ORAL PRESENTATIONS P.6-344

Back to Table of contents

Back to Table of contents

POSTERS PRESENTATIONS P.345-910

Back to Table of contents

Back to Table of contents

ORAL PRESENTATION
PLENARY LECTURES

PLEN1

Fighting the enemy – Understanding SARS-CoV-2 and its disease causing mechanisms - Joakim Esbjörnsson[1]

[1]Department of Translational Medicine, Lund University - Lund (Sweden)

Coronaviruses are single stranded RNA viruses, and the size of the virus genome ranges from 27,000-34,000 bp and encodes approximately 23 proteins. This include the spike (S) protein, a surface glycoprotein that is crucial for viral attachment and entry into the host cell. The currently ongoing SARS-CoV-2 pandemic has caused more 500 million confirmed infections worldwide with over 6 million confirmed deaths since the start in late 2019. Still, more than 11 billion vaccine doses has been administered. The development and administration of an effective vaccine in this short time represents an unparalleled achievement of the research community and industry. This lecture will highlight some of the main discoveries that made this possible and provide an overview of the current knowledge about what SARS-CoV-2 looks like, how it evolves and adapts to the human population, and the current antiviral strategies and vaccines and how our current understanding has been impacted by structural studies of the virus.

PLEN2

Code crack of color diversity - Maguy Jaber

[1]Sorbonne University - Paris (France)

Research on pigments formulations is not only a current trend in contemporary conservation science and technical art history, but is something that has preoccupied painters and researchers in cosmetic field throughout the centuries. Most painters and researchers are constantly looking for new materials or paint techniques in order to achieve new effects, for their works to last longer, to better express their intentions than before.
A pigment is an insoluble material in the medium where it is dispersed in. Depending on its particle size, the presence of defects in its structure, the reactive sites that allow interaction with other additives, a wide colour diversity can be obtained. To fully understand the physico-chemical mechanisms involved in the colour process will be of inestimable value.
Tuning the colour properties by a better control of the crystalline structure will be the concern of the present talk. Several examples will be discussed: inorganic pigments such as green earths, lake pigments and cadmium sulphides. The preparation of these inorganic and hybrid materials is described according to historical recipes. Grinding of green earth induce a complete change in their properties due to a modification in their particle size and reactivity. Cadmium sulphide pigments assume different hues from yellow to orange, depending on their conditions of formation and the presence of defects in their structure.

Back to Table of contents

ORAL PRESENTATION KEYNOTES

KN1

XFEL- and synchrotron-based serial crystallography studies of the membrane-bound proton pump cytochrome c oxidase

Gisela Brändén[1]
[1]University of Gothenburg - Goteborg (Sweden)

Serial crystallography is a relatively novel method within macromolecular crystallography that allows determination of protein structures at room temperature and enables time-resolved studies of protein dynamics. We use this method to study the membrane-bound respiratory enzyme cytochrome c oxidase, with the hope of being able to describe the mechanistic details of proton pumping. I will present our work on microcrystallization of membrane proteins, developments within crystal injection, and show results from recent static and time-resolved X-ray diffraction experiments at synchrotrons and XFELs.

Back to Table of contents

KN2
Experience and outlook for crystallography at the first MBA based synchrotron MAX IV
Marjolein Thunnissen

/

Back to Table of contents

KN3

The orchestration of NHEJ factors at DNA double-strand breaks by the Ku70/Ku80 heterodimer

M. Seif El Dahan 1, A.K. Stavridi 2, P. Frit 3, P. Legrand 4, S. Baconnais 5, E. Le Cam 5, P. Calsou 3, T.L. Blundell 2, A.K. Chaplin 2, J.B. Charbonnier 1, V. Ropars 1

1Université Paris-Saclay, CEA, CNRS, Institute for Integrative Biology of the Cell (I2BC) - Gif-sur-Yvette (France), 2Department of Biochemistry, University of Cambridge - Cambridge (United Kingdom), 3Institut de Pharmacologie et Biologie Structurale (IPBS), Université de Toulouse - Toulouse (France), 4Synchrotron Soleil - Saint-Aubin (France), 5Genome Integrity and Cancer UMR 9019 CNRS, Université Paris Saclay, Gustave Roussy 114 rue Edouard Vaillant - Villejuif (France)

Double Strand Breaks (DSB) are among the most toxic DNA lesion for the cells. A default during the repair process can lead to chromosomic aberrations, genes rearrangements and cancers. Without sister chromatid, the non-homologous end-joining (NHEJ) represent the major pathway of DSB repair in eukaryote cells. The ring-shaped Ku70/80 heterodimer rapidly senses broken DNA ends forming a recruiting hub (1, 2). Through protein-protein contacts eventually reinforced by protein-DNA interactions, the Ku-DNA hub attracts a series of specialized protein. To repair simple DSBs, such as 5’ phosphorylated blunt-ended DNA ends, the only additional requirement is the activity of DNA Ligase 4 (LIG4) in complex with its co-factor, the XRCC4 homodimer. Ku and LIG4/XRCC4 form the minimal core machinery of the c-NHEJ that can further be stimulated by the XLF or PAXX homodimers. We combined structural, biochemical and cellular analyses to unveil the role of Ku-Binding Motifs (KBM) present on several NHEJ factors. We determined crystal and CryoEM structures of Ku70/80/DNA complexes with different KBM motifs and unveiled their relative position on the heterodimer (3, unpublished data). We characterized the competition and synergies between these KBM motifs and used separation of function mutants of these KBM to precise the role of these interaction both in terms of recruitment at the DSB sites and in terms of repair efficiency. We then contributed to analyse the role of these KBM motifs in the context of the NHEJ super-complexes formation.

References

(1) Zahid, S & al. (2021) Int J Mol Sci;

(2) Frit, P & al (2019) Prog Biophys Mol Biol

(3) Nemoz C & al (2018) Nat Struct Mol Biol

Back to Table of contents

KN4

The extracellular juncture domains of Type 5 autotransporters

Julia Weikum,1,2 Alina Kulakova,3 Giulio Tesei,4 Shogo Yoshimoto,5 Line Vejby Jægerum,1 Monika Schütz,6 Katsutoshi Hori,5 Marie Skepö,7 Pernille Harris,3 Jack C. Leo,8,9 and J. Preben Morth1,2,10

1 Membrane Transport Group, Centre for Molecular Medicine Norway (NCMM), Nordic EMBL Partnership, University of Oslo, P.O. Box 1137 Blindern, 0318 Oslo, Norway
2 Enzyme and Protein Chemistry, Section for Protein Chemistry and Enzyme Technology, Department of Biotechnology and Biomedicine, Technical University of Denmark, Søltofts Plads, 2800, Kgs. Lyngby, Denmark
3 Department of Chemistry, Technical University of Denmark, Kemitorvet building 207, 2800 Kgs. Lyngby, Denmark
4 Structural Biology and NMR Laboratory, Linderstrøm-Lang Centre for Protein Science, Department of Biology, University of Copenhagen, Ole Maaloes Vej 5, Copenhagen 2200, Denmark
5 Department of Biomolecular Engineering, Graduate School of Engineering, Nagoya University, Furo-cho, Chikusa-ku, Nagoya 464-8603, Japan
6 Interfaculty Institute for Microbiology and Infection Medicine, University Clinics Tübingen, 72076 Tübingen, Germany.
7 Division of Theoretical Chemistry, Department of Chemistry, Lund University, 221 00 Lund, Sweden
8 Department of Biosciences, University of Oslo, P.O. Box 1137 Blindern, 0318 Oslo, Norway.
9 Department of Biosciences, Nottingham Trent University, Nottingham NG11 8NS, UK
10 Institute for Experimental Medical Research (IEMR), Oslo University Hospital, Ullevål PB 4956 Nydalen, NO-0424 Oslo, Norway.

Enterohemorrhagic and enteropathogenic Escherichia coli are among the most important food-borne pathogens. The virulence factor intimin is essential for attachment of pathogenic E. coli to intestinal host cells in human. Intimin is a surface exposed bacterial adhesion receptor which consists of four extracellular bacterial immunoglobulin-like (Big) domains, extending into the fifth subdomain which resemble a lectin like fold. The fifth domain binds to the Tir-receptor We have determined the crystal structures of the inner two Ig domains, called (D00 and D0) at 1.5 Å and the next domain pair D0-D1 at 1.8 Å resolution. With this we can confirm that the passenger of intimin has five distinct domains, only recently proposed. We describe that D00-D0 linker region exhibits a higher degree of rigidity and that D00 likely functions as a juncture domain exposed to the outer membrane and always anchored next to the inner membrane beta barrel inserted into the membrane. The accumulated data allows us to model the complete passenger of intimin and allows us to propose functionality through the degree of flexibility and rigidity inherent to the Big domains, D00-D0-D1, extending directly from the membrane.

Back to Table of contents

KN5
Electron diffraction of 3D nanocrystals: an emerging technique in structural biology

C. Moriscot [1], W.L. Ling [1], G. Schoehn [1], D. Housset [1]

[1]Institut de Biologie Structurale, UGA, CEA, CNRS - Grenoble (France)

Electron diffraction of 3D nanometer sized crystals, most commonly named microED, has recently emerged as a new technique to solve the structure of both small organic molecules and proteins (1–3). MicroED is clearly a promising technique in structural biology, both quite easy to implement and very complementary to X-ray crystallography and single particle cryo-EM. Electrons are actually a very interesting probe for small samples as they strongly interact with matter, and more importantly, they deposit much less energy than X-rays per diffracted particle (4). The drawback of strong interaction is the presence of multiple diffraction events that make the relationship between diffracted intensities and structure factor much complicated than with the kinematical theory of diffraction. Nevertheless, sub-atomic resolution data can routinely be collected for small organic compounds and data up to 1.5 Å resolution can be obtained from protein crystals. Phasing can be done by either direct methods for sub-atomic resolution data or by molecular replacement and refinement can easily be performed with programs developed for X-ray crystallography, such as Refmac or Shelxl. When the number of atoms is small, multiple diffraction can be taken into account at the refinement stage to improve the final Coulomb potential map (5, 6). During the past few years, microED has been very successful for solving the the structures of small organic molecules, metallo organic framework and proteins up to 100-200 kDa. However, a quick look at the Protein Data Bank shows that among the 66 protein structures determined so far by microED, only 10 are not model proteins, and just 2 were solved with models sharing less than 99% sequence homology. 9 years after the first articles marking the emergence of microED in structural biology (7, 8), this indicate that the technique is still far from routinely used. Based on examples either studied at IBS, thanks to our hybrid pixel direct detector mounted on an F20 200 kV electron microscope, or picked up in the literature, I will give an overview of the main results of the technique but also focus on remaining bottlenecks.

References

1. Clabbers, M. T. B., E. van Genderen, W. Wan, E. L. Wiegers, T. Gruene, and J. P. Abrahams. 2017. Protein structure determination by electron diffraction using a single three-dimensional nanocrystal. Acta Crystallogr. Sect. Struct. Biol. 73: 738–748.
2. Gemmi, M., E. Mugnaioli, T. E. Gorelik, U. Kolb, L. Palatinus, P. Boullay, S. Hovmöller, and J. P. Abrahams. 2019. 3D Electron Diffraction: The Nanocrystallography Revolution. ACS Cent. Sci. 5: 1315–1329.
3. Gruene, T., J. T. C. Wennmacher, C. Zaubitzer, J. J. Holstein, J. Heidler, A. Fecteau-Lefebvre, S. De Carlo, E. Müller, K. N. Goldie, I. Regeni, T. Li, G. Santiso-Quinones, G. Steinfeld, S. Handschin, E. van Genderen, J. A. van Bokhoven, G. H. Clever, and R. Pantelic. 2018. Rapid Structure Determination of Microcrystalline Molecular Compounds Using Electron Diffraction. Angew. Chem. Int. Ed Engl. 57: 16313–16317.
4. Henderson, R. 1995. The potential and limitations of neutrons, electrons and X-rays for atomic resolution microscopy of unstained biological molecules. Q. Rev. Biophys. 28: 171–193.
5. Palatinus, L., P. Brázda, P. Boullay, O. Perez, M. Klementová, S. Petit, V. Eigner, M. Zaarour, and S. Mintova. 2017. Hydrogen positions in single nanocrystals revealed by electron diffraction. Science 355: 166–169.
6. Blum, T. B., D. Housset, M. T. B. Clabbers, E. van Genderen, M. Bacia-Verloop, U. Zander, A. A. McCarthy, G. Schoehn, W. L. Ling, and J. P. Abrahams. 2021. Statistically correcting dynamical electron scattering improves the refinement of protein nanocrystals, including charge refinement of coordinated metals. Acta Crystallogr. Sect. Struct. Biol. 77: 75–85.
7. Nederlof, I., E. van Genderen, Y. W. Li, and J. P. Abrahams. 2013. A Medipix quantum area detector allows rotation electron diffraction data collection from submicrometre three-dimensional protein crystals. Acta Crystallogr. D Biol. Crystallogr. 69: 1223–1230.
8. Shi, D., B. L. Nannenga, M. G. Iadanza, and T. Gonen. 2013. Three-dimensional electron crystallography of protein microcrystals. eLife 2: e01345

Back to Table of contents

KN6

Atomic resolution structure determination of larger macromolecular complexes by cryo-EM and X-ray crystallography

Ashwin Chari & Holger Stark (Göttingen,Germany)

The technological advances in electron microscopy hardware, in detector development and in available image processing tools made cryo-EM a highly successful and rapidly developing method for protein structure determination. Based on the exponentially growing numbers of protein structures determined by this method, cryo-EM is even likely to become the dominant method for protein structure determination within the next few years assuming the current growth in database deposition continues. Since cryo-EM does not require crystalline material, many structures of complexes have been solved in the last decade that were evasive targets to X-ray crystallography for a long time. In cryo-EM there is also an increasing level of automation that allows even beginners to obtain a high-resolution structure of a biochemically well-defined complex within days or weeks.
Furthermore, the resolution limits in cryo-EM have been pushed constantly over the last couple of years. For highly stable and rigid complexes, even true atomic resolution structures are now possible1. The image processing in cryo-EM also often allows the user to determine structures of several conformational states from one single dataset and therefore provides information about dynamic structural elements in a complex.
Because of the cryo-EM success story, the attention in structural biology has recently been shifted away from X-ray crystallography in spite of the long-term success and power of this technique. It is however noteworthy that several important developments were also made in the field of crystallography. Especially the possibilities to do time-resolved crystallographic experiments by XFEL but also by standard synchrotrons do provide access to detailed dynamic information in macromolecular complexes that is not yet obtainable by cryo-EM.
There is therefore absolutely no good reason to play the two techniques off against each other. Cryo-EM and crystallography have both advantages and disadvantages. Using both techniques in parallel indeed provides complementary information which greatly helps our structural and functional understanding of macromolecular complexes.

(1) Yip, K.M., Fischer, N., Paknia, E., Chari, A., and Stark, H. (2020). Atomic-resolution protein structure determination by cryo-EM. Nature 587, 157-161.

Back to Table of contents

KN7

Structural Chemistry of Layered Hybrid Perovskites

Philip Lightfoot (St Andrews, United Kingdom)

Lead halide perovskites (LHPs) have recently revolutionised the field of solar cells, in addition to showing novel and promising properties in several other areas, such as luminescence, ferroelectricity etc. The solid-state chemistry and crystallography of these materials is fascinating and complex, with a bewildering array of different compositions and structure types. Recently1, we have tried to systematise part of this complex structural diversity, by using an approach based on symmetry mode analysis to understand crystallographic relationships amongst layered phases of the type AA'PbX4 (X=Cl, Br, I), which are based on (001)-oriented corner-sharing octahedral layers, related to perovskite. This talk will first discuss this classification, revealing some trends across structural behaviour versus chemical composition. We shall then discuss some examples of related structures from our own work; for example, the less common (110)-oriented layered lead halide perovskites2, and some novel structural behaviour and physical properties in halide hybrids based on tin3 and copper4.

References
1. J. A. McNulty and P. Lightfoot, IUCrJ, 8, 485-513 (2021).
2. Y.-Y. Guo et al., Chem. Commun., 55, 9935-9938 (2019).
3. J. A. McNulty and P. Lightfoot, Chem. Commun., 56, 4543-4546 (2020).
4. C. Han et al., Inorg. Chem., 61, 3230-3239 (2022).

Back to Table of contents

KN8

Microstructures induced by phase transformations under extreme conditions

A. Dewaele 1, L. Henry 2, R. Fréville 3, C. Denoual 2, N. Guignot 4, A. King 4, B. Nicolas 3, E. Boulard 5, Y. Legodec 5, G. Garbarino 6
[1]CEA-Arpajon - Arpajon (France), [2]CEA - Arpajon (France) - Arpajon (France), [3]CEA - Arpajon (France), [4]Synchrotron Soleil - Saint-Aubin (France), [5]IMPMC - Paris (France), [6]ESRF - Grenoble (France)

Phase transitions in metals have a drastic influence on their mechanical response and thus have a fundamental bearing for the industry. Some of them are described as martensitic, a displacive mechanism involving small but collective atomic displacements which induces characteristic microstructures. Metals also exhibit a rich polymorphism under extreme conditions (high pressure – high temperature), but the mechanism of transitions were unknown as the microstructures formed could not be measured with conventional techniques such as powder X-ray diffraction.
We characterized pressure-induced phase transformations in iron (alpha-epsilon) and cerium (gamma-alpha), pressurizing samples in diamond anvil cells or Paris-Edinburg presses in the 0-20 GPa, 300-100 K pressure-temperature range. The use of samples with controlled microstructures, together with in situ measurements – single and multigrain X-ray diffraction, X-ray computed tomography coupled with diffraction – allows constraining their mechanisms and observing transient states. The in situ observables are transformation conditions, elastic strains, orientation relations, surfaces of coexistence between the two phases. They are complemented by ex-situ scanning electron microscope analysis (EBSD technique) and interpreted using mechanic modelings.
For iron, we find that the first displacive step along Burgers path (see Figure) can be followed by a reconstructive stage, the microstructure keeping a memory of the first step. This memory triggers the reverse transformation path. Transformation twinning affects a limited volume of the sample. For cerium, the transformation microstructure exhibits martensitic features, such as platelets, which could be explained by an elastic softening in gamma-Ce.
Such monitoring of allotropic transitions can be used to tailor materials with outstanding mechanical or thermal properties.

References

E. Boulard, C. Denoual, A. Dewaele, A. King, Y. LeGodec, N. Guignot, Following the phase transitions of iron in 3D with X-ray tomography and diffraction under extreme conditions, Acta Mat. 192, 30-39, 2020
A. Dewaele, V. Svitlyk, F. Bottin, J. Bouchet and J. Jacobs, Iron under conditions close to the alpha-gamma-epsilon triple point, Appl. Phys. Lett. 112, 201906, 2018
A. Dewaele, C. Denoual, S. Anzellini, F. Occelli, M. Mezouar, P. Cordier, S. Merkel, M. Véron and E. Rausch, « Mechanism of the alpha-epsilon transformation in iron », Phys. Rev. B 91, 174105, 2015

epsilon-Fe platelets orientation variants predicte

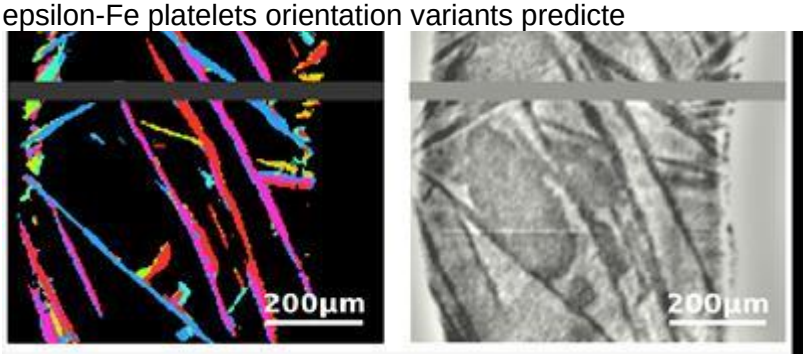

Back to Table of contents

KN9

Multivariate innovative methods for the analysis of in situ X-ray powder diffraction data collected in the presence of chemical, spatial, temperature or time gradients

M. Lopresti [1], L. Palin [1], E. Conterosito [1], B. Mangolini [2], C. Rocco [3], M. Marco [1]
[1]Università del Piemonte Orientale (Italy), [2]Cold Car SpA (Italy), [3]IC CNR (Italy)

X-ray powder diffraction (XRPD) is a key technique for the characterization of phases in solid samples, with applications spanning from materials and earth science to chemistry, pharmaceutics and engineering. The obtained information can be either qualitative or quantitative, related to phase composition, crystallite size, stress, texture. In the last decades in situ experiment allowed to evaluate such properties while the samples evolve by internal (e.g. chemical) and/or external (e.g. temperature, pressure…) stimuli. Such experiments allow exploring the structural properties in presence of gradients of several types. Chemical (when composition is changing, or a gas pressure is applied) and energetic (when temperature and/or pressure are being modified during the experiment) are the most investigated gradients within in situ XRPD experiments. When a static sample is studied by microdiffraction, a spatial gradient can be studied by collecting XRPD pattern scanning the surface of the sample itself: in other words, the structural features are studied depending on the xy coordinates of the sample surface. In all these cases, large dataset can be collected both by lab instruments and synchrotron facilities. Facing such datasets requires new approaches, complementary to traditional XRPD analysis methods, which are very powerful but time and resource consuming.
The amount of useful information that can be extracted from a XRPD dataset can be maximized exploiting multivariate analysis techniques such as principal component analysis (PCA), while reducing the experimental noise. Within the presentation, the application of multivariate approaches to X-ray diffraction will be described presenting both assessed and under development approaches. Particular attention will be given to pre-processing selection in relation to specific data features. Then, case studies are presented to show potentialities and limitations of each approach. At first, regression and PCA methods are applied to chemical gradient, to carry out a quantitative of some ad hoc designed mixtures showing preferred orientation and microabsorption, illustrating how they can overperform traditional Rietveld-based approaches. The PCA is then used to analyze the temperature gradient, studying the crystallization and melting of eutectic mixtures by an XRPD experiment run at variable temperature conditions. By combining multivariate analysis and in situ XRPD, a new approach called differential scanning diffraction (DSD) can be defined and implemented. A phase transition can be now analyzed like a traditional differential scanning calorimetry (DSC) but probing structural effect instead of energy ones. Finally, spatial gradients are analyzed, applying PCA analysis to microdiffraction data collected on the surface of metal object and mineralogic samples.

Back to Table of contents

KN10

Quantum crystallography of (macro)molecular crystals for everyone

P. Dominiak
Biological and Chemical Research Centre, Department of Chemistry, University of Warsaw - Warsaw (Poland)

At the heart of X-ray crystallography is the scattering of the X-ray photon beam at the electron density of the crystal. Similarly, the electron beam is scattered at the electrostatic potential of the crystal or single particle. When analyzing the experimental diffraction(scattering) data, it is necessary to use the appropriate atomic scattering factors. To obtain them, the widely used model of independent atoms (IAM) with spherical symmetry was proposed about 100 years ago. However, the electron densities and electrostatic potentials of atoms in a molecule or crystal are not perfectly spherical, and the associated point charges are rarely close to formal ones. Currently, thanks to better measuring equipment, the shortcomings of the IAM are clearly visible in X-ray crystallography. To take advantage of more accurate, routinely collected data, more accurate electron density models should be used. The same soon happen with electron crystallography and modelling of electrostatic potential.

Quantum crystallography is usually associated with highly complex modeling using quantum chemistry methods and collecting experimental diffraction data of exceptional quality and resolution. Indeed, this is the heart of quantum crystallography. However, there is a branch of quantum crystallography which focuses on delivering new scattering models, data interpretation methods, and fast and reliable software tools to be applicable to standard measurements. The goal is to extract more information from routinely collected data. On the one hand, these new methods allow to achieve better fitting of the model to the data and improve the quality of the geometric data typically obtained from such measurements. On the other hand, they provide access to new types of information, i.e. electron density, electrostatic potential, interaction energy, and many more. Thus, quantum crystallography can be useful to all crystallographers, chemists, and structural biologists in their daily practice.

During the lecture, I will give general overview to the recent developments on the Hirshfeld Atom Refinement (HAR) and the Transferable Aspherical Atom Model (TAAM) refinement. I will focus on the Multipolar Atom Types from Theory and Statistical clustering (MATTS, formerly UBDB) data bank used to parametrize TAAM. I will present the results of TAAM refinements of organic crystal structures on the data from X-ray and 3D electron diffraction (3D ED). Prove that the time and effort needed to do TAAM refinement for organic crystals is almost the same as for IAM, including crystals with disorder and twinning. I will discuss how TAAM may help in the refinement of protein crystal structures against 3D ED (microED) data.

Acknowledgements: This work is supported by the National Centre of Science (Poland) through grant OPUS No.UMO-2017/27/B/ST4/02721.

Back to Table of contents

KN11

Electron crystallography – diverse facets of nanocrystalline materials

Tatiana E. Gorelika, b, c

[a]Ulm University, Albert Einstein Allee 11, 89081 Ulm, Germany
[b]Helmholtz Centre for Infection Research, Inhoffenstr. 7, 38124 Braunschweig, Germany
[C]Helmholtz Institute for Pharmaceutical Research Saarland, Campus E8.1, 66123 Saarbrücken, Germany

Electron crystallography came on the scientific scene 15 years ago with the introduction of automated procedure for stepwise electron diffraction data acquisition – automated diffraction tomography (Kolb, et al., 2007). Later, diverse instrumental variants of the method appeared (Gemmi et al., 2019, Gruene & Mugnaioli, 2021), including rotation electron diffraction (RED), precession-assisted electron diffraction tomography (PEDT), and continuous rotation electron diffraction (cRED, essentially equivalent to microcrystal electron diffraction, microED). In the meantime, all these techniques are located under an umbrella term of 3D electron diffraction – 3D ED. The success of 3D ED for structure analysis is given by the simplicity of the data acquisition and the possibility to use procedures established within X-ray crystallographic community. Successful structure analysis from 3D ED data were reported for different classes of materials, featuring a structure determination of an unknown protein (Xu et al., 2019), structure analysis of twinned orthocetamol crystals (Andrusenko et al., 2019), MOFs and COFs (Huang et al, 2021a) and zeolites (Su et al., 2014). Potential of the method as high-throughput technique is demonstrated by Bruhn (Bruhn et al., 2021) and Burch (Burch et al., 2021).
Possibilities to automate the data collection have opened a new facet of the method – serial electron crystallography – the collection of series of small datasets with partial completeness or single diffraction patterns from individual randomly oriented crystals. The method has been effectively used to identify and solve structures of inorganic (Smeets et al., 2018) and biological (Buecker et al., 2020) compounds. Cluster analysis of the serial electron diffraction data allowed identifying and analysing individual components in a complex polyphasic system (Wang et al., 2019).
Analysis of electron scattering intensities between the Bragg peaks allows for structure analysis of features beyond the average crystalline structure (Mugnaioli & Gorelik, 2019) of nanocrystalline materials. Models of stacking faults in nanocrystalline layered materials can be constructed from quantitative analysis of diffuse scattering lines within the reciprocal space (Krysiak et al., 2018). Furthermore, 3D ΔPDF maps obtained from 3D ED data (Schmidt et al., 2021), allow for analysis of interatomic distances correlation in materials with high amount of point defects just as it can be done from X-ray or neutron diffraction data.
Crystal size confinement produces extended features in the reciprocal space. In the extreme case of 2D crystals, the reciprocal space consists of continuous lines – relrods – which can be seen as a special case of diffuse scattering. Analysis of scattering intensities distribution along the relrods allows to assign the number of repetition units in a crystal, i.e. determine the number of layers in a 2D crystal (Gorelik et al., 2021).
Finally, the structure of amorphous material on nanoscale can be studied using electron Pair Distribution Function (ePDF) and Fluctuation Electron Microscopy (FEM), where ePDF (Gorelik et al., 2019; Ehrhardt et al., 2021) allows for “bulk” structure analysis of the material, whereas FEM (Voyles & Muller, 2002) provides information on the local atomic arrangement (Huang et al., 2021b).

Andrusenko et al., 2019. Angew. Chem., Int. Ed., 58, 10919; Bruhn et al., 2021. Front. Mol. Biosci., 12 July 2021; Buecker et al., 2020, Nature Comm. 11:996; Burch et al., 2021, ChemRxiv; Ehrhardt et al., 2021. Chem. Mater. 33, 8990; Gemmi et al., 2019. ACS Cent. Sci. 5, 1315; Gorelik et al., 2019. Acta Cryst. B75, 532; Gorelik et al., 2021. Micron 146, 103071; Gruene & Mugnaioli, 2021. Chem Rev. 121, 11823; Huang et al., 2021a. Coord. Chem. Rev. 427, 213583; Huang et al., 2021b. Microscopy and Microanalysis 27, 748; Kolb et al., 2007. Ultramicroscopy, 107, 507; Krysiak et al., 2018. Acta Cryst. A74, 93; Mugnaioli & Gorelik 2019. Acta Cryst. B75, 550; Schmidt et al., 2021. Oral contribution at IUCr Congress, Prague; Smeets et al., 2018. J. Appl. Crystallogr. 51, 1; Su et al., 2014. Microporous and Mesoporous Materials 189, 115; Voyles & Muller, 2002. Ultramicroscopy 93, 147; Wang et al., 2019. IUCrJ. 6, 854; Xu et al. 2019. Sci. Adv. 5, 1.

Back to Table of contents

KN12

Diversity in Crystallography: fact or fiction?

Elspeth Garman (Oxford, United Kingdom)

During the 20th century, the discipline of crystallography has attracted a number of outstanding female researchers, among them the publically famous Kathleen Lonsdale, Dorothy Hodgkin, Helen Megaw and Rosalind Franklin. In addition, many other women became card-carrying crystallographers, partly due to the 'gender blind' recruitment of researchers by the Bragg father and son [1]. What allowed this field to provide an environment in which women could significantly contribute, and how has this developed historically and up to the present time? Using observations from a variety of sources [e.g. 2], I will endeavour to present some thoughts on this question, and efforts to address the current imbalances in equity and diversity in the 21st century [3].

References

[1] Maureen M. Julian, "Women in Crystallography," in Women of Science: Righting the Record, ed. G. Kass-Simon and Patricia Farnes (Bloomington: Indiana University Press, 1990), pp. 342

[2] https://blogs.iucr.org/crystallites/2018/03/07/women-in-crystallography-we%E2%80%99re-not-just-historical/

[3] https://www.iucr.org/iucr/governance/advisory-committees/gedc

Back to Table of contents

KN13

Analyzing single crystal diffuse scattering

R. Neder
Friedrich-Alexander-Univeristät Erlangen-Nürnberg - Erlangen (Germany)

Materials with a disordered structure still pose a challenge with respect to an accurate and complete description of their structure. The analysis of just the Bragg reflection intensities will yield a different structural model compared to the analysis of the diffuse scattering. While the former yields a structure projected into a single unit cell, the latter yields an structural model that allows to view the local deviations from the average structure.

In recent years experimental data collection of the diffuse scattering has become much less tedious. Compared to pure Bragg data the challenges imposed are due to the very different local intensity scales of Bragg and diffuse scattering, inversely coupled to very different extend in reciprocal space. New neutron based instruments like Corelli, new low background X-ray detectors and the rise of electron diffraction techniques allow a faster and better data collection strategy.

The data analysis has greatly benefited from the development of the 3D-Delta-PDF technique. This technique yields a much less difficult access to starting models and offers a good complementary approach to quantitative data analysis based on reciprocal space data.

The lecture will review the current experimental and data analysis developments.

Back to Table of contents

KN14

Configuring material properties by crystal engineering

Alessia Bacchi (Parma, Italia)

Crystal engineering is a powerful tool to design materials with high technological added value to address health and environment protection through mild and nature friendly components and methods. Some compounds relevant to human health and nutrition are liquid at ambient conditions (L-API); widely known examples are propofol, vitamin E, nicotine, and terpenoids and phenolic derivatives used as natural antioxidants such as carvacrol, eugenol , eucalyptol, and valproic acid. A practical way to manufacture some of these compounds in a solid dosage form is to modify their molecular structures by synthetic derivatization, or to turn them into salts, provided that the molecule may be reacted with a convenient acid or base, and that these are acceptable from a regulatory point of view. However, not all the molecules may become salts, and derivatization may alter molecular bioavailability. Recently, cocrystallization has proven to be a powerful method to control the release of liquid ingredients in the environment, thanks to the engineering of ad hoc intermolecular interactions which strengthen or weaken the tendency of the ingredient to be retained inside the solid matrix. [1-2]. Similarly, L-API have been encapsulated within adaptable cavities of Metal Organic Frameworks purposedly designed to uptake such guests; the evolution in time of the supramolecular arrangement of the nano-confined guests in the cavities has been monitored by SCXRD and related to the observed selectivity ofthe material towards different L-API guests [3-4].
We here present some proofs of concept that a rational design of crystalline materials such as MOFs and cocrystals capable to store and release L-API guests is feasible (Figure 1), and that the release profile can be related to the solid state arrangement of the material, offering a strong and rational tool to afford a vast range of materials capable of controlled release of L-APIs.

References

[1] Turning Liquid Propofol into Solid (without Freezing It): Thermodynamic Characterization of Pharmaceutical Cocrystals Built with a Liquid Drug, Alessia Bacchi, Davide Capucci, Marco Giannetto, Monica Mattarozzi, Paolo Pelagatti, Nair Rodriguez-Hornedo, Katia Rubini, and Andrea Sala, Cryst. Growth Des. 2016, 16, 11, 6547–6555
[2] Designing a Palette of Cocrystals Based on Essential Oil Constituents for Agricultural Applications, Paolo P. Mazzeo, Claudia Carraro, Andrea Monica, Davide Capucci, Paolo Pelagatti, Federica Bianchi, Silvia Agazzi, Maria Careri, Aida Raio, Marina Carta, Felicia Menicucci, Mattia Belli, Marco Michelozzi, and Alessia Bacchi, ACS Sustainable Chem. Eng. 2019, 7, 21, 17929–17940
[3] Stepwise Evolution of Molecular Nanoaggregates Inside the Pores of a Highly Flexible Metal–Organic Framework. Davide Balestri, Paolo P. Mazzeo, Claudia Carraro, Nicola Demitri, Paolo Pelagatti, Alessia Bacchi. , 2019, Angew. Chem. Int. Ed., vol. 58, p. 17342-17350
[4] Deciphering the Supramolecular Organization of Multiple Guests Inside a Microporous MOF to Understand their Release Profile. Davide Balestri, Paolo P. Mazzeo, Roberto Perrone, Fabio Fornari, Federica Bianchi, Maria Careri, Alessia Bacchi, Paolo Pelagatti P. Angew. Chem. Int. Ed., 2021, vol. 60, p. 10194-10202

Figure 1.

Back to Table of contents

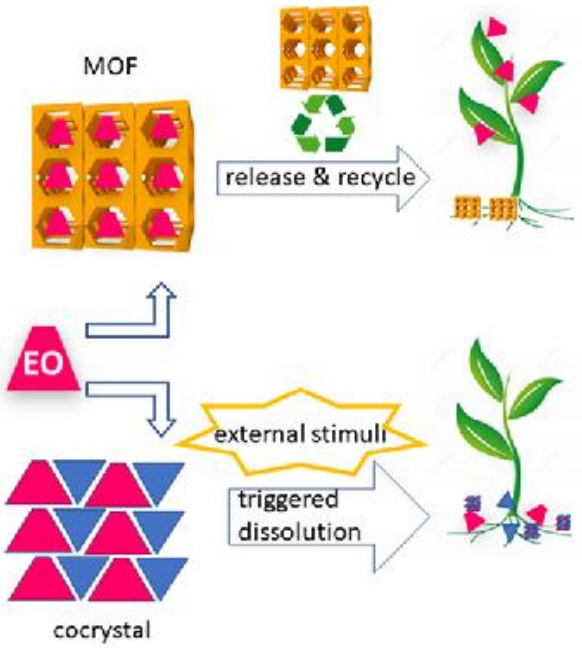

Back to Table of contents

KN16

Battery cathode crystal structures: seeking to simplify complexity

Bill David
University of Oxford / STFC - Oxford (United Kingdom)

The crystallographic analysis of high performance rechargeable batteries is, from a commercial viewpoint, essential for the achievement of optimal performance. From an academic perspective, the precise experimental measurement of these simple pristine materials can pose significant analytical and theoretical challenges.
There is a conundrum at the basis of this research. For example, pristine high-power lithium-ion cathode materials have a very simple crystal structure based on an ordered, layered rock-salt structure. LiCoO2, the prototypic cathode material, adopts a rhombohedral structure with a single variable atomic coordinate; both lithium and cobalt have octahedral moieties. NaCoO2 adopts a similar structure but, on one-third de-intercalation, transitions to a hexagonal symmetry where the oxygen coordination around sodium is trigonal pyramidal.
This talk discusses the challenges of building a simple and accurate model of the crystal structures of sodium-ion battery cathode materials during charging and discharging. Multiple structures have been reported that are based on the octahedral and trigonal-pyramidal prototypes but these structure alone are not sufficient to describe the complexity of the observed powder diffraction data. The approach presented in this talk is based around the analysis of the shearing of neighbouring layers using the minimal number of stacking fault probabilities that precisely model the observed complex powder diffraction patterns.

Back to Table of contents

KN17

Intermolecular interactions "stabilising" a crystal structure – truth or wishful thinking?

Catharine Esterhuysen (Stellenbosch, South Africa)

Noncovalent intermolecular interactions are often the most discussed aspect of a crystal structure, with a common statement (particularly in students' writing) being that "the crystal structure is stabilised by XYZ interactions". But are such statements warranted? When can one say with reasonable certainty that a short distance between two atoms is genuinely indicative of an attraction, and when should one be more circumspect? For instance, when can a C–H···H interaction reasonably be considered stabilising?
In this presentation we will look at the nature of various intermolecular interactions and the ways in which crystal structures can (and should) be analysed before such broad statements regarding a "stabilising" interaction can be made.

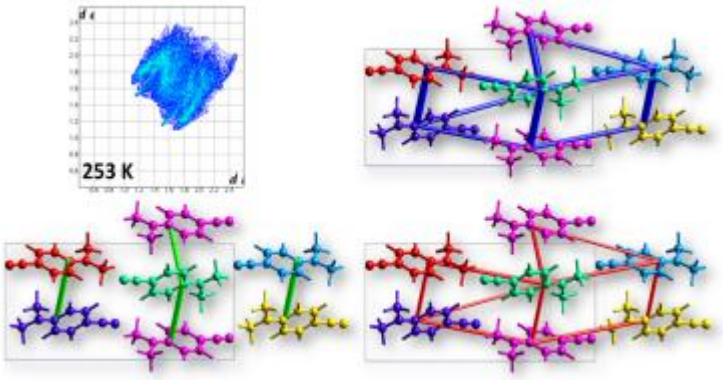

Back to Table of contents

ORAL PRESENTATION
PUBLIC LECTURES

PL1

René-Just Haüy and the birth of modern crystallography

D. Cabaret , J.C. Boulliard
Sorbonne Université - Paris (France)

In 1784, a small book entitled "Essai d'une théorie sur la structure des crystaux" was published marking the beginning of modern crystallography.
A crystallography that releases from its first purely descriptive vocation using mathematics.
A crystallography that predicts shapes and reveals molecules that would be debated for almost a century.

Its author, René-Just Haüy, a French abbot living in Paris, began at almost forty years old into a scientific career focused on the crystal study. His successes made him one of the greatest scientists of his time.

To mark the bicentenary of his death, we propose to present the milestones of his uncommon career, in the troubled historic context of the end of the 18th century.
We will highlight his work, from the birth of a myth to that of a theory that made crystallography and mineralogy real sciences as physics or chemistry.

PL2

A scientific yard next to the restoration yard of Notre-Dame de Paris

Philippe Dillmann
LAPA IRAMAT and NIMBE, CNRS, CEA Saclay, Université de Paris Saclay, 91191 Gif sur Yvette Cedex

Following the tragedy of 15 April 2019, a formidable restoration project was set up around Notre-Dame. In parallel to this work and in close interaction with it, a scientific project was developed, coordinated by the CNRS and the Ministry of Culture, with nearly 200 scientists, nine working groups, interdisciplinary research, a necessary link between the scientific project and the restoration project, and a synergy between institutions, skills and diversified practices.

On the scientific yard of Notre-Dame, the sciences of measurement and modelling rub shoulders with, for example, engineers specialized in structural calculations, acousticians or digital experts, physical chemists who try to understand how matter is arranged at the atomic and molecular level, but also archaeologists who study the medieval building, art and technical historians, anthropologists and sociologists. For several decades now, the boundaries between these disciplines have been blurred and have become interactive, articulating concepts and practices in a demanding dialogue. The archaeological and heritage sciences bring together all the disciplines that intersect in order to grasp the totality of an object from ancient times, as it may have been conceived at a given moment in history; it is this interdisciplinary approach that is at work at Notre-Dame.

Back to Table of contents

ORAL PRESENTATION

MS

MS01 MX/Cryo-EM software development

MS1-01

Fitting, refinement and validation of atomic models in cryo-EM maps using TEMPy2

D.M. Topf [1]
[1]*CSSB/LIV/UKE Hamburg - Hamburg (Germany)*

Abstract
As the resolutions of cryo-EM reconstructions of macromolecular assemblies are being improved, there is a need for better fitting and refinement methods of atomic models in medium-to-high resolutions. There is also a strong need for robust approaches for model assessment. Here, we present the current capabilities of our software TEMPy2 to fit, refine and validate atomic models in cryo-EM maps. We demonstrate it on a large benchmark of assemblies from EMDB (at 1.8-7.1 Å resolution) and CASP14 cryo-EM targets (2.1-3.8 Å resolution). We also present new capabilities of TEMPy2 to process cryoEM maps.

References
1. Cragnolini T, Sahota H, Joseph AP, Sweeney A, Malhotra S, Vasishtan D, Topf M (2021) TEMPy2: a Python library with improved 3D electron microscopy density-fitting and validation workflows. Acta Crystallogr D Struct Biol 77:41–47.
2. Cragnolini T, Kryshtafovych A, Topf M (2021) Cryo-EM targets in CASP14. Proteins 89(12):1949-1958.

Back to Table of contents

MS01 MX/Cryo-EM software development

MS1-02

New Tools and Pipelines for Continuous Heterogeneity Analysis from Cryo-EM using Normal Modes and 3D Zernike Polynomials

J. Krieger [1], D. Herreros [1], C.O.S. Sorzano [1], J.M. Carazo [1]
[1]*Centro Nacional de Biotecnologia - Madrid (Spain)*

Abstract

Cryo-EM is now able to reveal continuous heterogeneity and dynamics with many groups developing methods to analysis this, including ours, which we are making available in Scipion [1], which integrates multiple software packages into pipelines.

Simple computational biophysics models and methods such as elastic network models (ENMs) and normal mode analysis (NMA) can efficiently identify key motions of biological relevance, even for large system studied by Cryo-EM [2]. These methods have been demonstrated to be beneficial for Cryo-EM continuous heterogeneity analysis some years ago with the hybrid electron microscopy normal mode analysis (HEMNMA) [3], which has recently been integrated into Scipion through the ContinuousFlex plugin [4], and its extension HEMNMA-3D for tomography [5].

We now extend the capabilities for using such approaches further by integrating the ProDy Python package for protein dynamics [6] into a Scipion plugin with new protocols for atom selection and alignment, analysis of deformation vectors associated with pairwise conformational changes, ENM NMA, construction of structural ensembles and principal component analysis (PCA) of them, and comparison of these different motions derived from theory and experiments.

Another approach that is proving successful in our lab, which is being implemented with Xmipp [7] and associated Scipion plugins, makes use of 3D Zernike polynomials to describe conformational changes [8]. This approach can combine information from images, volumes and atomic structures into a common framework, optimising the coefficients of the polynomials to describe transitions between them and create a rough conformational space. Applying these polynomials and coefficients creates new volumes and structures corresponding to particular regions of the space.

We can also convert Zernike bases and coefficients to corresponding ones for normal modes and vice versa, providing a more direct connection between Cryo-EM data and physically realistic motions. There is also the potential to integrate with other computational biophysics methods, such as molecular dynamics simulations, and other molecular modelling procedures, allowing refinement of the resulting structures and landscapes.

We demonstrate using the SARS-CoV-2 spike and AMPA-type ionotropic glutamate receptors how such new pipelines combining different approaches within Scipion will allow a richer ability to understand protein dynamics, landscapes and mechanisms.

References

Scipion: A software framework toward integration, reproducibility and validation in 3D electron microscopy. de la Rosa-Trevín JM, Quintana A, Del Cano L, Zaldívar A, Foche I, Gutiérrez J, Gómez-Blanco J, Burguet-Castell J, Cuenca-Alba J, Abrishami V, Vargas J, Otón J, Sharov G, Vilas JL, Navas J, Conesa P, Kazemi M, Marabini R, Sorzano CO, Carazo JM. J Struct Biol. 2016 Jul;195(1):93-9

Protein dynamics developments for the large scale and cryoEM: case study of ProDy 2.0. Krieger JM, Sorzano COS, Carazo JM, Bahar I. Acta Crystallogr D Struct Biol. 2022 Apr 1;78(Pt 4):399-409

Iterative elastic 3D-to-2D alignment method using normal modes for studying structural dynamics of large macromolecular complexes. Jin Q, Sorzano CO, de la Rosa-Trevín JM, Bilbao-Castro JR, Núñez-Ramírez R, Llorca O, Tama F, Jonić S. Structure. 2014 Mar 4;22(3):496-506

Hybrid Electron Microscopy Normal Mode Analysis with Scipion. Harastani M, Sorzano COS, Jonić S. Protein Sci. 2020 Jan;29(1):223-236

HEMNMA-3D: Cryo Electron Tomography Method Based on Normal Mode Analysis to Study Continuous Conformational Variability of Macromolecular Complexes. Harastani M, Eltsov M, Leforestier A, Jonic S. Front Mol Biosci. 2021 May 19;8:663121

Back to Table of contents

ProDy 2.0: Increased Scale and Scope after 10 Years of Protein Dynamics Modelling with Python. Zhang S, Krieger JM, Zhang Y, Kaya C, Kaynak B, Mikulska-Ruminska K, Doruker P, Li H, Bahar I. Bioinformatics. 2021 Apr 5;37(20):3657-9
Advances in Xmipp for Cryo-Electron Microscopy: From Xmipp to Scipion. Strelak D, Jiménez-Moreno A, Vilas JL, Ramírez-Aportela E, Sánchez-García R, Maluenda D, Vargas J, Herreros D, Fernández-Giménez E, de Isidro-Gómez FP, Horacek J, Myska D, Horacek M, Conesa P, Fonseca-Reyna YC, Jiménez J, Martínez M, Harastani M, Jonić S, Filipovic J, Marabini R, Carazo JM, Sorzano COS. Molecules. 2021 Oct 15;26(20):6224
Approximating deformation fields for the analysis of continuous heterogeneity of biological macromolecules by 3D Zernike polynomials. Herreros D, Lederman RR, Krieger J, Jiménez-Moreno A, Martínez M, Myška D, Strelak D, Filipovic J, Bahar I, Carazo JM, Sanchez COS. IUCrJ. 2021 Oct 14;8(Pt 6):992-1005

Back to Table of contents

MS01 MX/Cryo-EM software development

MS1-03

Automatic decision on optimal resolution cut-off with PAIREF

M. Maly [1], K. Diederichs [2], J. Stránský [3], K. Adámková [3], J. Dohnálek [3], P. Kolenko [1]
[1]Czech Technical University in Prague, Faculty of Nuclear Sciences and Physical Engineering - Prague (Czech Republic), [2]University of Konstanz - Konstanz (Germany), [3]Institute of Biotechnology of the Czech Academy of Sciences, Biocev - Vestec near Prague (Czech Republic)

Abstract

High-resolution cut-off is an often carelessly estimated parameter during diffraction data processing despite its apparent impact on the quality of a solved structure model. Nevertheless, the paired refinement protocol has been shown to be a 'golden standard' for the determination of the cut-off. To provide this procedure to be run easily and effortlessly, we developed its automation – program *PAIREF* [1]. The resulting comprehensive analysis allows linking the data and structure model quality.
PAIREF has been included in the *CCP4 Suite* and can be run from its graphical user interface or the command line. For refinement, two engines are supported: *REFMAC*5 and *Phenix.refine* [2].
Recently, we developed a new feature: an automatic interpretation of the calculated results that suggests an optimal resolution cut-off. The decision-making algorithm takes into account several statistics: overall R-values and their trends, *R*-values from high-resolution shells, CC_{work} and CC*. This allows *PAIREF* to be involved in automated data-processing pipelines.
The automatic evaluation of results can be illustrated on a particular example of interferon gamma from *Paralichthys olivaceus* (PDB entry 6f1e). This structure was originally solved at 2.3 Å resolution [3]. We ran paired refinement with an increment of 0.1 Å up to the resolution of 1.9 Å using *PAIREF*; the interpretation of results is shown in Figure 1. The data in resolution shells 2.3-2.2 Å and 2.2-2.1 Å satisfy all the criteria as the overall R_{free}-values have a decreasing trend. However, in the next shell 2.1-2.0 Å, high-resolution *R*-values are close to exceeding an *R*-value of a perfect model against random data that is approximately 0.42 [4]. Thus, a warning sign is displayed for this shell. Finally, the last shell 2.0-1.9 Å does not comply with several criteria. To conclude, a strict cut-off of 2.1 Å and a permissive cut-off of 2.0 Å are suggested by the program. This interpretation is in good agreement with our previously published results [1].

References

[1] Malý, M., Diederichs, K., Dohnálek, J., Kolenko, P. (2020). *IUCrJ* **7**, 681–692.
[2] Malý, M., Diederichs, K., Dohnálek, J., Kolenko, P. (2021). *Acta Cryst. F***77**, 226–229.
[3] Zahradník, J., Kolářová, L., Pařízková, H., Kolenko, P., Schneider, B. (2018). *Fish Shellfish Immunol.* **79**, 140–152.
[4] Evans, P. R., Murshudov, G. N. (2013). *Acta Cryst. D***69**, 1204–1214.

The decision-making algorithm of PAIREF results in

Shell	Accepted?	Reason
2.30-2.20 A	Yes	Overall Rfree decreased while using data in the shell 2.30-2.20 A
2.20-2.10 A	Yes	Overall Rfree decreased while using data in the shell 2.20-2.10 A
2.10-2.00 A	Warning	Overall Rfree decreased while using data in the shell 2.10-2.00 A Rfree in high resolution is higher than 0.40 while using data in the shell 2.10-2.00 A Rwork in high resolution is higher than 0.40 while using data in the shell 2.10-2.00 A
2.00-1.90 A	No	Overall Rwork increased and Rfree remained constant while using data in the shell 2.00-1.90 A Rfree in high resolution is higher than 0.40 while using data in the shell 2.00-1.90 A Rwork in high resolution is higher than 0.40 while using data in the shell 2.00-1.90 A CC1/2 in high resolution is negative or undefined while using data in the shell 2.00-1.90 A But statistics deteriorate in a previous resolution shell.

Back to Table of contents

MS01 MX/Cryo-EM software development

MS1-04

Slice'N'Dice: Maximising predicted models for structural biologists

A.J. Simpkin [1], L.G. Elliot [1], D.J. Rigden [1], R.M. Keegan [2]
[1]University of Liverpool - Liverpool (United Kingdom), [2]CCP4, STFC - Oxford (United Kingdom)

Abstract

With the advent of next generation modelling methods such as Alphafold 2, structural biologists are increasingly using predicted structures as search models for Molecular Replacement (MR) (Barbarin-Bocahu, 2022). Predicted model conformation, especially for multi-domain proteins, is often a key limitation when using predicted models for MR. Slice'N'Dice is a software package designed to solve conformational problems by first slicing models into distinct structural units and then automatically placing these units with Phaser. Predicted models can be clustered based on the xyz coordinates of the C-alpha atoms or, if available, using predicted aligned error (PAE). In a single job, users can select a range of different splits so that the optimal number of splits can be taken forward to MR. Slice'N'Dice is available in CCP4 8.0 and is currently being adapted for cryo-EM.

References

Barbarin-Bocahu, I. & Graille, M. (2022). Acta Cryst. D78, 517-531.

Back to Table of contents

MS01 MX/Cryo-EM software development

MS1-05

Exploring generality of experimental conformational changes with AlphaFold predictions

A. Castellví [1], A. Medina [1], G. Petrillo [1], T. Sagmeister [2], T. Pavkov-Keller [2], F. Govantes [3], K. Diederichs [4], M. Sammito [1], I. Usón [1]
[1]IBMB-CSIC - Barcelona (Spain), [2]Universität Graz - Graz (Austria), [3]UPO-CSIC - Sevilla (Spain), [4]Universität Konstanz - Konstanz (Germany)

Abstract

Structural predictions (Jumper et al., 2021) have matched the accuracy of experimental structures in the case of close homologues, outperformed docking methods for multimeric complexes and helped sampling the conformational landscape of transporters and receptors. Such successes prompt the question whether predictions can be used to relate experimental structures in the context of available knowledge. LysR-type transcriptional regulators (LTTR) constitute the most common family of bacterial regulators. Intriguingly, their experimental structures are remarkably diverse. The active species, composed of flexible monomers dimerizing through their N- and C-terminal domains in a circular arrangement, differ across LTTR, due to intrinsic sequence differences or because crystals stabilize diverse snapshots of a common dynamic mechanism. We have used AlphaFold2 (AF) to interrogate the experimental AtzR structure in the context of predictions guided towards the different hetero-multimeric conformations known for other LTTR (Castellví et al., 2022). Our approach drives AF prediction with the structure-based selection of the information input through sequence alignment and template conformation, linked to examination of the energy with PISA (Krissinel 2011) and interactions with ALEPH (Medina et al., 2020).

References

Jumper, J., Evans, R., Pritzel, A., Green, T., Figurnov, M., Ronneberger, O., Tunyasuvunakool, K., Bates, R., Žídek, A., Potapenko, A., Bridgland, A., Meyer, C., Kohl, S. A. A., Ballard, A. J., Cowie, A., Romera-Paredes, B., Nikolov, S., Jain, R., Adler, J., Back, T., Petersen, S., Reiman, D., Clancy, E., Zielinski, M., Steinegger, M., Pacholska, M., Berghammer, T., Bodenstein, S., Silver, D., Vinyals, O., Senior, A. W., Kavukcuoglu, K., Kohli, P. & Hassabis, D. (2021). Highly accurate protein structure prediction with AlphaFold. Nature, 1–11. https://doi.org/10.1038/s41586-021-03819-2

Castellví, A., Medina, A.,, Petrillo, G.,, Sagmeister, T., Pavkov-Keller T., Govantes, F., Diederichs, K., Sammito, M D. and Usón, I. (2022). Exploring generality of experimental conformational changes with AlphaFold predictions. https://biorxiv.org/cgi/content/short/2022.04.12.488086v1

Medina, A., Triviño, J., Borges, R. J., Millán, C., Usón, I., & Sammito, M. D. (2020). ALEPH: A network-oriented approach for the generation of fragment-based libraries and for structure interpretation. Acta Crystallogr., D76, 193–208. https://doi.org/10.1107/S2059798320001679

Krissinel, E. (2011). Macromolecular complexes in crystals and solutions. Acta Crystallogr., D67(4), 376–385. https://doi.org/10.1107/S0907444911007232

Back to Table of contents

MS02 Infection and Disease/hot structures

MS2-01

B12-dependent radical SAM enzymes: Structural and mechanistic perspectives of emerging catalytic machineries involved in antibiotic biosynthesis and the microbiome.

A. Benjdia [1]
[1]*INRAE - Université Paris-Saclay - Jouy-en-Josas (France)*

Abstract

In the last ten years, radical SAM enzymes have emerged as central catalysts for the biosynthesis of myriad natural products including major antibiotics such as carbapenems and antimicrobial peptides (RiPPs). These enzymes are arguably the most diverse and versatile biocatalysts in living systems and represent novel opportunities to face the current antibiotic resistance crisis. Among them, one of the largest and least explored group are the "B_{12}-dependent radical SAM enzymes" with more than 200,000 members identified in genomes and metagenomes. These enzymes use the dual catalytic power of S-adenosyl-L-methionine (SAM) and vitamin B_{12} (cobalamin) to notably form carbon-carbon bonds on unactivated atoms. However, despite years of efforts, we have still a poor knowledge of these enzymes which are the only biocatalysts capable to perform such reaction.

To gain mechanistic insights into these emerging enzymes, we investigated the methanogenesis marker protein 10 (Mmp10) which catalyzes a key post-translational modification (arginine methylation) in methyl-coenzyme M reductase (MCR). By combining biochemical and biophysical techniques including X-ray crystallography and electron paramagnetic resonance, we discovered an unprecedented enzyme architecture containing four distinct metallic centers and key structural features involved in the control of catalysis [1]. Crystallographic snapshots of the reaction showed that, contrary to current paradigm, major and unprecedented active-site reorganization occurred upon following substrate binding in radical SAM enzymes. Notably, we demonstrated that the unique [4Fe4S] cluster can be transiently coordinated by a tyrosine residue which enables the enzyme to alternate between radical and nucleophilic chemistry. This study not only discloses how B_{12}-dependent radical SAM enzymes catalyze chemically challenging alkylation reactions, but also opens new avenues for the biosynthesis and engineering of natural products [2].

References

1 - Fyfe CD, Bernardo-García N, Fradale L, Grimaldi S, Guillot A, Brewee C, Chavas LMG, Legrand P, Benjdia A*, Berteau O.* - 2022 - Crystallographic snapshots of a B_{12}-dependent radical SAM methyltransferase. *Nature* (7896):336-342.

2 - Soualmia F, Guillot A, Sabat N, Brewee C, Kubiak X, Haumann M, Guinchard X, Benjdia A*, Berteau O*. - 2022 - Exploring the Biosynthetic Potential of TsrM, a B_{12}-dependent Radical SAM Methyltransferase Catalyzing Non-radical Reactions. *Chemistry*. in press

Back to Table of contents

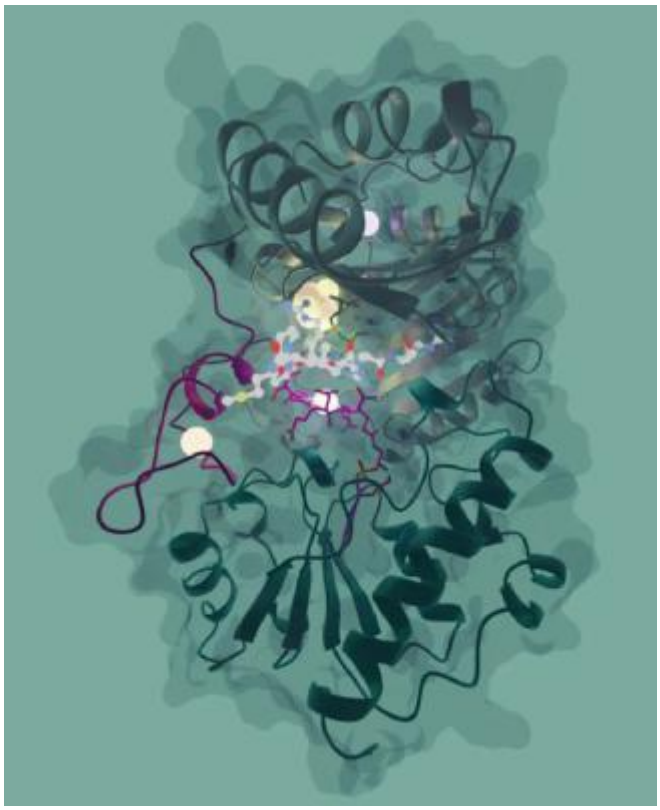

Back to Table of contents

MS02 Infection and Disease/hot structures

MS2-02

The coronavirus structural taskforce

G. Santoni [1], A. Thorn [2]
[1]ESRF - Grenoble (France), [2]University of Hamburg - Hamburg (Germany)

Abstract

During the COVID-19 pandemic, structural biologists rushed to solve the structures of the 28 proteins encoded by the SARS-CoV-2 genome in order to understand the viral life cycle and to enable structure-based drug design. In addition to the 204 previously solved structures from SARS-CoV-1, over 2000 structures covering SARS-CoV-2 viral proteins have been released in a span of a 2 years. As structural models are available, researchers from different backgrounds use them as a basis for further analysis. Molecular dynamics simulations, docking studies and bioinformatics modelling are just an example of the possible use of those data. However, all modelling is prone tov error and structural biology is not immune to that. I will present here the efforts of the Coronavirus Structural Task Force [1], a spontaneous gathering of scientists who tried to target the issue by fixing errors when possible, sharing our findings with the broader community and communicating about the culture of errors in structural biology. A few key findings, as well as a wider discussion about the role of open science in the current days will be the core of my presentation.

References

Croll, T., Diederichs, K., Fischer, F., Fyfe, C., Gao, Y., Horrell, S., Joseph, A., Kandler, L., Kippes, O., Kirsten, F., Müller, K., Nolte, K., Payne, A., Reeves, M.G., Richardson, J., Santoni, G., Stäb, S., Tronrud, D., Williams, C, Thorn, A*. (2021) Making the invisible enemy visible (2021) Nature Structural & Molecular Biology 28, 404–408 https://doi.org/10.1038/s41594-021-00593-7

Back to Table of contents

MS02 Infection and Disease/hot structures

MS2-03

Structural and Functional Characterization of TraA, the Relaxase a Gram-positive Type IV Secretion System (T4SS).

T. Berger [1], A. Reisenbichler [1], C. Michaelis [2], E. Grohmann [2], W. Keller [1]
[1]Institute of Molecular Biosciences, University of Graz - Graz (Austria), [2]Faculty of Life Sciences and Technology, Department of Microbiology, Berliner Hochschule für Technik - Berlin (Germany)

Abstract

The occurrence of multi-resistant strains among pathogenic bacteria, in particular those causing nosocomial infections, is one of the most pressing problems of our health system. Bacterial conjugation is one important route of DNA transfer between bacteria and mediates the rapid spread of bacterial resistances within bacterial communities. Type IV secretion systems (T4SS) are responsible for the efficient transport of nicked, single-stranded plasmid DNA across the cell walls of the donor as well as the recipient cell (1). The T4SS from the antibiotic resistance plasmid pIP501, occurring in *Enterococci* and related Gram-positive bacteria, is encoded within a single operon comprised of 15 putative transfer factors. The 1st open reading frame encodes TraA, a relaxase, which causes a single-strand DNA cleavage at the *nic* site of the origin of transfer, *oriT*, of plasmid pIP501 and initiates the transfer of the nicked DNA strand. Here we present the crystal structure of the N-terminal domain comprising the relaxase activity, which shows structural homology with NES, the nicking enzyme in *S. aureus*. (2) The solution structure of both the N-terminal domain and full-length TraA are investigated by SAXS and CD spectroscopy methods.

References

(1) Alvarez-Martinez CE, and Christie PJ (2009) Biological diversity of prokaryotic type IV secretion systems. *Microbiol Mol Biol Rev* 73, 775-808.
(2) Edwards JS, et al. (2013) Molecular basis of antibiotic multiresistance transfer in Staphylococcus aureus. *Proc Natl Acad Sci U S A* 110, 2804-2809.

Back to Table of contents

MS02 Infection and Disease/hot structures

MS2-04

Control of phosphodiesterase activity in RbdA, a regulator of biofilm dispersal

C. Cordery [1], J. Craddock [2], J. Webb [2], M. Walsh [3], I. Tews [2]
[1]University of Southampton/Diamond Light Source - Southampton/Didcot (United Kingdom), [2]University of Southampton - Southampton (United Kingdom), [3]Diamond Light Source - Didcot (United Kingdom)

Abstract

Bacteria can exist as a sessile biofilm or in the planktonic, free-swimming form, the switching is regulated by nucleotide messenger c-di-GMP. Phosphodiesterases are required for c-di-GMP breakdown, leading to dispersal. RbdA (regulator of biofilm dispersal) of the opportunistic human pathogen Pseudomonas aeruginosa has been highlighted to be involved in a cascade responsible for the dispersal of biofilms, in addition to its phosphodiesterase domain, it contains a sensory PAS domain which is of further interest. Furthermore, this cascade of dispersal is responsive to redox potential and nitric oxide (NO). The full mechanism and function of proteins of this cascade are currently poorly understood with the overall aim of discovering treatments for antimicrobial tolerant *Pseudomonas aeruginosa* biofilm infections. These infections are the leading cause of death among cystic fibrosis sufferers. Previous data on the multi-domain membrane protein RbdA have shown involvement in NO-induced biofilm dispersal and allosteric GTP regulation. Here, we show that the diguanylate cyclase domain N-terminal to the phosphodiesterase is an inverse regulator of c-di-GMP hydrolysis. The crystallographic structure of this active, substrate-free, dimeric phosphodiesterase allows insight into the structural mechanism controlling this inhibition. This will springboard further research to characterise these diguanylate cyclase-phosphodiesterase double domain proteins and more broadly the sensing mechanism of PAS domains, particularly in response to RedOx. This will enable us to better understand the pathway of dispersal of bacterial biofilms.

Determination of PDE activity of RbdA constructs

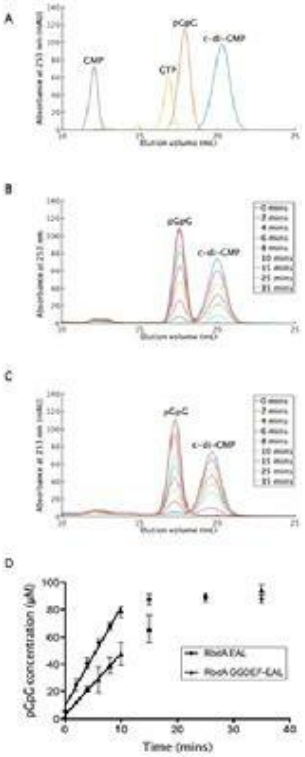

Back to Table of contents

MS02 Infection and Disease/hot structures

MS2-05

Using crystallographic “failures” to identify artificial and endogenous inhibitors for plant growth and defence pathways

U. Shahul Hameed [1], R. Zarban [1], I. Haider [1], M. Jamil [1], S. Al-Babili [1], S. Arold [1]
[1]*King Abdullah University of Science and Technology (KAUST) - Thuwal (Saudi Arabia)*

Abstract

Plants cannot move to obtain nutrients or avoid predation. To cope with this constraint, plants have developed an arsenal of regulatory mechanisms that are markedly more sophisticated and influential than those used by animals. Understanding and controlling the molecular basis for plants’ decision-making on growth and defence strategies may help improve food security.
We present two converging tales of how “failed” X-ray crystallography experiments provided not only a novel lead compound for specific enzyme inhibition but also helped reveal regulation feedback mechanisms that determine plant growth and pathogen resistance. Based on more than a dozen different crystal structures, biophysical and in planta data we show how members of two enzyme families (the HTL/D14/KAI2 hydrolases and NATA1/2 acetyltransferases) integrate endogenous and external stimuli to allow plants to make informed decisions [1,2 and unpublished]. Collectively, our findings expand the range of molecular regulatory mechanisms used in plants to balance growth and defence, and reveal unexpected lead compounds to control them.

References

[1] Shahul Hameed U, Haider I, Jamil M, Guo X, Zarban RA, Kim D, Al-Babili S, Arold ST.; EMBO Rep 2018; doi: 10.15252/embr.201745619
[2] Zarban Zarban RA, Hameed UFS, Jamil M, Ota T, Wang JY, Arold ST, Asami T, Al-Babili S; Plant Physiol. 2022; doi: 10.1093/plphys/kiab547

Striga hermonthica HTL7 and NATA1 with ligands

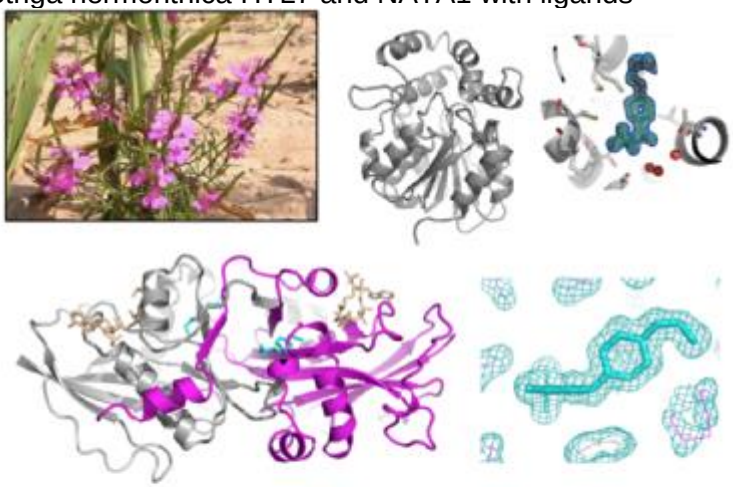

TOP *Left*: The parasitic plant *Striga hermonthica* (pink flowers) causes billions of USD of losses every year by draining nutrients from crops. *Middle*: The crystallographic structure of *Sh*HTL7, the key sensor used by Striga to identify the host plant. *Right*: Serendipitously identified specific inhibitor in its 2fofc electron density map [1]. **BOTTOM** *Left*: Dimeric NATA1 with cofactors and inhibitor [unpublished]. *Right*: Serendipitous inhibitor in 2fofc map.

Back to Table of contents

MS03 Crystallization and biophysical characterization

MS3-01

Successful sample preparation for serial crystallography at synchrotrons and XFELs

John Beale (Villigen, Switzerland)

The applications and potential advantages of serial crystallography, at both synchrotron and XFEL light sources, are growing. Despite advances in delivery methods, the sample volumes of micro-crystals required for serial crystallography, particularly time-resolved experiments, are still demanding. Batch crystallisation methods are the primary means in crystallographers toolbox to create these samples. However, the process to convert single crystals grown by vapour diffusion to large volumes (> 100 µL) of micro-crystalline slurry can be exceptionally challenging.

To try and ease the process, we have formulated a strategy to perform this translation. It is divided into three stages: (1) optimising crystal morphology, (2) transitioning to batch, and (3) scaling. Given the variation of protein crystallisation, we hope that this protocol can act as a useful framework when attempting the conversion from vapour diffusion to batch.

In this talk, I will explain how this process was developed and applied to model proteins. Then I will talk about some of the experiences, good and bad, we have had with user proteins at the SLS and SwissFEL. I will finish with a peak at some results from how this user crystals fared at the new SwissFEL endstation, Cristallina.

Back to Table of contents

MS03 Crystallization and biophysical characterization

MS3-02

Protein quality control for improved data reproducibility and reliability

K. Remans [1], A. De Marco [2], N. Berrow [3], M. Lebendiker [4], M. Garcia-Alai [5], S. Knauer [6], B. Lopez-Mendez [7], A. Matagne [8], A. Parret [9], S. Uebel [10], B. Raynal [11]

[1]EMBL - Heidelberg (Germany), [2]University of Nova Gorica - Vipava (Slovenia), [3]IRB - Barcelona (Spain), [4]Hebrew University of Jerusalem - Jerusalem (Israel), [5]EMBL - Hamburg (Germany), [6]University of Bayreuth - Bayreuth (Germany), [7]Novo Nordisk Foundation Center for Protein Research - Copenhagen (Denmark), [8]University of Liège - Liège (Belgium), [9]EMBL (present address: Charles River Laboratories, Beerse) - Hamburg (Germany), [10]Max Planck Institute of Biochemistry - Martinsried (Germany), [11]Institut Pasteur - Paris (France)

Abstract

Purified proteins are used in various types of scientific experiments and fields. For example, in structural biology insights into the functional mechanisms can be obtained by elucidating the 3D molecular structure of proteins and protein complexes using technologies such as X-ray crystallography, cryo-EM and NMR. In biochemistry and biophysics, interactions with other proteins, nucleic acids and small molecules can be studied by determining affinities and specificities. Proteins can function as antigens to generate specific antibodies or as reagents in cell biology experiments. Furthermore, recombinant proteins can be used as tool molecules in genomics, chemical biology and microscopy assays. In order for these experiments to produce reliable and biologically relevant results, they must be performed using high-quality proteins that are active, properly folded, in the right oligomeric state and contain correctly inserted co-factors. Ensuring that these parameters are fulfilled requires quality control. As researchers inexperienced in handling proteins are not always aware of how to validate the quality of protein samples used in downstream experiments, a working group comprised of members of professional European biophysics (https://arbre-mobieu.eu) and protein production networks (https://p4eu.org) put together a number of guidelines addressing this problem. These guidelines comprise the minimal information that needs to be present to reliably reproduce the expression and purification of the protein of interest, minimal quality control checks for assessing purity, homogeneity/dispersity and identity and more extended quality control tests that need to be performed depending on the specific downstream application of the protein sample. An evaluation by the network members over a one-year period indicated that implementing these quality control guidelines facilitates the optimisation of the protein purification process and improves the reliability of downstream experiments. Therefore, investing in protein quality control benefits all life science stakeholders (researchers, editors and funding agencies alike) by increasing data veracity and minimising loss of valuable time and resources.

References

Berrow N., de Marco A., Lebendiker M., Garcia-Alai M., Knauer S.H., Lopez-Mendez B., Matagne A., Parret A., Remans K., Uebel S. and Raynal B. (2021) Quality control of purified proteins to improve data quality and reproducibility: results from a large-scale survey. European Biophysics Journal 50(3-4): 453-460

de Marco A., Berrow N., Lebendiker M., Garcia-Alai M., Knauer S.H., Lopez-Mendez B., Matagne A., Parret A., Remans K., Uebel S. and Raynal B. (2021) Quality control of protein reagents for the improvement of research data reproducibility.Nature Communications 12(1): 2795

Remans K., Lebendiker M., Abreu C., Maffei M., Sellathurai S., May M.M., Vaněk O. and de Marco A. (2022) Protein purification strategies must consider downstream applications and individual biological characteristics. Microbial Cell Factories 21(1): 52

Back to Table of contents

MS03 Crystallization and biophysical characterization

MS3-03

Serial crystallography: a game-changer in crystallization and crystal handling

K. Rollet [1], R. De Wijn [1], P. Pachl [1], L. Coudray [1], P. Bénas [1], C. Sauter [1]
[1]*ARN - IBMC - CNRS - Unistra - Strasbourg (France)*

Abstract

Over the past decade, the advent of X-ray free electron lasers delivering ultra intense X-ray beams has revolutionized biocrystallography. With a brilliance a billion times higher than at synchrotrons, the XFEL beam destroys the sample just after the emission of its diffraction signal in a process called “diffraction before destruction”. While this firepower allows the characterization of smaller crystals than ever (micro or even nanocrystals), the sample needs to be refreshed after each shot and the collection of a full dataset requires series of thousands of crystals. Also, crystal cryocooling is no longer necessary and this type of analysis is mostly performed at room temperature. In these near-to-physiological conditions and thanks to the temporal resolution of XFEL pulses (<100 fs), the dynamics of biological systems (conformational changes, catalytic events) can be probed in crystallo. Similar protocols have been implemented at synchrotron facilities and are widely accessible.

To take advantage of these new approaches, crystal growers need to adapt current protocols mainly devoted to the production of large single crystals, to the preparation of showers of microcrystals with homogeneous size and diffraction quality. Based on crystal growth principles and examples of alternative crystallization approaches including advanced crystallization control or microfluidics technologies [1,2,3], we will describe new routes of sample preparation and crystal delivery for serial crystallography.

References

[1] de Wijn, Rollet et al. Monitoring the production of high diffraction-quality crystals of two enzymes in real time using in situ dynamic light scattering. Crystals (2020), 10: 65-77.
[2] de Wijn et al. A simple and versatile microfluidic device for efficient biomacromolecule crystallization and structural analysis by serial crystallography. IUCrJ (2019), 6: 454–464.
[3] de Wijn, Rollet et al. Crystallization and structure determination of an enzyme:substrate complex by serial crystallography in a versatile microfluidic chip. Journal of Visualized Experiments (2021), 169: e61972.

Back to Table of contents

MS03 Crystallization and biophysical characterization

MS3-04

Screening approaches that explore chemical space in order to identify suitable starting conditions for structure determination by cryoEM or other methods

P.D. Shaw Stewart [1], T.O. Kwan [2], S.A. Kolek [1], A.E. Danson [2], R.I. Reis [2], I. Moraes [2], I.S. Camacho [2]
[1]Douglas Instruments Ltd - Hungerford (United Kingdom), [2]National Physical Laboratory - Teddington (United Kingdom)

Abstract

Protein structure determination by cryoEM requires expensive equipment that has low throughput. It is therefore wasteful to examine samples that can be shown in advance to be aggregated, since such samples are unlikely to be suitable for structure determination by any method. It may, however, be possible to break up aggregated samples by adding low concentrations of additives such as denaturants, detergents, osmolytes, etc. This study used a high-throughput screening approach to explore chemical space with premixed screens using several biophysical methods, focusing on dynamic light scattering (DLS), differential scanning fluorimetry (DSF) and circular dichroism (CD). DLS was found to be particularly suitable for additive screening because 96 conditions could be explored with as little as 10 µL of protein solution, and screens could be run automatically e.g. overnight.

References

Kwan TOC, Kolek SA, Danson AE, Reis RI, Camacho IS, Shaw Stewart PD and Moraes I (2022) "Measuring Protein Aggregation and Stability Using High-Throughput Biophysical Approaches." *Front. Mol. Biosci.* 9:890862. doi: 10.3389/fmolb.2022.890862

Workflow for HTP biophysical probes

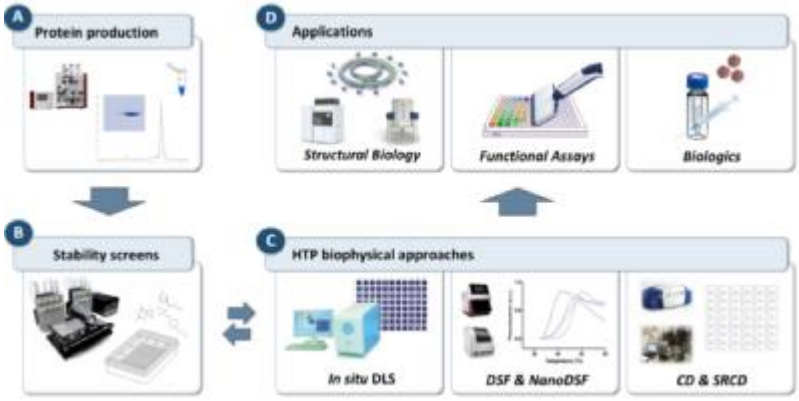

Back to Table of contents

MS03 Crystallization and biophysical characterization

MS3-05

Nucleation and reproducibility in protein crystallization assisted by the crystallophore.

E. Girard [1], Z. Alsalman [1], A. Robin [2], S. Engilberge [1], A. Roux [3], F. Riobé [3], O. Maury [3]
[1]Univ. Grenoble Alpes, CEA, CNRS, IBS - Grenoble (France), [2]European Molecular Biology Laboratory - Grenoble (France), [3]Univ. Lyon, ENS de Lyon, CNRS UMR 5182, Université Claude Bernard Lyon 1, Laboratoire de Chimie - Lyon (France)

Abstract

Obtaining crystals remains the major hurdle encountered by bio-crystallographers in their race to get new high-quality structures. The crystallophore, Xo4, is a family of nucleating and phasing molecules based on lanthanide complexes. Tb-Xo4 was the first molecule of this family to be described [1].

Tb-Xo4 crystallization properties will be first described through results obtained on more than fifteen proteins and will show that Tb-Xo4 is an efficient tool as:
(i) Tb-Xo4 increases the number of crystallization conditions by promoting unique ones [1,2]
(ii) The crystalline forms promoted by the crystallophore bypass crystal defects often encountered by crystallographers such as low-resolution diffracting samples or crystals with twinning [3]
(iii) Crystals can be obtained from enriched fractions containing several proteins, contrary to the dogma that crystallization can only be promoted from pure protein sample [3] leading to the structure determination of a protein complex [4].
(iv) Even more unexpected, the crystallophore is able to induce nucleation directly from the protein solution, as exemplified by the crystallization of hen egg white lysozyme in water [5].

Then, we will focus on the crystallization reproducibility, a prerequisite and particular issue in structure-based drug design. Reproducibility is largely improved with the crystallophore. This will be illustrated by results with three different proteins obtained in the framework of a collaborative project with the High throughput Crystallization Platform (HTX-lab) at EMBL-Grenoble, the Polyvalan startup (https://crystallophore.fr) and Edelris company (https://www.edelris.com).

Altogether, crystallophore is an efficient solution for protein crystallization and structure determination in the bio-crystallographer toolbox.

Authors acknowledge financial supports from the Fondation Maison de la Chimie, Agence Nationale de la Recherche (ANR Ln23-13-BS07-0007-01) and Region Auvergne Rhône Alpes (programs Xo4-2.0 and Crysfrag).

References

[1] Engilberge, S., Riobé, F., Di Pietro, S., Lassalle, L., Coquelle, N., Arnaud, C.-A., Pitrat, D., Mulatier, J.-C., Madern, D., Breyton, C., Maury, O. & Girard, E. (2017). Chem. Sci. 8, 5909–5917.
[2] Jiang, T., Roux, A., Engilberge, S., Alsalman, Z., Di Pietro, S., Franzetti, B., Riobé, F., Maury, O. & Girard, E. (2020). Crystal Growth & Design. 20, 5322–5329.
[3] Engilberge, S., Wagner, T., Santoni, G., Breyton, C., Shima, S., Franzetti, B., Riobé, F., Maury, O. & Girard, E. (2019). Journal of Applied Crystallography. 52, 722–731.
[4] Vögeli, B., Engilberge, S., Girard, E., Riobé, F., Maury, O., Erb, T. J., Shima, S. & Wagner, T. (2018). Proceedings of the National Academy of Sciences. 115, 3380–3385.
[5] de Wijn, R., Rollet, K., Engilberge, S., McEwen, A. G., Hennig, O., Betat, H., Mörl, M., Riobé, F., Maury, O., Girard, E., Bénas, P., Lorber, B. & Sauter, C. (2020). Crystals. 10, 65.

Back to Table of contents

MS04 Structure in Cancer Biology

MS4-01

Conformational regulation in anti-CD40 antibodies

C. Orr [1], H. Fisher [2], I. Elliott [2], X. Yu [2], M. Glennie [2], A. White [3], A. Pearson [4], J. Essex [2], M. Cragg [2], I. Tews [2]
[1]Diamond Light Source - Didcot (United Kingdom), [2]University of Southampton - Southampton (United Kingdom), [3]UCB Pharma - Slough (United Kingdom), [4]Hamburg Centre for Ultrafast Imaging CFEL - Hamburg (Germany)

Abstract

Antibodies are an increasingly important therapeutic modality comprising ~eighty percent of therapeutic biologics. Despite this, further improvements in therapeutic antibody design are required. Although the majority of the 100+ antibodies approved for use in the clinic are of the hIgG1 isotype, other isotypes are now being increasingly investigated. For example, the hIgG2 isotype is unique in its ability to exhibit a range of different disulfide orientations in its hinge region which may afford additional therapeutic functionality. While this is a natural phenomenon, occurring in the blood through a red-ox process, it can also be exploited in therapeutic antibodies to enhance signalling (agonism) of certain important immune receptor targets, such as CD40. However, the underpinning mechanism is unknown.

Therefore, here, we studied the hinge of hIgG2 in the context of the clinically relevant anti-CD40 monoclonal antibody chiLob7/4. Cysteines in the hinge region were exchanged to serine in a number of different variants with subsequent biological activity and hinge disulfide structure evaluated using an anomalous scattering approach. In these anti-CD40 Lob7/4 hIgG2 antibodies, which all bind to the same epitope and retain high affinity binding, activity correlated with formation of a specific disulfide crossover structure. SAXS analysis showed that the crossover restricts conformational freedom of the antibody. A full-atomistic simulation and evaluation of the conformational pool against the SAXS data using ensemble methods showed that fewer conformations exist in solution in antibodies that are agonistic. This study highlights that specific modifications of monoclonal antibody hinge regions to introduce covalent disulfide links can modulate receptor signaling in an epitope-independent manner, which may be applicable in future therapeutics.

References

Yu X, Chan HTC, Orr CM, Dadas O, Booth SG, Dahal LN, Penfold CA, O'Brien L, Mockridge CI, French RR, Duriez P, Douglas LR, Pearson AR, Cragg MS, Tews I, Glennie MJ, White AL. Complex Interplay between Epitope Specificity and Isotype Dictates the Biological Activity of Anti-human CD40 Antibodies. Cancer Cell. 33 (2018), 664-675.
Yu X, Chan HTC, Fisher H, Penfold CA, Kim J, Inzhelevskaya T, Mockridge CI, French RR, Duriez PJ, Douglas LR, English V, Verbeek JS, White AL, Tews I, Glennie MJ, Cragg MS. Isotype Switching Converts Anti-CD40 Antagonism to Agonism to Elicit Potent Antitumor Activity. Cancer Cell. 37 (2020), 850-866.

Back to Table of contents

MS04 Structure in Cancer Biology

MS4-02

Anaplastic Lymphoma Kinases and ligands: Structure, mechanism, and antagonism in cancer and metabolism

S. Savvides [1]
[1]*VIB & Ghent University - Ghent (Belgium)*

Abstract

Anaplastic lymphoma kinase (ALK) and the related leukocyte tyrosine kinase (LTK) are recently deorphanized receptor tyrosine kinases. Together with their activating cytokines, ALKAL1 and ALKAL2 they are involved in neural development, cancer and autoimmune diseases. Furthermore, mammalian ALK recently emerged as a key regulator of energy expenditure and weight gain. Despite such functional pleiotropy and growing therapeutic relevance structural insights into ALK and LTK and their complexes with cognate cytokines have remained scarce. To facilitate our mechanistic understanding of ALK/LTK function and therapeutic targeting, we pursued crystal structures of ALK/LTK-cytokine complexes. Our structures revealed unprecedented protein architectures and receptor-cytokine assemblies, whereby a single cytokine molecule without any apparent symmetry dimerizes ALK and LTK proximal to the cell membrane to initiate signaling. The cytokine-binding segments of human ALK and LTK comprise a novel architectural chimera of a permuted TNF-like module that braces a glycine-rich subdomain featuring a hexagonal lattice of long polyglycine type II helices. The cognate cytokines ALKAL1 and ALKAL2 are monomeric three-helix bundles, yet their binding to ALK and LTK elicits similar dimeric assemblies with two-fold symmetry, that tent a single cytokine molecule proximal to the cell membrane. We show that the membrane-proximal EGF-like domain dictates the apparent cytokine preference of ALK. Assisted by these diverse structure–function findings, we propose a structural and mechanistic blueprint for complexes of ALK family receptors, and thereby extend the repertoire of ligand-mediated dimerization mechanisms adopted by receptor tyrosine kinases.

References

De Munck S., Provost M., Kurikawa M., Omori I., Mukohyama J., Felix J. Bloch Y. Abdel-Wahab O., Bazan J.F., Yoshimi. A., Savvides S.N.* Structure and mechanism of cytokine-mediated activation of ALK family receptors. Nature (2021), 600:143-147.

ALK/LTK-cytokine complexes

Back to Table of contents

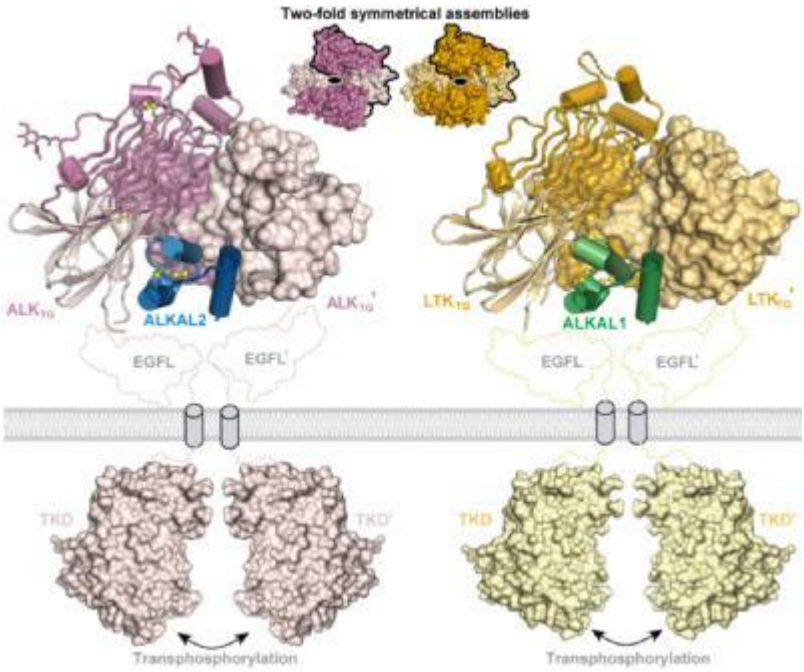

ALK/LTK complexes are novel among RTK

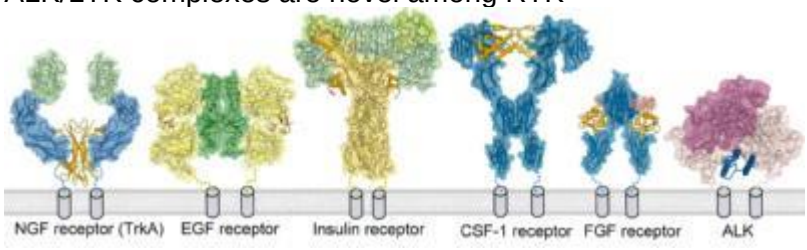

Back to Table of contents

MS04 Structure in Cancer Biology

MS4-03

Equilibria between conformational states of the Ras oncogene protein revealed by high pressure crystallography

N. Colloc'h [1], P. Lopes [2], M. Spoerner [2], A.C. Dhaussy [3], T. Prangé [4], H.R. Kalbitzer [2], E. Girard [5]
[1]ISTCT UMR 6030 CNRS Université de Caen-Normandie - Caen (France), [2]Institute of Biophysics and physical biochemistry, University of Regensburg - Regensburg (Germany), [3]CRISTMAT UMR 6508, Normandie Univ. Ensicaen CNRS - Caen (France), [4]CiTCoM UMR 8038 CNRS Université de Paris - Paris (France), [5]IBS Univ. Grenoble Alpes CEA CNRS - Grenoble (France)

Abstract

The small GTPase Ras protein, involved in central regulatory processes such as cell differentiation, proliferation and apoptosis, possesses multiple conformational states and acts as a molecular switch between active GTP-bound, and inactive GDP-bound states, controlling essential signal transduction pathways. Ras is anchored to the membrane via its C-terminal domain and activated through cell surface receptors. An allosteric network of interactions between the effector binding regions and the membrane interacting regions is involved in Ras cycling. The different conformational states which coexist simultaneously in solution with low occupancies possess higher Gibbs free energy than the ground state. Equilibria between these states can be shifted by applying high hydrostatic pressure favoring conformations with lower molar partial volumes and has been previously analyzed by high-pressure NMR spectroscopy.

High-pressure macromolecular crystallography is a powerful tool to characterized at the molecular level the different allosteric states involved in Ras cycling. High resolution structures of Ras(wt).Mg2+.GppNHp and Ras(D33K).Mg2+.GppNHp at pressures up to 900 MPa give insight to per-residue descriptions of the structural plasticity involved in allosteric equilibria between conformers. A transition above 300 MPa in the crystal leads to more stable conformers. The different segments of Ras protein which remains in the ground-state conformation or undergo structural changes, adopting excited-energy conformations corresponding to transient intermediate states, have been mapped out at atomic resolution. Such in-crystallo phase transitions induced by pressure opens the possibility to finely explore the structural determinants related to switching between Ras allostric sub-states without any mutations nor exogenous partners.

References

Girard et al., Chem. Sci., 2022, 13:2001-2010

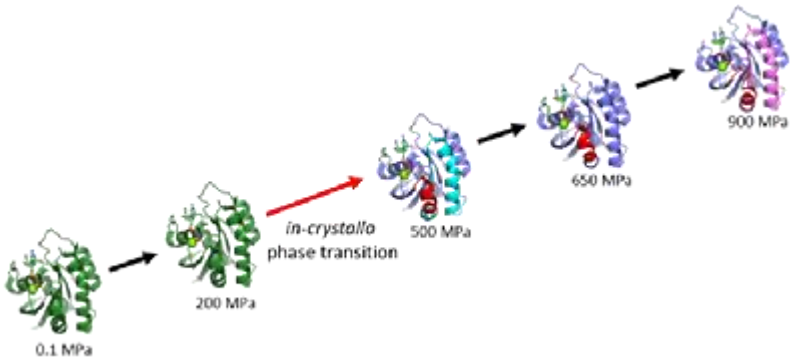

Back to Table of contents

MS04 Structure in Cancer Biology

MS4-04

Structure-assisted design of Carborane inhibitors of human Carbonic Anhydrase IX

J. Brynda [1], P. Rezacova [1], M. Kugler [1], K. Pospisilova [1], B. Gruner [2], J. Nekvinda [2], J. Holub [2], W. Das [3], M. Hajduch [3]
[1]Institute of Organic Chemistry and Biochemistry AS CR - Praha (Czech Republic), [2]Institute of Inorganic Chemistry AS CR - Praha (Czech Republic), [3]Institute of Molecular and Translational Medicine - Olomouc (Czech Republic)

Abstract

Carbonic anhydrases (CAs) are zinc metalloenzymes playing an important role in many physiological processes. Several CAs are also involved in various pathological processes in humans and represent thus targets for drug development. Specifically, human carbonic Anhydrase IX (CA IX), isoform overexpressed in solid hypoxic tumours, is a target for cancer therapy and diagnostics. We have previously identified carboranes as a promising class of specific inhibitors of CA IX [1]. Here we report recent advances in the structure-assisted design of carborane and metallacarborane inhibitors targeting CA IX.

We chose carboranes, three-dimensional scaffolds, which act as as space-filling fragments. We modified boron cages to synthetize carboranes and metallacarboranes substituted by sulfamide, sulfonamide or sulfamate groups, i.e. functions known to bind tightly to the zinc atom in the active site of CAs. Consequently, the small library of ca. 70 substituted carboranes and metallacarboranes was. Several compounds exhibit selective inhibitory activity toward CAIX with Ki values in low nanomolar or even picomolar range. Selected inhibitors were tested for their effect on tumor growth in BALB/c mice orthotopically implanted with 4T1 cells and SCID mice subcutaneous transplanted with HT-29 cells.

References

Metallacarborane Sulfamides: Unconventional, Specific, and Highly Selective Inhibitors of Carbonic Anhydrase IX.
Grüner B, Brynda J, Das V, Šícha V, Štěpánková J, Nekvinda J, Holub J, Pospíšilová K, Fábry M, Pachl P, Král V, Kugler M, Mašek V, Medvedíková M, Matějková S, Nová A, Lišková B, Gurská S, Džubák P, Hajdúch M, Řezáčová P. J Med Chem. 2019 Nov 14;62(21):9560-9575. doi: 10.1021/acs.jmedchem.9b00945.
Carborane-based carbonic anhydrase inhibitors.
Brynda J, Mader P, Šícha V, Fábry M, Poncová K, Bakardiev M, Grüner B, Cígler P, Řezáčová P.Angew Chem Int Ed Engl. 2013 Dec 16;52(51):13760-3. doi: 10.1002/anie.201307583.

Structure of CA with Carboran Inhibitor

Back to Table of contents

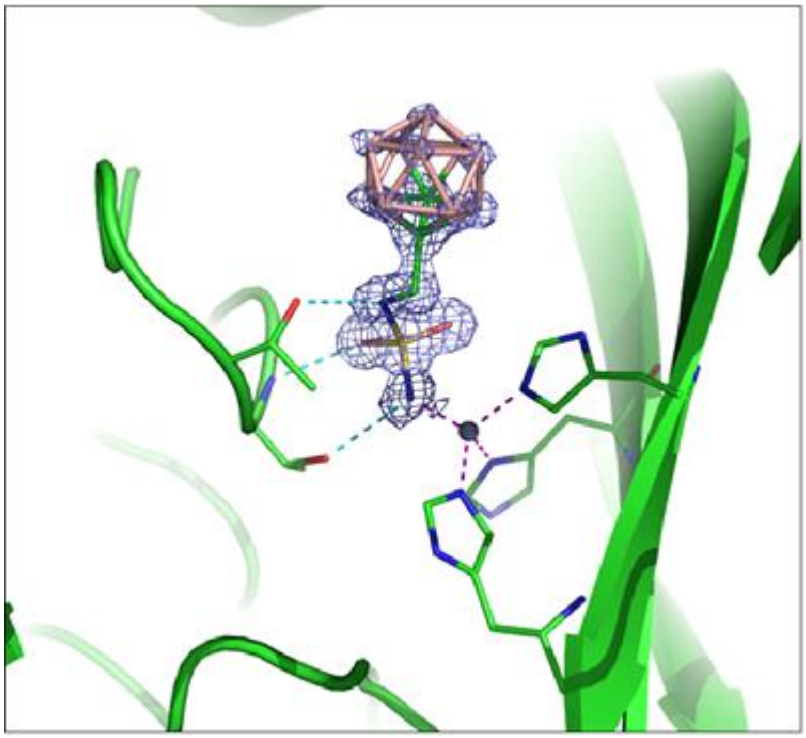

Back to Table of contents

MS05 Nucleic acids and their interaction

MS5-01

The Interactions between Guanine and Uracil

E. Westhof [1]
[1]*IBMC ARN CNRS Université de Strasbourg - Strasbourg (France)*

Abstract

Decoding during ribosomal translation occurs through complex and interdependent molecular recognition networks between mRNA, tRNAs, and rRNAs. Among those, the stability of codon-anticodon triplets, the fold of the tRNA anticodon hairpin, the modified nucleotides, and the interactions with rRNA bases at the decoding site constitute key contributors. Based on biochemical and genetic data in the literature, coupled with many crystal structures of fully active ribosomes, nucleotide modifications in the anticodon loop are better understood molecularly. They contribute to the pre-organization of the anticodon loop with helicoidal stacking of the anticodon triplet (34-35-36) for efficient recognition and binding to the complementary mRNA triplet (3-2-1). The structures demonstrated that the ribosomal grip grasps the geometry and the steric volumes of the triplet pairs. Thus, at the first and second positions of the mini helix, the geometrical constraints imposed by the ribosomal grip at the decoding site stabilize a keto-enol tautomeric shift, either of the G or the U, in a GoU pair leading to a Watson-Crick-like configuration, isosteric to G=C or A-U pairs. Such near-cognate interactions are at the source of the most frequent translational errors observed. At the third position, GoU wobbles are expected. However, three forms are observed: the standard GoU with the U in the major groove, a new GoU* pair with U* in the minor groove, and the tautomeric Watson-Crick-like GoU or GoU*. The first two types are isosteric between themselves (G34oU3 occupies the same volume than U34*oG3). The last two types require base modifications in an asymmetric fashion: when the U is on the tRNA (U34) a modification is necessary (forming G3oU34*) but with G on the tRNA it is not necessary but can occur (forming U3oG34). In summary, the first two isosteric wobble GoU configurations are necessary to satisfy the wobbling rules for proper decoding, while the last tautomeric Watson-Crick-like configuration leads to translational errors. It is striking how molecular biology exploits the full physico-chemical spectrum of the keto bases G and U during the central process of translation for both controlling fidelity and accommodating errors.

References

Demeshkina, N., Jenner, L., Westhof, E., Yusupov, M. and Yusupova, G. (2012) A new understanding of the decoding principle on the ribosome. Nature 484, 256.

Grosjean, H. and Westhof, E. (2016) An integrated, structure- and energy-based view of the genetic code. Nucleic Acids Res. 44, 8020.

Rozov, A., Demeshkina, N., Khusainov, I., Westhof, E., Yusupov, M. and Yusupova, G. (2016) Novel base-pairing interactions at the tRNA wobble position crucial for accurate reading of the genetic code. Nat Commun 7, 10457.

Rozov, A., Wolff, P., Grosjean, H., Yusupov, M., Yusupova, G. and Westhof, E. (2018) Tautomeric G*U pairs within the molecular ribosomal grip and fidelity of decoding in bacteria. Nucleic Acids Res. 46, 7425.

Westhof, E., Yusupov, M. and Yusupova, G. (2014) Recognition of Watson-Crick base pairs: constraints and limits due to geometric selection and tautomerism. F1000Prime Reports 6, 19.

Westhof E, Yusupov M, Yusupova G. (2019) The multiple flavors of GoU pairs in RNA. J Mol Recognit. 2019:e2782.

Back to Table of contents

Three types of GoU pairs

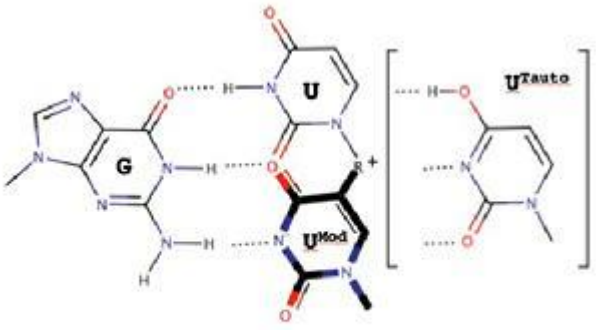

The three observed types of GoU pairs in the ribosomal decoding center: the standard wobble (above), the Watson-Crick-like (left and right), and the minor groove GoU pair with U34 modified on C5 (noted U34*).

Back to Table of contents

MS05 Nucleic acids and their interaction

MS5-02
Structural studies of repressors from SorC/DeoR family

P. Rezacova [1], M. Soltysova [1], J. Skerlova [1], J. Brynda [1], P. Pachl [1], K. Skubnik [2], J. Novacek [2]
[1]*Institute of Organic Chemistry and Biochemistry of Czech Academy of Sciences - Prague (Czech Republic),*
[2]*2CEITEC Central European Institute of Technology, Masaryk University - Brno (Czech Republic)*

Abstract
In bacteria, gene expression is controlled at the transcriptional level through interactions between regulatory proteins and DNA operators. Exploration of bacterial genomes led to the discovery of a large number of putative transcriptional regulators with the assignment of new families and subfamilies. One of these is the SorC family that embraces proteins that control the expression of genes and operons involved in the metabolism of sugar substrates. To date hundreds of putative transcriptional regulators have been classified into SorC family with only several members of SorC family functionally characterized: CggR [1] and DeoR [2] from B. subtilis, SorC from Klebsiella pneumonie [3] and LsrR from E. coli [4].
SorC family repressors contain conserved helix-turn-helix domain DNA-binding (DBD) at their N-terminus and an effector-binding domain (EBD) at their C-terminus. The DBD recognizes palindromic operator sequence usually located downstream of the promotor while the EBD (PF04198) has a phosphosugar binding function and plays role in oligomerization.
We performed extensive structural studies of two repressors from B. subtilis: DeoR and CggR [5-7]. By combining techniques of X-ray crystallography and cryo-electron microscopy we explored the mechanism of effector binding and modulation of oligomerization, characterized the DNA recognition and allosteric changes induced by effector binding. Structural studies of these two representatives provided information crucial for understanding the general mechanisms of gene regulation by SorC repressors.

The work was supported from European Regional Development Fund; OP RDE; Project: "ChemBioDrug" (No. CZ.02.1.01/0.0/0.0/16_019/0000729).

References
1. Zorrilla, S., Chaix, D., Ortega, A., Alfonso, C., Doan, T., Margeat, E., Rivas, G., Aymerich, S., Declerck, N. & Royer, C. A. (2007) Fructose-1,6-bisphosphate acts both as an inducer and as a structural cofactor of the central glycolytic genes repressor (CggR), Biochemistry. 46, 14996-5008.
2. Zeng, X., Saxild, H. H. & Switzer, R. L. (2000) Purification and characterization of the DeoR repressor of Bacillus subtilis, J Bacteriol. 182, 1916-22.
3. de Sanctis, D., McVey, C. E., Enguita, F. J. & Carrondo, M. A. (2009) Crystal structure of the full-length sorbitol operon regulator SorC from Klebsiella pneumoniae: structural evidence for a novel transcriptional regulation mechanism, J Mol Biol. 387, 759-70.
4. Wu, M., Tao, Y., Liu, X. & Zang, J. (2013) Structural basis for phosphorylated autoinducer-2 modulation of the oligomerization state of the global transcription regulator LsrR from Escherichia coli, J Biol Chem. 288, 15878-87.
5. Rezacova, P., Kozisek, M., Moy, S. F., Sieglova, I., Joachimiak, A., Machlus, M. & Otwinowski, Z. (2008) Crystal structures of the effector-binding domain of repressor Central glycolytic gene Regulator from Bacillus subtilis reveal ligand-induced structural changes upon binding of several glycolytic intermediates, Mol Microbiol. 69, 895-910.
6. Skerlova, J., Fabry, M., Hubalek, M., Otwinowski, Z. & Rezacova, P. (2014) Structure of the effector-binding domain of deoxyribonucleoside regulator DeoR from Bacillus subtilis, Febs J. 281, 4280-4292.
7. Soltysova, M., Sieglova, I., Fabry, M., Brynda, J., Skerlova, J. & Rezacova, P. (2021) Structural insight into DNA recognition by bacterial transcriptional regulators of the SorC/DeoR family, Acta Crystallogr D Struct Biol. 77, 1411-1424.

Back to Table of contents

MS05 Nucleic acids and their interaction

MS5-03
DciA, the ancestral replicative helicase loader

C. Cargemel [1], S. Marsin [1], Y. Adam [1], M. Chan-Yao-Chong [2], J. Andreani [1], S. Baconnais [3], P. Legrand [4], M. Ould Ali [5], I. Gallay-Li De La Sierra [1], A. Humbert [1], D. Durand [1], M. Aumont-Nicaise [6], C. Velours [6], F. Ochsenbein [1], E. Le Cam [3], C. Possoz [1], T. Ha-Duong [2], H. Walbott [1], J.L. Ferat [1], S. Quevillon-Cheruel [1]
[1]Université Paris-Saclay, CEA, CNRS, Institute for Integrative Biology of the Cell (I2BC) - Gif-sur-Yvette (France), [2]Université Paris-Saclay, CNRS, BioCIS - Châtenay-Malabry (France), [3]Genome Integrity and Cancer UMR 9019 CNRS, Université Paris Saclay, Gustave Roussy - Villejuif (France), [4]Synchrotron SOLEIL, L'Orme des Merisiers - Gif-sur-Yvette (France), [5]Cryo-Electron Microscopy Plateform of iI2BC - Gif-sur-Yvette (France), [6]Protein Interaction Platform (PIM) of I2BC - Gif-sur-Yvette (France)

Abstract

DNA replication is a crucial step for the proliferation of all organisms. Multi-subunits complex termed replisome carried out strand synthesis while controlling the replication fidelity. In front of the replisome, the replicative helicase unwinds DNA by its translocation on the lagging strand. One of the essential steps of replication is the recruitment and loading of the helicase at the replication initiation site. In bacteria, the initiation protein DnaA localized at the unique origin of replication *oriC* recruits two helicases DnaB, but the loading depends on a protein loader. DnaB loading has been well described within the *Escherichia coli* model, where DnaC ensures DnaB loading by cracking open the helicase. Yet, DnaC distribution is marginal in the bacterial domain. It was established phylogenetically that the *dnaC* gene is a domesticated phage element that has replaced several times, through the evolution, the ancestral gene *dciA* (1). Despite the preponderance of *dciA* in bacteria, the loading mechanism of DnaB managed by DciA was not yet studied.
Our work focused on the biochemical and structural characterization of DciA and DnaB from *Vibrio cholerae*. Like other bacterial replicative helicases, *Vc*DnaB adopts a toroid-shaped homo-hexameric structure but with a slight opening (2). Performing helicase assays and SPR analyses, we showed that *Vc*DnaB can load itself on DNA and that *Vc*DciA stimulates this function, resulting in an increased DNA unwinding (2). We obtained a crystal structure of the *Vc*DnaB•*Vc*DciA complex, which we compared to the DnaB•DnaC complex from *E. coli*. Surprisingly, despite no structural nor sequence similarity between the two loaders, both target the same binding site. We determined that *Vc*DciA is composed of two structural domains: a globular NTD (structure solved by NMR), which binds to DNA, and an unstructured CTD, which can fold transitory in two small helices (3) and bind to *Vc*DnaB. We combined a multi-disciplinary approach to study the structural and functional interplay between the three partners of the *Vc*DnaB•*Vc*DciA•DNA complex in order to understand the loading mechanism of DnaB by DciA. We expect a completely different mechanism than the one known for DnaC.

References

(1) Brezellec P, Vallet-Gely I, Possoz C, Quevillon-Cheruel S and Ferat JL. (2016) DciA is an ancestral replicative helicase operator essential to bacterial replication initiation. Nature Communications. 7:13271. DOI: 10.1038/ncomms13271. PMCID: PMC5109545
(2) Marsin S§, Adam Y§, Cargemel C§, Andreani J, Baconnais S, Legrand P, Li de la Sierra-Gallay I, Humbert A, Aumont-Nicaise M, Velours C, Ochsenbein F, Durand D, Le Cam E, Walbott H, Possoz C, Quevillon-Cheruel S* and Ferat JL*. (2021) Study of the DnaB:DciA interplay reveals insights into the primary mode of loading of the bacterial replicative helicase. Nucleic Acids Res. 49(11):6569-6586. DOI: 10.1093/nar/gkab463. PMID: 34107018
(3) Chan-Yao-Chong M, Marsin S, Quevillon-Cheruel S, Durand D and Ha-Duong T. (2020) Structural ensemble and biological activity of DciA intrinsically disordered region. J Struct Biol. 212(1):107573. DOI: 10.1016/j.jsb.2020.107573. Epub 2020 Jul 15. PMID: 32679070

Back to Table of contents

MS05 Nucleic acids and their interaction

MS5-04

High resolution cryo-EM structure of a type II topoisomerase cleavage core-complex with bound 18mer dsDNA

S. Najmudin [1], X.S. Pan [2], A.J. Beavil [1], N.B. Cronin [3], A. Ilangovan [4], L.M. Fisher [2], M.R. Sanderson [1]
[1]Randall Centre for Cell and Molecular Biophysics, 3rd Floor New Hunt's House, Faculty of Life Sciences and Medicine, King's College London - London SE1 1UL (United Kingdom), [2]Molecular and Clinical Sciences Research Institute, St. George's, University of London, Cranmer Terrace - London SW17 0RE (United Kingdom), [3]LonCEM Facility, The Francis Crick Institute, 1 Midland Road - London NW1 1AT (United Kingdom), [4]Abernethy Building, School of Biological and Behavioural Sciences, Queen Mary University of London, Newark Street, Whitechape - London E1 2AT (United Kingdom)

Abstract

Type II topoisomerases perform essential roles in DNA replication, chromosome segregation and recombination [1]. Bacteria have two type II enzymes: DNA gyrase, whose function is to supercoil chromosomal DNA and remove positive supercoils ahead of replication forks, and topoisomerase (topo) IV which unlinks catenated daughter chromosomes at cell division [2]. They use ATP to cross one DNA segment through a transient double-stranded DNA break in another DNA duplex involving a 'DNA cleavage complex'. This covalent enzyme-DNA intermediate is formed by reversible attack of the ParC or GyrA active-site tyrosines of the tetrameric topo IV (ParC2ParE2) or gyrase (GyrA2GyrB2) complex. Many important antibacterial and anticancer agents exert their cytotoxic effects by stabilising the cleavage complex. Thus, both topo IV and gyrase are targets for clinically important quinolones such as ciprofloxacin and moxifloxacin and quinazolinedione inhibitors, and human topo IIα and IIβ are targets for the anticancer drugs etoposide and doxorubicin [3]. Structures of several quinolone-topo IV/gyrase (and drug-topo II) core cleavage complexes have been determined by X-ray crystallography [4-6] but the approach has limitations. For example, not all topoisomerases and quinolones yield suitable crystals. Moreover, X-ray crystal structures of full-size holoenzyme complexes [7] are not easily obtained and the few cryoEM structures available are at relatively low resolution. Here we describe the use of cryoEM to solve the structure to 2.7 Å of a DNA-core complex of a type II topoisomerase, that of topo IV from Streptococcus pneumoniae, a major cause of pneumonia. To our knowledge, this is the first reported sub-3 Å cryoEM structure of a topoisomerase and provides high resolution insights on novel enzyme-DNA-interactions.

References

[1] Schoeffler, A.J. and Berger, J.M. (2008) Q. Rev. Biophys. 41, 41-101.
[2] Hirsch J. and Klostermeier D. (2021) Nucleic Acids Res. 49, 6027-6042.
[3] Jaswal S., Nehra B., Kumar S. and Monga V. (2020) Bioorg. Chem. 104, 104266
[4] Laponogov, I., Sohi, M.K., Veselkov, D.A., Pan, X.-S., Sawhney, R., Thompson, A.W., McAuley, K., Fisher, L.M. and Sanderson M.R. (2009) Nat. Struct. Mol. Biol. 16, 667-9.
[5] Veselkov, D.A., Laponogov, I., Pan, X.-S., Selvarajah, J., Skamrova, G.B., Branstrom, A., Narasimhan, J., Vara Prasad, J.V.N., Fisher, L.M. and Sanderson, M.R. (2016) Acta Cryst. D 72, 488-496.
[6] Laponogov, I., Pan, X.-S., Veselkov, D.A., Cirz, R.T., Wagman, A., Moser, H.E., Fisher, L.M. and Sanderson, M.R. (2016) Open Biol. 6, 160157.
[7] Laponogov, I., Veselkov, D.A., Crevel, I.M.-T., Pan, X.-S., Fisher, L.M. and Sanderson, M.R. (2013) Nucleic Acids Res. 41, 9911-9923.

Back to Table of contents

MS05 Nucleic acids and their interaction

MS5-05

RNA X-ray Structures at Atomic Resolution that Contain an Essential Constituent of the mRNA Vaccines: N1-Methylpseudouridine

B. Spingler [1], P. Nievergelt [1], F. Berliat [1], K.E. Mcauley [2]
[1]University of Zurich - Zurich (Switzerland), [2]Paul Scherrer Institute - Villigen (Switzerland)

Abstract

In the two COVID-19 mRNA vaccines of Pfizer-BioNTech[1] and Moderna, all uridines of the mRNA have been substituted by N1-methylpseudouridine (m1Ψ).[2, 3] N1-Methylpseudouridine has been characterized as a natural product already more than 40 years ago [4, 5] and has been identified in a multitude of ribosome structures [6, 7, 8, 9, 10], however only at a resolution of 2.9 angstroem or even lower. Given the relevance of this topic, we set out to crystallize N1-methylpseudouridine alone and as part of high-resolution double-stranded RNA structures. We will report about our success in achieving both goals, the latter at a resolution of up to 1.05 angstroem.
We thank for support by the company Biosynth Carbosynth.

References

[1] Polack, F. P., Thomas, S. J., Kitchin, N., Absalon, J., Gurtman, A., Lockhart, S., Perez, J. L., Pérez Marc, G., Moreira, E. D., Zerbini, C., Bailey, R., Swanson, K. A., Roychoudhury, S., Koury, K., Li, P., Kalina, W. V., Cooper, D., Frenck, R. W., Hammitt, L. L., Türeci, Ö., Nell, H., Schaefer, A., Ünal, S., Tresnan, D. B., Mather, S., Dormitzer, P. R., Şahin, U., Jansen, K. U. & Gruber, W. C. (2020). New Engl. J. Med. 383, 2603.
[2] Nance, K. D. & Meier, J. L. (2021). ACS Cent. Sci. 7, 748.
[3] Morais, P., Adachi, H. & Yu, Y.-T. (2021). Front. Cell Dev. Biol. 9, 789427.
[4] Argoudelis, A. D. & Mizsak, S. A. (1976). J. Antibiot. 29, 818.
[5] Brand, R. C., Klootwijk, J., Planta, R. J. & Maden, B. E. H. (1978). Biochem. J. 169, 71.
[6] Natchiar, S. K., Myasnikov, A. G., Kratzat, H., Hazemann, I. & Klaholz, B. P. (2017). Nature 551, 472.
[7] Brown, A., Baird, M. R., Yip, M. C. J., Murray, J. & Shao, S. (2018). eLife 7, e40486.
[8] Coureux, P.-D., Lazennec-Schurdevin, C., Bourcier, S., Mechulam, Y. & Schmitt, E. (2020). Commun. Biol. 3, 58.
[9] Matzov, D., Taoka, M., Nobe, Y., Yamauchi, Y., Halfon, Y., Asis, N., Zimermann, E., Rozenberg, H., Bashan, A., Bhushan, S., Isobe, T., Gray, M. W., Yonath, A. & Shalev-Benami, M. (2020). Nucleic Acids Res. 48, 11750.
[10] Liang, X., Zuo, M.-Q., Zhang, Y., Li, N., Ma, C., Dong, M.-Q. & Gao, N. (2020). Nature Commun. 11, 3542.

Back to Table of contents

MS06 Structural Enzymology

MS6-01

Capturing Snapshots of Metalloenzymes in Action

C. Drennan [1]
[1]*Departments of Chemistry and Biology, MIT - Cambridge (United States)*

Abstract

How do microbes live on the pollutant carbon monoxide? How do microbes split the triple bond of nitrogen gas? When it comes to performing difficult chemistry, microbes often combine a protein scaffold with a highly reactive metallocofactor, employing a hired gun if you will. Some metallocofactors are relatively simple – a single iron atom bound to an enzyme, whereas others are complex, and are best described as multi-metal assemblies or as “great metallocofactors.” In this presentation, audience members will hear about the “great metallocofactors” involved in one-carbon metabolism: nickel-iron-sulfur containing metallocofactors that perform the biological equivalent of the water-gas shift reaction and of the Monsanto process.

Back to Table of contents

MS06 Structural Enzymology

MS6-02

Time-resolved studies on Oxygenase Catalysis

C. Schofield [1]
[1]*University of Oxford - Oxford (United Kingdom)*

Abstract

The 2-oxogluterate oxygenase structural family are ubiquitous in aerobic biology. They catalyse a very wide range of oxidative reactions, most commonly hydroxylation, but also more exotic reactions, such as penicillin formation from a tripeptide, as catalysed by isopenicillin N synthase (IPNS). They have roles ranging from penicillin biosynthesis in microbes to epigenetic regulations in humans, where they play key roles in hypoxic sensing. Static cryo-crystallography has revealed they have a conserved distorted double stranded beta-helix core fold that supports ferrous iron and 2-oxoglutarate binding residues. Although a consensus mechanism for them has emerged, how the protein fold moves to enable robust catalysis and control the reactivity of intermediates is unclear, though modelling studies suggest correlated motions are important in catalysis. The lecture will describe how XFEL analysis coupled with cryo-crystallographic and solution studies have provided new insight into catalysis by IPNS, including on the role of conformational changes in the protein fold during covalent bond making steps in catalysis. Challenges in initiating and coordinating reaction in crystals will also be discussed.

References

Rabe et al. Sci Adv, 2021, 7, eabh0250

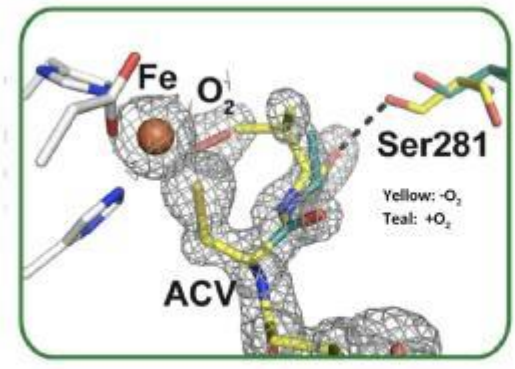

Back to Table of contents

MS06 Structural Enzymology

MS6-03

Visualizing bi-enzyme complex dynamics by time-resolved crystallography

S. Sung [1], D. Von Stetten [1], P. Mehrabi [2], E. Schulz [2], R. Sterner [3], A. Kneuttinger [3], T.R. Schneider [1], A. Pearson [2], M. Wilmanns [1]
1EMBL - Hamburg (Germany), 2University of Hamburg - Hamburg (Germany), 3University of Regensburg - Regensburg (Germany)

Abstract

Bi-enzyme complexes with tunnel-mediated product/substrate transport between two active sites are intricate enzyme factories, in which two spatially separated catalytic steps are coordinated by sophisticated allosteric mechanisms. Tryptophan synthase (TS) assembles into a heterotetrameric TrpA/(TrpB)2/TrpA complex, in which the TrpA product indole is transported to the TrpB subunit through a ~25 Å long intermolecular tunnel to form the final product tryptophan[1,2]. We used TS as a pilot system to apply Time-Resolved serial crystal X-ray crystallography (TRX)[3] and Cryo-Trapping X-ray crystallography (CTX) to investigate the structural details of catalysis, allostery and product/substrate transport within a timely resolution that matches its biochemical properties. To date, we have structurally characterized eight out of 13 previously established reaction states by TRX and CTX[4,5]. By ensuring indole delivery from the TrpA active site into the intermolecular tunnel to the TrpB active site, we have identified distinct indole locations within this tunnel. In summary, our data provide an well-defined basis to unravel the biochemistry of a complex bi-enzyme system by a structure-based molecular movie presentation.

References

1. M. F. Dunn, Arch. Biochem. Biophys. 2012, 519, 154.
2. A. C. Kneuttinger, et al., Int. J. Mol. Sci. 2019, 20, 5106.
3. P. Mehrabi, E. C. et al., Nat. Methods 2019, 16, 979.
4. K. S. Anderson, et al., JBC, 1991, 266, 8020.
5. S.Sung et al., Unpublished

Back to Table of contents

MS06 Structural Enzymology

MS6-04

X-ray induced reduction of heme metal centers is protein-independent –implications for structural studies of redox sensitive proteins

V. Pfanzagl 1, J.H. Beale 2, T. Gabler 1, K. Djinovic-Carugo 3, C. Obinger 1, E. Beale 4, S. Hofbauer 1.

1University of Natural Resources and Life Sciences, Department of Chemistry - Wien (Austria), 2Paul Scherrer Institute - Villigen (Switzerland) - Villigen (Switzerland), 3University of Vienna, Max F. Perutz Laboratories - Wien (Autriche), 4Paul Scherrer Institute - Villigen (S Switzerland uisse)

Abstract

X-ray crystallography is one of the main resources to obtain information on the coordination of molecules within the active site of metalloproteins on an atomistic level. Based on ligand coordination, interatomic distances and relative positioning of catalytic amino acids enzymologists try to understand the underlying electronic reaction mechanism. Therefore the exact redox status and conformation of the cofactor in question is of utmost importance. Unfortunately the redox active nature of metal cofactors makes them especially susceptible to irradiation induced photoreduction, making structural information obtained by photo-reducing X-ray sources the least trustworthy [1,2]. Here we present a study of the pre-steady state reduction kinetics of X-ray induced photo-reduction of six different model heme proteins to identify a reasonable dose-limit for the collection of non-reduced datasets for redox-active metallo enzymes. Using online-UV-vis spectroscopy we examined the reduction kinetics of the heme cofactor to understand the impact of sample-derived variables (protein, crystallization conditions, crystal morphology and cofactor) and irradiation-derived variables (dose and dose rate). We can show that the reduction kinetics solely depend on the dose, irrespective of the sample-derived variables (Figure 1) and define a protein-independent dose-limit of ~40 kGy, which corresponds to a 50% reduction. Furthermore, using standard macromolecular crystallography tools, we were able to collect and solve time-resolved low dose structures. We present structures of a model heme protein (KpDyP) in different defined redox states obtained by serial crystallography and dose-specific data splitting. These structures show photoreduction induced rearrangements in water coordination and conformation of the catalytically relevant residue Asp 143 [3] (Figure 2). The observed effects of photo-reduction highlight that care has to be taken when in-solution data of ferric proteins are rationalized by structural constraints derived from crystal structures of reduced enzymes [4]. Finally, we will present data for a pristine unreduced XFEL structure of KpDyP in its biologically relevant iron (III) oxidation state.

References

[1] G. I. Berglund, G. H. Carlsson, A. T. Smith, H. Szöke, A. Henriksen, J. Hajdu, Nature 417 (2002), 463-468 [2] T. Beitlich, K. Kühnel, C. Schulze-Briese, R. L. Shoeman, I. Schlichting, J Synchrotron Radiat 14 (2007), 11-23 [3] V. Pfanzagl, K. Nys, M. Bellei, H. Michlits, G. Mlynek, G. Battistuzzi, K. Djinović-Carugo, S. Van Doorslaer, P.G. Furtmüller, C. Obinger, J. Biol Chem 293 (2018), 14823-14838 [4] V. Pfanzagl, J.H. Beale, H. Michlits, D. Schmidt, T. Gabler, C. Obinger, K. Djinovic-Carugo, S.Hofbauer, J. Biol Chem 295 (2020), 13488-13501

Back to Table of contents

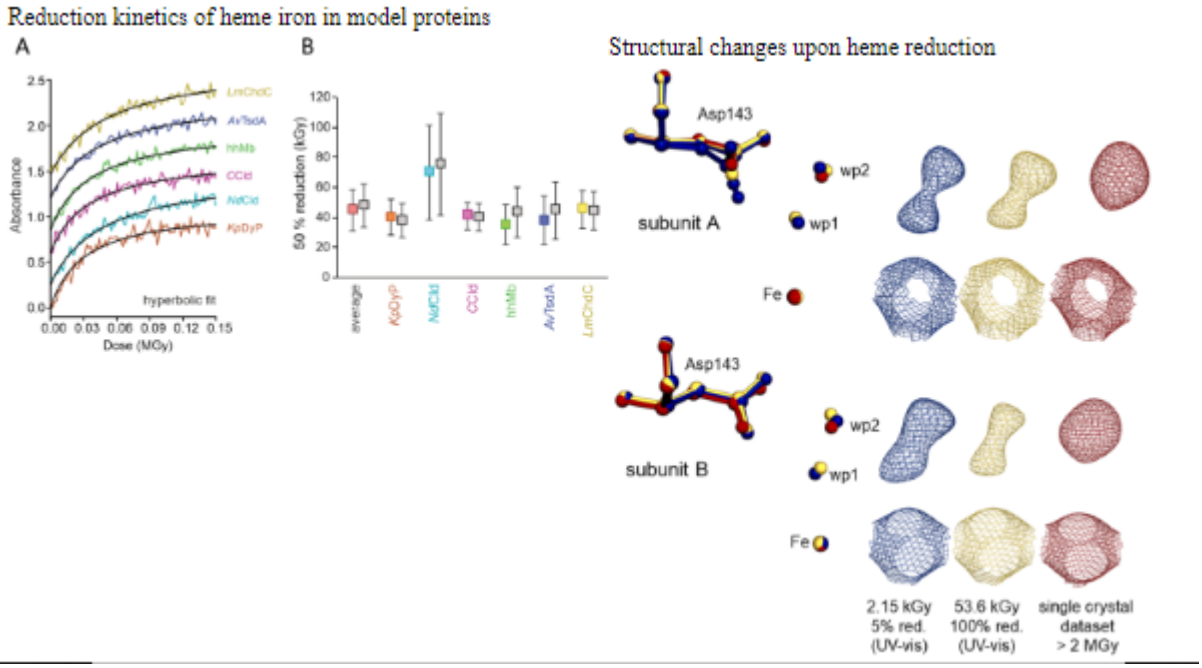

Back to Table of contents

MS06 Structural Enzymology

MS6-05

Multimetal Methyltransferase Making Methanogenesis

C. Fyfe [1]
[1]*Micalis Institute - Jouy en Josas* ***(France)***

Abstract

B12-dependent radical SAM enzymes are one of the largest groups of radical SAM enzymes with more than 200,000 members. This family of metalloenzymes are unique in their ability to form carbon-carbon bonds between unactivated sp3-hybridized carbons. Using biochemical and biophysical techniques including X-ray crystallography and electron paramagnetic resonance we have investigated methanogenesis marker protein 10 (Mmp10). Mmp10 has been shown to perform a post-translational methylation of an arginine within the active site of methyl-coenzyme M reductase. This is one of many post-translational modifications that are profoundly important for the methane production by microbes using methyl-coenzyme M reductase. Our crystallographic snapshots of Mmp10 reveal unique features including four distinct metal centres and a tyrosine that can coordinate the radical SAM clusters fourth iron allowing it to switch between radical and nucleophilic chemistry. The various snapshots we obtain have shown not only how this enzyme binds it protein substrate but also how it can utilise SAM in multiple ways to methylate its substrate[1].

References

[1] Fyfe CD, Bernardo-García N, Fradale L, Grimaldi S, Guillot A, Brewee C, Chavas LMG, Legrand P, Benjdia A, Berteau O. - 2022 - Crystallographic snapshots of a B12-dependent radical SAM methyltransferase. Nature (7896):336-342.

Mmp10 with its substrate and four metal centres

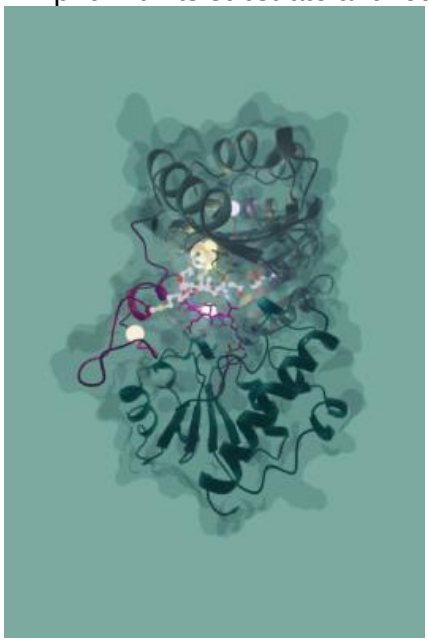

Back to Table of contents

MS07 Membrane Proteins

MS7-01

Mammalian rhodopsin dynamics using an X-ray free electron laser

V. Panneels [1]
[1]*PSI - PSI-Villigen* ***(Switzerland)***

Abstract

Mammalian rhodopsin dynamics using an X-ray free electron laser.
.
Thomas Gruhl1, Tobias Weinert1, Matthew Rodrigues1, Schertler group1,2, Nango group3, Neutze group4, Nogly group2, SACLA group5, Standfuss group1, SwissFEL group6, Gebhard Schertler1,2, Valérie Panneels1.
1 Division of Biology and Chemistry, Laboratory for Biomolecular Research, Paul Scherrer Institute, 5232 Villigen, Switzerland
2 Department of Biology, ETH Zurich, 5232 Villigen PSI, Switzerland.
3 RIKEN SPring-8 Center, 1-1-1 Kouto, Sayo-cho, Sayo-gun, Hyogo 679-5148, Japan.
4 Department of Chemistry and Molecular Biology, University of Gothenburg, Sweden.
5 Japan Synchrotron Radiation Research Institute (JASRI), 1-1-1 Kouto, Sayo-cho, Sayo-gun, Hyogo, 679-5198, Japan.
6 SwissFEL, Paul Scherrer Institute, 5232 Villigen, Switzerland
---
Mammalian Rhodopsin, a prototype of the largest druggable G Protein-Coupled Receptors family (GPCRs), is our light receptor for night vision. Upon photon absorption, its chromophore 11-cis retinal undergoes one of the fastest events in biology, which happens in the femtosecond range, the isomerization into the agonist form, all-trans retinal. We have developed a new crystal form of rho-dopsin in LCP, diffracting to better than 2 Å, which is suitable for room temperature time-resolved serial crystallography. At the japanese SACLA and SwissFEL X-ray free electron lasers (XFELs), we were able to collect a number of time-resolved data sets. The rhodopsin microcrystals grown in the dark are successively injected in the light of a pump laser and probed with the XFEL beam after various time-delays from femtoseconds to milliseconds (see **Figure**), revealing important insights on the detailed mechanism of rhodopsin activation, e.g. retinal isomerization, rearrangements of amino acid side chains and water molecules.
We have been able to observe how the 11-cis retinal isomerizes, undergoing a severe twist inside the tight rhodopsin binding pocket after 1 picosecond of photoactivation, followed by a thermal relaxation, which will later lead to various changes in the protein conformation. The results can be compared to those of the prokaryotic proton pump bacteriorhodopsin studied using the same method **[1-3]**, but also to spectroscopic studies and numerous computational models of rhodopsin. Time-resolved serial femtosecond crystallography on rhodopsin will not only give details on the photophysical trigger of retinal excitation upon photon absorption, but also general insights on the molecular activation of a class A GPCR.

References

[1] Nango et al. Science. (2016) 354(6319):1552-1557.
[2] Nogly et al. Nat Commun. (2016) 7:12314.
[3] Nogly et al. Science. (2018) 13;361(6398).

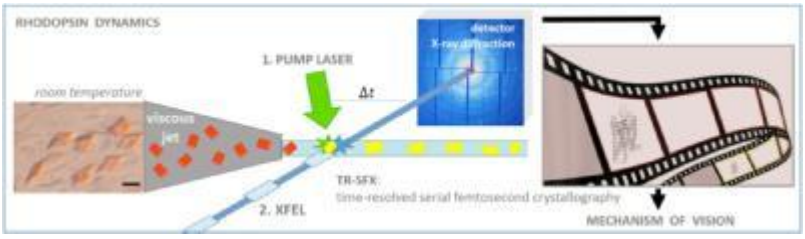

Back to Table of contents

MS07 Membrane Proteins

MS7-02

Mechanism of a proton-dependent lipid transporter involved in teichoic acid synthesis

C. Perez [1]
[1]*Biozentrum, University of Basel - Basel (Switzerland)*

Abstract
Transport of lipids across membranes is fundamental for diverse biological pathways in cells. Multiple ion-coupled transporters take part in lipid translocation, but their mechanisms remain largely unknown. Major facilitator superfamily (MFS) lipid transporters play central roles in cell wall synthesis, brain development and function, lipids recycling, and cell signaling. LtaA is a flippase that mediates the translocation of the lipid-anchor of lipoteichoic acid, an essential cell wall biopolymer in the Gram-positive pathogen Staphylococcus aureus. We used X-ray crystallography, cysteine disulfide trapping, molecular dynamics simulations, mutagenesis analysis, and transport assays in vitro and in vivo, to elucidate the mechanism of LtaA and reveal its importance for bacterial fitness. We demonstrate that while the entire amphipathic central cavity of LtaA contributes to lipid binding, its hydrophilic pocket dictates substrate specificity. We show that cycling through outward- and inward-facing conformations is essential for transport, while LtaA lateral openings are asymmetric in their function. We propose that LtaA catalyzes lipid translocation by a 'trap-and-flip' mechanism that might be shared among MFS lipid transporters.

Back to Table of contents

MS07 Membrane Proteins

MS7-03

The antibiotic darobactin mimics a β-strand to inhibit outer membrane insertase

R. Jakob [1], H. Kaur [1], J.K. Marzinek [2], R. Green [3], Y. Imai [3], J.R. Bolla [4], E. Agustoni [1], C.V. Robinson [4], P.J. Bond [2], K. Lewis [3], T. Maier [1], S. Hiller [1]

[1]University of Basel - Basel (Switzerland), [2]National University of Singapore - Singapore (Singapore), [3]Northeastern University - Boston, MA (United States), [4]University of Oxford - Oxford, UK (United Kingdom)

Abstract

Antibiotics that target Gram-negative bacteria in new ways are needed to resolve the antimicrobial resistance crisis. Gram-negative bacteria are protected by an additional outer membrane, rendering proteins on the cell surface attractive drug targets. The natural compound darobactin targets the bacterial insertase BamA - the central unit of the essential BAM complex, which facilitates the folding and insertion of outer membrane proteins. BamA lacks a typical catalytic centre, and it is not obvious how a small molecule such as darobactin might inhibit its function. Here we resolve the mode of action of darobactin at the atomic level using a combination of cryo-electron microscopy, X-ray crystallography, native mass spectrometry, in vivo experiments, and molecular dynamics simulations. Two cyclizations pre-organize the darobactin peptide in a rigid β-strand conformation. This creates a mimic of the recognition signal of native substrates with a superior ability to bind to the lateral gate of BamA. Because the interaction between darobactin and BamA is largely mediated by backbone contacts, it is particularly robust against potential resistance mutations. Our results identify the lateral gate as a functional hotspot in BamA and will allow the rational design of antibiotics.

References

Nature, 2021 May;593(7857):125-129. doi: 10.1038/s41586-021-03455-w.

Back to Table of contents

MS07 Membrane Proteins

MS7-04

Toward the comprehension of the assembly and opening of the MexAB-OprM efflux pump involved in the antibiotic resistance of Pseudomonas aeruginosa

Y. Ntsogo [1], M. Lustig [1], E. Boyer [2], L. Daury [2], G. Phan [1], O. Lambert [2], I. Broutin [1]
[1]University Paris Cité - Paris (France), [2]University de Bordeaux - Bordeaux (France)

Abstract

Bacterial infections remain a major public concern due to the accelerated increase in the appearance of antibiotic resistance. Among the different mechanisms used by bacteria to resist to antibiotics, the active efflux plays a major role. In Gram-negative bacteria, this is achieved by tripartite efflux pumps that form a macromolecular assembly spanning both membranes of the cellular wall. In Pseudomonas aeruginosa, an opportunistic pathogen highly involved in nosocomial diseases, the constitutive pump is MexAB-OprM.
Along with functional studies, many crystal structures were solved for the individual components of this pump and homologous ones [1-6]. Nevertheless, a lot of questions concerning the assembly recognition and specificity, the mechanism of efflux, and the opening of the whole pump are still a matter of active research, as the blockage of these pumps could restore the utility of the actual therapeutic arsenal. By a combined approach involving crystallography and cryo-EM together with biophysical analysis and in cellulo complementation experiments, we were able to bring new insides into the comprehension of these mechanisms.

References

[1] Ma, M., Lustig, M., Salem, M., Mengin-Lecreulx, D., Phan, G. & Broutin I. (2021) MexAB-OprM Efflux Pump Interaction with the Peptidoglycan of Escherichia coli and Pseudomonas aeruginosa. Int. J. Mol. Sci., 22, 5328. https://doi.org/10.3390/ijms22105328
[2] Glavier, M., Puvanendran, D., et al. (2020). Antibiotic export by MexB multidrug efflux transporter is allosterically controlled by a MexA-OprM chaperone-like complex, Nat Commun, Nat Comm., 11:4948, https://doi.org/10.1038/s41467-020-18770-5
[3] Tsutsumi, K., Yonehara, R., et al. (2019). Structures of the wild-type MexAB-OprM tripartite pump reveal its complex formation and drug efflux mechanism. Nat Commun 10(1): 1520-1529.
[4] Du, D., Wang, Z., et al. (2014). Structure of the AcrAB-TolC multidrug efflux pump. Nature 509(7501), 512-515.
[5] Ntsogo Enguéné, Y.V., Phan, G., Garnier, C., Ducruix, A., Prange, T., Broutin, I. (2017). Xenon for tunnelling analysis of the efflux pump component OprN. PLoS ONE, 12(9):e0184045. doi: 10.1371/journal.pone.0184045
[6] Phan, G., Benabdelhak, H., et al. (2010). Structural and Dynamical Insights into the Opening Mechanism of P. aeruginosa OprM Channel. Structure 18(4), 507-517. doi: 10.1016/j.str.2010.01.018.

Cryo-EM structure of the MexAB-OprM efflux pump

Back to Table of contents

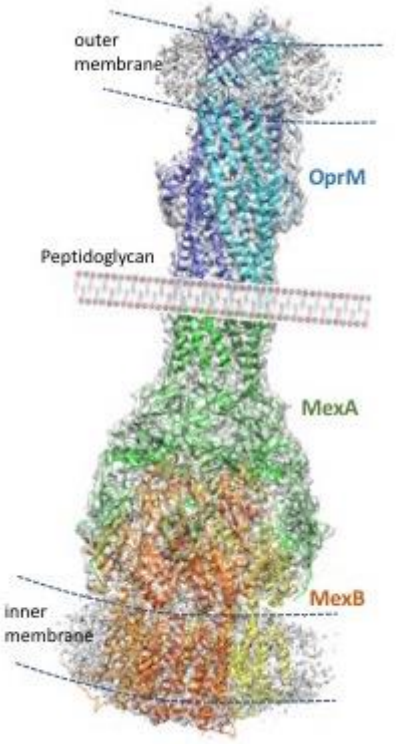

Back to Table of contents

MS08 Serial crystallography, obtaining structures from many crystals

MS8-01

Mechanism and dynamics of fatty acid photodecarboxylase

I. Schlichting [1]
[1]*Max Planck Institute for Medical Research - Heidelberg (Germany)*

Abstract

Light is important for organisms from all domains of life, serving as an energy resource or carrier of information initiating intra- or intercellular signaling. Photosensitive proteins, endowed with a light-absorbing chromophore, enable this. Detailed insights, including the initial events on the ultrafast time scale, were obtained by various forms of spectroscopy and computation. However, direct structural information necessary to understand the underlying molecular mechanisms has been inaccessible until recently. The unique properties of X-ray free electron lasers open the sub-ps time domain for time-resolved crystallography using small crystals that can be efficiently photolyzed, thus providing access to the long sought-after excited state and intermediate structures.
Photodecarboxylation is a well-established reaction in chemistry; however, no photoenzymatic equivalent was known until the discovery of Fatty Acid Photodecarboxylase (FAP), a flavin containing photoenzyme [1]. The enzymatic mechanism was investigated in detail by a large interdisciplinary consortium [2]: decarboxylation occurs directly upon reduction of the photo-excited flavin by the fatty acid substrate. Along with flavin reoxidation by the alkyl radical intermediate, a major fraction of the cleaved carbon dioxide unexpectedly transforms in 100 ns into another species, assigned to be bicarbonate based on IR-spectroscopy. Despite a great deal of insight into the catalytic mechanism and the role of two strictly conserved residues for substrate stabilization and functional charge transfer [2], a number of questions remain. To address these, including the nature of the transiently generated CO2-derivative we performed a follow-up time-resolved serial femtosecond crystallography experiment at SwissFEL spanning time-delays from ns to ms after photoexcitation. The results will be discussed.

References

[1] Sorigué et al An algal photoenzyme converts fatty acids to hydrocarbons, Science 357: 903-907 (2017)
[2] Sorigué et al Mechanism and dynamics of fatty acid photodecarboxylase, Science 372, eabd5687 (2021)

Back to Table of contents

MS08 Serial crystallography, obtaining structures from many crystals

MS8-02
Structural insights into mechanism of glycine reuptake inhibition

A. Shahsavar [1], P. Stohler [2], G. Bourenkov [3], I. Zimmermann [4], M. Siegrist [2], W. Guba [2], E. Pinard [2], S. Sinning [5], M. Seeger [6], T. Schneider [3], R. Dawson [4], P. Nissen [5]
[1]University of Copenhagen (Denmark), [2]Roche (Switzerland), [3]EMBL Hamburg (Germany), [4]Linkster Therapeutics (Switzerland), [5]Aarhus University (Denmark), [6]University of Zurich (Switzerland)

Abstract
Glycine transporter GlyT1 is the main regulator of neuronal excitation and inhibition mediated by neurotransmitter glycine in the brain. Prolonging glycinergic signalling through selective inhibition of GlyT1 has been pursued extensively over the past two decades as a key strategy for the treatment of a broad range of neurological/psychiatric disorders including schizophrenia. GlyT1 inhibitors achieve antipsychotic and pro-cognitive effects against many symptoms of schizophrenia, however a successful drug candidate has to come. To elucidate structure-based mechanism for inhibition in GlyT1, we have investigated its complex with a benzoylpiperazine chemotype inhibitor. We have combined a variety of tools including protein engineering to introduce stabilising mutations and grafting stable protein scaffolds as fusion constructs, exploring various expression systems, as well as generating stabilising inhibition state-specific sybodies to enable structure determination. Lipidic cubic phase crystallisation yielded microcrystals (< 10 µm) of GlyT1 in complex with the small-molecule inhibitor and the sybody. Diffraction data were collected from hundreds of microcrystals using serial helical line scans as available on the EMBL P14 beamline at the PETRA III storage ring (DESY, Hamburg). Merging the oscillation patterns yielded a complete dataset at 3.4 Å resolution. The GlyT1 structure reveals the selective inhibitor-bound state, adopting an inward-open conformation. The data unveil a dual nature of non-competitive inhibitors of functional transport exhibiting also competitive binding to the substrate binding site of glycine. Catching the transporter in a clinically relevant conformation helps re-evaluate the efforts for the development of efficacious GlyT1 inhibitors and provides insight in finding new strategies to target glycine reuptake transporter.

Back to Table of contents

MS08 Serial crystallography, obtaining structures from many crystals

MS8-03

Molecular snapshots of drug release from tubulin

M. Wranik [1], J. Standfuss [1]
[1]*Paul-Scherrer-Institut - Villigen* ***(Switzerland)***

Abstract

The dynamic interplay between proteins and their ligands is central to molecular biology, pharmacology, and drug development. Simple static models of ligand-protein interactions such as the “lock-and-key” mechanism have long been known to be insufficient. Much needed molecular insight can be obtained by resolving structural intermediates, but the relevant transitions extend over many orders of magnitude in time and cannot be resolved with conventional structural biology.

We have used time-resolved serial crystallography at a synchrotron and X-ray laser, to study the release of the photochemical affinity switch azo-Combretastatin A4 from the anti-cancer target tubulin. Thirteen logarithmically spaced temporal snapshots at near-atomic resolution are complemented by time-resolved spectroscopy and molecular dynamics simulations. They show how the photoinduced cis to trans isomerization of the azobenzene bond stretches the ligand in the picoseconds, the formation of a metastable binding pose in the nanosecond range which is followed by stepwise opening of a gating loop within microseconds, and the completion of the unbinding reaction within milliseconds. Ligand unbinding is accompanied by a collapsing binding pocket and global tubulin-backbone rearrangements. Our results have implications for the molecular basis of photopharmacology, the mechanism of action of anti-tubulin drugs and provide an experimental framework to study protein-ligand interaction dynamics.

Back to Table of contents

MS08 Serial crystallography, obtaining structures from many crystals

MS8-04

Xtrapol8: automatic elucidation of low-occupancy intermediate states in crystallographic studies

E. De Zitter [1], N. Coquelle [2], T. Barends [3], J.P. Colletier [1]
[1]Institut de Biologie Structurale (IBS), Univ. Grenoble Alpes, CEA, CNRS - Grenoble (France), [2]Structural Biology Group, European Synchrotron Radiation Facility (ESRF) - Grenoble (France), [3]Department of Biomolecular Mechanisms, Max Planck Institute for Medical Research - Heidelberg (Germany)

Abstract

The ultimate goal of structural biology is to link structure to function but this connection remains difficult to make when only a single inanimate structural model is available. Accordingly, the structural characterization of intermediate states is of high interest and pursued by many structural biology groups. A big leap forward was taken with the advent of time-resolved serial crystallography at XFELs and synchrotrons, which enables researchers to follow the structural evolution of the crystalline structure after a specific trigger, opening avenues to produce movies of proteins at work. However, a major limitation remains that the occupancy of the intermediate state has to be large enough to become visible in the electron density map. This is generally not the case, with triggered crystals existing as mixtures of initial, intermediate and final state(s). Fortunately, powerful data processing strategies exist that can extract the intermediate state signal. Indeed, differences between the triggered and untriggered dataset can be visualized in Fourier difference (Fobs,triggered-Fobs,untriggered) electron density maps and extrapolated structure factor amplitudes (Fextr,triggered)[1] can be calculated that solely describe the intermediate state and can be used in crystallographic structure refinement. In the past, such data processing has been performed by some well-experienced crystallographers but remains up until today out of reach for most researchers.

Here we will present Xtrapol8, a program written in python, using the cctbx toolbox[2] (Phenix)[3] modules and CCP4 programs,[4] to make these approaches accessible to a wide audience of structural biologists, from well-experienced crystallographers to newcomers in the field. Briefly, Xtrapol8 allows the calculation of high-quality Fourier difference maps, estimation of the occupancy of the intermediate state(s) in the crystals, and generation of extrapolated structure factor amplitudes (Fig. 1). The program uses Bayesian statistics to weight structure factor amplitude differences[5,6] which are then used to generate extrapolated structure factor amplitudes for a range of possible intermediate state occupancies.[1,7] The correct occupancy of the intermediate state is determined based on the extrapolated electron densities and the automatically refined structures. With the possibility to launch Xtrapol8 via the command line or graphical user interface, and to control various parameters of which defaults are carefully chosen, the program is highly adapted to the user's expertise. We anticipate that it will ease and accelerate the handling of time-resolved structural data, and thereby the understanding of molecular processes underlying function in a variety of proteins.

References

[1] Genick, U. K., Borgstahl, G. E., Ng, K., Ren, Z., Pradervand, C., Burke, P. M., Srajer, V., Teng, T. Y., Schildkamp, W., McRee, D. E., Moffat, K., Getzoff, E. D. (1997), Science, 275, 1471-1475.
[2] Grosse-Kunstleve, R. W., Sauter, N. K., Moriarty, N. W, Adams, P. D. (2002), Journal of Applied Crystallography, 35, 126-136.
[3] Liebschner, D., Afonine, P. V., and others, Adams, P. D. (2019), Acta Crystallogr D, 75, 861-877.
[4] Winn, M. D., Ballard, C. C., Cowtan, K. D., and others, Wilson, K. S. (2011), Acta Crystallogr D, 67, 235-42.
[5] Ursby, T. & Bourgeois, D. (1997), Acta Crystallogr. A, 53, 564-575.
[6] Ren, Z., Perman, B., Srajer, V., Teng, T. Y., Pradervand, C., Bourgeois, D., Schotte, F., Ursby, T., Kort, R., Wulff, M., Moffat, K. (2001), Biochemistry, 40, 13788-801.
[7] Coquelle, N., Sliwa, M., Woodhouse, J., and others, Colletier, J.-P., Schlichting, I. & Weik, M. (2018), Nature chemistry, 10, 31–37.

Back to Table of contents

The main steps followed by Xtrapol8.

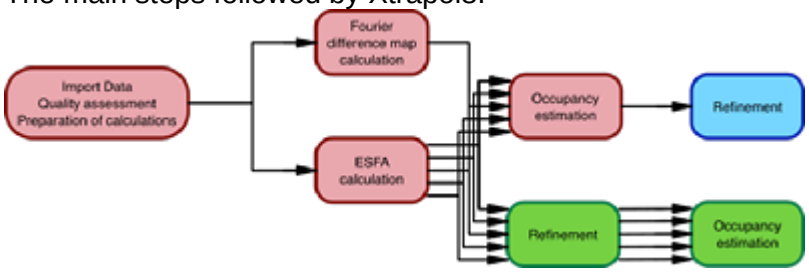

Back to Table of contents

MS08 Serial crystallography, obtaining structures from many crystals

MS8-05

Photoactivation in a Fluorescent Protein Proceeds via the Hula-Twist Mechanism : Revealed through TR-SFX

A. Fadini [1], J. Van Thor [1]
[1]*Imperial College London - London* ***(United Kingdom)***

Abstract

The light-induced cis/trans isomerization of a chromophore double bond is a fundamental reaction in photochemistry and it has been shown to be the primary activation event for a variety of protein photoreceptors. A detailed understanding of the reaction pathway and of how it is steered by protein environment is key for the rational design of more effective photosystems.

In the 1980s, Liu&Asato coined and proposed a mechanism for chromophore photoisomerization in proteins: the hula twist. This was supposed to be volume conserving and therefore favorable inside a sterically-crowded binding pocket. By exploiting the time resolution available at XFELs and the insertion of a heavy atom to break the symmetry of the chromophore ring, we capture the ultrafast photoproduct of the trans-to-cis reaction in a fluorescent protein. This, to our knowledge, is the first direct experimental structural evidence that unequivocally supports hula-twist chromophore photoisomerization in a protein, more than 30 years after it was first hypothesized. By analyzing data from time points that span from 300 fs to 1 µs, we also resolve how photoisomerization leads to the sequential movement and relaxation of secondary structure elements. This data demonstrates the power of time-resolved crystallography for elucidating the ultrafast dynamical response in photoactivated systems.

References

Work so far unpublished.
Key relevant references :
Liu, R. S. H. & Asato, A. E. The primary process of vision and the structure of bathorhodopsin: A mechanism for photoisomerization of polyenes* (lumirhodopsin/hypsorhodopsin/binding site/concerted twist). Proc. Nail. Acad. Sci. USA 82, 259–263 (1985)
Chang, J., Romei, M. G. & Boxer, S. G. Structural Evidence of Photoisomerization Pathways in Fluorescent Proteins. J. Am. Chem. Soc. 141, 15504–15508 (2019)
Colletier, JP., Schirò, G., Weik, M. (2018). Time-Resolved Serial Femtosecond Crystallography, Towards Molecular Movies of Biomolecules in Action. In: Boutet, S., Fromme, P., Hunter, M. (eds) X-ray Free Electron Lasers. Springer, Cham. https://doi.org/10.1007/978-3-030-00551-1_11

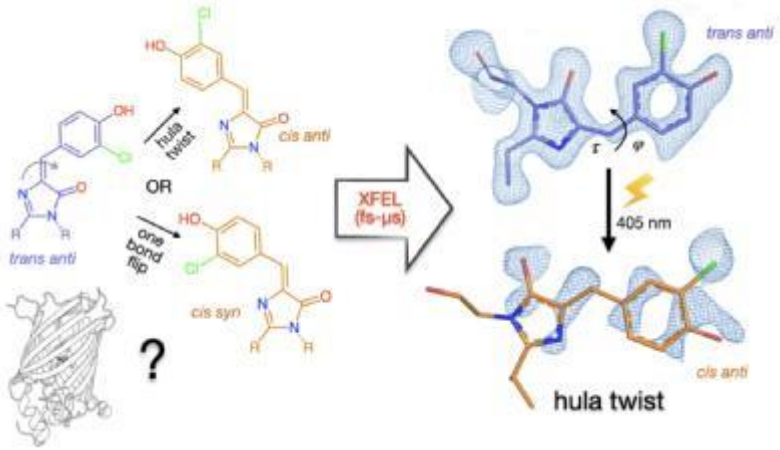

Back to Table of contents

MS09 Structural Biology combining methods/High resolution

MS9-01

Fully autonomous end-to-end protein to structure pipelines: the CrystalDirect harvester at MASSIF-1

S. Rocchio [1], M. Andrew [1], M. José [1], B. Matthew [1]
[1]*EMBL - Grenoble (France)*

Abstract

Recent advances in automation and method development at synchrotron facilities increased the interest in developing different data collection pipelines and plate-to-beam applications to respond to modern structural biology projects and to improve the efficiency for high throughput applications [1,2].
The combination of the CrystalDirect harvester with the automation on MASSIF-1 beamline will help to respond to multiple technical and experimental challenges [3,4,5]. The CrystalDirect harvester gives access to a fully automated protein crystallography workflow, integrating protein crystallization, sample harvesting and cryocooling into an automated process [3,6,7], while the automation of MASSIF-1 allows large amounts of high-quality data to be efficiently collected [1,2].
To date, room temperature (RT) data collection and dehydration experiments require a large number of manual steps and the experimental set-up is time-consuming; the automation of this process will render those experiments more reliable and reproducible, and facilitate their access to non-expert users [8,9,10,11].
The beamline commissioning is currently ongoing, with the main goal to develop different approaches for data collection that are both target-based and automated, and the initial focus on defining pipelines for room temperature data collection and dehydration experiments.
The CrystalDirect harvester has been installed in the beamline environment and the software integration, that permit the communication of the harvester with different software interfaces (CRIMS, MXCuBE3, and ISPyB), has enabled multiple and sequential crystal harvesting, sample mounting, and data collection to be executed in automated mode. The proper operation of each pipeline has been validated, showing the potential to develop multiple data collection approaches at both cryogenic and room temperature. Initial results indicate the possibility to collect complete datasets from single crystals at room temperature; the optimization of the automated data collection pipeline for different protein target is currently ongoing.
The beamline upgrade will, therefore, open new experimental opportunities and help respond to the dynamic change of scientific needs, such as the increased interest in structural data at physiological temperatures [10,11,12].

References

1. Bowler et al. J. Sync. Rad (2015). 22 1540-1547 http://dx.doi.org/10.1107/S1600577515016604
2. Svensson, et al. Acta Cryst. (2018). D74, 433- 440, http://dx.doi.org/10.1107/S2059798318003728
3. Cornaciu I et al., J Vis Exp. (2021); https://doi.org/10.3791/62491
4. Munzker et al. ChemBioChem (2020). 21, 21, 3096-3111; https://doi.org/10.1002/cbic.202000246
5. Helaey et al. BioRxiv (2021) https://doi.org/10.1101/2021.06.03.446146
6. Cipriani et al. Acta Cryst. (2012). D68, 1393-1399; https://doi.org/10.1107/s0907444912031459
7. Zander et al. Acta Cryst. (2016). D72, 454-466; http://dx.doi.org/10.1107/S2059798316000954
8. Bowler et al. J. Appl. Cryst (2017). 50, 631-638; https://doi.org/10.1107/S1600576717003636
9. Bowler et al. Cryst. Growth Des (2015). 15, 3, 1043-1054; https://doi.org/10.1021/cg500890r
10. Fisher Q Rev Biophys (2021) . 54, E1. https://doi.org/10.1017/S0033583520000128
11. Doukov et al. J Appl Cryst (2020) . 53, 1493-1501, https://doi.org/10.1107/S1600576720013503
12. Fraser et al. PNAS (2011). 08 (39) 16247-16252; https://doi.org/10.1073/pnas.1111325108

Back to Table of contents

MS09 Structural Biology combining methods/High resolution

MS9-02

Mechanistic basis for environment-controlled gene silencing by the histone-like nucleoid-structuring (H-NS) protein

U. Shahul Hameed [1], C. Liao [2], X. Zhao [2], M. Jaremko [1], J. Ladbury [3], L. Jaremko [1], J. Li [2], S. Arold [1]
[1]KAUST - Thuwal (Saudi Arabia), [2]U Vermont - Burlington (United States), [3]U Leeds - Leeds (United Kingdom)

Abstract

As an environment-dependent pleiotropic gene regulator in Gram-negative bacteria, the H-NS protein is crucial for adaptation and toxicity control of human pathogens such as *Salmonella*, *Vibrio cholerae* or enterohaemorrhagic *Escherichia coli.* Changes in temperature affect the capacity of H-NS to form multimers that condense DNA and restrict gene expression. However, the molecular mechanism through which H-NS senses temperature and other physiochemical parameters remains unclear and controversial. Combining structural (X-ray crystallography, NMR and SAXS), biophysical and computational analyses, we show that H-NS forms superhelical filaments in crystals and in solution through the joint action of N-terminal and central dimerization domains. The handedness and pitch of these filaments are in agreement with plectonemic DNA supercoils. The human body temperature promotes the unfolding of the central dimerization domain, breaking up H-NS multimers. This unfolding event enables an autoinhibitory compact H-NS conformation that blocks DNA binding. High-resolution proton-less NMR analyses reveal fuzzy electrostatic interactions as the driving force for self-inhibition. We use computational multiscale modelling and simulations to obtain detailed insights into the mechanism of H-NS filament's sensitivity to environmental changes. We then combined molecular simulations and biophysical and structural analysis to reveal, at an atomistic level, how the same general mechanism was adapted through specific amino acid substitutions to suit bacteria that target plants and insects. Collectively, our results reveal the molecular basis of a mechanism that allows bacteria to sense their environment and adapt to it.

References

[1] Zhao et al, (2021), Molecular Basis for Environment Sensing by a Nucleoid-Structuring Bacterial Protein Filament. J. Phys. Chem. Lett. DOI: 10.1021/acs.jpclett.1c01710
[2] Zhao et al, (2021) Molecular basis for the adaptive evolution of environment-sensing by H-NS proteins. eLIFE, DOI: 10.7554/eLife.57467
[3] Shahul Hameed et al. (2018), H-NS uses an autoinhibitory conformational switch for environment-controlled gene silencing., NAR, doi: 10.1093/nar/gky1299
[4] Arold, S.T. et al. (2010) H-NS forms a superhelical scaffold for DNA condensation. PNAS, 107:15728-32

Composite figure showing H-NS states

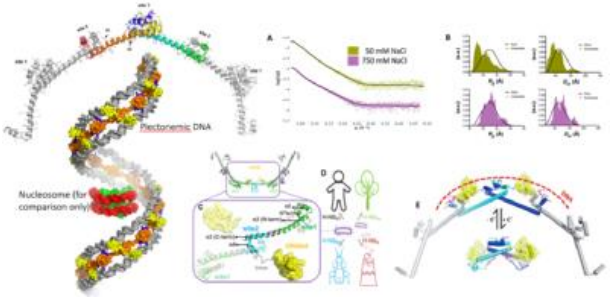

Back to Table of contents

MS09 Structural Biology combining methods/High resolution

MS9-03

Probing ligand-binding modes by “temperature-resolved” macromolecular crystallography

C.Y. Huang [1], S. Aumonier [1], S. Engilberge [2], D. Eris [1], K.M.L. Smith [1], F. Leonarsky [1], J.A. Wojdyla [1], J.H. Beale [1], D. Buntschu [1], A. Pauluhn [1], M.E. Sharpe [1], V. Olieric [1], M. Wang [1]
[1]Paul Scherrer Institut - Villigen PSI (Switzerland), [2]European Synchrotron Radiation Facility - Grenoble (France)

Abstract

Continuous developments of cryogenic X-ray crystallography have provided most of our knowledge in 3D protein structures, which has been further augmented by the revolutionary advances in cryoEM recently. However, a single structure conformation identified at cryogenic temperatures may introduce a misleading interpretation as a result of cryogenic cooling artifacts. This can limit the overview of inherent protein physiological dynamics, which can play a critical role in protein biological functions. We developed an ambient temperature X-ray crystallography method using temperature as a trigger to record movie-like structure snapshots. The method has been used to show how TL00150, a 175.15 Da fragment, undergoes structural changes in its binding modes with the aspartic protease endothiapepsin (EP). We observed a surprising fragment binding discrepancy between the cryocooled and the physiological temperature structures, and captured multiple binding poses and their interplay with DMSO. The observations here open up new promising prospects for structure determination and interpretation at physiological temperatures, their implication in structure-based drug discovery and also providing more accurate starting models for molecular dynamics simulations.

References

Probing ligand binding of endothiapepsin by “temperature-resolved” macromolecular crystallography, Huang *et al.* Acta Cryst. D, under revision

Ligand binding modes of EP upon temperature change

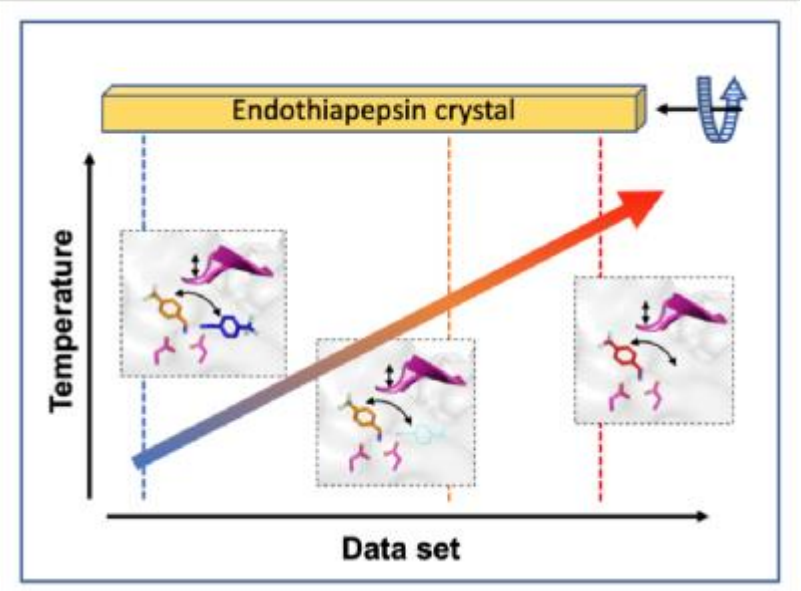

Back to Table of contents

MS09 Structural Biology combining methods/High resolution

MS9-04

Enabling high-energy, large-unit-cell, ultra-high-resolution X-ray crystallography on the P14@PETRAIII beamline

G. Bourenkov [1], T. Schneider [1], U.L. Dakshinamoorthy [2], E. Paknia [2], R. Fogh [3], P. Keller [3], C. Flensburg [3], C. Vonrhein [3], G. Bricogne [3], C. Schulze-Briese [4], A. Chari [2]
[1]EMBL Hamburg - Hamburg (Germany), [2]MPI for Multidisciplinary Sciences - Göttingen (Germany), [3]Global Phasing Limited - Cambridge (United Kingdom), [4]Dectris - Baden-Dättwil (Switzerland)

Abstract

The undulator beamline P14 is a part of the Integrated Facility for Structural Biology operated by the European Molecular Biology Laboratory at the PETRA III storage ring at DESY (Hamburg, Germany). At high energies, a white beam compound refractive lens transfocator in 2:1 geometry is used to deliver a top-hat beam that can be shaped to any size between 20 and 300 µm at the sample position. Variable-size top-hat beams are particularly important in structural studies of large macromolecular complexes [1] and ultra-high-resolution studies of enzymatic mechanisms under precise dose control [2].

In early 2021, the Dectris CdTe 16M EIGER2 detector was installed at the P14 beamline. A high-flux collimated mode at an energy of 26.687 keV was established as a new standard beamline setting, in order to boost data quality by reducing radiation damage [3]. To further improve data quality, Global Phasing Ltd's workflow has been deployed on P14 through its interface to MXCuBE2 ([4], § 4.4.7). Crystal symmetry and orientation are first determined, then used together with knowledge of the MD3-goniostat's reorientation capabilities to design a multi-orientation strategy aiming to achieve completeness (no cusps) and uniformity of redundancy, within a "dose budget" adapted to the target resolution. The workflow then directly drives the execution of that strategy via MXCuBE2.

The potential of the combined use of these technical advances is highlighted by two ultra-high-resolution datasets from large-unit cell systems: 1) A primitive orthorhombic system with 560 kDa per asymmetric unit (a.u.), that yielded a 0.98 Å resolution dataset (almost 100M reflections, 2.75M unique, at a dose of 2.5 MGy); 2) A C-centered orthorhombic system with 280 kDa per a.u., yielding a 0.96 Å resolution dataset (over 40M reflections, 1.375M unique, 2.5 MGy). Data collection times, including characterization and strategy design, were 15 minutes for both datasets.

We conclude that the combination of optimized beamline optics, an advanced data-collection workflow, and CdTe detectors with small pixels enables the collection of highly precise and accurate high-resolution data on large unit-cell systems at high energies, capable of supporting the most demanding applications of X-ray crystallography to Structural Biology, and enzyme mechanistic studies. The increasing availability of high-energy beamlines will allow for the standardization of the setup to the benefit of the structural researchers.

References

[1] Singh et al. (2020) Cell 6, 1130-1133.
[2] Dai et al. (2019) Nature 573, 609-613
[3] Storm et al. (2021) IUCrJ 8(6)
[4] Oscarsson et al. (2019) Journal of Synchrotron Radiation 26, 393-405.

Back to Table of contents

MS09 Structural Biology combining methods/High resolution

MS9-05

The interaction of the Lactobacilli surface layer proteins with the lipotheichoic acids from the cell wall

N. Gubensäk [1], M. Eder [1], D. Vejzovic [1], T. Sagmeister [1], C. Grininger [1], F. Berni [2], E. Damisch [1], N. Malanovic [1], J. Codee [2], T. Pavkov-Keller [3]
[1]University of Graz, IMB - Graz (Austria), [2]Leiden University - Leiden (Netherlands), [3]University of Graz, IMB; BioTechMed - Graz (Austria)

Abstract

Surface layers (S-layers) are 2D crystalline lattices of proteins which cover the whole surface of many archaeal and bacterial cells. Since these proteins are in close contact with their environment they fulfil many vital tasks like bacterial adherence to other cells, protection against life-threatening conditions, maintenance of the cell shape and auto-coaggregation. These S-layer proteins are attached to the cell wall by interaction with lipoteichoic acids (LTA). The domain involved in this interaction, the LTA-binding domain, is found in a variety of bacterial cell surface proteins.

Our goal is to structurally characterize the LTA-biding domain and its interaction with the LTA. The soluble fragments of Lactobacili S-layer protein, containing the LTA-binding domain, were purified and subjected to crystallization. The obtained crystal structures show a unique domain with phosphate molecules bound in the putative binding regions. Isothermal titration calorimetry and thermofluor measurements with LTA and synthetized fragments as well as mutagenesis experiments were performed to characterize the binding. Via Nuclear Magnetic Resonance titration experiments, residues affected upon binding of LTA-fragments and the interaction region could be determined. Furthermore, combining the experimental data and in silico calculations, we propose a model for LTA-binding.

Acknowledgment: This work has been supported by the Austrian Science Fund (FWF, Project P29432 and doc.fund BioMolStruct DOC 130).

Back to Table of contents

MS10 Protein-carbohydrate interactions

MS10-01
Integrative methods in structural glycobiology

J. Agirre [1]
[1]*University of York - York (United Kingdom)*

Abstract
The introduction of intuitive graphical software (Potterton et al., 2018) has enabled structural biologists who are not experts in crystallography to build complete protein or nucleic acid models rapidly. In contrast, up until recently carbohydrates were in a completely different situation: scant automation existed, and users building models manually frequently tripped over legacy issues such as incorrect dictionaries or non-standard atom naming, which evidenced a historical lack of methodological support for carbohydrates (Agirre, 2017). Sugars are stereochemically complex and, as pyranose rings, have clear conformational preferences. And despite this, all refinement programs produced high-energy conformations at medium to low resolution, without any support from the electron density (Atanasova et al., 2020); this problem rendered the affected structures unusable in glyco-chemical terms. More recently, the AlphaFold revolution has delivered glycan-less but generally accurate structures of glycoproteins, once again enlarging the gap between protein and carbohydrates (Bagdonas et al., 2021). Bringing structural glycobiology up to 'protein standards' is requiring a total methodological overhaul. Time is of the essence, as the community is steadily increasing the production rate of glycoproteins, and electron cryo- microscopy is imaging them in the resolution range where crystallographic methods falter most. In this talk, I will introduce our latest methodological developments, which integrate prior knowledge from multiple techniques to streamline and automate hitherto error-prone processes (Bagdonas et al., 2020), helping structural biologists to produce correct atomic models with confidence.

References
- Potterton, L., Agirre, J., Ballard, C., Cowtan, K., Dodson, E., et al (2018). *Acta Crystallographica Section D: Structural Biology*, **74(2)**, 68-84.
- Agirre, J. (2017). *Acta Crystallographica Section D: Structural Biology*, **73(2)**, 171-186.
- Atanasova, M., Bagdonas, H., & Agirre, J. (2020). *Current opinion in structural biology*, **62**, 70-78.
- Bagdonas, H., Fogarty, C. A., Fadda, E., & Agirre, J. (2021). *Nature Structural & Molecular Biology*, **28(11)**, 869-870.
- Bagdonas, H., Ungar, D., & Agirre, J. (2020). *Beilstein Journal of Organic Chemistry*, **16(1)**, 2523-2533.

Back to Table of contents

MS10 Protein-carbohydrate interactions

MS10-02

Unveiling the substrate specificity of sulfatases, another important group of carbohydrate active enzymes

M. Dalgaard Mikkelsen [1], T. Barbeyron [2], E. Ficko-Blean [2], A. Naretto [2], R. Larocque [2], S. Genicot [2], T. Roret [3], M. Czjzek [2], A.S. Meyer [1], G. Michel [2]

[1]Protein Chemistry and Enzyme Technology Section, DTU Bioengineering, Department of Biotechnology and Biomedicine, Technical University of Denmark, 2800 Kgs Lyngby, Denmark - Kongens Lyngby (Denmark), [2]Sorbonne Université, CNRS, Integrative Biology of Marine Models, Station Biologique de Roscoff, 29680 Roscoff, France - Roscoff (France), [3]Sorbonne Université, CNRS, FR2424, Station Biologique de Roscoff, 29680 Roscoff, France - Roscoff (France)

Abstract

Sulfated glycans represent an essential part of polysaccharides present in marine environments and mammalian host. Bacterial carbohydrate sulfatases are enzymes that remove sulfate esters from sulfated glycans, and are essential for microbes to utilize sulfated glycans [1-2]. Interestingly, many genomes of marine but also of gut bacteria revealed that polysaccharide degraders contain a surprisingly high number of sulfatases [3-4], many of which have no associated function. Despite their importance, carbohydrate sulfatases are some of the most poorly characterized carbohydrate active enzymes to date. In the context of the explosion of genomic data, the functional annotation of sulfatases is thus particularly prone to flaws and misinterpretations. A recent sulfatase classification system allowing for a better prediction of clades or subfamilies [5], together with intense biochemical characterizations [2,4, 6,7] have shown that, likewise to other enzyme families of the CAZy database, sulfatase clades generally coincide with diversity in substrate specificity. Here we will briefly present the classification of sulfatases and will expose recent examples of sulfatase crystal structures, highlighting how substrate specificity is obtained by subtle sequence variations.

References

1. Tuncil, Y. E. et al. mBio 8, doi:10.1128/mBio.01068-17 (2017).
2. Cartmell, A. et al. PNAS 114, 7037-7042, doi:10.1073/pnas.1704367114 (2017).
3. Barbeyron, T., et al. Environ Microbiol. 18, 4610-4627, doi:10.1111/1462-2920.13584. (2016)
4. Luis, A. S. et al. Nature 598, 332-337, doi:10.1038/s41586-021-03967-5 (2021).
5. Barbeyron, T., et al. PLoS One. 11, e0164846. doi: 10.1371/journal.pone.0164846. (2016)
6. Hettle, A. G. et al. Structure 26, 747-758 e744, doi:10.1016/j.str.2018.03.012 (2018).
7. Mikkelsen, M.D., et al. Sci Rep. 11, 19523. doi: 10.1038/s41598-021-98588-3. (2021)

Active site of a marine fucan-sulfatase

Back to Table of contents

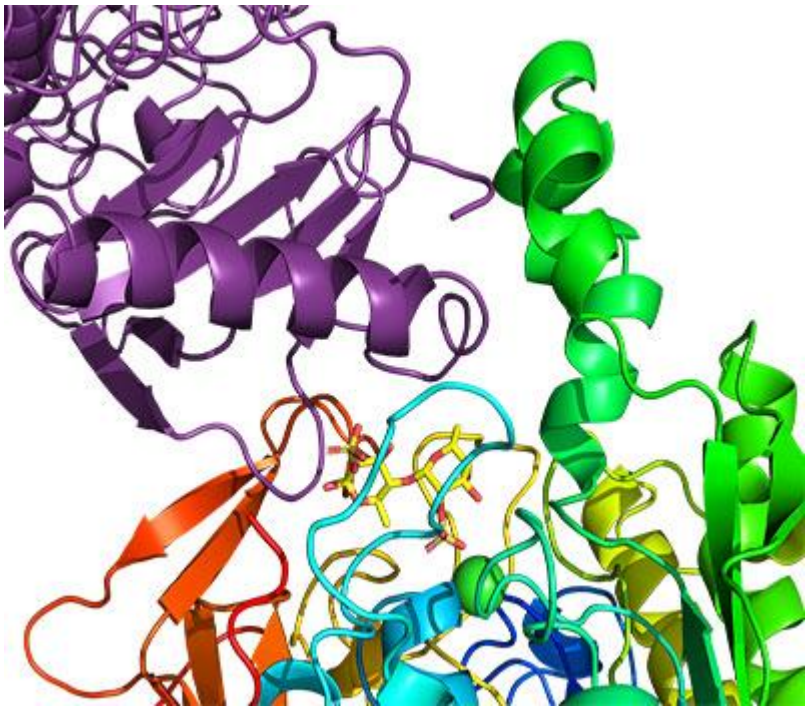

Back to Table of contents

MS10 Protein-carbohydrate interactions

MS10-03

Glycan-mediated activation of B cells in chronic lymphocytic leukaemia subsets

P. Cocomazzi [1], C. Minici [1], A. Iatrou [2], P. Maity [3], H. Jumaa [3], P. Ghia [4], K. Stamatopoulos [2], M. Degano [1]
[1]IRCCS Scientific Institute San Raffaele - Milano (Italy), [2]CERTH - Thessaloniki (Greece), [3]University of Ulm - Ulm (Germany), [4]Università Vita-Salute San Raffaele - Milano (Italy)

Abstract

Chronic lymphocytic leukaemia (CLL) is the most common form of adult blood cancer, characterized by the clonal expansion of neoplastic B cells that ultimately invade the circulation and secondary lymphoid organs. The importance of B-cell receptor (BCR)-mediated signalling is highlighted by several findings. CLL displays very heterogeneous clinical courses, ranging from indolent to highly aggressive, but patients expressing highly homologous BCRs can be grouped into subsets with homogenous clinico-biological characteristics [1]. Moreover, inhibition of specific kinases along of the BCR signalling cascade is effective, albeit resistance develops upon prolonged treatment of patients. The self-antigen(s) so far characterized that select the leukemic B-cells are quite heterogeneous, but a shared, unifying feature of CLL B-cells is their apparent ability to proliferate in absence of added exogenous antigens through a mechanism of cell-autonomous signalling [2]. Three CLL-derived BCRs have been previously shown to activate signalling through protein-protein homotypic interactions [3,4]. Here, we show that two BCRs from CLL subsets that differ in heavy and light chain usage bind via their combining sites to N-linked glycans of glycoproteins. Crystal structures demonstrated that in both cases the α-1-3 arm of hybrid or complex glycans is recognized via specific interactions with the CDR3 loops of both heavy and light chains of the BCR. However, the modes of interactions are distinct, thus showing that autoreactive BCRs directed towards a common, ubiquitous self-ligand can originate through different genetic rearrangements. The binding of glycans to the two BCRs activates intracellular signalling in a B lymphocyte model cell line, and thus pinpoints the molecular basis of the hallmark cell-autonomous signalling of CLL in these subsets. These findings suggest that a strategy based on antagonists of the glycan-BCR interaction may be highly effective in a personalized approach to CLL treatment.

References

[1] Stamatopoulos, K. et al. Over 20% of patients with chronic lymphocytic leukemia carry stereotyped receptors: Pathogenetic implications and clinical correlations. Blood 109, 259–270 (2007).
[2] Dühren-von Minden, M. et al. Chronic lymphocytic leukaemia is driven by antigen-independent cell-autonomous signalling. Nature 489, 309–312 (2012).
[3] Minici, C. et al. Distinct homotypic B-cell receptor interactions shape the outcome of chronic lymphocytic leukaemia. Nat. Commun. 8, 15746 (2017).
[4] Gemenetzi, K. et al. Higher-order immunoglobulin repertoire restriction in CLL: the illustrative case of stereotyped subsets 2 and 169. Blood 137, 1895-1904 (2021).

Glycan binding to a CLL-derived BCR

Back to Table of contents

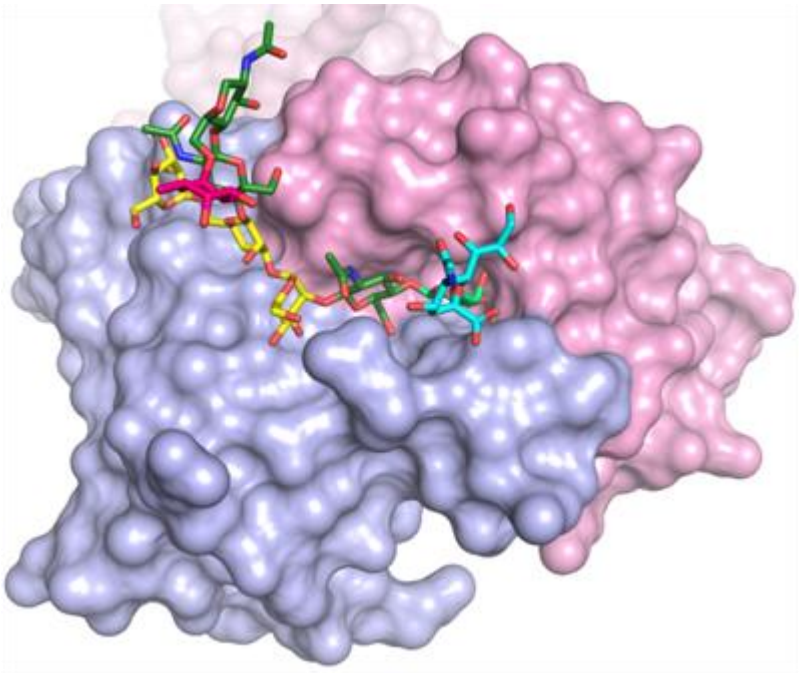

Back to Table of contents

MS10 Protein-carbohydrate interactions

MS10-04

Molecular recognition mechanism for the galactoside binding in a melibiose transporter MelB

L. Guan [1], P. Hariharan [1]
[1]*Texas Tech University Health Sciences Center - LUBBOCK* ***(United States)***

Abstract

The major facilitator superfamily (MFS) is one of the largest transporter families containing uniporters and secondary active transporters. *Salmonella typhimurium* melibiose transporter $MelB_{St}$ is a prototype of the Na^+-coupled MFS transporters, and it catalyzes stoichiometric transport of galactosides with Na^+, Li^+, or H^+. $MelB_{St}$ exhibits a loose sugar specificity with affinities for a wide range of galactosides of various modifications at the non-galactosyl moiety but with no affinity for glucose or glucosides. This sugar recognition mechanism was a long-unsolved puzzle till our crystal structures were resolved. We so far obtained seven structures of $MelB_{St}$ bound with different sugars or sugar analogs and deciphered the molecular recognition mechanism for the sugar binding. $MelB_{St}$ has a charged- and Trp residues-clustered narrow pocket to select for the specific galactosyl moiety and a large non-specific pocket to accommodate the chemically diverse non-galactosyl moieties. The cation-binding pocket is directly connected to the galactosyl-specific binding site, setting the structural basis for the coupled transport. These key structural findings have laid a solid foundation for understanding the cooperative binding and symport mechanisms in Na^+-coupled MFS transporters, including eukaryotic transporters such as MFSD2A.

References

Guan L, Hariharan P. X-ray crystallography reveals molecular recognition mechanism for sugar binding in a melibiose transporter MelB. Commun Biol. 2021;4(1):931. doi: 10.1038/s42003-021-02462-x.

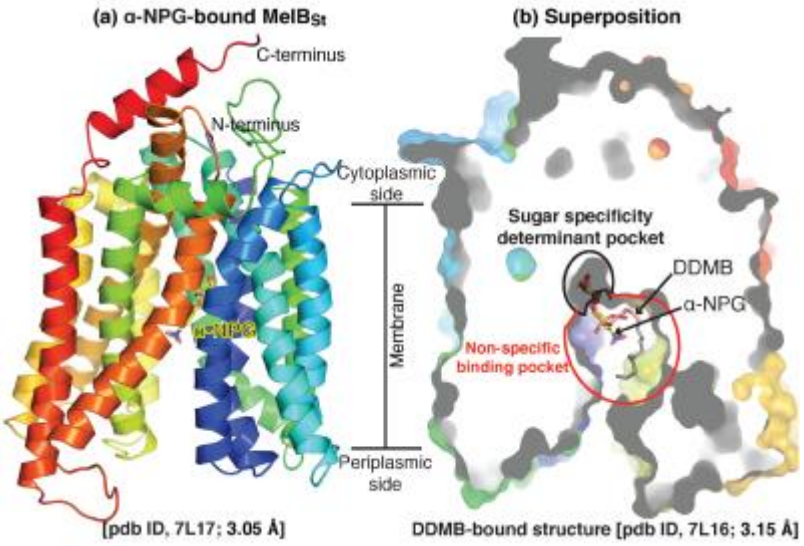

Back to Table of contents

MS10 Protein-carbohydrate interactions

MS10-05

Polyuronic acid degradation by polysaccharide lyase family 7

M. Vuillemin [1], J. Fernandez [2], L. Klau [3], B. Pilgaard [1], E. Kiehn [1], F. Meilleur [4], F. Fredslund [1], D. Welner [1], A. Meyer [1], J.P. Morth [1], C. Rovira [2], F. Aachmann [3], C. Wilkens [1]
*[1]Technical University of Denmark - Kongens Lyngby **(Denmark)**, [2]University of Barcelona - Barcelona **(Spain)**, [3]Norwegian University of Science and Technology - Trondheim **(Norway)**, [4]Oak Ridge National Laboratory - Oak Ridge **(United States)***

Abstract

Polysaccharide lyases (PLs) are in general efficient enzymes that generate short oligosaccharides not longer oligosaccharides that from an industrial perspective are far more promising. Unfortunately, the enzymatic mechanisms of PLs is not clearly understood preventing protein engineering leading to longer oligosaccharides. PLs are hypothesized to catalyze glycosidic linkage clevage *via* a 3-step β-elimination mechanism generating an unsaturated uronic acid residue and a new reducing end. First, the carboxylate group of an uronic acid moiety is neutralized by an amino acid residue or a Ca^{2+} ion, which will lower the pK_a of the C5 proton allowing its abstraction by the catalytic base in step 2. In the 3rd step, an amino acid or water acts as a catalytic acid and donates a proton to the glycosidic linkage. This cleaves the glycosidic bond and creates the unsaturated bond between C4 and C5. Further, PLs catalyze bond cleavage by *syn*- or *anti*-β-elimination. In *syn*, the C5-proton to be abstracted and protonation of the glycosidic oxygen at the new reducing end are on the same side of the sugar ring, while in *anti* on opposite sides. In theory, in the *syn* mechanism, the same residues can abstract the proton and donate it to the glyosidic bond, whereas in *anti* two catalytic groups are needed, however, this remains to be shown.
We have discovered PL7 members acting on β-glucuronan and alginate that are excellent model systems for studying PL7 mechanisms. Previously, it was suggested that a histidine acts as the general base and a tyrosine the general acid. We identified a β-glucuronan lyase with a k_{cat} of 3119 s^{-1} lacking the histidine. The high k_{cat} enabled a mutational analysis based on the crystal structure (1.45 Å) in which residual activity could be detected for all mutated residues except the tyrosine, which suggests this enzyme acts *via* a *syn* mechanism. Crystal structures (>0.82Å) of two alginate lyases in complex with alginate oligosaccharides – both Michaelis-Menten-like complex' and products after catalysis, were solved indicating the histidine's role is to distort the sugar moiety at subsite +1, which positions the scissile glyosidic linkage within reach of the tyrosine that can then act as both the general acid and base. A neutron crystal structure (2.33 Å) shows that the tyrosine is deprotonated, enabling it to abstract the proton. QM/MM is currently on-going to determine if the tyrosine can donate the proton to the glyosidic linkage.

PsAlg7A in complex with products

Back to Table of contents

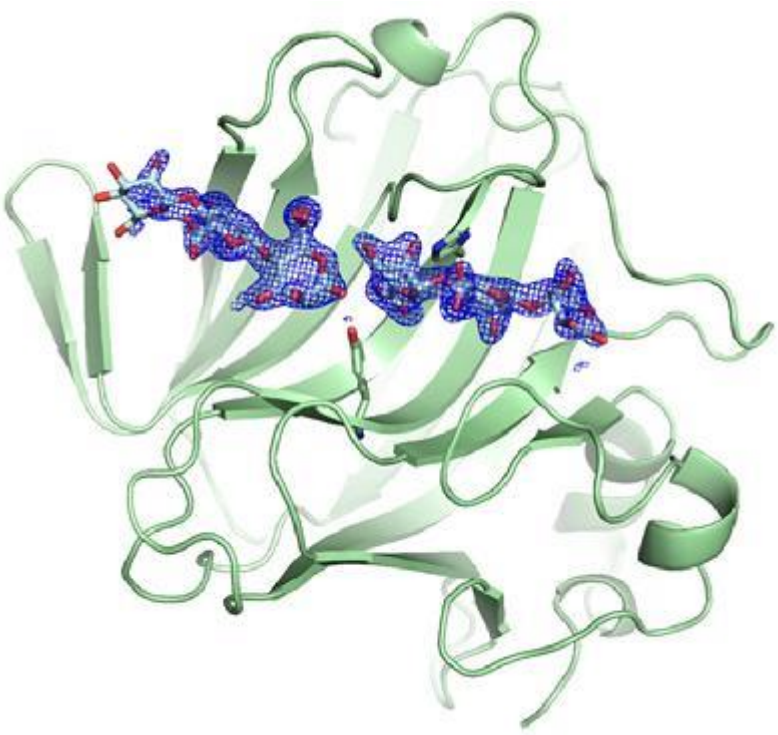

PsAlg7A Michaelis-Menten-like complex

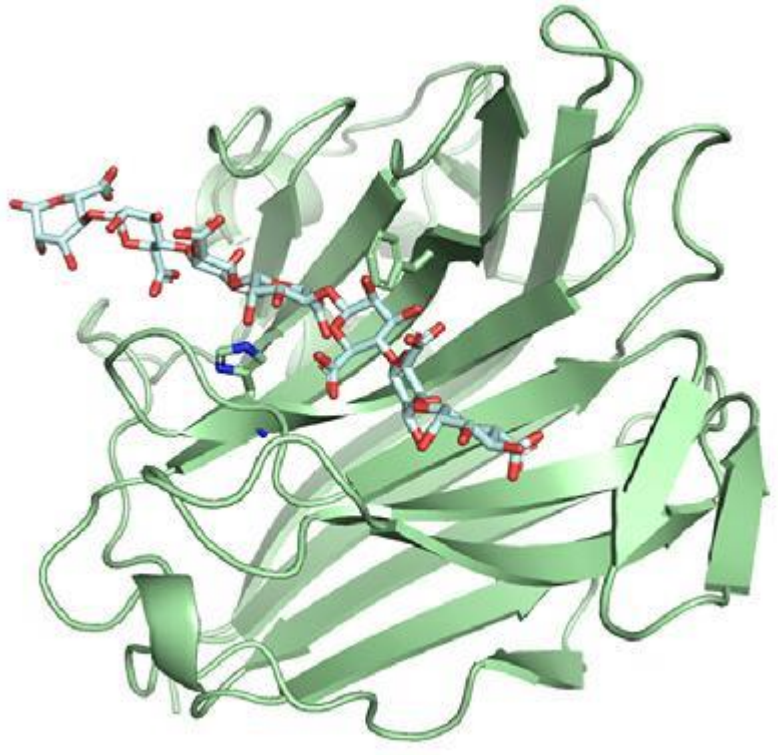

Back to Table of contents

MS11 Opportunities from combining structural biology and fold prediction

MS11-01

How predicted protein models help to illuminate the full protein universe

J. Pereira [1], J. Durairaj [1], L. Pantolini [1], G. Studer [1], X. Robin [1], A. Waterhouse [1], S. Bienert [1], G. Tauriello [1], T. Schwede [1]
[1]*Biozentrum and SIB Swiss Institute of Bioinformatics, University of Basel - Basel* ***(Switzerland)***

Abstract

Protein structural biology is going through a major revolution, with deep learning-based methods enabling the prediction of three-dimensional protein structures and complexes at an unprecedented level of accuracy. Together with the availability of large amounts of computational power, these methods facilitate the large-scale modelling of millions of proteins across the tree of life and thus complement the experimental structural information deposited in the Protein Data Bank. For example, there are currently about 1 million protein structure models in the AlphaFold database, and this number is expected to increase 150-fold by the summer of 2022 by including models for all proteins in UniRef90. This means that structural biologists will have structural models for virtually all catalogued proteins at their disposal.
But what does this mean exactly? Is experimental structural biology obsolete now, or is this a turning point and an accelerator for further developments? In this talk, I will discuss what the implications of such a structural coverage are and how large-scale protein structure prediction accelerates our understanding of natural proteins.

Back to Table of contents

MS11 Opportunities from combining structural biology and fold prediction

MS11-02

Deep learning based hallucination of de novo protein assemblies accross the nanoscale

A. Courbet [1]
[1]*Department of Biochemistry, University of Washington - Seattle (United States)*

Abstract

A. Courbet1,2,3†,B. I. M. Wicky1,2†, L. F. Milles1,2†, , R. J. Ragotte1,2, J. Dauparas1,2, E. Kinfu1,2, S. Tipps1,2, R. D. Kibler1,2, M. Baek1,2, F. DiMaio1,2, X. Li1,2, L. Carter1,2, A. Kang1,2, H. Nguyen1,2, A. K. Bera1,2, D. Baker1,2,3*
1 Department of Biochemistry, University of Washington, Seattle, WA, USA.
2 Institute for Protein Design, University of Washington, Seattle, WA, USA.
3 Howard Hughes Medical Institute, University of Washington, Seattle, WA, USA.
† These authors contributed equally to this work.

Deep learning generative approaches provide an opportunity to broadly explore protein structure space beyond the sequences and structures of natural proteins. In this work, we use deep network hallucination to generate a wide range of de novo symmetric protein homo-oligomers given only a specification of the number of protomers and the protomer length. Crystal structures of 7 designs are very close to the computational models (median RMSD: 0.6 Å), as are 3 cryoEM structures of giant ring like structures with up to 1550 residues, C42 symmetry, and 12 nanometer in diameter; all display complex folds and topologies that differ considerably from previously solved structures. Our results highlight the rich diversity of new protein structures that can be created using deep learning, and pave the way for the design of increasingly complex nanomachines and biomaterials.

Back to Table of contents

MS11 Opportunities from combining structural biology and fold prediction

MS11-03

A novel self-assembly mechanism for the S-layer in Lactobacillus acidophilus

T. Sagmeister [1], C. Buhlheller [1], N. Gubensaek [1], M. Eder [1], C. Grininger [1], L. Petrowitsch [1], A. Medina [2], C. Millán [2], I. Usón [2], Đ. Vejzović [1], E. Damisch [1], W. Keller [1], T. Pavkov-Keller [1]
[1]Institute of Molecular Biosciences, University of Graz, Austria - Graz (Austria), [2]Structural Biology, Crystallographic Methods group at IBMB-CSIC, Barcelona - Barcelona (Spain)

Abstract

The surface layer or S-layer represents the outermost cell envelope in many bacteria and archaea and is formed by individual (glyco)protein subunits. These surface layer proteins organize and self-assemble into highly regular two-dimensional crystalline arrays. In general, S-layer proteins have two functional regions, whereas one region is responsible for the attachment to the cell wall and another region responsible for the self-assembly of the S-layer array. Since the S-layer is in close contact with the environment these arrays fulfil various functions like bacterial adherence to other cells or receptors, protection against life-threatening conditions and maintenance of the cell shape. In *L. acidophilus*, a naturally occurring host of the human gut microbiome, the S-layer is relevant for the adherence to the gut epithelia cells and is associated with probiotic properties.
In this study we present the crystal structure of both major S-layer proteins, SlpA and SlpX, of *L. acidophilus* and SlpA of the close relative *L. amylovorus*. For crystallization, each of the three proteins were split into three functional regions, whereas the two N-terminal parts are responsible for the self-assembly. The crystal structures gave us insight and understanding of the mechanism of how the self-assembly occurs. In combination with AlphaFold Multimer predictions we propose a model for the fully assembled S-layer of SlpA from *L. acidophilus*. Our model suggests several possible interactions that are all important for the formation of the S-layer. The N-terminal region shows a very interesting mechanism of a flexible linker that interacts with the next molecule and the middle region of the protein is crucial for dimer formation, that is responsible for the P2 symmetry of the S-layer. Predictions of the S-layer of close relatives in the Lactobacillus genus support our proposed model. For future research we aim, that our unique model helps in the understanding of the interaction of *Lactobacillus* with the host.

Back to Table of contents

MS11 Opportunities from combining structural biology and fold prediction

MS11-04

PDB-wide model validation using deep learning-based predictions of distances and contacts

F. Sanchez Rodriguez [1], G. Chojnowski [2], R. Keegan [3], D. Rigden [1]
[1]Institute of Structural, Molecular and Integrative Biology, University of Liverpool - Liverpool (United Kingdom), [2]European Molecular Biology Laboratory, Hamburg Unit - Hamburg (Germany), [3]UKRI-STFC, Rutherford Appleton Laboratory, Research Complex at Harwell - Didcot (United Kingdom)

Abstract

Structural determination of proteins may be carried out using a range of different techniques, of which Macromolecular X-Ray Crystallography (MX) and cryogenic Electron Microscopy (cryoEM) are currently the two most popular. These experiments typically culminate into the creation of a model that satisfies the experimental observations collected for the structure of interest, which is later deposited in the Protein Data Bank (PDB) (Berman et al. 2000). However, experimental limitations can lead to unavoidable uncertainties during model building resulting in regions that require validation and potentially further refinement. Many metrics are available for model validation, but most are limited to the consideration of the physico-chemical aspects of the model or its match to the map.

Recent developments in the field of evolutionary covariance and machine learning have enabled the precise prediction of residue-residue contacts and increasingly accurate inter-residue distance predictions. Access to this accurate covariance information has played an essential role in the latest advances observed in the field of protein bioinformatics, particularly the improvement of prediction of protein folds by ab initio protein modelling, with the most notable examples being AlphaFold2 (Jumper et al. 2021) and RoseTTAFold (Baek et al. 2021).

Here we attempt to validate all PDB entries solved through cryoEM or MX at resolutions of 3.0-5.0Å, using a series of new methods for model validation based on the availability of accurate inter-residue distance predictions. These new methods include a support-vector machine classifier trained to compare the distance predictions obtained using AlphaFold2 with the distances observed in the protein model in order to detect possible modelling errors. Further analysis of possible sequence register errors is also done by performing an alignment of the predicted residue contact map and the map inferred from the contacts observed in the model. Regions of the deposited model where the maximum contact overlap is achieved through a sequence register different to that observed in the model are flagged and the optimal sequence register can then be used to fix the possible error.

Results obtained for this PDB-wide model validation suggest the presence of possible modelling and sequence register errors among the deposited models that have gone previously unnoticed and can be detected with these new methods.

References

Baek, Minkyung, Frank DiMaio, Ivan Anishchenko, Justas Dauparas, Sergey Ovchinnikov, Gyu Rie Lee, Jue Wang, et al. 2021. “Accurate Prediction of Protein Structures and Interactions Using a Three-Track Neural Network.” Science 373 (6557): 871–76.

Berman, Helen M., John Westbrook, Zukang Feng, Gary Gilliland, T. N. Bhat, Helge Weissig, Ilya N. Shindyalov, and Philip E. Bourne. 2000. “The Protein Data Bank.” Nucleic Acids Research 28 (1): 235–42.

Jumper, John, Richard Evans, Alexander Pritzel, Tim Green, Michael Figurnov, Olaf Ronneberger, Kathryn Tunyasuvunakool, et al. 2021. “Highly Accurate Protein Structure Prediction with AlphaFold.” Nature 596 (7873): 583–89.

Back to Table of contents

MS11 Opportunities from combining structural biology and fold prediction

MS11-05

AlphaFold-2 revolution for crystallographic software

E. Krissinel [1], R. Keegan [1], C. Ballard [1], A. Lebedev [1], V. Uski [1]
[1] *Science and Technology Facilities Council UK - Didcot (United Kingdom)*

Abstract

Understanding protein function through its structure is one of main motivations behind the structural biology research, which is closely related to the question of the relationship between sequence and structure. Over the past 40 years, significant progress has been made in this direction, both experimentally and in terms of computational methods for protein homology analysis. The Smith and Waterman algorithm, proposed in 1981 [1], laid the foundation for homology studies. By 2002, algorithms for secondary structure prediction have reached ~80% accuracy, giving more structural insight in sequence-based analysis [2]. Profile matching techniques (see, e.g., [3,4]) boosted the sensitivity of sequence matching so that structural homology could be detected deep in the twilight zone. Computation of protein folds from sequence was a very challenging task for a long time. It was largely solved by AlphaFold-2 and RoseTTAFold by 2021 [5,6].

Each of the above achievements has had a significant impact on structural biology research and computational methods for structure determination. In this context, the emergence of AlphaFold-2, which produces structures that are incredibly accurate by computational standards, is perceived as a revolution, since it solves the very problem of the sequence-structure relationship. While the full scope of this event is yet to be realised, we would like to discuss its impact from a narrower perspective of a large project in crystallographic software, the Collaborative Computational Project Number 4 (CCP4). The presentation will deliver on CCP4's response to the emergence of AlphaFold-2 as a powerful instrument for homology modelling; overview the new tools included in CCP4 Software Suite, its online services and CCP4 Cloud; discuss changes in approaches to computational structure determination; and outline possible directions for further development. What will be the role of methods developed in pre-AlphaFold era, and do we expect a leap toward full automation of structure determination?

References

[1] Smith, T.F. & Waterman, M.S. (1981) J. Mol. Biol. 147(1) 195-197.
[2] Aloy, P., Stark, A., Hadley, C. & Russell, R.B. (2003) Proteins: Struct. Funct. Bioinf. 53(S6) 436-456.
[3] Yona, G. & Levitt, M. (2002) J. Mol. Biol. 315(5) 1257-1275.
[4] Söding, J. (2005) Bioinformatics 21, 951-960.
[5] Jumper, J., Evans, R., Pritzel, A. et al. (2021) Nature 596, 583–589.
[6] Baek, M., DiMaio, F., Anishchenko, I. et al. (2021) Science 373(6557) 871-876.

Back to Table of contents

MS13 Structural Characterization of Functional Materials

MS13.1-01

Crystal structure, characterization and physical properties of lead-free organic-inorganic hybrid perovskites

S. Abdel-Aal [1], A. Abdel-Rahman [1], N. Claiser [2], M. Souhassou [2], J. Martorell [3], C. Lecomte [2]
*[1]Cairo university **(Egypt)**, [2]Lorraine university **(France)**, [3]ICFO **(Spain)***

Abstract

Organic- inorganic hybrid perovskites gain considerable attention recently and more studies have been done as changing the halide, metal ion or /and the ligand enables to tune the optical, electric, magnetic, ferroelectric and multiferroic properties. Halide perovskites in particular lead halides are interesting semiconductors with a direct band gap (1.5 eV) which enables collecting visible photons. These luminescent crystals have no future for safety and ecological reasons. Diammonium halide perovskite hybrids [NH3(CH2)nNH3]MClxBr4-x ; x= 0, 2, 4; M= Co, Mn; n= 4-9 allow mixing of organic and inorganic components in one molecule which possesses a property that may not exist in either of the parent components. The complete structure information as well as lattice parameters for Co series n= 4-9 are provided, and for n = 3-6 for Mn hybrid. Differential thermal analysis DSC shows reversible order - disorder transition for both the Co and Mn hybrids. Permittivity studies confirm the phase transition. The optical properties of Co series show strong absorption in the visible range, the band gap (1.73 eV) which is promising for photovoltaic applications.

References

1-Seham K. Abdel-Aal, A. Ouasri,."Crystal structure, Hirshfeld surfaces and vibrational studies of tetrachlorocobaltate hybrid perovskite salts NH3(CH2)nNH3CoCl4 (n = 4, 9)" Journal of Molecular Structure , 2022, 1251, 131997

2-Seham. K. Abdel-Aal, A. S. Abdel-Rahman, G. Bortel, Á. Pekker, K. Kamarás, G. Faigel, "Structure investigation and vibrational spectroscopy of two prospective hybrid perovskites based on Mn and Co" Journal of Physics and Chemistry of Solids, 2022, 161, 110400

3-Seham K. Abdel-Aal, Moh. F.Kandeel, Ashraf F. El-Sherif, Ahmed S. bdel- Rahman, Synthesis, Characterization and optical properties of new Organic-Inorganic Hybrid Perovskites [(NH3)2(CH2)3]CuCl4 and [(NH3)2(CH2)4]CuCl2Br2, 218 (12) 2021 Physica Status Solidi (A)

4-Seham K. Abdel-Aal, et al, Crystal Structure, Vibrational Spectroscopy, and Optical Properties of 1D - Organic-Inorganic Hybrid Perovskite of [NH3CH2CH(NH3)CH2]BiCl5, Acta Cryst. B75, (2019)

5- Seham K. Abdel-Aal, Ahmed S. Abdel-Rahman, "Fascinating Physical Properties of 2D Hybrid Perovskite [(NH3)(CH2)7(NH3)]CuClxBr4_x, x = 0, 2 and 4" Journal of electronic materials, 48(3) (2019) 1686-1693,

6-Mohga Farid Mostafa, Shimaa Said El-khiyami, Seham K. Abdel-Aal, Structure, thermal, and impedance study of a new organic–inorganic hybrid [(CH2)7(NH3)2]CoCl4, Journal of Physics and Chemistry of Solids, (2018), (DOI: 10.1016/j.jpcs.2018.02.048

7-Seham K. Abdel-Aal, Ahmed S. Abdel-Rahman, Gudrun Kocher-Oberlehner, Andrey Ionov, R.N. Mozhchil, "Structure, optical studies of two-dimensional hybrid perovskite for photovoltaic applications" Acta Cryst, A73, (2017), C1116.

8-Seham K. Abdel-Aal, Ahmed S. Abdel-Rahman, "Synthesis, structure, lattice energy and enthalpy of 2D perovskite hybrid [NH3(CH2)4NH3]CoCl4, compared to [NH3(CH2)nNH3]CoCl4, n = 3 - 9, J. Cryst. Growth. 457 (2017) P 282-288.

9-Mohga Farid Mostafa, Shimaa Said El-khiyami, Seham Kamal Abdel-Aal, Crystal structure, phase transition and conductivity study of two new organic-inorganic hybrids: [(CH2)7(NH3)2]X2, X = Cl/Br, Journal of Molecular Structure 1127 (2017) P 59-73.

Back to Table of contents

MS13 Structural Characterization of Functional Materials

MS13.1-02

The cation-dependent structural, optical, and magnetic properties of molecular hypophosphite perovskites

A. Gagor [1], M. Mączka [1], D. Stefańska [1], A. Pikul [1]
[1] *Institute of Low Temperature and Structure Research, Polish Academy of Sciences - Wrocław* ***(Poland)***

Abstract

Organic-inorganic hybrids that crystallize in a perovskite architecture of a general formula ABX_3 are perspective multifunctional materials showing ferroelectric, multiferroic photovoltaic, photoluminescent (PL), and barocaloric properties [1]. The crystal structure of these compounds is built of B-metal centers (usually Pb^{2+}, Sn^{2+}, Mn^{2+}, Cd^{2+}, Zn^{2+} etc.) coordinated octahedrally by X-molecular units (halide, formate, azide, cyanate, dicyanamide, or hypophosphite ions $H_2PO_2^-$) which also act as bridging-ligands. Organic A-site molecular cations, which in contrast to inorganic perovskites have a non-spherical shape and often possess a dipole moment, occupy the large voids and interact via hydrogen bonds with the metal-ligand framework having the potential to strongly modify it [2].

The multiatomic, extended X-site ligands, like hypophosphite ions, produce unconventional octahedral tilts, columnar shifts, and unprecedented off-center shifts of organic cations that are absent in inorganic perovskites. This high tendency for symmetry breaking was expected to favor improper ferroelectricity or other functional properties but, starting from 2017 when the first hypophosphite perovskite was reported up to now, all reported hypophosphite perovskites had centrosymmetric structures.

Herein we report the crystal structures, magnetic and photoluminescent properties of new hypophosphites based on imidazolium, pyrrolidinium, and guanidinium. We show that replacing Mn^{2+} with Cd^{2+} and Co^{2+} tunes the physical properties. The Co-based analogs are weak ferromagnets with a stronger ferromagnetic response and higher ordering temperatures compared to manganese counterparts. The Cd analogs have broadband emission correlated with distortion of the cadmium-hypophosphite framework. The most interesting discovery in this family, however, is the polar symmetry of pyrrolidinium-based cadmium hypophosphite. The non-centrosymmetric structure hasn't been reported for any known hybrid hypophosphite. The new hypophosphites exhibiting magnetic or polar order, and photoluminescent properties show that hypophosphite perovskites are a promising platform for the creation of new functional materials, including light-emitting, ferroelectric, and multiferroic.

This research was supported by the National Science Centre (Narodowe Centrum Nauki) in Poland under project no. 2018/31/B/ST5/00455

References

[1] B. Saparov and D. B. Mitzi; Organic-Inorganic Perovskites: Structural Versatility for Functional Materials Design, Chem. Rev., 2016, 116 , 4558 —4596;
[2] Boström, Hanna L. B.; Senn, Mark S.; Goodwin, Andrew; L. 2018; Recipes for improper ferroelectricity in molecular perovskites, Nature Communications, 2380, 9, 1

Back to Table of contents

MS13 Structural Characterization of Functional Materials

MS13.1-03
Structural Chemistry of ABX3 Molecular Perovskites
G. Kieslich [1]
[1]*Technical University of Munich - Munich* ***(Germany)***

Abstract
A recent research direction related to ABX_3 perovskites is the use of molecules on the A and/or X-site, a development that has proved fruitful for photovoltaics, (improper) ferroelectrics and barocalorics. Replacing atoms by molecules increases the chemical space for the synthesis of materials with new properties, conceptually translating chemical, synthetic freedom to novel opportunities in material design. In my presentation I will discuss how the use of molecular building units in molecular materials introduces new structural degrees of freedom of rotational, translational, and conformational nature that can be exploited for material design. I will discuss how understanding and controlling these structural degrees of freedom is key for efficiently harnessing their chemical diversity by drawing on my group's recent research results such as the discovery of a new type of polymorphism in ABX_3 molecular perovskites, the application of information theory to calculate the complexity of (molecular) perovskites, and how to integrate new geometric degrees of freedom through the use of divalent A^{2+} cations.

References
[1] S. Burger, S. Grover, K. T. Butler, H. L. B. Boström, R. Grau-Crespo, G. Kieslich. Tilt and Shift Polymorphism in Molecular Perovskites. *Mater. Horiz*. **2021**, 8, 2444.
[2] S. A. Hallweger, C. Kaußler. The structural complexity of perovskites. *Phys. Chem. Chem. Phys*. **2022**, 24, 9196.
[3] S. Burger, K. Hemmer, D. C. Mayer, D. Daisenberger, J. K. zareba, G. Kieslich. Designing Geometric Degrees of Freedom in ReO3-type coordination polymers. **2022**, *ChemRxiv*: 10.26434/chemrxiv-2022-mkcw8.

Back to Table of contents

MS13 Structural Characterization of Functional Materials

MS13.1-04

Dynamic, adaptive and self-healing crystals

P. Naumov [1]
[1]*New York University Abu Dhabi - Abu Dhabi* ***(United Arab Emirates)***

Abstract

The anticipated shift in focal point of interest of solid-state chemists, crystal engineers and crystallographers from structure to properties to function of organic solids parallels the need to apply our accumulated understanding of the intricacies of crystal structure to explaining the related properties, with the ultimate goal of harnessing that knowledge in applications that require soft, light-weight, and/or biocompatible organic solids.[1] In these developments, the adaptive molecular single crystals warrant a particular attention as an alternative choice of materials for light, flexible, and environmentally benign devices, primarily memories, capacitors, sensors, and actuators. Some of the outstanding requirements for application of these dynamic materials as high-efficiency energy storage devices are strongly induced polarization, high switching field, and narrow hysteresis in case of reversible dynamic processes. However, having been studied almost exclusively by chemists, molecular crystals still lack the appropriate investigations that reliably evaluate their reproducibility, scalability, and actuating performance, and some important drawbacks have diverted the interest of engineers from these materials in applications. United under the umbrella term crystal adaptronics, the recent research efforts aim to realistically assess the appositeness of dynamic crystals for applications that require fast, reversible and continuous operation over prolonged periods of time. With the aim to highlight the most recent developments in the research of adaptive molecular crystals, this Perspective article discusses their assets and pitfalls. It also provides some hints on the likely future developments that capitalize on the untapped, sequestered potential for applications of this distinct materials class.

References

[1] P. Naumov, D. P. Karothu, E. Ahmed, L. Catalano, P. Commins, J. Mahmoud Halabi, M. B. Al-Handawi, L. Li, The Rise of the Dynamic Crystals (perspective article), J. Am. Chem. Soc. 142 (2020) 13256.

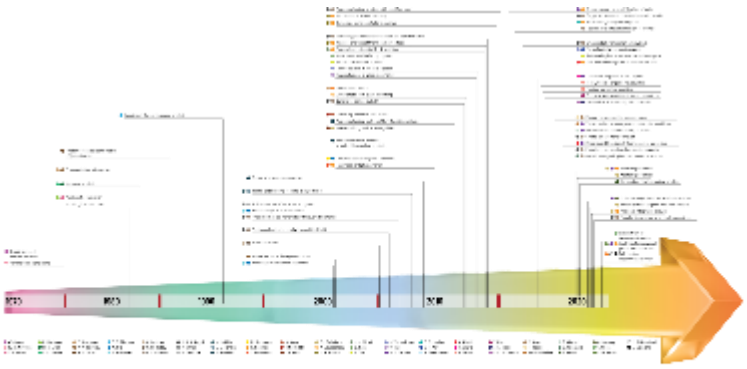

Back to Table of contents

MS13 Structural Characterization of Functional Materials

MS13.1-05

Pressure induced phase transition in the ferroelectric hybrid perovskite (C6H11NH3)2[PbBr4]

S. Pillet [1], M. Deutsch [1], A. Yangui [2], O. Pages [3], M. Baker Shoker [3], G. Bouchez [4], K. Boukheddaden [4]
[1]CRM2 - Vandoeuvre les Nancy (France), [2]Chalmers University of Technology - Gothenburg (Sweden), [3]LCPA2MC - Metz (France), [4]GEMAC - Versailles (France)

Abstract

Organic-inorganic hybrid perovskites have recently emerged as highly efficient optoelectronic materials, and are being intensively investigated and developed for high performance photovoltaics, photodetections, light-emitting diodes and laser devices. Applying external pressure on hybrid perovskite materials can be used as a clean physical way to modify continuously the underlying crystal structure and consequently tune the resulting physical properties (band gap, light emission), or even generate new properties that could not be obtained at ambient conditions. Crystallographic investigations on single crystal, as a function of applied hydrostatic pressure, is in this case required to explore structure-properties relationships, and provide a clear understanding of the underlying mechanisms at the atomic level.

(C6H11NH3)2[PbBr4] is a hybrid perovskite exhibiting a 2D structural architecture with semi-conducting inorganic layers of corner-sharing PbBr6 octahedra separated by bilayers of C6H11NH3+ cations. (C6H11NH3)2[PbBr4] presents intense white light emission and ferroelectricity, characterized by a para-electric to ferro-electric transition at 360K. We have discovered that this compound undergoes a pressure induced structural phase transition, revealed by combined crystallographic and Raman studies conducted on single crystal under pressure in a diamond anvil cell. The phase transition is driven by a disorder to order phase transition of the organic framework, and proceeds without any space group change. The evolution of the unit cell parameters evidences a strongly anisotropic compressibility, in line with the low dimensionality of the structural architecture. Interestingly, the structural results indicate a stabilization of the ferroelectric phase under pressure, which opens interesting perspectives for improved performances in photovoltaics or light emitting devices.

The complete properties, including structural and vibrational ones, as a function of applied pressure will be discussed, and put in a broad perspective.

References

A. Yangui, D. Garrot, J. S. Lauret, A. Lusson, G. Bouchez, E. Deleporte, S. Pillet, E. E. Bendeif, M. Castro, S. Triki, Y. Abid, and K. Boukheddaden, J. Phys. Chem. C, (2015), 119, 23638−23647.
M. Szafranski, and A. Katrusiak, J. Phys. Chem. Lett, (2017), 8, 2496-2506.

Back to Table of contents

MS13 Structural Characterization of Functional Materials

MS13.1-06

A walk through the valley of weak interactions and diverse mechanical responses of crystals

M. Pisacic [1], L. Balen [1], M. Djakovic [1]
[1]*University of Zagreb, Faculty of Science - Zagreb* ***(Croatia)***

Abstract

The amazing ability of crystalline matter to adapt to external stimuli while consequently achieving outstanding mechanical movements, such as bending, jumping, crawling, or exploding, has enabled the evolution of a new direction in advanced materials design and development. [1] However, with a growing number of literature reports describing dynamic crystalline compounds, it becomes clear that the structural background behind these materials is not straightforward, and to get to the point where mechanically responsive crystalline solids become the material of choice, a thorough structure-property correlation must be delivered.

One-dimensional crystalline cadmium(II) coordination polymers emerged as a perfect model system to investigate structure-property interconnection, as they displayed an unexpected diversity of mechanically induced responses – a wide spectrum from purely elastic bending motions to variable plasticity. [2–5] These motions were found to be dependent not only on the crystals' composition but also on the direction of the force application, therefore making a clear distinction between 1D and 2D bendable crystals. Recently, it was observed that the latter could additionally be divided into two subcategories, 2D-isotropically and 2D-anisotropically flexible. Upon investigation of this intricate spindle of crystal flexibility and structural characteristics, intermolecular interactions were found to be one of the key factors which guide the behavior of the crystal towards the desired mechanical output. [5]

To investigate the influence of the weak intermolecular interactions on the mechanically induced crystal adaptability more closely, we opted for another family of crystalline Cd(II) coordination polymers equipped with methyl derivatives of pyridine or pyrazine. By introducing slight structural changes around the cadmium(II) metal center, via exchanging bridging anion or inducing small changes in heterocyclic ligand, we were able to alter the crystals' morphology, the dimensionality of resulting polymers, crystal packing arrangement, the strength of the intermolecular interactions, and consequently the crystals' mechanical response. While with pyridine-based ligands we isolated 1D coordination polymers whose crystals displayed a variety of elastic mechanical responses, crystalline compounds with pyrazine-based ligands formed 2D polymeric networks and displayed primarily plastic flexibility upon the applied stress. Furthermore, a detailed inspection of mechanical and structural properties using a variety of advanced and custom-designed experimental methods provided us with a deeper insight into the origin and a mechanism of mechanically induced bendability, thereby allowing us to get one step closer to unraveling the puzzle of an extraordinary world of flexible crystals.

References

[1] P. Naumov, S. Chizhik, M. K. Panda, N. K. Nath, E. Boldyreva, *Chem. Rev.* **115** (2015) 12440–12490.
[2] M. Đaković, M. Borovina, M. Pisačić, C.B. Aakeröy, Ž. Soldin, B.-M. Kukovec, I. Kodrin, *Angew. Chem. Int. Ed.* **57** (2018) 14801–14805.
[3] M. Pisačić, I. Biljan, I. Kodrin, N. Popov, Ž. Soldin, M. Đaković, *Chem.Mater.* **33** (2021) 3660–3668.
[4] M. Pisačić, I. Kodrin, I. Biljan, M. Đaković, *CrystEngComm* **23** (2021) 7072–7080.
[5] M. Pisačić, I. Kodrin, A. Trninić, M. Đaković, *Chem.Mater*. **34** (2022) 2439–2448.

Acknowledgements
This work has been fully supported by the Croatian Science Foundation under project "From form to function: Mechanically flexible crystalline materials with controllable responses" (IP-2019-04-1242).

Back to Table of contents

MS13 Structural Characterization of Functional Materials

MS13.2-01

Ultra-Fast Rotor Dynamics and Gas Reorientation in Crystalline Nanoporous Architectures

S. Bracco [1], C.X. Bezuidenhout [1], J. Perego [1], S. Piva [1], A. Daolio [1], A. Comotti [1], P. Sozzani [1]
[1]*Università di Milano-Bicocca - Milano* ***(Italy)***

Abstract

Crystalline nanoporous architectures offer stimulating opportunities in designing rotors and motors in the solid state and exploring sorptive properties and gas transport.
Molecular rotors in the solid state have been successfully engineered in porous materials, such as Metal Organic Frameworks (MOFs), thanks to their large free volume, which allows for fast dynamics. In particular, a ultra-fast molecular rotor, whose rotation speed approaches that of unhindered rotations in organic moieties even at very low temperatures, has been realized.(1) The rotor based on bicyclo[1.1.1]pentane–dicarboxylate (BCP) moiety was installed in the 3D cubic structure of a highly porous Zn-MOF, thus isolating the individual rotor from each another (Fig. 1a, b). Solid state NMR relaxation measurements ^{1}H T_1 and muon-spin spectroscopy(2) performed at temperatures as low as 2 K allowed the determination of an activation energy as low as 6.2 cal mol^{-1}, consistent with fast molecular reorientation in the GHz regime even at the lowest temperatures. Furthermore, pillared-MOFs built from two distinct ultrafast and interacting molecular rotors form a multidynamical architecture wherein the rotors experience sequential motional behaviour activated at distinct temperatures. The manipulation by chemical stimuli, such as CO2, which diffused from the gas phase into the porous matrix, resulted in the selective control over rotary dynamics.(3)
CO_2 diffusion in a porous crystalline material, in which the channels are decorated by double helices of electrostatic charges, has been described by solid state NMR. The remarkable CO_2-matrix association allowed direct observation of the gas exploring the nanochannels and the identification of the specific interaction sites by 2D ^{1}H-^{13}C HETCOR MAS NMR experiments (Fig. 2), providing peculiar details about the role of electrostatic interactions in gas transport phenomena. The sorption performances and the extraordinary thermal stability up to 450 °C highlighted the perspective of applying these materials for selective removal of CO_2 from other gases.(4)

References

1) J. Perego, S. Bracco, M. Negroni, C. X. Bezuidenhout, G. Prando, P. Carretta, A. Comotti, and P. Sozzani, Nat. Chem. 2020, 12, 845.
2) G. Prando, J. Perego, M. Negroni, M. Riccò, S. Bracco, A. Comotti, P. Sozzani, P. Carretta, Nano Lett. 2020, 20, 7613.
3) J. Perego, C. Bezuidenhout, S. Bracco, G. Prando, L. Marchio', M. Negroni, P. Carretta, P. Sozzani, A. Comotti J. Am. Chem. Soc. 2021, 143, 13082.
4) G. Xing, I. Bassanetti, S. Bracco, M. Negroni, C. Bezuidenhout, T. Ben, P. Sozzani, A. Comotti, Chemical Science 2019, 10, 730.

Molecular rotors in the cubic structure of Zn-MOF

Back to Table of contents

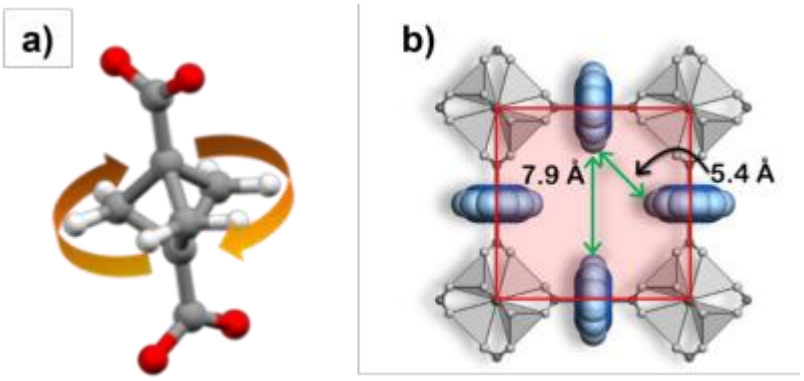

Detection of CO2 in porous crystals by ss-NMR

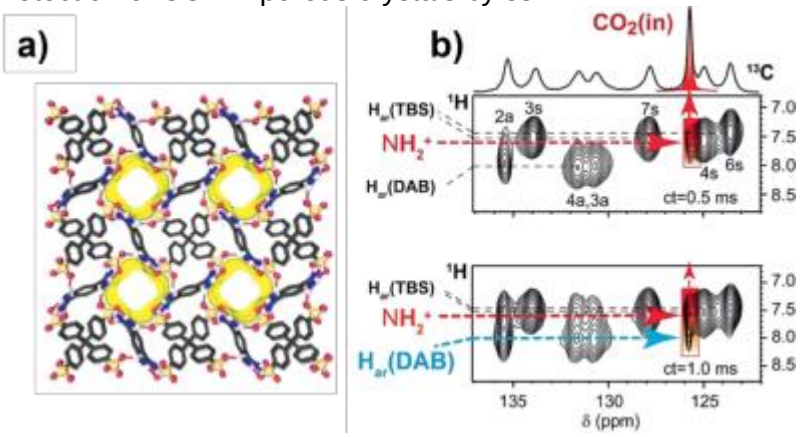

Back to Table of contents

MS13 Structural Characterization of Functional Materials

MS13.2-02

Insights into battery materials by electron microscopy

K. Volz [1]
[1]*Philipps-University Marburg - Marburg* ***(Germany)***

Abstract

Scanning transmission electron microscopy (STEM), especially when aberration-correction is used, can be applied to investigate all kind of functional materials at an atomic level. When compared to image simulations, the information on the sample structure and composition can be quantitative. Combining STEM with a fast, pixelated detector allows for the acquisition of a full diffraction pattern at each scan point. From this, four-dimensional STEM (4D-STEM) datasets are available, which can be used to generate different data, e.g. annular dark field (ADF) as well as (annular) bright field ((A)BF) images, angular resolved STEM (ARSTEM) or differential phase contrast (DPC) data.
We use a double aberration corrected JEOL 2200FS, equipped with an in-column energy filter and a pnCCD detector to acquire 4D-STEM data sets.
With the example of cathode materials for battery applications (e.g. LiNi0.85Co0.10Mn0.05O2), we track the formation of different phases of and defects within the oxide in dependence on cycling conditions of the material and derive ABF as well as BF images from 4D datasets. These are used to also obtain difference images (ABF-BF). It will be shown that the composition of the materials and especially the Lithium content can be derived from the contrast of the different atomic columns in the structure, which has a characteristic specimen thickness dependence for the different data sets. This is possible by comparing the experimental data sets to state of the art multi-slice simulations.
Moreover, we will investigate the co-sintering of the cathode material with several solid electrolytes as well as the influence of electrochemical cycling on (nano)structure of the battery materials.

This contribution will hence summarize the material science aspects of the energy materials investigated but also elucidate the potential of quantitative 4D-STEM to investigate materials.

References

Acknowledgement: We gratefully acknowledge support of the German Research Foundation (DFG) in the framework of the SFB 1083 “Structure and Dynamics of Internal Interfaces” as well as support of the BMBF in the framework of the FestBatt consortium.

Back to Table of contents

MS13 Structural Characterization of Functional Materials

MS13.2-03

Structural determination of a photoemissive chiral 3D silver(I)-benzenedithiolate coordination polymer

S. Hawila [1], A. Abdallah [1], J.L. Rukemampunzi [1], N. Guillou [2], A. Mesbah [1], A. Fateeva [3], G. Ledoux [4], S. Pailhès [4], R. Debord [4], F. Massuyeau [5], R. Gautier [5], A. Demessence [1]

*[1]IRCELYON, UMR CNRS 5256, Université Lyon 1 - Villeurbanne **(France)**, [2]ILV, UMR CNRS 8180, UVSQ, Université Paris-Saclay - Versailles **(France)**, [3]LMI, UMR CNRS 5615, Université Lyon 1 - Villeurbanne **(France)**, [4]IML, UMR CNRS 5306, Université Lyon 1 - Villeurbanne **(France)**, [5]IMN, UMR CNRS 6502, Université de Nantes - Nantes **(France)***

Abstract

These last few years, Metal Organic Chalcogenolate (MOC) coordination polymers (CPs) have received increasing interest due to the formation of new materials with interesting electrical transport and photoluminescence properties [1]. 1D and 2D MOCs, showing great photoluminescence properties in the solid state, have been synthesized from numerous functionalized monothiolate ligands [2, 3]. This study has recently been extended to copper and silver networks obtained with a multithiolate ligand, the benzenehexathiolate (BHT). These MOCs exhibit up to now the highest room temperature conductivity among the CPs and Metal-Organic Frameworks (MOFs), with 250 $S.cm^{-1}$ for the 3D $[Ag_5(BHT)]_n$ compound and 1580 $S.cm^{-1}$ for the 2D $[Cu_3(BHT)]_n$ one [4, 5]. In order to control their band gap to either get photoluminescent or conducting materials, there is a tremendous need to understand their structure-properties relationships and therefore to develop new d^{10} coinage MOCs with other thiolate ligands. In this context, the first d^{10} coinage MOC based on silver and a ditopic thiolate linker, the 1,3-benzenedithiolate (1,3-BDT) ligand, $[Ag_2(1,3\text{-BDT})]_n$ has been obtained. Its structure was solved *ab initio* from powder X-ray diffraction (PXRD) collected at the CRISTAL beamline of the SOLEIL synchrotron facility (Gif-Sur-Yvette, France). The final Rietveld plot shows the perfect agreement between the calculated data obtained from the structural model and the observed ones (Fig. 1). $[Ag_2(1,3\text{-BDT})]_n$ crystallizes in the cubic chiral $P2_13$ space group with a = 12.88562(3) Å, V = 2139.52(1) $Å^3$ and Z = 12. The asymmetric unit contains four independent silver atoms with one in general position, and the three others on the threefold axes, as well as one 1,3-BDT ligand ($C_6H_4S_2$) in general position. Each silver atom is coordinated to three sulphur atoms to form a near planar triangular geometry, and each sulphur atom is also coordinated to three silver atoms. The 3D framework can be described from a sulphur network constructed from two independent empty octahedra, Ag_4S_6 and Ag_2S_6 (Fig. 2, in dark and light blue, respectively), centred on the threefold axes and connected through sharing edges to generate eight membered ring channels filled by the organic moiety of the bridging 1,3-BDT ligands. In situ PXRD have shown that $[Ag_2(1,3\text{-BDT})]_n$ is stable up to 400°C under air. Although, this new MOC behaves as an insulator, it exhibits low temperature solid state photoemission and a Second Harmonic Generation (SHG) response.

References

[1] Y. Kamakura & D. Tanaka, Chem. Lett., 2021, 50, 523.
[2] O. Veselska & A. Demessence, Coord. Chem. Rev., 2018, 355, 240.
[3] Q. Wang, S.-L. Dong, D.-D. Tao, Z. Li & Y.-B. Jiang, Coord. Chem. Rev., 2021, 432, 213717.
[4] X. Huang, H. Li, Z. Tu, L. Liu, X. Wu, J. Chen; Y. Liang, Y. Zou, Y. Yi, J. Sun, W. Xu & D. Zhu, J. Am. Chem. Soc., 2018, 140, 15153.
[5] Q. Wang, S.-L. Dong, D.-D. Tao, Z. Li & Y.-B. Jiang, Coord. Chem. Rev., 2021, 432, 213717.

Fig.1: Final Rietveld plot of [Ag2(1,3-BDT)]n

Back to Table of contents

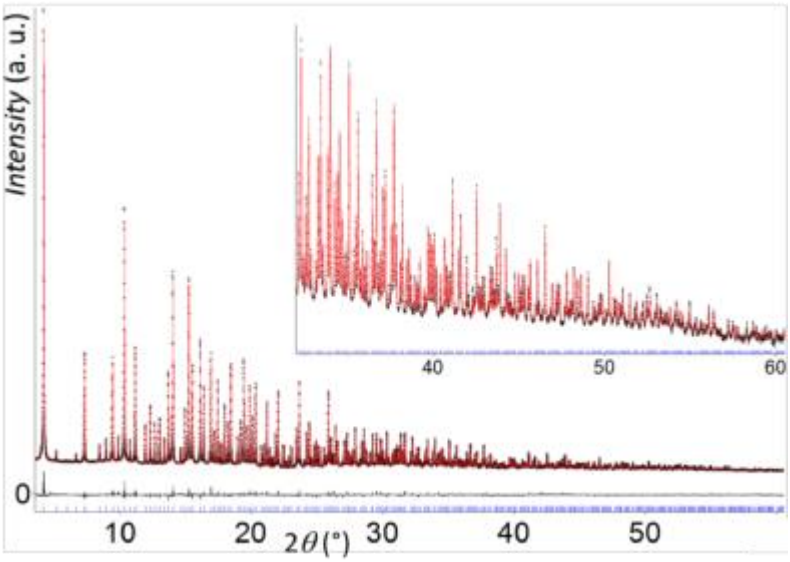

Fig. 2: Structure of [Ag2(1,3-BDT)]n

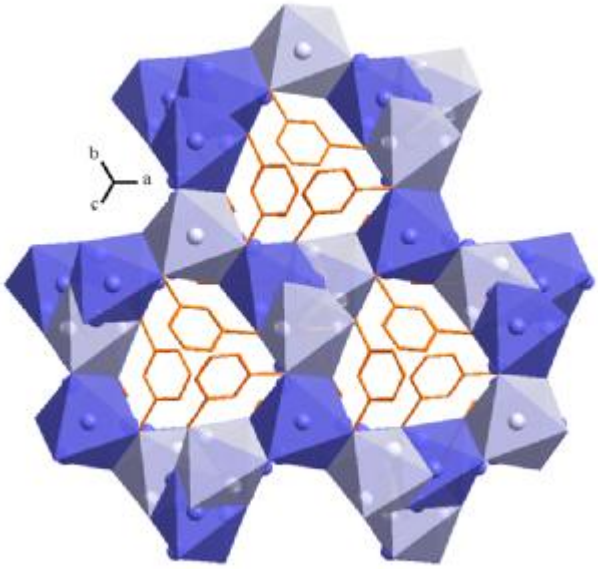

Back to Table of contents

MS13 Structural Characterization of Functional Materials

MS13.2-04

TTF-based Hydrogen-bonded Organic Frameworks: porous conducting crystalline materials

G. Mínguez Espallargas [1], M. Vicent-Morales [1], M. Esteve-Rochina [1], J. Calbo [1], E. Ortí [1], I.J. Vitórica-Yrezábal [2]

*[1]ICMol - Univ. Valencia - Valencia **(Spain)**, [2]University of Manchester - Manchester **(United Kingdom)***

Abstract

Hydrogen-bonded organic frameworks, or HOFs, are porous molecular-based crystalline materials that are self-assembled through H-bonding interactions.1 Similar to other porous materials such as MOFs and COFs, HOFs have been used in multiple applications, including gas storage, separation, encapsulation, or proton conductivity, among others.2 A major advantage of HOFs is the lack of formation of strong coordination bonds (as in MOFs) or covalent bonds (as in COFs), thus being easily synthesised in mild conditions, which facilitates their processing, one of the major drawbacks of MOFs and COFs.

Herein we will present the preparation of porous conducting HOFs through the use of tetrathiafulvalene-tetrabenzoic acid, H4TTFTB, a molecule that has been previously used in the construction of conductive MOFs and COFs.3 By tuning the synthetic conditions, three different polymorphs have been obtained, all of them presenting open structures and suitable TTF stacking for efficient orbital overlap.3 Interestingly, two of these polymorphs present a zwitterionic character with a positively charged TTF core and a negatively charged carboxylate group, resulting in an efficient charge transport with no need of post-synthetic treatment (e.g., electrochemical oxidation or doping). In fact, experimental conductivities of 10–6 S·cm–1 are observed. On the contrary, a non-zwitterionic HOF based on the same ligand behaves as an insulator despite the suitable stacking of the TTF units.

References

[1] B. Wang, B.; R. B. Lin, Z. Zhang, S. Xiang, B. Chen, J. Am. Chem. Soc. 2020, 142, 14399–14416.
[2] R. B. Lin, Y. He, P. Li, H. Wang, W. Zhou, B. Chen, B. Chem. Soc. Rev. 2019, 48, 1362–1389
[3] See for example: a) J. Castells-Gil, S. Mañas-Valero, I. J. Vitórica-Yrezábal, D. Ananias, J. Rocha, R. Santiago, S. T. Bromley, J. J. Baldoví, E. Coronado, M. Souto, G. Mínguez Espallargas, Chem. - A Eur. J. 2019, 25, 12636–12643; b) T. C. Narayan, T. Miyakai, S. Seki, M. Dincă, J. Am. Chem. Soc. 2012, 134, 12932–12935; c) H. Ding, Y. Li, H. Hu, Y. Sun, J. Wang, C. Wang, C. Wang, G. Zhang, B. Wang, W. Xu, D. Zhang, Chem. - A Eur. J. 2014, 20, 14614–14618.
[4] M. Vicent-Morales, M. Esteve-Rochina et al., J. Am. Chem. Soc. accepted.

Back to Table of contents

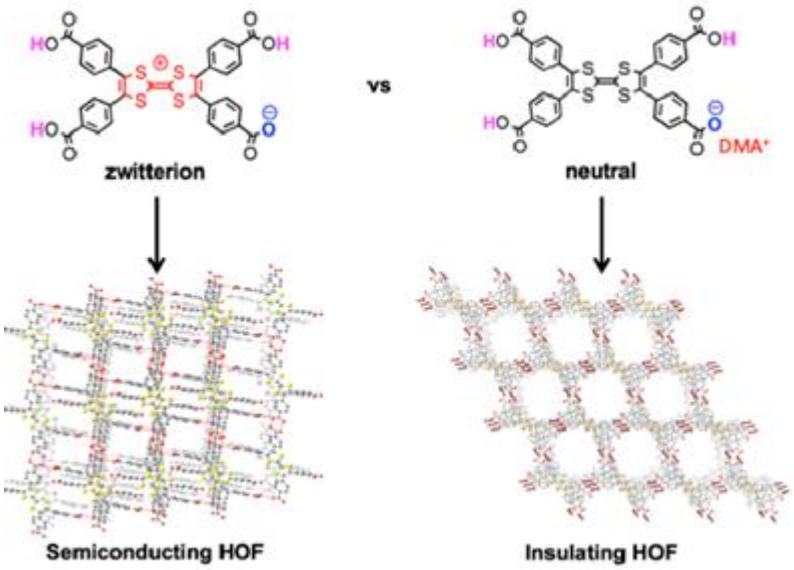

Back to Table of contents

MS13 Structural Characterization of Functional Materials

MS13.2-05

Negative thermal expansion and organic semiconductors

A. Van Der Lee [1]
[1]*CNRS - Montpellier* ***(France)***

Abstract

Negative thermal expansion is usually considered to be an extremely rare phenomenon, but this is mainly due to the fact that structure determinations as a function of temperature are not done systematically, and whenever structural data are available at different temperatures negative thermal expansion is not always recognized as such. We show here that approximately 35% of the organic structures in the Cambridge Structural Database for which structural data at different temperatures exist display negative thermal expansion along at least one of the orthogonal axes. About one hundred structures have been identified which could present negative volumetric expansion.

We give a detailed description of colossal uniaxial negative thermal expansion in a dense organic benzothieno-benzothiophene compound which shows high mobility values of up to 0.17 $cm^2V^{-1}s^{-1}$ under an inert atmosphere, but also in air. We show that the uniaxial negative thermal expansion persists beyond a supercritical-like first-order phase transition. The origin of the extreme negative and positive thermal expansion is due to a steric hindrance between adjacent tilted thiophene units and strongly enhanced by attractive S···S and S···C interactions within the highly anharmonic mixed-domain phase. This material could trigger the tailoring of optoelectronic devices highly sensitive to strain and temperature.

Back to Table of contents

MS14 Materials for energy storage and Conversion

MS14-01

Structural evolution of nanoparticles under realistic conditions observed with Bragg coherent x-ray imaging

M.I. Richard [1], M. Dupraz [1], C. Chatelier [1], C. Atlan [1], E. Bellec [2], N. Li [1], S. Labat [3], T. Schülli [2], E. Rabkin [4], O. Thomas [3], J. Eymery [1], S. Leake [2]

*[1]Université Grenoble Alpes, CEA Grenoble, IRIG, MEM, NRS - Grenoble **(France)**, [2]ESRF - The European Synchrotron - Grenoble **(France)**, [3]Aix Marseille Université, CNRS, Univ. Toulon, IM2NP UMR 7334 - Marseille **(France)**, [4]Technion-Israel Institute of Technology - Haifa **(Israel)***

Abstract

The advent of the world's first coherent hard X-ray sources represents an unprecedented opportunity to conduct in situ and operando studies on the structure of nanoparticles in reactive liquid or gas environments in synchrotrons. In this talk, I will illustrate how Bragg coherent x-ray imaging [1] allows to image in three dimensions (3D) and at the nanoscale the strain and defect dynamics inside nanoparticles as well as their refaceting during catalytic reactions [2–5]. I will also highlight the potential of machine learning to predict characteristic structural features in nanocrystals just from their 3D Bragg coherent diffraction patterns [6].

References

[1] I. Robinson and R. Harder, Coherent X-Ray Diffraction Imaging of Strain at the Nanoscale, Nat. Mater. 8, 291 (2009).
[2] S. Fernández et al., In Situ Structural Evolution of Single Particle Model Catalysts under Ambient Pressure Reaction Conditions, Nanoscale 11, 331 (2018).
[3] M.-I. Richard et al., Crystallographic Orientation of Facets and Planar Defects in Functional Nanostructures Elucidated by Nano-Focused Coherent Diffractive X-Ray Imaging, Nanoscale 10, 4833 (2018).
[4] J. Carnis, L. Gao, S. Fernández, G. Chahine, T. U. Schülli, S. Labat, E. J. M. Hensen, O. Thomas, J. P. Hofmann, and M.-I. Richard, Facet-Dependent Strain Determination in Electrochemically Synthetized Platinum Model Catalytic Nanoparticles, Small Weinh. Bergstr. Ger. e2007702 (2021).
[5] J. Carnis et al., Twin Boundary Migration in an Individual Platinum Nanocrystal during Catalytic CO Oxidation, Nat. Commun. 12, 5385 (2021).
[6] B. Lim et al., A Convolutional Neural Network for Defect Classification in Bragg Coherent X-Ray Diffraction, Npj Comput. Mater. 7, 1 (2021).

Back to Table of contents

MS14 Materials for energy storage and Conversion

MS14-02

Space and time-resolved operando XRD investigation of the (de)lithiation in Liion batteries electrodes materials

Samuel Tardif (Grenoble, France)

/

Back to Table of contents

MS14 Materials for energy storage and Conversion

MS14-03

Uncovering the interplay of competing distortions in the Prussian blue analogue K2Cu[Fe(CN)6]

J. Cattermull [1], A. Goodwin [1]
[1]*University of Oxford - Oxford* ***(United Kingdom)***

Abstract

We report the synthesis, crystal structure, thermal response, and electrochemical behaviour of the Prussian blue analogue (PBA) K2Cu[Fe(CN)6]. From a structural perspective, this is the most complex PBA yet characterised: its triclinic crystal structure results from an interplay of cooperative Jahn-Teller order, octahedral tilts, and a collective `slide' distortion involving K-ion displacements. These different distortions give rise to two crystallographically-distinct K-ion channels with different mobilities. The crystal structure was solved by Rietveld refinement of synchrotron X-ray powder diffraction (XRD) pattern using ISODISTORT and TOPAS. The low symmetry can be explained in theory by the combination of the aforementioned distortion modes, and is justified from good fit to data in the diffraction pattern (Rwp = 1.95%).

Variable-temperature X-ray powder diffraction measurements show that K-ion slides are the lowest-energy distortion mechanism at play, as they are the only distortion to be switched off with increasing temperature. At higher temperatures we propose a decomposition pathway to form a different Prussian blue material from exsolving the copper ions in the framework.

Electrochemically, the material operates as a K-ion cathode with a high operating voltage, and an improved initial capacity relative to higher-vacancy PBA alternatives. On charging, K+ ions are selectively removed from a single K-ion channel type and the slide distortions are again switched on and off accordingly. We discuss the functional importance of various aspects of structural complexity in this system, placing our discussion in the context of other related PBAs.

Figure: Schematic representation of the structural transformations in K2Cu[Fe(CN)6] that take place as a function of temperature and electrochemical cycling.

References

J. Cattermull, K. Sada, K. Hurlbutt, S. J. Cassidy, M. Pasta and A. L. Goodwin, (2022), 10.26434/ChemRxiv-2022-zr5nn

schematic of structural changes

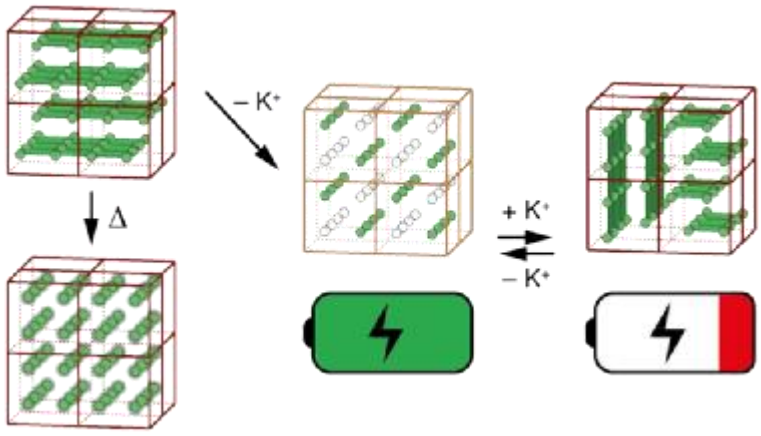

Back to Table of contents

MS14 Materials for energy storage and Conversion

MS14-04

Crystalline silicon gels as anode material for lithium ion batteries

S.L. Flores-Lopez [1], L.D. Santos-Gomez [2], N. Rey-Raap [2], I. Camean [1], A.B. Garcia [1], A. Arenillas [1], S. Garcia-Granda [2]

[1]Instituto de Ciencia y Tecnología del Carbono (INCAR), CSIC - Oviedo (Spain), [2]University Oviedo - Oviedo (Spain)

Abstract

A silica gel has been synthesized via an efficient sol-gel method under microwave radiation, using tetraethylorthosilicate (TEOS) as the silica precursor and acid-basic conditions during the sol-gel process [1]. This approach makes it possible to obtain mesoporous silica gels in a short time, but amorphous in all cases, with presence of a broad peak at 2θ = 17–29° that corresponds to the formation of amorphous silica according to JCPDS-card 96-900-1582.

Among the reduction methods used to obtain crystalline silicon, the magnesio-thermal reduction process stands out for its speed, control and yields [2,3]. Thus, our amorphous silica gels were mixed with Mg in a Mg:Si molar ratio of 2.5:1 and treated at 750 °C under an inert atmosphere (Ar, 300 mL/min). During the heat treatment, different heating ramps were used to avoid overheating of the sample and to maintain the gel structure. The phases produced from the reduction process of SiO_2, such as MgO and Mg_2Si, were eliminated by washing with HCl (1 M) for 4 hours.

The structural properties of the obtained silicon gels were analyzed and measured by SEM, X-ray diffraction (XRD) and high-resolution transmission electron microscopy (HR-TEM). Fig. 1 shows the XRD data for all the reduced silicon gels obtained, illustrating the complete removal of SiO_2, with only Si peaks remaining in the structure. The major diffraction peaks at 2θ = 28.4°, 47.4° and 56.2° are presented at (111), (202) and (131) planes, respectively, which can be attributed to high-purity silicon gel according to JCPDS-card 96-901-3109. However, such peaks reduce their intensity when the heating ramp decrease. Through SEM analysis we can appreciate variations on the final morphology of the reduced species. In sample treated with ramp at 1°C/min the nodular morphology is well maintained, whilst in sample reduced at 50°C/min fused nodules can be observed. The electrochemical performance of the reduced silicon gels as anodes for lithium ion batteries have been also investigated by prolonged galvanostatic cycling vs. Li/Li^+.

Acknowledgement: thanks to the grants PID2020-113001RB-100, PID2020-113558RB-C41, and PCI2020-112039 funded by MCIN/AEI/10.13039/501100011033 and by the European Union NextGenerationEU/PRTR; and the grants from Principado de Asturias IDI/2021/50921 and IDI/2021/50997. NRR y LdSG gratefully acknowledge to the MICIN for their postdoctoral grants (IJC2019-040875-I and IJC2020-044746-I, respectively); SFL thanks to the Principado de Asturias for the grant received through Severo Ochoa program.

References

[1] S.L. Flores-López, S.F. Villanueva, M.A. Montes-Morán, G. Cruz, J.J. Garrido, A. Arenillas, Advantages of microwave-assisted synthesis of silica gels, Colloids Surf. Physicochem. Eng. Asp. 604 (2020) 125248. https://doi.org/10.1016/j.colsurfa.2020.125248.

[2] A. Xing, J. Zhang, Z. Bao, Y. Mei, A.S. Gordin, K.H. Sandhage, A magnesiothermic reaction process for the scalable production of mesoporous silicon for rechargeable lithium batteries, Chem. Commun. 49 (2013) 6743. https://doi.org/10.1039/c3cc43134g.

[3] L. Zhang, X. Liu, Q. Zhao, S. Dou, H. Liu, Y. Huang, X. Hu, Si-containing precursors for Si-based anode materials of Li-ion batteries: A review, Energy Storage Mater. 4 (2016) 92–102. https://doi.org/10.1016/j.ensm.2016.01.011.

Figure 1. XRD data of the reduced silicon gels

Back to Table of contents

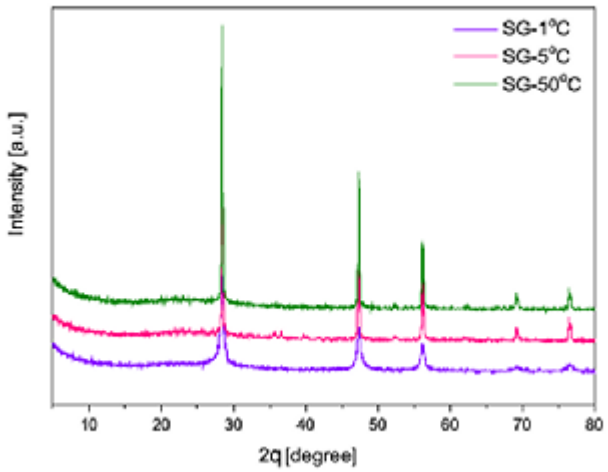

Back to Table of contents

MS14 Materials for energy storage and Conversion

MS14-05

Cation order determination in Cu-based quaternary chalcogenide semiconductors by Multiple Edge Anomalous Diffraction

D.M. Többens [1], S. Schorr [1]
[1]*Helmholtz-Zentrum Berlin - Berlin (Germany)*

Abstract

The quaternary chalcogenide semiconductors $Cu_2B^{II}C^{IV}X_4$ (B^{II} = Zn, Fe; C^{IV} = Sn, Ge, Si; X = S, Se) have drawn wide attention for their potential applications in many fields [1]. Depending on their band gaps these materials are interesting for thin film solar cells, high-temperature thermoelectric materials, and nonlinear optics. Solid solutions of both cations and anions allow fine tuning of physical properties. It is well established that the cation arrangement in the respective structure is crucial for the electronic properties. However, often the cations involved are isoelectronic or nearly so and cannot be distinguished by routine laboratory X-ray diffraction. Neutron and anomalous X-ray diffraction have been used to overcome this problem. A variant of the later, Multiple Edge Anomalous Diffraction (MEAD) [2] was found by us to work particularly well in a number of cases. This method calls for measuring the energy dependency of the intensity of individual Bragg peaks around the X-ray absorption edge of a chemical element. By selecting peaks that are particularly sensitive to specific aspects of the cation order, correlation problems can be lifted. In addition, MEAD provides results in a way clearer and more convincing than other methods (Figure 1).
These compounds listed above crystallize in structure types derived by cation ordering from the cubic sphalerite type or the hexagonal wurtzite type crystal structure. The particular cation arrangement results either in kesterite or wurtz-kesterite structures, which are characterized by the presence of Cu^{I}-B^{II} and Cu^{I}-C^{IV} layers (perpendicular to the longest crystallographic axis). Alternatively, stannite or wurtz-stannite structures are formed, with cations arranged in B^{II}-C^{IV} and pure Cu^{I} layers. The actual type is often hard to establish and literature structures are sometimes just based on assumptions. MEAD was used to confirm the cation structure type of Cu_2FeSnS_4, $Cu_2ZnSnSe_4$, $Cu_2Zn(Ge,Si)Se_4$ and also $CuGaGeS_4$. Materials crystallizing in the kesterite structure in particular are prone to cation disorder within the Cu^{I}-B^{II} layers. Depending on the compound, the degree of cation disorder can change heavily with off-stoichiometry or thermal treatment. In these cases, MEAD spectra supply a robust way of quantification. This works particularly well for compounds where all cations are isoelectric, like $Cu_2ZnGeSe_4$. In other cases, joint Rietveld refinement of powder diffraction patterns taken at multiple energies close to the absorption edges of the chemical elements is the best way to determine cation occupation factors. This method, too, profits from prior MEAD analysis firmly establishing the overall distribution, thus limiting the range of potential options.

References

1. Schorr, S. and G. Gurieva, Energy band gap variations in chalcogenide compound semiconductors: influence of crystal structure, structural disorder, and compositional variations, in *Crystallography in Materials Science: From Structure-Property Relationships to Engineering*, S. Schorr and C. Weidenthaler, Editors. 2021, Walter de Gruyter GmbH & Co KG: Berlin, Bosten. p. 123 - 138.
2. Többens, D.M., *et al.*, Cation distribution in $Cu_2ZnSnSe_4$, Cu_2FeSnS_4 and $Cu_2ZnSiSe_4$ by multiple-edge anomalous diffraction. *Acta Crystallographica Section B - Structural Science Crystal Engineering and Materials*, 2020. 76: p. 1027-1035.

Cu2ZnSnSe4 adopts Kesterite type cation order.

Back to Table of contents

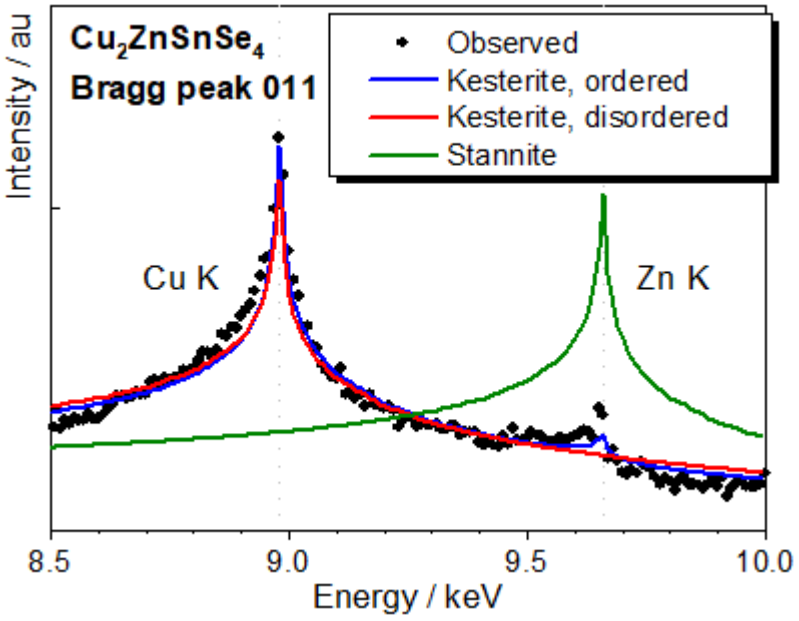

Back to Table of contents

MS15 Mineralogical and inorganic crystallography

MS15-01

Structural characterization of pink MgCoxNi1-xSiO4 (0 ≤ x ≤ 1) solid solutions with olivine structure

M.A. Tena [1], R. Mendoza [2], C. Trobajo [2], J.R. Garcia [2], S. Garcia-Granda [2]
[1]University Jaume I - Castellon de la Plana (Spain), [2]University Oviedo - Oviedo (Spain)

Abstract

Yellow-green Ni_2SiO_4 olivine and blue Co_2SiO_4 olivine are in the DCMA Classification of the Mixed Metal Oxide Inorganic Coloured Pigments (DCMA-5-45-3 and DCMA-5-08-2) [1]. These compounds can be used as ceramic dyes when they are dissolved in glazes. Formation of solid solutions with Mg(II) decreases the high content of nickel or cobalt in them and makes these materials less hazardous. White Mg_2SiO_4 also crystallizes in this structure. M(II) ions are in two octahedral positions in olivine. M1 is a 4a site and M2 4c. The transition metal ions prefer the M2 site and Mg^{2+} ions (without electrons in d orbitals) the more ionic M2 site [2, 3].

In this study $MgCo_xNi_{1-x}SiO4$ (0.0 ≤ x ≤ 1.0) solid solutions with olivine structure have been synthetized via the chemical coprecipitation method obtaining materials with a smaller M(II) (M = Co, Ni) amount. Increasing the unit cell parameters with x is consistent with the replacement of Ni(II) by the larger Co(II) ion, confirming the formation of olivine solid solutions. At 1200 °C, the unit cell parameters increase linearly with x according to the Vegard´s law. Thus, the Co(II) and Ni(II) are randomly distributed in the $MgCo_xNi_{1-x}SiO_4$ (0.0 ≤ x ≤ 1.0) solid solutions with the olivine structure. The different scattering factor of Mg(II) ion allows to refine occupations considering the occupation of (Ni(II)/Co(II)) + Mg(II) as 1.0. The occupation of Co(II) ions in M1(4a) was found higher than in M2(4c) sites.

At 1000 and 1200 °C, only small amounts of minor crystalline phases are detected with olivine. The composition without cobalt (x = 0.0) is green and pink samples are obtained with cobalt (x > 0.0) at these temperatures. The pink colour of samples with x > 0.0 is due to the absorbance between 440 and 630 nm, assigned to third transition band in octahedral Co(II), $^4T_1 \rightarrow {}^4T_1(P)$. The absorbance increases with x (cobalt amount), the a* colour parameter (+, red amount) increases with x and the b* colour parameter (yellow amount (+) to blue amount (-)) decreases with x.

Colour and distances in the coordination of Co(II) in these materials will be compared with other Co(II) compounds to explain the reason for the pink $MgCo_xNi_{1-x}SiO_4$ (0.25 ≤ x ≤ 1.0) solid solutions and the blue or violet in Co_2SiO_4.

Fig. 1. The diffraction profile refinement by Rietveld´s method from pink $MgCoSiO_4$ composition fired at 1200 °C (The CIEL*a*b* colour parameters: 66.67, +12.55, -5.61; L* is the lightness axis (black (0) → white (100)), a* is the green (-) → red (+) axis, and b* is the blue (-) → yellow (+) axis [4]).

Thanks to the Spanish Agencia Estatal de Investigación. Ministerio de Ciencia e Innovación, PID2020-113558RB-C41 and CrysFact Network Red2018-10102574-T (AEI/MCI).

References

[1]] Dry Color Manufacturer's Ass. (1982). DCMA Classification and Chemical description of the Mixed Metal Oxide Inorganic Coloured Pigments. 2nd ed. Metal Oxides and Ceramics Colours Subcommittee, Washington DC.

[2] D. Boström, Cation Ordering at 1300 °C in the (Ni,Mg)-Olivine Solid Solutions Series, Acta Chemica Scandinavica 43 (1989) 116-120.

[3] M. Müller-Sommer, R. Hock, A. Kirfel, Rietveld refinement study of the cation distribution in (Co,Mg)-olivine solid solution. Physical Chemistry Mineral 24 (1997) 17-23. https://doi.org/10.1007/s002690050013

[4] Commission Internationale del'Eclairage (1971) Recommendations on Uniform Color Spaces, Color Difference Equations, Phychometrics Color Terms. 1978. Supplement nº 2of CIE Publication Nº 15 (E1-1.31). Bureau Central de la CIE, Paris

Back to Table of contents

Pink MgCoSiO4 composition fired at 1200 ºC

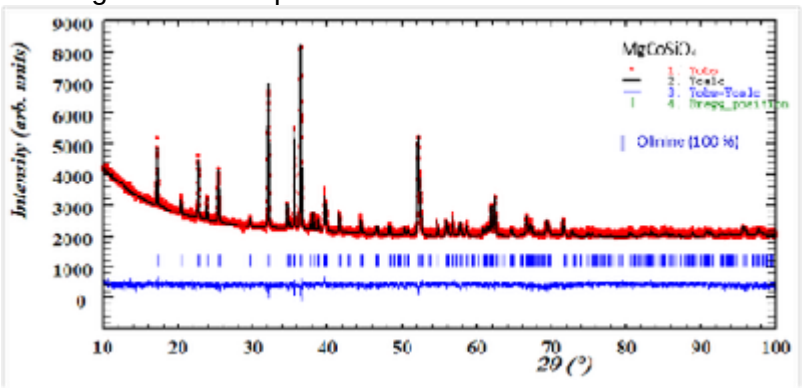

Back to Table of contents

MS15 Mineralogical and inorganic crystallography

MS15-02

Beam-sensitive nano-crystals: why only lowest doses yield the correct structures

H. Klein [1], E. Yörük [1], S. Kodjikian [1]
[1] *Institut Néel, Université Grenoble Alpes and CNRS - Grenoble (France)*

Abstract

There is a wealth of materials that are beam sensitive and only exist in nanometric crystals, because the growth of bigger crystals is either impossible or so complicated that it is not reasonable to spend enough time and resources to grow bigger crystals before knowing their potential for research or applications. In these cases, characterization methods need to be optimized to get the most information out of these particles before the radiation damages them to a point where their structure is altered.

Both, the small size and beam sensitivity, call for electron diffraction as a privileged investigation tool. The strong interaction of electrons (as compared to X-rays) with matter allows single crystal diffraction experiments on nanometer-sized crystals and for the same amount of beam damage, electron diffraction yields more information than X-rays [1]. These inherent advantages of electron diffraction are optimized in the recently developed low-dose electron diffraction tomography (LD-EDT) [2].

Here we present two examples of beam sensitive nanometric crystals: the notoriously beam sensitive metal organic framework Mn-formiate $[Mn(HCOO)_2(H_2O)_2]_\infty$ [3] and the mineral bulachite $[Al_6(AsO_4)_3(OH)_9(H_2O)_4]\cdot 2H_2O$ [4]. In both cases, even small electron doses of a few $e^-/Å^2$ are enough to damage the structure. Comparing the diffraction patterns before and after an irradiation of 3.9 $e^-/Å^2$ of Mn-formiate shows that the high resolution reflections have disappeared (Figure 1).

A much smaller total dose had to be chosen for the structure solution and refinement. We therefore recorded a dataset of 60 frames corresponding to a total dose of 0.15 $e^-/Å^2$. The obtained data quality is high, allowing not only the solution of the structure, but also its refinement taking into account the dynamical diffraction effects (Figure 2).

Likewise, on bulachite the electron dose had to be drastically reduced in order not to destroy the structure and conserve the free water molecules. We acquired a LD-EDT data set containing 105 frames with a total dose of 3 $e^-/Å2$. The obtained structure solution contained all non-hydrogen atom positions including the free water molecules. The charge valence sums calculated from the model allowed distinguishing the O^{2-}, OH^- and H_2O. A dynamical refinement improved the accuracy of the atom positions with an average distance to the XRD refined positions of 0.1 Å for bonded oxygen (Figure 2).

In this contribution we show that beam sensitive crystals need the extremely low doses that can be obtained by LD-EDT to obtain the correct structures of complex crystals.

References

[1] Henderson, R., Q. Rev. Biophys. 1995, 28, 171–193.
[2] Kodjikian, S.; Klein, H., Ultramicroscopy 2019, 200, 12–19, https://doi.org/10.1016/j.ultramic.2019.02.010.
[3] Poulsen, R.D.; Jørgensen, M.R.V.; Overgaard, J.; Larsen, F.K.; Morgenroth, W.; Graber, T.; Chen, Y.-S.; Iversen, B.B., Chem. Eur. J. 2007, 13, 9775–9790
[4] Grey, I.E.; Yoruk, E.; Kodjikian, S.; Klein, H.; Bougerol, C.; Brand, H.E.A.; Bordet, P.; Mumme, W.G.; Favreau, G.; Mills, S.J., Mineral. Mag. 2020, 84, 608–615, https://doi.org/10.1180/mgm.2020.52.

Back to Table of contents

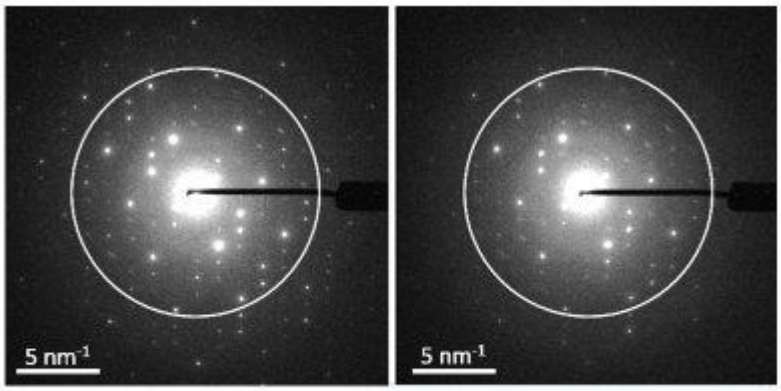

***Figure 1**: diffraction patterns of the pristine Mn-formiate (left) and in the same orientation, but after an irradiation dose of 3.9 $e^-/Å^2$ (right). The circle represents a resolution of 1 Å.*

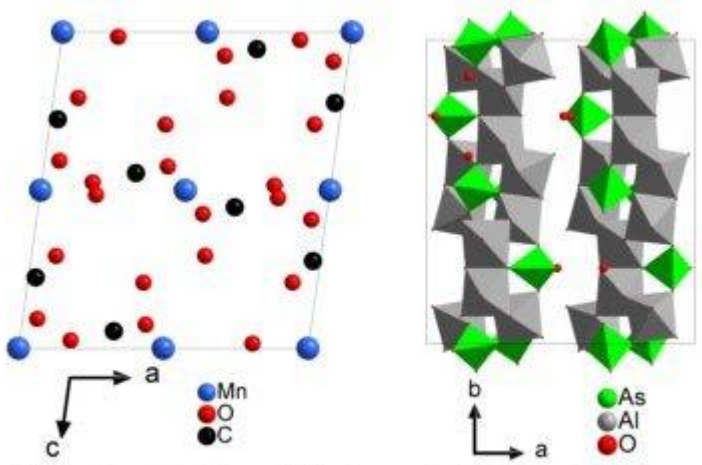

Figure 2 : projections of the dynamically refined structures of Mn-formiate (left) and bulachite (right)

Back to Table of contents

MS15 Mineralogical and inorganic crystallography

MS15-03

Design of High-Temperature Syntheses for Cluster Compounds (Bi2xA1-3x)[PtBi6I12] with A = Mn, Fe, Sn, Pb

M.A. Herz [1], K. Finzel [1], M. Ruck [1]
[1]Technische Universität Dresden - Dresden (Germany)

Abstract

During the search for new topological insulators[1][2], we discovered pseudo one-dimensional compounds $(Bi_{2x}A_{1-3x})[PtBi_6I_{12}]$ with $0 \leq x \leq 1/3$. Reacting Bi with Pt, BiI_3 and a divalent metal A = Mn, Fe, Sn[3], Pb[4] above 300 °C yielded shiny, black, air insensitive crystals of these subiodides. Synthesis of pure samples and growth of single-crystals with x = 0 was achieved through extensive investigations into the synthetic pathways with the help of differential scanning calorimetry and phase analysis of samples annealed at the temperatures of the identified thermal effects.

The isostructural title compounds crystallize in the rhombohedral space group –R . The crystal structures contain cuboctahedral $[PtBi_6I_{12}]^{2-}$ cluster anions. A^{2+} cations in octahedral voids between trigonal faces of two adjacent cuboctahedra concatenate them into infinite linear chains. If x is not equal to 0, the higher charge of the Bi^{3+} cations in the octahedral voids is compensated by vacancies that break the chain into finite strands. In $Bi_2[PtBi_6I_{12}]3$[5], i.e. for x = 1/3, these are cluster triples. The crystals' cube-like morphology originates from six Bi···I inter-cluster bridges per cluster connecting the chains.

The heavy elements show strong spin-orbit coupling, which, if it exceeds the width of the chemical band gap, would be expected to result in a nontrivial topology. In the case of magnetic cations, spin polarization could lead to surface states that all share the same chirality. The full-relativistic electronic band structures and the topological invariants are presented.

References

[1] a) M. Z. Hasan, C. L. Kane, Rev. Mod. Phy. 2010, 82, 3045
[2] Y. Ando, J. Phys. Soc. Jpn. 2013, 82.
[3] M. A. Herz, K. Finzel, M. Ruck, Z. Anorg. Allg. Chem. 2022, e202200080.
[4] M. A. Herz, M. Knies, K. Finzel, M. Ruck, Z. Anorg. Allg. Chem. 2020, 647, 53.
[5] A. Günther, F. Steden, M. Ruck, Z. Anorg. Allg. Chem. 2008, 634, 423.

Fig.1 The different analytical methods involved.

Back to Table of contents

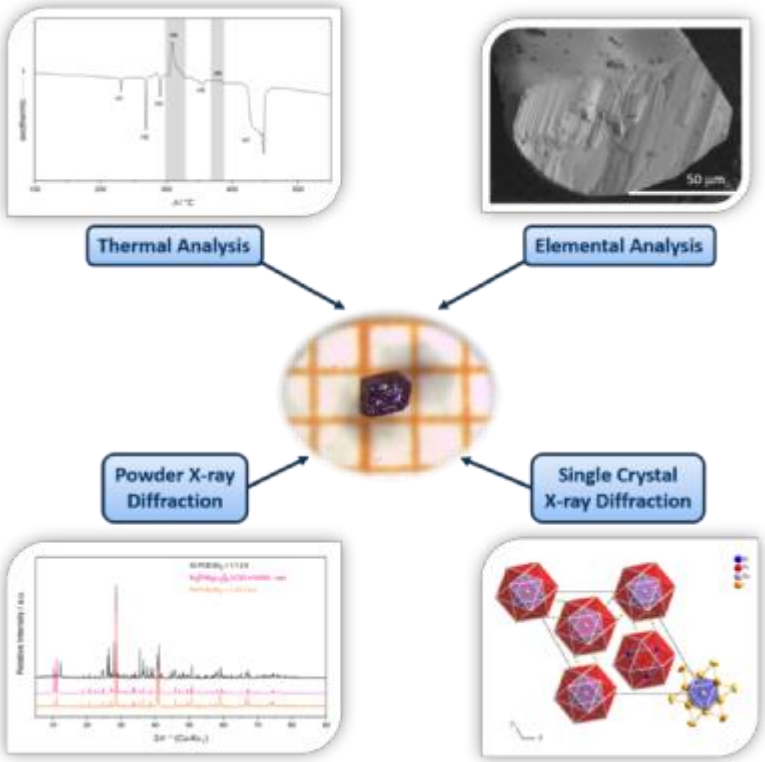

Back to Table of contents

MS15 Mineralogical and inorganic crystallography

MS15-04

Epitaxial intergrowths and local oxide displacements in natural bixbyite

K.A.H. Støckler [1], N. Roth [2], T.B.E. Grønbech [1], B.B. Iversen [1]
[1]Aarhus University - Aarhus (Denmark), [2]University of Oxford - Oxford (United Kingdom)

Abstract

The naturally occurring mineral bixbyite, $Fe_{2-x}MnxO_3$, was recently studied due to its low temperature transition to a disordered spin-glass state [1,2]. However, the mineral also exhibits correlated disorder of structural origins as evidenced by elastic room-temperature single crystal neutron diffuse scattering, Fig. 1(left), and single crystal x-ray diffuse scattering, Fig. 1(right). The one-dimensional nature of the single crystal x-ray scattering suggests the presence of two-dimensional order and one-dimensional disorder. Here we show that this disorder arises from epitaxial intergrowths of the mineral braunite. This is consistent with reports of such intergrowths in natural bixbyite samples based on transmission electron microscopy experiments [3]. Additional short-range order is indicated by the presence of broad diffuse scattering features in the room temperature single crystal neutron scattering data. As these features are not observed in the x-ray data it is natural to expect them to originate from correlations involving Fe^{3+} and Mn^{3+} which have low x-ray but high neutron contrast. We show that the diffuse scattering can be modelled by a size effect where the displacements of oxide ions are correlated with the substitutional disorder on the cation sites. This can be rationalized by the approximately octahedral sites being occupied by Jahn-Teller inactive (Fe^{3+}, d^5) and active (Mn^{3+}, d^4) ions which results in preferences for local octahedral or tetragonally distorted octahedral coordination, respectively. The different contrasts and experimental requirements in single crystal x-ray and neutron scattering experiments allow us to analyze the two modes of disorder in natural bixbyite separately giving a more complete overview of the structure of disordered bixbyite.

References

[1] N. Roth, F. Ye, A. F. May, B. C. Chakoumakos, and B. B. Iversen, Phys. Rev. B 100 (2019).
[2] N. Roth, A. F. May, F. Ye, B. C. Chakoumakos, and B. B. Iversen, IUCrJ 5, 410 (2018).
[3] J. Peter, M. Trapp, S. Lauterbach, P. Golle-Leidreiter, U. Kolb, and H. J. Kleebe, Am. Mineral. 106, 1163 (2021).

Figure 1

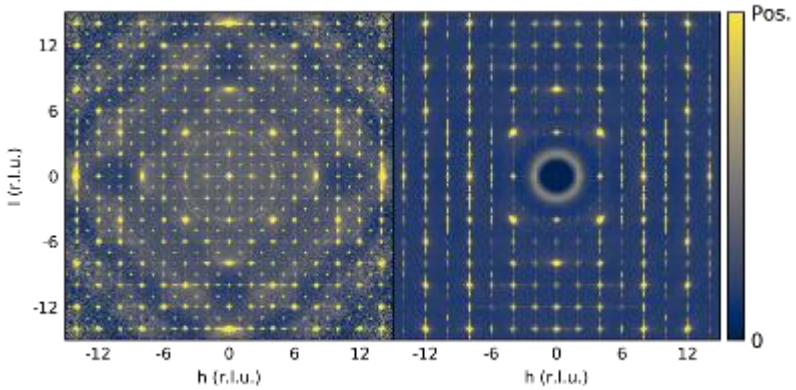

Back to Table of contents

MS15 Mineralogical and inorganic crystallography

MS15-05

Accurate Crystal Structure of Ice VI from X-Ray Diffraction with HAR

M.L. Chodkiewicz [1], R. Gajda [1], K. Wozniak [1]
[1]*University of Warsaw - Warszawa (Poland)*

Abstract

Water is an essential chemical compound for living organisms, and twenty of its different crystal solid forms (ices) are known. Still, there are many fundamental problems with these structures such as establishing the correct positions and thermal motions of hydrogen atoms. The list of ice structures is not yet complete as DFT calculations have suggested existence for additional as of yet unknown phases. In many ice structures, neither neutron diffraction nor DFT calculations nor X-ray diffraction methods can easily solve the problem of hydrogen atom disorder or accurately determine their atomic displacement parameters. Here we present accurate crystal structures of H2O, D2O and mixed (50%H2O/50%D2O) ice VI obtained by Hirshfeld Atom Refinement (HAR) against high pressure single crystal synchrotron and laboratory X-ray diffraction data. It was possible to obtain O-H bond lengths and anisotropic atomic displacement parameters for disordered hydrogen atoms which are in excellent agreement with the corresponding results of single crystal neutron diffraction data. Our results show that Hirshfeld atom refinement against X-ray diffraction data is a tool which can compete with neutron diffraction in detailed studies of polymorphic forms of ice and crystals of other hydrogen rich compounds. As neutron diffraction is relatively expensive, requires larger crystals which might be difficult to obtain, and access to neutron facilities is restricted, cheaper and more accessible X-ray measurements combined with HAR can facilitate the verification of the existing ice polymorphs and the quest for the new ones.

References

References
[1] M. L. Chodkiewicz, R. Gajda, B. Lavina, S. Tkachev, V. B. Prakapenka, P. Dera, K. Woźniak, Accurate crystal structure of ice VI from X-ray diffraction with Hirshfeld Atom Refinement, IUCRJ, 2022, Submitted
Acknowledgements:
Financial support of this work by the National Science Centre, Poland, through OPUS 21 grant number DEC-2021/41/B/ST4/03010 is gratefully acknowledged. The work was accomplished at the TEAM TECH Core Facility for crystallographic and biophysical research to support the development of medicinal products sponsored by the Foundation for Polish Science (FNP). The synchrotron radiation experiments were performed at the APS (Proposal No. GUP-71134) and DESY (Proposal I-20200083 EC).

Examples of water clusters considered.

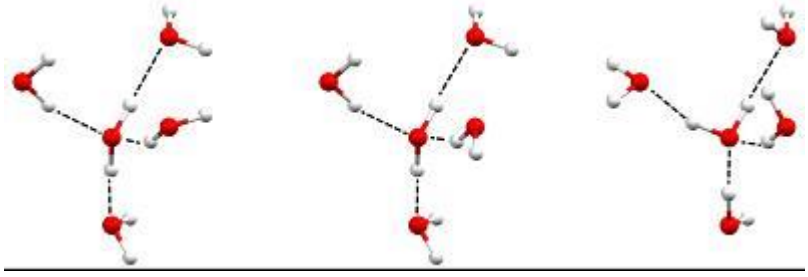

Back to Table of contents

MS16 Time-resolved diffraction and scattering techniques

MS16-01

Making ultrafast phase transition movie with streaming crystallography and femtosecond XANES in Prussian blue analogues

E. Collet [1], M. Herve [2], G. Privault [1], I. Chaban [1], E. Trzop [2], M. Cammarata [3], C. Mariette [3], K. Imoto [4], M. Yoshikiyo [4], H. Tokoro [5], S. Ohkoshi [4]

[1]University Rennes 1 - Rennes (France), [2]CNRS - Rennes (France), [3]ESRF - Grenoble (France), [4]University Tokyo - Tokyo (Japan), [5]University Tsukuba - Tsukuba (Japan)

Abstract

The development of modern ultrafast technologies has recently opened new perspectives in controlling bistable materials, where light can be used to switch between different phases and thus different properties [1], by accessing the ultrashort timescales. Specifically, following the dynamics of photo-induced phase switching gives access to the complex couplings between electronic and structural reorganizations, which can be ultimately tuned using ultrafast stimuli. Among the available bistable materials, Prussian Blue Analogues (PBAs) are cyano-bridged bimetallic compounds exhibiting a phase transition based on a charge transfer between two stable states [2]. The electronic charge transfer in these molecular materials is coupled to symmetry-breaking and large volume change, leading to a wide bistability regime [3]. Studying the ultrafast dynamics associated to the photo-induced switching within thermal hysteresis is however hindered by the non-reversible character of the transformation in the bistability range, which is necessary for applications but precludes the use of conventional pump-probe spectroscopy on static material samples. In this work, we overcame this limitation by developing a new Streaming Crystallography methodology, where laser pump – X-ray probe measurements are performed on a continuously-refreshed liquid jet containing micro-crystals in the ground state. We used Time-Resolved X-Ray Diffraction (TR-XRD) at the European Synchrotron Radiation Facility (ESRF) to follow the multiscale phase transition dynamics within the thermal hysteresis of a MnFe PBA driven by optical excitation at 650 nm (Fig. 1) [4,5]. Our results reveal that complete photo-transformation from tetragonal to cubic phase can be achieved in micro-crystals, and leads to a permanent photo-induced phase. The out-of-equilibrium and multiscale dynamical behavior results from the coupling of volume strain driven by photoinduced charge transfer towards less bonding states and symmetry change related to Bragg peak splitting [5]. More generally, these results open a broad field of dynamical studies for photo-switching resulting in permanent or long-lived states in bistable molecular materials and photo-active devices through ultrafast crystallography.

References

[1] Sato, O. Nat. Chem. 2016, 8(7), 644-656
[2] Cammarata, M. Nature Chem. 2021, 13, 10-14
[3] Azzolina, G. et al., Phys. Rev. B 2020, 102, 134104
[4] Azzolina, G. et al., Eur. J. Inorg. Chem. 2019, 2019, 3142-3147
[5] Azzolina, G. et al., J. Mater. Chem. C 2021, 9, 6773

TR-XRD pattern of MnFe PBA

Back to Table of contents

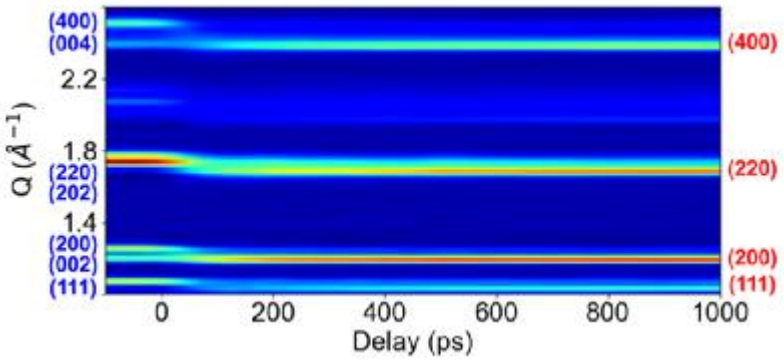

Back to Table of contents

MS16 Time-resolved diffraction and scattering techniques

MS16-02

Time-resolved serial synchrotron crystallography for the functional characterization of proteins

P. Mehrabi [1], E. Schulz [1]
[1]Universität Hamburg - Hamburg (Germany)

Abstract

Functional characterization of proteins requires insights into the interplay between structure and dynamics. Classical approaches to X-ray crystallography via populating intermediate states by mutation or chemical trapping only provide static time-averaged data sets. Acquiring dynamic data is thus highly important. This leads to dynamic models which better represent the true behaviour of the system. However, elucidating models of protein dynamics that are related to functional characteristics is often rife with difficulty, as enzyme systems are highly complex, and require structural data as a function of time where key insights can be obtained by visualizing the wide range of both internal motions and interactions with the solvent environment. Considering this, serial time-resolved approaches are powerful tools to elucidate time-dependent structures. To this end we have combined and established novel fixed target approaches which enable unique data collection strategies, such as the “Hit And REturn” (HARE) approach. As well as novel reaction initiation strategies with the use of piezo droplet injectors. The “Liquid Application Method for time-resolved Analysis” (LAMA) method simplifying reaction initiation for systems that are not naturally amenable to light activation. Building upon and advancing these current technologies with the use of environmental control of both temperature and humidity and further advances in sample handling and data acquisition strategies are enabling us to delve further into the regulatory mechanisms of allostery and water networks for proteins, inevitably providing insights into fundamental enzymology.

Back to Table of contents

MS16 Time-resolved diffraction and scattering techniques

MS16-03

Steady-state and time-resolved X-ray scattering demonstrate that oligomerization processes limit photoactivation and recovery of the cyanobacterial Orange Carotenoid Protein

E.A. Andreeva [1], J.P. Colletier [2]

[1]Institut de Biologie Structurale (IBS), Univ. Grenoble Alpes, CEA, CNRS, 38044 Grenoble, France; Max-Planck-Institut für medizinische Forschung, Jahnstraße 29, 69120 Heidelberg, Germany - Grenoble (France), [2]Institut de Biologie Structurale (IBS), Univ. Grenoble Alpes, CEA, CNRS, 38044 Grenoble, France; - Grenoble (France)

Abstract

The photoactive Orange Carotenoid Protein (OCP), involved in cyanobacterial photo-protection [1], is a two-domain protein which upon light absorption transitions from a compact inactive “dark” state (OCP^O) to an extended photoactive “light” state (OCP^R) [2,3]. The molecular mechanism enabling photoactivation involves migration of the carotenoid pigment from the interface between the two domains into the NTD, and subsequent domain dissociation. It remains unclear what the exact structure of OCP^R is, on which timescale it forms, and whether or not oligomerization [2,4] is involved in the regulation of OCP function – either in the inactive or photo-activated state. Here, we used a combination of steady-state and time-resolved (TR) X-ray scattering and spectroscopy to address these three specific issues. Our results inform on the time scales associated to the dissociation and reassociation of domains in monomeric OCP, yielding OCP^R and enabling recovery of OCP^O, respectively. They furthermore demonstrate that oligomerization occurs at the OCP^O and OCP^R level, limiting the photoactivation of OCP^O and the OCP^O to OCP^R thermal recovery, respectively [5].

References

[1] Kirilovsky D. & Kerfeld C. A., (2016). Cyanobacterial photoprotection by the orange carotenoid protein. Nat. Plants 2, 16180.
[2] Wilson A. et al., (2008). A photoactive carotenoid protein acting as light intensity sensor. PNAS, 105 (33): 12075-12080
[3] Haijun L. et al., (2016). Dramatic Domain Rearrangements of the Cyanobacterial Orange Carotenoid Protein upon Photoactivation. Biochemistry,55 (7): 1003–1009
[4] Golub M. et al., (2019). Solution Structure and Conformational Flexibility in the Active State of the Orange Carotenoid Protein: Part I. Small-Angle Scattering. J. Phys. Chem. B, 123, 9525−9535
[5] Andreeva E.A. et al., (2022). Oligomerization processes limit photoactivation and recovery of the Orange Carotenoid Protein. Biophysical Journal (in review).

TR X-ray scattering monitors OCP photoactivation

Back to Table of contents

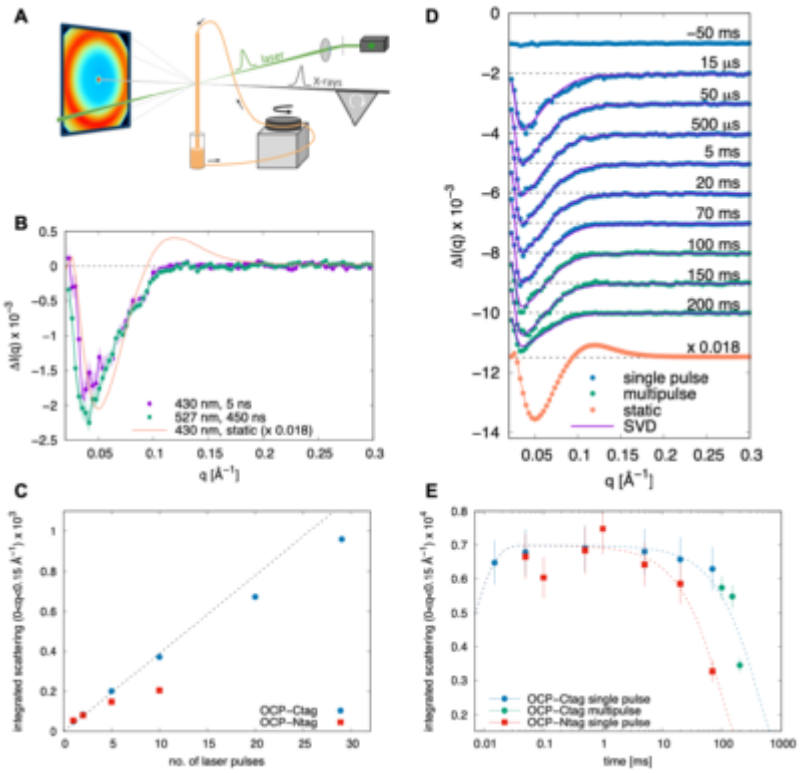

Proposed model for OCP photoactivation

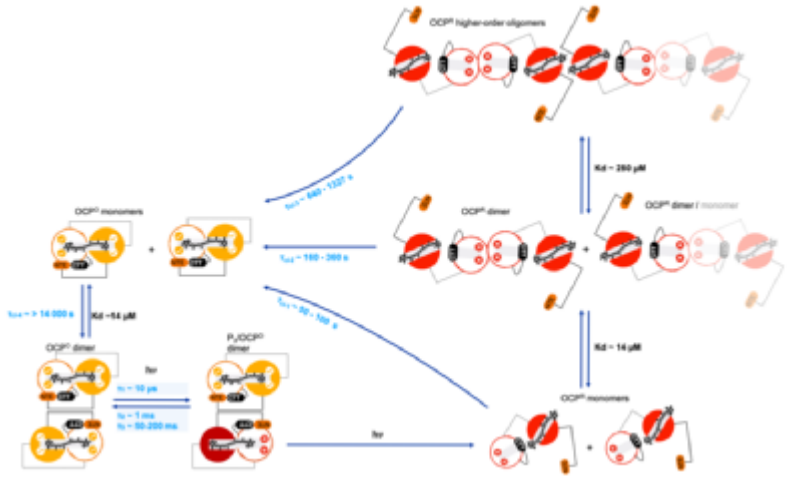

Back to Table of contents

MS16 Time-resolved diffraction and scattering techniques

MS16-04

Randomness in time-resolved serial crystallography data: alternatives to the binning and averaging approach

C. Casadei [1], A. Hosseinizadeh [2], G. Schertler [1], A. Ourmazd [2], R. Santra [3]
[1]ETHZ - Zürich (Switzerland), [2]University of Wisconsin - Milwaukee (United States), [3]CFEL - Hamburg (Germany)

Abstract

Time binning approaches have proved successful in dealing with the issues of data incompleteness and partiality in time-resolved serial crystallography and produced molecular movies that offer unprecedented insight into the function of biomolecules in action. Yet the averaging procedure that underlies such approaches normally requires large numbers of frames: this often means binning over large time windows, which implies a loss of timing information.

While the data manifold of the time-evolving system is intrinsically one-dimensional - and its trajectory likely explores only a low-dimensional subspace of the high-dimensional data space, the physical specificities of the diffraction experiment introduce incompleteness and partiality, artificially increasing the apparent dimension of the subspace in which the data points lie. Time-lagged embedding mitigates such issues and allows - at least in favourable situations - to reconstruct the underlying system dynamics by singular value decomposition in the supervector space (Singular Spectrum Analysis). Nonetheless this procedure is impractical in the case of large data sets, and in some circumstances may not be able to provide a low-rank approximation of the system dynamics [1]. Time-lagged embedding can be combined with data filtering in supervector space to ease these issues. This can be done - for instance, by using a set of orthonormal trigonometric functions as subspace basis, or alternatively a data-driven set of basis functions. The latter approach is called the nonlinear Laplacian spectral analysis (NLSA) [1], which was first applied to serial crystallography in [2].

These concepts are exemplified using synthetic models and preliminary serial crystallography results from the membrane protein bacteriorhodopsin in the first ps after photoactivation.

References

[1] D. Giannakis et al., PNAS 2012, 109 (7), DOI: 10.1073/pnas.1118984109
[2] A. Hosseinizadeh et al., Nature 2021, 599, DOI: 10.1038/s41586-021-04050-9

Back to Table of contents

MS16 Time-resolved diffraction and scattering techniques

MS16-05

Transient hexatic phase observed by ultrafast high-coherence nanobeam diffraction

T. Domröse [1], T.H. Danz [1], S. Yalunin [1], C. Ropers [1]
[1]*Max Planck Institute for Multidisciplinary Sciences - Göttingen (Germany)*

Abstract

Ultrafast transmission electron microscopy (UTEM) is a powerful technique that enables the investigation of non-equilibrium structural dynamics by means of diffraction in a laser pump/electron probe approach [1]. The sensitivity of such experiments to structural modifications induced by the optical excitation is often limited by the coherence of the electron source. In order to achieve sufficient reciprocal-space resolution, diffractive probing typically averages over nanoscale heterogeneity by forming probes with a diameter of several 100 µm.

In the Göttingen UTEM, ultrashort electron pulses are generated by linear photoemission from a tip-shaped field-emitter, yielding a particularly high coherence (Fig. 1a). This enables ultrafast diffraction experiments with a collimated nanometer-sized electron beam and sub-picosecond temporal resolution (Fig. 1b) [2]. In this work, we harness these capabilities to investigate the formation kinetics of an incommensurate charge-density wave (CDW) phase following optical excitation of a layered material [3]. The high-coherence electron source in conjunction with the small probing volume allows us to track the establishment of three-dimensional long-range order encoded in the temporal evolution of the CDW reciprocal lattice rods.

At early times and within the material layers, the CDW is characterised by a strongly anisotropic broadening of the associated diffraction spots, suggesting a transient state with intact bond-orientational order, but reduced translational symmetry (Fig. 1d). This anisotropy decays after around 10 ps, followed by ongoing spot sharpening on longer timescales.

Along the out-of-plane directions, a reconstruction of the CDW rocking curve from a time-dependent tilt series reveals an initial increase of scattered CDW intensities that is broadly spread across the entire out-of-plane wave vector component (Fig. 1c). Only afterwards, a well-defined diffraction peak indicative of the equilibrium CDW stacking sequence emerges.

This behavior implies an initial loss of interlayer correlations and the formation of a quasi-two-dimensional intermediate at early times. We identify this intermediate as a transient hexatic phase characterised by a high density of unbound topological defects. Induced by the optical excitation, their presence translates into the observed characteristic broadening of diffraction spots along the azimuthal direction (green arrow in Fig. 1d) [4]. From here, the ongoing pairwise recombination of dislocations and the transition into a three-dimensional system lead to the establishment of long-range order associated with the thermalised crystalline IC phase found at late times.

In the future, we expect our experimental approach to provide further insights into phase formation kinetics in other correlated materials and to elucidate the impact of spatial heterogeneity on ultrafast structural dynamics.

References

[1] A. H. Zewail, Science 328, 187-193 (2010).
[2] A. Feist et al., Ultramicroscopy 176, 63-73 (2017)
[3] T. Domröse, Th. Danz, S. Yalunin, C. Ropers, in preparation
[4] D. Nelson, B. Halperin, Physical Review B 19, 2457-2484 (1979)

Ultrafast CDW dynamics probed by UTEM

Back to Table of contents

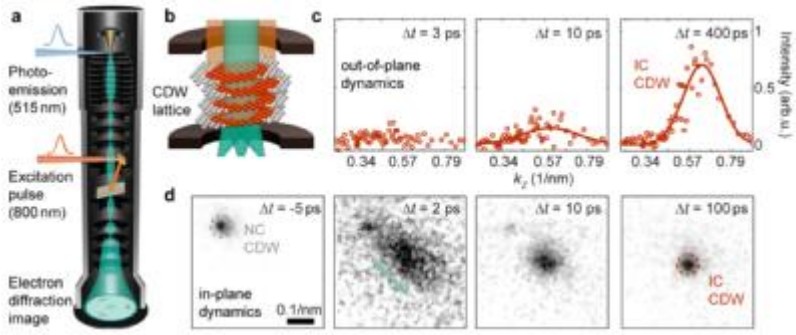

Back to Table of contents

MS17 Total scattering studies and disorder

MS17-01

Recent advances in data quality and versatility of laboratory PDF experiments

N. Prinz [1], D. Tsymbarenko [2], M. Zobel [1]
[1]RWTH Aachen University - Aachen (Germany), [2]Lomonosov Moscow State University - Moscow (Russian Federation)

Abstract

Although the very first laboratory-based X-ray pair distribution function (PDF) analysis had been carried out in the 1930s [1], laboratory PDF studies have been pretty uncommon till a few years back. [2] Limited momentum transfer vector Qmax, insufficient instrumental resolution and very long measurement times impeded a routine use for structural refinements. A few years ago, we have significantly pushed instrumental resolution of PDF data in the laboratory by reducing air scattering and optimizing beamstop positioning for a diffractometer in transmission geometry, using a MYTHEN2 4K module to cover a large angular range. [3] The use of monochromatic Ag Kα1 radiation permitted laboratory PDF data to be fitted over interatomic distance ranges of several dozens of Angstroms, e.g. to refine PDF data of 7 nm TiO2 nanoparticles with a goodness-of-fit R_w as low as 0.222 over 70 Å. This paved the way to study local disorder in superionic conductors [4] and the structure of 1D lanthanide polymer powders in the laboratory [5]. Since then and as very specialized PDF setups are not available in many laboratories, more diverse attempts to optimize laboratory PDF analysis have been carried out. Diffractometers using Goebel mirrors provide $Kα_{1,2}$ mixtures, which results in overlap of PDF peaks beyond 20 Å, preventing a continuous and simultaneous fit of the short-range order < 20 Å and the medium- to long-range order beyond. However, recent advanced data processing evolved and TOPAS can nowadays deconvolute the instrumental contributions such as wavelength mixtures, emission profiles or axial divergence, yielding less instrumentally dampened PDF data [6] – in particular for crystalline materials. This approach is showcased and compared to monochromatically measured laboratory PDF data. To conclude, and in light of recent pushes in high-energy X-ray detectors such as the HyPix-Arc series (Rigaku) or Photon III (Bruker) combined with high-flux microfocus sources, single crystal diffractometers can accomplish very decent PDF data in only about two hours. This approach is based again on Kα2 stripping, necessary for data fitting beyond 30 Å, and highlighted for poorly crystalline powders and solutions of polynuclear lanthanide complexes. [7]

References

[1] B. E. Warren, N. S. Gingrich, Phys. Rev. (1934) 46 (368)
[2] M. J. Nijenhuis, J. T. Gateshki, M. Fransen, *Z. Kristallogr. Suppl.* (2009) 163
[3] S.L.J. Thomä, et al., *Rev. Sci. Instr.* (2019) 90 (4), 043905-1 - 043905-5
[4] A. A. Coelho, P. A. Chater, M. J. Evans, *J. Appl. Cryst.* (2021) 54, 444-453
[5] R. Schlem, et al., *Adv. Energy Mater.* (2020), 10, 1903719(1-10),
[6] D. Grebenyuk, et al., *Inorg. Chem. (*2021), 60, 11, 8049-8061
[7] D. Tsymbarenko, D. Grebenyuk, M. Burlakova, M. Zobel, *submitted*

Back to Table of contents

MS17 Total scattering studies and disorder

MS17-02

Neutron total scattering measurements under hydrostatic high pressure

N. Funnell [1]
[1]*UKRI - ISIS Neutron and Muon Facility - Didcot (United Kingdom)*

Abstract

Total scattering measurements have proved invaluable for in-situ studies on numerous materials, providing structural information over short-range length scales. Though it is now common to explore crystalline samples as, e.g., a function of temperature, flow gas, chemical composition, or electric current, it remains challenging to perform local structure studies under pressure. Amorphous substances comprise the majority of total scattering studies under pressure [1] because crystalline materials necessitate the inclusion of a pressure transmitting medium (PTM) in order to avoid sample strain. The PTM has its own local structure scattering signature, and untangling its contribution from that of the sample is non-trivial. This is particularly severe for neutron measurements, where common PTM materials are deuterated, making them significantly more powerful scatterers than in the analogous diffraction experiment with X-rays, using their hydrogenous counterparts.
This talk describes some of the recent efforts on the PEARL instrument at the ISIS Neutron and Muon Facility toward developing approaches for obtaining pair distribution function data from samples under hydrostatic pressure, as well as some early science studies. [2-4]

References

[1] P. S. Salmon, J. W. E. Drewitt, D. A. J. Whittaker, A. Zeidler, K. Wezka, C. L. Bull, M. G. Tucker, M. C. Wilding, M. Guthrie and D. Marrocchelli, *J. Phys.: Condens. Matter*, (2012), **24**, 415102
[2] A. Herlihy, H. S. Geddes, G. C. Sosso, C. L. Bull, C. J. Ridley, A. L. Goodwin, M. S. Senn and N. P. Funnell, *J. Appl. Crystallogr.*, (2021), **54**, 1546–1554
[3] A. Herlihy, T. A. Bird, C. J. Ridley, C. L. Bull, N. P. Funnell and M. S. Senn, *Phys. Rev. B*, (2022), **105**, 094114
[4] N. P. Funnell, C. L. Bull, S. Hull and C. J. Ridley, *J. Phys.: Condens. Matter*, accepted – in press

Back to Table of contents

MS17 Total scattering studies and disorder

MS17-03

The local structure of oxygen deficient perovskite Sr2ScGaO5 polymorphs explored by total neutron scattering and EXAFS

M. Ceretti [1], G. Agostini [2], M. Brunelli [3], G. Cuello [4], W. Paulus [1]
[1]ICGM - Montpellier (France), [2]Alba - Barcelona (Spain), [3]ESRF - Grenoble (France), [4]ILL - Grenoble (France)

Abstract

Oxygen deficient perovskite oxides have been extensively investigated in the last decades because of their rich chemistry, structural complexity, interesting properties and applications, such as ionic conductors.[1-5] We have recently reported on oxygen diffusion mechanisms in a new oxygen deficient perovskite, Sr_2ScGaO_5 (SSGO), containing exclusively open or closed shell B-cations and fixed oxygen stoichiometry.[5-8] Depending on the synthesis route, it adapts two polymorphs: the orthorhombic brownmillerite (*I2mb*), or an oxygen deficient perovskite structure (*Pm-3m*). Once synthesized, both phases are surprisingly kinetically stable up to 1400°C, making them as a model system to study oxygen diffusion mechanisms6. We report here on a multi-technical approach to characterize structural changes as a function of temperature using X-ray and neutron diffraction techniques. To further investigate the local structure, neutron pair distribution function (PDF) analysis together with the extended X ray absorption fine structure (EXAFS) analysis were carried out on both SSGO polymorphs. Our studies confirm a 2nd order phase transition for SSGO with Brownmillerite framework, implying an order/disorder transition of the 1D (GaO_4) tetrahedral chains indicating dynamical switching activated above 300°C. For the oxygen deficient SSGO perovskite, oxygen vacancies do not show a statistical distribution but are correlated. From PDF analysis we clearly proof that on a local scale the brownmillerite type vacancy structure exists, suggesting that the average cubic perovskite framework is consisting of a complex microstructure. In addition to this, EXAFS first shell analysis, indicate for both polymorphs an identical local environment for the Ga atoms. Temperature dependent structure and local structure (PDF) analysis, combined with EXAFS spectroscopy, are discussed in terms of lattice dynamical aspects obtained from ^{17}O-NMR and Raman spectroscopy .

References

[1] Abakumov A. M., et al., J. Solid State Chemistry (2003) 174 (2), 319
[2] Hadermann J., et al., J. Mat. Chem. (2007) 17 (7), 692
[3] Shaula, A. L., et al., Solid State Ion. (2006) 177 (33-34), 2923
[4] Wu J. W., et al., App. Phys. Lett. (2014) 105 (22), 222906
[5] Corallini S., et al., J. Phys. Chem. C (2015) 119 (21), 11447
[6] Ceretti M., et al., Crystals (2016) 6 (11), 146
[7] Corallini S., et al., Inorg. Chem. (2017) 56 (5), 2977
[8] Ceretti M., et al, Inorg. Chem. (2020) 59 (13) 9434

Neutron G(r) refinements for the cubic SSGO

Back to Table of contents

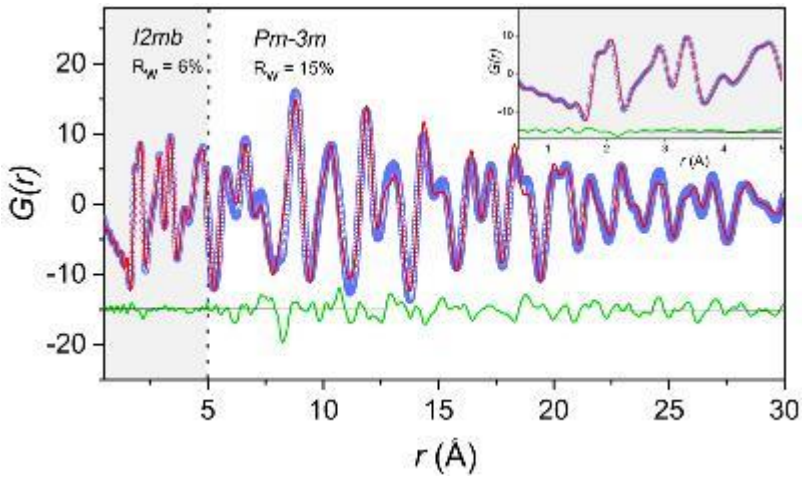

Back to Table of contents

MS17 Total scattering studies and disorder

MS17-04

Elucidating 2D Charge-Density-Wave Atomic Structure in an MX–Chain by the 3D-ΔPair Distribution Function Method

L. Guérin [1], T. Yoshida [2], A. Simonov [3], B. Toudic [1], S. Takaishi [4], M. Yamashita [4]
[1]Rennes 1 University - Rennes (France), [2]University of Electro-Communications - Chofu (Japan), [3]ETH - Zurich (Switzerland), [4]Tohoku University - Sendai (Japan)

Abstract

Many solids, particularly low-dimensional systems, exhibit charge density waves (CDWs). In one dimension, charge density waves are well understood, but in two dimensions, their structure and their origin are difficult to reveal. Herein, the 2D charge-density-wave atomic structure and stabilization mechanism in the bromide-bridged Pd compound [Pd(cptn)2Br]Br2 (cptn=1R,2R-diaminocyclopentane) is investigated by means of single-crystal X-ray diffraction employing the 3D-Δpair distribution function (3D-ΔPDF) method. Analysis of the diffuse scattering using 3D-ΔPDF shows that a 2D-CDW is stabilized by a hydrogen-bonding network between Br− counteranion and the amine (NH2) group of the cptn in-plane ligand, and that 3D ordering is prevented due to a weak plane to plane correlation. We extract the effective displacements of the atoms describing the atomic structure quantitatively and discuss the stabilization mechanism of the 2D-CDW. Our study provides a method to identify and measure the key interaction responsible for the dimensionality and stability of the CDW that can help further progress of rational design.

References

L. Guérin, T. Yoshida, E. Zatterin, A. Simonov, D. Chernyshov, H. Iguchi, B. Toudic, S. Takaishi, and M. Yamashita, Elucidating 2D Charge-Density-Wave Atomic Structure in an MX–Chain by the 3D-ΔPair Distribution Function Method**, ChemPhysChem 23, (2022).

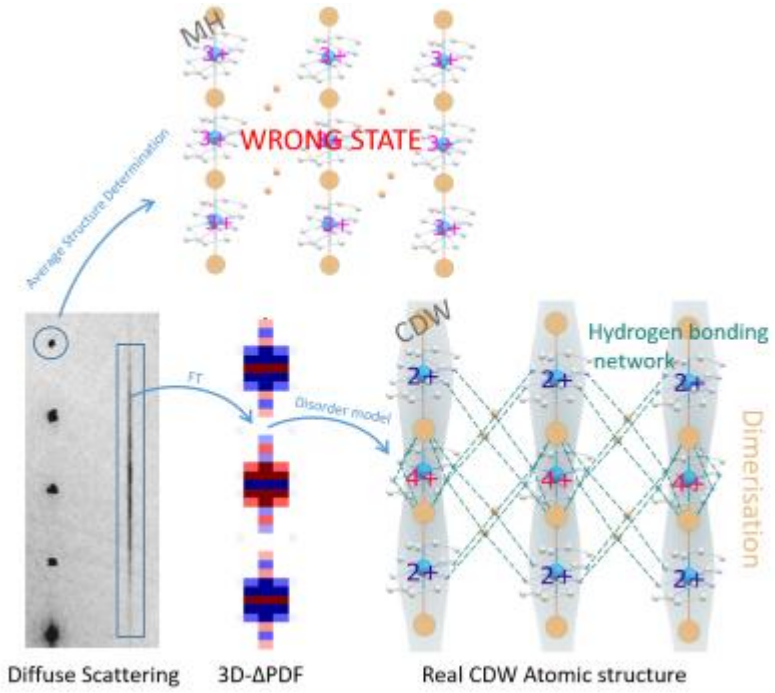

Back to Table of contents

MS17 Total scattering studies and disorder

MS17-05

Correlated linker disorder in a metal-organic framework

E. Meekel [1], A. Goodwin [1]
[1]*University of Oxford - Oxford (United Kingdom)*

Abstract

Having long focused on the elegant control possible over crystalline metal-organic framework (MOF) structures[1], the field is now increasingly exploiting the presence and nature of disorder in MOFs as an important design tool with which to tune their physical and chemical properties[2]. The objective of this work is to purposely introduce correlated disorder in a MOF structure and characterize the disorder by means of diffuse scattering and Monte Carlo modelling. Ultimately, we want to understand how to control disorder in MOFs, as well as how to systematically characterize disorder and how it can affect MOF properties.

Combining the low symmetry linker 1,3-BDC (BDC = benzene dicarboxylic acid) with a Zn salt resulted in TRUMOF-1. The structure is disordered both orientationally and occupationally (Fig. 1). Monte Carlo simulations confirmed the disorder to be correlated, extracting the local from the average structure. Further DFT studies indicate a correlation between the pore volume and energy, hinting towards the coupling of topological disorder and porosity percolation.

In conclusion, in this work we show how to approach the design of a correlated disordered MOF and successfully analyse its local structure by means of diffuse scattering and Monte Carlo simulations. Ultimately, DFT studies enabled us to show how the disorder directly translates to the pore network and thus porosity.

References

[1] O. M. Yaghi, et al., Nature, 2003, 423, 705–714.
[2] E. G. Meekel and A. L. Goodwin, CrystEngComm., 2021.

Fig. 1: TRUMOF-1 characterisation summary.

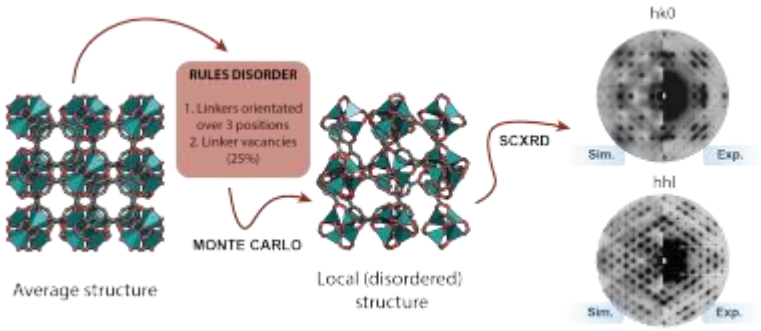

Back to Table of contents

MS18 Biomineralogy and bioinspired materials

MS18-01

The concomitant role of amorphous precursors and organic molecules in forming colorful single crystalline biominerals with convoluted porous structures

M. Albéric [1]
[1]*Sorbonne University - Paris (France)*

Abstract

Some biomineralized structures with intricate shapes and morphologies, such as the colorful skeletal elements of sea urchins grow via the deposition of hydrated amorphous calcium carbonate (ACC) that subsequently transforms in anhydrous ACC and finally crystallizes into single-crystalline calcite. Applying the heat-stimulated crystallization of remnant anhydrous ACC and destruction of intra-crystalline organic molecules in those biominerals, we evidenced by HR-XRD, calcite lattice distortions originating in strong atomic interactions at the organic-inorganic interfaces and showed by *in situ* heating SAXS measurements, the evolution of nano-pores, which likely compensate mineral volume shrinkage during ACC crystallization and organics removal.

Our results suggest that ACC crystallization proceeds as far as organics can serve as space-filling and accommodate for density changes due to the amorphous to crystalline transformation. Beyond that point, crystallization is hindered and ACC kinetically trapped within the biominerals in the form of thin layers. We propose that ACC thin layers are adjacent to the organic/inorganic interfaces and may serve as buffer layers between intracrystalline organics and crystalline calcite with elastic energy stored in the form of lattice strains.

In addition, studying *in vitro* ACC systems with pair distribution function analysis during heat induced crystallization we showed that water governs the local structural rearrangement prior to crystallization.

Finally, we are recently extending our approach to study the role of organic pigments in the biomineralization pathways of these colorful biominerals in which polyhydroxylated naphthoquinones are entrapped and may very well be involved in shaping these large single crystalline biominerals.

References

Albéric, M., Bertinetti, L., Zou, Z.Y., Fratzl, P., Habraken, W. Politi, Y. (2018a). The Crystallization of Amorphous Calcium Carbonate is Kinetically Governed by Ion Impurities and Water. Advanced Science, 5(5).

Albéric, M., Caspi, E.N., Bennet, M., Ajili, W., Nassif, N., Azais, T., Berner, A., Fratzl, P., Zolotoyabko, E., Bertinetti, L. Politi, Y. (2018b). Interplay between Calcite, Amorphous Calcium Carbonate, and Intracrystalline Organics in Sea Urchin Skeletal Elements. Crystal Growth & Design,18(4), 2189-2201.

Albéric, M., Zolotoyabko, E., Spaeker, O., Chenghao, L., Tadayon, M., Schmitt, C.N.Z., Politi, Y., Bertinetti, L., Fratzl, P. (2022). Heat-Mediated Micro- and Nano-Pore Evolution in Sea Urchin Biominerals. Crystal Growth & Design, https://doi.org/10.1021/acs.cgd.2c00083.

Back to Table of contents

MS18 Biomineralogy and bioinspired materials

MS18-02

Biomimetic and biological crystallization of amorphous precursors: from spherulites to functionally graded materials

S.E. Wolf [1]
[1]*Friedrich-Alexander University - Erlangen (Germany)*

Abstract
Biominerals are hybrid ceramics evolutionary honed to high-performance materials with exceptional damage tolerance. Their biosynthesis typically involves the biologically-controlled crystallization of transient amorphous precursors in a shape-preserving, thus “pseudomorphic” manner. Biominerals are often praised for their exquisite control over this process, as some biominerals are known to be (nearly) single-crystalline. While earlier studies highlighted the homogenous textures of specific biominerals, complex textures are far more widespread yet challenging to account for. Here, we propose that polycrystalline biominerals with textures gradually varying with depth can be interpreted as functionally graded materials that enhance their endurance against sharp and blunt contact damage by stress delocalization [1]. We further demonstrate that spherulitic transformation bio-inspired crystallization setup readily yields such complex texture in techniques if reaction parameters are well-controlled [2]. Ultimately, a closer look at the mechanistic preconditions for spherulitic growth and the ultrastructure of ACC [3] allows for a conceptional understanding of the underlying physicochemical processes.

References
[1] D Wallis, J Harris, CF Böhm, D Wang, P Zavattieri, P Feldner, B Merle, V Pipich, K Hurle, S Leupold, LN Hansen, F Marin and SE Wolf. Progressive changes in crystallographic textures of biominerals generate functionally graded ceramics. Mater. Adv. 3, 1527–1538 (2022). DOI: 10.1039/d1ma01031j
[2] J Harris, I Mey, M Hajir, M Mondeshki, and SE Wolf. Pseudomorphic transformation of amorphous calcium carbonate films follows spherulitic growth mechanisms and can give rise to crystal lattice tilting. CrystEngComm 17, 6831–6837 (2015). DOI: 10.1039/C5CE00441A
[3] SM Clark, B Colas, DE Jacob, JC Neuefeind, HW Wang, AK Soper, PI Schodder, P Duchstein, B Apeleo Zubiri, T Yokosawa, V Pipich, D Zahn, E Spiecker and SE Wolf. The nano- and meso-scale structure of amorphous calcium carbonate. Sci. Rep. 12, 6870 (2022). DOI: 10.1038/s41598-022-10627-9

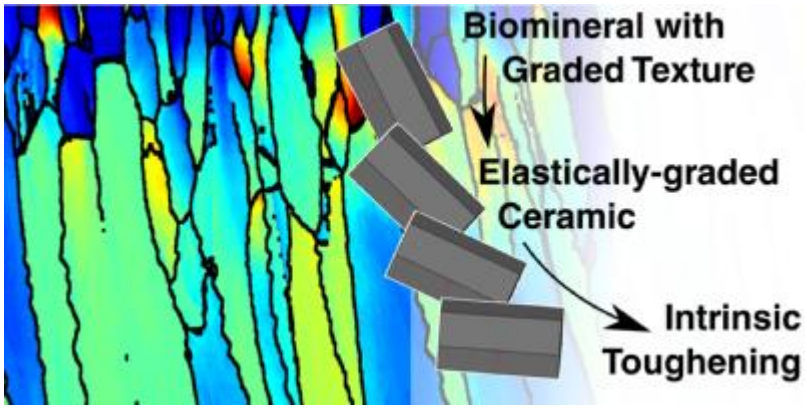

Back to Table of contents

MS18 Biomineralogy and bioinspired materials

MS18-03

Bio-inspired films of crystalline calcium carbonate: 2D patterning by surface-driven liquid-liquid phase separation and hybrid amorphous-to-crystal transformation.

C. Colas [1], T. Grunewald [2], F. Gobeaux [1], A. Campos [3], M. Burghammer [4], A. Baroni [5], P. Ferrand [2], V. Chamard [2], C. Chevallard [1]

[1]Université Paris-Saclay, CEA, CNRS UMR 3685 - Gif-sur-Yvette (France), [2]Aix-Marseille Univ, CNRS, Centrale Marseille, Institut Fresnel - Marseille (France), [3]Aix Marseille Univ, CNRS, Centrale Marseille, FSCM (FR1739), CP2M - Marseille (France), [4]European Synchrotron Radiation Facility - Grenoble (France), [5]Aix-Marseille Univ, CNRS, Centrale Marseille, Institut Fresnel - Marseille (France) - Marseille (France)

Abstract

Calcareous biominerals, widely found in the living world (shell, skeleton, vision device), present a great variety of forms and biological functions. They, however, gather a number of shared structural characteristics suggesting a common mechanism of formation. In particular, they are in their great majority, composed of a dense assembly of spheroidal crystalline nanoparticles,[1] while having crystalline properties close to those of a single crystal. The formation pathway of these complex materials is not fully established to date, triggering the interest of physico-chemists. As a matter of fact, an increasing amount of evidences suggests that non-classical crystallization involving disordered transient states[2,3] takes place during calcareous biomineralization. Namely, amorphous calcium carbonate has been reported in several aquatic mineralizing species, while the observed space-filling nature of the nanoparticles is suggestive of a mechanism involving a liquid precursor. To assess the relevance of such intermediate states during biomineralization of calcium carbonate, we have developed a model syntheses, involving dense liquid and amorphous phases,[4] further used to produce synthetic calcite crystals. In particular, transiently stabilized amorphous films were produced by exposure of a calcium and polyelectrolyte solution to gaseous carbon dioxide. The resulting films have a sub-micronic thickness and are composed of a dense arrangement of nanoparticles. A newly identified formation mechanism of the films is proposed, which corresponds to the formation of an interfacial 2D pattern by liquid-liquid phase separation, followed by the thickening of the pre-defined 2D pattern by the aggregation of amorphous nanoparticles formed in bulk. The observed peculiar 2D pattern, an assembly of micronic discs, is then used as a morphological marker to explore the crystallization processes triggered under three different conditions: exposure to a high relative humidity, to a high temperature, or during undisturbed aging at the air–solution interface. The investigation of the resulting 2D crystals, in terms of micro- and nanoscale morphologies, allows the determination of the amorphous-to-crystal transformation mechanisms related to each condition. Thus, the crystalline properties resulting from either solid/solid, or hybrid (dissolution/crystallization and solid/solid) transition are investigated and finally compared to those of biogenic crystals. In particular, Bragg ptychography[5] measurements reveal that the crystalline coherence length and the spatial distribution of crystalline defects (tilting and modification of the inter-reticular space) depend on the crystallization conditions. We show that crystals produced by solid-solid transformation in different conditions are not equivalent in terms of crystalline properties, and that they can, in specific conditions, show comparable values of crystalline deformation to the ones of the black lip pearl oyster Pinctada margaritifera.[5]

This work received funding from the European Research Council (European Union's Horizon H2020 research and innovation program grant agreements No 724881.

References

1. Wolf, S. E. et al. Nonclassical crystallization in vivo et in vitro (I): Process-structure-property relationships of nanogranular biominerals. Journal of Structural Biology 196, 244–259 (2016).
2. Gong, Y. U. T. et al. Phase transitions in biogenic amorphous calcium carbonate. PNAS 109, 6088–6093 (2012).

Back to Table of contents

3. Politi, Y. Sea Urchin Spine Calcite Forms via a Transient Amorphous Calcium Carbonate Phase. Science 306, 1161–1164 (2004).
4. Gower, L. B. & Odom, D. J. Deposition of calcium carbonate "lms by a polymer-induced liquid-precursor (PILP) process. Journal of Crystal Growth 16 (2000).
5. Mastropietro, F. et al. Revealing crystalline domains in a mollusc shell single-crystalline prism. Nature Materials 16, 946–952 (2017).

Back to Table of contents

MS18 Biomineralogy and bioinspired materials

MS18-04

Preferred orientation of freshwater shells of the species Sinanodonta woodiana and Anodonta anatina studied by neutron and X-ray diffraction

M. Kucerakova [1], J. Rohlicek [2], S. Vratislav [1], L. Kalvoda [1], K. Douda [3]
[1]Czech Technical University - Prague (Czech Republic), [2]Institute of Physics - Prague (Czech Republic), [3]Czech University of Life Sciences Prague - Prague (Czech Republic)

Abstract

Using neutron and X-ray diffraction, the texture of the prismatic and nacreous layer of several shells of the species Sinanodonta woodiana was studied and compared with the preferred orientation of the shells of the species Anodonta anatina. The shells of both molluscs were collected in freshwater streams in the Czech Republic. The neutronographic texture measurements were performed on the KSN-2 neutron diffractometer located at the research reactor LVR-15 in the Nuclear Research Institute, plc. Rez, Czech Republic. X-ray texture measurements were performed on a SmartLab Rigaku X-ray diffractometer (with Cu Kα rotating anode) located at the Institute of Physics of the Academy of Sciences of the Czech Republic. It was found that during the growth of the shell the a and b axes of aragonite are reoriented and the direction of the c-axis does not change alignment. The texture strength is increasing with the shell growth.

Back to Table of contents

MS18 Biomineralogy and bioinspired materials

MS18-05

Mg-rich nanoparticles within Mg-poor calcite matrices: from coralline red algae to a widespread phenomenon in Biomineralization

I. Polishchuk [1], N. Bianco-Stein [1], B.P.O.K.R. Pokroy [1]
[1]Technion - Haifa (Israel)

Abstract

In the course of biomineralization, organisms utilize various biostrategies to enhance the mechanical durability of their skeletons. In this research, we investigated the structure and chemical composition of high-Mg biomineralized tissues of several marine organisms. The case study of articulated coralline red algae unraveled that their high-Mg calcite cell wall nanocrystals are arranged in layers with alternating Mg concentrations and that this organization facilitates crack deflection, thereby preventing catastrophic fracture. (1-2) We also discovered that these nanocrystals contain incoherent Mg-rich nanoparticles which self-arrange periodically throughout the alga's mineralized cell wall. We further show the evidence of high-Mg calcite nanoparticles in the cases of six biologically different organisms belonging to different phyla and even kingdoms.(3) Our experimental results lead us to suggest that Mg-rich nanoparticles form via spinodal decomposition of the Mg-ACC precursor. Such decomposition is independent of the biological characteristics of the studied organisms but rather originates from their similar chemical composition and a specific Mg content within their skeletons, which generally ranges from 14 to 48 mol % of Mg. We establish that the presence of high-Mg nanoparticles embedded within lower Mg-calcite matrices is a widespread strategy utilized by various organisms to improve the mechanical properties of their high-Mg calcite skeletons. The valuable knowledge gained from this biostrategy significantly impacts the understanding of how biominerals, though comprised of intrinsically brittle materials, can effectively resist fracture.In the course of biomineralization, organisms utilize various biostrategies to enhance the mechanical durability of their skeletons. In this research, we investigated the structure and chemical composition of high-Mg biomineralized tissues of several marine organisms. The case study of articulated coralline red algae unraveled that their high-Mg calcite cell wall nanocrystals are arranged in layers with alternating Mg concentrations and that this organization facilitates crack deflection, thereby preventing catastrophic fracture. We also discovered that these nanocrystals contain incoherent Mg-rich nanoparticles which self-arrange periodically throughout the alga's mineralized cell wall. We further show the evidence of high-Mg calcite nanoparticles in the cases of six biologically different organisms belonging to different phyla and even kingdoms. Our experimental results lead us to suggest that Mg-rich nanoparticles form via spinodal decomposition of the Mg-ACC precursor. Such decomposition is independent of the biological characteristics of the studied organisms but rather originates from their similar chemical composition and a specific Mg content within their skeletons, which generally ranges from 14 to 48 mol % of Mg.(3) We establish that the presence of high-Mg nanoparticles embedded within lower Mg-calcite matrices is a widespread strategy utilized by various organisms to improve the mechanical properties of their high-Mg calcite skeletons. The valuable knowledge gained from this biostrategy significantly impacts the understanding of how biominerals, though comprised of intrinsically brittle materials, can effectively resist fracture.

References

1. Bianco-Stein N, Polishchuk I, Seiden G, Villanova J, Rack A, Zaslansky P and Pokroy B*. Helical Microstructures of the Mineralized Coralline Red Algae Determine Their Mechanical Properties. Adv Sci 2020; 7:2000108.
2. Bianco-Stein N, Polishchuk I, Lang A, Atiya G, Villanova J, Zaslansky P, Katsman A and Pokroy B*. Structural and Chemical Variations in the Calcitic Segments of Coralline Red Algae Lead to Improved Crack Resistance. Acta Biomater 2021; 130:362.

Back to Table of contents

3. Bianco-Stein N, Polishchuk I, Lang A, Portal L, Dejoie C, Katsman A and Pokroy B*. High-Mg calcite Nanoparticles within a Low-Mg Calcite Matrix: a Widespread Phenomenon in Biomineralization. PNAS 2022, DOI: 10.1073/pnas.2120177119.

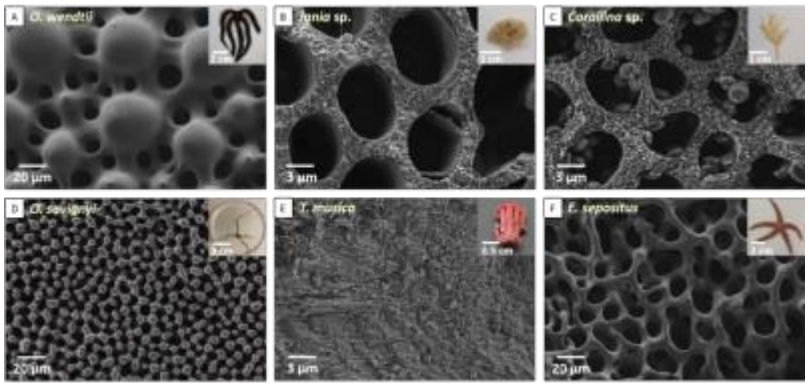

Back to Table of contents

MS19 Experimental and theoretical advances in quantum crystallography

MS19-01

Dynamic Quantum Crystallography – where are we now?

A.A. Hoser [1], A.Ø. Madsen [2]
[1]University of Warsaw - Warsaw (Poland), [2]University of Copenhagen - Copenhagen (Denmark)

Abstract

Nowadays we observe fast development of experimental diffraction techniques: new, strong X-ray sources and modern hybrid pixel detectors, enable the collection of the diffraction patterns with accuracy and precision about which no one dreamed a few years ago. It requires state of the art models to extract all information present in collected experimental results as the intensity of the diffracted beam depends on both: electron density and thermal motion. Whereas much work was done with the electron density modelling (e.g. Hansen-Coppens multipole model[1], Hirshfeld atom refinement (HAR)[2]), thermal motion description still requires improvements. Anisotropic displacement parameters usually do not attract attention and are treated as a dustbin for all experimental errors (there are only few remarkable exceptions).

Within dynamic quantum crystallography we reinstate thermal motion to its rightful place. We enrich the analysis of thermal motion in crystals with information from periodic DFT calculations. As a benefit we obtain hydrogen atoms ADPs and accurate thermodynamic properties (heat capacity, entropy) for molecular crystals, which are still difficult to obtain for purely from theoretical calculations.

In this contribution the normal mode refinement (NoMoRe) approach[3,4]: current developments, applications[5,6], and future directions will be presented.

References

1. N. K. Hansen and P. Coppens, Acta Crystallographica Section A, 1978, 34, 909-921.
2. S. C. Capelli, H.-B. Burgi, B. Dittrich, S. Grabowsky and D. Jayatilaka, IUCrJ, 2014, 1, 361-379.
3. A. A. Hoser and A. Ø. Madsen, Acta Crystallographica Section A, 2016, 72, 206-214.
4. A. A. Hoser and A. Ø. Madsen, Acta Crystallographica Section A, 2017, 73, 102-114.
5. A. A. Hoser, M. Sztylko, D. Trzybiński and A. Ø. Madsen, Chemical Communications, 2021, 57, 9370-9373.
6. A. A. Hoser, T. Rekis, A. Ø. Madsen, Acta Crystallographica Section B, 2022 - accepted

Free energies of pyrazinamide polymorphs.

Back to Table of contents

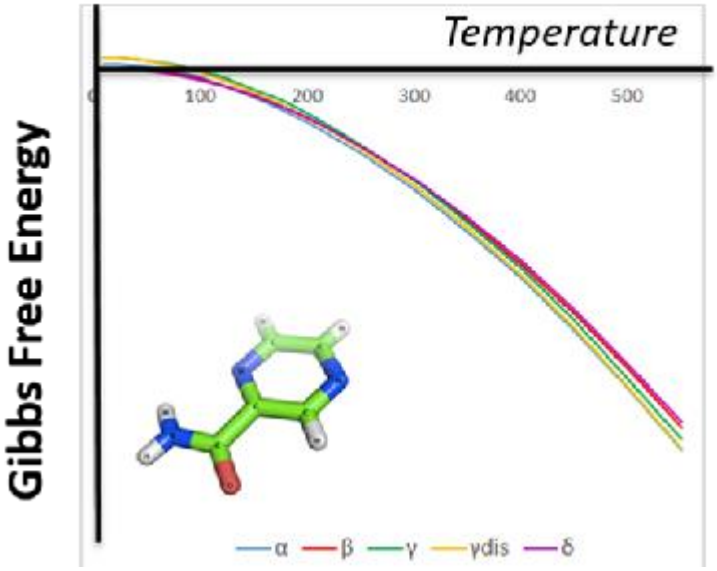

Specific heat capacity estimated for α-glycine.

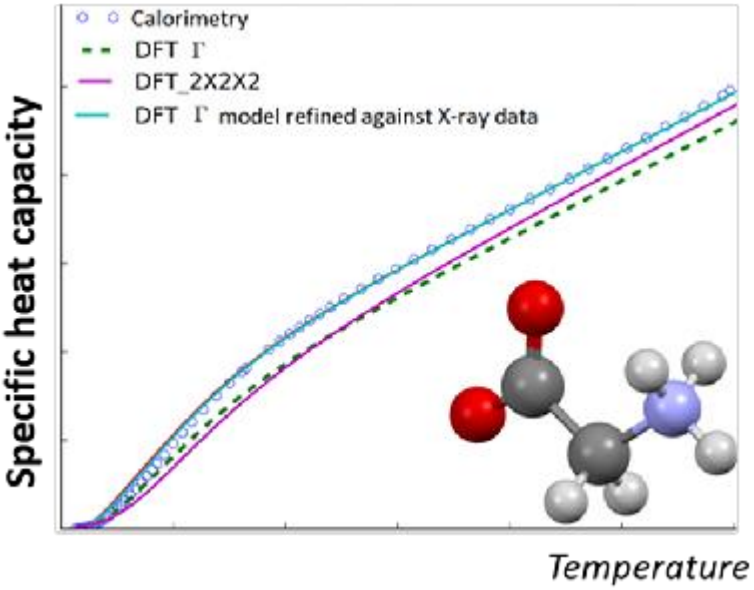

Back to Table of contents

MS19 Experimental and theoretical advances in quantum crystallography

MS19-02

Can we witness proteins traversing conical intersections via FEL-based crystallography?

T. Lane [1]
[1]*DESY - Hamburg (Germany)*

Abstract

Many photochemical reactions are thought to proceed via conical intersections, including biochemically mediated photochemistry. With the advent of hard x-ray free electron lasers, we have the ability to witness nuclear motions during conical intersection transversal with femtosecond and Ångström resolution. I will give a brief overview of the technical advances that have enabled this work, discuss why we think CIs play an important role in biology, and focus on one case study from my own work on photochemical DNA repair.

Back to Table of contents

MS19 Experimental and theoretical advances in quantum crystallography

MS19-03

X-ray diffraction - a suitable probe for superconductivity?

J. Langmann [1], G. Eickerling [1], W. Scherer [1]
[1]*Institute of Physics, University Augsburg - Augsburg (Germany)*

Abstract

X-ray diffraction (XRD) techniques clearly have their merits in superconductor research: Over the past years, they have provided valuable information on the atomic structure of superconducting materials as a basis for further experimental and theoretical work. Temperature-dependent XRD experiments have also helped to elucidate subtle structural rearrangements linked to the onset of superconductivity in low-dimensional compounds like *1T*-$TiSe_2$ [1] or high-T_c superconductors like $YBa_2Cu_3O_{7-\delta}$ [2].
But may the sensitivity of XRD to the (one-)electron density distribution in a crystal be leveraged to directly track not only structural but also electronic changes connected to the onset of superconductivity? Previous powder XRD work on the BCS superconductor MgB_2 seems to imply this: Analysis of experimental data at 15 K and at room temperature by means of the maximum entropy method (MEM) pointed out an accumulation of additional electron density at the locations of bond-critical points between the boron atoms in MgB_2 below $T_c \approx 39$ K [3].
Yet, the large temperature difference between the experiments and the model-free nature of MEM leave open questions about the precise physical origin of these findings. We therefore tracked electron density changes across T_c by collecting temperature-dependent single-crystal XRD data with high resolution and refining flexible multipolar models [4]. In this way, detected electron density differences (see figures) could be decomposed into contributions from changes in lattice parameters, dynamic or static atomic displacements or bonding-induced density shifts. It turned out that the increase of electron density at the location of the boron-boron bond-critical point upon cooling from room temperature to 13.5 K is rather related to changes in thermal smearing than to changes in bonding density. We could furthermore show that previous reports on magnesium vacancy concentrations in the range of 5 % in MgB_2 [5-8] may be related to the lacking flexibility of the independent atom model (IAM) to account for significant bonding-induced density shifts in the compound.

References

[1] Y. I. Joe *et al.*, Nature Phys. **10**, 421 (2014).
[2] J. Chang *et al.*, Nature Phys. **8**, 871 (2012).
[3] E. Nishibori *et al.*, J. Phys. Soc. Jpn. **70**, 2252 (2001).
[4] A. Fischer *et al.*, J. Phys. Chem. A **115**, 13061 (2011).
[5] A. Serquis *et al.*, Appl. Phys. Lett. **79**, 4399 (2001).
[6] H. Mori *et al.*, Phys. Rev. B **65**, 092507 (2002).
[7] V. Tsirelson *et al.*, Acta Cryst. **B59**, 575 (2003).
[8] N. D. Zhigadlo *et al.*, Phys. Rev. B **81**, 054520 (2010).

Observed electron density at 13.5 K.

Back to Table of contents

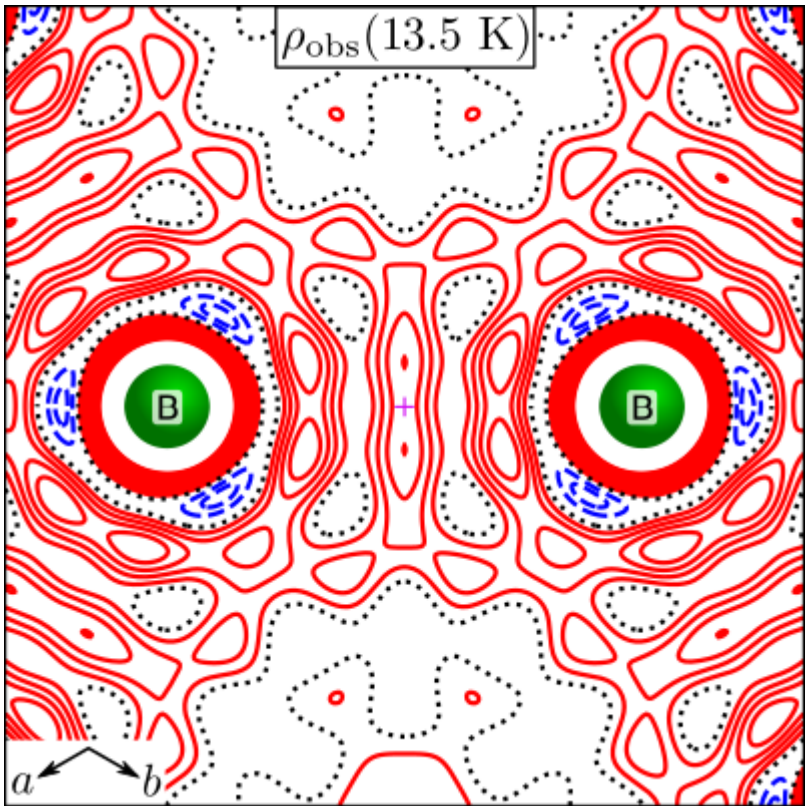

Observed electron density at room temperature.

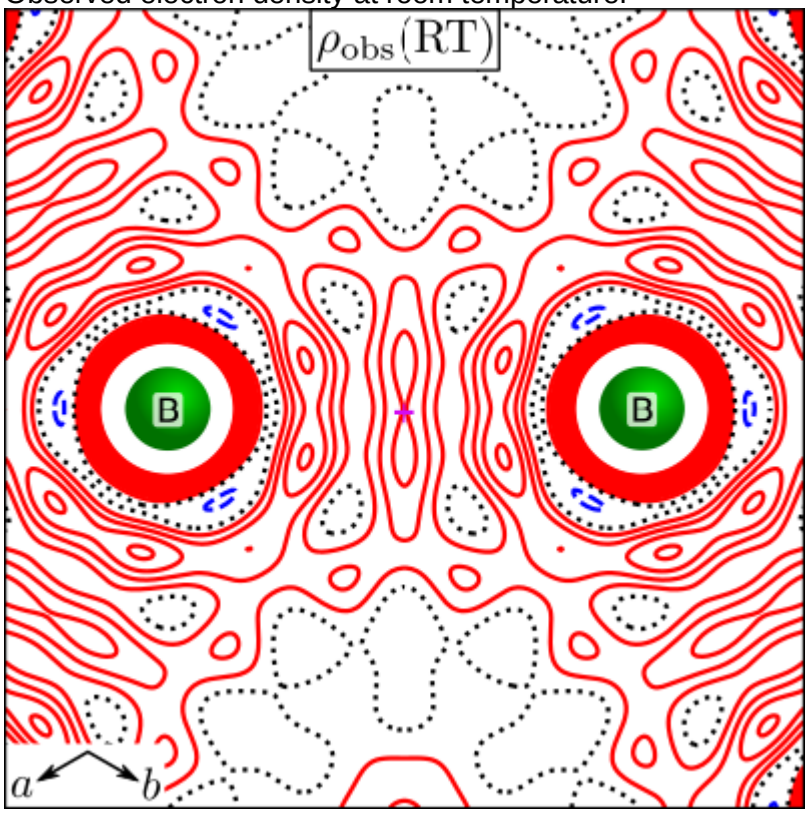

Back to Table of contents

MS19 Experimental and theoretical advances in quantum crystallography

MS19-04

Toward a total interaction potential from experimental transferred electron density

E. Mocchetti [1], C. Jelsch [1], C. Didierjean [1], B. Guillot [1]
[1]Université de Lorraine, laboratoire CRM2, UMR-CNRS 7036 - Nancy (France)

Abstract

The development of a fast, accurate and transferable model for the calculation of total interaction energy between two molecular charge densities has been a long-standing challenge in numerous research fields including quantum crystallography. For that, accurate but generally time-consuming quantum chemistry calculations have been performed and fast but often system specific empirical models have been developed. Here, we propose to base the interaction potential calculations on the knowledge of the charge density originated from X-ray diffraction data. In this purpose, the so-called Hansen and Coppens multipolar model [1] for the charge density has been used. In order to overcome the need of experimental diffraction data to refine the parameters of the density model, we transferred them from the ELMAM2 database [2]. This database provides atomic density parameters averaged over experimental molecular electron densities from high resolution X-Ray diffraction data, along with corresponding averaged atomic anisotropic polarizabilities. Thus, an accurate molecular charge density can be reconstructed, while accounting for the local environment thanks to the polarizabilities [3], in a very fast way. From this transferred charge density, we derived the total interaction energy divided into four terms, following the SAPT decomposition [4]. These terms include: an electrostatic (Coulombian) term, a dipolar induction (polarization) term, a dispersion term and a repulsion or exchange term. We designed each term with as few empirical parameters as possible to reproduce the SAPT reference data, using the benchmark database NENCI-2021 [5] for training and cross-validation. The electrostatic term, based on the unperturbed transferred charge density, needed no empirical parameter to reach a correlation coefficient R = 97% with the SAPT data. The dipolar induction term, based on the transferred atomic polarizabilities, reached with no fitted parameters a correlation up to R = 90%. For the dispersion term, we started from the London dispersion energy, which depends also on atomic polarizabilities. By introducing parameters for chemical species, we obtained a correlation of R = 98% for this dispersion term. It is well-known that the exchange energy is correlated to the density overlap, namely the integral of the product of interacting charge densities. Comparing these integrals to the SAPT exchange energies we already obtained a correlation about R = 92%. During this lecture, we will describe how we built these models based on the transferred electron density and show the details of the interaction energy results. Furthermore, this method would enable to compute accurately, in a fast and transferable way, the total intermolecular interaction energies in various systems such as organic dimers and crystals or protein-ligand complexes.

References

[1] Hansen, N. K., & Coppens, P. (1978). Testing aspherical atom refinements on small-molecule data sets. Acta Crystallographica Section A: Crystal Physics, Diffraction, Theoretical and General Crystallography, 34(6), 909-921.
[2] Domagała, S., Fournier, B., Liebschner, D., Guillot, B., & Jelsch, C. (2012). An improved experimental databank of transferable multipolar atom models–ELMAM2. Construction details and applications. Acta Crystallographica Section A: Foundations of Crystallography, 68(3), 337-351.
[3] Leduc, T., Aubert, E., Espinosa, E., Jelsch, C., Iordache, C., & Guillot, B. (2019). Polarization of Electron Density Databases of Transferable Multipolar Atoms. The Journal of Physical Chemistry A, 123(32), 7156-7170.
[4] Patkowski, K. (2020). Recent developments in symmetry-adapted perturbation theory. Wiley Interdisciplinary Reviews: Computational Molecular Science, 10(3), e1452.
[5] Sparrow, Z. M., Ernst, B. G., Joo, P. T., Lao, K. U., & DiStasio Jr, R. A. (2021). NENCI-2021. I. A large benchmark database of non-equilibrium non-covalent interactions emphasizing close intermolecular contacts. The Journal of Chemical Physics, 155(18), 184303.

Back to Table of contents

SAPT vs our ELMAM Model dispersion energies

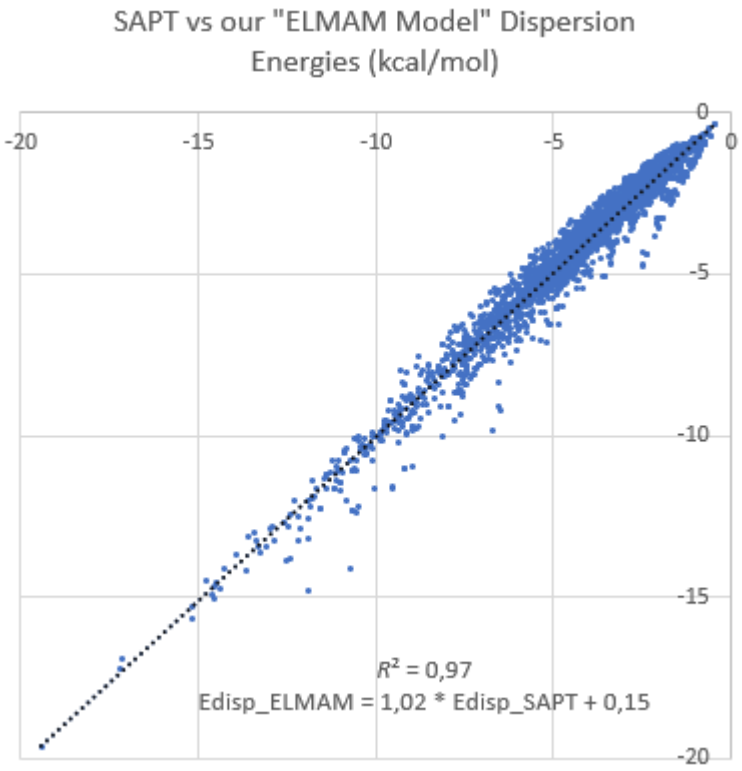

Back to Table of contents

MS19 Experimental and theoretical advances in quantum crystallography

MS19-05

Tackling anomalous X-ray scattering via Waller's dispersion formula

N. Peyerimhoff [1], F. Kleemiss [2], M. Bodensteiner [2], F. Meurer [2]
[1]Durham University - Durham (United Kingdom), [2]Regensburg University - Regensburg (Germany)

Abstract

In standard X-ray refinements, the effects due to anomalous dispersion are routinely mitigated using tabulated dispersion values (the real (dispersive) and imaginary (absorptive) parameters f' and f'') for each element. These tabulated values can be unreliable for X-rays with wavelengths near absorption edges and do not take any bonding into account.

One approach is to include these dispersion parameters as refinement parameters within the refinement process. This has recently been verified in [1] by comparison with an experimentally measured absorption spectrum for the determination of f'' and using the Kramers-Kronig relationship for the derivation of f'.

Another approach is to calculate the dispersion parameters f' and f'' quantum mechanically, for example, by employing Waller's dispersion formula [2]. Waller's dispersion formula takes excitation phenomena of electrons via the incoming X-rays into account, extending classical Thomson scattering. This method of deriving the contributions to the dispersion parameters from the electrons in the K- and L-shell of atoms (viewing them as hydrogen-like) has been discussed in the classical papers by Hoenl [3] and Eisenlohr-Mueller[4]. Mathematically this is done via the inclusion of energy-dependent matrix coefficients into the scattering moment.

The aim of this work is to extend the theorical aspects of the approach in [3,4] to the M-shell and to prepare the ground for a successful implementation in *Olex2*. By this approach, we will calculate specific dispersion parameters for each atom in any given structure. This is in some sense akin to modern refinement procedures in which specific form factors are calculated quantum mechanically, for example in Hirshfeld atom refinement (HAR) as implemented in *Olex2* via NoSpherA2 [5,6].

References

[1] F. Meurer, O. V. Dolomanov, Ch. Hennig, N. Peyerimhoff, F. Kleemiss, H. Puschmann, and M. Bodensteiner, Refinement of dispersion correction parameters in single-crystal structure determination, submitted.
[2] I. Waller, *Z. Physik*, vol. 51, **1928**.
[3] H. Hoenl, *Ann. Physik*, vol. 18, **1933**.
[4] H. Eisenlohr and G. L. J. Mueller, *Z. Physik*, vol. 136, **1954**.
[5] F. Kleemiss, O. V. Dolomanov, M. Bodensteiner, N. Peyerimhoff, L. Midgley, L. J. Bourhis, A. Genoni, L. A. Malaspina, D. Jayatilaka, J. L. Spencer. F. White, B. Grundkoetter-Stock, S. Steinhauer, D. Lentz, H. Puschmann, and S. Grabowsky, *Chem. Sci.*, vol. 12, **2021**.
[6] L. Midgley, L. J. Bourhis, O. V. Dolomanov, S. Grabowsky, F. Kleemiss, H. Puschmann, and Norbert N. Peyerimhoff, *Acta Cryst.*, vol A77, **2021**.

Back to Table of contents

MS20 Electric, opto-electronic and magnetic properties from elastic and inelastic scattering plus properties of materiels from quantum crystallography

MS20-01

Accessing the electronic structure and magnetism of linearly coordinated transition metal dopants with X-ray dichroism and resonant inelastic scattering

M. Baker [1]
[1]*The University of Manchester - Manchester (United Kingdom)*

Abstract

Lithium nitride (alpha-Li3N) is proven to be an excellent high symmetry (P6/mmm) host crystal to investigate the single-ion magnetism of linearly coordinated transition metal dopants [1]. Dopants, from Mn(I) through to Cu(I) can be hosted, occupying a linearly coordinated position between nitride ions (figure 1). The basic magnetic properties of the transition metal dopant series include remarkably large easy-plane (Mn, Co) and easy-axis (Fe and Ni) magnetic anisotropy[2]. Fe doped lithium nitride exhibits a magnetic coercivity field exceeding many rare-earth-based permanent magnets with a hysteresis that persists up to 16 K[3]. The magnetism of the series is found to be strongly influenced by 3dz2-4s hybridisation (figure 2). Direct access to 3d-4s mixing and metal-ligand bonding via π and δ channels can be resolved by X-ray absorption and magnetic circular dichroism for the late transition metals. However, for Fe, overlapping multiplet excitations inhibit clear spectral assignment. It is only via high-energy resolution 2p3d resonant inelastic scattering X-ray scattering measurements that access to 3dz2 mixing enhanced 4s excitations can be observed in Fe doped lithium nitride. The results provide a comprehensive interpretation of the electronic structure, bonding and magnetism of linearly coordinated single-ion magnets. Challenges associated with the precise study of single-ion dopants are shown to be ameliorated by the element sensitivity of X-ray absorption and inelastic scattering.

References

[1] M. S. Huzan, et al. Chem. Sci., 2020, 11, 11801.
[2] A. Jesche, et al. Phys. Rev. B 2015, 91, 18040(R).
[3] A. Jesche, et al. Nat. Commun., 2014, 5, 3333.

Figure 1

Back to Table of contents

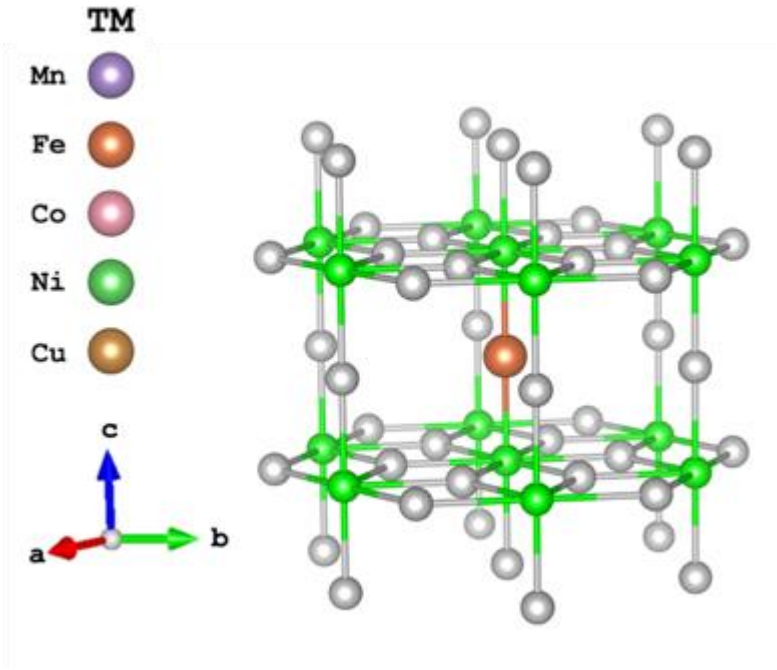

Figure 2

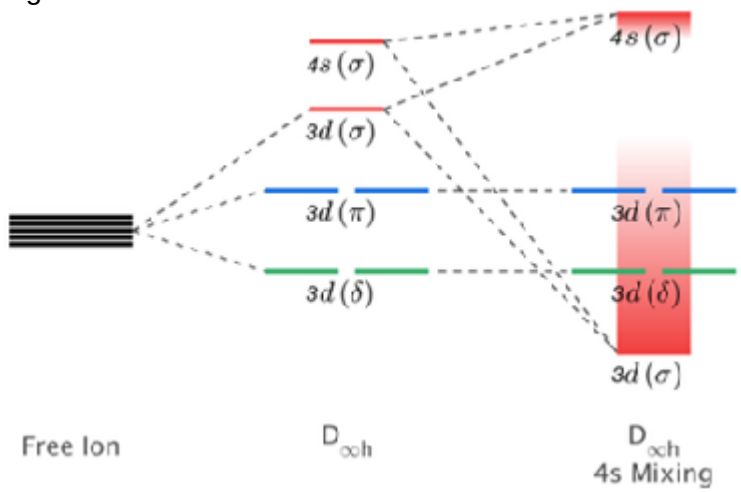

Back to Table of contents

MS20 Electric, opto-electronic and magnetic properties from elastic and inelastic scattering plus properties of materiels from quantum crystallography

MS20-02

Understanding the high-voltage crystallographic and electronic structure evolution in Li-ion battery cathodes through X-ray diffraction, scattering and spectroscopy

A. Sreekumar Menon [1], D. Walker [1], P. Thomas [1], L. Piper [1]
[1]*University of Warwick - Covertry (United Kingdom)*

Abstract

Increasing the nickel content of Li-M-O2 (M = transition metal) layered oxide cathodes in Li-ion batteries has led to the development of LiNi0.8Mn0.1Co0.1O2 (NMC811), which is touted to be a key player in the next-generation of electric vehicle batteries. NMC 811 is nearing industrial maturity when operated standard voltage window i.e. 3.0−4.2 V. Increasing the voltage window will further increase energy density by extracting more lithium ions but leads to rapid degradation associated with bulk structural and electronic changes together with surface oxygen loss. In the degradation regime, bulk O2- participate in the charge compensation but it remains unclear its role in driving degradation.

Here, we report on the latest in-house operando X-ray diffraction and the Ni K-edge X-ray absorption near-edge structure (XANES) studies of NMC811–Graphite LIB pouch cells built on the Battery Pilot Line at WMG (Warwick Uni.). This approach enables the synchronous tracking of the dynamic crystallographic and electronic structure changes in NMC811, specifically the collapse of the layered structure during delithiation and the associated changes in the Ni oxidation, over extended periods of cycling. We correlate the high voltage transformations with changes in the oxygen oxidation state using O K-edge resonant inelastic x-ray scattering in the regime where oxygen-loss induced degradation is pronounced.

Back to Table of contents

MS20 Electric, opto-electronic and magnetic properties from elastic and inelastic scattering plus properties of materiels from quantum crystallography

MS20-03

Experimental charge density and phase transition studies of a new hybrid perovskite: the complementarity between powder, single crystal diffraction and magnetic measurements.

N. Claiser [1], M. Souhassou [1], P. Durand [1], C. Lecomte [1], D. Luneau [2], A.S. Abdel-Rahman [3], S.K. Abdel-Aal [3]

[1]CRM2, Université de Lorraine - Nancy (France), [2]LMI, Université Claude Bernard Lyon1 - Lyon (France), [3]Physics department, Faculty of Science, Cairo University - Cairo (Egypt)

Abstract

Crystal structure of bis(1,2diamine propane) di-μ-chloro-bis[diaquadichloromanganate(II)] dichloride, is built as layers of centrosymmetric dinuclear units made of two (MnIICl4(H2O)2)- octahedra (figure 1) sharing one edge along the a direction and distributed in the basal ac plane. These doubly negative charged layers are separated along the b axis positively charged di-amine propane layers. Non-coordinated chloride anions make the electroneutrality and stabilize the structure through hydrogen bonds with coordinated water molecules, and the ammonium groups of organic layers. We modeled the experimental charge density based on high-resolution single crystal diffraction experiment in order to calculate the electrostatic properties of this material, explaining how the electrostatic interactions contribute largely to the stability of the structure.

Differential scanning calorimetry (DSC) reveal a two-step transition (main peaks at T= 366 K and T= 375 K) ascribed to the release of the coordinated water molecules. Meanwhile, SQUID magnetometry show very different magnetic behavior after the transitions. Below 346 K the temperature dependence of the product of the magnetic susceptibly with temperature (cT) is almost constant down to 10K (Figure 1). After heating up to 390 K the cT temperature dependence is no more constant but decrease rapidly with temperature. To understand such a change and using combined powder and single crystal diffraction experiments we investigate the determination of the high temperature resulting structure. This reveals that the dinuclear Mn(II) units rearrange in trinuclear Mn(II) units. This structural description is according perfectly with simulation of the magnetic behavior.

Figure 1. a) 3D view of the structures at 100K before (along the a axis) and after (along the b axis) high temperature h
b) Temperature dependence of magnetic behavior.

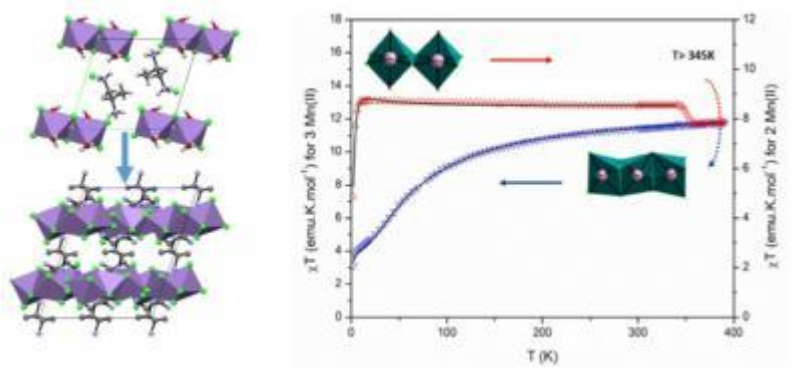

Back to Table of contents

MS20 Electric, opto-electronic and magnetic properties from elastic and inelastic scattering plus properties of materiels from quantum crystallography

MS20-04

Tuning the band structure and Van Hove singularity in $Sr_3Ru_2O_7$ via isovalent out-of-plane Ba doping

C. O' Neil [1], M. Pelly [1], A.J. Browne [2], B. Gade [2], D.A.F. Almeida [2], A.W. Rost [1], A.S. Gibbs [2]
[1]School of Physics and Astronomy, University of St Andrews - St Andrews (United Kingdom), [2]School of Chemistry, University of St Andrews - St Andrews (United Kingdom)

Abstract

The orthorhombic n = 2 Ruddlesden-Popper compound $Sr_3Ru_2O_7$ (structure see Fig. 1a) is a prime example of a strongly correlated oxide, displaying phenomena associated with a quantum critical end point and the formation of complex electronic phases [1,2] at high magnetic fields. The physics of this material is associated with an underlying Van Hove singularity in the band structure (a point at which, in general terms, there is a singularity in the density of states and the Fermi surface undergoes a topological transition, e.g. by different Fermi surfaces touching) [3]. Tuning the properties of $Sr_3Ru_2O_7$ has been pursued through a number of strategies including magnetic field, pressure, uniaxial strain and doping.

Here, we utilise isovalent Ba doping on the Sr sites as a chemical pathway to expand the lattice and increase the tolerance factor, driving the system closer to the tetragonal aristotype structure (Fig. 1b). Being an out-of-plane dopant, it is expected to minimally affect impurity scattering and thereby transport. Through detailed magnetisation and specific heat measurements, we have discovered a shift towards T = 0 K of the low-temperature specific heat peak known for the x = 0 compound $(Sr_{1-x}Ba_x)_3Ru_2O_7$. This suggests the Van Hove singularity crossing the chemical potential at approximately x = 0.08, with a subsequent sharp decrease in the density of states. We have investigated this further using high resolution neutron diffraction to probe the link between the crystal and electronic structure in this intriguing set of materials, allowing precise structure-property relationships to be obtained.

We will discuss the details of this tuning of the band structure via structural distortions. In particular we will show how such tuning can provide a clear pathway to increasing the strength and impact of the Van Hove singularity on the physics of $Sr_3Ru_2O_7$, and by extension Ruddlesden-Popper ruthenates in general [4].

References

[1] A. P. Mackenzie et al., Physica C 481, 207 (2012).
[2] C. Lester et al., Nature Communications 12, 5798 (2021).
[3] A. Tamai et al., Physical Review Letters 101, 026407 (2008)
[4] D.V. Efremov et al., Physical Review Letters 123, 207202 (2019)

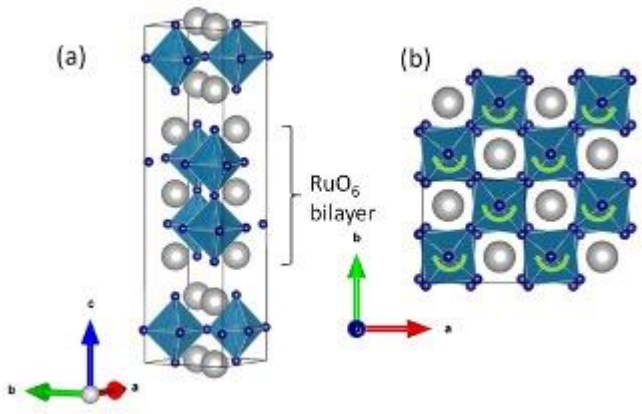

Back to Table of contents

MS20 Electric, opto-electronic and magnetic properties from elastic and inelastic scattering plus properties of materiels from quantum crystallography

MS20-05

Influence of non-covalent interactions on solid-state emission of halogenated diphenyl phosphanyl anthracenes

A. Krawczuk [1], T. Patten [1], S. Friedl [1], N. Graw [1]
[1]Georg-August Universität Göttingen - Göttingen (Germany)

Abstract

With applications in OLEDs, sensors, and field-effect transistors, organic solid-state luminescent materials have drawn a great deal of attention of the past two decades as alternatives to inorganic luminophores. One challenge still to overcome is the observed, dramatic quenching of their emission when passing from dilute solutions to solid-state. An avenue to reduce the quenching lies in intramolecular modification of a fluorophore or by controlling the formation of weak non-covalent intermolecular interactions in a crystalline phase, with halogenation as a potential modification. In certain chromophores, halogens atoms substituted along the heavy atom backbone promote intermolecular halogen bonding and, in turn, can increase the mixing of the singlet and triplet stated of the excited chromophore and enhance intersystem crossing.

In this work,[1] we present three newly synthesized halogenated anthracene derivatives, 9-PPh_2-10-Cl-($C_{14}H_8$) (**1**), 9-PPh_2-10-I-($C_{14}H_8$) (**2**) and 9-PPh_2-10-Br-($C_{14}H_8$) (**3**), that exhibit solid-state luminescence, enhanced by the presence of halogen atoms. By introducing halogen substituents, we observe a significant red-shift of emission when comparing to other photoactive non-halogenated anthracene derivatives.[2,3] In particular, for compound 3 a maximum emission wavelength of 452 nm was observed, whereas compound 1 was red-shifted to 552 nm (Figure 1). We will discuss the structure-property correlation in the studied systems supported by X-ray diffraction experiments and quantum crystallography tools with a special focus on C-X…π and X…X interactions (X=Cl, Br, I) considered as main driving force promoting Aggregation-Induced-Emission (AIE).

References

[1] T. Patten, N. Graw, S. Friedl, A. Krawczuk, D. Stalke, To be submitted, 2022; [2] T. Schillmöller, P. N. Ruth, R. Herbst-Irmer, D. Stalke, *Chem. Eur. J.*, 2020, **26**, 17390-17398; [3] T. Schillmöller, R. Herbst-Irmer, D. Stalke, *Adv. Optical Mater.*, 2021, **9**, 2001814.

Solid-state luminescence spectra of 1 and 3

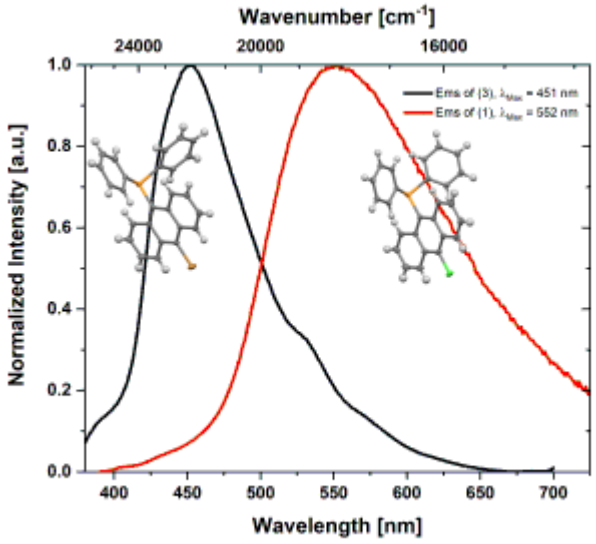

Back to Table of contents

MS21 Aperiodic crystals in organic and inorganic compounds and soft condensed matter

MS21-01

Commensurate and Incommensurate Superstructures in Rare Earth Metal Tellurides RETe2–δ

T. Doert [1], H. Poddig [1]
[1]*Technische Universität Dresden - Dresden (Germany)*

Abstract

The structures of the rare earth metal polychalcogenides $REX_{2-\delta}$ (*RE* = La-Nd, Sm; Gd-Lu; *X* = S, Se, Te; $0 \leq \delta \leq 0.2$) attracted some attention due to their distorted square planar chalcogenide layer and the motives observed within these layers. All structures share a common structural pattern, namely an alternating stacking of puckered [*REX*] and planar [*X*] layers, and are closely related to the ZrSSi structure (space group *P*4/*nmm*), which is regarded as their common aristotype [1].

For electronic reasons, the planar [*X*] layer shows distortions from a perfect square net, forming dianions X_2^{2-} for the non-deficient REX_2 compounds. By reducing the chalcogenide content, vacancies are observed within the planar layers, resulting in different commensurate or incommensurate superstructures for the $REX_{2-\delta}$ compounds depending on the vacancy concentration. The [*REX*] slabs are not involved in the internal charge re-balancing associated with the vacancy formation and, hence, merely change. For the sulfides and selenides we find additional X^{2-} anions along the vacancies to maintain a charge balanced [*X*] layer in $REX_{2-\delta}$. Tellurides, however, show different ordering patterns in the planar [Te] layer for the non-deficient $RETe_2$ compounds, but also a tendency to form larger anionic fragments for the deficient $RETe_{2-\delta}$ compounds, as seen for the commensurate structure of $GdTe_{1.8}$, e.g. [2].

$LaTe_{1.94}$ and $LaTe_{1.82}$ are two distinct examples of incommensurate crystal structures for $RETe_{2-\delta}$ compounds, differing in the number of vacancies in their planar [Te] layers [3, 4]. Both compounds share an average tetragonal unit cell with a ≈ 4.50 Å and c ≈ 9.17 Å, i.e. the structure of their common aristotype. The major difference between these compounds are their respective *q* vectors, which are compatible with tetragonal symmetry for $LaTe_{1.94}$, but indicate a loss of the fourfold rotational axis for $LaTe_{1.82}$, ending up in an orthorhombic superspace group. The [Te] layer of $LaTe_{1.94}$ is mainly composed of single vacancies (point defects), isolated Te^{2-} anions and Te_2^{2-} anions. $LaTe_{1.82}$ is more Te deficient and features adjacent vacancies in addition to linear Te_3^{4-} anions to guarantee charge balance.

References

[1] Doert, T. & Müller, C. J. (2016). Reference Modules in Chemistry, Molecular Sciences and Chemical Engineering, Elsevier.
[2] Poddig, H., Donath, T., Gebauer, P., Finzel, K., Kohout, M., Wu, Y., Schmidt, P. & Doert, T. (2018). Z. Anorg. Allg. Chem. 644, 1886–1896.
[3] Poddig, H., Finzel, K., Doert, T. (2020) Acta Crystallogr. Sect. C 76, 530–540.
[4] Poddig, H., Doert, T. (2020), Acta Crystallogr. Sect. B, 76, 1092–1099.

GdTe1.8: hk0.5 layer of the diffraction image.

Back to Table of contents

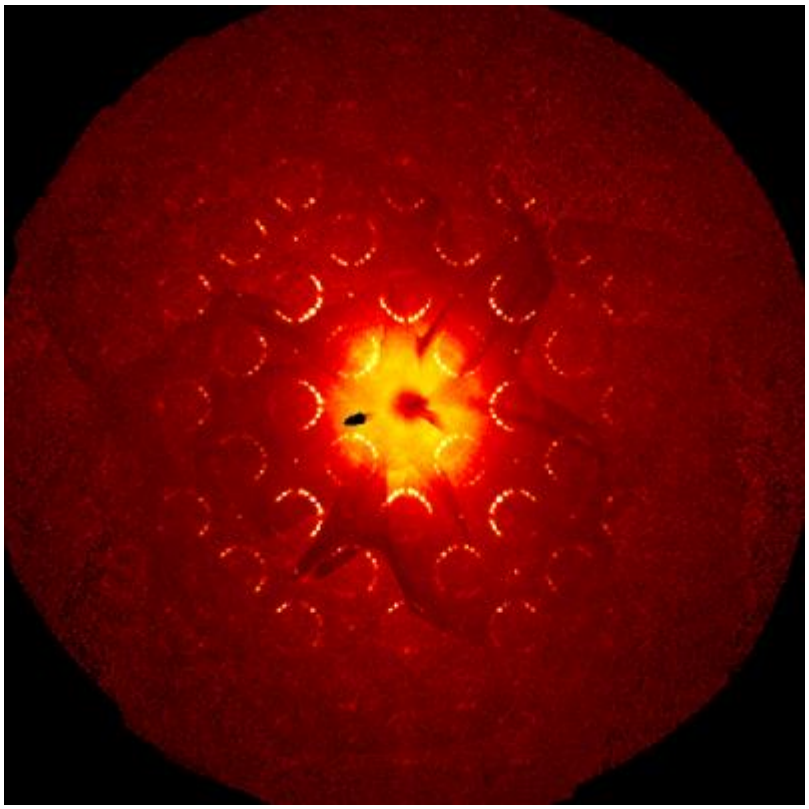

LaTe1.82: de Wolff sections through Te(2)

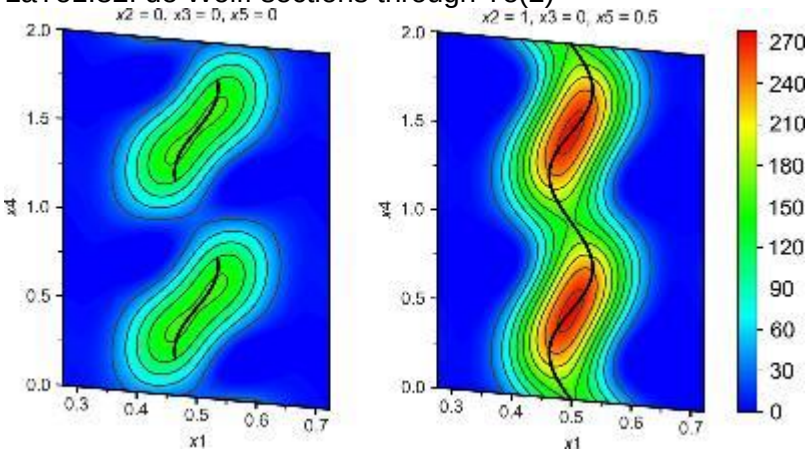

Back to Table of contents

MS21 Aperiodic crystals in organic and inorganic compounds and soft condensed matter

MS21-02

Symmetry breaking and short-range order in aperiodic urea inclusion crystals

P. Rabiller [1], A. Simonov [2], C. Mariette [1], L. Guérin [1], A. Bosak [3], B. Toudic [1]
[1]Univ. Rennes, CNRS, IPR - Rennes (France), [2]ETH Zurich, Mat. Dept. - Zurich (Switzerland), [3]ESRF - Grenoble (France)

Abstract

Here we will focus on the phase transitions and disorder within a prototype family of aperiodic compound n-alkane (n-CnH2n+2/urea), n varying from 7 (n-heptane) to 24 (n-tetracosane). A very rich sequence of phases is reported. All these phase transitions are described in terms of group/sub-group symmetry breaking within crystallographic superspace. Such phase transitions may either keep, decrease or increase the dimension of the crystallographic superspace This result shows the multiplicity of structural solutions that aperiodicity offers. For short-chain guest molecules (from octane to dodecane), diffuse scattering is present in the form of sharp 2D-layers, depicting para-crystal features. The strong modulation of diffuse scattering within these layers shows that the positions of alkane molecules in neighboring channels are correlated. Using the 3D-ΔPDF method, we have extracted the effective interaction potentials and have shown that the interaction is mediated by the relaxation of urea molecules.

References

A.Simonov, P.Rabiller, C.Mariette, L.Guérin, A.Bosak, A.Popov, and B.Toudic, Phys. Rev. B, in press.

(hk01) diffuse layer in n-octane-urea (exp & calc)

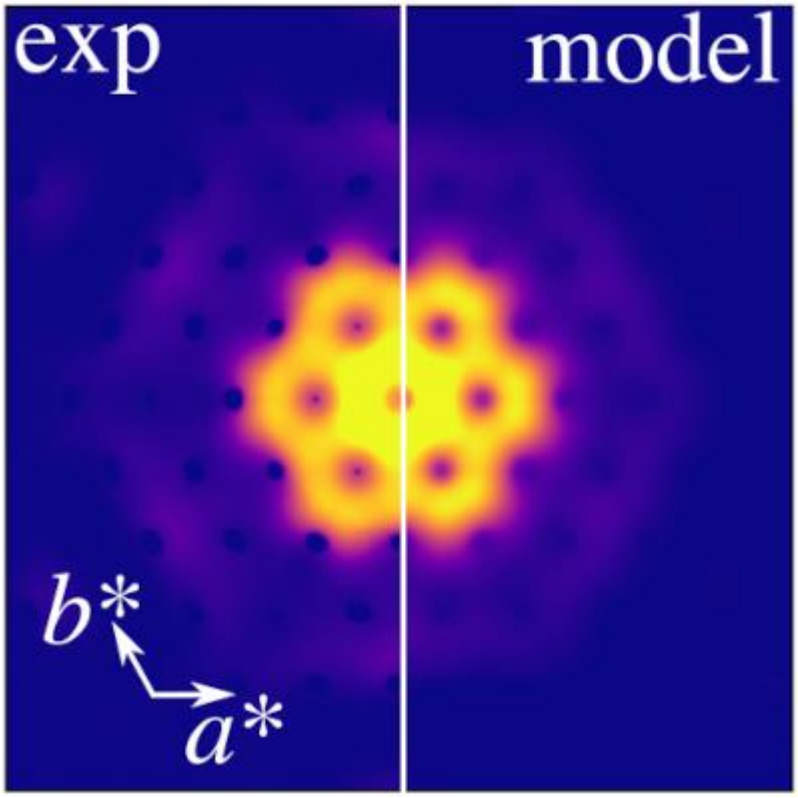

Back to Table of contents

MS21 Aperiodic crystals in organic and inorganic compounds and soft condensed matter

MS21-03

The importance of characterizing incommensurately modulated structures for the study of physical properties

A. Arakcheeva [1], A. Arakcheeva [1], A. Arakcheeva [1]
[1]Ecole Polytechnique Fédérale de Lausanne - Lausanne (Switzerland)

Abstract

The presentation focuses on the practical significance of the results of the study of different incommensurable modulated structures. Details of these studies can be found in the cited publications.

Layered transition metal dichalcogenides are usually classified as materials with quasi-two-dimensional metallic conductivity appearing in layered planes. It was shown that this rule does not hold for 1T-TaS_2, where the in-plane temperature (pressure) dependent conductivity is not metallic, whereas the out-of-plain one is metallic [1]. This phenomenon was explained on the basis of determining the incommensurately modulated crystal structures of 1T-TaS_2 at different temperatures and pressures [1].

The effect of the incommensurately modulated structure of iron-deficient $Fe_{1.35}Ge$ on the temperature dependence of its resistivity shows that a large number of ordered Fe-vacancies introduce strong backscattering similar to disordered structures. The $Fe_{1.35}Ge$ system is on the verge of the Mooij correlation [2]. A similar effect resulting in saturated metal resistivity is also observed for the $Sr_2Pt_{8-x}As$ incommensurately modulated structure [3].

The luminescence properties of $Na_xEu_{3+(2-x)/3}MoO_4$ scheelite-like structures were shown as a function of Eu-dimers occurring in their incommensurately modulated structure [4].

$Ba_4Fe_4ClO_{9.5-x}$ crystals, are interesting cases of tunable structure modulations [5]. The exact properties of these newly obtained compounds have not yet been studied, but they seem very promising.

The importance of methylammonium lead iodide, $MAPbI_3$, for solar cell development is well established. However, the properties of this compound are very sensitive to a phase transition around 330 K, which is expected to occur at the operating temperature of this compound. Cycling the compound around this temperature shows stabilization of an incommensurately modulated structure [6], which reduces the efficiency factor. This knowledge will allow appropriate operational adjustments to be made.

References

[1] Martino, E., Pisoni, A., Ćirić, L., Arakcheeva, A., Berger, H., Akrap, A., Putzke, C., Moll, P.J.W., Batistić, E., Tutiš,E., Forró, L. and Semeniuk, K. npj 2D Mater. Appl. 2020, 4, 7. https://doi.org/10.1038/s41699-020-0145-z.

[2] Jacimovic, J., Popcevic, P., Arakcheeva, A., Pattison, P., Pisoni, A., Katrych, S., Prsa, K., Berger, H., Smontar, A. and Forró, L. Journal of Alloys and Compounds, 2019, 794, 108. DOI 10.1016/j.jallcom.2019.04.159.

[3] Martino, E., Arakcheeva, A., Autès, G., Pisoni, A., Bachmann, M.D., Modic, K.A., Helm, T., Yazyev, O.V., Moll, P.J.W., Forró, L. and Katrych, S. IUCrJ, 2018, 5(4), 470. DOI: 10.1107/S2052252518007303.

[4] Arakcheeva, A., Logvinovich, D., Chapuis, G., Morozov, V., Eliseeva, S.V., Bunzlide, J.-C. G. and Pattison, P. Chemical Science, 2012, 3, 384. DOI: 10.1039/c1sc00289a.

[5] Arakcheeva, A., Bi, W.H., Baral, P.R. and Magrez, A., CrystEngComm., 2022, https://doi.org/10.1039/D1CE01657A.

[6] Glushkova, A., Mantulnikovs, K., Giriat, G., Semeniuk, K., Forró, L., Horvath, E. and Arakcheeva, A. Sol. RRL, 2019, 1900044. https://doi.org/10.1002/solr.201900044.

Sketch of the MAPbI3 transformation during cycling

Back to Table of contents

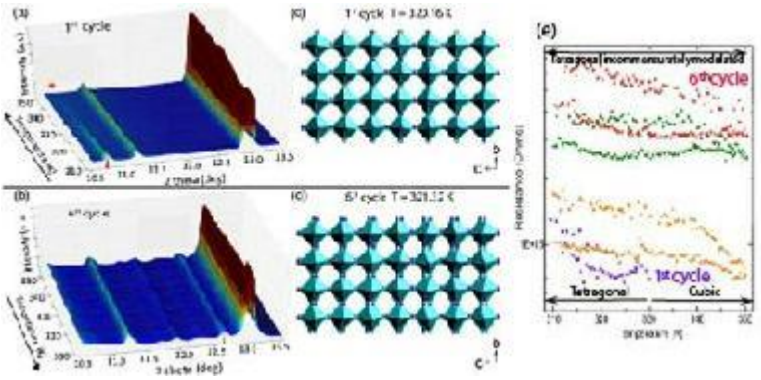

Back to Table of contents

MS21 Aperiodic crystals in organic and inorganic compounds and soft condensed matter

MS21-04

Fingerprinting Phason Strain

G. Nisbet [1], G. Beutier [2], M. De Boissieu [2], T. Yamada [3], H. Takakura [4]
[1]Diamond Light Source - Didcot (United Kingdom), [2]Univ. Grenoble Alpes, CNRS, SIMAP - Grenoble (France), [3]Department of Applied physics, Tokyo University of Science, - Tokyo (Japan), [4]Faculty of Engineering, Hokkaido University - Sapporo (Japan)

Abstract

Diffuse Multiple Scattering (DMS) [1] occurs in single crystals when an elastic internal divergent source of X-rays is subsequently scattered by diffracting planes. This source is provided by the diffuse scatter arising from a disruption in the long-range order of the crystal such as structural defects or crystal-surface truncation. DMS manifests as diffraction lines similar to Kossel lines which, unlike DMS line, arise due to fluorescence. The elastic nature of DMS lines means that multiple line intersections can be forced using synchrotron radiation by changing the incident energy [2].

The DMS pattern of the icosahedral quasicrystal is indexed using a 6 dimensional cubic reciprocal lattice (6 integer indices). The 6D reciprocal vector is expressed as the sum of the physical space component (3D) and the so-called perpendicular or phason component (3D). Any departure from the perfect icosahedral symmetry can be expressed in term of a strain of the 6D lattice along the ‘phason' component, using the so-called phason strain matrix [3].

By selecting a scattering geometry such that the 5-fold axis is perpendicular to the incident beam and parallel to the detector normal, a 5-fold pattern is observed. By selecting an appropriate energy or wavelength, 5 equivalent triple line intersections can be observed simultaneously. However, a departure from the icosahedral symmetry results in some of the intersections being split, providing a binary fingerprint for the presence of phason strain. Furthermore, precise determination of the phason strain can be achieved by fitting the DMS lines which only requires a few minutes of data collection. Because multiple projections are collected simultaneously without moving the sample, the technique offers high precision and flexibility in terms of crystal orientation and in situ experiments in the presence of various external stimuli.

References

[1] Nisbet, A. G. A., Beutier, G., Fabrizi, F., Moser, B. & Collins, S. P. Acta Cryst. A71, 20-25 (2015)

[2] A. G. A. Nisbet, F. Fabrizi, S. C. Vecchini, M. Stewart, M. G. Cain, T. Hase, P. Finkel, S. Grover, R. Grau-Crespo, and S. P. Collins Phys. Rev. Materials 5, L120601 (2021)

[3] Ted Janssen et al., Aperiodic crystals, Oxford University press, 2018

Back to Table of contents

MS21 Aperiodic crystals in organic and inorganic compounds and soft condensed matter

MS21-05

Charge-density waves in EuAl4 and SrAl4

S. Van Smaalen [1], S. Ramakrishnan [2], S. Rohith Kotla [1], T. Rekis [1], J.K. Bao [3], C. Eisele [1], H. Agarwal [1], L. Noohinejad [4], M. Tolkiehn [4], C. Paulmann [4], B. Singh [5], R. Verma [5], B. Bag [5], R. Kulkharni [5], A. Thamizhavel [5], B. Singh [5], S. Ramakrishnan [5]

[1]University of Bayreuth - Bayreuth (Germany), [2]Hiroshima University - Hiroshima (Japan), [3]Shanghai University - Shanghai (China), [4]Deutsches Elektronen-Synchrotron DESY - Hamburg (Germany), [5]Tata Institute of Fundamental Research - Mumbai (India)

Abstract

A charge-density wave (CDW) may develop in quasi-1-dimensional (1D) metallic crystals at low temperatures. It describes a modulation of the density of the conduction electrons and of the positions of the atoms according to a wave with a single modulation wave vector **q** [1]. The classical CDW is explained by the mechanism of Fermi-surface nesting (FSN), where **q** connects to each other different parts of the Fermi surface. The atomic displacements can be measured by x-ray diffraction (XRD). More recently, CDWs have been found in metals whose crystal structures and physical properties lack obvious 1D features [1, 2]. Mechanisms have been put forward, that provide alternative explanations for the formation of CDWs. In particular this includes **q**-dependent electron-phonon coupling (EPC).

Here, we present comprehensive studies towards the CDWs in the materials $EuAl_4$ and $SrAl_4$ with strong electron correlations [3,4]. Both materials crystallize in the tetragonal $BaAl_4$ structure type with space group I4/mmm. For $EuAl_4$ we have found that the incommensurate CDW has orthorhombic symmetry with superspace group Fmmm(0 0 s)s00 (No. 69.1.17.2), while the periodic basic or average structure remains tetragonal I4/mmm [3]. We will discus the mutual influence of CDW order and magnetism, as present in $EuAl_4$, and of the CDW without magnetism, as found in $SrAl_4$.

Acknowledgements: Single-crystal x-ray diffraction data were collected at Beamline P24 of PETRA-III at DESY, Hamburg, Germany. This research has been funded by the Deutsche Forschungsgemeinschaft (DFG, German Research Foundation)—No. 265092781, and the Alexander-von-Humboldt Foundation.

References

[1] Chen, C.-W., Choe, J. & Morosan, E. (2016). Charge density waves in strongly correlated electron systems. Rep. Prog. Phys. **79**, 084505.

[2] Ramakrishnan, S. & van Smaalen, S. (2017). Unusual ground states in $R_5T_4X_{10}$ (R = rare earth; T = Rh, Ir; and X = Si, Ge, Sn): a review. Rep. Prog. Phys. **80**, 116501. Doi: 10.1088/1361-6633/aa7d5f.

[3] Ramakrishnan, S., Rohith Kotla, S., Rekis, T., Bao, Jin-Ke, Eisele, C., Noohinejad, L., Tolkiehn, M., Paulmann, C., Singh, B., Verma, R., Bag, B., Kulkarni, R., Thamizhavel, A., Singh, B., Ramakrishnan, S., van Smaalen, S. (2022). Orthorhombic charge density wave on the tetragonal lattice of $EuAl_4$. IUCrJ, in press.

[4] Kaneko, K., Kawasaki, T., Nakamura, A., Munakata, K., Nakao, A., Hanashima, T., Kiyanagi, R., Ohhara, T., Hedo, M., Nakama, T., Onuki, Y. (2021). Charge-Density-Wave Order and Multiple Magnetic Transitions in Divalent Europium Compound $EuAl_4$. J. Phys. Soc. Jpn **90**, 064704.

Back to Table of contents

MS22 Complex order in magnetic materials

MS22-01

Variety and complexity of magnetic structures of rare earth-based nano-lamellar i-MAX phases

C. Colin [1], M. Barbier [2], T. Ouisse [2], E. Ressouche [3], Q. Tao [4], J. Rosen [4], R. Ballou [1], C. Opagiste [1], V. Petříček [5]

[1]Univ. Grenoble Alpes, CNRS, Grenoble INP, Inst. NEEL - Grenoble (France), [2]Univ. Grenoble Alpes, CNRS, Grenoble INP, LMGP - Grenoble (France), [3]Univ. Grenoble Alpes, Grenoble INP, CEA, IRIG-MEM - Grenoble (France), [4]Thin Film Physics Division, Department of Physics, Chemistry, and Biology (IFM), Linköping University - Linköping (Sweden), [5]Institute of Physics CAS - Praha (Czech Republic)

Abstract

MAX phases (where M is an early transition metal, A is an element of groups 13 to 16 and X is either C or N) make up a large family of nano-lamellar and quasi two-dimensional compounds, many of which remain to be discovered and understood. One of the most notable advances in the recent years has been the prediction and the synthesis of the magnetic (Mo2/3RE1/3)2AC series, called i-MAX phases, through partial substitution of Mo atoms by rare-earth (RE) elements [1-4]. The first interest of these phases is based on their layered structure in which bilayers of quasi-2D magnetic skewed triangular lattice overlay a Mo honeycomb arrangement and an A Kagomé lattice. The second interest is related to the fact that these phases display a wide range of magnetic characteristics. This results from intra and inter-planes exchanges caused by Ruderman-Kittel-Kasuya-Yosida indirect coupling mechanism of localized inner 4f-shell electron spins though the conduction electrons [2,5]. The interaction of the aspherical 4f orbitals with the CEF results in magneto-crystalline anisotropy and magnetization measurements performed on i-MAX single crystals revealed a strong anisotropy and interesting magnetic behaviors strongly dependent of the nature of the RE element included in the structure [5-6]. The confluence of oscillating RKKY couplings of 4f magnetic moments, competing interactions and CEF can then induce a complicated magnetic behavior, including incommensurability and metamagnetism.

We have determined the magnetic structures of several i-MAX phases with different rare earths by powder and single crystal neutron diffraction under magnetic field [6]. In this talk, I will present different cases, illustrating the wide variety of magnetic structures ranging from simple commensurate to rather complicated doubly modulated incommensurate magnetic structures that can be described in (3+2)D superspace group.

References

[1] A.S. Ingason, et al., J. Phys.: Condens. Matter. 28(43) 433003 (2016)
[2] Q. Tao, et al., Chem. Mater. 31, 2476−2485 (2019)
[3] A. Champagne et al., Phys. Rev. Mater. 3 053609 (2019)
[4] A. Petruhins et al., Mater. Res. Lett. 7 446–52 (2019)
[5] Q. Tao et al., J. Phys.: Condens. Matter. 34 215801 (2022)
[6] M. Barbier et al., Submitted

Back to Table of contents

MS22 Complex order in magnetic materials

MS22-02

Search for long-range magnetic order in icosahedral quasicrystals

R. Tamura [1]
[1]*Tokyo University of Science - Tokyo (Japan)*

Abstract

Since the discovery of QCs in 1984 [1], one of the fundamental issues in this field is to realize a long-range magnetic order in QCs, such as ferromagnetic and antiferromagnetic ones. In this respect, the discoveries of rare-earth (R) containing QCs, such as Zn-Mg-R [2], Cd-Mg-R [3] and Cd-R [4] i QCs, opened up a new field to investigate the magnetism of localized moments on a quasiperiodic lattice, and their magnetism has been extensively investigated. However, all the R containing QCs commonly exhibited a spin-glass behavior and no long-range magnetic order (LRMO) was observed. On the contrary, Tsai-type 1/1 approximants (ACs) were found to exhibit rich magnetic orders including ferromagnetic, antiferromagnetic and spin-glass states, which may suggest that LRMO is unfavored in a quasiperiodic lattice.

The magnetism of Tsai-type approximants has been extensively investigated for the last decade in order not only to gain insight into the magnetism of QCs but also to understand the magnetism of ACs itself. As a result, the magnetism of ACs has been found to be well classified by the average electron-per-atom (e/a) ratio [5]: The physical quantities such as the Weiss temperature (Qp) and Curie temperature (Tc) are well described by the e/a ratio. In addition, the study of the magnetism in the composition-tunable Tsai-type 1/1 ACs has helped us to understand and also predict the magnetism of Tsai-type QCs to considerable extent. The absence of the LRMO in the previously studied QCs is now partly understood by the fact that their e/a ratio happens to be located in the strongly frustrating region. Recently, new Au-Ga-R QCs were synthesized in the ferromagnetic region by the melt-spinning method and they were found to exhibit ferromagnetic transitions as expected [6], which is the first LRMO observed in i QCs.

Acknowledgements: This work was supported by JSPS KAKENHI Grant Numbers JP19H05817, JP19H05818, JP21H01044.

References

[1] D. Shechtman, et al., Phys. Rev. Lett. 53 (1984) 1951.
[2] Z. Luo, et al., Scr. Metall. Mater. 28, (1993) 1513.
[3] J. Guo et al., Jpn. J. Appl. Phys. 39 (2000) L770.
[4] A. I. Goldman, et al., Nat. Mater. 12, (2013) 714.
[5] S. Suzuki et al., Mater. Trans. 62, (2021) 298.
[6] R. Tamura et al., J. Am. Chem. Soc. 143, (2021) 19938.

Back to Table of contents

MS22 Complex order in magnetic materials

MS22-03

Revealing the faulted structure of α-FeB and its implications

F. Igoa [1], E. Defoy [1], G. Rousse [2], Y. Le Godec [3], D. Portehault [1]

[1]Sorbonne Université, CNRS, Laboratoire de Chimie de la Matière Condensée de Paris (LCMCP), Paris, France. - Paris (France), [2]Sorbonne Université, Collège de France, CNRS, Chimie du Solide et de l'Energie (CSE), Paris, France. - Paris (France), [3]Sorbonne Université, CNRS, Institut de Minéralogie, Physique des Matériaux et Cosmochimie (IMPMC), Paris, France. - Paris (France)

Abstract

Iron borides are a family of materials that has attracted considerable attention due to its properties relevant to the fields of powder metallurgy, magnetism, catalysis and metal-air batteries.[1] The compositions cover a wide range from Fe_9B to FeB_{49}, out of which Fe_2B and β-FeB outstand as well-described thermodynamic phases.[2] The **low temperature modification** of the former, so-called **α-FeB**, can be synthesized as **nanostructures** of different sizes and shapes, which has opened the door to the tailoring of specific properties.[2] For instance, nanosized α-FeB displays a very open magnetic hysteresis, in contrast to the soft ferromagnetism of β-FeB, relevant for applications in data storage.[3] A big problem for the fundamental research of α-FeB though, is the fact that **its structure is not well understood**, which obstructs results interpretation. The discord lies in the fact that the powder **diffractogram of α-FeB resembles that of β-FeB**, with the exception that **some Bragg reflections are missing** (Figure 1). Several **models** have been suggested to explain these features: (i) a point defect modification of β-FeB where the B and Fe atoms are exchanged, (ii) the crystallization in the CrB structure type of space group Cmcm and (iii) a **random stacking between CrB and β-FeB structure types**.[3] However, none of the models has been critically examined nor proved to reproduce an experimental diffraction dataset.

In the present work we have synthesized and deeply characterized the structure of α-FeB. All structure propositions are exhaustively analyzed. Electron microscopy images, shown in the inset of Figure 1, suggests the presence of stacking faults as the most plausible model. Indeed, while no accurate agreement was obtained for models (i) and (ii), model (iii) explains the experimental diffractogram. The **stacking faults model** was built on the basis of **4-layer types of β-FeB**, each corresponding to different origin choices, such that, depending on the stacking sequence, **β-FeB or CrB-type clusters are formed** (Figure 1 inset). The average interference wavefunction from each layer is computed by exploiting the recursive nature of the patterns found in randomized stacking sequence. The powder pattern is modeled as a function of the faults probability (p), as shown in Figure 2. It can be seen that for an intermediate faulted system, **the simulated pattern reproduces the corresponding absences** in the experimental diffractogram, thus **putting an end to the long-standing structural controversy**. Examples of the implications of the faulted structure for the chemical use of FeB will be discussed.

References

[1] Wei, Y., et al. J. Mater. Res. (2017), 32, 883. [2] Rades, S., et al. ChemPhysChem. (2011), 12, 1756. [3] Rades, S., et al. Chem. Mater. (2014), 26, 1549.

Figure 1.

Back to Table of contents

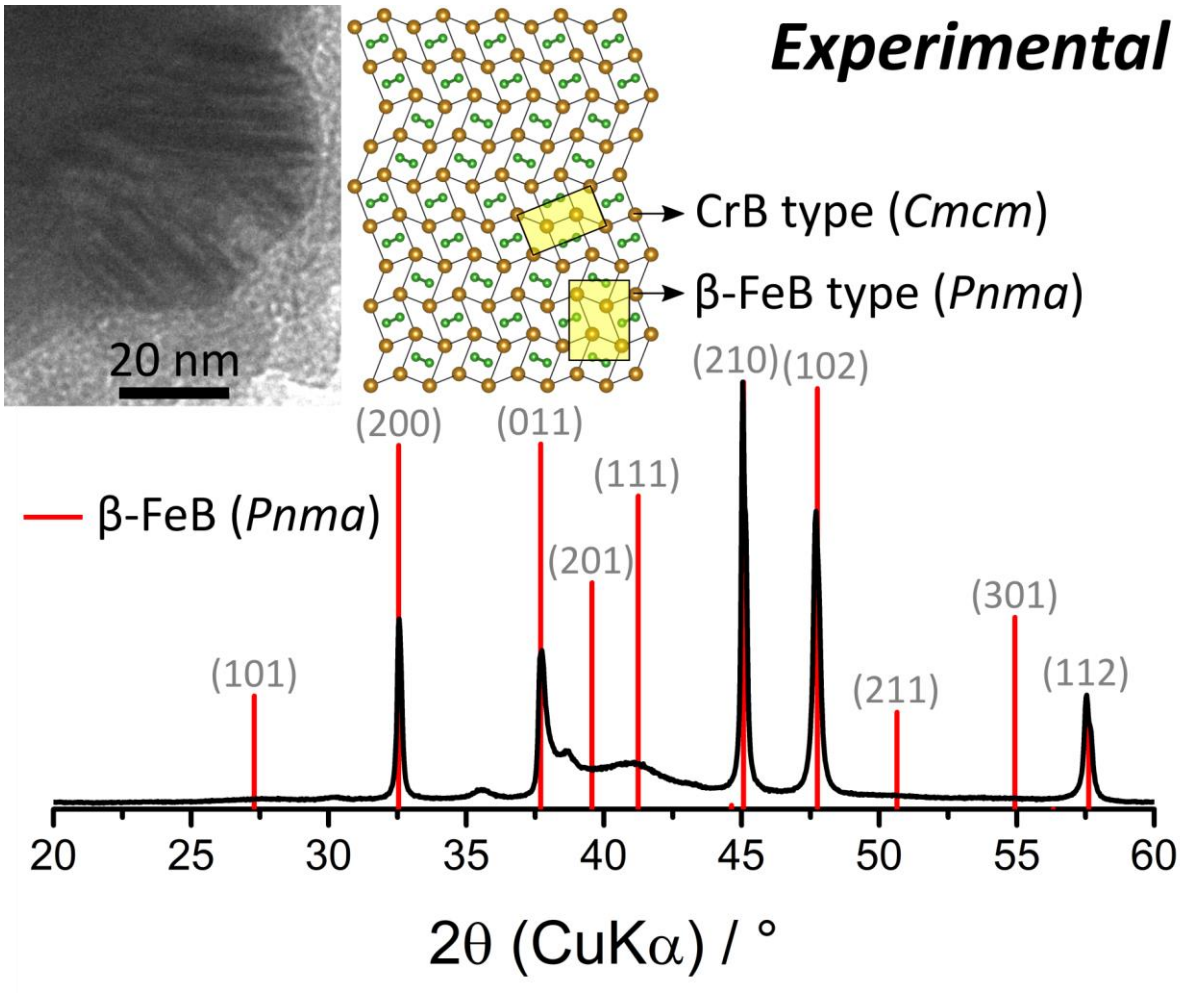

Figure 2.

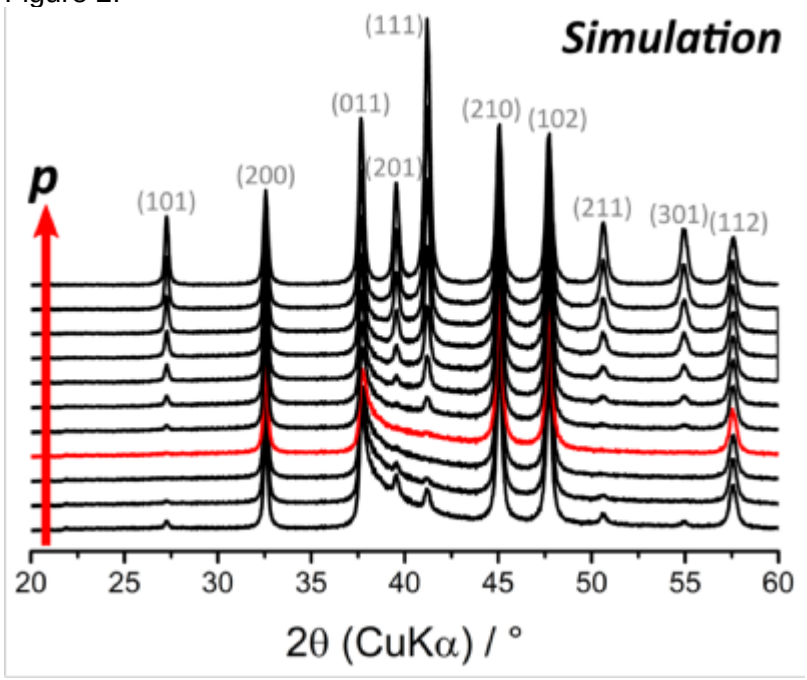

Back to Table of contents

MS22 Complex order in magnetic materials

MS22-04

Chemical solution deposited strongly oriented thin films with potential magnetoelectric effect

R. Kužel [1], J. Buršík [2], M. Soroka [2], J. Prokleška [1]
[1]Charles University, Faculty of Mathematics and Physics - Prague (Czech Republic), [2]Institute of Inorganic Chemistry of the Czech Academy of Sciences - Husinec-Rez (Czech Republic)

Abstract

Although bulk hexaferrites are known to exhibit strong magnetoelectric (ME) effects near room temperature, the same effects have not been realized much in a thin-film form.
The hexaferrite thin films of different phases (M, Y, W, X and Z) were prepared by chemical solution deposition method, and several processing parameters were tested and optimized with the aim of minimizing the amount of impurities that could spoil the magnetic properties of the final material. For the preparation of highly oriented ferrite films, several substrates were used, and different substrate/seeding layer/ferrite layer architectures were proposed [1]. The preparation of strongly oriented films appeared to be complicated for some of the phases. With respect to the ME effect, the Y and Z phases seem to be the most promising.
New Y-ferrite phases were prepared with the composition $BaSrZnCoFe_{11}(Me)O_{22}$ (Me = Al, Ga, In, Sc), and it was found that for Me = Al, Ga the magnetic structure is of noncolinear ferrimagnetic type with an unspecified helical magnetic structure. For Me = Ga this is a new system with potential ME effect. These films could be prepared with good out-of-plane and in-plane orientation directly on STO - SrTiO3(111) substrate, but M-phase seeding layer usually leads to better results.
The ME Z-type ferrite $Sr_3Co_2Fe_{24}O_{41}$ and $Ba_xSr_{3-x}Co_2Fe_{24}O_{41}$ thin films with strong out-of-plane and in-plane orientation were prepared and characterized for the first time [2]. In the former case, the analysis was complicated by the presence of M and S (spinel) phases that were also oriented (aligned with the substrate and with another). Consequently, many weak asymmetric reflections were overlapped and careful selection of reflections suitable for the analysis had to be made. The magnetization data show anomalies in the magnetic behavior occurring at temperatures close to the room temperature that are characteristic for collinear to noncollinear spin structure transitions. For the latter film, it has been found that the ME effect can be stronger for the oriented film, but still with some disorder, than for a single crystal [3].
XRD studies were performed by a combination of different scans to characterize both out-of-plane orientation and in-plane orientations. Strong out-of-plane orientations were found, and only basal (00l) reflections were available in symmetric scans. Therefore, the lattice parameters, profile analysis (crystallite size and strains), and residual stresses were studied by combination of several asymmetric reflections scanned at specific suitable angles of inclinations [4].

References

[1] R. Uhrecký, J. Buršík, M. Soroka, R. Kužel, J. Prokleška, *Thin Solid Films*, **622** (2017) 104-110.
[2] J. Buršík, R. Uhrecký, M. Soroka, R. Kužel, J. Prokleška, *Journal of Magnetism and Magnetic Materials*, **469** (2019) 245-252.
[3] Kwang Woo Shin, M. Soroka, Aga Shahee, Kee Hoon Kim, J. Buršík, R. Kužel, M. Vronka, M. Haydee Aguirre, *Advanced Electronic Materials*, (2022), 2101294.

Back to Table of contents

MS22 Complex order in magnetic materials

MS22-05

Charge density waves in the heavy fermion systems LaPt2Si2 and UPt2Si2: similar but different

Philipp Hans (Marseille, France)

/

Back to Table of contents

MS23 Quasicrystals and complex intermetallic materials

MS23-01

From honeycomb structures to 2D quasicrystals: Alkaline earth metal decorated Ti_2O_3 monolayers

S. Förster [1], S. Schenk [1], E. Cockayne [2], F. Wührl [1], L.V. Tran [1], M. Haller [1], O. Krahn [1], H. Meyerheim [3], M. De Boissieu [4], W. Widdra [1]

[1]Martin-Luther-Universität Halle-Wittenberg - Halle (Saale) (Germany), [2]National Institute of Standards and Technology - Gaithersburg (United States), [3]Max Planck Institute of Microstructure Physics - Halle (Saale) (Germany), [4]Universite Grenoble Alpes, CNRS, SIMaP - St Martin d'Heres (France)

Abstract

Honeycomb structures are two-dimensional networks with hexagonal symmetry. Most famous is the elemental honeycomb of graphene, but also binary honeycomb structures are well-known like h-BN, transition metal chalcogenides and binary oxides. Binary oxide honeycomb structures are characterized by six-membered rings formed from transition metal atoms, e.g. Ti or V, which are covalently linked via oxygen atoms. Expressed in a tiling decoration scheme, oxide honeycomb structures are represented by a unit cell containing two equilateral triangles, each decorated with one Ti atom in its center and oxygen atoms at the centeres of the sides as shown in Figure 1.

This talk bridges from binary oxide honeycomb structures to two-dimensional ternary oxide quasicrystals of dodecagonal symmetry that are formed from three tiling elements: equilateral triangles, squares and rhombuses [1]. The atomic structure of oxide quasicrystals has been under dispute in the past. By investigating a complex periodic quasicrystal approximant containing 48 triangles, 18 squares and 6 rhombusses (shown in Figure 2) we were able to decide between the competing structural models. Using scanning tunneling microscopy, surface x-ray diffraction and density functional theory calculations, we provide the experimental evidence that this extraordinary structure consists of an aperiodically ordered Ti_2O_3 network with rings of four, seven or ten Ti atoms (blue in Fig. 2) covalently linked via oxygens (red). These unfamiliar ring sizes are stabilized by the decoration with alkaline earth metal ions (green) [2]. The tiling decoration scheme derived from this model is able to explain the atomic structure of all experimentally observed periodic and aperiodic phases in two-dimensional ternary oxides and allows a classification of all structures according to their alkaline earth metal ion concentration[3].

Furthermore, we will show that an alkaline earth metal ion decorated honeycomb structure can be transformed into a dodecagonal oxide quasicrystal. This transition is accompanied with a workfunction change in the 2D oxide layer reporting on a change in the surface dipole induced by the alkaline earth metal ions in the two different geometries. The relation between honeycomb structures and dodecagonal oxide quasicrystals established here paves the way towards the exploration of new aperiodic two-dimensional oxide systems.

References

[1] S. Förster, K. Meinel, R. Hammer, M. Trautmann, and W. Widdra, Nature 502, 215 (2013).
[2] E. Cockayne, M. Mihalkovič, and C. L. Henley, Phys. Rev. B. 93, 026102 (2016).
[3] F. E. Wührl et al., Phys. Stat. Solidi B, 2100389 (2021).

Binary oxide honeycomb given as triangular tiling.

Back to Table of contents

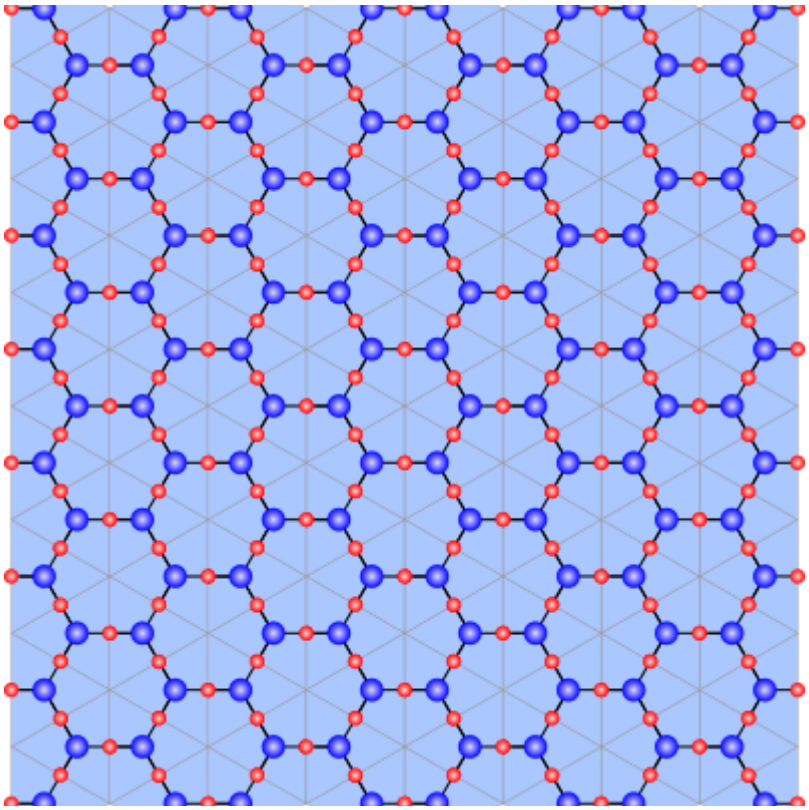

Unit cell of the 48:18:6 approximant in Sr-Ti-O.

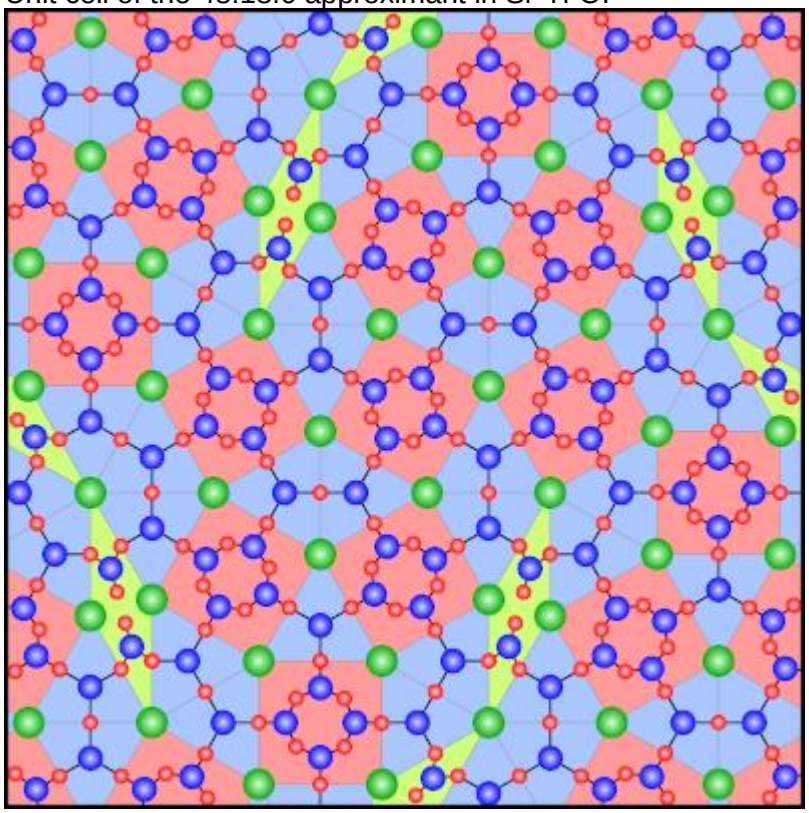

Back to Table of contents

MS23 Quasicrystals and complex intermetallic materials

MS23-02

Square-triangle tilings: an infinite playground for soft matter

M. Imperor [1]
[1]*CNRS - Orsay (France)*

Abstract

Regular square and triangle, two very simple geometrical figures, can be used to construct a fascinating variety of tilings which cover the 2D plane without any overlaps or holes. Such tilings are observed in many soft matter systems. We follow a geometrical approach based on the lifting of a tiling in a four-dimensional superspace. A classification of all possible globally uniform square-triangle phases is obtained by taking into account both the overall composition and the orientations of the two kinds of tiles [1]. Special square-triangle phases encountered in soft matter systems are described in this context: The Archimedean Σ and H phases, the striped phases and the 12-fold maximally symmetric phases. Geometrical constraints on boundary lines and junction points between domains of different compositions are predicted, a situation likely to be encountered in experimental and numerical studies.

Recent numerical simulations evidence new quasicrystal phases with octagonal symmetry [2]. They are observed in the self-assembly on a plane of a binary mixture of small and large hard spheres. Remarkably, the octagonal symmetry results from the association of three type of tiles: isosceles triangle combined with small and large squares. The relative concentration of the three tiles can be continuously varied by tuning the number of smaller spheres present in the system. Such octagonal quasicrystals open the way to a new family of square-triangle tilings.

References

[1] M. Impéror-Clerc, A. Jagannathan, P. Kalugin and J.-F. Sadoc, Soft Matter 17 (2021) 9560 – 9575 DOI: 10.1039/D1SM01242H

[2] E. Fayen, M. Impéror-Clerc, L. Filion, G. Foffi and F. Smallenburg, under review, arXiv:2202.12726v1

Back to Table of contents

MS23 Quasicrystals and complex intermetallic materials

MS23-03

(3+3)D incommensurately modulated structure of the τ phase in the Al-Cu-Zn system

M. Klementova [1], L. Palatinus [1], J. Bursik [2], O. Zobac [2]
[1]FZU - Institute of Physics of the Czech Academy of Sciences - Prague (Czech Republic), [2]Institute of Physics of Materials of the Czech Academy of Sciences - Brno (Czech Republic)

Abstract

Dural alloys based on the Al-Cu-Zn system are of great technological importance for superior mechanical properties. They also exhibit shape-memory effect [1]. Recently, phase equilibria in this system were experimentally studied [2]. At 400°C, a single-phase field was found, containing three structural modifications of the ternary phase τ: cubic CsCl structure (τC), related rhombohedral structure type (τR), and an unknown structure with incommensurate modulation (τi), which is the topic of this study.

A sample was prepared from pure elements in the 40Al:45Cu:15Zn ratio (at%), i.e. in the region of the phase τi. It was then melted in evacuated quartz-glass ampoules, annealed at 400 °C for 648 hours and quenched in water. Overall composition was measured by SEM-EDX and the structure was analyzed by powder XRD, which confirmed the ternary phase τi.

More detailed structural evaluation of the incomensurate structure τi was done by electron diffraction (3D ED) [3]. A thin lamella cut out with FIB as well as a crushed sample prepared under liquid nitrogene were investigated. Data were collected on an FEI Tecnai G2 20 transmission electron microscope operated at 200 kV with LaB6 cathode, equipped with an ASI Cheetah direct detection camera (512x512 pixels) using the continuous rotation approach (tilt range +/-50deg, step 0.25deg). The data were processed in the PETS software [4]. Structure solution and refinement were performed in the computing system Jana2020 [5]. The structure was solved by the charge flipping algorithm using the program Superflip [6].

The basic structure has cubic symmetry and it is of the CsCl type with lattice parameter a = 2.91(1) Å. The modulation is quite complex (Fig. 1a) consisting of three independent modulation vectors and a non-standard centering, which only effects the satellite reflections. The centering vectors are (0,0,0,0.5,0.5,0), (0,0,0,0.5,0,0.5) and (0,0,0,0,0.5,0.5). The corresponding (3+3)D superspace group is Xm-3m (a,0,0) (0,a,0) (0,0,a) with a=0.386. The simple CsCl-type structure, in this case with the sites occupied by Al and Cu, is modified by the addition of Zn on the Al-site and vacancies on the Cu-site. The number of the vacancies increases from 4at% in τC to 17at% in τR and it is likely the cause of the modulation. The modulation (Fig. 1b) is mostly occupational even though slight deviations from the average atomic positions are also visible (Al shown in grey, Cu in green, electrostatic potential in yellow).

References

[1] L. Gomidzelovic et al., Trans. Nonferrous Met. Soc. China 25 (2015) 2630.
[2] O. Zobac et al., J. Material Science 55 (2020) 10796.
[3] M. Gemmi et al., ACS Cent. Sci. 5 (2019) 1315.
[4] L. Palatinus et al., Acta Cryst. B75 (2019) 512.
[5] V. Petricek, M. Dusek, L. Palatinus, Z. Krist 229-5 (2014) 345.
[6] L. Palatinus and G. Chapuis, J. Appl. Cryst. 40 (2007) 786.
CzechNanoLab project LM2018110 funded by MEYS CR is gratefully acknowledged as well as the EXPRO project 21-05926X supported by the Czech Grant Agency.

(a) Reciprocal space sections, (b) structure model

Back to Table of contents

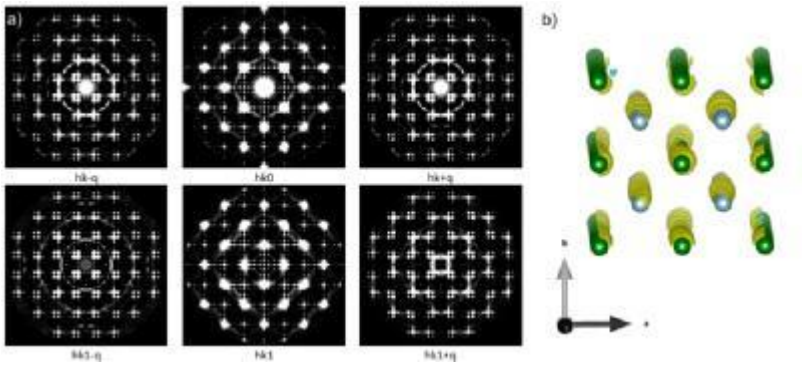

Back to Table of contents

MS23 Quasicrystals and complex intermetallic materials

MS23-04

Atomic Resolution Holography to Study the Local Structure in Quasicrystals

J.R. Stellhorn [1], K. Kimura [2], K. Hayashi [2], N. Happo [3], N. Fujita [4], S. Ohhashi [4], M. De Boissieu [5]
[1]Hiroshima University - Higashi-Hiroshima (Japan), [2]Nagoya Institute of Technology - Nagoya (Japan), [3]Hiroshima City University - Hiroshima (Japan), [4]Tohoku University - Sendai (Japan), [5]University Grenoble Alpes - Saint-Martin-d'Hères (France)

Abstract

The atomic-resolution holography (ARH) technique [1-3] offers the possibility to experimentally determine the local atomic-scale structure of complex systems. This method can selectively investigate specific elements and their 3-dimensional local atomic environment in a range of up to around 2 nm, without the need of *a priori* information on the structure. Therefore, it can provide a novel perspective for the visualization of the structure of aperiodic systems, like quasicrystals. Owing to the high complexity of the atomic arrangements in these systems, techniques targeted at the local atomic structure can provide valuable complementary information to understand the crystal chemistry (in addition to e.g. superspace crystallography approaches).

The local perspective of the structure by ARH provides an average view around a specific element in 3-dimensional space. In this presentation, we will show the recent developments for the ARH structure determination for decagonal and for Tsai-type icosahedral systems, in particular the evolution from approximant to quasicrystalline systems. Due to the 3D information available from ARH, we can for example distinguish between intra- and inter-cluster correlations of the icosahedral clusters. Some results from the investigation of a 2/1 approximant (AP) of the Ag-In-Yb system are illustrated in the figures below.

Fig.1: (a) The spherical hologram of a AgInYb 2/1 AP measured at 9.5 keV.
(b, c) 3D reconstructions of the ARH data, highlighting the atomic images related to the connections inside (blue) and between (purple) the Yb icosahedra, both having interatomic distances of about 5.7 Å.
(d) Structural view in real space along the pseudo-5-fold axis of the approximant.

References

[1] M. Tegze, G. Feigel, Nature 380 (1996) 49
[2] K. Hayashi et al., J. Phys.: Condens. Matter 24 (2012) 093201
[3] J. R. Stellhorn et al., Mater. Trans. 62, (2021) 342-349

Figure 1

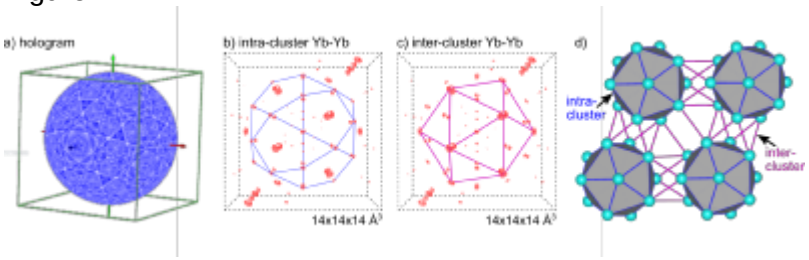

Back to Table of contents

MS23 Quasicrystals and complex intermetallic materials

MS23-05

4D crystallographic model for twisted homophase lilayers

M. Quiquandon [1], D. Gratias [1]
[1]CNRS UMR 8247 - PARIS (France)

Abstract

/

Back to Table of contents

MS24 3D electron diffraction

MS24-01

3D ED on epitaxial thin films

P. Boullay [1], S. Passuti [1], A. David [1], E. Rauch [2]
[1]CRISMAT, Normandie Université, ENSICAEN, UNICAEN, CNRS - Caen (France), [2]SIMAP, Grenoble INP, Université Grenoble Alpes, CNRS - Grenoble (France)

Abstract

Using strain engineering, metastable phases can be stabilized in the form of epitaxial thin films. Besides their intrinsically small diffracting volume, these films are clamped onto a thick crystalline substrate that significantly complicate their analysis by X-ray diffraction methods and usually prevents any structure determination of unknown complex phases stabilized in the form of thin films. Over the past decade, 3D Electron Diffraction (3D ED) [1] and, in particular, precession-assisted electron diffraction tomography (PEDT) has proven to be a powerful tool to address this challenge. To introduce the topic and the method, some results obtained on a series of Bismuth-based films [2,3] will be briefly outlined.

While challenging, the determination of unknown structures does actually not represent the primary need for epitaxial thin films. In most cases, the deposited materials have a known structure. The question is not to solve the structure but to know how it differs from a reference structure (bulk). In a second part, we will address the accurate structure refinement of our film based on the dynamical diffraction theory. Although this type of refinement is now well established for PEDT [4], we will be confronted here with a complication related to the microstructure of epitaxial thin films which generally resemble more polycrystalline samples with a strong texture than single crystals. The influence of the presence of oriented domains (twinned domains) on our ability to obtain relevant information about the structure of a film will be illustrated with results obtained on tilted perovskite films [5].

In the last part, we will present a 3D ED protocol adapted for a systematic analysis of epitaxial thin films with the use of scanning precession-assisted electron diffraction tomography (see 3D SPED approach already used for nanocrystalline microstructures analysis [6]). In this approach, a parallel electron nanobeam (typically less than 10nm) is scanned along the film growth direction in order to collect series of PEDT data as a function of film thickness for different tilt angles of the sample holder. This can be a line scan or an area scan which will allow us to extract relevant crystallographic information from a specific part of the film. This will be illustrated with our most recent results obtained on 35 nm thick PrVO3 films deposited on SrTiO3 [7].

The most recent results are obtained within the framework of the European project NanED (Electron Nanocrystallography – H2020-MSCA-ITN GA956099).

References

[1] M. Gemmi et al., “3D Electron Diffraction: The Nanocrystallography Revolution”, ACS Central Science 5 (2019) 1315-1329.
[2] L. Li, P. Boullay et al., “Novel Layered Supercell Structure from Bi2AlMnO6 for Multifunctionalities”, Nano Lett. 17 (2017) 6575-6582.
[3] L. Li, P. Boullay et al., “Self-assembled two-dimensional layered oxide supercells with modulated layer stacking and tunable physical properties”, Materials Today Nano 6 (2019) 100037.
[4] L. Palatinus et al., “Structure refinement using precession electron diffraction tomography and dynamical diffraction: tests on experimental data”, Acta Cryst. B 71 (2015) 740-751.
[5] G. Steciuk, A. David et al., “Precession electron diffraction tomography on twinned crystals: application to CaTiO3 thin films”, J. Appl. Cryst. 52 (2019) 626-636.
[6] E. F. Rauch et al., “New Features in Crystal Orientation and Phase Mapping for Transmission Electron Microscopy”, Symmetry 13 (2021) 1675.
[7] D. Kumar, A. David et al., “Strong Magnetic Anisotropy of Epitaxial PrVO3 Thin Films on SrTiO3 Substrates with Different Orientations”, ACS Appl. Mater. Interfaces 12 (2020) 356060-35613.

Back to Table of contents

MS24 3D electron diffraction

MS24-02

Using 3D-ΔPDFs from electron diffraction data to determine local structure

E.M. Schmidt [1], Y. Krysiak [2], P.B. Klar [3], L. Palatinus [3], A.L. Goodwin [4]
[1]University of Bremen - Bremen (Germany), [2]University of Hannover - Hannover (Germany), [3]Czech Academy of Sciences - Prague (Czech Republic), [4]Oxford University - Oxford (United Kingdom)

Abstract

Many functional materials have surprisingly simple average structures, but often partially occupied sites indicate disorder. To understand structure property relationships in complex ordered materials a description including local order is needed. Powder pair distribution functions are often used quantitatively to analyse the local structure of a material. While the experimental setup is very simple, the determination of three-dimensional local order principles requires complex modelling. Experimentally the analysis of single crystal diffuse scattering is more complex, but the recently established three-dimensional delta pair distribution function (3D-ΔPDF) is the perfect tool to map local deviations from the average structure and provides a straightforward interpretation of local ordering principles [1].

Here, we demonstrate how the 3D-ΔPDF can be obtained from electron diffraction data to understand the complete local structure of the high temperature ion conductor yttrium stabilized zirconia $Zr_{0.82}Y_{0.18}O_{1.91}$ (YSZ). YSZ crystallizes in the fluorite structure and shows composition disorder on both the metal and oxygen site. The substitution of Y^{3+} for Zr^{4+} on the metal site results in oxygen vacancies for charge compensation. Locally, O^{2-} ions relax towards the vacancies, while the metal-ions relax away from them.

Single crystals of YSZ were investigated with electron, X-ray and neutron diffraction. Highly structured diffuse scattering is observed alongside the sharp Bragg reflections (see Figure 1). By comparing the results from our electron ΔPDF to X-ray and neutron ΔPDFs we demonstrate the reliability of the 3D-ΔePDF (see Figure 2). A detailed analysis of the intensity distribution in the 3D-ΔPDF in the vicinity of the nearest neighbour inter-atomic vectors allows us to quantify the local structure relaxations.

To our knowledge, this is the first 3D-ΔePDF ever reported and this proof of principle is an important step towards the full description of a disorder model. This has important implications for the large variety of disordered materials of which single crystals for X-ray or neutron techniques are not available. In those cases, the 3D-ΔePDF will pave the way to understanding and tailoring physical properties.

References

[1] Weber, T., & Simonov, A. (2012). Z. Kristallogr., 227(5), 238-247.

hk0 layer

Back to Table of contents

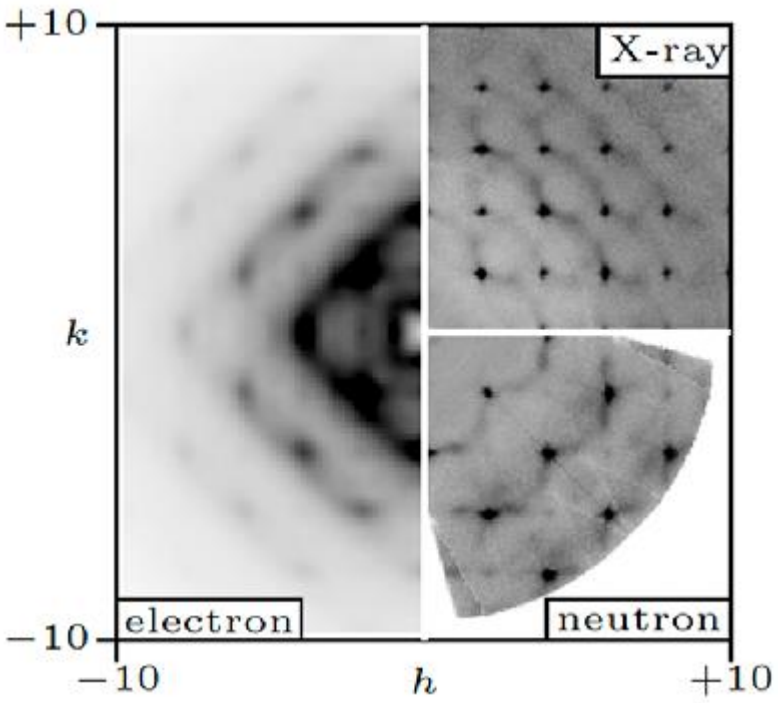

3D-ΔPDF in the ab0.25-layer

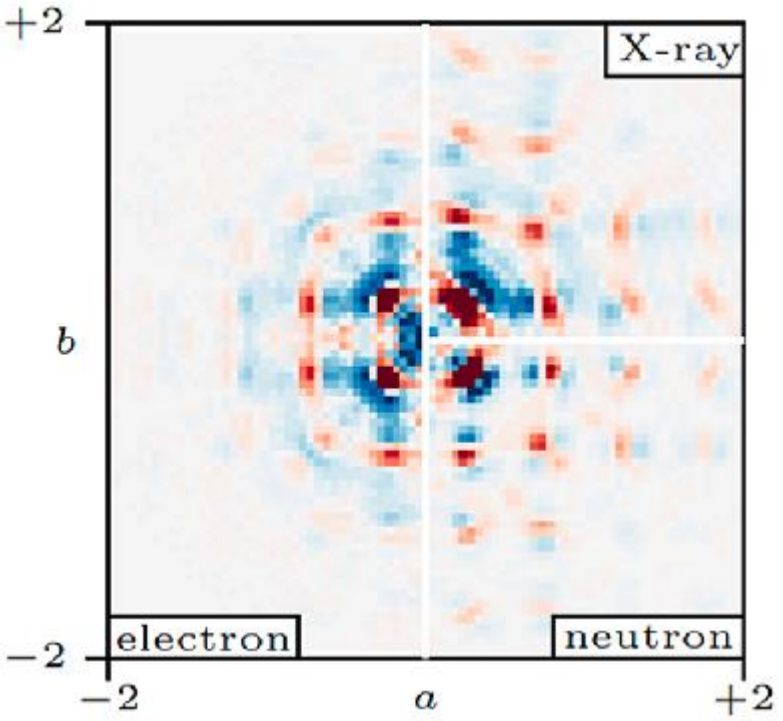

Back to Table of contents

MS24 3D electron diffraction

MS24-03

Single-Crystal Analysis of Nanocrystalline Materials: Revealing Details at Atomic Levels

Z. Huang [1]
[1]*Stockholm University - Stockholm (Sweden)*

Abstract

Porous crystalline materials, such as zeolites, metal-organic frameworks (MOFs), and covalent organic frameworks (COFs), have been widely used as absorbents, ion-exchangers, selective catalysts, etc. The unique properties of such materials are associated with their well-defined pores and channels of molecular dimensions. As three-dimensional (3D) arrangement of atoms, their chemical nature and connectivities determine the physical and chemical properties of a material. Knowing the precise structural information at an atomic level will not only help us fundamentally understand a material, but also predict its properties and guide the further development of new materials and technologies.

X-ray diffraction is the predominant technique used for structural determination of crystalline materials. However, challenges are remaining on the structural analysis of nanocrystalline materials which are too small to be studied by single crystal X-ray diffraction. Three-dimensional electron diffraction (3DED) has been developed to tackle the challenges. By taking advantage of the strong interaction between electrons and matter, 3DED allows single crystal structural analysis even when the crystal sizes are down to the range of nanometers[1]. This turns a polycrystalline powder into millions of analytes of single crystals. Moreover, with a short data collection time of 2-5 minutes per crystal, it is possible to analyze individual crystals in a high throughput manner and determine the structure of each tiny crystal.

Here, I give an example of using 3DED technique in high-throughput discovery of a new MOF material among a phase mixture[2]. The new MOF, ZIF-EC1, was discovered with a trace amount in a ZIF-CO3-1 material. Interestingly, the structure of ZIF-EC1 is rather dense, which is built by mono- and binuclear Zn clusters. This offers a high density of N and Zn, which are active sites for electrocatalysis. Furthermore, I will present our recent development by using 3DED to probe molecular motions in MOF nanocrystals, where different degrees of motions can be identified[3]. Last but not least, I will present using 3DED to directly locate guest molecules in open framework materials, where different configurations of the guest molecule can be identified ab initio and atom-by-atom. We believe that 3DED can be used as a powerful analytical tool for discovering new materials and revealing unique atomic properties, which could easily be extended to other crystalline materials.

References

[1] Z. Huang, T. Willhammar, X. Zou, Chem. Sci. 2021, 12, 1206–1219.
[2] M. Ge, Y. Wang, F. Carraro, W. Liang, M. Roostaeinia, S. Siahrostami, D. M. Proserpio, C. Doonan, P. Falcaro, H. Zheng, X. Zou, Z. Huang, Angew. Chem. Int. Ed. 2021, 60, 11391–11397.
[3] L. Samperisi, A. Jaworski, G. Kaur, K. P. Lillerud, X. Zou, Z. Huang, J. Am. Chem. Soc. 2021, 143, 17947–17952.

Back to Table of contents

MS24 3D electron diffraction

MS24-04

Characterization of the atomic structure of the Al79.5Mn16Pt4.5 R-phase by 3D electron diffraction

L. Meshi [1], S. Syniakina [1], B. Grushko [2]
[1]Department of Materials Engineering, Ben Gurion University of the Negev - Be'er Sheva (Israel), [2]Peter-Grünberg-Institut, Forschungszentrum Jülich - Jülich (Germany)

Abstract

An investigation of the Al-Mn-Pt alloys revealed an extension of the compositional region of the high-temperature "Al_3Mn" T-phase towards ~$Al_{79.5}Mn_{16}Pt_{4.5}$ [1]. The grains of the $Al_{79.5}Mn_{16}Pt_{4.5}$ T-phase, annealed at 800°C, contained nanometric plate-like inclusions [1], which were asserted to the so-called R-phase. Similar co-existence of the T and R phases was reported in the Al-Mn-Pd system at equivalent compositions ([2] and references therein). The precipitation of the R-phase from a supersaturated T-phase matrix was supposed to take place during cooling from the annealing temperature. The small size of the precipitates and their low fraction did not allow study of their structure. Investigation of the relevant Al-Mn-Pt alloys, annealed at 700 °C, confirmed the formation of the stable R-phase in a small compositional region around $Al_{79.5}Mn_{16}Pt_{4.5}$, its equilibrium with the T-phase of very close composition, and allowed to construct a partial 700°C isothermal section.
Regarding structural model of the R-phase, it is noteworthy to mention the $Al_{60}Mn_{11}Ni_4$ R-phase, which has been reported to exist in the Al-Mn-Ni system [3]. Although its presence was not confirmed in more recent Ref. [2], atomic model of this phase, proposed in [3], was found to be applicable to the Al-Mn-Cu R-phase. From another hand, this model did not fit the Pd and Pt containing R-phases. Latter is a subject of current investigation.
The atomic structure of the $Al_{79.5}Mn_{16}Pt_{4.5}$ R-phase was studied using the 3D electron diffraction (3DED) method. Its crystal structure was revealed as orthorhombic, C*mcm* (63), a = 7.730 Å, b = 24.035 Å and c = 12.597 Å. An atomic model of the R-phase was deduced using direct methods applied to the 3DED data and compared to that of the Al-Mn-Pt T-phase of very close composition. Some discrepancies between the present model and that of Ref. [3] were noted and explained.

References

[1] R. Tamari, B. Grushko, L. Meshi, J. Alloys Comp. 861 (2021) 158328. Structural study of $Al_{78}Mn_{17.5}Pt_{4.5}$ and (re)constitution of the Al–Mn–Pt system in its vicinity. https://doi.org/10.1016/j.jallcom.2020.158328
[2] B. Grushko, D. Pavlyuchkov, S.B. Mi, S. Balanetskyy, Ternary phases forming adjacent to Al_3Mn-Al_4Mn in Al–Mn–TM (TM = Fe, Co, Ni, Cu, Zn, Pd). J. Alloys Comp. 677 (2016) 148-162.
[3] K. Robinson, The determination of the crystal structure of $Ni_4Mn_{11}Al_{60}$, Acta Cryst. 7 (1954) 494-497. https://doi.org/10.1107/S0365110X54001570

Back to Table of contents

MS24 3D electron diffraction

MS24-05

Frame-based kinematical refinement: a way to quantify dynamical effects in 3D electron diffraction

L. Palatinus [1], P. Klar [1]
[1]*Institute of Physics of the CAS - Prague (Czech Republic)*

Abstract

3D electron diffration (3D ED) is a technique that allows single-crystal structure analysis from submicrometric crystals. However, the acuracy of the structure models is still lower than what is achievable from single-crystal x-ray diffraction. One way to improve the accuracy of the structure model is to use the dynamical theory of diffraction to calculate model intensities (so-called dynamical refinement, [1]). The extent to which dynamical diffraction effects are responsible for the lower accuracy of structure refinements that do not involve dynamical diffraction theory (so-called *kinematical refinement*) is a subject of an ongoing debate.

It is dificult to compare directly the kinematical and dynamical refinement, because they require different data processing. The main difference is that kinematical refinement allows averaging over symmetrically related reflections. In dynamical diffraction, the intensities depend on crystal orientation. Thus, each diffraction pattern (aka frame) needs to be treated separately, and symmetry-related reflections cannot be averaged. As a result of the different treatment of the data, the number of parameters and reflections is not the same in dynamical and kinematical refinement, and the figures of merit cannot be easily compared.

We developed a method to circumvent the problem [2]. The amount of multiple scattering depends on the scattering power of the atoms, and it is thus possible to decrease the dynamical scattering in the model calculation by lowering the occupancy of all atoms. In the limit of almost zero occupancy, the calculation corresponds to the case with essentially no dynamical diffraction effects. Such refinement, while involving kinematical diffraction, preserves the same number of reflections and refined parameters as a full dynamical refinement. As this refinement keeps the frame-specific data treatment, we call it frame-based kinematical refinement.

Figure 1 shows a plot of wRall for an inorganic mineral natrolite and an organic compound limaspermidine as a function of the occupancy reduction. Both structures are non-centrosymmetric, and therefore wRall for both the correct and inverted model are shown.

The results of the calculations lead to the following observations:

- The dynamical effects are present in the data even for organic, weakly diffracting materials. Their description, albeit with an approximate model assuming a perfect crystal, substantially improves the fit to the data.
- The improvement of the fit obtained by dynamical refinement over kinematical refinement is not due to the different data treatment, but indeed due to the description of the dynamical effects.
- Making the data "partially kinematical", i.e. progressively lowering the atomic occupancies, does not improve the fit. Thus, when the dynamical refinement does not fit the data perfectly, it cannot be improved by assuming that the diffraction is not entirely dynamical. Instead, a different, better model of the dynamical effects in an imperfect crystal is needed.

References

[1] Palatinus L., Petricek V., Correa C. A., Acta Cryst. A **71**, 235-244 (2015)
[2] Klar P, Krysiak Y, Xu H, Steciuk G, Cho J, Zou X, et al.,ChemRxiv 2021. doi:10.26434/chemrxiv-2021-4jh14 (2021)

wRall factors as a function of occupancy reduction

Back to Table of contents

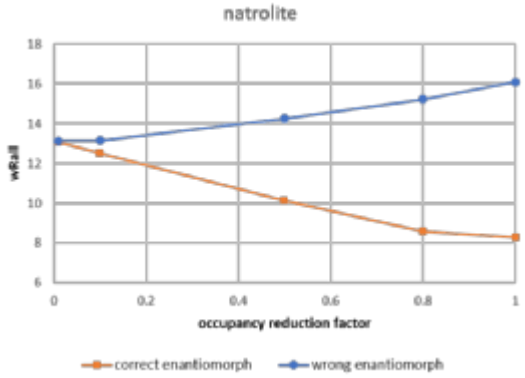

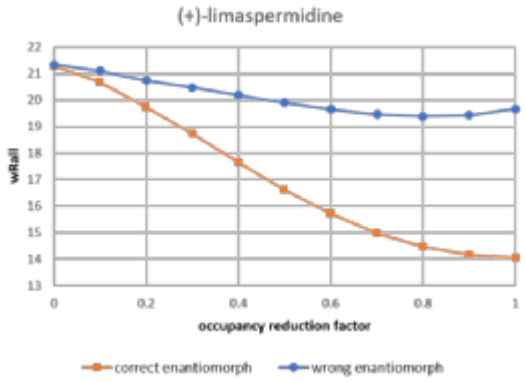

Back to Table of contents

MS25 3D electron diffraction for structure solution of organics and proteins

MS25-01

Serial Electron Diffraction: Strategies for Data Collection and Analysis

R. Bücker [1], P. Hogan-Lamarre [2], P. Mehrabi [3], E.C. Schulz [3], G.H. Kassier [4], R.J.D. Miller [2]
[1]Centre for Structural Systems Biology - Hamburg (Germany), [2]University of Toronto - Toronto (Canada), [3]University of Hamburg - Hamburg (Germany), [4]DESY - Hamburg (Germany)

Abstract

Serial electron diffraction (SerialED) [1] is an emerging three-dimensional electron diffraction (3D ED/MicroED) [2] method performed in a scanning transmission electron microscope (STEM), where, in analogy to fixed-target serial X-ray crystallography at XFELs or synchrotrons, data from a large ensemble of nano-crystals is merged into a high-resolution structure solution. The characteristics of electron diffraction, such as high interaction cross sections at relatively low inelastic energy deposition, and high sensitivity to hydrogens and charge states, are combined with the ability of serial data collection to provide virtually damage-free structures, pushing the boundaries of 3D ED to the smallest and most sensitive of crystals, and opening up new avenues towards time-resolved measurements.

Like its X-ray counterpart, SerialED is typically performed in the limit of rapidly acquired single or dose-fractionated diffraction snapshots, minimizing deleterious effects of radiation damage. However, the flexibility of a STEM enables a much broader range of data collection strategies, blurring the lines between serial crystallography (SX), momentum-resolved STEM (4D-STEM), and massively automated rotation electron diffraction [3].

I will present results from a range of highly radiation-sensitive biological and organic small-molecule samples, discuss approaches for collection, data processing [4] and sample preparation, and give an outlook on ongoing projects towards time-resolved SerialED and new sample classes.

References

[1] R. Bücker, et al., Serial Protein Crystallography in an Electron Microscope, Nature Communications 11, 996 (2020). S. Smeets, et al., Serial electron crystallography for structure determination and phase analysis of nanocrystalline materials, Journal of Applied Crystallography 51, 1 (2018).

[2] M. Gemmi, et al., 3D Electron Diffraction: The Nanocrystallography Revolution, ACS Central Science 5, 1315 (2019).

[3] B. Wang, X. Zou, and S. Smeets, Automated Serial Rotation Electron Diffraction Combined with Cluster Analysis: An Efficient Multi-Crystal Workflow for Structure Determination, IUCrJ 6, 854 (2019).

[4] R. Bücker, P. Hogan-Lamarre, and R. J. D. Miller, Serial Electron Diffraction Data Processing With Diffractem and CrystFEL, Front. Mol. Biosci. 8, (2021).

SerialED: (a) grid mapping; (b) data collection

Back to Table of contents

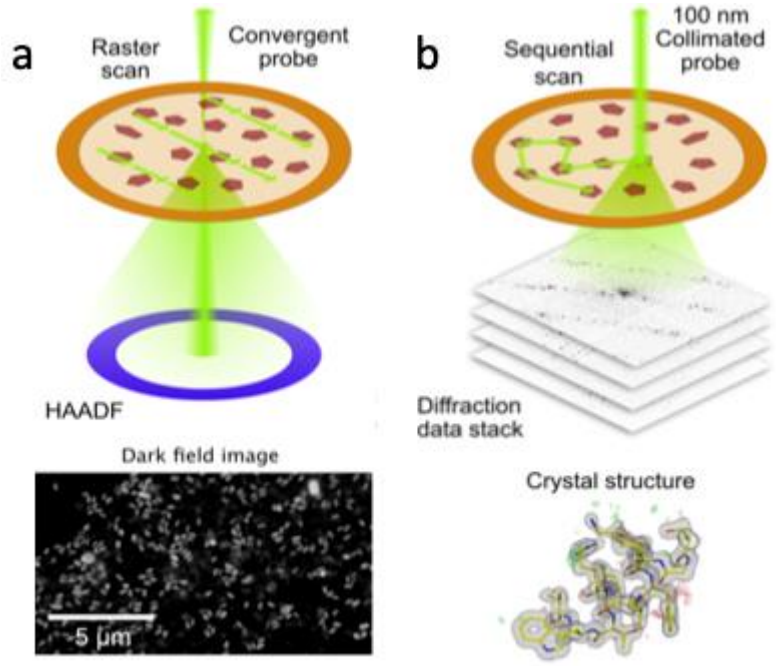

Back to Table of contents

MS25 3D electron diffraction for structure solution of organics and proteins

MS25-02

Absolute structure of pharmaceutical salts of vilanterol using 3D ED – from Earth to the space station and back

P. Brazda [1], L. Palatinus [1], A. Jegorov [2], A. Gavenda [2], P. Vraspir [2]
[1]Institute of Physics of the Czech Academy of Sciences, Na Slovance 1999/2, 18221 Prague 8 - Prague (Czech Republic), [2]Teva Czech Ind., s.r.o., Ostravska 29, 74770 Opava Komarov - Opava (Czech Republic)

Abstract

Crystallographic analysis plays an important role in the development and characterization of new pharmaceutical substances. An essential part of a complete structure analysis is the determination of absolute configuration of chiral molecules. We showed that 3D electron diffraction (3D ED) can determine the absolute configuration of the pharmaceutical molecules [1] by the so-called dynamical refinement – a structure refinement against 3D ED data taking into account the dynamical diffraction theory [2]. This contribution will review the tedious but finally successful journey towards the determination of the absolute configuration of a pharmaceutical molecule vilanterol (Figure 1).

Two different salts were prepared in this project. The first material was a salt of vilanterol with triphenylacetic acid. It was grown at the International Space Station with the aim to obtain crystals large enough for using synchrotron radiation for structure solution and absolute structure determination. Unfortunately, the quality of the crystals turned out to be insufficient even for structure solution. We therefore embarked the project and decided to attempt the absolute structure determination by 3D ED. The crystals grown in microgravity [3] turned out to be more than sufficiently large for the application of 3D ED. The structure could be solved and refined. However, the combination of the poor crystallinity of the material and the fact that the symmetry of the structure (space group $P2_1$) was very close to $P2_1/n$ symmetry did not allow us to draw a clear conclusion on the absolute configuration. Therefore, a new salt was prepared in laboratory. This time the 1,5-naphtalene disulphonic acid was chosen instead of triphenylacetic acid. The size of the crystals was again too small for the synchrotron experiments. The material crystallized in space group $P1$ and again the structure was very strongly pseudocentrosymmetric. However, better quality of the crystals allowed us to determine the absolute structure of the material and thus the absolute configuration of vilanterol, which demonstrates that 3D ED can substantially speed up the pharmaceutical research even for very challenging materials and make it more cost effective.

References

[1] Brazda, P., Palatinus, L., Babor, M. Science 364 (2019) 667.
[2] Palatinus, L., Petricek, V., Correa, C. A. Acta Crystallogr. A 71 (2015) 235.
[3] Patent US 2021/0300861 A1.
[4] We thank SpacePharma Inc. for the experiments in microgravity on the International Space Station.
[5] Financial support from the Czech Science Foundation (project no. 21-05926X) is greatly acknowledged.

Figure 1 Vilanterol

Back to Table of contents

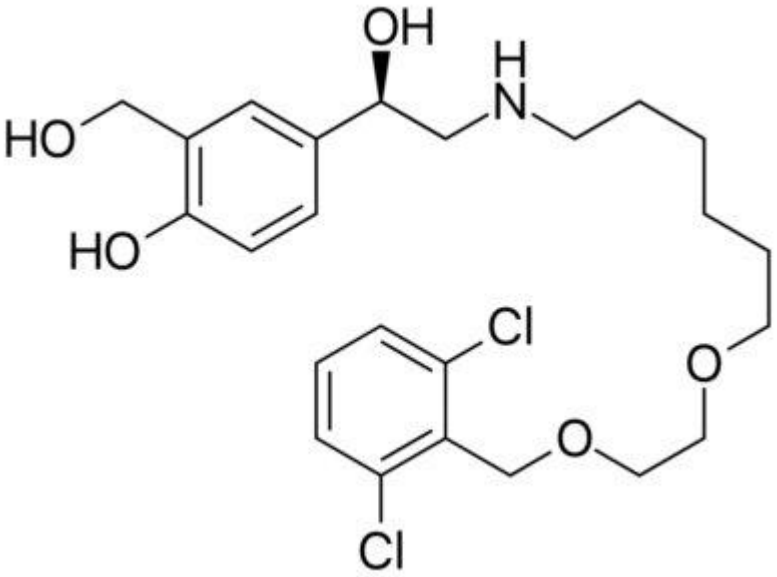

Back to Table of contents

MS25 3D electron diffraction for structure solution of organics and proteins

MS25-03

Dare to spin – well diffracting protein nanocrystals through on-vortex crystallisation

G. Hofer [1], L. Calmanovici Pacoste [1], L. Wang [1], H. Xu [1], X. Zou [1]
[1]Stockholm University - Stockholm (Sweden)

Abstract

Protein crystallisation has been extensively studied for X-ray and neutron diffraction. The hunt for optimised conditions yielding large single crystals has become the staple of protein crystallography labs around the world. Recently new advances in synchrotron beam lines and free electron X-ray lasers have opened the world of smaller (<40 µm a side) crystals being used for structure determination.

Electron diffraction (3D ED / microED) brings altogether new challenges to the field. Not only can it utilise even smaller crystals, it even requires one dimension to be sub 1 µm to allow the electron beam to pass through. Additionally, it benefits from the other dimensions being significantly larger, since that allows for more protein to participate in the diffraction measurement - which in turn improves signal strength while reducing beam damage effects. Such ideal plate shaped crystals are often created by focused ion beam milling of larger crystals, but this approach is time consuming and requires specialised machinery.

We have found that leaving behind the careful and slow techniques of X-ray protein crystallography and instead employing rapid crystallisation on a vortex mixer can offer surprisingly good control over crystal size in the range required for 3D ED. The optional addition of metal or PTFE beads to create shear forces capable of fragmenting larger crystals provides a feedback loop that seeds new crystal growth should the seed count be insufficient at first.

With an optimized protocol taking only minutes, we have succeeded in creating solutions containing countless well diffracting crystal plates of a urate oxidase (UOX), a ribonucleotide reductase R2 and two arginine kinases amongst others. Diffraction data sets to 2 Å are commonly obtainable from these plates with both the diffraction quality and resolution improving with decreasing plate thickness. In the case of UOX the achievable resolution changed from 3 Å to 1.4 Å when switching to the new method.

Back to Table of contents

MS25 3D electron diffraction for structure solution of organics and proteins

MS25-04

Structure determination of a protein-peptide complex using microcrystal electron diffraction

A. Shaikhqasem [1], L. Machner [2], F. Hamdi [3], C. Parthier [1], F.L. Kyrilis [3], S.M. Feller [2], P.L. Kastritis [3], M.T. Stubbs [1]

[1]Institute for Biochemistry und Biotechnology, Charles Tanford Protein Center, Martin Luther University Halle-Wittenberg - Halle (Saale) (Germany), [2]Institute of Molecular Medicine (Tumor Biology), Charles Tanford Protein Center, Martin Luther University Halle-Wittenberg - Halle (Saale) (Germany), [3]ZIK HALOmem, Charles Tanford Protein Center, Martin Luther University Halle-Wittenberg - Halle (Saale) (Germany)

Abstract

Developments in microcrystal electron diffraction (MicroED) allow the determination of protein structures from crystals that are too small to be analyzed by conventional X-ray crystallography [1]–[3]. Although the method has been used to determine novel protein structures, it is limited to micro/submicron ultra-thin protein crystals [4], [5]. Due to the limited rotation range of the sample stage in a MicroED setup, completeness of the collected data is restricted by crystal shape, symmetry and orientation on the grid [4], [6]. Here we applied MicroED to determine the structure of a novel complex between an enzyme regulatory domain and an intrinsically disordered peptide. Needle-like crystals in the space group $P2_12_12_1$ were grown using the hanging drop vapor diffusion method. Diffraction data were collected on a 200 kV Thermo Scientific Glacios Cryo-TEM equipped with a CetaD detector. Data were collected along multiple sections of several crystal needles within the limiting rotation range of the sample stage. The performed collection strategy allowed data processing from only two crystals that were oriented perpendicular to each other on the grid, resulting in a 3.2 Å resolution dataset with a merged completeness of 89.3%. Our work represents an effective workflow for obtaining a complete electron diffraction dataset from needle-like protein crystals.

References

[1] B. L. Nannenga, D. Shi, A. G. W. Leslie, and T. Gonen, “High-resolution structure determination by continuous-rotation data collection in MicroED,” Nat. Methods 2014 119, vol. 11, no. 9, pp. 927–930, Aug. 2014.

[2] B. L. Nannenga and T. Gonen, “The cryo-EM method microcrystal electron diffraction (MicroED),” Nat. Methods 2019 165, vol. 16, no. 5, pp. 369–379, Apr. 2019.

[3] M. T. B. Clabbers, A. Shiriaeva, and T. Gonen, “MicroED: conception, practice and future opportunities,” urn:issn:2052-2525, vol. 9, no. 2, pp. 169–179, Jan. 2022.

[4] H. Xu et al., “Solving a new R2lox protein structure by microcrystal electron diffraction,” Sci. Adv., vol. 5, no. 8, pp. 4621–4628, Aug. 2019.

[5] C. Nguyen and T. Gonen, “Beyond protein structure determination with MicroED,” Curr. Opin. Struct. Biol., vol. 64, p. 51, Oct. 2020.

[6] B. L. Nannenga, “MicroED methodology and development,” Struct. Dyn., vol. 7, no. 1, p. 014304, Feb. 2020.

Back to Table of contents

MS25 3D electron diffraction for structure solution of organics and proteins

MS25-05

Electron diffraction as a tool to study novel organometallic complexes

E.A. Thompson [1], A.A. Antson [1], H.T. Jenkins [1]
[1]University of York - York (United Kingdom)

Abstract

3D electron diffraction (3DED) is a technique that is sparking huge interest within the chemistry community as a tool to rapidly determine the structures of newly synthesised compounds. At the York Structural Biology Laboratory (YSBL) we collected our first 3DED data in late 2019 from paracetamol using a T12 microscope with a retrofitted Ceta camera. This was a manual and laborious process. Since April 2021 we have been using our Glacios microscope with Ceta-D camera to collect 3DED data from hundreds of crystals of small molecule compounds and have determined multiple structures. Our focus is on applying 3DED to determine structures of novel and challenging samples, in particular air-sensitive organometallic compounds, synthesised by our colleagues at the University of York. This has enabled us to characterise materials that were precluded from earlier structure determination by X-ray crystallography. I will describe our workflow for collecting and processing 3DED data from small molecule complexes, highlight our recent results from an air-sensitive σ-alkane complex[1] and illustrate how 3DED can be incorporated into a pipeline for synthetic chemists to accelerate research.

References

1 L. R. Doyle, E. A. Thompson, A. L. Burnage, A. C. Whitwood, H. T. Jenkins, S. A. Macgregor and A. S. Weller, Dalt. Trans., 2022, **51**, 3661–3665.

Electron diffraction from organometallic crystals

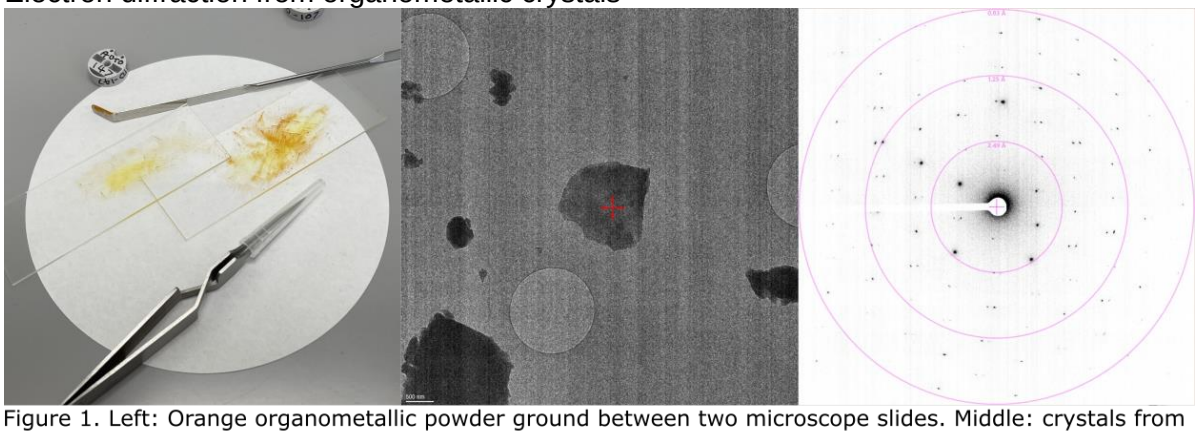

Figure 1. Left: Orange organometallic powder ground between two microscope slides. Middle: crystals from orange powder deposited on a TEM grid. Right: representative electron diffraction pattern from a single crystal.

Back to Table of contents

MS26 Quantum mechanical models for dynamics and diffuse scattering

MS26-01

Thermal diffuse scattering and ab initio phonons in LaPdSb

M. Gutmann [1], D. Adroja [1], B. Rainford [2], K. Refson [1], M. Von Zimmermann [3]
[1]Rutherford Appleton Laboratory - Chilton Didcot (United Kingdom), [2]University of Southampton - Southampton (United Kingdom), [3]DESY - Hamburg (Germany)

Abstract

LaPdSb has been found experimentally to be a potential high temperature thermoelectric material[1]. The compound crystallises in a hexagonal structure with layers of La alternating with layers containing Pd and Sb [2]. Here, we present results combining ab-initio phonons computed using the CASTEP code along. These show a number of low-energy phonon modes supporting the thermoelectric properties. The ab-initio phonons are used to compute thermal diffuse scattering. Neutron diffuse scattering patterns were collected using the SXD beamline at the ISIS spallation neutron source and complementary high-energy X-ray diffuse patterns were obtained using beamline BW5 at DESY. These patterns are compared with the theoretical thermal diffuse scattering patterns. Alternatively, the thermal diffuse scattering can also be modelled using a simple balls-and-springs model. This gives complementary information on the bonding-strength between the various metal ions.

References

[1] T. Sekimoto et al., Appl. Phys. Lett _89_, 092108 (2006).
[2] The crystals for our experiments were grown by Drs. K. Kathoh (National Defense Academy, Yokosuka, Japan) and H. Aoki (Dept. of Physics, Tohoku University, Sendai, Japan).

Back to Table of contents

MS26 Quantum mechanical models for dynamics and diffuse scattering

MS26-02

Solution of single crystal diffuse scattering problem using 3D-ΔPDF deconvolution

A. Simonov [1], Y. Kholina [2]
[1]Department of Materials, ETH Zurich - Zurich (Switzerland), [2]Department of Materials, ETH Zurich - Zürich (Switzerland)

Abstract

Properties of many materials depend crucially on the structure and distribution of defects in their crystal lattice. Defects can be probed by single crystal diffuse scattering of x-rays or neutrons, however the problem of construction of a model disordered solid consistent with the observed diffuse scattering is still unsolved since currently it relies on either trial-and-error or Patterson function based methods. Ideally one would seek a method which would allow to solve diffuse scattering in the same sense as direct methods provide a solution to the phase problem of the Bragg peaks crystallography.

In this work we show that such a general method indeed exists for the special case of binary disordered solids. Our method relies on the deconvolution of the 3D-ΔPDF function into two parts: one encoding the structure of the defect, and the other encoding the correlation between defects. The structure of the defect can then be solved by using standard algorithms similar to charge flipping, while the interaction between the defects can be found using the method called the density consistency matching. We illustrate the use of the method using the experimental data from tris-tert-butyl-1,3,5-benzene tricarboxamide single crystal.

Back to Table of contents

MS26 Quantum mechanical models for dynamics and diffuse scattering

MS26-03

Pauflerite β-$VOSO_4$ as a 1D S = 1/2 Heisenberg antiferromagnetic system: crystal structure, disorder, and thermal expansivity

C. Fuller [1], D.L. Quintero-Castro [2], A. Bosak [3], D. Chernyshov [1]
[1]SNBL at ESRF - Grenoble (France), [2]University of Oslo - Oslo (Norway), [3]ESRF - Grenoble (France)

Abstract

Low-dimensional antiferromagnets are of interest both from a fundamental point of view, and as perspective materials for future spintronics applications. Similar to some vanadyl phosphates, Pauflerite β-$VOSO_4$ is a quasi–one-dimensional S = 1/2 Heisenberg system[1]. We report on the low-temperature thermal expansion of a synthetic β-$VOSO_4$, revealing a structural rationale for the magnetic chain direction in agreement with inelastic neutron scattering measurements and DFT calculations, as well as the observation of diffuse scattering. We provide a microscopic interpretation of the underlying correlated disorder, which is linked to the inversion of the short-long V-O distance pairs along the chains, forming a local defect state. Diffuse scattering indicates that such defects are correlated and form thin layers, destroying alternation of V-O bonding pattern in the neighbouring chains. Using direct Monte Carlo (MC) modelling[2], we present here an atomistic realization of the disordered crystal structure. 2D defects in anisotropic magnetic systems may perturb, or even destroy, long-range magnetic ordering. In particular, the lack of inversion symmetry in the 2D defect layers opens the possibility for the Dzyaloshinskii-Moriya interaction (DMI) and, consequently, chiral magnetism localized in the defect planes. In this respect, the defect β-$VOSO_4$ structure offers a new, and as yet unexplored, playground.

References

[1] D. L. Quintero-Castro, G. J. Nilsen et al., One dimensional magnetism in β-$VOSO_4$, in preparation
[2] T.R. Welberry, M. J. Gutmann et al., Single-crystal neutron diffuse scattering and Monte Carlo study of the relaxor ferroelectric $PbZn_{1/3}Nb_{2/3}O_3$ (PZN), J. Appl. Cryst., 2005, 38, 639-647

Back to Table of contents

MS26 Quantum mechanical models for dynamics and diffuse scattering

MS26-04

X-ray diffraction and periodic DFT calculations for modelling of hydrogen atoms in a mineral - pinnoite

M. Stachowicz [1], A. Huć [1], A. Hoser [2], K. Woźniak [2]
[1]Department of Geochemistry, Mineralogy and Petrology, Faculty of Geology, University of Warsaw - Warsaw (Poland), [2]Department of Chemistry, Biological and Chemical Research Centre, University of Warsaw - Warsaw (Poland)

Abstract

High resolution charge density experiments are still rarely carried out in the studies of minerals. Accurate modelling of hydrogen atoms from X-ray diffraction is challenging due to low scattering power of H. Here, we present a combined dynamic quantum crystallography approach to overcome the experimental shortcomings from X-rays.

Pinnoite, $Mg[B_2O(OH)_6]$ was first described by Staute in 1884 [1]. This diborate mineral, consists of $Mg(OH)_6$ octahedra sharing all OH groups with $B_2O(OH)_6$ double tetrahedra. The lattice framework forms void channels along [001]. The exact structure of pinnoite was under review over the last decades. It was solved in $P4_2$ or $P4_2/n$ space groups [2,3].

High-resolution single-crystal X-ray diffraction data were collected up to 0.4 Å resolution at 293 K for natural pinnoite. Based on reflection extinction conditions the space group, $P4_2/n$ was chosen. The specimen originated from an Inder boron deposit in Kazakhstan. It contained needle-like crystals of excellent quality, free of any elemental impurities. The morphology and chemical composition of single crystals were examined on scanning electron microscope, equipped with energy dispersive spectrometer.

We obtained lattice dynamics model of pinnoite, from periodic DFT calculations, run in Crystal17 [4] software. Next, we refined the vibrational frequencies against the single crystal x-ray diffraction data, using NOMORE [5] package. The resultant accurate ADPs of hydrogen atoms, were further implemented to the charge density refinement (XD package [6]) of pinnoite.

The quantitative experimental charge density distribution was determined with Hansen-Coppens multipole formalism [7], getting R(F)=1.48%. Each boron atom is tetrahedrally coordinated by four oxygen atoms, three of which form O(1) - H(1), O(2)-H(2), O(3)-H(3) hydroxyl groups, whereas O(4) links two symmetrically equivalent boron atoms. The Bader [8] atomic basins were determined and charges were integrated from electron density within each basin: q^{Mg} =+1.5; $q^{O(1)}$ = -1.3; $q^{O(2)}$ = -1.2; $q^{O(3)}$ = -1.3; $q^{O(4)}$ = -1.5; $q^{B(1)}$ = +2.5; $q^{H(1)}$ = +0.5; $q^{H(2)}$ = +0.6; $q^{H(3)}$ = +0.5. The crystal maintained $P4_2/n$ symmetry, in pressures of 2.7GPa and 4GPa, generated in a diamond anvil cell. The model of electron density distribution determined here serves as a reference for ongoing high pressure studies.

We acknowledge financial support within the Polish National Science Centre (NCN) OPUS17 grant number DEC-2019/33/ B/ST10/02671.

References

1. H. Staute, Berichte Der Deutschen Chemischen Gesellschaft, 17 (1884) 1584–1586.
2. J. Krogh-Moe, Acta Cryst, 23 (1967) 500–501.
3. F. Paton, S.G.G. MacDonald, Acta Cryst, 10 (1957) 653–656.
4. R. Dovesi, R. Orlando, A. Erba, C.M. Zicovich-Wilson, B. Civalleri, S. Casassa, L. Maschio, M. Ferrabone, M. De La Pierre, P. D'Arco, Y. Noël, M. Causà, M. Rérat, B. Kirtman, International Journal of Quantum Chemistry, 114 (2014) 1287–1317.
5. A.A. Hoser, A.Ø. Madsen, Acta Cryst A, 72 (2016) 206–214.
6. A. Volkov, P. Macchi, L.J. Farrugia, C. Gatti, P. Mallinson, T. Richter, T. Koritsanszky, XD2016 - A Computer Program Package for Multipole Refinement, Topological Analysis of Charge Densities and Evaluation of Intermolecular Energies from Experimental and Theoretical Structure Factors (2016).

Back to Table of contents

7. N.K. Hansen, P. Coppens, Acta Crystallographica Section A: Crystal Physics, Diffraction, Theoretical and General Crystallography, 34 (1978) 909–921.
8. R.F.W. Bader, Atoms in Molecules: A Quantum Theory, Clarendon Press, (1994).

Back to Table of contents

MS26 Quantum mechanical models for dynamics and diffuse scattering

MS26-05

Diffuse scattering from crystals - quantifying the contribution of lattice dynamcis and disorder

B. Wehinger [1]
[1]*ESRF - The European Synchrotron - Grenoble (France)*

Abstract
I will present quantitative modelling of diffuse scattering intensities from first principles including contributions from lattice dynamics and disorder and illustrate its application to quantum materials. I will show how high-precision measurements of diffuse scattering intensities together with a rigorous data analysis allow for the determination of the full elasticity tensor [1]. Modelling diffuse scattering from first principles allows to understand unusual features in the distribution of scattering intensities and allows for quantitative statements on the microscopic origin [2]. Finally, I will show how the application of diffuse scattering to quantum materials allow us to discover new fundamental phenomena at the forefront of quantum-many-body physics [3].

References
[1] Björn Wehinger, Alessandro Mirone, Michael Krisch and Alexeï Bosak, Full Elasticity Tensor from Thermal Diffuse Scattering, Phys. Rev. Lett. 118, 035502 (2017).
[2] Björn Wehinger, Dmitry Chernyshov, Michael Krisch, Sergey Bulat, Victor Ezhov and Alexeï Bosak, Diffuse scattering in Ih ice, J. Phys.: Condens. Matter 26 265401 (2014).
[3] Sándor Tóth, Björn Wehinger, Katharina Rolfs, Turan Birol, Uwe Stuhr, Hiroshi Takatsu, Kenta Kimura, Tsuyoshi Kimura, Henrik M. Rønnow and Christian Rüegg, Electromagnon dispersion probed by inelastic X-ray scattering in LiCrO2, Nat. Comm. 7, 13547 (2016).

Diffuse scattering in ice Ih [2]

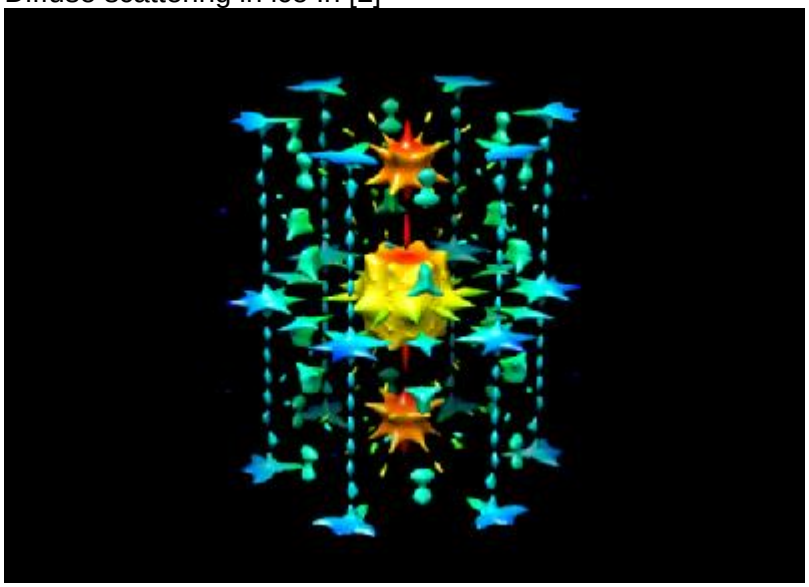

Back to Table of contents

MS27 Minerals and Materials Under Extreme Conditions

MS27-01

Structural and chemical versatility in iron oxides at extreme conditions

E. Bykova [1]
[1]*Bayerisches Geoinstitut - Bayreuth (Germany)*

Abstract

Being the only geochemically profuse element in Earth's interior with a variable oxidation state, iron controls oxygen fugacity and affects all global planetary processes. Numerous iron oxides with unexpected compositions recently identified at high-pressure and high-temperature conditions demonstrate rich crystal chemistry and intriguing physical properties.

We applied methods of single-crystal X-ray diffraction and Moessbauer spectroscopy in laser-heated diamond anvil cells to study phase transformations, chemical stability and crystal chemistry of compounds belonging to Fe-O system at pressures up to 200 GPa and temperatures over 3000 K. We observed that conventional iron oxides (FeO, Fe_3O_4 and Fe_2O_3) exhibit rich polymorphism at high pressures and high temperatures which is in significant degree governed by magnetic and electronic changes in Fe atoms. We will discuss how chemical, electronic, and magnetic states of iron oxides are influenced by pressure, giving rise to unexpected chemical reactions, structural and other types of transformations.

Back to Table of contents

MS27 Minerals and Materials Under Extreme Conditions

MS27-02

Structure of high-pressure ices revealed from single and powder neutron diffraction

K. Komatsu [1]
[1]*Geochemical Research Center, Graduate School of Science, The University of Tokyo - Tokyo (Japan)*

Abstract

Water ice has remarkable structural diversity, at least 20 crystalline phases are known up to date. Most of those polymorphs exist at relatively low pressures below 2 GPa, and above the pressure, they are limited to ices VII, VIII, X with bcc structures and ice XVIII with a fcc structure, and their structural diversity has seemingly disappeared. However, many unresolved questions about the apparently simple structures of those high-pressure ice phases remain. For example, ice VII shows many anomalous properties at around 10 – 15 GPa, such as electric conductivity enhancing, self-diffusion of protons, x-ray diffraction peak broadening, Raman peak narrowing, and those structural origins are not fully understood (e.g., [1)] and see references therein). Another example is a phase transition from ice VII to ice X which involves hydrogen-bond symmetrisation. It has long been considered that the transition may occur at 60 GPa for H2O and 70 GPa for D2O from spectroscopic studies over 20 years ago[2-4)], but the succeeding studies have suggested multiple changes for hydrogen disordering and proposed different transition pressures ranging from 30 to 110 GPa[5-8)].

Neutron diffraction is a key technique to unravel such unresolved questions of high-pressure ices, because neutrons can interact with hydrogen as well as oxygen and elucidate the detailed crystal structure including hydrogen positions. However, in-situ experiments of neutron diffraction under very high pressure, or the detailed structure analyses by single-crystal neutron diffraction have been limited due to the technical difficulty. Our group recently developed new high-pressure cells for single-crystal neutron diffraction up to 5 GPa [9, 10)] and for powder neutron diffraction up to 80 GPa[11)]. The key material for both high-pressure cells is nano-polycrystalline diamond. In this presentation, I will show several neutron diffraction studies for ice VII using the newly developed high-pressure cells, and discuss the detailed crystal structure of ice VII.

References

1) Yamane R. et al. (2021) Phys. Rev. B, 104, 214304.
2) Aoki K. et al. (1996) Phys. Rev. B, 54, 15673-7.
3) Goncharov A.F. et al. (1996) Science, 273, 218-20.
4) Pruzan P. et al. (1997) J. Phys. Chem. B, 101, 6230-3.
5) Meier T. et al. (2018) Nat. Commun., 9, 2766.
6) Guthrie M. et al. (2019) Phys. Rev. B, 99, 184112.
7) Méndez A.S.J. et al. (2021) Phys. Rev. B, 103, 064104.
8) Grande Z.M. et al. (2022) Phys. Rev. B, 105, 104109.
9) Yamashita K. et al. (2020) High. Press. Res., 40, 88-95.
10) Yamashita K. et al. (2022) High. Press. Res., 42, 121-35.
11) Komatsu K. et al. (2020) High. Press. Res. 40, 184-193.

Back to Table of contents

MS27 Minerals and Materials Under Extreme Conditions

MS27-03

Polymerization of CO4-groups in carbonates

L. Bayarjargal [1], D. Spahr [1], J. König [1], V. Milman [2], B. Winkler [1]
[1]Institute of Geosciences, Goethe University Frankfurt - Frankfurt am Main (Germany), [2]Dassault Systèmes BIOVIA - Cambridge (United Kingdom)

Abstract

The building blocks of 'conventional' carbonates such as calcite or magnesite are trigonal planar $[CO_3]^{2-}$-groups [1,2]. These CO_3-groups remain stable as isolated groups up to pressures of ~70 GPa. At higher pressures and high temperatures above ~2000 K the formation of $[CO_4]^{4-}$-groups was observed and explained by the formation of carbon with sp^3-hybridized orbitals [2]. In contrast to sp^2-hybridized CO_3-groups, CO_4-groups may polymerize based on half-occupied orbitals that allow for additional bonding. However, extensive investigation of the polymerization of CO_4-groups was hindered by experimental difficulties to achieve such extreme conditions. In contrast to CO_4-groups, polymerizations of other orthoanions $[MO_4]$ have been extensively investigated in the past. $[SiO_4]^{4-}$-tetrahedra are the main building blocks in silicates and play a major role in crystallography and mineralogy [3,4]. Tetrahedral SiO_4-groups can polymerize and build pairs, chains, rings, sheets or networks [3,4]. In addition to the SiO_4-tetrahedra in silicates, further anions such as $[BO_4]^{5-}$ -groups of borates are key-components in basic chemistry and polymerize with BO_4-groups and even with other BO_3 building blocks [5].
Recently, we demonstrated the synthesis of carbonates containing CO_4-groups at moderately high pressures (20-30 GPa) by reacting carbonates with either oxides or CO_2 [6-8]. These carbonates have chemical compositions other than the well-known 'conventional' carbonates ($MeCO_3$) and are either enriched in a metal oxide or CO_2 [6-8]. Some of them can even be recovered at ambient conditions [6,7]. The favorable synthesis pressure conditions allowed us to investigate different structural aspects and the polymerization of CO_3-groups in large detail. As a result of the polymerization, carbonates with isolated CO_4-tetrahedra or carbonates with groups, rings, chains or pyramids can be formed (see the figure). The structural variety of those carbonates resembles that of silicates and some borates. In the present study, we will give an overview of carbonates containing CO_4-groups and present crystal-chemical aspects of CO_4-groups in comparison to SiO_4 and other MO_4 complex anions.

We acknowledge funding from the DFG (BA4020/2, WI1232, FOR2125) and DESY for the provision of experimental facilities and beamtime. B.W. is grateful for support by the BIOVIA Science Ambassador program.

References

[1] Bayarjargal et al. Phys. Earth Planet. Inter., 281, 31 (2018)
[2] Binck et al. Phys. Rev. Mater., 4, 055001 (2020)
[3] Liebau, F., Structural Chemistry of Silicates, Berlin (1985)
[4] Okrusch, M., Matthes, S., (Eds.) Mineralogie: Berlin (2014)
[5] Mutailipu et al. Chem. Rev., 121, 1130 (2021)
[6] Spahr et al. Inorg. Chem., 60, 14504 (2021)
[7] Spahr et al. Inorg. Chem., 60, 5419 (2021)
[8] König et al. Earth Space Chem., 6, 73 (2022)

Polymerization of CO4-groups

Back to Table of contents

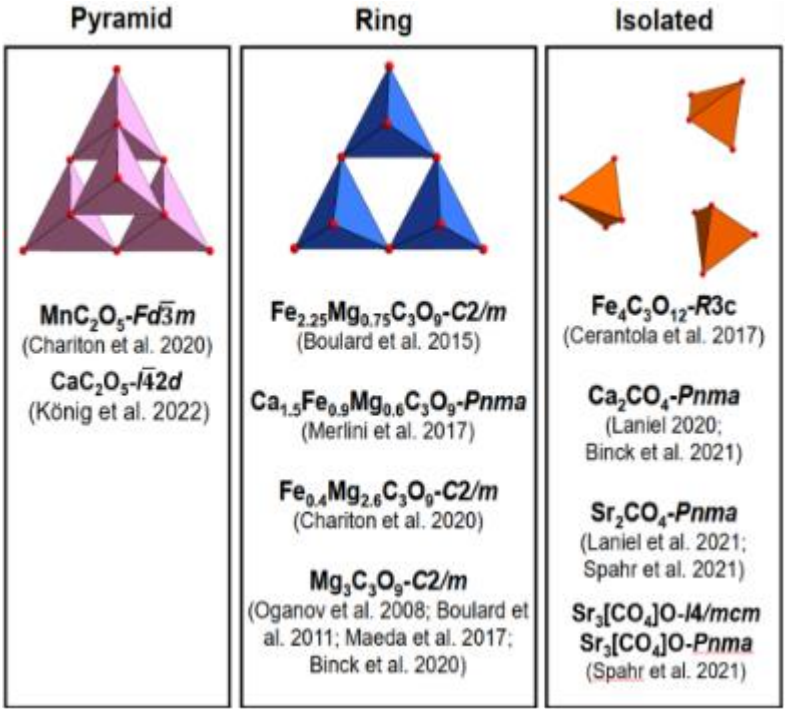

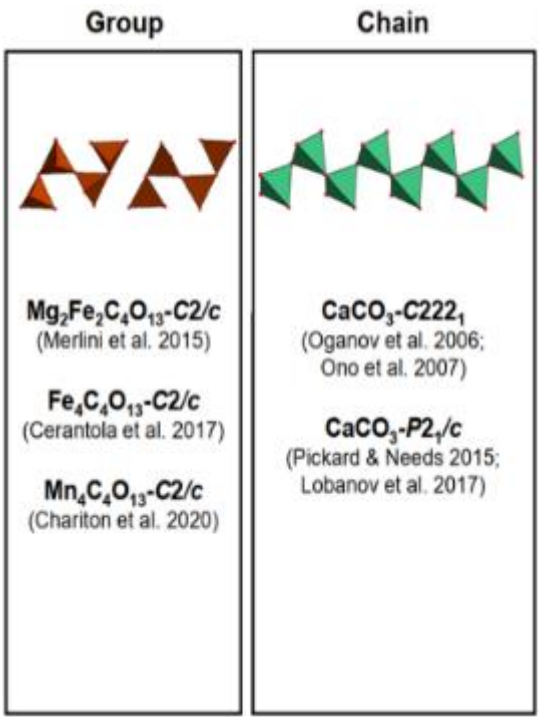

Back to Table of contents

MS27 Minerals and Materials Under Extreme Conditions

MS27-04

Comprehensive determination of the high-pressure structural behaviour of $BaTiO_3$

C. Bull [1], C. Ridley [1], K. Knight [1], N. Funnell [1], A. Gibbs [1]
[1]STFC (United Kingdom)

Abstract

We have mapped the phase diagram of the archetypal ferroelcetric material $BaTiO_3$ more extensively than previous attempts using high-pressure neutron-powder diffraction.[1] The mapping of the phase diagram has been performed using isothermal compression at fixed temperatures (175, 225, 290, 480 K) within each of the known crystallographic phases, up to ~6 GPa using a large volume press. The crystallographic structure of each phase has been measured, and using the unique information neutron diffraction provides we have determined the absolute atomic displacements of all atoms within the cell, obtained detailed information on the order of the phase transitions observed, and the behaviour of the ferroelectric dipole moment.

References

[1] Bull C.L. et al Materials Advances, 2,6094 (2021)

Phase Diagram of BaTiO3

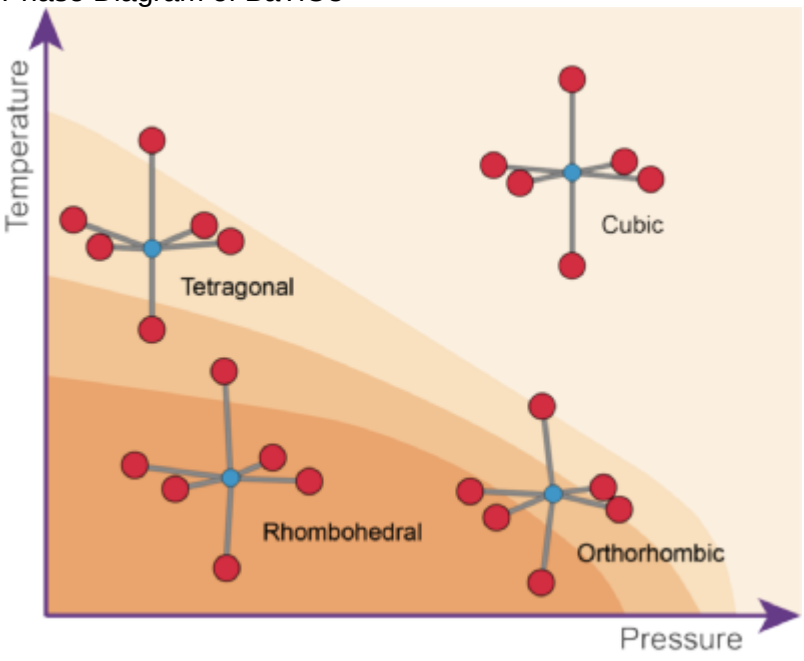

Back to Table of contents

MS27 Minerals and Materials Under Extreme Conditions

MS27-05

Binary arsenic nitride synthesized from elements under pressure

K. Dziubek [1], M. Ceppatelli [2], D. Scelta [1], M. Serrano-Ruiz [3], M. Morana [4], V. Svitlyk [5], G. Garbarino [5], T. Poręba [5], M. Mezouar [5], M. Peruzzini [3], R. Bini [6]

[1]LENS - Sesto Fiorentino (Italy), [2]LENS, CNR-ICCOM - Sesto Fiorentino (Italy), [3]CNR-ICCOM - Sesto Fiorentino (Italy), [4]Univeristy of Pavia - Pavia (Italy), [5]ESRF - Grenoble (France), [6]LENS, University of Florence - Sesto Fiorentino (Italy)

Abstract

Synthetic nitride chemistry is a very rapidly developing field. Many nitrides and nitride-based heterostructures are promising materials that can find application as superhard compounds, wide-bandgap semiconductors *etc*. Applying different high pressure-high temperature techniques facilitates nitridation and is the key to the synthesis of novel phases directly from elements.

Both nitrogen and arsenic belong to group 15 of the periodic table, although they exhibit completely different physical and chemical properties. At normal conditions nitrogen consists of very stable (945 kJ mol^{-1}) N≡N molecules, while the ground state of arsenic, so-called grey modification, is a solid-state structure consisting of extended layers. The direct chemical reaction between arsenic and nitrogen has not been reported. Indeed, except for the $As(N_3)_3$ and $As(N_3)_5$, the unstable and explosive molecular azides synthesized from the precursors, no binary compound of As and N has been revealed so far.

We report for the first time the high-pressure high-temperature synthesis of extended covalent AsN from elements at P > 25 GPa and T > 1400 K [1]. The cubic crystal structure (space group $P2_13$), in which each arsenic atom is single-bonded to three neighboring nitrogen atoms and vice versa (Fig. 1), has been reported so far for only several binary compounds: yellow *α*-indium (I) chloride InCl, *π*-cubic tin (II) sulfide SnS, and intermetallic phases strontium aluminide SrAl and strontium gallide SrGa. The arrangement of atomic or ionic units in these crystals resembles a severely distorted rocksalt structure, with a doubled lattice parameter. The new material was investigated also on compression and decompression, confirming its (meta)stability at room temperature in the pressure range of 10-50 GPa.

References

[1] Ceppatelli, M.; Scelta, D.; Serrano-Ruiz, M.; Dziubek, K.; Morana, M.; Svitlyk, V.; Garbarino, G.; Poręba, T.; Mezouar, M.; Peruzzini, M.; Bini, R. *Angew. Chem. Int. Ed. Engl.* **2022**, *61*, e202114191.

Back to Table of contents

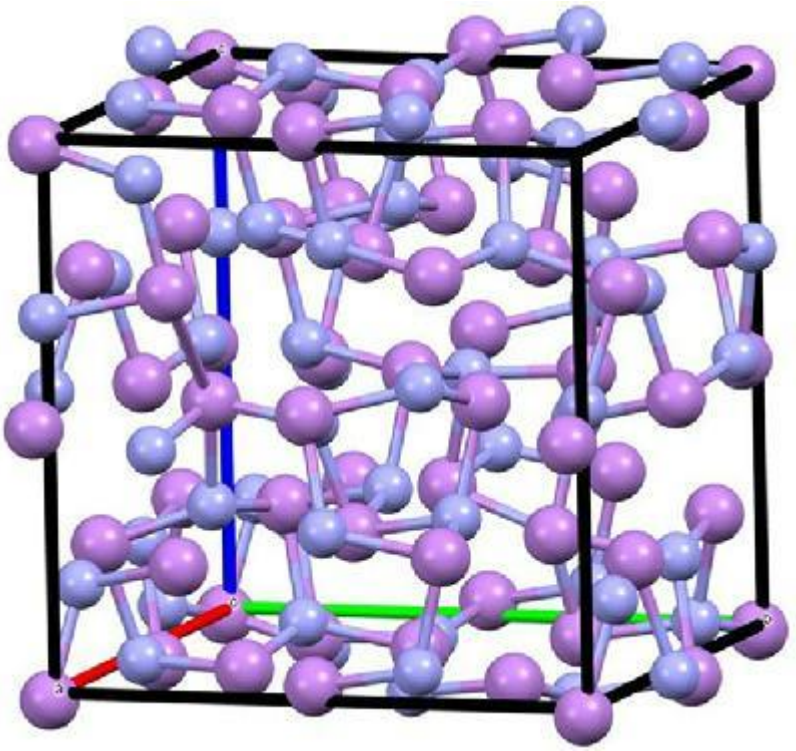

Back to Table of contents

MS28 Navigating crystal forms in molecular and pharmaceutical materials

MS28-01

Cocrystal polymorphs & Mechanochemistry - Mechanism & Kinetics

F. Emmerling [1]
[1]*Federal Institute for Materials Research and Testing (BAM) - Berlin (Germany)*

Abstract

Mechanochemistry is an effective, environmentally benign, and facile method for the synthesis of new crystal forms. Different milling parameters are known to affect the mechanisms and rates of product formation: milling frequency, milling time, filling degree of the milling jar, ball diameter and vessel size, degree of milling ball filling, and material of jars. The increasing interest in mechanochemistry is contrasted by a limited mechanistic understanding of mechanochemical reactivity and selectivity. Control over ball milling transformations is needed before the transformative potential of mechanochemical processing can be realized. Different analytical methods and their combinations have been developed for the time-resolved in situ monitoring of mechanochemical transformations, including powder X-ray diffraction, X-ray absorption spectroscopy, NMR, Raman spectroscopy, and thermography.[1] Here we will discuss our recent results investigating the formation of polymorphic cocrystals[2–3] thereby elucidating the influence of milling parameters (solvent, temperature, time) and reaction sequences on the formation mechanism and kinetics.[2-4] For the mechanochemical chlorination reaction of hydantoin normalizing the kinetic profiles to the volume of the milling ball showed clearly that milling reaction kinetics are conserved.[5] Here physical kinetics dominate reaction rates in a ball-milling transformation. Attempting to interpret such kinetics in purely chemical terms risk misinterpreting the results. Our results indicate that time-resolved in situ investigations of milling reactions offer a new approach to tune and optimize mechanochemical processes.

References

[1] Michalchuk, A. A. L.; Emmerling, F. Angew. Chem. Int. Ed. 2022, https://doi.org/10.1002/anie.202117270.
[2] Kulla, H.; Michalchuk, A. A.; Emmerling, F. Chem. Commun. 2019, 55, 9793–9796.
[3] Martins, I. C.; Emmerling, F. Carbamazepine Dihydroxybenzoic Acid Cocrystals: Exploring Packing Interactions and Reaction Kinetics. Cryst. Growth Des. 2021, 21, 6961–6970.
[4] Linberg, K; Szymoniak, P.; Schonhals, A.; Emmerling, F.; Michalchuk, A. Emmerling, A. Michalchuk, 2022, https://doi.org/10.26434/chemrxiv-2022-04jdf
[5] Martins, I. C.; Carta, M.; Haferkamp, S.; Feiler, T.; Delogu, F.; Colacino, E.; Emmerling, F. ACS Sustain. Chem. Eng. 2021, 9, 12591–12601.

Back to Table of contents

MS28 Navigating crystal forms in molecular and pharmaceutical materials

MS28-02

Complex Structures for a Simple Organic Salt: The Extraordinary Self-Assembly of Fampridine Hydrochloride

R. Montis [1]
[1]*Università degli Studi di Urbino Carlo Bo - Urbino (Italy)*

Abstract

Crystals are the result of a highly symmetric and periodic arrangement of molecules, assembled together via a set of intermolecular interactions and weak forces. Depending on the nature of the interacting entities, (their molecular shape and the type and the strength of the intermolecular interactions involved), atoms, molecules and ions can self-assemble generating different types of crystal packing. In general, small organic molecules tend to form simple supramolecular arrangements. Excluding rare cases, this usually produces crystal structures with simple and relatively small unit cells. Although molecular self-assembly in solid state has been extensively investigated and remains the focus of continuous and growing interest, sometime, a simple serendipitous discovery can remind us that we are still far to understand the rules governing the crystallization process.
In this contribution one of these fortuitous discoveries is described. A simple hydrochloride salt of fampridine crystallized as four different crystalline phases, two of which adopted an incredibly complex self-assembly. [1] The two structures represent the first observation of Frank-Kasper phases in small organic systems, a special class of crystalline phases previously observed only in metal alloys and different classes of supramolecular soft matter. The two FK structures crystallized from a precursor dense liquid obtained after a liquid-liquid phase separation. Investigation of the liquid phase by cryogenic electron microscopy reveals the presence of spherical aggregates, suggesting that a complex pre-organization is in place prior the nucleation. These structures, together with the experimental procedure used for their preparation, invite interesting speculation about their formation and open different perspectives for the design of organic crystalline materials.

References

[1] Montis, R., Fusaro, L., Falqui, A. et al. Nature, 2021, 590, 275–278. https://doi.org/10.1038

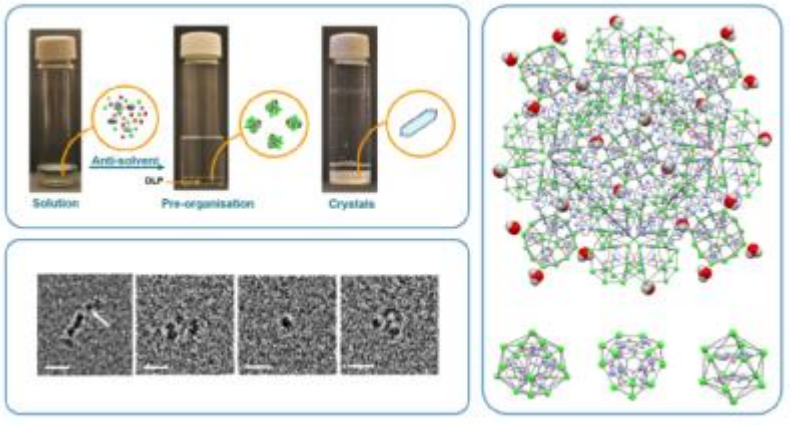

Back to Table of contents

MS28 Navigating crystal forms in molecular and pharmaceutical materials

MS28-03

The mystery of a co-crystal disappearing polymorph – case solved with quantum crystallography methods

M. Gryl [1], M. Kozieł [1], K. Nowakowska [1]
[1]Jagiellonian University, Faculty of Chemistry, Gronostajowa 2, 30-387 - Kraków (Poland)

Abstract

In the last decade, with the variety of possible applications of multicomponent materials, polymorphism in co-crystals has become more common or maybe more investigated by the scientific community. [1]
On the one hand, obtaining different forms of a co-crystal can lead to new materials with significantly different physical properties. However, in many cases, control over the obtained crystal phases containing more than one building block can be more challenging than in single-component materials. Performed experiments can lead to the concomitant polymorphs being difficult to separate and to so-called disappearing crystal phases.
Here we present the case of three polymorphs of urea barbituric acid co-crystals, which were obtained for the first time in 2008 by one of us [2]. Two phases were centrosymmetric ($P2_1/c$ and P-1), whereas the third was polar, crystallizing in the Cc space group. After the form $P2_1/c$ was obtained the Cc polymorph was not reproduced using the same or modified experimental conditions, neither in our home lab, nor by other researchers [3]. Therefore, it was considered to be one of the cases of metastable, disappearing polymorphs.
Using modern quantum crystallography tools, we understood the process of the polar co-crystal formation. Electron density studies combined with calculations of interaction energies gave us an idea for an advanced cocrystallization experiment used to reproduce the missing co-crystal form. Not only were we successful, but we also established ideal conditions for obtaining the remaining two polymorphic modifications [4,5]. This work gives a foundation for using quantum crystallography to study concomitant polymorphism phenomena in multicomponent materials.

References

[1] S. Aitipamula, P. Shan Chowa, R. B. H. Tan. CrystEngComm, 2014,16, 3451-3465.
[2] (a) M. Gryl, A. Krawczuk and K. Stadnicka. Acta Cryst., 2008. B64, 623-632; (b) M. Gryl, A. Krawczuk-Pantula and K. Stadnicka. Acta Cryst., 2011. B67, 144-154.
[3] K. A. Powell, G. Bartolini, K. E. Wittering, A. N. Saleemi, C. C. Wilson, C. D. Rielly, and Z. K. Nagy. Cryst. Growth Des., 2015, 15, 10, 4821–4836.
[4] L. M. Malec, M. Gryl, M. T. Oszajca, M. Z. Brela, and K. M. Stadnicka. Cryst. Growth Des. 2021, 21, 12, 6902-6912.
[5] M. Gryl et al., 2022, in preparation for publication.

Figure 1

Back to Table of contents

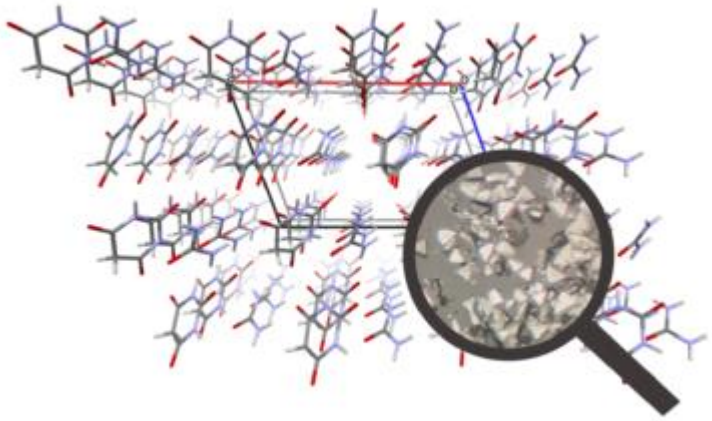

If we look in-depth at the crystal structure, we can see and understand how the crystals are formed

Back to Table of contents

MS28 Navigating crystal forms in molecular and pharmaceutical materials

MS28-04

Learning the intermolecular history of an API through the application of Hirshfeld Surface analysis tools

V. Psycharis [1]
[1]*Institute of Nanoscience and Nanotechnology NCSR 'Demokritos', - Agia Paraskevi (Greece)*

Abstract

Cocrystals have attracted the intense interest of researchers working on pharmaceuticals because there is a need in many cases to change the physical properties of Active Pharmaceutical Ingredients (APIs) [1]. The packing and arrangement of APIs, in pharmaceutical crystals, where they exist as molecular entities or as molecular adducts, influence the physical and in some cases the chemical properties and thus their overall performance [2]. Further to this research area, another field that has been emerged in parallel is the use of APIs as ligands in transition metal complexes which have been used as therapeutic and diagnostic agents [3]. Following the path of crystallization of different APIs in the structure of a polymorph, an adduct or a complex and studying the specific intermolecular interactions that play the major role in the packing of the corresponding structure, the complete information for the behavior of the API molecule in the crystalline phase is gathered. In the present study, the intermolecular interactions of two APIs (Levofloxacin and Acetylsalicylic Acid) are examined in all of crystalline forms found in CSD with the analysis tools of Crystal Explorer software, which are based on the Hirshfeld Surface (HS) concept [4,5]. Ball and stick model, dnorm and Shape index Hirshfeld surfaces for the Levofloxacin molecule in its free (top three pictures, [6]) and coordinated forms (bottom three pictures [7]) are shown in Figure-1. Points within ellipses are contact points of the API that they are observed in both compounds. As the HS analysis tools consider all the intermolecular interactions that are involved in the packing of the API molecule in the crystal structure under study, and not only those that are deemed important, the role of each specific active atomic site of the API can be revealed. Thus, through this study, all information concerning the protected, the available donor or the acceptor sites of an API for intermolecular interactions, upon coordination or adduct formation, and the corresponding sites of the API in its polymorphs will be gained. All this information is expected to help in the design of new cocrystals with improved performance of the specific API or to passivate specific sites upon coordination which are involved in side effects during its bioactivity.

References

[1] S. L. Morissette et al. Advanced Drug Delivery Reviews 56 (2004) 275.
[2] S. Datta & D. J.W. Grant, Nat Rev Drug Discov 3(2004):42-57.
[3] M. Selvaganapathy & N. Raman, J Chem Biol Ther 1 (2016) 1000108.
[4] M.A. Spackman and D. Jayatilaka, Cryst. Eng. Comm. 11(2009)19.
[5] J. J. McKinnon, M. A. Spakman and A. S. Mitchell Acta Cryst. B 60 (2004) 627.
[6] J.T. J. Freitas et al. Crystal Growth and Design18 (2018) 3558.
[7] P. Drevensek et al. J. Inorg. Biochem. 100 (2006) 1755.

Ball and stick models, dnorm & Shape decorated HSs

Back to Table of contents

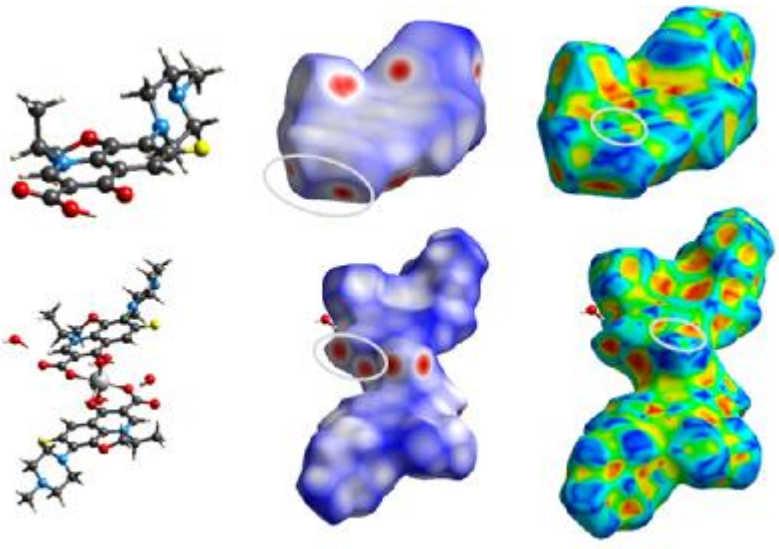

Back to Table of contents

MS28 Navigating crystal forms in molecular and pharmaceutical materials

MS28-05

The pressure-temperature phase diagram of tetramorphic pyrazinamide by vapour pressure and synchrotron X-ray diffraction under pressure

I. Rietveld [1], K. Li [1], G. Gbabode [1]
[1]*University of Rouen - Mont Saint Aignan (France)*

Abstract

The phase behaviour of drug molecules is important to control the desired polymorph in drug formulations, whether it is to ensure better stability of the formulation or better solubility (solubilization) of the drug. In the case of pyrazinamide, a drug against tuberculosis, four polymorphs are known to exist labelled α, β, γ, and δ [1,2]. Stability studies of this active pharmaceutical ingredient have been complicated due to the very slow transition kinetics observed in DSC measurements [1,2]. Using vapour pressure measurements, in which the reluctance of phase transformation is in fact an advantage, all solid-solid phase transformation temperatures have been determined. This method has been key to map the phase behaviour of pyrazinamide.

The use of high-pressure measurements with synchrotron X-ray diffraction at several temperatures from room temperature up to 120 °C has allowed to construct the pressure-temperature phase diagram of the four solid phases of pyrazinamide and the liquid phase (Figure 1). The equations of state of the four polymorphs have been determined at various temperatures in addition to the thermal expansion.

The α form was found to be the stable form at room temperature. One striking feature of pyrazinamide is that one polymorph, the δ form, has a very large thermal expansion and strong compressibility, which was not found in the other three forms. This gives rise to curved solid-solid transition equilibria in the pressure-temperature phase diagram, which is not commonly observed in the pressure range of 0 to 1 GPa for transitions between polymorphs.

References

(1) Castro, R. A. E.; Maria, T. M. R.; Evora, A. O. L.; Feiteira, J. C.; Silva, M. R.; Beja, A. M.; Canotilho, J.; Eusebio, M. E. S., A New Insight into Pyrazinamide Polymorphic Forms and their Thermodynamic Relationships Cryst. Growth Des. 2010,10, 274-282.

(2) Cherukuvada, S.; Thakuria, R.; Nangia, A., Pyrazinamide Polymorphs: Relative Stability and Vibrational Spectroscopy Cryst. Growth Des. 2010, 10, 3931-3941

Pressure-temperature phase diagram of pyrazinamide

Back to Table of contents

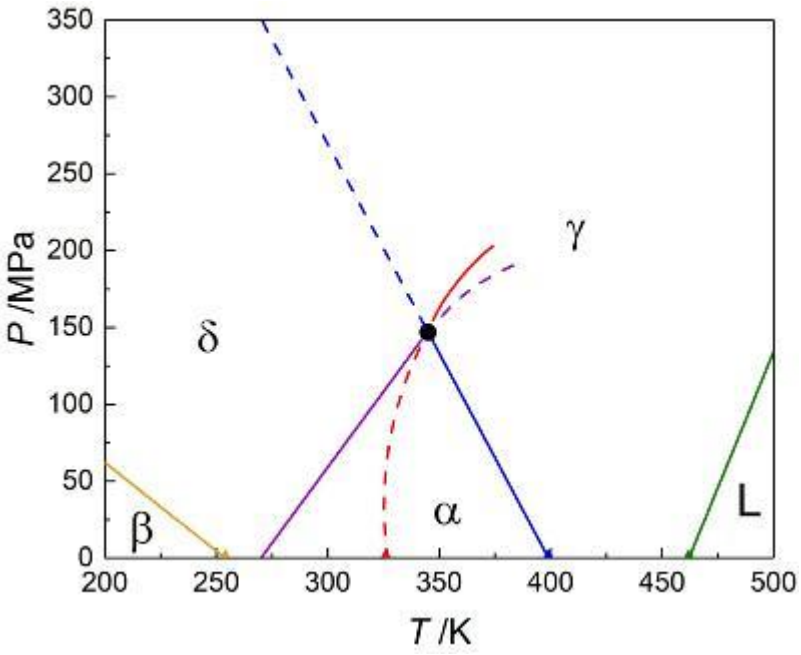

Back to Table of contents

MS29 Crystal engineering: structural flexibility, phase transitions and non-standard manipulation of synthons

MS29-01

More thoughts on the (un)predictability of supramolecular interactions in molecular crystals [1]

C. Ponan [1], G.R. Williams [1], O. Magdysyuk [2], K. Bucar [1]
[1]University College London - London (United Kingdom), [2]Diamond Light Source - Didcot (United Kingdom)

Abstract

We report the use of real-time and *in situ* X-ray diffraction monitoring of thermal and mechanochemical cocrystallisation reactions (using a modified differential scanning calorimeter and an adapted ball mill) to discern hierarchies of supramolecular synthons in multi-component molecular crystals.[2] The cocrystallisation experiments uncovered a series of solids with unexpected supramolecular structures (along with peculiar and previously unobserved mechanochemical crystallization phenomena[3]), thus highlighting limitations of our current abilities to understand, engineer, and maintain molecular crystals.[4]

This presentation aims to critically assess a range of concepts and ideas that form the basis of contemporary crystal engineering research,[5] with the aim to prompt a community-wide conversation about the current state of the art.

References

1. M. K. Corpinot, S. A. Stratford, M. Arhangelskis, J. Anka-Lufford, I. Halasz, N. Judaš, W. Jones and D.-K. Bučar, *CrystEngComm*, 2016, **18**, 5434–5439.
2. unpublished results
3. M. Arhangelskis, D.-K. Bučar, S. Bordignon, M. R. Chierotti, S. A. Stratford, D. Voinovich, W. Jones and D. Hasa, *Chem. Sci.*, 2021, **12**, 3264-3269.
4. D.-K. Bučar, *Cryst. Growth Des.,* 2017, **17**, 2913–2918
5. M. K. Corpinot and D.-K. Bučar, *Cryst. Growth Des.*, 2019, **19**, 1426–1453.

Back to Table of contents

MS29 Crystal engineering: structural flexibility, phase transitions and non-standard manipulation of synthons

MS29-02

Metal centers as electron donors in σ-hole interactions

A. Frontera [1]
[1]*Universitat de les Illes Balears - Palma de Mallorca (Spain)*

Abstract

In this communication, the role of metal centers as electron donors is analyzed from two perspectives. Firstly, it highlights recent studies discovering unconventional halogen and chalcogen bonding (HaB and ChB, respectively) that involves positively charged metal centers. These centers provide their filled d-orbitals for HaB/ChB, and thus behave as nucleophilic components toward the σ-holes at the halogen or chalcogen atoms (see Figure 1a). This role of some electron-rich transition metal centers can be regarded as an oxymoron in the sense that the metal is, in most cases, formally cationic; consequently, its nucleophilic function is surprising. The importance of Ha···d-[M] (Ha=halogen; M is Group 9 (Rh, Ir), 10 (Ni, Pd, Pt), or 11 (Cu, Au)) interactions in crystal engineering is emphasized by showing remarkable examples reported and uncovered by processing of the Cambridge Structural Database (CSD),[1] where this Ha···d-[M] directional interaction guides the formation of solid supramolecular assemblies of different dimensionalities.

Secondly, by exploring the CSD and using DFT calculations it is shown that the metal center can also enhance the σ-hole interaction (in particular ChBs) by metal coordination (see Figure1b). Moreover, the new σ-hole that is formed opposite to the M–Ch bond provides an extra possibility of binding. In fact, an example where Pd–Te···Cl chalcogen bond is provided that has a strong directing role and is responsible for the formation of an interesting supramolecular polymer.

The results derived from this study might be useful to those scientists working in the fields of supramolecular chemistry and crystal engineering as well as to inspire chemists working in supramolecular catalysis.

References

[1] D. M. Ivanov, N. A. Bokach, V. Yu. Kukushkin, A. Frontera, Metal Centers as Nucleophiles: Oxymoron of Halogen Bond-Involving Crystal Engineering. Chem Eur. J., 2022, 28, e202103173.

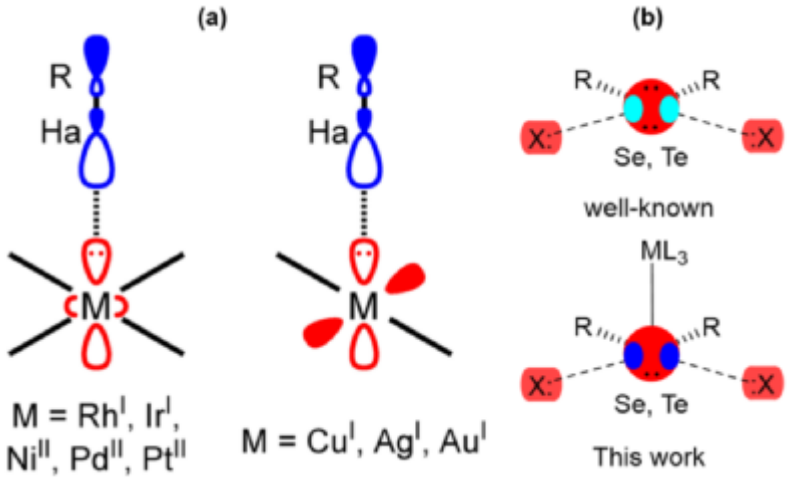

Back to Table of contents

MS29 Crystal engineering: structural flexibility, phase transitions and non-standard manipulation of synthons

MS29-03

Carboxylate metallogels and coordination networks: the role of non-covalent interactions

S. Bourne [1], G. Ramon [1], S.C. Zacharias [1]
[1]University of Cape Town - Cape Town (South Africa)

Abstract

Supramolecular interactions form the basis for a range of functional materials. The study of non-covalent interactions (NCIs), and the supramolecular synthons they form, has reached a mature phase. Thus crystal engineering of functional solid materials has grown into a vibrant and exciting field. Related to crystal engineering, through the use of the same NCIs and supramolecular synthons is the field of soft materials. Together, these areas allow researchers to prepare a range of stimuli-responsive materials,[1-3] such as supramolecular gels, metal-organic networks (MOFs), covalent organic frameworks (COFs), and other porous coordination networks. These materials are then of use in catalysis, drug delivery, gas storage, separation and sensing.

As part of a study investigating the factors affecting the formation of supramolecular gels,[4] we considered a range of di- and tri-carboxylic acid linkers, including 2,6-pyridinedicarboxylic acid(26pca), 3,5-pyridinedicarboxylic acid (35pca), and benzene-1,3,5-tricarboxylic acid (btc). The key factors required in linkers are the capacity to form porous networks; having three groups capable of forming NCIs is favourable, eg. btc and 35pca. 26pca was not useful in producing gels, as it lacks the 3rd anchoring point. However, three crystalline compounds of this linker with Fe(III) provided a case study[5] in the influence of reaction time and temperature on the nature of the NCIs and hence the complexity and stability of the structures obtained (Figure 1). We found that btc could be used to form both gels and single crystals, through similar NCIs. A survey of related structures in the CSD[6] found there are four common topological motifs (Figure 2), which cannot be predicted from either the composition or space group of the compound.[7]

References

1. S. Panja and D. J. Adams, *Chem. Soc. Rev.*, 2021, **50**, 5165.
2 T. Wang, E. Lin, Y.-L. Peng, Y. Chen, P. Cheng and Z. Zhang, *Coord. Chem. Rev.*, 2020, **423**, 213485.
3 Y. Wang, W. Wang, Z. Zhang and P. Li, *Appl. Surf. Sci.*, 2022, **571**, 151355.
4. S.C. Zacharias, G. Ramon and S.A. Bourne, *Soft Matter*, 2018, **14**, 4505.
5. S.C. Zacharias, G. Ramon and S.A. Bourne, *Acta Cryst.* 2018, *B***74**, 354.
6. C. R. Groom, I. J. Bruno, M. P. Lightfoot and S. C. Ward, *Acta Cryst*. 2016, *B***72**, 171.
7. S.C. Zacharias, G. Ramon and S.A. Bourne, *CrystEngComm*, 2022, **24**, 2393.

Fig 1.Structures of 26pca with Fe(III)

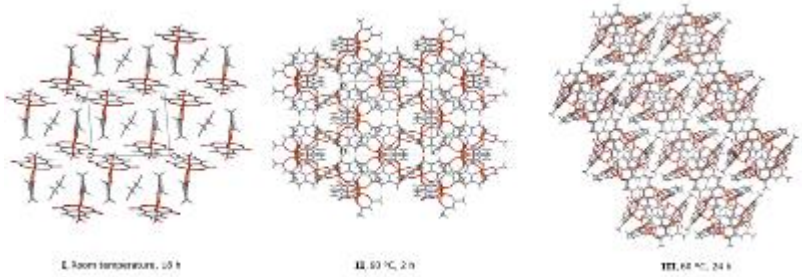

Fig 2 Motifs observed in btc coordination polymers

Back to Table of contents

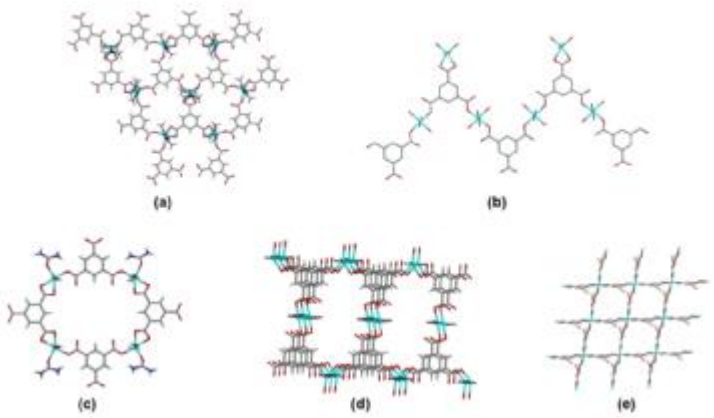

Back to Table of contents

MS29 Crystal engineering: structural flexibility, phase transitions and non-standard manipulation of synthons

MS29-04

Mechanically responsive crystals: Tuning flexibilty through fine-tuning intermolecular interactions

M. Đaković [1], M. Pisačić [1], O. Mišura [1]
[1]*Universit of Zagreb, Faculty of Science - Zagreb (Croatia)*

Abstract

Responsiveness of crystalline solids, in particular molecular crystals, to a variety of external stimuli has become a highly desired property as it enables their application in emerging technologies. Although adaptability of crystals to external stimuli other than sole mechanical force has been widely reported, mechanically stimulated flexibility is still relatively rarely observed among molecular crystals and the rationale behind those responses is far from being fully understood [1].

Coordination polymers, in addition to being ideal model systems for exploring structural prerequisites for delivery of a specific mechanical response [2], have recently offered a range of not hitherto observed mechanical behaviours of crystalline materials [3-5]. Supramolecular interactions, in particular hydrogen and halogen bonds, emerged as one of the key structural features in the delivery of a targeted mechanical response, and their role in fine-tuning those responses, as well as a correlation of their influence in crystal packing and mechanical response, will be demonstrated on several recent examples [3-7].

This work has been fully supported by the Croatian Science Foundation under Project IP-2019-04-1242.

References

[1] P. Commins, I. T. Desta, D. P. Karothu, M. K. Panda, P. Naumov, *ChemCommun*, 52 (2016) 13941-13954.
[2] M. Đaković, Ž. Soldin, B.-M. Kukovec, I. Kodrin, C. B. Aakeröy, N. Baus, T. Rinovec, *IUCrJ* 5 (2018) 13-21.
[3] M. Đaković, M. Borovina, M. Pisačić, C. B. Aakeröy, Ž. Soldin, B.-M. Kukovec, I. Kodrin, *Angew. Chem. Int. Ed.* 57 (2018) 14801–14805.
[4] M. Pisačić, I. Biljan, I. Kodrin, N. Popov, Ž. Soldin, M. Đaković, *Chem.Mater.* 33 (2021) 3660–3668.
[5] M. Pisačić, I. Kodrin, A. Trninić, M. Đaković, *Chem.Mater.* 34 (2022) 2439–2448.
[6] M. Pisačić, I. Kodrin, I. Biljan, M. Đaković, *CrystEngComm* 23 (2021) 7072–7080.
[7] O. Mišura, M. Pisačić, M. Đaković, *in preparation*

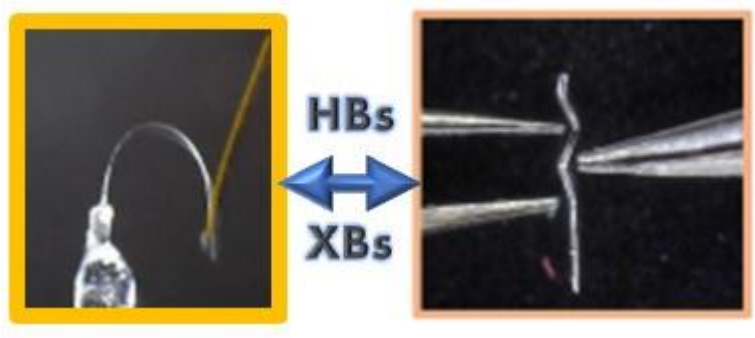

Back to Table of contents

MS29 Crystal engineering: structural flexibility, phase transitions and non-standard manipulation of synthons

MS29-05

Less is more: How the lack of strong H-bonds highlights the role of weak interactions.

C. Tedesco [1], G. Pierri [1], R. Schettini [1], F. De Riccardis [1], I. Izzo [1]
[1]*University of Salerno - Fisciano (Italy)*

Abstract

Peptoids are N-substituted polyglycines with useful biological activities and interesting chemical properties both in solution and in the solid state [1].
Recently, our group evidenced how environmental changes such as temperature, humidity, gas pressure, etc.) may trigger the dynamic behavior of cyclic peptoids in the solid state [2]. We established the solvatomorphic behavior of a cyclic hexapeptoid decorated with four propargyl and two methoxyethyl side chains, which led to the discovery of two pure crystalline forms and four solvates [2,3]. Interestingly, the methanol solvate and the hydrate form result in a stable porous molecular framework, which adsorbs gases as propyne or carbon dioxide, but not methane [4].
By conformational energy and lattice energy calculations we demonstrated that intermolecular CH···OC backbone-to-backbone interactions are able to tighten a peptoid porous framework upon guest release by triggering a reversible single crystal to single crystal transformation at above 40°C. Thus, two propargyl side chains move by 113° and form an unprecedented “CH-π zipper”, which may be unzipped by new CH···OC and CH-π interactions by exposure to guest vapors [5].
We also evidenced that the formation of stable porous frameworks based on cyclic peptoids can be triggered by strategic choice of appropriate side chains. We demonstrated that substitution of distal propargyl side chains with methoxyethyl groups in a fully propargylated cyclic octamer peptoid greatly improves the solid state stability inducing permanent one-dimensional porosity of the compound [6]. More recently we evidenced the role of intramolecular backbone-to-backbone CO···CO interactions and CH···OC hydrogen bonds in the stabilization of enantiomorphic right- and left-handed polyproline type I helices in cyclic dodecapeptoids [7].
In this contribution we will show how the lack of the amide proton prevents the formation of NH···CO H-bonds and makes peptoids the ideal platform for evidencing the influence of weak interactions, as CH···OC and CO···OC interactions, in stabilizing molecular conformations, triggering conformation polymorphism and phase transitions, and ultimately determine their dynamic solid state behavior.

References

[1] C. Tedesco , L. Erra , I. Izzo, F. De Riccardis, *CrystEngComm*, **2014**, *16* , 3667 —3687.
[2] A. Meli, E. Macedi, F. De Riccardis, V. J. Smith, L. J. Barbour,I. Izzo, C. Tedesco, *Angew. Chem., Int. Ed.,* **2016**, *55*, 4679– 4682.
[3] E. Macedi, A. Meli, F. De Riccardis, P. Rossi, V. J. Smith, L. J. Barbour, I. Izzo, C.Tedesco, CrystEngComm, **2017**, *19*, 4704– 4708.
[4] G. Pierri, A. Landi, E. Macedi, I. Izzo, F. De Riccardis, R. Dinnebier, C. Tedesco , *Chem. – Eur. J.*, **2020**, *26* , 14320 —14323.
[5] G. Pierri, M. Corno , E. Macedi , M. Voccia, C. Tedesco, *Cryst. Growth Des.*, **2021**, *21* , 897 — 907.
[6] C. Tedesco, R. Schettini, V. Iuliano, G. Pierri, A. N. Fitch, F. De Riccardis, I. Izzo, *Cryst. Growth Des.*, **2019**, *19* , 125 —133.
[7] G. Pierri, R. Schettini, F. F. Summa, F. De Riccardis, G. Monaco, I. Izzo,Consiglia Tedesco, *Chem. Comm.,* **2022**, DOI: 10.1039/D2CC00682K

Back to Table of contents

MS30 Advanced porous materials : MOFs, COFs, SOFs....and what else?

MS30-01

Exploring the guest-induced structural dynamics in MOFs by in situ PXRD techniques

V. Bon [1]
[1]*Technische Universität Dresden - Dresden (Germany)*

Abstract

Metal-Organic Frameworks (MOFs) are crystalline porous solids, constructed from metal clusters and organic ligands, connected in 2D-Networks or 3D-Frameworks using the modular building principle [1]. Benchmark values of specific surface area and pore volume, but also target and precise design of pore aperture and its functionalization makes them quite promising for gas storage, separation, catalysis, sensors and many other applications [2]. Several dozens of MOFs show a unique feature of framework flexibility and can adapt their pore confinement upon adsorption and desorption of guest molecules, which is accompanied by the structural transitions in adsorbent [3, 4]. These solids are actively discussed for several applications, such as gas storage and separation, sensing and mechanical energy storage [5].

Monitoring the gas and vapour adsorption by PXRD allows to follow the structural changes of MOF and represents an important tool for the understanding of intrinsic framework dynamics. In the following contribution, we present multipurpose instrumentations, dedicated to monitoring the gas and vapour adsorption in MOFs by PXRD or X-ray absorption spectroscopy in a wide range of pressure and temperatures [6]. Instrumentations are commissioned at KMC-2 beamline of BESSY II synchrotron and are available for the users of the large scale facility. Several archetypical studies of guest-induced structural dynamics in micro- and mesoporous MOFs will be discussed.

However, the access to synchrotron instrumentation is limited and strongly connected to the beamtime proposals, work cycles of the large scale facility and other factors. This motivated us to develop *in situ* PXRD/adsorption chamber for the laboratory powder X-ray diffractometer. Herein, we introduce the instrumentation and the first results of PXRD studies using a laboratory *in situ* adsorption chamber.

References

[1] M. Eddaoudi, M. O'Keeffe, O.M. Yaghi et al., *Acc. Chem. Res.*, **34** (2001) 319-330.
[2] S. Kitagawa, R. Kitaura, S.-i. Noro, *Angew. Chem. Int. Ed.*, **43** (2004) 2334-2375.
[3] A. Schneemann, V. Bon, S. Kaskel, et al., *Chem. Soc. Rev.*, **43** (2014) 6062-6096.
[4] S. Krause, N. Hosono and S. Kitagawa, *Angew. Chem. Int. Ed.*, **59**, 2020, 15325.
[5] Special issue MOFs, *Chem. Soc. Rev.*, **43**, 2014.
[6] V. Bon, E. Brunner, A. Pöppl and S. Kaskel, *Adv. Funct. Mater.*, **30**, 2020, 1907847.

Back to Table of contents

MS30 Advanced porous materials : MOFs, COFs, SOFs....and what else?

MS30-02

Multivariate frameworks and the eye of the beholder

S. Canossa [1]
[1]*Max Planck Institute for Solid State Research - Stuttgart (Germany)*

Abstract

Multivariate frameworks are reticular structures where specific sites can host chemically different building block alternatives. Or… are they?

The ever-astounding diversity of reticular structures such as metal–organic frameworks (MOFs) entered new territories since chemists started to explore the synthesis of crystalline MOFs with aperiodic composition.[1] Most importantly, short-range sequences of functionalities in these so-called 'multivariate' frameworks were found to confer functions otherwise unachievable.[2] While the resulting enthusiasm drives the pursuit of better synthetic control and the search for new functional behaviours, crystallographers and structural chemists might wonder: What precisely is multivariation? Is it limited to composition? How can we classify multivariate frameworks according to sensible and useful criteria?[3]

This contribution will delve into these still largely unanswered questions, thereby highlighting another prominent issue in reticular chemistry: How can we characterize framework multivariation? Our recent research on single-crystal total scattering of MOFs offered some insights on how all these questions could be addressed, leading to a renewed viewpoint on reticular materials and their structural understanding.

References

1. H. Furukawa, U. Müller, O. M. Yaghi, "Heterogeneity within Order in Metal–Organic Frameworks". *Angewandte Chemie International Edition* 54, 3417–3430 (2015).
2. Q. Liu, H. Cong, H. Deng, "Deciphering the Spatial Arrangement of Metals and Correlation to Reactivity in Multivariate Metal–Organic Frameworks". *Journal of the American Chemical Society* 138, 13822–13825 (2016).
3. S. Canossa, Z. Ji, C. Gropp, Z. Rong, E. Ploetz, S. Wuttke, O. M. Yaghi, "System of sequences in multivariate reticular structures", *Nature Reviews Materials* (2022; accepted)

Back to Table of contents

MS30 Advanced porous materials : MOFs, COFs, SOFs....and what else?

MS30-03

A combined experimental and theoretical approach to interpret the anomalous thermal behavior of Pb-exchanged zeolite (STI)

G. Cametti [1], D. Roos [1], S.V. Churakov [2], D. Prieur [3], A.C. Scheinost [3]

[1]Institute of Geological Sciences, Baltzerstrasse 1+3, 3012 - Bern (Switzerland), [2]Paul Scherrer Institut, Forschungstrasse 111, 5232 - Villigen (Switzerland), [3]The Rossendorf Beamline at the European Synchrotron Radiation Facility (ESRF), Avenue des Martyrs 71, 38043 - Grenoble (France)

Abstract

Pb-exchanged zeolites are of interest because of their applications in environmental-related issues and in industrial processes. The thermal stability of these materials is an important aspect to consider if the retaining capacity of the incorporated heavy metals has to be assessed. In our recent study, we characterized and determined the crystal structure of a natural zeolite stellerite (with **STI** framework type), exchanged with Pb^{2+} [1] and we further investigated its thermal behavior as a function of increasing temperature [2]. It was found that Pb-STI showed an anomalous thermal behavior with respect to the natural counterpart and the other metal-exchanged zeolites with **STI** framework type [3]. In particular, after an initial contraction of the unit-cell volume (-3.5%), accompanied by dehydration, the framework expands (+2%) and adopts a structural topology equivalent to that observed at room temperature. Thus, in contrast to natural stellerite and to the Cd-, Ag-, and Na- exchanged forms [4,5] no breaking of the tetrahedral bonds is observed upon heating and, most important, the thermal stability significantly increased.

The interpretation of the mechanism, which leads to the change from negative to positive thermal expansion during the dehydration process, is still unclear and complicated by: i) the occurrence of different extraframework (EF) species (i.e. Pb^{2+}, $Pb(OH)^{+}$ and H_2O), and ii) their severe disorder within the voids. In this contribution, different hypotheses and eventual reactions occurring upon heating were experimentally and theoretically tested to shed light on the observed anomalous dehydration behavior.

The following scenario were considered: i) dehydration of the structure, i.e. loss of H_2O without any further reaction. ii) dehydration accompanied by hydrolysis of the water molecules according to the reaction $H_2O \rightleftharpoons OH^- + H^+$ [6]. iii) loss of H_2O and subsequent formation of Pbx(OH)x or PbxOx clusters. iv) oxidation of Pb^{2+} in Pb^{4+}, according to the reaction $Pb^{2+} + 2\ H_2O \rightleftharpoons Pb^{4+} + 2OH^- + H_2(g)$ [7].

The best agreement between experimental data and theoretical predictions was observed for models iii) and iv). However, we did not have any experimental evidence of Pb oxidation. The Pb-L3 XANES spectra of Pb-stellerite collected from 25 to 400°C showed the expected increase of thermal disorder with increasing temperature, but no change of local symmetry or oxidation state during the dehydration process. For model (iv), the formation of different kind of clusters ($Pb_2(OH)_2$, Pb_2O_2, $Pb_4(OH)_4$, etc.) was tested. The best agreement between model and observation corresponds to a structure with 33% of Pb forming $Pb_4(OH)_4$ clusters, located inside the bigger cavity of stellerite (Fig. 1).

References

[1]Roos, D., Scheinost, A. C., Churakov, S. V., Nagashima, M., Cametti, G. (2021) On the nature of Pb species in Pb-exchanged zeolite stellerite (STI): a combined experimental and theoretical study. Microporous and Mesoporous Materials, 327, 111444.

[2]Roos, D. (2021) Crystal structure and thermal stability of STI and LEV zeolites after Pb^{2+} incorporation. Master Thesis, University of Bern, Switzerland, 59 pp.

[3]Arletti, R., Mazzucato, E. Vezzalini, G. (2006) Influence of dehydration kinetics on T-O-T bridge breaking in zeolites with framework type STI: The case of stellerite. American Mineralogist, 91, 628-634.

[4]Cametti, G., Scheinost, A.C., Giordani, M. Churakov, S.V. (2019) Framework modifications and dehydration path of a Ag^{+}-modified zeolite with STI framework type. Journal of Physical Chemistry C, 123, 13651-13663.

Back to Table of contents

[5]Cametti, G., Scheinost, A. C., Churakov, S. V. (2019) Structural modifications and thermal stability of Cd^{2+}-exchanged stellerite, a zeolite with STI framework type. Journal of Physical Chemistry C, 123, 25236-25245.
[6]Albuquerque, R. Q., Calzaferri, G. (2007) Proton activity inside the channels of zeolite L. Chemistry a European Journal, 13, 8939-8952.
[7]Ronay, C., Seff, K. (1985) Crystal structure of Pb_6-A and $Pb_9(OH)_8(H_2O)_3$-A. Zeolite A ion exchanged with Pb_{2+} at pH 4.3 and 6.0 and evacuated. Journal of Physical Chemistry, 89, 1965-1970.

Fragment of the simulated Pb-STI structure showing

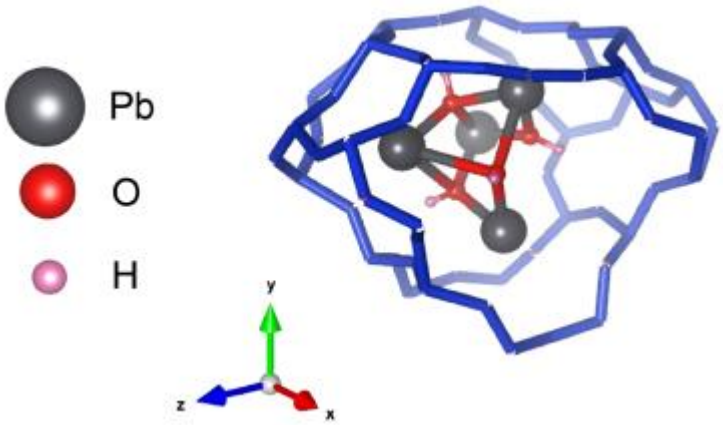

Back to Table of contents

MS30 Advanced porous materials : MOFs, COFs, SOFs....and what else?

MS30-04

Pore architecture of the MIL-53(Al) mechanically controlled to intelligently modulate CO2 adsorption

P. Yot [1], I. Paul [1], F. Alabarse [2], C. Thessieu [3], S. Wang [4], S. Christian [4], M. Guillaume [1]
[1]University of Montpellier - Montpellier (France), [2]Elettra Sincrotrone Trieste - Basovizza (Italy), [3]Almax Easy-Lab - Diksmuide (Belgium), [4]Ecole Normale Supérieure - ESPCI Paris - Paris (France)

Abstract

External control over the pore size of flexible Metal-Organic Frameworks (MOFs) such as MIL-53(Al) (MIL: Matériaux de l'Institut Lavoisier) has recently emerged as an innovative and promising concept, with possible applications to gas storage and separation [1]. In this work we have designed a new type of pressure cell capable of studying by in situ powder X-ray diffraction the structural behavior of the MOF MIL-53(Al) under the combined application (i) of a mechanical stress (σ_{mech}≤1 GPa) and (ii) a gas pressure (P_{gas}≤20 bar). This new cell developed in collaboration with Almax-easyLab or "combined stress-pressure clamp" (CSPC) was successfully validated on the XPress line at Elettra Sincrotrone Trieste by following the structural modifications of MIL-53 (Al) which as it is well known presents different crystalline forms with variable volumes: (i) large-pore form (lp, V_{uc}~1450 Å^3), narrow-pore form (np, V_{uc}~900-1150 Å^3) under gas adsorption (CO_2, H_2O,...) and (ii) closed-pore form (cp, V_{uc}~890 Å^3) only obtained by compression and stabilized by the π-π interactions between the benzene rings of the organic linkers in the wine-rack 1D porous network of the solid [2]. An excellent consistency of the switchabilty of the structure with previous work was demonstrated under uniaxial mechanical stress (Figure 1a) and then under CO_2 adsorption with the identification of the three possible forms of MIL-53(Al). When the two stimuli (σ_{mech}+P_{gas}) are combined, the results obtained show: (i) for the first time the reopening of the cp form of MIL-53(Al) towards the np then lp form and (ii) a dependence of the adsorption pressures leading to the formation of these forms with applied mechanical pressures (Figure 1b-d). This work has therefore allowed a better understanding of the interaction between mechanical stress and the adsorption of host molecules and thus opens the door to other opportunities for innovative applications, such as external control over separation performance, stress-swing adsorbent regeneration, actuated gas storage and fluid-solid barocaloric for example.

References

[1] N. Chanut et al., Nat. Commun. (2020), 11, 1216.
[2] P. G. Yot et al, Chem. Commun. (2014), 50, 9462–9464.
[3] P. Iacomi et al., Angew. Chem. Int. Ed. (2022), e202201924.

Figure 1: Selected sweeps of P under increase σ

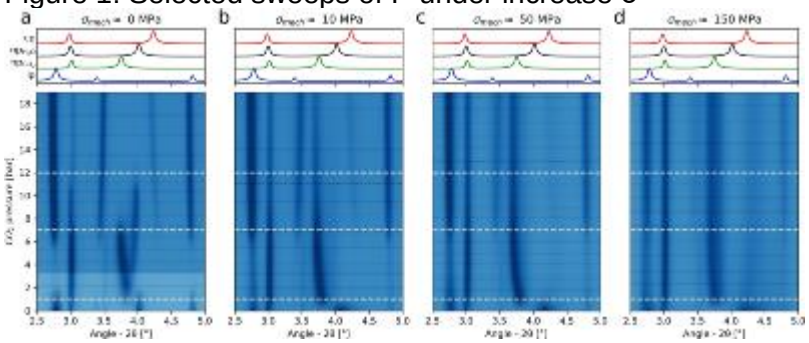

Back to Table of contents

MS30 Advanced porous materials : MOFs, COFs, SOFs....and what else?

MS30-05

Dynamic Behaviour of a Tetrapyridine-Based Crystalline Supramolecular Organic Framework

D. Marchetti [1], F. Portone [2], F. Mezzadri [2], E. Dalcanale [2], M. Gemmi [1], A. Pedrini [2], C. Massera [2]
[1]Istituto Italiano di Tecnologia - Pontedera (Italy), [2]Università di Parma - Parma (Italy)

Abstract

In recent years, supramolecular organic frameworks (SOFs) have emerged as an important class of functional porous materials, alongside metal-organic frameworks (MOFs) and covalent organic frameworks (MOFs)[1-2]. Herein we report a dynamic responsive SOF obtained through the self-assembly of rigid aromatic tetrahedral molecules (tetra-4-(4-pyridil)phenylmethane, **TPPM**) *via* van der Waals interaction and non-conventional hydrogen bonds. It presents a responsive behaviour, in its crystalline form, based on the reversible switch from an empty to a filled phase framework and *vice-versa*, when exposed to specific organic solvents vapours and heat, respectively.

The phase transition between filled and empty phase goes through a single-crystal to single-crystal path, despite that after the solvent removal the obtained phase presents high defectivity and nanometric crystalline domains. The Empty phase single crystals were too small and defective to be characterized by standard X-ray diffraction experiments. Their crystal structure could be determined only by 3D electron diffraction (3D ED)[3-4] working in low dose mode with a parallel nanobeam of 150 nm in size, which matches perfectly with the grain size of the compound. The structural model obtained ab-initio by 3D ED was also refined taking into account dynamical scattering to a final R-value of 13%, with thermal parameters that mimic the rotational flexibility of the biarylic wings.

References

1. Atwood, J. L.; Barbour, L. J.; Jerga, A. A New Type of Material for the Recovery of Hydrogen from Gas Mixtures. Angew. Chem. Int. Ed. 2004, 43, 2948 –2950.

2. Yang, W.; Greenaway, A.; Lin, X.; Matsuda, R.; Blake, A. J.; Wilson, C.; Lewis, W.; Hubberstey, P.; Kitagawa, S.; Champness, N. R.; Schröder, M. Exceptional Thermal Stability in a Supramolecular Organic Framework: Porosity and Gas Storage. J. Am. Chem. Soc. 2010, 132, 14457–14469.

3. Gruene, T.; Wennmacher, J. T. C.; Zaubitzer, C.; Holstein, J. J.; Heidler, J.; Fecteau-Lefebvre, A.; De Carlo, S.; Müller, E.; Goldie, K. N.; Regeni, I.; Li, T.; Santiso-Quinones, G.; Steinfeld, G.; Handschin, S.; van Genderen, E.; van Bokhoven, J. A.; Clever, G. H.; Pantelic, R. Rapid Structure Determination of Microcrystalline Molecular Compounds Using Electron Diffraction. Angew. Chem. Int. Ed., 2018, 57, 16313-16317.

4. Gemmi, M.; Mugnaioli, E.; Gorelik, T. E.; Kolb, U.; Palatinus, L.; Boullay, P.; Hovmoller, S.; Abrahams, J. P. 3D Electron Diffraction: The Nanocrystallography Revolution. ACS Cent. Sci., 2019, 5, 1315-1329.

Dynamic Behaviour of the proposed SOF

Back to Table of contents

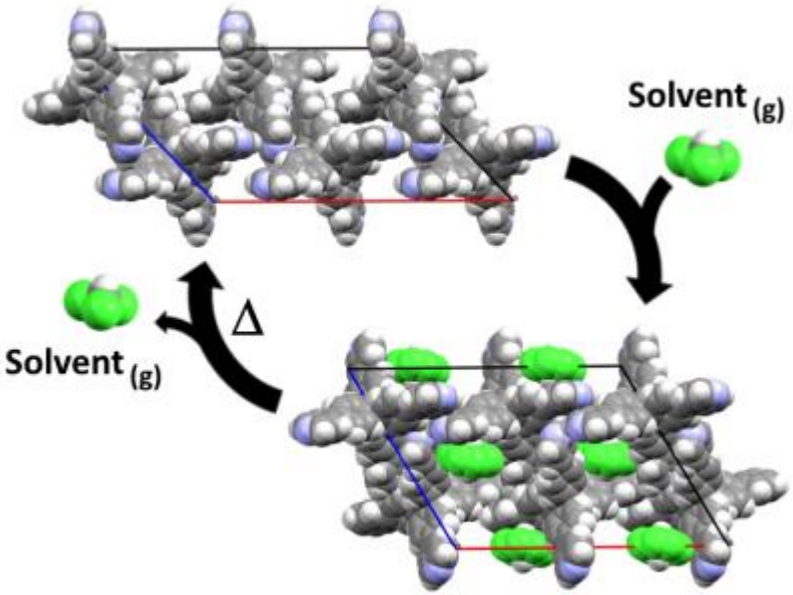

3D ED Reciprocal Space Reconstruction

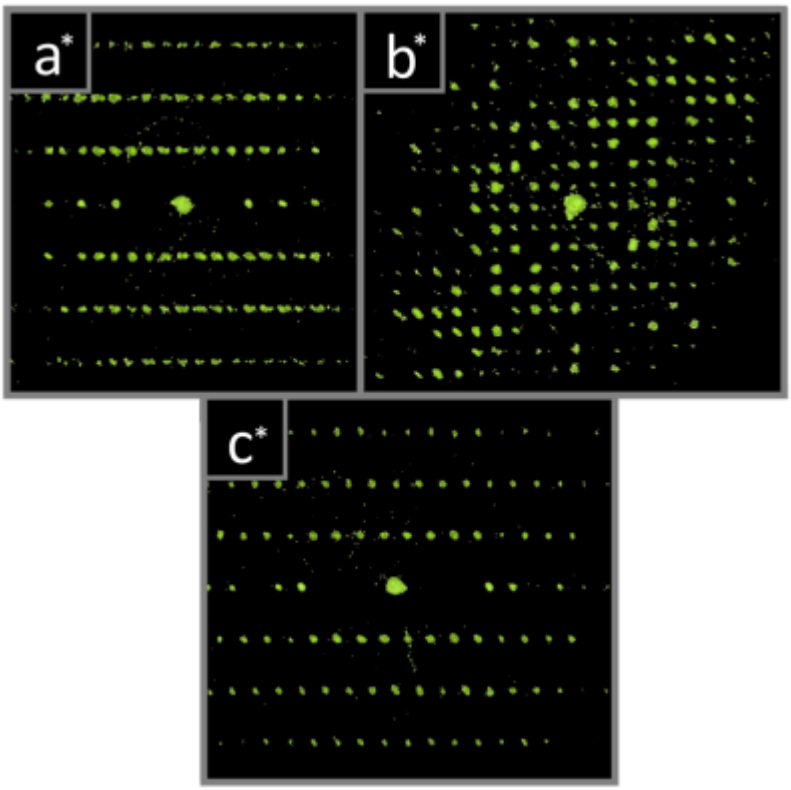

Back to Table of contents

MS31 Unconventional interactions or symmetries for optimized and new properties, including chirality

MS31-01

Anion-Anion Self-assembly via Matere Bond and other σ-Hole Interactions

G. Resnati [1], A. Pizzi [1], M. Calabrese [1]
[1]*Politecnico di Milano - Milano (Italy)*

Abstract

Several attractive interactions can effectively balance the coulombic repulsion between ions with the same charge and, for instance, can allow for the self-assembly of anions into stable adducts. An example is the hydrogen bond (HB) that can drive the formation of anion-anion dimers stable in the gas, liquid, and solid phases thanks to the force localized in the region of the HB between two protic hydroxyanions (e.g., HCO_3^-, HSO_4^-, and $H_2PO_4^-$).

The anisotropic distribution of the electron density in the anion, namely the formation of a pnictogen bond (PnB), has been used to rationalize the formation of adducts involving polyatomic anions of group 15 elements [1]. An analogous approach will be presented in this lecture in order to rationalize the self-assembly of polyatomic anions wherein the central atom of the polyatomic anion is an element of group 7 or 11 of the Periodic Table. Specifically, it will be described how the matere bond (MaB) can drive the organization of permanganate and perrhenate anions into dimers and infinite chains [2] and how tetrachlorido aurate anions self-assemble into infinite chains under coinage bond (CiB) control [3].

References

[1] A. Bauza, A. Frontera, T. J. Mooibroek, *Nature Comm.* **2017**, *8*, 14522.
[2] Daolio, A.; Pizzi, A.; Terraneo, G.; Frontera, A.; Resnati, G., *ChemPhysChem* **2021**, *22*, 2281-2285.
[3] A. Daolio, A. Pizzi, G. Terraneo, M. Ursini, A. Frontera, G. Resnati, *Angew. Chem. Int. Ed.* **2021**, *60*, 14385–14389.

Back to Table of contents

MS31 Unconventional interactions or symmetries for optimized and new properties, including chirality

MS31-02

Interactions of aromatic ligands in sandwich and half-sandwich compounds

D. Malenov [1], S. Zaric [1]
[1]*University of Belgrade-Faculty of Chemistry - Belgrade (Serbia)*

Abstract

Aromatic rings in sandwich and half-sandwich compounds can form the same types of interactions as non-coordinated aromatic molecules. However, in organometallic compounds, because of the coordination, the electrostatic potential of the aromatic ring can be changed, causing some changes in the interactions [1,2].

Stacking interaction between coordinated and uncoordinated benzene has the energy of −4.40 kcal/mol, while the calculated staking between two coordinated benzenes has the energy of −4.01 kcal/mol. These energies are significantly stronger than stacking between two uncoordinated benzenes (−2.73 kcal/mol). In crystal structures coordinated benzene and coordinated cyclopentadienyl anion form stacking interactions that dominantly have large horizontal displacements (more than 4.5 Å). This dominance is caused by the relatively strong stacking interactions at large displacements [1].

Electrostatic potential surfaces of aromatic ligands in half-sandwich compounds are entirely positive, making them capable of forming strong anion-pi and C-H/anion interactions [2,3,4] Our calculations of energies of interactions between half-sandwich compounds and halide anions showed that aromatic ligands in half-sandwich compounds can bind to anions. Anion-pi interactions with half-sandwich compounds are stronger than with most of organic aromatic compounds, while C-H/anion interactions are even stronger than anion-pi interactions [2].

Our studies show that transition metal coordination makes aromatic moieties suitable for strong stacking interactions, as well as strong interactions with anions and gives new insights into the molecular design.

References

[1] Malenov, D. P.; Zarić, S. D., Coord. Chem. Rev. 2020, 419, 213338.
[2] Malenov, D. P.; Zarić, S. D., Chem. Eur. J. 2021, 27, 17862.
[3] Rather, I. A.; Wagay, S. A.; Ali, R., Coord. Chem. Rev. 2020, 375, 213327.
[4] Frontera, A.; Gamez, P.; Mascal, M.; Mooibroek, T. J.; Reedijk, J., Angew. Chem. Int. Ed. 2011, 123, 9736.

Back to Table of contents

MS31 Unconventional interactions or symmetries for optimized and new properties, including chirality

MS31-03

Solid solutions as a mean to investigate and exploit the structure property relationships in molecular crystals

M. Lusi [1]
[1]*University of Limerick - Limerick (Ireland)*

Abstract

Current strategies for the rational design of crystal structure and the optimization of their properties rely on the exploitation of known supramolecular interactions and the application of rough practical experimental rules on thumbs. This approach enable the prediction of general structural features but does not allow for fine tuning and properties optimization. On the contrary the continuous stoichiometry variation that is typical of substitutional solid solutions offers a better control of structures and properties.
Here a series of solid solutions are presented to control solubility and thermal stability in multidrug solid forms. At the same time, stoichiometry variation in these phases give insight into the relative strength of different supramolecular interactions. In particular, a cocrystals that combines enantiomers of a chiral drug and a multiple chiral conformer exemplifies the potential of these materials to synthetic crystallography and crystal engineering.

Back to Table of contents

MS31 Unconventional interactions or symmetries for optimized and new properties, including chirality

MS31-04

n→π* charge transfer between an iodide anion and a quinoid ring

K. Molcanov [1], V. Milašinović [1], V. Vuković [2], A. Krawczuk [3], C. Hennig [4], M. Bodensteiner [2]
[1]Rudjer Bošković Institute - Zagreb (Croatia), [2]Universitat Regensburg - Regensburg (Germany), [3]Universitat Goettingen - Goettingen (Germany), [4]ESRF - Grenoble (France)

Abstract

π-hole interaction between an iodide anion and a quinoid ring in a co crystal of 3-chloro-*N*-methylpyridinium iodide with tetrabromoquinone (**3-Cl-*N*-MePy·I·Br$_4$Q**) involves a sandwich-like I$^-$···quinone···I$^-$ moiety with close contacts between the iodide anion and carbon skeleton of the quinoid ring (Fig 1). Distance between the iodide and the ring mean plane is 3.73 Å, which is slightly shorter than the sum of van der Waals radii for C and I. This close contact forms because the quinoid ring with four electron-withdrawing substituents is severely electron-depleted, resulting in a large π-hole at the carbonyl C atom [1,2]. In the studied case there is also a partial electron transfer between the iodide and the quinone which is noted by a change of colour: the neutral quinone is yellow, while the co-crystals and the semiquinone crystals are black.

This unusual interaction is studied by quantum crystallography, combining X-ray charge density with quantum chemical modelling; a study under a wide range of conditions involves variable-temperature crystallography (80 - 400 K) and high-pressure crystallography.

The interaction involves an *n*→π* charge transfer, so the quinoid ring has a partial negative charge (estimated to 0.08 - 0.11 e) and a partial radical character. The X-ray charge density study revealed two symmetry-independent bonding critical points between the iodide and carbon atoms of the ring with maximum electron density of 0.065 e Å^{-3}, which were reproduced by quantum chemical modelling. Energy of the interaction is estimated to -13 kcal mol^{-1}, which is comparable to hydrogen bonding; it is dominantly of electrostatic nature, with a considerable dispersion component.

References

[1] K. Molčanov, G. Mali, J. Grdadolnik, J. Stare, V. Stilinović, B. Kojić-Prodić (2018). *Cryst. Growth Des.*, **18**, 5182-5193.
[2] V. Milašinović, K. Molčanov (2021). *CrystEngComm*, **21**, 2304-2315.

A sandwich-like I−···Br4Q···I− unit.

Back to Table of contents

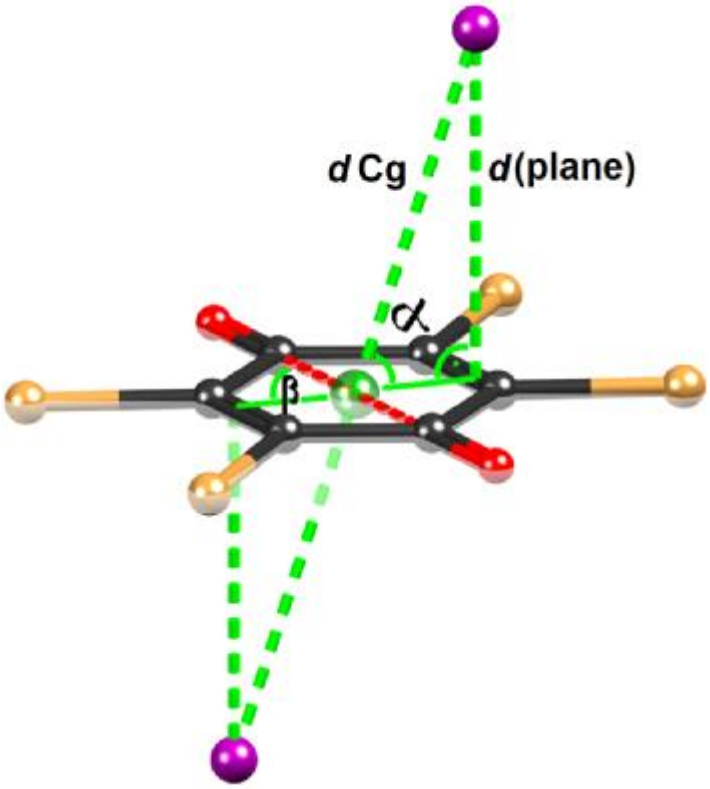

Back to Table of contents

MS31 Unconventional interactions or symmetries for optimized and new properties, including chirality

MS31-05

Simulation of lattice defects in quinacridone

M.U. Schmidt [1], B. Scherer [1], D. Brey [1]
[1]Goethe Universität - Frankfurt (Germany)

Abstract

Various lattice defects in the alpha-I-phase of quinacridone (C20H12N2O2) were simulated using lattice-energy minimisations. alpha-I-Quinacridone forms a chain structure in P -1, Z = 1. The molecules are connected by hydrogen bonds along [010], by pi-stacking along [100] and by weak van der Waals interactions along [001]. alpha-I-Quinacridone is inherently nanocrystalline. Lattice defects were calculated in correspondingly large supercells with up to 4464 atoms, using a previously evaluated force-field. Vacancies, vacancy aggregates and interstitial molecules are energetically very unfavourable. A misorientation of a single molecule (flip around [010] by 180°) causes an energy increase of 243.7 kJ/mol. Various edge defects and screw defects were investigated. A screw defect along [010] leads to E = + 76.1 kJ/mol, all other defects cause even greater energy increases. In contrast, the rotation of an entire chain around [010] by 180° leads to a very small energy increase only (E = 1.57 kJ/mol), and the real crystals probably contain a high number of such defects. Various planar defects were calculated, including different stacking disorders, anti-phase domains and commensurately modulated structures with two different types of layers having different lateral periodicities. Stackings faults along [001] with herringbone packing instead of parallel packing are energetically quite favourable; the same is true for antiphase domains in the [001] direction. As an example for a bulk defect we calculated antiphase domains, in which blocks of 4*4 chains are rotated by 180° around [010], which increases the energy only very slightly. Twinning by mirroring at the (001) plane is energetically favourable, and was observed in an HRTEM image. A rotation of chains, layers or block around [010] by 180° causes only a very slight modification of the molecular packing, which was not observable in the HRTEM. These investigations of lattice defects in alpha-I-quinacridone provide an insight to lattice defects, their energies and local structures in other similar organic chain structures, too.

References

D. Brey, B. Scherer, M.U. Schmidt, submitted.

Back to Table of contents

MS32 Advanced techniques to disclose Structure-Property Relationships

MS32-01

Cooperative dynamics in metal–organic frameworks: from free-and-isolated to interacting synchronous rotors

C. Bezuidenhout [1], J. Perego [1], S. Bracco [1], P. Sozzani [1], A. Comotti [1]
[1]*University of Milano Bicocca - Milan (Italy)*

Abstract

Owing to their modular nature, Metal-Organic frameworks (MOFs) represent a new platform for achieving and exploring structural framework that allows for control over the ligand environment. This allows for tuning of the ligand properties towards potentially desired outcomes. Traditionally when inserting molecular rotors as struts into MOFs, the gaol is to isolate them and consequently lowering their reorientation energy barriers for fast rotary dynamics. We have achieved such a system of isolated bicyclo[1.1.1]pentandioate (**FTR**) rotors within a MOF structure which yielded an energy barrier for rotation of a couple calories per mole. [1]
The outstanding synthetic versatility of MOFs allows us to insert the **FTR** rotor into a pillar-and-layer Zn-MOF where the rotors can interact with their neighbours (Fig 1 and 2). Contrary to expectations, these rotors navigate the rotational potential energy landscape in such a way to produce co-rotating pairs of rotors or geared molecular rotors. These *geared molecular rotors* have a very low energy barriers for rotation (24 cal/mol) owing to the synchroneity of their rotation. Additionally, the collective bipy-ring rotation are in concert with the framework structural dynamics that gives rise to controllable swinging between two identical arrangements in a dynamically disordered structure. Upon cool down to 160 K the framework become more ordered thus indicating that the reorientation dynamics of the bipy pyridyl rings are being stopped. This framework gymnastics is a good example of structural dynamics controlled by rotor reorientation dynamics. [2]

References

[1] J. Perego, S. Bracco, M. Negroni, C. X. Bezuidenhout, G. Prando, P. Carretta, A. Comotti, P. Sozzani *Nature Chem*. **2020**, 12, 845.
[2] J.Perego, C. X. Bezuidenhout, S. Bracco, G. Prando, L. Marchiò, M. Negroni, P. Carretta, P. Sozzani, and A. Comotti *Journal of the American Chemical Society* **2021**,143 (33), 13082-13090.

Pillared MOF containing two types of rotors

Back to Table of contents

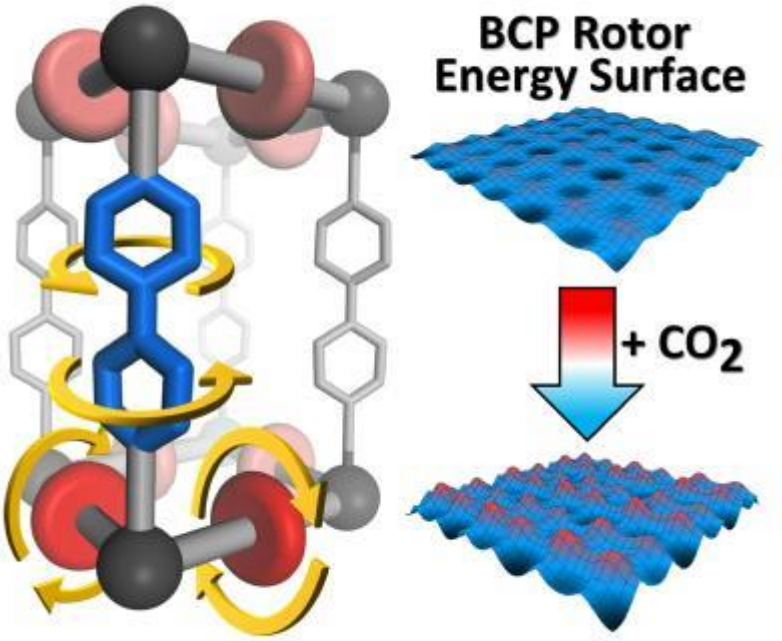

The structure of the bi-ligand pillared MOF system

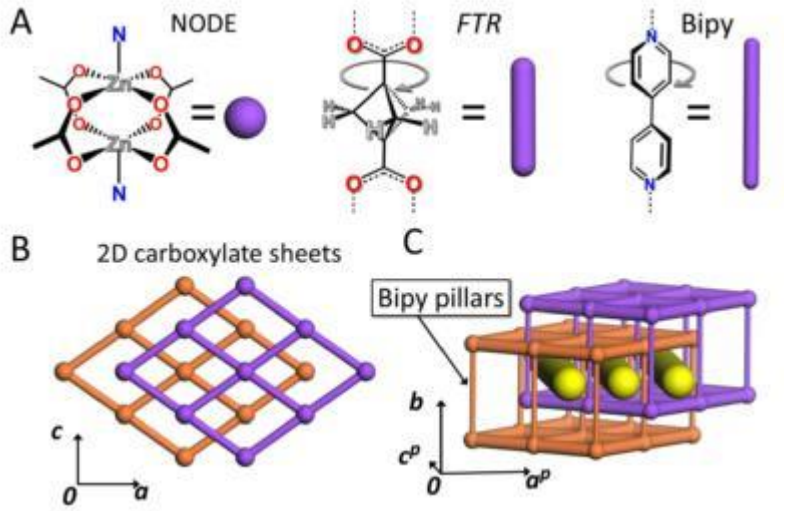

Back to Table of contents

MS32 Advanced techniques to disclose Structure-Property Relationships

MS32-01
Understanding photoswitchable ferroelectrics by combined in-situ XRD with light and electric field

L. Hatcher [1], M. Warren [2], B. Coulson [1], M. Joshua [1]
[1]Cardiff University - Cardiff (United Kingdom), [2]Diamond Light Source - Didcot (United Kingdom)

Abstract
Ferroelectric switches are of great and continuing interest for a wide range of applications including ultrafast electronics (e.g. ferroelectric capacitors, RAM etc.), solid-state cooling, energy harvesting and solar energy solutions.[1, 2] These materials display spontaneous electrical polarisation that can be reversed by the application of an external stimulus, e.g. electric field.[3] Where the direction of polarisation can be controlled by photoactivation, these materials become desirable for photovoltaic applications. Hybrid pervoskites, e.g. methyl ammonium lead iodide, are a class of photoactive ferroelectric materials that have received particular attention in recent years, and have been successfully applied in new generation solar cell technologies.[4] Despite this, understanding of the key structure-property relationships in these, and related, perovskite-like ferroelectrics remains limited[4] and would benefit significantly from in-situ studies with advanced diffraction techniques.
We present the synthesis, crystallisation, dielectric characterisation and in-situ crystallographic investigation of the photoactive ferroelectric $(CH_5N_2)[NaFe(CN)_5(NO)].H_2O$ (1), which is designed in analogy with hybrid perovskites. By incorporating the known linkage isomer photoswitch $[Fe(CN)_5(NO)]^{2-}$ into the hybrid material, predicable photoactive behaviour is introduced that could be used to control the electric properties of the system with light. Using an in-situ electric field cell[5] at the Small Molecule Single Crystal Diffraction Beamline I19 at Diamond Light Source, UK, we identify a new low-temperature phase on cooling a single crystal of 1 in the presence of a +40 kV cm^{-1} applied field, with associated framework distortions and the $CH_5N_2^+$ cations shifting significantly to align with the field. This result provides unique insight into the structure-property relationships responsible for switching in hybrid organic-inorganic materials. Photoswitching in 1 is also confirmed by photocrystallographic studies, with the crystal illuminated in-situ on the diffractometer using 500 nm and 950 nm LED light.

References
1. Scott, J.F. Applications of Modern Ferroelectrics. *Science* 315, 954-959 (2007).
2. Zhang, S., Malič, B., Li, J.-F. & Rödel, J. Lead-free ferroelectric materials: Prospective applications. *Journal of Materials Research* 36, 985-995 (2021).
3. Bowen, C.R. et al. Pyroelectric materials and devices for energy harvesting applications. *Energy & Environmental Science* 7, 3836-3856 (2014).
4. Tsai, H. et al. Light-induced lattice expansion leads to high-efficiency perovskite solar cells. *Science* 360, 67 (2018).
5. Saunders, L.K. et al. An electric field cell for performing in situ single-crystal synchrotron X-ray diffraction. *Journal of Applied Crystallography* 54, 1349-1359 (2021).

Back to Table of contents

MS32 Advanced techniques to disclose Structure-Property Relationships

MS32-03

Quantum crystallography of titanium amides with agostic interactions

L. A. Malaspina [1], S. Grabowsky [1]
[1]*University of Bern - Bern (Switzerland)*

Abstract

C-H bond activation by metal-hydrogen bonding (agostic interactions) plays a central role in catalytic processes [1]. These processes are directly dependent on metal-hydrogen bond energies. The versatility of the coordination modes of the heavy metals allows wide structure and topology variations of the complexes. Therefore, it is of major importance to accurately describe these chemical bonds.

One important drawback is the difficulty of deriving accurate and precise hydrogen atom positions by any kind of experiment. Neutron-diffraction experiments would be the only reliable source of such information, but there is a lack of available accurate X-H bond distances with X being a transition metal from neutron diffraction. Therefore, it would be desirable to determine the elongation of the C-H bonds in agostic interactions and the metal-hydrogen bonding parameters from standard X-ray diffraction experiments. In this context, the capabilities of Hirshfeld Atom Refinement [2] to obtain precise and accurate C-H/C-H…Ti bond parameters in a series of titanium amides are tested. The compounds were synthesized in the group of Prof. Beckhaus, University of Oldenburg, Germany.

Experimental and theoretical charge densities of agostic interactions involving transition metal compounds have been determined and analysed in the past [3]. Here, we use a combination of HAR with subsequent X-ray constrained wavefunction fitting [4] and purely theoretical calculations on the accurate HAR geometries to analyse the related chemical bonding beyond a charge-density analysis. We discuss how signatures of agostic interactions manifest themselves in the classical C-H…Ti agostic interactions found in titanium amides (Figure 1).[5]

References

[1] Bäckvall, J. E. (2002). J. Organomet. Chem. 652(1-2), 105-111.
[2] Jayatilaka, D., Dittrich, B. (2008). Acta Cryst. A, 64, 383-393.
[3] (a) Scherer, W., Wolstenholme, D. J., Herz, V., Eickerling, G., Bruck, A., Benndorf, P., Roesky, P. W. (2010). Angew. Chem., Int. Ed., 49, 2242-2246. (b) Hauf, C.; Barquera-Lozada, J. E.; Meixner, P.; Eickerling, G.; Altmannshofer, S.; Stalke, D.; Zell, T.; Schmidt, D.; Radius, U.; Scherer, W. (2013). Z. Anorg. Allg. Chem., 639, 1996-2004.
[4] (a) Jayatilaka, D. (1998). Phys. Rev. Lett. 80, 798-801. (b) Jayatilaka, D., Grimwood, D. J. (2001). Acta Cryst. A, 57, 76-86.
[5] Adler, C., Bekurdts, A., Haase, D., Saak, W., Schmidtmann, M., & Beckhaus, R. (2014). Eur. J. Inorg. Chem., 8, 1289-1302.

Investigated titanium amide compounds

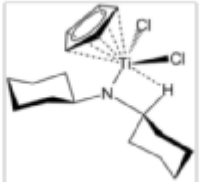

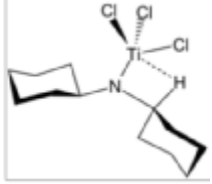

Back to Table of contents

MS32 Advanced techniques to disclose Structure-Property Relationships

MS32-04

Refinement of anomalous dispersion parameters

F. Meurer [1], O.V. Dolomanov [2], C. Hennig [3], N. Peyerimhoff [4], F. Kleemiss [1], H. Puschmann [5], M. Bodensteiner [1]

[1]University of Regensburg - Regensburg (Germany), [2]OlexSys - Durham (United Kingdom), [3]ESRF/Helmholtz-Zentreum - Grenoble/Dresden-Rossendorf (France), [4]Durham University - Durham (United Kingdom), [5]OlexSys Ltd - Durham (United Kingdom)

Abstract

Correcting for anomalous dispersion is part of any model during an X-ray crystal structure determination. The procedure takes the inelastic scattering in the diffraction experiment into account.[1] This X-ray absorption effect is specific to each chemical compound and is particularly sensitive to radiation energies in the region of the absorption edges of the elements in the compound. Therefore, the widely used tabulated values for these corrections can only be approximations as they are based on calculations for isolated atoms.[2] Features of the unique spatial and electronic environment that are directly related to the anomalous dispersion are ignored, although these can be spectroscopically observed. This significantly affects the fit between the crystallographic model and the measured intensities when the excitation wavelength in an X-ray diffraction experiment is close to an element's absorption edge. The dispersive (f´) and absorptive (f´´) terms of the anomalous dispersion can be refined as independent parameters in the full-matrix least-squares refinement.[3] This procedure has now been implemented as a new feature in the well-established Olex2 software suite.[4] These refined parameters are in good agreement with independently recorded X-ray absorption spectra and the resulting crystallographic models show significant improvement compared to those employing tabulated values (Fig. 1&2). The presentation will report on synchrotron multi-wavelength single-crystal X-ray diffraction as well as X-ray absorption spectroscopy experiments which we performed on the molecular compound $Mo(CO)_6$ at energies around the molybdenum K edge (20,000 eV). It will further provide an outlook into the application to determine oxidation states of organometallic compounds.

References

[1] S. Caticha-Ellis, Anomalous Dispersion of X-rays in Crystallography, **1981**.
[2] a) B. L. Henke, E. M. Gullikson, J. C. Davis, *At. Data Nucl. Data Tables*, **1993**, *54*, 181–342; b) S. Brennan, P. L. Cowan, *Rev. Sci. Instrum.*, **1992**, *63*, 850–853; c) S. Sasaki, *KEK Report*, **1989**, *88*, 1-136.
[3] O. Einsle, S. L. A. Andrade, H. Dobbek, J. Meyer, D. C. Rees, *J. Am. Chem. Soc.*, **2007**, *129*, 2210–2211.
[4] O. V. Dolomanov, L. J. Bourhis, R. J. Gildea, J. A. K. Howard, H. Puschmann, *J. Appl. Cryst.*, **2009**, *42*, 339–341.

Experimental (line) and refined (cross) f´ and f´´

Back to Table of contents

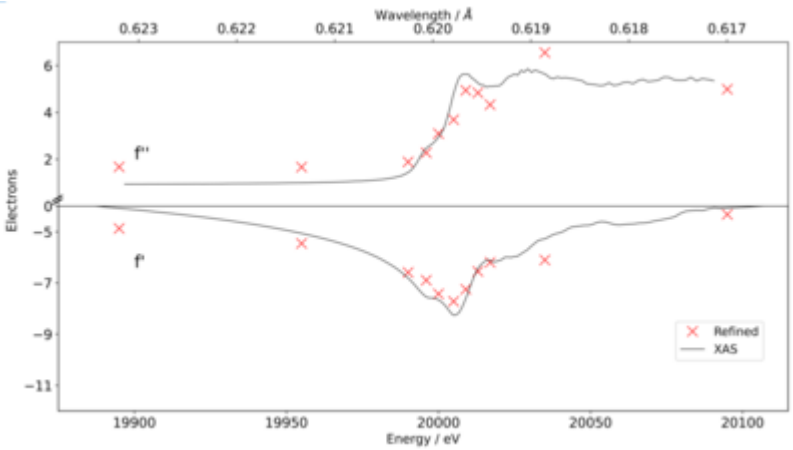

Residual density a)tabulated b)refined dispersion

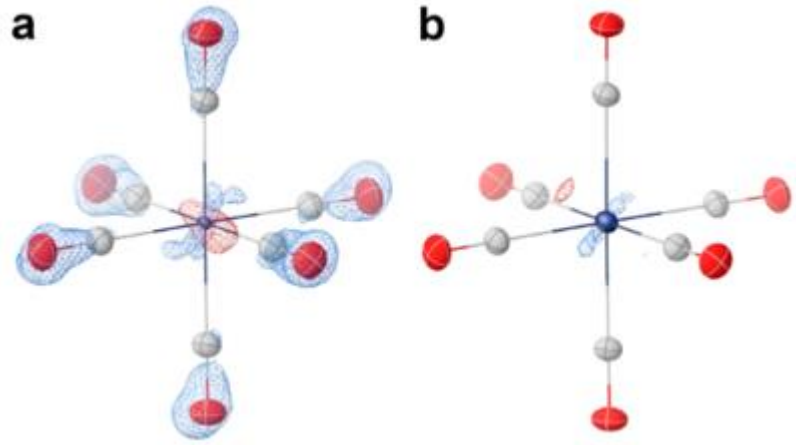

Back to Table of contents

MS32 Advanced techniques to disclose Structure-Property Relationships

MS32-05

Structural investigations of a magnetoelectric plastic-crystal by complementary in situ multi-constrains (T, P, E) SC-XRD experiments

E. Tailleur [1], E. Wenger [1], M. Deutsch [1], M. Romanini [2], D. Aguilà-Avilés [2]
[1]CRM2-University of Lorraine - Vandoeuvre-Lès-Nancy (France), [2]Universitat de Barcelona - Barcelona (Spain)

Abstract

Materials presenting a coupling between two ferroic orders, such as ferroelectricity and (anti)ferromagnetism, are of particular interest owing to their high potential for applications in memory devices [1]. Therefore, there is an important research effort to design new multiferroic materials with improved magnetoelectric coupling. Molecule-based materials are particularly appealing to achieve magnetoelectric coupling since the versatility of each molecular components offers the possibility to tune the physical properties [2].

On the other hand, plastic crystalline molecular materials have attracted significant interest in the past few years because the solid-solid phase transition from the ordered crystal phase to the disordered plastic-crystal phase (PC) is generally accompanied by large enthalpy/entropy variations [3]. Recent investigations have been carried out on so-called ferroelectrics PC where the PC-crystal transition is associated to the para-ferroelectric transition giving rise to barocaloric, electrocaloric and multicaloric effects [4].

The ferroelectric PC triethylmethylammonium tetrabromoferrate (III) reported in 2012 by H. Chai et al [5] is particularly attractive as the para-ferroelectric transition, taking place around 355K, is accompanied by a change in the magnetic properties. At room temperature, $[(Et_3NMe)^+(FeBr_4)^-]$ crystallizes in polar space group P63mc and presents a structural transition leading to a new ferroelectric phase around 170K. More recently, we observed a color change from dark red to yellow as function of temperature. The structural properties at the origin of this wide range of physical properties, especially the ferroelectricity, are almost unexplored. Indeed, $[(Et_3NMe)^+(FeBr_4)^-]$ shows an important disorder, complicating the atomic structure determination of the cationic part. To overcome these difficulties, we investigated the structural behavior of this compound by in situ X-ray diffraction in different non-ambient conditions. First, we explored the phase diagram from room temperature to 5K and we quenched the room temperature phase at low temperature. Then, we performed in situ SC-XRD under pressure from ambient pressure to 4.5 GPa. Both experiments, at low temperature and under pressure, evidence an absence of correlation between the structural phase transition and the color change. Finally, thanks to the new experimental setup we develop in our lab, we realized an in situ SC-XRD under a static electric field of 2kV/mm. All these non-routine measurements allowed us to have a better description of the cationic part disorder of $[(Et_3NMe)^+(FeBr_4)^-]$. This is a first step to establish structure-properties relationships of this multifunctional material.

References

[1] N. A. Spaldin and R. Ramesh, Nat. Mater., 2019, 18, 203–212
[2] T. Akutagawa et al., Nat. Mater., 2009, 8, 342–347.
[3] J. Ll. Tamarit et al, Mol. Cryst. Liq. Cryst, 1994, 250, 347
[4] Harada J. et al., J. Am. Chem. Soc., 2018, 140, 346
[5] H.L. Cai et al, J. Am. Chem. Soc, 2012, 134, 18487

Back to Table of contents

MS33 Supramolecular recognition

MS33-01

Host-guest chemistry in the solid state: stories on the concomitant and sequential crystallization

O. Danylyuk [1]
[1]*Institute of Physical Chemistry Polish Academy of Sciences - Warsaw (Poland)*

Abstract

The molecular recognition between protein and ligand is a delicate balance of multiple attractive and repulsive interactions affected by solvation/desolvation phenomena and conformational changes of one or both molecular partners. The same can refer to the simpler supramolecular host-guest systems composed of flexible partners with multiple binding interactions.[1] In reality at least some of the aqueous host-guest complexes are characterized not by one single crystal structure, but by ensemble or snap shots of various host-guest crystal forms. These crystal forms can differ in the supramolecular interactions, conformation of host or guest, and even host-guest stoichiometry. The situation is additionally complicated by solute-solvent interactions, as in aqueous supramolecular chemistry water cannot be treated as pure spectator in the host-guest complexation and crystallization. Unfortunately, the experimental crystal structure data on the host-guest supramolecular recognition rarely mirror the whole structural landscape.

Here the host-guest systems of bizarre crystallization behavior will be discussed. The host-guest complexes with competing sets of strong non-covalent interactions and/or constrictive binding can exhibit two-step complexation and crystallization. Some cucurbit[6]uril host-guest systems reveal sequential or concomitant crystallization of metastable and equilibrium host-guest complexes. These crystal forms differ in the host-guest interaction and hydration mode. The metastable crystal complexes interconvert spontaneously into stable crystal forms *via* the solution-mediated transformation at ambient conditions. The host-guest system of carboxylated pillar[5]arene with bis-amidinium guest pentamidine is manifested as an ensemble of three host-guest crystal forms. These crystal complexes, although all based on the cavity inclusion of guest inside host, differ in the supramolecular interactions and solvation type.

Our results show that there are many challenges in terms of ruling out the principles and conditions for the concomitant or sequential crystallization of the host-guest complexes. But they also open up an exciting opportunity in terms of more holistic models of the host-guest systems. It is time to shift our focus from ‘visible interactions’ in one crystal structure to the appreciation of many subtle effects playing combined role in the host-guest complexation and crystallization.

References

[1] Yang, L. P.; Zhang, L.; Quan, M.; Ward, J. S.; Ma, Y.-L.; Zhou,H.; Rissanen, K.; Jiang. W. A Supramolecular System that Strictly Follows the Binding Mechanism of Conformational Selection. Nat. Commun. 2020, 11, 2740.

Back to Table of contents

MS33 Supramolecular recognition

MS33-02

Prevalent Polymorphism in Ternary Complexes using Robust Supramolecular Synthons

A. Lemmerer [1], A. Salajee [1]
[1]*University of the Witwatersrand - Johannesburg (South Africa)*

Abstract

Crystal engineering pertains to the control of the assembly of organic and inorganic components to a desired structure or a desired property. Organic components can be either one-component molecular solids, two-component, three-component, and higher with a predictable and stoichiometric combination of different molecules. Complexes between two or more organic compounds (in any physical state at room temperature) that remain neutral can result in a multi-component molecular complex. This scenario is often referred to colloquially as a co-crystal (or cocrystal). An additional scenario is for two (or more) components to undergo an intermolecular proton transfer with complimentary acid and basic functional groups. Such complexes are known as molecular salts as they do not contain inorganic acids or bases. We have found that we can easily make ternary complexes, consisting of a charge transfer binary complex hydrogen bonded to a third component using neutral and charge-assisted hydrogen bonding.[1] The colours of the ternary complexes change from yellow to orange to red depending on the identity of the third component, being a number of pyridines with nitro, amino or halogen atom substituents. Additionally, we have found that members of this series show colour polymorphism, whereby the different polymorphs can show the same range of colours. So far, we have systems that are dimorphic[2] and trimorphic.[3]

References

[1] Tania Hill, Rudolph M. Erasmus, Demetrius C. Levendis and Andreas Lemmerer. Combining two distinctive intermolecular forces in designing ternary co-crystals and molecular salts of 1,3,5-trinitrobenzene, 9-anthracenecarboxylic acid and ten substituted pyridines. CrystEngComm, 2019, 21, 5206–5210.
[2] Atiyyah Salajee, Caitlin Morrison and Andreas Lemmerer. Polymorphism of the ternary complex (2-amino-5-chloropyridine)·(9-anthracenecarboxylic acid)·(trinitrobenzene). An example of salt/cocrystal polymorphism. CrystEngComm, 2022, submitted.
[3] Andreas Lemmerer. All good things come in threes: first example of a trimorphic, ternary molecular salt complex. CrystEngComm, 2020, 22, 6091–6095.

Figure 1. (a) The three components of the ternary

Back to Table of contents

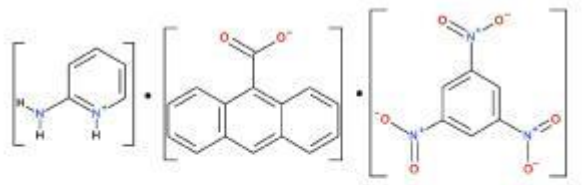

(a) (2-aminopyridinium)·(9-anthracenecarboxylate)·(trinitrobenzene)

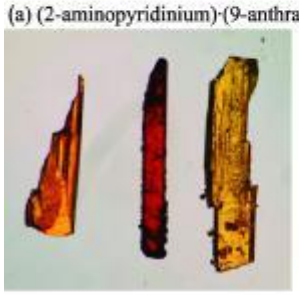

(b) Forms **I, II & III**

(c) Forms **I & II**

Back to Table of contents

MS33 Supramolecular recognition

MS33-03

Supramolecular recognition in solution towards co-crystal formation

K. Edkins [1], Y. Shen [1]
[1]School of Health Sciences, University of Manchester - Manchester (United Kingdom)

Abstract

Crystallisation is an important unit operation in the chemical industry and is usually performed as a 'wet' process, among which, nucleation is vital to the final crystal structure. But solute molecules can interact already in undersaturated solution forming supramolecular aggregates potentially influencing the final crystal form. Such pre-nucleation aggregates can be detected before the initial crystalline nucleation[1] and their presence and nature may be linked to the final crystal form and inform the crystallization experiment itself.

The formation of co-crystals from solution during a screening experiment is still unpredictable and based on serendipity-driven trial and error. One major issue is the choice of the correct host to co-former ratio to ensure that the co-crystal can nucleate, which can vary between different solvents. Thermodynamically, this range can be defined in a ternary phase diagram connecting host, co-former and solvent concentrations [2], but the preparation thereof is work-intensive and time-consuming. Without the knowledge of the phase diagram, though, the screening process becomes guesswork. With the model system of caffeine-benzoic acid, we will show that the detection of pre-nucleation aggregates can facilitate this process for individual solvents and predict co-crystal formation in a timely manner.

Using carbamazepine with the two co-formers nicotinamide and saccharin as second model system, we will show that it may even be possible to connect the nature of the pre-nucleation clusters with the nucleation pathway. Classical nucleation theory describes nucleation as a liquid to solid phase transition in which the solid exhibits the structure of the final crystal form. Non-classical nucleation theory defines nucleation as a liquid-liquid phase separation with the formation of a liquid dense phase, from which the final crystalline solid will nucleate at a later stage. In our model system, we observe pre-nucleation aggregation with significantly different strength leading to homodimers in one system and heterodimers in the other. This can be connected by the observation of a co-amorphous phase for one of the systems [3] and points towards a non-classical nucleation pathway.

References

[1] Crystal Growth & Design 2022, 22, 1476–1499
[2] Crystal Growth & Design 2007, 7, 1223–1226
[3] Molecular Pharmaceutics, 2019, 16, 1294-1304

Back to Table of contents

MS33 Supramolecular recognition

MS33-04

Crystal engineering of supramolecular assemblies of bowl-shaped host molecules

C. Oliver [1]
[1]*University of Cape Town - Rondebosch (South Africa)*

Abstract

Small-molecule supramolecular chemists are inspired by large, supramolecular assemblies, such as viruses, produced by nature.[1] However, large, synthetic, multi-component (n > 3) supramolecular assemblies which enclose chemical space are still relatively rare phenomena in the field of small-molecule, supramolecular chemistry. Atwood and MacGillivray reported the first example of such an assembly by showing that the bowl-shaped host molecule *C*-methylcalix[4]resorcinarene **1** can spontaneously assemble in a nitrobenzene solution to form a large, chiral, supramolecular assembly consisting of 6 molecules of 1 and 8 water molecules, the latter 'stitching' molecules of **1** into a hexameric assembly, $\mathbf{1}_6$•$(H_2O)_8$ via O-H•••O hydrogen bonds.[2] Despite > 140 structures reported since this discovery containing **1** co-crystallised with various guest and/or solvent molecules, only one similar hexameric assembly of **1** was reported by Holman et al. where 6 of the 8 water molecules were replaced by 2-ethylhexanol molecules.[3] Here we present a crystallisation of **1** from a number of alcohols, which yielded similar hexameric assemblies to that of the MacGillivray-Atwood and Ugono-Holman hexamers. However, interesting differences were found, including the first case where two unique multi-component assemblies are found within the same crystal structure for these types of structures.[4] In addition, we report the hexameric assembly of **1** with 1-propanol as the solvent, increases the interior cavity size by simultaneous insertion of water and 1-propanol as the 'stitching' molecules, indicating a possible means of engineering the size of these cavities.[5]

References

[1] Ariga, K., Hill, J. P., Lee, M. V., Vinu, A., Charvet, R., Acharya, S., Science and Technology of Advanced Materials, 2008, 9, 014109.
[2] MacGillivray, L. R., Atwood, J. L., Nature, 1997, 389, 469-472.
[3] Ugono, O., Holman, K. T., Chem.Commun., 2006, 2144-2146.
[4] Oliver, C. L, Bathori, N. B., Jackson, G. E., Kuter, D., Cruickshank, D. L., 2016, CrystEngComm, 18, 3015-3018.
[5] Payne, R. M., Oliver, C. L., CrystEngComm, 2018, 20, 1919-1922.

Back to Table of contents

MS33 Supramolecular recognition

MS33-05

Driving the release of active compounds through cocrystallization

M. Prencipe [1], P.P. Mazzeo [1], B. Famiani [1], A. Bacchi [1]
[1]University of Parma - Parma (Italy)

Abstract

The use of pesticides for chemical treatment of plants and soil is still an alarming issue since contributes to the accumulation of harmful by-products in the environment [1]. Some of most sustainable and effective alternatives have been found in essential oil (EOs), which are natural compounds based on terpenoids and directly produced by plants. EOs have been shown antibacterial, antifungal and insecticide effects, but their physical properties, such as low melting point and high volatility, have limited their application in agrochemical industry.
Cocrystallization has proved to be a practical solution for tuning the physical properties of EOs [2], giving new crystalline materials with an enhanced thermal stability and able to deliver the active compounds in a more prolonged way. Cocrystals are indeed multi-component crystalline compounds obtained by the interaction of two or more different molecules, called coformers, in a defined stoichiometric ratio. However, the coformers often have just played a rule of “co-builders” of a new crystalline scaffold, remaining their molecular properties untapped for further applications [3].
The purpose of this work is thus to exploit cocrystalisation to drive the release of EOs and control their availability. We here report several examples of cocrystals where the release of the active components is triggered by external stimuli as a function of the coformer used. To this end, XRPD measurements were performed before and after the triggering and were compared between the individual conformer and its cocrystals. Crystals structures were characterized through SCXRD and physical properties were opportunely described by calorimetric measurements (DSC, TGA).

References

[1] M. B. Isman, ACS Symp. Ser. 2014, 1172, 21–30.
[2] A. Bacchi, P. P. Mazzeo, https://doi.org/10.1080/0889311X.2021.1978079, 2021, 27, 102–123.
[3] P. P. Mazzeo et al, ACS Sustainable Chem. Eng. 2019, 7, 17929−17940.

Back to Table of contents

MS34 Crystallization Techniques and chemical reactions driven by solid state interactions

MS34-01

Heterogeneous nucleation of protein crystals

E. Saridakis [1]
[1]*NCSR DEMOKRITOS - Athens (Greece)*

Abstract

The inducement of crystal nucleation on foreign substrates, usually called heterogeneous nucleation, is a long-established technique for the optimisation of protein crystals. It allows not only the improvement of protein crystals by allowing them to grow under supersaturations lower than those required for spontaneous nucleation, but also the discovery of new conditions during initial screening. Indeed, it has been found that many screen conditions, although suitable for crystal growth, provide insufficient supersaturation for nucleation, thus going undetected in the absence of a heterogeneous nucleant.

Scores of possible substrates have been tested as heterogeneous nucleants, but those that yield good results for a reasonably wide range of proteins are scarce. Furthermore, using such nucleants requires a good grasp of how and over what range of conditions they are expected to function, and often some dexterity. They are therefore often been overlooked and underused. A range of heterogeneous nucleants, designed and tested by our team[1-5] and by others, will be surveyed and the rationale of their function will be explained in a more theoretical way. Some examples of their successful use in our hands will also be given.

References

1. Sears, R., Saridakis, E. & Chayen, N.E. *Proc. Natl. Acad. Sci. U.S.A.* (2006) 103, 597.
2. Saridakis, E. *et al. Proc. Natl. Acad. Sci. USA* (2011) 108, 11081.
3. Nanev, C.N.,Saridakis, E. & Chayen, N.E. *Sci. Rep.* 7 (2017) DOI: 10.1038/srep35821.
4. Nanev, C.N., Saridakis, E., Govada, L., Kassen, S.C., Solomon H.V. & Chayen, N.E. *ACS Appl. Mater. Interfaces* (2019) 11, 12931.
5. Govada, L. *et al.* Accepted in *Adv. Funct. Mater.* (2022).

Back to Table of contents

MS34 Crystallization Techniques and chemical reactions driven by solid state interactions

MS34-02

Encapsulated Nanodroplet Crystallisation – unlocking structural resolution for sample limited and complex molecular systems

M. Probert [1]
[1]*Newcastle University - Newcastle Upon Tyne (United Kingdom)*

Abstract

The explosion of technologies, enabling the application of diffraction science to ever more complex materials, is truly staggering. With microfocus in-house X-ray sources through to the international XFEL facilities now being used to help resolve structural properties and molecular characteristics. However, all of these and their related instruments still have a common requirement, the prior preparation of a suitably crystalline sample for analysis. Increasingly exotic molecular systems are now being prepared synthetically, or isolated from natural sources, as targets of interest. These targets suffer greatly from difficulties in structure elucidation outside the solid-state due to the complexities of data and information loss from spectroscopic methods. Therefore, the reliance on solid-state methods has increased for categoric materials characterisation. However, these increasingly complex molecular species have associated complications in determining suitable crystallisation conditions to provide samples of suitable quality for analysis.

Additionally, as both academia and industry strive to reduce the timescales for research projects bringing solid-state analysis earlier in the development pipeline is imperative. It has the advantage of reducing costs on projects that are less likely to come to fruition but has the major disadvantage that the quantity of material available is generally significantly reduced. The reduction in sample quantity available for analysis makes many classical crystallisation routes non-viable or extremely cost inefficient due to the sample recycling and additional processing required.

High throughput Encapsulated Nanodroplet Crystallisation[1] is a recently developed technique that has the capability to provide solutions to the problems outline. It has been successfully employed on a diverse range of structurally challenging compounds from small molecules through inorganic complexes to natural products and their synthetic analogues. The method has the major advantages of the limited amount of material required for crystallisation screening (<10 mg material gives >1000 crystallisations) and ease of polymorph screening across a wide range of chemical environments.

The methodologies employed in the technique will be discussed with case studies highlighting the structural diversity of the method's applicability, along with the mechanisms for easy access to the technique.

References

[1] Tyler ARM, Ragbirsingh R, McMonagle CJ, Waddell PG, Heaps SE, Steed JW, Thaw P, Hall MJ, Probert MR. Encapsulated Nanodroplet Crystallisation of Organic-Soluble Small Molecules. Chem 2020, (7), 1755-1765

Back to Table of contents

MS34 Crystallization Techniques and chemical reactions driven by solid state interactions

MS34-03

Chaperone Compounds for Co-Crystallization of Small Molecules

C. Richert [1], T. Berking [1], W. Frey [1], T. Stuerzer [2], M. Adam [2]
[1]University of Stuttgart - Stuttgart (Germany), [2]Bruker AXS GmbH - Karlsruhe (Germany)

Abstract

Modern instrumentation and processing techniques enable high-quality 3D structure analysis – including absolute structure determination – often in less than an hour, i.e. faster and more comprehensively than many spectroscopic methods can achieve. However, many small or highly flexible organic molecules remain intractable to current crystallization methods, including the crystal-sponge method[1]. A new chaperone-aided crystallization method[2] based on tetraaryladamantanes (Figure1) has delivered high quality co-crystals in a fair number of cases, allowing for the structure determination of analytes, including their stereochemistry. The adamantane chaperone approach works well for analytes that are liquid at room temperature and adds an important tool to the toolbox for both synthetic organic chemists and crystallographers, facilitating the investigation of small molecules, such as new natural products, synthetic intermediates, pharmaceutically active ingredients, or fragrances.

The chaperone-aided crystallization method is easy to apply and crystals suitable for the determination of absolute configuration are typically obtained within minutes or hours. With modern X-ray instrumentation the method can provide very fast access to the full 3D structure of an important class of organic analytes.

Salient features include:
- Structures in hours or days rather than weeks
- Small quantities of analyte required
- No solvent screening required

Four chaperone compounds are being made available, helping to obtain suitable crystals with ordered analyte in the unit cell, allowing for determination of relative or absolute configuration.

We will discuss the method and demonstrate rapid crystal growth for examples, such as the two enantiomers of limonene.

References

[1] Inokuma, Y.; Yoshioka, S.; Ariyoshi, J.; Arai, T.; Hitora, Y.; Takada, K.; Matsunaga, S.; Rissanen, K.; Fujita, M. *Nature* **2013**, *495*, 461-466.
[2] Krupp, F.; Frey, W. ; Richert, C. *Angew. Chem. Int. Ed*. **2020**, *59*, 15875–15879.

Fig1: Chaperones based on tetraaryladamantanes

Back to Table of contents

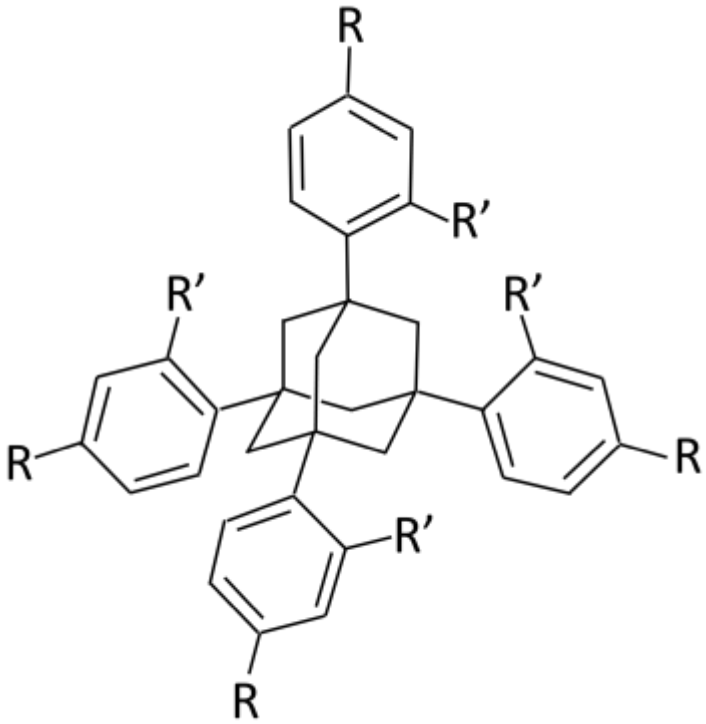

Back to Table of contents

MS34 Crystallization Techniques and chemical reactions driven by solid state interactions

MS34-04
Sublimation of multi-component crystals

D.A. Haynes [1]
[1]*Stellenbosch University - Stellenbosch (South Africa)*

Abstract
Sublimation is a powerful but unexplored technique for crystallisation of molecular crystals. [1] We have recently begun exploring sublimation to produce crystals of organic co-crystals. [2] We have investigated competition between hydrogen and halogen bonding during sublimation [3], and have assessed the general utility of sublimation to produce multi-component crystals. [4]
Unexpectedly, we have found that organic salts can be crystallised by sublimation. [5] It is clear from our experiments that in some cases proton transfer takes place after the neutral molecules enter the gas phase. Our attempts to understand this process will be described.
We have also shown that crystals of hydrates can be produced via sublimation, and that changing the sublimation conditions can affect the nature of the products obtained. Control of morphology and polymorph through the inclusion of additives during sublimation will also be discussed. Finally, we compare our results using sublimation to those obtained using mechanochemistry.

References
1. P. McArdle and A. Erxleben, *CrystEngComm*, 2021, **23**, 5965-5975.
2. T. Carstens, D. A. Haynes and V. J. Smith, *Cryst. Growth Des.*, 2020, **20**, 1139-1149.
3. J. Lombard, T. le Roex and D. A. Haynes, *Cryst. Growth Des.*, 2020, **20**, 7384-7391.
4. J. Lombard, T. le Roex and D. A. Haynes, *Cryst. Growth Des.*, 2020, **20**, 7840-7849.
5. J. Lombard, V. J. Smith, T. le Roex and D. A. Haynes, *CrystEngComm*, 2020, **22**, 7826-7831.

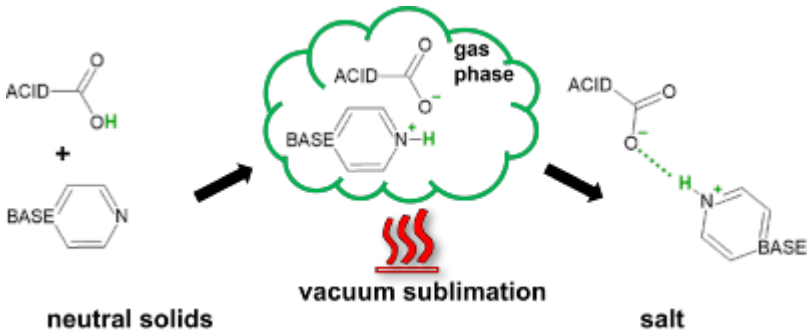

Back to Table of contents

MS34 Crystallization Techniques and chemical reactions driven by solid state interactions

MS34-05

Synthesis of spin crossover (SCO) complexes through accelerated aging contact reactions

R. Lonergan [1], H. Shepherd [1]
[1]*University of Kent - Canterbury (United Kingdom)*

Abstract

Accelerated aging (AA) refers to diffusion-controlled reactions between initially solid materials which are effected by mild changes to their environment. Zeolitic imidazolate frameworks (ZIFs), metal organic frameworks (MOFs), nanoparticles and more have been made using AA.[1] SCO complexes can switch between high spin (HS) and low spin (LS) states when exposed to external stimuli such as light, heat or pressure.[2] This change in spin state is often accompanied by a dramatic change of colour as well as changes to the magnetic and structural properties. For this reason they have applications as sensors. The inexpensive and facile nature of AA syntheses will allow for cheap largescale production of these sensors. Relative humidity (RH) and reactant hygroscopy have both been reported as important mechanistic factors.[1,3] Here we show the synthesis of SCO active materials and a copper analogue through accelerated aging and show our initial mechanistic investigations into the effect of hygroscopy and relative humidity on these reactions which reveals that the rate of reaction is dependent on atmospheric moisture.

The most recent research on these AA reactions and their products will be presented. Their potential in regards to the creation of novel materials that cannot be made with solution-state reactions will be discussed, as well as results of the investigation into the roles of hygroscopy and humidity as the possible driving forces behind these solid-state reactions.

References

1 - S.L. James, C. J. Adams, C. Bolm, D. Braga, P. Collier, T. Friščˇ, F. Friščˇic´, F. Grepioni, K. D. M. Harris, G. Hyett, W. Jones, A. Krebs, J. Mack, L. Maini, A. G. Orpen, I. P. Parkin, W. C. Shearouse, J. W. Steed and D. C. Waddell, Chem. Soc. Rev, 2012, 41, 413–447.
2 - O. Kahn, Curr. Opin. Solid State Mater. Sci., 1996, 1, 547–554.2
3 - J. L. Do and T. Friščić, ACS Cent. Sci., 2017, 3, 13–19.

Contact reaction of single crystals of reactants

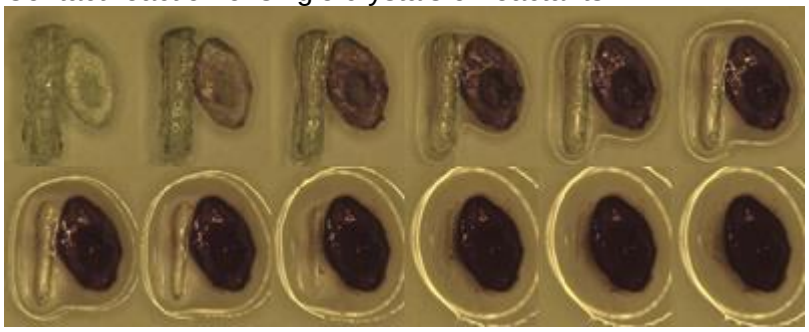

Back to Table of contents

MS35 Artificial intelligence in photon and neutron crystallography, data mining, machine learning

MS35-01

Improve neutron measurements performances with AI and machine learning

P. Mutti [1], M. Boehm [1], Y. Le Goc [1], T. Weber [1], M. Noack [2], J. Sethian [2]
[1]Institut Laue-Langevin - Grenoble (France), [2]Lawrence Berkeley National Laboratory - Berkeley (United States)

Abstract

Artificial Intelligence and machine learning are, nowadays, powerful methods to increase the performances of neutron scattering experiments, both in terms of data collection strategy and in instrument parameters optimization. In the present talk we will present two different use-cases covering both aspects. Small Angle Neutron Scattering (SANS) is a growing technique especially in biology and it is characterized by short measuring time and, therefore, high throughput of samples per experiment. This high-volume data contains rich scientific information about structure and dynamics of materials under investigation. Deep learning could help researchers better understand the link between experimental data and materials properties. We applied deep learning techniques to evaluate the quality of experimental neutron scattering images [1], which can be influenced by instrument configuration, sample and sample environment parameters. Sample structure can be deduced on-the-fly during data collection that can be therefore optimised. The neural network model can predict the experimental parameters to properly setup the instrument and derive the best measurement strategy. A three-axis neutron spectrometer represent the opposite situation in terms of quantity of collected data although an experiment last typically several days. With the aim to optimize the beam-time usage, it is therefore very important to concentrate the data acquisition in those regions of the reciprocal space where a maximum of information on our physical system can be acquired. Autonomous data acquisition becomes increasingly important for the execution and analysis of ever more complex experiments. In autonomous learning, algorithms learn from a comparatively little amount of input data and decide themselves on the next steps to take in a closed-loop. We have performed a series of experiments fully driven by the computer without any human intervention. The used algorithm was able to explore the reciprocal space and fully reconstruct the signal without any prior knowledge of the physics case under study. Thanks to autonomous learning gpCAM [2], developed by Marcus Noack of the CAMERA team at Berkeley Lab, estimates the posterior mean and covariance and uses them in a function optimization to calculate the optimal next measurement point. The posterior is based on a prior Gaussian probability density function, which is repeatedly retrained on previously measured points. The main advantage of such an approach is clearly the possibility to drastically reduce the number of measurements with respect to a classical grid scan (i.e. const- Q, const-E scans) and therefore optimize the beam-time usage [3]. In this talk we will compare these new experimental approaches and compare them to traditional data acquisition. We try to show a perspective of the future possibilities and howthe scientific measurements could evolve in conjunction with modern algorithms.

References

[1] Deep learning in neural networks: An overview, Schmidhu- ber, Jürgen, Neural networks, 61, 85–117, 2015, Elsevier
[2] Marcus Noack and Petrus Zwart. Computational strategies to increase efficiency of gaussian- process-driven autonomous experiments. In 2019 IEEE/ACM 1st Annual Workshop on Large-scale Experiment-in-the-Loop Computing (XLOOP), pages 1–7. IEEE, 2019.
[3] Noack, M.M., Zwart, P.H., Ushizima, D.M. et al. Gaussian processes for autonomous data acquisition at large-scale synchrotron and neutron facilities. Nat Rev Phys (2021). https://doi.org/10.1038/s42254-021-00345-y

Back to Table of contents

MS35 Artificial intelligence in photon and neutron crystallography, data mining, machine learning

MS35-02

A Critical Review of Neural Networks for the Use with Spectroscopic Data

J. Schuetzke [1], N. Szymanski [2], G. Ceder [2], M. Reischl [1]
[1]Karlsruhe Institute of Technology - Karlsruhe (Germany), [2]Lawrence Berkeley National Laboratory - Berkeley (United States)

Abstract

In recent years, neural networks have found increased use in the analysis of crystallographic characterization data, such as X-ray diffraction (XRD) patterns. Previous work has shown that neural networks can successfully identify crystalline phases from XRD patterns and classify their symmetry, even in multiphase mixtures. When compared with classical machine learning methods, such as Support Vector Machines or Decision Trees, CNNs show improved performance in the classification of XRD patterns and can even handle experimental artifacts such as peak shifts caused by strain, whereas the classification models would fail. Such an approach is readily extended to other spectroscopic techniques, including NMR, Raman or NIR. Those network models usually employ a convolutional neural network (CNN) architecture which has been developed for the use with images.
Despite these promising results, our work reveals several key limitations of the CNN architecture with respect to spectroscopic analysis, and we show that these limitations can lead to failed classifications on relatively simple patterns. Convolutional layers are demonstrated to have very little benefit for classification, and their only important contribution comes from the pooling operations that shrink the size of the input while keeping relevant information regarding peak intensities. Those pooling operations compensate for peak shifts, and therefore classical models applied to the shrunken input perform equally well as the presented neural networks. Nonetheless, we show how to adapt various parameters in the neural networks, such as the choice of activation function, to train more robust models with improved accuracy on classification tasks. Based on our findings, we believe that neural networks have their place for use with spectroscopic data but require careful design of their architecture to handle peculiarities inherent to spectral data.

Back to Table of contents

MS35 Artificial intelligence in photon and neutron crystallography, data mining, machine learning

MS35-03

Cocrystal Discovery with Network Science and Machine Learning

J.J. Devogelaer [1], H. Meekes [1], P. Tinnemans [1], E. Vlieg [1], R. De Gelder [1]
[1]Radboud University - Nijmegen (Netherlands)

Abstract

Physicochemical and biopharmaceutical properties of pure compounds can be modified by the formulation of multicomponent crystals, such as salts, solvates and cocrystals, which are crystalline aggregates containing multiple ionic and/or neutral species in the crystal lattice [1]. The formation of salts is rather straightforward but the design of cocrystals remains challenging. Experimental screening of cocrystals is time-consuming and therefore computational tools to understand and predict cocrystals can be crucial for an efficient and successful screening process.

Recently we constructed a network of coformers from the information present in the Cambridge Structural Database (CSD). Analysis of this network shows that the coformers in the network behave primarily in a bipartite manner, demonstrating the importance of combining complementary coformers [2].

Using link-prediction algorithms, missing links in the network can be identified: cocrystals that are not yet present in the CSD but are likely to exist based on the information in the network [3]. For a target compound unknown to the CSD, in-house data on cocrystallization can be combined with the entire CSD coformer network and link-prediction may quite accurately predict new combinations for the target compound [4]. Moreover, using link prediction an invalid cocrystal set can be generated that can serve as negative input data for an approach based on artificial intelligence. The cocrystals present in the CSD, together with the results from link prediction applied to the coformer network, were used as input to a machine learning approach. We trained artificial neural networks (ANNs) to recognize fruitful combinations of coformers. Validation of the ANN model showed that high accuracies are obtained and that the combination of network science and machine learning delivers a powerful prediction tool for discovering new cocrystals [5].

References

[1] Grothe, E., Meekes, H., Vlieg, E., ter Horst, J. H., de Gelder, R. *Cryst. Growth Des.*, 2016, **16**, 3237–3243.
[2] Devogelaer, J.J., Meekes, H., Vlieg, E., de Gelder, R. *Acta Cryst. B*, 2019, **75**, 371-383.
[3] Devogelaer, J.J., Brugman, S.J.T., Meekes, H., Tinnemans, P., Vlieg, E., de Gelder, R. *Crystengcomm*, 2019, **21**, 6875-6885.
[4] Devogelaer, J.J., Charpentier, M.D., Tijink, A., Dupray, V., Coquerel, G., Johnston, K., Meekes, H., Tinnemans, P., Vlieg, E., ter Horst, J.H., de Gelder, R. *Cryst. Growth Des.*, 2021, **21**, 3428−3437.
[5] Devogelaer, J.J., Meekes, H., Tinnemans, P., Vlieg, E., de Gelder, R. *Angew. Chem. Int. Ed.*, 2020, **59**, 21711-21718.

Back to Table of contents

MS35 Artificial intelligence in photon and neutron crystallography, data mining, machine learning

MS35-04

LaueNN: Neural network based hkl recognition of Laue spots and its application to polycrystalline materials

R.R.P. Purushottam Raj Purohit [1], S. Tardif [2], O. Castelnau [3], J. Eymery [1], R. Guinebretiere [4], O. Robach [1], J.S. Micha [5]

[1]Univ. Grenoble Alpes, CEA, IRIG, MEM, NRS, 17 avenue des Martyrs, Grenoble, 38000, France - Grenoble (France), [2]Univ. Grenoble Alpes, CEA, IRIG, MEM, NRS, 17 avenue des Martyrs, Grenoble, 38000, France - Grenoble (France) - Grenoble (France), [3]PIMM, Arts et Metiers Institute of Technology, CNRS, ENSAM, 151 Bd de l'hopital, Paris, 75013, France - Paris (France), [4]Université de Limoges, IRCER, UMR 7315, CNRS, Centre Européen de la Céramique, Limoges, 87068, France - Limoges (France), [5]Univ.Grenoble Alpes, UMR SYMMES CNRS-CEA, 17 avenue des Martyrs, Grenoble, 38000, France - Grenoble (France)

Abstract

A feedforward neural network (FFNN) model is introduced for efficient and accurate prediction of Laue spots hkl in single/multi-grain/multiphase Laue images. Laue micro-diffraction is an X-ray scattering technique for the determination of local structural parameters (strain, stress and orientation) in materials from microstructure mapping (2D and 3D). The use of a polychromatic beam offers many experimental advantages (no rotation of the sample, many diffraction spots, signal that can be used even in the presence of strong orientation disorder). However, in the case of polycrystalline microstructures, the determination of the structural parameters (lattice parameters) from the fine analysis of the relative position of the spots requires identifying unambiguously all the spots forming the Laue pattern corresponding to an individual crystal among all other spots. The indexation step of the data analysis must be reliable to input unambiguous experimental dataset to the structural model refinement (final step in analysis) and rapid; since production rate of data on the synchrotron line can amount to several 10000s diffraction images per hour, each Laue image being able to contain contribution from multi-grain/ multi-phase present in the probed volume of the material.

Several approaches have been carried out by different groups allowing to index single crystals [1, 2] and polycrystals (for example: XMAS, LaueTools [3-5]). In the latter case, the most time consuming, in the whole data analysis workflow, is the indexation step i.e., determination of Laue spot hkl Miller indices from sets of spots related to the probed crystal. To this effect, we propose [6] employing a FFNN based model to tackle the bottleneck of indexation thereby providing considerable speed over the classical indexation techniques for complex Laue patterns. The model is completely trained on the relative angular distribution of spots present in simulated Laue patterns. With the feature engineering and an optimized FFNN model, accuracies of at-least 90% is easily achieved irrespective of crystal system. The training and validation accuracies and losses that define the metrics of the model learning is presented in Figure 1(a,b). While Figure 1(c,d) shows the ground truth and prediction results for a copper Laue pattern. The present model is also validated on several experimental campaigns performed at the French CRG-IF beamline BM32 at the European Synchtrotron (ESRF). Real-time/ on-the-fly HKL indexation of polycrystalline or complex Laue patterns is now possible with the proposed FFNN architecture, thereby providing users valuable and rapid feedback during data collection on the beamline and accelerate the data treatment from raw data to reliable and interpretable structural parameters.

References

[1] Dejoie, C., Tamura, N. (2020). J. Appl. Cryst., 53, 824-836
[2] Gupta, V.K., Agnew, S.R. (2009). J. Appl. Cryst., 42, 116-124
[3] Kou, K., Chen, K., Tamura, T. (2018). Scripta Materialia, 143 (2018) 19-53
[4] Song, Y., Tamura, N., Zhang, C., Karami, M., Chen, X. (2019). Acta Crysta, A75, 876-888
[5] Micha, J.-S., Robach, O., Tardif, S. https://gitlab.esrf.fr/micha/lauetools
[6] Purushottam raj purohit, R.R.P. , et al., accepted for publication in J. Appl. Cryst., (2022)

LaueNN model accuracy and losses with evaluation

Back to Table of contents

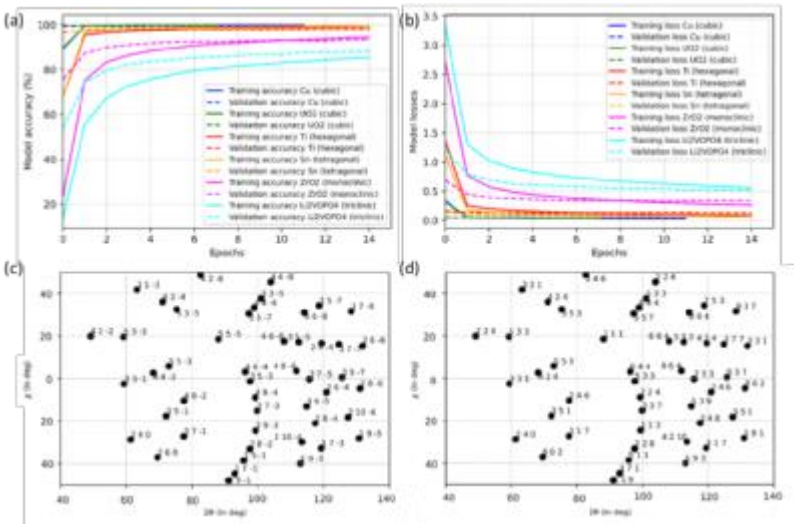

Back to Table of contents

MS35 Artificial intelligence in photon and neutron crystallography, data mining, machine learning

MS35-05

Understanding Allostery in Purine Nucleoside Phosphorylases by Machine Learning and Molecular Dynamics Interaction Databases

Z. Štefanić [1], B. Gomaz [1]
[1]Ruđer Bošković Institute - Zagreb (Croatia)

Abstract

Despite it's fundamental importance, the mechanism of allostery is yet to be fully revealed in many proteins. One class of enzymes where allostery plays an intriguing role are Purine Nucleoside Phosphorylases (PNPs). These enzymes appear both in bacteria where they are homohexamers, and in higher organisms where they are present in homotrimeric form. They catalyse the synthesis of purine nucleotides in the purine salvage pathway and represent an ideal case for studying allostery. Although many 3D structures have been determined so far, understanding the mechanism by which monomeric subunits communicate in these enzymes has proven a daunting task by relying exclusively on structural data.

To understand allostery, which is in essence a dynamical phenomenon, it is necessary to employ not only static structures from X-ray crystallography, but also their dynamic counterparts from molecular dynamics simulations. If allosteric communication between amino acids is transmitted through non-covalent interactions, then the most natural way of tracing the allosteric pathways through protein is by following the time evolution of underlying interaction networks. Proteins can naturally be represented as networks, where nodes are amino acids and edges are various interactions between them, be it peptide bonds along the main chain, or various non-covalent interactions that may be present during time evolution.

However, tracing different communication pathways in static proteins structure provided by the X-ray experiments can be challenging. Adding a time evolution in form of molecular simulations on top of that multiplies the complexity of the problem many times, making it often unmanagable without using programmatic ways of processing the enormous amounts of data that are generated. To the rescue come powerful methods of machine learning that are specially adapted to process such quantities of data.

Helicobacter pylori represents a major global health threat. It is estimated that around 50% of the world population is infected with this bacterium. Because of the ever increasing number of antibiotic-resistant strains, there is a constant need for new drug targets of H. pylori. We have identified that PNP is a promissing drug target [1] against that pathogen. Specially designed molecular interaction databases have been applied in search for allosteric pathways in PNPs recently as part of the project Allosteric communication pathways in oligomeric enzymes (ALOKOMP, https://alokomp.irb.hr/). By enhancing the static information obtained from X-ray crystallography with dynamic time evolution obtained via molecular dynamics simulations and combining both in form of specially designed databases to which automated machine learnig algorithms can be applied, it is hoped that elusive allosteric pathways can be identified in this class of enzymes.

References

[1] Marta Narczyk, Marta Ilona Wojtyś, Ivana Leščić Ašler, Biserka Žinić, Marija Luić, Elżbieta Katarzyna Jagusztyn-Krynicka, Zoran Štefanić & Agnieszka Bzowska (2022) Interactions of 2,6-substituted purines with purine nucleoside phosphorylase from Helicobacter pylori in solution and in the crystal, and the effects of these compounds on cell cultures of this bacterium, Journal of Enzyme Inhibition and Medicinal Chemistry, 37:1, 1083-1097, DOI: 10.1080/14756366.2022.2061965

Back to Table of contents

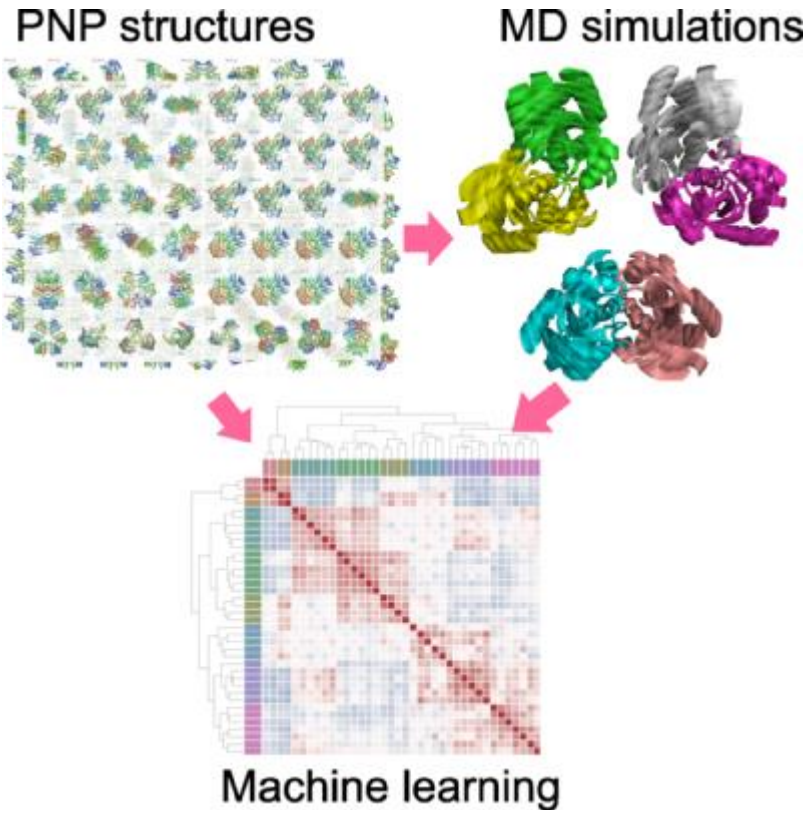

Back to Table of contents

MS36 Software development in quantum mechanics-based methods of crystallography

MS36-01

The multipolar model: still alive!

P.M. Macchi [1]
[1]*Politecnico di Milano, Department of Chemistry, Materials and Chemical Engineering - Milano (Italy)*

Abstract

In the recent years, the way of modelling accurate x-ray diffraction data has abruptly changed, because of the emerging technique of wavefunction fitting [1]. While this method opens the way to more information because the wavefunction enables calculation of one and two-electron properties, the traditional multipolar model [2,3] has still an important appeal for many reasons. First, the model is not restrained to a theoretical ansatz and to a fixed electronic state. Second, the transferability of multipoles is much easier, and it allows full confrontation with standard models based on the independent atom approximation. In this respect, the estimation of the errors adheres with the same statistical interpretation of routine crystal structure models. Moreover, many robust and well tested approximations enable prediction of two-electron properties as well, for example the energy densities [4]. The multipolar model finds also an easy interplay with polarized neutron diffraction data for the refinement of charge and spin density distribution [5]. The calculation of electrostatic properties and interaction energies has now reached a very high and sophisticated level of precision [6]. Finally, yet importantly, the multipolar approximation enables a rapid calculation, that seamlessly fit with the extremely rapid data collections that are nowadays possible also at laboratory scale.
The recent developments and improvement will be illustrated and discussed, within the framework of the XD program package [7].

References

[1] Jayatilaka, D. (1998) Phys. Rev. Lett., 80, 798–801.
[2] Stewart R.F. (1976) Acta Cryst., A32, 565–574.
[3] Hansen, N.K. & Coppens, P. (1978) Acta Cryst., A34, 909-921.
[4] Tsirelson, V. & Stasch, A. (2021) Acta Cryst., B76, 769-778.
[5] Deutsch, M., Gillon, B., Claiser, N., Gillet, J. M., Lecomte, C. & Souhassou, M. (2014). IUCrJ, 1, 194–199.
[6] Weatherly, J., Macchi, P. & Volkov, A. Acta Cryst. (2021). A77, 399-419
[7] Volkov, A., Macchi, P., Farrugia, L. J., Gatti, C., Mallinson, P., Richter, T. & Koritsanszky, T. (2016) XD2016 - A Computer Program Package for Multipole Refinement, Topological Analysis of Charge Densities and Evaluation of Intermolecular Energies from Experimental and Theoretical Structure Factors

Back to Table of contents

MS36 Software development in quantum mechanics-based methods of crystallography

MS36-02

Neural network predictors in Quantum Chemical Topology

Á. Martín Pendás [1], M. Gallegos González [1]
[1]*Universidad de Oviedo - Oviedo (Spain)*

Abstract

Quantum Chemical Topology (QCT) [1] has played a prominent role in the interpretation of high accuracy XRD experiments and in the development of Quantum Crystallography [2]. Basic to this framework are atomic charges, which need from expensive 3D numerical integrations. QCT charges are particularly attractive given their invariance against orbital transformations. Given that Machine Learning (ML) techniques have been shown to accelerate orders of magnitude the computation of a number of quantum mechanical observables, we take advantage of of ML knowledge to develop NNAIMQ [3], an intuitive and fast Neural Network (NN) model for the computation of QTAIM charges for C, H, O and N atoms with high accuracy. Our model has been trained and tested using data from quantum chemical calculations in more than 45 000 molecular environments of the near-equilibrium CHON chemical space. The reliability and performance of NNAIMQ have been analyzed in a variety of scenarios. Altogether, NNAIMQ yields remarkably small prediction errors, well below the 0.03 electron limit in the general case, while accelerating the calculation of QTAIM charges by several orders of magnitude. Generalization to other descriptors is also proposed.

References

[1] R. Bader, Atoms in Molecules: A Quantum Theory, International series of monographs on chemistry (Clarendon Press, Oxford, 1990), ISBN 9780198551683
[2] S. Grabowsky, A. Genoni, H. Bürgi, Hans-Beat Chemical Science. 8, 4159–4176, 2017.
[3] M. Gallegos, J. M. Guevara-Vela, A. Martín Pendás, J. Chem. Phys. 156 014112, 2022

Back to Table of contents

MS36 Software development in quantum mechanics-based methods of crystallography

MS36-03

DiSCaMB - a package for computations with aspherical atom form factors (HAR, TAAM).

M. Chodkiewicz [1], K. Woźniak [1], L. Patrikeev [1], P. Dominiak [1]
[1]Biological and Chemical Research Centre, Department of Chemistry, University of Warsaw, Żwirki i Wigury 101, Warszawa 02-089 (Poland)

Abstract

DiSCaMB is a C++ library (python interface is also planned) for performing crystallographic calculations related to atomic form factors. It is accompanied by programs which both exemplifies use of the library and can be applied in real life crystallographic calculations – for example to generate (*.tsc) file [1,2] with atomic form factors which can be subsequently use for refinement with e.g. Olex2[3]. DiSCaMB provides functionalities related to models used in quantum crystallography such as Hirshfeld Atom Refinement (HAR) and to Transferable Aspherical Atom Model (TAAM).

Atomic form factors in HAR are based on atomic densities obtained by partition of electron density derived from wave function calculations. TAAM relies on transferability of atomic densities between atoms in similar chemical environments. TAAM implementations uses banks of atomic density parameters (e.g. Invariom [4], ELMAM2 [5], MATTS – successor of UBDB [6](which is used by DiSCaMB), etc.)). The densities are expressed in terms of Hansen-Coppens[7] multipole model. DiSCaMB includes tools for performing all of the intermediate step from acquiring information about crystallographic structure to obtaining atomic form factors (see Fig.1).

Since its public release [8] which have had rather limited functionality, DiSCaMB developed into a software for exploring new approaches in quantum crystallography, including application of alternative electron density partitions in HAR [9], speeding up HAR with fragmentation and testing its relation to TAAM [10] and applying TAAM approach including a refinement against X-ray [11] and electron [12] scattering data.

Here we present full spectrum of DiSCaMB capabilities which will be available with the upcoming major new release of the library.

References

[1] Midgley, L., Bourhis, L.J., Dolomanov, O., Peyerimhoff, N., Puschmann, H. (2019). https://arxiv.org/abs/1911.08847v1

[2] Kleemiss, F., Dolomanov, O. V., Bodensteiner, M., Peyerimhoff, N., Midgley, L., Bourhis, L. J., Genoni, A., Malaspina, L. A., Jayatilaka, D., Spencer, J. L., White, F., Grundkötter-Stock, B., Steinhauer, S., Lentz, D., Puschmann, H. & Grabowsky, S. (2021). Chem. Sci. 12, 1675–1692.

[3] Dolomanov, OV; Bourhis, LJ; Gildea, RJ; Howard, JAK; Puschmann, H. J. (2009). Appl. Cryst., 42, 339-341

[4] Dittrich, B., Hübschle, C. B., Pröpper, K., Dietrich, F., Stolper, T. & Holstein, J. (2013). Acta Crystallogr. B 69, 91.

[5] Domagała, S., Fournier, B., Liebschner, D., Guillot, B. & Jelsch, C. (2012). Acta Crystallogr. A 68, 337.

[6] Kumar, P., Gruza, B., Bojarowski, S. A. & Dominiak, P. M. (2019). Acta Crystallogr. A 75, 398.

[7] Hansen, N. K. & Coppens, P. (1978). Acta Cryst. A34, 909–921.

[8] Chodkiewicz, ML; Migacz, S; Rudnicki, W; Makal, A; Kalinowski, JA; Moriarty, NW; Grosse-Kunstleve, RW; Afonine, PV; Adams, PD; Dominiak, PM. (2018). J. Appl. Cryst., 51, 193–199.

[9] Chodkiewicz, M. L., Woinska, M. & Wozniak, K. (2020). IUCrJ 7, 1199-1215.

[10] Chodkiewicz, M., Pawledzio, S., Woinska, M. & Wozniak, K. (2022). IUCrJ 9, 298-315.

[11] Jha, K. K., Gruza, B., Kumar, P., Chodkiewicz, M. L. & Dominiak, P. M. (2020). Acta Cryst. B76, 296-306.

[12] Gruza, B., Chodkiewicz, M. L., Krzeszczakowska, J. & Dominiak, P. M. (2020). Acta Cryst. A76, 92-109.

Fig. 1. Some of DiSCaMB functionalities.

Back to Table of contents

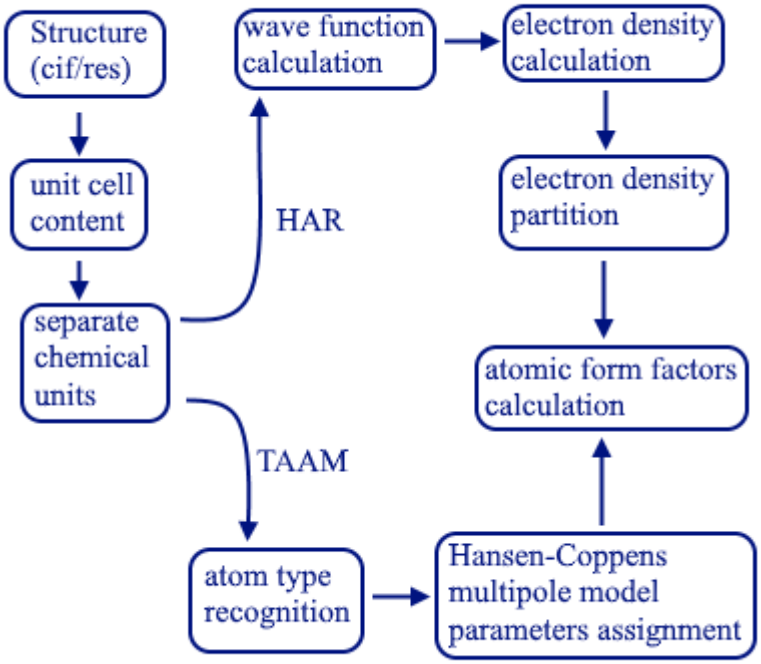
Structure (cif/res)
unit cell content
separate chemical units
HAR
TAAM
wave function calculation
electron density calculation
electron density partition
atomic form factors calculation
Hansen-Coppens multipole model parameters assignment
atom type recognition

MS36 Software development in quantum mechanics-based methods of crystallography

MS36-04

A Periodic Density Source for a Periodic System: Using PAW-DFT for Hirshfeld Atom Refinement in XHARPy

P.N. Ruth [1], R. Herbst-Irmer [1], D. Stalke [1]
[1]*Institute of Inorganic Chemistry, University of Göttingen - Göttingen (Germany)*

Abstract

Hirshfeld atom refinement was first conceived in 2008, when Jayatilaka and Dittrich proposed using the Fourier Transform of atomic densities, which are obtained by Hirshfeld stockholder partitioning (Hirshfeld, 1971) of theoretically derived densities (Jayatilaka & Dittrich, 2008) source for atomic form factors used in the refinement against X-ray diffraction data. Previous implementations used non-periodic calculations to obtain the density, which is subsequently partitioned into the individual atomic contributions.

Using the Numpy/Jax/GPAW libraries in Python we have built a new refinement library called XHARPy, which enables users to do Hirshfeld Atom Refinement using partitioned periodic densities calculated in the projector augmented wave DFT method (Ruth *et al.*, 2022), in addition to refinement against Hirshfeld densities from non-periodic source via NoSpherA2 (Kleemiss *et al.*, 2021). A basic command line interface is also available.

In an evaluation of the accuracy of the determined atomic displacement parameters and bond lengths of hydrogen from X-ray data (Birkedal et al., 2004) for urea, the periodic description compares favourably to non-periodic descriptions using cluster charges (Figure 1) in the reproduction of results from neutron diffraction (Swaminathan *et al.*, 1984). Evaluated quality indicators were: The crystallographic agreement factor $wR_2(F^2)$, the absolute difference between neutron diffraction and HAR derived X-H bond distances $|\Delta r|$, the absolute difference between atomic displacement parameters $|\Delta U_{ij}|$ and the disagreement of the resulting probability distributions S_{12} (Whitten & Spackman, 2006).

P.N.R. and D.St thank the GRK BENCh, which is funded by the Deutsche Forschungsgemeinschaft (DFG, German Research Foundation) - 389479699/GRK2455.

References

Birkedal, H., Madsen, D., Mathiesen, R. H., Knudsen, K., Weber, H.-P., Pattison, P. & Schwarzenbach, D. (2004). *Acta Cryst.* A**60**, 371–381, DOI: 10.1107/S0108767304015120.
Hirshfeld, F. L. (1971). *Acta Cryst.* B**27**, 769–781, DOI: 10.1107/S0567740871002905.
Jayatilaka, D. & Dittrich, B. (2008). *Acta Cryst.* A**64**, 383–393, DOI: 10.1107/S0108767308005709.
Kleemiss, F., Dolomanov, O. V., Bodensteiner, M., Peyerimhoff, N., Midgley, L., Bourhis, L. J., Genoni, A., Malaspina, L. A., Jayatilaka, D., Spencer, J. L., White, F., Grundkötter-Stock, B., Steinhauer, S., Lentz, D., Puschmann, H. & Grabowsky, S. (2021). *Chem. Sci.* **12**, 1675–1692, DOI: 10.1039/D0SC05526C.
Ruth, P. N., Herbst-Irmer, R., Stalke, D., (2022). *IUCrJ* **9**, 286–297, DOI: 10.1107/S2052252522001385.
Swaminathan, S., Craven, B. M. & McMullan, R. K. (1984). *Acta Cryst*. B**40**, 300–306, DOI: 10.1107/S0108768184002135.
Whitten, A. E. & Spackman, M. A. (2006). *Acta Cryst*. B**62**, 875–888, DOI: 10.1107/S0108768106020787

Comparison of Hirshfeld atom refinement methods

Back to Table of contents

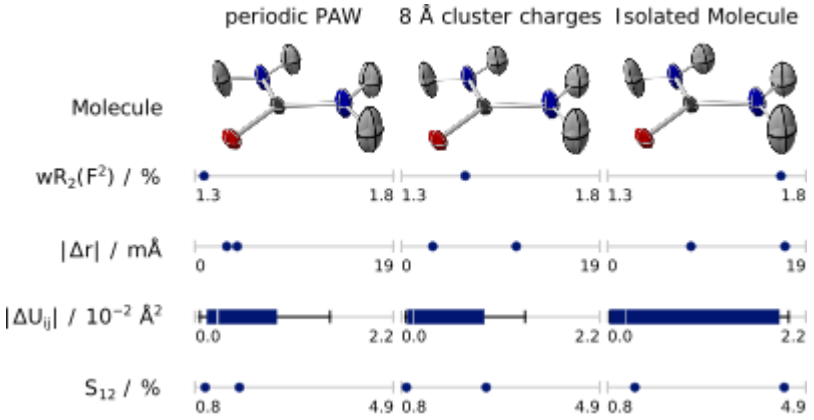

Back to Table of contents

MS36 Software development in quantum mechanics-based methods of crystallography

MS36-05

MATTS2021 data bank: application of cluster analysis to interpret electron density of atom types

P. Rybicka [1], M. Kulik [1], M.L. Chodkiewicz [1], P.M. Dominiak [1]
[1]Biological and Chemical Research Centre, Department of Chemistry, University of Warsaw - Warsaw (Poland)

Abstract

An electron density model is necessary to interpret data from X-ray diffraction. In contrast to spherical Independent Atom Model (IAM), the Multipole Model (MM) uses aspherical approach to describe electron density, which includes the deformation of electron density arising from lone electron pairs and covalent bonds. The MATTS (Multipolar Atom Types from Theory and Statistical clustering) data bank gathers Multipole Model parameters specific for various atom types in proteins, nucleic acids, and organic molecules. However, the relations between and within atom types, how electron density of particular atoms responds to their surroundings, and which factors describe the electron density in molecules within the Multipole Model, were not yet investigated in details. By implementing data analysis methods such as clustering, we captured similarities in the spatial distribution of electron density for atom types and found out which of their features influence the multipole parameters of electron density the most. The resemblance between atom types gives potential for improving quality of the data bank by adding better parametrization, definitions, and local coordinate systems for atom types. The further development of the MATTS data bank and introducing atom types on various levels of generality and specificity, will lead to achieving the eventual goal of having a wider range of atom types necessary to construct the electron density of any molecule.
Acknowledgements: Support by the National Centre of Science (Poland) through grant OPUS No.UMO-2017/27/B/ST4/02721 is gratefully acknowledged.

References

[1] N. K. Hansen, P. Coppens, Acta Cryst., 1978, A34, 909–921.
[2] P. Kumar, B. Gruza, S. A. Bojarowski, P. M. Dominiak, Acta Cryst., 2019, A75, 398-408.

Back to Table of contents

MS37 Advances in Structure determination of new materials by multi-technique approach including imaging techniques

MS37-01

Investigating reaction intermediates under realistic conditions with diffraction, imaging and spectroscopy

A. Lagrow [1]
[1]*International Iberian Nanotechnology Laboratory - Braga (Portugal)*

Abstract

Reaction intermediates are complex to characterize as they are often unstable outside of their reaction environment, are metastable, amorphous or poorly crystalline. However, despite these difficulties they are important to the understanding and control of a materials growth mechanism. To investigate these materials, characterization techniques carried out under close to reaction conditions are required, such as in-line, in-situ or cryo characterization techniques. These techniques allow access to the material under realistic or simulated conditions, either in solution or under reactive gases. Several techniques such as synchrotron X-ray scattering and diffraction, Raman spectroscopy, infrared spectroscopy and ultraviolet-visible spectroscopy can be used in solution due to the large penetration depth of the technique, where-as transmission electron microscopy (TEM) can be utilized for in-depth analysis, trying to preserve the materials while transferring them into the TEM or generating that form in-situ.

In this talk I will detail several examples of reaction intermediates studied by combining electron microscopy techniques with a range of spectroscopic and diffraction techniques under realistic reaction conditions. In particular the materials explored are metastable and form during a reaction, either during growth or under reactive conditions such as corrosion or catalysis. The examples focused on will be materials studied during growth and corrosion to investigate reaction intermediates and reaction kinetics. Nanoparticle intermediates studied during solution synthesis showed the formation of amorphous materials, nanocluster formation and also crystalline structures that rapidly broke down when removed from solution. A range of solution based techniques including cryo electron microscopy were utilized to determine the initial forms of these materials and their growth mechanisms.[1-3] For metallic nanoparticles and their oxides and carbides, reaction dynamics and corrosion mechanisms were explored. A particular example that will be discussed is on the oxidation of iron carbides to iron oxide, utilizing high resolution scanning transmission electron microscopy and electron energy loss spectroscopy to determine the intermediate structures that form and the fate of the carbon in the structure.[4] Finally the growth and passivation of copper indium gallium selenide (CIGSe) thin films will be discussed focusing on reactions at the boundaries between grains and their passivation with alkali metals.

References

1) A. P. LaGrow, L. Sinatra, A. Elshewy, K-W. Huang, K. Katsiev, A. R. Kirmani, A. Amassian, D. H. Anjum, O. M. Bakr. Journal of Physical Chemistry C, 2014, 118, 19374−19379.
2) A. P. LaGrow, T. M. D. Besong, N. M. AlYami, K. Katsiev, D. H. Anjum, A. Abd Elkader, P. M. F. J. Costa, V. M. Burlakov, A. Goriely, O. M. Bakr. Chemical Communications, 2017, 53, 2495 – 2498.
3) A. P. LaGrow, M. O. Besenhard, A. Hodzic, A. Sergides, L. Bogart, A. Gavriilidis, N. T. K. Thanh. Nanoscale. 2019, 11, 6620-6628.
4) A. P. LaGrow, S. Famiani, A. Sergides, L. Lari, D. C. Lloyd, M. Takahashi, S. Maenosono, E. D. Boyes, P. L. Gai, N. T. K. Thanh. Materials, 2022, 15, 1557.

Back to Table of contents

MS37 Advances in Structure determination of new materials by multi-technique approach including imaging techniques

MS37-02

X-Ray Nano-Analysis for Energy related Materials at ESRF

V. Vanpeene [1], A. Léon [2], S. Schlabach [3], L. Roué [4], B. Lestriez [5], E. Maire [6], R. Tucoulou [1], J. Segura-Ruiz [1], J. Villanova [1]

[1]ESRF, The European Synchrotron - Grenoble (France), [2]European Institute For Energy Research - Karlsruhe (Germany), [3]Institute for Applied Materials, Institute of Nanotechnology, and Karlsruhe Nano Micro Facility, Karlsruhe Institute of Technology - Eggenstein-Leopoldshafen (Germany), [4]Institut National de la Recherche Scientifique (INRS) - Centre Énergie, Matériaux, Télécommunications (EMT) - Varennes (Canada), [5]Nantes université, CNRS, Institut des Matériaux de Nantes Jean Rouxel, IMN - Nantes (France), [6]MATEIS - CNRS UMR 5510 INSA Lyon - Villeurbanne (France)

Abstract

Nowadays, the energy related materials are key actors in our energetical and ecological transition towards more sustainability. As a result, high-performance electrochemical devices, such as fuel cells and batteries, have rapidly spread worldwide for energy conversion and storage, respectively. Both systems are made of advanced materials, which can be multi-layered, poly-phased including various chemistries based on either low and/or light elements and complex multi-scaled microstructures. In order to develop efficient, durable and reliable devices, a deep understanding of the degradation processes occurring at the nano-scale is required within those structures [1-3].

In this context, X-ray nano-characterization provides unique opportunities. More especially, ultimate state-of-the-art synchrotron X-ray techniques offer an exclusive combination of spatial and temporal resolution. This presentation will focus on the capabilities of the nano-analysis beamline ID16B at the ESRF [4]. The beamline offers a multi-modal approach allowing for the characterization of heterogeneous materials in a non-destructive way using a combination of several powerful nano-scale techniques such as X-ray fluorescence (XRF), X-ray absorption spectroscopy (XANES), X-ray diffraction (XRD), and 3D phase contrast imaging (nano-CT). Each technique will be detailed along different case studies focused on Solid Oxide Cells (SOCs) and Li-ion battery degradation. First, new insights into chemical diffusion and formation of secondary phases at the interface of active layers will be illustrated using a multi-technique approach. Then, 3D morphological information obtained thanks to in situ nano-CT along a battery cycle will be depicted. Finally, the new opportunities for materials science investigation opened by the EBS upgrade at the ID16B nano-analysis beamline will be presented.

References

[1] A. Léon, A. Micero, B. Ludwig, A. Brisse, Effect of scaling-up on the performance and degradation of long-term operated electrolyte supported solid oxide cell, stack and module in electrolysis mode, Journal of Power Sources 510 (2021)230346

[2] A. Brisse, J. Schefold, A. Léon, High-temperature steam electrolysis, Chapter 7 in Hydrogen production by water electrolysis edited by T. Smolinka & J. Garche (2021)

[3] X. Han, L. Lu, Y. Zheng, X. Feng, Z. Li, J. Lia, M. Ouyang, A review on the key issues of the lithium ion battery degradation among the whole life cycle, eTransportation, 1, 1000005 (2019).

[4] Martínez-Criado G., Villanova J., Tucoulou R., et al., ID16B: A hard X-ray nanoprobe beamline at the ESRF for nano-analysis, J. Synchr. Radiat., 23, 344-352 (2015).

Back to Table of contents

MS37 Advances in Structure determination of new materials by multi-technique approach including imaging techniques

MS37-03

HRXRD and micro-CT Investigation of Stress and Defects Induced by a Novel Packaging Design for MEMS Sensors

A. Borzì [1], R. Zboray [1], S. Dolabella [1], S. Brun [2], F. Telmont [2], P. Kupferschmied [2], J.F. Le Neal [3], P. Drljaca [3], G. Fiorucci [4], A. Dommann [1], A. Neels [1]

[1]Center for X-ray Analytics, Empa - Dübendorf (Switzerland), [2]Sy&Se SA - La Chaux-de-Fonds (Switzerland), [3]TE Connectivity - Bevaix (Switzerland), [4]eHaute Ecole Arc Ingénierie - La Chaux-de-Fonds (Switzerland)

Abstract

Advanced methods such as high-resolution X-ray diffraction and X-ray micro CT allow highly precise determination of residual stress, volume, and lattice defects in functional materials. Their conjoint exploitation allows a multiscale approach to investigating the materials' microstructure [1] and offers a powering tool to facilitate the industrial implementation of novelties in microfabrication. The wafer-level packaging is a critical step of the MEMS microfabrication resulting in an airtight interface, stress-free and devoid of defects [2-4]. In this work, such critical parameters are investigated for the first time related to a novel wafer-bonding process, namely Impulse Current Bonding (ICB) [5-6]. Moreover, they are compared to the same characteristics associated with the standard anodic bonding technology used for MEMS production [7-9]. The microstructural investigations by HRXRD prove that the ICB does not induce any relevant residual stress at the interface above the limit of 1 MPa, determined by the unrivaled strain detectability of HRXRD. The bonding interface is devoid of any defects, as defined by X-ray micro-CT studies.

The ICB technology is promising related to the reduction of the energy footprint of the microelectronic industry in virtue of the outstanding reduction of the thermal budget of the packaging up to 85% compared to the anodic bonding. Moreover, the extension of ICB to other materials systems such as glass to ceramic or metals makes this technology a promising candidate for numerous applications, including the design of biocompatible devices for bio-implants.

References

[1] A. Borzì, R. Zboray, S. Dolabella, J.F. Le Neal, P. Drljaca, G. Fiorucci, A. Dommann, A. Neels, A holistic X-ray analytical approach to support sensor design and fabrication: strain and cracking analysis in wafer bonding process, Materials & Design. (2021) 110052. https://doi.org/10.1016/j.matdes.2021.110052

[2] S.-H. Choa, Reliability of MEMS packaging: vacuum maintenance and packaging induced stress, Microsyst Technol. 11 (2005) 1187–1196. https://doi.org/10.1007/s00542-005-0603-8.

[3] O. Brand, H. Baltes, Microsensor packaging, Microsystem Technologies. 7 (2002) 205–208. https://doi.org/10.1007/s005420100110.

[4] G. Kelly, J. Alderman, C. Lyden, J. Barrett, Microsystem packaging: lessons from conventional low cost IC packaging, J. Micromech. Microeng. 7 (1997) 99–103. https://doi.org/10.1088/0960-1317/7/3/004.

[5] Patented in Europe EP3320403-B1

[6] Patented in the US US 10,788,793-B2

[7] S. Kobayashi, K. Ohwada, T. Hara, T. Oguchi, Y. Asaji, K. Yaji, Double-frame silicon gyroscope packaged under low pressure by wafer bonding, IEEJ Trans. SM. 120 (2000) 111–115. https://doi.org/10.1541/ieejsmas.120.111.

[8] M. Esashi, N. Ura, Y. Matsumoto, Anodic bonding for integrated capacitive sensors, in: [1992] Proceedings IEEE Micro Electro Mechanical Systems, IEEE, Travemunde, Germany, 1992: pp. 43–48. https://doi.org/10.1109/MEMSYS.1992.187688.

[8] G. Wallis, D.I. Pomerantz, Field Assisted Glass-Metal Sealing, Journal of Applied Physics. 40 (1969) 3946–3949. https://doi.org/10.1063/1.1657121.

Back to Table of contents

HRXRD analyses on the ICB and AB assembled samples

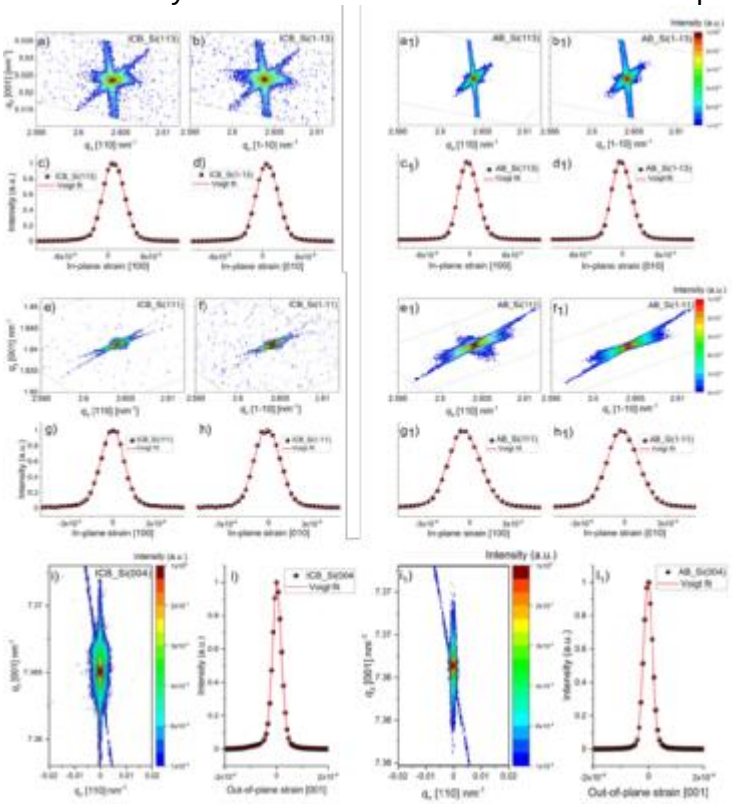

X-ray micro-CT and SEM analyses on one sample asse

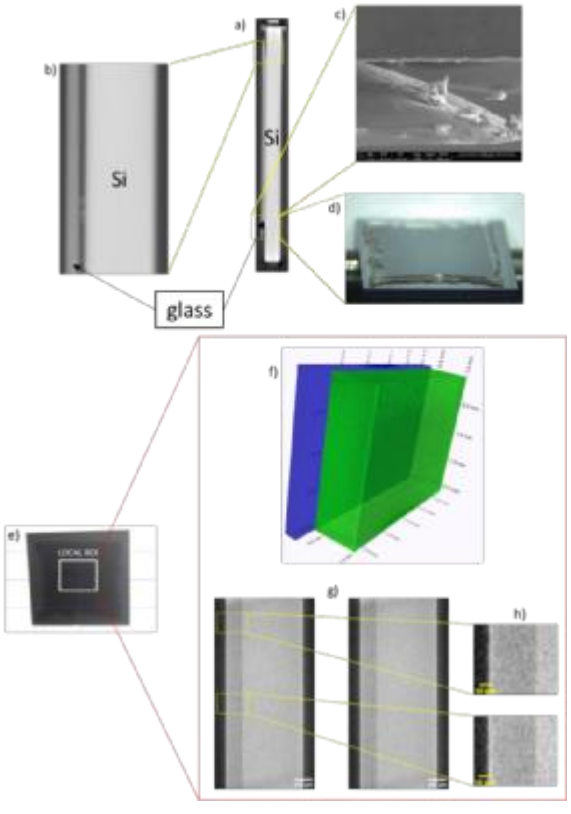

Back to Table of contents

MS37 Advances in Structure determination of new materials by multi-technique approach including imaging techniques

MS37-04

In-situ XRD and PDF investigation of battery fluoride materials MF3.3H2O (M = Fe, Cr) in controlled atmosphere: accessing new phases with controlled chemistry

J. Gertenbach [1], G. Nénert [1], K. Forsberg [2], C. Colin [3]
[1]Malvern Panalytical - Almelo (Netherlands), [2]Royal Institute of Technology - Stockhlom (Sweden), [3]Néel Institute - Grenoble (France)

Abstract

Iron fluoride ($FeF_3.nH_2O$) shows high capacity as cathode material for lithium-ion batteries combined to low toxicity and low cost. The water content of iron fluoride has been shown to be of prime importance in the performances of the cathode. So far, the various synthesis route doesn't allow for a precise water content control, especially on the low amount regime which is the most interesting range of composition [1]. In addition, CrF_3 has been shown to increase significantly the conductivity of LiF film [2]. Consequently, it is of interest to look for the in-situ formation of the various $MF_{3-x}(OH)_x.nH_2O$ phases (M = Cr, Fe).

In this contribution, we report on the in-situ formation of $MF_{3-x}(OH)_x.nH_2O$ (M = Fe, Cr) phases using self-generated atmosphere. Traditionally, the heating $MF_3.3H_2O$ in open air results in the full oxidation and decomposition of the fluorides giving rise to nano based oxides. Here, we make use of self-generated atmosphere to control the precise crystal chemistry of those phases upon heating preventing full oxidation at mild temperatures while stabilizing new phases relevant for battery applications.

Some of the results are presented in Figure 1 about the $FeF_{3-x}(OH)_x.nH_2O$ phases. Precise controlled of the water content of the $FeF_{3-x}(OH)_x.nH_2O$ series could be reached with n ranging from 1/3 to 0 with about 10 new pure phases. We demonstrate experimentally the initial assumption on the role played by the water in the stabilisation of the $FeF_3.1/3H_2O$ phase, phase which is relevant for battery application [1]. In addition, the controlled in-situ decomposition of $CrF_3.3H_2O$ led to the formation of a new CrF3-x(OH)x pyrochlore which was characterized structurally and magnetically. This work demonstrates the added value of in-situ experiment using self-generated atmosphere for synthetising new phases.

References

[1] Kim et al., (2010) Adv. Mater. 22, 5260; Ma et al. (2012), Energy Environ. Sci. 5, 8538.
[2] Tetsu O. (1984), Materials Research Bulletin 19, 451.

Isoline plot of the FeF3.3H2O in-situ diffraction

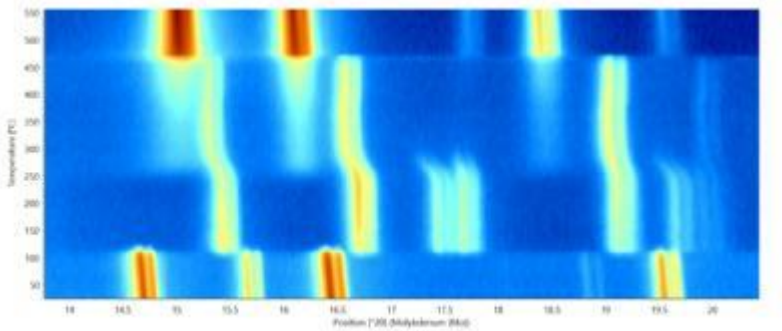

Back to Table of contents

MS37 Advances in Structure determination of new materials by multi-technique approach including imaging techniques

MS37-05

Structural elucidation of novel metal-organic frameworks using 3D electron diffraction

A. Mansouri [1], B. Chen [1], P. Boullay [2], I. Dovgaliuk [1], G. Patriarche [3], G. Mouchaham [1], C. Serre [1]
[1]Institut des Matériaux Poreux de Paris, Ecole Normale Supérieure, ESPCI Paris, CNRS, PSL University, 75005 - Paris (France), [2]Normandie Université, ENSICAEN, UNICAEN, CNRS, CRISMAT, 14050 - Caen (France), [3]Center for Nanoscience and Nanotechnology, C2N UMR 9001, CNRS, Université Paris Sud, Université Paris Saclay - Palaiseau (France)

Abstract

Metal-organic frameworks (MOFs) are hybrid crystalline porous solids demonstrating potential applications in different domains related to energy, environment or health [1]. The structural elucidation of nano-sized MOFs is essential as it provides a better understanding of their unique properties. However, the synthesis of robust MOFs often leads to polycrystalline compounds rendering the structure elucidation by single-crystal and powder X-ray diffraction often challenging. A good alternative is to solve the structure from 3-dimensional electron diffraction (3DED) data [2], a method allowing to solve the structure from much smaller particles by using electrons instead of X-rays.

Titanium-based MOFs (Ti-MOFs) are of interest due to their photoactive character, good biocompatibility and tunability in terms of pore engineering, which makes them attractive candidates in photocatalysis or energy-related reactions [3,4]. However, the design of new Ti-MOFs is still driven by serendipity due to the complexity of titanium chemistry in solution [5]. Here, we present a new robust nanoporous nitro functionalized titanium terephthalate MOF labelled MIP-209 (MIP stands for Materials from Institute of Porous Materials of Paris) constructed from Ti12O15 oxo-clusters, similarly to MIP-177 [1] as revealed first by X-ray Pair distribution function analysis (PDF). The structure has been then solved by ab initio methods using continuous rotation electron diffraction (cRED) data and refined kinematically.

In this communication, the structural characterization of MIP-209 by 3DED will be presented. in combination with complementary structural characterization methods such as pair distribution function (PDF) analysis and low-dose high-resolution TEM (LD-HRTEM). Due to the high electron beam sensitivity of MOFs, the latter was only made possible by the use of a microscope equipped with a direct detection electron counting camera (DDEC) [6], enabling the imaging of MOFs with low dose rates.

The authors acknowledge the Region Ile-de-France in the framework of DIM Respore for the financial support and the Nanomax Platform (Ecole Polytechnique) for the use of a cutting edge microscope and camera. The authors acknowledge financial support from the CNRS-CEA "METSA" French network (FR CNRS 3507) on the platform IRMA (CRISMAT-Caen) for 3DED experiments.

References

[1] Wang, S., & Serre, C. et al. (2018). *Nature Communication*, 9, 1660.
[2] Gemmi, M., & Abrahams, J. P. (2019). *ACS central science*, 5(8), 1315-1329.
[3] Chen, X., & Xia, Q. (2020). *Chemical Engineering Journal*, 395, 125080.
[4] Nguyen, H. L. (2017). *New Journal of Chemistry*, 41(23), 14030.
[5] Assi, H., Mouchaham, G., Steunou, N. et al. (2017) *Chemical Society Reviews Journal*, 46, 343
[6] Zhang, D., & Han, Y. (2018). *Science*, 359(6376), 675.

Structural model (left) and HRTEM images (right).

Back to Table of contents

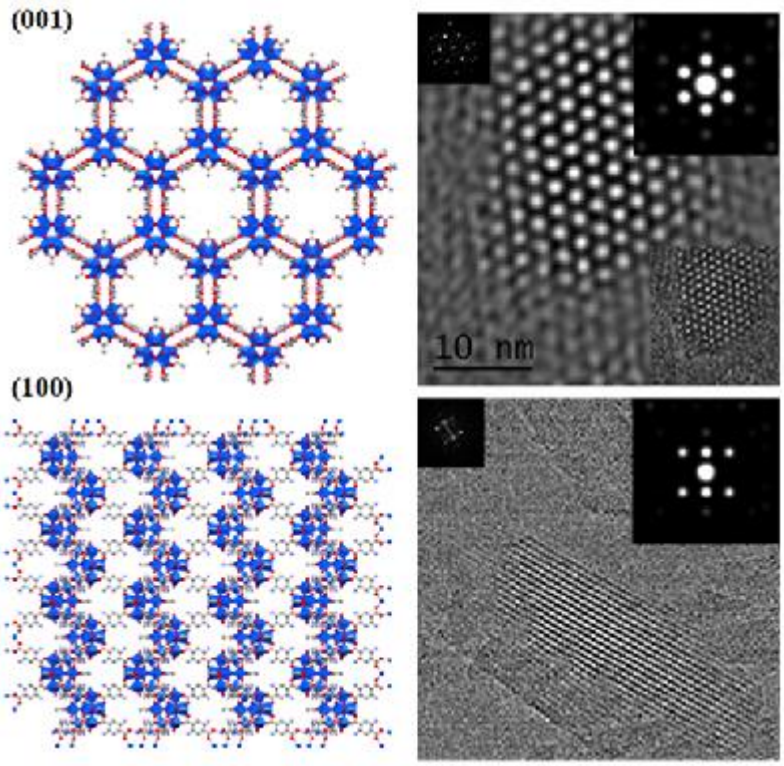

Back to Table of contents

MS38 Computations with/for Pair Distribution Functions

MS38-01

Nanostructure characterization with Pair Distribution Function analysis: Tools for automated analysis

K.M.Ø. Jensen [1]
[1]*University of Copenhagen - Copenhagen Ø (Denmark)*

Abstract

The development of advanced, functional materials builds on an understanding of the intricate relationship between material structure and properties, and over the past century, crystallographic methods using scattering and diffraction have thus been essential for materials science. Crystallography allows ab initio determination of crystal structures from diffraction data, and has provided us with the vast knowledge of crystal chemistry that is now used in design of functional materials. However, in the case of nanomaterials with limited long-range order, crystallographic methods are challenged, and ab initio structure determination, or structure solution, is not currently possible. Over the past decades, total scattering with Pair Distribution Function (PDF) analysis has become an essential tool for characterisation of nanomaterial structure.[1] However, structure solution from the PDF is not possible except in a very few simple cases.[2-4] In the absence of broadly applicable ab initio nanostructure determination methods, it is therefore necessary to propose reasonable starting models and to then 'refine' the model parameters against the data using local minimization methods. The step of finding a starting model can be a major challenge and is thus a bottleneck in complex material characterization. Recently, new automated approaches have made it possible to test thousands of models against a dataset,[5-7] but these methods are computationally expensive, and analysing the output, i.e., extracting structural information from the resulting fits in a meaningful way is challenging. Here, we show how machine learning (ML) methods cain aid. Our Machine Learning based Motif Extractor[8] (ML-MotEx) trains an ML algorithm on thousands of automatically generated fits, which means that a larger strucural space can be invesigated. The use of explainale ML furthermore allows to use SHAP (SHapley Additive exPlanation) values to identify which model features are important for the fit quality. We have used the method on several different systems, and shown how it can be applied for PDF analysis of nanoclusters in solutions as well as disordered oxide materials.

As a second example of the use of ML for scattering data analysis, we show how autoencoders can be a step towards structure solution directly from PDF. Our algorithm DeepStruc[9] can solve a simple, monometallic nanoparticle structure from a Pair Distribution Function (PDF) obtained from total scattering data by using a conditional variational autoencoder. We show that this is possbile from both simulated and experimental PDFs, and illustrate how it learns to identify e.g. stacking faulted strcutures between fcc and hcp nanoparticles. These tools illustrate how new computational methods can aid in analysis of scattering data, and opens for new approaches to nanostucture characterization.

References

1: Billinge, S. J. L. & Kanatzidis, M. G. Beyond crystallography: the study of disorder, nanocrystallinity and crystallographically challenged materials with pair distribution functions. Chem. Commun., 749-760 (2004).
2: Cliffe, M. J., Dove, M. T., Drabold, D. & Goodwin, A. L. Structure determination of disordered materials from diffraction data. Phys. Rev. Lett. 104, 125501 (2010).
3: Juhás, P., Cherba, D. M., Duxbury, P. M., Punch, W. F. & Billinge, S. J. L. Ab initio determination of solid-state nanostructure. Nature 440, 655-658 (2006).
4: Juhás, P., Granlund, L., Duxbury, P. M., Punch, W. F. & Billinge, S. J. L. The Liga algorithm for ab initio determination of nanostructure. Acta Cryst. A 64, 631-640 (2008).

Back to Table of contents

5: Banerjee, S., Liu, C.-H., Jensen, K. M. O., Juhas, P., Lee, J. D., Tofanelli, M., Ackerson, C. J., Murray, C. B. & Billinge, S. J. L. Cluster-mining: an approach for determining core structures of metallic nanoparticles from atomic pair distribution function data. Acta Crystallogr. A 76, 24-31 (2020).
6: Christiansen, T. L., Kjær, E. T. S., Kovyakh, A., Röderen, M. L., Høj, M., Vosch, T. & Jensen, K. M. Ø. Structure analysis of supported disordered molybdenum oxides using pair distribution function analysis and automated cluster modelling. J. Appl. Crystallogr. 53, 148-158 (2020).
7: Yang, L., Juhas, P., Terban, M. W., Tucker, M. G. & Billinge, S. J. L. Structure-mining: screening structure models by automated fitting to the atomic pair distribution function over large numbers of models. Acta Crystallogr. A 76, 395-409 (2020)
8: Anker, A. S. et al. Extracting Structural Motifs from Pair Distribution Function Data of Nanostructures using Explainable Machine Learning. ChemRxiv (2022). doi:10.26434/chemrxiv-2022-v1vfx (2022)
9: Kjær, E. S. T., Anker, A. S., Weng, M. N., Billinge, S. J. L., Selvan, R. & Jensen, K. M. Ø. DeepStruc: Towards structure solution from pair distribution function data using deep generative models. ChemRxiv doi:10.26434/chemrxiv-2022-0zrdl (2022).

Back to Table of contents

MS38 Computations with/for Pair Distribution Functions

MS38-02

Unsupervised and supervised machine learning for total scattering and PDF analyses

S. Billinge [1]
[1]*Columbia University and Brookhaven National Laboratory - New York (United States)*

Abstract

I will describe recent efforts to apply machine learning to the analysis of total scattering and PDF data and modeling. This includes the use of deep neural nets for finding the unknown space-group of a measured PDF and automaticallly finding chemically reasonable components in large sets of powder diffraction and PDF measurements from, for example, an in situ synthesis experiment, using unsupervised machine learning methods. I will also present preliminary results of applying variational conditional autoencoders to do structure solution from PDF data, at least in a very limited way. Some of these tools are available as cloud-hosted web services at PDFitc.org and are free to use by the community.

References

[1] Liu, C.-H., Tao, Y., Hsu, D., Du, Q., Billinge, S.J.L., 2019. Using a machine learning approach to determine the space group of a structure from the atomic pair distribution function. Acta Cryst A 75, 633–643. https://doi.org/10.1107/S2053273319005606

[2] Liu, C.-H., Wright, C.J., Gu, R., Bandi, S., Wustrow, A., Todd, P.K., O'Nolan, D., Beauvais, M.L., Neilson, J.R., Chupas, P.J., Chapman, K.W., Billinge, S.J.L., 2021. Validation of non-negative matrix factorization for rapid assessment of large sets of atomic pair distribution function data. J Appl Cryst 54. https://doi.org/10.1107/S160057672100265X

[3] Thatcher, Z., Liu, C.-H., Yang, L., McBride, B.C., Thinh Tran, G., Wustrow, A., Karlsen, M.A., Neilson, J.R., Ravnsbæk, D.B., Billinge, S.J.L., 2022. nmfMapping: a cloud-based web application for non-negative matrix factorization of powder diffraction and pair distribution function datasets. Acta Cryst A 78. https://doi.org/10.1107/S2053273322002522

[4] Emil T. S. Kjr, Andy S. Anker, Marcus N. Weng, Simon J. L. Billinge, Raghavendra Selvan, and Kirsten M. . Jensen. DeepStruc: Towards structure solution from pair distribution function data using deep generative models". In: arXiv (2022). url: https://arxiv.org/abs/2110.14820

Back to Table of contents

MS38 Computations with/for Pair Distribution Functions

MS38-03

Symmetry-Adapted Pair Distribution Function Analysis

T. Bird [1], P. Chater [1], M. Senn [2]
[1]Diamond Light Source (United Kingdom), [2]University of Warwick (United Kingdom)

Abstract

Symmetry-Adapted Pair Distribution Function Analysis (SAPA)[1] is a novel technique for obtaining information on local dynamics and disorder from pair distribution function (PDF) data of crystalline materials. In the SAPA method, the crystal structure is expanded to a supercell of a given size and then broken down into a symmetry-mode basis using the *ISODISTORT* online software. Using the TOPAS command line functionality, groups of modes transforming as the same irreducible representation can be tested in turn, in order to find the modes most responsible for any deviation of the local structure from the average. With the python programming language, this technique can be performed as an automated process. Using this method, we have been able to elucidate the underlying symmetry of the successive ferroelectric phase transitions in $BaTiO_3$[2] and have highlighted the importance of structural flexibility in determining the range and magnitude of negative thermal expansion in ReO_3[3] and related structures[4].

References

[1] T. A. Bird, A. Herlihy and M. S. Senn, *J. Appl. Cryst.*, **54** (2021), 1514-1520
[2] M. S. Senn, D. A. Keen, T. C. A. Lucas, J. A. Hriljac and A. L. Goodwin, *Phys. Rev. Lett.*, **116** (2016), 207602
[3] T. A. Bird, M. G. L. Wilkinson, D. A. Keen, R. I. Smith, N. C. Bristowe, M. T. Dove, A. E. Phillips and M. S. Senn, *Phys. Rev. B*, **104** (2021), 214102
[4] T. A. Bird, J. Woodland-Scott, L. Hu, M. T. Wharmby, J. Chen, A. L. Goodwin and M. S. Senn, *Phys. Rev. B.,* **101** (2020), 064306

A flowchart of the steps for the SAPA method

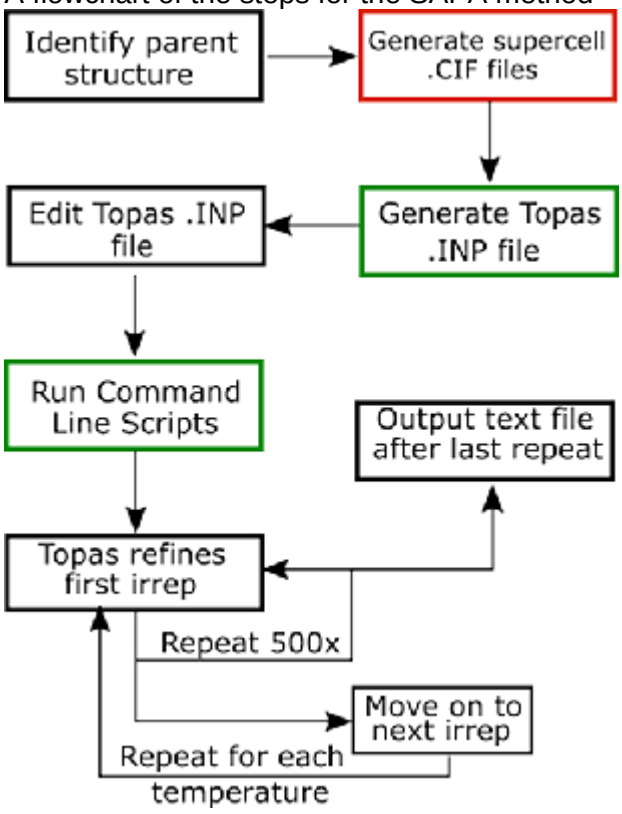

Back to Table of contents

MS38 Computations with/for Pair Distribution Functions

MS38-04

Direct visualization of magnetic correlations in frustrated spinel ZnFe2O4

J.R. Sandemann [1], T.B.E. Grønbech [1], K.A.H. Støckler [1], F. Ye [2], B.C. Chakoumakos [2], B.B. Iversen [1]
[1]Aarhus University - Aarhus (Denmark), [2]Oak Ridge National Laboratory - Oak Ridge (United States)

Abstract

Magnetic materials with the spinel structure (AB_2O_4) form the core of numerous magnetic devices, but $ZnFe_2O_4$ constitutes a peculiar example where the nature of the magnetism is still unresolved [1,2]. Here the Fe atoms sit on the octahedral sites which constitutes a pyrochlore lattice whose geometry, a network of corner-sharing tetrahedra, is very conducive to exotic magnetic ground states. Using a combination of AC and DC susceptibility measurements in conjunction with heat capacity data we have established the presence of a spin-glass phase in $ZnFe_2O_4$ at low temperature.

Recently, we introduced the magnetic 3D-ΔPDF method, which through a model-free approach allowed us to directly reconstruct the magnetic correlations in magnetically disordered systems [3]. We have collected Single crystal neutron scattering patterns down to 1.5K which revealed clear structured diffuse scattering showing that despite the lack of long-range order, the spins are correlated on short length scales. The elastic diffuse scattering signal was isolated which enabled the use of 3D-mΔPDF analysis to determine the local magnetic correlations present in $ZnFe_2O_4$ at low temperatures which clearly shows the nature of the magnetic frustration in the compound.

Integration of the peaks in the 3D-mΔPDF revealed the behaviour of the individual correlations, and thus also the correlation length, with temperature. The correlations can be rationalized by orbital interaction mechanisms for the magnetic pathways giving insight into the underlying magnetic exchange mechanisms. Using the 3D-mΔPDF results in conjunction with the magnetic exchange considerations a preferred spin-cluster around any given Fe atom has been proposed.

Our study demonstrates how analysis of the detailed 3D single crystal neutron diffuse scattering offers a means to build microscopic understanding of magnetic exchange mechanisms in magnetically disordered materials, which is not possible from merely the Bragg scattering.

References

[1] Watanabe, T., Takita, S., Tomiyasu, K. & Kamazawa, K., *Phys. Rev. B* 92, 174420 (2015).
[2] Kremenović, A., Antić, B., Vulić, P., Blanuša, J. & Tomic, A., *J. Magn. Magn. Mater.* 426, 264-266 (2017).
[3] Roth, N., May, A. F., Ye, F., Chakoumakos, B. C. & Iversen, B. B., *IUCrJ* 5, 410-416 (2018)

The spinel unit cell

Back to Table of contents

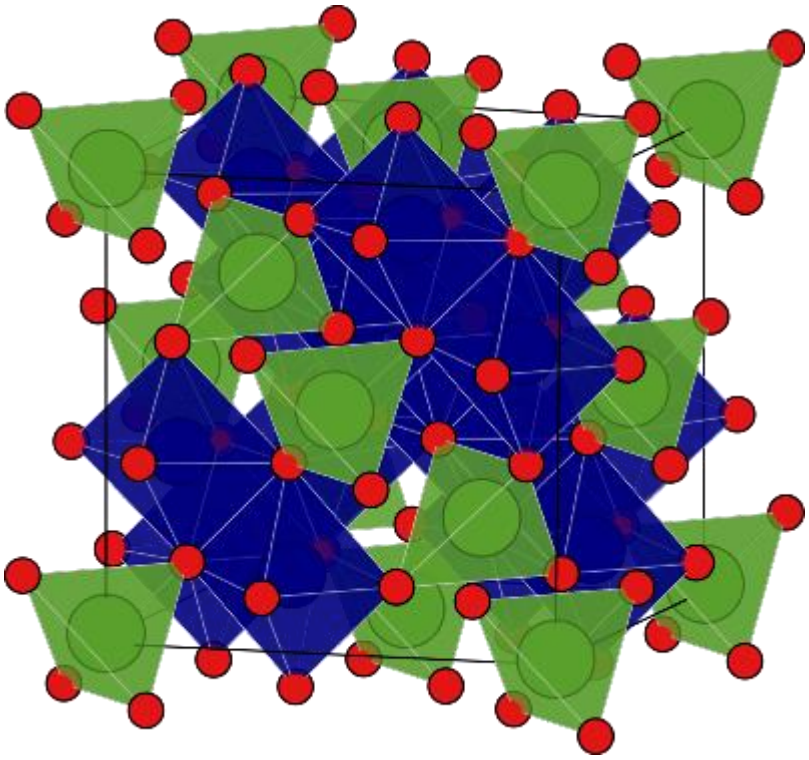

Isolated diffuse scattering at 1.5 K

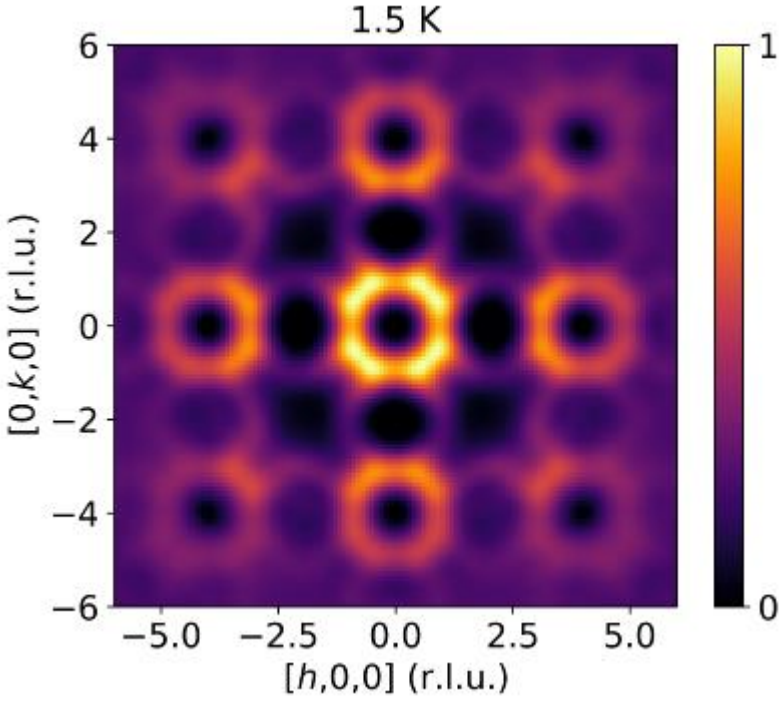

Back to Table of contents

MS38 Computations with/for Pair Distribution Functions

MS38-05

Most recent development big box modelling in RMCProfile7

W. Slawinski [1], Y. Zhang [2], M. Tucker [2], H. Playford [3]
[1]University of Warsaw - Warsaw (Poland), [2]Oak Ridge National Laboratory - Oak Ridge (United States), [3]ISIS Nautron and Muon Source - Didcot (United Kingdom)

Abstract

Big box modelling of Pair Distribution Function (PDF) is becoming more and more popular and powerful tool to describe local structure of materials. To a large extent this id because it allows move freely and create a structure having non-symmetry restrained distortions. Therefore, this enable the solution which complies both the average structure (as obtained from Bragg diffraction data) and local order/disorder as obtained from Pair Distribution Function. In order to follow the increasing need in the PDF analysis tools, we are currently implementing new capabilities in new RMCProfile7 program. This piece of software grown out from very well-known RMCProfile6, gives multiple of new capabilities implemented very recently.
Here, we present new functionalities which are now available in RMCProfile7:
1. Multiple phase refinement
2. Variety of experimental dataset types (real space, reciprocal space, Bragg)
3. Multiples of datasets of the same type (i.e. multiple of Bragg datasets, joint X-Ray and neutron refinements)
4. Real space data calculation also possible as back Fourier transform of reciprocal space data
5. Variety of constraints (minimum distance, moveout) and restraints (bond valence sum; broad variety of potentials – bond, angles, torsion angles, inversion angle, planarity, planar rings; tails)
6. Multiple atom type swaps, fully compatible with all constraints/restraints
7. Implementation of molecule type move (collective move, rotation and/or swap for a rigid molecule or rigid group of atoms)
8. Implementation of Bragg profile calculation based on GSAS-II program for both X-ray and neutron time of flight data
9. Scale and offset refinement, also background for Bragg datasets
RMCProfile7 is freely available in beta form on https://rmcprofile.pages.ornl.gov/

Back to Table of contents

MS39 Crystallography at the nanoscale

MS39-01

2D nanostructures at atomic scale: from energy an environmental applications to quantum devices

J. Arbiol [1]
[1]*Catalan Institute of Nanoscience and Nanotechnology (ICN2), CSIC and BIST - Bellaterra (Spain)*

Abstract

Technology at the nanoscale has become one of the main challenges in science as new physical effects appear and can be modulated at will. As developments in materials science are pushing to the size limits of physics and chemistry, there is a critical need for understanding the origin of these unique properties and relate them to the changes originated at the atomic scale, e.g.: linked to structural changes of the material, many times related to the presence of crystal defects or crystal surface terminations. Especially on 2D materials designed for electrocatalysis in energy and environmental applications, crystallography and distribution of the atomic species are of outmost importance in order to determine the active sites that will improve the reaction performance, including efficiency and selectivity towards certain reactions. In 2D nanomaterials the distribution and coordination of metal species at the surface are determining their final electrocatalytic behavior as the reactions of interest mainly occur at the surface. The presentation will show how pristine and perfect crystalline surfaces may tend to be inert versus certain reactions, while creation of certain types of defects or even a predetermined surface amorphization may highly improve the catalytic activity of these 2D nanomaterials.
In the present work, I will show how combining advanced electron microscopy imaging with electron spectroscopy, in an aberration corrected STEM will allow us to probe the elemental composition and structure in unprecedented spatial detail, while determining the growth mechanisms and correlating the structural properties to their electrocatalytic performance.

References

[1] Y. He, et al. (2020) Nature Communications, 11, 57.
[2] Y. He, et al. (2022) Nature Catalysis, 5, 212-221.
[3] T. Zhang, et al. (2021) Energy & Environmental Science, 14, 4847-4857.
[4] Z. Liang, et al. (2021) Advanced Energy Materials, 11, 2003507.

Back to Table of contents

MS39 Crystallography at the nanoscale

MS39-02

Investigation of Materials at the Nanoscale Using Hard X-ray Nanoprobes

G. Martinez [1]
[1]*ESRF - Grenoble (France)*

Abstract

Owing to the spatial resolution and sensitivity (i.e., signal to background ratio), synchrotron nanobeams are promising tools with a strong impact in nanoscience [1]. Although the optical quality of the X-ray focusing optics has limited the progress of hard X-ray nanoprobes, recent progresses in fabrication approaches have pushed the spatial resolution towards the diffraction limit. Consequently, the exploitation of X-ray nanobeams has begun to extend towards the atomic domain, with concomitant and continuous developments of multiple analytical techniques. The study of nanoscale objects, small embedded nanodomains with weak signals and/or heterogeneous nanostructures has demanded the use of intense X-ray pencil beams. In addition, the extreme brilliance with reduced emittance of new synchrotron sources and novel X-ray detection schemes have boosted nowadays intense X-ray nanobeams using several focusing devices. Due to the multiple interactions of X-rays with matter these X-ray nanoprobes present manifold capacities, such as ultra-sensitive elemental/chemical detection by X-ray fluorescence/X-ray absorption, or identification of minority polytypes, and/or strain fields by X-ray diffraction with nanometer resolution. In the present talk I describe how hard X-ray nanobeams are produced and exploited currently for space-resolved determination of structural and electronic properties, as well as for chemical speciation of nanosized materials even under in-situ conditions. Selected recent examples will range from phase separation in single nanowires to visualization of degradation mechanisms under device operation, inversion domains and buried interfacial defects, to structural distortions and quantum confinement effects at low temperatures.

References

[1] L. Mino, E. Borfecchia, J. Segura-Ruiz, C. Giannini, G. Martinez-Criado, and C. Lamberti, Materials characterization by synchrotron x-ray microprobes and nanoprobes, Reviews of Modern Physics, 90 (2018) 025007.

Back to Table of contents

MS39 Crystallography at the nanoscale

MS39-03

True molecular conformation and structure determination of remarkable polycyclic aromatic hydrocarbons

I. Andrusenko [1], E. Mugnaioli [2], M. Gemmi [1], W. Schmidt [3]
[1]Istituto Italiano di Tecnologia, Center for Materials Interfaces, Electron Crystallography - Pontedera (Italy), [2]Università di Pisa, Dipartimento di Scienze della Terra - Pisa (Italy), [3]PAH Research - Igling-Holzhausen (Germany)

Abstract

The true molecular conformation and the crystal structure of four large (30 – 46 C atoms) polycyclic aromatic hydrocarbons (PAHs)[1,2] were determined by direct methods from 3D electron diffraction (3D ED)[3] data, a result that could not be achieved by single crystal X-ray diffraction (XRD) due to limited crystal size and the thin leaflet morphology of the samples. Additionally, three of such compounds were isolated as by-products in the synthesis of similar materials and, therefore, were available only in very limited amount.

The main strength of 3D ED is the ability to perform single crystal diffraction on sub-micrometric areas. Therefore, this technique can be used for structure determination when crystal size is the limiting factor for single crystal XRD. Remarkably, this analytical protocol can be performed even on extremely small sample batches, which cannot be conveniently prepared for conventional powder XRD.

Moreover, the molecular conformation of two compounds could not be determined via classical spectroscopic methods due to the large size of the molecules and the occurrence of multiple and reciprocally connected aromatic rings. On the other hand, 3D ED data provided not only ab-initio structure solution, but also the unbiased determination of the internal molecular conformation. It is noteworthy that ab-initio crystal structure determination does not require information about the molecular conformation, but only a rough estimation of the atomic content of the unit cell.

The other two compounds were synthesised more than 50 years ago, but have hitherto remained structurally unsolved. All molecules have a considerable interest due to their optoelectronic properties, which led to the creation of a number of functionalised materials based on PAH backbones. Detailed synthetic routes, spectroscopic analyses and promising properties are also discussed.

References

1. Hall, C. L., Andrusenko, I., Potticary, J., Gao, S., Liu, X., Schmidt, W., Marom, N., Mugnaioli, E., Gemmi, M. & Hall, S. R. (2021) 3D Electron Diffraction Structure Determination of Terrylene, a Promising Candidate for Intermolecular Singlet Fission. ChemPhysChem 22(15), 1631-1637.
2. Andrusenko, I., Hall, C. L., Mugnaioli, E., Potticary, J., Schmidt, W., Gao, S., Marom, N., Hall, S. R. & Gemmi, M. (2022) True Molecular Conformation and Structure Determination by 3D Electron Diffraction of PAH By-Products Potentially Useful for Electronic Applications, in preparation.
3. Gemmi, M., Mugnaioli, E., Gorelik, T. E., Kolb, U., Palatinus, L., Boullay, P., Hovmöller, S. & Abrahams, J. P. (2019) 3D Electron Diffraction: The Nanoctystallography Revolution. ACS Cent. Sci. 5, 1315-1329.

Back to Table of contents

MS39 Crystallography at the nanoscale

MS39-04

Evaluating the Accuracy of Rietveld Analysis for Diffraction Data from Nanocrystalline Powders

H. Hekmatjou [1], H. Ozturk [1]
[1]*Ozyegin University - Istanbul (Turkey)*

Abstract

Powder X ray diffraction is a widely used method to evaluate the structural properties of nanocrystalline powders. However, direct application of crystallographic solution algorithms are not compatible with the true structural characteristics of such materials [1, 2]. In this study, we present a computational workflow based on first-principle atomistic formulations of diffraction data to evaluate the performance of Rietveld refinement analysis in quantifying average atomic displacements of monodispersed and ideally random powders of gold nanocrystals. We show that the accuracy of the extracted thermal displacements of atoms (isotropic displacement parameters and microstrains) depend strongly on the average sizes of the investigated nanocrystals.

References

[1] Xiong, S.; Ozturk, H.; Lee, S.-Y.; Mooney, P. M.; Noyan, I. C., The nanodiffraction problem. Journal of Applied Crystallography 2018, 51 (4), 1102-1115.
[2] Xiong, S.; Lee, S.-Y.; Noyan, I. C., Average and local strain fields in nanocrystals. Journal of Applied Crystallography 2019, 52 (2), 262-273.

Back to Table of contents

MS39 Crystallography at the nanoscale

MS39-05

Crystallography of clay nanotubes and one-dimensional periodic organization of water inside

A. D' Angelo [1], S. Rols [2], E. Paineau [3], S. Rouzière [3], P. Launois [3]
[1]CNRS/ILL - Orsay/Grenoble (France), [2]ILL - Grenoble (France), [3]CNRS - Orsay (France)

Abstract

Imogolite nanotubes (INTs) of stoichiometry Al2SiO7H4 are clay nanomaterials formed of a rolled gibbsite sheet with isolated SiO3(OH) entities inside [1]. Present in soils, they can also be synthesized by soft chemistry. The inner diameter of these hydrophilic nanotubes is truly nanometric (1.5 nm).

We first present here the determination of the atomic structure of these nanotubes. Their powder X-ray diffractogram inherently exhibits rather broad features due to their nanometric lateral size, giving access to a very limited number of structural parameters. We employed a specific methodology, based on the use of helical symmetries and on simple semi-empirical energy minimization, to reduce the number of fitted variables needed to determine the atomic structure [2]. Then we performed molecular dynamics (MD) simulations using a recently proposed interaction potential [3]. Good agreement between experimental and calculated XRS diagrams is found [4].

Based on this determination of the nanotube structure at the atomic scale, we studied water under confinement in the INTs [4]. We performed X-ray scattering (XRS; synchrotron and in situ laboratory measurements) and elastic neutron scattering experiments, combined with MD simulations. The complementarities between the experimental approaches for the determination of the water content inside and outside the nanotubes will be underlined. Moreover, at room temperature, a one-dimensional periodic structuration of nanoconfined water is revealed by MD (Fig. (a)) and XRS (Fig. (b)), for the first time. Fig. (a) shows an atomic density map for a section of a water-filled INT, from MD simulations; z-axis: long axis of the nanotube, black dots: atoms in the nanotube, gray ones: water inside; fig. (b) shows XRS diagrams of the nanotubes (SOLEIL synchrotron) for increasing amount of water inside (dry nanotube: top curve, most hydrated: bottom curve). The arrow points to the 002 periodicity peak of the nanotube and its intensity variation highlights the periodic arrangement of water molecules along the nanotube axis. We find that the molecules in the wetting layer are the most ordered but, interestingly, the periodicity remains beyond the water layer in contact with the inner wall of the nanotube. The influence of this structuring on the transport properties of the nanoconfined water will be discussed.

References

[1] E., Paineau and P., Launois, Nanomaterials from Clay Minerals, Elsevier, (2019), pp 257-284
[2] G., Monet et al., Nature Comm., 9, (2018), 2033
[3] L., Scalfi et al., Langmuir, 34, (2018), 6748
[4] A., D'Angelo et al., article in preparation

Figure: atomic density map and XRS diagrams

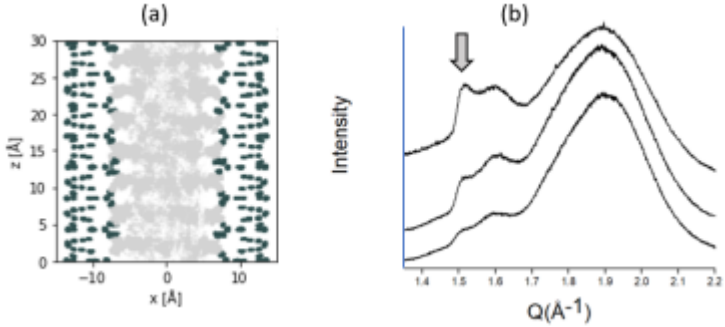

Back to Table of contents

MS40 Operando and in-situ crystallographic studies

MS40-01

Operando X-Ray diffraction studies of NASICON-type positive electrodes for Na-Ion batteries

S. Park [1], J.N. Chotard [2], A. Iadecola [3], D. Carlier [4], F. Fauth [5], L. Croguennec [4], C. Masquelier [2]
[1]Tiamat Energy - Amiens (France), [2]LRCS - UPJV - Amiens (France), [3]SOLEIL Synchrotron - Saint-Aubin (France), [4]ICMCB Bordeaux - Pessac (France), [5]ALBA Synchrotron - Cerdanyola del Vallès (Spain)

Abstract

Polyanionic materials (phosphates in particular) are of special interest as positive electrodes for Li-Ion or Na-ion batteries since they offer competitive electro-chemical performances compared to sodiated or lithiated transition metal oxides [1,2]. They are based upon stable 3D frameworks, which provide long-term structural stability and demonstrate a unique variety of atomic arrangements in their crystal structures. Recent electrochemical and structural investigations of vanadium-based phosphate compounds ($LiVPO_4O$-$LiVPO_4F$, $Na_3V_2(PO_4)_2F_3$, $Na_3V_2(PO_4)_3$ …..) revealed promising perspectives [3-5].

The NASICON structural family with its large panel of compositions, $Na_xMM'(PO_4)_3$ ($0 \leq x \leq 4$; M,M' = Ti, Fe, V, Cr, Mn) is among the most widely investigated due to its specific three-dimensional framework structure, stable long-term cycling ability and high Na+ mobility [1-2, 5-6]. Among them, the vanadium phosphate $Na_3V_2(PO_4)_3$ [7] is of particular interest. We will present several new structures that we determined, from pristine powders or for intermediate compositions spotted by operando X-Ray diffraction.

Recently, we succeeded in synthesizing Fe-substituted $Na_4FeV(PO_4)_3$ that allows the reversible extraction of close to 3 Na^+ (for two transition metals) and we will report on its crystal structure and on that of $Na_3FeV(PO_4)_3$ for which new Na^+ order-disorder phenomena have been spotted [8, 9]. Even more recently, we reported on the existence of an intriguing definite phase of composition $Na_2V_2(PO_4)_3$ through computational methods [10] and operando X-ray diffraction and X-ray absorption spectroscopy during battery operation [11].

References

[1] C. Masquelier, L. Croguennec, *Chemical Reviews*, 113(8), 6552-6591 (2013)
[2] P. Adelhelm, M. Casas-Cabanas, L. Croguennec, I. Hasa, A. Koposov, S. Mariyappan, C. Masquelier, D. Saurel, *J. Power Sources*, 482, 228872 (2021)
[3] E. Boivin, J. N. Chotard, C. Masquelier, L. Croguennec, *Molecules*, 26(5), 1428 (2021)
[4] T. Broux, F. Fauth, N. Hall, M. Bianchini, T. Bamine, J.-B. Leriche, E. Suard, D. Carlier, L. Simonin, C. Masquelier & L. Croguennec, *Small Methods*, 3, 1800215 (2019)
[5] F. Chen, V. Kovrugin, R. David, J. N. Chotard, O. Mentré, F. Fauth & C. Masquelier, *Small Methods*, 3, 1800218 (2019)
[6] B. Singh, Z. Wang, S. Park, G. Sai Gautam, J.N. Chotard, L. Croguennec, D. Carlier, A. K. Cheetham, C. Masquelier & P. Canepa, *J. Mater. Chem. A*, 9(1), 281-292 (2021)
[7] J.N. Chotard, G. Rousse, R. David, O. Mentré, C. Masquelier, *Chem. Mater*., 27(17),5982-5987 (2015)
[8] S. Park, J. N. Chotard, D. Carlier, I. Moog, M. Courty, M. Duttine, F. Fauth, A. Iadecola, L. Croguennec, C. Masquelier, *Chem. Mater*., 33(13), 5355 (2021)
[9] Z. Wang, S. Park, Z. Deng, F. Fauth, D. Carlier, L. Croguennec, C. Masquelier, J. N. Chotard, P. Canepa, *J. Mater. Chem. A*., 10, 209-217 (2022)
[10] S. Park, Z. Wang, Z. Deng, I. Moog, P. Canepa, F. Fauth, D. Carlier, L. Croguennec, C. Masquelier & J. N. Chotard, *Chem. Mater*., 34, 451-462 (2022)
[11] S. Park, J. N. Chotard, D. Carlier, I. Moog, M. Duttine, F. Fauth, A. Iadecola, L. Croguennec & C. Masquelier, *Chem. Mater*., 34, 4442- (2022)

Back to Table of contents

MS40 Operando and in-situ crystallographic studies

MS40-02

Lithiation heterogeneities in full cells by combined neutron and synchrotron scattering techniques

S. Lyonnard [1]
[1]*CEA-IRIG/SyMMES - Grenoble (France)*

Abstract

Operando characterization techniques are key to understand the electrochemical processes that dictate battery performance and the concomitant materials transformations during cycling. In particular, synchrotron and neutron techniques are increasingly employed as they provide unique insights into the chemical, morphological and structural properties inside electrodes and electrolytes across multiple length scales with, potentially, high time/spatial resolutions. Horse techniques such as XRD/NPD, as well as advanced methods such as coherent bragg imaging or ptychography, are constantly developed to better characterize the structure of crystalline battery materials e.g. phase transitions, strain, defects, etc… - extending the experimental limits towards high fidelity and high resolution data. However, the usual rules at Large Scale Facilities is to perform stand-alone experiments providing one type of information at one scale, therefore leading to a fragmented knowledge. Bridging scales and heterogeneous datasets is a challenge that require correlative data acquisition and analysis integrated in multimodal multi-techniques workflows, an approach that is still in its infancy [1]. In this talk, we will present combined and/or coupled operando experiments performed on full batteries of different types, using both neutrons & x-rays, and/or both atomic scale and nanoscale techniques, including scattering computed tomography. We will focus on lithiation heterogeneities at the scale of electrodes, in the depth and/or in 3D, revealed in different types of materials as hierarchical composite anodes based on silicon nanodomains [2] or silicon nanowires [3], and layered intercalation compounds such as LNO [4].

References

[1] Advanced Energy Materials, 2021, 2102694. D. Atkins, E. Capria, K. Edström, T. Famprikis, A. Grimaud, Q. Jacquet, M. Johnson, A. Matic, P. Norby, H. Reichert, J-P. Rueff, C. Villevieille, M. Wagemaker*, S. Lyonnard*. Accelerating Battery Characterization Using Neutron and Synchrotron Techniques: Toward a Multi-Modal and Multi-Scale Standardized Experimental Workflow. DOI:10.1002/aenm.2021026944]
[2] C. Berhaut et al, ACS Nano (2019), 13, 10, 11538-11551 ; C. Berhaut et al, Energy Storage Materials (2020), 29 190-197 ; M. Mirolo et al, in preparation.
[3] C. Keller et al, in preparation
[4] Q. Jacquet et al, in preparation.

Back to Table of contents

MS40 Operando and in-situ crystallographic studies

MS40-03

In-situ PXRD studies of Cs-ion exchange in the zeolite chabazite

D. Parsons [1], A. Nearchou [2], J. Hriljac [1]

[1]Diamond Light Source Ltd - Didcot (United Kingdom), [2]University of Birmingham - Birmingham (United Kingdom)

Abstract

The removal of relatively long-lived radionuclides such as ^{137}Cs ($t_{½}$ = 30.2 years) from aqueous nuclear waste streams, or from aqueous environments contaminated with nuclear waste, is of high importance. A favoured option for the removal of radioactive cations are zeolites: porous crystalline aluminosilicates adopting framework structures comprising corner-shared [SiO_4] and [AlO_4] tetrahedra, with exchangeable cations occupying the hydrated pores and cages of the framework. Chabazite is a particular zeolite that is efficacious in the selective removal of aqueous Cs^+ by ion exchange and has been applied in decontamination efforts at Fukushima.[1] The crystallographic positions occupied by extraframework cations, such as Na, K and Cs, within the chabazite crystal structure are well established when the material contains exclusively one type of cation;[2][3] however, the mechanism by which ion exchange occurs in these materials has not been previously probed despite the inherent advantages to enhancing the understanding of this process. Very few *in situ* PXRD studies have been reported on structural changes in solids as they contact solutions under flow, owing to the specialised sample environment required, the need for synchrotron sources to provide high counting statistics and appropriate detectors to permit rapid acquisition of high-quality datasets. Nevertheless, this approach has been successfully employed previously to reveal mechanistic information on ion exchange processes.[4] In this study, PXRD patterns have been collected, on beamline I11 at the Diamond Light Source synchrotron, on chabazite samples as ion exchange occurs, facilitated by a liquid flow cell (Fig. 1.) which elutes a desired solution through the sample as data is recorded *in situ*. Cs-ion exchange has been studied for two chabazite samples, one containing sodium (Na-CHA) and the other potassium (K-CHA). Time-resolved changes observed in PXRD patterns as Cs-ion exchange proceeds are highlighted in Fig. 2, which shows changes in the (0 -2 -2) reflection during the experiment. Through applying Rietveld refinement to the in-situ datasets, time-resolved structural changes are observed as the constitution of extraframework cations changes within the zeolite, providing a mechanistic understanding of how Cs-ion exchange occurs in these materials.

References

[1] T. Tsukada, K. Uozimi, T. Hijikata, T. Koyama, K. Ishikawa, S. Ono, S. Suzuki, M. S. Denton, R. Keenan and G. Bonhomme, *J. Nucl. Sci. Technol*., 2014, **51**, 886 – 893. (n.b. 'chabazite' is referred to by the less common term 'herschelite' in this publication)

[2] M. Calligaris, A. Mezzetti, G. Nardin and L. Randaccio, *Zeolites*, 1986, **6**, 137 – 141.

[3] A. Alberti, E. Galli, G. Vezzalini, E. Passaglia and P. F. Zanazzi, *Zeolites*, 1982, **2**, 303 – 309.

[4] A. J. Celestian and A. Clearfield, *J. Mat. Chem*., 2007, **17**, 4839 – 4842.

The liquid flow cell installed on beamline I11.

Back to Table of contents

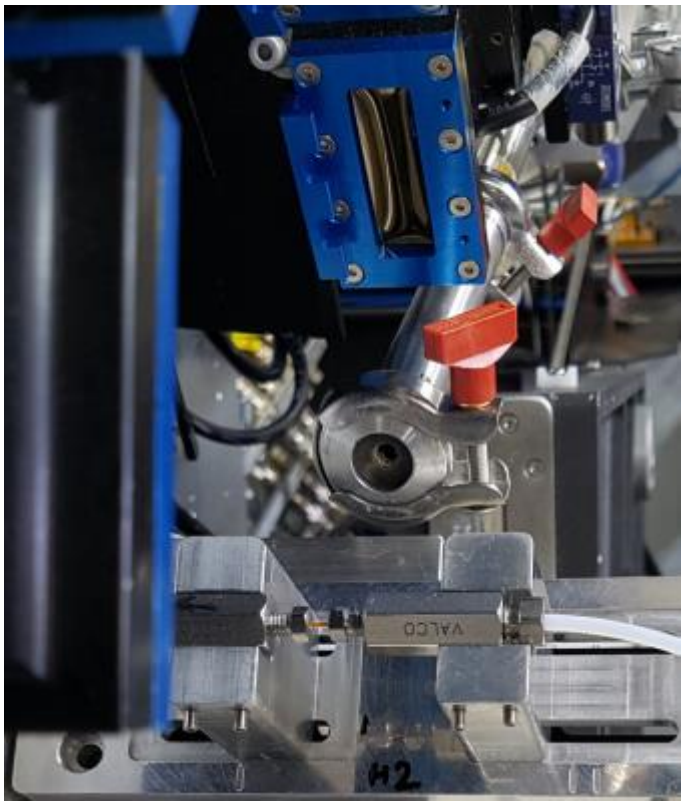

Changes in 0-2-2 reflection for K-CHA with time

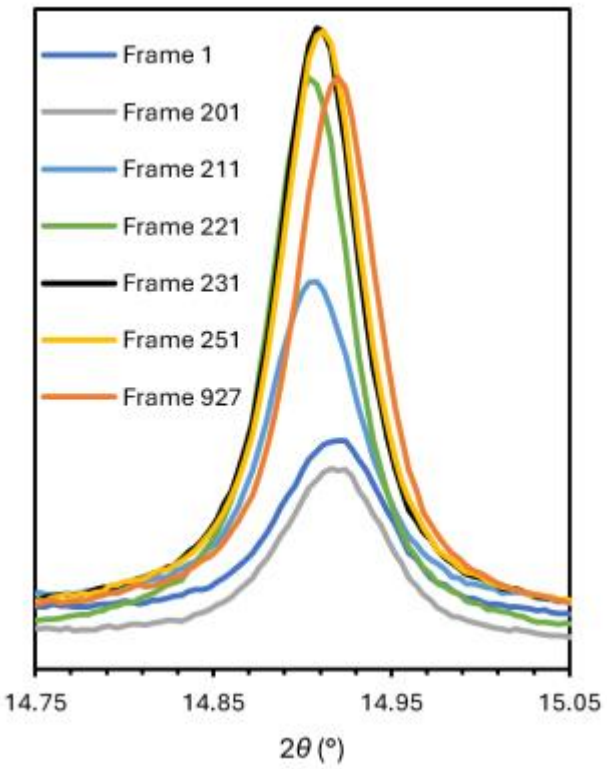

Back to Table of contents

MS40 Operando and in-situ crystallographic studies

MS40-04

Understanding the material formation of high entropy alloy nanoparticles: in-situ study using coupled X-ray diffraction/ absorption spectroscopy

R. Pittkowski [1], D. Stoian [2], M. Arenz [3], K. Jensen [1]
[1]University of Copenhagen - Copenhagen (Denmark), [2]ESRF - Grenoble (France), [3]Universität Bern - Bern (Switzerland)

Abstract

High entropy alloy (HEA) catalysis has recently emerged as a new research topic.[1] So far, HEAs have been mainly used in engineering applications. It is, however, expected that these multi-metallic compounds also provide exciting new possibilities for catalysis.[2] This has often been cited as a paradigm shift from “using the materials we have” to “engineering the materials we need”.[2] Recent theoretical analyses predict a great potential for HEAs as new catalysts due to the almost unlimited number of unique surface sites.[3] By changing the alloy composition, the catalytic properties can be optimized to enable a new, statistical approach in materials design. From an experimental viewpoint, however, HEAs come with new challenges regarding their synthesis and characterization. While HEA nanoparticles are essential for catalysis to provide sufficiently large surfaces, their synthesis is only in its infancy. My work focuses on the formation mechanism of noble metal HEA particles, which is compared with the formation of binary alloys of the same noble metals (Pt, Ir, Os, Ru, Rh). Characterizing multi-metallic HEA particles is a challenge that requires novel approaches in material characterization techniques. In-situ crystallographic studies using advanced synchrotron-based techniques can provide new insights into the HEA material formation pathways. Coupled in-situ powder X-ray diffraction/ X-ray absorption spectroscopy (XRD/XAS) [see Fig.1] is an analytical tool, which allows following both the crystallization processes as well as the changes in the oxidation state of the individual elements. In the in-situ XRD/XAS reaction set-up, the precursor powder is placed in a capillary and heated in a reductive atmosphere, while diffraction pattern and absorption spectra are recorded quasi-simultaneously [see Fig. 2]. With this, we can directly track the alloy formation pathway of both the binary alloys and HEA nanoparticles. By understanding the material formation pathway in detail, we can deduce the parameters that determine the phase formation behavior in the multi-metallic systems (single phase vs multiple phases). This gives new insights into alloy crystallization mechanisms and ultimately can provide guidelines for the design and synthesis of new multi-metallic alloy nanoparticles.

References

[1] George, E.P., Raabe, D., Ritchie, R.O. High-entropy alloys. Nat. Rev. Mater. 2019, 4 515–534.
[2] Löffler, T., Ludwig, A., Rossmeisl, J, Schuhmann, W. What Makes High-Entropy Alloys Exceptional Electrocatalysts? Angew. Chem. Int. Ed. 2021, 60, 2-12.
[3] Batchelor, T. A. A, Pedersen, J. K., Winther, S.H., Castelli, I.E., Jacobsen, K. W., Rossmeisl, J. High-Entropy Alloys as a Discovery Platform for Electrocatalysis, Joule 2019, 3, 834-845.

Schematic representation of the in-situ setup

Back to Table of contents

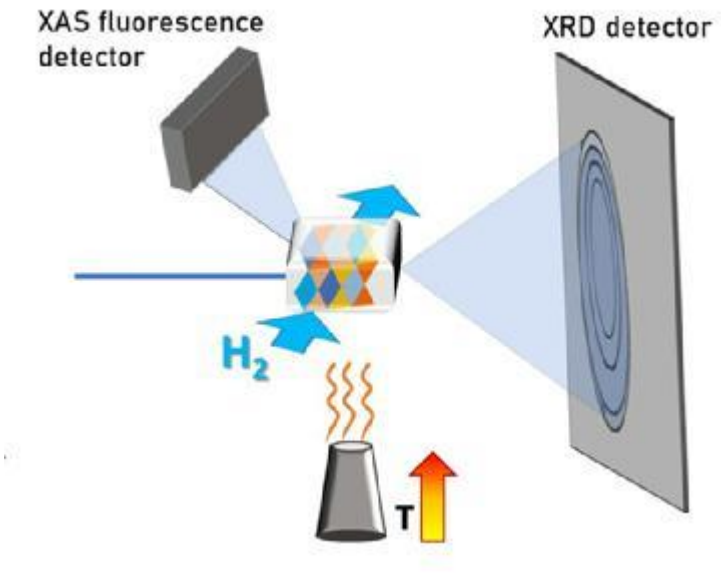

Following particle formation with XRD and XANES

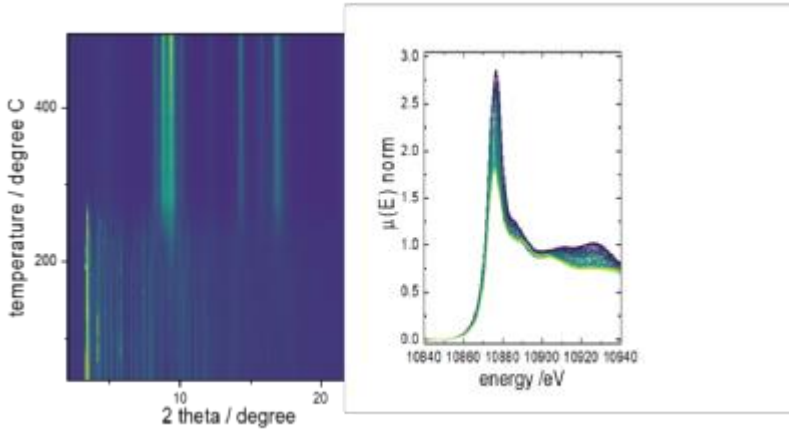

Back to Table of contents

MS40 Operando and in-situ crystallographic studies

MS40-05

Local order structural studies during electrochemical (de)intercalation by operando PDF analysis of the systems $LiMoO_2$ and $NaMoO_2$

M. Suchomel [1], M. Guignard [1]
[1]*Univ. Bordeaux, CNRS, Bordeaux INP, ICMCB, UMR 5026 - Pessac (France)*

Abstract

The electrochemical (de)intercalation of alkaline ions in a battery is a very powerful technique to determine the phase diagrams in MO_2-AMO_2 lamellar systems (where A is an alkaline ion and *M* is a 3d or 4d transition metal ion) by combining *in situ* X-ray scattering probes and electrochemistry. In MoO_2-AMoO_2 (A = Li or Na) systems, many phase transitions occur during the deintercalation of alkali ions. It was proposed that these phase transitions arise in part from the rearrangement of molybdenum sites within the MoO_2 sheets formed from MoO_6 octahedra. [1,2]

In order to validate this hypothesis, operando Pair Distribution Function (PDF) analysis experiments have been performed during electrochemical cycling using $A_{2/3}$MoO2 phases as positive electrode materials in batteries. These experiments were performed on the XPDF beamline (I15-1) of the Diamond synchrotron. As PDF analysis from X-ray scattering data are particularly sensitive to heavier elements, it proved possible to follow the evolution of Mo-Mo bond lengths during the intercalation and deintercalation of alkaline ions in both the Li_xMoO_2 and Na_xMoO_2 systems.

As an example, Figure 1 illustrates the evolution of operando battery PDF G(*r*) curves obtained during intercalation and deintercalation of sodium ions in Nax*M*oO_2. The analysis of G(r) for interatomic distances between 2.4 Å and 3.3 Å, largely dominated by Mo-Mo distances, clearly shows that these distances evolve continuously during cycling. This indicates that the molybdenum atoms shift slightly from the center of their MoO_6 octahedron to form molybdenum "clusters". We have identified several types of "clusters" according to the alkaline content, *i.e.* according to the average degree of oxidation of the molybdenum ions. Figure 2 illustrates the "zig-zag" chain clusters of molybdenum forming in $Na_{0.5}MoO_2$ (Figure 2a) and "diamond" type clusters stabilizing the structure of the compound $NaMoO_2$ (Figure 2b).

In this work, the complex structural phase diagrams of these materials will be reviewed, and using these new results, it will be shown how operando PDF measurements under electrochemical cycling can provide new insight into the role of short Mo-Mo bond formation during (de)intercalation in the Li_xMoO_2 and Na_xMoO_2 systems.

References

[1] L. Vitoux, M. Guignard, M. R. Suchomel, J. C. Pramudita, N. Sharma, C. Delmas "The Na_xMoO_2 Phase Diagram ($1/2 \leq x < 1$) : An Electrochemical Devil's Staircase" *Chemistry of Materials* **2017**, 29, 7243-7254.

[2] L. Vitoux, M. Guignard, J. Darriet, C. Delmas "Exploration of the Na_xMoO_2 phase diagram for low sodium contents ($x \leq 0.5$)" *Journal of Materials Chemistry A* **2018**, 6, 14651-14662.

Figure 1:

Back to Table of contents

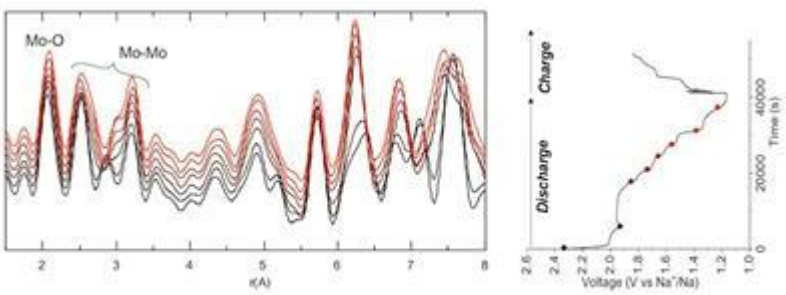

Figure 1: Operando Pair Distribution Function G(r) curves (left) for the system Na_xMoO_2 measured during the electrochemical intercalation and deintercalation of Na^+ (right).

Figure 2:

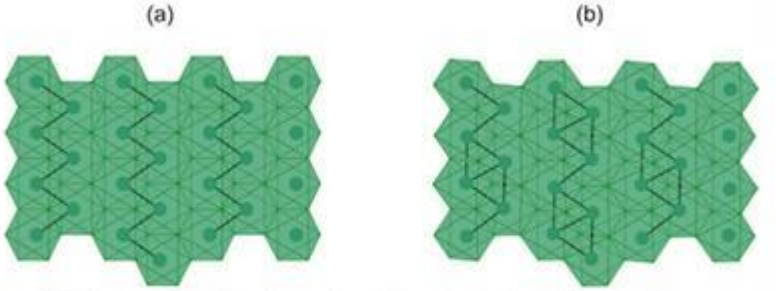

Figure 2: Projection of $(MoO_2)_n$ sheets formed by edge-sharing MoO_6. Only Mo atoms are shown to highlight clustering. Black lines represent short (< 2.8 Å) Mo-Mo bonds in (a) "zig-zag" type clusters for $Na_{0.9}MoO_2$ and (b) "diamond" type clusters for b) $NaMoO_2$

Back to Table of contents

MS41 Automation in data collection and processing

MS41-01

Supporting High Quality Experiments through Beter use of Sample Optical Images

M. Savko [1]
[1]*Synchrotron SOLEIL - Saint-Aubin (France)*

Abstract

This work is about sample optical images and how they can aid in better experiment design. Specifically we ask the following: Can we build an artificial system that recognizes, localizes and segments out a sample? Can it further tell apart pin from stem, stem from loop and crystal from either of them? Can it do it at arbitrary scale, orientation and varying lighting conditions? Can all of that be done in real time?
The main thesis of the present work is that answer to all of the questions above is yes.
If that is indeed true the following becomes possible: Upon sample mount we can instantly zoom in on sample areas that are most likely to contain interesting objects and dedicate costlier evaluation methods e.g. x-ray based raster to relatively small areas. By performing sample optical segmentation at multiple orientations we can gain information sufficient for reconstruction of a 3d model of the sample which can be then used as a natural reference for any automatically or manually defined point, line, area or a higher dimensional object. The great advantage of this natural reference is its invariance with respect to arbitrary reorientation particularly in a multiaxis goniometer setting. We believe this last point is of great importance in supporting wider use of experiment design benefiting from sample probing at multiple orientation by solving a problem of achieving submicron precision when reorienting samples with goniometers of much lesser expected precision, alleviating necessity of costly and unreliable manual re-alignments.
The main contributions of the present work are the following: I. Pixel annotated dataset of ~1200 high resolution sample images II. An artificial network network [1] based program capable to segment out a sample image in real time (including discussion of finer points of how it was trained) III. A program for rapid 3d sample shape reconstruction and registration at arbitrary orientation.
A practical demonstration of how a system based on those contribution can serve in day to day operation on an MX beamline concludes the talk.

References

[1] S. Jégou, M. Drozdzal and D. Vazquez, A. Romero and Y. Bengio, The One Hundred Layers Tiramisu: Fully Convolutional DenseNets for Semantic Segmentation, https://doi.org/10.48550/arxiv.1611.09326

Back to Table of contents

MS41 Automation in data collection and processing

MS41-02

Real-time pre-processing of serial crystallography

J. Kieffer [1], N. Coquelle [1], G. Santoni [1], S. Basu [2], S. Debionne [1], A. Homs [1], D. De Sanctis [1]
[1]ESRF - Grenoble (France), [2]EMBL - Grenoble (France)

Abstract

This contribution presents recent advances on real-time analysis of diffraction images acquired at high frame-rate (1 kHz) and their application to macro-molecular serial crystallography. A new signal separation algorithm is presented, able to distinguish amorphous (or powder diffraction) component from the signal originating from larger (single) crystals. The main improvement comes from the calculation of azimuthal uncertainties and relies on the ability to work efficiently in azimuthal space. This work is built on top of pyFAI, the fast azimuthal integration library and take benefits of running on graphical processors.
Two applications, built upon this separation algorithm are presented:
1. A lossy compression algorithm whose performances are evaluated on rotational and serial crystallography data. Performances are compared with uncompressed data using the XDS tool for the rotational part and CrystFEL for serial data.
2. A peak-picking algorithm which is able to assess the diffraction quality of crystals in real-time, with fast user feed-back using the NanoPeakCell application. The quality of picked peaks is evaluated through the indexing rate in CrystFEL.
This algorithm will be the core of data processing of the new serial crystallography beam-line at ESRF-ID29.

References

Debionne, S., Homs, A., Claustre, L., Kieffer, J., De Sanctis, D., Santoni, G., Goetz, A. & Meyer, J. (2022). In Proceedings of the 14 th international conference on Synchrotron Radiation Instrumentation (SRI2021). https://indico.desy.de/event/27430/abstracts/

Background analysis of MX diffraction frame

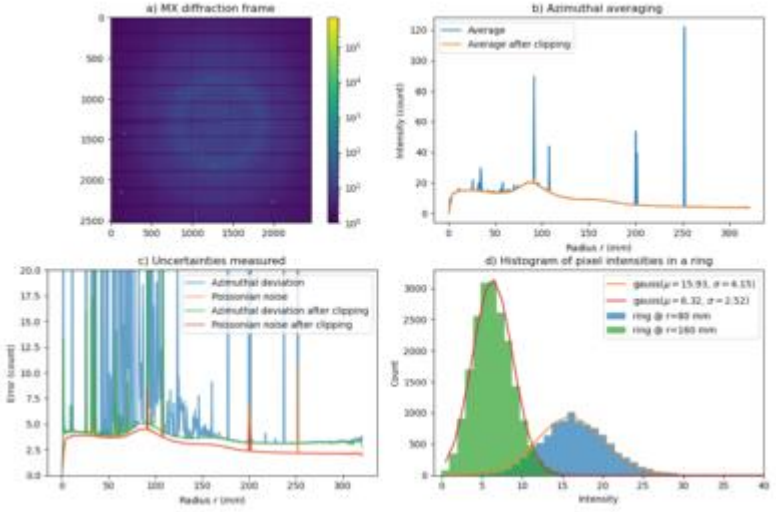

Back to Table of contents

MS41 Automation in data collection and processing

MS41-03

Interactive and unattended data collection driven by target dose at the Diamond Light Source I04 beamline

D. Aragao [1], R. Flaig [1], P. Romano [1], M. Mazzonana [1]
[1]Diamond Light Source - Didcot (United Kingdom)

Abstract

Diamond Light Source currently operates seven beamlines for macromolecular crystallography [1]. I04 [2,3] is an energy (6-18 keV) and beam size (5-100 microns) tuneable microfocus beamline suitable for projects ranging from large scale high throughput ligand screening to difficult single or multiple anomalous dispersion experiments. These large spectrum capabilities are built on top state of the art hardware equipment and software developments. The hardware highlights are a multi-axis goniometer for crystal alignment and X-ray centring, a large and very fast frame rate pixel array detector for diffraction data collection and the use of compound refractive index lenses for focusing. The software stack includes the diamond wide data acquisition and GUI software GDA [4-5] as well as the SyncWeb interface [6] for ISPYB [7]. Collecting at its full potential I04 can load a sample, centre it automatically using X-ray diffraction at two different orientations and collect a 7.2 second rotation dataset of 360 degrees in less than 2 minutes providing on average over 32 samples throughput per hour. I04 is also part of the recent Diamond MX beamline developments on the use of Unattended Data Collection (UDC) [8] where the only interaction of the users with the beamline is done prior to the beamtime on defining how do they want to collect their data based on a series of pre-set recipes (unpublished). In addition to UDC, I04 provides onsite and remote access capabilities and has special tools like built-in Raddose3D [9] calculator to help design experiments for optimal data. Here we present a brief overview of the beamline automation in data collection including the recent enhancements on using dose to increase efficiency on both the unattended data collection as well as driving queues of experiments dialling dose instead of an exposure (Figure 1, Figure 2). The latter enhancement was critical to open the automation avenue for the available beamline energy range and beam sizes without compromising on radiation damage as well as not under exposing a well diffracting crystal.

References

[1] https://www.diamond.ac.uk/Instruments/Mx.html
[2] R. Flaig et all, Acta Cryst. (2017). A73, a71
[3] https://www.diamond.ac.uk/Instruments/Mx/I04.html
[4] http://www.opengda.org/
[5] https://alfred.diamond.ac.uk/documentation/
[6] https://diamondlightsource.github.io/SynchWeb/
[7] S. Delagenière et all. Bioinformatics, (2011) 27. 22:3186–3192
[8] https://www.diamond.ac.uk/Instruments/Mx/I03/I03-Manual/Unattended-Data-Collections.html
[9] CS Bury et all. Protein Sci. (2018). 27:217–228.

1)Using dose as the target to drive the experiment

Back to Table of contents

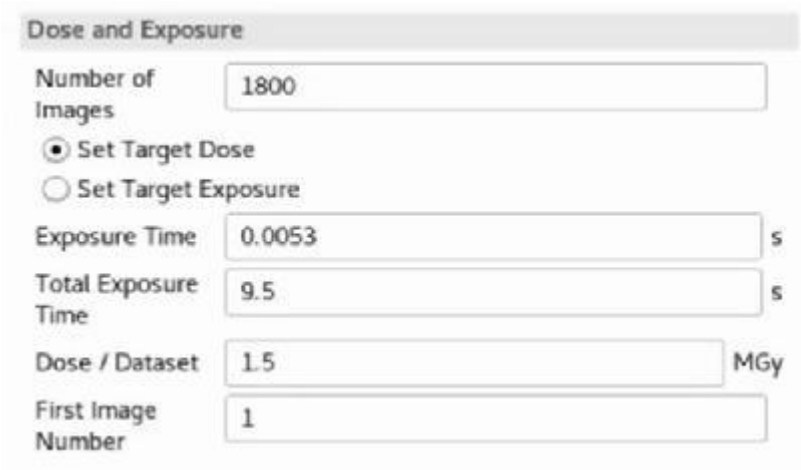

2)Data collection queues driven by dose

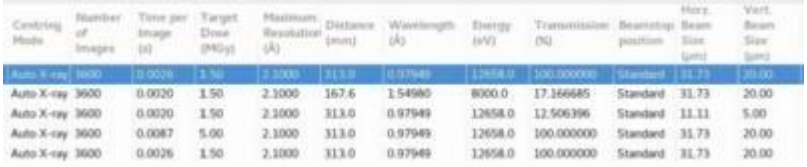

Centring Mode	Number of Images	Time per Image (s)	Target Dose (MGy)	Maximum Resolution (Å)	Distance (mm)	Wavelength (Å)	Energy (eV)	Transmission (%)	Beamstop position	Horz. Beam Size (µm)	Vert. Beam Size (µm)
Auto X-ray	3600	0.0026	1.50	2.1000	313.0	0.97949	12658.0	100.000000	Standard	31.73	20.00
Auto X-ray	3600	0.0020	1.50	2.1000	167.6	1.54980	8000.0	17.166685	Standard	31.73	20.00
Auto X-ray	3600	0.0020	1.50	2.1000	313.0	0.97949	12658.0	12.506396	Standard	11.11	5.00
Auto X-ray	3600	0.0087	5.00	2.1000	313.0	0.97949	12658.0	100.000000	Standard	31.73	20.00
Auto X-ray	3600	0.0026	1.50	2.1000	313.0	0.97949	12658.0	100.000000	Standard	31.73	20.00

Back to Table of contents

MS41 Automation in data collection and processing

MS41-04

Data reduction in protein crystallography

M. Galchenkova [1], A. Tolstikova [2], O. Yefanov [1], H. Chapman [1]
[1]DESY, CFEL - Hamburg (Germany), [2]DESY - Hamburg (Germany)

Abstract

Area X-ray detectors became bigger (having more megapixels) and faster (measuring more frames per second). This allows to measure dynamical processes in protein crystals with high resolution and below 1ms time scale. The price to pay is the amount of data that such detectors generate. Unfortunately, storage volume is growing much slower. Therefore, there is an increasing gap between the data generation volume and the possibility to store it.

One of the most disk consuming type of experiments is macromolecular crystallography (MX) and especially serial crystallography (SX). Such experiments often require many Mpix detectors and usually can be done with very high speed – modern facilities produce enough photons to measure at 1kHz rate. Unfortunately, the lossless compression rate of such diffraction patterns is rather poor due to the high background. In standard MX experiments at synchrotrons, due to the well-established processing pipeline, only the averaged intensities of the Bragg peaks are kept. Unfortunately for FELs and synchrotron SX experiments such luxury is not possible yet – reprocessing of raw data can improve the result a lot. Recently we have shown that reprocessing of the data measured 10 years ago at LCLS led to resolution improvement from 3.5A to 2.5A.

We have tested different approaches for SX data reduction: compressing with different lossless algorithms, binning the data, saving only hits, quantization, etc. Data from different experiments at synchrotrons and FELs with various detectors and different samples were used. Checking the resulting statistics of compressed data (like CC*/Rsplit, Rfree/Rwork, anomalous signal) we have demonstrated that the volume of the measured data can be greatly reduced (10-100 times!) while the quality of the resulting data was kept almost constant. Some compression strategies, tested on SX and MX datasets, can be applicable to other type of experiments.

Back to Table of contents

MS41 Automation in data collection and processing

MS41-05

MASSIF-1, the macromolecular beamline dedicated to automation

D. Nurizzo [1], M. Bowler [2]
[1]ESRF - GRENOBLE (France), [2]EMBL - GRENOBLE (France)

Abstract

From the beginning back in 2014, Massif-1 [1] at ESRF has been designed to be fully automated from crystal mounting up to data collection and processing [2]. To profit from the Extremely Brilliant Source project and the drastic increase of performance of the storage ring, the beamline entered in a depth refurbishment and upgrade of the entire experimental hutch in august 2020. It is now equipped with a micro-diffractometer with kappa option (MD2S) and fitted with an ESRF-FlexHCD sample changer taking up to 368 samples in Unipuck (Figure 1). The CrystalDirect harvester for automatic harvesting of crystals is also installed since May 2021.

With the experience gleaned from more than 70,000 crystals collected since the kick-off [3], we manage to specify experimental roadmaps conforming to the user requirements. Our aim is to design the best data collection protocol allowing the best quality of the final data set and helping the scientist in solving their biological questions in an automated manner. The workflows in charge of the setting up the experiment, is also the decision maker and according to the previous results will follow the best data collection strategy taking advantage of the beamline setup. As examples: we strengthen the quality of the services by adapting the beam diameter to match the best diffracting volume with the help of DOZOR software; we collect two different kappa orientation with low symmetry space groups; we constantly check the state of the beam and the hardware and report any misbehaviour and correct suitably and more will be revealed during the presentation. The automation has been further pushed in data processing and data solving. The data sets collected on the beamline are screened for anomalous signal and/or molecular replacement and small molecule fitting.

References

[1] Journal of synchrotron Radiation. Volume 22 Part 6 November 2015, 1540-1547. [2] Acta Cryst. (2015). D71, 1757-1767. [3] IUCR Journal. Volume 6 Part 5 September 2019, 822-831

MASSIF-1 Experimental Hutch

Back to Table of contents

MS42 Solving Structures Through Combination of Reciprocal and Direct Space Methods

MS42-01
Correlated disorder in thermoelectric materials
B. Brummerstedt Iversen [1]
[1]*Aarhus University - Aarhus (Denmark)*

Abstract
X-ray diffraction from powders and single crystals has for decades been the key analytical tool in materials science. Bragg intensities provide information about the average crystal structure, but often it is disorder and specific local structure that control key material properties. This is especially the case for thermoelectric materials where disorder for example strongly affects the thermal conductivity. For 1D data there has been an immense growth in combined analysis of Bragg and diffuse scattering using the Pair Distribution Function (PDF), and for example we frequently use 1D PDF analysis to study nanocrystal nucleation [1]. For single crystals, diffuse scattering studies have a long history with elaborate analysis in reciprocal space, whereas direct space analysis of the 3D-PDF is still in its infancy. We have used 3D-PDF analysis to study the crystal structures of high-performance thermoelectric materials Cu2Se [2], PbTe and PbS [3, 4], 19-e half-heusler Nb1-xCoSb [5, 6] and InTe [7], where the true local structure is essential for understanding the unique properties.

References
[1] E. D. Bøjesen, B. B. Iversen, The chemistry of nucleation, CrystEngComm 18, 8332 – 8353 (2016)
[2] N. Roth et al., Solving the disordered structure of β-Cu2-xSe using the three-dimensional difference pair distribution function, Acta Crystallogr. Sect. A, 75, 465–473 (2019)
[3] K. A. U. Holm et al., Temperature Dependence of Dynamic Dipole Formation in PbTe, Phys. Rev. B 102, 024112 (2020)
[4] K. A. U. Holm et al., Anharmonicity and correlated dynamics of PbTe and PbS studied by single crystal X-ray scattering, Phys. Rev. B 103, 224302 (2021)
[5] N. Roth et al., A simple model for vacancy order and disorder in defective half-Heusler systems, IUCrJ 7, 673-680 (2020)
[6] N. Roth et al., Tuneable local order in thermoelectric crystals, IUCR-J. 8, 695-702 (2021)
[7] J. Zhang et al, Direct observation of one-dimensional disordered diffusion channel in a chain-like thermoelectric with ultralow thermal conductivity, Nat. Commun. 12, 6709 (2021)

Back to Table of contents

MS42 Solving Structures Through Combination of Reciprocal and Direct Space Methods

MS42-02

Automated and meta-structure solution from powder diffraction in python using pyobjcryst

V. Favre-Nicolin [1]
[1]*ESRF-The European Synchrotron - Grenoble (France)*

Abstract

Twenty years ago the Fox software [1,2] was written to solve crystal structures from powder diffraction using global optimisation methods. The application was since improved to include all steps used in structure solution, including indexing and profile fitting. Despite the availability of powerful algorithms, solving structures can remain a tedious tasks with the lack of *a priori* knowledge, because the actual building blocks as well as the spacegroup (and thus the multiplicity and the number of independent atoms) are often ambiguous: solving a structure may require to test a large number of possible parametrisations, useually by hand.

A few years ago the objcryst library behind Fox was interfaced in python as part of the diffpy [3] suite in the pyobjcryst library, and more recently all the library components which can be used to solve structures (indexing, profile fitting, Monte Carlo, parallel tempering algorithms...) have been added to pyobjcryst. This allows to use most of the functionality of Fox inside a python notebook and a web browser, as shown in Figure 1.

We will also show that beyond the ability to solve structure solutions using a python script or notebook, it is possible to automatically loop through possible crystal configurations like building blocks (molecules, polyedra) and spacegroups, including parallelising the search using python's multiprocessing module, as is shown in the example notebooks available from pyobjcryst's online documentation [4].

References

[1] V. Favre-Nicolin and R. Cerný, J. Appl. Cryst. (2002). 35, 734-743
[2] V. Favre-Nicolin and R. Cerný, Z. Kristallogr. 219 (2004) 847–856
[3] P. Juhas, C. L. Farrow, X. Yang, K. R. Knox, and S. J. L. Billinge, Acta Crystallogr. A 71, 562 (2015)
[4] https://pyobjcryst.readthedocs.io/

3D crystal structure from COD in a python notebo

```
[3]: c1 = create_crystal_from_cif("http://crystallography.net/cod/4506702.cif",
                                 oneScatteringPowerPerElement=True,
                                 connectAtoms=True)

     print(c1.GetFormula())
     c1.widget_3d()

     C29 H32 N4 O5
```

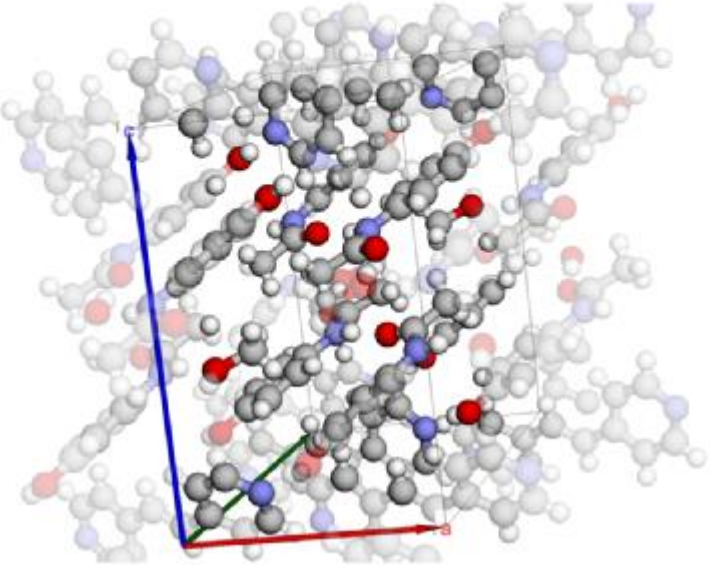

Back to Table of contents

MS42 Solving Structures Through Combination of Reciprocal and Direct Space Methods

MS42-03

The crystal chemistry of binary beryllium dipnictides – new binary structure types between Zintl polyanions and Grimm Sommerfeld compounds

A. Feige [1], L. Bradaczek [1], M. Michak [1], D. Günther [1], M. Grauer [1], B. Mondal [2], C. Giacobbe [3], E. Lawrence Bright [3], C. Benndorf [1], R. Tonner-Zech [2], O. Oeckler [1]

[1]Institute for Mineralogy, Crystallography and Materials Science - Leipzig (Germany), [2]Wilhelm-Ostwald-Institute for Physical and Theoretical Chemistry - Leipzig (Germany), [3]European Synchrotron Radiation Facility - Grenoble (France)

Abstract

Compounds with an average valence electron concentration of four often form coloring variants of diamond-like frameworks according to the Grimm Sommerfeld concept. Although the crystal structure of sphalerite was determined already in the 1920s,[1] there are still binary main group compounds with diamond-like frameworks lacking investigation. This is the case for binary beryllium pnictides Be*Pn*$_2$ – not only because of the high toxicity of beryllium, but mainly because of complications concerning structure analyses. We have now elucidated the structures of BeP_2, $BeAs_2$ and $BeSb_2$ by combining single-crystal diffraction using microfocused synchrotron radiation with HRTEM imaging as well as electron crystallography for very precise data sets of crystallites on the sub-micron scale.[2] Phase-pure samples [3,4] were obtained by solid-state reactions or in salt flux, but the syntheses result in microcrystalline powders that do not allow data collection on laboratory diffractometers.

$BeSb_2$ features a diamond-like framework consisting of spiral-like antimony chains with ten atoms per translation period, which are interconnected by beryllium atoms. The antimony substructure represents a new homonuclear Zintl ion. *Ab initio* DFT calculations for this new structure type reveal semiconducting properties and confirm the considerations based on the Zintl and Grimm Sommerfeld concept, respectively: Valence electron density is almost fully located on the antimony substructure to form the corresponding chains and diamond-like framework. Bader charges nearly correspond to the expected formal oxidation states, while *Electron Localized Function* suggests the presence of homonuclear Sb–Sb bonds within the polyanions.

$BeAs_2$ and isotypic BeP_2 exhibit stacking disorder in a typical *OD* structure. This results from different possibilities of stacking layers built up from arsenic eight-rings and beryllium atoms. The cyclic Zintl polyanions were first revealed by electron crystallography. A disorder model was derived from the diamond-like average structure taking into account twinning as well as diffuse streaks in diffraction patterns. A second polymorph of $BeAs_2$ that adopts the $BeSb_2$ structure type could also be characterized.

References

[1] W. M. Lehmann, *Z. Kristallogr.* **1924**, *60*, 379.
[2] F. Fahrnbauer, T. Rosenthal, T. Schmutzler, G. Wagner, G. B. Vaughan, J. P. Wright, O. Oeckler, *Angew. Chem. Int. Ed.* **2015**, *54*, 10020.
[3] R. Gerardin, J. Aubry, *J. Solid State Chem.* **1976**, *17*, 239.
[4] J. F. Brice, R. Gérardin, M. Zanne, *Mater. Res. Bull.* **1975**, *10*, 1237.

Back to Table of contents

Chain-like structure of beryllium antimonide.

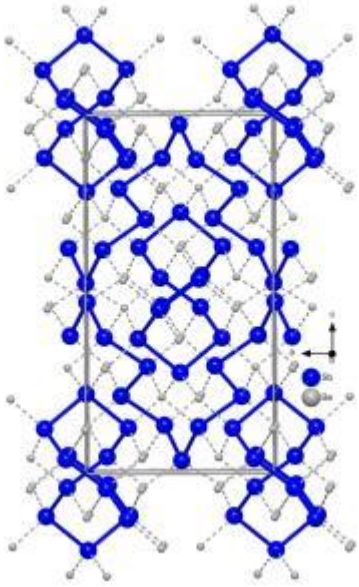

Ring-like structure of beryllium arsenide.

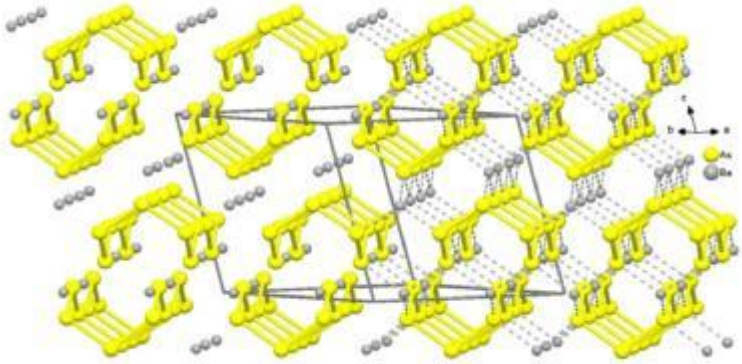

Back to Table of contents

MS42 Solving Structures Through Combination of Reciprocal and Direct Space Methods

MS42-04

Structure of the active ingredient of Pepto-Bismol by 3D ED and STEM imaging

E. Svensson Grape [1], V. Rooth [1], M. Nero [1], T. Willhammar [1], A.K. Inge [1]
[1]Stockholm University - Stockholm (Sweden)

Abstract

Bismuth subsalicylate (BSS) is textbook[1] example of a metallodrug and has been used to treat upset stomachs for 120 years. It is the active ingredient of Pepto-Bismol, an over-the-counter medication and household brand name across North America and other countries. Tens of billions of doses have been consumed, and it remains as the most sold stomach remedy in countries such as the US. BSS is administered as a crystalline substance. Despite its history and current significance, the crystal structure has remained unknown due to small crystallite size, complexity of the structure, and disorder. At last, we reveal the crystal structure of BSS by 3D electron diffraction (3D ED), and disorder by scanning transmission electron microscopy (STEM).[2]

In order to solve the structure, 3D ED data were collected on 18 crystals of BSS which had a particularly high degree of order. Due to the low symmetry of the triclinic crystals individual datasets had low completeness. Select datasets were merged using hierarchical clustering analysis. All non-hydrogen atoms were then located in the crystal structure using the merged dataset.

The crystal structure of BSS is made of Bi_{3+} cations and bridging O^{2-} anions surrounded by organic salicylate anions ($Hsal^-$) in a 2D layered structure. All carboxylate groups coordinate to Bi_{3+} cations, while only half of the $Hsal^-$ anions also coordinate through the phenol group. The layered structure has been compared to that of a sugar wafer[3a] or an ice cream sandwich[3b], where the Bi^{3+} and O^{2-} ions form the inner filling and the $Hsal^-$ anions form the outer wafer or biscuit.

BSS crystals isolated from Pepto-Bismol appeared to have disorder. STEM imaging with integrated differential phase contrast (iDPC) was applied to visualize the disorder. In the ordered part of the crystal the stacked layers have the same orientation. However in the disordered parts neighbouring layers had opposite orientations. In some parts the layer orientation alternated periodically while in other parts the orientation appeared random.

Structure determination provides insight into some of the properties of BSS such as its poor solubility in water, which also may influence bioavailability. The disorder in the stacking of the layers indicates that crystals of BSS from different sources are somewhat different, which may be of interest for tuning the structure and properties of this compound.

References

[1] Inorganic Chemistry 7th ed., Oxford University Press 2018, Editted by Mark Weller, Tina Overton, Jonathan Rourke, and Fraser Armstrong.
[2] Svensson Grape, E., Rooth, V., Nero, M. et al. *Nature Commun.* **13**, 1984 (2022).
[3] a) *Nature* 604, **601** (2022), b) Kira Welter, *Chemistry World*, (April 25, 2022).

Fig. 1 Structure of BSS determined by 3D ED

Back to Table of contents

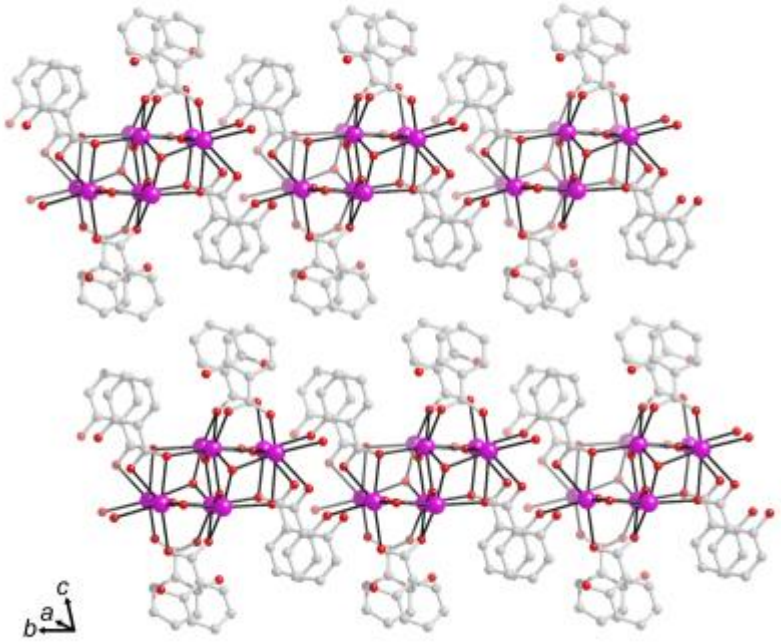

Fig. 2 iDPC STEM image of BSS with disorder

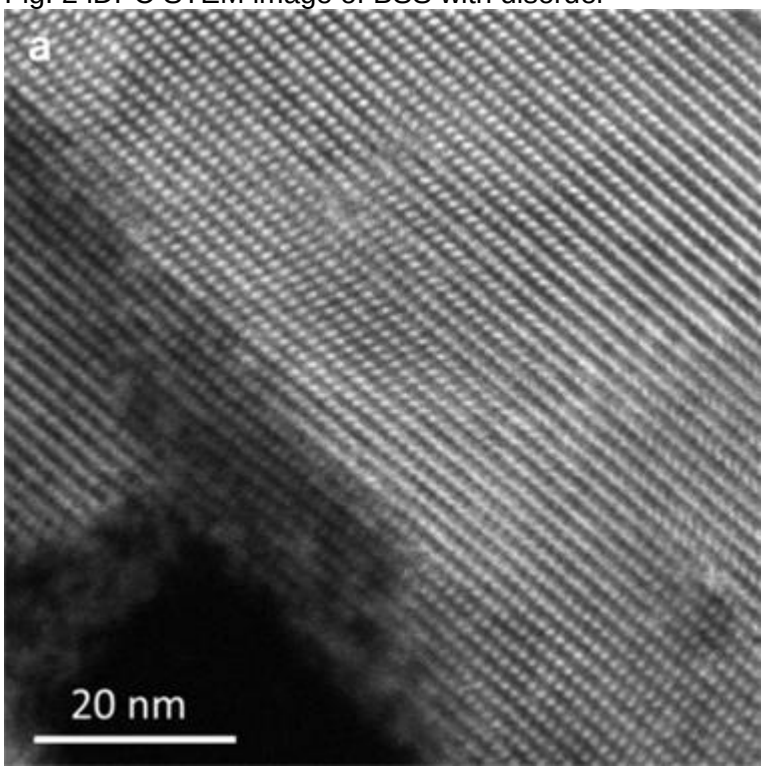

Back to Table of contents

MS42 Solving Structures Through Combination of Reciprocal and Direct Space Methods

MS42-05

Multi-methodological approach to solve SBDS protein involved in the molecular mechanism of Shwachman Diamond Syndrome

D. Siliqi [1], G.F. Mangiatordi [1], N. Sánchez-Puig [2], A. Gijsbers [3], M. Saviano [4], G. Lattanzi [5], E. Spinetti [6]

[1]Istituto di Cristallografia -CNR - Bari (Italy), [2]Departamento de Química de Biomacromoléculas, Instituto de Química, Universidad Nacional Autónoma de México - Mexico City (Mexico), [3]Maastricht MultiModal Molecular Imaging Institute (M4I), Maastricht University - Maastricht (Netherlands), [4]Istituto di Cristallografia -CNR - Caserta (Italy), [5]Università di Trento - Trento (Italy) - Trento (Italy), [6]Frankfurt Institute for Advances Studies - Frankfurt (Germany)

Abstract

The Shwachman-Diamond Syndrome (SDS, OMIM #260400 and #617941) is an autosomal recessive disease that affects many parts of the body, including bone marrow, pancreas, bones, immune and central nervous systems [1], with an increased risk of progression to myelodysplastic syndrome [2]. In most cases (90%), SDS is associated with mutations in the Shwachman-Bodian-Diamond Syndrome gene (SBDS, OMIM gene #607444), located in chromosome 7q11 and encoding for a protein, named SBDS, structurally organized into three highly conserved domains [2–4]. SBDS is required for the assembly of mature ribosomes and ribosome genesis. Together with the Elongation Factor Like-1 EFL1 (OMIM gene #617538) [5], SBDS triggers the GTP-dependent release of eIF6 (eukaryotic initiation factor 6) from 60S pre-ribosomes in the cytoplasm [2,6,7], thereby activating the ribosomes for translation competence by allowing 80S ribosome assembly and by facilitating eIF6 recycling to the nucleus, where it is required for 60S rRNA processing and nuclear export. In this mechanism, SBDS acts as the nucleotide exchange factor (GEF) for EFL1[8,9], increasing its affinity for GTP over GDP [6]. In this presentation, we aimed to show the *Archaeoglobus fulgidus* SBDS (AfSBDS) protein structure solved by the crystallographic method (data collected at the Diamond Light Source beamline I24) [10], as well as the conformations of the protein (both archaeal and yeast orthologues) in the solution obtained small-angle X-ray scattering (SAXS) technique (data collected at the Diamond Light Source beamline B21) [10, 11]. Furthermore, starting from the observation that SBDS single-point mutations, localized in different domains of the proteins, are responsible for an SDS phenotype, we carried out the first comparative Molecular Dynamics simulations on three SBDS mutants [manuscript in preparation].

References

1. Dror, Y.; Donadieu, J.; Koglmeier, J.; Dodge, J.; Toiviainen-Salo, S.; Makitie, O.; Kerr, E.; Zeidler, C.; Shimamura, A.; Shah, N.; et al. Draft Consensus Guidelines for Diagnosis and Treatment of Shwachman-Diamond Syndrome. Ann. N. Y. Acad. Sci. 2011, 1242, 40–55, doi:10.1111/j.1749-6632.2011.06349.x.
2. Finch, A.J.; Hilcenko, C.; Basse, N.; Drynan, L.F.; Goyenechea, B.; Menne, T.F.; Gonzalez Fernandez, A.; Simpson, P.; D'Santos, C.S.; Arends, M.J.; et al. Uncoupling of GTP Hydrolysis from EIF6 Release on the Ribosome Causes Shwachman-Diamond Syndrome. Genes & Development 2011, 25, 917–929, doi:10.1101/gad.623011.
3. Ng, C.L.; Waterman, D.G.; Koonin, E.V.; Walters, A.D.; Chong, J.P.; Isupov, M.N.; Lebedev, A.A.; Bunka, D.H.; Stockley, P.G.; Ortiz-Lombardía, M.; et al. Conformational Flexibility and Molecular Interactions of an Archaeal Homologue of the Shwachman-Bodian-Diamond Syndrome Protein. BMC Structural Biology 2009, 9, 32, doi:10.1186/1472-6807-9-32.
4. Savchenko, A.; Krogan, N.; Cort, J.R.; Evdokimova, E.; Lew, J.M.; Yee, A.A.; Sánchez-Pulido, L.; Andrade, M.A.; Bochkarev, A.; Watson, J.D.; et al. The Shwachman-Bodian-Diamond Syndrome Protein Family Is Involved in RNA Metabolism. Journal of Biological Chemistry 2005, 280, 19213–19220, doi:10.1074/jbc.M414421200.
5. Stepensky, P.; Chacón-Flores, M.; Kim, K.H.; Abuzaitoun, O.; Bautista-Santos, A.; Simanovsky, N.; Siliqi, D.; Altamura, D.; Méndez-Godoy, A.; Gijsbers, A.; et al. Mutations in EFL1 , an SBDS Partner, Are Associated with

Back to Table of contents

Infantile Pancytopenia, Exocrine Pancreatic Insufficiency and Skeletal Anomalies in AShwachman-Diamond like Syndrome. Journal of Medical Genetics 2017, 54, 558–566, doi:10.1136/jmedgenet-2016-104366.
6. Menne, T.F.; Goyenechea, B.; Sánchez-Puig, N.; Wong, C.C.; Tonkin, L.M.; Ancliff, P.J.; Brost, R.L.; Costanzo, M.; Boone, C.; Warren, A.J. The Shwachman-Bodian-Diamond Syndrome Protein Mediates Translational Activation of Ribosomes in Yeast. Nat. Genet. 2007, 39, 486–495, doi:10.1038/ng1994.
7. Warren, A.J. Molecular Basis of the Human Ribosomopathy Shwachman-Diamond Syndrome. Adv Biol Regul 2018, 67, 109–127, doi:10.1016/j.jbior.2017.09.002.
8. Gijsbers, A.; García-Márquez, A.; Luviano, A.; Sánchez-Puig, N. Guanine Nucleotide Exchange in the Ribosomal GTPase EFL1 Is Modulated by the Protein Mutated in the Shwachman–Diamond Syndrome. Biochemical and Biophysical Research Communications 2013, 437, 349–354, doi:10.1016/j.bbrc.2013.06.077.
9. García-Márquez, A.; Gijsbers, A.; de la Mora, E.; Sánchez-Puig, N. Defective Guanine Nucleotide Exchange in the Elongation Factor-like 1 (EFL1) GTPase by Mutations in the Shwachman-Diamond Syndrome Protein. J. Biol. Chem. 2015, 290, 17669–17678, doi:10.1074/jbc.M114.626275.
10. Siliqi, D.; Foadi, J.; Mazzorana, M.; Altamura, D.; Méndez-Godoy, A.; Sánchez-Puig, N. Conformational Flexibility of Proteins Involved in Ribosome Biogenesis: Investigations via Small Angle X-Ray Scattering (SAXS). Crystals 2018, 8, 109, doi:10.3390/cryst8030109
11. Gijsbers, A.; Montagut, D.; Méndez-Godoy, A.; Altamura, D.; Saviano, M.; Siliqi, D.; Sánchez-Puig, N. Interaction of the GTPase Elongation Factor Like-1 with the Shwachman-Diamond Syndrome Protein and Its Missense Mutations. International Journal of Molecular Sciences 2018, 19, 4012, doi:10.3390/ijms19124012

Crystallographic model of SBDS and its crystal

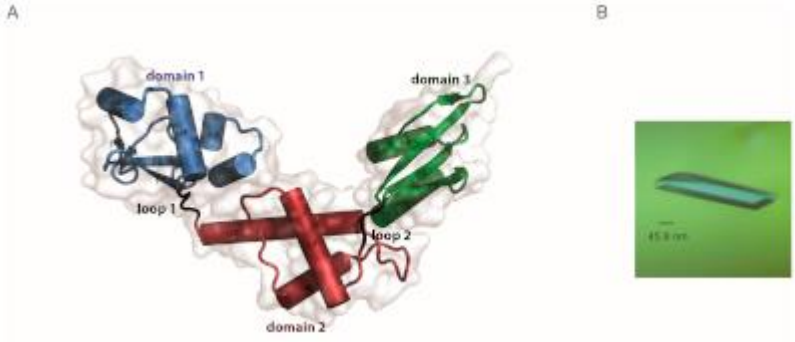

Ensemble of SBDS conformations obtained by SAXS

Back to Table of contents

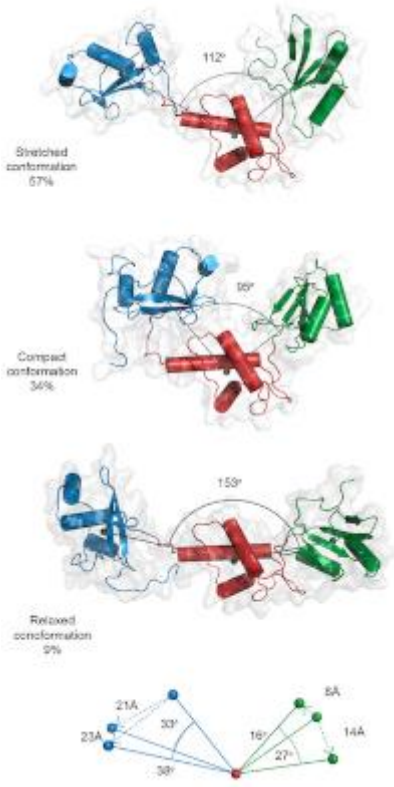

Back to Table of contents

MS43 Crystallography for cultural heritage materials

MS43-01

Characterisation of heterogenous phases in wood from the Mary Rose: Insight from computed tomography Pair Distribution Function analysis

K.M.Ø. Jensen [1], E. Rani Aluri [2], E. Sanchez Perez [2], G.B.M. Vaughan [3], M. Di Michiel [3], E.J. Schofield [4], S.J.L. Billinge [5], S.A. Cussen [2]

[1]University of Copenhagen - Copenhagen (Denmark), [2]University of Sheffield - Sheffield (United Kingdom), [3]ESRF - Grenoble (France), [4]The Mary Rose Trust - Portsmouth (United Kingdom), [5]Columbia University - New York (United States)

Abstract

Salvaged in 1982 after spending 437 years under the sea bed, the Mary Rose hull has provided unprecedented insight into Tudor society and technology.[1] However, preserving this artefact for future generations remains a challenge. For example, the presence of sulfur, in combination with iron from corroded fixtures, is capable of forming destructive acids under atmospheric conditions,[2-4] and development of effective conservation strategies requires detailed knowledge of the nature and distribution of these species in the wood. We have applied the recently developed computed tomography Pair Distribution Function analysis (ctPDF) to wood from the Mary Rose keelson.[5] As well as occasional large salt particles, we find nanoparticles with diameters of less than 5 nm distributed through the wood at depths greater than 5 mm from the surface, most likely deposited by anaerobic bacteria. Surprisingly, nanocrystal structural analysis reveals these to be predominantly $Zn_{1-x}Fe_xS$. Polyethylene glycol, a polymer that has been introduced to stabilize the wood, is shown to penetrate only into the surface-region to 5 mm depth. This use of ctPDF to map and characterize crystalline but also amorphous and nanostructured phases in the wood results in crucial insights on the nature of compounds responsible for wood degradation, allowing the development of targeted conservation treatments.

References

1: Marsden, P., Sealed by time: The Loss and Recovery of the Mary Rose. The Mary Rose Trust, Portsmouth, U.K, 2003; Vol. 1.
2: Wetherall, K. M.; Moss, R. M.; Jones, A. M.; Smith, A. D.; Skinner, T.; Pickup, D. M.; Goatham, S. W.; Chadwick, A. V.; Newport, R. J. Journal of Archaeological Science 2008, 35, (5), 1317-1328.
3: Sandstrom, M.; Jalilehvand, F.; Damian, E.; Fors, Y.; Gelius, U.; Jones, M.; Salome, M. Proceedings of the National Academy of Sciences of the United States of America 2005, 102, (40), 14165-14170.
4: Schofield, E. J., Nat. Rev. Mater. 3, 285-287 (2018)
5: Jensen, K. M. Ø.; Eluri, E. R.; Perez, E. S., Vaguhan, G. M. B.; Di Michiel, M.; Schofield, E. J.; Billinge, S.J.L.; Cussen, S. A. Matter, 5, 1, 150-161

Back to Table of contents

MS43 Crystallography for cultural heritage materials

MS43-02

Coordinated Development of Tubes and Optics for Microfocus Sources: New possibilities for X-ray Analytics of Cultural Heritage Materials

J. Wiesmann [1], J. Graf [1], P. Radcliffe [1]
[1]incoatec GmbH - Geesthacht (Germany)

Abstract

In recent years, interest in the non-destructive examination of cultural objects has increased considerably. In addition to infrared and optical imaging and spectroscopy techniques, X-ray methods such as X-ray fluorescence, X-ray diffraction, X-ray radiography and X-ray imaging are often used to analyse objects such as paintings and books. In particular, the development of air-cooled microfocus sources with high brilliance that can be used in mobile devices has changed the quality of XRF and XRD analysis in this context. An example is the publication of K. Janssens et al. [1].

Incoatec has long offered these solutions for applications in crystallography and beyond. In addition to our key area of multilayer X-ray optics, we started to develop X-ray sources ourselves in 2011. The aim was to offer the best combination of optics and sources for specific applications in the analysis of small and macromolecular structures. We succeeded in bringing new solutions to the market that offer a flux density of more than 5*10^10 ph/s/mm² in a spot of less than 100µm. In the meantime, we have developed several new metal-ceramic tubes and suitable multilayer optics for different applications.

In our contribution we will summarise the most important parameters for combining multilayer optics and microfocus sources to achieve collimated or focused X-rays with high brilliance. We will present examples of the use of these sources for the analysis of cultural heritage materials using different XRD and XRF methods.

References

[1] Macroscopic X-ray powder diffraction scanning : possibilities for quantitative and depth-selective parchment analysis
Vanmeert Frederik, de Nolf Wout, Dik Joris, Janssens Koen; Analytical chemistry - ISSN 0003-2700 - 90:11(2018), p. 6445-6452
Full text (DOI uitgever): https://doi.org/10.1021/ACS.ANALCHEM.8B00241

Back to Table of contents

MS43 Crystallography for cultural heritage materials

MS43-03

Metal carboxylates in paintings – the study of their structure and behaviour

R. Barannikov [1], P. Bezdička [2], E. Kočí [2], S. Garrappa [2], L. Kobera [3], J. Rohlíček [4], J. Plocek [2], S. Švarcová [2]

[1]Institute of Inorganic Chemistry of the Czech Academy of Sciences, ALMA Laboratory, Husinec-Řež 1001, 250 68 Husinec-Řež, Czech Republic; Department of Inorganic Chemistry, Faculty of Science, Charles University in Prague, Hlavova 2030/8, 128 43 Prague 2, Czech Republic - Prague (Czech Republic), [2]Institute of Inorganic Chemistry of the Czech Academy of Sciences, ALMA Laboratory, Husinec-Řež 1001, 250 68 Husinec-Řež, Czech Republic - Prague (Czech Republic), [3]Institute of Macromolecular Chemistry of the Czech Academy of Sciences, Heyrovského nám. 2, 162 06 Praha 6, Czech Republic - Prague (Czech Republic), [4]Institute of Physics of the Czech Academy of Sciences, Na Slovance 1999/2, 182 21 Praha 8, Czech Republic - Prague (Czech Republic)

Abstract

Saponification, resulting from pigment-binder interactions is one of the most dangerous degradation phenomena affecting the appearance and stability of paintings. The crystallization of metal carboxylates (soaps) is assumed as a critical point for the development of undesirable changes manifested as protrusions, efflorescence, darkening and etc. However, factors triggering this process are not fully understood, limiting the development of a suitable strategy for conservation and preservation of precious works of art.

Previous research of the portrait miniatures[1] has revealed presence of different types of crystalline metal carboxylates frequently in a conjoined occurrence of lead white ($2PbCO_3 \cdot Pb(OH)_2$) and cinnabar (HgS) pigments in paint layers, exceptionally even without presence of any lead-based pigment (Fig. 1). These findings indicated that HgS assists to the formation of Pb and/or Hg carboxylates. Nevertheless, its role in the reaction mechanism has to be clarified.

The paucity of reliable reference structural data limited the experimental research of HgS effect on the pigment-binder interactions on molecular level. In our previous research[2], the long chain simple and mixed mercury (II) carboxylates in the series $Hg(C16)_x(C18)_{2-x}$ (x= 0.0; 0.2; 0.5; 0.8; 1.0; 1.2; 1.5; 1.8; 2.0) were synthesized in the form of pure polycrystalline powders and characterized by XRPD, ssNMR, FTIR and DSC. The crystal structure of the studied mercury carboxylates was described on the basis of complementary ssNMR and XRPD measurements, Rietveld refinement and DFT calculations. All the subjected compounds crystallize in a monoclinic lattice of the C2/c symmetry. Mercury atoms are arranged in a slightly distorted square antiprismatic geometry and are monodentatically bonded to carboxylate anions. The structural disorder at the aliphatic end of the stearic acid chains was detected in the mixed carboxylates.

The synthesized and characterized metal carboxylates have been applied for the study of formation of metal soaps in model experiments simulating egg and/or oil-based paint systems consisted of lead and/or mercury-based pigments, and furthermore for the study of their crystallization in oil-based polymeric matrix.

References

1. S. Garrappa, D. Hradil, J. Hradilová, et al., Anal. Bioanal. Chem., 2021, 413, 263-278.
2. R. Barannikov, E. Kočí, P. Bezdička, et. al. Dalton Trans., 2022, 51, 4019–4032.

Miniature portrait of Emperor Joseph I of Habsburg

Back to Table of contents

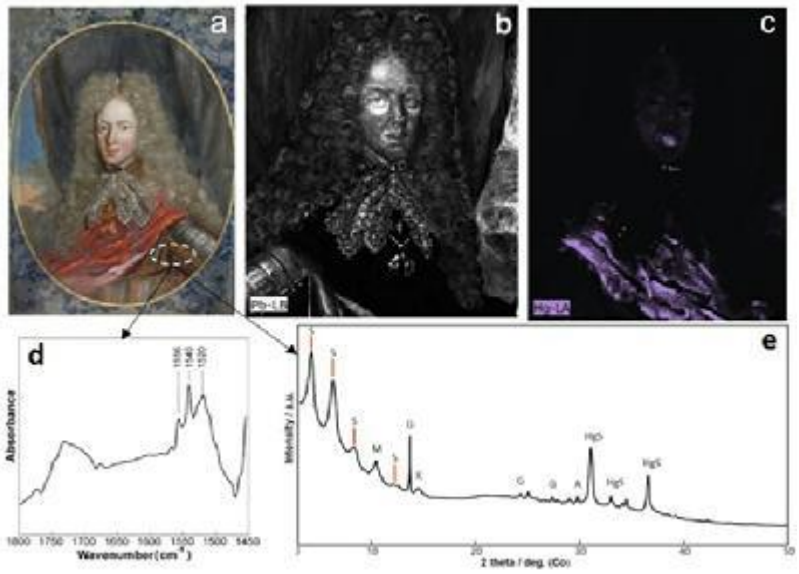

Back to Table of contents

MS43 Crystallography for cultural heritage materials

MS43-04

Application of multivariate analysis to X-ray diffraction tomography: the study of medieval applied brocades.

P. Bordet [1], F. Kergourlay [1], A. Pinto [2], N. Blanc [1], P. Martinetto [1]
[1]Institut Neel CNRS - Grenoble (France), [2]Institut Neel CNRS & ArcNucleart CEA - Grenoble (France)

Abstract

X-ray diffraction tomography (XRD-CT) is a recognized technique for structural investigation of heterogeneous materials, which makes it a tool of choice for the non-destructive analysis of cultural heritage micro-samples. Characterization of such complex samples with a sufficiently high spatial resolution requires the acquisition of a large number of diffraction images (typically several tens of thousands), followed by a sequence of multiple data manipulations and corrections to locate the various phases in the samples. Here we propose to use multivariate analysis to automatically break down the data into a small set of components, each representing the diffraction pattern of one or a small number of phases. This makes the identification of phases and the quantification of each component much more efficient and leads to a quantitative determination of the phase content of each voxel of the tomographic reconstruction, without a priori knowledge about the sample composition. We show that the NMF (Non-negative Matrix Factorization) method is very effective for this purpose, with a computation time suitable for online data analysis in order to e.g. assess the quality of measurements during synchrotron experiments. Here, we apply this method to the study of micro-samples of medieval applied brocade decorations taken from a wooden statue [1,2] which was found to contain as many as 11 different phases. The figure shows an exemple of tomographic reconstruction of the 11 phase concentrations after 6-component NMF multivariate analysis. From left to right and top to bottom: gypsum, cinnabar, beeswax, romarchite, cassiterite, cerussite, hydrocerussite, goethite, minium, gold, chlorargyrite.The results are validated a posteriori by comparison with analytical techniques requiring sample preparation and therefore destructive (SEM- EDX, IRTF, Raman) and sequential Rietveld refinement.
Acknowledgement: This study received state aid managed by the National Research Agency under the program Investissements d'Avenir with reference: ANR-15-IDEX-02 (Cross Disciplinary Program IDEX UGA PATRIMALP).

References

[1] Martinetto, P., Blanc, N., Bordet, P., Champdavoine, S., Fabre, F., Guiblain, T., Hodeau, J.-L., Lelong, F., Leynaud, O., Prat, A., Pouyet, E., Uher, E., Walter, Ph. (2021). J. Cult. Herit., 47, 89-99.
[2] Bordet P., Kergourlay F., Pinto A., Blanc N., Martinetto P. (2021). J. Anal. At. Spectrom., 36, 1724

Phase concentrations from NMF

Back to Table of contents

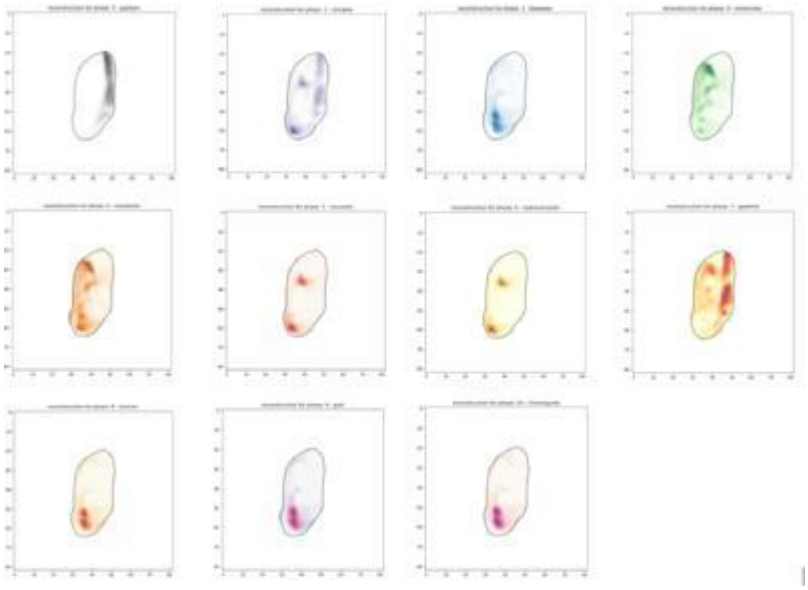

Back to Table of contents

MS43 Crystallography for cultural heritage materials

MS43-05

Scanning Electron Diffraction microstructural studies to differentiate between ancient black glazed pottery and its contemporary replica

P.P. Das [1], S. Nicolopoulos [1], E.F. Rauch [2], E. Palamara [3], N. Zacharias [3]
[1]NanoMEGAS SPRL - Brussels (Belgium), [2]SIMaP - Grenoble (France), [3]University of the Peloponnese - Kalamata (Greece)

Abstract

In the present work, Scanning Electron Diffraction in Transmission Electron Micrsocope (TEM-ASTAR) (1,2) was applied to characterize phases present in the black glazed surfaces of Hellenistic pottery down to nm scale resolution and to investigate the potential to differentiate between archaeological pottery with contemporary replicas (3). Two samples were analyzed: one archaeological sample (AL49) originating from Aliartos, Boeotia, Greece dated to the Hellenistic period; and one authentic replica (TH3) produced by Thetis Ltd, using the same raw materials and manufacturing processes as the original pottery. Additionally, Thetis products undergo a process of artificial weathering, to ensure the maximum similarity with the archaeological samples. Both samples contain a high-quality glaze, as observed by their black and shiny surface. Previous crystallographic analyses of the ceramic body and the glaze have suggested the presence of various phases. Most commonly, quartz, feldspar, hercynite, maghemite and hematite are identified on the body and hematite, hercynite, magnetite, magnetite, titanomagnetite on the glaze (4); however EDS analysis has revealed similar chemical composition for both samples (original & its replica) with systematic differentiations on only EDS glaze profiling studies (3). In order to reveal possible differences between two samples, thin lamellas (from AL49 and TH3) were prepared by FIB technique and studied in a Jeol 2100F TEM equipped with ASTAR (2). Scanning Precession (precession angle 1.2 deg) ED data was collected using ASTAR from an area of 300x300 pixels with step size 2 nm. The examination of several areas shows that the two samples show significant difference in magnetite Fe3O4 content (46% in TH3 vs 70% in AL49, 20% amorphous area in TH3 vs < 5% in AL49, where the hematite Fe2O3 phase is equally present in both samples. As an exmaple; ASTAR phase (colour) and relibility map (grey scale) from one area for TH3 contemporary sample is shown in Figure 1: 46% magnetite Fe3O4 (blue), 2% FeO Wüstite (red), 32% Fe2O3 hematite (green) and 20% amorphous phase (black) and in Figure 2 one area of AL49 archaeological is shown: 70 % magnetite (blue), 3% Wüstite (red), 27% hematite (green). Although our results are “preliminary”, they highlight the potential of scanning electron diffraction based crystallographic techniques to reveal differences between various archaeological artifacts, having similar chemical composition.

References

1. P. H. Sciau, “Chapter two - transmission electron microscopy: emerging investigations for cultural heritage materials,” Advances in Imaging and Electron Physics, vol. 198, pp. 43–67, 2016.
2. S. Nicolopoulos, P. P. Das, A. G. Pérez et al., “Novel TEM Microscopy and Electron Diffraction Techniques to Characterize Cultural Heritage Materials: From Ancient Greek Artefacts to Maya Mural Paintings,” Scanning, 2019.
3. N. Zacharias, G. Mastrotheodoros, M. Katsiotis, N. Laskaris, Glazed Pottery Surfaces Under the Microscope: Which Criteria to Decide About Archaeological and Modern Items, ISA 2012, Tampa Florida May 18-22, Book of Abstracts p.85, 2012.
4. Y. Maniatis, E. Aloupi, A.D. Stalios, New evidence for the nature of the Attic black gloss. Archaeometry 35, 1: 23-34, 1993.

ASTAR Phase and Reliability Map for TH3 sample

Back to Table of contents

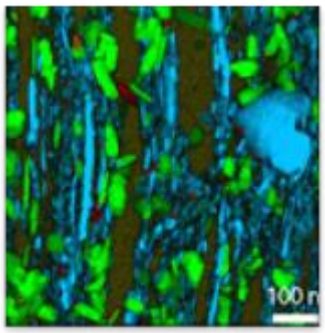

ASTAR Phase and Reliability Map for AL49 sample

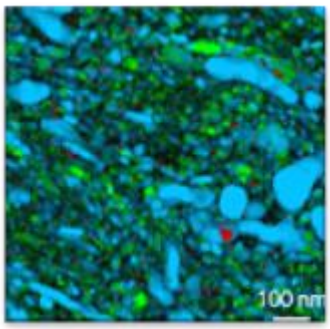

Back to Table of contents

MS44 Crystallography in large scale facilities

MS44-01

Battery materials and diagnostics using advanced operando techniques

Claire Villevieille (Grenoble, France)
Univ. Grenoble Alpes, Univ. Savoie Mont Blanc, CNRS, Grenoble INP, LEPMI,38000 Grenoble, France

Since the commercialization of lithium-ion (Li-ion) batteries by Sony in 1991, researchers have been extensively working on increasing the specific energy of both negative and positive electrode materials by replacing, respectively, graphite and LiCoO2 used therein. Although the specific energy of Li-ion batteries can be slightly increased, this nearly 30-year-old intercalation-chemistry-based battery technology is approaching its limitations. Thus, other battery chemistries based on Na-ion chemistry or on solid electrolytes have received considerable attention. During electrochemical cycling, these battery systems exhibit several changes at the bulk and the interface/surface levels, the investigation and understanding of which require new characterization tools. There are two different approaches to understand the reaction mechanism of electroactive materials during cycling, namely using either *ex situ* or *in situ/operando* modes. For the latter approach, the development of reliable electrochemical cells is of a prime importance (Figure 1). This is never an easy task though, since the design of such cells has to be adequate to the technique of a choice and its individual requirements. Once a proper design is, however, found, the surface, the bulk, the interphases, and finally the combination of these can be studied and the reaction mechanisms can be better understood and/or elucidated, thus further improving the battery technology. Through this talk, we will focus on the analysis of the electrochemical reactions occurring during cycling of selected materials by combination of different *operando/in situ* studies like X-ray diffraction, neutron diffraction, neutron imaging and X-ray tomographic microscopy etc.

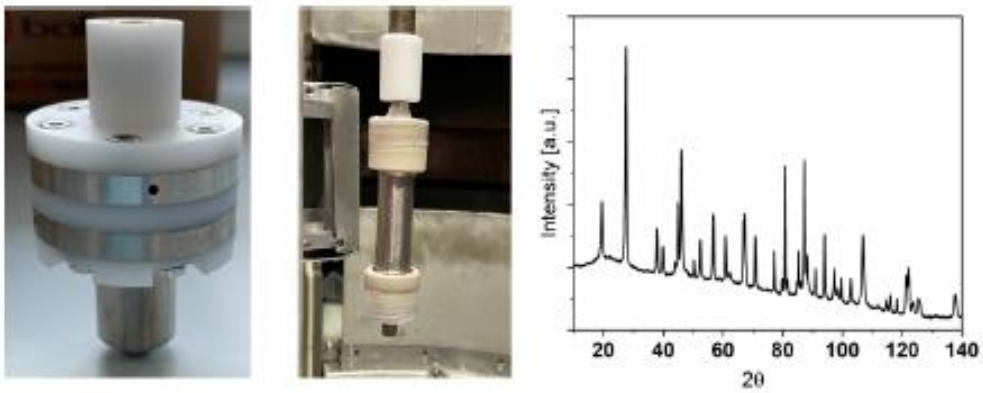

Figure 1, from left to right: Operando neutron diffraction cell for solid state batteries, operando neutron diffraction cell for liquid-based batteries, and the corresponding neutron diffraction pattern of a full cell composed of Li-rich NMC and graphite.

Back to Table of contents

MS44 Crystallography in large scale facilities

MS44-02

From XFELs to Synchrotrons and back: High output serial crystallography to image the structure and dynamics of biological macromolecules.

D. Oberthuer [1]
[1]*CFEL/DESY - Hamburg (Germany)*

Abstract
The establishment of serial methods in macromolecular crystallography since the seminal experiments by Chapman et al. at LCLS in 2008 led, together with the re-discovery of crystallography under ambient conditions to a re-emergence of time-resolved studies to track the dynamic properties of functioning proteins. It also enabled structure determination using sub-micron sized crystals and - using an XFEL - circumvents many challenges related to radiation damage. Initially many critics doubted that serial crystallography would work, but from experimental phasing to superior difference maps from time-resolved experiments, the critics could be proven wrong every single time. Today it is a robust method, thanks also to strong developments in sample delivery procedures and data processing algorithms. One challenge still remains, however: the availability of beamtime and access for novice user groups, even with five XFELs in operation. It is therefore necessary to strongly consider for which scientific question an XFEL is needed, what could be done by serial crystallography at synchrotron light sources (SSX), where experiments at both XFELs and Synchrotrons would complement each other and how such decisions can be made in a way that benefits science and at the same time lowers the access barriers for users. To address these issues, results from recent experiments at both the European XFEL and PETRAIII will be shown here, ranging from new protein structures using native nano-crystals and de novo structure determination through a combination of nanoSFX and Alphafold2, to approaches to data collection under (almost) physiological conditions.

Back to Table of contents

MS44 Crystallography in large scale facilities

MS44-03

Coherent diffraction imaging at space-group forbidden reflections

G. Beutier [1], J. Eymery [2], M. Dupraz [3], M.I. Richard [2], A. Wartelle [1], M. Verdier [1], M. De Boissieu [1], S. Collins [1], E. Bellec [4], V. Favre-Nicolin [4], S. Leake [4]

[1]Univ Grenoble Alpes - CNRS - SIMaP - Saint-Martin-d'Hères (France), [2]CEA - IRIG - Grenoble (France), [3]Institut Néel - Grenoble (France), [4]ESRF - Grenoble (France)

Abstract

On one hand, coherent diffraction imaging (CDI) in Bragg geometry has emerged as a unique 3D microscopy of nanocrystals thanks to 3rd generation synchrotron sources. Away from absorption edges and at space-group allowed reflections, it provides not only the electronic density, but also, encoded in the phase, the atomic displacement field with respect to the mean lattice, which in turn reveals crystal strain, defects and domains [1–3]. On the other hand, some crystal structures have crystallographic reflections which are forbidden by the space-group symmetry but can nevertheless be observed at a suitable X-ray absorption edge, due to the anisotropy of the tensor of scattering (ATS) [4]. They are several orders of magnitude weaker than allowed reflections, but the absence of Thomson scattering allows the observation of various electronic phenomena related to electronic orders (magnetic, charge, orbital), as well as static and dynamic atomic displacements.
The new generation of synchrotron sources, such as the ESRF “Extremely Bright Source”, opens opportunities to perform CDI on such weak reflections. Here we report on the measurement of the (115) forbidden reflection of a GaN nanopillar at the Ga K edge (Figure 1). Sufficient statistics could be obtained in a total accumulation time of ~30 minutes for an entire rocking curve to retrieve the phase of the scattering function (Figure 2). Such measurement at high temperature would provide an image of the inhomogeneity of thermal motion in the crystal [5], which would be particularly interesting close to surfaces, inversion domain boundaries [3] and crystal defects. This proof-of-principle experiment demonstrates that forbidden reflections are a new opportunity for CDI with the new synchrotron sources.

References

[1] Robinson, I. & Harder, R. (2009). Nature Materials 8, 291.
[2] Clarke, J., Ihli, J., Schenk, A. S., Kim, Y.-Y., Kulak, A. N., Campbell, J. M., Nisbet, G., Meldrum, F. C. & Robinson, I. K. (2015). Nature Materials 14, 780.
[3] Labat, S., Richard, M.-I., Dupraz, M., Gailhanou, M., Beutier, G., Verdier, M., Mastropietro, F., Cornelius, T. W., Schülli, T. U., Eymery, J. & Thomas, O. (2015). ACS Nano 9, 9210.
[4] Dmitrienko, V. E. (1983). Acta Cryst. A 39, 29.
[5] Beutier, G., Collins, S. P., Nisbet, G., Ovchinnikova, E. N. & Dmitrienko, V. E. (2012). Eur. Phys. J. Special Topics 208, 53.

Reciprocal space map at the forbidden reflection

Back to Table of contents

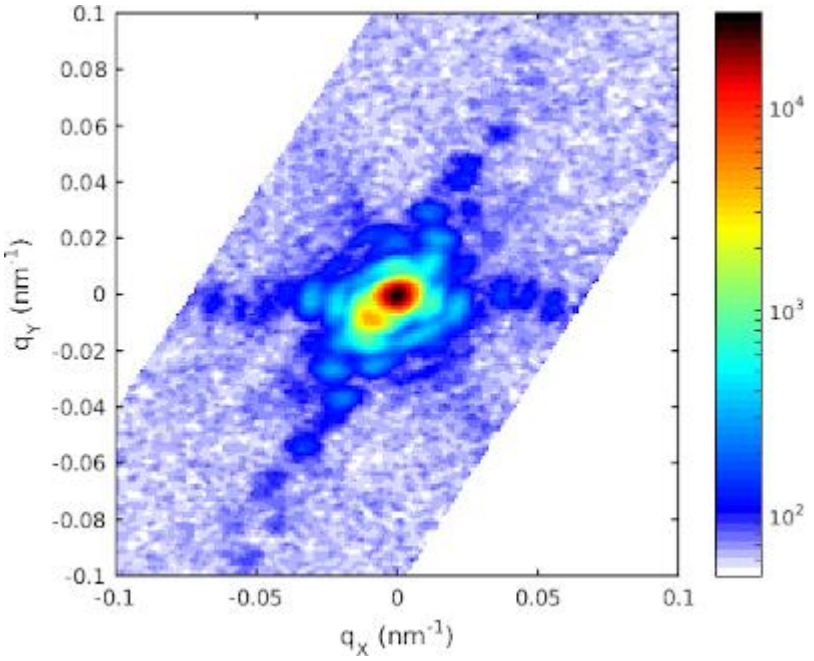

Direct space image from phase retrieval

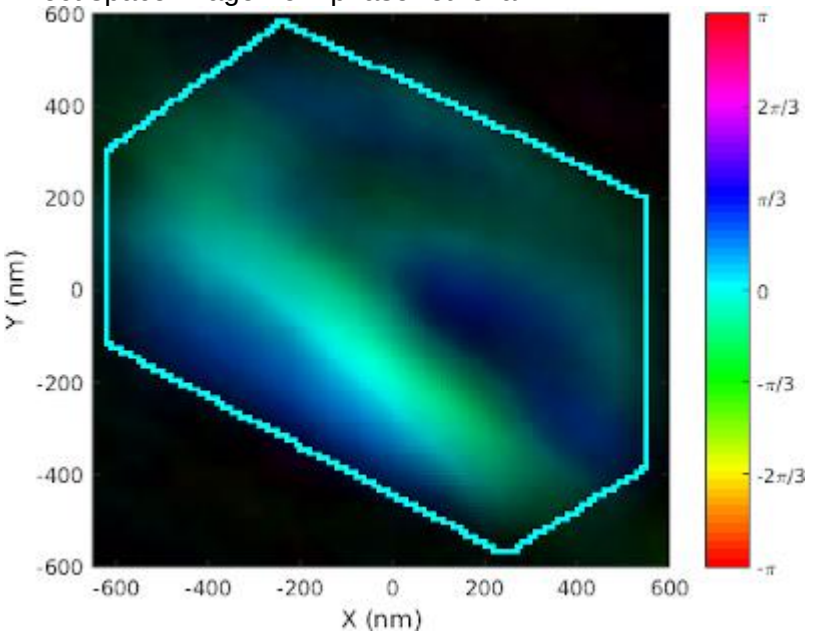

Back to Table of contents

MS44 Crystallography in large scale facilities

MS44-04

Structural Complexity in the RP phase La2CoO4+δ Explored by Synchrotron X-ray Single Crystal Diffraction and Neutron Powder Diffraction.

R. De Barros [1], M. Ceretti [1], W. Paulus [1], A. Bosak [2], V. Nassif [3]
[1]ICGM - Montpellier (France), [2]ESRF - Grenoble (France), [3]Institut Néel - Grenoble (France)

Abstract

Oxides with K_2NiF_4 type structure have been extensively studied those past decades, showing a large variety of physical and transport properties, i.e. spin, charge, orbital ordering and ionic-electronic conductivity [1]. In particular, this latter, highlighted the transition metal oxides ($RE_2MO_{4+\delta}$, RE = rare earthrare earth, M =Mn, Co, Ni, Cu), being promising materials compounds for intermediate temperature solid oxide fuel cells and oxygen separation membranes. Among them, thereby $La_2CoO_{4+\delta}$ is a special case, due to the higher stability of Co^{3+} with respect to Cu and Ni, allowing to take up more interstitial oxygen quantities, the non-stoichiometric region being 0 <= δ <= 0.25. This system is also interesting in terms of its chemical reactivity, as $La_2CoO_{4.0}$ is able to uptake oxygen spontaneously at room temperature. This kind of oxygen mobility at ambient temperature is extremely surprising, as it involves an unusual high oxygen diffusion coefficient (about 10^{-10} cm^2/s), making this system a unique case so far [2,3]. On the other hand, rare earth cobaltates are an outstanding example of strongly correlated electron materials, which provide a remarkable opportunity to study interplay between dimensionality, lattice, charge, spin and orbital momentum degrees of freedom.

In this study we relied on large scale facilities in order to investigate structural changes and complexity in $La_2CoO_{4+\delta}$. By neutron in situ powder diffraction (D1B @ILL, Grenoble), we followed the structural evolution occuring in the stoichiometric $La_2CoO_{4.00}$, under oxidizing atmosphere. By Synchroton X-ray single crystal thermodiffraction on the beamline ID28 (ESRF, Grenoble) we explore the structural complexity of $La_2CoO_{4.25}$. From NPD, we report on the extremely rich phase diagram (Figure 1), from a stoichiometric orthorhombic *Bmab* phase, passing via an ordered intermediated tetragonal phase (*F4/mmm*), to the oxygen rich orthorhombic (*Fmmm*) phase $La_2CoO_{4.25}$ and a more orthohrombic phase. Synchrotron single crystal diffraction highlights a very complex modulated structure, where all the satellites reflections, up to alteast the 5^{th} order could be indexed using a propagation vectore q = 0.75a*+0.5b* (Figure 2), except some reflection (in green) corresponding to a checkerboard charge ordering. These reflections are also visible in NPD, suggesting a sub-mesoscopic oxygen ordering at room temperature. Surprisingly, the oxygen order persists up to 843K, corresponding to the orthogonal to tetragonal phase transition.

This study highlights the complementarity of the two diffraction techniques, neutrons and synchrotron, for the study of complex structures in which oxygen creates superstructures.

References

[1] Goodenough, J. B. Reports on Progress in Physics 2004, 67 (11), 1915-1993.
[2] Girgsdies, F.; Schöllhorn, R. Solid State Communications 1994, 91 (2), 111-112.
[3] Nemudry, A.; Rudolf, P.; Schöllhorn, R. Solid State Ionics 1998, 109 (3), 213-222.

Back to Table of contents

FIG.1 Phase transition of La2CoO4 (powder), f(T).

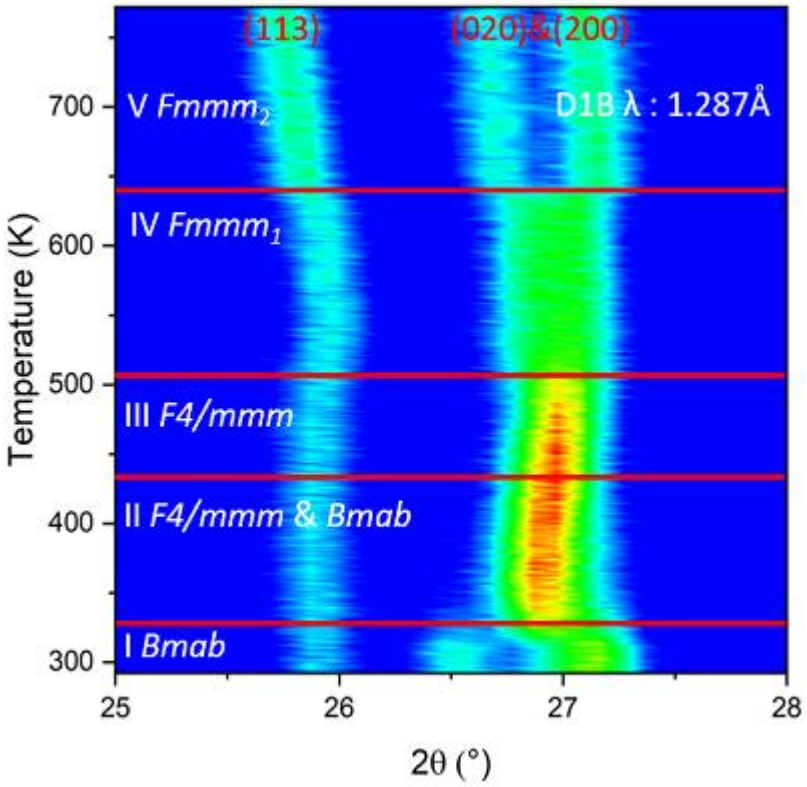

FIG.2 HK4 plane of La2CoO4.25 @RT(single crystal).

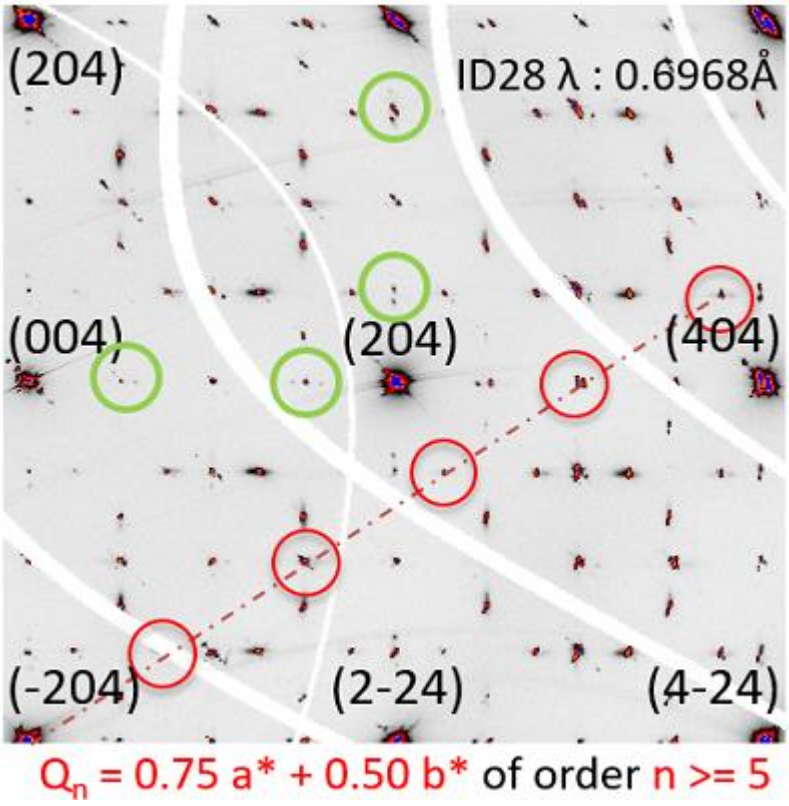

Back to Table of contents

MS44 Crystallography in large scale facilities

MS44-05

EMBL@PETRA4 – an Integrated Facility for Structural Biology and Imaging

S.L.S. Storm [1], G. Bourenkov [1], D. Liz [1], B. Clement [1], M. Agthe [1], D. Von Stetten [1], J. Albers [1], S. Fiedler [1], D. Svergun [1], M. Wilmanns [1], T.R. Schneider [1]
[1]EMBL Hamburg - Hamburg (Germany)

Abstract

As a partner of DESY in the planning towards the fourth generation synchrotron radiation source PETRA IV to be established in Hamburg, EMBL is proposing to contribute an Integrated Facility for Structural Biology and Imaging. The facility will offer both easy-to-use, robust, and remotely accessible measurement services and cutting-edge capabilities for tackling the most challenging experiments. As presently implemented for MX and BioSAXS in EMBL@PETRA3, upstream services supporting the preparation of samples, and downstream services for the analysis and interpretation of experimental data will be offered in an integrated fashion.
The core of the Integrated Facility is proposed to consist of a set of endstations receiving X-ray from three insertion devices implementing a range of functionalities for structural biology and X-ray imaging:

- Static and time-resolved small-angle X-ray scattering (BioSAXS) for biological systems,
- Static and time-resolved macromolecular crystallography (MX),
- Medium resolution high throughput phase-contrast X-ray imaging (HiTT) for biological systems.

The next generation BioSAXS beamline will benefit from PETRA IV beam by shorter data collection times, lower sample consumption and unprecedented time resolution for studying biomolecular dynamics. Furthermore, novel SAXS experiments will become possible to bridge the gap between the synchrotron-based and XFEL studies.
For MX, the increased brilliance of PETRA IV in combination with advanced optics will increase throughput and enable the collection of diffraction data to higher resolution from small and/or less-ordered crystals. The time-scales accessible by time-resolved crystallography will be significantly shortened.
The increased coherence of PETRA IV will revolutionize phase-contrast based X-ray imaging. We will provide X-ray imaging in an operational mode (‘HiTT’ – High-Throughput Tomography) facilitating its use by a wide user community for answering biological questions. Scale-bridging and correlative imaging will be offered in cooperation with other providers of imaging technologies.

Back to Table of contents

MS45 What is inside the black box?

MS45-01

Space groups, the Final Frontier: a tutorial guide to some entries in International Tables Volume A

W. Clegg [1]
[1]*Newcatle University - Newcastle upon Tyne (United Kingdom)*

Abstract
Crystallographers of previous generations were well acquainted with the contents of International Tables Volume A (and its predecessor Volume I in the earlier series); most of this weighty tome is taken up with extensive graphical, mathematical and other information about each of the 230 space groups relevant to three-dimensional crystal structures. With the increasing use of automatic procedures in the collection and processing of diffraction data and the solution and refinement of crystal structures from the data, the need to refer to these tables has largely disappeared as far as many users are concerned, and younger practitioners may well never have opened the Big Book any more than they have opened Black Boxes. Automation, however, is not infallible and there is much to be said for knowing what useful information is available when it is needed. I will begin with a few basic concepts and principles regarding space group symmetry and then go on to examine a few specific space groups in some detail. Those who are familiar with Volume A can take time off and visit a parallel session!

Back to Table of contents

MS45 What is inside the black box?

MS45-02

You have the molecular structure – are you out of the black box?

P. Bombicz [1]
[1]*Research Centre for Natural Sciences - Budapest (Hungary)*

Abstract

There are several techniques a crystallographer may apply occasionally as a black box: using the software of data collection and structure solution, or the physical chemistry of nucleation at crystal growth, etc.; but being lucky enough to have the molecular structure – are you ready and can you sit back? You have to explore how the crystal structure is constructed from the molecules, how the crystal structure and the macroscopical properties are related to each other. Understanding the rules, the hows and whys of crystal architecture, offers often challenges, and this way is often flanked by pitfalls. I will speak about the relation of chirality and crystallizability, surprizing stoichiometry, long uncovered crystal symmetries and pseudo-symmetries, week intramolecular interactions which completely change crystal properties, ways and reasons of solvent inclusion. Selected examples prove that understanding of crystal architecture is not necessarily straightforward.

References

Figure 1 Challenges offered by the exploration of crystal architecture.

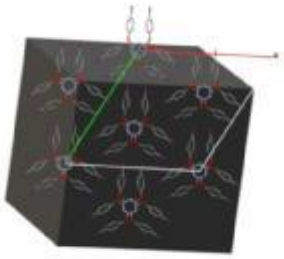

Back to Table of contents

MS45 What is inside the black box?

MS45-03

Efficient determination of possible twin laws using modified Rodrigues parameters

C.L. Hall [1], L.N. Midgley [2], C.G. Böhmer [3], N. Peyerimhoff [2], H. Puschmann [4]
[1]University of Bristol - Bristol (United Kingdom), [2]University of Durham - Durham (United Kingdom), [3]University College London - London (United Kingdom), [4]OlexSys - Durham (United Kingdom)

Abstract

In many situations, it is difficult to obtain crystals that produce perfect diffraction patterns and instead structures need to be determined using crystals with structures or defects that affect the diffraction pattern. One important example is twinning, which leads to the appearance of multiple sets of reflections associated with the different twin domains; represented in reciprocal space, these sets of reflections are related by rotation about the origin [1,2]. If the reciprocal lattices of the different twin domains do not overlap, then structure determination for a twinned crystal is relatively straightforward [1]. However, overlap of the lattices (especially the partial overlap associated with some non-merohedral twins) makes structure determination difficult as it is necessary to disentangle the data from the different twin domains [1,2]. We present a new method for determining twin laws that would lead to possible overlaps between the reciprocal lattices associated with different twin domains. This method depends on representing 3D rotations using "modified Rodrigues parameters" (MRPs), which are stereographic projections of the unit quaternions into 3D Euclidean space and which can be used to represent all 3D rotations [3]. Using MRPs, we have developed a computationally-efficient method that determines which rotations of a given reciprocal lattice could lead to some or all of the rotated reflections being within a specified tolerance of the original reflections. The error control on small perturbations in MRPs [3] means that we are guaranteed to find all possible twin laws that would cause a given number of rotated reflections to be within tolerance of the observed original reflections. The output of our algorithm is a list of possible twin laws in order of severity (i.e., the number of bad reflections that they would cause). These could then be used as twin candidates for further algorithms to perform the detwinning and automatically correct the integration of the bad reflections.

References

[1] Herbst-Irmer, R. (2016) “Twinning in chemical crystallography – a practical guide”, Zeitschrift für Kristallographie - Crystalline Materials 231(10):573-581, doi:10.1515/zkri-2016-1947
[2] Sevvana, M., Ruf, M., Usón, I., Sheldricke, G. M., and Herbst-Irmer, R. (2019) “Non-merohedral twinning: from minerals to proteins”, Acta Crystallographica D: Structural Biology 75(12):1040-1050, doi:10.1107/S2059798319010179
[3] Terzakis, G., Lourakis, M., and Ait-Boudaoud, D. (2018) “Modified Rodrigues parameters: an efficient representation of orientation in 3D vision and graphics”, Journal of Mathematical Imaging and Vision 60:422–442, doi:10.1007/s10851-017-0765-x

Back to Table of contents

MS45 What is inside the black box?

MS45-04
The Crystal Isometry Principle
V. Kurlin [1], D. Widdowson [1], A. Cooper [1], M. Bright [1]
[1]*University of Liverpool - Liverpool (United Kingdom)*

Abstract
'Black box' approaches to the prediction of properties are greatly hindered by ambiguities in data representation [1]. A crystal structure can be represented by infinitely many different bases and motifs. Crystal Structure Prediction produces numerous near-duplicates among millions of simulated crystals, obtained as slightly different approximations of the same local energy minimum, which must be distinguished from genuinely different structures [2].
Since crystal structures are determined in a rigid form, their strongest equivalence is rigid motion or isometry also including reflections. Their classification up to isometry requires invariants and metrics that are continuous under perturbations because any conventional or reduced basis may double in size under small perturbations.
Density functions [3], the isoset (a complete invariant of periodic structures) [4], Average Minimum Distances (AMD) open up the 'black box' of crystallographic data with unambiguous representations of periodic structures [5]. The simplest Gaussian regression on AMD invariants [6] achieved the state-of-the-art Mean Absolute Error (less than 5kJ/mole, 0.05eV/atom) on 5679 crystals [2].
Pointwise Distance Distributions (PDD) are stronger invariants, which can be continuously compared by the Earth Mover's Distance. This distance was used for visualising the Inorganic Crystal Structure Database [7]. More than 200 billion pairwise comparisons between all 660K+ periodic crystals (full 3D structure; no disorder) in the Cambridge Structural Database (CSD) was completed over two days on a modest desktop PC.
PDD computations detected five pairs of entries that have identical geometry but differ by one pair of atoms, for example, Cd<->Mn in HIFCAB vs JEPLIA [8, section 7]. Since these coincidences seem physically impossible, five journals are now investigating the integrity of publications based on these duplicates.
These experiments justify the Crystal Isometry Principle, which states that any periodic crystal is uniquely determined by its geometric structure. Indeed, replacing any atom with a different one inevitably perturbs distances between neighbours. Then all periodic crystals live in a common Crystal Isometry Space (CRISP), so that Mendeleev's periodic table representing individual elements, categorised by atomic number and group, can be extended into a continuous space for all solid crystalline materials. For instance, diamond and graphite, both consisting purely of carbon, have different locations in CRISP.
In the case of 2-dimensional lattices [9], the first map of CRISP shows that among all real crystals in the CSD about 45% of 2-dimensional lattices are oblique and nicely fill the expected continuous space [10] except towards the point representing very thin long cells.

References
[1] Sacchi, P., Matteo Lusi, M., Cruz-Cabeza, A.J., Nauhac, E.Joel Bernstein, J. Same or different – that is the question: identification of crystal forms from crystal structure data. CrystEngComm 22 (43), 7170-7185, 2020.
[2] Pulido, A., Chen, L., Kaczorowski, T., Holden, D., Little, M., Chong, S., Slater, B., McMahon, D., Bonillo, B., Stackhouse, C., Stephenson, A., Kane, C., Clowes, R., Hasell, T., Cooper, A., Day, G. Functional materials discovery using energy-structure maps. Nature 543, 657-664, 2017.
[3] Edelsbrunner, H., Heiss, T., Kurlin, V., Smith, P., Wintraecken, M. The Density Fingerprint of a Periodic Point Set. Peer-reviewed Proceedings of Symposium on Computational Geometry 2021, 32:1--32:16. Available at http://kurlin.org/projects/projects/periodic-geometry-topology/density-functions-periodic-point-set.pdf
[4] Anosova, O., Kurlin, V. An isometry classification of periodic point sets. Peer-reviewed Proceedings of Discrete Geometry and Mathematical Morphology 2021, p. 229-241. Available at http://kurlin.org/projects/projects/periodic-geometry-topology/crystal-isosets-complete.pdf

Back to Table of contents

[5] Widdowson, D., Mosca, M.M., Pulido, A., Kurlin, V., Cooper, A.I. Average Minimum Distances of periodic point sets - fundamental invariants for mapping all periodic crystals. MATCH Communications in Mathematical and in Computer Chemistry, v.87(3), p.529-559, 2022. Available at http://kurlin.org/projects/periodic-geometry-topology/AMD.pdf
[6] Ropers, J., Mosca, M.M, Anosova, O., Kurlin, V., Cooper, A.I. Fast predictions of lattice energies by continuous isometry invariants of crystal structures. Peer-reviewed Proceedings of DACOMSIN 2021: Data and Computation for Materials Science and Innovation. Available at https://arxiv.org/abs/2108.07233.
[7] Hargreaves, C., Dyer, M., Gaultois, M., Kurlin, V., Rosseinsky, M.The Earth Mover's Distance as a Metric for the Space of Inorganic Compositions. Chemistry of Materials, v.32 (24), p.10610-10620. The ICSD map appeared on the cover of volume 32, issue 24 (December 2020).
[8] Widdowson, D., Kurlin, V., Pointwise Distance Distributions of finite and periodic point sets. arxiv.org:2108.04798. The latest version is at http://kurlin.org/projects/periodic-geometry-topology/PDD.pdf
[9] Kurlin, V. Mathematics of 2-dimensional lattices. arxiv:2201.05150. The latest version is at http://kurlin.org/projects/periodic-geometry-topology/lattices2Dmaths.pdf
[10] Bright, M., Cooper, A.I., Kurlin, V. Geographic-style maps for 2-dimensional lattices. arxiv:2109.10885. The latest version is at http://kurlin.org/projects/periodic-geometry-topology/lattices2Dmap.pdf

Ambiguity and discontinuity of reduced cells

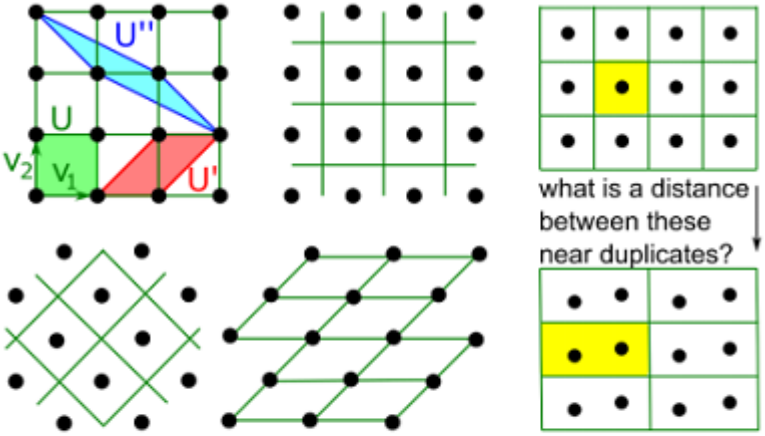

Figure 1. Left: the square lattice can be given by many bases.

Right: reduced cells are discontinuous under perturbations.

Invariants of crystals and maps of 2D lattices

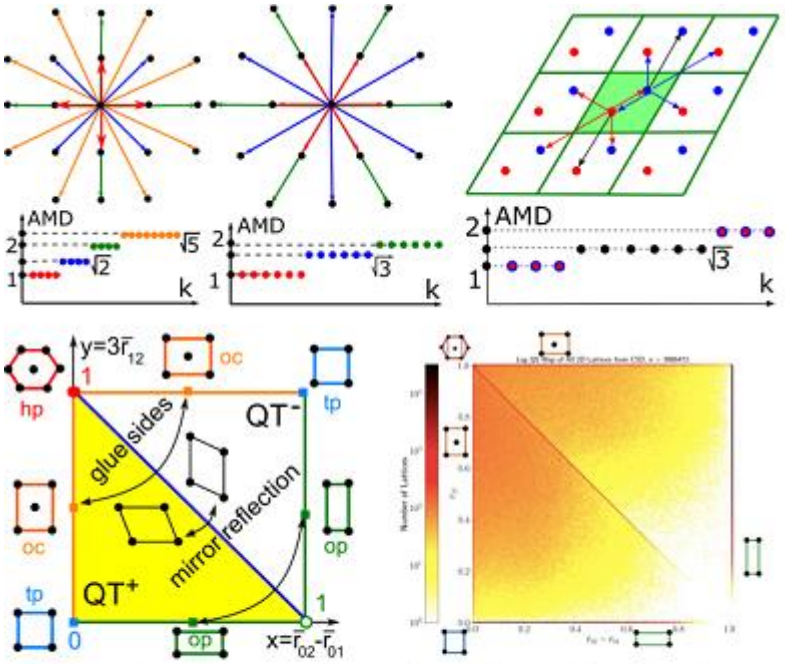

Figure 2. Top: the AMD sequence of distances from motif points to k neighbours for the square lattice, hexagonal lattice, a honeycomb structure (with averages over motif points).

Bottom left: the space of all 2D lattices up to isometry and scaling. Bottom right: the log scale density map of 2D lattices in all periodic crystals from the Cambridge Structural Database.

Back to Table of contents

MS45 What is inside the black box?

MS45-05

Peering at the data inside the Black Box

R. Oeffner [1], A. Mccoy [1], C. Millán [1], T. Croll [1], R. Read [1]
[1]*Cambridge Institute for Medical Research, University of Cambridge - Cambridge (United Kingdom)*

Abstract

The availability of high-quality predicted models of proteins, from machine-learning tools such as *AlphaFold2* and *RoseTTAFold*, is accelerating the automation of structural biology and making it more accessible to novices. This trend makes it even more important to have intuitive tools that help inexperienced users to peer inside the black box when things go wrong.

With phasing of crystallographic data and subsequent model refinement being greatly simplified by reliable starting models, undiagnosed data pathologies are much more likely to be the remaining barrier to success [1]. Likelihood-based methods, which power the automation machinery, rely on a variety of assumptions about the data. When pathologies that violate those assumptions cannot automatically be identified and mitigated, the user needs help to explore the data. Tables of statistics and one-dimensional plots, such as those produced by *phenix.xtriage* [2], are helpful, but direct visualization of the data provides a new dimension.

The *HKLviewer* [3], which is included in Phenix [4] and CCTBX [5], is a 3D visualisation program for inspecting X-ray diffraction data. It can launch the *xtricorder* tool in *phasertng* [6] to carry out statistical analyses characterizing features such as anisotropy in the data, the information gained by the diffraction measurements, and the potential presence of translational non-crystallographic symmetry (tNCS). Properties of the data can be visualized by varying the sizes and colours of diffraction spots, and axes corresponding to tNCS translations or twin operators can be superimposed. The reflection data can either be examined as an asymmetric unit wedge or quickly expanded to P1 in a computationally lightweight manner. Derived properties (such as the intensity divided by its standard deviation) can be calculated, using simple Python commands invoking CCTBX, and then displayed as well.

The *HKLviewer* has been designed to help raise awareness of potential issues that might be encountered in downstream structure solution software. It can also be deployed as a teaching aid to educate novice crystallographers about the issues that can arise in data collection.

References

[1] McCoy et al. Acta Crystallogr D Struct Biol Crystallogr. 78, 1–13 (2022).
[2] Zwart et al. CCP4 Newsletter 43 (2005). http://legacy.ccp4.ac.uk/newsletters/newsletter43.pdf.
[3] Oeffner et al. Computational Crystallography Newsletter 12, 15-25 (2021).
[4] Liebschner et al. Acta Crystallogr D Struct Biol 75, 861–877 (2019).
[5] Grosse-Kunstleve et al. J. Appl. Cryst. 35, 126-136 (2002).
[6] McCoy et al. (2022). Acta Crystallogr D Struct Biol Crystallogr. 77, 1–10

Back to Table of contents

MS46 Reproducibility in crystallography

MS46-01

The Role of Archiving Raw Diffraction Data in Ensuring Reproducibility in Crystallography

L.M.J. Kroon-Batenburg [1]
[1]*Utrecht University - Utrecht (Netherlands)*

Abstract
Structure determination with (X-ray) crystallography from single crystals has become a seemingly routine technique. The workflow is rather well established in the community. Its starts with recording diffraction images on an area detector, finding positions of diffraction spots and indexing of the unit cell, predicting and integrating all spots (to a certain resolution) while subtracting the (incoherent) background, data reduction including scaling of the Bragg intensities by matching independent observations, solving the structural model (basically solving the phase problem) and refining (by least-squares or maximum likelihood methods) the model against the intensities or structure factors, improving the models through chemical knowledge or rebuilding in the electron density. A range of metrics is used to show the reliability of the results and the final model is validated through checkCIF or a PDB validation report. In all these steps choices are made by the software and the researcher, based on prior knowledge and experience. However, the choices are rarely documented. Why did the researcher decide to cut off the data at a certain resolution? Could the limit be chosen differently? Did the researcher index the reflection correctly? Is the lattice symmetry correct? Do the structure factors have this symmetry? Did the researcher miss additional lattices, so dealing in fact with a non-merohedral twin? Are some features in the diffraction pattern neglected, like diffuse scattering or incommensurate modulation? In chemical crystallography many efforts were made to check the validity of the model and refinement protocols of the (unmerged) structure factor data through checkCIF, ensuring its reliability when permanently archived, while in macromolecular crystallography PDB validation reports and the OneDep system guarantee the correct version of record of the publication. However, the validation metrics may not show the problems mentioned above.
True reproducibility in crystallography can only be reached if all steps and choices in the workflow can be repeated. Open Science policies require that no research data should be lost but should be made available to the research community according to the FAIR principles. These are compelling reasons for the deposition of raw data in freely accessible repositories at the moment of publication. See also an editorial on FAIR diffraction data coming to Macromolecular Crystallography in Acta Cryst. D, Acta Cryst. F, IUCrJ and J. Appl. Cryst. in 2019 [1]. Recent developments in archiving capabilities such as large-scale repositories have made this feasible. IUCrData journal will be opening a new section: Raw Data Letters. The papers in this section will describe interesting features in raw data sets [2]. The publication promotes retrieval by other scientists for purposes such as reanalysis by newer methods or protocols and for software and methods development and supports our aim of achieving true reproducibility in crystallography.

References
[1] Editorial on FAIR diffraction data coming to Macromolecular Crystallography in Acta Cryst. D, Acta Cryst. F, IUCrJ and J. Appl. Cryst. in 2019 (https://doi.org/10.1107/S2053230X19005909).
[2] https://iucrdata.iucr.org/x/services/journal_news.html

Back to Table of contents

MS46 Reproducibility in crystallography

MS46-02
Reliability and Reproducibility in Small-Molecule Crystallography
A. Linden [1]
[1]*University of Zurich, Department of Chemistry - Zurich (Switzerland)*

Abstract
Most reported small-molecule crystal structures have only been determined once from one crystal selected from a crystallization batch, often the first attempt. Multiple determinations of the structures of some compounds are found in the CSD, but these are relatively rare compared with the size of the database. How, then, do we assess the reliability or each of these "one-off" results and how reproducible is that result? Validation via *checkCIF* and by other means goes a long way towards verifying the veracity of the archived results. The inclusion of refinement instructions and reflection data or structure factors in the deposited record allows reviewers and readers to know exactly how the authors developed their model and, if interested, to investigate and tinker with the structure further from that point. However, even though CCD, image plate, pixel array and other area detectors have been commonplace since the early 1990s, up to now, in the single-crystal world, there is usually no public record of the original frame images from the diffractometer. Even if a laboratory is lovingly archiving their frames locally, do they still have a functioning version of the software or hardware to be able to reprocess them? One of the challenges with establishing repositories for frame data is to have enough metadata to know exactly how the original data reduction was performed. There are many options in modern data reduction software and it is hard to know how the original scientist tweaked the options to optimise the outcome. Very likely identical strategies are not used from one structure to the next. Without such knowledge, exact reproducibility might not be achievable. Nonetheless, the overall structure result may well be sufficiently reproducible and reliable for the purpose of the study, even if not quite identical. "Fit for purpose" is a key consideration and users of deposited data must remain cognisant of the intentions of the original investigation and not try to extract more significance out of a result than might be possible given the data collected at the time. Despite best efforts, some crystal structures can never entirely unambiguously answer even the original question behind the study. At the same time, it is important that the original report or deposited data is properly annotated with details of any special data handling or model refinement strategies that were used and any caveats about the sample, data and results that future users of the data should be aware of. With automated CIF generation software, attention to this last aspect is sometimes insufficient.

Back to Table of contents

MS46 Reproducibility in crystallography

MS46-03

The 'coloring' problem in the delafossite PdRhO2 vanished?

H. Borrmann [1], J. Henn [2]
[1]Max Planck Institute for Chemical Physics of Solids - Dresden (Germany), [2]DataQ Intelligence - Bayreuth (Germany)

Abstract

Outstanding properties of metallic delafossites , e.g. $PtCoO_2$, $PdCoO_2$, $PdRhO_2$, are largely attributed to exceptional quality of single crystals which are typically obtained without special efforts [1]. X-ray diffraction experiments on single crystals of very high quality containing heavy elements are typically suffering from severe extinction effects. The pronounced anisotropic structure is well reflected in a plate-like shape of the crystals. The associated severe absorption effects need to be taken into account with great care. Fortunately, we have been able to optimize crystal shape via micro-structuring using focused ion beam (FIB) techniques. Without any particularly sophisticated additional data treatment the structure refinement for $PdRhO_2$ revealed truly surprising results [2]. The anticipated "coloring" problem seems not to exist, as among the four obvious possibilities to occupy the two metal sites the 'correct' one clearly gives the best fit to the experimental data. In order to check if this unexpected result is just accidental, e.g. a consequence of remaining systematic errors in the data, several statistical and analytical tests were applied in order to unravel associated bias in the final structural model. Ultimate goal are clear indicators which are helping to improve the significance of experimentally derived parameters and to establish an approach to identify and experimentally minimize contributions from systematic errors in diffraction data.

References

[1] V. Sunko et al., *Phys. Rev. X* **10** (2020), 021018. DOI: 10.1103/PhysRevX.10.021018
[2] P. Kushwaha et al., *Cryst. Growth Des.* **17** (2017), 4144. DOI: 10.1021/acs.cgd.7b00418

Back to Table of contents

MS46 Reproducibility in crystallography

MS46-04

Reproducibility and the CSD

N.T. Johnson [1], S.C. Wiggin [1], I.J. Bruno [1], S.C. Ward [1]
[1]Cambridge Crystallographic Data Centre - Cambridge (United Kingdom)

Abstract

The Cambridge Structural Database (CSD) is a powerful resource for scientists around the world, containing over 1.1 million small molecule organic and metal-organic crystal structures.[1] As a repository for experimental structural data, it has an important role to play in helping the community set and maintain good data practises for sharing crystallographic data to help ensure that the data stored in the CSD is FAIR.[2]

Although FAIR data is important, we recognise that this does not completely capture our responsibility as a data repository. Alongside other factors, like securing the sustainability of our resource, we need to play our role to help ensure data is not only reusable but also reproducible. The CCDC's web deposition service encourages users to provide structure factor information, share a DOI to any raw experimental data, as well as supply additional experimental information (such as the crystallisation details or any properties of the material) to help capture as much metadata as possible. Through our education and outreach work, we aim to help scientists understand the importance of providing rich metadata and how it benefits them and the wider academic community.

We will highlight some of the steps we have taken to promote the reproducibility of experimental crystal structure data and beyond. We will also reflect on what we can learn from the CSD to help us on this journey and conclude by exploring some of the challenges and opportunities in striving towards the reproducibility of data.

References

1. Groom, C., Bruno, I., Lightfoot, M., & Ward, S. (2016). Acta Crystallographica Section B Structural Science, Crystal Engineering And Materials. 72, 171-179.
2. Helliwell, J. (2019). Structural Dynamics. 6, 054306.

Back to Table of contents

MS46 Reproducibility in crystallography

MS46-05

Analysis of common buffer molecules' conformations in ligand-protein complexes

J. Macnar [1], D. Brzezinski [2], D. Gront [3]
[1]College of Inter-Faculty Individual Studies in Mathematics and Natural Sciences, University of Warsaw - Warsaw (Poland), [2]Institute of Computing Science, Poznan University of Technology - Poznan (Poland), [3]Faculty of Chemistry, Biological and Chemical Research Center, University of Warsaw - Warsaw (Poland)

Abstract

Structural information about ligand-macromolecule complexes is key for biomedical sciences, especially for structure-based drug design and structural bioinformatics. Most of the experimental information about macromolecules complexed with ligands is coming from X-ray crystallography. The accessibility of synchrotron sources with modern appliances and software has resulted in the availability of approximately 190,000 structures deposited in the Protein Data Bank (PDB)[1]. Alas, a small number of the crystal structures available in the PDB are of suboptimal quality, including some with poorly identified and modeled ligands in protein-ligand complexes. BioShell 3.0[2] is an advanced structural bioinformatics toolkit that includes the analysis of ligand-protein complexes. By combining a graph-theoretical approach, kernel density estimators, bioinformatics methods, and chemical knowledge, we present an analysis verifying the accuracy of HEPES and MES molecules, frequent components of crystallization buffers, selected from PDB deposits. This analysis will lead to a better refinement of ligand-protein complexes.

References

[1] Berman HM, Westbrook J, Feng Z, Gilliland G, Bhat TN, Weissig H, Shindyalov IN, Bourne PE (2000) The Protein Data Bank. Nucleic Acids Res. 28:235–42.
[2] Macnar JM, Szulc NA, Kryś JD, Badaczewska-Dawid AE, Gront D (2020) BioShell 3.0: Library for Processing Structural Biology Data. Biomolecules 10:461

Back to Table of contents

MS47 New horizons in teaching crystallography in the 21st century

MS47-01

How should we teach crystallography?

J. Helliwell [1]
[1]*University of Manchester - Manchester (United Kingdom)*

Abstract

In this talk I reflect on how we teach crystallography. As educators we perform multiple roles providing courses to undergraduates and graduates as well as explaining our crystallographic research to the public and schoolchildren. Firstly then, an audience of undergraduates in practice presents different challenges to the teacher depending on whether they are physicists, chemists or biologists; these being the specific courses I have taught in the last 40 years or so and for which I, therefore, have extensive experience. Secondly, for graduate courses, these are organized by our crystallographic societies and associations. Such courses might be tailored to a given subject, as with undergraduates, or more likely might be for a broad, across the subjects, set of students. I have also taught on and/or organized these. Thirdly, as researchers, we are increasingly called upon to explain our research to broad audiences such as of the public, and/or of school children, and these cross sections of society do not necessarily have much science training, or if they have it has been long forgotten. As educators, I am sure all of us wrestle with just how we teach our crystallography concepts in these situations. Overall, we seek to ensure trust in our results and to inspire enthusiasm for what we study. In University of Manchester Open Days to prospective students and their parents I found it important to focus on tangible examples to begin with to capture the interest of the non-expert. Also explaining the same thing with multiple media helps; physical molecular models, crystals such as calcite and quartz, molecular graphics on a laptop, as well as books and journals. Diffraction patterns are the hardest to explain, and how we use them; the microscope analogy helps a lot.

References

Helliwell, J.R. (2016) Perspectives in Crystallography Chapter 1: Explaining 'What is crystal structure analysis? for a general audience. Published by CRC Press Taylor and Francis Group, Boca Raton, Florida, USA.
Helliwell, J.R. (2021) How should we teach crystallography? A review of teaching books' contents pages, Crystallography Reviews, 27:3-4, 135-145.

How should we teach crystallography to the Public

Back to Table of contents

MS47 New horizons in teaching crystallography in the 21st century

MS47-02

Communicating crystallography to little people, the Bragg your Patterns project

H. Maynard-Casely [1], O. Patel [2], S.R. Batten [3], L. Lin [4], A. Duncan [4]
[1]ANSTO - Sydney (Australia), [2]WEHI - Melbourne (Australia), [3]Monash University - Melbourne (Australia), [4]ICMS Australia - Melbourne (Australia)

Abstract

Many programs for science communication are targeted towards secondary school-ages (11 +), and for good reason as this is when students make choices on subjects, and it is vital that they are supported in their continuing science education. But are we missing out on inspiring them in the first place? Can we inspire students to see the bigger picture of science, beyond grades and textbooks? What if we run programs that target younger students, as well as the families around them? For younger students it is vital to have strong visual and hands on components to science communication activities. Crystallography lends itself very well to the former of these, but can we build resources to help the latter (hands on) component?

In 2023 we in Australia and New Zealand are hosting the International Crystallographic Congress (iucr2023.org) and have instigated the 'Bragg your Pattern' project to engage younger students in patterns and crystallography. The plan is that after 2023 we will have a group of established activities, a network of partners and an engaging website for the community to use going forward. We are planning a series of activities, starting in Australia's national Science Week in August 2022 and running through to the IUCr Congress in August 2023. In this contribution we will present our plans – our focus and planned activities and invite comment and participation from the ECM community.

Back to Table of contents

MS47 New horizons in teaching crystallography in the 21st century

MS47-03

An interactive tool to explore the two-dimensional Fourier transform

B. Stöger [1]
[1]*TU Wien - Vienna (Austria)*

Abstract

According to the kinematic model of diffraction, the diffraction pattern of an object is the square of the norm of its Fourier transform. Therefore, understanding the Fourier transform is crucial in understanding diffraction phenomena. However, the Fourier transform is highly counterintuitive. The best and perhaps only way to come to terms with the Fourier transform is by applying it.

In this context we developed a tool that can be used to interactively explore the two-dimensional Fourier transform in the classroom and demonstrate many of its properties. Two-dimensional source data (arbitrary images, polygons, lattices, Gaussian distributions) can be processed and combined (Fourier transformed, convoluted, added, multiplied, taken to the power, rotated, split into phases and magnitudes) in arbitrary ways and finally displayed.

Thus, numerous fundamental properties of the Fourier transform (linearity, scaling, origin shift, convolution theorem, complex numbers, Fourier transform of real and/or symmetric functions) as well as properties of the diffraction pattern (termination effects, Patterson function, displacement parameters, homometry, quasi-periodicity and countless more) can be demonstrated. For example, Fig. 1 shows the effect of Fourier termination, which might be due to an extreme absorption profile, on a benzene ring. Fig. 2 shows that the inverse Fourier transform of intensity data gives the autocorrelation (Patterson) function of the object under investigation.

All parameters, such as for example the shape of the absorption profile in Fig. 1, can be modified interactively and give immediate results even on modest hardware. Thus, questions and ideas that arise in class can be experimented with spontaneously. The high speed is due to usage of the FFTW library [1]. The code is available under an open-source license.

References

[1] M. Frigo, *Proceedings of the 1999 ACM SIGPLAN Conference on Programming Language Design and Implementation (PLDI '99)*, Atlanta, Georgia, May **1999**

Truncation effect owing to absorption

Back to Table of contents

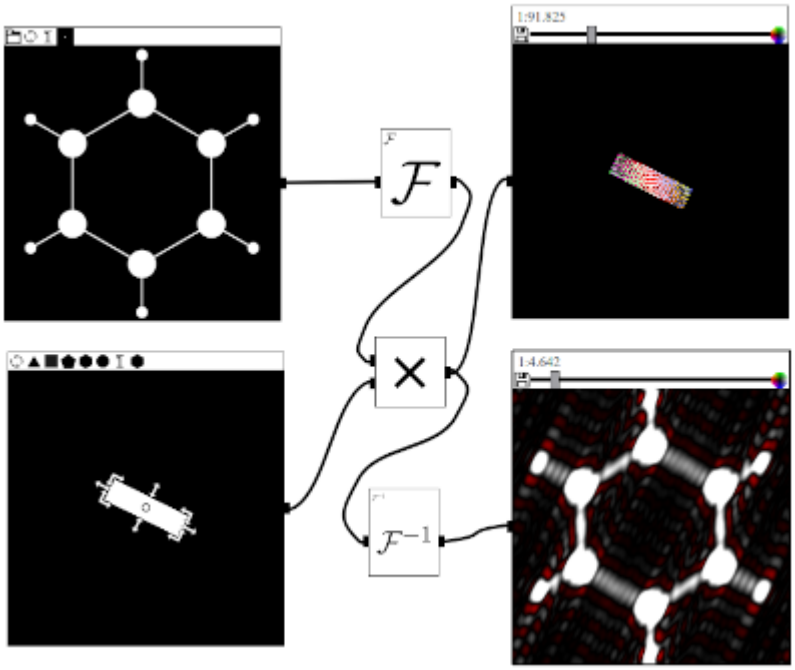

Patterson function

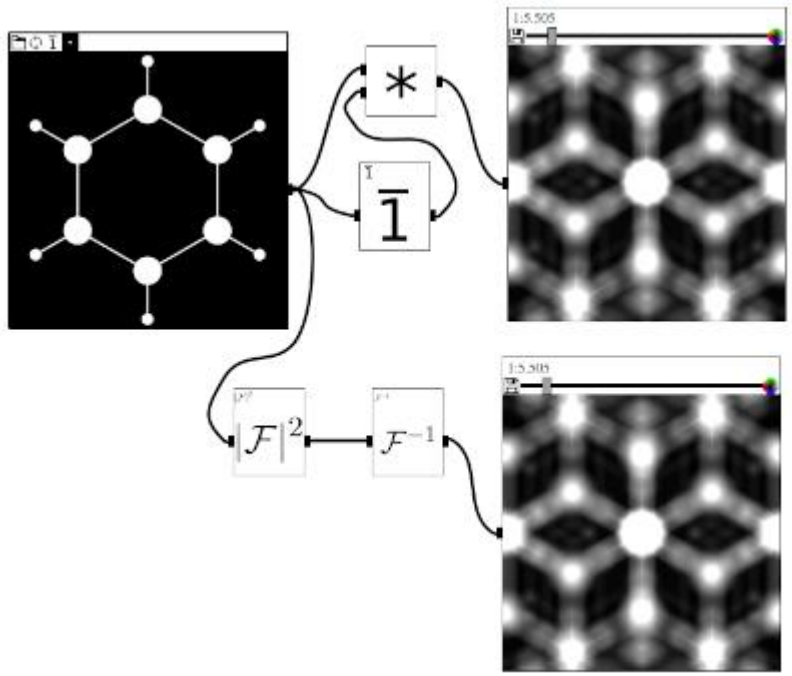

Back to Table of contents

MS47 New horizons in teaching crystallography in the 21st century

MS47-04

CCP4 Cloud as a system for crystallography teaching

M. Fando [1], E. Krissinel [2], I. Tews [3]

[1]Translational and Clinical Research Institute - Newcastle University, Framlington Place, Newcastle Upon Tyne (United Kingdom), [2]Scientific Computing Department, Science and Technology Facilities Council UK - Didcot (United Kingdom), [3]Faculty of Environmental and Life Sciences, University of Southampton - Southampton (United Kingdom)

Abstract

The impressive progress in macromolecular crystallography is owed in considerable part to advances in structure solution software. While this simplifies the structure determination process, the structure determination becomes more accessible to the newcomers. Today, in many cases, structures can be solved without understanding the theoretical underpinnings or an understanding of the methods and algorithms used. However, this creates a risk of diminishing expertise in both theoretical background and efficient use of new tools in software packages, such as CCP4.

CCP4 therefore invests considerable effort into educational programs and software documentation. The educational capabilities of the CCP4 Cloud [1], a new front-end for the CCP4 Software Suite [2], are presented here. CCP4 Cloud has attractive new features, which make it particularly suitable for teaching MX to a range of audience, from undergraduate students to experienced post-doctoral researchers:

1) Web interface, i.e no need for dedicated software installation or specialised computing facilities for most task;
2) Possibility of sharing structure solution projects with teachers and other students, and working on them simultaneously in real-time, irrespectively of geographic location;
3) Provision of CPU power for experimenting with complex automatic software and difficult data on a reasonable time scale;
4) Highly systematic approach to the development of structure solution projects with an ergonomic interface;
5) Developed documentation for individual structure solution tasks, MX methods, and techniques;
6) Availability of specific tutorials that include data, demo projects, as well as seed projects for guided training and self-education;
7) Open architecture for contributing to the documentation, tutorials;
8) Provision of mechanisms that allow creating setups for own crystallography courses and sharing them with colleague teachers.

Since its first release, CCP4 Cloud is routinely used for teaching crystallography at International Schools and Workshops (e.g. CCP4/DLS Virtual Workshop, South American School, IUCr CCP4/CCP-EM Workshop) as well as university courses. As a community-driven project CCP4 welcomes contributions to software documentation and educational materials from users of these teaching resources and the structural biology community.

References

[1] Krissinel, E., Uski, V., Lebedev, A., Winn, M., Ballard, C. (2018) Distributed computing for macromolecular crystallography. Acta Cryst. D74: 143-151; doi:10.1107/S2059798317014565;

[2] Winn M., Ballard C., Cowtan K., Dodson E., Emsley P., Evans P., Keegan R., Krissinel E., Leslie A., McCoy A., McNicholas S., Murshudov G., Pannu N., Potterton E., Powell H., Read R., Vagin A., Wilson K. (2011) Overview of the CCP4 suite and current developments. Acta Crystallogr D67(Pt 4):235-42. doi:10.1107/S0907444910045749

Back to Table of contents

MS47 New horizons in teaching crystallography in the 21st century

MS47-05

Ducks in space groups! Grasping arrangements of symmetry elements with 3D models

N. Graw [1], A. Krawczuk [1], D. Stalke [1]
[1]Georg-August-Universität - Göttingen (Germany)

Abstract

Symmetry considerations are vital in chemistry and even more so in crystallography.[1,2] In a typical chemistry curriculum, students are taught symmetry on a molecular basis. Learning and teaching about symmetry naturally requires spatial imagination. To develop and refine this ability, molceular models and model kits are of outmost importance and are readily available for a broad range of purposes[3]. Moving on to the solide state though, the variety of available or reported models becomces smaller. The description of crystalline matter from a crystallographer's point of view necessitates translational symmetry to be considered. From our teaching experience the introduction of translational symmetry components is difficult and something students struggle with. These difficulties culminate when it comes to the assembly of symmetry elements to give space groups.

We herein present large scale (i. e. typically 50 x 50 x 50 cm), physical 3D models of complete space groups (Fig. 1) to promote student's spatial imagination and to help understanding the construction of space groups by symmetry elements.[4] The models were designed and built to fulfil three basic requirements: (1) to be accurate space group representations containing conventional symbols to depict symmetry elements, (2) to visually resemble the conventional 2D space group notation used in the International Tables of Crystallography, Section A[5] if viewed along the respective crystallographic axis and, (3) to allow students to assemble asymmetric units within the unit cell by themselves. These models allow to connect conventional 2D depictions to a 3D representation, which can be moved and inspected by students. Furthermore being able to assemble objects freely within the models underlines the governing role of symmetry in solid-state structures.

While physical models have their benefits in face-to-face teaching, they are usually only available during a lecture. In order to create a digital version of the developed models that can be used by students outside the classroom (e.g. for revision at home), a virtual reality approach is pursued. The VR environment allows to keep the design principles and interactivity of the physical models, but makes them available at any time. First results of this work will be outlined.

Acknowledgements: We are grateful for the help of our faculty's workshop in constructing the models, and the help of Xiaobai Wang and the SUB Videoteam in taking the photographs. This work was funded by the Niedersächsisches Ministerium für Wissenschaft und Kultur (2018-2019, 2022-2023).

References

[1] H. H. Jaffé, *Symmetry in Chemistry*, New York: Dover Publications, **2013.**
[2] L. Glasser, *J. Chem Educ*. **1967**, *44*, 502.
[3] E. B. Flint, *J. Chem Educ*. **2011**, *88*, 907-909.
[4] N. Graw, D. Stalke, *J. Appl. Cryst*. **2022**, *55*, 144-148.
[5] C. P. Brock, T. Hahn, H. Wondratschek, U. Müller, U. Shmueli, E. Prince, A. Authier, V. Kopský, D. B. Litvin, E. Arnold, D. M. Himmel, M. G. Rossmann, S. Hall, B. McMahon, M. I. Aroyo, *International Tables for Crystallography*, International Union of Crystallography, Chester, England, **2016**.

Figure 1: Model of space group P21/c.

Back to Table of contents

Back to Table of contents

MS48 What should undergraduate students learn about crystallography?

MS48-01

Condensing a degree into a few hours of lectures

C.W. Lehmann [1]
[1]*Max-Planck-Institut für Kohlenforschung - Mülheim an der Ruhr (Germany)*

Abstract
Crystallography is a highly interdisciplinary subject and basic knowledge at the undergraduate level should be taught in chemistry, physics, biology, material sciences and other related subjects. With the exception of mineralogy, there is usually only very limited time available to introduce undergraduates to crystallography, which makes it even more important to bring across the right message. How to condense the knowledge of a whole degree into a few hours of lectures? As far as I am concerned symmetry and in particular solid state symmetry has to occupy a large portion of the available time. On the other hand, some form of motivation has to be given, such that students become interested in this field. As a chemist, chemical crystallography is introduced by reference to an actual publication, containing a molecular structure determined by X-ray crystallography and a more or less elaborate footnote or supplementary information, with the crystallographic details. The challenge put in front of the students is to decipher terms like triclinic, Fddd or GooF. Subsequently translational symmetry is introduced in contrast to the (hopefully) known point group symmetry of molecules. Wooden models of the crystal systems are distributed in the classroom and students are asked to identify symmetry elements, which are translated from Schoenflies to Hermann-Mauguin notation. After the introduction of screw-axes and glide-planes examples of space groups are discussed. This completes the symmetry part. The practical aspects of X-ray diffraction have to be given some room, in order to combine the material introduced so far to an actual experiment. This is then continued with a step-by-step process involving some simple geometrical diffraction considerations, a derivation of Bragg's law, the origin of diffraction intensities and finally a brief comment on the phase problem and its possible solution. At the end the results of a successful single crystal structure determination are re-examined and the cryptic terms of the initial crystallographic footnote are put into context. Time permitting differences and similiarities to powder diffraction are presented and further examples are given in the course. As part of this ECM-lecture there will be a discussion on the pros and cons of online teaching, including a review of personal experiences during three corona terms.

Back to Table of contents

MS48 What should undergraduate students learn about crystallography?

MS48-02

Developing a playful crystallography learning method for undergraduate students - Experiences from Benin

M.Y. Agbahoungbata [1], S.A. Bonou [1], T. D'almeida [1], C. Borna [1]
[1]X-TechLab / Agence de Développement de Sèmè City - Cotonou (Benin)

Abstract

The applications of crystallography and related sciences extend to many sectors of activity essential to the daily life including health, energy, agriculture, environment, etc. Most of these applications have the potential to contribute significantly to the development of Benin. However, the application of crystallography in these key sectors requires capacity building and training to allow for a real appropriation of the know-how in the field. To date, training in crystallography in national universities is very limited and is restricted to a general and exclusively theoretical courses within the classical physics and chemistry programs, which leave almost no room for practice or experimentation.
Changing this situation and “Fostering high-standard education, Technical and vocational training” becomes a national priority [1].
Within the “Agence de Développement de Sèmè City”, one of the flagship projects of Benin Government whose three pillars are Training, Research and Entrepreneurship, there is a platform named X-TechLab whose genesis, design and missions are closely related to the applications of x-ray techniques (crystallography, tomography, spectrometry, etc.). Thanks to an agreement between X-TechLab and the Chemistry Department of the University of Abomey-Calavi (UAC), the biggest public university in Benin, a training program titled “Initiation to Crystallography and crystal symmetry” has been carried out [2]. The aim was to endow the participants with the skills that will allow them to better understand the symmetry operations in crystallography. The training was fully practical and has been completed as tutorials. First, the students built their own motifs by following a guideline and then they used the motif for paving a plan using translation and inversion as symmetry operations (crystallographic group P1 and P2) to get some wallpapers. This led them to revise and to use most of the geometry rules they have studied in High school, and it allowed them to understand the key role played by symmetry operations in several fields such as architectural, aesthetics, etc.

The program has reached over a thousand learners, i.e. undergraduate students whose age range is approximately 18 to 22 years old. Almost 97% of them have succeeded the final test at the end of the training. The aim of this presentation is to highlight the impact of this learning method and its capability to raise students’ awareness about the importance of Crystallography & applications.

References

[1]https://www.gouv.bj/download/309/presentation_pag-2021-2026-seance-appropriation-06-01-2021.pdf
[2] https://www.xtechlab.co/en/general/breve-description-du-programme-de-formation-a-luac-benin/

X-TechLab training_UAC 2020

Back to Table of contents

Back to Table of contents

MS48 What should undergraduate students learn about crystallography?

MS48-03

Four Editions of Polish Crystallographic Olympiad

J. Chojnacki [1]
[1]*Gdańsk University of Technology - Gdańsk (Poland)*

Abstract

A brief overview of four editions of Polish Crystallographic Olympiad will be presented. Two modes of operation: stationary (I, II and III editions) and virtual (IV edition) will be compared and tentative conclusions drawn. Some attention will be given to the importance of type od tasks (tests, open questions, oral examination) and expected scope of knowledge for correct evaluation of crystallographic competences of the attenders. Finally, personal comments about required correlation with regular crystallography courses' programmes for undergraduate students will be given.

Logo of the IV Polish Crystallographic Olympiad

Back to Table of contents

MS48 What should undergraduate students learn about crystallography?

MS48-04

Using crystallographic databases in undergraduate education – The example of the Cambridge Structural Database

I. Gimondi [1], Y. Olatunji-Ojo [1], S.C. Ward [1]
[1]The Cambridge Crystallographic Data Centre - Cambridge (United Kingdom)

Abstract

Crystallography underpins and informs lots of different subjects, such as chemistry and biology, and fields, from pharmaceutical to agrochemical, from energy storage to the food industry. It is not a surprise then how extensively crystallographic data can be used in education.
In this talk we will focus on what undergraduate students can learn from crystallographic databases, taking the Cambridge Structural Database (CSD) and the associated software, the CSD Software as a case study.
First, we will present the CSD Teaching Subset and relevant teaching material, and how it can be used for teaching in combination with WebCSD and our visualization software Mercury. The CSD Teaching Subset is a collection of over 750 structures selected by the CCDC in collaboration with educators in the community, free for download and use in education. The structures in the CSD Teaching Subset are particularly good to demonstrate and exemplify a range of topics, from isomerism to chirality, from VSEPR theory to symmetry operations, from molecular interactions to reaction mechanisms. One of the strong suits that make using the CSD in education an asset is the possibility to visualise molecules and structures in 3D in Mercury. Indeed, being able to explain a three-dimensional concept in a 3D space rather than on a 2D board is considered of crucial importance by educators in the communities who shared their experiences with us.
Another great advantage of using crystal structures in teaching is to provide real examples and case studies, thus connecting theory to scientific challenges.
There is even more that undergraduates can learn from crystallographic databases and from the crystallographic community. Indeed, the crystallographic community is regarded as an example to follow for the way they format their data using the CIF file and how data are shared and maintained in databases such as the CSD. Using more advanced functionality form the CSD Software, students can learn how to search a database with over 1.1 million structures. This is per se a gateway for students to develop and improve a range of skills: from performing a literature review to good data sharing practices, and learning not only how to answer a research question, but also how to interrogate the data.
There is a lot that undergraduates can learn from crystallography and the crystallographic community and we believe that the use of crystallographic databases like the CSD can support them and enhance their learning.

References

- Gary M. Battle, Frank H. Allen, and Gregory M. Ferrence, *Journal of Chemical Education* **2010** *87* (8), 809-812. DOI: 10.1021/ed100256k
- Gary M. Battle, Frank H. Allen, and Gregory M. Ferrence, *Journal of Chemical Education* **2010** *87* (8), 813-818. DOI: 10.1021/ed100257t
- Gary M. Battle, Frank H. Allen, and Gregory M. Ferrence, *Journal of Chemical Education* **2011** *88* (7), 886-890. DOI: 10.1021/ed1011019
- Gary M. Battle, Frank H. Allen, and Gregory M. Ferrence, *Journal of Chemical Education* **2011** *88* (7), 891-897. DOI: 10.1021/ed1011025
- *CSD Educators blogs collection*. https://www.ccdc.cam.ac.uk/Community/blog/tags/CSD%20Educators

Back to Table of contents

MS48 What should undergraduate students learn about crystallography?

MS48-05

Teaching Crystallography Without a Diffractometer

A. Royappa [1]
[1]*University of West Florida - Pensacola (United States)*

Abstract

Crystallography has been, and remains, the principal method of obtaining structural information at the molecular level, and therefore is of paramount importance in chemistry (particularly synthetic chemistry). Since the Cambridge Structural Database (CSD) is the world's largest repository of crystal structures, with well over a million structures deposited, it is an invaluable resource for structural information on molecules. In the absence of a diffractometer (a common situation in universities the world over), the CSD is a valuable resource for teaching crystallographic concepts. It is used in several different courses across the undergraduate Chemistry curriculum at the University of West Florida, a primarily undergraduate institution. In this presentation, we will describe how the CSD is integrated into our lecture and laboratory courses as well as into our research programs.

Back to Table of contents

POSTERS PRESENTATION

MS01 MX/Cryo-EM software development

MS01-1-1 Analytic representation of inhomogeneous-resolution density maps and real-space refinement

A. Ourjoumtsev [1], L. Urzhumtseva [2], V.Y. Lunin [3]
[1]IGBMC / UdL - Illkirch / Nancy (France), [2]IBMC - Strasbourg (France), [3]IMPB, Keldysh Institute, RAS - Pushchino (Russian Federation)

Abstract
Real-space refinement of atomic models improves such models by their fit to experimental density maps in crystallography or to scattering electrostatic potential maps in cryo electron microscopy. This procedure has a number of advantages in comparison with reciprocal-space refinement, is complementary to it in crystallographic studies and is the principal technique in cryo EM. An accurate real-space refinement of atomic models can be done by comparison of the model maps with the experimental ones, when the former mimic imperfections of the latter, mainly a limited resolution and an atomic disorder. Model maps can be calculated as a sum of atomic contributions, i.e., atomic images at given conditions. In three-dimensional space, such image is represented by a peak surrounded by spherically symmetric Fourier ripples. To describe a solitary spherical wave, a function Ω(x;μ,v) with required properties has been especially designed (Urzhumtsev & Lunin, 2022). A three-dimensional interference function G(x), which is an image of an immobile point atom, can be highly accurately decomposed into a sum of 'shell' terms, each being a function Ω(x;μ,v) with appropriate parameters. This decomposition leads to a series of conclusions (Urzhumtsev & Lunin, 2022):
- An image of an atom of any chemical type at any resolution and with any displacement factor can be presented analytically as a sum of Ω(x;μ,v) terms.- Atomic displacement parameter and resolution are arguments of these analytic functions; function parameters are coefficients of a multi-Gaussian approximation to the atomic scattering factors and those of the G(x) shell-decomposition, both sets are known.- Model density map, even when its resolution varies from one its region to another, can be calculated in a single run, with no Fourier transform used.- In each its point, a model density map becomes an analytic function of atomic parameters, i.e., their coordinates, displacement parameter and the local resolution associated now with atom.- As a consequence, for a score function describing the model-to-experimental maps fit, its partial derivatives with respect to all atomic parameters become also analytic functions; all these parameters, including the local resolution, can be really 'real-space' refined using gradient methods, with no need in structure factors and Fourier transform.- Being associated with atoms, the local resolution can be reported in the PDB files together with the coordinates and displacement factors; this value is a measure of confidence of the atomic parameters charactering the map region in which the atom has been identified.- When the variation of the local resolution can be neglected, one can use a simplified form of a decomposition of images at a given resolution into a sum of Ω(x;μ,v); this reduces the number of terms, in turn reducing CPU time and improving convergence; this is an option at earlier and intermediate stages of refinement.
To decompose oscillating spatial curves, such as atomic images of a limited resolution, programs in fortran77, their equivalents in python3, as well as a GUI version, have been developed. Implementation of these algorithms into phenix.refine (Afonine et al., 2012) is in progress.

References
Afonine, P.V., Echols, N., Grosse-Kunstleve, R.W., Headd, J.J., Moriarty, N.W., Mustyakimov, M., Terwilliger, T., Urzhumtsev, A., Zwart, P.H., Adams, P.D. (2012). "Toward automated crystallographic structure refinement with phenix.refine". Acta Cryst. D68, 352-367.
Urzhumtsev, A.G. & Lunin, V.Y. (2022). "Analytic representation of inhomogeneous-resolution maps of three-dimensional scalar fields". BioRxiv, 10.1101/2022.03.28.486044

Back to Table of contents

MS01 MX/Cryo-EM software development

MS01-1-2 Trends in macromolecular structure data across 50 years of the Protein Data Bank #MS01-1-2

D. Harrus [1], C. Wwpdb Consortium [2]
[1]EMBL-EBI - Cambridge (United Kingdom), [2]wwPDB (United Kingdom)

Abstract
The worldwide PDB (wwPDB) is the international consortium responsible for managing the Protein Data Bank (PDB) - the single global repository for three-dimensional structures of biological macromolecules and their complexes. Over the past decade, the size and complexity of macromolecular complexes deposited to the PDB has increased significantly. The PDB archive now contains more than 190,000 experimentally determined structures of biological macromolecules, all of which are publicly accessible without restriction. These structures provide essential information worldwide, to a diverse user community. There are more than 2 billion downloads of data files from the PDB archive each year, with more than 1 million unique IP addresses accessing the archive within the same period.
In 2014, in an effort to fulfil the evolving archive requirements of the scientific community over the coming decades, the wwPDB partners launched OneDep, a global unified system for deposition, biocuration, and validation of macromolecular structures. It replaced legacy pipelines across PDB, EMDB, and BMRB deposition sites and is able to interface with other archival resources. Since then, the goal of the developments of the OneDep system has been to ensure data quality and completeness across all three archives, while supporting growth in the number and complexity of depositions.
In 2021, we celebrated 50 years of the PDB archive, making it one of the longest-running open access scientific databases. Throughout these 50 years, there has been significant evolution of the data in the PDB archive. This evolution has been driven by a number of factors including development in structural determination techniques, adaptation of biocuration practices, and increase in data capture via updated file formats.
In this poster, we present some of the key trends in data across the PDB archive, highlighting how structural biology data has changed over time and how wwPDB biocuration practices have adapted to handle these changes.

References
The Protein Data Bank Archive. Methods in Molecular Biology. 01 Jan 2021, 2305:3-21DOI: 10.1007/978-1-0716-1406-8_1 PMID: 33950382

Modernized uniform representation of carbohydrate molecules in the Protein Data Bank. Glycobiology. 01 Sep 2021, 31(9):1204-1218DOI: 10.1093/glycob/cwab039 PMID: 33978738

Enhanced validation of small-molecule ligands and carbohydrates in the Protein Data Bank. Structure. 02 Mar 2021, 29(4):393-400.e1DOI: 10.1016/j.str.2021.02.004 PMID: 33657417

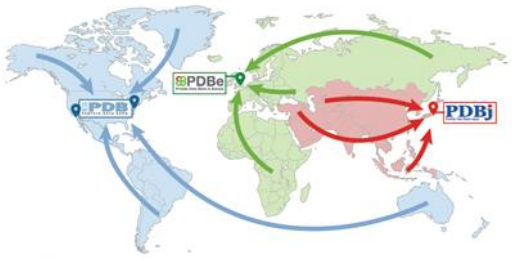

WORLDWIDE PDB
PROTEIN DATA BANK

Back to Table of contents

MS01 MX/Cryo-EM software development

MS01-1-3 Search for optimal phasing parameters with SHELIXIR
#MS01-1-3

P. Kolenko [1], J. Stránský [2], T. Kovaľ [2], M. Malý [1], J. Dohnálek [2]
[1]Czech Technical University in Prague - Prague (Czech Republic), [2]Institute of Biotechnology CAS - Vestec near Prague (Czech Republic)

Abstract
Experimental phasing represents a minority of phasing procedures in macromolecular crystallography. Nevertheless, it is an inevitable option when no model suitable for the molecular replacement method is available or the diffraction limit of the crystal is too low for the ab initio methods.
Experimental phasing frequently requires data collection at non-standard wavelengths, special crystal treatment, or multiple combinations of both. Data collection at multiple wavelengths is time consuming, and a special crystal treatment usually represents a work with chemicals that burden the environment. Therefore, minimization of both time and consumption is the desired approach. In both cases, optimized phasing pipelines may help. Especially when difficult experimental phasing at synchrotron is performed.
SHELIXIR [1] is a simple and efficient tool for both routine and difficult experimental phase-problem solutions. It utilizes the *SHELX C/D/E* [2] program package. It works as a pipeline that links the processes together and provides the user with a comprehensive output in form of an HTML page. Beyond the standard protocols, *SHELIXIR* can screen through the following parameters: space groups, solvent content, and high- and low-resolution diffraction limit.
Parallelized screening for optimal solvent content minimizes the computational time. Moreover, it helps to find better experimental phases using the parameter that can significantly differ from the real solvent content (by more than 16%). In some cases, the screening played a crucial role in successful experimental phasing.

References
[1] P. Kolenko, J. Stransky, T. Koval, M. Maly, J. Dohnalek. (2021). *J. Appl. Cryst.*, **54**, 996-1005.
[2] I. Uson & G.M. Sheldrick (2018). *Acta Cryst. D***74**, 106-116.

Examples of screening procedures.

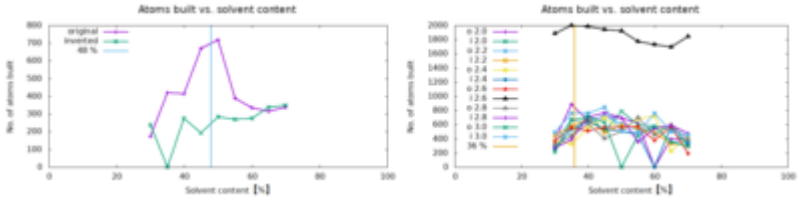

Back to Table of contents

MS01 MX/Cryo-EM software development

MS01-2-1 PDBe-KB: collaboratively defining the biological context of structural data
#MS01-2-1

D. Armstrong [1]
[1]PDBe (EMBL-EBI) - Cambridge (United Kingdom)

Abstract
AbstractThe Protein Data Bank in Europe – Knowledge Base (PDBe-KB, https://pdbe-kb.org) is a collaborative resource between world-leading specialist data resources striving towards a two-fold goal: (i) to increase the visibility and reduce the fragmentation of annotations contributed by specialist data resources, and to make these data more findable, accessible, interoperable and reusable (FAIR) and (ii) to place macromolecular structure data in their biological context, thus facilitating their use by the broader scientific community in fundamental and applied research. Since we described PDBe-KB in 2019, there have been significant improvements in the variety of available annotation data sets and user functionality. Here we highlight all these additional annotations and new features such as a bulk download data service and a novel superposition service that generates clusters of superposed protein chains weekly for the whole PDB archive.
Scientific Justification To date, the PDB contains over 190,000 structures of 57,000 distinct proteins. However, structures by themselves are not necessarily of intrinsic biological value, unless they can be related to additional functional information. Many data resources can derive additional annotations related to structures. While most of these annotations are openly accessible, they may not be easily findable, and the lack of standard data formats often hinders interoperability and reusability. To make these annotations FAIR (i.e. findable, accessible, interoperable, reusable), we established PDBe-KB in 2018 through a global collaboration between PDBe and leading specialist data resources. Currently, PDBe-KB integrates data from 30 partner resources providing over 1.2 billion residue-level annotations. These annotations are made available on PDBe-KB web-pages, programmatically via an API, and distributed as a Neo4J graph database.
The PDBe-KB web pages- Aggregated Views of Proteins recently reached over a million unique users since its first release. These aggregated views offer a “one-stop-shop” to users providing a comprehensive view of the functional context of the protein structure. We are actively updating these pages, and a few recent features include (i) a superposition service to visualise protein chains clustered by structural similarity; (ii) annotations for small molecules and macromolecular interaction partners. (iii) a section highlighting all the mature and processed proteins for a polyprotein; and (iv) a bulk download service that provides easy access to all the coordinate files, validation reports, sequences for a given proteinECCB is a great platform to showcase all these new features to the scientific community. It provides a good opportunity to enhance further collaborations and collate valuable feedback which will help us improve our PDBe-KB service offerings.

References
PDBe-KB consortium, PDBe-KB: collaboratively defining the biological context of structural data Nucleic Acids Research, Database Issue (2022)
PDBe-KB consortium, PDBe-KB: a community-driven resource for structural and functional annotations. Nucleic Acids Research, Database Issue (2020)

Overview of PDBe-KB

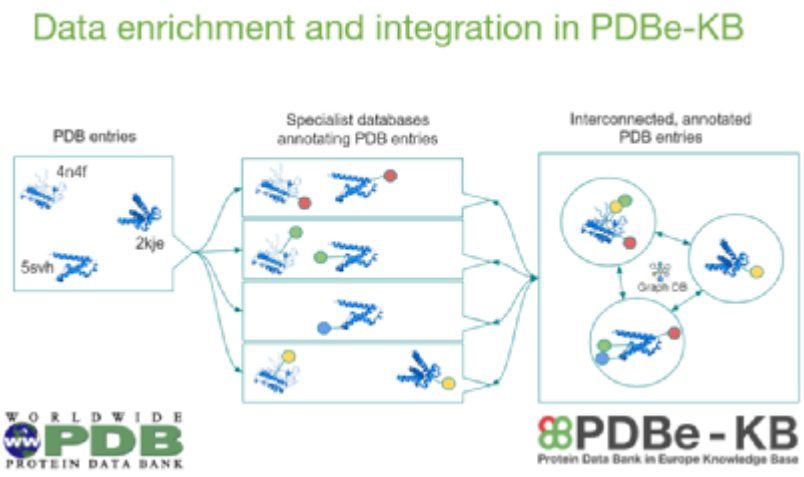

Back to Table of contents

MS01 MX/Cryo-EM software development

MS01-2-2 Efficient automated matching of protein structural entities from a database to partitioned cryo-EM maps #MS01-2-2

L. Elliott [1]
[1]University of liverpool - Liverpool (United Kingdom)

Abstract
Cryo-electron microscopy (Cryo-EM) has undergone a recent resolution revolution; however, the majority of maps deposited are below 3.0Å resolution. The current methods for model generation, such as ARP/wARP, rely on high resolution maps (<4.0Å) and take hours to complete. Here is proposed a pipeline that takes an input Cryo-EM map and returns a protein structure. The input map could be over a range of resolutions and will be sequence independent. The proposed pipeline starts by model segmentation, a method of splitting Cryo-EM map files into components of a larger macro assembly or 'Segments'. Once the map has been segmented, each segment will be run in a database search to find corresponding protein structures. The two search methods currently being investigated are 3D Zernike Descriptors: describing the shape of the protein map which is invariant to rotation; and FTIP, a software which finds representative points on the map to describe its shape. The top ranking matches for each segment will then undergo fitting and metrics from this process will determine a correct match or not. From this matching models will be determined and a structure realting to the input map will be outputted.

Back to Table of contents

MS02 Infection and Disease/hot structures

MS02-1-1 Disulfide bond formation between T-cell receptor and peptide epitope lowers the threshold of activation #MS02-1-1

C. Szeto [1], P. Zareie [2], A. Riboldi-Tunnicliffe [3], N. La Gruta [2], S. Daley [4], S. Gras [1]
[1]Department of Biochemistry and Chemistry, La Trobe Institute for Molecular Science, La Trobe University - Bundoora (Australia), [2]Infection and Immunity Program, Monash Biomedicine Discovery Institute and Department of Biochemistry and Molecular Biology, Monash University - Clayton (Australia), [3]Australian Synchrotron, Australian Nuclear Science and Technology Organisation - Clayton (Australia), [4]Centre for Immunology and Infection Control, School of Biomedical Sciences, Faculty of Health, Queensland University of Technology - Brisbane City (Australia)

Abstract
The immune system is vigilant in detecting foreign pathogens. Our cells present peptide epitopes (p) atop Major Histocompatibility Complex (MHC) glycoproteins on the cell's surface. They are monitored by T cells that use their unique T cell receptors (TCRs) to recognize and bind to pMHCs, where the quality of binding influences T cell activation. Activated T cells can eliminate and control infection, clearing the body of infectious diseases. The binding parameters that dictate T cell activation for this inter-cellular TCR-pMHC interaction remains unclear. The long reigning hypothesis is that a binding affinity threshold controls T cell activation. However, T cell therapeutics that engineer T cell receptors to increase binding affinity have had limited success in generating safe and efficacious therapeutics. Here, we have engineered a disulfide bond (S-S) between a TCR and peptide epitope within a well-studied TCR-pMHC model. The formation of this S-S bond was validated using X-ray crystallography and biophysical assays. We show that the covalent S-S bond does not allow dissociation of the TCR-pMHC complex and indefinitely prolongs the bond lifetime. This leads to a 50-fold increase in sensitivity for T cell activation, without loss of epitope specificity or change in binding affinity. Thus, we reveal a novel design for the engineering of T cell receptors that could be useful in future T cell therapeutics.

Back to Table of contents

MS02 Infection and Disease/hot structures

MS02-1-2 More than a single effect by a single point mutation: Molecular dynamics simulation of NPC1 #MS02-1-2

H. Yoon [1], J. Jeong [2], H.H. Lee [1], S. Jang [2]
[1]Seoul National University - Seoul (Korea, Republic of), [2]Sejong University - Seoul (Korea, Republic of)

Abstract

The Niemann-Pick type C1 (NPC1) protein is one of the key players of cholesterol trafficking from the lysosome and its function is closely coupled with the Niemann-Pick type C2 (NPC2) protein. The dysfunction of one of these proteins can cause problems in the overall cholesterol homeostasis and leads to a disease, which is called the Niemann-Pick type C (NPC) disease. The parts of the cholesterol transport mechanism by NPC1 have begun to recently emerge, especially after the full-length NPC1 structure was determined from a cryo-EM study, so many details about the overall cholesterol trafficking process by NPC1 still remain to be elucidated. Notably, the NPC1 could act as one of the target proteins for the control of an infectious disease due to its role as the virus entry point into the cells as well as for cancer treatment due to the inhibitory effect of tumor growth. A mutation of NPC1 can leads to dysfunctions and understanding this process can provide valuable insights into the mechanisms of the corresponding protein and the therapeutic strategies against the disease that are caused by the mutation. It has been found that patients with the point mutation R518W (or R518Q) on the NPC1 shows the accumulation of lipids within the lysosomal lumen. In this paper, we report how the corresponding mutation can affect the cholesterol transport process by NPC1 in the different stages for a proper function by the molecular dynamics simulations. The simulation results show that the point mutation intervenes at least at three different steps during the cholesterol transport by NPC1 and NPC2 in combination, which includes the association step of NPC2 with the NPC1 transfer of the cholesterol step from NPC2 to NPC1-NTD and the passage within the NPC1 via a channel. The detailed analysis of the resulting simulation trajectory reveals the important structural features that are essential for the proper functioning of the NPC1 for the cholesterol transport, and it shows how the overall structure, which thereby include the function, can be affected by a single mutation.

References

[1] Saha, P., et al. (2020) Inter-domain dynamics drive cholesterol transport by NPC1 and NPC1L1 proteins. Elife 9, e57089.
[2] Dubey, V., et al. (2020) Cholesterol binding to the sterol-sensing region of Niemann Pick C1 protein confines dynamics of its N-terminal domain. PLoS Comput Biol 16, e1007554.

Back to Table of contents

MS02 Infection and Disease/hot structures

MS02-1-3 Structural bases for the higher adherence to ACE2 conferred by the SARS-CoV-2 spike Q498Y substitution
#MS02-1-3

E. Erausquin [1], J. López-Sagaseta [1]
[1]1 Unit of Protein Crystallography and Structural Immunology, Navarrabiomed, 31008, Navarra, Spain. 2 Public University of Navarra (UPNA), Pamplona, 31008, Navarra, Spain. 3 Navarra University Hospital, Pamplona, 31008, Navarra, Spain. - Pamplona (Spain)

Abstract
A remarkable amount of SARS-CoV-2 variants and other yet unmonitored lineages harbour amino acid substitutions with potential to modulate the interface between the spike receptor binding domain (RBD) and its receptor ACE2. The naturally-occurring Q498Y substitution currently present in circulating SARS-CoV-2 variants has drawn the attention of several investigations[1-4], and recent studies have detected this substitution in previously unidentified SARS-CoV-2 lineages found in wastewater samples of New York City[5].
To decipher the structural bases that underlie the enhanced affinity attributed to this substitution, I have crystallized the RBD Q498Y mutant bound to its human ACE2 receptor. Compared to the structure with its wild type counterpart, the RBD Q498Y:ACE2 complex reveals conservation of major H-bond interactions and a more populated, non-polar set of contacts mediated by the bulky side chain of Tyr498, as well as one additional π-π stacking interaction, that collectively lead to this increase in the binding affinity.
Our studies contribute to a deeper understanding on the impact of a relevant mutation present in current SARS-CoV-2 circulating variants and which might lead to stronger host-pathogen interactions.

References
1. Yi, C., Sun, X., Ye, J., Ding, L., Liu, M., Yang, Z., Lu, X., Zhang, Y., Ma, L., Gu, W., Qu, A., Xu, J., Shi, Z., Ling, Z. & Sun, B. *Key residues of the receptor binding motif in the spike protein of SARS-CoV-2 that interact with ACE2 and neutralizing antibodies* (2020). Cell. Mol. Immunol. 17, 621–630 doi: 10.1038/s41423-020-0458-z
2. Capponi, S., Wang, S., Navarro, E. J. & Bianco, S. *AI-driven prediction of SARS-CoV-2 variant binding trends from atomistic simulations* (2021). Eur. Phys. J. E. Soft Matter. 44, 123 doi: 10.1140/epje/s10189-021-00119-5
3. Ahamad, S., Kanipakam, H. & Gupta, D. *Insights into the structural and dynamical changes of spike glycoprotein mutations associated with SARS-CoV-2 host receptor binding* (2022). J. Biomol. Struct. Dyn. 40, 263–275 doi: 10.1080/07391102.2020.1811774
4. Li Y, Zhang Z, Yang L, Lian X, Xie Y, Li S, Xin S, Cao P, Lu J. *The MERS-CoV Receptor DPP4 as a Candidate Binding Target of the SARS-CoV-2 Spike* (2020) iScience. Jun 26;23(6):101160. doi: 10.1016/j.isci.2020.101160
5. Smyth, D. S., Trujillo, M., Gregory, D. A., Cheung, K., Gao, A., Graham, M., Guan, Y., Guldenpfennig, C., Hoxie, I., Kannoly, S., Kubota, N., Lyddon, T. D., Markman, M., Rushford, C., San, K. M., Sompanya, G., Spagnolo, F., Suarez, R., Teixeiro, E., Daniels, M., Johnson, M. C. & Dennehy, J. J. *Tracking cryptic SARS-CoV-2 lineages detected in NYC wastewater* (2022). Nat. Commun. 13, 635. https://doi.org/10.1038/s41467-022-28246-3

Back to Table of contents

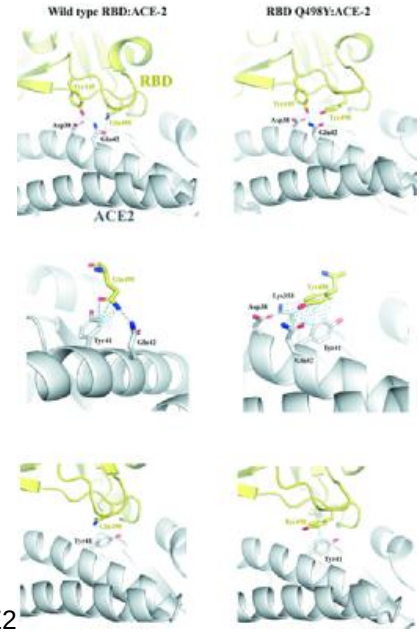

Interatomic contacts between RBD Q498Y and ACE2

Back to Table of contents

MS02 Infection and Disease/hot structures

MS02-1-4 Structure of the diabetogenic I-Ag7 receptor with a bound hybrid insulin peptide
#MS02-1-4

E. Erausquin [1], P. Serra [2], D. Parras [2], P. Santamaria [3], J. López-Sagaseta [1]
[1]1Unit of Protein Crystallography and Structural Immunology, Navarrabiomed, 31008, Navarra, Spain. 2Public University of Navarra (UPNA), Pamplona, 31008, Navarra, Spain. 3Navarra University Hospital, Pamplona, 31008, Navarra, Spain. - Pamplona (Spain), [2]Institut D'Investigacions Biomèdiques August Pi i Sunyer (IDIBAPS), Barcelona, Spain. - Barcelona (Spain), [3]4Institut D'Investigacions Biomèdiques August Pi i Sunyer (IDIBAPS), Barcelona, Spain. 5Julia McFarlane Diabetes Research Centre (JMDRC) and Department of Microbiology, Immunology and Infectious Diseases, Snyder Institute for Chronic Diseases and Hotchkiss Brain Institute, Cumming School of Medicine - Barcelona (Spain)

Abstract
The NY4.1 T cell clone was originally isolated from pancreatic islet-infiltrating lymphocytes from nonobese diabetic (NOD) mice[1]. Recently, evidence was provided for promiscuous recognition of several different hybrid insulin peptides (HIPs) by the highly diabetogenic, I-Ag7-restricted 4.1-T cell receptor (TCR)[2]. In TCR-transgenic NOD mice, recognition of these peptide-MHCII complexes triggers the activation and recruitment of 4.1-CD4+ T cells into pancreatic islets, leading to rapid destruction of pancreatic beta cells and over type 1 diabetes within the first few weeks of life.
To understand, at an atomic level, how this diabetogenic receptor binds HIP antigens, I solved the crystal structure of an agonistic HIP/I-Ag7 complex at 1.8 Å resolution.
The HIP39 epitope is tightly packaged into the peptide-binding groove of the MHCII molecule through a nourished net of interactions with both the I-Aad and I-Abg7. These include Van der Waals (VDW), hydrogen bonding (H-bonds), ionic interactions (salt bridges) and water bridges. Positions P5, P7 and P8 in the peptide are occupied by acidic residues (Glu/Glu/Asp) that expose side chains outwardly, making them available for potential interactions with cognate TCRs. Importantly, these acidic residues and positions are highly abundant in HIPs derived from a human lymphoblastoid cell line[3].
Altogether, this crystal structure provides high-resolution data that enable an accurate definition of the HIP/I-Ag7 binding signature and contribute to a better understanding on how HIP antigens bind diabetogenic receptors. These complexes are known to trigger T cell autoreactivity to self tissues in type I diabetes.

References
1. Verdaguer J., Schmidt D., Amrani A., Anderson B., Averill N., Santamaria P.; *Spontaneous Autoimmune Diabetes in Monoclonal T Cell Nonobese Diabetic Mice.* J Exp Med 17 November 1997; 186 (10): 1663–1676. doi: https://doi.org/10.1084/jem.186.10.1663
2. Parras D, Solé P, Delong T, Santamaría P, Serra P. Recognition of Multiple Hybrid Insulin Peptides by a Single Highly Diabetogenic T-Cell Receptor. Front Immunol. 2021 Aug 30;12:737428. doi: 10.3389/fimmu.2021.737428
3. Tran, M.T., Faridi, P., Lim, J.J. et al. T cell receptor recognition of hybrid insulin peptides bound to HLA-DQ8. Nat Commun 12, 5110 (2021). https://doi.org/10.1038/s41467-021-25404-x

Structure of the 4.1-TCR:HIP39/I-Ag7 complex

Back to Table of contents

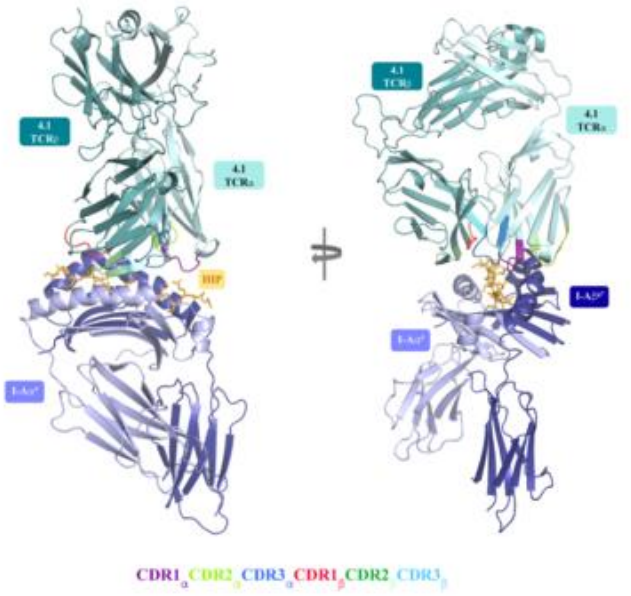

Back to Table of contents

MS02 Infection and Disease/hot structures

MS02-1-5 Schistolysin 2, a new parasporin-related protein from Schistosoma mansoni: structural and functional studies
#MS02-1-5

A. Parpinel [1], P. Poteaux [2], S. Dos-Reis [1], C. Bon [1], B. Gourbal [2], L. Mourey [1], D. Duval [2], L. Maveyraud [1]
[1]Institut de Pharmacologie et de Biologie Structurale - CNRS UMR 5089 - Toulouse (France), [2]Laboratoire Interaction Hôtes-Pathogènes-Environnements - CNRS UMR 5244 - Perpignan (France)

Abstract
Schistolysin 2 is a member of one of the two aerolysin-related families recently discovered by David Duval and colleagues [1, 2]: the Schistolysins and the Biomphalysins. They identified 2 genes in *Schistosoma mansoni* and 23 in *Biomphalaria glabrata*, respectively. The snail *Biomphalaria glabrata* is the intermediary host of the worm *Schistosoma mansoni,* the causative agent of intestinal schistosomiasis [3]. This neglected tropical disease affected 236 million people worldwide in 2019, 90% in sub-Saharan Africa. In 2020, the WHO called for new therapies to support the action of Praziquantel, the recommended treatment against all forms of schistosomiasis, and eliminate the disease [4].
Our goal is to determine the biochemical and structural properties, as well as the biological role and activity, of proteins from both families, in order to characterise their structure-function relationships. To date, the structural study of Schistolysin 2 is the most advanced. It is produced as a stable octamer, the crystal structure of which has been determined at 2.6 Å resolution. SAXS experiments brought complementary data.
Two questions arise: does the observed octamer correspond to a (pre)pore state and does it possess cytotoxic activity? According to the comparison carried out using the DALI server, the most structurally similar protein is a non-toxic crystal protein from *Bacillus thuringiensis* (PDB: 2D42) [5]. Interestingly, this protein and Schistolysin 2 display a very similar structure to the *Clostridium perfringens* epsilon toxin (PDB: 1UYJ), an aerolysin-like β-pore-forming toxin [6]. To determine the role and activity of Schistolysin 2, its gene expression is studied by in situ hybridization and its production by immunofluorescence assays in the adult worm. In addition, cellular toxicity tests with the purified form are being carried out. The combination of structural and functional data should allow us to understand the role of this protein in *Schistosoma mansoni*, and possibly help in the development of new therapies against schistosomiasis or for other applications.

References
[1] Galinier, R. et al. Biomphalysin, a New β Pore-forming Toxin Involved in Biomphalaria glabrata Immune Defense against Schistosoma mansoni. PLOS Pathogens 9, e1003216 (2013).
[2] Pinaud, S. and al. New Insights Into Biomphalysin Gene Family Diversification in the Vector Snail Biomphalaria glabrata. Front. Immunol. 12, 635131 (2021).
[3] McManus, D. P. and al. Schistosomiasis. Nat Rev Dis Primers 4, 1–19 (2018).
[4] Geneva: World Health Organization. Ending the neglect to attain the Sustainable Development Goals: a road map for neglected tropical diseases 2021–2030. (2020). Licence: CC BY-NC-SA 3.0 IGO.
[5] Akiba, T. et al. Nontoxic crystal protein from Bacillus thuringiensis demonstrates a remarkable structural similarity to β-pore-forming toxins. Proteins: Structure, Function, and Bioinformatics 63, 243–248 (2006).
[6] Cole, A. R. et al. Clostridium perfringens ε-toxin shows structural similarity to the pore-forming toxin aerolysin. Nat Struct Mol Biol 11, 797–798 (2004).

Orthogonal views of the octameric Schistolysin 2.

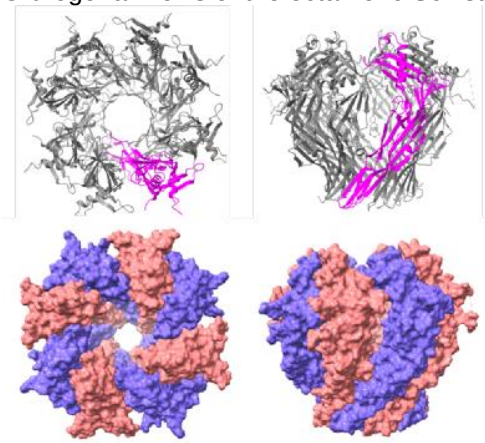

Back to Table of contents

MS02 Infection and Disease/hot structures

MS02-1-6 A highly specific N7-guanine RNA cap methyltransferase in an unusual locus of large RNA virus genome #MS02-1-6

A. Shannon [1], B. Sama [1], P. Gauffre [1], B. Makem-Tamekem [2], E. Decroly [1], B. Canard [1], F. Ferron [1]
[1]CNRS - UMR7257 - MARSEILLE (France), [2]Aix-Marseille Université - MARSEILLE (France)

Abstract
The order Nidovirales is a diverse group of (+)RNA viruses, with a common genome organization and conserved set of replicative and editing enzymes (1). In particular, RNA methyltransferases plays a central role in mRNA stability and are considered beneficial to genome expansion (2). In Coronaviridae ; the best Nidovirales characterized family ; two separate methytransferases, nsp14 (3,4) and nsp16 (5-7), perform the RNA-cap N7-guanine and 2'-OH methylation respectively, for generation of the m7GpppNm type I cap structure (8). Both enzymes are located in the ORF1b genomic region. The other Nidovirales families are however far less well characterized, and are sequentially distant making the identification of RNA / N7-guanine methyltransferase signature sequence difficult, obscuring our understanding about how RNA-caps are N7-methylated for these families. White Bream virus a Tobaniviridae, was lacking a N7-MTase signature at the expected genomic location. Recently it was proposed its presence in ORF1a, an odd genomic location for such an enzyme (9). Here, we demonstrate that the enzyme activity is N7-specific, and present the structure of a new N7-Mtase. This discovery helps to define better the N7-MTase family in its whole and we discuss the evolutionary advantages of such an appearance in this location of the genome

References
1. A.E. Gorbalenya et al. Virus Res 2006, 17,17–37.
2. F. Ferron, et al. . Trends Biochem Sci. 2021 Nov;46(11):866-877.
3. Y. Ma, et al. Proc. Natl. Acad.Sci. U.S.A., 2015 112, 9436–9441.
4. F. Ferron,et al. Proc. Natl. Acad. Sci.U.S.A. 2018, 115, E162–E171.
5. E. Decroly,et al. J. Virol.,2008, 82, 8071–8084.
6. E. Decroly,et al. PLoS Pathog., 7, e1002059. 2011
7. Y. Chen, et al. PLoS Pathog., 7, e1002294. 2011
8. E. Decroly,F. Ferron, J. Lescar,J. and B. Canard, Nat. Rev.Microbiol 2011, 10, 51–65.
9. F. Ferron et al., NAR Genomics and Bioinformatics, 2020, Vol. 2, No. 1 1-10

Tobaniviridae N7-MTase

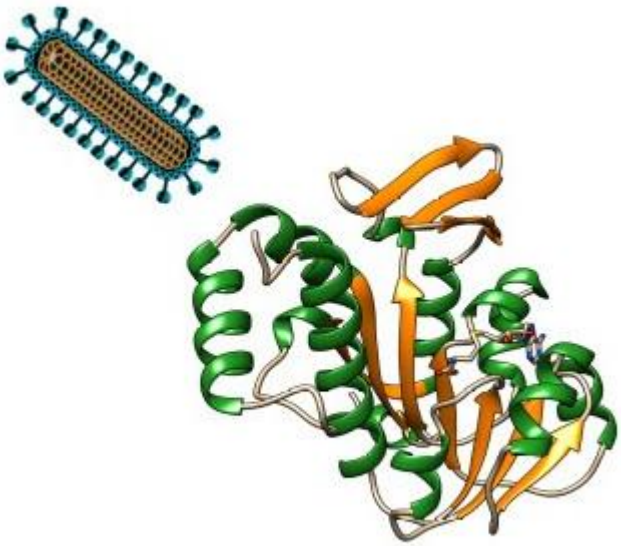

Key enzymes driving RNA virus evolution

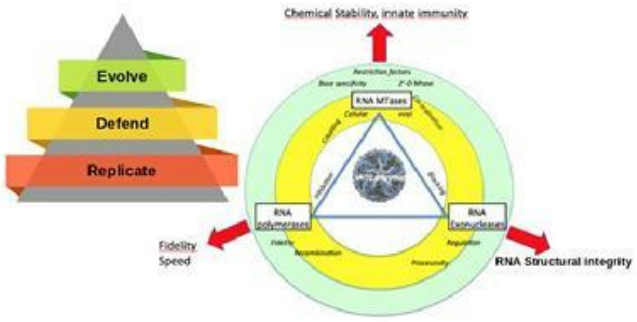

Back to Table of contents

MS02 Infection and Disease/hot structures

MS02-1-7 Structural characterization of SARS-CoV-2 spike derived peptides presented by the Human Leukocyte Antigen A*29:02
#MS02-1-7

L. Murdolo [1], S. Swaminathan [2], C. Szeto [1], C. Smith [2], S. Gras [1]
[1]La Trobe Univeristy - Melbourne (Australia), [2]QIMR Berghofer Medical Research Institute - Herston (Australia)

Abstract
The rapid emergence of SARS-CoV-2 out of Wuhan China in late 2019, has resulted in the current COVID-19 pandemic which has crippled social and economic development worldwide. With over 6.2 million deaths, significant efforts are being made to generate a viable treatment option. It has been well established that T cells destroy cells infected with a virus. These T cells also produce long lasting immunity through the maintenance of memory cells which can recognize future viral invasion.
Activation of T cells is achieved through the Human Leukocyte Antigens (HLA) surface molecule on infected cells. These HLA molecules present viral peptides to T cells that are then able to recognize these as antigens. However, due to the highly polymorphic nature of HLA molecules, it remains unclear how different peptides bound to the vast number of HLA molecules affect the stimulation of the adaptive immune response.
This project focuses on a single HLA, that is HLA-A*29:02, found in approximately 3% of the world population. Here we have structurally characterise a peptide and its Omicron mutated homologue derived from the spike protein. Using X-ray crystallography to solve the structure of a purified peptide complex, we have gained deeper insights into how viral mutation in the Omicron variant is capable of abrogating T lymphocyte recognition by destabilising the bound peptide.
We have solved the first structure of HLA-A*29:02 showing how it present viral peptide, and used stability assay to determine the impact of mutations on peptides presentation to T cells. Overall, this research has furthered our understanding of how our own immune system responds to these antigens. It may also help to develop long lasting therapies such as vaccines which stimulate T cell activation.

Back to Table of contents

MS02 Infection and Disease/hot structures

MS02-2-1 HLA-B*57-restricted immune response to HIV TW10 epitope drives for selection of specific TCR gene usages regardless of the viral load
#MS02-2-1

D. Chatzileontiadou [1], C.A. Lobos [1], H. Robson [2], C.A. Almeida [3], C. Szeto [1], L.J. D'orsogna [3], S. Gras [1]
[1]La Trobe University - Bundoora, VIC (Australia), [2]Monash University - Clayton, VIC (Australia), [3]University of Western Australia - Perth, WA (Australia)

Abstract
HIV infects and depletes CD4$^+$ T cells leading to severe immunosuppression. Currently almost 38 million people live with HIV worldwide[1]. Rare individuals, termed HIV controllers, can control viral load and remain healthy while infected. Despite Human Leukocyte Antigen (HLA) gene diversity in the population, almost 50% of HIV controllers express the HLA-B57 molecule which presents, among others, the Gag derived epitope, TW10[2]. Given the strong T-cell responses to this epitope and its presentation in early infection, TW10, could therefore shape the long-term control of HIV[3,4]. However, the mechanisms contributing to HIV control related to this epitope remain unclear. Here, we study the CD8$^+$ T cell responses to the TW10 epitope presented in HLA-B*57:01$^+$ HIV$^+$ individuals. We determine the αβ T cell receptor (TCR) repertoire in both HIV controller and non-controller individuals revealing similarities and the existence of a public TCR and public clonotypes in both groups. We further determine the polyfunctionality of selected T cell clones from each group that reveal strong CD8$^+$ T cell responses, shaped by the specific TCR repertoire biases regardless of the viral load. Furthermore, affinity measurements of selected TCRs and the first crystal structure of HLA-B*57:01-TW10 in complex with a CD8$^+$ TCR reveal the basis of the TW10 TCR repertoire biases and their impact on antigen recognition. The link between HIV viral load and T cell function driven by immunodominant epitopes may further our understanding of immunologic control of HIV.

References
[1] Global HIV & AIDS statistics — 2021 fact sheet
[2] Migueles SA, Sabbaghian MS, Shupert WL, Bettinotti MP, Marincola FM, Martino L, et al. HLA B*5701 is highly associated with restriction of virus replication in a subgroup of HIV-infected long term nonprogressors. Proc Natl Acad Sci U S A. 2000;97(6):2709-14.
[3] Brumme ZL, Brumme CJ, Carlson J, Streeck H, John M, Eichbaum Q, et al. Marked epitope- and allele-specific differences in rates of mutation in human immunodeficiency type 1 (HIV-1) Gag, Pol, and Nef cytotoxic T-lymphocyte epitopes in acute/early HIV-1 infection. J Virol. 2008;82(18):9216-27.
[4] Brennan CA, Ibarrondo FJ, Sugar CA, Hausner MA, Shih R, Ng HL, et al. Early HLA-B*57-restricted CD8+ T lymphocyte responses predict HIV-1 disease progression. J Virol. 2012;86(19):10505-16.

Back to Table of contents

MS02 Infection and Disease/hot structures

MS02-2-2 Autoimmunity and molecular recognition in type I diabetes
#MS02-2-2

J. Lopez Sagaseta [1], E. Erausquin [1], P. Serra [2], D. Parras [2], P. Santamaria [2]
[1]Unit of Protein Crystallography and Structural Immunology, Navarrabiomed - Pamplona (Spain), [2]Institut D'Investigacions Biomèdiques August Pi i Sunyer (IDIBAPS), Barcelona, Spain. - Barcelona (Spain)

Abstract
The NY4.1 T-cell clone was originally isolated from pancreatic islet-infiltrating lymphocytes from non-obese diabetic (NOD) mice. We have recently shown that the NY4.1 T cell receptor (4.1-TCR) recognizes pancreatic beta cell-derived hybrid insulin peptides (HIPs) in the context of the Major Histocompatibility Complex class II (pMHCII) molecule I-Ag7. In TCR-transgenic NOD mice, recognition of these peptide-MHCII (pMHCII) complexes triggers the activation and recruitment of NY4.1-CD4+ T cells into pancreatic islets, leading to rapid destruction of pancreatic beta cells and overt type 1 diabetes within the first few weeks of life.
We present the crystal structure of a HIP peptide/I-Ag7 complex at 1.80 Å resolution, as well as the structure of this pMHCII bound to the 4.1-TCR at 2.6 Å resolution. Comparison of the two structures reveals a previously unrecognized mode of interaction between a pMHCII and its cognate TCR, whereby TCR engagement entails exquisite conformational motions in I-Ag7 and the HIP that are essential for stable binding.
This observation suggests that some pMHCII complexes are malleable and that some TCRs trigger conformational motions on their cognate pMHCIIs to optimize binding.

References
1. Babad J, Geliebter A, DiLorenzo TP. T-cell autoantigens in the non-obese diabetic mouse model of autoimmune diabetes. Immunology (2010) 131:459–465. doi: 10.1111/j.1365-2567.2010.03362.x
2. Purcell AW, Sechi S, DiLorenzo TP. The Evolving Landscape of Autoantigen Discovery and Characterization in Type 1 Diabetes. Diabetes (2019) 68:879–886. doi: 10.2337/dbi18-0066
3. Gioia L, Holt M, Costanzo A, Sharma S, Abe B, Kain L, Nakayama M, Wan X, Su A, Mathews C, et al. Position β57 of I-A(g7) controls early anti-insulin responses in NOD mice, linking an MHC susceptibility allele to type 1 diabetes onset. Sci Immunol (2019) 4: doi: 10.1126/sciimmunol.aaw6329
4. Baker RL, Jamison BL, Wiles TA, Lindsay RS, Barbour G, Bradley B, Delong T, Friedman RS, Nakayama M, Haskins K. CD4 T Cells Reactive to Hybrid Insulin Peptides Are Indicators of Disease Activity in the NOD Mouse. Diabetes (2018) 67:1836–1846. doi: 10.2337/db18-0200
5. Anderson B, Park BJ, Verdaguer J, Amrani A, Santamaria P. Prevalent CD8(+) T cell response against one peptide/MHC complex in autoimmune diabetes. Proc Natl Acad Sci U S A (1999) 96:9311–9316. doi: 10.1073/pnas.96.16.9311
6. Han B, Serra P, Amrani A, Yamanouchi J, Marée AFM, Edelstein-Keshet L, Santamaria P. Prevention of diabetes by manipulation of anti-IGRP autoimmunity: high efficiency of a low-affinity peptide. Nat Med (2005) 11:645–652. doi: 10.1038/nm1250
7. Lieberman SM, Evans AM, Han B, Takaki T, Vinnitskaya Y, Caldwell JA, Serreze D V, Shabanowitz J, Hunt DF, Nathenson SG, et al. Identification of the beta cell antigen targeted by a prevalent population of pathogenic CD8+ T cells in autoimmune diabetes. Proc Natl Acad Sci U S A (2003) 100:8384–8388. doi: 10.1073/pnas.0932778100
8. Trudeau JD, Chandler T, Soukhatcheva G, Verchere CB, Tan R. Prospective prediction of spontaneous but not recurrent autoimmune diabetes in the non-obese diabetic mouse. Diabetologia (2007) 50:1015–1023. doi: 10.1007/s00125-007-0600-9
9. Verdaguer J, Schmidt D, Amrani A, Anderson B, Averill N, Santamaria P. Spontaneous autoimmune diabetes in monoclonal T cell nonobese diabetic mice. J Exp Med (1997) 186:1663–1676. doi: 10.1084/jem.186.10.1663
10. Verdaguer J, Yoon JW, Anderson B, Averill N, Utsugi T, Park BJ, Santamaria P. Acceleration of spontaneous diabetes in TCR-beta-transgenic nonobese diabetic mice by beta-cell cytotoxic CD8+ T cells expressing identical endogenous TCR-alpha chains. J Immunol (1996) 157:4726–4735.
11. Santamaria P. The long and winding road to understanding and conquering type 1 diabetes. Immunity (2010) 32:437–445. doi: 10.1016/j.immuni.2010.04.003
12. Barrett JC, Clayton DG, Concannon P, Akolkar B, Cooper JD, Erlich HA, Julier C, Morahan G, Nerup J, Nierras C, et al. Genome-wide association study and meta-analysis find that over 40 loci affect risk of type 1 diabetes. Nat Genet (2009) 41:703–707. doi: 10.1038/ng.381
13. Barton NH, Keightley PD. Understanding quantitative genetic variation. Nat Rev Genet (2002) 3:11–21. doi: 10.1038/nrg700

Back to Table of contents

14. Robertson CC, Inshaw JRJ, Onengut-Gumuscu S, Chen W-M, Santa Cruz DF, Yang H, Cutler AJ, Crouch DJM, Farber E, Bridges SLJ, et al. Fine-mapping, trans-ancestral and genomic analyses identify causal variants, cells, genes and drug targets for type 1 diabetes. Nat Genet (2021) 53:962–971. doi: 10.1038/s41588-021-00880-5
15. Zhang M, Wang Y, Li X, Meng G, Chen X, Wang L, Lin Z, Wang L. A Single L/D-Substitution at Q4 of the mInsA(2-10) Epitope Prevents Type 1 Diabetes in Humanized NOD Mice. Front Immunol (2021) 12:713276. doi: 10.3389/fimmu.2021.713276
16. Tisch R, McDevitt H. Insulin-dependent diabetes mellitus. Cell (1996) 85:291–297. doi: 10.1016/s0092-8674(00)81106-x
17. Vyse TJ, Todd JA. Genetic analysis of autoimmune disease. Cell (1996) 85:311–318. doi: 10.1016/s0092-8674(00)81110-1
18. Corper AL, Stratmann T, Apostolopoulos V, Scott CA, Garcia KC, Kang AS, Wilson IA, Teyton L. A structural framework for deciphering the link between I-Ag7 and autoimmune diabetes. Science (2000) 288:505–511. doi: 10.1126/science.288.5465.505
19. Schmidt D, Amrani A, Verdaguer J, Bou S, Santamaria P. Autoantigen-independent deletion of diabetogenic CD4+ thymocytes by protective MHC class II molecules. J Immunol (1999) 162:4627–4636.
20. Schmidt D, Verdaguer J, Averill N, Santamaria P. A mechanism for the major histocompatibility complex-linked resistance to autoimmunity. J Exp Med (1997) 186:1059–1075. doi: 10.1084/jem.186.7.1059
21. Thiessen S, Serra P, Amrani A, Verdaguer J, Santamaria P. T-cell tolerance by dendritic cells and macrophages as a mechanism for the major histocompatibility complex-linked resistance to autoimmune diabetes. Diabetes (2002) 51:325–338. doi: 10.2337/diabetes.51.2.325
22. Tsai S, Santamaria P. MHC Class II Polymorphisms, Autoreactive T-Cells, and Autoimmunity. Front Immunol (2013) 4:321. doi: 10.3389/fimmu.2013.00321
23. Tsai S, Serra P, Clemente-Casares X, Yamanouchi J, Thiessen S, Slattery RM, Elliott JF, Santamaria P. Antidiabetogenic MHC class II promotes the differentiation of MHC-promiscuous autoreactive T cells into FOXP3+ regulatory T cells. Proc Natl Acad Sci U S A (2013) 110:3471–3476. doi: 10.1073/pnas.1211391110
24. Tsai S, Serra P, Clemente-Casares X, Slattery RM, Santamaria P. Dendritic cell-dependent in vivo generation of autoregulatory T cells by antidiabetogenic MHC class II. J Immunol (2013) 191:70–82. doi: 10.4049/jimmunol.1300168
25. Parras D, Solé P, Delong T, Santamaría P, Serra P. Recognition of Multiple Hybrid Insulin Peptides by a Single Highly Diabetogenic T-Cell Receptor. Front Immunol (2021) 12:737428. doi: 10.3389/fimmu.2021.737428
26. Serra P, Garabatos N, Singha S, Fandos C, Garnica J, Solé P, Parras D, Yamanouchi J, Blanco J, Tort M, et al. Increased yields and biological potency of knob-into-hole-based soluble MHC class II molecules. Nat Commun (2019) 10:4917. doi: 10.1038/s41467-019-12902-2
27. Boulter JM, Glick M, Todorov PT, Baston E, Sami M, Rizkallah P, Jakobsen BK. Stable, soluble T-cell receptor molecules for crystallization and therapeutics. Protein Eng (2003) 16:707–711. doi: 10.1093/protein/gzg087
28. Lopez-Sagaseta J, Dulberger CL, Crooks JE, Parks CD, Luoma AM, McFedries A, Van Rhijn I, Saghatelian A, Adams EJ. The molecular basis for Mucosal-Associated Invariant T cell recognition of MR1 proteins. Proc Natl Acad Sci U S A (2013) 110:E1771-8. doi: 10.1073/pnas.1222678110
29. Armstrong KM, Piepenbrink KH, Baker BM. Conformational changes and flexibility in T-cell receptor recognition of peptide-MHC complexes. Biochem J (2008) 415:183–196. doi: 10.1042/BJ20080850
30. Borbulevych OY, Piepenbrink KH, Baker BM. Conformational melding permits a conserved binding geometry in TCR recognition of foreign and self molecular mimics. J Immunol (2011) 186:2950–2958. doi: 10.4049/jimmunol.1003150
31. Borbulevych OY, Piepenbrink KH, Gloor BE, Scott DR, Sommese RF, Cole DK, Sewell AK, Baker BM. T cell receptor cross-reactivity directed by antigen-dependent tuning of peptide-MHC molecular flexibility. Immunity (2009) 31:885–896. doi: 10.1016/j.immuni.2009.11.003
32. Tynan FE, Reid HH, Kjer-Nielsen L, Miles JJ, Wilce MCJ, Kostenko L, Borg NA, Williamson NA, Beddoe T, Purcell AW, et al. A T cell receptor flattens a bulged antigenic peptide presented by a major histocompatibility complex class I molecule. Nat Immunol (2007) 8:268–276. doi: 10.1038/ni1432
33. Bulek AM, Cole DK, Skowera A, Dolton G, Gras S, Madura F, Fuller A, Miles JJ, Gostick E, Price DA, et al. Structural basis for the killing of human beta cells by CD8(+) T cells in type 1 diabetes. Nat Immunol (2012) 13:283–289. doi: 10.1038/ni.2206
34. Nakayama M, Abiru N, Moriyama H, Babaya N, Liu E, Miao D, Yu L, Wegmann DR, Hutton JC, Elliott JF, et al. Prime role for an insulin epitope in the development of type 1 diabetes in NOD mice. Nature (2005) 435:220–223. doi: 10.1038/nature03523
35. Dai S, Huseby ES, Rubtsova K, Scott-Browne J, Crawford F, Macdonald WA, Marrack P, Kappler JW. Crossreactive T Cells spotlight the germline rules for alphabeta T cell-receptor interactions with MHC molecules. Immunity (2008) 28:324–334. doi: 10.1016/j.immuni.2008.01.008
36. Maynard J, Petersson K, Wilson DH, Adams EJ, Blondelle SE, Boulanger MJ, Wilson DB, Garcia KC. Structure of an autoimmune T cell receptor complexed with class II peptide-MHC: insights into MHC bias and antigen specificity. Immunity (2005) 22:81–92. doi: 10.1016/j.immuni.2004.11.015

Back to Table of contents

37. Tran MT, Faridi P, Lim JJ, Ting YT, Onwukwe G, Bhattacharjee P, Jones CM, Tresoldi E, Cameron FJ, La Gruta NL, et al. T cell receptor recognition of hybrid insulin peptides bound to HLA-DQ8. Nat Commun (2021) 12:5110. doi: 10.1038/s41467-021-25404-x
38. Wang Y, Sosinowski T, Novikov A, Crawford F, White J, Jin N, Liu Z, Zou J, Neau D, Davidson HW, et al. How C-terminal additions to insulin B-chain fragments create superagonists for T cells in mouse and human type 1 diabetes. Sci Immunol (2019) 4: doi: 10.1126/sciimmunol.aav7517
39. Garcia KC, Adams EJ. How the T cell receptor sees antigen--a structural view. Cell (2005) 122:333–336. doi: 10.1016/j.cell.2005.07.015
40. López-Sagaseta J, Sibener L V, Kung JE, Gumperz J, Adams EJ. Lysophospholipid presentation by CD1d and recognition by a human Natural Killer T-cell receptor. (2012) 31:2047–2059. https://www.scopus.com/inward/record.uri?eid=2-s2.0-84859906269&doi=10.1038%2Femboj.2012.54&partnerID=40&md5=bb36d6c7039bc907381cb4df187a2a16
41. Garcia KC, Degano M, Pease LR, Huang M, Peterson PA, Teyton L, Wilson IA. Structural basis of plasticity in T cell receptor recognition of a self peptide-MHC antigen. Science (1998) 279:1166–1172. doi: 10.1126/science.279.5354.1166
42. Garboczi DN, Ghosh P, Utz U, Fan QR, Biddison WE, Wiley DC. Structure of the complex between human T-cell receptor, viral peptide and HLA-A2. Nature (1996) 384:134–141. doi: 10.1038/384134a0
43. Li Y, Huang Y, Lue J, Quandt JA, Martin R, Mariuzza RA. Structure of a human autoimmune TCR bound to a myelin basic protein self-peptide and a multiple sclerosis-associated MHC class II molecule. EMBO J (2005) 24:2968–2979. doi: 10.1038/sj.emboj.7600771
44. Vonrhein C, Flensburg C, Keller P, Sharff A, Smart O, Paciorek W, Womack T, Bricogne G. Data processing and analysis with the autoPROC toolbox. Acta Crystallogr D Biol Crystallogr (2011) 67:293–302. doi: 10.1107/S0907444911007773
45. Kabsch W. XDS. Acta Crystallogr D Biol Crystallogr (2010) 66:125–132. doi: 10.1107/s0907444909047337
46. Evans PR, Murshudov GN. How good are my data and what is the resolution? Acta Crystallogr D Biol Crystallogr (2013) 69:1204–1214. doi: 10.1107/S0907444913000061
47. McCoy AJ, Grosse-Kunstleve RW, Adams PD, Winn MD, Storoni LC, Read RJ. Phaser crystallographic software. J Appl Crystallogr (2007) 40:658–674. doi: 10.1107/S0021889807021206
48. Vagin A, Teplyakov A. Molecular replacement with MOLREP. Acta Crystallogr D Biol Crystallogr (2010) 66:22–25. doi: 10.1107/S0907444909042589
49. López-Sagaseta J, Kung JE, Savage PB, Gumperz J, Adams EJ. The molecular basis for recognition of CD1d/α-galactosylceramide by a human non-Vα24 T cell receptor. PLoS Biol (2012) 10:e1001412. doi: 10.1371/journal.pbio.1001412
50. Reinherz EL, Tan K, Tang L, Kern P, Liu J, Xiong Y, Hussey RE, Smolyar A, Hare B, Zhang R, et al. The crystal structure of a T cell receptor in complex with peptide and MHC class II. Science (1999) 286:1913–1921. doi: 10.1126/science.286.5446.1913
51. Kovalevskiy O, Nicholls RA, Murshudov GN. Automated refinement of macromolecular structures at low resolution using prior information. Acta Crystallogr Sect D, Struct Biol (2016) 72:1149–1161. doi: 10.1107/S2059798316014534
52. Adams PD, Afonine P V, Bunkoczi G, Chen VB, Davis IW, Echols N, Headd JJ, Hung LW, Kapral GJ, Grosse-Kunstleve RW, et al. PHENIX: a comprehensive Python-based system for macromolecular structure solution. Acta Crystallogr D Biol Crystallogr (2010) 66:213–221. doi: 10.1107/s0907444909052925
53. Emsley P, Lohkamp B, Scott WG, Cowtan K. Features and development of Coot. Acta Crystallogr D Biol Crystallogr (2010) 66:486–501. doi: 10.1107/s0907444910007493

Structure of the 4.1-TCR:HIP39/I-Ag7 complex.

Back to Table of contents

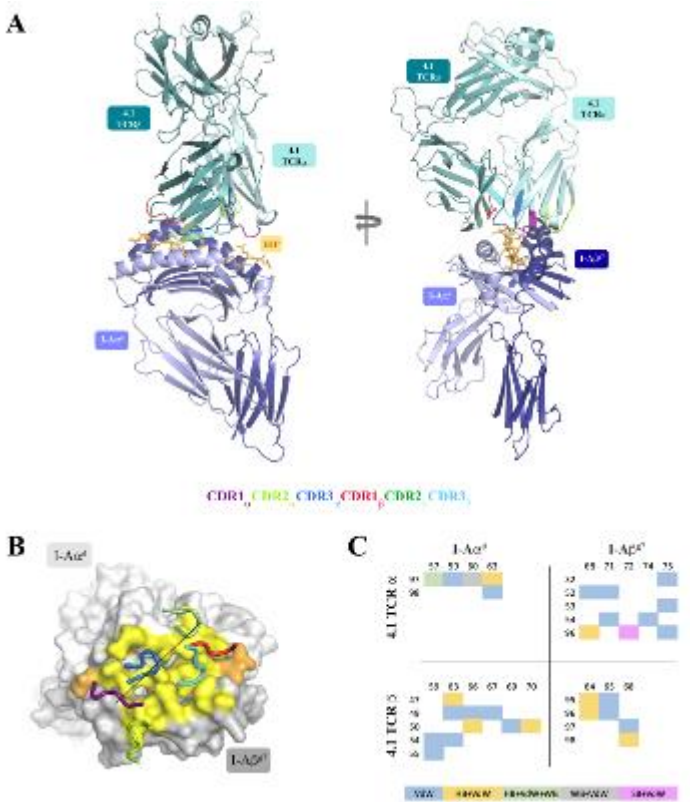

Structural plasticity of both I-Ag7 and peptide co

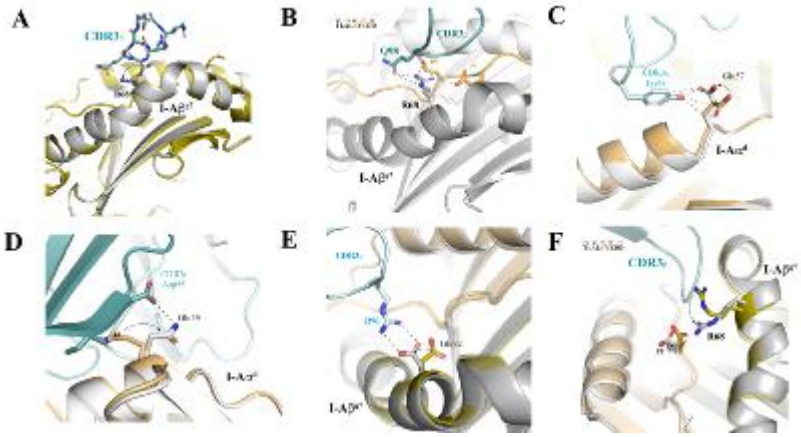

Back to Table of contents

MS02 Infection and Disease/hot structures

MS02-2-3 Structure-based design and synthesis of piperidinol-containing molecules as new Mycobacterium abscessus inhibitors
#MS02-2-3

J. De Ruyck [1]
[1]University of Lille - Villeneuve Ascq (France)

Abstract
Non-tuberculous mycobacterium (NTM) infections, such as those triggered by *Mycobacterium abscessus*, are increasing globally. *M. abscessus* pulmonary diseases in particular are of health concern as they are often recalcitrant to standard chemotherapy due to the intrinsic drug resistance mechanisms developed by this mycobacterium. We previously demonstrated that a piperidinol derivative, named PIPD1, is an efficient molecule both against *M. abscessus* and *Mycobacterium tuberculosis*, the agent of tuberculosis that targets the mycolic acid transporter MmpL3. In order to refine the properties of PIPD1 we determined the pharmacokinetics properties of PIPD1 and showed, that intraperitoneal administration of PIPD1 led to serum concentration of 600 ng/ml, to the distribution in different organs and an elimination half-life of 3.2 hours. We also designed, synthesized and determined the biological activity of a series of piperidinol derivatives against *M. abscessus*. Structure–activity relationship (SAR) studies pointed to the sites on the scaffold that can tolerate slight modifications. Interestingly, the Van der Waals radius of substituents present on the ortho position of the aromatic ring B seems to have a great importance for the biological activity. These results allow identifying FMD-88 with a similar antimycobacterial activity as PIPD1.

References
Structure-Based Design and Synthesis of Piperidinol-Containing Molecules as New Mycobacterium abscessus Inhibitors de Ruyck *et al*, ChemistryOpen, 2020, 9, 351-365

Model of Mmpl3

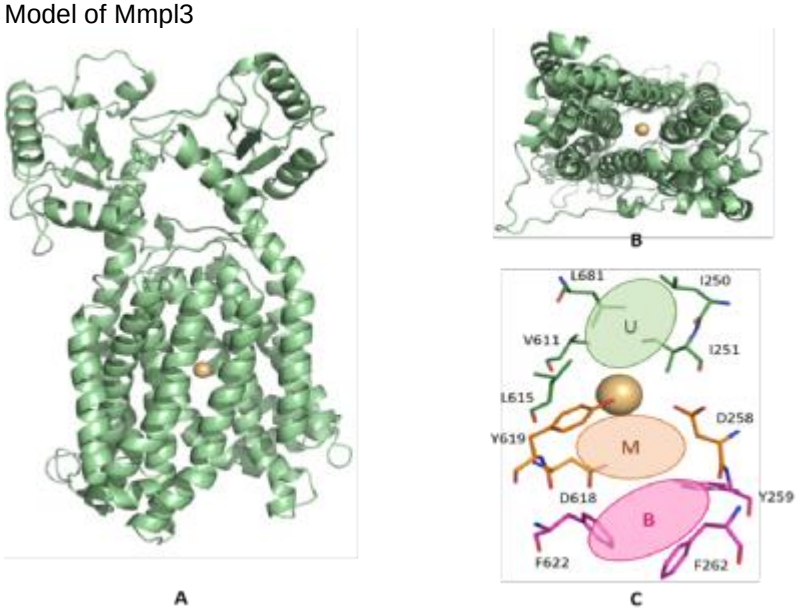

Putative binding site of FMD-88

Back to Table of contents

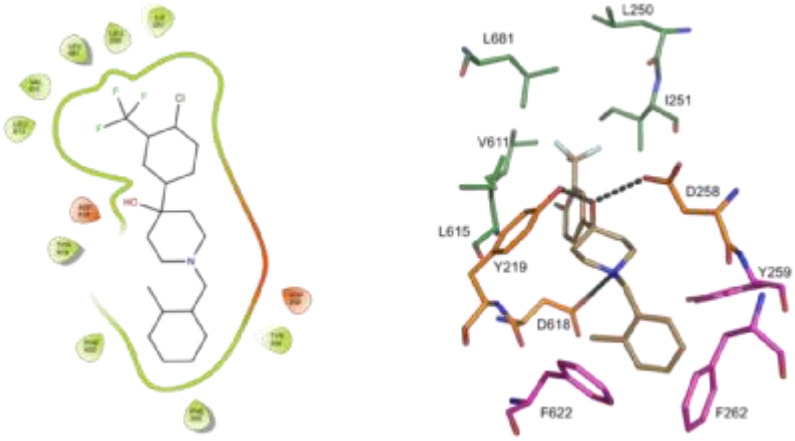

Back to Table of contents

MS02 Infection and Disease/hot structures

MS02-2-4 Toward new inhibitors of InhA, an essential protein from Mycobaterium tuberculosis, discovered by dynamic combinatorial X-ray crystallography
#MS02-2-4

R. Tamhaev [1], L. Maveyraud [1], L. Mourey [1], C. Lherbet [2]
[1]IPBS - Toulouse (France), [2]SPCMIB - Toulouse (France)

Abstract
Tuberculosis, one of the most ancient disease, is caused by Mycobacterium tuberculosis (MTB) and remains a major health burden as a leading cause of mortality due to an infectious disease worldwide. The first-line antituberculosis drug, Isoniazid (INH), acts as a prodrug that requires prior activation by the catalase-peroxydase KatG. The resulting adduct NAD-INH is the effective inhibitor and targets InhA, an enoyl acyl carrier protein reductase (ENR) from the Fatty Acid Synthase II (FAS-II) system, involved in the biosynthesis of mycolic acids and essential for MTB survival. With the rise of drug-resistant bacteria, particularly to INH, different classes of direct inhibitors of InhA, requiring no prior activation by KatG, have also been discovered but none of them has been approved for clinical use so far. Based on this observation, there is currently a need to identify new inhibitors of InhA to fight efficiently against MTB.
In this project, we use Dynamic Combinatorial X-ray crystallography (DCX) as a tool to facilitate the discovery of new inhibitors of InhA by X-ray crystallography. This method uses building blocks or fragments with compatible chemical functions that combine at specific conditions to generate a Dynamic Combinatorial Library called DCL. The reversibility of the combinations makes it possible to generate compounds adapted to their environment and the confinement associated with the InhA binding site. This work focuses on the identification of new InhA inhibitors by screening suitable fragments that can span from entry to the depth of the substrate-binding site. Combination of X-ray and enzymatic data will be crucial to identify most impactful interactions and may lead to new potential inhibitors of InhA.

References
1. Global tuberculosis report 2021, World Health Organisation
2. Chollet et al., J Struct Biol. 2015, vol 190, 328-337
3. Congreve, M.S. et al. Angew. Chem. Int. Ed. 2003, 42, 4479 –4482
4. Milon Mondal and Anna K. H. Hirsch. Chem. Soc. Rev., 2015, 44, 2455-2488

Back to Table of contents

MS02 Infection and Disease/hot structures

MS02-2-5 Inhibitor screening and structural characterization of virulence factors from SARS-CoV-2 #MS02-2-5

S. Chatziefthymiou [1], M. Kuzikov [2], S. Afandi [3], E. Crosas [4], G. Pompidor [1], H. Taberman [1], B. Windschügel [2], J. Labahn [5], M. Kolbe [3], J. Hakanpää [1]
[1]Photon Science, DESY - Hamburg (Germany), [2]Fraunhofer ITMP ScreeningPort - Hamburg (Germany), [3]Helmholtz-Center for Infection Research (HZI) - Hamburg (Germany), [4]ITT DESY - Hamburg (Germany), [5]Forschungszentrum Jülich, Institute of Complex Systems (ICS-6) - Hamburg (Germany)

Abstract
Coronavirus induced zoonotic diseases can cause pandemics with unforeseeable consequences to human health and global economy. Our project aims to screen and develop effective therapeutics against SARS-CoV-2, targeting its replication-transcription complex (RTC). Following an interdisciplinary research approach, compound libraries of approved drugs are used for the discovery of potent inhibitors for proteins of the RTC and the binding mode of these enzyme-inhibitor complexes is studied by X-ray crystallography.
Our workflow includes the production of proteins involved in the coronavirus RTC, the high-throughput inhibitor screening with fluorescence-based assays using drug repurposing libraries and the structure/function analysis of the identified enzyme-inhibitor complexes. The advantages of this approach is that it is cost efficient, high-throughput, allows the direct identification of potent inhibitors and ensures optimal beamtime usage. Furthermore, such a platform can be successfully used in future viral outbreaks.
In this presentation we will give an overview of this project and the results achieved to date. We will focus on one of the target proteins, namely the uridine-specific endoribonuclease nsp15, and apart from the results from its inhibitor screening we will also present findings that allowed us to shed light on important activity determinants of this enzyme.

References
1. Malone B, Urakova N, Snijder EJ, Campbell EA. Structures and functions of coronavirus replication-transcription complexes and their relevance for SARS-CoV-2 drug design. Nat Rev Mol Cell Biol. 2022 Jan;23(1):21-39
2. Deng X, Baker SC. An "Old" protein with a new story: Coronavirus endoribonuclease is important for evading host antiviral defenses. Virology. 2018 Apr;517:157-163

Back to Table of contents

MS02 Infection and Disease/hot structures

MS02-2-6 Structural determination of Mycobacterium tuberculosis and Rhodococcus erythropolis mycothiol disulphide reductases
#MS02-2-6

J. Gutiérrez-Fernández [1], M. Hammerstad [2], H.P. Hersleth [2]
[1]Structural Biology Team, Norway Center for Molecular Medicine, University of Oslo - Oslo (Norway), [2]Department of Biosciences, University of Oslo, Section for Biochemistry and Molecular Biology - Oslo (Norway)

Abstract
Low molecular thiols are involved in many processes in all organisms playing a protective role against reactive oxygen, chlorine and electrophilic species, heavy metals, toxins and antibiotics. Not only they maintain the reduced state of cytosolic proteins but also act as cofactors of many oxidoreductases. This is the case of the mycothiol disulphide reductase (Mtr), an oxidoreductase of Actinobacteria that is able to reduce mycothiol disulphide (MSSM) to mycothiol (MSH) which could be oxidized again by reactive species, thus contributing to the redox homeostasis. To catalyze the reduction of MSSM, Mtr oxidizes NADP+H^+ into $NADP^+$ through a flavin cofactor ($FADH_2$ to FAD). In this work we aim to obtain high-resolution three-dimensional structures of *Mycobacterium tuberculosis* and *Rhodococcus erythropolis* mycothiol disulphide reductases (MtMtr and ReMtr respectively) to unveil their mechanism of action, the binding of mycothiol disulphide and to analyze the increased affinity ReMtr shows by certain additional substrates, such as the telluride oxyanion tellurite ($TeO3_2^-$). This information will also allow us to design potential compounds targeting Mtr with therapeutic purposes.

References
Hammerstad, M. *et al.* (2020) The Crystal Structures of Bacillithiol Disulfide Reductase Bdr (YpdA) Provide Structural and Functional Insight into a New Type of FAD-Containing NADPH-Dependent Oxidoreductase. *Biochemistry*, 59, 4793-4798.
Arenas-Salinas, M. *et al.* (2016) Flavoprotein-Mediated Tellurite Reduction: Structural Basis and Applications to the Synthesis of Tellurium-Containing Nanostructures. *Front. Microbiol.* 7, 1160.
Kumar, A. *et al.* (2017) Structural and mechanistic insights into Mycothiol Disulphide Reductase and the Mycoredoxin-1-alkylhydroperoxide reductase E assembly of *Mycobacterium tuberculosis*. *BBA*, 1861, 9, 2354-2366.

Back to Table of contents

MS02 Infection and Disease/hot structures

MS02-2-7 Structural characterisation of influenza epitopes presented by a prevalent Indigenous Australian Human Leukocyte Antigen
#MS02-2-7

A. Nguyen [1], L. Hensen [2], P. Illing [3], C. Szeto [4], A. Purcell [1], K. Kedzierska [5], S. Gras [4]
[1]Department of Biochemistry and Molecular Biology and Infection and Immunity Program, Biomedicine Discovery Institute, Monash University, Clayton, VIC 3800, Australia - Melbourne (Australia) - Melbourne (Australia), [2]Department for Internal Medicine II, University Hospital Tübingen, Tübingen, BW 72076, Germany - Tübingen (Germany), [3]Department of Biochemistry and Molecular Biology and Infection and Immunity Program, Biomedicine Discovery Institute, Monash University, Clayton, VIC 3800, Australia - Melbourne (Australia), [4]Department of Biochemistry and Chemistry, La Trobe Institute for Molecular Science, La Trobe University, Melbourne, VIC 3086, Australia - Melbourne (Australia), [5]Department of Microbiology and Immunology, The Peter Doherty Institute for Infection and Immunology, University of Melbourne. - Melbourne (Australia)

Abstract
Influenza is a highly infectious respiratory disease caused by the influenza virus. Previous research has shown that Indigenous Australians are at higher risk of developing severe symptoms associated with influenza infection than non-Indigenous Australians. In the event of a pandemic outbreak, Indigenous Australians are more likely to be hospitalised due to influenza infection (16%) than non-Indigenous Australians, despite only making up a small portion (2.5%) of the total population. The underlying immunological reason for this susceptibility is still unclear, but may be due to their distinct immunogenetics. In particular, Indigenous Australians have distinctive Human Leukocyte Antigen (HLA) expression profiles that impact on the selection and presentation of peptide antigens to anti-viral T cells, which plays a critical role in the clearance of the virus.
Our work is focused on HLA-B*13:01, a prevalent HLA allele in the Indigenous Australian population. There is no data regarding how the HLA-B*13:01 molecule might select and bind to peptide antigens for subsequent presentation to T cells. Here, we have characterised HLA-B*13:01 presenting influenza epitopes and their recognition by T cell receptors at the atomic level using X-ray crystallography at the Australian Synchrotron. This provides the first insight into HLA-B*13:01 peptide presentation and the T cell recognition mechanism in great detail. Our structures of HLA-B*13:01 revealed characteristics unique to this HLA molecule which are important for T cell recognition and could help further understand the T cell-mediated response restricted to this HLA.

Back to Table of contents

MS03 Crystallization and biophysical characterization

MS03-1-1 Targeting the sphingolipid biosynthesis pathway of protozoan parasites as drug targets #MS03-1-1

D. Cazzola [1]
[1]Durham University - Durham (United Kingdom)

Abstract
The protozoa are a large group of single-cell eukaryotes which include important human pathogens such as Toxoplasma gondii (the causative agent of Toxoplasmosis) and Plasmodium falciparum (which causes malaria). Often, these parasitic infections are asymptomatic, however, they become life threatening in critical conditions, such as pregnancy, or in immuno-compromised patients. In fact, it is estimated that up to 50% of the world's population is chronically but asymptomatically infected with Toxoplasma. Other members of the protozoa kingdom are considered genuine pathogens, such as Plasmodium. Recent research has identified several enzymes involved in the biosynthesis of sphingolipids as attractive drug targets, as these take part in a plethora of cellular functions such cellular membrane stability, and important signalling pathways, including cell differentiation and apoptosis.
This project aims to investigate the structure and function of the enzymes involved in the biosynthesis of sphingolipids, with primary focus on Serine Palmitoyltransferase (SPT), which catalyzes the first, rate-limiting step in the de-novo synthesis of sphingolipids. To achieve this, a vastly multidisciplinary approach will be undertaken, starting with the use of novel, state-of-the-art bioinformatic tools, such as Alphafold2, which will be used for the rational design of protein constructs, with the aim to optimise the protein production, purification, and crystallization processes. Following the attainment of crystal structures, novel ligand and fragment screening methods will be employed, and successful leads will be optimised with a rational approach, to maximize efficacy across pathogens and minimize detriment to human health.

Back to Table of contents

MS03 Crystallization and biophysical characterization

MS03-1-2 From fragment screening to fragment growing - new methods for drug discovery #MS03-1-2

D. Gasparikova [1]
[1]Durham University - Durham (United Kingdom)

Abstract
Human glucokinase (GK) is a hexokinase isozyme (hexokinase IV) present in both the liver and pancreas. Glucokinase plays an important role in the phosphorylation of glucose to glucose-6-phosphate, which is a key step in glucose metabolism. In the beta cells of the pancreas, glucokinase acts as a glucose sensor for insulin secretion, while in the liver it facilitates the transformation of glucose into glycogen, which allows glucose to be stored for later use. The role of glucokinase in the reduction of glucose concentration leads to the pharmacological desire to develop glucokinase activators with the potential to counterbalance the glycaemic imbalance related to type-2 diabetes. Furthermore, applying fragment-based methods to identify fragment hits binding to glucokinase can lead to the recognition of allosteric activators of glucokinase, which can be used as lead compounds in the future. In combination with docking experiments, which aid the binding pose prediction, X-ray crystallography is utilised to understand the interactions between GK and its lead compounds.

Back to Table of contents

MS03 Crystallization and biophysical characterization

MS03-1-3 A fundamental study of protein dynamism to the rescue of drug design: application to hIDO1 #MS03-1-3

M. Mirgaux [1], L. Leherte [1], J. Wouters [1]
[1]Laboratoire de Chimie Biologique Structurale (CBS), Namur Research Institute for Life Sciences (NARILIS), Namur Institute of Structured Matter (NISM), University of Namur (UNamur) - Namur (Belgium)

Abstract
Protein dynamics govern most of the fundamental processes in the human body. In particular, the dynamics of loops located near an active site may be involved in the positioning of the substrate and the reaction mechanism. The understanding of this dynamism is therefore crucial for the development of drugs affecting the active site. This is the case for the hemoprotein hIDO1, a therapeutic target involved in immunotherapy resistance. The overexpression of this enzyme leads to a local depletion in L-Trp. This depletion exerts an immunosuppressive respond by a decrease of the T cells activation. [1] The hIDO1 protein has an active site composed of a heme cofactor and a dynamic loop. However, few information was available on the conformations adopted by this loop and its folding mechanism. Being essential in the reaction catalyzed by the enzyme, its understanding is crucial for drug development.
In this work, a fundamental study of the folding mechanism of the dynamic loop in hIDO1 has been performed in order to trace its closure by a multidisciplinary approach. Combining crystallography, modelling methods and Molecular Dynamics, the behavior of this loop has been studied in the presence of different ligands such as substrate, substrate analogs or product analogs [2, 3]. For the first time, the loop was resolved in intermediate and closed conformation by crystallography (2.4Å and 2.3Å respectively). This work highlights the central role of this loop in the maintenance of the cofactor in the active site and opens the door to new strategies for drugs design.

References
[1] A. L. Mellor et al. Nature Reviews Immunology, 4(10):762–774, 2004.
[2] M. Mirgaux et al. Acta Crystallographica Section D: Structural Biology, 76(12), 1211-1221, 2020.
[3] M. Mirgaux. et al. International Journal of Tryptophan Research, 14, 1-11, 2021.

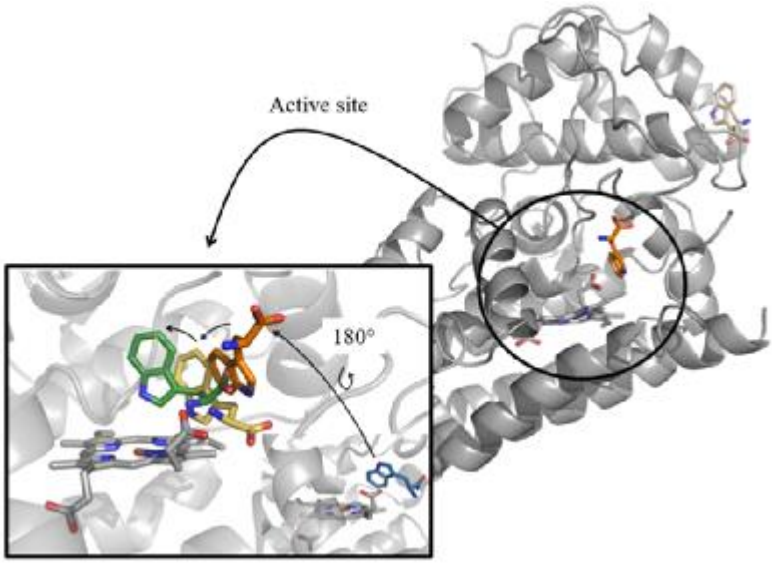

Back to Table of contents

MS03 Crystallization and biophysical characterization

MS03-1-4 Structural and Functional Studies of TBEV Non-Structural Protein 5
#MS03-1-4

P. Havlickova [1], J. Crossley [1], Z. Gardian [1], F. Dycka [1], I. Kuta Smatanova [1], Z. Franta [1]
[1]Institute of Chemistry, Faculty of Science, University of South Bohemia, Branišovská 1760, České Budějovice, Czech Republic - Ceske Budejovice (Czech Republic)

Abstract
Tick-borne encephalitis virus (TBEV) is a major human pathogen, transmitted by ticks from family Ixodidae. TBEV is an enveloped virus with a ~ 11 kb positive-sense single-strand RNA genome, encoding a single 375 kDa polyprotein. During the infection, the polyprotein is cleaved into three structural and seven non-structural (NS) proteins. While structural proteins are involved in the assembly of new virions, non-structural proteins are responsible for the virus replication [1].
NS5 is a large conserved protein comprising of two domains connected by a highly flexible linker, which is important for the activity as well as for the overall shape of the protein. N-terminal methyltransferase (MTase) domain is involved in the capping process. C-terminal RNA-dependent RNA polymerase (RdRp) is crucial for virus replication [2].
This project focuses on structural and functional studies of TBEV NS5 protein. Various constructs were designed – NS5 full length, RdRp domain and MTase domain. Expression and purification of individual constructs have been optimized and pure samples were used for initial crystallization screening, cryo-EM analysis and functional assays.
So far, we have obtained cryo-EM data for RdRp domain, using Titan Krios equipped with Falcon 4 camera and Relion processing pipeline yielded a reconstruction of 6 Å resolution. Tiny protein crystals of RdRp grew in several crystallization conditions. Furthermore, fluorescence-based binding assays revealed substrate affinity and specificity.

References
1. Mackenzie, J. (2005). Traffic. 6, 967-977.
2. Bollati, M. et al. (2009). Antiviral Res. 87, 125-148.
This research is supported by ERDF No. CZ.02.1.01/0.0/0.0/15_003/000041, GAJU 106/2021/P and GAJU 04-17/2019/P.

Back to Table of contents

MS03 Crystallization and biophysical characterization

MS03-1-5 Structural insight into the salivary serpins of Ixodes ricinus
#MS03-1-5

B. Kaščáková [1], P. Havlíčková [1], T. Prudniková [1], J. Kotál [2], A. Chlastáková [2], Z. Beránková [2], H. Langhansová [2], J. Chmelař [2], I. Kutá Smatanová [1]
[1]Department of Chemistry, Faculty of Science, University of South Bohemia, Branišovská 1760, České Budějovice, Czech Republic - České Budějovice (Czech Republic), [2]Department of Medical Biology, Faculty of Science, University of South Bohemia, Branišovská 1760, České Budějovice, Czech Republic - České Budějovice (Czech Republic)

Abstract
Serine protease inhibitors – serpins are one of the largest superfamilies of structurally conserved proteins that are widely distributed in nature [1]. They have many regulatory functions that make them one of the most studied protein families. Many serpins lost their inhibitory function during their evolution and work as chaperons or storage proteins. Serpins with protease inhibition function form covalent complexes with target protease [2]. This process leads to a suicide mechanism that inactivates the protease as well as serpin. The serpin inhibitory activity requires rearrangement of the conformation. The typical secondary structure is made of 3 β-barrels, 9 α-helices and an exposed, flexible reactive center loop (RCL) that contains a proteinase recognition site. During crystallographic attempts, different types of conformation were solved and each of these structural rearrangements was important to understanding the inhibitory pathway. The successful process of serine proteinase inhibition results in an irreversible suicide substrate mechanism, by which serpin is covalently bound to the target protease [3].
Here are presented results of the X-ray structural analysis of four *Ixodes ricinus* serpins named Iripin-3, Iripin-5, Iripin-4, and Iripin-1. All of them help the tick in different ways to stay attached to the host for sufficient time for feeding necessary for reproduction and distribution of ticks by inhibiting the proteases involved in host immune defense responses to a tick bite. These serpins are mainly expressed in salivary glands and thus are present at the site of first contact with a host. This group of proteins has primarily immunological and haemostatic functions, but their functions can vary according to their specificity. The tick serpins act as modulators of immune responses by using their anti-coagulation, and anti-complementary functions and play role in immunosuppression [4]. Serpins are good candidates for drug development in combination with protein engineering.

References
1. J. Potempa, E. Korzus & J. Travis (1994) J. Biol. Chem. 269, 15957-15960.
2. Ooi, C. P., Haines, L. R., Southern, D. M., Lehane, M. J., & Acosta-Serrano, A. (2015). PLoS Negl. Trop. Dis. 9:e3448. doi: 10.1371/journal.pntd.0003448
3. P. G. W. Gettins, P. A. Patston & S. T. Olson(eds) (1996) Serpins: Structure, Function and Biology, Molecular biology Intelligence Unit, R. G. Landes Co., and Chapman & Hall, Austin, TX
4. J. Chmelar, C. J. Oliveira, P. Rezacova, I. M. B. Francischetti, Z. Kovarova, G. Pejler, P. Kopacek, J.M. C. Ribeiro, M. Mares, J. Kopecky & M. Kotsyfakis; Blood 2011; 117 (2): 736–744. doi: https://doi.org/10.1182/blood-2010-06-293241

Back to Table of contents

MS03 Crystallization and biophysical characterization

MS03-1-6 Interactions of probiotic bacteria with the human dendritic cell receptor DC-SIGN #MS03-1-6

C. Grininger [1], T. Sagmeister [1], L. Petrowitsch [1], M. Eder [1], T. Pavkov-Keller [1]
[1]University of Graz - Graz (Austria)

Abstract
Surface layers (S-layers) are protein coats displayed on the external surface of many bacterial and archaeal species. They provide a large surface area for interaction with host cells which implies tremendous implications for the immune response and human disease. It was shown that the extracted S-layer from *Lactobacillus acidophilus*, one of the major species found in human intestines, and its interaction with dermal dendritic cell receptors, especially DC-SIGN, can act as a potent inhibitor of viral and bacterial infections[1]. However, it is not clear whether the non-glycosylated S-layer protein alone or together with lipoteichoic acids (LTA), an integral part of the bacterial cell wall that serves as an anchor for the S-layer, is responsible for the interaction. Characterization of the exact interaction partner(s), its binding mode and kinetics as well as comparison to known receptor-glycan binding regions from e.g. viral glycoproteins is essential for understanding the role of these interactions in triggering signaling pathways to achieve anti-viral or anti-bacterial effects. Since L. acidophilus and S-layer protein are both categorized as “generally recognized as safe” (GRAS), there is interest in characterizing this novel mechanism of inhibition in order to develop new therapeutics that would address infections of specific viruses or pathogenic bacteria.

References
1. Acosta, M. P., Ruzal, S. M. & Cordo, S. M. S-layer proteins from Lactobacillus sp . inhibit bacterial infection by blockage of DC-SIGN cell receptor. International Journal of Biological Macromolecules 92, 998–1005 (2016).

Back to Table of contents

MS03 Crystallization and biophysical characterization

MS03-1-7 Getting it right from the start – collecting best data with the D8 VENTURE platform #MS03-1-7

M. Adam [1], V. Smith [1]
[1]Bruker AXS GmbH - Karlsruhe (Germany)

Abstract
In house X-ray data collection is still a gold standard for obtaining precise atomic coordinates in a timely manner. Highly integrated platforms like our D8VENTURE are available 24/7 and enable even the novice user to work effectively on ever complex crystallographic targets as well as they provide experts with a variety of tools to collect the best data possible. New features, both in automation hardware and software design have been developed to be at your service as the projects become more challenging and productivity is a requirement.
Here we demonstrate that how the D8 VENTURE platform available with the IµS DIAMOND or METALJET X-ray source and combined with the latest generation of photon counting CPAD (PHOTON III) detectors and SCOUT automated sample changer can collect data of protein crystals with a broad array of properties ranging from highest resolution to extremely large unit cells or very small crystal size in a high throughput manner.
We will discuss new options for the tailoring of source parameters with a focus on beam divergence and beam size. Both allow an optimized diffraction experiment for your specific crystal and can be crucial for resolving reflections and minimizing background scattering.

D8 VENTURE with SCOUT sample changer

Back to Table of contents

MS03 Crystallization and biophysical characterization

MS03-1-8 Interactions Between Hydrophilic Polymers and Biomacromolecules
#MS03-1-8

J. Hašek [1], T. Koval [1], P. Kolenko [1], T. Skálová [1], J. Dušková [1], J. Dohnálek [1]
[1]Institute of Biotechnology, Academy of Sciences, Pr;myslov8 595 - Vestec (Czech Republic)

Abstract
Hydrophilic polymers of polyethyleneglycol type are often used as precipitants for crystallization of bio-macromolecules. It is the reason why many of experimental structures deposited in Protein databank [1] show PEG type polymers bound on the protein surface. We inserted these structures in the Database of Protein-Polymer Interactions (DPPI) [2].
The DPPI contains presently 3667 PDB structures of bio-macromolecules (proteins and nucleic acids) complexed with PEG type fragments at least 4 monomers long (-OCC-OCC-OCC-OCC-O-). The script of the program PYMOL [3] allows quick identification and inspection of configurations of polymer chain bound on the protein surface. It automatically zooms and displays distances of all relevant interatomic contacts between polymer and protein. As some proteins bind more polymer chains, the DPPI contains many thousands experimentally verified interactions. To help quick inspection of many situations, the DPPI users deposit the pictures in special directory using the command PNG
Correct localization of the polymer chains on the protein surface does not lie in the center of crystallographer's interest. This is the reason why, we can meet some evident misinterpretations. Of course, it is not allowed to make any corrections in the PDB file. Instead, the user can write the corresponding comment into the text box inserted in the picture similarly as it is shown in the Figure.
Visual inspection of the DPPI provides surprisingly high number of various types of protein-polymer interactions. Classification of these interactions is a useful background for explaining the success of the poly(ethyleneglycol)-type polymers in many economically important applications in the industry, science, medicine and pharmaceutics, e.g. crystallization of proteins, protection of drugs against enzymatic cleavage, development of antifouling surfaces, etc.
The research is supported by the project CZ.02.1.01/0.0/0.0/15_003/0000447 from the ERDF.

References
1. wwPDB consortium Protein Data Bank: Nucleic Acids Research, (2018) 47, D520-D528. DOI: 10.1093/nar/gky9492. Hašek, J., Z. Kristallogr. (2011) 28, 475-480. DOI: 10.1524/9783486991321-0773. Schrödinger, L., & DeLano, W. (2020). Program PyMOL. Retrieved from http://www.pymol.org/pymol

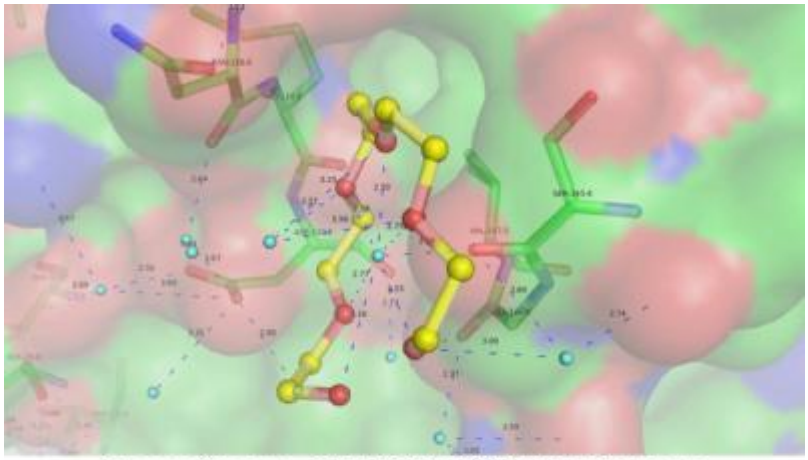

File name of the picture **1Y33-15P-O6 C=O-M@O6 inhibited-Subtilisin.png**
Meaning: **1Y33**=PDB code, **15P**=name of ligand, **O6**=six oxygens of PEG bind the protein, **C=O-M@O6** = protein carbonyl binds metal atom trapped in the center of six ether oxygens of PEG. As the modelled oxygen lies in the plane of the six oxygens, it is probably natrum **ion Na⁺**.

Back to Table of contents

MS03 Crystallization and biophysical characterization

MS03-1-9 Structural and functional studies of cyclodipeptide synthases with RNA microhelices mimicking their tRNA susbtrates
#MS03-1-9

Z. Marouf [1], P. Fernández Varela [2], C. Tellier [2], M. Glousieau [2], J.C. Cintrat [3], N. Morellet [1], M. Gondry [2], E. Lescop [1], J.B. Charbonnier [2]
[1]Université Paris-Saclay,CNRS, Institut de Chimie des Substances Naturelles (ICSN) - Gif-sur-Yvette (France), [2]Université Paris-Saclay, CEA, CNRS, Institute for Integrative Biology of the Cell (I2BC) - Gif-sur-Yvette (France), [3]Université Paris Saclay, CEA, INRAE, Département Médicaments et Technologies pour la Santé (DMTS), SCBM - Gif-sur-Yvette (France)

Abstract
Cyclodipeptide synthases (CDPS) divert aminoacyl-tRNAs to produce cyclodipeptides and complex derivatives, diketopiperazines, which constitute a broad class of natural products synthesized by microorganisms and possessing pharmacological properties. Most CDPS have a relaxed specificity and often produce several cyclopeptides. This hinders the identification of specificity determinants. To overcome this problem, we selected Nbra-CDPS from Nocardia Brasiliensis. Nbra-CDPS has the advantage of using different substrates, Ala and Glu tRNA that target the first and second CDPS pocket respectively, thus, synthesizing cyclo-Ala-Glu (cAE) as the main product. A recent study of Gondry's team (Canu et al, 2020) shows that CDPS interact mainly with the acceptor arms of tRNAs (also termed miHx). A major objective of our study is to identify the CDPS amino acid residues responsible for substrate specificity. The substitution of these residues will allow to generate enzymes that can use non canonical amino acids. Ultimately, the intent of the project is to produce by an ecological biosynthesis process, various diketopiperazines with high therapeutic potential.
We aim in this study to solve by X-ray crystallography the high resolution structure of the complex between Nbra-CDPS and miHx and to prove the interest of using miHx as mimick of tRNA substrates for functional and structural studies. We determined twelve crystal structures of Nbra-CDPS crystallized in presence of acylated and nonacylated-miHx. Data analysis showed the presence of the enzyme alone, without MiHx. We have identified some obstacles that may hinder the study of the complex. In particular, the substrate Ala-miHxAla is not stable and deacylates significantly. Thus, we recently developed the use of more stable analogues of the substrate through amide bond formation (miHx-NHAla) for structural and biophysical studies. Functional studies are in progress to study new small molecules binders of Nbra-CDPS.
To explore the interaction of Nbra-CDPS with the tRNA substrate we use a catalytic-dead mutant by introducing a S34A mutation that blocks the first substrate at the pocket. Recently we produced another variant of the protein without the C-terminal his-tag to avoid any interference with interaction area access nearby. We measured the affinity of these CDPS variants for miHx by BioLayer Interferometry and EMSA. We deduced a KD in the nanomolar range for miHxAla by both approaches.
NMR studies were performed on isotopically labeled Nbra-CDPS and highlighted its interaction with a non-acylated miHxAla by 15N HSQC spectra. The preliminary NMR assignment provided first molecular information of residues involved in the recognition with MiHx.
In addition, new strategies are being deployed to further characterize the interaction. Firstly, synthesis of miHx with functional groups allowing to specifically cross-link the miHx with the CDPS pocket are in progress. Secondly, we initiated a study to analyse by cryoEM the 3D structure of a dimeric form of Nbra-CDPS in complex with two Ala-tRNA (MW about 100kDa). Preliminary negative staining images of this complex have been collected.
In conclusion, the combination of all these approaches will allow us to decipher the molecular mechanism of recognition between CDPS and their substrates and thus guide the engineering of these enzymes.

References
Nicolas Canu, Carine Tellier, Morgan Babin, Robert Thai, Inès Ajel, et al.. Flexizyme-aminoacylated shortened tRNAs demonstrate that only the aminoacylated acceptor arms of the two tRNA substrates are required for cyclodipeptide synthase activity. Nucleic Acids Research, 2020, 48 (20)

Back to Table of contents

MS03 Crystallization and biophysical characterization

MS03-2-1 SorC protein family: the structural insight into their DNA recognition
#MS03-2-1

M. Nováková [1], J. Škerlová [1], J. Brynda [1], I. Sieglová [1], M. Fábry [2], P. Řezáčová [2]
[1]Institute of Organic Chemistry and Biochemistry, CAS - Prague (Czech Republic), [2]Institute of Organic Chemistry and Biochemistry, CAS; Institute of Molecular Genetics, CAS - Czech Republic - Prague (Czech Republic)

Abstract
SorC family is a family of bacterial transcription regulators involved in the control of carbohydrate metabolism and quorum-sensing (1,2). SorC protomers consist of a DNA-binding domain (DBD) and an effector-binding domain (EBD). Several SorC structures have been determined so far (3-6), however, there has been no structural information of their complex with the cognate DNA.
We performed X-ray crystallographic studies of two functionally characterized SorC family members from Bacillus subtilis: bsDeoR and bsCggR. Each selected protein represents one of the subgroups that are recognized within the family. To gain insight into the protein/DNA atomic interactions, we determined 2.3 and 2.1 Å resolution crystal structures of bsDeoR and bsCggR DBDs in complex with DNA duplexes representing halves of the operator sequences. However, the molecular packing in the crystal allowed us to make assumptions on recognition of the full operator sequence.
Besides the interest of basic research, our work has potential even for a biotechnological industry, where, recently, transcriptional repressors started to be used as molecular sensors of the metabolic flux of microorganisms.

References
1. Fillinger, S., Boschi-Muller, S., Azza, S., Dervyn, E., Branlant, G. and Aymerich, S. (2000) Two glyceraldehyde-3-phosphate dehydrogenases with opposite physiological roles in a nonphotosynthetic bacterium. J Biol Chem, 275, 14031-14037.
2. Taga, M.E., Semmelhack, J.L. and Bassler, B.L. (2001) The LuxS-dependent autoinducer AI-2 controls the expression of an ABC transporter that functions in AI-2 uptake in Salmonella typhimurium. Mol Microbiol, 42, 777-793.
3. Řezáčová, P., Kožíšek, M., Moy, S.F., Sieglová, I., Joachimiak, A., Machius, M. and Otwinowski, Z. (2008) Crystal structures of the effector-binding domain of repressor Central glycolytic gene Regulator from Bacillus subtilis reveal ligand-induced structural changes upon binding of several glycolytic intermediates. Mol Microbiol, 69, 895-910.
4. Škerlová, J., Fábry, M., Hubálek, M., Otwinowski, Z. and Řezáčová, P. (2014) Structure of the effector-binding domain of deoxyribonucleoside regulator DeoR from Bacillus subtilis. FEBS J, 281, 4280-4292.
5. de Sanctis, D., McVey, C.E., Enguita, F.J. and Carrondo, M.A. (2009) Crystal structure of the full-length sorbitol operon regulator SorC from Klebsiella pneumoniae: structural evidence for a novel transcriptional regulation mechanism. J Mol Biol, 387, 759-770.
6. Ha, J.H., Eo, Y., Grishaev, A., Guo, M., Smith, J.A., Sintim, H.O., Kim, E.H., Cheong, H.K., Bentley, W.E. and Ryu, K.S. (2013) Crystal structures of the LsrR proteins complexed with phospho-AI-2 and two signal-interrupting analogues reveal distinct mechanisms for ligand recognition. J Am Chem Soc, 135, 15526-15535.

Back to Table of contents

MS03 Crystallization and biophysical characterization

MS03-2-2 Mechanism of regulation and neutralization of tRNA-phosphorylating small RelA-SpoT Homolog toxins #MS03-2-2

L. Dominguez Molina [1], T. Kurata [2], A. Talavera Perez [1], V. Hauryliuk [2], A. Garcia Pino [1]
[1]Université Libre de Bruxelles (ULB) - Brussels (Belgium), [2]Lund University - Lund (Sweden)

Abstract
RelA-SpoT Homolog (RSH) enzymes control bacterial physiology in order to overcome and survive to stressful conditions through synthesis and degradation of a nucleotide second messenger, the guanosine penta and tetraphosphate (also known as a (p)ppGpp). Small alarmone synthetases (SASs) are single-domain RSH enzymes that contains the (p)ppGpp synthesis (SYNTH) domain, but absence of the hydrolysis (HD) domain and regulatory C-terminal domains characteristic from long RSHs family members such as RelA and SpoT. These catalytic domains are found as part of different subfamilies and can be functionally divided into small pyrophosphotransferases including the well-studied RelP, RelQ, TAS1 alarmone synthetases (SASs) that catalyze ATP hydrolysis and pyrophosphate transfer to nucleotides or uncharged tRNA, and small alarmone hydrolases that catalyze the cleavage of phospho-ribose nucleotides.
The faRel2-atFaRel2 operon from Coprobacillus sp. D7 was recently identified as a type II toxin-antitoxin (TA) module in which the toxin FaRel2 that targeted protein synthesis by pyrophosphorylating uncharged tRNAs at the free 3'OH of the CAA end is neutralised by the antitoxin AtFaRel2[1]. The antitoxin from the faRel2-atFaRel2 system has a novel fold that has not been observed associated with toxins from other TA families. While the activity of the aforementioned tRNA-phosphorylating toxins can be counteracted by bacterial SAHs, the natural regulation of these type II TAs toxins by their cognate antitoxin remains unknown. Tas1, the effector enzyme from Pseudomonas aeruginosa PAO1 type VI secretion system (T6SS) is a remote homologue of FaRel2. Once processed and secreted into the target cell, Tas1 produces (p)ppApp, mounting a strong toxic response via depletion of the ATP pool and inhibition of purine biosynthesis [2]. The action of Tas1 is counteracted by the immunity factor Tis1 via blocking of the acceptor nucleotide binding site. However, sequence analysis could not detect meaningful similarity between Tis1 and AtFaRel2 suggesting that tRNA-modifying small RSH toxins may be neutralised via a different mechanism representing a new way of control RSH enzymes.

References
[1] Kurata, T. et al. RelA-SpoT Homolog toxins pyrophosphorylate the CCA end of tRNA to inhibit protein synthesis. Mol. Cell. P3160-3170 (2021)
[2] Ahmad, S. et al. An interbacterial toxin inhibits target cell growth by synthesizing (p)ppApp. Nature 575, 674–678 (2019)

Back to Table of contents

MS03 Crystallization and biophysical characterization

MS03-2-3 Molecular insights into the HLA-B35 molecules' classification associated with HIV control #MS03-2-3

C. Lobos [1], D. Chatzileontiadou [2], B. Sok [1], C.A. Almedia [3], H. Halim [1], L. D'orsogna [4], S. Gras [2]
[1]Monash University - Clayton (Australia), [2]La Trobe University - Bundoora (Australia), [3]The University of Western Australia - Perth (Australia) - Perth (Australia), [4]The University of Western Australia - Perth (Australia)

Abstract
Human leukocyte antigen (HLA) class I molecules have been shown to strongly influence the immune response to HIV infection and acquired immunodeficiency syndrome (AIDS) progression. Polymorphisms within the HLA-B35 molecules divide the family into 2 groups Px and Py. The Px group is associated with deleterious effects and an accelerated disease progression in HIV+ patients, while the Py group is not. The classification is based on the preferential binding of a Tyrosine at the C-terminal part of the peptide in the Py group, and a non-Tyrosine residue in the Px group. However, there is lack of knowledge on the molecular differences between the two groups. Here, we have investigated three HLA-B35 molecules, namely HLA-B*35:01 (Py), HLA-B*35:03 (Px), and HLA-B*35:05 (unclassified). We selected an HIV-derived peptide, NY9, and demonstrated that it can trigger a polyfunctional CD8+ T cell response in HLA-B*35:01+/HIV+ patients. We also provided the first αβTCR repertoire analysis of the NY9-specific T cells. We determined that in complex with the NY9 peptide, the Py molecule was more stable than the Px or the unclassified molecule. We solved the structures of the three HLA molecules in complex with the NY9 peptide, and structural similarities with HLA-B*35:01 would classify the HLA-B*35:05 within the Py group.

Graphical Abstract

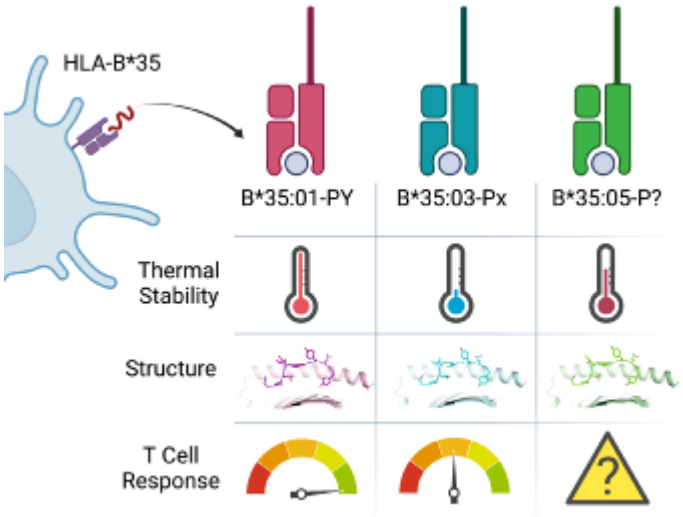

Back to Table of contents

MS03 Crystallization and biophysical characterization

MS03-2-4 Mitochondrial COA7 is a heme-binding protein with disulfide reductase activity, which acts in the early stages of complex IV assembly
#MS03-2-4

S. Maghool [1]
[1]bio21 Institute, The University of Melbourne - Melbourne (Australia)

Abstract
Shadi Maghool[a], Luke E. Formosa[b], Alice J. Sharpe[b], Boris Reljicb[c], Linden Muellner-Wong[b,c], David A. Stroud[c,d], Michael T. Ryan[b], and Megan J. Maher[a,e]
aSchool of Chemistry and Bio21 Molecular Science and Biotechnology Institute, The University of Melbourne, Parkville, Victoria 3010, Australia.
bDepartment of Biochemistry and Molecular Biology, Biomedicine Discovery Institute, Monash University, Clayton 3800, Australia.
cDepartment of Biochemistry and Pharmacology and The Bio21 Molecular Science and Biotechnology Institute, The University of Melbourne, Parkville, Victoria 3010, Australia.
dMurdoch Childrens Research Institute, The Royal Children's Hospital, Parkville, Victoria 3052 Australia.
eDepartment of Biochemistry and Genetics, La Trobe Institute for Molecular Science, La Trobe University, Melbourne 3086, Australia.

Cytochrome c oxidase (complex IV) catalyses the transfer of electrons from cytochrome c in the intermembrane space, to molecular oxygen in the matrix. Assembly of complex IV requires the participation of a host of cysteine-rich proteins of the mitochondrial intermembrane space, which take part in a tightly choreographed series of intermolecular interactions for complex IV assembly. In addition, complex IV requires the incorporation of three copper ions, heme a and heme a3cofactors for the assembly and activity of the complex. Crucially, disruptions in this pathway lead to defects in complex IV assembly and inhibition of oxidative phosphorylation and, in humans, manifests in mitochondrial disease [1].
Despite the importance of complex IV assembly in health and mitochondrial disease, we have only a limited understanding of the molecular basis of its biogenesis, due to a lack of knowledge about structures and precise functions of the individual assembly factors. Cytochrome c oxidase assembly factor 7 (COA7) is a metazoan-specific assembly factor, the absence or mutation of which in humans accompanies complex IV assembly defects and neurological conditions. COA7 binds heme with micromolar affinity, even though the protein structure does not resemble previously characterized heme-binding proteins. The heme-bound COA7 can redox cycle between oxidation states Fe(II) and Fe(III) and shows disulfide reductase activity toward copper metallochaperones SCO1 and SCO2 [2]. This presentation will describe the role of COA7 in the early stages of complex IV assembly using structural and functional approaches and importantly, explain the disulfide reductase activity of the heme bound COA7.

References
[1] Timon-Gomez, A., Nyvltova, E., Abriata, L. A., Vila, A. J., Hosler, J., and Barrientos, A. (2018) Mitochondrial cytochrome c oxidase biogenesis: Recent developments, Seminars in cell & developmental biology 76, 163-178.
[2] Formosa*, L. E., **Maghool*, S.**, Sharpe, A. J., Reljic, B., Muellner-Wong, L., Stroud, D. A., Ryan, M. T., & Maher, M. J. (2022). Mitochondrial COA7 is a heme-binding protein with disulfide reductase activity, which acts in the early stages of complex IV assembly. Proceedings of the National Academy of Sciences of the United States of America, 119(9), e2110357119. https://doi.org/10.1073/pnas.2110357119.*equal first author.

Back to Table of contents

MS03 Crystallization and biophysical characterization

MS03-2-5 Structural and molecular characterization of the Aminoglycoside PHosphotransferase APH(3')-IIb from Pseudomonas aeruginosa
#MS03-2-5

J. Kowalewski [1], M. Gelin [1], J.F. Guichou [1], G. Labesse [1], C. Lionne [1]
[1]Centre de Biologie Structurale - Montpellier (France)

Abstract
The World Health Organization (WHO) has warned on the importance to find new strategies to encounter the major health problem that is the antimicrobial resistance [1]. Bacterial pathogens have been classify in different groups function of there threat, Priority-1 group includes gram negative bacterial pathogens such as *Pseudomonas aeruginosa*, *Klebsiella pneumoniae*, *Acinetobacter baumannii* and *Enterobacteriaceae*. Aminoglycosides are broad spectrum antibiotics reserved for severe infections, most of the time associated with Priority-1 bacteria. They are characterize as bactericidal, concentration-dependent, and show a marked post-antibiotic effect [2].
However, bacteria have developed different mechanisms of resistance to these antibiotics. One of the most important mechanism is the expression of Aminoglycosides Modifying Enzymes (AME). These enzymes are able to inactivate aminoglycosides leading to a decreased affinity for their ribosomal target [3]. This modification is the major source of resistance against this class of antibiotics [4]. Among this class of enzymes we can notice the Aminoglycosides Phosphotransferases (APH). They catalyze the transfer of the γ-phosphate of a nucleotide (ATP or GTP) on a free hydroxyl group of an aminoglycoside. Structural and biochemical characterization are crucial to better understand this class of enzyme and develop effective inhibitors to circumvent their activity and to thus rejuvenate the antibacterial action of the aminoglycosides [5]. There have been significant advances providing structural, mechanistic, and inhibitory insights into many members of the aminoglycoside phosphotransferases (APHs) family [for example, 6;7].
In the present work and for the first time, we have solved the structure of the APH(3')-IIb of *P. aeruginosa* alone and in presence of MgATP and Kanamycin, two of its natural ligands. We have characterized its catalytic specificities and affinity for aminoglycosides and for phosphate donors. Preliminary results, obtained on the inhibition of this enzyme in order to resensitize bacteria to these antibiotics, would also be presented. Our results will be discussed from the of the drug resistances observed in clinical therapy, as well as the potential ways for reversing them. This work was supported by an ANR contract (SIAM project, ANR-19-AMRB-0001-01).

References
[1] https://www.who.int/news-room/detail/27-02-2017-who-publishes-list-of-bacteria-for-which-new-antibiotics-are-urgently-needed, accession 22th January 2019.
[2] Kotra LP, Haddad J and Mobashery S (2000) Aminoglycosides: perspectives on mechanisms of action and resistance and strategies to counter resistance *Antimicrob. Agents Chemother.* 44(12):3249.
[3] Ramirez MS, Tolmasky ME (2010) Aminoglycoside modifying enzymes. *Drug Resist. Updat.* 13:151–71.
[4] Vakulenko SB, Mobashery S (2003) Versatility of aminoglycosides and prospects for their future. *Clin. Microbiol. Rev.* 16: 430–50.
[5] Labby KJ, Garneau-Tsodikova S (2013) Strategies to overcome the action of aminoglycoside-modifying enzymes for treating resistant bacterial infections. *Future Med. Chem.* 5:1285–1309.
[6] Lallemand P, Leban N, Kunzelmann S, Chaloin L, Serpersu EH, Webb MR, Barman T, Lionne C (2012) Transient kinetics of aminoglycoside phosphotransferase(3')-IIIa reveals a potential drug target in the antibiotic resistance mechanism. *FEBS Lett.* 586:4223–7.
[7] Stogios PJ, Spanogiannopoulos P, Evdokimova E, Egorova O, Shakya T, Todorovic N, Capretta A, Wright GD, Savchenko A (2013) Structure-guided optimization of protein kinase inhibitors reverses aminoglycoside antibiotic resistance. *Biochem. J.* 454:191–200.

Back to Table of contents

MS03 Crystallization and biophysical characterization

MS03-2-6 TNA: Apply for access to laboratories of excellence in MOlecular Scale Biophysics Research Infrastrure (MOSBRI)
#MS03-2-6

S. Hoffmann [1], N. Jones [1], B. Raynal [2], E. Von Castelmur [3], D. Derbyshire [3], M. Sunnerhagen [3]
[1]ISA, Aarhus University - Aarhus (Denmark), [2]Plateforme de biophysique,Institut Pasteur - Paris (France), [3]Department of Physics, Chemistry and Biology, Linköping university - Linköping (Sweden)

Abstract
MOSBRI provides free of charge trans-national (TNA) access to molecular-scale biophysics instrumentation and expertise, aiming at studying biological systems at an intermediate level between atomic-resolution structural descriptions and cellular-scale observations. The MOSBRI programme offers TNA to 13 European biophysical laboratories, widely distributed over Europe and selected to ensure a comprehensive portfolio of technologies and expertise. Access to the MOSBRI TNA sites is based on a proposal submitted via the MOSBRI web-site.
MOSBRI has a range of access modalities:
MOSBRI pipelines: This means an integrated access to a synergistic set of biophysical instruments and technologies. This will allow the TNA user to fully exploit the expertise of the TNA site to tackle advanced questions.
Access to instruments and methodologies: This proposal submission method may be used if you have a focused research question and already know which instrument/methodology your project needs access to.
Project maturation: If you are unsure which pipeline or instrument suite will best answer your project's scientific question, the MOSBRI's moderator panel experts can offer to guide you via project maturation.
In this poster we will present what MOSBRI TNA can offer and explain our different access modalities in detail.

Back to Table of contents

MS04 Structure in Cancer Biology

MS04-1-1 Structure-assisted drug discovery: cyclin-dependent kinase 2
#MS04-1-1

S. Djukic [1], J. Škerlová [1], M. Peřina [2], J. Radek [2], V. Kryštof [2], P. Řezáčová [3]
[1]Institute of Organic Chemistry and Biochemistry - Prague (Czech Republic), [2]Palacký University - Olomouc (Czech Republic), [3]Insitute of Organic Chemistry and Biochemistry - Prague (Czech Republic)

Abstract
Cyclin-dependent kinase 2 (CDK2) is a Ser/Thr protein kinase that is active during G1 and S phase of the cell cycle and works as check point control. During the G1 phase of the cell cycle, it is activated by binding to cyclin E and in S phase by binding to cyclin A [1]. It is dispensable in healthy cells, as other CDKs can take over its role, but it is essential for proliferation of cancer cells. This makes CDK2 an interesting target in discovery of anticancer compounds [2].We are using X-ray crystallography in the structure-assisted drug discovery approach to study CDK2/cyclin A complex in design of new inhibitors of this protein and to understand the protein-inhibitor interactions.Enzyme was prepared by heterologous expression in E. coli and purified in high yields and purity necessary for crystallographic studies. Crystallization conditions for CDK2/cycA were identified through wide screening and optimization. Diffraction data have been collected on BL14.1 at the BESSY II electron storage ring operated by the Helmholtz-Zentrum Berlin and crystal structures were determined at high resolution (1.7-2.5 Å). Structural study of the crystal structures allowed us to analyse protein-inhibitor interactions and to identify essential residues in the active site (Figure1).The knowledge we obtained from these structures will play an important part in future design of inhibitors specific to CDK2 and other enzyme isoforms.

References
1.Echalier A, Endicott JA, Noble ME: Biochimica et Biophysica Acta (BBA) - Proteins and Proteomics 2015, 1804 (3): 511–92. Wood DJ et al. Cell Chemical Biology. 2018; 26 (1): 121–130.e5.3. Dayal N et al. J Med Chem 2021; https://doi.org/10.1021/acs.jmedchem.1c00330

Figure1: Crystal structure of CDK2/cyclin A in com

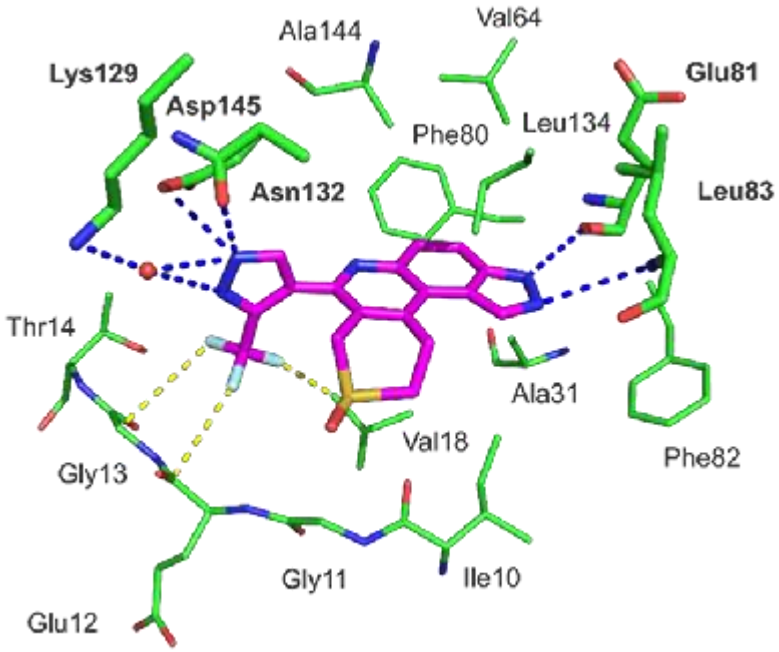

Back to Table of contents

MS04 Structure in Cancer Biology

MS04-1-2 Structure of ErbB3, ISU104 exhibits potent anti-tumorigenic activity
#MS04-1-2

M. Choi [1], M. Hong [2], Y. Yoo [1], M. Kim [2], J.Y. Kim [2], J.S. Cha [1], U. Kim [1], H.S. Cho [1], S.B. Hong [2]
[1]Yonsei university - Seoul (Korea, Republic of), [2]ISU ABXIS - Sungnam (Korea, Republic of)

Abstract
ErbB3, a member of the ErbB receptor family, is a potent mediator in the development and progression of cancer, and its activation plays pivotal roles in acquired resistance against anti-EGFR therapies and other standard-of-care therapies. Upon ligand (NRG1) binding, ErbB3 forms heterodimers with other ErbB proteins (i.e., EGFR and ErbB2), which allows activation of downstream PI3K/Akt signaling. In this study, we developed a fully human anti-ErbB3 antibody, named ISU104, as an anticancer agent. ISU104 binds potently and specifically to the domain 3 of ErbB3. The complex structure of ErbB3-domain 3::ISU104-Fab revealed that ISU104 binds to the NRG1 binding region of domain 3. The elucidated structure suggested that the binding of ISU104 to ErbB3 would hinder not only ligand binding but also the structural changes required for heterodimerization. Biochemical studies confirmed these predictions. ISU104 inhibited ligand binding, ligand-dependent heterodimerization and phosphorylation, and induced the internalization of ErbB3. As a result, downstream Akt phosphorylation and cell proliferation were inhibited. The anticancer efficacy of ISU104 was demonstrated in xenograft models of various cancers. In summary, a highly potent ErbB3 targeting antibody, ISU104, is suitable for clinical development.

References
Mirim Hong, Youngki Yoo, Miyoung Kim, Ju Yeon Kim, Jeong Seok Cha, Myung Kyung Choi, Uijin Kim, Kyungyong Kim, Youngsoo Sohn, Donggoo Bae, Hyun-Soo Cho, Seung-Beom Hong; A Novel Therapeutic Anti-ErbB3, ISU104 Exhibits Potent Antitumorigenic Activity by Inhibiting Ligand Binding and ErbB3 Heterodimerization. Mol Cancer Ther 1 June 2021; 20 (6): 1142–1152. https://doi.org/10.1158/1535-7163.MCT-20-0907

Structural analysis of the ErbB3 and ISU104.

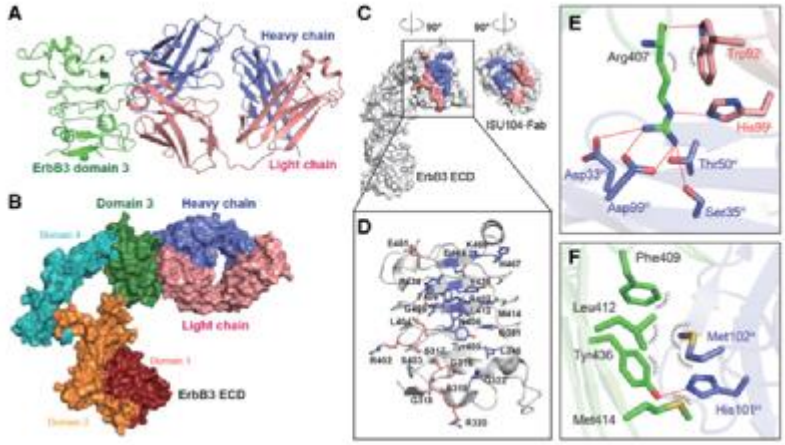

ISU104 blocks NRG1 binding to ErbB3.

Back to Table of contents

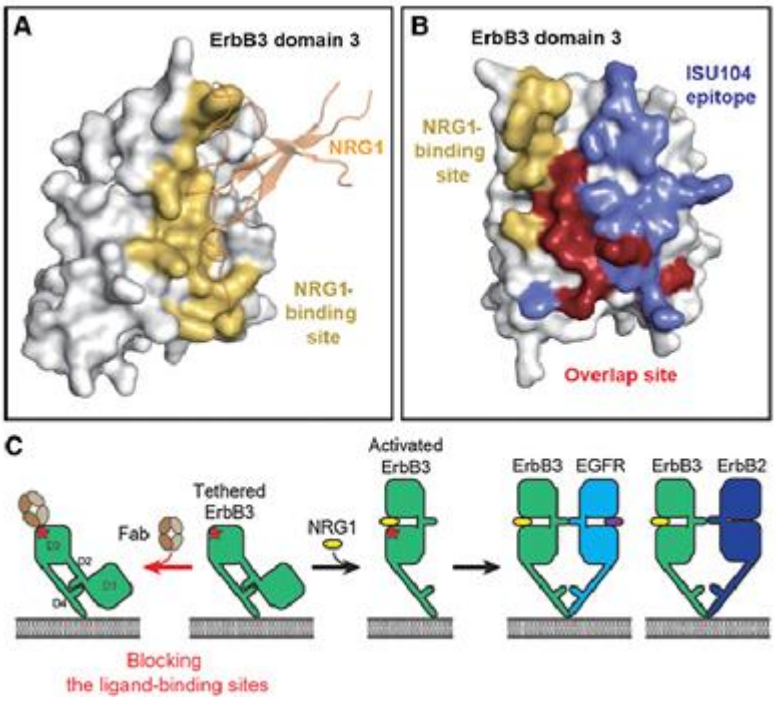

Back to Table of contents

MS04 Structure in Cancer Biology

MS04-2-1 Structural investigation of HER2 specific protein binder
#MS04-2-1

U. Kim [1], T.T.T. Kim [2], J.S. Cha [1], H. Kim [1], H.S. Cho [1], H.S. Kim [2]
[1]Yonsei University - Seoul (Korea, Republic of), [2]Korea Advanced Institute of Science and Technology - Daejeon (Korea, Republic of)

Abstract
A protein binder with a desired epitope and binding affinity is critical to the development of therapeutic agents. Here we present computationally- guided design and affinity improvement of a protein binder recognizing a specific site on domain IV of human epidermal growth factor receptor 2 (HER2). As a model, a protein scaffold composed of Leucine-rich repeat (LRR) modules was used. We designed protein binders which appear to bind a target site on domain IV using a computational method. Top 10 designs were expressed and tested with binding assays, and a lead with a low micro- molar binding affinity was selected. Binding affinity of the selected lead was further increased by two-orders of magnitude through mutual feedback between computational and experimental methods. The utility and potential of our approach was demonstrated by determining the binding interface of the developed protein binder through its crystal structure in complex with the HER2 domain IV.

References
Tae Yoon Kim#, Jeong Seok Cha#, Hoyoung Kim, Yoonjoo Choi*, Hyun-Soo Cho* and Hak- Sung Kim* “Computationally-guided design and affinity improvement of a protein binder targeting a specific site on HER2.” Computational and Structural Biotechnology Journal, Volume 19, 1325-1334, 2021.03.

overall workflow of repebody development

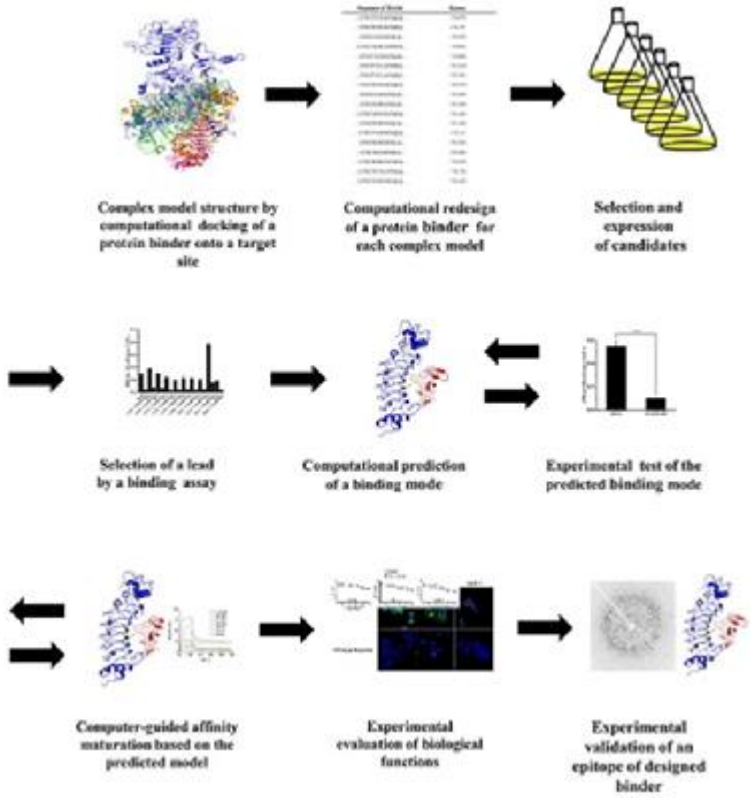

structure of Rb-H2 in complex with HER2 domain IV

Back to Table of contents

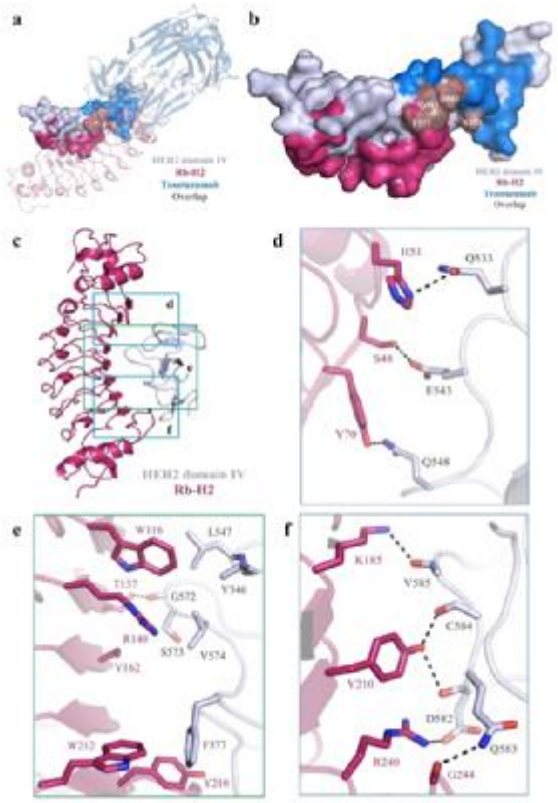

Back to Table of contents

MS04 Structure in Cancer Biology

MS04-2-2 The genetic biomarker of cervical cancer: An application of Statistical and Bioinformatics techniques #MS04-2-2

M. Kumar [1]
[1]**Banaras Hindu University - Varanasi (India)**

Abstract
Malignant tissues in the cervical lead to cervical cancer. It is increasing women's mortality in the world. Statistical and Bioinformatics approaches are generally used to explore the genome data. To find the significant differentially expressed genes and associated pathways related to cervical cancer. From the gene expression omnibus database GSE44001, A total of 300 cervical cancer patients has been extracted for analysis. Non-parametric, semi-parametric, and parametric models have been used to find the significant genes based on clinical parameters. The survival of cancer patients highly depend on tumor diameter size and stage. The risk of death 2.92 and 2.35 times higher among patients who had tumor diameter size (4.1 mm & above) and (3.1-4.0 mm) as compared to tumor diameter size (0-3.0 mm) respectively. Total 4 genes (ABCB7, THOC2, PKN3, and HIST1H3C) were upregulated and 8 (TP63, IGF1, AIM2, ARHGAP6, RAP2B, TRIM66, CNBP, and ATG3) were downregulated. This study explores the notable genes that may responsible for cervical cancer.

References
Bray, F., Ferlay, J., Soerjomataram, I., Siegel, R. L., Torre, L. A., & Jemal, A. (2018). Global cancer statistics 2018: GLOBOCAN estimates of incidence and mortality worldwide for 36 cancers in 185 countries. CA: a cancer journal for clinicians, 68(6), 394-424.HLA-B, N. (2017). Integrated genomic and molecular characterization of cervical cancer. Nature, 543, 16.Kumar, M., Sonker, P. K., Saroj, A., Jain, A., Bhattacharjee, A., & Saroj, R. K. (2020). Parametric survival analysis using R: Illustration with lung cancer data. Cancer Reports, 3(4), e1210.Rajput, M., Kumar, M., Kumari, M., Bhattacharjee, A., & Awasthi, A. A. (2020). Identification of key genes and construction of regulatory network for the progression of cervical cancer. Gene Reports, 21, 100965.Saroj, R. K., Murthy, K. N., Kumar, M., Bhattacharjee, A., & Patel, K. K. (2021). Bayesian competing risk analysis: An application to nasopharyngeal carcinoma patients data. Computational and Systems Oncology, 1(1), e1006.Scheike, T. H., & Zhang, M. J. (2002). An additive–multiplicative Cox–Aalen regression model. Scandinavian Journal of Statistics, 29(1), 75-88.Utada, M., Chernyavskiy, P., Lee, W. J., Franceschi, S., Sauvaget, C., de Gonzalez, A. B., & Withrow, D. R. (2019). Increasing risk of uterine cervical cancer among young Japanese women: Comparison of incidence trends in Japan, South Korea and Japanese-Americans between 1985 and 2012. International journal of cancer, 144(9), 2144-2152.
Tripathi, N., Keshari, S., Shahi, P., Maurya, P., Bhattacharjee, A., Gupta, K., ... & Kumar, M. (2020). Human papillomavirus elevated genetic biomarker signature by statistical algorithm. Journal of Cellular Physiology, 235(12), 9922-9932.Wei, L. J. (1992). The accelerated failure time model: a useful alternative to the Cox regression model in survival analysis. Statistics in medicine, 11(14-15), 1871-1879.Zhang, J., Späth, S. S., Marjani, S. L., Zhang, W., & Pan, X. (2018). Characterization of cancer genomic heterogeneity by next-generation sequencing advances precision medicine in cancer treatment. Precision clinical medicine, 1(1), 29-48.

Back to Table of contents

MS05 Nucleic acids and their interaction

MS05-1-1 Crystallization of Alzheimer DNA Promoter Sequences from Amyloid Precursor Gene with Thioflavin T and Other Fluorescent Markers
#MS05-1-1

H. Dimitrova [1], R. Rusev [1], B. Shivachev [1], Z. Delcheva [1], N. Kuvandjiev [1]
[1]Institute of Mineralogy and Crystallography "Acad. Ivan Kostov", Bulgarian Academy of Sciences, Acad. G. Bonchev str., bl. 107, 1113 Sofia, Bulgaria - Sofia (Bulgaria)

Abstract

The object of the present work is the detection of binding interactions and co-crystallization of Alzheimer's DNA promoter sequences of the amyloid precursor (APP) gene with Thioflavin T (ThT), new ThT analogues and other fluorescent markers.

Thioflavin T fluorescence is often used as a diagnostic of amyloid structure, but it is not completely specific for amyloid [1]. Depending on the particular protein and experimental conditions, Thioflavin T may or may not undergo a spectroscopic change upon binding to precursor monomers, small oligomers, and unaggregated material with high β-sheet content or even alpha helix-rich proteins. Conversely, some amyloid fibrils do not affect Thioflavin T fluorescence, raising the prospect of false negative results [1]. However, the in depth analysis of the binding of ThT to DNA can significantly contribute to shed light on the optical properties of ThT and their possible dependence on the hydrophobic local characteristics of the binding pocket. This information can be of use in the improvement of the biomedical/biological applications of ThT or similar sensors.

The variety DNA oligonucleotide sequences from the promoter region of the APP gene containing 5'-CAGCTG-3' (S1) sector [2] and/or 5'-AATGAGGTGGAGAATGT-3' (S2) part [3] were crystallized by the vapor diffusion method. The crystallization conditions contained cacodylate buffer (pH 6.5-7.5), alcohol (2-propanol or methylpentanediol (MPD)), cations (Mg^{2+}, Ba^{2+}, Zn^{2+}), cobalt hexamine $[Co(NH_3)_6]^{3+}$ and polyamines (Spermine). As found in the process of optimization of the crystallization conditions, for the tested sequences, crystal growth was observed only in the conditions featuring Spermine. Crystals were grown by the "hanging drop" method and 1.5μl (2mM) ligand was added to 1.5 μl DNA (2mM) for a 3 μl total drop volume (room temperature) and the drop was equilibrated against 50% MPD. Crystals suitable for single crystal X-ray analysis, formed within a month (Fig. 1).

The improvement of the optimal conditions for crystallization and co-crystallization of selected sequences from the promoter region of the APP gene as well as their subsequent co-crystallization with Thioflavin T and other fluorescent markers, represents a cutting-edge research. Chemical synthesis of homologous Thioflavin T molecules was performed. Thioflavin T analogues were prepared by a two-step procedure consisting of a condensation reaction to obtain Schiff bases and subsequent quaternization with CH_3I or $(CH_3)_2SO_4$. The reactions were performed both in solution and solid phase.

It is expected that single crystal samples of the co-crystallized Alzheimer DNA Promoter Sequences from Amyloid Precursor Gene to be structurally determined on the basis of single crystal X-ray analysis. The structural determination of the ThT binding site will contribute to the most accurate determination of the sequence specificity of this DNA marker or the exclusion of such affinity for particular bases from the DNA sequence.

References

[1] A. Biancardi, T. Biver, and B. Mennucci, Fluorescent dyes in the context of DNA-binding: The case of Thioflavin T., International Journal of Quantum Chemistry (2017) 117(8).
[2] Chernak, J.M., Structural features of the 5′ upstream regulatory region of the gene encoding rat amyloid precursor protein., Gene (1993) 133(2).
[3] Brohede, J., et al., A DNA methylation study of the amyloid precursor protein gene in several brain regions from patients with familial Alzheimer disease., Journal of neurogenetics (2010) 24(4).

Obtained crystals

Back to Table of contents

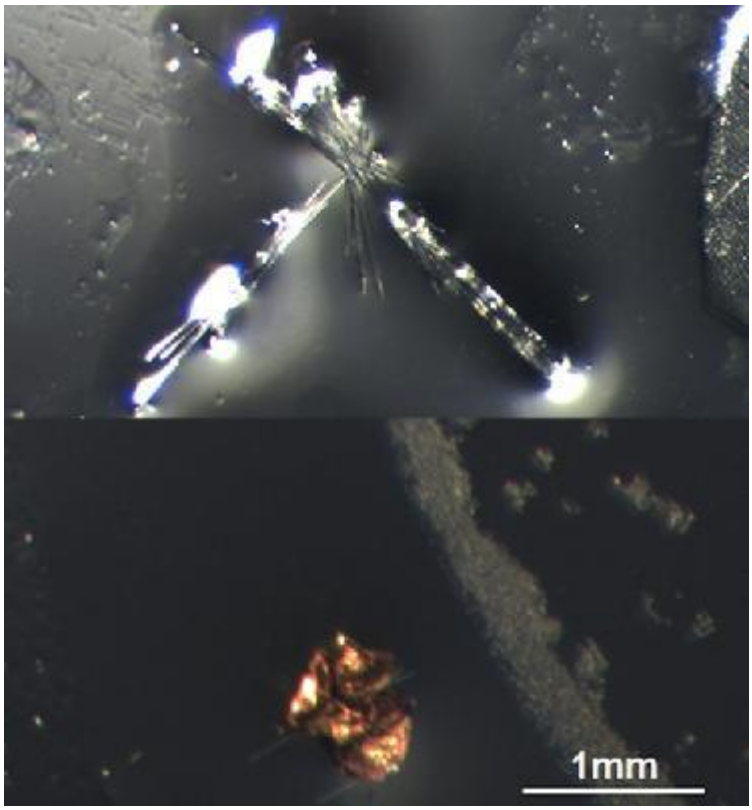

Back to Table of contents

MS05 Nucleic acids and their interaction

MS05-1-2 Uncovering the role of protein HelD in bacterial transcription – the growing picture based on structural and functional data
#MS05-1-2

J. Dohnálek [1], T. Kouba [2], T. Kovaľ [1], P. Sudzinová [3], J. Pospíšil [3], H. Šanderová [3], M. Trundová [1], B. Husťáková [1], K. Murakami [4], L. Krásný [3]
[1]Institute of Biotechnology, Czech Academy of Sciences - Vestec near Prague (Czech Republic), [2]Institute of Organic Chemistry and Biochemistry, Czech Academy of Sciences - Prague (Czech Republic), [3]Institute of Microbiology of Czech Academy of Sciences - Prague (Czech Republic), [4]Pennsylvania State University - State College (United States)

Abstract
RNA synthesis is central to life. The complex responsible for RNA synthesis – RNA polymerase (RNAP) – depends in its function on a number of accessory factors, some of which play a role in recovery from stalled states and adaptation to environmental changes. The helicase-like protein HelD discovered in 2011 [1] has been shown to be a multi-domain partner of RNAP [2,3], capable of tight binding to RNAP in an unprecedented manner [4]. The current picture of the HelD structure-function relationship has been so far depicted using small angle X-ray scattering, crystallography and Cryo-EM, together with biophysical measurements, and specifically designed transcription assays. Our cryo-EM structure of a complex between the *Mycobacterium smegmatis* RNAP and HelD shows the crescent-shaped HelD simultaneously penetrating deep into two RNAP channels that are responsible for nucleic acids binding and substrate delivery to the active site, thereby locking RNAP in an inactive state. Three structural classes suggest three states of the process of HelD binding to RNAP and of its interference with transcription. HelD is expected to help release RNAP from stalled elongation complexes. While the mechanism of its binding and nucleic acids release is largely explained by the current results, the mechanism of HelD unbinding from RNAP is yet to be explained. New structural and functional data bring insights into the intereference of HelD with the transcriptional cycle of RNAP and the role of its so far not fully understood NTPase activity.

This work was supported by MEYS (LM2015043, LM2018127, and CZ.1.05/1.1.00/02.0109), CSF (20-12109S and 20-07473S), NIH (grant R35 GM131860), AS CR (86652036), ERDF (CZ.02.1.01/0.0/0.0/15_003/0000447), EMBL (EI3POD) and Marie Skłodowska-Curie grant (664726).

References
1. Delumeau O, Lecointe F, Muntel J, Guillot A, Guédon E, Monnet V, Hecker M, Becher D, Polard P, Noirot P. (2011) The dynamic protein partnership of RNA polymerase in *Bacillus subtilis*. Proteomics 11, 2992-3001.
2. Wiedermannová J, Sudzinová P, Kovaľ T, Rabatinová A, Šanderova H, Ramaniuk O, Rittich Š, Dohnálek J, Fu Z, Halada P, Lewis P, Krásny L. (2014) Characterization of HelD, an interacting partner of RNA polymerase from *Bacillus subtilis*. Nucleic Acids Res. 42, 5151-5163.
3. Kovaľ T, Sudzinová P, Perháčová T, Trundová M, Skálová T, Fejfarová K, Šanderová H, Krásný L, Dušková J, Dohnálek J. (2019) Domain structure of HelD, an interaction partner of *Bacillus subtilis* RNA polymerase. FEBS Lett. 593, 996-1005.
4. Kouba T, Koval' T, Sudzinová P, Pospíšil J, Brezovská B, Hnilicová J, Šanderová H, Janoušková M, Šiková M, Halada P, Sýkora M, Barvík I, Nováček J, Trundová M, Dušková J, Skálová T, Chon U, Murakami KS, Dohnálek J, Krásný L. (2020) Mycobacterial HelD is a nucleic acids-clearing factor for RNA polymerase. Nat Commun. 11:6419.

Back to Table of contents

MS05 Nucleic acids and their interaction

MS05-1-3 Prediction of DNA hydration based on data mining of crystallographic structures
#MS05-1-3

L. Biedermannova [1], B. Schneider [1]
[1]Institute of Biotechnology - Vestec (Czech Republic)

Abstract
Water plays an important role in stabilizing DNA structure and in mediating its interactions. In our work, we utilize crystallographic data to compile the average hydration patterns around biomolecules - proteins [1,2,3] and nucleic acids [4,5,6]. Recently, we investigated hydration of DNA as a function of its conformation and sequence. We analyzed hydration of DNA dinucleotides from an ensemble of 2,727 non-redundant DNA chains containing 41,853 dinucleotides and 316,265 associated first-shell water molecules [6].
The dinucleotides were classified into categories based on their 16 sequences and the previously determined structural classes, so called nucleotide conformers (NtCs). The construction of hydrated dinucleotide building blocks allowed dinucleotide hydration to be calculated as probability of water density distributions (Figure 1). Peaks in the water densities - Hydration Sites (HSs) - uncovered the interplay between the base and the sugar-phosphate hydration in the context of sequence and structure.
Here, we present the overview of these results and the potential application of the the hydrated building blocks for the prediction of DNA hydration (Figure 2). The data for the hydrated building blocks and the predictions are available for browsing and visualization at the website watlas.datmos.org/watna.

References
[1] Biedermannová L. & Schneider B.: Structure of the ordered hydration of amino acids in proteins: analysis of crystal structures. Acta Crystallographica D71: 2192-2202 (2015).[2] Černý J., Schneider B. & Biedermannová L.: WatAA: Atlas of Protein Hydration. Exploring synergies between data mining and ab initio calculations. Phys. Chem. Chem. Phys. 19, 17094 (2017).[3] Biedermannová L. & Schneider B.: Hydration of proteins and nucleic acids: Advances in experiment and theory. A review. Biochimica et Biophysica Acta - General Subjects 1860: 1821-1835 (2016). [4] Schneider B. & Berman H.M.: Hydration of the DNA Bases Is Local. Biophysical J. 69: 2661-2669 (1995). [5] Schneider B., Patel K. & Berman H.M.: Hydration of the Phosphate Group in Double-Helical DNA. Biophysical J. 75: 2422-2434 (1998). [6] Biedermannová L. et al., Acta Cryst D, under consideration (2022).

Calculation of hydrated building blocks

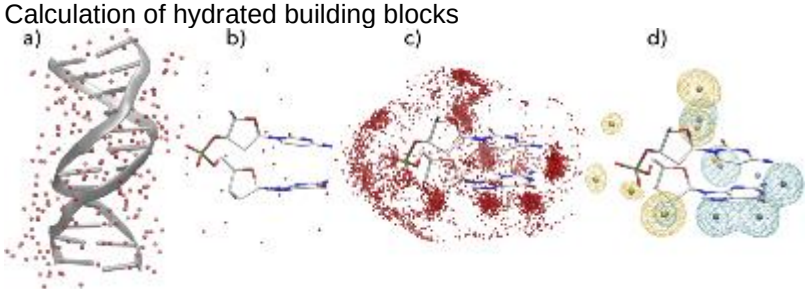

Predicted (yellow and cyan) vs crystal water (red)

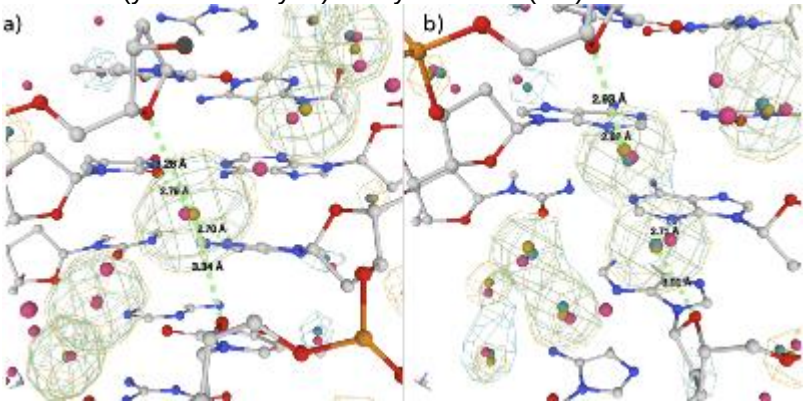

Back to Table of contents

MS05 Nucleic acids and their interaction

MS05-2-1 Crystallographic structures of aIF5B from Pyrococcus abyssi in its GDP and GTP-bound forms #MS05-2-1

Y. Mechulam [1], G. Bourgeois [1], R. Kazan [1], P.D. Coureux [1], E. Schmitt [1]
[1]Laboratoire de Biologie structurale de la cellule,CNRS-Ecole polytechnique-Institut polytechnique de Paris - Palaiseau (France)

Abstract
e/aIF5B is a eukaryotic and archaeal translational GTPase involved in the late steps of translation initiation. After start codon recognition on the small ribosomal subunit and e/aIF2 release, e/aIF5B-GTP binds the initiator tRNA and catalyzes the joining of the large ribosomal subunit to form a ribosome competent for elongation. e/aIF5B is then released in a GDP-bound form. Despite their central role, the mechanisms of GTP-dependent conformational switching is still debated. Here, we present two crystal structures of aIF5B from the hyperthermophilic archeon *Pyrococcus abyssi*. The structure of the full-length protein bound to GDP was refined 2.9 Å resolution. The structure of a C-terminally truncated form of the protein bound to GTP was refined to 1.7 Å resolution. In this structure, one magnesium ion and one sodium ion are tightly bound to the nucleotide. Comparison of both structures highlights the conformational changes associated to the binding of the nucleotides. As for all translational GTPases, the GDP/GTP binding is controlled by the OFF/ON movements of two switch regions. However, other specific regions of aIF5B change their conformation during the GTP/GDP transition. The movement of these regions could be involved in the mechanism of action of the factor on the ribosome.

Back to Table of contents

MS05 Nucleic acids and their interaction

MS05-2-2 Role of aIF5B in archaeal translation initiation
#MS05-2-2

R. Kazan [1], G. Bourgeois [1], C. Lazennec-Schurdevin [1], Y. Mechulam [1], P.D. Coureux [1], E. Schmitt [1]
[1]Laboratoire De Biologie Structurale De La Cellule- CNRS-UMR7654-Ecole Polytechnique-Institut Polytechnique de Paris - Palaiseau (France)

Abstract
Translation initiation (TI) allows accurate selection of the initiation codon on a messenger RNA (mRNA) and defines the reading frame. In all domains of life, translation initiation generally occurs within a macromolecular complex made up of the small ribosomal subunit, the mRNA, a specialized methionylated initiator tRNA and translation initiation factors (IFs). Once the start codon is selected at the P site of the ribosome and the large subunit is associated, the IFs are released and a ribosome competent for elongation is formed. However, even if the general principles are the same in the three domains of life, the molecular mechanisms are different in bacteria, eukaryotes, and archaea.
In eukaryotes and in archaea late steps of translation initiation involve the two initiation factors e/aIF5B and e/aIF1A. In eukaryotes, the role of eIF5B in ribosomal subunit joining is established and structural data showing eIF5B bound to the full ribosome were obtained. To achieve its function, eIF5B collaborates with eIF1A. However, structural data illustrating how these two factors interact on the small ribosomal subunit have long been awaited. The role of the archaeal counterparts, aIF5B and aIF1A, remains to be extensively addressed. We studied the late steps of Pyrococcus abyssi translation initiation. Using in vitro reconstituted initiation complexes and light scattering, we show that aIF5B bound to GTP accelerates subunit joining without the need for GTP hydrolysis. We report the crystallographic structures of aIF5B bound to GDP and GTP and analyze domain movements associated to these two nucleotide states. Finally, we present the cryo-EM structure of an initiation complex containing 30S bound to mRNA, Met-tRNAiMet, aIF5B and aIF1A at 2.7 Å resolution. Structural data shows how archaeal 5B and 1A factors cooperate to induce a conformation of the initiator tRNA favorable to subunit joining. Archaeal and eukaryotic features of late steps of translation initiation are discussed.

Back to Table of contents

MS05 Nucleic acids and their interaction

MS05-2-3 UBDB+EPMM approach as a tool for investigating electrostatic interactions between proteins and RNA #MS05-2-3

U. Budniak [1], P. Dominiak [1]
[1]CNBCh, Department of Chemistry, University of Warsaw - Warsaw (Poland)

Abstract
I would like to present the method for characterization of protein-RNA interaction on the example of IFIT-RNA complexes. IFITs proteins (Interferon-induced proteins with tetratricopeptide repeats) are expressed in cells infected by viruses and by binding foreign RNA they prevent synthesis of viral proteins in human host cell. They can bind different forms of RNA: with triphosphate group, guanine or cap at 5' end of RNA. I calculated electrostatic interactions in selected complexes of IFIT1 and IFIT5 proteins with RNA on the basis of the known structures deposited in Protein Databank and compared the results with experimental values of binding affinity.
I decided to focus on the electrostatic interaction energy because it has been shown, that electrostatic energy is a sufficient approximation of total interaction energy. Biomacromolecules (proteins, nucleic acids) are too complex systems for precise quantum mechanical computations and calculations of total energy are yet too demanding. Furthermore, electrostatic energy is the best component of total energy, because it is the least sensitive to errors in geometry of investigated systems. Such errors are often encountered while determining structures of big, biological complexes, for which it is very difficult to properly define position of all atoms. There are computational methods, which enable to estimate electrostatic interaction energy in macromolecules, however, most of them base on simplified methods taken from classical mechanic (force fields), where electrostatics is usually approximated by Coulomb interactions of point charges. I used the UBDB+EPMM approach, by which it is possible to compute electrostatic energies with similar accuracy as with quantum chemistry methods, for wide range of types of interactions (hydrogen bonds, π-π stacking) and distances (not only at equilibrium geometry but also below or above). University at Buffalo Pseudoatom DataBank (UBDB) enables reconstruction of charge density for macromolecules in quantitative manner. Exact Potential Multipole Method (EPMM) evaluates the exact Coulomb integral in the inner region (≤4.5 Å) and combines it with a Buckingham-type multipole approximation for long-range interatomic interactions, hence computational time is shortened. The UBDB+EPMM method has been successfully used in previous research to analyze interactions in peptides, proteins and various complexes e.g. aminoglycosides with RNA or proteins with DNA.
Energy calculations were based on the structures of IFIT5 proteins with pppRNA and IFIT1 with different 5'end of RNA deposited in PDB. The UBDB was transferred to reconstruct electron density distribution and thorough calculations of interactions between ligand and particular amino acids in the biding site were conducted to indicate significant residues influencing interaction energy. I showed that according to the calculations of electrostatic energy, the interactions of the IFIT5 protein with RNA do not depend on the sequence of the first three nucleotides of the RNA. Moreover, the IFIT1 protein should bind pppRNA with a similar strength as it binds cap0RNA. In addition, I identified energy-important amino acids, the mutations of which may affect the strength of RNA binding by the protein.
Project was financed from the grant PRELUDIUM11 of National Science Centre, Poland nr 2016/21/N/ST4/03722.

References
Jarzembska, K. N. & Dominiak, P. M. (2012) *Acta Cryst*. A68, 139–147.Volkov A. *et al.* (2004) *Chem. Phys. Lett.* 391, 170–175.Dominiak P. M. *et al.* (2009) *Acta Cryst*. D65, 485-499.Kulik M. *et al.* (2015) *Biophys. J*., 108(3):655-665.Abbas, Y. M. *et al.* (2013) *Nature* 494(7435), 60-64.Abbas, Y.M. *et al.* (2017) *PNAS*, 114(11), E2106-E2115.

Back to Table of contents

MS05 Nucleic acids and their interaction

MS05-2-4 TREN and TMPA capped calix[6]arene metal complexes as ds-DNA/RNA binders
#MS05-2-4

A. Višnjevac [1], N. Nyssen [2], I. Nikšić-Franjić [1], I. Piantanida [1], B. Colasson [2], O. Reinaud [2]
[1]Institut Ruđer Bošković - Zagreb (Croatia), [2]Universite de Paris - Paris (France)

Abstract
TMPA and TREN capped calix[6]arene derivatives are specially designed for an easy coordination of variety of transition metal dications and specific intra-cavity inclusion of small organic species attracted (and coordinated) by this cations. Within the frame of a project aimed to investigate capability of these remarkable edifices to recognize various ds-DNA or ds-RNA structures and to study structural particularities of so formed non-covalent assemblies, we are reporting single crystal X-ray structures of a TMPA capped calixarene copper (II) complex, [Cu(II)X6(NMe3+)3tmpaOMe(MeCN)][NO3-]5 (1) and two isostructural TREN capped calix[6]arene cobalt (II) complexes, [Co(II)X6trenOMe(MeCN)][ClO4-]2 (2) and [Co(II)X6trenOMe(OH)]ClO4- (3). In all complexes, four metal coordination valences are occupied by four nitrogen donor atoms from TMPA (in 1) and TREN (in 2 and 3). While the fifth coordination site in 1 and 2 is occupied by an intra-cavity coordinated acetonitrile molecule, in 3, this site is taken by a hydroxide anion. In all three structures, metal lies in a centre of a slightly distorted trigonal bipyramid, with an apical compression in the case of Cu(II) complex 1, and elongation in the case of Co(II) complexes 2 and 3. The apical compression of the pyramid as observed in 1 indirectly confirms the oxidation state of the copper, which was impossible to establish crystallographically, due to an overwhelming disorder of the two nitrate counter anions. Charge of the Co(II) is expectedly balanced by two extra cavity perchlorate counter anions in 2 and by one in 3 (as the other negative charge here emanates from the intra-cavity bound OH). While there are no classic H-bonds in the structure of 1, in cobalt complexes 2 and 3, a network of H-bonds involving the perchlorate anion guides crystallographic packing by a formation of H-bonded perchlorate bridged head-to-tail molecular chains.
Both, experimentally (fluorimetric experiments by Ethidium bromide and DAPI displacement) and computationally (molecular dynamics simulations), it was confirmed that the metal complex 1, with water or hydroxide instead of acetonitrile bound in the cavity, efficiently binds to the DNA minor groove, as well as corresponding calixarene with no metal cation attached. In contrast, the calixarene analogue in which the positively charged trimethylammonium feet are replaced with neutral amino groups does not bind to the ds-DNA, whereas its Cu (II) complex does. These findings confirm the crucial role of the positive charge in these molecules for the efficient DNA binding.

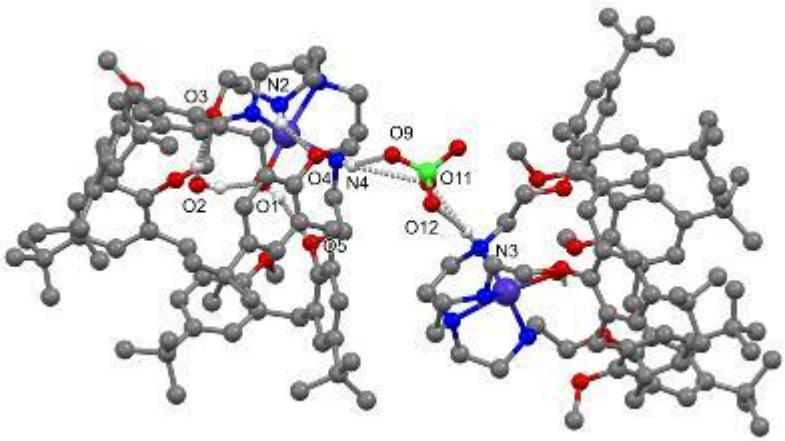

Back to Table of contents

MS05 Nucleic acids and their interaction

MS05-2-5 Racemic crystal structures of A-DNA duplexes
#MS05-2-5

B. Kauffmann [1], P.K. Mandal [2], I. Huc [2]
[1]IECB, University of Bordeaux, CNRS, INSERM - Pessac (France), [2]Department of Pharmacy and Center for Integrated Protein Science, Ludwig-Maximilians-University - Munich (Germany)

Abstract
The ease with which racemic mixtures crystallize compared to equivalent chiral systems is a phenomenon with which chemists are highly familiar. However, biological macromolecules such as DNA and proteins are naturally chiral, and thus the limited range of chiral space groups available hampers crystallisation of such molecules. Inspiring work over the past 15 years has shown that racemic mixtures of proteins – made possible by impressive advances in protein chemical synthesis – can indeed improve the success rate of protein crystallisation experiments. More recently, the racemic crystallisation approach was extended to include nucleic acids. Thus, the use of racemic mixtures of nucleic acids may aid in the determination of enantiopure DNA crystal structures. Here, we report findings that suggest that benefits may extend beyond this. We describe two racemic crystal structures of the DNA sequence d(CCCGGG) which we find to fold into A-form DNA. This form differs from the Z-form DNA conformation adopted by the chiral equivalent in the solid state, showing that the use of racemates may also favour the emergence of new conformations. Importantly, the racemic mixture forms interactions in the solid state that differ from the chiral equivalent (including the formation of racemic pseudo-helices), suggesting that the use of racemic DNA mixtures could provide new possibilities towards the design of precise self-assembled nano-materials and nano-structures.

References
Jacques, J., Collet, A. & Wilen, S. (1994). Enantiomers, Racemates and Resolutions. Malabar, Florida: Krieger Publishing Co.
Mathews, B. W. (2009). Protein Sci. 18, 1135–1138.
Mandal, P. K., Collie, G. W., Kauffmann, B. & Huc, I. (2014). Angew. Chem. Int. Ed. 53, 14424–14427.

L/D- d(CCCGGG)2 in two racemic crystal forms

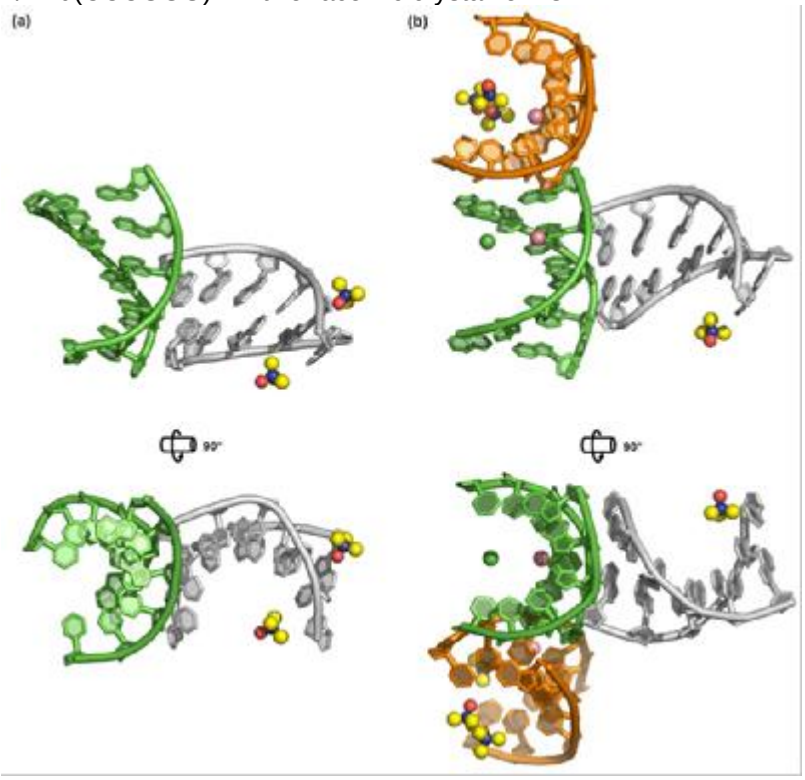

Back to Table of contents

MS05 Nucleic acids and their interaction

MS05-2-6 Target sequence recognition and gene regulation by Grainyhead/CP2 transcription factors #MS05-2-6

U. Heinemann [1], Q. Ming [1], Y. Roske [1], M. Rutkiewicz [1], J. Wang [1]
[1]Max-Delbrück Center Mol. Medicine - Berlin (Germany)

Abstract
Recognition of and binding to specific target sequences on double-stranded (ds) DNA are the initial steps in gene regulation by transcription factors (TFs). In humans, TFs of the Grainyhead/CP2 family are involved in regulating a variety of genes both during embryogenesis and in different tissues of the adult organism. Based on their sequences these TFs are ordered in the Grainyhead-like subfamily comprising GRHL1, GRHL2 and GRHL3, and the CP2 subfamily comprising TFCP2, TFCP2L1 and UBP1. In earlier work, we biochemically analyzed dsDNA binding and determined crystal structures of the DNA-binding domains (DBDs) and oligomerization domains of GRHL1 and GRHL2. The structural basis of target DNA recognition by Grainyhead-like TFs was established by co-crystallizing the GRHL1 DBD with a dsDNA fragment centered around the core binding motif AACCGGTT (1). Unexpectedly, a recent survey of GRHL1-binding DNA motifs using neural networks identified target DNA sequences not containing the previously known core binding motif (Proft et al., unpublished). To extend this study, crystal structures of the DBDs of TFCP and TFCP2L1 from the CP2 branch of the larger protein family were determined. In addition, a structure of dsDNA-bound TFCP2L1 DBD was analyzed and binding parameters were measured by isothermal titration calorimetry (Wang et al., unpublished). These analyses indicated that the TFs of the Grainyhead/CP2 family share a common mode of DNA recognition by binding as apparent dimers to symmetric target sequences, forming specific hydrogen-bonded contacts in the major groove and less specific contacts in the minor groove of dsDNA that displays a largely unperturbed B-form structure. Although the DNA recognition is similar in Grainyhead and CP2 TFs, other aspects of their gene regulation mechanisms are expected to differ, because the N-terminal transactivation domains in both subfamilies are distinct.

References
1. Ming, Q., Roske, Y., Schuetz, A., Walentin, K., Ibraimi, I., Schmidt-Ott, K.M. & Heinemann, U. (2018) Structural basis of gene regulation by the Grainyhead/CP2 transcription factor family. Nucleic Acids Res. 46, 2082-2095.

Back to Table of contents

MS06 Structural Enzymology

MS06-1-1 Cysteine Synthase: A key enzyme in the cysteine synthesis pathway and a novel drug target for Chagas Disease
#MS06-1-1

K. Sowerby [1]
[1]Durham University - Durham (United Kingdom)

Abstract
Trypanosoma cruzi, the causative agent of Chagas' disease, affects 8 million people worldwide, largely in Latin America. In the last century, this disease has begun to spread with more than 25 million people at risk of infection. Chagas' disease often has no symptoms or non-specific effects leading to the disease developing into a chronic and life-threatening infection. Cysteine is an essential amino acid for the survival of *T. cruzi* as it allows the parasite to survive oxidative bursts imposed by the human immune system. Cysteine synthase is one of two of proteins responsible for cysteine synthesis within the *de novo* synthesis pathway of the parasite. Cysteine synthase facilitates the β-elimination of the acetate group of O-acetyl serine (produced by serine acetyltransferase) to produce cysteine. This pathway is not found in human cells and is essential to the parasite so represent a potential drug target against Chagas' disease.
Determination of the structure of cysteine synthase is critical to understanding of protein functionality and of this pathway in the parasite. Here I will present the structure of cysteine synthase from *T. cruzi*, as well as from related trypanosomatids *L. infantum* and *T. theileri*. I will also show the initial results of a fragment-based screen that will be used to produce novel inhibitors of this enzyme.

Back to Table of contents

MS06 Structural Enzymology

MS06-1-2 Structural Enzymology on EMBL beamlines at PETRA III
#MS06-1-2

T.R. Schneider [1], M. Agthe [1], I. Bento [1], G. Bourenkov [1], K. Kovalev [1], S. Panneerselvam [1], D. Von Stetten [1], S.L. Storm [1]
[1]EMBL c/o DESY - Hamburg (Germany)

Abstract
EMBL is operating three endstations – P13, P14, T-REXX - for macromolecular crystallography on the PETRA III synchrotron in Hamburg. T-REXX is operated in collaboration with HARBOR (https://www.cui.uni-hamburg.de/en/harbor.html). Instrumentation for sample characterization and crystallization are available in the adjacent Sample Preparation and Characterization Facility. We will present an overview of recent applications of the facilities in structural enzymology including:
- Atomic resolution: Rindfleisch .. Tittmann (2022): Ground-state destabilization by electrostatic repulsion is not a driving force in orotidine-5′-monophosphate decarboxylase catalysis. Nature Catalysis 5: 332.
- Time-resolved: Mehrabi .. Pai (2019): Time-resolved crystallography reveals allosteric communication aligned with molecular breathing. Science 365:1167
- Micro-crystals: Shahsavar ... Nissen (2021): Structural insights into the inhibition of glycine reuptake. Nature 591:677
- Large complexes: Singh ... Chari (2020): Discovery of a Regulatory Subunit of the Yeast Fatty Acid Synthase. Cell. 180:1130.
- S-SAD phasing: Loch ... Jaskolski (2021): Crystal structures of the elusive Rhizobium etli L-asparaginase reveal a peculiar active site. Nat Commun. 12:6717.
New opportunities arising with the recently installed EIGER2 16M CdTe detector and the planned fourth generation synchrotron PETRA IV will be discussed.
We gratefully acknowledge funding from the BMBF and iNext-Discovery. For access: smis.embl-hamburg.de/, inext-discovery.eu/.

Back to Table of contents

MS06 Structural Enzymology

MS06-1-3 Identifying the key determinants of enzyme specificity in two Stereo-complementary Class II Pyruvate Aldolases of Bacterial Origin
#MS06-1-3

I. Justo [1], S. Marsden [2], U. Hanefeld [2], I. Bento [3]
[1]EMBL - Hamburg (Germany), [2]Technische Universiteit Delft - Delft (Netherlands), [3]EMBL-Hamburg - Hamburg (Germany)

Abstract
Class II pyruvate aldolases are enzymes capable of catalyzing the formation of new carbon-carbon bonds in a stereospecific and reversible manner, having lately attracted great attention as potential biocatalysts. In their enzymatic mechanism, these enzymes use a divalent metal cation as a cofactor and are highly specific for the nucleophile donor substrate. Some enzymes are able to take besides pyruvate, hydroxy- and fluoro- pyruvate as a donor substrate [1]. Regarding the acceptor aldehyde substrate, these hydroxy-ketoacid aldolases accept a diverse range of acceptor aldehydes. With the goal of identifying key residues that underlie the enzymatic mechanism and the stereospecificity of such enzymes, the structural and enzymatic characterization of two different hydroxyketoacid aldolases, namely SwHKA from Sphingomonas wittichii RW1 (3S,4S selective) [1] and BpHKA Burkholderia phytofirmans (3S,4R selective) [1] that show opposite stereoselectivity, was performed. Based on several high-resolution crystal structures of native and mutant enzymes, soaked with substrates that were obtained for both SwHKA [2] and BpHKA enzymes, and on the enzymatic characterization of such enzymes, we were able to identify a new resting state for SwHKA and key residues in the active site of both SwHKA and BpHKA responsible for the stabilization and for the correct orientation of the acceptor aldehyde for catalysis.

References
1. V. De Berardinis, C. Guérard-Hélaine, E. Darii, K. Bastard, V. Hélaine, A. Mariage, J.-L. Petit, N. Poupard, I. Sánchez-Moreno, M. Stam, Green Chemistry 2017, 19, 519-526.2. S.R. Marsden, L. Mestrom, I. Bento, D.G.G. McMillan, P.-L. Hagedoorn, and U. Hanefeld, Adv. Synth. Catal. 2019, 361, 2649– 2658.

Back to Table of contents

MS06 Structural Enzymology

MS06-1-4 The icOS laboratory: time-resolved optical spectroscopy on crystals
#MS06-1-4

S. Engilberge [1], T. Giraud [1], P. Jacquet [2], M. Byrdin [2], D. De Sanctis [1], P. Carpentier [3], A. Royant [2]
[1]Structural Biology Group, European Synchrotron Radiation Facility - Grenoble (France), [2]Univ. Grenoble Alpes, CNRS, CEA, Institut de Biologie Structurale - Grenoble (France), [3]Institut de Recherche Interdisciplinaire de Grenoble, Laboratoire Chimie et Biologie des Métaux, Université Grenoble Alpes, CNRS, CEA - Grenoble (France)

Abstract
The *in crystallo* optical spectroscopy (*ic*OS) laboratory located at the European Synchrotron Radiation Facility (ESRF) hosts a recently upgraded microspectrophotometer for the measurement of UV/vis absorption, fluorescence emission or Raman spectra from protein crystals, providing complementary information to X-ray crystallography.[1] These experiments can serve to assess the physiological state of the protein *in crystallo*.[2,3] As these states can be affected by the absorbed X-ray dose, the spectroscopic measurements potentially serve as a metric of the extent of the radiation damage.[4,5,6] Besides, it can be used to characterize, within crystals, the presence and occupancy of photoreactions intermediate states either at room temperature,[5,7] with a temporal resolution up to the millisecond, or, quenched at cryogenic temperature.[5,6,7,8] Recently, we developed a time-resolved *ic*OS setup (TR-*ic*OS) for the measurement of transient UV-Vis absorption spectra on the microsecond to millisecond time scale. The setup is based on a pump-probe approach with a tunable nanosecond laser as the pump and a xenon flash lamp as the probe. The TR-*ic*OS setup will be used to characterize various biological systems that will be studied by time-resolved diffraction on the brand new serial crystallography beamline ID29-SMX (https://www.esrf.fr/id29).

References
1. von Stetten D *et al*. In crystallo optical spectroscopy (icOS) as a complementary tool on the macromolecular crystallography beamlines of the ESRF. *Acta Crystallogr. D*, **2015**, 71, 15-26.
2. de Zitter E *et al*. Mechanistic investigations of green mEos4b reveal a dynamic long-lived dark state. *J Am Chem Soc*. **2020**, 142, 10978-10988.
3. Bou-Nader C *et al*. An enzymatic activation of formaldehyde for nucleotide methylation. *Nat Commun.* **2021**, 12:4542.
4. Bui S *et al*. Direct evidence for a peroxide intermediate and a reactive enzyme–substrate–dioxygen configuration in a cofactor-free oxidase. *Angew. Chem. Int. Ed.* **2014**, 53, 13710-13714.
5. Gotthard G *et al*. Specific radiation damage is a lesser concern at room temperature. *IUCrJ*. **2019**, 12, 665-680.
6. Sorigué D *et al*. Mechanism and dynamics of fatty acid photodecarboxylase. *Science* **2021**, 372, (6538):eabd5687.
7. Aumonier S *et al*. Millisecond time-resolved serial oscillation crystallography of a blue-light photoreceptor at a synchrotron. *IUCrJ*, **2020**, 7, 728-736.
8. Kovalev K *et al*. Molecular mechanism of light-driven sodium pumping. *Nat Commun*. **2020**, 11:2137.

Back to Table of contents

MS06 Structural Enzymology

MS06-1-5 Protein dynamics probed by time-resolved crystallography on the second to hour time scale #MS06-1-5

N. Caramello [1], S. Engilberge [1], S. Aumonier [2], D. Von Stetten [3], G. Gotthard [4], G.A. Leonard [1], C. Mueller-Dieckmann [1], A. Royant [5]
[1]Structural Biology Group, European Synchrotron Radiation Facility - Grenoble (France), [2]Photon Science Division – Laboratory for Macromolecules and Bioimaging (LSB), Paul Scherrer Institut - Villigen (Switzerland), [3]European Molecular Biology Laboratory (EMBL) c/o DESY - Hamburg (Germany), [4]Laboratory of Biomolecular Research, Biology and Chemistry Division, Paul Scherrer Institute - Villigen (Switzerland), [5]Univ. Grenoble Alpes, CNRS, CEA, Institut de Biologie Structurale (IBS) - Grenoble (France)

Abstract
Over the last decade, the development of serial crystallography (SX) has rejuvenated room temperature macromolecular crystallography (RTMX) and led to technical and methodological breakthroughs [1]. Time-resolved SX usually addresses phenomena occurring on the picosecond to second time scale, but RTMX can be applied to study protein dynamics on slower time scales. We have applied RTMX to study the relaxation of a photostationary equilibrium built within a crystal of the LOV2 domain of phototropin 2 from *Arabidopsis thaliana*, whose photoadduct decays on the minute time scale [2]. We have monitored its relaxation in the dark by recording 1 s data sets using an Eiger X 4M detector, as a follow-up to a study on the population build-up of the same photoadduct [3]. We could observe bond breakage in the photoadduct using both *in crystallo* UV-vis absorption spectroscopy and X-ray crystallography with similar decay time constants. Surprisingly, the return to the ground state of the chromophore is followed by additional protein rearrangements, which slow down the full recovery of the protein ground state. Our work demonstrates the possibility of performing time-resolved protein crystallography experiments from a small number of crystals using standard beamline equipment at synchrotrons for phenomena occurring on the second to hour time scale.

References
1. Schlichting, I. Serial femtosecond crystallography: the first five years. IUCrJ 2, 246–255 (2015).
2. Iuliano, J. N. et al. Unraveling the Mechanism of a LOV Domain Optogenetic Sensor: A Glutamine Lever Induces Unfolding of the Jα Helix. ACS Chem. Biol. 15, 2752–2765 (2020).
3. Aumonier, S. et al. Millisecond time-resolved serial oscillation crystallography of a blue-light photoreceptor at a synchrotron. IUCrJ 7, 728–736 (2020).

Back to Table of contents

MS06 Structural Enzymology

MS06-1-6 Examples of the functional and structural diversity of NYN nucleases
#MS06-1-6

L. Coudray [1], M. Arrive [2], A. Gobert [2], P. Giege [2], C. Sauter [1]
[1]ARN - IBMC - CNRS - Unistra - Strasbourg (France), [2]IBMP - CNRS - Unistra - Strasbourg (France)

Abstract
RNA maturations and modifications play a crucial role in the living by enabling a variety of RNAs to fulfil their functions. These include the cleavages carried out by ribonucleases, which are characterised by binding domains enabling them to interact with RNAs (RBDs) or other partners and catalytic domains responsible for their cleavage function. In 2006, a new globular domain associated with RBDs was identified in several eukaryotic and prokaryotic proteins including YacP and N4BP1. Structural predictions suggested an α/β domain with 5 strands (S) and 4 helices (H), perfectly congruent with secondary structures observed in the PIN (PilT N-terminal) and FLAP catalytic domains. The presence of 2 conserved Asp (D) at the end of S1 and S4 as well as 2 acidic residues in the N-terminal part of H2 and H4 suggests a potential nuclease function for this new domain, which was then named NYN for N4BP1, YacP-like Nuclease domain[1]. Subsequently, this PIN-like domain superfamily was split into 5 major structural subclasses including “NYN” (true NYN) and “PRORP” (Protein only RNase P[2])[3]. Although several proteins with NYN domains have already been identified, the huge diversity of domains associated with NYN suggests a variety of functions and targets, from which very little is known at present.
The structural (X-ray crystallography, SAXS), biophysical (DLS, NanoDSF) and functional (*in vitro* cleavages, RNA-seq) study of these proteins can lead to a better understanding of their role *in vivo* and, in the longer term, to the possibility of diverting their function to solve agronomic[4] or health problems.

References
[1] Anantharaman, V., and Aravind, L. (2006). The NYN domains: novel predicted RNAses with a PIN domain-like fold. RNA Biol 3, 18–27.
[2] Gobert, A., Gutmann, B., Taschner, A., Gößringer, M., Holzmann, J., Hartmann, R.K., Rossmanith, W., and Giegé, P. (2010). A single Arabidopsis organellar protein has RNase P activity. Nat Struct Mol Biol 17, 740–744.
[3] Matelska, D., Steczkiewicz, K., and Ginalski, K. (2017). Comprehensive classification of the PIN domain-like superfamily. Nucleic Acids Res 45, 6995–7020.
[4] Gobert, A., Quan, Y., Arrivé, M., Waltz, F., Da Silva, N., Jomat, L., Cohen, M., Jupin, I., and Giegé, P. (2021). Towards plant resistance to viruses using protein-only RNase P. Nat Commun 12, 1007.

Back to Table of contents

MS06 Structural Enzymology

MS06-1-7 Structure based modification of Omega Transaminases from Pseudomonas putida KT2440 for industrial use
#MS06-1-7

P. Das [1], S. Noronha [2], P. Bhaumik [1]
[1]Dept. of Biosciences and Bioengineering,Indian Institute of Technology Bombay - Mumbai (India), [2]Dept. of Chemical Engineering, Indian Institute of Technology Bombay - Mumbai (India)

Abstract
Transaminases are enzymes that catalyse the exchange of an amino group between an amino acceptor and an amino donor, resulting in the formation of chiral products. A class of these enzymes, known as omega transaminase (ω-TA), can mediate this chiral amination without the requirement of an α-COOH group. These enzymes are also reported to accept unnatural substrates[1], thus increasing their relevance in the production of several pharmaceutical intermediates of commercial interest. However, product inhibition and poor substrate tolerance are some of the several factors that hinder the industrial application of these enzymes despite recent developments in the field of enzyme and process engineering[2]. This study aims at understanding the active site architecture of wild-type transaminases, followed by rational design of the active site to enhance the biotransformation of (*R*)-Phenylacetylcarbinol ((*R*)-PAC) to (*1R*, *2S*)-Norephedrine. Two such ω-transaminases (TA_5182 and TA_2799) were identified in the *P. putida* KT2440 strain and overexpressed in *E. coli* BL21 hosts. Crystals of the purified recombinant enzymes were grown; and the structures of both the enzymes in their apo and co-factor (PLP) bound holo forms were solved. The crystal structure of TA_5182 reveals the position of two flexible loops over the cofactor binding pocket, which are not modelled due to lack of features in the electron density in most of the reported apo structures of the similar enzymes. TA_2799 was solved in the co-factor bound state with a PLP molecule covalently bonded to the catalytic Lys286 as an internal aldimine. Based on their crystal structures, the FoldX stability enhancement algorithm was used to predict probable mutations in sites away from the active site to enhance the stability of the enzymes (Figure 1). Enzyme activity assays show that TA_2799 requires significantly higher concentrations of co-factor than TA_5182 to achieve satisfactory biotransformation of R-PAC. In-silico analyses were performed to generate mutants of TA_2799 to reduce the co-factor dependency of the enzyme. Based on substrate docking studies, several mutants are proposed to modify the substrate-binding pocket of the enzymes to accommodate a wider range of substrate molecules. The results of our studies will generate Pseudomonad ω-TAs with high efficiency for asymmetric synthesis, to be used in host systems for optimal large-scale industrial biotransformation.

References
1. Zhang, Z., Liu, Y., Zhao, J., Li, W., Hu, R., Li, X., ... & Ma, L. (2021). Active-site engineering of ω-transaminase from Ochrobactrum anthropi for preparation of L-2-aminobutyric acid. *BMC biotechnology, 21*(1), 1-9.2. Kelefiotis-Stratidakis, P., Tyrikos-Ergas, T., & Pavlidis, I. V. (2019). The challenge of using isopropylamine as an amine donor in transaminase catalysed reactions. *Organic & Biomolecular Chemistry, 17*(7), 1634-1642.

Overall structure and rational design of ω-TA

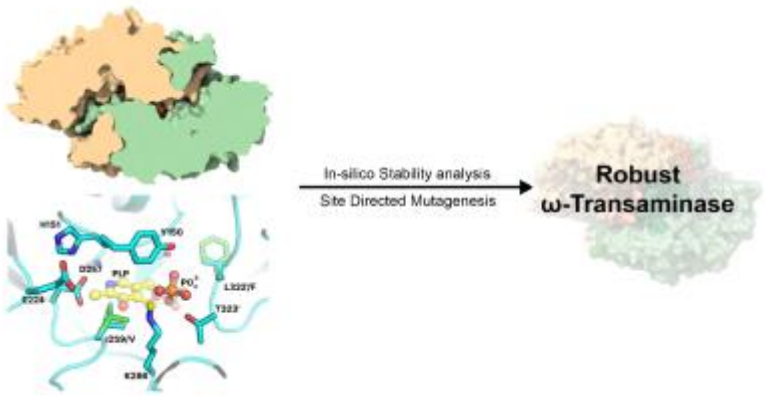

Back to Table of contents

MS06 Structural Enzymology

MS06-1-8 Structural and functional insight into Glycocin-Glycosyltransferases
#MS06-1-8

M. Krummhaar [1], A. Langhans [2], B. Koksch [2], C. Roth [1]
[1]Max Planck institute of colloids and interfaces - Potsdam (Germany), [2]Freie Universität Berlin - Berlin (Germany)

Abstract
Antimicrobial resistance is on the rise and thus, there is an urgent need to discover novel antimicrobial compounds and determine their mechanism of action.A promising class of such antimicrobials are bacteriocins: Short ribosomally synthesized and post-translationally modified peptides (RiPPs).One subclass of these peptides requires a glycosylation to show antimicrobial activity and thus have been termed glycoactive bacteriocins, Glycocins.[1]Despite their high potency, the challenging synthesis renders the elucidation of the mechanism of action difficult. The correct glycosylation is installed by a dedicated glycosyltransferase that is able to either glycosylate a serine or threonine, resulting in canonical *O*-glycosylation or a cysteine resulting in a rare type of *S*-glycosylation.[2-4]Insights into the function of the cognate Glycocin-Glycosyltransferases (GGTs) will help to understand the unusual specificity of theses transferases of cysteine and/or serine and threonine. Furthermore, these transferases might be useful tools to synthesise glycocins, glycopeptides and neo-glycopeptides in general.We were able to discover several putative Glycocins and their cognate GGTs based on sequence similarity and cluster characterisation.The recombinant production and subsequent purification of five GGTs from *Bacillus subtilis*, *Gottfriedia acidiceleris*, *Laceyella sacchari*, *Enterococcus faecalis* and *Streptomyces platensis*, was established.The recombinant GGTs were characterised in regard of the metal ion dependency and the carbonucleotide specificity by direct measurements of the binding constants with isothermal titration calorimetry.To investigate the molecular determinants for the observed differences in specificity in terms of preferred sugars and their *S*/*O*-selectivity, we use X-ray crystallography as method of choice. For four GGTs crystals could be obtained and the crystal structure for the *B. subtilis* GGT could be solved to 2.6 Å resolution.

References
1. Norris, G. E.; Patchett, M. L., The glycocins: in a class of their own. Current Opinion in Structural Biology 2016, 40, 112-119.2. Nagar, R.; Rao, A., In Vitro Synthesis of Bioactive Glycovariants of Enterocin 96, an Antimicrobial Peptide from Enterococcus faecalis. Methods Mol Biol 2019, 1954, 279-296.3. Biswas, S.; Garcia De Gonzalo, C. V.; Repka, L. M.; van der Donk, W. A., Structure-Activity Relationships of the S-Linked Glycocin Sublancin. ACS Chem Biol 2017, 12 (12), 2965-2969.4. Stepper, J.; Shastri, S.; Loo, T. S.; Preston, J. C.; Novak, P.; Man, P.; Moore, C. H.; Havlicek, V.;Patchett, M. L.; Norris, G. E., Cysteine S-glycosylation, a new post-translational modification found in glycopeptide bacteriocins. FEBS Lett 2011, 585 (4), 645-50

Crystal structure of the B. subtilis GTase

Back to Table of contents

MS06 Structural Enzymology

MS06-1-9 Tale of pesticide removal: atrazine degradation by hydroxyatrazine ethylaminohydrolase (AtzB) #MS06-1-9

A. Sharma [1], P. Kesari [1], P. Bhaumik [1]
[1]Indian Institute of Technology Bombay - Mumbai (India)

Abstract
Atrazine is a triazine ring containing herbicide introduced in the 1950s, applied to control weeds in the agricultural fields. Repeated applications and misuse of atrazine has polluted soil and surface water leading to adverse effects on humans and animals (Kumar et al. 2014). However, extensive studies have been done on atrazine degradation (Sharma et al., 2019) for more than a decade. Multiple pathways have been deduced, of which the product hydroxyatrazine is more recalcitrant and persistent in nature. Hitherto, hydroxyatrazine ethylaminohydrolase (AtzB) is the only enzyme reported that catalyses the deamination reaction of hydroxyatrazine and thus is the most important enzyme involved in atrazine degradation. Interestingly, it can mediate dechlorination reactions as well. AtzB belong to amidohydrolase family that generally catalyses hydrolysis of amidine bonds. Sequence analysis and experimental evidences reveal that AtzB is a metalloezyme containing a Zn(II) ion at the active site. However, the molecular details of the active site and catalytic mechanism of the enzyme is not known yet. Sequence optimized synthetic AtzB gene from *Pseudomonas* sp. was cloned, expressed and purified in recombinanat form. The pH optimum of AtzB ranges between 6.5-7.0. Kinetic studies show that AtzB activity is inhibited at high hydroxyatrazine (substrate) concentration and the K_m was found to be 33 µM. Structural alignment of our modelled AtzB with other homologous proteins show conservation of the Zn-coordinating residues (His74, His76, His245 and Asp331) and the catalytic active site residues comprising of Asp331, His280 and Glu248. Site directed mutations of the active site residues resulted in complete loss of activity implying their importance for AtzB function. Docking and molecular dynamics (MD) simulation studies indicated the structural features responsible for the accommodation of multiple substrates at the active site of AtzB. Based on our results we also propose a novel catalytic mechanism of AtzB and such mechanism has not been observed for other amidohydrolases.

References
1) Kumar, V., Kumar, V., Upadhyay, N. and Sharma, S., 2014. Chemical, biochemical and environmental aspects of atrazine. J Biodivers Environ Sci, 5, pp.149-165.
2) Sharma, A., Kalyani, P., Trivedi, V.D., Kapley, A. and Phale, P.S., 2019. Nitrogen-dependent induction of atrazine degradation pathway in Pseudomonas sp. strain AKN5. FEMS microbiol lett, 366(1), p.fny277. https://doi.org/10.1093/femsle/fny277

Back to Table of contents

MS06 Structural Enzymology

MS06-1-10 Structural exploration of FemX interaction with tXNA conjugates : identification of one potential antibiotic.
#MS06-1-10

I. Li De La Sierra Gallay [1], L. Rietmeyer [2], G. Schepers [3], D. Dorchêne [2], L. Iannazzo [4], D. Patin [1], T. Touzé [1], H. Van Tilbeurgh [1], P. Herdewijn [3], M. Ethève-Quelquejeu [4], M. Fonvielle [2]
[1]I2BC, UMR9198 - Gif-sur-Yvette (France), [2]CRC, UMRS1138 - Paris (France), [3]LMC - Leuven (Belgium), [4]LCBPT, UMR8601 - Paris (France)

Abstract
FemX is a non-ribosomal aminoacyl transferase. This enzyme transfers an alanyl residue from Ala-tRNAAla to the L-Lys side chain in the peptidoglycan precursor UDP-N-acetyl-muramyl-pentapeptide, a crucial reaction for the production of bacterial cell walls. This reaction is the first step of synthesis of the L-Ala-L-Ser-L-Ala side chain, which is completed by other Fem transferases. Because of their key role in the peptidoglycan metabolism, Fem transferases are considered as attractive targets for the development of novel antibiotics.
We have previously analyzed the interaction of several in vitro synthetized peptidyl-RNA conjugates and solved the X-ray structure of one peptidyl-RNA conjugate in complex with FemXWv of Weissella viridescens, a model enzyme of Fem family (1). We are now interesting on the study of Xenobiotic Nucleic Acids (XNA) analogs as substrates or inhibitors of FemX. XNAs, are characterized by replacement of the ribose (or deoxy-ribose) by a non-natural sugar, to create a nucleic acid that usually possesses unaltered Watson-Crick (or other) base-pairing properties and a similar 3D structure when compared to its natural DNA or RNA analogue.
In the present work we explored the impact of the XNA modification in aminoacyl-tRNA (aa-tRNA) analogs. We synthetized and characterized a subset L-Ala-tXNA microhelices and solved the Xray-structure of four complexes of FemXWv / tXNA conjugates. Where the tRNA in the tXNA conjugates is replaced with an 8nt XNA microhelix, the lysine-side chain branch is replaced with an artificial 1,4-triazole linkage and the sugar is replaced with : six-carbon sugars (HNA), 2'-F ribose (2'F-RNA), 2'-F arabinose (2'-FANA) and deoxyribonucleic acids (DNA). The combination of structural and enzymatic information allowed us to shed some light on the chemical groups implicated in the FemX inhibition at the molecular level. HNA and 2'F-RNA aminoacylated substrates have essentially unaltered catalytic and structural properties relative to L-Ala-tRNA microhelix controls. DNA and 2'F-ANA, conversely, abolish catalysis and substrate binding. These are all shown to be FemX inhibitors, with the 2'F-RNA being the most potent. A stabilizing interaction with one of the F atoms is thought to account for the high affinity in the case 2'F-RNA compound.

References
(1)Fonvielle M e*t al.* Angew. Chem. Int. Ed 2013 Jun 6. doi: 10.1002/anie.201301411

Back to Table of contents

MS06 Structural Enzymology

MS06-2-1 Time resolved crystallographic studies on chlorite dismutase
#MS06-2-1

J. Kamps [1], A.M. Orville [1]
[1]Diamond Light Source

Abstract
Chlorite dismutase (Cld) is essential to chlorate and perchlorate respiring cyanobacteria, due to its ability to convert chlorite (ClO_2^-), a toxic metabolite, into chloride (Cl^-) and molecular oxygen (O_2).[1] Cld from *Cyanothece* sp. is a homodimeric heme *b*-containing enzyme located in the cytosol. Production of O_2 by Cld involves the formation of an O–O bond, which is a rare occurence both biologically and abiotically, and was long thought to be exclusive to photosystem II. According to the current understanding of the mechanism (Figure 1), a high spin Fe(IV)=O (compound II) is formed as an intermediate. In order to futher understand the structural dynamics and intermediates formed during enzymatic catalysis, we are working towards time resolved crystallographic and complementary methods to study this reaction. Here we present the latest results.

References
1) I. Schaffner et al., Mol. Microbiol., 96, 1053-1068 (2015); 10.1111/mmi.12989

Figure 1: Chlorite dismutase mechanism

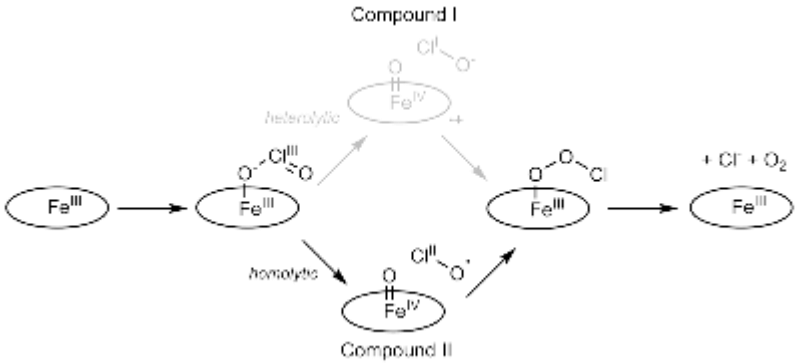

Back to Table of contents

MS06 Structural Enzymology

MS06-2-2 Structural and functional characterization of altronate oxidoreductase from Escherichia coli #MS06-2-2

S. Berger [1], P. Hinse [1], S. Eschenburg [1], T.F. Reubold [1]
[1]Hannover Medical School - Hannover (Germany)

Abstract
Gram-negative bacteria metabolize various hexuronic acids, which is essential for the colonization of the intestine (1,2). Furthermore, enzymes that metabolize hexuronic acids are of high interest for the industrial utilization of pectin-rich biomass from, for instance, sugar beet pulp (3). In the metabolization of the hexuronic acid D-galacturonate, the enzyme altronate oxidoreductase (AOR, also known as tagaturonate reductase, EC1.1.1.58) catalyzes the reduction of D-tagaturonate to D-altronate. We have solved the crystal structure of AOR from Escherichia coli to a resolution of 2.2 Å in the absence of its substrate. The structure was solved by single anomalous dispersion utilizing the anomalous signal of tungsten present in the telluro-polyoxotungstate cluster anion [TeW6O24]6− included in the crystallization experiment. The polypeptide chain of AOR, comprising 483 amino acid residues, folds into two distinct domains, which are separated by a solvent-accessible cleft. Comparison with known crystal structures of other sugar and sugar acid metabolizing enzymes confirm that AOR belongs to the family of polyol-specific long-chain dehydrogenases (4) and that the cleft is the binding site for the substrates D-tagaturonate and NADH. Using molecular docking of D-tagaturonate and NADH, we identified amino acid residues that likely determine substrate specificity. To verify these findings, we established an absorption-based activity assay and showed that mutation of these residues abolishes the enzymatic activity.

References
1. Maltby R, Leatham-Jensen MP, Gibson T, Cohen PS, Conway T. Nutritional basis for colonization resistance by human commensal Escherichia coli strains HS and Nissle 1917 against E. coli O157:H7 in the mouse intestine. PLoS One. 2013;8(1):e53957. doi: 10.1371/journal.pone.0053957.
2. Fabich AJ, Jones SA, Chowdhury FZ, Cernosek A, Anderson A, Smalley D, McHargue JW, Hightower GA, Smith JT, Autieri SM, Leatham MP, Lins JJ, Allen RL, Laux DC, Cohen PS, Conway T. Comparison of carbon nutrition for pathogenic and commensal Escherichia coli strains in the mouse intestine. Infect Immun. 2008 Mar;76(3):1143-52. doi: 10.1128/IAI.01386-07.
3. Kuivanen J, Biz A, Richard P. Microbial hexuronate catabolism in biotechnology. AMB Express. 2019 Jan 30;9(1):16. doi: 10.1186/s13568-019-0737-1.
4. Klimacek M, Nidetzky B. A catalytic consensus motif for D-mannitol 2-dehydrogenase, a member of a polyol-specific long-chain dehydrogenase family, revealed by kinetic characterization of site-directed mutants of the enzyme from Pseudomonas fluorescens. Biochem J. 2002 Oct 1;367(Pt 1):13-8. doi: 10.1042/BJ20020932.

Back to Table of contents

MS06 Structural Enzymology

MS06-2-3 Trapping a novel intermediate of vitamin B6 biosynthesis in PLP synthase, using in crystallo spectroscopy
#MS06-2-3

M. Rodrigues [1], N. Giri [2], A. Royant [3], Y. Zhang [4], R. Bolton [1], G. Evans [5], S. Ealick [4], T. Begley [2], I. Tews [1]
[1]University of Southampton - Southampton (United Kingdom), [2]Texas A&M University - College Station (United States), [3]Institut de Biologie Structurale - Grenoble (France), [4]Cornell University - Ithaka (United States), [5]Diamond Light Source - Didcot (United Kingdom)

Abstract
The major pathway of natural vitamin B6 biosynthesis is the ribose-5-phosphate dependent pathway. PLP is an active form of vitamin B6 that is synthesised by PLP synthase, an enzyme complex consisting of up to 24 protein subunits of the two proteins Pdx1 and Pdx2. Pentose and triose carbohydrates and ammonia, derived from glutamine hydrolysis catalysed by Pdx2, are the substrates of vitamin B6 biosynthesis. The Pdx1 synthase subunit catalyses a complex sequence of chemical reactions through formation of covalent enzyme-intermediate complexes, using lysine amino acid residues in an unusual double Schiff base mechanism.
We have characterised the I333 intermediate, named after its characteristic absorbance, using a lysine-arginine exchange variant. Using in crystallo UV-vis absorption spectroscopy, mass spectrometry analyses and structure determination we propose I333 as an on-pathway intermediate. The structure of the enzyme intermediate complex rationalises stereoselective deprotonation and subsequent substrate assisted phosphate elimination, which are central to our understanding of PLP biosynthesis.

References
Rodrigues MJ, Windeisen V, Zhang Y, Guédez G, Weber S, Strohmeier M, Hanes JW, Royant A, Evans G, Sinning I, Ealick SE, Begley TP, Tews I. Lysine relay mechanism coordinates intermediate transfer in vitamin B6 biosynthesis. Nat Chem Biol. 13 (2017), 290-294.Rodrigues MJ, Giri N, Royant A, Zhang Y, Bolton R, Evans G, Ealick SE, Begley T, Tews I. Trapping and structural characterisation of a covalent intermediate in vitamin B6 biosynthesis catalysed by the Pdx1 PLP synthase. RSC Chem Biol. 3 (2021), 227-230.

Back to Table of contents

MS06 Structural Enzymology

MS06-2-4 XFEL investigation of redox crosstalk within the ribonucleotide reductase R2b-NrdI complex #MS06-2-4

J. John [1], M. Högbom [1]
[1]Department of Biochemistry and Biophysics, Stockholm University, Arrhenius Laboratories for Natural Sciences - Stockholm (Sweden)

Abstract
Ribonucleotide reductase R2b contains a di-manganese carboxylate centre that generates an organic radical with the help of the oxygen-activated flavoprotein NrdI, making the R2b-NrdI complex a system with two different redox-active centres. Redox-active protein centres are a challenging target for investigation with standard single crystal synchrotron crystallography. The extended exposure to intense X-rays during data collection often leads to photoreduction of the redox-active species, impeding the determination of defined oxidation states. Serial femtosecond crystallography (SFX) utilizing an X-ray free electron laser mitigates the problem of photoreduction by shortening the X-ray exposure by several orders of magnitudes. Here we present two SFX structures of the ribonucleotide reductase R2b-NrdI complex in defined oxidation states and demonstrate structural rearrangements and crosstalk within the complex (1).

References
(1) "Redox-controlled structural reorganization and flavin strain within the ribonucleotide reductase R2b-NrdI complex monitored by serial femtosecond crystallography"Juliane John, Oskar Aurelius, Vivek Srinivas, In-Sik Kim, Asmit Bhowmick, Philipp S. Simon, Medhanjali Dasgupta, Cindy Pham, Sheraz Gul, Kyle D. Sutherlin, Pierre Aller, Agata Butryn, Allen M. Orville, Mun Hon Cheah, Shigeki Owada, Kensuke Tono, Franklin D. Fuller, Alexander Batyuk, Aaron S. Brewster, Nicholas K. Sauter, Vittal K. Yachandra, Junko Yano, Jan Kern, Hugo Lebrette, Martin HögbombioRxiv 2022.04.14.488295; doi: https://doi.org/10.1101/2022.04.14.488295

Back to Table of contents

MS06 Structural Enzymology

MS06-2-5 Exploring the Structure and Mechanism of heme peroxidases using SFX and multicrystal composite approaches
#MS06-2-5

M. Rozman [1], D. Svistunenko [1], M. Wilson [1], D. Axford [2], A. Ebrahim [2], T. Tosha [3], H. Sugimoto [3], I. Tews [4], R. Owen [2], J. Worrall [1], M. Hough [2]
[1]University of Essex - Colchester (United Kingdom), [2]Diamond Light Source - Didcot (United Kingdom), [3]RIKEN SPring8 Center - Harima (Japan), [4]University of Southampton - Southampton (United Kingdom)

Abstract
Heme peroxidases access Fe(III) and Fe(IV) states of Fe in their catalytic mechanism. These states are exquisitely sensitive to radiation damage, creating a significant challenge to obtain intact structures and hence to relate these accurately to mechanistically relevant states of the enzymes. Dye decolourising peroxidases have a largely unknown physiological function although certain enzymes of this class have been suggested to have significant potential industrial application in the breakdown of recalcitrant polysaccharides such as lignin as part of the production of biofuels.
We used serial femtosecond crystallography at SACLA with fixed targets and extruder sample delivery to obtain intact room temperature structures of the Fe(III) and Fe(IV) states of several different dye-decolourising peroxidases from Streptomyces lividans. Structures were corroborated using multicrystal datasets at 100 K for each state, where the UV-visible spectrum of each crystal was measured prior to and following x-ray data collection to validate the redox state in the resulting multicrystal dataset and structure. Moreover, we explored the effects of X-Ray dose on the crystals, observing elongation of Fe(III)-OH2 and Fe(IV)=O bond lengths as a function of the absorbed dose.
The results of these studies [1,2], in combination with extensive kinetic and spectroscopic data reveal key features of enzyme mechanisms and differences between the three Streptomyces lividans Dyps studied including the role of 'dry' versus 'wet' distal heme pockets and the manner in which mechanism is tuned to utilise aspartate or arginine residues for the rates enhancement of peroxide heterolysis.

References
Lucic, M, Svistunenko, DA, Wilson, M.T, Chaplin, AK, Davy, B, Ebrahim, A, Axford, D, Tosha, T, Sugimoto, H, Owada, S, Dworkowski, FSN, Tews, I, Owen, R, Hough, MA, Worrall, JAR. (2020) Serial femtosecond zero dose crystallography captures a water-free distal heme site in a dye-decolourising peroxidase to reveal a catalytic role for an arginine in FeIV=O formation. Angewandte Chemie Int. Ed. 132, 12840.
Aspartate or arginine? Validated redox state X-ray structures elucidte mechanistic subtleties of FeIV = O formation in bacterial dye-decolorizing peroxidases (2021) Marina Lučić, Michael T. Wilson, Dimitri A. Save file Svistunenko, Robin L. Owen, Michael A. Hough & Jonathan A. R. Worrall. JBIC Journal of Biological Inorganic Chemistry 26, 743–761

Back to Table of contents

MS06 Structural Enzymology

MS06-2-6 Different roles of protease binding sites of ecotin in inhibiton of complement proteases MASP-1, 2 and 3 #MS06-2-6

V. Harmat [1], Z.A. Nagy [2], D. Héja [2], D. Bencze [2], B. Kiss [2], E. Boros [2], D. Szakács [2], K. Fodor [3], M. Wilmanns [4], A. Kocsis [5], J. Dobó [5], P. Gál [5], G. Pál [2]
[1]Laboratory of Structural Chemistry and Biology, Institute of Chemistry, Eotvos Lorand University; and ELKH-ELTE Protein Modelling Research Group - Budapest (Hungary), [2]Department of Biochemistry, Eotvos Lorand University - Budapest (Hungary), [3]Department of Biochemistry, Eotvos Lorand University; and European Molecular Biology Laboratory, Hamburg Unit, Hamburg - Budapest (Hungary), [4]European Molecular Biology Laboratory, Hamburg Unit - Hamburg (Germany), [5]Institute of Enzymology, Research Centre for Natural Sciences, ELKH - Budapest (Hungary)

Abstract
Ecotin is a serine protease inhibitor with broad specificity, amongst it targets there are pancreatic proteases trypsin and chymotrypsin and elastase, as well as various enzymes of the blood coagulation, contact and complement cascade systems, making it a main virulence factor of various microbes. It is a homodimeric protein with two protease binding sites in both of its monomers: the canonical primary binding loop and a secondary binding region, which is able to ensure that strong binding is established even if the S1/P1 interaction of the primary binding loop is not optimal. Focusing on the interactions of ecotin and mannan binding proteases (MASP-1, 2 and 3), essential enzymes in activating the lectin and alternative pathways of the complement system, we solved the crystal structures of MASP-2/ecotin and MASP-1/ M84R ecotin complexes [1] and compared them with the previously published MASP-3/ecotin complex structure [2]. Using these data, together with our functional studies, we could explain independent roles of the primary and secondary binding sites of ecotin in inhibiting these three related enzymes [1].
ESRF, Grenoble is acknowledged for providing beam time. The crystallographic study was supported by grants VEKOP-2.3.2-16-2017-00014, and VEKOP-2.3.3-15-2017-00018 by the EU and the State of Hungary, co-financed by the European Regional Development Fund.

References
[1] Z. A. Nagy et al., Synergy of protease binding sites within the ecotin homodimer is crucial for inhibition of MASP enzymes and for blocking lectin pathway activation. , J. Biol. Chem. 2022, in press, https://doi.org/10.1016/j.jbc.2022.101985
[2] C. Gaboriaud et al., The Serine Protease Domain of MASP-3: Enzymatic Properties and Crystal Structure in Complex with Ecotin. PLOS ONE. 2013 8e67962

Back to Table of contents

MS06 Structural Enzymology

MS06-2-7 Structural and functional characterization of novel enzymes from targeted probiotic Lactic bacterial strains for the production of new generation prebiotics
#MS06-2-7

I. Feliciotti [1], S. Kolida [2], B. Rastal [3], K. Watson [1]
[1]University of Reading, University of Reading, School of Biological Sciences - Reading (United Kingdom), [2]OptiBiotics Health PLC - Reading (United Kingdom), [3]University of Reading, Food and Nutritional Science - Reading (United Kingdom)

Abstract
The human gut microbiome is a complex ecosystem, which plays a crucial role in human health. However, the gut microbiome equilibrium is delicate and as such different strategies to modulate it have been proposed. One approach involves the use of prebiotics and probiotics as supplements able to alter the microbial composition in the gut and increase its beneficial effects.
This project focuses on lactobacillae probiotic strains already used for its beneficial effects in lipid metabolism.
Recent sequencing of specific lactobacillae strains has revealed potential novel enzymes responsible for beneficial effects in human health: beta-galactosidases which are responsible for galacto-oligosaccharide (GOS) synthesis.
Select enzymes have been targeted for detailed structure-function studies to elucidate their functional role: bioinformatics tools have been utilized to identify important functional and structural domains and X-ray crystallography will be used for their structural characterisation.

We anticipate that this work will be valuable for understanding detailed mechanisms of action of specific enzymes involved in the production of new prebiotics.

Back to Table of contents

MS06 Structural Enzymology

MS06-2-8 Combining X-ray emission spectroscopy with X-ray crystallography to study metalloprotein catalysis at synchotron sources
#MS06-2-8

R. Bosman [1], M. Chithirai Pandi [1], J. Kamps [1], J. Weatherby-Sanchez [1], U. Neuman [1], J. Sutter [1], J. Sandy [1], P. Aller [1], M. Hough [1], J. Kelly [1], A.M. Orville [1]
[1]Diamond Light Source ltd - Oxford (United Kingdom)

Abstract
Understanding enzyme structure in atomic detail is vital to understanding the mechanisms governing enzyme function. However, high spatial resolution provides only a partial picture of an enzymes chemistry. The XFEL-hub at Diamond Light Source (DLS) is designing and commissioning a von Hàmos spectrometer to combine time-resolved x-ray emission spectroscopy (tr-XES) and time-resolved crystallography (tr-XRD). XES is a bulk sensitive element specific spectroscopy that probes orbital configuration and is therefore sensitive to the metals oxidation, spin state and ligand bonding[1]. This setup allows in-depth studies of metalloenzymes where protein function is closely tied with, typically, first-row transition metals electronic configuration.
Building on previous seminal work[2,3], the spectrometer will accommodate 16 crystals at 400mm to provide high spectral resolution, improved solid-angle per eV, and large total solid angle. Multiple crystal mounting positions allows configurations for improved resolution or signal-to-noise, and the possibility to perform multiple simultaneous spectral measurements (Kα and Kß spectral lines)[4]. Importantly, the spectrometer will be able to integrate with a drop-on-tape sample delivery system, also under development at DLS, targeted towards sample efficient tr-XRD mixing experiments. This sample delivery system will facilitate mixing or pumped-probe time-resolved experiments in both aerobic and anaerobic environments. Together this provides a comprehensive setup for tr-XRD/tr-XES measurements for metalloenzymes. Initial commissioning will be for iron and copper spectra with deployment at the VMXi beamline at DLS. Future work includes use at other beamlines, deployment at XFELs and more elements (e.g. Nickel). Here we present the optical and design work, and on-beam benchmarking tests at VMXi.

References
References:
1. Glatzel, P. & Bergmann, U. High resolution 1s core hole X-ray spectroscopy in 3d transition metal complexes—electronic and structural information. Coordination Chemistry Reviews 249, 65–95 (2005).
2. Fuller, F. D. et al. Drop-on-demand sample delivery for studying biocatalysts in action at X-ray free-electron lasers. Nat Methods 14, 443–449 (2017).
3. Alonso-Mori, R. et al. A multi-crystal wavelength dispersive x-ray spectrometer. Rev Sci Instrum 83, 073114 (2012).
4. Kinschel, D. et al. Femtosecond X-ray emission study of the spin cross-over dynamics in haem proteins. Nature Communications 11, 4145 (2020).

Back to Table of contents

MS06 Structural Enzymology

MS06-2-9 Amino acids mediated active site control in Pseudomonads aeruginosa native Ketopantoate reductase PaKPR PanE2
#MS06-2-9

G. Basu Choudhury [1]
[1]CSIR-IICB - Kolkata (India)

Abstract
Pseudomonas aeruginosa possesses two copies of Ketopantoate reductase (KPRs) enzyme that catalyses cofactor dependent conversion of Ketopantoate to Pantoate, one of the steps involved in the biosynthesis of pantothenate and coenzyme A. Although these two copies are similar in function but they widely vary in their sequence with only 30% similarity between them. Evolutionary studies made in our recent work have shown one of the copy was attained via horizontal gene transfer whereas the other one was conserved. A detailed structural and functional characteristics of the acquired copy of PaKPR (PanE1) was also studied. In this current work we have thoroughly studied the differences present between the wild type conserved PaKPR (PanE2) and the acquired one, and tried to figure out whether any structural implications are present for the co existence of the 2 copies of the same functional proteins in the same genome. For successfully addressing these facts, we have solved the crystal structures of this native PaKPR PanE2, cofactor(NADP+) bound panE2 and a ternary complex of panE2+NADP+Pantoate. And we found several changes in the secondary structure organisation while overall shape of the protein was same. However, Cofactor and substrate binding active site is a bit squeezed in the PaKPR panE2 that may cause a problems in entry and exit of the ligands into it. Moreover, crystallographic evidences have shown that F132 and Y148 together act as a gate for the entry and exit of the substrate and product, present at the outside of the active site . Their movements were clearly visible in native and ligand bound states. This control over the movements of the substrate and product can cause a delay is the conversion process.

References
1.Genome-wide survey and crystallographic analysis Suggests a role for both horizontal gene transfer and duplication in pantothenate biosynthesis pathway.Khanppanavar,B. et al BBA Gen Subj 2019

2. Crystal structure of Escherichia coli ketopantoate reductase in a ternary complex with NADP+ and pantoate bound: substrate recognition, conformational change, and cooperativity. Alessio Ciulli et al. J Biol Chem. 2007.

Back to Table of contents

MS06 Structural Enzymology

MS06-2-10 Structural and biochemical studies on a GH5 cellulase from Aspergillus oryzae with β-glucosidase activity.
#MS06-2-10

B. Banerjee [1], C. Kamale [1], A. Suryawanshi [1], A. Mishra [2], R. Gupta [2], S. Noronha [2], P. Bhaumik [1]
[1]Dept of Biosciences and Bioengineering, Indian Institute of Technology Bombay - Mumbai (India), [2]Dept. of Chemical engineering, Indian Institute of Technology Bombay - Mumbai (India)

Abstract
Saccharification of cellulose to yield glucose holds particular commercial interest in the biofuel industry. This glucose can be fermented and distilled to produce fuel grade ethanol. The hydrolysis of cellulose is carried out by cellulase, an ensemble of enzymes that includes exoglucanases, endoglucanases and β-glucosidases, which act synergistically on cellulose. The endoglucanases act initially, followed by exoglucanases to produce cellobiose which is hydrolysed to glucose by β-glucosidases[1]. The reaction involving β-glucosidases is the rate determining step in the entire process of cellulose saccharification. β-glucosidases are inhibited by accumulation of the product glucose in the reaction chamber[2]. Apart from glucose, these enzymes are also inhibited by conditions of high temperature and acidic pH. As a result of these factors, thermotolerant β-glucosidases which have higher tolerance towards glucose and can function in lower pH, are considered important for the industrial bioethanol production processes. In this study, we report a GH5 cellulase of *Aspergillus oryzae* (AoBgl) which has β-glucosidase activity. The gene coding for aobgl has been cloned and over-expressed in *Escherichia coli* BL21 (DE3). The protein was purified using Ni-NTA affinity chromatography, followed by anion exchange and size exclusion chromatography. The purified protein was crystallized and structures of both the apo as well as cellobiose-bound forms of the enzyme was solved at high resolutions (1.65 Å for apo form and 1.73 Å for cellobiose bound complex). AoBgl has an overall TIM barrel like structural fold that is similar to β-glucosidases of GH1 family, this structural feature might be responsible in conferring β (1-4) glycosidic linkage hydrolysing features to this GH5 enzyme. On substrate binding, a change in conformation in a loop region has been observed. This loop region involves residues present in the +2 subsite of substrate binding (Figure 1) . Biochemical studies on AoBgl revealed that the optimum temperature of its activity is 55 ˚C and optimum pH of activity was 5.5 (Figure 2 A, B). Apart from these features, the enzyme had a very high glucose tolerance of 1.35 M (Figure 2 C). These biochemical properties indicate that AoBgl is highly suitable candidate for industrial bioethanol production processes. Guided by these structural and biochemical characteristics, further superior variants of AoBgl can be generated for use in biofuel industry.

References
1. Taherzadeh, M. J., & Karimi, K. (2007). Enzyme-based hydrolysis processes for ethanol from lignocellulosic materials: a review. BioResources, 2(4), 707-738.
2. Sawant, S., Birhade, S., Anil, A., Gilbert, H., & Lali, A. (2016). Two-way dynamics in βglucosidase catalysis. Journal of Molecular Catalysis B: Enzymatic, 133, 161-166.

Figure 1: Structural changes on cellobiose binding

Back to Table of contents

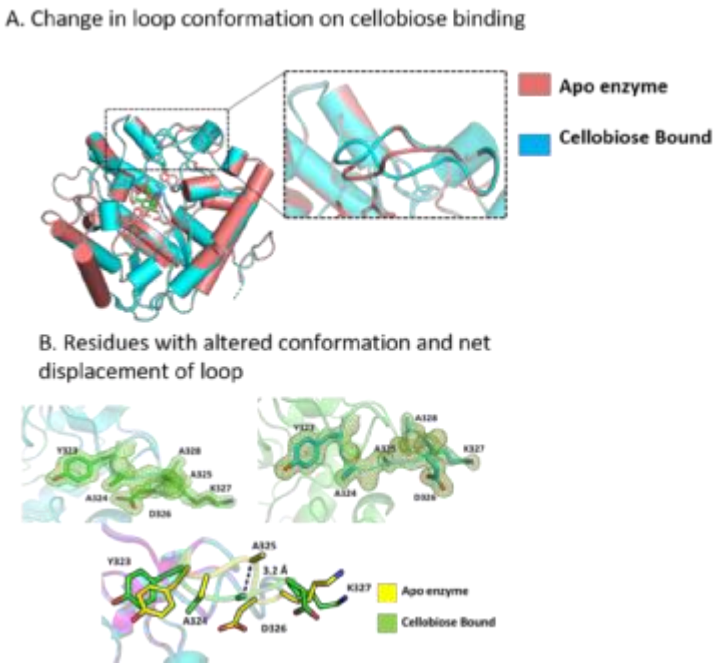

Figure 2: Biochemical characterization of AoBgl

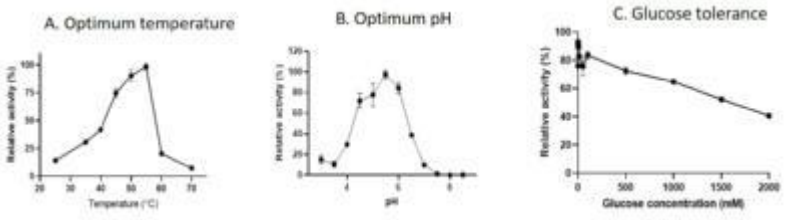

Back to Table of contents

MS06 Structural Enzymology

MS06-2-11 Structural insights of plasmepsin X from P. falciparum uncovering a novel inactivation mechanism of zymogen
#MS06-2-11

A. Deshmukh [1], P. Kesari [1], N. Pahelkar [1], A. Suryawanshi [1], I. Rathore [1], V. Mishra [1], J. Dupuis [2], H. Xiao [3], A. Gustchina [4], J. Abendroth [5], M. Labaied [5], R. Yada [2], A. Wlodawer [4], T. Edwards [5], D. Lorimer [5], P. Bhaumik [6]
[1]Department of Biosciences and Bioengineering, Indian Institute of Technology Bombay, Powai - Mumbai (India), [2]Food, Nutrition, and Health Program, Faculty of Land and Food Systems, University of British Columbia, - Vancouver (Canada), [3]Summerland Research and Development Center, Agriculture and Agri-Food Canada - Summerland (Canada) - Summerland (Canada), [4]Protein Structure Section, Center for Structural Biology, National Cancer Institute - Frederick (United States), [5]UCB Pharma - Bainbridge Island (United States), [6]IIT Bombay - MUMBAI (India)

Abstract
Plasmodium falciparum is a deadliest *Plasmodium* species responsible for human malaria. Plasmepsin X (PMX) from *Plasmodium falciparum* is a pepsin-like aspartic protease that plays essential role in the invasion and egress of the parasite (1,2). Invasion and egress processes involve a cascade of events and are essential for the survival and dissemination of infection in the parasite life cycle. Plasmepsin X is an upstream protease in this cascade of events and hence, is an attractive drug target (3). We have reported the first crystal structure of *Plasmodium falciparum* Plasmepsin X (*Pf*PMX) zymogen, with a novel prosegment fold (4). The zymogen structure has five disulphide bonds with a unique disulfide bond formed by two adjacent cysteine residues (C447-C448). The twisted loop from prosegment occupies the active site forming several hydrophobic interactions with mature enzyme, and arginine 244 from the initial mature region forms the salt bridge interactions with catalytic aspartates inactivating the *Pf*PMX zymogen. Such an inactivation mechanism has not been observed previously for any other pepsin-like aspartic proteases. Sequence and structural alignment studies also showed that such a unique zymogen inactivation mechanism could be applicable to other PMX-like proteases from other apicomplexan parasites. The biochemical data suggest the conversion of zymogen to mature enzyme occurs through cleavage of the prosegment at multiple cleavage sites. The structural features of *Pf*PMX presented would aid in developing potent inhibitors of this enzyme and similar proteases from apicomplexan parasites in efforts to combat malaria and other apicomplexan diseases.

References
1. Pino P, Caldelari R, Mukherjee B, Vahokoski J, Klages N, Maco B, Collins CR, Blackman MJ, Kursula I, Heussler V (2017) A multistage antimalarial targets the plasmepsins IX and X essential for invasion and egress. Science. 358:522–528.
2. Nasamu AS, Glushakova S, Russo I, Vaupel B, Oksman A, Kim AS, Fremont DH, Tolia N, Beck JR, Meyers MJ (2017) Plasmepsins IX and X are essential and druggable mediators of malaria parasite egress and invasion. Science. 358:518–522.
3. Favuzza P, de Lera RM, Thompson JK, et al. Dual Plasmepsin-targeting antimalarial agents disrupt multiple stages of the malaria parasite life cycle. Cell Host and Microbe. 27:642-658.
4. Kesari, P, Deshmukh, A, Pahelkar, N, Suryawanshi, AB, Rathore, I, Mishra, V, Dupuis, JH, Xiao, H, Gustchina, A, Abendroth, J, Labaied, M, Yada, RY, Wlodawer, A, Edwards, TE, Lorimer, DD, Bhaumik, P (2022) Structures of plasmepsin X from P. falciparum reveal a novel inactivation mechanism of the zymogen and molecular basis for binding of inhibitors in mature enzyme. Protein Science. 31: 882-899.

Structure of PfPMX zymogen

Back to Table of contents

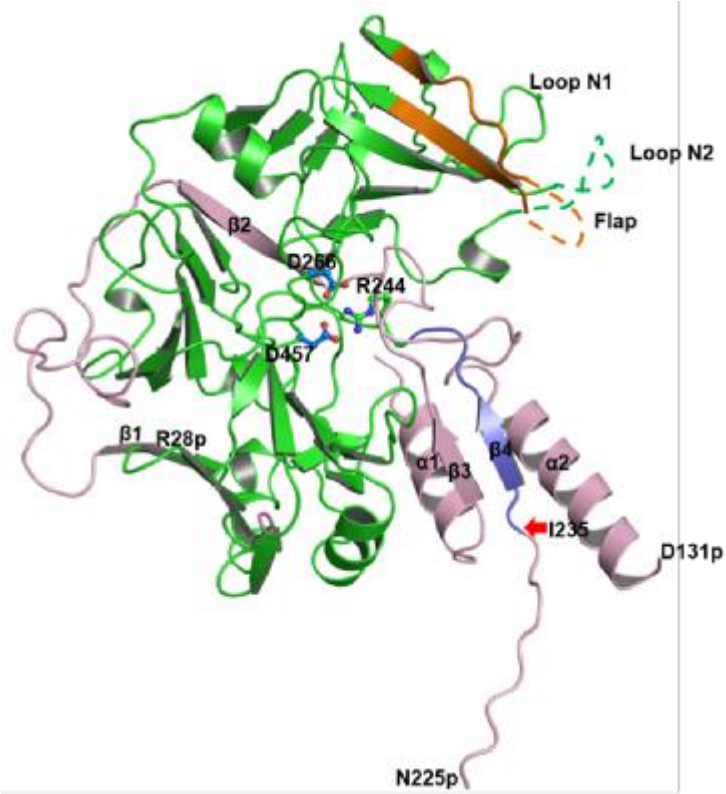

Back to Table of contents

MS06 Structural Enzymology

MS06-2-12 Role of flexible domain II in the homotropic cooperativity of Aspergillus niger glutamate dehydrogenase #MS06-2-12

B.K.J. Godsora [1], P. Prakash [1], N.S. Punekar [1], P. Bhaumik [1]
[1]Department of Biosciences and Bioengineering, Indian Institute of Technology Bombay, Powai, Mumbai 400076, India - Mumbai (India)

Abstract
Homotropic cooperativity is a part of allosteric mechanism mostly observed in the multimeric proteins such as haemoglobin, ATCase, etc. (1). The atomic details on inter-subunit communications during the homotropic cooperativity are scanty. Thus we attempt to understand this fundamental phenomenon in an important metabolic enzyme, glutamate dehydrogenase (GDH). It reversibly catalyzes the reductive amination of α-ketoglutarate to L-glutamate in presence of ammonia and the coenzyme NAD(P)H, and thus interlinks the carbon and nitrogen cycles (2). The hexameric NADP-specific GDHs from *Aspergillus niger* (AnGDH) and *Aspergillus terreus* (AtGDH) share 88% sequence identity. Interestingly, AnGDH shows homotropic cooperativity towards its substrate α-ketoglutarate (n_H = 3.0) while AtGDH shows Michaelian kinetics (3). Therefore, structural analysis of AnGDH and AtGDH will help to unravel the mechanistic details about the homotropic cooperativity. In that context, we have recently solved the crystal structures of AtGDH as dimer in the asymmetric unit, which generates into a biologically functional hexamer on applying the three fold crystallographic symmetry operation. There are two different conformational states in each dimer – open (~17 Å) and partial closed state (~13 Å). Each subunit of AtGDH consists of two domains -- rigid domain I for substrate binding and hexamerization, and flexible domain II involved in coenzyme binding. Structural comparison between AtGDH and AnGDH (5XVI) shows differential domain II dynamics. In AnGDH (5XVI) the maximal mouth opening distance measured between the cleft residues Lys122 (domain I) and Arg282 (domain II) is ~21 Å, and in AtGDH the same is ~17 Å. The amino acid substitutions in domain II probably regulate the extent of mouth openings in these two enzymes. Based on the structural analysis, twelve mutants of AtGDH have been generated sequentially on *Atgdh* gene background and their responses to α-ketoglutarate substrate saturation of the purified mutants were performed. Further the kinetic studies on AtGDH sequential mutants (Ala220Lys, Arg246Ser and Ile433Val located in the domain II) showed changes in the substrate affinity (K_m) and maximum reaction velocity (V_{max}). Thus, our findings suggest that the extent of mouth opening might regulates the rate of enzyme catalysis, and thus ultimately likely to be linked to the homotropic cooperativity. The findings of our study would help in understanding the homotropic cooperativity in hexameric GDHs from lower organisms.

References
1) Goodey, N. M. and Benkovic, S. J. (2008). Allosteric regulation and catalysis emerge via a common route. *Nat. Chem. Biol.*, **4**, 474-82.2) Godsora, B. K. J., Prakash, P., Punekar, N. S., & Bhaumik, P. (2022). Molecular insights into the inhibition of glutamate dehydrogenase by the dicarboxylic acid metabolites. *Proteins*, **90(3)**, 810–823.3) Agarwal, N., Walvekar, A. S., and Punekar, N. S. (2019). 2-Oxoglutarate cooperativity and biphasic ammonium saturation of Aspergillus niger NADP-glutamate dehydrogenase are structurally coupled. *Arch. Biochem. Biophys*., **669**, 50-60.

Dynamics of domain II in hexameric AtGDH

Back to Table of contents

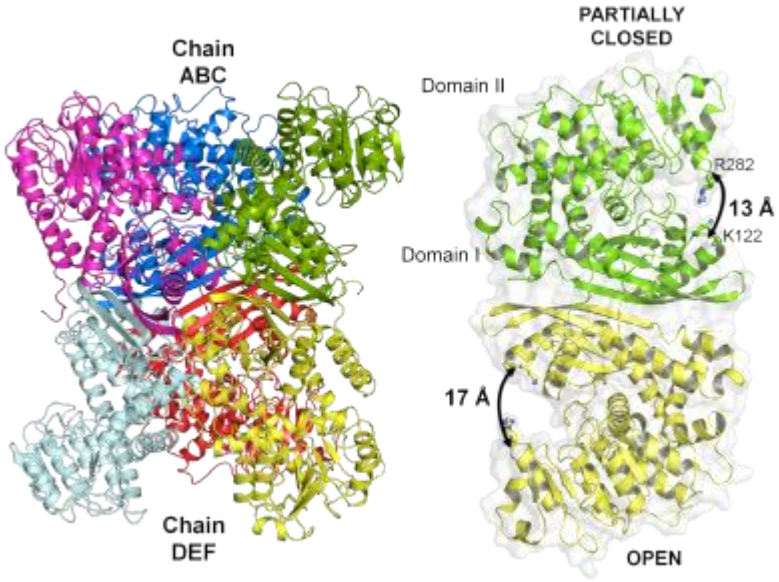

Back to Table of contents

MS06 Structural Enzymology

MS06-2-13 Understanding the mechanism of lipid – enzyme interactions in the limbus region of lipases at atomic resolution
#MS06-2-13

M. Cianci [1]
[1]**Università Politecnica delle Marche - Ancona (Italy)**

Abstract
Lipases (E.C. 3.1.1.3) are ubiquitous hydrolases for the carboxyl ester bond of water-insoluble substrates such as triacylglycerols, phospholipids, and other insoluble substrates, acting in aqueous as well as in low-water media, thus being of considerable physiological significance with high interest also for their industrial applications. The hydrolysis reaction follows a two-step mechanism, or 'interfacial activation', with adsorption of the enzyme to a heterogeneous interface and subsequent enhancement of the lipolytic activity. Among lipases, Candida antarctica Lipase B (CALB) has never shown any significant interfacial activation, and a closed conformation of CALB has never been reported leading to the conclusion that its behaviour was due to the absence of a lid regulating the access to the active site. The lid open and closed conformations and their protonation states are observed in the crystal structure of CALB at 0.91 Å resolution [1]. Having the open and closed states at atomic resolution allows relating protonation to the conformation, indicating the role of Asp145 and Lys290 in the conformation alteration. Once positioned within the catalytic triad, substrates are then hydrolysed, and products released. However, the intermediate steps of substrate transfer from the lipidic-aqueous phase to the enzyme surface and then down to the catalytic site are still unclear. By inhibiting CALB with ethyl phosphonate and incubating with glyceryl tributyrate (2,3-di(butanoyloxy)propyl butanoate), the crystal structure of the lipid-enzyme complex, at 1.55 Å resolution, shows the tributyrin in the limbus region of active site [2]. The substrate is found above the catalytic Ser, with the glycerol backbone readily pre-aligned for further processing by key interactions via an extended water network with α-helix10 and α-helix5. These findings explain the lack of 'interfacial activation' of CALB and offer new elements to elucidate the mechanism of substrate recognition, transfer and catalysis of Candida antarctica Lipase B (CALB) and lipases in general.

References
[1] Stauch, B., Fisher, S. J., Cianci, M. (2015). Journal of Lipid Research, 56, 2348-2358.
[2] Silvestrini, L. & Cianci, M. (2020). International Journal of Biological Macromolecules, 158, 358-363.

Figure 1. Tributyrate bound to CALB lipase

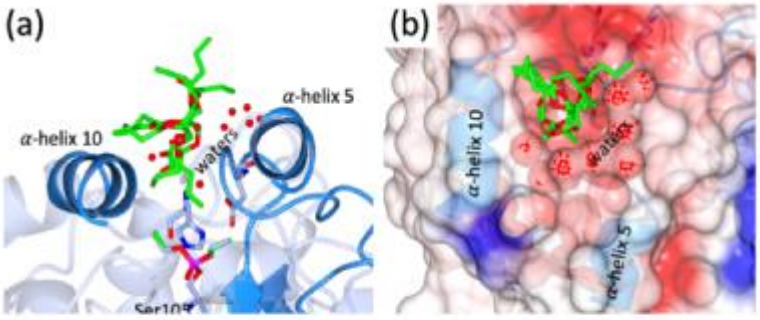

a) relative side position of glycerol tributyrate to the active site, α-helix 5, α-helix 10, and water network; b) electrostatic potential of CALB surface. Red areas have a negative potential, blue areas a positive potential, white areas are neutral.

Back to Table of contents

MS06 Structural Enzymology

MS06-2-14 Shortcut to hypusine. Structural characterization of putative bifunctional deoxyhypusine synthase from Trichomonas vaginalis.
#MS06-2-14

E. Wator [1], P. Wilk [1], P. Grudnik [1]
[1]Malopolska Centre of Biotechnology, Jagiellonian University in Krakow - Krakow (Poland)

Abstract
Deoxyhypusine synthase (DHS) is a transferase catalysing the formation of deoxyhypusine, which is the first, rate-limiting step of unique post-translational modification: hypusination. During the first step, DHS catalyses the transfer of 4-aminobutyl moiety of spermidine to a specific lysine of eIF5A precursor in a NAD-dependent manner and emergent deoxyhypusine is further hydroxylated to hypusine by deoxyhypusine hydroxylase (DOHH). This modification occurs exclusively on only one protein: eukaryotic initiation factor 5A (eIF5A) and it is essential for cell proliferation and enzymes involved in hypusination are highly conserved in eukaryotes. However, in 2016 Quintas-Granados and colleagues identified that deoxyhypusine synthase from Trichomonas vaginalis (Tv-DHS) has bifunctional activity and it is able not only to form deoxyhypusine, but also to further hydroxylate it to hypusine.
The presented study aimed to investigate putative bifunctional deoxyhypusine synthase from Trichomonas vaginalis using biochemical and structural biology methods.
Bifunctional Tv-DHS and its substrate Tv-eIF5A were expressed and purified. Our crystallization attempts lead us to high-resolution crystal structures determination allowing for detailed analysis and comparison to the human proteins. Based on the Tv-DHS crystal structure we identified putative additional active site, which was further confirmed by site-directed mutagenesis studies. Additionally, we determined binding affinity of Tv-DHS for small molecules ligands and protein substrate. In contrast to the human enzyme, Tv-DHS seems to be less polyamine-specific as spermine activates it to almost the same extent as the preferred substrate – spermidine.
Availability of high-quality structural and biochemical data can significantly advance our understanding of this unique posttranslational modification and probably will aid the design of novel tvDHS inhibitors for potential applications in sexually transmitted diseases therapy.

The research has been supported by National Science Centre (NCN, Poland) research grant no. 2019/33/B/NZ1/01839 to P.G and 2019/35/N/NZ1/02805 to E.W.

References
1. Park MH, Wolff EC. Hypusine, a polyamine-derived amino acid critical for eukaryotic translation. J Biol Chem. 2018;293(48):18710-18718.
2. Wątor E, Wilk P, Grudnik P. Half Way to Hypusine-Structural Basis for Substrate Recognition by Human Deoxyhypusine Synthase. Biomolecules. 2020;10(4):522.
3. Quintas-Granados LI, Carvajal Gamez BI, Villalpando JL, Ortega-Lopez J, Arroyo R, Azuara-Liceaga E, Álvarez-Sánchez ME. Bifunctional activity of deoxyhypusine synthase/hydroxylase from Trichomonas vaginalis. Biochimie. 2016 Apr;123:37-51

Back to Table of contents

MS07 Membrane Proteins

MS07-1-1 Obligate respiratory chain complex III2IV2 supercomplexes of Actinobacteria
#MS07-1-1

T. Kovalova [1], A. Moe [1], S. Król [1], D. Sjöstrand [1], P. Brzezinski [1], M. Högbom [1]
[1]Department of Biochemistry and Biophysics, The Arrhenius Laboratories for Natural Sciences, Stockholm University, 106 91 Stockholm - Stockholm (Sweden)

Abstract
Many pathogens including *Mycobacterium tuberculosis* and *Mycobacterium leprae* belong to the phylum *Actinobacteria*. With rising antibiotic resistance among bacteria, research of new drug targets is necessary. While respiratory chain proteins usually share significant structural and functional similarities across the different domains of life, in the *Mycobacteria* genus, there are structural differences that provide an interesting research target. Their most significant structural distinction is the requirement for respiratory chain protein complexes to form an obligate supercomplex (assembled from two copies of complex III and IV) in order to maintain standard function. To this day, there are two cryo-EM determined wild type structures of obligate respiratory chain supercomplexes, from *M. smegmatis* (3.3 Å; Wiseman et al. 2018) and *Corynebacterium glutamicum* (3.0 Å; Moe; Kovalova et al. 2021). Comparison of the structures of these sequence homolog reveals multiple differences, including the binding site of periplasmic superoxide dismutase of the M. smegmatis being occupied by a new unknown subunit in *C. glutamicum* structure. Two possible menaquinone binding positions were observed in the QP site of *C. glutamicum.* Furthermore, occurrence of two different additional menaquinone binding sites in both structures was observed. In our work we focused on gaining insight into supercomplex formation and the role of individual subunits on its functionality and stability which will include a structure-function study of various mutants.

References
Moe, A., Kovalova, T., Król, S. Yanofsky, D.J., Bott, M., Sjöstrand, D., Rubinstein, J.L., Brzezinski, P., Högbom, M. The respiratory supercomplex from C. glutamicum. Structure 30(3), 338-349.e3. (2022).
Wiseman, B., Nitharwal, R.G., Fedotovskaya, O., Schäfer, J., Guo, H., Kuang, Q., Benlekbir, S., Sjöstrand, D., Ädelroth, P., Rubinstein, J.L., Brzezinski, P., Högbom, M. Structure of a functional obligate complex III2IV2 respiratory supercomplex from Mycobacterium smegmatis. Nat Struct Mol Biol 25, 1128–1136 (2018).

Back to Table of contents

MS08 Serial crystallography, obtaining structures from many crystals

MS08-1-1 Sample delivery techniques to perform serial crystallography at the XFEL Hub of Diamond Light Source. #MS08-1-1

A. Shilova [1], P. Aller [1], R. Owen [1], R. Bosman [1], J. Kamps [1], J. Glerup [1], A.M. Orville [1]
[1]Diamond Light Source - Harwell (United Kingdom)

Abstract
Serial crystallography experiments have been continuously performed and developed at X-ray free-electron lasers (XFELs) and synchrotron beamlines over the last decade. In this method, a complete diffraction dataset is collected from a large number of microcrystals serially delivered and exposed to an X-ray beam in random orientations at room-temperature. Short X-ray exposure minimizes radiation damage, and data collection at room-temperature provides more biologically reliable data on structural dynamics in proteins compared to the data collection at cryo-temperatures.
Serial crystallography experiments at XFELs have inspired novel sample delivery techniques, which are now also being used at synchrotrons. The XFEL Hub at Diamond is developing several techniques to enable time-resolved serial crystallography experiments at synchrotrons and XFELs. This development relies on a growing variety of sample presentation methods each with unique requirements, including different fixed target supports (1), injection methods using high-viscosity extrusion injectors, and on-demand acoustic droplet ejection or piezoelectric injection of nanolitre to picolitre (2,3) droplets either into the X-ray beam or onto a tape drive. Some of the drop-on-demand methods are also compatible with complementary X-ray emission spectroscopy measurements from the same sample and X-ray pulse. This allows to follow the oxidation/spin states changes of biologically relevant metals during catalysis. Our goals include promoting the efficient use of samples and accessibility of serial crystallography experiments for academic and industry users, in part, by transferring/ adapting appropriate technology between different facilities.

References
1. A modular and compact portable mini-endstation for high-precision, high-speed fixed target serial crystallography at FEL and synchrotron sources. Sherrell DA, Foster AJ, Hudson L, Nutter B, O'Hea J, Nelson S, et al., Owen RL. J Synchrotron Radiat. 2015 Nov;22(6):1372-8.
2. Drop-on-demand sample delivery for studying biocatalysts in action at X-ray free-electron lasers. Fuller FD, Gul S, Chatterjee R, Burgie ES, Young ID, Lebrette H, et al., Yano J. Nat Methods. 2017 Apr;14(4):443-449.
3. An on-demand, drop-on-drop method for studying enzyme catalysis by serial crystallography. Butryn A, Simon sisPS, Aller P, Hinchliffe P, Massad RN, Leen G, et al, Orville AM. Nat Commun. 2021 Jul 22;12(1):4461.

Back to Table of contents

MS08 Serial crystallography, obtaining structures from many crystals

MS08-1-2 User support for time-resolved SFX data processing at XFELs
#MS08-1-2

T. Zhou [1], P. Aller [1], R. Bosman [1], J.J.A.G. Kamps [1], A. Shilova [1], A. Brewster [2], F. Dall'antonia [3], A.M. Orville [1]
[1]XFEL Hub, Diamond Light Source - Harwell Science and Innovation Campus, Didcot OX11 0DE (United Kingdom), [2]Molecular Biophysics and Integrated Bio imaging Division, Lawrence Berkeley National Laboratory - 1 Cyclotron Road, Berkeley, CA 94720, (United States), [3]European XFEL - Holzkoppel 4, 22869, Schenefeld (Germany)

Abstract
A frontier challenge of structural biology is to determine high-resolution structures of catalytic systems in the fourth dimension (time) to reveal the intermediate state of catalysis. Serial crystallography methods at synchrotrons (SSX) and XFELs (SFX) are particularly well suited for time-resolved studies using micro-crystal slurries. Specifically, the intense beam generated at XFEL enables the study of smaller crystals and, thereby, reduces the ligand diffusion time allowing for more reaction time control.
Two important questions that need to be answered during the SFX experiments are: **a)** “Have we obtained sufficient data?” During SSX and SFX experiments, “still” diffraction patterns are collected at random orientations, which need to be processed individually and merged for a complete dataset. Merging statistics and assessment of the quality of electrons density maps ultimately determines whether sufficient data has been collected. **b)** “Does the equilibration/reaction time need to be adjusted?” Again, the electron density maps for a given time point must be checked during time-resolved studies to evaluate interpretability of atomic models with respect to the proposed reaction mechanisms and/or anticipated catalytic reaction intermediates. Therefore, answering both questions during SSX/SFX experiments requires collected data to be processed in as near to real-time as possible. Further, the fast data collection rate at XFELs, which currently can go up to 3520 images per second with an AGPID 1M at the European XFEL, makes real-time data processing challenging and an optimized data processing strategy is required for maximum data processing efficiency. The XFEL Hub at Diamond Light Source has been helping users/collaborators during SSX and SFX experiments, from set up software packages to process collected data. I will present our works relating to user support at several XFELs (LCLS, PAL-XFEL and EuXFEL), focusing on real-time data processing using dials and cctbx packages (script based data processing and cctbx.xfel GUI)[1, 2].

References
[1] Winter, G., *et al.*, (2018). "DIALS: implementation and evaluation of a new integration package." *Acta Crystallogr D Struct Biol* 74(Pt 2): 85-97.
[2] Brewster AS, *et al.*, (2019): Processing serial crystallographic data from XFELs or synchrotrons using the cctbx.xfel GUI. *Computational Crystallography Newsletter* 10, 22 - 39

Back to Table of contents

MS08 Serial crystallography, obtaining structures from many crystals

MS08-1-3 Serial Crystallography Made Simple: Easing the learning curve of multi-crystal diffraction experiments with new fixed-target methods
#MS08-1-3

A. Finke [1], G. Illava [2], R. Jayne [3], D. Closs [3], W. Zeng [2], S. Milano [2], Q. Huang [2], I. Kriksunov [2], B. Apker [3], R. Thorne [2], M. Szebenyi [2]
[1]MAX IV Laboratory - Lund (Sweden), [2]Cornell University - Ithaca (United States), [3]MiTeGen - Ithaca (United States)

Abstract
Serial crystallography (SX) is a powerful method for structural determination in macromolecular crystallography (MX), especially for samples and experimental conditions not amenable to single-crystal cryocrystallography. Much effort has been put on sample delivery and analysis of diffraction data, to great success. With SX, protein structures can be gleaned from room temperature diffraction with little radiation damage, protein dynamics can be measured, and pump-probe experiments can elucidate biochemifcfal pathways in large biological systems. But from a user service (specifically, storage ring MX beamline) perspective, we find that the largest barrier to getting users interested in trying SX for their own samples is not inertia (users would do it if they knew how to), nor is it infrastructural (nearly every MX beamline nowadays has some capacity to do SX). The hurdle is not making sample preparation and sample delivery accessible to most structural biology laboratories' MX structure pipelines. Easier access to SX sample delivery systems would enable users to the many possibilities of SX.
With accessibility in mind, we have developed an integrated fixed-target sample delivery system for SX with a target of commercialization and mass production.[1] The sample holders are thin, photopatterned Kapton sheets containing hundreds of wells for samples, with sealable gaskets that can be easily mounted on a standard magnetic base and transported in Unipucks for shipping. In addition, we have developed a portable sample mounting station for room temperature sample preparation, under a humidified atmosphere so sensitive crystalline samples do not dry out.
Our new sample delivery system has been commercialized and has already made promising results. We demonstrate the utility of this system on a pair of Glutaminase C-drug complexes, in which an explanation of the large difference in enzyme inhibition could only be determined by room temperature SX analysis.[2]

References
1. Illava, G., *et al*. *Acta Cryst.* **2021**, *D77*, 628-644.
2. Milano, S. K., *et al. J. Bio. Chem.* **2022**, *298*, 101535.

Kapton-based fixed target mount.

Back to Table of contents

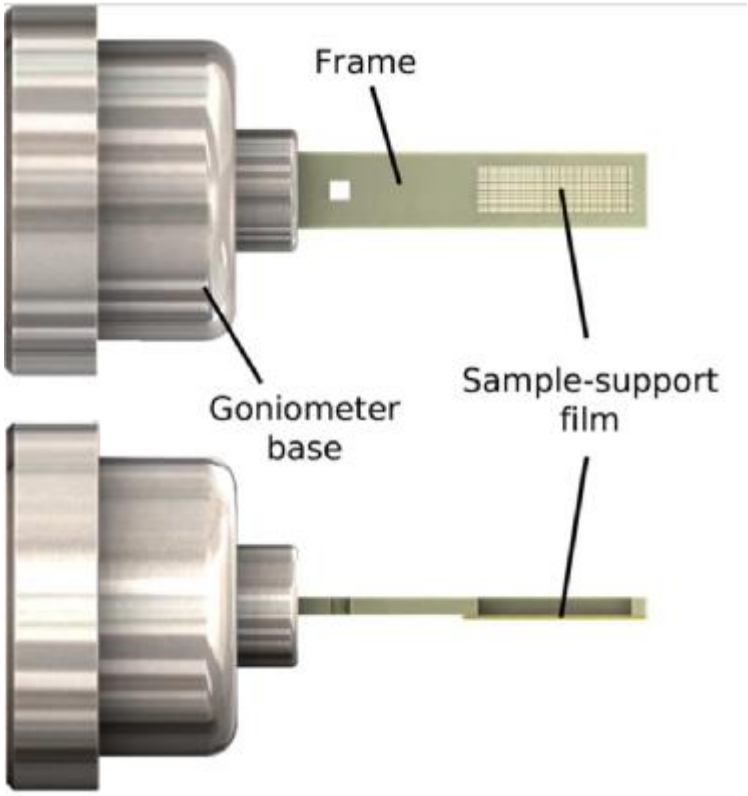

Humidor for sample deposition.

MS08 Serial crystallography, obtaining structures from many crystals

MS08-1-4 ID29, a versatile beamline for time-resolved serial crystallography at the EBS-ESRF #MS08-1-4

J. Orlans [1], S. Basu [2], D. De Sanctis [1]
[1]European Synchrotron Radiation Facility, 71 Avenue des Martyrs - Grenoble (France), [2]European Molecular Biology Laboratory, 71 Avenue des Martyrs - Grenoble (France)

Abstract
With its recent upgrade to the fourth-generation synchrotron called “Extremely Brilliant Source” (EBS), the ESRF is developing a new sub-microfocus beamline for the time-resolved study of serial synchrotron crystallography (TR-SSX) at room temperature with extremely high photon flux (up to 10^{16} ph/sec). The combination of two choppers generates a pulsed beam allowing the data collection from tens of microsecond to millisecond time delays; the double multilayer mirror monochromator (DMM) allows tuning ID29 beam on a wide energy range (from 10 to 20 keV) with variable bandwidth. A new developed diffractometer for fixed-target[1-4] experiments is adapted to accommodate different other sample delivery devices such as high viscosity injector[5-7], microfluidic[8], and tape-drive[9-11]. This high versatility will make possible to perform mixing experiments but also pump-probe experiments with the support of a high repetition rate nanosecond laser, which runs synchronously with the pulsed beam. In addition to the beamline, users have access to a laboratory in order to prepare their sample and characterise them offline before their beamtime.

We thank Victor Armijo 2, Raymond Barrett 1, Antonia Beteva 1, Anne-Lise Buisson 1, Paolo Busca 1, Hugo Caserotto 1, Florent Cipriani 2, Nicolas Coquelle 1, Samuel Debionne 1, Fabien Dobias 1, Franck Felisaz 2, David Flot 1, Jonathan Gigmes 1, Thierry Giraud 1, Hervé Gonzalez 1, Andrew Gotz 1, Alejandro Homs-Puron 1, Nicolas Janvier 1, Jérôme Kieffer 1, Gordon Leonard 1, Marcos López-Marrero 2, Daphné Lorphèvre 1, Christian Morawe 1, Carlos Muñoz Pequeño 1, Marcus Oscarsson 1, Gergely Papp 2, Anton Popov 1, Antoine Royant 1, Jérémy Sinoir 2, Olof Svensson 1, Pascal Theveneau 1 & Amparo Vivo 1.for their contribution to ID29 upgrade project.

1European Synchrotron Radiation Facility, 71 Avenue des Martyrs - Grenoble (France), 2European Molecular Biology Laboratory, 71 Avenue des Martyrs - Grenoble (France)

References
1. Ebrahim, A. et al. Resolving polymorphs and radiation-driven effects in microcrystals using fixed-target serial synchrotron crystallography. Acta Crystallogr. Sect. D Struct. Biol. 75, 151–159 (2019).
2. Ebrahim, A. et al. Dose-resolved serial synchrotron and XFEL structures of radiation-sensitive metalloproteins. IUCrJ 6, 543–551 (2019).
3. Mehrabi, P. et al. The HARE chip for efficient time-resolved serial synchrotron crystallography. J. Synchrotron Radiat. 27, 360–370 (2020).
4. Doak, R. B. et al. Crystallography on a chip – without the chip: sheet-on-sheet sandwich. Acta Crystallogr. Sect. D Struct. Biol. 74, 1000–1007 (2018).
5. Weierstall, U. et al. Lipidic cubic phase injector facilitates membrane protein serial femtosecond crystallography. Nat. Commun. 5, 3309 (2014).
6. Botha, S. et al. Room-temperature serial crystallography at synchrotron X-ray sources using slowly flowing free-standing high-viscosity microstreams. Acta Crystallogr. Sect. D Biol. Crystallogr. 71, 387–397 (2015).
7. Shimazu, Y. et al. High-viscosity sample-injection device for serial femtosecond crystallography at atmospheric pressure. J. Appl. Crystallogr. 52, 1280–1288 (2019).
8. van der Linden, P. J. E. M., Popov, A. M. & Pontoni, D. Accurate and rapid 3D printing of microfluidic devices using wavelength selection on a DLP printer. Lab Chip 20, 4128–4140 (2020).
9. Fuller, F. D. et al. Drop-on-demand sample delivery for studying biocatalysts in action at X-ray free-electron lasers. Nat. Methods 14, 443–449 (2017).
10. Beyerlein, K. R. et al. Mix-and-diffuse serial synchrotron crystallography. IUCrJ 4, 769–777 (2017).
11. Butryn, A. et al. An on-demand, drop-on-drop method for studying enzyme catalysis by serial crystallography. Nat. Commun. 12, 4461 (2021).

ID29 Experimental Hutch

Back to Table of contents

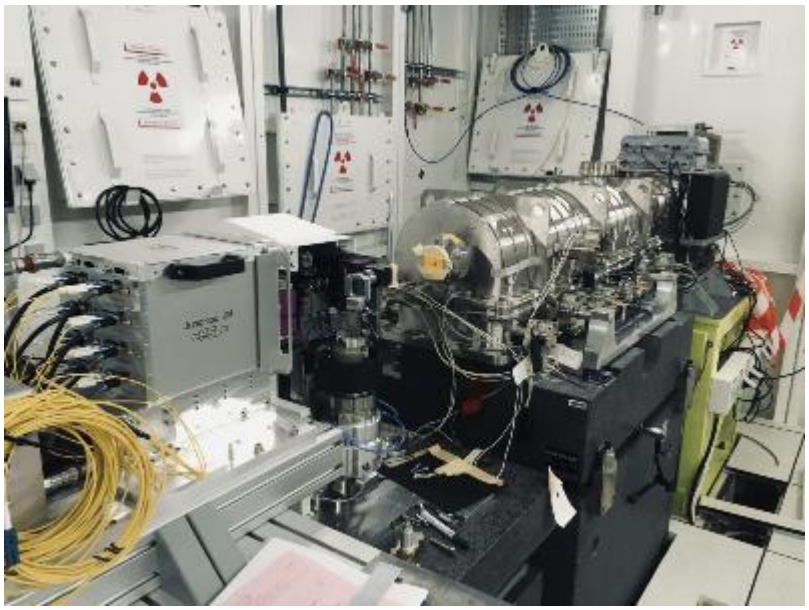

Back to Table of contents

MS08 Serial crystallography, obtaining structures from many crystals

MS08-1-5 Microfluidic Tools for Serial Protein Crystallography and Imaging at Synchrotron Facilities #MS08-1-5

R. Vasireddi [1], G. David [2]
[1]Scientist - Saint-Aubin (France), [2]BIOLABs & MFLab Manager Ingénieur R&D Biologie / Biology R&D Engineer - Saint-Aubin (France)

Abstract
Recent developments in ultra-brilliant synchrotron and hard X-ray free electron lasers (FEL) open very exciting possibilities in structural biology, such as serial protein crystallography (1) and time resolved structural studies of bio-macromolecules. These techniques already contribute to high impact science, yet both require high consumption of crystals and generate large data volumes for structural analysis, potentially requiring long periods of beamtime acquisition on oversubscribed central facilities. These issues can be somewhat mitigated with efficient sample delivery under the X-ray beam. Microfluidic and microscale technologies have played a critical role in facilitating both protein crystallization and structure determination (2). The transfer of microfluidic technology experiments is, however, technically challenging due to the requirement of X-ray compatibility of the different device materials. In the current presentation we will review the impact of microfluidic device technologies on protein crystal growth and X-ray diffraction analysis. We focus on applications of microfluidics for use in serial protein crystallography experiments and imaging at synchrotron sources. At Synchrotron SOLEIL, the microfluidic team, together with the life sciences scientists provides expertise in the design, manufacturing, and experimental implementation of microfluidic devices optimized for X-ray experiments. We also provide facilitated means of sample handling and specialized sample environments that address specific experimental conditions at synchrotrons and XFEL facilities. Finally, we are attempting to prepare standardized microfluidic trapping devices for biomacromolecular structural studies at Synchrotron SOLEIL and other synchrotron facilities (3).

References
[1] Chapman, H. N., Fromme, P., Barty, A., White, T. A., Kirian, R. A., Aquila, A., Weierstall, U. “Femtosecond X-ray protein nanocrystallography”. Nature, 470(7332), 73-77 (2011).
[2] R.Vasireddi, A. Gardais and L. M. G. Chavas “Diffusion-based crystal formation in microdevice for high-throughput in situ X-ray screening and data collection at room temperature” (Under Review)-2022.
[3] I. Chaussavoine, A. Beauvois, T. Mateo, R. Vasireddi, N. Douri, J. Priam, Y. Liatimi, S. Lefrançois, H. Tabuteau, M. Davranche, D. Vantelon, T. Bizien, L. M. G. Chavas and B. Lassalle-Kaiser; “The microfluidic laboratory at the synchrotron SOLEIL” Journal of Synchrotron Radiation 27,230-237, 2020.

Back to Table of contents

MS08 Serial crystallography, obtaining structures from many crystals

MS08-1-6 Iron binding and photoreduction in the ABC transporter subunit FutA
#MS08-1-6

R. Bolton [1], M. Machelett [1], D. Axford [2], A. Royant [3], T. Schrader [4], T. Tosha [5], H. Suigimoto [5], J. Worrall [6], G. Evans [2], M. Hough [2], R. Owen [2], I. Tews [1]
[1]University of Southampton - Southampton (United Kingdom), [2]Diamond Light Source - Didcot (United Kingdom), [3]Institut de Biologie Structurale - Grenoble (France), [4]Jülich Centre for Neutron Science - Garching (Germany), [5]RIKEN SPring-8 Center - Hyogo (Japan), [6]University of Essex - Colchester (United Kingdom)

Abstract
Oceanic primary production by marine cyanobacteria is a main contributor to carbon and nitrogen fixation on earth. *Prochlorococcus* is the most abundant photosynthetic organism on Earth, responsible for a comparable carbon fixation to the net global primary production from agriculture. The ecological success is rooted in genome reduction and ability to thrive in nutrient depleted waters. The single FutA protein in *Prochlorococcus* has a function in iron uptake through as a periplasmatic binding protein to the specialised ABC where it would bind iron in the ferric state (Fe^{3+}). However, in the cytosol FutA proteins are known to bind ferrous iron (Fe^{2+}).

Studies of metal binding proteins are hampered by X-ray induced photoreduction, in this case leading to conversion from the ferric to the ferrous oxidation state. We used serial femtosecond crystallography (SFX) and neutron diffraction to obtain crystallographic structures of the oxidised state, revealing penta-fold coordination of the metal. X-ray induced photoreduction using rotation methods and serial synchrotron dose series (SSX) then gave access to the reduced ferrous state. Structural changes were mapped at room temperature several dose points up to 110 kGy before global radiation damage becomes too severe, defining the sweet spot of such analyses in this case.

References
Beale JH, Bolton R, Marshall SA, Beale EV, Carr SB, Ebrahim A, Moreno-Chicano T, Hough MA, Worrall JAR, Tews I, Owen RL. Successful sample preparation for serial crystallography experiments. J Appl Crystallogr. 52 (2019), 1385-1396.Horrell S, Axford D, Devenish NE, Ebrahim A, Hough MA, Sherrell DA, Storm SLS, Tews I, Worrall JAR, Owen RL. Fixed Target Serial Data Collection at Diamond Light Source. J Vis Exp. 2021 Feb 26, 168.

Back to Table of contents

MS08 Serial crystallography, obtaining structures from many crystals

MS08-1-7 A metal-binding GFP-derivative reused as novel standard sample for serial crystallography approaches at FELs
#MS08-1-7

C. Schmidt [1], K. Dörner [1], J. Schulz [1], K. Lorenzen [1]
[1]European XFEL GmbH - Schenefeld (Germany)

Abstract
Since (time-resolved) serial crystallography experiments at an FEL source differ vastly from conventional cryo-crystallography measurements, sample requirements do as well. Hence, standard samples for FELs are needed for several reasons. There is an ongoing need for improving sample delivery methods as well as for data analysis of diffraction images for serial crystallography and time-resolved experiments.
One potential standard sample is iq-mEmerald, a GFP-derivative, with an engineered metal binding-site close to its chromophore, which was initially designed by Yu et al. (2014) as a metal sensor for live cell imaging [1]. Upon metal binding, fluorescence quenching and small reversible conformational changes can be induced, making it a candidate for mixing experiments, as well as for phase determination approaches.
A simple, one day, three-step purification procedure results in up to 300 mg of iq-mEmerald per liter *Escherichia coli* BL21 (DE3) cell culture. Microcrystals of various sizes can be obtained by batch crystallization by varying the pH and ammonium sulfate concentration of the precipitant solution. Crystals can be soaked, among others, with a $ZnCl_2$ solution, resulting in a change of the space group. The anomalous signal of the zinc atoms was exploited for single-wavelength anomalous dispersion (SAD) phasing and a structural model could be built using automatic model-building tools.
Thus, iq-mEmerald is a possible standard sample for serial mixing experiments and phasing approaches.

References
Yu, Xiaozhen, Marie-Paule Strub, Travis J. Barnard, Nicholas Noinaj, Grzegorz Piszczek, Susan K. Buchanan, und Justin W. Taraska. „An Engineered Palette of Metal Ion Quenchable Fluorescent Proteins“. PLoS ONE 9, Nr. 4 (21. April 2014): e95808. https://doi.org/10.1371/journal.pone.0095808.

Back to Table of contents

MS08 Serial crystallography, obtaining structures from many crystals

MS08-1-8 Towards time resolved structural studies of tryptophan 2,3-dioxygenase #MS08-1-8

A. Bailey [1]
[1]**Diamond Light Source - Oxford (United Kingdom)**

Abstract
Structural studies of heme proteins have historically been complicated by radiation damage manifesting around the heme active site. As a result, an outstanding challenge in the field is the determination of time-resolved structural intermediates of oxygen activation at room temperature and pressure. Tryptophan 2,3-dioxygenase (TDO) is a tetrameric heme protein containing one heme cofactor per monomer. The active site binds divalent oxygen, filling the vacant distal ligand of the heme iron, and catalyses the oxygenation of L-tryptophan via the activation of oxygen. The study of TDO has clinical relevance – the product of this reaction, n-formylkynurenine, is upregulated in certain cancer cells and contributes to the suppression of anti-tumour immunity [1]. Recently, using cryo-trapped X-ray and neutron methods, a consensus on the precise chemical nature of the heme protein Fe(IV)=O reactive intermediates have been developed [2]. However, these methods are technically difficult to achieve and interpret while avoiding photon-induced radiation damage to the vulnerable heme active site. X-ray free electron lasers (XFELs) provide a new method to probe reaction mechanisms through serial femtosecond crystallography: the resulting structures are pristine, and when combined with simultaneous x-ray emission spectroscopy, the redox state of the heme iron can be validated. Here we present rotation and serial crystal X-ray structures of TDO from Diamond Light Source and PAL-XFEL, and an optimisation protocol to produce microcrystalline slurries suitable for serial diffraction experiments. We also present spectra from cryo-cooled single crystal microspectrophotometry of TDO macrocrystals, this data represents progress towards understanding oxygen diffusion through TDO crystals relevant for time-resolved XFEL studies.

References
[1] Pilotte L et al. Proc Natl Acad Sci U S A. 2012;109(7):2497-2502
[2] Moody PCE et al. Acc Chem Res. 2018;51(2):427-435

Back to Table of contents

MS08 Serial crystallography, obtaining structures from many crystals

MS08-1-9 Routine room temperature structure determination from protein crystals in situ at Diamond beamline VMXi using the Crystallisation Facility at Harwell
#MS08-1-9

H. Mikolajek [1], M. Hough [1], J. Sandy [1], J. Sanchez-Weatherby [1]
[1]Diamond Light Source - Didcot (United Kingdom)

Abstract
The need for rapid turnaround times from the appearance of protein crystals to the determination of high quality crystal structures has driven many aspects of automation. Moreover, it is increasingly recognised that room temperature structures allow access to protein dynamics, may reveal ligand binding modes not apparent at cryogenic temperatures and allow for time resolved structures to be determined. We present the current pipeline of the Crystallisation Facility at Harwell and Diamond Beamline VMXi [1] and the capability of the pipeline to produce high quality structures at room temperature from small numbers of crystals in situ, for example within crystallisation plates. Protein samples in solution are provided by users, with automated crystallisation and data collection offering datasets and structure solution in many cases within days. In situ data collection allows for rapid feedback on crystallisation conditions for further optimisation and is particularly suitable for crystals challenging to cryo-protect or that are not robust to mechanical handling or other stresses. Operation is typically completely remote with data measured using a queueing system, providing convenience for the scientist. Recent developments in sample delivery and data analysis will also be described. We will also present illustrative examples in which the approach described above has led to effective structure solution on user projects.

References
1. VMXi: a fully automated, fully remote, high-flux in situ macromolecular crystallography beamline (2019) Juan Sanchez-Weatherby, James Sandy, Halina Mikolajek, Carina M. C. Lobley, Marco Mazzorana, Jon Kelly, Geoff Preece, Rich Littlewood and Thomas L.-M. Sørensen. Journal of Synchrotron Radiation. 26, 291-301.

Back to Table of contents

MS08 Serial crystallography, obtaining structures from many crystals

MS08-1-10 [Re(CO)2(dppv)(pbi)] complexes containing cis-1,2-bis(diphenylphosphino)-ethene and 2-(2-pyridyl)benzimidazolate ligands
#MS08-1-10

A. Kamecka [1], A. Kapturkiewicz [2], S. Shova [3], K. Suwinska [4]
[1]Siedlce University of Natural Sciences and Humanities, Faculty of Sciences, Institute of Chemical Sciences, Siedlce, 3 Maja 54, 08-110 Siedlce, Polandaculty of Mathematics and Natural Sciences, Cardinal Stefan Wyszyński University in Warsaw, K. Woycickiego 1/3, 01-938 Warszawa, Poland - Siedlce (Poland), [2]Siedlce University of Natural Sciences and Humanities, Faculty of Sciences, Institute of Chemical Sciences, Siedlce, 3 Maja 54, 08-110 Siedlce, Poland - Siedlce (Poland), [3]"Petru Poni" Institute of Macromolecular Chemistry, alley G, Ghica Vodă, 41A, 700487 Iași, Romania - Iași (Romania), [4]Faculty of Mathematics and Natural Sciences, Cardinal Stefan Wyszyński University in Warsaw, K. Woycickiego 1/3, 01-938 Warszawa, Poland - Warsaw (Poland)

Abstract
Simple reaction procedure, boiling of an equimolar mixture of $[Re(Cl)(CO)_3(dppv)]$, pbiH, and $TlClO_4$ in o-dichlorobenzene solutions, leads to two, chromatographically separable, isomers of $[Re(CO)_2(dppv)(pbi)]$ complex. The obtained species, the yellow emissive and the orange emissive isomers, have been identified using FT-IR, ^1H NMR, and ^{31}P NMR spectroscopy and their structures confirmed by X-ray examinations. According to obtained crystallography results, the investigated isomers differ mainly in the arrangement of the 2-(2-pyridyl)benzimidazolate (pbi) anion in their structures. Diverse arrangement of the P^P and N^N$^-$ ligand around the central cis-$Re(CO)^{2+}$ core results in well pronounced changes in luminescence properties of the studied luminophores, caused by different nature of their lowest excited triplet state.
Detailes of the molecular structures of the two [Re(Cl)(CO)3(dppv)] isomers will be discussed.

Back to Table of contents

MS08 Serial crystallography, obtaining structures from many crystals

MS08-1-11 Automated data processing and analysis of serial crystallography experiments
#MS08-1-11

G.M. Assmann [1], F. Leonarski [1], F. Dworkowski [1], T. Tomizaki [1], C.Y. Huang [1], M. Wang [1], J.A. Wojdyla [1]
[1]Swiss Light Source, Paul Scherrer Institute - Villigen (Switzerland)

Abstract
To collect a complete data set with little radiation damage, serial crystallography (SX) data collection strategies have recently experienced a renaissance. In serial synchrotron crystallography (SSX) experiments either partial data sets from a few degrees of rotation or zero-rotation stills are collected. Serial femtosecond crystallography (SFX) collects stills using X-ray pulses generated by a FEL before destruction of the crystal occurs (Chapman *et al*., 2011; Boutet *et al*., 2012). SX experiments produce large datasets, which require automated data-processing pipelines and sufficient merging strategies. An automated pipeline should analyze and archive raw data and support users in decision-making on merging strategies.
At the beamline X06SA at the Swiss Light Source, VESPA, a dedicated, versatile and universal endstation for SSX experiments supporting sample delivery methods including HVE (high viscosity ejectors), ALD (acoustic levitation diffractometry) and FT (fixed targets), was recently installed. The SSX stills, collected during commissioning beamtime at the VESPA endstation with a Jungfrau 4M detector (Leonarski *et al*., 2018), were used to compare different data processing steps (spot finding, indexing, integration and merging) offered by existing SFX data processing packages (such as CrystFEL (White, 2019), nXDS (Kabsch, 2014)). The VESPA setup, the first results of comparative analysis and the implementation of a combined automated data-processing pipeline, to be deployed at the SLS and the SwissFEL facilities, will be presented.

References
Boutet, S. *et al.* (2012). Science, 337, 362–364 ; Chapman, H., *et al.* (2011). Nature, 470, 73–77 ; Kabsch, W., (2014) Acta Cryst., D70, 2204-2216; Leonarski F., *et al.* (2018) Nature Methods, 15(10): 799-804; White, T.A., (2019) Acta Cryst., D75.

Back to Table of contents

MS08 Serial crystallography, obtaining structures from many crystals

MS08-2-1 Optimization of capillary-based serial synchrotron crystallography sample delivery for soluble proteins #MS08-2-1

M. Bjelcic [1], O. Aurelius [1], J. Nan [1], S. Ghosh [2], R. Neutze [2], T. Ursby [1]
[1]MAX IV Laboratory - Lund (Sweden), [2]University of Gothenburg - Gothenburg (Sweden)

Abstract
Serial Synchrotron Crystallography (SSX) is an emerging data-collection approach in which diffraction data are collected from multiple protein microcrystals. Some of the most common sample delivery setups for SSX include LCP extruder, GDVN, and fixed target[1,2].
The Neutze group developed a flow cell system called Serial-X[3] for LCP membrane protein crystal samples at synchrotrons (Figure 1). The system has been tested and its proof of principle confirmed with data collected at BioMAX (paper in manuscript, Figure 2). This project is taking the setup on the next level of use by showing it can be used for non-LCP crystals.
The idea was to test non-LCP crystals if they can be modified to mock-up LCP samples and to test all samples with different viscous matrices to show flexibility of the set-up. Hemoglobin, lysozyme and Rubisco crystals were used for the study. Based on literature search, monoolein, vacuum grease, HEC and Vaseline® have been chosen as viscous matrices for the study since those are the most common carrier media[4].
The first step was to test how crystals mix with the matrices, what the consistency of the LCP samples are (since for the set-up it needs to be a certain density to go and not clog the system) and how long the crystals can survive in the mixture. After establishing the test protocol it was used on all crystal and matrix pairings. The next step was data collection at BioMAX, where flow rate, exposure time, transmission and number of images per spot were needed to be tested. Initial data processing shows the system can be used for non-LCP samples and achieving good resolution of 1.8 to 2Å.

References
1. Diederichs K., Wang M. (2017) *Serial Synchrotron X-Ray Crystallography (SSX)*. In: Wlodawer A., Dauter Z., Jaskolski M. (eds) Protein Crystallography. Methods in Molecular Biology, vol 1607. Humana Press, New York, NY.
2. Grünbein M.L., Kovacs G-N.; *Sample delivery for serial crystallography at free-electron lasers and synchrotrons*, Acta Cryst. (2019) D75, 178-191
3. S. Ghosh, D. Zoric, P. Dahl, M. Bjelcic, J. Johansson, E. Svensson, P. Borjesson, A. Banacore, P. Edlund, O. Aurelius, M. Milas, J. Nan, A. Shilova, A. Gonzales, U. Muller, G. Branden, R. Neutze; *Serial synchrotron crystallography using goniometer compatible 3D-printed flow cells*; paper in manuscript
4. K. H. Nam; *Sample Delivery Media for Serial Crystallography*; Int. J. Mol. Sci. (2019), 20, 1094. (10.3390/ijms20051094)

Back to Table of contents

MS08 Serial crystallography, obtaining structures from many crystals

MS08-2-2 OM and Cheetah: a common framework for online and offline analysis in serial crystallography #MS08-2-2

A. Tolstikova [1], V. Mariani [2], T.D. Grant [3], A. Barty [1]
[1]DESY - Hamburg (Germany), [2]SLAC - Menlo Park (United States), [3]Jacobs School of Medicine and Biomedical Sciences - Buffalo (United States)

Abstract
OM, formerly known as OnDA [1], is a software framework for real-time monitoring of X-ray imaging experiment data and experimental conditions. OM provides users with a set of stable and efficient real-time monitors for the most common types of experiments, which can be used immediately without modifications or can be easily adapted to meet the users' requirements. Since its first release OM has proven to be an invaluable tool for monitoring of diffraction data and quick decision making during serial crystallography experiments at both free-electron laser and synchrotron sources. OM focuses on scalability and portability, to facilitate its adoption for a wide array of current and future instruments, and strives for stability and performance, relying on free and open-source libraries and protocols.
Although OM has been originally designed for real-time data processing, the flexibility of its core parallelization and data recovery strategies as well as its highly modular architecture have allowed it to be used as a new processing core for Cheetah, a software package for high-throughput reduction and analysis of serial diffraction data [2]. Merging online and offline analysis for serial crystallography into a single software framework offers numerous advantages. Support for new facilities, detectors and data sources can be shared between the OM and Cheetah packages, facilitating the development work and reducing the time needed to adapt both packages to new experiments and processing workflows. Using the same algorithms and features in both OM and Cheetah, additionally, allows the processing parameters optimized for one of the packages to be used for the other, avoiding duplication of effort. OM has, for example, recently gained the ability to stream data via a network socket to the CrystFEL software package [3], to get real-time feedback on the indexing rate and unit cell parameters during data collection. Cheetah can use the same technology to send detector frame to CrystFEL for further processing, without writing intermediate file to disk. As new, high-throughput facilities and detectors come online, and generate data at an unprecedented rate, avoiding writing files to disk can result in a strong reduction of storage needs, with its associate costs.
This contribution will give an overview of the new features in both the OM and Cheetah software packages, introducing recent development and discussing possible directions of future development.

References
1. Mariani, V., Morgan, A., Yoon, C.H., Lane, T.J., White, T.A., O'Grady, C., Kuhn, M., Aplin, S., Koglin, J., Barty, A. and Chapman, H.N., 2016. OnDA: online data analysis and feedback for serial X-ray imaging. Journal of applied crystallography, 49(3), pp.1073-1080.
2. Barty, A., Kirian, R.A., Maia, F.R., Hantke, M., Yoon, C.H., White, T.A. and Chapman, H., 2014. Cheetah: software for high-throughput reduction and analysis of serial femtosecond X-ray diffraction data. Journal of applied crystallography, 47(3), pp.1118-1131.
3. White, T.A., Kirian, R.A., Martin, A.V., Aquila, A., Nass, K., Barty, A. and Chapman, H.N., 2012. CrystFEL: a software suite for snapshot serial crystallography. Journal of applied crystallography, 45(2), pp.335-341.

Back to Table of contents

MS08 Serial crystallography, obtaining structures from many crystals

MS08-2-3 On the fly crystallization for nucleation studies by Serial Femtosecond Crystallography at the European X-ray Free Electron Laser
#MS08-2-3

R. De Wijn [1], G. Mills [1], R. Bean [1], J. Bielecki [1], H. Han [1], F.H.M. Koua [1], S. Kantamneni [1], C. Kim [1], J. Koliyadu [1], R. Letrun [1], D. Melo [1], A. Round [1], T. Sato [1], R. Schubert [1], M. Vakili [1], A. Wrona [1], A. Mancuso [1], A. Mancuso [2]
[1]European X-Ray Free-Electron Laser Facility GmbH - Schenefeld (Germany), [2]Department of Chemistry and Physics, La Trobe Institute for Molecular Science, La Trobe University - Melbourne (Australia)

Abstract
The study of nucleation or early crystallization events, while being very relevant for structural biology or even pharmaceutical applications, is a demanding topic with X-rays. Capturing highly dynamic processes at the desired moment in time while trying to keep the sample undamaged and preserving its quality remains a challenging hurdle. Recent studies were published using cryo-transmission electron microscopy, cryo-STEM tomography or dynamic light scattering (DLS) [1-3], but early stage crystallization remains not completely understood. The In-line crystallization method, presented here, is a novel concept for a rapid crystallization system to overcome some of the current limitations with X-rays and using the Serial Femtosecond Crystallography (SFX) method at the European X-Ray Free-Electron Laser (EuXFEL). This system allows the crystallization of lysozyme within one minute inside a capillary, with a nucleating agent (Tb-Xo4) and in conditions suitable for the use of a liquid jet with a Gas Dynamic Virtual Nozzle (GDVN), compatible with megahertz data collection at the scientific instrument SPB/SFX. In-line crystallization opens up two key possibilities: firstly, to be able to systematically control and optimize the size of crystals during an experiment. Ultimately, this control provides the very exciting possibility to systematically observe nucleation of protein crystals with XFEL pulses. Secondly, the possibility to reduce clogging of crystals in the sample delivery system, which is a key limitation to the good running of a SFX experiment using GDVN. The commercially available nucleating agent Tb-Xo4 from Polyvalan (https://crystallophore.fr/) is a lanthanide complex which was developed at the IBS (Grenoble, France) primarily as a phasing agent. Its nucleating property was then characterized in various assays [4, 5]. Our injection setup is optimized to allow for rapid nucleation of lysozyme at low salt concentrations via the addition of the nucleating agent Tb-Xo4. For lysozyme, such fast crystallization is difficult to achieve with other precipitants such as poly-ethylene glycol or salts while retaining good injectability of the liquid. The effect of Tb-Xo4 on lysozyme was already studied using DLS [3] and showed an immediate effect by triggering nucleation within seconds even in pure water in the absence of any other crystallant.
The in-line crystallization allows a rapid and controlled crystallization mainly suited for nucleation and early crystallization studies while still using the full advantage of the European XFEL: high brilliance and high repetition rate. Optical microscopy, electron microscopy and early X-ray data supporting this setup will be presented here.

References
[1] Van Driessche A.E.S., et al. 2021. Nucleation of protein mesocrystals via oriented attachment. Nat Commun 12:3902.
[2] Houben L., et al. 2020. A mechanism of ferritin crystallization revealed by cryo-STEM tomography. Nature 579:540-543.
[3] de Wijn R, et al. 2020. Monitoring the production of high diffraction-quality crystals of two enzymes in real time using in situ dynamic light scattering. Crystal. 10:65.
[4] Engilberge S, et al. 2017. Cristallophore: A versatile lanthanide complex for protein crystallography combining nucleating effects, phasing properties, and luminescence. Chem Sci 8:5909-5917.
[5] Engilberge S, et al. 2018. Unveiling the binding modes of the crystallophore, a terbium-based nucleating and phasing molecular agent for protein crystallography. Chem - A Eur J 24:9739-9746.

Back to Table of contents

MS08 Serial crystallography, obtaining structures from many crystals

MS08-2-4 Development of metric(s) for validation of automated processing of X-ray free-electron SFX data #MS08-2-4

S.M. Kantamneni [1], O. Turkot [1], R. De Wijn [1], D. Melo [1], F.H.M. Koua [1], F. Dall'antonia [1], L. Gelisio [1], A.P. Mancuso [1]
[1]European XFEL - Hamburg (Germany)

Abstract
Data processing in Serial Femtosecond X-ray Crystallography(SFX) collected at X-ray free-electron laser sources is carried out using software packages such as OnDA [1], Cheetah [2] and CrystFEL [3]. At the European X-Ray Free-Electron Laser (EuXFEL) Facility, an in-house automated analysis software package based on CrystFEL is used for offline analysis of calibrated detector data. The in-house or other automated pipelines offer a robust implementation of processing subsets for offline SFX data on different worker nodes in a cluster computing systems. They provide advantages such as ease of use and firsthand results. However, the trade-off between simplicity in usage and processing success rate when using these pipelines in comparison to manual data analysis is yet to be fully understood. To explore this-, a metric, or a combination of metrics, is being developed which can be used to evaluate the success rate of the data processing. Metric(s) such as CC*, CC_1/2, and R_split computed after the data processing step as well as the phase error computed after the phasing step in the structure solution process are currently under study towards this aim. In later stages, these metrics are used to validate the success rate of automated and manual processing.

References
[1] Barty, A. *et al.* (2014). J. Appl. Crystallogr. 47, 1118–1131.
[2] Mariani, V. *et al.* (2016). J. Appl. Crystallogr. 49, 1073–1080.
[3] White, T. A. *et al.* (2012). J. Appl. Crystallogr. 45, 335–341.

Back to Table of contents

MS08 Serial crystallography, obtaining structures from many crystals

MS08-2-5 Efficient sample delivery for serial protein crystallography with low background
#MS08-2-5

J.M. Lahey-Rudolph [1], L. Holthusen [1], M. Rößle [1]
[1]University of Applied Sciences Lübeck/ TH Lübeck - Lübeck (Germany)

Abstract
Serial crystallography experiments require a continuous delivery of microcrystals to the X-ray beam. An ideal sample delivery should have several features: First, owing to the small crystal size, a high signal to noise ratio (SNR) is vital for successful experiments. Second, high hit-rates are desirable that minimize both necessary beamtime and sample consumption. Last but not least, the setup should be robust and easy to use, but flexibly adaptable to experimental different designs. In cooperation with Suna Precision, we have developed a sample environment designed to fulfil these criteria. Here, a slurry of microcrystals in mother liquor is transported onto an ultrathin porous polymer foil, across an interaction-point and into the X-ray beam.
With this new tapedrive version, liquid scattering is reduced and SNR optimized by blotting away excess mother liquor and if applicable for TR-SX ligand buffer before the quasi-naked crystals are illuminated. The tapedrive setup will be installed at the new ESRF ID29 beamline in Grenoble. It allows time-resolved observation of conformational changes in crystallized proteins using different triggers like light-activation, pH jump or chemical mixing via diffusion. This contribution offers solutions and advice against the frequent problem of crystal settling and highlights ongoing experiments on preferential crystal orientation.

References
Martiel *et al., Acta Cryst*., **D75**, 160-177 (2019), doi:10.1107/S2059798318017953
Beyerlein *et al.*, *IUCrJ,* **4** (2017), doi:10.1107/S2052252517013124

Back to Table of contents

MS08 Serial crystallography, obtaining structures from many crystals

MS08-2-6 Living cells: Crystallization chambers for serial synchrotron crystallography
#MS08-2-6

J. Blaha [1], S. Panneerselvam [1], D. Schraivogel [2], B. Ramsz [2], D. Ordonez [2], M. Paulsen [2], T.R. Schneider [1], L.M. Steinmetz [2], M. Wilmanns [1]
[1]EMBL-Hamburg - Hamburg (Germany), [2]EMBL-Heidelberg - Heidelberg (Germany)

Abstract
Despite the advent of AlphaFold and the resolution revolution in cryo-electron microscopy, the x-ray crystallography remains a powerful tool for structural biology. While the focus of crystallographers is shifting from conventional crystallography methods towards more advanced techniques elucidating mechanisms of enzymatic reactions in time-resolved manner. In cellulo crystallization is one such emerging alternate technique that directly utilizes living cells for generation of protein crystals [1-3]. In cellulo crystallography circumvents the conventional and laborious steps of heterologous expression, purification, and in vitro crystallization. Moreover, it allows to study the protein structure in the environment of living cells and thus provides a platform for drug discovery in cellular conditions. However, the underlying mechanisms of the intracellular protein crystallization are still poorly understood, and the identification of novel in cellulo crystallization targets is not at all straightforward. In recent years several techniques were developed that allow for fast screening of suitable novel in cellulo targets and improve hit rates of low efficacy in cellulo crystals [4-5]. Here we present our approach to the in cellulo crystallization method pipeline that is applied at EMBL – Hamburg at the PETRA III beamlines to identify novel in cellulo crystallization targets, to improve the crystal containing cells concentration and to prepare cryo-samples for serial synchrotron diffraction data collection in robust and reliable manner.

References
1. Hasegawa, H., et al., In vivo crystallization of human IgG in the endoplasmic reticulum of engineered Chinese hamster ovary (CHO) cells. J Biol Chem, 2011. 286(22): p. 19917-31.
2. Redecke, L., et al., Natively inhibited Trypanosoma brucei cathepsin B structure determined by using an X-ray laser. Science, 2013. 339(6116): p. 227-230.
3. Nass, K., et al., In cellulo crystallization of Trypanosoma brucei IMP dehydrogenase enables the identification of genuine co-factors. Nat Commun, 2020. 11(1): p. 620.
4. Norton-Baker, B., et al., A simple vapor-diffusion method enables protein crystallization inside the HARE serial crystallography chip. Acta Crystallogr D Struct Biol, 2021. 77(Pt 6): p. 820-834.
5. Lahey-Rudolph, J.M., et al., Rapid screening of in cellulo grown protein crystals via a small-angle X-ray scattering/X-ray powder diffraction synergistic approach. J Appl Crystallogr, 2020. 53(Pt 5): p. 1169-1180.

Back to Table of contents

MS08 Serial crystallography, obtaining structures from many crystals

MS08-2-7 Identifying bacteriorhodopsin light-induced artefacts in time-resolved crystallography #MS08-2-7

Q. Bertrand [1], T. Weinert [1], J. Standfuss [1]
[1]PSI - Villigen (Switzerland)

Abstract
Time-resolve crystallography at X-ray free electron lasers (XFELs) allows the investigation of ultrafast protein reactions on the femtosecond time scale. However, getting insight on such rapid structural movements implies that the protein reactions of interest have to be triggered on the same time scale. This forces the use of photosensitive samples for which the reaction can be triggered in the femtosecond time range using lasers. However due to the crystal inherent properties, lasers are not able to trigger reaction for all proteins within one crystal. If the amount of molecules for which the reaction of interest has been triggered is too low, the structural signal from the reaction is unrecoverable. To counter this issue, the laser power applied to the sample might be increased, to simply deliver more photon to the crystal thus increasing the chances to trigger a reaction.
But any excessive laser power used during the experiment may lead to multi-photon excitation and may increase the probability of observing artefacts rather than native protein motion. Although structural effects of this multi-photon absorption are unknown, they are discussed in the X-ray laser field as a potential risk that could make data from femtosecond laser experiments unrelated to physiological protein motions.
Those questions were raised and the subject was largely discussed for Bacteriorhodopsin (bR), a model protein for which the photo-cycle has been extensively studied in the past years. To answer interrogations about the correct behavior of bR's photo-cycle under various laser power, we performed a power-titration experiment. This latter was performed through a typical pump probe time-resolve serial crystallography (TR-SX) experiment using a single time delay of 10 ps, but registered with different laser power applied to the sample.
Our experiment shows that clear new retinal features appear in the difference maps and extrapolated maps when an extreme laser power is used. Those features are additional peaks in the difference maps around the retinal that could be modelized as a second retinal conformation in extrapolated maps and only appears using high laser power. This conformation closely resembles one only visible later on the photo-cycle and it seems that the use of extreme laser power accelerates the behavior of the retinal through its photo-cycle. This delay of 10 ps provides overlaps with available datasets from several experiments already recorded with various laser powers and the comparison with those data will give insight about the impact of different laser setups on this light induced artefact.

References
Nango et al., 2016; Nogly et al., 2018; Weinert et al., 2019; Nass Kovacs et al., 2019; Grünbein et al., 2020.

Back to Table of contents

MS09 Structural Biology combining methods/High resolution

MS09-1-1 Insulin plasma concentration determination – details of a well-established sandwich assay #MS09-1-1

E. Johansson [1], X. Wu [2], B. Yu [2], Z. Yang [2], Z. Cao [2], C. Wiberg [1], C. Jeppesen [1], F. Poulsen [1]
[1]Novo Nordisk A/S - Maaloev (Denmark), [2]Novo Nordisk A/S - Beijing (Denmark)

Abstract
Insulin is a hormone produced in the pancreatic beta cells from which it is released after food intake, when the blood glucose level rises. Insulin signals cells to absorb glucose from the blood for energy usage or storage for future use. Insulin thereby helps to keep the blood glucose level in balance. A certain amount of circulating insulin is needed, even in phases without food intake, because the liver keeps producing glucose and releasing it into the bloodstream to supply cells with glucose all the time. A fasting insulin level should never be zero, which it might be in a person with untreated Type 1 diabetes. However, an excessive insulin level is just as problematic as a sign of insulin resistance, prediabetes or Type 2 diabetes. Thus, it is important from a diagnostic point of view to know the concentration of insulin in blood.
The monoclonal antibodies (mAbs) HUI-018 and OXI-005 were developed and found to work in a sandwich immunoassay for human insulin (HI) by Novo Nordisk in the 1980's and have since been used extensively. Initially, the approximate epitopes of different insulins for HUI-018 and OXI-005 were identified by indirect methods. In this study, the insulin epitopes for OXI-005 and HUI-018 were determined using X-ray crystallography in order to achieve a more thorough understanding. The crystal structure of the HUI-018 Fab in complex with HI was determined and OXI-005 Fab crystal structures were determined in complex with HI and porcine insulin (PI) as well as on its own. Based on the Fab complex crystal structures with the insulins a molecular model for simultaneous binding of the Fabs to PI was built and this model was validated by small angle X-ray scattering. The epitopes for the mAbs on insulin were found well separated from each other as expected from luminescent oxygen channelling immunoassay results for different insulins. The affinities of the OXI-005 and HUI-018 Fabs for HI, PI and DesB30 HI were determined using surface plasmon resonance. The KDs were found to be in the range of 1-4 nM for the HUI-018 Fab, while more different for the OXI-005 Fab (50 nM for HI, 20 nM for PI and 400 nM for DesB30 HI) supporting the importance of residue B30 for binding to OXI-005.
Finally, the design of other insulin and insulin analogue specific concentration determination assays is discussed on the background of a number of experimental structures of other insulin recognising Fabs in complex with their targets.

References
Johansson E., Wu X., Yu B., Yang Z., Cao Z., Wiberg C., Jeppesen C.B., Poulsen F. (2021) Insulin binding to the analytical antibody sandwich pair OXI-005 and HUI-018: Epitope mapping and binding properties. Protein Sci 30(2), 485-496.

Insulin bound to the Fabs of HIU-018 and OXI-005:

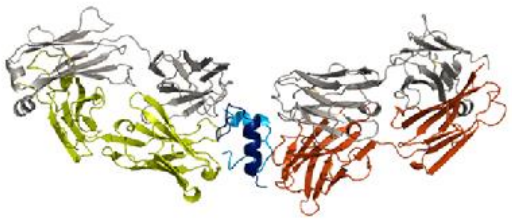

Back to Table of contents

MS09 Structural Biology combining methods/High resolution

MS09-1-2 Myoglobin as a model for heme peroxidase intermediate determination via integrative structural biology #MS09-1-2

S. Foster [1], H. Kwon [1], R. Liddington [1], J. Basran [1], P. Moody [1]
[1]Leicester Institute of Structural and Chemical Biology - University of Leicester - Leicester (United Kingdom)

Abstract
Heme-peroxidases were amongst the earliest enzymes investigated, and function to catalyse a breadth of substrates in a H2O2- dependent oxidation reaction. The progress of their reactions can be monitored by observing the electronic absorption spectra in the near UV-visible region as well as other indirect techniques. The distinct spectral signatures are due to structural and electronic changes at the heme moiety iron centre(1). Two major intermediate states, Compounds I and II, have iron oxidised above the resting Fe(III) “ferric” state to Fe(IV)-oxo “ferryl” state. Whilst readily identifiable via spectroscopic measurements, crystallographic and spectroscopic determinations of their precise nature is often conflicting. As the protonation state of these intermediates, being protonated (Fe(IV)–OH) or deprotonated (Fe(IV)=O), directly determines the enzymes reactivity, it is therefore apropos to correctly characterise them (2).
Despite not being a formal peroxidase, myoglobin is an excellent model as it exhibits low level basal peroxidase activity with analogous ferryl intermediates that can be monitored spectroscopically (3-5). Furthermore myoglobin readily forms high resolution crystals, has been used as a model system for the development of serial crystallography (6-8) and forms stable long-lived intermediates including Compound II. Our research aims to take an integrative structural biology approach to unequivocally address the ambiguity surrounding the peroxidase intermediates of myoglobin. Historically, the Fe-O bond length was taken as a proxy as bond order, however accurately measuring bond lengths with the precision needed with traditional X-ray diffraction, and being confident of avoiding X-ray induced photoreduction (despite multicrystal analyses and cryo-cooling) does not give the certainty of direct observation that is available via high resolution neutron crystallography, or X-ray free-electron laser (XFEL) diffraction. Similarly, the rise of microcrystal electron diffraction (microED) and the Coloumbic potential maps generated would permit direct observation of charge states, and facilitate a proof of principal for a pump-probe experiment at SFX-XFEL sources. Accumulation of a reaction intermediate has be validated with in crystallo and solution state UV-spectroscopy. Combining our solution spectroscopic results with the precise hydrogen positioning of a perdeuterated crystal amenable to neutron diffraction would begin to clarify the heme site protonation state. Additionally, microcrystalline slurries of hydrated crystals interrogated with microED and XFEL crystallography would incorporate charge potentials and radiation damage free structures surrounding the heme centre, respectively, supplementing the neutron studies. Integrating these results would build an intimate understanding of the chemistry driving this model peroxidase. Our group has previously collected Neutron and XFEL diffraction of two formal peroxidases (cytochrome c peroxidase and Ascorbate Peroxidase). With the Compound II intermediate protonation states appearing to contrast one another in these systems (9-11), describing the heme chemistry which drives the peroxidase activity within myoglobin succinctly using this integrative approach, will address a four decade long question and deepen our understanding of heme peroxidases.

References
1 Dunford, H. B. Peroxidases and catalases : biochemistry, biophysics, biotechnology, and physiology. 2nd ed.. edn, (Wiley-Blackwell, 2010).
2 Moody, P. C. E. & Raven, E. L. The Nature and Reactivity of Ferryl Heme in Compounds I and II. Accounts Chem. Res. 51, 427-435, doi:10.1021/acs.accounts.7b00463 (2018).
3 Hersleth, H.-P., Hsiao, Y.-W., Ryde, U., Görbitz, Carl H. & Andersson, K. K. The crystal structure of peroxymyoglobin generated through cryoradiolytic reduction of myoglobin compound III during data collection. Biochemical Journal 412, 257-264, doi:10.1042/bj20070921 (2008).
4 Matsui, T., Ozaki, S.-i. & Watanabe, Y. Formation and Catalytic Roles of Compound I in the Hydrogen Peroxide-Dependent Oxidations by His64 Myoglobin Mutants. J. Am. Chem. Soc. 121, 9952-9957, doi:10.1021/ja9914846 (1999).
5 Tew, D. & Ortiz de Montellano, P. R. The myoglobin protein radical. Coupling of Tyr-103 to Tyr-151 in the H2O2-mediated cross-linking of sperm whale myoglobin. J. Biol. Chem. 263, 17880-17886 (1988).
6 Barends, T. R. M. et al. Direct observation of ultrafast collective motions in CO myoglobin upon ligand dissociation. Science 350, 445, doi:10.1126/science.aac5492 (2015).
7 Oghbaey, S. et al. Fixed target combined with spectral mapping: approaching 100% hit rates for serial crystallography. Acta crystallographica. Section D, Structural biology 72, 944-955, doi:10.1107/S2059798316010834 (2016).
8 Owen, R. L. et al. Low-dose fixed-target serial synchrotron crystallography. Acta crystallographica. Section D, Structural biology 73, 373-378, doi:10.1107/S2059798317002996 (2017).

Back to Table of contents

9 Casadei, C.M . et al. Neutron cryo-crystallography captures the protonation state of ferryl heme in a peroxidase. Science (American Association for the Advancement of Science) 345, 193-197, doi:10.1126/science.1254398 (2014).
10 Kwon, H. et al. Direct visualization of a Fe(IV)–OH intermediate in a heme enzyme. Nature Communications 7, 13445, doi:10.1038/ncomms13445 (2016).
11 Kwon, H. et al. XFEL Crystal Structures of Peroxidase Compound II. Angewandte Chemie International Edition, doi:10.1002/anie.202103010 (2021).

Back to Table of contents

MS09 Structural Biology combining methods/High resolution

MS09-1-3 TraM – a DNA binding protein of pIP501 – a broad-host-range plasmid
#MS09-1-3

T.M.I. Berger [1], N.K. Gubensäk [1], C. Michaelis [1], A. Reisenbichler [1], E. Grohmann [1], W. Keller [1]
[1]University of Graz - Graz (Austria)

Abstract
The spread of resistances to antibiotics in bacteria is a serious global health problem. Conjugative plasmid transfer mediated by Type IV Secretion Systems (T4SS) is the most important means to transfer antibiotic resistance genes among bacteria. It is present in Gram- positive (G+) and in Gram- negative (G-) bacteria as well as in archaea. Conjugative plasmids of incompatibility group Inc18, primarily found in enterococci and streptococci, have a remarkably broad host range of conjugative transfer and hence play an important role in the propagation of multi drug resistant germs [1]. Several human pathogens are among them. Their abundance in wild life and farm animals increases the potential of its circulation. Till date there is no excisting structure of a T4SS of G+ bacteria, but several of G- bacteria [2]. pIP501 is one of the best studied Inc18 plasmids. Its transfer region is organized in a single operon encoding 15 putative transfer proteins.One of them is the DNA binding transmembrane protein TraM. TraM has three domains, an extracellular and an intracellular domain connected by a transmembrane domain. The investigation of TraM includes biophysical, biochemical and structural characterization. We are on the way to determine the residues of TraM, which are involved in DNA binding. We designed two different N-terminal constructs varying in length, TraM94 and TraM167. The structure of TraM94 was recently solved in our group. In contrast to the monomeric TraM94 TraM167 is a trimer in solution like the C-terminal domain of TraM, whose structure was solved in our group already some years ago [3].

References
[1] Verena Kohler, Ankita Vaishampayan, and Elisabeth Grohmann, 'Broad-Host-Range Inc18 Plasmids: Occurrence, Spread and Transfer Mechanisms', Plasmid, 99 (2018), 11–21 <https://doi.org/10.1016/j.plasmid.2018.06.001>.
[2] Jeong Min Chung and others, 'Structure of the Helicobacter Pylori Cag Type IV Secretion System', ELife, 8 (2019), 1–15 <https://doi.org/10.7554/eLife.47644.001>.
[3] Nikolaus Goessweiner-Mohr and others, 'The 2.5 Å Structure of the Enterococcus Conjugation Protein TraM Resembles VirB8 Type IV Secretion Proteins', Journal of Biological Chemistry, 288.3 (2013), 2018–28 <https://doi.org/10.1074/jbc.M112.428847>.

Back to Table of contents

MS09 Structural Biology combining methods/High resolution

MS09-1-4 Identification of BAZ2A bromodomain hit compounds

#MS09-1-4

A. Dalle Vedove [1], G. Cazzanelli [1], J. Corsi [1], M. Sedykh [2], L. Batiste [2], J.R. Marchand [2], D. Spiliotopoulos [2], V.G. D'agostino [1], A. Caflisch [2], G. Lolli [1]
[1]University of Trento - Trento (Italy), [2]University of Zurich - Zurich (Switzerland)

Abstract

BAZ2A is an epigenetic regulator affecting nucleolar transcription of ribosomal RNA. It is overexpressed in aggressive and recurrent prostate cancer where, in concert with EZH2, promotes cellular migration. Its bromodomain is characterized by a shallow and difficult-to-drug pocket. Here, we describe the identification of two hit compounds, based on different scaffolds, of the BAZ2A bromodomain. In a first approach (fragment-joining), a benzimidazole-triazole fragment was identified by a molecular docking campaign and validated by competitive binding assays and X-ray crystallography. Another ligand was observed in close proximity by soaking experiments using the BAZ2A bromodomain pre-incubated with the benzimidazole-triazole fragment. The crystal structure of BAZ2A with the two ligands was employed to design a few benzimidazole-triazole derivatives with increased affinity. In a second approach, a structure-based fragment-growing campaign was followed. By combining docking, competition binding assays and protein crystallography, we have extensively explored the interactions of the ligands with the rim of the binding pocket, and in particular ionic interactions with the side chain of Glu1820, which is unique to BAZ2A. We determined twenty-three high-resolution crystal structures of the holo BAZ2A bromodomain and analyzed common bromodomain/ligand motifs and favorable intra-ligand interactions. Binding of some of the compounds to the BAZ2A bromodomain is enantiospecific as also confirmed by isothermal titration calorimetry.

References

Dalle Vedove A., Cazzanelli G., Corsi J., Sedykh M., D'Agostino V.G., Caflisch A. and Lolli G. (2021) Identification of a BAZ2A bromodomain hit compound by fragment joining. ACS Bio & Med Chem Au 1, 5-10.

Back to Table of contents

MS09 Structural Biology combining methods/High resolution

MS09-1-5 VMXm: A new micro/nanofocus protein crystallography beamline at Diamond Light Source #MS09-1-5

A. Crawshaw [1], A. Warren [1], J. Trincao [1], M. Lunnon [1], G. Duller [1], G. Evans [1]
[1]Diamond Light Source - Didcot (United Kingdom)

Abstract
The Versatile Macromolecular Crystallography Microfocus (VMXm) beamline is a new micro/nanofocus beamline joining the suite of macromolecular crystallography beamlines at Diamond Light Source. The beamline has been designed to enable rotation data collection from microcrystals down to 0.5 microns in size. The beamline had its first users in Autumn 2018 and currently a user commissioning call is open for microcrystals measuring <10 µm in any dimension. The beamline optics deliver a beamsize of 0.4 - 9 µm vertically and horizontally between 1.3 - 13 µm to the sample position. The beamline operates at energies between 10-22 keV, delivering ~10^{12} ph/s to the sample (at 12.5 keV). VMXm is equipped with two detectors, a Pilatus3 6M (Si sensor) and an Eiger2 X 9M (CdTe sensor) which are fully interchangeable. The quantum efficiency of the CdTe detector is improved at higher energies compared to the Si detector. As such, it is possible to exploit photoelectronic escape from microcrystals using higher energy data collections, which in turn can prolong the lifetime of the crystals in the beam.
Microcrystals are prepared on electron microscopy grids using techniques borrowed from cryo-EM, including grid blotting and plunge freezing using liquid ethane. Samples are prepared in advance of beam time using the VMXm support laboratory, with grid preparation being validated through visualization using an offline Scanning Electron Microscope (SEM). Once grids are introduced to the beamline, crystals can be visualized and aligned to the X-ray beam using either an on-axis optical microscope or the integrated SEM. Signal-to-noise of the diffracted X-rays is greatly improved due to the mounting technique of the crystals which are held under vacuum for diffraction measurements, reducing background scatter to a minimum.
An outline of the beamline will be shown along with recent data collection results. The beamline has been used to collect data on crystals ranging from 2-5 µm in size. The first novel structure has recently been solved using Se derivatized samples. We have also seen improvements in microcrystal data collections where previously data was solved from 20 small wedges of merged data. Here, we were able to exploit photoelectron escape and low background images to solve the structure to a higher resolution from a single crystal.

Back to Table of contents

MS09 Structural Biology combining methods/High resolution

MS09-1-6 Structural basis of TIR-domain assembly formation in TRAM- and TRIF- dependent TLR signalling #MS09-1-6

M. Pan [1], A. Hedger [1], J. Nanson [1], S. Pospich [2], T.V.E.A. Ve [3], S. Raunser [2], M. Landsberg [1], B. Kobe [1]
[1]the University of Queensland - Brisbane (Australia), [2]Max Planck Institute of Molecular Physiology - Dortmund (Germany), [3]Griffith University - Gold Coast (Australia)

Abstract
Toll-like receptors (TLRs) detect pathogens and endogenous danger, initiating immune responses that lead to the production of pro-inflammatory cytokines. Recruitment of signalling adaptors such as MyD88, MAL, TRIF and TRAM to the TLR requires Toll/interleukin-1 receptor (TIR)-domain interactions. Except for TLR3, all TLRs utilize the MyD88-dependent pathway, and TLR3 and endosomal TLR4 use the TRIF-dependent pathway. However, knowledge of how receptors recruit downstream adaptor proteins and the structural basis of these interactions remains limited, only BB-loop has been identified to play a key role in the interface. Here we show that TRAM TIR domains spontaneously and irreversibly form filaments in vitro. The TRAM TIR domain also forms co-filaments with TLR4 TIR domains. A 5.5 Å-resolution cryo-EM structure shows a stable TRAM filament involving two parallel strands of TIR-domain subunits in a BB-loop-mediated head-to-tail arrangement. The two-stranded head-to-tail arrangement of TRAM TIR filaments is similar to that observed for TIR domain assemblies of MAL and MyD88, which have previously been shown to signal through a mechanism involving cooperative assembly formation. A BB-loop mutant that prevents filament formation validates the key role of the BB loop in filament formation. Using this mutant, we determined the crystal structure of TRAM TIR to 3 Å-resolution. The BB-loop of the crystal structure adopts a different conformation to that observed in the filament structure and may represent a monomeric non-signalling state. Cell-based signalling assays are used to validate TRAM TIR assembly interfaces. This information is crucial for a mechanistic understanding of TLR signalling, the development of therapeutic strategies, and understanding of the molecular basis of the consequences of the human disease of adaptor polymorphic variants.

Back to Table of contents

MS09 Structural Biology combining methods/High resolution

MS09-2-1 Disulfide bridge explains dimer formation for rsCherryRev1.4.
#MS09-2-1

T. Bui [1], P. Dedecker [1], L. Van Meervelt [1]
[1]Biochemistry, Molecular and Structural Biology, Department of Chemistry, KU Leuven - Leuven (Belgium)

Abstract
Since the green fluorescent protein (GFP) was first discovered in the early 1960s [1], there is a vast number of novel fluorescent proteins (FPs) that have been found in nature or successfully engineered. The spectral diversity and the special photophysical behaviors of fluorescent protein have enabled their applications in many biology-related studies. However, one of the major handicaps of FPs that restricts greatly their utility as a label in studying live-cell systems is the oligomerization tendency to some extent. Extensive efforts were devoted to preventing their oligomer formations and generating monomeric FPs. Previous structural studies revealed that the oligomerization in FPs was mainly formed by electrostatic interactions and/or hydrogen bonds between monomers. Hence, the common strategy to create a monomeric form of most FPs is to mutate key residues at their interfacing positions to break down the interactions between units [2].
rsCherryRev1.4 was reported as a monomeric red reversible photo-switchable FPs that was developed from rsCherryRev by introducing six mutations: G24C, R36H, R125C, V144F, R149Q, and E160L [3]. Compared to rsCherryRev, rsCherryRev1.4 is considered as an improved version exhibiting faster off-switching speed and lower switching fatigue at a high light intensity, thus increasing the application of rsCherryRev1.4 in the RESOFLT technique. Nevertheless, rsCherryRev1.4 has some limitations such as dimerization tendency and complex photophysical properties. We now have determined the crystal structure of rsCherryRev1.4 and discovered that its dimer formation is the result of disulfide bonding.
A plate-like crystal of rsCherryRev1.4 was obtained by the sitting drop vapor diffusion method after a few weeks. Diffraction data up to 2 Å resolution were collected at the I04 beamline of Diamond Light Source at 100K using an EIGER detector. The structure was solved in space group I2 by molecular replacement using mCherry (PDB code 2h5q) [4] as the phasing model. The orientation and interface regions between two monomers in rsCherryRev1.4 are very similar to those observed in the AB interface of DsRed [5],[6]. However, structural analysis using PDBePisa reveals that only CYS24 and SER21 are involved in one disulfide bond and one hydrogen bond formed between the two monomers in rsCherryRev1.4. In DsRed, there are 13 hydrogen bonds and three salt bridges created between chain A and chain B. This comparison suggests a crucial contribution of CYS24 to the dimerization tendency of rsCherryRev1.4, and CYS24 is one of the mutations introduced in rsCherryRev that is not prone to form a dimer. Other experiments including mutagenesis, electrophoresis and chromatography were also performed. Obtained results give further evidence for the disulfide link formed by two residues CYS24 as observed in the rsCherryRev1.4 dimer.

References
[1] Tsien, R. Y. Annu. Rev. Biochem. 67, 509-544 (1998).
[2] Chudakov, D.M. et al. Physiol. Rev. 90, 1103-1163 (2010).
[3] Lavoie-Cardinal, F. et al. ChemPhysChem 15, 655-663 (2014).
[4] Shu, X. et al. Biochemistry 45, 9639-9647 (2006).
[5] Tubbs, J. L. et al. Biochemistry 44, 9833-9840 (2005).
[6] Campbell, R. E. et al. Proc. Nat. Acad. Sci. 99, 7877-7882 (2002).

Back to Table of contents

MS09 Structural Biology combining methods/High resolution

MS09-2-2 Structures and interactions of anti-CRISPR AcrIF2 and AcrIF7
#MS09-2-2

E. Bae [1], N. Suh [2], J.Y. Suh [1]
[1]Seoul National University - Seoul (Korea, Republic of), [2]Soon Chun Hyang University - Asan (Korea, Republic of)

Abstract
Clustered regularly interspaced short palindromic repeats (CRISPRs) and CRISPR-associated (Cas) proteins form a microbial adaptive immune system against phage infection. In response, phages evolved anti-CRISPR (Acr) proteins to neutralize the host CRISPR-Cas immune system as a counter-defense mechanism. AcrIF2 and AcrIF7 were discovered in *Pseudomonas aeruginosa* phages and strongly inhibit the type I-F CRISPR-Cas systems. Here we determined the structures of AcrIF2 and AcrIF7 using X-ray crystallography and NMR spectroscopy, respectively. AcrIF2 contains a four-stranded antiparallel β-sheet sandwiched between two pairs of antiparallel α-helices. AcrIF7 features a three-stranded antiparallel β-sheet with flanking two α-helices. Both Acr inhibitors interact strongly with the Cas8f:Cas5f heterodimer, which is a subcomplex of the type I-F CRISPR surveillance complex. They compete for the same binding interface on Cas8f without common structural motifs. Our findings suggest that Acrs of divergent origin may have acquired specificity to a common target through convergent evolution of their surface charge configurations.

Back to Table of contents

MS09 Structural Biology combining methods/High resolution

MS09-2-3 The detailed structure of a flavodoxin from Bacillus cereus revealed at ultrahigh resolution combined with in situ single-crystal spectroscopy.
#MS09-2-3

M. Lofstad [1], I. Gudim [1], M. Hammerstad [1], H-P. Hersleth [1]
[1]University of Oslo, Department of Biosciences - Oslo (Norway)

Abstract
To obtain the correct structure of metallo- and redox proteins complementary *in situ* spectroscopic methods are needed to prove the redox state of these proteins. We have previously with single-crystal UV-vis and Raman spectroscopy followed the radiation-induced reduction of different haem- and flavoproteins [1,2]. For flavoproteins a bending of the flavin group due to radiation damage have been observed [2,3]. For a flavodoxin from *Bacillus cereus* previously solved to 1.3 Å, some negative electron density difference on the flavin group was observed [3]. The structural implication and whether this was due to radiation damage could not be explained. New crystallographic data to 0.8 Å presented here gives a more detailed explanation indicating some sort of flavin disorder. This study shows the added value of combining protein crystallography with *in situ* spectroscopy and ultrahigh resolution in the study of cofactor proteins.

References
[1] Hersleth, H.-P. & Andersson, K.K. How different oxidation states of crystalline myoglobin are influenced by X-rays. *Biochim. Biophys. Acta, Proteins Proteomics* (2011), 1814 , 785-796.

[2] Røhr, Å.K., Hersleth, H.-P. & Andersson, K.K. Tracking Flavin Conformations in Protein Crystal Structures with Raman Spectroscopy and QM/MM Calculations. *Angew. Chem. Int. Ed.* (2010), 49, 2324-2327.

[3] Gudim, I., Lofstad, M., van Beek, W. & Hersleth, H.-P. High-resolution crystal structures reveal a mixture of conformers of the Gly61-Asp62 peptide bond in an oxidised flavodoxin from *Bacillus cereus*. *Protein Sci*. (2018), 27, 1439-1449.

The previously unexplained electron density

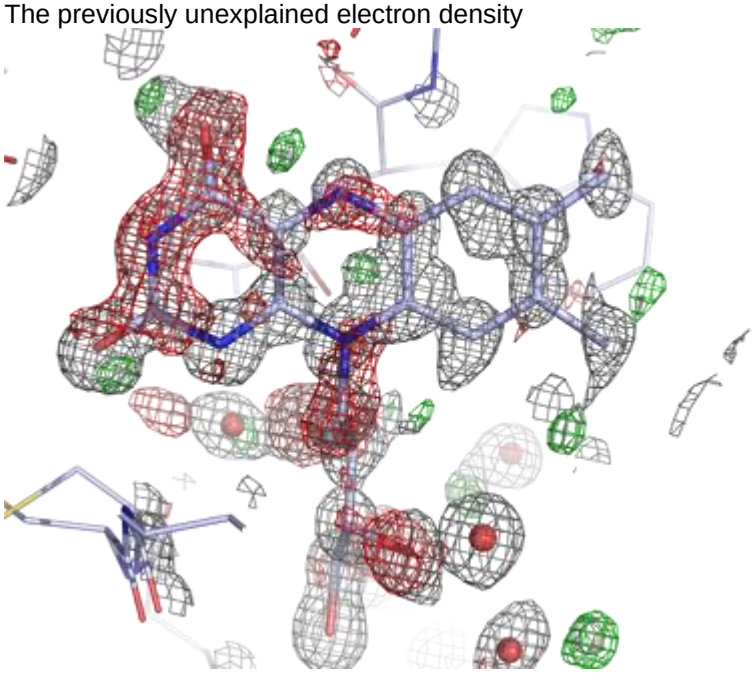

Back to Table of contents

MS09 Structural Biology combining methods/High resolution

MS09-2-4 New Opportunities for Integrated Structural Biology at 4th generation synchrotron sources. #MS09-2-4

A. Thompson [1], L. Chavas [1], T. Isabet [1], F. Jamme [1], P. Montaville [1], J. Perez [1], B. Pineau [1], J. Susini [1], B. Lassalle [1], L. Eric [2], C. Pierre-Damien [2]
[1]Synchrotron Soleil - Gif Sur Yvette (France), [2]ecole Polytechnique - Palaiseau (France)

Abstract
A proposal for a high brilliance upgrade to the SOLEIL synchrotron radiation source is expected to increase the beam brightness by > 50 times on beamlines used for life sciences. At the same time revolutions in Cryo-electron microscopy and the prediction of protein folds, and accessibile super resolution microscopy techniques have changed the way we look at an integrative approach. The combined expertise of the life sciences beamline teams at SOLEIL form the HelioBiology section, which has been, for the last 4 years, developing a post-upgrade approach to structural biology. This approach will be presented, paying particular attention to facilities that are novel to SOLEIL including in-vivo crystallisation [1] , microfluidic devices and their synchrotron applications [2], and concrete efforts towards an integrated approach to structural problems including the addition of new methods, such as cryo-electron microscopy and soft x-ray end cryo-electron tomography. Recent examples will illustrate opportunities for integrated studies at SOLEIL and elsewhere, and some potential evolutions discussed. This work is presented on behalf of the members of the HelioBio scientific section at SOLEIL (https://www.synchrotron-soleil.fr/en/research/house-research/biology-health-heliobio).

References
References[1]. Banerjee, S., Montaville, P., Chavas, L.M.G., Ramaswamy, S. "The New Era of Microcrystallography" Journal of the Indian Institute of Science., 98(3): 273–281. (2018).[2]. Chaussavoine, I., Beauvois, A., Mateo, T., Vasireddi, R., Douri, N., Priam, J., Liatimi, Y., Lefrançois, S., Tabuteau, H., Davranche, M., Vantelon, D., Bizien, T., Chavas, L.M.G., Lassalle-Kaiser, B. "The microfluidic laboratory at Synchrotron SOLEIL" Journal of Synchrotron Radiation., 27(1): 230-237. (2020).

Back to Table of contents

MS09 Structural Biology combining methods/High resolution

MS09-2-5 Identification of Potentially Bioactive Argon Binding Sites in Protein Families
#MS09-2-5

I. Hammami [1], G. Farjot [2], M. Naveau [3], A. Rousseaud [2], W.E. Shepard [4], P. Nioche [5], L. Chatre [6], T. Prangé [7], I. Katz [2], N. Colloc'h [6]
[1]CNRS UMR6030 / Air Liquide Santé International - Caen / Les Loges-En-Josas (France), [2]Air liquide Santé International - Les Loges-En-Josas (France), [3]UAR 3408 US 50 CNRS INSERM - Caen (France), [4]Synchrotron SOLEIL - l'Orme des merisiers Saint-Aubin (France), [5]Structural and molecular analysis platform, BioMedTech Facilities INSERM US36 - Paris (France), [6]CNRS UMR6030 - Caen (France), [7]CNRS CiTCoM UMR 8038 - Paris (France)

Abstract
Argon belongs to the group of chemically inert noble gases, which display a remarkable spectrum of clinically useful biological properties. In an attempt to better understand noble gases, notably argon's mechanism of action, we mined a massive noble gas modelling database which lists all possible noble gas binding sites in the proteins from the Protein Data Bank. We developed a method of analysis to identify among all predicted noble gas binding sites, the potentially relevant ones, based on their conservation, binding energy, hydrophobicity, shape and localization within structurally aligned protein families which are likely to be modulated by Ar.[1]This method allowed us to identify relevant noble gas, in particular Ar, binding sites that have potential pharmacological interest in several protein families such as Nitric Oxide Synthase (NOS), and soluble Guanylate Cyclase heme-NO and oxygen binding domain (sGC H-NOX domain). These potential Ar targets are currently undergoing crystallographic studies under Ar pressure to confirm our in-silico predictions. We have already identified a crystallographic Ar binding site under 5 MPa pressure within Thermolysin, that corresponds to a predicted noble gas binding site that meets all our suggested criteria. *In vitro* validation experiments are being performed with Ar on a few identified putative physiological targets in order to improve the understanding of its interaction mechanism of action.

References
(1) Hammami, I.; Farjot, G.; Naveau, M.; Rousseaud, A.; Prangé, T.; Katz, I.; Colloc'h, N. Method for the Identification of Potentially Bioactive Argon Binding Sites in Protein Families. J. Chem. Inf. Model. 2022. https://doi.org/10.1021/acs.jcim.2c00071.

Back to Table of contents

MS09 Structural Biology combining methods/High resolution

MS09-2-6 Modelling Diffuse Scattering in Protein X-Ray Crystallography using Internal Motion Models #MS09-2-6

J. Van Der Horn [1], L. Kroon-Batenburg [1]
[1]Utrecht University - Utrecht (Netherlands)

Abstract
Protein structures obtained through X-ray crystallography represent an average conformation of all protein molecules in a crystal. In reality, proteins are very flexible and dynamic. Even in a crystal, they can adopt many different conformations. Clues about their disorder can be captured during X-ray diffraction experiments, in the form of diffuse scattering. The observed diffuse signal can be attributed to correlated motions on various scales. Here, we make the distinction between rigid-body motions and internal motions, like those of secondary structures and single residues. We devised a model which can selectively simulate various types of internal disorder and calculate the diffuse signals associated with them. It is shown that the primary features of the total diffuse signal be attributed to rigid-body motions, whereas the internal motions mainly affect the contrast of the signal.

References
Ferreira, C. et al. (2020). Protein crystals as a key for deciphering macromolecular crowding effects on biological reactions. Physical Chemistry Chemical Physics, 22(28), 16143–16149. https://doi.org/10.1039/d0cp02469dChapman, H. N. et al. (2017). Continuous diffraction of molecules and disordered molecular crystals. Journal of Applied Crystallography, 50(4), 1084–1103. https://doi.org/10.1107/s160057671700749xPearce, N. M., & Gros, P. (2021). A method for intuitively extracting macromolecular dynamics from structural disorder. Nature Communications, 12(1). https://doi.org/10.1038/s41467-021-25814-xUrzhumtsev, A. et al. (2016). From deep TLS validation to ensembles of atomic models built from elemental motions. Addenda and corrigendum. Acta Crystallographica Section D Structural Biology, 72(9), 1073–1075. https://doi.org/10.1107/s2059798316013048

Back to Table of contents

MS09 Structural Biology combining methods/High resolution

MS09-2-7 X-ray structure of AvrLm1 effector from Leptosphaeria maculans in complex with the Mitogen Activated protein Kinase MPK9 from Brassica napus and their interaction
#MS09-2-7

H. Van Tilbeurgh [1], S. Djouadou [1], I. Li De La Sierra-Gallay [1], N. Lazar [1], K. Blondeau [1], C. Sizun [2], I. Fudal [3]
[1]I2BC-Orsay (France) - Gif-sur-Yvette (France), [2]Icsn - Gif-Sur-Yvette (France) - Gif-sur-Yvette (France), [3]Bioger - Thiverval-Grignon (France)

Abstract
Fungi are the most devastating pathogens of plants, including crops of major economic importance. Host invasion relies on effectors, key elements of pathogenesis, which modulate plant immunity and facilitate infection. Fungal effectors are typically small proteins with no or only weak homologs in databases, and known motifs are absent from their sequences. Their function in pathogenesis is also mostly unknown. Effectors have a dual role in microbe-plant interactions, both targeting plant components and being targeted by resistance (R) proteins and then termed avirulence (AVR) proteins. The 3D structure of several fungal and oomycete avirulence effectors have been reported and have been provided key advances in the understanding of plant-pathogen interactions (Boutemy L.S. et al 2011; Blondeau K. et al 2015; Ma L. et al 2018). In this study, we purified, characterized and determined the 3D structure of the AvrLm1 / MPK9 complex. We solved the X-ray structure by molecular replacement using an AlphaFold 3D model for the effector. The crystal structure at 3.9Å resolution reveled a ß-barrel fold never observed before in other effectors from L. maculans and provides insight into recognition of the MAP protein kinase MPK9. The structure of AvrLm1 revealed a structural homolog called SnTox3, which is a K2PP-like protein. From the comparison of both structures and biochemical experiments we concluded that AvrLm1 is synthesized as a pre-pro protein and that the pro-domain can be cleaved in vitro by the Kex2 protease. Finally, we determined quantitatively the interaction between AvrLm1 and MPK9 by ITC.

References
Ma, Lisong et al. “Leptosphaeria maculans Effector Protein AvrLm1 Modulates Plant Immunity by Enhancing MAP Kinase 9 Phosphorylation.” iScience vol. 3 (2018): 177-191. doi:10.1016/j.isci.2018.04.015

Back to Table of contents

MS09 Structural Biology combining methods/High resolution

MS09-2-8 Advanced in-house X-ray diffraction and scattering instruments as a service for structural biology #MS09-2-8

J. Stransky [1], J. Pavlicek [1], J. Dohnalek [1]
[1]Institute of Biotechnology, Czech Academy of Sciences - Vestec near Prague (Czech Republic)

Abstract
The Centre of Molecular Structure (CMS) provides services and access to state-of-art instruments, which cover a wide range of techniques required by not only structural biologists. CMS operates as part of the Czech Infrastructure for Integrative Structural Biology (CIISB), and European infrastructures Instruct-ERIC and MOSBRI. CMS is organized in 5 core facilities: CF Protein Production, CF Biophysics, CF Crystallization of Proteins and Nucleic Acids, CF Diffraction Techniques, and CF Structural Mass Spectrometry.
CF Diffraction Techniques employs two laboratory X-ray instruments equipped with high flux MetalJet X-ray sources: a single crystal diffractometer D8 Venture (Bruker) and a small angle X-ray scattering instrument SAXSpoint 2.0 (Anton Paar). The configurations of both instruments represent the top tier of possibilities of laboratory instrumentation. Apart from standard applications, the instruments are also extended for advanced experiments: the diffractometer is equipped with the stage for in-situ crystal diffraction and crystal dehydration, SAXS is equipped with in-situ UV-Vis spectroscopy and a liquid chromatography system for SEC-SAXS. The setups enable easy access and fast turn-around of samples under different conditions, but also collection of high quality end-state data without further need for synchrotron data collection in many cases. CF Diffraction Techniques provides services in synergy with the other CFs on-site, therefore scientific questions can be quickly answered as they emerge from the experiments.
The Centre of Molecular Structure is supported by: MEYS CR (LM2018127); project Czech Infrastructure for Integrative Structural Biology for Human Health (CZ.02.1.01/0.0/0.0/16_013/0001776) from the ERDF; UP CIISB (CZ.02.1.01/0.0/0.0/18_046/0015974), ELIBIO (CZ.02.1.01/0.0/0.0/15_003/0000447), and MOSBRI from EU Horizon 2020 (No. 101004806).

Back to Table of contents

MS10 Protein-carbohydrate interactions

MS10-1-1 Extensive substrate recognition by the streptococcal antibody-degrading enzymes IdeS and EndoS #MS10-1-1

A.S.L. Sudol [1], M. Crispin [1], I. Tews [1], J. Butler [1], D.P. Ivory [1]
[1]University of Southampton - Southampton (United Kingdom)

Abstract
The cleavage of human IgG antibodies is a potent immune evasion mechanism utilised by some pathogenic bacteria. The Streptococcus pyogenes bacterium, which has the capacity to cause necrotising fasciitis, employs multiple enzymes to deactivate the human adaptive immune system. Two such proteins, IdeS and EndoS, prevent immune detection by ablating the immune effector functions of IgG, by cleavage and deglycosylation of its Fc region, respectively. Their fine specificity for IgG has led to a wide range of clinical and biotechnology applications, with IdeS having received clinical approval facilitating organ transplantation in hypersensitised individuals, while EndoS has found application in engineering antibody glycosylation. Here, we present crystal structures of IdeS and EndoS in complex with their IgG1 Fc substrate, with both enzymes exhibiting exquisite target specificity. The IdeS protease is shown encasing the antibody hinge target, but also recognises the Fc globular domains. In contrast, the glycan hydrolase domain in EndoS traps the Fc glycan in a flipped-out conformation, while additional antibody specificity is driven by protein recognition by the so-called carbohydrate binding module. Understanding the molecular basis of antibody recognition by bacterial enzymes will facilitate the development of next-generation enzymes.

Back to Table of contents

MS10 Protein-carbohydrate interactions

MS10-2-1 FimH bacterial lectin switches arms between monovalent and multivalent binding of N-glycans #MS10-2-1

J. De Ruyck [1], S. Semwal [1], J. Bouckaert [1]
[1]Unité de Glycobiologie Structurale et Fonctionnelle - Villeneuve d'Ascq (France)

Abstract
The lectin domain of the fimbrial adhesin FimH from *Escherichia coli* recognizes, with a similar high affinity (K_d < 20 nM) and in a monovalent fashion (1), oligomannoside-3 and -5 *N*-glycans, on the condition that these ligands are present in a molar excess. Oligomannose-6 is generated with the first transfer of a mannose in α1,2-linkage, to the mannose that is itself α1,3-linked to the common core of *N*-glycans (Fig. 1). This extra mannose, C, causes a 10-fold affinity loss compared to oligomannose-3 and -5 but permits divalent binding that is sustained beyond a molar excess of the ligand (2).
Oligomannose-6 co-crystals with FimH lectin occurred only at the surface of a large lithium sulphate crystal. In these crystals, oligomannose-6 is a divalent ligand bridging two FimH lectins (Fig. 2). Oligomannose-6 bound via two non-reducing mannosides, A and B, that sprout from the central mannose, 4' (Fig. 1), that is α1,6-linked to the common *N*-glycan trimannose core. In contrast, in the co-crystal structure of FimH lectin with core(α1,6)-fucosylated oligomannose-3, no change is observed in the monovalent capture of mannose 4 of oligomannose-3, or the precursor of arm C (Fig. 1).
We profiled the binding of the FimH lectin on a glycan microarray and measured the kinetics of FimH interactions with oligomannosidic *N*-glycans and glycoproteins. To transition to oligomannose-6, we measured the kinetics of FimH binding with Manα1,2Man, Manα1,3Man, Manα1,6Man and Manα1,4Man coupled with bovine serum albumin, and compared affinities with direct binding in a FimH Lectprofile assay. Both earlier studies (3), mixed interfaces of the three different non-reducing *N*-glycan dimannosides of oligomannose-6 (Fig. 1) and molecular dynamics simulations suggest a positive cooperativity in the simultaneous binding by FimH (Fig. 2) of Manα1,3Manα1 and Manα1,6Manα1 (Fig. 1) on arms A and B of oligomannose-6.

References
(1) Bouckaert, J., Mackenzie, J., de Paz, J. L., Chipwaza, B., Choudhury, D., Zavialov, A., Mannerstedt, K., Anderson, J., Pierard, D., Wyns, L., Seeberger, P. H., Oscarson, S., De Greve, H., Knight, S. D. (2006) The affinity of the FimH fimbrial adhesin is receptor-driven and quasi-independent of Escherichia coli pathotypes. Molecular Microbiology 61, 1556-1568
(2) Sauer, M. M., Jakob, R. P., Luber, T., Canonica, F., Navarra, G., Ernst, B., Maier, T., Glockshuber, R. (2019) Binding of the bacterial adhesin FimH to its natural, multivalent high-mannose type glycan targets. J Am Chem Soc 141, 936-944
(3) Dumych, T., Bridot, C., Gouin, S. G., Paryzhak, S., Szunerits, S., Bilyy, R., Bouckaert, J., (2018) A novel integrated way for deciphering the glycan code for the FimH lectin. Molecules 23, 2794

Oligomannose-6

Back to Table of contents

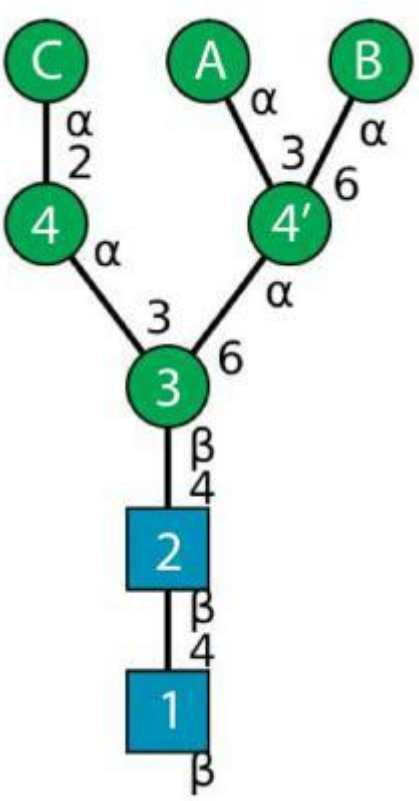

Oligomannose-6 bridging two FimH lectins

Back to Table of contents

MS11 Opportunities from combining structural biology and fold prediction

MS11-1-1 Fantastic bacteriophages and where to find them
#MS11-1-1

A. Butler [1]
[1]**Durham University - Durham (United Kingdom)**

Abstract
Viruses are highly diverse, sophisticated infectious agents that replicate solely inside living organisms by exploiting host cell metabolic machinery. The virosphere is comprised of all viruses that are found in the environment and therefore presents high degrees of genetic diversity. The Horizon 2020 Virus-X—Viral Metagenomics for Innovation Value—project was established in 2016 with a central aim to better understand genetic diversity amongst viruses found in extreme natural environments like geothermal springs. These insights could then be utilised to develop novel gene products for uses in a wide range of biotechnological applications, including novel therapeutics and molecular diagnostics.
The project established a highly intertwined and collaborative pipeline, which covered the initial retrieval of viral metagenomes and processing using bioinformatics to protein characterisation and progression onto innovation. This unique approach allowed for the careful selection of target genes, with the greatest potential for innovation, to be taken forward for functional and structural characterisation. These were a combination of non-structural viral proteins, where their functions were largely understood; as well as those with uncharacterised properties, allowing for the discovery of new functionalities. The structures of many of these proteins have been successfully determined experimentally using X-ray crystallography. Protein structure determination proved complementary to bioinformatics, and thus a total of 97 proteins have been thoroughly characterised including robust lytic enzymes from thermophilic bacteriophages. Here, I will present the structure of one of these phage lytic enzymes, which was solved using an integrative approach of standard crystallographic phasing techniques alongside structure prediction models generated from artificial intelligence systems such as AlphaFold.

Back to Table of contents

MS11 Opportunities from combining structural biology and fold prediction

MS11-1-2 MAXS reveals the conformational changes of intrinsically disordered regions of MAP2K6 #MS11-1-2

T. Matsumoto [1], S. Hasegawa [2], T. Hasegawa [1], T. Kinoshita [2]
[1]Rigaku Corporation - Tokyo (Japan), [2]Osaka Metropolitan University - Osaka (Japan)

Abstract
Mitogen-activated protein kinase kinase 6 (MAP2K6) plays a crucial role in the MAP2K6/p38 MAP kinase signaling cascade that regulates various stress-induced responses. This cascade is involved in inflammatory responses and apoptosis, and has attracted attention as a drug target for inflammatory and immune system diseases.
Crystal structure analysis of full-length MAP2K6 was solved at 2.6 Å resolution showing the N-terminal 43 residues were disordered1. The docking domain, which is important for correct recognition and facilitating signal transduction of p38 MAP kinase, is located at this disordered N-terminus. This disordered docking domain is flexible, and therefore, we speculate that it is usually intrinsically disordered, but may transition to an ordered state on binding to the p38 kinases. The structure prediction of MAP2K6 with AlphaFold also strongly suggested that the N-terminus is an intrinsically disordered region2, 3.
If the structure and conformational changes of molecules in solution can be directly visualized, it is possible to confirm that areas of intrinsically disorder region are transitioning to an ordered state by complex formation. X-ray solution scattering experiments are a powerful technique for analysing structures and conformational changes.
In addition, the scattering from the middle range of the resolution region [q values between 0.30 to 0.65 Å-1] contains important information such as the inter-domain distances and inter-secondary structure distances in the molecule. This data allows us to visualize more detailed molecular behaviours and conformational changes. The solution scattering that contains this important middle-angle region information is called mid-angle X-ray scattering (MAXS).
Therefore, we performed MAXS analysis of the MAP2K6/p38 complex and found that the solution structure of MAP2K6/p38α complex revealed compact state. We also succeeded in observing order state of n-terminus.
In this presentation will discuss solution structure analysis by MAXS and show that is essential to evaluate the conformational changes of intrinsically disordered regions.

References
1. Matsumoto, T., et al. Crystal structure of non-phosphorylated MAP2K6 in a putative auto-inhibition state. *J. Biochem.* (2012). **151**, 541-549.2. Jumper, J., et al. Highly accurate protein structure prediction with AlphaFold. *Nature* (2021). **596**, 583-589.3. Varadi, M., et al. AlphaFold Protein Structure Database: massively expanding the structural coverage of protein-sequence space with high-accuracy models. *Nucleic Acids Research* (2021). **50**, D439-D444.

Back to Table of contents

MS11 Opportunities from combining structural biology and fold prediction

MS11-1-3 Evolutionary covariance to assess the biological relevance of putative homo-oligomeric interfaces #MS11-1-3

J.J. Burgos-Mármol [1], R.M. Keegan [2], E. Krissinel [2], D.J. Rigden [1]
[1]ISMIB, University of Liverpool - Liverpool (United Kingdom), [2]UKRI-STFC, Rutherford Appleton Laboratory, Research Complex at Harwell - Didcot (United Kingdom)

Abstract

Evolutionary covariance to assess the biological relevance of putative homo-oligomeric interfaces
J. Javier Burgos-Mármol[1], Ronan M. Keegan[2], Eugene Krissinel[2], Daniel J. Rigden[1]
[1] Institute of Systems, Molecular and Integrative Biology, University of Liverpool, Liverpool L69 7ZB, UK[2] UKRI-STFC, Rutherford Appleton Laboratory, Research Complex at Harwell, Didcot OX11 0FA, UK
Evolutionary covariance is a phenomenon that occurs due to natural selection of mutations that tend to preserve the structure and, consequently, the function of a protein. When a mutation appears in a protein, the interaction with the surrounding residues can be affected, modifying the structure and possibly its functionality in a detrimental way. However, if a second compensating mutation occurs so that the contact is preserved, the functionality may not be adversely affected and the new variant could pass down to new individuals. By studying a protein's homologues, these pair correlations that signal structural contacts can be found.
This principle has been employed in the last decades to develop software tools that are able to predict contacts within a protein chain by looking at the sequence alone, with accuracy related to the number of homologues available. While more recent tools, using machine learning algorithms, have been trained mostly to predict intramolecular contacts, previous programs with little or no training to distinguish intramolecular contacts from those within oligomer interfaces can be used to infer intermolecular contacts.
We present project PISACov, a tool that exploits first-generation contact-prediction programs as well as novel algorithms to evaluate interfaces in homo-oligomeric proteins. To this end, the workflow includes widely used tools to produce sequence alignments and contact predictions that are finally put together to assess the interface. The application involves the use of PISA, a CCP4 program that determines the stability of the interfaces observed in a crystal structure by calculating their solvation free-energy. With this method, PISACov acts a an independent source of information to determine which of the crystal interfaces are likely biologically relevant. Other uses beyond validation of PISA results are possible. For instance, alternative computationally generated interfaces (e.g. from AlphaFold) can be evaluated by PISACov to be assessed with this approach.

Back to Table of contents

MS11 Opportunities from combining structural biology and fold prediction

MS11-1-4 Analysis of interfaces and packing of amyloid peptide structures
#MS11-1-4

M. Sulyok-Eiler [1], Z. Dürvanger [1], V. Dr. Harmat [1], A. Dr. Perczel [1]
[1]Laboratory of Structural Chemistry and Biology, Eötvös University - Budapest (Hungary)

Abstract
Amyloid fibrils are a type of protein aggregates that are associated with both diseases (Alzheimer's, Parkinson's and type 2 diabetes) and biological functions (folding and reservoir). Amyloids feature a common cross beta spine but they are very diverse in overall structure [1]. The dry interface has a particular interest; they are thought to be a main driving force behind the amyloid formation. These interfaces have been studied with smaller peptide sequence models that are still capable of self-assembly. In the last 15 years since the description of the 8 main amyloid classes [2], 180 peptide structures have been deposited in the PDB. In this review we summarize the characteristics of the known structures and analyze them for 3D classification. For assessing their interfaces we utilize novel metrics together with existing ones. Using these tools of structural characteristics of amyloid structures and their protein counterparts are compared.
The project was supported grants VEKOP-2.3.2-16-2017-00014, and VEKOP-2.3.3-15-2017-00018 by the European Union and the State of Hungary, co-financed by the European Regional Development Fund.

References
[1] Horváth, D; Menyhárd K., D. and Perczel, A. Protein Aggregation in a Nutshell: The Splendid Molecular Architecture of the Dreaded Amyloid Fibrils. Current Protein & Peptide Science, 20(11) (2019).
[2] Sawaya, M., Sambashivan, S., Nelson, R. et al. Atomic structures of amyloid cross-β spines reveal varied steric zippers. Nature 447, 453–457 (2007).

Back to Table of contents

MS11 Opportunities from combining structural biology and fold prediction

MS11-2-1 High-accuracy protein structure models in AlphaFold DB
#MS11-2-1

M. Varadi [1], M. Deshpande [1], S. Nair [1], S. Anyango [1], D. Bertoni [1], S. Velankar [1]
[1]EMBL-EBI - Hinxton (United Kingdom)

Abstract
Proteins are essential macromolecules with vital biological functions. They are involved in a wide range of research activities and medical and biotechnological applications, from fighting infectious diseases to tackling environmental pollution. Knowledge of the three-dimensional (3D) arrangement of the atoms of a protein can provide essential clues to understanding the roles and mechanisms underpinning protein functions. However, while the Universal Protein Resource (UniProt) archives almost 230 million unique protein sequences, the Protein Data Bank (PDB) holds only over 190,000 3D structures (178,000 based on X-ray diffraction) for over 58,000 distinct proteins, thus severely limiting the use of structural information to support biomolecular research globally [1, 2].
One way to attempt to decrease this gap is to predict the structures of millions of proteins. Increasingly, researchers deploy Artificial Intelligence (AI) techniques to predict a protein's structure computationally from its amino-acid sequence alone [3, 4].
AlphaFold DB is an openly accessible, extensive database of high-accuracy protein-structure predictions [5]. Powered by AlphaFold v2.0 of DeepMind, it has enabled an unprecedented expansion of the structural coverage of the known protein-sequence space. While the AlphaFold AI system has certain limitations, especially in terms of modelling complexes, high accuracy models are helpful even in determining the crystal structure of more complex target proteins. AlphaFold DB provides programmatic access to and interactive visualisation of predicted atomic coordinates, per-residue and pairwise model-confidence estimates and indicated aligned errors. The current version of AlphaFold contains approximately 1 million predicted structures across 37 model-organism proteomes, with significant increases expected in terms of the data size sets.

References
[1] UniProt: the universal protein knowledgebase in 2021; UniProt Consortium; Nucleic Acids Res.; 2021 Jan 8;49(D1):D480-D489[2] PDBe: improved findability of macromolecular structure data in the PDB; Armstrong D. et al; Nucleic Acids Res.; 2020 Jan 8;48(D1):D335-D343[3] Highly accurate protein structure prediction with AlphaFold; Jumper J. et al; Nature; 2021 Aug;596(7873):583-589[4] Accurate prediction of protein structures and interactions using a three-track neural network; Baek M. et al; Science; 2021 Aug 20;373(6557):871-876[5] AlphaFold Protein Structure Database: massively expanding the structural coverage of protein-sequence space with high-accuracy models; Varadi M. et al; Nucleic Acids Res.; 2022 Jan 7;50(D1):D439-D444

Back to Table of contents

MS11 Opportunities from combining structural biology and fold prediction

MS11-2-2 C-type lectin-(like) fold interaction patterns in protein:protein complex formation #MS11-2-2

T. Skalova [1], J. Dohnalek [1]
[1]Institute of Biotechnology,Czech Academy of Sciences - Vestec (Czech Republic)

Abstract
C-type lectins are carbohydrate-binding proteins which utilize calcium for the carbohydrate binding. The fold typically consists of two α-helices, two small β-sheets and a long surface loop, with two or three disulfide bridges. C-type lectin-like (CTL) proteins are proteins of the same fold, not necessarily containing calcium or binding carbohydrates, with miscellaneous functions in organisms and often forming protein:protein complexes. Recently, we have solved the structure of a CTL:CTL complex, human natural killer cell receptor NKR-P1 in complex with its ligand LLT1 ([1], PDB code 5MGT). This opened for us the question of general principles of CTL:protein complex formation.
In order to get a more complex view, the PDB database has been scanned and 77 structurally known CTL:protein complexes have been found [2]. There are complexes of CTL snake venom proteins, NK receptor complexes, complexes with immunoglobulin, intimin:TIR complexes, complexes of Epstein-Barr virus gp42 glycoprotein, lectican:tenascin complex and complex of artificial binder, TNFalpha antagonist. Moreover, CTL proteins often act as homodimers (NK receptors) or heterodimers (snake venom proteins, NK receptors, SPL-1 protein). To compare the mutual positions of binding partners in the complexes, all CTL partners were superimposed to selected CTL protein, CD69 (PDB code 3HUP). Complex-forming residues were denoted by color on the surface of CD69.
It was found that CTL:protein binding varies in its form and strength, from picomolar to milimolar K_D and with various interaction interfaces. In projection to CD69, nearly all surface is covered by contact residues in CTL:protein complexes (heterodimers included). When heterodimeric contacts are excluded, still a large part of the surface is covered. However, when the frequency of residue usage in interactions is highlighted, “canonical” binding clearly predominates (Fig. 1).
This work was supported by the Czech Science Foundation (18-10687S), by the ERDF fund (CZ.02.1.01/0.0/0.0/16_013/0001776 and CZ.02.1.01/0.0/0.0/15_003/0000447), and by the Czech Academy of Sciences (86652036).

References
[1] Blaha, J., Skalova, T., Kalouskova, B., Skorepa, O., Cmunt, D., Pazicky, S., Polachova, E.,
Abreu, C., Stranský, J., Koval, T., Duskova, J., Zhao, Y., Harlos, K., Hasek, J., Dohnalek, J., Vanek, O., 2021. Crystal structure of the human NKR-P1 bound to its lymphocyte ligand LLT1 reveals receptor clustering in the immune synapse (preprint). bioRxiv 2021.06.16.448687. https://doi.org/10.1101/2021.06.16.448687.
[2] Dohnalek, J., Skalova, T. C-type lectin-(like) fold – Protein-protein interaction patterns and utilization, Biotechnology Advances, in press, https://doi.org/10.1016/j.biotechadv.2022.107944

Interactions mapped on CD69. Taken from [2].

Back to Table of contents

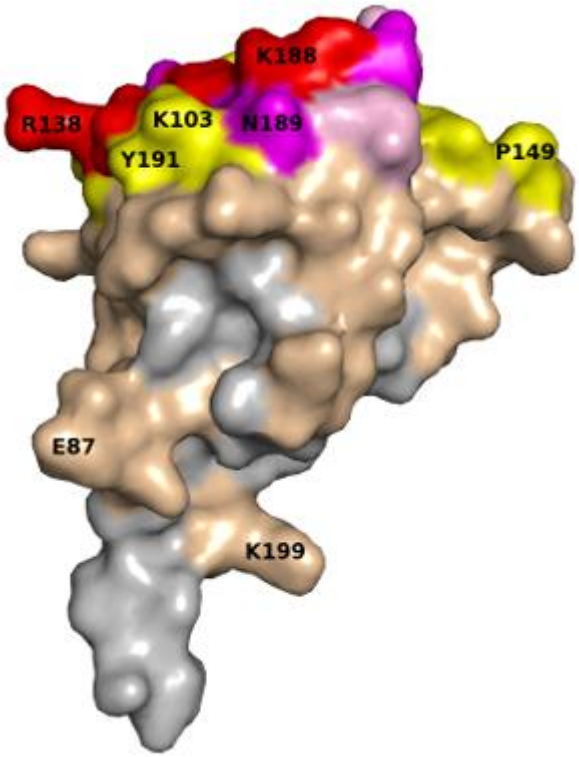

Back to Table of contents

MS13 Structural Characterization of Functional Materials

MS13-1-1 Structure-properties correlation in metal halide perovskites containing diammonium cations #MS13-1-1

M. Morana [1], R. Chiara [1], L. Malavasi [1]
[1]University of Pavia - Pavia (Italy)

Abstract
Metal halide perovskites (MHPs) are materials of great interest that have been proposed for manifold applications. However, the classic perovskite structure, corresponding to the ABX3 formula (where A = small cation, B = metal and X = halide) shows a low stability to air and humidity limiting the actual application. On the other hand, layered perovskites, whose structure is made of alternating layers of organic cations and metal-halide octahedra, are gaining the spotlight thanks to their improved stability. Two main structure types are commonly formed Ruddlesden–Popper (RP) or Dion–Jacobson (DJ) perovskites. The former is characterized by staggered perovskite layers, whereas in DJ perovskites the layers are eclipsed, i.e. stacked without relative displacement [1]. In particular, ditopic ligands such as diammonium cations usually give DJ perovskites with formula A′An–1BnX3n+1 where A′ and A are organic cations, and n represents the number of inorganic layers. Correlating structural distortions and optical properties in layered perovskites is of key importance to modulate their properties and design novel and optimized materials. Thanks to the vast work performed on perovskites including monoammonium cations, well-defined parameters, such as the B-X bond distance and the B-X-B angle, have been defined and a careful materials design is now possible [2]. On the other hand, such kind of correlation is still partially missing on perovskites including a diammonium cations. In order to further enlarge the family of layered perovskites containing diammonium cations, a systematic and rationale investigation was performed, in particular the four diammonium cations represented in Figure 1 namely 1,3-phenylenediammonium (1,3-PDA), 1,3-xylylenediamimonium (1,3-XDA), 1,4-phenylenediammonium (1,4-PDA), and 1,4-xylylenediamimonium (1,4-XDA). We also explored the effect of different halides characterizing the structures and properties of Pb-Br and Pb-Cl layered perovskites. The structural data obtained from single-crystal XRD have been coupled to optical spectroscopy (absorbance and photoluminescence) investigation, allowing to highlight peculiar behaviors templated by the nature of the diammonium cation, such as broadband or narrowband emission.

References
[1] Huang, P.; Kazim, S.; Wang, M.; Ahmad, S. Toward Phase Stability: Dion-Jacobson Layered Perovskite for Solar Cells. ACS Energy Lett. 2019, 4, 2960– 2974, DOI: 10.1021/acsenergylett.9b02063

[2] Li, X.; Hoffman, J. M.; Kanatzidis, M. G. The 2D Halide Perovskite Rulebook: How the Spacer Influences Everything from the Structure to Optoelectronic Device Efficiency. Chem. Rev. 2021, 121 (4), 2230–2291. https://doi.org/10.1021/acs.chemrev.0c01006.

Starting diamines used for the synthesis

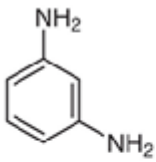

1,3-phenylenediammonium (1,3-PDA)

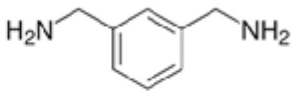

1,3-xylylenediamimonium (1,3-XDA)

1,4-phenylenediammonium (1,4-PDA)

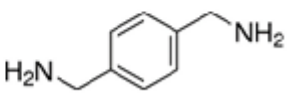

1,4-xylylenediamimonium (1,4-XDA)

Back to Table of contents

MS13 Structural Characterization of Functional Materials

MS13-1-10 Structure of Tetragonal Tungsten Bronze Materials by X-ray Diffraction and Electron Techniques #MS13-1-10

J. Tidey [1], A. Sanchez [1], M. Senn [1], R. Beanland [1]
[1]University of Warwick - Coventry (United Kingdom)

Abstract
Doped tetragonal tungsten bronze (TTB) materials based upon the filling of niobium-IV oxide sublattices with alkali and alkaline earth metals are receiving increasing interest for their ferroelectric and ferrorelaxor properties. Key to the development of improved materials is a firm understanding of the structure-property relationships, yet in many cases the results of structural assessments prove controversial. Of note for the present report is that of Sr2NaNb5O15 (SNN) which is reported in the literature (García-González *et al.*, 2007) as crystallising with space group *Im*2*a* in cell setting [2 -2 0][2 2 0][0 0 2] with respect to the *P*4*mbm* aristotype. However, this is clearly at odds with the understanding of *c*-axis polarisation in these materials (Olsen *et al.*, 2016), and a recent group theoretical study (Whittle *et al.*, 2021) suggests a structure in space group *Ama*2 and the supercell [1 -1 0][2 2 0][0 0 2] be most probable. We employ X-ray diffraction and electron techniques (Figure 1) to experimentally identify the principal structure of SNN and related materials, identifying an incommensurate phase that approximates the theoretically deduced *Ama*2 structure.

Figure 1. (a) Dark field image and (b,c) selected area diffraction patterns of different twin domains at the indicated areas of a crystallite of SNN oriented along [1 1 0]. Imaging in (a) employs a diffracted beam at *l*=0.5 where arrows in (b) and (c) show reciprocal lattice vectors with respect to the aristotype cell. Note the differing systematic absences between (b) and (c), apparent in the zero (ZOLZ) and first-order (FOLZ) Laue zones.

References
García-González, E., Torres-Pardo, A., Jiménez, R. & González-Calbert, J. M. Chem. Mater. (2007) 19, 3575-3580.
Olsen, G. H., Aschauer, U., Spaldin, N. A., Selbach, S. M. & Grande, T. Phys. Rev. B (2016), 93, 18010(R).
Whittle, T. A., Howard, C. J. & Schmid, S. Acta Cryst. (2021) B77, 981-985.

Figure 1.

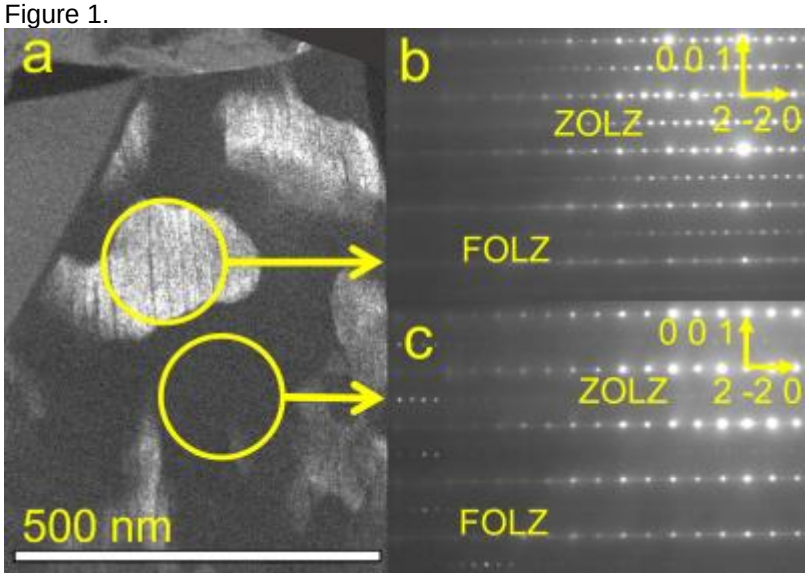

Back to Table of contents

MS13 Structural Characterization of Functional Materials

MS13-1-11 Symmetry, Structural and Electronic Correlations in a Family of Bismuth-based Layered Materials #MS13-1-11

E. Carrillo-Aravena [1], A. Consiglio [2], J. Heßdörfer [3], R. Friedrich [3], D. Di Sante [4], M. Ruck [5]
[1]Faculty of Chemistry and Food Chemistry, Technische Universität Dresden and Würzburg-Dresden Cluster of Excellence ct.qmat - Dresden (Germany), [2]Institut für Theoretische Physik und Astrophysik, Universität Würzburg and Würzburg-Dresden Cluster of Excellence ct.qmat - Würzburg (Germany), [3]Experimentelle Physik VII, Universität Würzburg and Würzburg-Dresden Cluster of Excellence ct.qmat - Würzburg (Germany), [4]Center for Computational Quantum Physics, Flatiron Institute - New York (USA), Institut für Theoretische Physik und Astrophysik, Universität Würzburg and Würzburg-Dresden Cluster of Excellence ct.qmat - Würzburg (Germany), [5]Faculty of Chemistry and Food Chemistry, Technische Universität Dresden, Max Planck Institute for Chemical Physics of Solids and Würzburg-Dresden Cluster of Excellence ct.qmat - Dresden (Germany)

Abstract
Topological insulators (TIs) are semiconductors with protected electronic surface states that allow dissipation-free transport. They are proposed as ideal materials for spintronics and quantum computing.
The first verified 3D weak TI, $Bi_{12}Rh_3I_9$[1-5], consists of two types of alternating charged layers. The anionic layer of edge-sharing $[Bi_2I_8]^{2-}$ octahedra and the topological non-trivial layer $[Bi_{12}Rh_3I]^{2+}$ (**Figure 1**). The latter determines the electronic states with inverted parity around the Fermi level and consists of a net of edge-sharing Rh-centered Bi cubes forming a prismatic rhombitrihexagonal honeycomb lattice, with an iodide ion at the center of each hexagonal prism.
The TI layer has been observed in the structurally similar, but topologically trivial compounds $Bi_{13}Pt_3I_7$[6,7] and $Bi_{12}Pt_3I_5$[7] that contain a different spacer, stacking sequence and electron count. Therefore, it was found that the anionic spacer played a decisive role in defining whether the topological properties of the material would be trivial or not.
Herewith, we present the structure and properties in a series of layered materials derived from those mentioned above: $Bi_{12}Rh_3Cu_2I_5$(**1**)[8] (**Figure 2**), $Bi_{12}Rh_3Ag_2I_5$(**2**), $Bi_{12}Pt_3CuI_5$(**3**), $Bi_{12}Pt_3AgI$(**4**) and $Bi_{12}Rh_3Ag_6I_9$(**5**). For those compounds, the TI layer is left unchanged, while the spacer layer is substituted for studying its impact on the topological properties. Full-relativistic DFT studies in conjunction with ARPES have shown a relationship between the size of the bulk bandgap and the thickness and chemical nature of the spacer layers. Structural characterization of these materials is challenging not only because of stacking faults — intrinsic to their layered structure — but also atomic disorder within the spacer layers. Furthermore, twinning by pseudo-merohedry is common for **1**, **2**, **3** and **4**, all of which share highly specialized metrics close to a hexagonal cell, but orthorhombic or monoclinic space groups.

References
[1] B. Rasche, A. Isaeva, A. Gerisch, M. Kaiser, W. Van den Broek, C. T. Koch, U. Kaiser, M. Ruck, *Chem. Mater*. **2013**, *25*, 2359–2364.
[2] B. Rasche, A. Isaeva, M. Ruck, M. Richter, K. Koepernik, J. van den Brink, *Sci. Rep*. **2016**, *6*, 20645.
[3] C. Pauly, B. Rasche, K. Koepernik, M. Liebmann, M. Pratzer, M. Richter, J. Kellner, M. Eschbach, B. Kaufmann, L. Plucinski, C. M. Schneider, M. Ruck, J. van den Brink, M. Morgenstern, *Nat. Phys*. **2015**, *11*, 338–343.
[4] C. Pauly, B. Rasche, K. Koepernik, M. Richter, S. Borisenko, M. Liebmann, M. Ruck, J. van den Brink, M. Morgenstern, *ACS Nano* **2016**, *10*, 3995– 4003.
[5] B. Rasche, A. Isaeva, M. Ruck, S. Borisenko, V. Zabolotnyy, B. Büchner, K. Koepernik, C. Ortix, M. Richter, J. van den Brink, *Nat. Mater*. **2013**, *12*, 422–425;
[6] M. Ruck, *Z. Anorg. Allg. Chem*. **1997**, *623*, 1535–1541.
[7] M. Kaiser, B. Rasche, A. Isaeva, M. Ruck, *Chem. Eur. J*. **2014**, *20*, 17152–17160.
[8] E. Carrillo-Aravena, K. Finzel, R. Ray, M. Richter, T. Heider, I. Cojocariu, D. Baranowski, V. Feyer, L. Plucinski, M. Gruschwitz, C. Tegenkamp, M. Ruck, *Phys. Status Solidi B* **2022**, 2100447.

Figure 1: TI layer $[Bi_{12}M_3I]^{x+}$ (M = Rh, Pt), overlaid with its layer group symmetry *p*6/*mmm*.
Figure 2: Crystal structure of the 3D weak TI $Bi_{12}Rh_3Cu_2I_5$. It consists of TI layers $[Bi_{12}Rh_3I]^{2+}$ separated by topologically trivial ic

Figure 1

Back to Table of contents

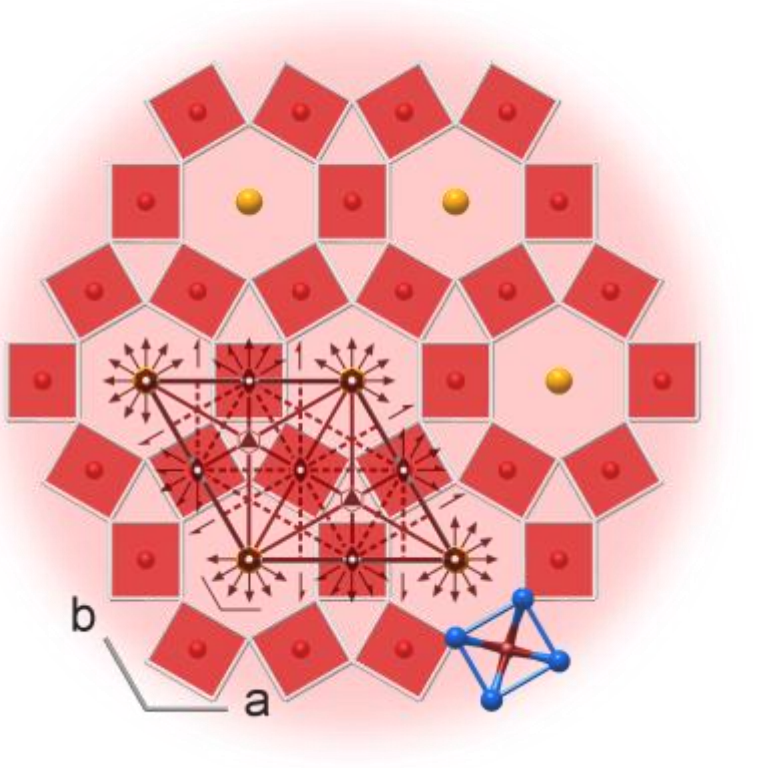

Figure 2

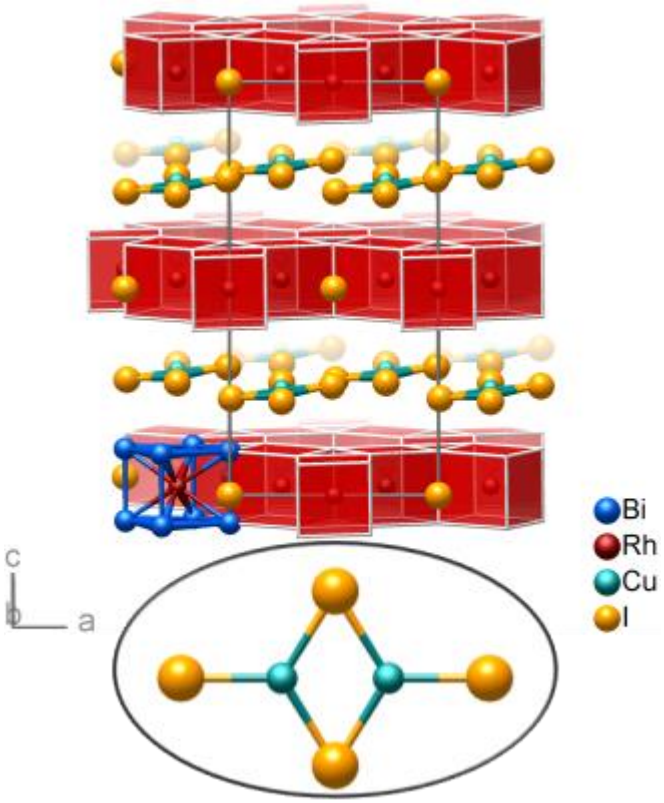

Back to Table of contents

MS13 Structural Characterization of Functional Materials

MS13-1-12 Comparative characterization of two new SiO2–CaO–P2O5 bioactive glasses #MS13-1-12

A. Ghneim [1], V. Legrand [1], C. Carteret [1], D. Schaniel [1], E.E. Bendeif [1]
[1]université de lorraine

Abstract
In the course of the last years, the emergence of a new generation of mesoporous bioactive glasses (MBGs) opened a wide range of new potential applications such as drug and gene deliveries [1], DNA vaccination or cellular treatment. These new MBGs are also used as implants in the human body for bone regenerative purposes due to their high biocompatibility and high reactivity with the human physiological medium. When exposed to physiological fluids, MBGs develop a layer of crystalline bone-like carbonate calcium phosphate [Hydroxy-Carbonate Apatite, HCA: Ca10(PO4) 6 (OH) 2 (HA)] on their surface shortly after interaction [2-4], thus promoting fast integration of the implant with the host tissue. layer which provides direct bonding with the host tissue. Therefore, the glass bioactivity is usually evaluated by measuring the rate of HCA formation at the bioglasses surface on its exposure either to body fluids in vivo or to a simulated body fluid (SBF) in vitro. The internal porosity of these materials further allows for progressive colonization of the tissues, ensures the vascularization and free circulation of cells, body fluids and nutriments. In order to understand the various steps in the formation of HCA after immersion of the bioactive glass in the physiological liquid, starting from the interaction of water molecules with the pore wall species to the formation of nanoparticles and finally layers of crystalline HCA, we propose to study the structural organization during this evolution and hence derive the key parameter influencing the bioactivity. That way, we conducted a comparative study on two new bioactive glass 70S30C (70% SiO2, 30% CaO (mol. %)) and 58S (60% SiO2, 36% CaO, 4% P2O5 (mol.%)) prepared by appropriate Sol-Gel process [3]. We will present in this study the different results obtained and in particular the evaluation of their bioactivity after immersion in in a simulated body fluid (SBF) for different interaction time (immersion time: 1d, 2d, 3d and 7 days).

References
(1) A. El-Fiqi, T.-H. Kim, M. Kim, M. Eltohamy, J.-E. Won, E.-J. Lee and H.-W. Kim, Nanoscale,2012, 4, 7475–7488.
(2) L. L, Hench. Journal of Materials Science: Materials in Medicine, 2006, 17(11), 967
(3) X. Yan, C. Yu, X. Zhou, J. Tang and D. Zhao, Angewandte Chemie International Edition, 2004,43, 5980–5984.
(4) I. Cacciotti, M. Lombardi, A. Bianco, A. Ravaglioli and L. Montanaro, Journal of MaterialsScience: Materials in Medicine, 2012, 23, 1849–1866.

Figure 1 Image that shows the full process of the

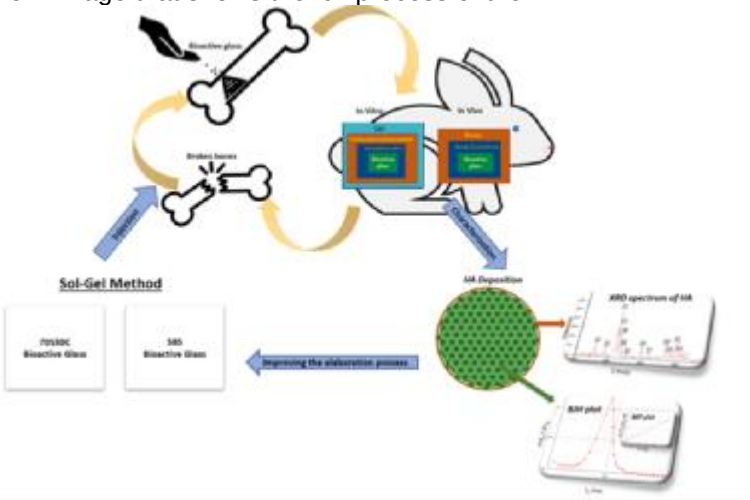

Back to Table of contents

MS13 Structural Characterization of Functional Materials

MS13-1-13 X-ray Diffraction and Diffusion Measurement Facility of the Institut Jean Barriol
#MS13-1-13

E. Wenger [1], P. Durand [1], Y. Vuillemard [1], A. Defez [1], C. Palin [1], V. Richalet [1], E.E. Bendeif [1]
[1]CRM2, Université de Lorraine, CNRS - Vandoeuves-les Nancy (France)

Abstract
The PMD²X (Plateforme de Mesures de Diffraction et de Diffusions des Rayons X) of the Institut Jean Barriol (FR 2843) [1-2] offers a first-class diffractometry service, both nationally and internationally. It was evaluated and certified in 2020 by the INFRA⁺ Lorraine University of Excellence quality programme to obtain the status of Structure d'Appui à la Recherche (StAR). Located in Vandoeuvre-lès-Nancy at the CRM2 laboratory (UMR UL-CNRS 7036), on which it relies instrumentally and methodologically, it provides the entire scientific community and industrial partners with analysis and characterization approaches appropriate for different types of functional materials (organic, inorganic, nanomaterials, etc.).

Equipped with a wide range and original devices allowing samples to be placed in non-ambient conditions, it allows:
- Measurements under extreme conditions (temperature, pressure, electric field, laser excitation, controlled humidity, gas flow, etc.)
- Phases identification and quantification from the structural parameters measured by X-ray diffraction
- Studies of phase transitions (coupled with DSC measurements)
- Nanoparticle and crystal domain sizes
- Interatomic bond lengths
- Molecular conformation
- Crystal packing
- High resolution crystallography and electron density modelling
- Energy calculations of inter-molecular interactions and electrostatic properties
- Analysis temperatures from 5 K to 720 K (-268°C to 450°C)

Single crystal studies: PMD²X performs on-demand and in routine, structure resolutions of small molecules. It provides crystallographic and structural information on your compounds (figures, CIF files, interatomic distances and angles)
- Crystal size = 50 to 200 µm (Recrystallisation possible)
- Temperature from 5K to 500K (by nitrogen or helium jet)
- X-ray sources available: Copper, Molybdenum, Silver.
- 4 circle goniometers and CCD detector, Bruker CMOS Photon III.

Powder studies:
- Reflection and transmission measurements.
- X-ray sources available: Copper Kalpha1 and Molybdenum.
- Identification and quantification of crystalline phases
- Monitoring of phase transitions (temperature: 11 K to 720 K)
- Analysis of mesoporous structures
- Characterization of nanomaterials, nanoparticles and confined liquids with the pair distribution function (PDF) method.

- PMD²X develops partnerships with large facilities (Synchrotrons) both through its involvement in the RECIPROCS network but also through new collaborative projects.
- The PMD²X platform is also strongly involved in the promotion of crystallography in Africa through the IUCr-UNESCO Open-Labs and the new Remote-Lab projects. These actions are also associated with hosting and training of young African researchers.

References
[1] www.crystallography.fr
[2] http://crm2.univ-lorraine.fr/lab/fr/services/pmd2x/

Examples of crystallographic analysis possibities

Back to Table of contents

MS13 Structural Characterization of Functional Materials

MS13-1-14 Synthesis of α-MoO3 nanofibers for enhanced field-emission properties
#MS13-1-14

S.K.S. Patel [1]
[1]Department of Chemistry, MMV, Banaras Hindu University - Varanasi-221005 (India)

Abstract
One-dimensional α-MoO_3 nanofibers of 280–320 nm diameters were synthesized by a hydrothermal method. The morphologies and compositions of as-synthesized α-MoO_3 nanofibers have been characterized by X-ray powder diffraction, Raman spectroscopy, and field-emission scanning electron microscopy. X-ray photoelectron spectroscopy showed the predominantly 6+ oxidation state with a small percentage of reduced δ+ (5 < δ < 6) oxidation state. The field-emission properties of α-MoO_3 nanofibers show a lower turn-on electric field of 2.48 V μm^{-1} and threshold electric field of 3.10 V μm^{-1}. The results suggest that the α-MoO_3 nanofibers are promising candidate for efficient and high performance field-emission devices.

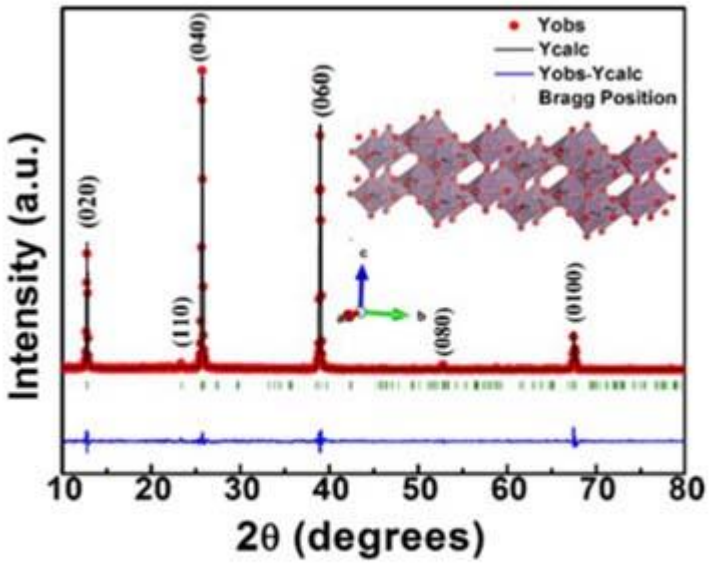

Fig. 1. Rietveld analysis of XRD data using orthorhombic structure with space group Pbnm of α-MoO_3 nanofibers and the insert shows the unit cell crystal structure.

Back to Table of contents

MS13 Structural Characterization of Functional Materials

MS13-1-15 3D ED of hybrid perovskites
#MS13-1-15

M. Gemmi [1], I. Andrusenko [1], D. Marchetti [1], A. Latini [2], M. Arciniegas [3]
[1]Electron Crystallography, Istituto Italiano di Tecnologia - Pontedera (Italy), [2]Dipartimento di Chimica, Sapienza Università di Roma - Roma (Italy), [3]NanoChemistry, Istituto Italiano di Tecnologia - Genova (Italy)

Abstract
Hybrid perovskites are a new class of materials that have raised a remarkable interest due to their promising properties for a variety of applications beyond photovoltaics. In particular, metal-halide organic-inorganic perovskites have been recognized as promising semiconductors with tunable optoelectronic properties, which make them excellent candidates for applications in chiroptics, spintronic, photodetectors, and light emitting devices. Often these structures cannot be crystallized in well-ordered and sufficiently large crystals to be studied by single crystal x-ray diffraction (XRD) and 3D electron diffraction (3D ED) becomes a valuable option. Unfortunately, they suffer from beam irradiation in part due to their intrinsic intercalated architecture of inorganic and organic layers, so that their TEM analysis is extremely challenging. Here we present two case studies of unknown metal halide perovskites whose structure is determined using 3D ED in low dose mode, avoiding excessive beam damage. The first structure is a 1D lead iodide hybrid perovskite where the inorganic part forms octahedral chains intercalated by a polycyclic aromatic hydrocarbon molecule with ethynyl pyridinium wings. The molecules are packed by π - π interaction. The inorganic part has been determined ab-initio with direct methods, while the location and the configuration of the organic molecule was derived using simulated annealing. The second type of structures are lead bromide hybrid perovskites where the organic part is made either by benzylamine (BZA) or thiophenemethylamine (TMA). These compounds crystallize in the sub-micrometer range, making standard crystallographic investigations for structure solution very difficult. Moreover, their structure analysis is complicated by twinning at the nanoscale. Also, the inorganic layer of both structures can be determined ab-initio, while the organic part cannot be found. We found that the TMA-based crystal is a 2D layered perovskite with the form TMA2PbBr4, while the BZA-based one is a 1D perovskite with the PbBr6 octahedra arranged in ribbons. We expect to locate the molecules in both cases using simulated annealing on powder XRD data. These results showcase how to implement 3D ED on complex hybrid structures, providing insight on their arrangement at the nanoscale that cannot be directly studied by X-ray diffraction analysis.

Back to Table of contents

MS13 Structural Characterization of Functional Materials

MS13-1-16 Tuning the colours with one luminescent host: Nitrides as promising phosphors
#MS13-1-16

C. Braun [1]
[1]KIT Karlsruhe - Eggenstein-Leopoldshafen (Germany)

Abstract
Tuning the colours with one luminescent host: Nitrides as promising phosphors
Phosphor-converted white light-emitting diodes (pc-LEDs) are emerging as an indispensable solid-state light source for the next generation lighting industry and display systems due to their unique properties.
Gallium nitride (GaN) is a key material when it comes to light-emitting diodes (LEDs) and has pushed the LED revolution in lighting and displays, triggered by the investigations of Nakamura and coworkers, being awarded the Nobel prize in 2014. The concept of down-conversion of a GaN-based blue LED offers the possibility to provide efficient generation of monochromatic, high-color purity light resulting in a highly efficient warm-white all-nitride phosphor-converted light emitting diode (pc-LED). To cover the colour range from blue, over green and orange to red (ca. 450 to 650 nm), a combination of InGaN und AlGa(In)P is necessary nowadays.
Several challenges have to be addressed here. The decrease of the external quantum efficiency versus emission wavelength around 560 nm, is termed the “yellow gap". The immiscibility of GaN and InN leads to a reduction in performance of InGaN-based LEDs with higher InN mole fractions. The lattice mismatch between GaN, InN, GaAlN, AlGaP, different thermal expansion coefficients and the variations of the In/Al content decrease the luminescence performance tremendously.
Nitrides and nitridosilicates with their wide-ranging applicability represent an essential component in industrial and materials applications due to their intriguing structural diversity, their auspicious chemical and physical properties. In particular, Eu^{2+}-doped (oxo)nitridosilicates and SiAlONs have been amply studied as important host lattices for phosphor-converted light-emitting diodes (pc-LEDs).
Here we demonstrate the doping of bulk GaN with europium, terbium and the combination of both and the successful adsorption of Eu and Tb at the grain boundaries of bulk β-Si_3N_4 and β-Ge_3N_4 as novel and promising components of the illustrious pc-LED family.
This colour tuning proves that one luminescence host can provide three colours (red, green and orange) and that even the so called “yellow gap” could be closed with a III-nitride. The green luminescence of GaN:Tb, Tb-β-Si_3N_4 and Tb-β-Ge_3N_4 demonstrates impressively that green emitting phosphors can be also achieved with purely nitridic compounds and not only with oxynitrides (e.g., β-SiAlON:Eu^{2+}) or oxonitridosilicates (e.g., $SrSi_2O_2N_2$:Eu^{2+}) as it was up to now.
By using one material for all colours, it will be possible to overcome technical challenges in building up LED devices, which will open up new capabilities for modern highly efficient phosphors.

Back to Table of contents

MS13 Structural Characterization of Functional Materials

MS13-1-17 New high-entropy oxides in a mullite-type structure
#MS13-1-17

A. Kirsch [1], N. Lefeld [2], J.K. Mathiesen [1], S.L. Skjærvø [1], E.D. Bøjesen [3], D. Sheptyakov [4], K.M.Ø Jensen [1]
[1]University of Copenhagen - Copenhagen (Denmark), [2]University of Bremen - Bremen (Germany), [3]Aarhus University - Aarhus (Denmark), [4]Paul Scherrer Institute - Villigen (Switzerland)

Abstract
Engineering compositional disorder into materials have attracted immense interest since the introduction of the high-entropy concept in 2004 [1]. High-entropy materials represent a class of compounds containing a high number of metal cations in ca. equal amounts statistically mixed in a single-phase solid solution. Only in 2015, the first high-entropy oxide (HEO) was synthesized [2]. Until now, it has been assumed that they crystallize in simple crystal structures [3] and mainly HEOs in a rock-salt, fluorite, spinel, perovskite and pyrochlore structure have been reported.
Yet, with this study we demonstrate the feasibility to synthesize HEOs possessing a complex connectivity of polyhedral units in a mullite-type structure (Figure 1). The parent compounds $Bi_2M_4O_9$ (M = Al^{3+}, Ga^{3+} and Fe^{3+}) and $REMn_4O_{10}$ (RE = rare earth elements, Y and Bi) show a variety of attractive properties including multiferroicity. To map out the synthesizability in this system, we produced 5 HEOs with compositions of $Bi_2(Al_{0.25}Ga_{0.25}Fe_{0.25}Mn_{0.25})_4O_9$, $(Eu_{0.2}HE)_2Mn_4O_{10}$ (HE = $Nd_{0.2}Sm_{0.2}Y_{0.2}Bi_{0.2}$), $(Er_{0.2}HE)_2Mn_4O_{10}$, $(Ce_{0.2}HE)_2Mn_4O_{10}$ and $(Nd_{0.2}Sm_{0.2}Y_{0.2}Er_{0.2}Eu_{0.2})_2Mn_4O_{10}$. We show that the materials represent statistically mixed solid solutions using a combination of neutron and X-ray powder diffraction (XRD) with subsequent Rietveld analysis, X-ray total scattering and Pair Distribution Function analysis, transmission electron microscopy, infrared and Raman spectroscopy. In addition, we follow their formation in situ by XRD. Surprisingly, all of them directly form out of an amorphous precursor without the formation of any other binary or ternary oxides.
On one hand, the targeted introduction of disorder into such a complex host lattice offers a great degree of freedom to fine-tune the material's properties. On the other hand, the feasibility to crystallize structurally complex HEOs is intriguing and encourages to search for additional structure-types to extend the landscape of high-entropy materials.

References
[1] Yeh, J.-W. et al. *Adv. Eng. Mater*., 6, 299-303 (2004)
[2] Rost, C. M. et al. *Nat. Commun.*, 6, 8485 (2015)
[3] Witte, R. et al. *Phys. Rev. Mater.* 3, 034406 (2019)

Crystal structures of the parent compounds.

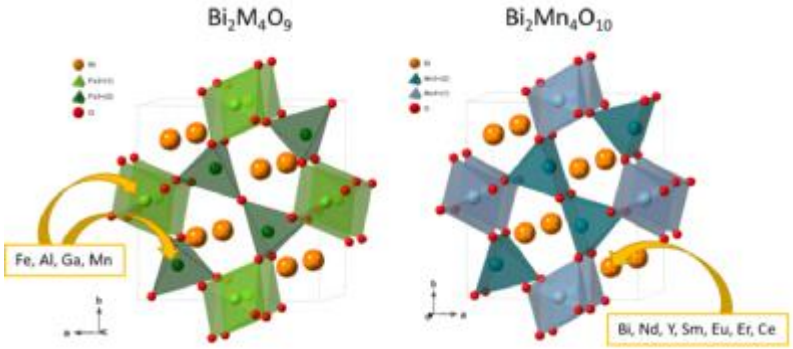

Back to Table of contents

MS13 Structural Characterization of Functional Materials

MS13-1-18 Elucidation of Barocaloric Effect in Spin Crossover Compounds
#MS13-1-18

H. Shahed [1], N. Sharma [1], M. Angst [1], J. Voigt [1], J. Persson [1], H. Gildenast [2], U. Englert [3], D. Chernyshov [4], K. Tornroos [5], A. Grzechnik [6], K. Friese [1]
[1]Jülich Centre for Neutron Science and Peter Grünberg Institute, JARA-FIT, Forschungszentrum Jülich GmbH, 52425 - Jülich (Germany), [2]RWTH Aachen University, Institute of Inorganic Chemistry, 52074 - Aachen (Germany), [3]RWTH Aachen University, Institute of Inorganic Chemistry, 52074 - Aachen (Germany), [4]Swiss-Norwegian Beamlines at the European Synchrotron Radiation Facility, 38000 - Grenoble (France), [5]Department of Chemistry, University of Bergen, Allégaten 41 - Bergen (Norway), [6]RWTH Aachen University, Institute of Crystallography, 52074 - Aachen (Germany)

Abstract
The search for new efficient materials and refrigeration mechanisms is a key challenge to replace the conventional vapor compression technology. An attractive alternative technology uses the caloric refrigeration cycle, which is based on the adiabatic temperature and isothermal entropy change upon tuning an external parameter such as pressure, electric field or magnetic field. Recently, spin crossover (SCO) compounds have been recognized as promising candidates, which exhibit large barocaloric effects: large isothermal entropy changes have been reported for some of these SCO compounds at fairly low hydrostatic pressures (< 1.2 GPa) [1]. In SCO complexes the central metal ion switches between a low spin (LS) state at low temperature / high pressure and a high spin (HS) state at high temperature/low pressure. The LS to HS transition involves an increase of the spin entropy, but a larger part of the entropy change originates from changes in the intramolecular vibrations [2].
In this work, we report on magnetization measurements and temperature dependent single crystal diffraction performed at the BM01 station (SNBL, ESRF) on SCO complexes consisting of Fe^{2+} as a central ion bound to six nitrogen atoms. Our focus is $Fe(PM\text{-}Bia)_2(NCS)_2$, ($FeN_6S_2C_{38}H_{28}$), which crystallizes in two polymorphs depending on the synthesis route. Polymorph A crystallizes orthorhombic (*Pccn*) and undergoes an abrupt spin transition around 175 K. Polymorph B crystallizes monoclinic ($P2_1/c$) and undergoes a gradual spin transition around 210 K [3].
From the structural data, we extracted the temperature dependence of the Fe-N distances (Figure 1). The width of the transition region differs strongly between the two polymorphs. This indicates the importance of intermolecular interactions (e.g. S—C contacts) for the spin transitions in both polymorphs. From the structural data based on the Fe-N distances, the entropy change at the HS-LS transition can be extracted. Our temperature dependent studies provide a good basis for the high pressure experiments on these compounds which are currently being performed by us.

References
[1] K. G. Sandeman, APL Mater., no. 11, pp. 4–9, 2016.
[2] S. P. Vallone et al., Adv. Mater., no. 23, pp. 1–7, 2019
[3] J. F. Létard et al., Monatshefte für Chemie, no. 2, pp. 165–182, 2003.
[4] J. F. Létard et al., Inorg. Chem., no. 17, pp. 4432–4441, 1998.

Fe-N bond lengths as function of temperature.

Back to Table of contents

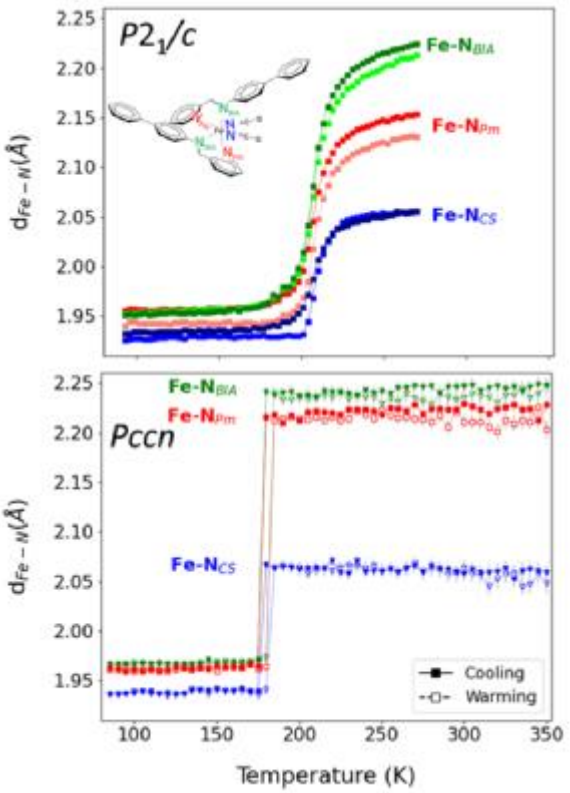

Back to Table of contents

MS13 Structural Characterization of Functional Materials

MS13-1-19 Raman spectroscopy approach to determine crystallographic and molecular orientation of rubrene molecular films
#MS13-1-19

B.A. Paez-Sierra [1]
[1]Physics Department, Universidad Militar Nueva Granada, Campus Nueva Granada - Cajicá (Colombia)

Abstract
Understanding and engineering molecular crystals are of great importance to reach a high performance of molecular-based electronics o biocompatible devices. Rubrene, a tetraphenyl derivative of tetracene, has been recognized to possess high mobility in single-crystal structures. We report ex-situ polarized Raman analysis of rubrene thin films grown by hot-wall epitaxy deposited onto mica substrates. Usually, polarized photons are used to distinguish molecular anisotropy in organic molecules, scaffolds for cell culture, and biological cell growth among other applications. Raman spectroscopy aid to determine both molecular anisotropy and chemical identity of the analyzed species.
We took the advantage of the Raman tensor properties i.e. group symmetry and polarized scattered photons to determine the molecular orientation of rubrene molecules in crystalline films. The Raman measurements were performed by shining the films at 90° with polarized laser light of 784 nm and collecting the Raman light in the backscattering configuration by rotating the in-plane sample at several angles. Since rubrene films exhibit three progressive stages of molecular growth i.e. from an amorphous matrix to spherulites and a final phase of coalescence, it is found that the Raman breathing mode 1003 cm–1 represents the rubrene fingerprint and is independent of the growth stage. Therefore, various internal modes of the phenyl groups were considered to compute the molecular orientation. In order to probe film anisotropy and molecular orientation, each angle was measured at two different polarizations. Thus, a set of Raman tensors was obtained and solved with an iterative “back-and-forth” method to determine the molecular orientation and to determine dipole-dipole interactions within the molecular crystal. Results revealed the advantage of Raman spectroscopy to probe crystallographic properties of molecular solids by using lower energies compared with other techniques.

References
Svenningsson, L., & Nordstierna, L. (2020). Polarized Raman Spectroscopy Strategy for Molecular Orientation of Polymeric Fibers with Raman Tensors Deviating from the Molecular Frame. ACS Applied Polymer Materials, 2(11), 4809–4813. https://doi.org/10.1021/acsapm.0c00762

Back to Table of contents

MS13 Structural Characterization of Functional Materials

MS13-1-2 Study on the crystal structure-antibacterial activity relationship of quaternary ammonium Schiff compounds based on difference in their electrostatic potential
#MS13-1-2

R. Rusev [1], K. Iliev [1], M. Simeonova [1], P. Peneva [1]
[1]Institute of Mineralogy and Crystallography, Bulgarian Academy of Sciences - Sofia (Bulgaria)

Abstract
The quaternary ammonium salts (QAS) are interesting class of N-containing organic compounds possessing wide range of applications derived from their unique structural properties - positively charged nitrogen “head” and lipophilic “tail”. The amphiphilic nature of QAS, together with the facile synthesis route determine their extensive use as surfactants, phase-transfer catalysts, antimicrobial and bactericidal agents etc.
This work is focused on the synthesis, physicochemical characterization and antibacterial properties of novel aromatic quaternary ammonium compounds derivatives of 4-pyridinecarboxaldehyde containing azomethine bridged aromatic fragments (e.g. Schiff bases). The developing of new quaternary ammonium Schiff bases is an expansion of our previous studies on the antibacterial properties of several QAS derivatives of quinoline (QN) and 4-pyrrolidino pyridine (4-PP) against the bacterial strains of *S. aureus*, *E. Coli*, *K. Pneumoniae* and *P. Aeruginosa* [1, 2]. The results from those studies concluded that QN and 4-PP QAS are predominantly active against the Gram positive bacteria – S. Aureus and in addition the antibacterial activity increases significantly with the replacement of the quinoline fragment with 4-pyrrolidino pyridine (Fig. 1a). The detailed analysis of the crystal structures of the studied compounds revealed that the drastic change in the antibacterial effect could be connected to the different properties of the 4-pyrrolidino pyridine and quinoline fragments but also could be related to variances in the electron density distribution in the molecule. Indeed, the calculated electrostatic potential [3] of the inactive/active pair of quaternary ammonium compounds (Fig. 1b) points out towards significant differences in the electron density distribution. One can notice that the molecule of the inactive quinoline derivative is predominantly positively charged whereas the active 4-pyrrolidino pyridine derivative is in the form of dipole.
From these findings it was clear that in order to further enhance the antibacterial effect of the studied QAS and/or to expand the possible bacterial targets, it is important to maintain the separation of the opposite charges in the molecule. Following this logic, new aromatic fragments bearing different functional groups with positive or negative induction effects (I^+ or I^-) were bonded to the main quaternary ammonium molecule via azomethine bridge (Fig. 1c). The electrostatic potential of the obtained quaternary ammonium Schiff compounds was calculated from their respective crystal structures. The synthesized compounds showed increased antibacterial activity towards *S. Aureus* with lower MIC values.
Acknowledgements: This work was supported by the Bulgarian Science Fund (project contract КП-06-М59/7).

References
1. Rusew, R., V. Kurteva, and B. Shivachev, Antibacterial activity of novel quaternary ammonium salts of quinoline and 4-pyrolidino pyridine. Bulg. Chem. Commun. F, 2018. 50: p. 115-125.2. Rusew, R., V. Kurteva, and B. Shivachev, Novel quaternary ammonium derivatives of 4-pyrrolidino pyridine: synthesis, structural, thermal, and antibacterial studies. Crystals, 2020. 10(5): p. 339.3. Spackman, P.R., et al., CrystalExplorer: A program for Hirshfeld surface analysis, visualization and quantitative analysis of molecular crystals. Journal of Applied Crystallography, 2021. 54(3).

Back to Table of contents

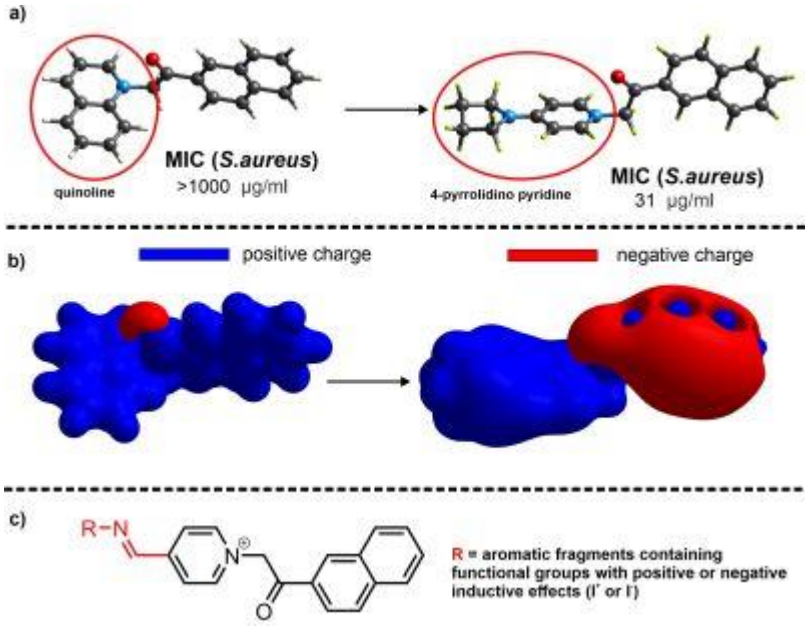

Back to Table of contents

MS13 Structural Characterization of Functional Materials

MS13-1-20 New layered titanate, $NaTi_2O_3(OH)_3$, obtained in hydrothermal environments at gigapascal pressures #MS13-1-20

A. Gordeeva [1], M. Antlauf [2], O. Andersson [2], U. Häussermann [1]
[1]Stockholm University - Stockholm (Sweden), [2]Umeå University - Umeå (Sweden)

Abstract
TiO_2-based materials are widely used in a variety of applications, such as photocatalysis, lithium-ion batteries and etc., due to their peculiar chemical and physical properties[1]. Since Kasuga et. al.[2] for the first time synthesized long uniform titanate nanotubes in hydrothermal conditions the interest in the method and its potential use for the development of titanates with novel morphologies and/or structures has only been increasing. Despite that, only subcritical hydrothermal conditions have been studied, with pressures (p) and temperatures (T) below the critical point (cp) of water (T_{cp} = 374 °C and p_{cp} = 22.1 MPa). In this work we are extending the synthesis to deep supercritical hydrothermal conditions in the range still accessible on industrial scale (T = 25 – 300 °C and p = 0.1 – 3 GPa). Such conditions are known[3] to allow access to kinetically favored phases and new morphologies.
Here we present new sodium hydroxo titanate, $NaTi_2O_3(OH)_3$, obtained by the hydrothermal conversion of amorphous titania and aqueous sodium hydroxide mixture at 1.3 – 1.5 GPa and 170 – 190 °C. Its crystal structure was characterized from powder X-ray and continuous rotational electron diffraction data (space group *C*2/m (No. 12), a = 5.2685(1) Å, b = 9.1256(2) Å, c = 9.4581(4) Å, β = 90.0503(9) °). The monoclinic structure constitutes layers of edge-condensed TiO_6 octahedra, one quarter of which is missing and replaced by basal triangles of NaO_6 octahedra from the adjacent layers. The channel-like layered structure and its stability in strongly acidic and alkaline environments promise a wide use of the novel sodium hydroxo titanate in adsorbent applications, such as the removal of organic molecules and radioactive toxic metal ions from water.

References
1. Zhang Y. et al. RSC Adv., 2015, 5, 79479–79510.
2. Kasuga T. et al. Langmuir, 1998, 14, 3160–3163.
3. Spektor K. et al. Inorg. Chem.I, 2016, 55, 8048−8058.

Structure, SEM and TEM images of the new titanate

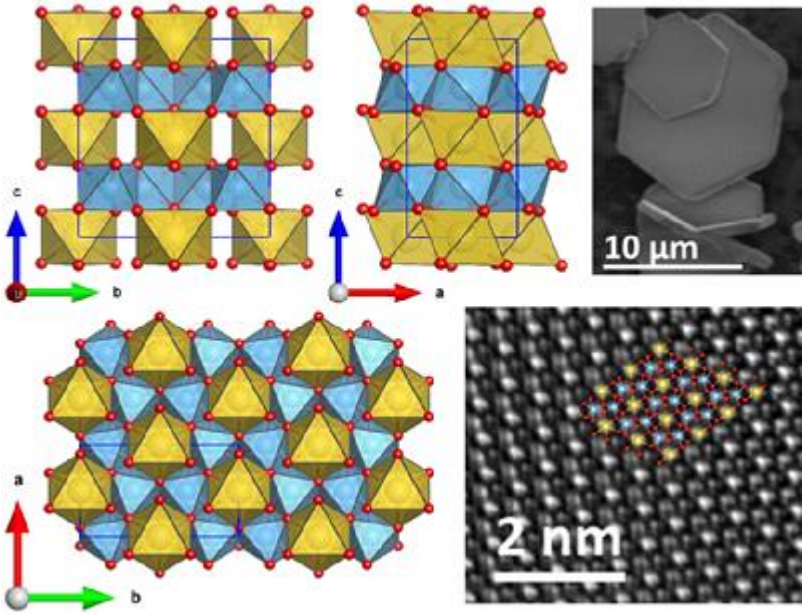

Back to Table of contents

MS13 Structural Characterization of Functional Materials

MS13-1-21 Higly Strained and Reactive Donor/Acceptor-Supported Metalla-Silanone
#MS13-1-21

N. Saffon-Merceron [1], T. Kato [2]
[1]ICT-UAR2599 - Toulouse (France), [2]LHFA - Toulouse (France)

Abstract
A novel stable donor/acceptor-supported Mn(I)-metallasilanone was synthesized and crystallized. The intramolecular silanone-Mn(I) interaction induces a highly strained structure, leading to an exceptionally high reactivity of this compound. Indeed, it readily reacts with several small molecules such as H2 or ethylene gas in mild conditions.

References
Angew. Chem. Int. Ed. 2021, 60, 18489–18493;
J. Chem. Soc. Trans. 1908, 93, 439;
J. Chem. Soc. Trans. 1901, 79, 449;

A new stable Mn(I)-metallasilanone

Molecular structure of Mn(I) metallasilanone

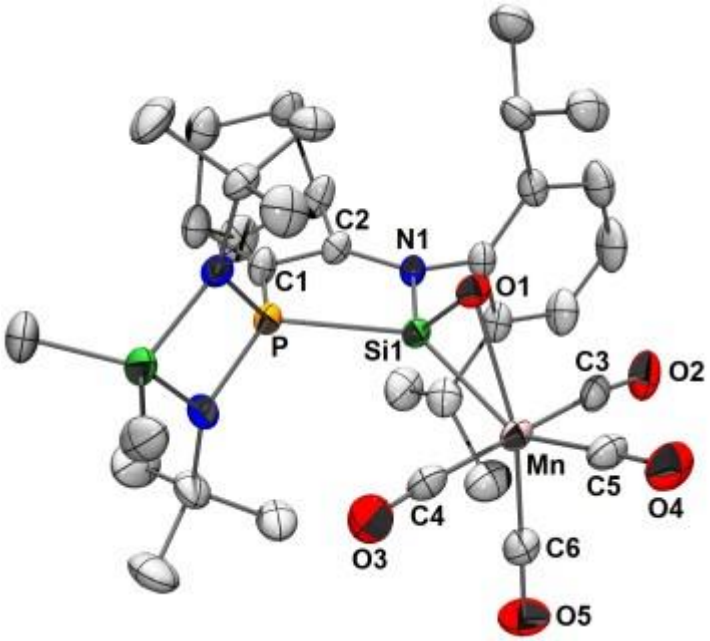

Back to Table of contents

MS13 Structural Characterization of Functional Materials

MS13-1-22 Novel iron fluoride based hybrid materials; Structural characterization, electric, dielectric and magnetic properties
#MS13-1-22

M. S. M. Abdelbaky [1], O. Guesmi [2], A. Moulahi [2], S. Garcia-Granda [1], M. Dammak [2]
[1]University of Oviedo - Oviedo (Spain), [2]University of Sfax - Sfax (Tunisia)

Abstract
Iron fluoride hybrid systems, in which fluoroferrate(II) or fluoroferrate(III) can be used to give rise to fluorescent materials, are a very promising class of materials in a wide range of technological applications exploiting their electric and dielectric properties. Herein, novel organic–inorganic hybrid compound based on iron fluoride, $(H_2Piper)_4$ $[(FeF_6)_2FeF5(H_2O)(H_2O)_4]$ (Piper = Piperazine), **1**, (8-HQN)6$[Fe_4F_{18}]$ (8-hyroxyquinoline = 8-HQN), **2**, were synthesized by hydrothermal method and characterized by X-ray single-crystal diffraction, thermogravimetric analysis (TGA) and differential scanning calorimetric (DSC). Single-crystal X-ray study showed that **1** crystallizes in *P*-1 space group while **2** in *R*3c one. The variation of the *dc* and *ac* conductivity confirmed two phase transitions of **1** and the temperature dependences of dielectric permittivity showed a relaxation process and highlighted the good protonic conduction of this material. The photoluminescence studies of **2** show a significate green emission at 2.14 eV associated with radiative recombination of excitons confined within the organic part when it was excited in UV-visible wavelength in the solid state at room temperature. Finally, the magnetic analysis of **2** exhibits a paramagnetic behavior above 100 K. [1,2]

Acknowledgment
Spanish Ministerio de Ciencia e Innovación (PID2020-113558RB-C41) and Gobierno del Principado de Asturias (GRUPIN-2021/50997) are acknowledged.

References
[1] A. Moulahi, O. Guesmi, M.S.M. Abdelbaky, S. García-Granda, M. Dammak. J. Alloys Compd.898 (2022) 162956
[2] O. Guesmi, M.S.M. Abdelbaky, S. García-Granda, M. Dammak. Inorg. Chim. Acta 496 (2019) 119033

Back to Table of contents

MS13 Structural Characterization of Functional Materials

MS13-1-23 A new germylene-β-sulfoxide hemilabile ligand and its apllications in coordination chemistry demonstrated by X-Ray diffraction.
#MS13-1-23

S. Mallet-Ladeira [1], D. Madec [2]
[1]CNRS- ICT - Toulouse (France), [2]UPS-CNRS-LHFA - Toulouse (France)

Abstract
The hemilabile ligands with a combination of strong and weak donor groups have become essential tools in transition-metal catalysis. On the other hand, the investigation of transition-metal germylene complexes has attracted considerable interest over the past few decades. However, the use of transition-metal germylene complexes in catalysis remains sporadic, with olny a few recent reports.
In this context, we report the synthesis of a germylene-β-sulfoxide ligand[2] **1** and its abilities in coordination chemistry. Its bridging capability as bidentate ligand towards transition metal complexes was clearly established by X-ray diffraction analysis with the metal complexes (**1**)-$W(CO)_4$, (**1**)-$Mo(CO)_4$ and (**1**)-Ni(cod) (cod = 1,5-cyclooctadiene).
Furthermore, the reaction of ligand (**1**) with $[Ru(PPh_3)_3Cl_2]$ afforded a complex which readily evolves during crystallization to an unprecedented bis-ruthenium complex. To the best of our knowledge, this complex is the first crystallographically characterized complex featuring two bridge chlorine atoms, and a trans-phosphine-sulfoxide arrangement.
Finally, the hemilabile character of **1** was clearly demonstrated by the nickel complex and a reaction with carbon monoxide giving a stable tricarbonyl Ni(0)-complex, its structure was confirmed by X-ray diffraction analysis.
Applications of this new germylene-β-sulfoxide ligand in enantioselective catalysis is under investigation.

References
1. Nicolas Lentz, Cynthia Cuevas-Chavez, Sonia Mallet-Ladeira, Jean-Marc Sotiropoulos, Antoine Baceiredo, Tsuyoshi Kato, and David MadecInorganic Chemistry 2021 60 (1), 423-430.
2. Nicolas Lentz, Sonia Mallet-Ladeira, Antoine Baceiredo, Tsuyoshi Kato, and David Madec, Dalton Trans., 2018,47, 15751-15756.

Molecular structures of W(0) and Mo(0) complexes

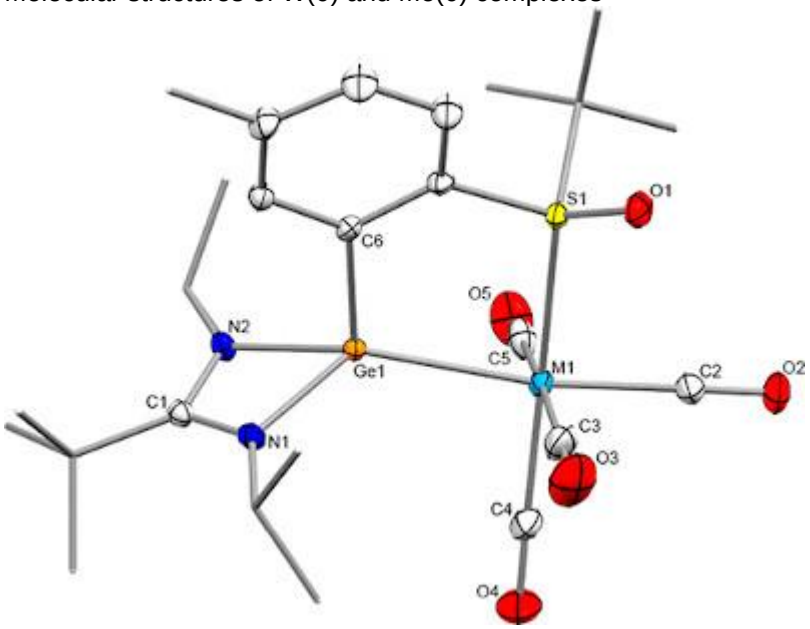

An unprecedented bridged bis-ruthenium complex

Back to Table of contents

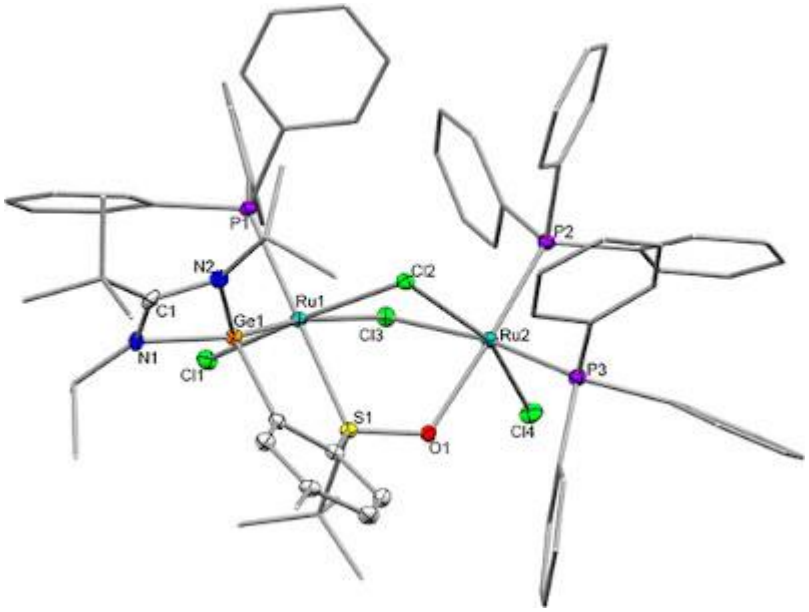

Back to Table of contents

MS13 Structural Characterization of Functional Materials

MS13-1-24 Synthesis and analyze structural of new materials ferroelectric Ba(2-x)SrxGdFeNb4O15 solid solution with (0 ≤ x ≤ 2)
#MS13-1-24

J. Farhan [1], A. Laaraj [1], H. Majdoubi [2], B. Ifegous [1], T. Lachhab [1], R. Adhiri [1]
[1]LIMAT FSBM - Casablanca (Morocco), [2]MSN UM6P - Ben Guerir (Morocco)

Abstract
The structural study of $Ba_{(2-x)}Sr_xGdFeNb_4O_{15}$ powders with (0 ≤ x ≤ 2) has been reported. All samples were prepared using the conventional solid-state reaction. XRD results confirmed that all compounds have a tetragonal tungsten bronze (TTB) structure with space group P4/mbm, where A 1 sites are exclusively occupied by Gd^{3+}. Ba^{2+} and Sr^{2+} ions are located in the A2 sites while the Fe^{3+} and Nb^{5+} ions are randomly distributed between the B1 and B2 sites. The Raman spectra of the powders showed mainly multi-component and broad bands related to the internal vibrations of the octahedral MO6 . The size of the A-site ions decreases when the Nb/Fe-O stretching changed. The evolution of the O–Nb/Fe–O bending vibrations as a function of the substitution rate x, seems to be a signature of the phase modifications. Infrared spectroscopy (IR) indicated the presence of stretching vibration bands as Nb/Fe-O, but also some strain vibration bands as H-O-H and O-H. Finally, Scattering Electron Microscopy (SEM) analyses show clearly the formation of TTB structure with uniform and dense grains with some phase of GdNbO4.

Back to Table of contents

MS13 Structural Characterization of Functional Materials

MS13-1-25 Development of cost-effective NdFeB permanent magnets by partial substitution of Ce and La #MS13-1-25

C.H. Kronbo [1], B.B. Iversen [1]
[1]Aarhus University - Aarhus (Denmark)

Abstract
$Nd_2Fe_{14}B$-based permanent magnets have been widely used for the last three decades as key components in many applications. We are working in collaboration with the global pump company Grundfos, who are using $Nd_2Fe_{14}B$-based permanent magnets in their motors driving their pumps, on developing $Nd_2Fe_{14}B$-based magnetic materials using low-cost, abundant materials such as Ce and La to substitute for Nd and thereby reducing the environmental footprint.
The crystal structure of $Nd_2Fe_{14}B$ is tetragonal with space group $P4_2/mnm$ and has six distinct Fe sites, two distinct Nd sites and one B site. The atomic structure, seen in Figure 1a, is layered with the atomic layers arranged perpendicular to the *c*-axis. The magnetic structure of $Nd_2Fe_{14}B$ adopts a ferromagnetic ordering at room temperature with the easy axis parallel to the *c*-axis. $Nd_2Fe_{14}B$ possesses a theoretical energy product as large as 64 MGOe and a Curie temperature of 585 K [1] which arise from exchange coupling between the magnetic moment of the rare-earth elements and the transition metals. Substituting Nd with other rare-earth elements such as Ce, or La creates isomorphic structures to the pure $Nd_2Fe_{14}B$ [2] but yield changes to the magnetic properties. Substitution with Ce and La is inevitably accompanied with magnetic dilution due to inferior intrinsic magnetic properties of $(Ce,La)_2Fe_{14}B$ but on the other hand reduces the environmental footprint. Ce in $Ce_2Fe_{14}B$ is in a mixed valence state (Ce^{3+}/Ce^{4+}) giving it one unpaired electron in the 4*f* orbital in the 3+ state and zero unpaired electrons in the 4+ state thus Ce needs to be in the 3+ state to contribute to the magnetic properties. It has been found that the Ce valence state is highly dependent on its steric environment and can be manipulated towards the favorable Ce^{3+} by co-substitution with La [3, 4].
Using synchrotron powder X-ray diffraction we are investigating substitution of Nd with Ce and La and an example of a diffractogram measured at Spring8 in Japan is shown in Figure1b. Using Rietveld refinement we are among other things looking at site occupancies to determine how Ce and La substitutes into the crystal structure. Comparing the crystallographic data with magnetic properties will enable us to find the optimal substitution stoichiometry for keeping a usable magnetic performance for applications.

References
[1] Sagawa, M., et al., *New material for permanent magnets on a base of Nd and Fe (invited)*. Journal of Applied Physics, 1984. 55(6): p. 2083-2087. [2] Herbst, J.F., *$R_2Fe_{14}B$ materials: Intrinsic properties and technological aspects*. Reviews of Modern Physics, 1991. 63(4): p. 819-898. [3] Poenaru, I., et al., *Ce and La as substitutes for Nd in $Nd_2Fe_{14}B$-based melt-spun alloys and hot-deformed magnets: a comparison of structural and magnetic properties.* Journal of Magnetism and Magnetic Materials, 2019. 478: p. 198-205. [4] Jin, J., et al., *Manipulating Ce Valence in $RE_2Fe_{14}B$ Tetragonal Compounds by La-Ce Co-doping*: Resultant Crystallographic and Magnetic Anomaly. Scientific Reports, 2016. 6(1): p. 30194.

Nd2Fe14B structure (P42/mnm).

Back to Table of contents

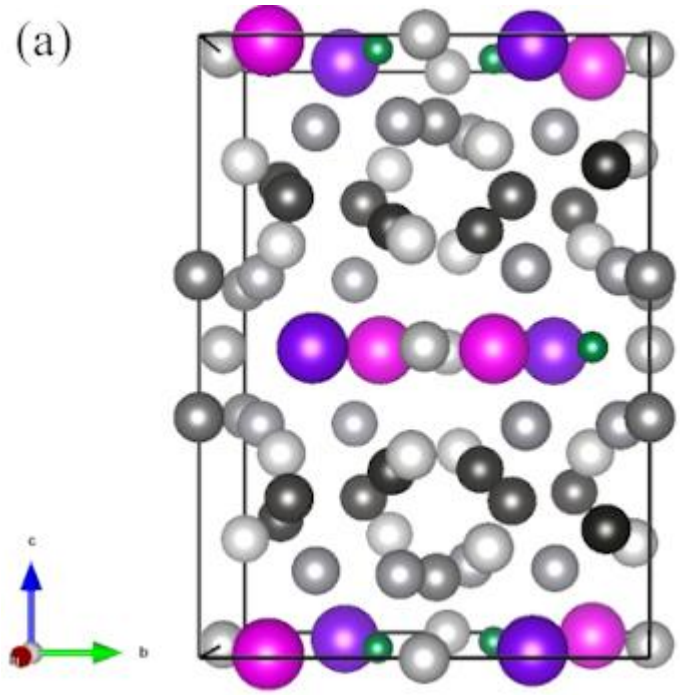

PXRD measured at Spring8, Japan (0.49009 Å)

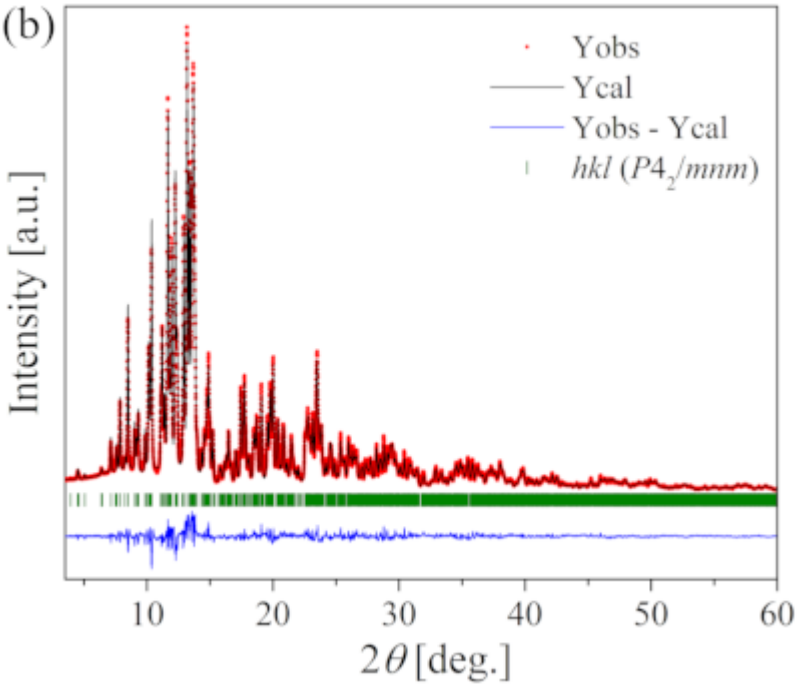

Back to Table of contents

MS13 Structural Characterization of Functional Materials

MS13-1-3 MgMn4Ga18: new structural type with three core-shell cluster packing
#MS13-1-3

N. Pavlyuk [1], V. Pavlyuk [1], G. Dmytriv [1], H. Ehrenberg [2], S. Indris [2], B. Schwarz [2]
[1]The Ivan Franko National University of Lviv - Lviv (Ukraine), [2]Institute of Applied Materials- Energy Storage Systems (IAM-ESS) of Karlsruhe Institut für Technologie (KIT) - Karlsruhe (Germany)

Abstract

$MgMn_4Ga_{18}$: new structural type with three core-shell cluster packing

Nazar Pavlyuk[1], Grygoriy Dmytriv[1], Volodymyr Pavlyuk[1], Sylvio Indris[2], Björn Schwarz[2] and Helmut Ehrenberg[2]
[1]Department of Inorganic Chemistry, Ivan Franko National University of Lviv, Kyryla and Mefodiya str. 6, 79005 Lviv, Ukraine[2]Karlsruhe Institute of Technology (KIT), Institute for Applied Materials (IAM), Hermann-von-Helmholtz-Platz 1, D-76344 Eggenstein-Leopoldshafen, Germany
Correspondence email: nazar.pavlyuk@gmail.com

Abstract. The new ternary gallide $MgMn_4Ga_{18}$ was synthesized by induction melting from the pure elements in a sealed tantalum crucible. The crystal structure was studied both by single crystal and powder X-ray diffraction. Single crystal diffraction data were collected at 20 degrees C on an Xcalibur™3 CCD diffractometer with graphite-monochromatized Mo- or Cu-Ka radiation. Scans were taken in the u-mode, the analytical absorption corrections were made by CrysalisRed [1]. Crystal structures of the compounds were solved by direct methods and refined using the SHELX-97 software package [2]. The $MgMn_4Ga_{18}$ structure (tP23, *P4/mmm*, *a* = 6.3116 (9) Å, *c* = 9.944 (2) Å) can be described as a three-core-shell cluster compound. The Mg atoms are surrounded by 16 adjacent Ga atoms [$MgGa_{16}$] in the form of an octadecahedron. The [$MgGa_{16}$] octadecahedron is encapsulated within the [Ga_{32}] icohexahedron, which is again encapsulated within a [Ga_{40}] pentacontaoctahedron, forming as a result three core–shell cluster [$MgGa_{16}@Ga_{32}@Ga_{40}$].The electronic structure calculations were performed by means of the TB-LMTO-ASA program and they confirm the core–shell packing of these clusters.

Table 1. Fractional atomic coordinates and isotropic displacement parameters (Å^2) for $MgMn_4Ga_{18}$

Atoms	*x*	*y*	*z*	U_{iso}/ U_{eq}
Ga1	0.23869(17)	0.23869(17)	0.23605(15)	0.0172 (5)
Ga2	0.5	0.5	0.3872(4)	0.0558 (17)
Ga3	0	0.3110(4)	0.5	0.0232 (7)
Ga4	-0.1870(4)	0.5	0	0.0183 (6)
Mn5	0	0	0.3433(4)	0.0059 (9)
Mn6	0.5	0.5	0.1526(4)	0.0077 (9)
Mg7	0	0	0	0.033 (4)

References

References

1. CrysAlis PRO, UK Ltd., Agilent Technologies, Yarnton, Oxfordshire, England, 2011.
2. G.M. Sheldrick, A short history of SHELX, Acta Cryst. A 64 (2008) 112e122.

Unit cell and coord. polyhedr. in MgMn4Ga18

Back to Table of contents

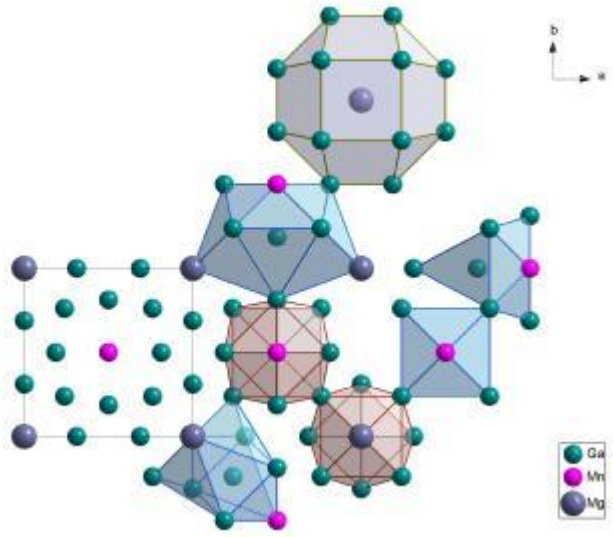

Cluster core shell packing in MgMn4Ga18

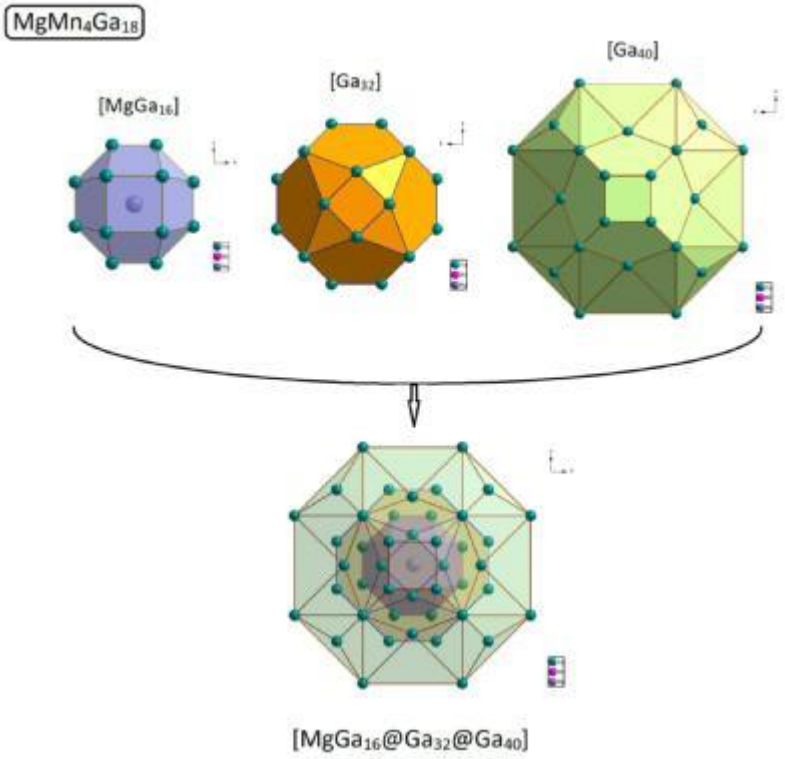

Back to Table of contents

MS13 Structural Characterization of Functional Materials

MS13-1-4 In Situ Temperature-Dependent X-ray Diffraction Study of Ferroelectric Single Crystal BCZT #MS13-1-4

A. Gadelmawla [1], S. Spreafico [1], F.W. Heinemann [1], D. Liu [2], Q. Li [2], Q. Yan [2], K. Hayashi [3], B. Meyer [1], K.G. Webber [1]

[1]Friedrich-Alexander-Universität Erlangen-Nürnberg - Erlangen (Germany), [2]Tsinghua University - Beijing (China), [3]Nagoya Institute of Technology - Nagoya (Japan)

Abstract

Perovskite ferroelectrics (ABO_3) are enabling components in numerous technological fields, including energy harvesting and storage and electromechanical transducer applications [1]. Among others, lead-free piezoelectric compositions based on $Ba_{1-x}(Zr_{0.2}Ti_{0.8})O_3$-$x(Ba_{0.7}Ca_{0.3})TiO_3$ (BCZT) have shown promising electromechanical response that can match the currently used $Pb(Zr,Ti)O_3$-based piezoelectrics [2]. To date, the average crystal structure has only been studied for polycrystalline BCZT, revealing rhombohedral (*R3m*), orthorhombic (*Amm2*), tetragonal (*P4mm*), and cubic ($Pm\bar{3}m$) phases in the 80–450 K temperature range [3–6]. Despite this, single crystal structure analysis is important, as it offers information about the crystal symmetry, phase transitions, static configurational displacement, and thermal vibration of each atom without the influence of grain structure. Although several previous studies have succeeded in growing BCZT single crystals [7–11], only Liu *et al.* have reported a high piezoelectric coefficient of 232 pC/N at room temperature for $Ba_{0.798}Ca_{0.202}Zr_{0.006}Ti_{0.994}O_3$ single crystal that was grown with the spontaneous nucleation method [12]. The relatively high makes the crystal reported by Liu *et al.* the best candidate for structure investigation.

In this study, and for the first time, *in situ* temperature-dependent single-crystal X-ray diffraction of lead-free ferroelectric perovskite BCZT is reported. The data were collected within the temperature range of 170–380 K, revealing rhombohedral (*R3m*), orthorhombic (*Pmm2*), and tetragonal (*P4mm*) crystal structures. In ferroelectric phases, both B-site and oxygen ions are displaced with respect to the A-site cations at their original position. This shift leads to spontaneous polarization in the crystal, which is the origin of ferroelectricity. Furthermore, the single crystal structure has been modeled via first-principles DFT simulations. The computational investigation aims to get an insight into the local atomic environment of the Zr and Ca dopants and the consequent spontaneous polarization ($\mathbf{P}_s$). Few previous computational works on BCZT focus on the local atomic environment [13], and the non-stoichiometry makes it challenging to model this single crystal via discreet atom representation and periodic boundary conditions. As a fair compromise, we employed a 3x3x3 supercell featuring 135 atoms, where the fractional proportions are reproduced employing 21, 6, 26, and 1 atoms for Ba, Ca, Ti, and Zr elements, respectively. Starting from pure $BaTiO_3$, we first introduced the single Zr atom in the Ti sublattice and, consequently, the 6 Ca atoms in the Ba sublattice, isolating and studying the contributions of the two dopants. The structural impact of Zr and Ca atoms is studied by looking at the distance between them and the neighboring atoms. Whereas the introduction of Zr atom leads to an expected structural expansion, the arrangements of Ca atoms had to be sampled because they play a discriminating role in the relaxation process. Ultimately, the $\mathbf{P}_s$ is evaluated via Berry Phase calculations and Born Effective Charges applied on the atomic displacements derived by computational and experimental structures. The adoption of multiple methods provides us clarity around the gray-zone of the evaluation of this property.

References

[1] B. Jaffe, Piezoelectric Ceramics, Elsevier Science, Saint Louis, 2014.
[2] W. Liu, X. Ren, Physical review letters 103 (2009) 257602.
[3] D.S. Keeble, F. Benabdallah, P.A. Thomas, M. Maglione, J. Kreisel, Appl. Phys. Lett. 102 (2013) 92903.
[4] M. Acosta, N. Khakpash, T. Someya, N. Novak, W. Jo, H. Nagata, G.A. Rossetti et al., Phys. Rev. B 91 (2015).
[5] I. Coondoo, N. Panwar, S. Krylova, A. Krylov, D. Alikin, S.K. Jakka, A. Turygin et al., Ceramics International 47 (2021) 2828–2838.
[6] M.B. Abdessalem, S. Aydi, A. Aydi, N. Abdelmoula, Z. Sassi, H. Khemakhem, Appl. Phys. A 123 (2017).
[7] Y. Zeng, Y. Zheng, X. Tu, Z. Lu, E. Shi, Journal of Crystal Growth 343 (2012) 17–20.
[8] I. Bhaumik, G. Singh, S. Ganesamoorthy, R. Bhatt, A.K. Karnal, V.S. Tiwari, P.K. Gupta, Journal of Crystal Growth 375 (2013) 20–25.
[9] G. Singh, I. Bhaumik, S. Ganesamoorthy, R. Bhatt, A.K. Karnal, V.S. Tiwari, P.K. Gupta, Appl. Phys. Lett. 102 (2013) 82902.
[10] F. Benabdallah, P. Veber, M. Prakasam, O. Viraphong, K. Shimamura, M. Maglione, Journal of Applied Physics 115 (2014) 144102.
[11] H. Palneedi, V. Annapureddy, H.-Y. Lee, J.-J. Choi, S.-Y. Choi, S.-Y. Chung, S.-J.L. Kang et al., Journal of Asian Ceramic Societies 5 (2017) 36–41.

Back to Table of contents

[12] D. Liu, J. Shim, Y. Sun, Q. Li, Q. Yan, AIP Advances 7 (2017) 95311.
[13] D. Amoroso, A. Cano, and P. Ghosez, Phys. Rev. B 97 (2018) 174108.

MS13 Structural Characterization of Functional Materials

MS13-1-5 Solid solutions of mono and dihalogen alkyl phosphonium salt derivatives and their photoluminescence properties
#MS13-1-5

K. Saršuns [1], I. Kļimenkovs [2], A. Bērziņš [2], T. Rekis [2]
[1]Faculty of Chemistry, University of Latvia - Riga (Latvia), [2]Faculty of Chemistry, University of Latvia - Rīga (Latvia)

Abstract
A neglected crystal engineering strategy that would allow to tune a variety of properties of a crystalline material in continuum is to obtain solid solutions. However, for organic systems, it has been observed that occasionally even very similar molecular entities cannot be interchanged in the crystal lattice. Up to date, there are only some rough, empirical guidelines indicating what kind of binary systems would possibly show component miscibility in the solid state. One type of binary systems deemed to form solid solutions is a system constituting two molecules differing by halogen atom type[1].
In this research work, halogenated alkyl phosphonium salts have been selected to attempt solid solution engineering. The compounds are known to exhibit long-persistent room-temperature solid-state luminescence phenomena[2].
We explored the solid solution formation in binary systems of mono and dihalogen alkyl phosphonium salt derivatives (**Figure 1.**). Solid solutions have been identified and characterized using powder X-ray diffraction and thermal methods of analysis. Photoluminescence spectra of the new crystalline phases were studied to explore the differences with respect to the luminescence properties of pure substances known from the literature[2].

References
(1) Corpinot M. K., Bučar D. K. A Practical Guide to the Design of Molecular Crystals. Crystal Growth & Design, 19(2), 1426-1453 (2019)(2) Alam, P, Leung N. L. C., Liu J., Cheung T. S., Zhang X., He Z., Kwok R. T. K., Lam J. W. Y., Sung H. H. Y., Williams I. D., Chan C. C. S., Wong K. S., Peng Q., Tang B. Z. Two Are Better Than One: A Design Principle for Ultralong-Persistent Luminescence of Pure Organics. Adv. Mater., 32(22), 2001026 (2020)

Acknowledgement
European Social Fund, project “Strengthening of the capacity of doctoral studies at the University of Latvia within the framework of the new doctoral model”, identification No. 8.2.2.0/20/I/006 and University of Latvia foundation through “Mikrotīkls” doctoral scholarship in the field of natural and medical sciences.

Molecular structures of mono (a) and dihalogen (b

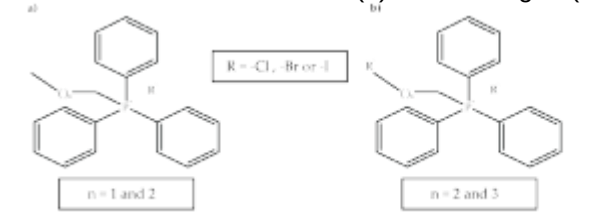

Figure 1. Molecular structures of mono (a) and dihalogen (b) alkyl phosphonium salt derivatives.

Back to Table of contents

MS13 Structural Characterization of Functional Materials

MS13-1-6 Temperature-dependent structural and spectroscopic properties of mullite-type $SnMBO_4$ #MS13-1-6

T. Gesing [1], S. Wittmann [2], A. Koldemir [3], R. Pöttgen [3], M.M. Murshed [2]
[1]Name should not appear here:Programming error by - Organizer (France), [2]University of Bremen, Institute of Inorganic Chemistry and Crystallography - Bremen (Germany), [3]Universität Münster, Institut für Anorganische und Analytische ChemieInstitute of Inorganic Chemistry and Crystallography - Münster (Germany)

Abstract
Mullite-type compounds $EMBO_4$ ($E_2M_2B_2O_8$ ≡ O8-phase) have drawn a considerable interest due to the influence of the stereochemical activity of the $6s^2$ lone electron pairs (LEPs) of the Pb^{2+} cation on the crystal-chemical and physical properties. The crystal structure of the O8-phase in the mullite-type setting is described in the orthorhombic space group Pnam, where the MO_6 octahedra build an edge-sharing chain running parallel to the crystallographic c-axis [1]. The octahedral chains are bridged by trigonal planar BO_3 groups connected by the distorted PbO_4 square pyramids. The influence of the LEP and the rigidity of the planar BO_3 groups play important roles to stabilize the O8-structures. In response to the toxicity of lead and the associated environmental issues, replacement of Pb^{2+} by suitable LEP-containing divalent cations is a demanding alternative. As such, mullite-type $SnAlBO_4$ and $SnGaBO_4$ are synthesized. Whereas the almost similar cationic size of Sn^{2+} and Pb^{2+} predict a complete replacement of Pb^{2+} by Sn^{2+} in the O8-structure, the significantly different Wang-Liebau eccentricity parameter [2] and the susceptibility of Sn^{2+} into Sn^{4+} oxidation requires ingenious exploitation of the solid-state reactions. Structural information's were obtained from Rietveld refinements and lattice parameters of a = 719.10(13) pm, b = 773.93(15) pm, c = 584.03(3) pm and V = 316.41(10)•10^6 pm^3 for SnAlBO4 and a = 727.60(4) pm, b = 791.20(4) pm, c = 584.03(3) pm and V = 336.47(13)•10^6 pm^3 for SnGaBO4 were refined. Bond valence sums indicate that tin and the M-elements are slightly under-bonded whereas boron is slightly over-bonded, which can be explained in terms of the contraction of the BO_3 group and the distortion of the MO_6 octahedra via strong influence of the $5s^2$ LEPs of Sn^{2+} cation. Temperature-dependent ^{119}Sn-Mössbauer spectra support the coordination and the oxidation state of tin. Temperature-dependent X-ray investigations (10 K – 850 K) show very small thermal expansion coefficients with a maximum of 10•10^{-6} K^{-1} at 800 K without any anomaly pointing to a phase transition. The vibrational features obtained from Raman spectroscopy complement both X-ray and Mössbauer spectroscopic results. $SnAlBO_4$ and $SnGaBO_4$ possess band-gap energies of 3.42(2) eV and 2.62(4) eV, respectively, determined from the UV/Vis diffuse reflectance spectra. The indirect nature of the electronic transition is analyzed using RATD (Reflection-Absorption-Tauc-DASF) analysis.

TMG and SW acknowledge support by DFG under grant number GE1981/14-1.

References
[1] T.M. Gesing, C.B. Mendive, M. Curti, D. Hansmann, G. Nenert, P.E. Kalita, K.E. Lipinska, A. Huq, A.L. Cornelius, M.M. Murshed, Structural properties of mullite-type $Pb(Al_{1-x}Mn_x)BO_4$, Z. Kristallogr. 228(10) (2013) 532-543. DOI:10.1524/zkri.2013.1640
[2] M. Curti, C.B. Mendive, T. Bredow, M. Mangir Murshed, T.M. Gesing, Structural, vibrational and electronic properties of $SnMBO_4$ (M = Al, Ga): a predictive hybrid DFT study, J. Phys.: Condens. Matter 31(34) (2019) 345701. DOI:10.1088/1361-648X/ab20a1

Figure 1: Crystal structure of $PbAlBO_4$

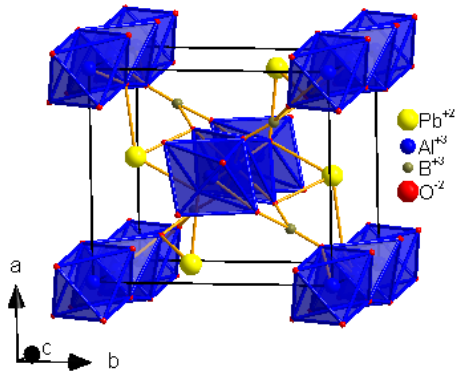

Back to Table of contents

MS13 Structural Characterization of Functional Materials

MS13-1-7 Solid solutions in the system Li4GeO4-Li2CaGeO4
#MS13-1-7

R. Nikolova [1], V. Nikolov [1], N. Kuvandjiev [1], N. Petrova [1]
[1]Institute of Mineralogy and Crystallography-Bulgarian Academy of Sciences - Sofia (Bulgaria)

Abstract
LISICON, $Li_{14}Zn(GeO_4)_4$ is one of the solid solutions with general formula $Li_{2+2x}Zn_{1-x}$ GeO_4 (-0.36 < x < 0.87). These solid solutions are derivatives of the stoichiometric compound Li_2ZnGeO_4 where Zn^{2+} is substituted by Li^+. These compounds are isostructural to Li_3PO_4 with crystal structure based on $[Li_nZn_m(GeO4)_p]$ framework and an “interstitial” loosely bonded Li^+. This unique arrangement predetermines ionic conductivity of the mentioned compounds. Li_2GeO_4 has been also tested as a laser and phosphor matrix, semiconductor and biosensor. It was reported that Mg, Co, Fe, Ni, Cd also form solid solutions isostructural to Li_3PO_4, and the substitution of Ge by Si, V, P is also acceptable. The general formula for these solid solutions is defined as Li_{2+2x}***Me1***$_{1-x}$ ***Me2***O_4, where ***Me1*** is divalent cation and ***Me2*** form a $(Me2O_4)^{4-}$ anion.
Here we report for first time the synthesis of solid solutions in the system Li_4GeO_4-Li_2CaGeO_4. As Ca^{2+} has a larger ionic radius than Zn^{2+} and the mentioned before cations, it could be expected that the framework "voids" in $Li_{2+2x}Ca_{1-x}GeO4$ will be larger, influencing the ionic conductivity and the luminescence properties. Compositions of $Li_{2+2x}Ca_{1-x}GeO_4$ with **x**=0,0.1,0.2,0.3,0.4,0.5,0.6,0.7,0.8,0.9,1.0 were prepared by conventional solid state reactions. The desired quantities of Li_2CO_3 (99,9), $CaCO_3$ (99,9), GeO_2(99,999) were mixed, milled and heated at 800°C for 3 h. The decarbonized samples were milled again and heated at 1050 °C for 6h. The resulting powders were studied using XRD, DSC-TG analyses. Two phase regions were defined between Li_2CaGeO_4 (x=0) and Li_4GeO_4 (x=1,0). For 1050 °C these regions are as follow: for **x** between 0 and 0.1 crystalizes $Li_{2+2x}Ca_{1-x}$ GeO_4 solid solutions owing tetragonal Li_2CaGeO_4 structure type; for **x** between 0.1 and 0.7 a mixture of $Li_{2+2x}Ca_{1-x}GeO_4$ solid solutions with Li_2CaGeO_4 tetragonal and orthorhombic type structures; for **x** between 0,7 and 0,9 solid solutions of $Li_{2+2x}Ca_{1-x}$ GeO_4 with orthorhombic Li_2CaGeO_4 type structure; and finally for **x** above 0.9 solid solutions with Li_4GeO_4 type structure. X-ray powder analyses for selected compositions (SiO_2 was used as an internal standard) are represented on the Figure 1. The studied samples were compared with the PDF data of the basic Li_2CaGeO_4 tetragonal and orthorhombic structures.
An interesting result is the presence of wide region of crystallization of Li2+2xCa1-x GeO4 solid solutions with two different structures. It would be important to look for relations between this phenomenon and the ionic conductivity of the obtained mixtures. It is also notable that in the orthorhombic Li2+2xMe21-xGeO4 phase the Me2 atoms are tetrahedraly coordinated. Such coordination is very unusual for Ca ion and it is important it to be confirmed for orthorhombic Li2+2xCa1-xGeO4 single crystal sample.
Acknowledgments: The research is financial supported by the National Science Fund of Bulgaria (Contract No. KP-06-H29/10).

X-ray powder data for selected compositions

Back to Table of contents

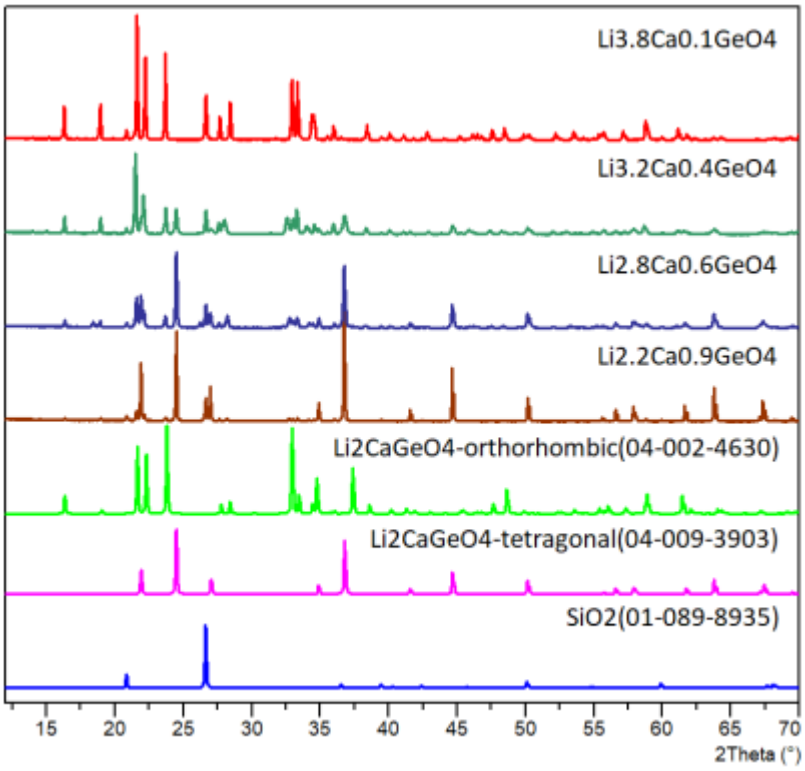

Back to Table of contents

MS13 Structural Characterization of Functional Materials

MS13-1-8 Phase transitions in flexible crystals of cocrystal solvate of caffeine
#MS13-1-8

S. Dey [1], S. Nandi [2], H. Gildenast [3], H. Shahed [4], V.B. Hakala [4], A. Grzechnik [5], C. Paulmann [6], M. Tolkiehn [6], U. Englert [3], G. Roth [1], L. Peters [1]
[1]Institute of Crystallography, RWTH Aachen University - Aachen (Germany), [2]Jülich Centre for Neutron Science JCNS and Peter Grünberg Institut PGI Quantum Materials and Collective Phenomena JCNS-2 / PGI-4, Forschungszentrum Jülich GmbH - Jülich (Germany), [3]Institute of Inorganic Chemistry, RWTH Aachen University - Aachen (Germany), [4]Forschungszentrum Jülich GmbH, Jülich Centre for Neutron Science JCNS, Germany - Jülich (Germany), [5]Institute of Crystallography, RWTH Aachen UniversityJülich GmbH, Jülich Centre for Neutron Science JCNS, Germany - Aachen (Germany), [6]Deutsches Elektronen-Synchrotron, Germany - Hamburg (Germany)

Abstract
Single crystals of 1:1:1 cocrystal solvate of caffeine, 4-chloro-3-nitrobenzoic acid and methanol are reported to demonstrate reversible bending up to large elastic strain at ambient conditions [1]. The compound has orthorhombic space group symmetry *Fdd*2 [T = 100 K: a = 32.784(9) Å, b = 55.541(15) Å, c = 3.9564(12) Å, V = 7191(4) Å3]. Elastic bending in these crystals is governed by changing distances between molecules within stacks and molecular rotations [2]. While combination of weak dispersive interactions viz. weak C–H···O hydrogen bonds, π-stacking and van der Waals forces between pseudo spherical functional groups aids flexibility, permanent plastic deformation in these crystals has been argued to be prevented by “interlocking”/ steric barriers in the supramolecular architecture [1,2]. Upon heating at Tc1 = 333 K, the crystals lose flexibility and are mechanically brittle [1]. Further heating leads to partial desolvation of methanol from their structure at Tc2 = 388 K [1].
Using temperature dependent specific heat capacity and single crystal X-ray diffraction experiments, the phase transition at Tc1 is found to be continuous. Crystal structures above Tc1 suggest reorganization of the stacking arrangement between the caffeine-acid dimers with respect to the longest growth direction of the crystals.
High temperature *in-situ* powder X-ray diffraction experiments suggest that the compound undergoes a phase transition at a significantly lower temperature. Additional peaks are observed in the diffraction pattern. These peaks violate the *F*-centered orthorhombic lattice. Alternatively, these peaks could be approximately described with an additional wave vector in (3+*d*) dimensions.

References
[1] Ghosh S, Reddy C. M. Elastic and bendable caffeine cocrystals: Implications for the design of flexible organic crystals. *Angew. Chem. Int. Ed*., **51**, 10319-10323 (2012)
[2] Thompson A. J., Price J. R., McMurtrie J. C., Clegg J. K. The mechanism of bending in co-crystals of caffeine and 4-chloro-3-nitrobenzoic acid. *Nat. Commun*., **12**, 5983 (2021)

Back to Table of contents

MS13 Structural Characterization of Functional Materials

MS13-1-9 In situ and ex situ electron diffraction revealing diverse structural transformations of LaxSr2-xMnO4-δ upon gas reduction
#MS13-1-9

D. Vandemeulebroucke [1], M. Batuk [1], P. Roussel [2], J. Hadermann [1]
[1]EMAT, University of Antwerp - Antwerp (Belgium), [2]Ecole Nationale Supérieure de Chimie de Lille - Lille (France)

Abstract
Stability under reducing working atmospheres is an important quality in electrode materials for solid oxide fuel cells. For Ruddlesden-Popper manganites $La_xSr_{2-x}MnO_{4-\delta}$ with $0.25 \leq x \leq 0.6$, this structure preservation has been demonstrated by in situ high-temperature neutron and X-ray powder diffraction. [1] However, in situ and ex situ 3D electron diffraction now reveal that $La_{0.5}Sr_{1.5}MnO_4$ nevertheless undergoes unexpected structure transformations upon heating in a reducing atmosphere such as diluted hydrogen gas.While previously unobserved, the extra reflections disclosing these transformations can be easily picked up by electron diffraction. This is because the interaction of matter with electrons is more than one million times stronger than with X-rays or neutrons, which makes them more suitable to elucidate subtle transitions. Electron diffraction allows to obtain two-dimensional single-crystal diffraction patterns for submicron sized crystals, of which X-ray and neutron diffraction can only produce one-dimensional powder data that contain less information.Using a dedicated environmental holder, 3D electron diffraction shows that $La_{0.5}Sr_{1.5}MnO_4$ partially transforms from its pristine K_2NiF_4-type symmetry to a perovskite phase, when it is heated inside the transmission electron microscope in diluted hydrogen. When the material is annealed ex situ in diluted H_2/Ar, the same phenomenon is detected for a part of the crystals, while other crystals show the occurrence of a superstructure accompanying oxygen-vacancy order. This oxygen-vacancy order was not observed in any of the in situ experiments.Similarly, in situ and ex situ 3D electron diffraction show different structural behaviour for the gas reduction of Sr_2MnO_4 when this happens inside or outside the electron microscope: Sr_2MnO_4 transforms to the monoclinic $P2_1/c$ supercell known in literature [2] when reduced ex situ, but maintains the tetragonal symmetry when reduced in situ. On the other hand, $LaSrMnO_4$ and $La_{0.25}Sr_{1.75}MnO_4$ indeed show no differences in their space groups upon reduction.In-depth study of the diverging reduction behaviour inside and outside the microscope could offer new insights on the degradation of real life working electrodes, and help to optimize their performance life time.
Financial support is acknowledged from FWO I003218N, University of Antwerp BOF TOP 38689 and the European Commission NanED Grant number 956099.

References
[1] Sandoval, M., Pirovano C., Capoen, E., Jooris, R., Porcher, F., Roussel, P., Gauthier, G. (2017). Int. J. Hydrog. Energy. 42 (34), 21930-21943.
[2] Broux, T., Bahout, M., Hernandez, O., Tonus, F., Paofai, S., Hansen, T., Greaves, C. (2013). Inorg. Chem. 52 (2), 1009-1017.

Back to Table of contents

MS13 Structural Characterization of Functional Materials

MS13-2-1 Two-dimensional methylhydrazinium lead chloride perovskites with temperature-controlled centrosymmetric, modulated, and polar crystal phases
#MS13-2-1

D. Drozdowski [1], A. Gągor [1]
[1]Institute of Low Temperature and Structure Research, Polish Academy of Sciences - Wroclaw (Poland)

Abstract
In the last few years one of the most compelling themes in materials science is the synthesis and physicochemical studies of hybrid organic-inorganic perovskites (HOIPs). The three-dimensional (3D) HOIPs, which consist of corner-sharing PbX_6 octahedra (X = Cl, Br, I) network with voids filled by small organic cations (e.g., methylammonium or formamidinium), have been described already as a breakthrough in optoelectronics, especially in photovoltaic technology [1]. These structures, however, possess meaningful drawbacks in the terms of possible applications, i.e., poor resistance to moisture and chemicals. One of the keys to overcoming these issues is to reduce structural dimensionality to the two-dimensional (2D) HOIPs, where the octahedra layers are separated by organic cations. This approach allows not only to improve stability and certain properties (e.g., photoluminescence quantum yield [2]), but also to incorporate larger organic cations, as the geometric limitations, coming from the 3D inorganic linkage, are no longer a blockage.
Indeed, our group effectively enriches the HOIPs family with the structures comprising methylhydrazinium (MHy^+) cation. It is worth noting that the MHy^+ is small enough to maintain 3D alignment (see $MHyPbBr_3$ and $MHyPbCl_3$ [3, 4]), and simultaneously sufficiently large to separate the 2D perovskite layers. We have already reported two 2D HOIPs with MHy^+ – MHy_2PbI_4 and MHy_2PbBr_4 [5, 6]. Herein, description of these newcomers will be limited to the phase transition (PT) mechanism. HT phase of MHy_2PbI_4 adopts *Pmmn* symmetry and undergoes a PT to *Pccn* at 298 K, and later to *P*-1 at 233 K on cooling. MHy_2PbBr_4 possesses HT phase isostructural to the iodide analogue but undergoes a PT at 368 K to modulated *Pmmn*, and eventually, at 343 K, to polar $Pmn2_1$ space group. This observation suggests that the halide substitution leads to formation of different crystal phases in 2D MHy lead halide HOIPs, which determine their properties.
Continuation of the halide substitution approach in the MHy_2PbX_4 (X = halide) 2D HOIPs has led to development of another representative, i.e., MHy_2PbCl_4. Unlike the counterparts described above, MHy_2PbCl_4 crystallizes at room temperature in a modulated *Pmmn*(00*γ*)*s*00 superspace group. While the HT phase, stabilized at 332 K (338 K) on cooling (heating), is isostructural to the Br- and I- analogues, cooling down to 205 K induces a PT to polar $P2_1$ symmetry. Origins of such interesting crystal phases sequence will be discussed, with expected influence on the optical and dielectric properties.

References
[1] Henry J. Snaith, *The Journal of Physical Chemistry Letters*, **2013**, 4 (21), 3623-3630, DOI: 10.1021/jz4020162
[2] Matthew D. Smith, Bridget A. Connor, and Hemamala I. Karunadasa, *Chemical Reviews*, **2019**, 119 (5), 3104-3139, DOI: 10.1021/acs.chemrev.8b00477
[3] Mirosław Mączka, Maciej Ptak, Anna Gągor, Dagmara Stefańska, Jan K. Zaręba, and Adam Sieradzki, *Chemistry of Materials*, **2020**, 32 (4), 1667-1673, DOI: 10.1021/acs.chemmater.9b05273
[4] Mirosław Mączka, Anna Gągor, Jan K. Zaręba, Dagmara Stefańska, Marek Drozd, Sergejus Balciunas, Mantas Šimėnas, Juras Banys, and Adam Sieradzki, *Chemistry of Materials*, **2020**, 32 (9), 4072-4082, DOI: 10.1021/acs.chemmater.0c00973
[5] Mirosław Mączka, Maciej Ptak, Anna Gągor, Dagmara Stefańska, and Adam Sieradzki, *Chemistry of Materials*, **2019**, 31 (20), 8563-8575, DOI: 10.1021/acs.chemmater.9b03775
[6] Mirosław Mączka, Jan K. Zaręba, Anna Gągor, Dagmara Stefańska, Maciej Ptak, Krystian Roleder, Dariusz Kajewski, Andrzej Soszyński, Katarzyna Fedoruk, and Adam Sieradzki, *Chemistry of Materials*, **2021**, 33 (7), 2331-2342, DOI: 10.1021/acs.chemmater.0c04440

Fragments of MHy+ cations alignment in MHy2PbCl4,

Back to Table of contents

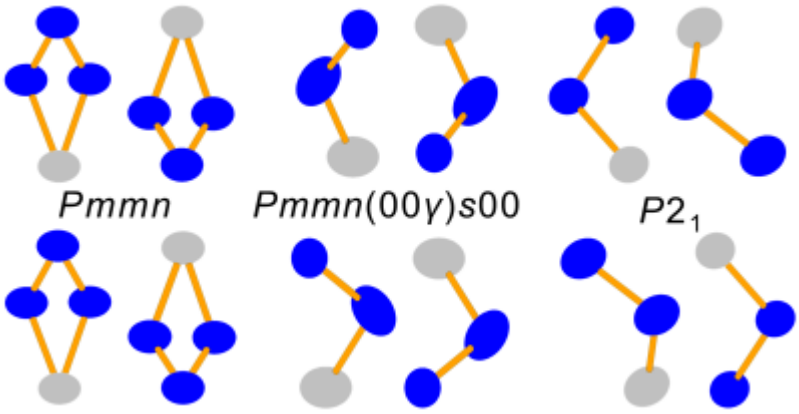

Back to Table of contents

MS13 Structural Characterization of Functional Materials

MS13-2-10 Following the path of temperature induced phase transitions in Pb(Mg1/3Nb2/3) – PbTiO3 ferroelectric crystals.
#MS13-2-10

I. Biran [1], S. Gorfman [1]
[1]department of material science and engineering, Tel Aviv University - Tel Aviv (Israel)

Abstract
(1-x) Pb(Mn1/3Nb2/3)O3 - x PbTiO3 (PMN-PT) is a functional ferroelectric material that has many technologically important applications as sonars for underwater communications, actuators and ultrasonic transducers [1]. The functionality of PMN-PT is underpinned by the flexibility of its perovskite-based structure and the ability to form complex domain microstructures through the various structural phase transitions. These transitions (between para- and ferroelectric as well as between different ferroelectric phases) have been in focus of much research [2] since the discovery of this material. The structure and symmetry of PMN-PT depends on its composition, x, and the temperature, T: it includes cubic, tetragonal, rhombohedral and two types of monoclinic phases. Because the delineation between these phases remains the major experimental challenge, certain areas of the x-T phase diagram are still rather vague. In addition, most of the existing structural studies of PMN-PT are performed with relatively coarse (> 15 K) temperature steps.
The aim of the work is to advance the understanding of the phase transitions in PMN-29PT and PMN-35PT crystals by tracing their cubic-tetragonal and tetragonal-to-monoclinic phase transitions using high-resolution single crystal X-ray diffraction. We collected a series of 3D reciprocal space volumes (RSV) which represent diffraction intensity distribution around certain families of Bragg peaks. Such Bragg peaks split into several components due to the presence of ferroelastic domains. The analysis of such splittings offers a powerful tool for elucidation of single-domain symmetry, and twin relationship between the domains [3]. We used a custom-built four-circle X-ray diffractometer, equipped with the microfocus X-ray source, double-crystal monochromator, Eulerian cradle, PILATUS 1M pixel area detector and fine-temperature control sample environment cell [4]. We measured RSVs around selected Bragg peaks with very fine (~0.1 K) temperature steps, both on heating and cooling. From their analysis we could follow the phase transitions path over between the room temperature and the transition to the cubic phase. We determined the phase transition temperatures on heating and cooling. By doing so, we characterised the order of the transition and checked the associate fine details. In addition, we were able to characterise the details of domain patterns occurring during each phase transition.
In the figure attached (Figure 1), one can see the change of the RSVs of PMN-29PT upon fine temperature steps. Noticeably, the shape of the peak differs as the phase transitions take place ((a) and (e) monoclinic phase; (b) and (d) tetragonal phase; (c) cubic phase).

References
[1] Park, S. E. & Shrout, T. R. (1997). J. App. Phys., 82, 1804-1811
[2] Noheda, B., Cox D. E., Shirane G., Gao, J. & Ye, Z.-G. (2002). Phys. Rev. B., 66, 054104.
[3] Gorfman, S.,Spirito, D.,Zhang, G., Detlefs, C. & Zhang, N. (2022). Acta Cryst. A78, 158-171.
[4] Gorfman, S., Spirito, D., Cohen, N., Siffalovic, P., Nadazdy, P. & Li, Y. (2021). J. Appl. Cryst., 54, 914-923.

Figure 1

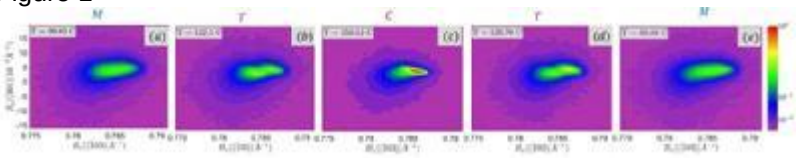

Back to Table of contents

MS13 Structural Characterization of Functional Materials

MS13-2-11 Magnesioreduction synthesis of Silicides: the structure-properties relationship
#MS13-2-11

C. Prestipino [1], M. Pasturel [1], S. Le Tonquesse [2], D. Berthebaud [2], T. Mori [3], E. Alleno [4]
[1]ISCR - Rennes (France), [2]CNRS NIMS - Tusukuba (Japan), [3]NIMS - Tusukuba (Japan), [4]Univ Paris Est, CNRS, ICMPE – UMR7182 - Thiais (France)

Abstract
Thermoelectric (TE) generators are all-solid-state devices that enable the conversion of heat, including heat losses, into electricity thanks to the Seebeck effect. These generators most commonly consist of an assembly of n- and p-type TE materials connected electrically in series and thermally in parallel between two ceramic plates. Important research efforts have been undertaken during the past two decades to increase TE efficiency of numerous materials such as Bi_2Te_3,$GeTe_2$ or $PdTe_3$ to enable a more extensive development of TE technology. However, many other factors must be taken into account when selecting materials for TE generator, such as the raw material costs and toxicity, mechanical properties, chemical and thermal stability, and thermal expansion coefficients. For all these reasons, Silicides (HMS and β-FeSi2) are considered as promising industrial thermoelectric materials for the mid-temperature applications (600 - 800 K), despite a moderate efficiency, however one of the main obstacle of a more diffuse application of such materilas remain their synthesis. For such reason we develop the magnesiothermic reduction (MR) synthesis for such compaunds. The MR rapidity and lower operating temperature synthesis is coupled with a reduction of average powder grain size, with a high cristallinity.
Such cristallinity has allowed us fine characterize by X-ray and electron diffraction the materials obtained and study the relationship between their complex crystallographic structure (incommensurability for MnSi1.74 and presence of stacking fault for β-$FeSi_2$), and microstructure with the synthesis conditions and how such parameter influence the thermoelectric properties of such materials. In particular to (i) to precisely determine the γ ratio of the composite structure of $V_xMn_{1-x}Si_\gamma$, which controls the VEC and therefore the transport properties [3,4], or (ii) to quantify the probability of stacking faults in β-$Co_yFe_{1-y}Si_2$ which can influence the lattice thermal conductivity[5].

References
(1)Le Tonquesse, S.; Alleno, É.; Demange, V.; Prestipino, C.; Rouleau, O.; Pasturel, M. Reaction Mechanism and Thermoelectric Properties of In0·22Co4Sb12 Prepared by Magnesiothermy. Materials Today Chemistry 2020, 16, 100223. https://doi.org/10.1016/j.mtchem.2019.100223.(2)Le Tonquesse, S.; Alleno, E.; Demange, V.; Dorcet, V.; Joanny, L.; Prestipino, C.; Rouleau, O.; Pasturel, M. Innovative Synthesis of Mesostructured CoSb3-Based Skutterudites by Magnesioreduction. Journal of Alloys and Compounds 2019, 796, 176–184. https://doi.org/10.1016/j.jallcom.2019.04.324.(3)Le Tonquesse, S.; Verastegui, Z.; Huynh, H.; Dorcet, V.; Guo, Q.; Demange, V.; Prestipino, C.; Berthebaud, D.; Mori, T.; Pasturel, M. Magnesioreduction Synthesis of Co-Doped β-FeSi2: Mechanism, Microstructure, and Improved Thermoelectric Properties. ACS Appl. Energy Mater. 2019, 2 (12), 8525–8534. https://doi.org/10.1021/acsaem.9b01426.(4)Le Tonquesse, S.; Joanny, L.; Guo, Q.; Elkaim, E.; Demange, V.; Berthebaud, D.; Mori, T.; Pasturel, M.; Prestipino, C. Influence of Stoichiometry and Aging at Operating Temperature on Thermoelectric Higher Manganese Silicides. Chemistry of Materials 2020, 32 (24), 10601–10609. https://doi.org/10.1021/acs.chemmater.0c03714.(5)Le Tonquesse, S.; Dorcet, V.; Joanny, L.; Demange, V.; Prestipino, C.; Guo, Q.; Berthebaud, D.; Mori, T.; Pasturel, M. Mesostructure - Thermoelectric Properties Relationships in V Mn1−Si1.74 (x = 0, 0.04) Higher Manganese Silicides Prepared by Magnesiothermy. J. Alloys Compd. 2020, 816, 152577. https://doi.org/10.1016/j.jallcom.2019.152577.

Rietveld refinement of washed MnSi1.74

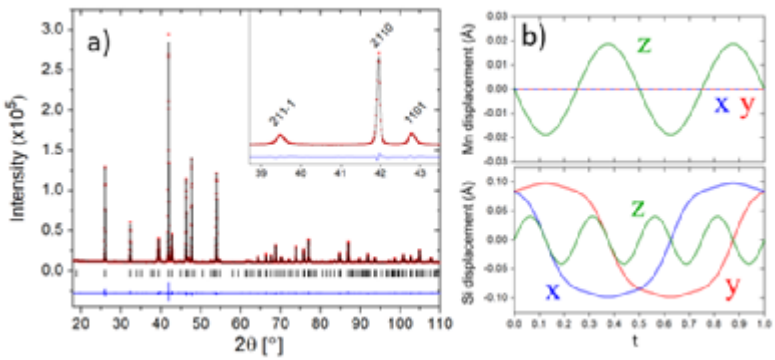

Back to Table of contents

MS13 Structural Characterization of Functional Materials

MS13-2-12 Structural Study of new family heteroleptic iron(III) [Fe(NSO)(N2O)] coordination compounds #MS13-2-12

V. Artigas [1], M.R. Probert [2], E. Olave [1], M. Fuentealba [1], B. Mitchell [3]
[1]Pontificia Universidad Católica de Valparaíso - Valparaíso (Chile), [2]Newcastle University - Newcastle upon Tyne (United Kingdom), [3]Universidad Andres Bello - Santiago (Chile)

Abstract
Spin-Crossover properties of homoleptic Iron(III) complexes containing two tridentate Schiff base ligands [FeN_4O_2] have been amply reported in the last decade[1]. However, to the best of our knowledge, few examples of a heteroleptic iron(III) coordination compound with Spin-Crossover (SCO) properties has been recently published[2]. According to this, and intending to develop new materials with SCO properties, we carried out the synthesis and characterisation of three new heteroleptic iron(III) [Fe(NSO)(N_2O)] **C1-3** coordination compounds. These complexes are the first complexes that contain tridentate organometallic Schiff base ligands derivate of ferrocenyl b-diketones.
The structural analysis, by single-crystal X-ray Diffraction, revealed that the structures of the compounds are isostructural and crystallize in the tetragonal space group I4/a, containing a molecule of the neutral Fe(III) complex in the asymmetric unit. In addition, this analysis showed that the metallic centre of iron is coordinated by the NSO atoms belonging to the organic ligand H_2thsa (thiosemicarbazone-salicylaldimine) L1 and the N_2O atoms corresponding to one of the different organometallic ligands **L2**. (**Fig 1**.). Regarding to this, the octahedral distortion parameters for **C1-3** exhibit large values, consistent with the high-spin electronic state (HS) of the Fe(III) complexes at 170K and 290K.
We are currently carrying out structural studies through XRD at 100K and magnetic properties through magnetic susceptibility, with the purpose of deepening key aspects that govern the structural and magnetic properties, crucial for the rational design of SCO systems.

References
[1] D.J. Harding, P. Harding, W. Phonsri, Coord. Chem. Rev. (2016) 313, 38–61.
[2] W. Phonsri, V. Martinez, C.G. Davies, G.N.L. Jameson, B. Moubaraki, K.S. Murray, Chem. Commun. (2016), 52, 1443–1446. W. Phonsri, L. C. Darveniza, S. R. Batten, K. S. Murray, Inorganics (2017), 5, 13747–13753.

Fig 1. Ball and Stick Diagram for C1-C3.

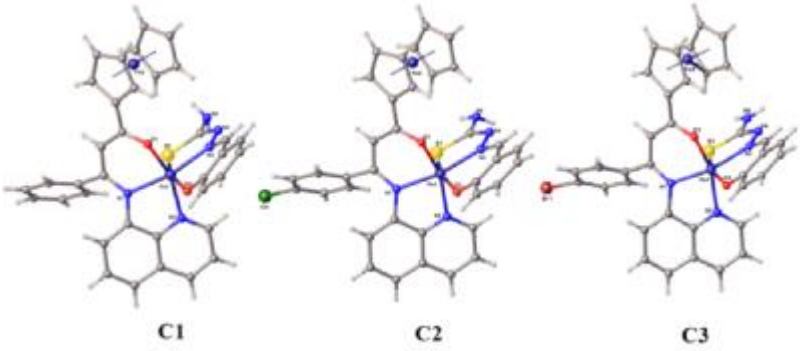

Back to Table of contents

MS13 Structural Characterization of Functional Materials

MS13-2-13 Tuning molecular crystallinity of vanadyl phthalocyanine (VOpc) layers for organic field effect transistors
#MS13-2-13

B.A. Paez-Sierra [1]
[1]Physics Department, Universidad Militar Nueva Granada, Campus Mueva Granada - Granada (Colombia)

Abstract
The effect of static magnetic fields on the molecular growth of vanadyl phthalocyanine (VOpc) layers was investigated. In order to probe device performance, organic field-effect transistors (OFETs) with bottom drain and source electrode configuration was carried out. OFET channels are formed with the organic semiconductor VOPc thin films with about 100 nm thickness. Organic molecules were grown under magnetic fields either parallel or perpendicular to the plane of the electrodes. The computed field-effect mobility was determined to be 2.40 cm2 V-1 s-1, 1.25 cm2 V-1 s-1, and 0.67 cm2 V-1 s-1 for VOpc layers under magnetic field parallel, perpendicular, and no field, respectively. Molecular orientation and crystallographic properties were investigated by polarized Raman spectroscopy measurements. The vibrational spectra reveal that for device production under a parallel magnetic field, VOpc molecules grow in the so-called face-to-face arrangement with the pc plane parallel to the substrate. VOpc layers grown under a magnetic field perpendicular to the substrate are face-to-face ordered with the pc plane tilted with respect to the source and drain plane. In the case of VOpc layers grown in absence of magnetic fields, molecules are face-to-face arranged with the pc plane parallel to the drain or source electrodes and tilted on the OFET channel.

Acknowledgments
This work was supported from funding provided by Vice-Rector for Research – Universidad Militar Nueva Granada, Campus Nueva Granada, grant number IMP-CIAS 3115.

References
Wang, Z., Lin, H., Zhang, X., Li, J., Chen, X., Wang, S., Gong, W., Yan, H., Zhao, Q., Lv, W., Gong, X., Xiao, Q., Li, F., Ji, D., Zhang, X., Dong, H., Li, L., & Hu, W. (2021). Revealing molecular conformation-induced stress at embedded interfaces of organic optoelectronic devices by sum frequency generation spectroscopy. Science advances, 7(16), eabf8555. https://doi.org/10.1126/sciadv.abf8555.

Back to Table of contents

MS13 Structural Characterization of Functional Materials

MS13-2-14 Development and characterization of electrospun nanofibers based on PCL and 4-chlorochalcone #MS13-2-14

D.M. Marulanda Cardona [1], M. Duarte Espinosa [1]
[1]Universidad Militar Nueva Granada - Bogota (Colombia)

Abstract
In this work, electrospun nanofibers mats based on poly caprolactone (PCL) and 3-(4-Chlorophenyl) -1-phenyl-2-propen-1-one (4-chlorochalcone) were developed. Chalcone family members, natural or synthetic, exhibit a wide variety of antibacterial, antiviral, anticancer and antidiabetic properties, among others [1]. 4-chlorochalcone is a chalcone derivative that is trans chalcone substituted by chloro group at position 4. The PCL nanofibrous mat containing 4-chlorochalcone was characterized using Scanning Electron Microscopy (SEM), Fourier Transform Infrared spectroscopy (FTIR), X-ray diffraction (XRD) and UV-visible spectroscopy (UV-vis). The results confirm the incorporation of 4-chlorochalcona into the matrix. The effect of 4-chlorochalcone concentration on the nanofiber mats morphology and crystallinity was studied.

References
[1] C. Zhuang, W. Zhang, C. Sheng, W. Zhang, C. Xing, Z. Miao, Chalcone: a privileged structure in medicinal chemistry, Chem Rev 117 (12) (2017) 7762-7810.

Back to Table of contents

MS13 Structural Characterization of Functional Materials

MS13-2-15 The synthesis and crystal structure of novel coordination polymers of cadmium(II) with hexamethylenetetramine ligand
#MS13-2-15

K. Nowakowska [1], M. Oszajca [1], W. Nitek [1], M. Gryl [1], M. Kozieł [1], W. Łasocha [2]
[1]Jagiellonian University, Faculty of Chemistry - Kraków (Poland), [2]Jagiellonian University, Faculty of Chemistry, J. Haber Institute of Catalysis and Surface Chemistry PAS - Kraków (Poland)

Abstract
Supramolecular chemistry is of great interest not only because of the rich architectural variety of compounds but also their unusual properties. Crystalline coordination polymers could have the potential application as molecular absorbents [1], heterogeneous catalysts [2], optical materials [3], gas storage substrates [4] and many more.
The most important element in the design of metal-organic crystalline phases is the choice of appropriate building blocks which symmetry and the ability to create specific interactions have a significant impact on the final product.
High symmetry ligands such as hexamethylenetetramine (hmt, urotropine) are of great significance to the design of novel metal – organic compounds. Urotropine has a considerable potential for application as a building block because of the four nitrogen atoms which are the metal ions coordination points and give the ability to create different coordination modes spanning from terminal monodentate to bridging bi-, tri-, and tetradentate. The topological features of urotropine and possibility of creating numerous intermolecular interactions increase the probability of obtaining coordination polymers with one-, two-, and tree-dimensional networks [5,6]. Divalent cadmium ions are one of the most commonly used metal ions in the design of coordination polymers due to their stable d^{10} closed-shell electron configuration. The associated absence of ligand field stabilization energy creates a specific coordination environment, ideal for the steric requirements imposed by a particular organic ligand. The lack of allowed d-d transitions facilitates optical properties such as luminescence [6,7] or, in the case of non-centrosymmetric compounds, provides a wide window for second harmonic generation experiments [8].
The result of this research are three novel multicomponent chemical compounds: $[Cd(hmt)_2(H_2O)_2Br_2]$ (**1**), $\{Cd_2(hmt)(H_2O)_2Br_4\}_n$ (**2**), $\{Cd_2(hmt)(DMF)Br_4\}_n$ 2n(DMF) (**3**). Two of them are coordination polymers with two- (**2**) and three-dimensional network (**3**). These products were obtained by the reaction of urotropine with cadmium bromide in the presence of three different solvents: isopropanol (**1**), ethanol (**2**) and N, N - dimethylformamide (DMF) (**3**). The interesting structural motifs stabilized by numerous hydrogen bonds are observed in the obtained coordination polymers. Hirshfeld surface analysis was applied to analyze the differences between the intermolecular interactions in obtained compounds.

References
[1] B. Parmar, K.K. Bisht, G. Rajput, E. Suresh, *Dalton Trans.*, (**2021**),50, 3083-3108
[2] P. Valvekens, F. Vermoortele, D. De Vos, *Catal. Sci. Technol*., (**2013**),3, 1435-1445
[3] Y. Zheng, Fang-Zhou Sun, X. Han, Jialiang Xu, Xian-He Bu, *Advanced Optical Materials*, (**2020**), 8,13, 2000110
[4] Hao Li, Libo Li, Rui-Biao Lin, Wei Zhou, Z. Zhang, S. Xiang, B. *Chen, Energy Chem.*, (**2019**),1, 1, 100006
[5] S. Hazra, B. Sarkar, S.Naiya, M.G.B. Drew, A. Ghosh, *Inorganica Chimica Acta*, (**2013**), 402, 12-19
[6] Yan Bai, Wei-Li Shang, Dong-Bin Dang, Ji-De Sun, Hui Gao, *Spectrochimica Acta*, (**2009**) 407–411
[7] A. Lan, Lei Han, D. Yuan, F. Jiang, M. Hong, *Inorganic Chemistry Communications*, (**2007**), 10, 9, 993-996
[8] N. Arunadevi, P. Kanchana, V. Hemapriya, S.S. Sankaran, M. Mayilsamy, P.D. Balakrishnan, Ill-Min Chung, P. Mayakrishnan, *Journal of Dispersion Science and Technology*, (**2021**), 1-18

Crystal structure of obtained compounds:1, 2, 3.

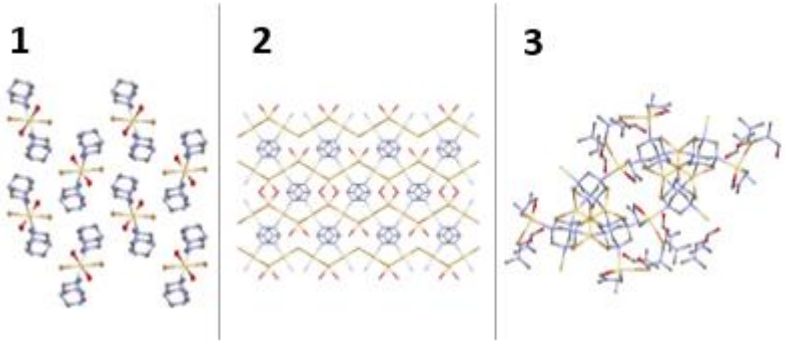

Back to Table of contents

MS13 Structural Characterization of Functional Materials

MS13-2-16 Li2IrO3 and KxLi2-xIrO3 - (Re)investigating magnetism-chemistry relationships in layered honeycomb iridates
#MS13-2-16

B. Gade [1], A. Gibbs [1]
[1]University of St Andrews - St Andrews (United Kingdom)

Abstract
The group I iridates – A2IrO3 – are one class of exotic magnets (specifically quantum spin liquid candidates following what's called the Kitaev model). Just like the other materials, these iridates suffer from innate defects, which in the alpha-polymorph of the Li-based compound show up most typically in the form of stacking faults. We have synthesised a range of samples with different stacking fault levels, under different atmospheres and doped with potassium - all of these show differing magnetic features.

References
T. Takayama, A. Krajewska, A. Gibbs, H. Takagi et al., Phys. Rev. B 99, 125127 (2019).
F. Bahrami et al., Phys. Rev. B 103, 094427 (2021)
H.Takagi et al., Nat Rev Phys 1, 264–280 (2019)
Sungkyun Choi et al., Phys. Rev B 99, 054426 (2019)
Freund, F. et al., Sci. Rep. 6, 35362 (2016)

Influence of atmosphere on mag. susceptibility

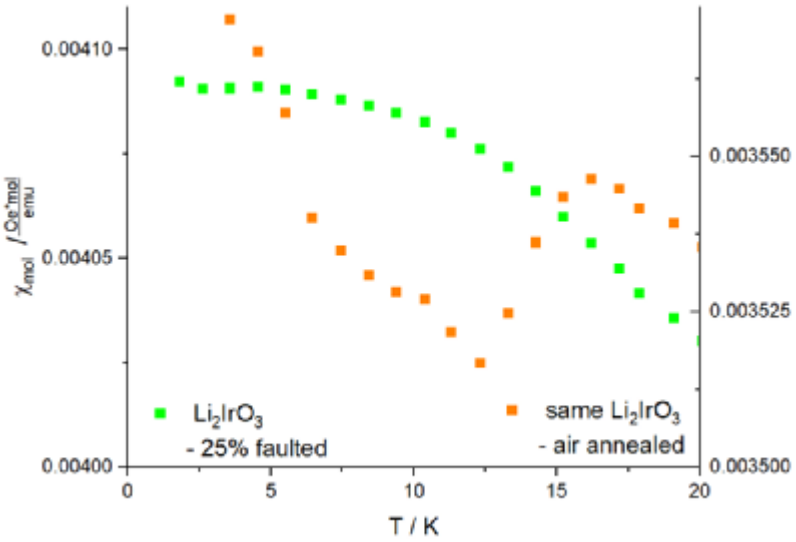

Effect of K-doping on Li2IrO3

Back to Table of contents

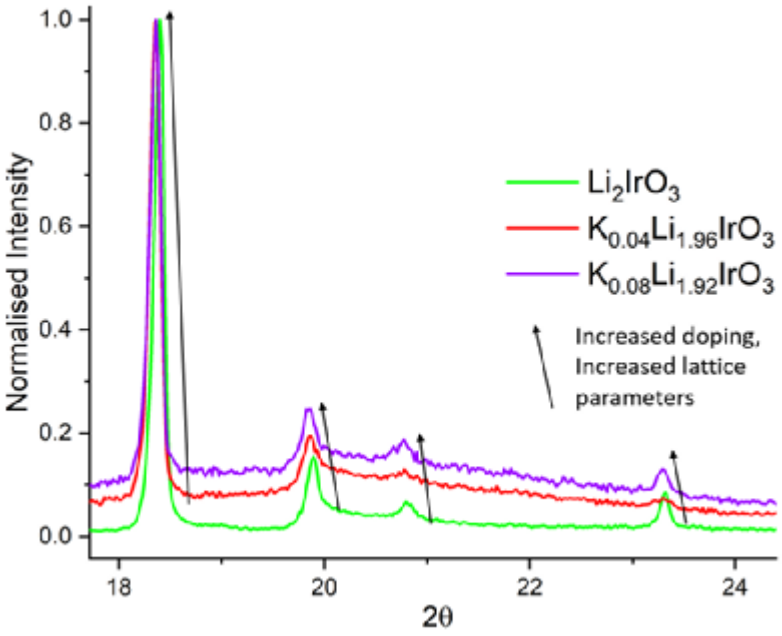

Back to Table of contents

MS13 Structural Characterization of Functional Materials

MS13-2-17 Engineered growth of polycrystalline amino acid films for eco-friendly piezoelectric sensing #MS13-2-17

K. Hari [1], S. Guerin [1]
[1]UNIVERSITY OF LIMERICK - LIMERICK (Ireland)

Abstract
In the past ten years, biological piezoelectric materials have emerged as the potential next generation of cost-effective, green electromechanical sensors[1, 2]. The piezoelectric voltages produced under an applied force are inversely proportional to the dielectric constant of the material and so even 'weak' organic piezoelectrics (with modest piezoelectric constants compared to inorganic ceramics[3, 4]), can generate large voltages in response to strain. Amino acids are the simplest biological units, and are inexpensive and easy to crystallise[5-7], and demonstrate measurable piezoelectricity in single crystal[8-10] and polycrystalline forms[11, 12].
Recently we have experimentally validated flexible glycine-based sensors for pipe leak detection and monitoring in real-time, for a variety of flow rates and leak sizes using a custom fluid test rig developed for the validation of PVDF patches[13]. This is the first time that glycine crystals have been grown and characterised as a high-concentration, polycrystalline aggregate for piezoelectric sensing[14]. However a key limitation of this study is that the piezoelectric response of the film was less than that of glycine single crystals due to the random orientation of glycine crystallites[11].
In this work, we will systematically study the effect of crystallisation growth parameters on a number of polycrystalline amino acid films in order to modulate the piezoelectric response and increase the detection sensitivity and voltage output of amino acid-based piezoelectric devices. Further, we will investigate how the use of multi-scale molecular modelling can help us to understand and design the polycrystalline amino acid films and emphasise the potential of computation guided crystal engineering to screen several candidate structures for optimised crystallisation properties that could be utilised for eco-friendly energy harvesting applications.

References
1. Guerin, S.; Tofail, S. A.; Thompson, D., Organic piezoelectric materials: milestones and potential. *NPG Asia Materials* **2019**, *11* (1), 1-5.

2. Chorsi, M. T.; Curry, E. J.; Chorsi, H. T.; Das, R.; Baroody, J.; Purohit, P. K.; Ilies, H.; Nguyen, T. D., Piezoelectric biomaterials for sensors and actuators. *Advanced Materials* **2019**, *31* (1), 1802084.

3. Zhang, S.; Xia, R.; Shrout, T. R., Lead-free piezoelectric ceramics vs. PZT? *Journal of Electroceramics* **2007**, *19* (4), 251-257.

4. Panda, P.; Sahoo, B., PZT to lead free piezo ceramics: a review. *Ferroelectrics* **2015**, *474* (1), 128-143.

5. Vijayan, N.; Rajasekaran, S.; Bhagavannarayana, G.; Ramesh Babu, R.; Gopalakrishnan, R.; Palanichamy, M.; Ramasamy, P., Growth and characterization of nonlinear optical amino acid single crystal: L-alanine. *Crystal growth & design* **2006**, *6* (11), 2441-2445.

6. Hod, I.; Mastai, Y.; Medina, D. D., Effect of solvents on the growth morphology of DL-alanine crystals. *CrystEngComm* **2011**, *13* (2), 502-509.

7. Moitra, S.; Kar, T., Growth and characterization of L-valine-a nonlinear optical crystal. *Crystal Research and Technology: Journal of Experimental and Industrial Crystallography* **2010**, *45* (1), 70-74.

8. Guerin, S.; Stapleton, A.; Chovan, D.; Mouras, R.; Gleeson, M.; McKeown, C.; Noor, M. R.; Silien, C.; Rhen, F. M.; Kholkin, A. L., Control of piezoelectricity in amino acids by supramolecular packing. *Nature materials* **2018**, *17* (2), 180-186.

9. Kumar, R. A.; Vizhi, R. E.; Vijayan, N.; Babu, D. R., Structural, dielectric and piezoelectric properties of nonlinear optical γ-glycine single crystals. *Physica B: Condensed Matter* **2011**, *406* (13), 2594-2600.

Back to Table of contents

10. Heredia, A.; Meunier, V.; Bdikin, I. K.; Gracio, J.; Balke, N.; Jesse, S.; Tselev, A.; Agarwal, P. K.; Sumpter, B. G.; Kalinin, S. V., Nanoscale ferroelectricity in crystalline γ-glycine. *Advanced Functional Materials* **2012**, *22* (14), 2996-3003.

11. Guerin, S.; Tofail, S. A.; Thompson, D., Longitudinal Piezoelectricity in Orthorhombic Amino Acid Crystal Films. *Crystal Growth & Design* **2018**, *18* (9), 4844-4848.

12. Guerin, S.; O'Donnell, J.; Haq, E. U.; McKeown, C.; Silien, C.; Rhen, F. M.; Soulimane, T.; Tofail, S. A.; Thompson, D., Racemic amino acid piezoelectric transducer. *Physical review letters* **2019**, *122* (4), 047701.

13. Okosun, F.; Cahill, P.; Hazra, B.; Pakrashi, V., Vibration-based leak detection and monitoring of water pipes using output-only piezoelectric sensors. *The European Physical Journal Special Topics* **2019**, *228* (7), 1659-1675.

14. Okosun, F.; Guerin, S.; Celikin, M.; Pakrashi, V., Flexible amino acid-based energy harvesting for structural health monitoring of water pipes. *Cell Reports Physical Science* **2021**, *2* (5), 100434.

Back to Table of contents

MS13 Structural Characterization of Functional Materials

MS13-2-18 Complex Magnetic Behavior in Rare Earth Rich Magnetocaloric Materials - R_3T
#MS13-2-18

S. Goswami [1], P.D. Babu [2], R. Rawat [3]
[1]Institute of Physics of the Czech Academy of Sciences - Prague (Czech Republic), [2]UGC DAE Consortium for Scientific Research, Mumbai Centre - Mumbai (India), [3]UGC DAE Consortium for Scientific Research - Indore (India)

Abstract
Rare earth rich intermetallic compounds of the type R_3T (R = rare earth, T = transition metal) are found to be very intersting class of materials as far as their complex magnetic structure is concerned. Tb_3Co is one such compound that orders antiferomagnetically below T_N = 84 K (Fig. 1) and goes through a first order transition below ~72 K (T_{FO}). In spite of the several studies attempted on this compound a sharp phase transition like feature (seen in ZFC magnetization) around 30 K was never got any proper explanation. From our temperature dependent neutron diffraction data (Fig. 2) it was found that the magnetic structure of this compound below 70 K remains unchanged. Rietveld refinement analysis confirmed that the phase transition like feature is mainly associated with the change in strength of spin-lattice coupling from weaker to stronger with decrease in temperature and it was never a real phase transition. [1] Besides, the analyses of the frequency dispersed linear and non-linear ac -susceptibility data confirms that the magnetic state below T_{FO} is coexisting with a spin-glass like phase and the glass temperature was found to coincide with T_{FO}. [1]
Further, this spin glass like behaviour in Tb_3Co persists even in the presence of external pressure up to P ~ 1 GPa although the glassiness was found to be weakened enough at P = 0.69 Gpa. Any furhter increase in pressure has negligible effect on the glassiness. [2] However, application of pressure shifts the magnetic transitions to lower temperature (T_N by 6 K, T_{FO} by 15 K, low temperature transition like feature by 3 K) and modulates the magnetic structure as well. In addition, the magnetocaloric effect (MCE) of Tb_3Co was improved by 37% in presence of pressure. [3]
Interstingly, other R_3T compounds (Ho_3Co, Dy_3Co, Dy_3Ni) was also examined and it was observed that R_3T compounds exhibit highly complex magnetic strucuture. The degree of complexity also varies with different R atom. The spin glass like state is found to be present in all these compositions, coexisting with long range magnetic order. This feature sustains even in presence of external pressure up to 1 Gpa. Low symmetry crystalline electric field plays a crusial role in magnetism of these materials. R_3T compounds can be used as potential magnetocalric material at lower tempearature and the enhancement in MCE in Tb_3Co with pressure can be realized in practice by some suitable chemical substitution.

References
[1] S. Goswami, P. D. Babu, R. Rawat, J. Phys. Condens. matter 2019. 31, 445801.
[2] S. Goswami, P. D. Babu, R. Rawat, J. Phys. Condens. matter 2019, 31, 505802.
[3] S. Goswami, P. D. Babu, R. Rawat, J. Phys. Condens. matter 2020, 32, 365803.

ZFC – FC of Tb3Co

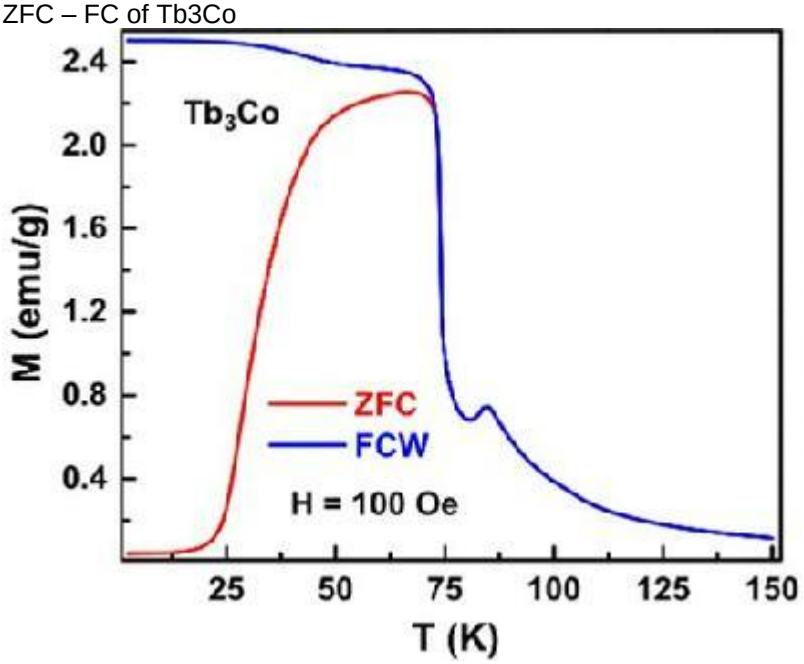

Back to Table of contents

Temperature dependent ND pattern of Tb3Co

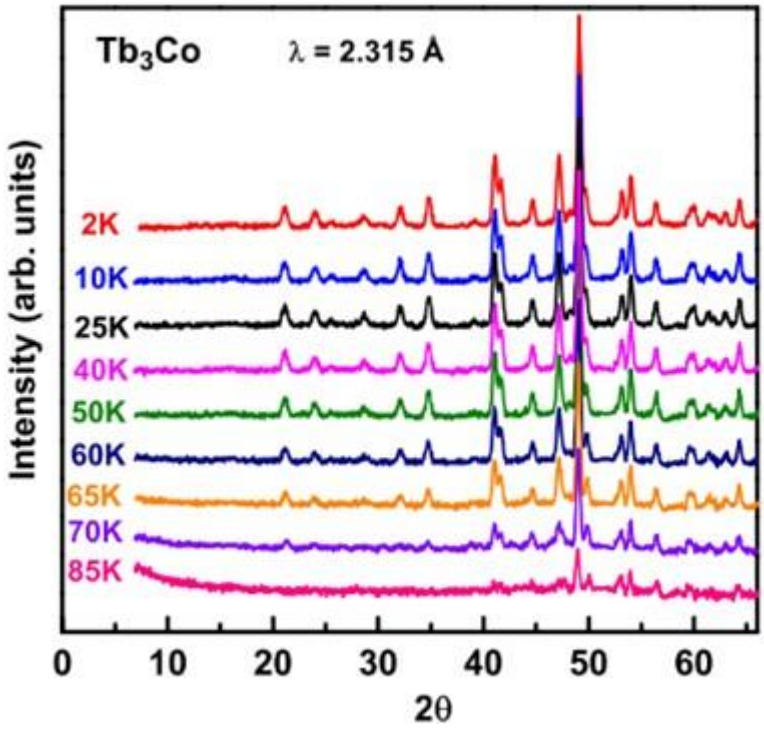

Back to Table of contents

MS13 Structural Characterization of Functional Materials

MS13-2-19 Perfluoroalkylation of the arenes by ligand-less Ni catalyst approach: new crystal structures of perfluorinated drug-derived molecules.
#MS13-2-19

S. Deolka [1], J. Khusnutdinova [1], E. Khaskin [1], S. Vasylevskyi [1]
[1]OIST, Okinawa Institute of Science and Technology Graduate University Onna-son, Kunigami-gun, Okinawa, Japan, 904-0495 - Okinawa (Japan)

Abstract
The synthetic strategy of perfluoroalkylation of the arenes is important for further improvement of the medical properties of the arene-derived drugs. Incorporation of fluoroalkyl groups can drastically change polarity and thus permeation of the drugs through blood-cell-brain barriers [1]. In addition, perfluoroalkylation enchances a methabolitic half-life by inhibiting drug degradation, resulting in long-lasting drug effects [2]. Nowadays there are only a few examples of perfluoroalkylation of arenes which involves, in rather complex synthetic routes, and the use of expensive metal-based catalysts [3]. Many approaches are energy inefficient for fluoralkylation and normally require a high temperatures 80-130 ºC, strong UV-irradiation, expensive ligands or additives to promote the reaction [4]. Herein we show ligand-free, room temperature, no additional light irradiation requires nickel-catalyzed perfluoalkylation of the arenes with high yields up to 95%. The highly efficient perfluoalkylation mechanism of the reaction will also be discussed, as well as intermediate products (Figure 1). The ligand-free Ni-catalyst is a simple fluoroalkylating Ni-precursor that can be easily prepared and the source of the fluoroalkyls is the commercially available Togni reagent. The single crystal X-Ray structures of the perfluoalkylated arenes with C_2F_5/C_3F_7-groups were obtained for the first time and will be presented at ECM33 (Figure 2).

References
[1]. F. D'Accriscio, P. Borja, N. Saffon-Merceron, M. Fustier-Boutignon, N. Mézailles, N. Nebra, Angewandte Chemie International Edition, **2017**, 56, 12898-12902
[2]. L. Amini-Rentsch, E. Vanoli, S. Richard-Bildstein, R. Marti, G. Vilé, Industrial & Engineering Chemistry Research, **2019**, 58, 10164-10171.
[3]. X. Zhao, D. W. C. MacMillan, Journal of the American Chemical Society, **2020**, 142, 19480-19486.
[4]. S. Zhang, N. Rotta-Loria, F. Weniger, J. Rabeah, H. Neumann, C. Taeschler, M. Beller, Chemical Communications, **2019**, 55, 6723-6726.

Proposed radical pathway for perfluoroalkylation

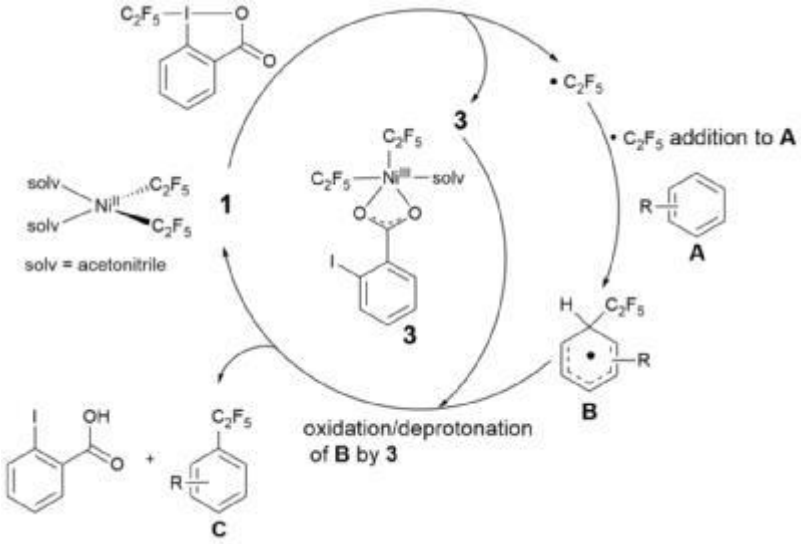

Substrates obtained by ligand-free Ni-catalyst.

Back to Table of contents

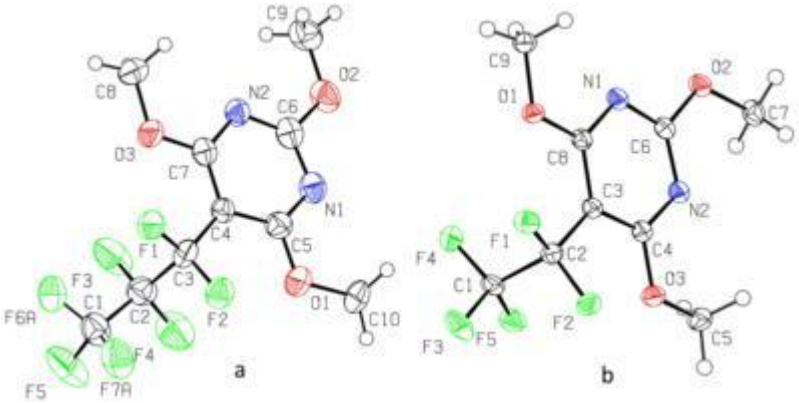

Back to Table of contents

MS13 Structural Characterization of Functional Materials

MS13-2-2 Crystal engineering of charge transfer complexes with TMPD (Wurster's blue) as electron donor and quinones as electron acceptors
#MS13-2-2

P. Stanic [1], K. Molčanov [1]
[1]Ruđer Bošković Institute - Zagreb (Croatia)

Abstract
Charge transfer complexes are systems of two or more molecules in which portion of charge is transferred between molecular units. Such complexes are stabilized by the electrostatic attraction between electron-rich donors and electron-deficient acceptors.[1] One of the well-known electron donors is N,N,N′,N′-tetramethyl-p-phenylenediamine (TMPD).[2] TMPD or Wurster's blue can form charge-transfer complexes as a radical cation with electronegative quinones or semiquinone radical anions (e.g. tetracyanoquinone and tetrachlorquinone).[3] Interest in charge-transfer complexes can be attributed to their conductive properties as well as their stability, interesting intermolecular interactions between components and easy preparation.
Here we report a study on π-stacking and multicentric bonding in charge-transfer complexes with partially charged TMPD radical cation. We have prepared a series of co-crystals of TMPD and different quinones; 2,3-dicyano-5,6-dichloroquinone (1), tetrafluorquinone (2), tetrachlorquinone (3), tetrabromquinone (4), 7,7,8,8-tetracyanoquinodimethane (5) and 2,3,5,6-tetrafluoro-7,7,8,8-tetracyanoquinodimethane (6). These systems were studied by means of variable-temperature crystallography (80 - 400 K) and X-ray charge density. Complexes of TMPD with 3 and 5 have been observed previously.[3] In prepared charge transfer compounds stacking interactions between TMPD and quinone molecules are present. There are three types of stacks observed (Figure 1.). First, in co-crystals with 1, 3, 4 and 5 moieties form equidistant stacks of alternating TMPD and quinones. The second type is pancake-bonded dimers of TMPD and quinone in complex with 2. And in co-crystal with 6 moieties form 2D arrays of alternating TMPD and quinone molecules. For crystals of TMPD with 3 and 4, a polymorphic phase transition at lower temperature was observed when moieties change the type of stacking to the second type mentioned, pancake-bonded dimers.
This work was funded by the Croatian Science Foundation, grant IP-2019-04-4674.

References
1. H. J. Wörner, C. A. Arrell, N. Banerji, et al., Struct. Dyn. 4, 061508 (2017)2. Wurster C.; Schobig E., Ber. Dtsch. Chem. Ges., 1879, 12, 1807-1813.3. de Boer J. L.; Vos A., Acta Crystallogr. B, 1968, B24, 720-725; Hanson A. W., Acta Crystallogr. B, 1968, B24, 768-778.

Three types of stacking in co-crystals of TMPD

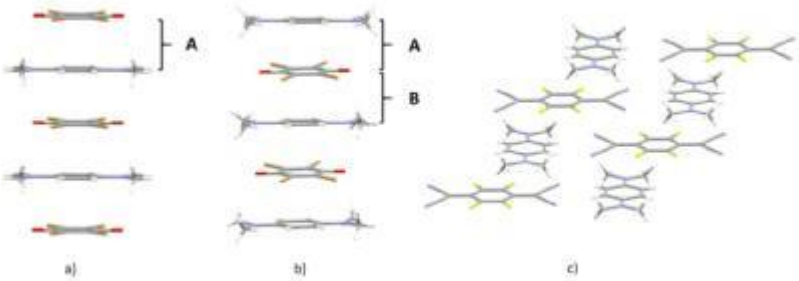

Back to Table of contents

MS13 Structural Characterization of Functional Materials

MS13-2-20 Thermodiffractometry study of $(NH_4)_{0.5}Co_{1.25}(H_2O)_2[BP_2O_8].(H_2O)_{0.5}$ with CZP framework topology #MS13-2-20

W. Mogodi [1], D. Billing [2], M. Fernandes [2], A. Fitch [3]
[1]Department of Chemistry, University of Cape Town - Cape Town (South Africa), [2]School of Chemistry, University of the Witwatersrand - Johannesburg (South Africa), [3]cEuropean Synchrotron Radiation Facility (ESRF) - Grenoble (France)

Abstract
Four CZP (chiral zincophosphate) zeolite topology compounds with the general formula $M^{I}M^{II}(H_2O)_2[BP_2O_8].yH_2O$ (M^{I} = Na, NH_4 and M^{II} = Mn, Co, y = 0.5, 1) have been prepared under mild hydrothermal conditions (at 180 °C). Such microporous compounds with aesthetically interesting crystal structures [1] can have interests in fields such as catalysis, storage, separation and ion-exchange. One compound of this family, $(NH_4)_{0.5}Co_{1.25}(H_2O)_2[BP_2O_8].(H_2O)_{0.5}$, has been studied by variable temperature high resolution powder X-ray diffraction experiments carried out from 298 to 1073 K. Complete Rietveld refinements were achieved by combining stereochemical restraints of the powder diffraction data. At room temperature, this compound crystallizes in the $P6_5$ (No. 170) space group with Z = 4 belonging to the hexagonal system. The unit cell parameters obtained were: a = 9.4330(2) Å, c = 15.5203(2) Å, V = 1196.01(5) $Å^3$. The crystal structure consists of a helical anionic framework, $\infty[BP_2O_8]^{3-}$, composed of corner sharing BO_4 and PO_4 tetrahedra. Water and ammonia molecules are found within the helical channels running along the [001] direction. This compound undergoes a series of dehydration, de-ammoniation (analysis augmented by thermogravimetric experiments) and finally diminished sharp Bragg peaks indicating loss of long-range order. Total scattering analysis [2] was applied for the first time coupled to the above conventional structural refinement approach to further unravel this gaseous dissociation and temperature induced amorphization of the rigid host structure. Preliminary X-ray PDF indicates that the local coordination environment found in the low temperature crystalline phases also persists in the amorphous phase.

References
[1] Kniep, R., Will, H.G., Boy, I. and Röhr, C. Angewandte Chemie International Edition, 1997, 36, 1013.
[2] Egami, T. and Billinge, S.J. Elsevier, 2003.

Diffraction behaviour of helical borophosphates

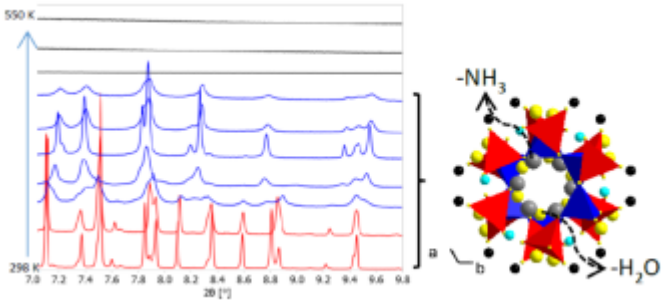

Back to Table of contents

MS13 Structural Characterization of Functional Materials

MS13-2-21 A structural study by single-crystal X-ray diffraction of iron(III) [Fe(5-X-Salmeen)$_2$]BF$_4$ #MS13-2-21

N. Nilo [1], M.A.U.R.I. Fuentealba [1], V. Artigas [1]
[1]Pontificia Universidad Católica de Valparaíso - Valparaíso (Chile)

Abstract
Spin-crossover (SCO) compounds are switchable between two electronic spin states, Low spin (LS) and High spin (HS). In general, the switching process in solid-state systems is controlled by cooperative intermolecular interactions.[1]
The correlation of structure with physical properties is crucial for identifying these interactions and ultimately understanding the complex processes controlling the SCO phenomenon.
Against this background, we carried out the synthesis and characterization of two coordination compounds candidates for SCO phenomenon, [Fe(5-Cl-Salmeen)$_2$]BF$_4$ and [Fe(5-Br-Salmeen)$_2$]BF$_4$, where substituted Salmeen result from the Schiff-base condensation of substituted salicylaldehyde with N-methylethylenediamine.
The structural study was performed by single-crystal X-ray diffraction for five temperatures between 170 to 293K, revealing that coordination compound cations 1-2 (Fig. 1) are isostructural with N4O2 donor atom set from tridentate ligands forming a distorted octahedron around the Fe(III) ion.
Both complexes crystallize in the monoclinic spacial group P21/n, containing two molecules of the cationic Fe(III) complex (Z'=2), where fragment 1 and fragment 2 have a different octahedral distortion, fragment 1 exhibits large values, consistent with the HS at 170 - 293K (Fig.2). While fragment 2 displays small values at 170K and high values at 293K, consistent with LS and HS states, respectively.
For both cases, the studies of the intermolecular interaction reveal differences in the percent of H-X, X-X, and X-F interactions between fragments 1 and 2.
Finally, the complex has been compared with the reported isostructural complex [Fe(5-Br-Salmeen)$_2$]ClO$_4$.[2]

References
[1] K. Ridier, G. Molnár, L. Salmon, W. Nicolazzi y A. Bousseksou. "Hysteresis, nucleation and growth phenomena in spin-crossover solids". Solid State Sciences 74 (2017), A1-A22. Doi: 10.1016/j.solidstatesciences.2017.10.014.[2] M. Wang, G Lee, Y. Wang, T. Dong y H. Wei. "Structure, magnetic properties, Mössbauer and catalase-like activity of spin crossover iron(III) complexes with salicylaldimine ligands". Journal of the Chinese Chemical Society 49(5) (2002), 825-832. Doi: 10.1002/jccs.200200118.

ORTEP diagram for fragment 1 of complexes 1 and 2.

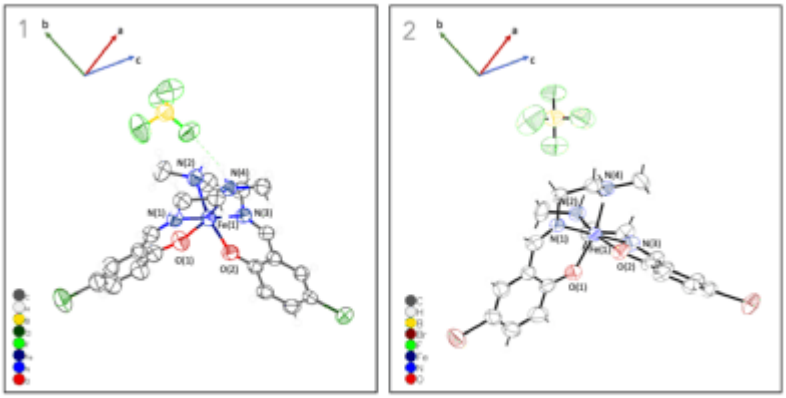

Multi-scale representation of structural changes

Back to Table of contents

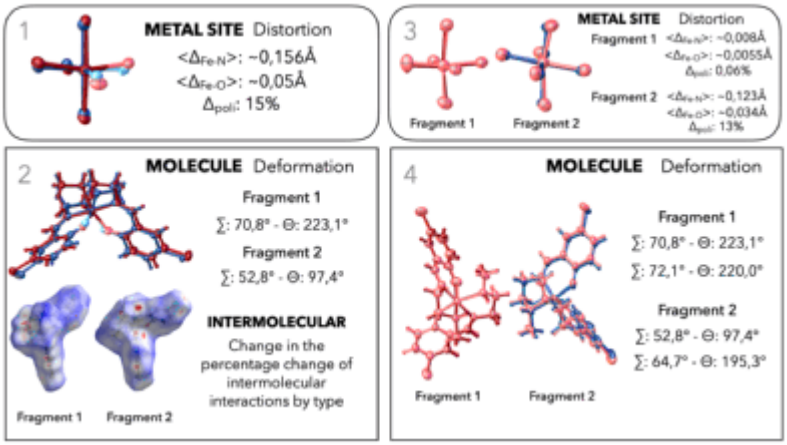

Back to Table of contents

MS13 Structural Characterization of Functional Materials

MS13-2-3 Structural and Magnetic Properties of the Oxalate-Based [CuIICrIII] Complexes: the Influence of the Tridentate Ligand and Simple Anions
#MS13-2-3

L. Molčanov [1], P. Šenjug [2], D. Barišić [2], D. Pajić [2], K. Molčanov [1], M. Jurić [1]
[1]Ruđer Bošković Institute - Zagreb (Croatia), [2]Faculty of Science - Zagreb (Croatia)

Abstract
Design of new materials with targeted physical properties is a very atractive field of research nowadays. In recent years, the structural diversity of metal-organic coordination systems has paved the way for the development of multifunctional materials that combine two or more different properties, especially magnetic and electrical ones. A very important role in the design and synthesis of such materials belongs to the oxalate moiety, $C_2O_4^{2-}$, due to its various possibilities of coordination to metal centres and its ability to mediate electronic effects between paramagnetic metal ions. The synthetic strategy for the preparation of (hetero)polynucelar species is "building block chemistry", in which a molecular anionic ligand, very often the tris(oxalato)metalate anion $[M^{III}(C_2O_4)_3]^{3-}$ (M^{III} = Cr, Fe, Ru, Rh, Mn or V), is used as a ligand towards other metal cations. Starting from the same reactants, the structural uncertainty of the obtained coordination compounds can lead to two basic cases: (i) both the structures and the chemical compositions are different; the obtained compounds differ significantly from each other, reflecting the great versatility of a self-assembly system; (ii) the structures are different, but the whole coordination networks have the same chemical composition, when the obtained compounds are classified as supramolecular isomers.[1]

Inspired by the structural versatility of oxalate-based [CuFe] compounds containing 2,2':6',2''-terpyridine (terpy)[2], seven novel oxalate-based [CuIICrIII] compounds: $[Cu_4(terpy)_4Cl_5][Cr(C_2O_4)_3]\cdot 9H_2O$ (1; terpy = 2,2′:6′,2″-terpyridine), $\{[Cr_2Cu_4(H_2O)_2(terpy)_4(C_2O_4)_7]\cdot 10H_2O\}_n$ (2), $[Cr_2Cu_4(H_2O)_2(terpy)_4(C_2O_4)_7]\cdot 12H_2O$ (3), $[Cu(H_2O)_3(terpy)][CrCu(H_2O)(terpy)(C_2O_4)_3]_2\cdot 9H_2O$ (4), $[Cu(H_2O)(terpy)(NO_3)][CrCu(H_2O)(terpy)(C_2O_4)_3]\cdot 6H_2O$ (5), $[CrCu_2(terpy)_2(C_2O_4)_3(NO_3)_2]\cdot 1.5H_2O\cdot CH_3OH$ (6) and $[Cr_2Cu_4(H_2O)_4(terpy)_4(C_2O_4)_6][Cr_2Cu_2(terpy)_2(C_2O_4)_6]\cdot 10H_2O$ (7) were obtained from the reaction of an aqueous solution of the building block $[Cr(C_2O_4)_3]^{3-}$ and a methanol solution containing Cu^{2+} ions and the terpyridine ligand by the layering technique. Interestingly, changing only the anion of the starting salt of copper(II), NO_3^- instead of Cl^-, resulted in an unexpected change in the bridge type, oxalate (compounds 2−7) versus chloride (compound 1), which affected the overall structural architecture. Compounds were studied by single-crystal X-ray diffraction, IR spectroscopy, magnetization measurements and density functional theory (DFT) calculations.

References
[1] J.-P. Zhang, X.-C. Huang and X.-M. Chen, Supramolecular isomerism in coordination polymers, Chem. Soc. Rev., 2009, 38, 2385–2396.
[2] L. Kanižaj, D. Barišić, F. Torić, D. Pajić, K. Molčanov, A. Šantić, I. Lončarić and M. Jurić, Structural, Electrical, and Magnetic Versatility of the Oxalate-Based [CuFe] Compounds Containing 2,2′:6′,2″-Terpyridine: Anion-Directed Synthesis, Inorg. Chem., 2020, 59, 18078–18089.

Back to Table of contents

MS13 Structural Characterization of Functional Materials

MS13-2-4 High brightness MetalJet x-ray source for MOFs/COFs structure determinations #MS13-2-4

J. Hållstedt [1], E. Espes [1]
[1]Excillum - Kista (Sweden)

Abstract
Organic Frameworks is the 3D porous materials that have been rapidly developed since 21st century, among which metal organic frameworks (MOFs) is so far the most well-known category in the family of organic frameworks. In recent decades, covalent organic frameworks (COFs) have also shown the great potential in the applications of gas absorption, chemical separation, catalysis, and energy storage and conversion, etc. Such applications are closely related to the physical and chemical properties of MOFs and COFs, which are determined by their crystal structures. Therefore, understanding the structure-property relationships from the level of atomic arrangement becomes crucial for a desired application. However, due to the interplay of nucleation and crystal growth processes, numerous cases have shown that it is often not easy to obtain large enough and well-ordered MOFs/COFs crystals for conventional in-house single crystal x-ray diffraction (SC-XRD) experiment. On the other hand, many MOFs/COFs crystals are relatively instable which undergo quick structure transitions during the SC-XRD data collections.

Therefore, high-end SC-XRD techniques for small size crystals such as MOFs/COFs are in high demand to overcome the above-mentioned challenges, which rely heavily on the x-ray source brightness for high-resolution data and short data collection time. Traditional solid or rotating anode x-ray tubes are typically limited in brightness by when the e-beam power density melts the anode. This limit is overcome by the liquid-metal-jet anode technology that has demonstrated brightness in the range of one order of magnitude above current state-of-the art solid anode sources. This is possible due to the regenerative nature of this anode and the fact that the anode is already molten, which allows for significantly higher e-beam power density compared to conventional solid anodes.

Over the last years, the liquid-metal-jet technology has developed from prototypes into fully operational and stable X-ray tubes running in more than 100 labs over the world, among which many researchers are focusing on the structure determinations of MOFs/COFs using SC-XRD since this application benefits greatly from small spot-sizes, high-brightness in combination with a need for stable output. To achieve a single-crystal-diffraction platform addressing the needs of the most demanding crystallographers, multiple users and system manufacturers has since installed the MetalJet x-ray source into their SCD set-ups with successful results.

This contribution reviews the evolvement of the MetalJet technology specifically in terms of flux and brightness and its applicability for pushing boundaries of what is possible in the home lab. Recent user examples will illustrate how the MetalJet has enabled faster turnaround time of research and also enabled easy and convenient 24/7 access to the highest quality of crystallography data.

Back to Table of contents

MS13 Structural Characterization of Functional Materials

MS13-2-5 Characterisation by X-Ray diffraction of Bidentate and Tridentate PCP and PCN NHC Core Pincer-Type Mn(I) Complexes
#MS13-2-5

C. Duhayon [1], R. Buhaibeh [1], D. Valyaev [1], J.B. Sortais [1], Y. Canac [1]
[1]LCC CNRS - Toulouse (France)

Abstract
Following the early generation of phosphines, N-heterocyclic carbenes (NHCs) have attracted much attention, leading to remarkable advances in different areas, such as organometallic chemistry, functional materials, and homogeneous catalysis. We turned our attention to the preparation, the coordinating properties, of novel NHC core tridentate ligands bearing phosphine and pyridine donor arms.
While only bidentate coordination was observed in all formed neutral Mn(I) complexes, a notable difference in the coordination mode was observed between two ligands bearing a pyridine extremity. When the pyridine is directly connected to the imidazole core, two isomeric complexes [1] and [2] were evidenced due to the possible formation of two thermodynamically favored five-membered metallacycles upon coordination of the phosphine or the pyridine arms. By contrast, when the pyridine is not directly connected, only bidentate complex [3] resulting from the concomitant coordination of NHC and PPh_2 donor units was observed, the coordination of pyridine would indeed have led to a less stable six-membered metallacycle.
On the other hand, cationic tridentate complexes [4](OTf), [5](OTf), and [6](OTf) were easily obtained as single isomers. These compounds are rare examples of NHC-containing manganese complexes pincer-type and constitute the first prototypes based on NHC core L_3-type ligand scaffolds.
The complete series of bi- and tridentate Mn(I) species have been fully characterized and systematically studied by single-crystal X ray diffraction. These studies allowed us to establish the solid-state structures of neutral bidentate Mn(I) complexes [1], [2], and [3] and their cationic tridentate congeners ([4](OTf), [5](OTf) and [6](OTf)). In all complexes, the hexacoordinate Mn(I) atom resides in a distorted octahedral environment. Three carbonyl coligands adopt a facial arrangement in all bidentate representatives. In the tridentate series, complexes [4](OTf) and [5](OTf) can be regarded as real pincers exhibiting the meridional coordination of the NHC core ligand with two CO coligands positioned in trans with respect to each other, while in [6](OTf) the PCN backbone acts as a tripodal ligand with the three CO coligands located cis to each other. Moreover, X-ray analyses reveal two different coordination modes for the nonsymmetrical PCN ligands in complexes mer-[$Mn(CO)_3(\kappa^3P,C,N)$](OTf) ([5](OTf)) and fac-[$Mn(CO)_3(\kappa^3P,C,N)$](OTf) ([6](OTf)) rationalized by the higher flexibility of ligand with CH_2Py extremity in the latter case.

References
Cationic PCP and PCN NHC Core Pincer-Type Mn(I) Complexes: From Synthesis to Catalysis
Organometallics 2021, 40, 231−241.
Ruqaya Buhaibeh, Carine Duhayon, Dmitry A. Valyaev, Jean-Baptiste Sortais, and Yves Canac

Figure 1. Perspective views of bidentate ([1], [2]

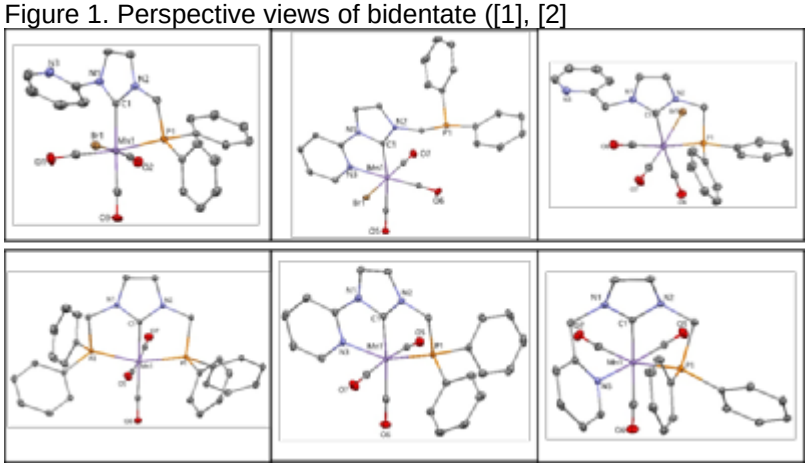

Back to Table of contents

MS13 Structural Characterization of Functional Materials

MS13-2-6 Comparative photocrystallographic study using CW and Pulse Laser irradiation on a photo-switchable ruthenium nitrosyl complex
#MS13-2-6

A. Hasil [1], K. Aleksander [1], S. Pillet [1], E. Wenger [1], D. Schaniel [1]
[1]University de Lorraine Nancy France - VANDOEUVRE-Les-Nancy (France)

Abstract
With the growing emphasis in solid state materials, Photoinduced linkage isomers (PLI) in nitrosyl complexes has been the subject of interest owing to its application as photoswitches. The generation of these PLI is induced by the photochromic and photorefractive response [1]. Potential applications of these materis are wide ranging, from data storage to smart window [2]. These applications are based on either CW or pulsed Laser irradiation. It is, therefore, important to understand the structural response of the material under these two excitation conditions. We present a photocrystallographic study of $[Ru(NH_3)_5(NO)]Cl_3.H_2O$ [3] in order to compare the PLI induced by CW and Pulsed laser irradiation. Firstly, CW laser was used for the irradiation of the ground state (GS) at 100K generating two PLI as verified in infrared spectroscopy and absorption measurements of the crystal (Fig.1). The PLI1 was generated at 422nm and a transfer by subsequent irradiation at 1064nm yields PLI2 with significant populations of 45 and 10.6% respectively. The PLI configurations were first identified on photodifference maps. Interestingly, in photodifference maps of PLI2, two distinct positions of nitrogen were found evidencing two PLI2 positions. Subequent refinement using isonitrosyl and side-on configuration of the NO ligand for PLI1 and PLI2 as PLI2A & PLI2B converged determining a structural model for these two states in *P*nma space group. Secondly, the experiment was repeated by using pulse laser irradiation at 100K. We obtained same results of structural dynamics, types of PLI and population of PLI1 and PLI2 as with the CW laser irradiation, demonstrating the pulsed and CW Laser irradiation generating the same structural response.This complex is thus a suitable candidate for next step of our in-house time resolved photocrystallographic study in order to study the dynamics of photoswitching.

References
[1] Stepanenko, I., Zalibera, M., Schaniel, D., Telser, J. Arion, V., Dalton Trans., 2022, 51, 5367-5393.
[2] Goulkov, M., Schaniel, D., Woike, T., J. Opt. Soc. Am. B., 2010, 27, 927-932.
[3] Bottomley, F. Journal of the Chemical Society, Dalton Trans., 1974,15, 1600-1605.

Steady state photocrystallographic analysis

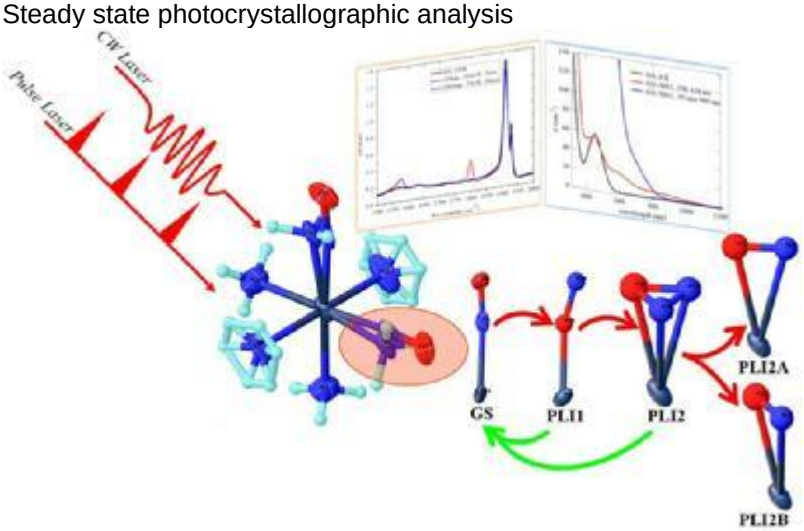

Back to Table of contents

MS13 Structural Characterization of Functional Materials

MS13-2-7 X-ray analyses on the variation of the surface and structure properties of GaN and AlN single crystals subject to femtosecond laser irradiation
#MS13-2-7

B. Shivachev [1], T. Petrov [2]
[1]Institute of Mineralogy and Crystallography "Acad. Iv. Kostov", Bulgarian Academy of Sciences - Sofia (Bulgaria),
[2]Institute of Solid State Physics, Bulgarian Academy of Sciences - Sofia (Bulgaria)

Abstract
GaN and AlN substrates are considered as hard-to-process materials due to their extreme hardness and strong stability against chemicals. Femtosecond laser sources can be used to treat GaN and AlN surfaces under ambient conditions, pressure and temperature supposedly without the destruction of their crystal structures and damaging the surface properties if laser parameters are adjusted. Specifically, the correct combination of exposure time and power are key for the conservation of the surface properties and structure and must be adjusted. In the present study GaN and AlN polished single crystals were exposed to femtosecond laser irradiation under ambient conditions. The irradiation treatment was carried out by a laser pulses having 350fs time duration on 1.03nm wavelength and a pulse power up to 2.1 mW. Repetition rate of the laser operation was 200kHz. The substrates before and after irradiation (Figure 1) were characterized by X-ray single crystal, X-ray micro-diffraction, 2D XRD and microscopy techniques in order to assess the presence of structural and surface effects: phase changes or conversion, oxidation, passivation etc. In parallel microthermal investigations (with the use of fast thermocouples) were carried out to assess the maximal temperature that can be attained under the irradiation. The single crystal micro-focus and powder microdiffraction studies were concentrated on different points (50 x 50 μm) of the GaN or AlN original and irradiated surfaces. With increasing irradiations exposure times and power, the surface of the GaN or AlN samples started to erode almost immediately. Nevertheless, the surface and bulk crystal structure was maintained up to certain time and power. In general, increasing the irradiations exposure times e.g. depth, led to the formation of pits and appearance of particles along the step edges, resulting in drastic roughening of the surface. Funding. This work was supported by the Bulgarian Science Research Found under grant DN-18/7 10.12.2017 (T.P. and B.Sh.)

Figure 1. Representation of GaN (a,b) and AlN c,d)

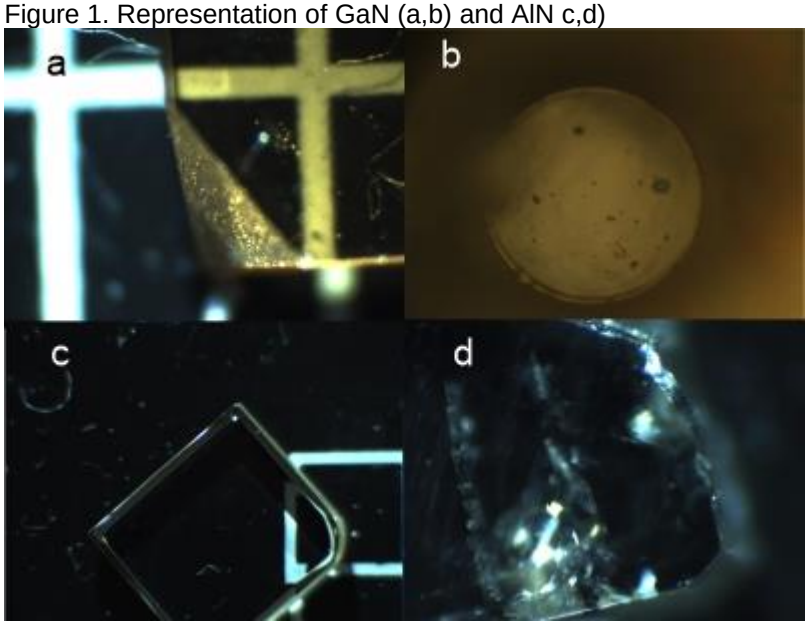

Back to Table of contents

MS13 Structural Characterization of Functional Materials

MS13-2-8 Emergence of High-Coercivity Ferromagnetism and R3c-to-Pn21a Phase Transition in Single-crystalline Gd-doped BiFeO3 nanowires
#MS13-2-8

S.K.S. Patel [1]
[1]Department of Chemistry, MMV, Banaras Hindu University - Varanasi (India)

Abstract
We fabricated single-crystalline, Gd-doped $BiFeO_3$ (BFO) nanowires using a hydrothermal technique. X-ray diffraction (XRD) data and high-resolution transmission electron microscopy (HRTEM) revealed pure single-phase crystalline $Bi_{1-x}Gd_xFeO_3$ (x = 0, 0.05, 0.10) nanowires of 40 - 60 nm diameter and their structural transformation from the rhombohedral R3c (for x = 0 and 0.05) to the orthorhombic Pn21a crystal structure (for x = 0.10). The addition of Gd^{3+} ions to the pure-phase BFO leads to remarkable changes in the structural and magnetic properties, which effects are caused by differences in the ionic-radii and magnetic moment between the Bi^{3+} and Gd^{3+} ions. According to the observed magnetization-field (M-H) and magnetization-temperature (M-T) curves, with increasing Gd^{3+} concentration, the saturation magnetization (M_S), squareness (Mr/Ms), coercivity (Hc), exchange-bias field (H_{EB}) and magnetocrystalline anisotropy (K) increased markedly, by Ms = 1.26 emu/g (640%), Mr/Ms = 0.19 (20.5%), Hc = 7788 Oe (4560%), H_{EB} = 501 Oe (880%) and K = 1.62 x 10^5 erg/cm^3 (3500%), for x = 0.10 relative to the data for x = 0. In such Gd-doped BFO nanowire samples, spin-canted Dzyaloshinskii–Moriya interaction, remarkable enhancements in the magnetocrystalline anisotropy as well as uncompensated surface ferromagnetic spin states in the antiferromagnetic core regions also were found. Such remarkable enhancements in Gd-doped BFO nanowires might offer a variety of spintronic applications.

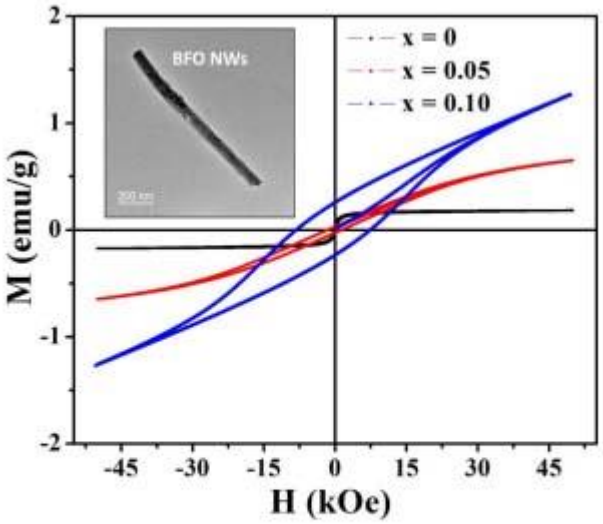

Fig. 1. Magnetization hysteresis (M–H) loops for samples measured at 300 K. The inset shows TEM images of BFO nanowire.

Back to Table of contents

MS13 Structural Characterization of Functional Materials

MS13-2-9 Germylene-β-sulfoxide hemilabile ligand in coordination chemistry
#MS13-2-9

S. Mallet-Ladeira [1], D. Madec [2]
[1]ICT- CNRS - Toulouse (France), [2]LHFA- UPS/CNRS - Toulouse (France)

Abstract
The use of transition-metal germylenes complexes in catalysis remains sporadic, with olny a few recent reports[1]. In this context, we described the synthesis of a germylene-β-sulfoxide ligand and its abilities in coordination chemistry[2]. We characterized transition metal complexes by X-ray diffraction and an unprecedented bridged bis-tuthenium complex.

References
1. (a) Brück, A.; Gallego, D.; Wang, W.; Irran, E.; Driess, M.; Harwig, J. F. Pushing the σ- Donor Strength in Iridium Pincer Complexes: Bis(silylene) and Bis(germylene) Ligands Are Stronger Donors than Bis(phosphorus(III)) Ligands. Angew. Chem. Int. Ed. 2012, 51, 11478-11482. (b) Wang, W.; Inoue, S.; Enthaler, S.; Driess, M. Bis(silylenyl)- and Bis(germylenyl)-Substituted Ferrocenes: Synthesis, Structure, and Catalytic Applications of Bidentate Silicon(II)Cobalt Complexes. Angew. Chem. Int. Ed. 2012, 51, 6167-6171. (c) Gallego, D.; Brück, A.; Irran, E.; Meier, F.; Kaupp, M.; Driess, M.; Harwig, J. F. From Bis(silylene) and Bis(germylene) Pincer-Type Nickel(II) Complexes to Isolable Intermediates of the NickelCatalyzed Sonogashira Cross-Coupling Reaction. J. Am. Chem. Soc. 2013, 135, 15617-15626. (d) Gallego, D.; Inoue, S.; Blom, B.; Driess, M. Highly Electron-Rich Pincer-Type Iron Complexes Bearing Innocent Bis(metallylene)pyridine Ligands: Syntheses, Structures, and Catalytic Activity. Organometallics 2014, 33, 6885-6897. (e) Álvarez-Rodríguez, L.; Cabeza, J. A.; Fernández-Colinas, J. M.; García-Álvarez, P.; Polo, D. Amidinatogermylene Metal Complexes as Homogeneous Catalysts in Alcoholic Media. Organometallics 2016, 35, 2516-2523. (f) Sharma, M. K.; Singh, D.; Mahawar, P.; Yadav, R.; Nagendran, S. Catalytic Cyanosilylation Using Germylene Stabilized Platinum(II) Dicyanide. Dalton Trans. 2018, 47, 5943-5947.
2. Lentz, N.; Mallet-Ladeira, S.; Baceiredo, A.; Kato, T.; Madec, D. Germylene–Sulfoxide as a Potential Hemilabile Ligand: Application in Coordination Chemistry. Dalton Trans., 2018, 47, 15751-15756.

An unprecedented bridged bis-ruthenium complex

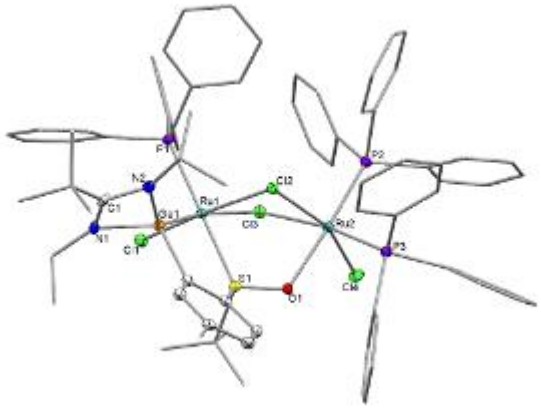

Ni(0)- complex

Back to Table of contents

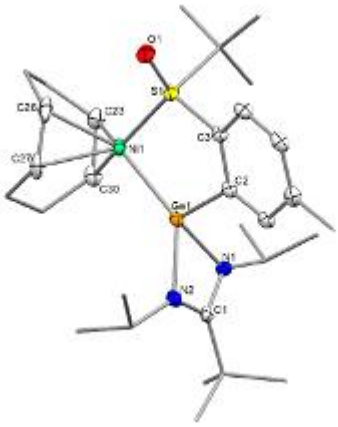

Back to Table of contents

MS14 Materials for energy storage and Conversion

MS14-1-1 Crystal structure and catalytic performance of a new vanadophosphate material #MS14-1-1

N. Hamdi [1], M. Akouibaa [1], S. Chaouch [1], M. Lachkar [1], B. El Bali [1]
[1]University Sidi Mohamed Ben Abdellah - FEZ (Morocco)

Abstract
A new vanadophosphate material, Li(C4N2H12)2[(HPO4)(VO)3(PO4)3], has been hydrothermally synthesized and structurally characterized by crystal x-ray diffraction (Fig1). The hybrid compound crystallizes in the orthorhombic system (SG: Pna21) with the following parameters (Å): a=14.6207, b=8.709, c=17.6208. its crystal packing, consisting of layers parallel to bc plane, is made of alternating rings of VO5, VO6 and PO4 polyhedral sharing vertices via oxygen atoms. The Li-ions are located in the eight membered rings, exactly at the opening window of the layers, while the protonated organic molecules reside between the interlayer space and interact with the inorganic moiety via hydrogen bonds in a three-dimensional arrangement. The thermal behavior leads to the formation of vanadium pyrophosphate precursor. The sorpativity and catalytic activity of the hybrid material were tested both as a sorbent for methylene blue (MB) dye in aqueous solutions and as a catalyst for the oxidation and degradation of (MB) in presence of H2O2, and the results showed the efficiency of the compound on the removal of the organic dye (MB).

Back to Table of contents

MS14 Materials for energy storage and Conversion

MS14-1-10 Electrochemical Oxygen Reduction Reaction Using Carbon nanotubes-graphene-manganese salen composite material
#MS14-1-10

P. Sonkar [1]
[1]Banaras Hindu University - Varanasi (India)

Abstract
Carbon nanotubes (CNT) and graphene oxide (GO) are good catalytic material due to their high-surface area, easy funtionalization, more conductivity and stability [1-3]. These materials have wide range of applications in the field of various sectors [1-2]. In this work, a composite material of CNT and GO has been prepared with manganese salen (CNT/GO/Mn(salen)). The composite material CNTs/GO/Mn(salen) has been used for electrochemical oxygen reduction reaction (ORR). It is suggesting that CNTs/GO/Mn(salen) could be a promising material for ORR electrocatalyst in fuel cells, metal-air-battery, chlor-alkali-electrolyzers and etc. It may be useful for the fuel work.

References
1. Bisen, Omeshwari Yadorao, et al. Reduction Reaction and Electrochemical Oxygen Sensing Thereof." ACS Applied Materials & Interfaces (2022).
2. P. K. Sonkar, V. Ganesan, S. K. Sen Gupta, D. K. Yadav, R. Gupta and M. Yadav, J. Electroanal. Chem., 807, 235 (2017).
3. P. K. Sonkar, M. Yadav, K. Prakash, V. Ganesan, M. Sankar, D. K. Yadav, and R. Gupta, J. Appl. Electrochem., (2018).

Back to Table of contents

MS14 Materials for energy storage and Conversion

MS14-1-11 Structure–performance relationships in NaxFexTi2-xO4 anodes for Na-ion batteries #MS14-1-11

M. Nowak [1], Z. Wojciech [1], J. Molenda [1]
[1]AGH University of Science and Technology - Kraków (Poland)

Abstract
Due to the tremendous growth of the electric vehicle industry and demand for Li-ion batteries recently, we may soon face a shortage of these crucial components. At the same time, we observe spiking prices of key elements such as lithium, nickel, cobalt and graphite necessary for battery production [1]. Na-ion technology emerges as an economically promising alternative to Li-ion because of the low price of raw elements (sodium, iron) as well as comparable performance. Though most of the proposed anode materials for Na-ion batteries are based on carbon chemistry, these exhibits very low Columbic efficiency during the first charging/discharging cycle and require a high temperature of pyrolysis. On the other hand elements such as Sn, Sb, Si, and P yield high capacities, but degrade rapidly due to volume changes up to 400%.Here we focus on iron-titanium-based oxide anodes that take employ intercalation mechanism to react with sodium and thus better retain the capacity because of minor changes in crystal structure during (de)sodiation. We prepared $NaFeTiO_4$, $Na_{0.9}Fe_{0.9}Ti_{1.1}O_4$ and $Na_{0.8}Fe_{0.8}Ti_{1.2}O_4$ via both citrate-assisted sol-gel methods as well as traditional high-temperature solid-state route and compared the performance in the Na-ion batteries [2]. Crystal structure, chemical composition and morphology were determined using X-ray diffraction (XRD), scanning electron microscopy (SEM) and nitrogen adsorption isotherms. The crystal structure of $NaFeTiO_4$ possesses single-barreled tunnels occupied by sodium that stand as a pathway for the rapid diffusion of sodium ions. During the synthesis, if the sodium content is reduced below one and some iron ions are replaced for titanium then the single-barreled tunnels become double-barreled and as a consequence, an additional diffusion path can be formed ($Na_{0.9}Fe_{0.9}Ti_{1.1}O_4$ and $Na_{0.8}Fe_{0.8}Ti_{1.2}O_4$). Impedance spectroscopy (IS) measurements in the temperature range of 25 – 300°C confirm that electrical conductivity of $Na_{0.9}Fe_{0.9}Ti_{1.1}O_4$ and $Na_{0.8}Fe_{0.8}Ti_{1.2}O_4$ is one order of magnitude higher than $NaFeTiO_4$ while the activation energy is lower (0.82 eV vs 0.86 eV) indicating better kinetics of combined sodium and electron migration. At the same time, double-barreled compounds are characterized by lower band-gap values (UV-VIS measurements). Among all of the investigated materials, $Na_{0.8}Fe_{0.8}Ti_{1.2}O_4$ has the highest charge capacity of about 180 mAh g^{-1} during the first cycle at C/20 and can retain 80% of the initial capacity after 30 cycles with an average charging voltage of 1.3 V vs. Na^+/Na. Ex-situ XRD of the recovered electrode layers after a full discharge as well as a complete discharging-charging cycle indicate minor changes in the volume of the elemental cell. Also, the changes in the local environment of Fe and Ti have been identified in X-ray absorption spectroscopy (XAS). Finally, the capacities exceeding 177 mAh g^{-1} measured at 60°C indicate that beside the Fe^{3+}/Fe^{2+} redox, also Ti^{4+}/Ti^{3+} may be involved during the sodiation process. We hope that due to the low cost and abundance of raw elements and promising electrochemical performance, $Na_{0.8}Fe_{0.8}Ti_{1.2}O_4$ may find application as anode material in the future generation of Na-ion batteries.Acknowledgments: This work was supported by the Polish Ministry of Science and Higher Education (MNiSW) under grant number 0046/DIA/2017/46

References
[1] IEA (2021), The Role of Critical Minerals in Clean Energy Transitions, IEA, Paris
[2] Nowak, W. Zając, J. Molenda, Energy, 2022, 239, 122388

Back to Table of contents

MS14 Materials for energy storage and Conversion

MS14-1-2 Synthesis, crystal structure, physico-chemical studies of two new nickel complexes used as precursor for preparation of Ni/NiO nanoparticles.
#MS14-1-2

M. Akouibaa [1], N. Hamdi [1], S. Chaouch [1], A. Bouayad [1], S. Rakib [1], M. Lachkar [1], B. El Bali [2]
[1]University Sidi Mohamed Ben Abdellah, Faculty of Sciences, Chemistry Department - Fez (Morocco), [2]Independent Scientist - oujda (Morocco)

Abstract
Two nickel complexes, namely, mer-[Ni(dien)2](NO3)2 (I) and mer-[Ni(dien)2]Cl2. H2O (II), have been synthesized under ambient conditions, where (dien = diethylenetriamine = bis(2-aminoethyl) amine and mer = meridional coordination). Their crystal and molecular structures have been determined by single-crystal X-ray diffraction methods. The complex (I) crystallizes in the orthorhombic system, space group, Pbca (no, 61), Z = 8, with a = 8.8117(6) Å, b = 14.0023(8) Å, c = 26.7603(17)Å, V = 3301.79 Å3 for (I), The complex (II) crystallizes in the monoclinic system, space group P21/c (no 14) a = 13.5000(4) Å, b = 8.7170(3) Å, c = 13.9430(4) Å, V = 1604.41 Å3 for (II). Meridional (mer) coordination promotes the generation of larger and lower-symmetry prismatic structures, in contrast with the facial (fac) coordination and higher-symmetry. For the complexes (I) and (II), the structures are formed by the cation [Ni(C4H13N3)2]2+, two nitrate anions for (I) and tow chloride anions and water molecule for (II). The nickel (II) atom is coordinated to six nitrogen donors from two neutral dien ligands, adopting a slightly distorted octahedral geometry. The newly complexes were also characterized by Infrared, TGA-DTA analysis and UV–Vis spectroscopy. Vibrational analysis of the two complexes was realized by infrared spectroscopy, which confirmed the characteristic bands of diethylenetriamine and nitrate groups. The morphology and the size of the two nickel complexes were monitored by scanning electron microscopy (SEM). Moreover, the thermal behavior of the complexes was investigated, and the calcination of the two complexes under air has led to the production of Ni/NiO nanoparticles.

ORTEP drawing of the asymmetric unit of mer-[Ni(di

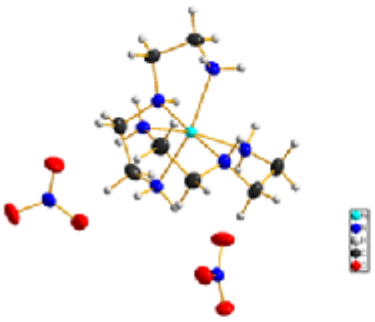

ORTEP drawing of the asymmetric unit of mer-[Ni(di

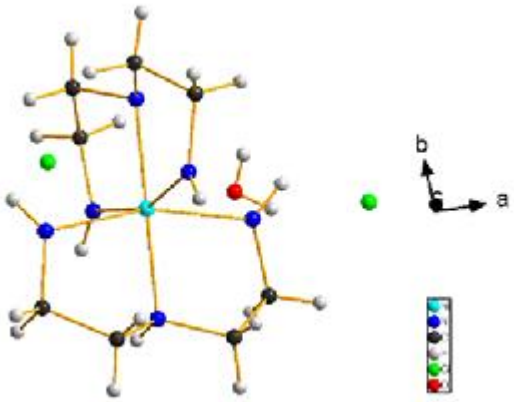

Back to Table of contents

MS14 Materials for energy storage and Conversion

MS14-1-3 Next generation MetalJet sources enabling 10µm high brightness high energy beams for high pressure diffraction application
#MS14-1-3

J. Hållstedt [1], E. Espes [1], A. Adibhatla [1], R. Drake [2]
[1]Excillum - Kista (Sweden), [2]PROTO Manufacturing Ltd. - Windsor (Canada)

Abstract
The interest of exploring new materials at more extreme condition is becoming increasingly important both for fundamental research as well as for application in e.g. superconductors and hydrogen storage. An important tool to characterize and understand these materials is by applying High pressure Xray diffraction (HPXRD). This application rely on high energy Xrays to achieve good transmission through the Diamond anvil cell (DAC) and in order to capture large part of the reciprocal space. In addition, with smaller crystals higher pressures can be achieved at the expense of diffraction intensity. For this reason more advanced application of this technology has so far been restricted to a rather limited number of synchrotron beam lines. To aid the scientists and to accelerate research we have recently demonstrated unprecedented high energy beams suitable for high pressure application utilizing the latest high power MetalJet microfocus Xray source. In this case the E1+ using I2 Indium alloy. The Xray source was coupled to a special high grade Montel optic with slits. The main beam characteristics were as follows: -Monochromatic 24keV (Indium kalfa) -Down to 10µm beam size (at sample position) -2-15 mRad divergence (slit controlled) -Flux approximately 1e7 photons /sec. for 10 µm beam. In this communication we demonstrate the setup and provide first glimpse of HPXRD results possible from this unique setup.

Illustration of X-ray spot in focus

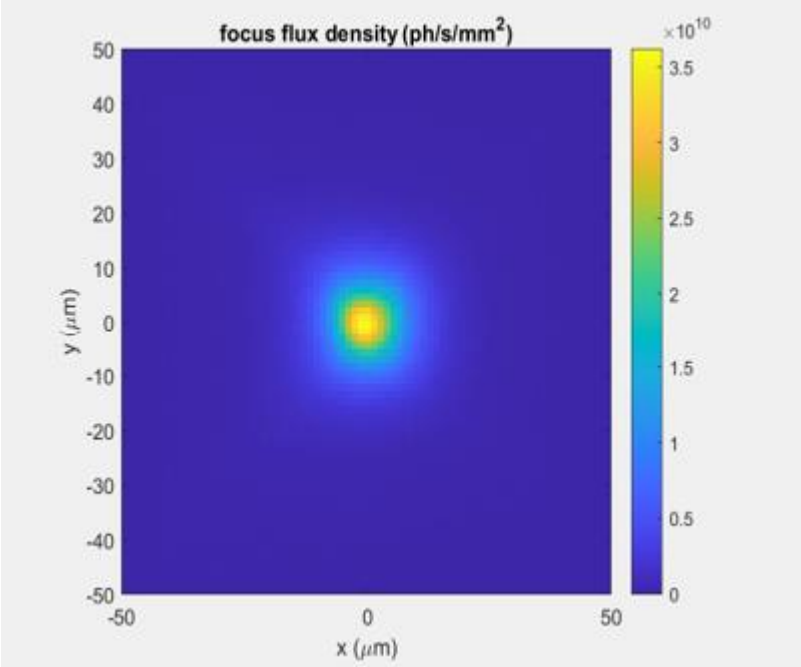

Back to Table of contents

MS14 Materials for energy storage and Conversion

MS14-1-4 Rotationally-driven piezoelectricity: Computational assessment of ionic plastic molecular crystals #MS14-1-4

E.D. Sødahl [1], J. Walker [2], S. Seyedraoufi [1], C.H. Gørbitz [3], K. Berland [1]
[1]Norwegian University of Life Science - Ås (Norway), [2]Norwegian University of Science and Technology - Trondheim (Norway), [3]University of Oslo - Oslo (Norway)

Abstract
Piezoelectric materials couple mechanical and electric responses making them suitable for a broad range of applications such as sonar, medical ultrasound, sensors and energy harvesting devices. In this work, we calculate dielectric, piezoelectric and ferroelectric properties of 11 hybrid molecular crystals using van der Waals density functional theory. We predict negative piezoelectric coefficients d_{33} for some of the hybrid molecular crystals. Negative d_{33} values have only been reported earlier for polymers and liquid crystals [1]. Further, the d_{ij}s of the hybrid molecular crystals are comparable to phase-pure inorganic piezoelectrics, such as AlN and $LiNbO_3$, see Fig. 1. The computed shear contributions to the piezoelectric response are large, with a d_{24} of -116 pC/N calculated for HdabcoReO$_4$[1]. The largest piezoelectric factor of anisotropy $|d_{16}/d_{33}|$=161 for HQReO$_4$[2] is also far larger than for typical inorganic systems such as $BaTiO_3$ with a $|d_{15}/d_{33}|$ of 6. We show the large piezoelectric anisotropy can in part be understood from rotations of constituent molecules similar to the polarization vector rotation observed in inorganic perovskites with compositions near to a morphotropic phase boundary [2].
[1]1,4 – diazabicyclo[2.2.2]octane perrhenate
[2]Quinuclidinium perrhenate

References
[1] I. Urbanaviciute, X. Meng, M. Biler, Y. Wei, T. D. Cornelissen, S. Bhattacharjee, M. Linares, and M. Kemerink, Negative piezoelectric effect in an organic supramolecular ferroelectric, Mater. Horiz. 6, 1688 (2019)
[2] M. Davis, M. Budimir, D. Damjanovic, and N. Setter, Rotator and extender ferroelectrics: Importance of the shear coefficient to the piezoelectric properties of domain- engineered crystals and ceramics, Journal of Applied Physics 101, 054112 (2007), publisher: American Institute of Physics

The calculated piezoelectric coefficients

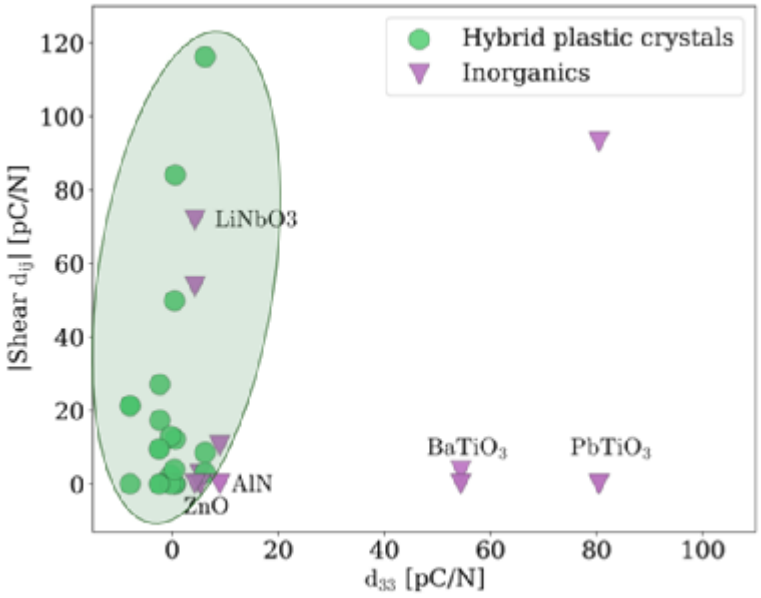

Back to Table of contents

MS14 Materials for energy storage and Conversion

MS14-1-5 Realising the relevance of pH on photocatalytic bismuth oxyhalides
#MS14-1-5

H. Jeppesen [1], M.M. Marks [2], H.C. Cavaye [3], S.F. Parker [3], M.C. Ceccato [2], N.L. Lock [4]
[1]Interdisciplinary Nanoscience Center (iNANO), Aarhus University and Deutsches Elektronen-Synchrotron (DESY) - Aarhus and Hamburg (Germany), [2]Interdisciplinary Nanoscience Center (iNANO), Aarhus University - Aarhus (Denmark), [3]ISIS Neutron and Muon Source, STFC Rutherford Appleton Laboratory - Chilton, Oxfordshire (United Kingdom), [4]Carbon Dioxide Activation Center (CADIAC), Department of Biological and Chemical Engineering and iNANO, Aarhus University - Aarhus (Denmark)

Abstract
Photocatalytic bismuth oxyhalides is a promising family of materials for high efficiency catalytic materials. Where these have traditionally been synthesised via hydrothermal methods[1,2], recent developments in synthesising the material via microwave assisted synthesis has gained significant attention due to their high photocatalytic efficiencies[3–5]. $Bi_{24}O_{31}Br_{10}$, synthesised via the latter method, proved highly efficient in alcohol oxidation reactions with quantum yields of 71 % at 410 nm[3] driven by a hydrogen transfer step and enhanced due to the presence of surface hydroxyls from the synthesis procedure at high pH[4].
Our work continued the investigation of the materials obtained via microwave assisted synthesis and post synthesis modifications and how this influences the material structure and morphology. This information is linked to the photocatalytic efficiencies investigated via benzylamine oxidation reactions under UV light. The bismuth oxyhalides were synthesised at 6 different pH - ranging from low to high, yielding in BiOX (X=Br, Cl) or $Bi_{24}O_{31}X_{10}$, respectively. Together with the phase change upon increased synthesis pH, particle sizes decreased and photocatalytic efficiency increased. Overall, BiOBr/$Bi_{24}O_{31}Br_{10}$ proved a higher activity than BiOCl/$Bi_{24}O_{31}Cl_{10}$, which matches our observations through inelastic neutron scattering. These spectra suggest a higher degree of hydrogen saturation on $Bi_{24}O_{31}Br_{10}$ compared to $Bi_{24}O_{31}Cl_{10}$, which as previously mentioned[4] are expected to be the driving force of the reaction. Finally, a phase transformation to BiOBr or BiOCl was observed by suspending $Bi_{24}O_{31}Br_{10}$ and $Bi_{24}O_{31}Cl_{10}$ in HBr or HCl. Despite final phases being structurally similar, a higher photocatalytic efficiency was observed in materials transformed from $Bi_{24}O_{31}Br_{10}$ compared to $Bi_{24}O_{31}Cl_{10}$.

References
(1) Li, K.-L., et al. *J. Taiwan Inst. Chem. E.* **2014**, *45 (5)*, 2688–2697. https://doi.org/10.1016/j.jtice.2014.04.001.
(2) Chen, H.-L., et al. *J. Taiwan Inst. Chem. E.* **2014**, *45 (4)*, 1892–1909. https://doi.org/10.1016/j.jtice.2013.12.015.
(3) Dai, Y., et al. *Angew. Chem. Int. Ed.* **2019**, *58 (19)*, 6265–6270. https://doi.org/10.1002/anie.201900773.
(4) Dai, Y., et al. *J. Am. Chem. Soc.* **2018**, *140 (48)*, 16711–16719. https://doi.org/10.1021/jacs.8b09796.
(5) Bijanzad, K., et al. *Physica B* **2015**, *475*, 14–20. https://doi.org/10.1016/j.physb.2015.06.013.

Back to Table of contents

MS14 Materials for energy storage and Conversion

MS14-1-6 Screening the Cambridge Structural Database for ferroelectric molecular crystals
#MS14-1-6

S. Seyedraoufi [1], E.D. Sødahl [1], O. Nilsen [2], C.H. Gørbitz [2], K. Berland [1]
[1]Norwegian University of Life Sciences - Ås (Norway), [2]University of Oslo - Oslo (Norway)

Abstract
The Cambridge Structural Database (CSD) holds more than 400 000 molecular crystal entries. Many of these crystals could hold great potential as functional materials, including for applications such as photovoltaics, energy harvesting, and computer memory. Recently, organic ferroelectrics have attracted much attention due to the need for environmentally friendly ferro- and piezoelectric materials. However, identifying which of these structures merits further investigation can be challenging due to the complex structure-property relationships of ferroelectrics, requiring both an intrinsic polarization and a well-defined polarization switching path. Here, we utilize existing and newly developed tools to extract a pool of material candidates for further assessment with density functional theory. Implemented filters include the existence of pseudo-center of symmetry and well-defined switching paths for proton-transfer ferroelectrics. For order-disorder ferroelectrics, we introduce geometric and bonding criteria to identify candidates. Moreover, we assess the potential of selected candidates using van der Waals' density functional theory. The results indicate that several candidates hold a sizeable spontaneous polarization and modest switching barriers.

Polarization switching of a proton-transfer FE

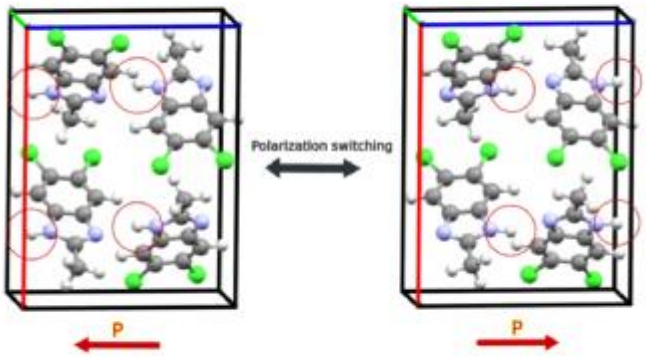

Back to Table of contents

MS14 Materials for energy storage and Conversion

MS14-1-7 Sintering and surface treatments for fabrication of $Na_3Zr_2Si_2PO_{12}$ NASICON solid electrolyte for sodium-metal solid state batteries
#MS14-1-7

A. Boroń-Filek [1], J. Mojecki [1], W. Zając [1]
[1]AGH University of Science and Technology - Kraków (Poland)

Abstract
Factors such as the growing number of electric cars and the need to balance the demand and supply of energy related to the constantly increasing share of renewable energy sources make energy storage a very important issue. Currently, the most common electrochemical energy storage technology is Li-ion cells, but due to the growing requirements for energy density, price and availability, new, more efficient solutions are sought. All-solid-state sodium metal batteries (Na-ASSB) may be the answer to these challenges. The use of a solid electrolyte should reduce the possibility of sodium dendrite build-up, and the use of a metallic anode will allow for high energy density. The basic element of this type of cell is a dense ceramic electrolyte with a high mobility of sodium ions, which forms a barrier to growth of dendrites. Good contact between the electrolyte and electrodes is also essential, ensuring a low resistance to charge transfer through the interface.
This work demonstrates the influence of synthesis conditions on properties of $Na_3Zr_2Si_2PO_{12}$ - a solid electrolyte for Na-ASSB. The influence of temperature, sintering time and sodium excess on the phase composition of NASICON was investigated using the X-ray diffraction method.
In order to improve the contact of the electrolyte with the electrodes, three methods of electrolyte surface modification were used: mechanical (controlling surface roughness), thermal (heat treatment in an inert atmosphere) and chemical (hydrochloric acid or sodium hydroxide eatching). The influence of the applied modifications were investigated using Raman, Fourier-transform infrared spectroscopy, X-ray photoelectron spectroscopy and scanning electron microscopy. Electrochemical performance and charge transfer resistance through the sodium metal electrode/electrolyte interface was determined in a symmetrical Na|NZSP|Na cells and evaluated using galvanostatic and impedance spectroscopy methods.
Ackonwledgement
Research project supported/partly supported by program „Excellence initiative – research university" for the AGH University of Science and Technology". This work was carried out using the infrastructure of Laboratory of Materials for Energy Conversion and Storage at the Centre of Energy, AGH University of Science and Technology. This work was supported by AGH University of Science and Technology under grant no. 16.16.210.476.

Back to Table of contents

MS14 Materials for energy storage and Conversion

MS14-1-9 A Polycationic Substituted Lithium Argyrodite Superionic Solid Electrolyte #MS14-1-9

J. Lin [1], M. Schäfer [2], S. Indris [3], J. Janek [4], A. Kondrakov [5], T. Brezesinski [1], F. Strauss [1]
[1]Battery and Electrochemistry Laboratory, Institute of Nanotechnology, Karlsruhe Institute of Technology (KIT) - Karlsruhe (Germany), [2]Institute for Applied Materials–Energy Storage Systems, Karlsruhe Institute of Technology (KIT) - Karlsruhe (Germany), [3]Institute for Applied Materials–Energy Storage Systems, Karlsruhe Institute of Technology (KIT) and Helmholtz Institute Ulm (HIU) for Electrochemical Energy Storage - Karlsruhe / Ulm (Germany), [4]Battery and Electrochemistry Laboratory (BELLA), Institute of Nanotechnology, Karlsruhe Institute of Technology (KIT) and Institute of Physical Chemistry, Justus-Liebig-University Giessen - Karlsruhe / Giessen (Germany), [5]Battery and Electrochemistry Laboratory, Institute of Nanotechnology, Karlsruhe Institute of Technology (KIT) and BASF SE - Karlsruhe / Ludwigshafen (Germany)

Abstract
Solid-state batteries are attracting great attention because of potentially higher energy and power densities than conventional Li-ion batteries based on liquid electrolytes.[1] Yet, they are plagued by the development of advanced solid electrolytes, mainly lacking in ionic conductivity and electrochemical stability; thus, the ongoing quest for exploration of new materials and compositions.[2-3] Despite increasing research interests in high-entropy materials, the effect that configurational entropy has on the charge transport properties remains largely elusive.[4] Recently, we have shown that high-entropy argyrodites can be achieved via polyanionic/cationic substitution, showing a low activation energy (E_A = 0.22 eV) and moderate r.t. ionic conductivity (~1 mS/cm).[5] However, the possibility of polycationic substitution and the resulting structure-property relationships have not been explored yet.
Within this context, we herein report about the influence of polycationic substitution on the Li-ion conductivity in argyrodite superionic conductors. Using electrochemical impedance spectroscopy and 7Li pulsed field gradient nuclear magnetic resonance (NMR) spectroscopy, it is found that polycationic substitution leads to a very low activation energy (E_A = 0.19 eV) for Li-ion conduction and a high r.t. ionic conductivity of ~13 mS/cm. These findings are rationalized via neutron powder diffraction (at 298 K and 10 K) in combination with magic angle spinning NMR spectroscopy. A high S^{2-}/I^- anion site disorder (up to ~10 %) and redistribution of Li lead to shortened jump distances and therefore facilitated long-range ion diffusion. Overall, our results show the possibility of polycationic substitution in lithium argyrodites, thereby opening up large compositional space for the development of novel superionic conductors with improved properties.

References
1. Janek, J.; Zeier, W. G. A Solid Future for Battery Development. Nat. Energy 2016, 1, 16141.
2. Kato, Y.; Hori, S.; Saito, T.; Suzuki, K.; Hirayama, M.; Mitsui, A.; Yonemura, M.; Iba, H.; Kanno, R. High-Power All-Solid-State Batteries Using Sulfide Superionic Conductors. Nat. Energy 2016, 1 (4), 16030.
3. Gao, Z.; Sun, H.; Fu, L.; Ye, F.; Zhang, Y.; Luo, W.; Huang, Y. Promises, Challenges, and Recent Progress of Inorganic Solid-State Electrolytes for All-Solid-State Lithium Batteries. Adv. Mater. 2018, 30 (17), 1705702.
4. Ma, Y.; Ma, Y.; Wang, Q.; Schweidler, S.; Botros, M.; Fu, T.; Hahn, H.; Brezesinski, T.; Breitung, B. High-Entropy Energy Materials: Challenges and New Opportunities. Energy Environ. Sci. 2021, 14 (5), 2883–2905.
5. Strauss, F.; Lin, J.; Duffiet, M.; Wang, K.; Zinkevich, T.; Hansen, A.-L.; Indris, S.; Brezesinski, T. High-Entropy Polyanionic Lithium Superionic Conductors. ACS Mater. Lett. 2022, 4 (2), 418–423.

Back to Table of contents

MS14 Materials for energy storage and Conversion

MS14-2-1 Structural changes during the sodiation of branch-like antimony-based anodes for Na-ion batteries #MS14-2-1

J. Płotek [1], A. Kulka [1], M. Moździerz [1], J. Molenda [1]
[1]AGH University of Science and Technology - Kraków (Poland)

Abstract
Anode materials based on alloying-type reactions are a promising solution to improve the capacity of the Na-ion batteries. This electrochemical process is characteristic for elements of group 14 and 15 of the periodic table which form various Na-Me (Me - metal, metalloid) alloys reversibly. Among them, antimony stands out with its high electrical conductivity, as well as the high theoretical capacity of 660 $mAh \cdot g^{-1}$. However, it is not flawless: with volume changes up to 293% and severe microstructure degradation, poor cyclability is inevitable. The prospective strategy to overcome these obstacles is to synthesize sub-micron and nanosized antimony composites with carbon.
This work aims to elucidate the sodiation and desodiation mechanism of the antimony-carbon composite with branch-like microstructure synthesized via a solvothermal reaction. Such microstructure enables good reversibility of the electrochemical reaction. Operando and ex-situ measurements revealed processes hidden during the discharge and charge processes.
The crystal structure of the material was characterized by the X-ray diffraction (XRD) method combined with Rietveld refinement and Raman spectroscopy. The main phase of the as-obtained sample was found to be rhombohedral antimony (R-3m space group), with the second monoclinic phase of $Sb_4O_5Cl_2$ (P21/a space group). The phase contribution was defined by linear fitting of the X-ray absorption spectra compared with the spectra of pure materials. Scanning electron microscopy revealed the presence of an extraordinary branch-like microstructure with a sub-micrometer particle size. The as-obtained material was mixed with a carbon additive and an eco-friendly carboxymethyl cellulose (CMC) binder to prepare an electrode. To gain a deep understanding of the structural changes during (de)sodiation, operando XRD and Raman spectroscopy measurements were conducted. The qualitative change of results of the X-ray absorption spectroscopy (XAS) for the L_1 and L_3-edge for Sb and the K-edge for Na as a function of sodium content (ex-situ measurements) in transmission mode, total electron and total fluorescence yields is also presented. Comparison of the three above-mentioned techniques allowed providing the detailed description of the processes occurring during first sodiation and desodiation into the antimony characterized by the remarkable microstructure. Moreover, numerous electrochemical measurements were performed: charge and discharge cycling, cycling voltammetry, and electrochemical impedance spectroscopy as a function of the state of charge.
The results confirm that during the alloying reaction, despite the application of a novel synthesis method, the Na_3Sb phase was formed, similar to that of commercial antimony. Not only crystal structure, but also oxidation state has been changed during the sodiation, which was proven by XAS. The application of a broad range of different operando and ex-situ characterization methods revealed structural changes in the electrode depending on the stage of the reaction. The obtained results contribute to the development of post-lithium-ion technology for energy storage.
Acknowledgments
The research were supported by the National Science Center Poland (NCN) based on decision number 2019/35/O/ST8/01799

Back to Table of contents

MS14 Materials for energy storage and Conversion

MS14-2-2 Influence of Li and Mg substitution on structural properties and electrochemical performance of NaxMnO$_2$-based cathode material for Na-ion batteries
#MS14-2-2

G. Ważny [1], K. Walczak [1], J. Molenda [1]
[1]AGH University of Science and Technology - Krakow (Poland)

Abstract
In the continuous search for high energy density post-lithium batteries, one should not forget the fundamental reasons for such research: providing earth-abundant, safe for the environment, and inexpensive materials [1]. At the same time, ensuring the high capacity and long cycle life of Na-ion battery is crucial. In this regard, agents activating oxygen redox seem to be especially promising. Here we present a complex investigation of Li and Mg substitutions in the Mn sublattice that affect crystal structure in layered $Na_{0.67}MnO_2$.
The samples were synthesized via sol-gel method using acetates and sucrose as a fuel. Crystal structure was determined using X-Ray diffractommetry, and transport properties were investigated by impedance spectroscopy. The most promising compositions were used as an active materials and mixed with carbon black and PVDF to prepare cathode layers. Then, the CR2032-type coin cells were assembled in an argon-filled glovebox with high purity, using metallic sodium as an anode and 1M $NaPF_6$ in EC:DEC as an electrolyte. Electrochemical performance was tested using cyclic voltammetry and cyclic charge/discharge techniques. Changes of the crystal structure in selected samples during cell performance were inspected via ex-situ and in-situ XRD measurements. X-ray absorption spectroscopy allowed to determine oxidation states of transition metal in selected samples and investigate the changes in sodium and oxygen behaviour during cycling.
All investigated materials crystalize in P2-type layered structure, described as *P6$_3$/mmc* or *P6$_3$/mcm* space group. X-ray diffraction measurements of cathode materials in the batteries showed that Mg substitution stabilises the crystal structure and prevents phase transition during cycling. Mg substitution enhances the capacity, reaching 112% of theoretical capacity for $Na/Na^+/Na_xMg_{0.25}Mn_{0.75}O_2$ cell in the first discharge, followed by 105% in the next one. The characteristic plateau on the first charge on charge/discharge plots can be associated with the activation of oxygen-related electrochemical processes. The first charge suggests the irreversible character of anionic redox process, which is confirmed by the cyclic voltammetry. This bahaviour applies to the whole $Na_xMg_yMn_{1-y}O_2$ system with various amounts of Mg. On the contrary, the mechanism is different for Li-substituted Na_xMnO_2. It is because alkali metal in transition metal sublattice affects the electronic structure in a different way [2]. To some extent, this phenomenon is visible in cyclic voltammetry and cyclic charge/discharge plots: CV shows plenty irregular peaks, which reflect in irregular charge/discharge curves.
A complex analysis of Mg- and Li-substituted Na_xMnO_2 system properties gives a huge insight into the work mechanisms induced by such different elements. This approach can have a great impact on designing and understanding advanced cathode materials for Na-ion batteries.
Acknowledgements
This work was funded by National Science Centre, Poland under grant no. 2018/31/N/ST8/01662.

References
[1] Raphaële J. Clément *et al* 2015 *J. Electrochem. Soc.* **162** A2589
[2] Robert A. House *et al* 2019 *Chem. Mater.* **31** 3293-3300

Back to Table of contents

MS14 Materials for energy storage and Conversion

MS14-2-3 Wurtzite-type nitrides and oxide nitrides: structural diversity and the effects of oxygen
#MS14-2-3

J. Breternitz [1], S. Schorr [2]
[1]Helmholtz-Zentrum Berlin für Materialien und Energie - Berlin (Germany), [2]Helmholtz-Zentrum Berlin für Materialien und Energie; Freie Universität Berlin - Berlin (Germany)

Abstract
Although solar cells are widely commercialised, the current dominant technology based on crystalline silicon suffers from the indirect bandgap of silicon. This dictates that such modules are comparably heavy, thick and inflexible. Substitutes, such as CdTe, Cu(Ga,In)S_2 or lead halide perovskites, on the other hand, contain very scarce elements – such as Te & In – or very toxic elements – such as Cd & Pb, which would prevent their large-scale use. Therefore, finding alternative semiconductor materials with suitable properties and their thorough characterisation remains a task of uttermost importance for the widespread use of renewable energies.
Herein, we emphasise on the class of ternary and multinary wurtzite-based nitride and oxide nitride materials.[1] Deriving from the hexagonal wurtzite-type, a plethora of different subgroup types are observed, typically through ordering of cations in these materials, and we will rationalise their relationships in the form of a Bärnighausen tree (figure 1).[2] As an example, we will highlight the structural relations on the example of Zn*IV*N_2 (*IV* = Sn, Ge), materials that are hotly debated as solar absorber candidate. They crystallise in the orthorhombic β-$NaFeO_2$-type (s.g. *Pna*2_1) when the cations are ordered. Interestingly, cation ordering has been identified as one way to tune the bandgap of these materials, and which is unique to those ternary nitrides. A different cation ordering obeying Pauling's rules was proposed for Zn*IV*N_2 in s.g. *Pmc*2_1 from computation.[3] This latter has nominally higher symmetry than the β-$NaFeO_2$-type due to the smaller unit cell size. However, it is unlikely to form, due to the specific symmetry in this space group that undermines the driving force for cation ordering.[2]
In real systems, a variable degree of oxygen incorporation can hardly be avoided in nitride materials. The structural effects of oxygen and cation disorder resemble at first sight, and we will highlight how they relate to each other with the aid of neutron diffraction in the model system $Zn_{1+x}Ge_{1-x}(N_{1-x}O_x)_2$. [4,5] In addition to the structural changes, the oxygen content also affects the bandgap, which narrows upon oxygen incorporation. Using bonding analyses based on DFT calculations, we will explain the oxygen induced bandgap narrowing as an upward shift of the conduction band that is due to orbital overlaps of the Zn(3d) with the O(2p) and N(2P) orbitals.[6]

References
[1] A. L. Greenaway, C. L. Melamed, M. B. Tellekamp, R. Woods-Robinson, E. S. Toberer, J. R. Neilson, A. C. Tamboli, *Ann. Rev. Mater. Res.* **2021**, *51*, 591–618.
[2] J. Breternitz, S. Schorr, *Acta Cryst. A* **2021**, *77*, 208–216.
[3] L. Lahourcade, N. C. Coronel, K. T. Delaney, S. K. Shukla, N. A. Spaldin, H. A. Atwater, *Adv. Mater.* **2013**, *25*, 2562–2566.
[4] Z. Wang, D. Fritsch, S. Berendts, M. Lerch, J. Breternitz, S. Schorr, *Chem. Sci.* **2021**, *12*, 8493–8500.
[5] J. Breternitz, Z. Wang, D. M. Többens, S. Savvin, S. Schorr, *in preparation*.
[6] J. Breternitz, S. Schorr, *Faraday Discuss.* **2022**, doi:10.1039/D2FD00041E.

Selected subgroup structures of the wurtzite-type.

Back to Table of contents

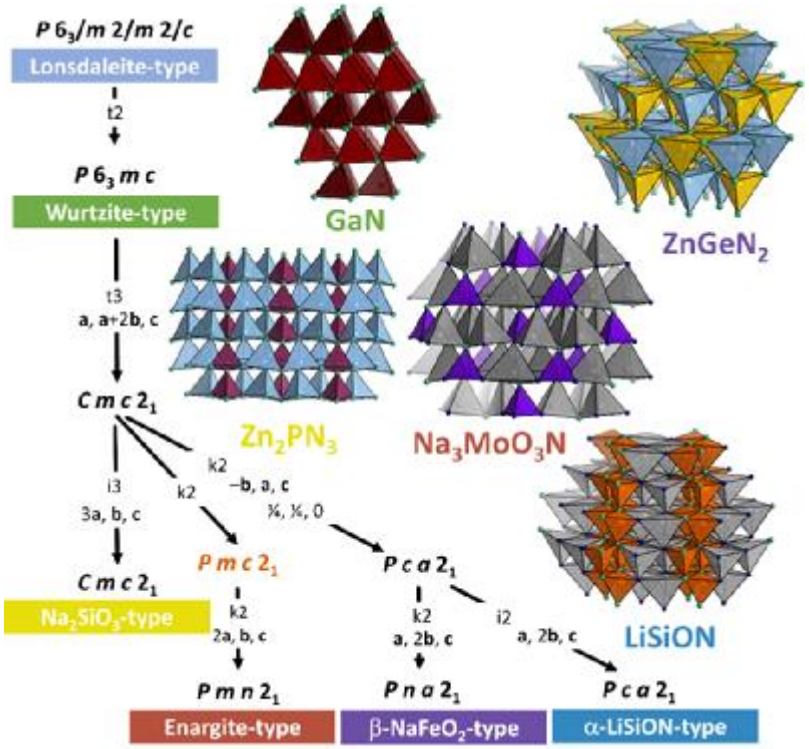

Back to Table of contents

MS14 Materials for energy storage and Conversion

MS14-2-4 Influence of Si on Hydrogen adsorption in SMoSe Janus host layer
#MS14-2-4

M. Vallinayagam [1], K. Jeyakumar [2], Z. Mattias [1], P. Matthias [3]
[1]TU Freiberg - Freiberg (Germany), [2]Rajiv Gandhi Institute of Petroleum Technology - Jais (India), [3]Helmholz Zentrum Dresden Rossendorf - Dresden (Germany)

Abstract
H adsorption on SMoSe Janus layer (JL) is enhanced by doping with Si dopant. The formation energy calculation reveals possibility of Si doing in SMoSe JL. Different sites are considered for Si doping, namely a) Si on Mo site (Si@Mo), b) Si on S site (Si@S), c) Si on Se site (Si@S), and d) Si on interstitial site (Si@int). The Si occupation on Mo sites is exothermic within Si-bulk chemical condition. Also doping on other sites, such as S or Se sites, are endothermic reaction with energy requirement about 0.4 eV. Careful analysis of the differential charge of each atom in Si-doped JLs paves the way to select possible sites for H inclusion. In the pristine JL layer the differential charge of both S and Se atoms is zero due to the uniform distortion of S-Mo and Se-Mo bond length. In Si@Mo case, the S and Se atoms in the first-nearest neighbor distance to Si acquire excess charge. On the other hand, Si@S and Si@Se cases induce no differential charge on S- or Se- atomic planes. All together lead to different choices for H adsorption sites, two sites in each S- and Se- atomic planes and top of doped element. The difference in Gibbs Free energy DG for H adsorption at different sites is calculated and compared with DG of H and H2. In conculsion, Si@Mo JLs are best candidate for H adsorption processes over pristine, Si@S and Si@Se JLs.

Schematic of pure and doped MoSSe Janus layer

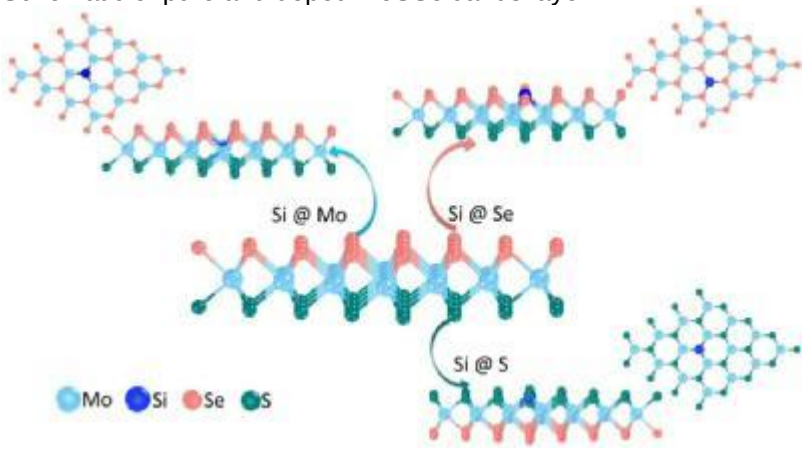

Gibbs free energy of H adsorption on Janus layer

Back to Table of contents

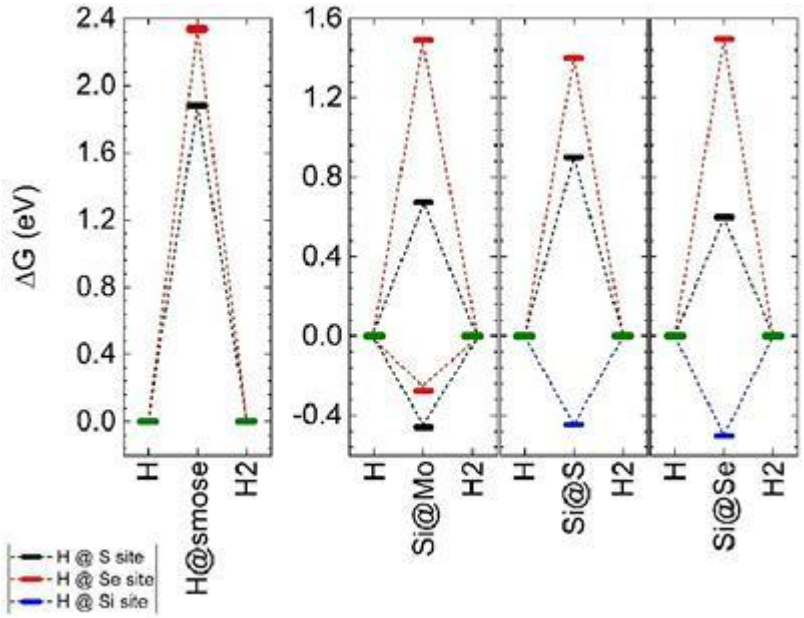

Back to Table of contents

MS14 Materials for energy storage and Conversion

MS14-2-5 Temperature and pressure stability of Li graphite intercalation compounds
#MS14-2-5

V. Baran [1], T. Hölderle [2], A. Méndez [1], A. Senyshyn [2]
[1]Deutsches Elektronen-Synchrotron (DESY) - Hamburg (Germany), [2]research neutron source heinz maier-leibnitz (frm ii) , technical university of munich - Garching (Germany)

Abstract
Nowadays, Li-ion batteries (LIBs) are dominating the electric energy storage market: powering electric vehicles, mobile devices, power tools, and off-grid storage systems. Modern Li-ion batteries, in the majority, use graphite as anode material due to its layered structure that allows relatively easy intercalation of species between them. Graphite intercalation compounds (GIC) have been known for some time and intensively studied but are still missing structure and properties data about some of the representatives[1, 2]. From this perspective, Li GICs have much attention to their synthesis, structure, and thermodynamic stability, with some controversial or inconsistent data, particularly temperature and pressure stability.
In the current contribution, we would like to present investigations on the temperature and pressure stability of Li GICs employing synchrotron x-ray diffraction. The temperature stability regime was investigated for a powder sample of Li_xC_6 (x = 0-0.9) extracted from LIB with high energy x-rays (60 keV) at the P02.1 beamline, PETRA III (DESY), in the temperature range from 180 K to 500 K. The pressure stability of Li_xC_6 (x = 0.7) was investigated at room temperature using a hydrostatic high-pressure cell [3] in the pressure range from 0 to 4000 bars.

References
[1] M. S. Dresselhaus and G. Dresselhaus, “Intercalation compounds of graphite”, Adv. Phys., 51:1, 1-186 (2002)
[2] E. Morinobu, M.S. Suzuki and T. Enoki. “Graphite Intercalation Compounds and Applications.” (2003)
[3] F. J. Wirkert, M. Paulus, J. Nase, J. Möller, S. Kujawski, C. Sternemann and M. Tola, “X-ray reflectivity measurements of liquid/solid interfaces under high hydrostatic pressure conditions”, J. Synchrotron Rad. 21, 76-81 (2014)

Back to Table of contents

MS14 Materials for energy storage and Conversion

MS14-2-6 MOF Catalysts for Energy Applications: Incorporation of Transition Metals at Atomic Levels #MS14-2-6

Z. Huang [1]
[1]Department of Materials and Environmental Chemistry, Stockholm University - Stockholm (Sweden)

Abstract
With the emergency call for carbon neutrality, development of new technologies to produce renewable and clean energy are attracting increasing attention recent years. Hydrogen energy is the most promising one due to that the consumption of hydrogen only produces water. With fuel cell hydrogen can be safely translated to electricity under mild conditions. However, the storage and transmission of hydrogen is still challenging. Ammonia borane as a promising hydrogen storage material can release a high amount of hydrogen with noble metals like Pt, Ru, Rh and Au as catalysts. Besides, in fuel cell devices, platinum group materials are the predominant class of materials that are used as the key component to catalyse the oxygen reduction reaction (ORR). However, the scarcity, high cost, and low efficiency of these noble metal catalysts prevent the widespread implementation of hydrogen as an affordable clean energy.
The low cost yet high tunability of metal−organic frameworks (MOFs) provide a unique platform for tailoring their characteristic properties as new catalysts. I will present stable MOFs with transition metal ions incorporated at atomic level as efficient catalysts. For example, we have developed a series of novel multivariate metal−organic frameworks (MTV-MOFs), MTV-MIL-100, through a solvent-assisted approach[1]. Two Co caions are anchored in each tri-nuclear cluster with ordered atomic arrangements with one Ti cation. These ordered and multivariate metal clusters offer an opportunity to enhance and fine-tune the electronic structures of the crystalline materials. Moreover, mass transport is improved by taking advantage of the high porosity of the MOF structure. Combining these key advantages, MTV-MIL-100(Ti,Co) exhibits a high photoactivity in the photocatalytic hydrolysis of ammonia borane. Moreover, we develop MOF catalysts by combining Zr-chains to promote high chemical stability and metalloporphyrin ligands to introduce transition metal ions as redox active-sites[2]. In addition, we tailor the immobilization and packing of the single redox active atoms at a density that is ideal for the reaction kinetics of ORR. The obtained MOF catalyst, PCN-226, thereby shows high ORR activity. We further demonstrate PCN-226 as a promising electrode material for practical applications in rechargeable Zn-air batteries. These examples represent two different strategies to design and incorporate transition metals in porous materials at an atomic level, which could further accelerate the development in searching for efficient catalysts.

References
[1] Y. Wang, H. Lv, E. S. Grape, C. A. Gaggioli, A. Tayal, A. Dharanipragada, T. Willhammar, A. K. Inge, X. Zou, B. Liu, Z. Huang, J. Am. Chem. Soc. 2021, 143, 6333–6338.
[2] M. O. Cichocka, Z. Liang, D. Feng, S. Back, S. Siahrostami, X. Wang, L. Samperisi, Y. Sun, H. Xu, N. Hedin, H. Zheng, X. Zou, H.-C. Zhou, Z. Huang, J. Am. Chem. Soc. 2020, 142, 15386–15395.

Back to Table of contents

MS14 Materials for energy storage and Conversion

MS14-2-7 Real structure of magnetron sputtered Pt-based nanocrystalline thin films
#MS14-2-7

M. Dopita [1], L. Horák [1], I. Khalakhan [1]
[1]Charles University - Prague (Czech Republic)

Abstract
Due to high energy-conversion efficiency, low operation temperatures, and environmental sustainability, proton exchange membrane fuel cells (PEMFCs) are among the most promising candidates for future green-energy systems. However several drawbacks hinder its wide commercialization. A high platinum price is a serious problem. Extensive studies have been performed to find the oxygen reduction reaction (ORR) catalyst, which is more active, less expensive and more stable than pure platinum. The promising strategy is the alloying of platinum with relatively cheap transition metals. It has been reported in literature that Pt alloyed with Ni, Co and Fe enhances the electrocatalytic activity toward ORR, while simultaneously lowers the catalyst cost due to reduction of used platinum quantity.
In our work the series of Pt, Pt-Ni, Pt-Cu, Pt-Y and Pt-CeO_2 nanocrystalline films were prepared by the magnetron co-sputtering process. The microstructure and the real structure of coatings were investigated in as-deposited as well as in as-treated - after the electrochemical treatment, simulating the real function of fuel cell (accelerated durability tests), using the combination of x-ray scattering methods (X-ray reflectivity, X-ray diffraction, GISAXS), SEM, TEM/HRTEM, and in situ electrochemical AFM and XPS.
A special emphasis was focused on detailed description of the real structure of the layers – its thickness, roughness, the phase composition, size of coherently diffracting domains – crystallite size, the defects of the crystal lattice, the preferred orientation of crystallites – the texture, the presence and the magnitude of the residual stress in layers, because of its undisputable role and influence in the deterioration processes occurring during the materials operation as a cathode in the PEMFCs. The results of microstructural investigations were correlated with the activity loss, dealloying and morphological changes induced by catalysts aging processes. Our study showed that the real structure of layers has an essential influence on the deterioration processes, significantly influencing the life time of PEMFCs cathodes.

References
[1] I. Khalakhan, M. Vorokhta, P. Kúš, M. Dopita, M. Václavů, R. Fiala, N. Tsud, T. Skála, V. Matolín, Electrochim. Acta 245, 2017, 760–769
[2] R. Brown, M. Vorokhta, I.Khalakhan, M. Dopita, T. Vonderach, T. Skála, N. Lindahl, I. Matolínová, H. Grönbeck, K. M. Neyman, V. Matolín, B. Wickman, ACS, Appl. Maters. and Interfaces, Volume 12, Issue 4, 2020, 4454-4462.
[3] I. Khalakhan, M. Bogar, M. Vorokhta,P. Kúš, Y. Yakovlev, M. Dopita, D.J.S. Sandbeck, S. Cherevko, I. Matolínová, H. Amenitsch, ACS App. Maters. and Interfaces, Volume 12, Issue 15, 2020, 17602-17610.
[4] X. Xie, I. Khalakhan, M. Vorokhta, Y. Yakovlev, T. N. Dinhová, J. Nováková, P. Kúš, M. Dopita, K. Veltruská, I. Matolínová, Adv. Mater. Interfaces, 8, 2021, 2100122.

Back to Table of contents

MS14 Materials for energy storage and Conversion

MS14-2-8 Predictive modeling of order-disorder phase transitions in hybrid organic materials with machine learning force fields
#MS14-2-8

R. Tranås [1], E.D. Sødahl [1], J.M. Carrete [2], G. Madsen [2], K. Berland [1]
[1]Norwegian University of Life Sciences NMBU - Ås (Norway), [2]TU Wien - Vienna (Austria)

Abstract
The caloric and ferroic properties of hybrid-organic materials make them attractive environmental-friendly materials for a range of technological applications, including actuators, sensors, energy harvesting, and solid-state refrigeration. However, progress in the development of such materials is hampered by the huge computational costs of ab-initio molecular dynamics modeling at finite temperatures which is required for predictive modeling of dynamical properties including phase transition temperatures. However, recent advances in machine-learning force fields (ML-FF) hold a promise of providing first-principles accuracy of dynamical properties at a fraction of the computational costs while retaining high accuracy. In this case study, we use the recently developed NeuralIL [1] ML-FF software to provide microscopic insight into the barocaloric (CH3)2NH2Mg(HCOO)3 system [2]. The simulations reveal the important role of methyl side group rotations in the vicinity of the phase transitions. The predictive phase transition temperature is also in close agreement with the experimental predictions, highlighting the potential of the method.

References
[1] Hadrián Montes-Campos, Jesús Carrete, Sebastian Bichelmaier, Luis M. Varela, and Georg K. H. MadsenJournal of Chemical Information and Modeling 2022 62 (1), 88-101
[2] Marek Szafranski, Wen-Juan Wei, Zhe-Ming Wang, Wei Li, and Andrzej Katrusiak, APL Materials 6, 100701 (2018)

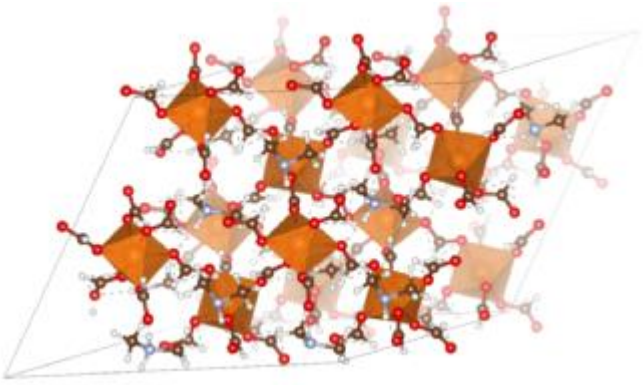

Back to Table of contents

MS14 Materials for energy storage and Conversion

MS14-2-9 Crystallographic studies of the Magnesium nitrate salt-hydrate eutectic system
#MS14-2-9

H.T. Logan [1], D.E. Oliver [2], C.R. Pulham [1]
[1]University of Edinburgh - Edinburgh (United Kingdom), [2]Sunamp Ltd. - Macmerry (United Kingdom)

Abstract
The advent of large-scale renewable energy sources has led to a growing requirement for energy-storage technologies whereby energy is stored at times of high production and low demand[1]. An important technology is thermal energy storage as 42% of the UK's energy demand is associated with heating and cooling. Phase-change materials (PCMs) enable the storage of thermal energy due to the material's high latent heat of fusion. A material of particular interest for PCM applications is magnesium nitrate. While it has been studied extensively for this purpose in the hexahydrate form[2], the low temperature eutectic composition has a melting temperature of approximately -31.5 °C [3], which is suitable for refrigeration applications. Such hydrates provide high cooling capacity at a composition for which the components crystallise at the temperature corresponding to the lowest melting point of the system. However, these PCMs suffer from several issues that must be overcome before integrating into cooling systems. Salt-hydrate eutectic systems frequently sub-cool[4] – a phenomenon whereby a material cools below its freezing point without crystallisation occurring.
Using the technique of 3-layer calorimetry, we have observed separate crystallisation events for each component (salt-hydrate and ice), suggesting that the phases sub-cool independently to different temperatures despite being at the eutectic composition. Using powder X-ray diffraction (PXRD) the low-temperature hydrate composition (suspected to be the nonahydrate) of the system has been studied, to gain structural and phase evolution information. Furthermore, a metastable magnesium nitrate hydrate (suspected to be the tetrahydrate) has also been studied. By solving the crystal structure of these low-temperature hydrates, we can begin to identify ways of eliminating the issue of sub-cooling through the use of heterogeneous nucleating agents. This will enable us to use these PCMs in energy-storage applications.

References
1. X. Luo et al., Appl. Energy, 2015, 137, 511-536.
2. K. Kauffman et al, Report No. NCEMP-20, University of Pennsylvania, Philadelphia, 1975.
3. W. Ewing et al, J. Am. Chem. Soc., 1933, 55, 4822-4824.
4. F. Bruno et al, Advances in Thermal Energy Storage Systems, Woodhead Publishing, Cambridge, 2014.

Back to Table of contents

MS15 Mineralogical and inorganic crystallography

MS15-1-1 Quantitative Phase Analysis of Anhydrous Clinker Portland using Rietveld Method #MS15-1-1

D. Tlamsamani [1], M. Ait Mouha [1], S. Slassi [1], Y. Khaddam [1], K. Yamni [1]
[1]Moulay Ismail University - Meknes (Morocco)

Abstract
Modern cements are complex materials with well-defined compositions that reach to high and consistent results. Automated techniques such as Rietveld analysis provide high precision controls of the composition and polymorphism of cement phases in order to optimize characteristics and consequently quality product. For the characterization of cements used in the construction sector, Rietveld method has significant benefits over other analytical techniques. The precise information about phase assemblage and polymorphism lets monitoring the hydration behavior of binder materials.
The objective of this paper is to report the quantitative Rietveld phase analyzes for three industrial clinkers, to review the most recent quantitative X-ray powder diffraction studies on anhydrous cement and to discuss the influence of the different parameters elaborated in the Rietveld method.

Back to Table of contents

MS15 Mineralogical and inorganic crystallography

MS15-1-10 Closing Some Gaps of Knowledge: Single Crystals of $Tm_2O[SiO_4]$ with the B-Type Structure #MS15-1-10

P. Djendjur [1], S. Greiner [1], T. Schleid [1]
[1]University of Stuttgart / Institute for Inorganic Chemistry - Stuttgart (Germany)

Abstract
Lanthanoid oxosilicates and their derivatives show a huge variety of compositions and structures. Since many solid-state reactions take place in glassy silica ampoules, a rather big proportion of side products from these reactions tend to yield oxosilicate derivatives. Compounds of the formula type $Ln_2O[SiO_4]$ (*Ln* = La, Nd, Eu, Gd, Ho – Lu) realize two different structure types. The $Gd_2O[SiO_4]$- or A-type structure is adopted by representatives all over the whole lanthanoid series (*Ln* = La, Nd, Eu, Gd, Ho – Tm and Lu) [1–6] and exhibits isolated $[SiO_4]^{4-}$ tetrahedra in combination with a porous network of distorted $[OLn_4]^{10+}$ tetrahedra connected via edges and corners forming $^{2}_{\infty}\{[O(Ln1)_{1/1}(Ln2)_{3/3}]^{4+}\}$ layers, which spread out parallel to the (100) plane. Another structure type is represented by the $Yb_2O[SiO_4]$- or B-type arrangement, which is so far only known with the heavier lanthanoids (*Ln* = Er, Yb – Lu) [7–9]. In this work, we present another representative of these B-type lanthanoid(III) oxide oxosilicates, namely $Tm_2O[SiO_4]$, which closes the gap in the short $Ln_2O[SiO_4]$ series with *Ln* = Er – Lu. It crystallizes in the monoclinic space group *C*2/*c* with the lattice parameters *a* = 1432.74(11) pm, *b* = 668.52(5) pm, *c* = 1033.67(8) pm, *β* = 122.183(3)° and *Z* = 8 (CSD-2169113).
The crystal structure consists of two crystallographically different Tm^{3+} cations (Figure 1). $(Tm1)^{3+}$ is surrounded by seven oxygen atoms to form a capped octahedron, whereas $(Tm2)^{3+}$ has a distorted octahedron with only six oxygen atoms as coordination sphere. With this in mind, it becomes clear, why the B-type structure can only be found with representatives of the later part of the lanthanoid series, offering rather small coordination spheres for both Ln^{3+} cations. Like in the A-type structure, silicon is surrounded by four of the five distinct oxygen atoms to form $[SiO_4]^{4-}$ tetrahedra (*d*(Si–O) = 161 – 164 pm), which remain isolated from one another. The single remaining oxygen atom (O5) is coordinated in a distorted tetrahedral manner by four Tm^{3+} cations, building $[OTm_4]^{10+}$ units, which are connected via common *trans*-oriented edges to two neighboring $[OTm_4]^{10+}$ units to form undulated $^{1}_{\infty}\{[O(Tm1)_{2/2}(Tm2)_{2/2}]^{4+}\}$ strands propagating parallel to the [001] direction (Figure 2).

References
[1] K. Fukuda, T. Iwata, E. Champion, *Powd. Diffr.* **2006**, *21*, 300–303.
[2] L. Leon-Reina, J. M. Porras-Vazquez, E. R. Losilla, L. Moreno-Real, M. A. G. Aranda, *J. Solid State Chem.* **2008**, *181*, 2501–2506.
[3] M. E. Bohem, Th. Schleid, *Z. Anorg. Allg. Chem.* **2016**, *642*, 1055–1055.
[4] Yu. I. Smolin, S. P. Tkachev, *Kristallografiya* **1969**, *14*, 22–25.
[5] I. Hartenbach, S. F. Meier, J. Wontcheau, Th. Schleid, *Z. Anorg. Allg. Chem.* **2002**, *628*, 2907–2913.
[6] H. Müller-Bunz, Th. Schleid, *Z. Anorg. Allg. Chem.* **1999**, *625*, 613–618.
[7] Yu. I. Smolin, *Kristallografiya* **1969**, *14*, 985–989.
[8] D. Phanon, R. Černý, *Z. Anorg. Allg. Chem.* **2008**, *11*, 1833–1835.
[9] T. Gustafsson, M. Klintenberg, S. E. Derenzo, M. J. Weber, J. O. Thomas, *Acta Crystallogr.* **2001**, *C 57*, 668–669.

Coordination polyhedra of $(Tm1)^{3+}$ and $(Tm2)^{3+}$.

Back to Table of contents

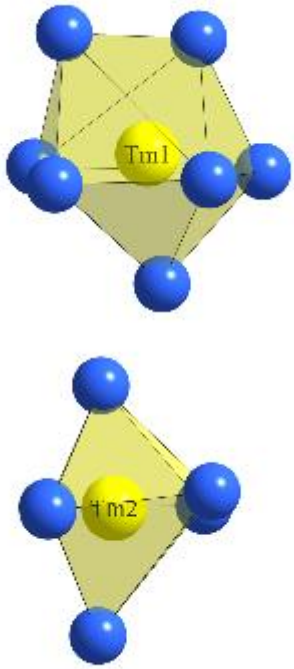

Unit cell of the B-type structure of $Tm_2O[SiO_4]$.

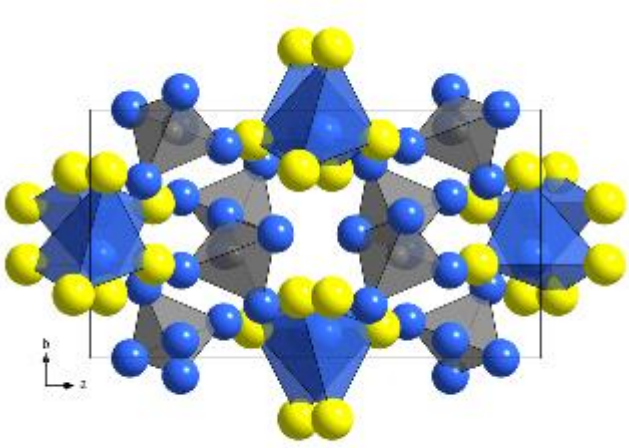

Back to Table of contents

MS15 Mineralogical and inorganic crystallography

MS15-1-11 Oxometalates A_3MO_2 with linear anions
#MS15-1-11

I. Zaytseva [1], C. Hoch [1]
[1]University of Munich (LMU) - Munich (Germany)

Abstract
A series of oxometalates A_3MO_2 (A = Na, K, Rb, Cs; M = Fe, Co, Ni, Cu, Ag, Au) with linear anions $[O–M^{I}– O]^{3–}$ have been characterised [1-6]. Their respective crystal structures have been described in multiple ways, complicating a comprehensive overview for this family of oxometalates. We present three new compounds and propose an overarching description on the basis of the structural relations of the cation packings in the majority of A_3MO_2 oxometalates to an idealised α-Uranium packing.
Dark red Cs_3NiO_2 crystals were prepared from NiO, Cs and Cs_2O at 250 °C in a closed tantalum crucible. It crystallises in the Cs_3AuO_2 structure type [1] ($P2_1/c$, Z = 12, a = 10.076(2) Å, b = 19.557(2) Å, c = 13.881(2) Å, β = 132.730(14)°, V = 2009.4(5) Å^3), in contrast to the reported modification described in $P4_2/mnm$ obtained by azide-nitrate route [2].
Yellow crystals of Cs_3CuO_2 were obtained in two modifications under similar synthesis conditions and were prepared from Cu metal and Cs_2O in closed silver or tantalum crucibles. One modification of Cs_3CuO_2 also adopts the Cs_3AuO_2 structure type [1] ($P2_1/c$, Z = 12, a = 10.0221(3) Å, b = 19.5023(5) Å, c = 13.8005(3) Å, β = 132.5160(10)°, V = 1988.19(9) Å^3). The other modification crystallises in a new structure type (P-1, Z = 6, a = 10.0322(10) Å, b = 10.0154(9) Å, c = 10.2089(8) Å, α = 93.815(4)°, β = 103.273(5)°, γ = 90.417(5)°, V = 995.8(2) Å^3).
The figure below shows various features of the Cs_3NiO_2 crystal structure. Constrictions of the linear $[NiO_2]^{3-}$ anions result in a particular sequence of edge and corner sharing distorted $[O(Cs_5Ni)]$ octahedra (red). These octahedral voids connect distorted hexagonal nets from both Cs and Ni atoms (blue and green, respectively). Atoms of one layer sit on top of the edge of triangles of an adjacent layer, giving an idealised α-U packing. Therefore, Cs_3NiO_2 can be described as *ADA'D'A''D''* sequence of Cs+Ni layers with ½ of the octahedral voids occupied by O. The structural analogies can be found in almost all representatives of this class of oxometalates and become even more striking for those compounds with higher symmetry. Starting from an idealised α-Uranium structure ($I4/mmm$, experimental α-Uranium structure in $Cmcm$ [7]), the A_3MO_2 structure family and occurring phase transitions can be described in a comprehensive way and, to some extent, be rationalised in a Bärnighausen tree.

References
[1] A.-V. Muding and M. Jansen (2012) Z. Anorg. Allg. Chem. 627, 77-80.
[2] K. Đuriš, O.V. Magdysyuk, M. Jansen (2012) Solid State Sci. 14, 1399-1404.
[3] W. Burow, J. Birx, F. Bernhardt, R. Hoppe (1993) Z. Anorg. Allg. Chem. 619 923-933
[4] F. Bernhardt, R. Hoppe (1950) Z. Anorg. Allg. Chem. 619, 969-975
[5] B. Darriet, M. Devalette, B. Lecart (1977) Rev. Chem. Miner. 14, 423-428.
[6] W. Carl, R. Hoppe (1989) Z. Anorg. Allg. Chem. 547, 79-88
[7] G.H. Lander, M.H. Mueller, (1970) Acta Crystallogr. B 26, 129-136.

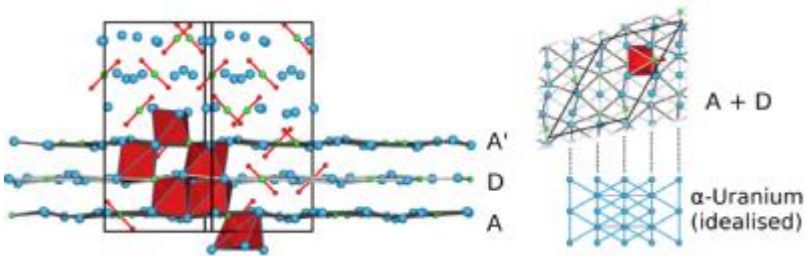

Back to Table of contents

MS15 Mineralogical and inorganic crystallography

MS15-1-12 Crystal structure and thermal behavior of Bi6Te2O15: investigation of synthetic and natural pingguite #MS15-1-12

G. Nénert [1], O. Missen [2], M. Weil [3], S. Mills [2]
[1]Malvern Panalytical - Almelo (Netherlands), [2]Geosciences, Museums Victoria - Melbourne (Australia), [3]TU Wien - Vienna (Austria)

Abstract
Pingguite was first reported in 1994 from the Yangjia Au deposit, as $Bi_6Te^{IV}_2O_{13}$ [1]. No crystal structure was determinable, and the valence of Te was determined by XPS. Subsequent occurrences of pingguite have been found in 4 additional countries, a more widespread distribution than many secondary tellurium minerals. Around half of the ~90 secondary Te minerals are found only in North America [2]. Despite its low planetary abundance, tellurium is found in an anomalously large number of minerals [3]. This is in part due to its complex chemistry in surface environments, including the stability of two higher oxidation states (Te^{IV} and Te^{VI}) which may coexist [2]. Pingguite is the most recently described mineral containing only bismuth, tellurium and oxygen.
The previously unknown crystal structure of pingguite was determined and refined from laboratory X-ray powder diffraction data using a synthetic sample [4]. We used this structural model to describe additional single crystal diffraction data of natural pingguite. This crystal structure calls for a revised chemistry of the rare mineral pingguite to $Bi_6Te_2O_{15}$ instead of the previously reported formula $Bi_6Te_2O_{13}$. Pingguite contains Te^{VI} only and not Te^{IV} as previously reported. Pingguite undergoes an irreversible phase transition around 840°C which is characterized by a loss of oxygen and a reduction from TeVI to TeIV resulting in a δ-Bi_2O_3 like type structure.

References
[1] Zhifu S, et al. (1994) Acta Mineral Sin 14:315
[2] Missen OP, et al. (2020) Earth-Sci Rev 204:103150.
[3] Christy AG (2015) Mineral Mag 79:33
[4] G. Nénert et al. (2020) Physics and Chemistry of Minerals (2020) 47:53

a) Crystal structure and b) picture of pingguite

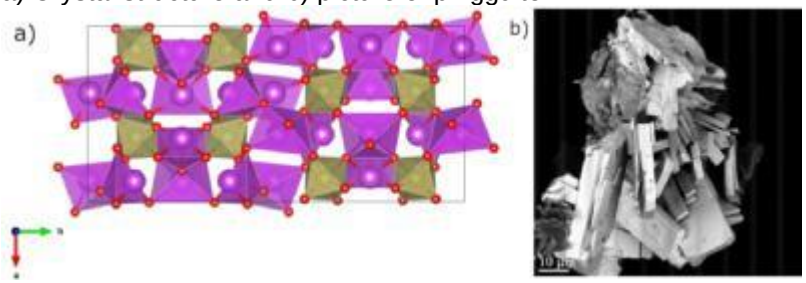

Back to Table of contents

MS15 Mineralogical and inorganic crystallography

MS15-1-13 The Hg-rich part of the binary system K-Hg revised: Synthesis, crystal and electronic structure of the new mercurides KHg_4, KHg_5 and KHg_8
#MS15-1-13

T. Hohl [1], C. Hoch [1], M. Wendorff [2], C. Röhr [2]
[1]LMU München - München (Germany), [2]ALU Freiburg - Freiburg (Germany)

Abstract
A thermoanalytical reinvestigation of the Hg-rich part of the binary phase diagram K-Hg (Fig. 1) revealed the three new incongruently melting compounds KHg_4, KHg_5 [1] and KHg_8, in addition to the known phases K_2Hg_7 [2], K_3Hg_{11} ([3], not reproduced), K_7Hg_{31} [3], KHg_6 [4] and KHg_{11} [5]. According to the revised phase diagram, KHg_4 and KHg_5 were obtained from melts of the elements using appropriate Hg-richer sample compositions.The Hg-rich compound KHg_8 was synthesized by slowly unfreezing a 31:7 mixture of Hg:K from -70 °C to r.t. The three title compounds all form new structure types, which were determined by means of single crystal X-ray data. In the structures of KHg_8 [triclinic, *P*-1, *a*=630.0(2), *b*=897.2(2) *c*=1263.7(3) pm, α=99.30(3), β=91.34(3), γ=98.36(3)°] and KHg_5 [monoclinic, $P2_1/c$, *a*=1148.3(1), *b*=1758.6(2), *c*=1031.5(1) pm, β=116.687(1)°], similar to KHg_6 [4] and related alkaline-earth compounds [6], the Hg atoms of all sites form nearly flat nets with 8/7-membered rings (yellow), regular pentagons (blue) and distorted pentagons, squares and triangles (red). The potassium cations are always centered in the 8/7-membered rings, which are completed by two nearly regular 5-membered rings (blue) of the shifted (cf. arrows in Fig. 2) adjacent nets to form overall 18/17 (5:8/7:5) cation coordination polyhedra (ccp). The space inbetween the columns of ccps, which increases with the Hg-content, consists of distorted trigonal prisms, octahedra and tetrahedra (red). These latter pure mercury polyhedra are formed by the smaller rings of the Hg nets. The orthorhombic structure of KHg_4 [*Cmcm*, *a*=937.4(3), *b*=873.5(3), *c*=645.6(2) pm] contains similar ccps and Hg_6 trigonal prisms, but an alternative structure description emphasizing flat square pyramids (green) relates this structure to those of other alkali and alkaline-earth mercurides in this composition range (e.g. K_3Hg_{11}, Rb_5Hg_{19} [7]). The calculated electronic structures show the expected metallic character of the compounds, but also a distinct electron transfer form K to Hg, which justifies to denote them 'mercurides'.

References
[1] M. Wendorff, C. Röhr, *Z. Kristallogr. Suppl.*, **41** 79-80 (2021).[2] E. Biehl, H. J. Deiseroth, *Z. Anorg. Allg. Chem.*, **625**, 1337-1342 (1999).[3] E. Todorov, S. C. Sevov, *J. Solid State Chem.*, **149**, 419-427 (2000).[4] F. Tambornino, C. Hoch, *J. Alloys Compd.*, **618**, 299-304 (2015).[5] E. Biehl, H. J. Deiseroth, *Z. Anorg. Allg. Chem.*, **625**, 1073-1080 (1999).[6] M. Wendorff, C. Röhr, *Z. Kristallogr.* **233**, 515-529 (2018).[7] E. Biehl, H. J. Deiseroth, *Z. Anorg. Allg. Chem.*, **625**, 389-394 (1999).[8] T. B. Massalski, H. Okamoto, P. R. Subramanian, L. Kacprzac (Hrsg.), Binary Alloy Phase Diagrams, 2nd. Edition, ASM International, Materials Park (OH, USA), 1990.

Revised phase diagram of the binary system K-Hg.

Back to Table of contents

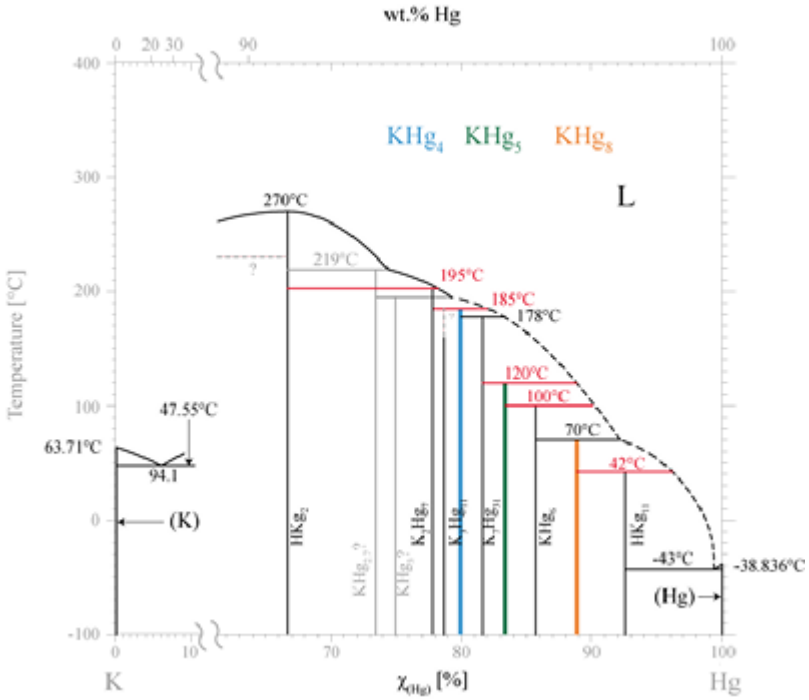

Comparison of the Hg nets in the crystal structure

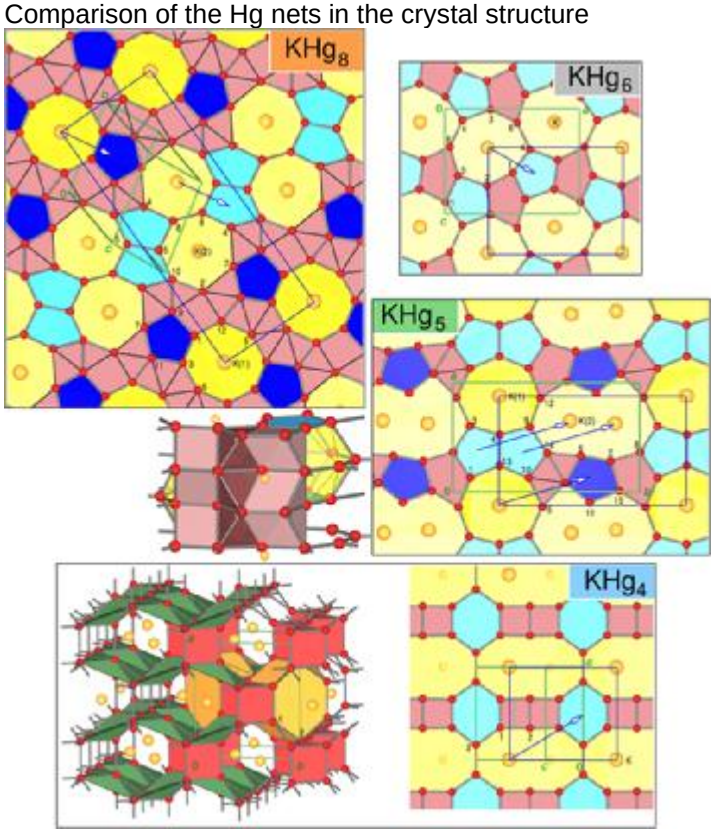

Back to Table of contents

MS15 Mineralogical and inorganic crystallography

MS15-1-14 Periodic trends of stereochemical activity of lone electron pairs
#MS15-1-14

M.M. Murshed [1], T. Gesing [1]
[1]University of Bremen - Bremen (Germany)

Abstract
In a series of papers, Wang and Liebau [1-3] pointed out that the bond valence sum calculated for a lone electron pair (LEP) cation increases as the cation's coordination environment becomes more distorted. They proposed to associate the geometric distortion of the LEP-coordination as the measures of the stereochemical activity of the LEP using the term eccentricity which we later coined as Wang-Liebau eccentricity (WLE) parameter [4]. Most of the polyhedral distortion indices [5-9] are purely geometric and cannot account for the interaction strength between the atoms. In contrast, the WLE parameter describes the weighted bond length with an exponential function, allowing the strength of a bond to exponentially decrease with increasing bond length. Sampling on crystal information data of As-, Se-, Sn-, Sb-, Te-, Tl-, Pb- and Bi-oxide coordinations, a statistical approach demonstrates that the WLE parameter of the LEP-cations follows a periodic trend. This study also includes a detailed comparison between the WLE and Hamani [10] model for the periodic trends of some LEP cations.

References
[1] X. Wang, F. Liebau, Z. Krist. 211 (1996) 437.
[2] X. Wang, F. Liebau, Acta Crystallogra. B 63 (2007) 216.
[3] F. Liebau, X. Wang, W. Liebau, Chem. - A Eur. J. 15 (2009) 2728.
[4] M. Curti, T.M. Gesing, M.M. Murshed et al., Z. Krist. 288 (2013) 629.
[5] K. Robinson, G. V. Gibbs, P.H. Ribbe, Science (80-.). 172 (1971) 567.
[6] J.M. Gaite, Phys. Chem. Miner. 6 (1980) 9.
[7] W.A. Dollase, Acta Crystallogr. A 30 (1974) 513.
[8] E. Makovicky, T. Balić-Žunić, Acta Crystallogr. Sect. B Struct. Sci. 54 (1998) 766.
[9] P.S. Halasyamani, Chem. Mater. 16 (2004) 3586.
[10] D. Hamani, O. Masson, P. Thomas, J. Appl. Cryst. 53 (2020) 1243.

Back to Table of contents

MS15 Mineralogical and inorganic crystallography

MS15-1-15 The new PHOTON III HE detector – unbeatable sensitivity for short wavelength crystallography #MS15-1-15

C. Lenczyk [1], T. Stuerzer [1], R. Durst [1], V. Smith [1]
[1]Bruker AXS GmbH - Karlsruhe (Germany)

Abstract
Recent years have seen strong growth in several areas of crystallography that require data collection using shorter wavelength X-rays emitted such as the development of new functional materials containing heavy elements, charge-density studies in quantum crystallography and studies on the effects of high-pressure on various types of crystals from the geosciences to improving pharmaceutical formulations. All typically require high precision data from advanced diffraction experiments.
The major technical drawback to crystallography using higher energy X-rays is that the quantum efficiency of many photon-counting direct detectors is very low at such high energies, and so it becomes increasingly difficult to obtain sufficiently precise data.
The new PHOTON III HE detector takes advantage of the advanced indirect detection employed in the PHOTON III series [1] to achieve very high quantum efficiency for the higher X-ray energies emitted from sources such as Mo, Ag and In.
Using a number of selected examples, we will demonstrate the improvements in data quality achieved by combining a hard radiation source with the new PHOTON III HE. We also will provide insights into modern indirect detector technology.

References
[1] B. Becker, J. Kaercher, M. Krug, S. Leo, T. Stuerzer, B. Weinhausen, R. Durst, "A large area detector with indirect conversion, charge integration and photon counting operation," Proc. SPIE 11838, Hard X-Ray, Gamma-Ray, and Neutron Detector Physics XXIII, 118380N (1 September 2021); https://doi.org/10.1117/12.2597029

Photon-counting PHOTON III HE detectors

Back to Table of contents

MS15 Mineralogical and inorganic crystallography

MS15-1-16 Synthesis and structural evaluation of a new copper(II) complex with a dithiocarbazate ligand #MS15-1-16

T. Leite [1], C. Gatto [1]
[1]University of Brasilia - Brasilia (Brazil)

Abstract
The dithiocarbazates are Schiff bases that present huge versatility, their chemical properties can be modified with the introduction of different substituent groups in their structure, allowing the formation of metal complexes with different coordination polyhedra.[1] In addition, dithiocarbazates and their complexes are reported in the literature showing biological properties such as antifungal, antibacterial and antitumoral.[2,3] The current work reports the synthesis and structural evaluation of a new dithiocarbazate ligand (2-acetylpiridine-S-p-clorobenzyl-dithiocarbazate) and its Cu(II) complex. Both complex and ligand have been characterized by spectral measurements such as IR, and UV-Vis and the ligand was characterized also by ^{1}H NMR and ^{13}C NMR. The crystal structure and molecular interactions were evaluated by single-crystal X-ray diffraction and the analysis of the Hirshfeld surface. The Cu(II) complex was observed with a square planar geometry, coordinated by *NS*-donor atoms of the dithiocarbazate and a chloride ion. The ligand is coordinated to the center atom with an anionic form and thiol tautomer. Intermolecular interactions were found between S1····H14 and Cl1····H2; those interactions contribute to the formation of the supramolecular arrangement in the crystal packing. Both compounds will be submitted for biological evaluation to investigate their promising biological properties.

References
[1] Cavalcante, C. D. Q. O. et al. (2019) New J. Chem, 48, 15501-15514.
[2] Yekke-Ghasemi, Z. et al (2020). New J. Chem, 44, 8878-8889.
[3] Lima, F. C. et al (2018). Inorg. Chim. Acta 483, 464-472.

Molecular structure of the copper(II) complex.

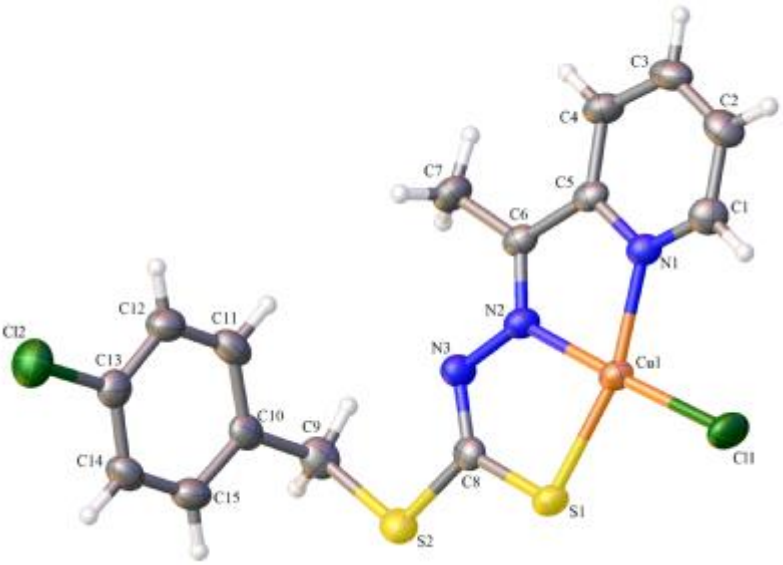

Back to Table of contents

MS15 Mineralogical and inorganic crystallography

MS15-1-17 A revised structure for the rare earth fluoride gagarinite-(Ce) from experimental synthesis by fluid induced alteration of chevkinite-(Ce)
#MS15-1-17

M. Stachowicz [1], P. Jokubauskas [1], B. Bagiński [1], R. Macdonald [1], D.E. Harlov [2]
[1]Department of Geochemistry, Mineralogy and Petrology, Faculty of Geology, University of Warsaw, Żwirki i Wigury 93, 02-089 - Warszawa (Poland), [2]Section 3-3, GeoForschungsZentrum, Telegrafenberg, 14473 - Potsdam (Germany)

Abstract

The Rare Earth Element (REE) fluoride, gagarinite-(Ce), $^{A}Na^{B}(REE,Ca)_2F_6$ has been synthesized in an experiment designed to examine the fluid-induced alteration of chevkinite-(Ce), $(Ce_{1.85}La_{0.79}Nd_{0.64}Ca_{0.39}Pr_{0.22})_{3.9}Fe^{2+}(Fe^{2+}_{1.03}Ti_{0.75}Mn_{0.16})_{1.9}Ti_2(Si_2O_7)_2O_8$. The experiments were conducted at 600 °C and 400 MPa for 21 days; 550 °C and 200 MPa for 63 days; and 600 °C and 200 MPa for 42 days. The formula of crystallized gagarinite-(Ce) analogue, calculated on the basis of 3 cations and 6 F *pfu*, can be written as: $(Na_{1.10}Ce_{0.69}Ca_{0.44}Nd_{0.31}La_{0.26}Pr_{0.12}Sm_{0.04}Sr_{0.03})_{3.0}F_{6.0}$.

The mineral, previously named zajacite-(Ce), is known from only one natural occurrence, a hypersolvus granite from the Strange Lake Zr-Y-REE-Nb-Be deposit, Quebec-Labrador. The space group was identified as $P\bar{3}$, with unit cell parameters *a*=6.099(1), *c*=11.064(2)(2) Å [1]. A subsequent single-crystal determination showed that it is isostructural with gagarinite-(Y) and its name was changed, with IMA-CNMNC approval, to gagarinite-(Ce), space group $P6_3/m$, with *a*=6.0861(12) and *c*=3.6810(8) Å [2].

The gagarinite-(Ce) in our experiments crystallized in $P\bar{6}$, with *a* = 6.1465(2), *c*= 3.75950(10), R_1=1.37%. We observed 26% twinning by a twin center. The structure is derived from that of UCl_3 [3] with the addition of extra $^{B}Na^{+}$ into the crystal lattice, where REE^{3+} and Ca^{2+} fill both the cation sites (*A*) of the uranium salt [4,5].

Previous studies assumed full occupancy of the REE+Ca, compositionally disordered, site. To charge balance the substitution $2^{A}REE^{3+} \rightarrow {}^{A}Ca^{2+} + {}^{A}REE^{3+} + {}^{B}Na^{+}$, the amount of extra Na^{+} must equal Ca^{2+} in the final formula, giving $Na_x(Ca_xREE_{2-x})F_6$. Gagarinite-(Ce) from the experiment shows surplus Na over Ca with a ratio close to 2:1, respectively. A vacancy in the REE site is necessary, equal to $\frac{1}{3}$ of the redundant Na to remain in charge balance. If the Na content exceeds 1 in the formula unit, Na has to substitute for REE in the cation site. Thus, the overall substitution mechanism is:

$(2x-y)REE^{3+} \rightarrow y\ {}^{B}Na^{+} + (x-y)\ {}^{A}Na^{+} + y\ {}^{A}Ca^{2+} + \frac{x-y}{3}\ {}^{A}\square$, where □ stands for vacancy and x > y.

We gratefully acknowledge funding by NCN Harmonia grant no. 2017/26/M/ST10/00407.

References

1. J.L. Jambor, A.C. Roberts, D.R. Owens, J.D. Grice, The Canadian Mineralogist, 34 (1996) 1299–1304.
2. M.J. Sciberras, P. Leverett, P.A. Williams, D.E. Hibbs, A.C. Roberts, J.D. Grice, The Canadian Mineralogist, 49 (2011) 1111–1114.
3. W.H. Zachariasen, Acta Crystallographica, 1 (1948) 265–268.
4. A.A. Voronkov, N.G. Shumyatskaya, Y.A. Pyatenko, Journal of Structural Chemistry, 3 (1962) 665–669.
5. J.M. Hughes, J.W. Drexler, The Canadian Mineralogist, 32 (1994) 563–565.

Back to Table of contents

MS15 Mineralogical and inorganic crystallography

MS15-1-18 Lead-free layered organic-inorganic double perovskite with novel interlayer halide structure #MS15-1-18

W. Wong [1], K.P. Loh [1], X. Wang [1]
[1]National University of Singapore - Singapore (Singapore)

Abstract
The structural flexibility of hybrid organic-inorganic perovskites is known and widely exploited for various applications. Here we present a new family of layered hybrid perovskites, which would be a subset of the Dion-Jacobson series of double perovskite. The organic 'spacer' layer now consists of a diammonium-halide-diammonium rather than one single layer of diammonium cation. Drawing comparison to the oxide perovskites, this new class can be seen to be closely related to the Aurivillus phase. This poster shows the key chemical and structural considerations arising from this family and such a configuration can be seen for the Cu+/Bi3+ and Ag+/Bi3+ systems using the 3-aminopyrroline cation. Through the organic cation selection, we show that chirality can be imparted into the system thereby inducing a chiral space group which potentially exhibits ferroelectricity.

graphical abstract

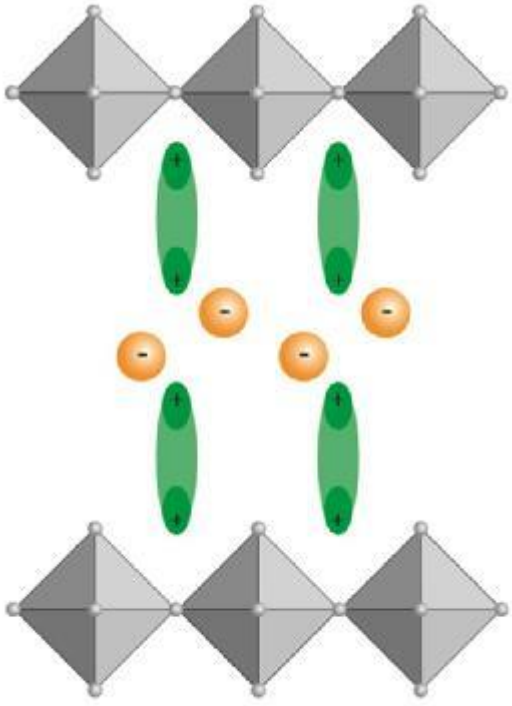

2D Perovskite with Interlayer Halide

Back to Table of contents

MS15 Mineralogical and inorganic crystallography

MS15-1-19 Evaluation of surrogate-models for the incorporation of tetravalent actinides in monazite phases #MS15-1-19

T. Lender [1], L. Peters [1]
[1]RWTH Aachen University - Aachen (Germany)

Abstract
Monazite has long been considered as one of the most promising crystalline host materials for long-term storage of radioactive waste, especially actinides. The main reasons for this are its chemical flexibility, its excellent chemical durability and its low recrystallization temperature which allows for rapid repair of radiation induced damage [1,2].
It has been shown that monazites can accommodate large amounts of trivalent actinides as well as various trivalent lanthanides (acting as surrogates for actinides) within its crystal structure [2]. However, the experimental incorporation of tetravalent dopants via a coupled substitution has proven challenging [3-4], even though natural monazite is known to contain up to 15 wt% UO2 and up to 32 wt% ThO2, respectively [5]. In this context, it has been suggested that the synthesis of single-phase Ca0.5Ce0.5PO4 was impossible [4], given the tendency of Ce4+ to partially reduce to Ce3+ at elevated temperatures. Here, we report on the successful synthesis of the solid solution series LaPO4 - Ca0.5Ce0.5PO4 in a metastable form via a co-precipitation method. This system will be investigated in view of acting as an inactive model system for comprehensive physical and chemical studies of coupled substitutions in monazite, comprising tetravalent metals.
The chemical composition of the samples was determined using EPMA; PXRD measurements show no evidence for a miscibility gap (see images attached; where not visible the error bars are smaller than the symbols used). Further XANES and EPR measurements are scheduled to verify the tetravalent oxidation state of cerium. The properties of the model system will be investigated, as well as their leaching resistance and the radiation stability.
The authors acknowledge support by BMBF under project number 02NUK060B.

References
[1] Schlenz H et al. Monazite as a suitable actinide waste form. Z. Kristallogr., 228, 113-123 (2013)
[2] Dacheux N, Clavier N, Podor R. Monazite as a promising long-term radioactive waste matrix: Benefits of high-structural flexibility and chemical durability. Am. Mineral., 98, 833-847 (2013)
[3] Popa K et al. The chemistry of the phosphates of barium and tetravalent cations in the 1:1 stoichiometry. J. Solid State Chem. 180, 2346-2355 (2007)
[4] Bregiroux D et al. Solid-State Synthesis of Monazite-type Compounds Containing Tetravalent Elements Inorg. Chem. 46, 10372-10382 (2007)
[5] Ewing RC, Weber WJ. Actinide waste forms and radiation effects. Chapter 35. In: Morss LR, Edelstein NM, Fuger J, editors. The chemistry of the actinide and transactinide elements. 4th ed. Springer, Dordrecht;3813–87 (2010)

PXRD of LaPO4-Ca0.5Ce0.5PO4 solid solution

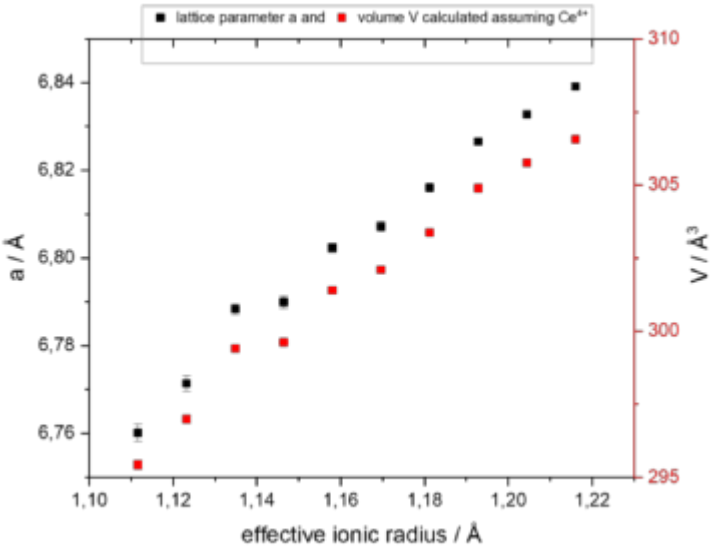

Back to Table of contents

EPMA of La0.5Ca0.25Ce0.25PO4

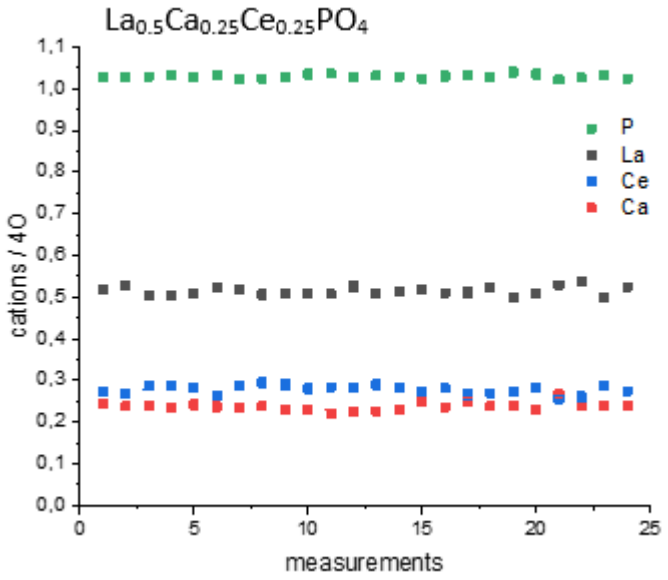

Back to Table of contents

MS15 Mineralogical and inorganic crystallography

MS15-1-2 $Sm_7F_{12}Cl_2$: Synthesis and Crystal Structure of a New Fluoride Rich Samarium(II) Fluoride Chloride #MS15-1-2

C. Buyer [1], S.A. Schumacher [1], T. Schleid [1]
[1]University of Stuttgart - Stuttgart (Germany)

Abstract
Red rod-shaped single crystals of $Sm_7F_{12}Cl_2$ (CSD-2126941) with a length up to 0.3 mm were obtained as a by-product in an experiment to obtain SmF_2 [1–4] from a NaCl flux. SmF_2 occurs as red plates in the CaF_2-type structure (cubic, $Fm\bar{3}m$, a = 580.31(4) pm, d(Sm−F) = 2501 pm, 8×) [4]. Both kinds of single crystals emerged after heating up a mixture of Sm, SmF_3 and NaCl (as flux) in a sealed niobium capsule to 850 °C and cooling down the product with 5 °C/h after four days. $Sm_7F_{12}Cl_2$ crystallizes in the $Ba_7F_{12}Cl_2$-type structure [5] with a = 1004.52(7) pm, c = 394.75(3) pm and Z = 1 (space group: $P\bar{6}$) analogous to $Eu_7F_{12}Cl_2$ [6]. For H^- instead of F^- anions, this structure is also known for $Sr_7H_{12}Cl_2$ [7] and $Ca_7H_{12}Cl_2$ [8]. There are three crystallographically independent Sm^{2+} cations, all coordinated by nine anions in the shape of tricapped trigonal prisms. While $(Sm1)^{2+}$ only enjoys coordination from F^- anions (d(Sm1−F) = 240 – 275 pm), $(Sm2)^{2+}$ and $(Sm3)^{2+}$ carry seven F^- anions at distances between 246 and 278 pm and two Cl^- anions with distances of about 314 pm as ligands. $(F1)^-$, $(F2)^-$ and $(F3)^-$ are coordinated tetrahedrally, while $(F4)^-$ has a square pyramidal Sm^{2+} environment. The coordination spheres of both Cl^- anions consist of six Sm^{2+} cations in shape of trigonal prisms. The atomic parameters are given in Table 1 and the unit cell of $Sm_7F_{12}Cl_2$ is shown in Figure 1 as viewed along [001]. A second samarium(II) fluoride chloride with the formula SmFCl adopts the PbFCl-type structure (tetragonal, a = 413.59(5) pm, c = 699.34(11) pm) [4] exhibiting four Sm−F distances of 252 pm and five Sm−Cl distances of 307 pm (1×) and 311 pm (4×) [4] in capped square antiprismatic coordination sphere.

Atomic coordinates, Wyckoff positions and equivalent isotropic displacement parameters for hexagonal $Sm_7F_{12}Cl_2$.

Atom	**Site**	***x*/*a***	***y*/*b***	***z*/*c***	U_{eq} / p
Sm1	1*a*	0	0	0	232(4)
Sm2	3*j*	0.40813(12)	0.11180(12)	0	121(3)
Sm3	3*k*	0.28971(11)	0.40317(11)	1/2	92(2)
F1	3*j*	0.1226(14)	0.2757(14)	0	179(26
F2	3*j*	0.4262(16)	0.3659(16)	0	233(37
F3	3*k*	0.0501(14)	0.4375(14)	1/2	110(27
F4	3*k*	0.2195(15)	0.1250(15)	1/2	211(29
Cl1	1*c*	1/3	2/3	0	193(19
Cl2	1*f*	2/3	1/3	1/2	110(17

References
[1] E. Catalano, R. G. Bedford, V. G. Silveira, H. H. Wickman, *J. Phys. Chem. Solids* **1969**, *30*, 1613 - 1627.
[2] T. Petzel, O. Greis, *Z. Anorg. Allg. Chem.* **1973**, *396*, 95 - 102.
[3] O. Greis, *J. Solid State Chem.* **1978**, *24*, 227 - 232.
[4] C. Buyer, Th. Schleid, *Acta Crystallogr.* **2021**, *A 77*, C1036.
[5] F. Kubel, H. Bill, H. Hagemann, *Z. Anorg. Allg. Chem.* **1999**, *625*, 643 - 649.
[6] O. Reckeweg, F. J. DiSalvo, S. Wolf, Th. Schleid, *Z. Anorg. Allg. Chem.* **2014**, *640*, 1254 - 1259.
[7] O. Reckeweg, J. C. Molstad, S. Levy, C. Hoch, F. J. DiSalvo, *Z. Naturforsch.* **2008**, *63b*, 513 - 518.
[8] O. Reckeweg, F. J. DiSalvo, *Z. Naturforsch.* **2010**, *65b*, 493 - 498.

Back to Table of contents

Extended unit cell of $Sm_7F_{12}Cl_2$ viewed along [001]

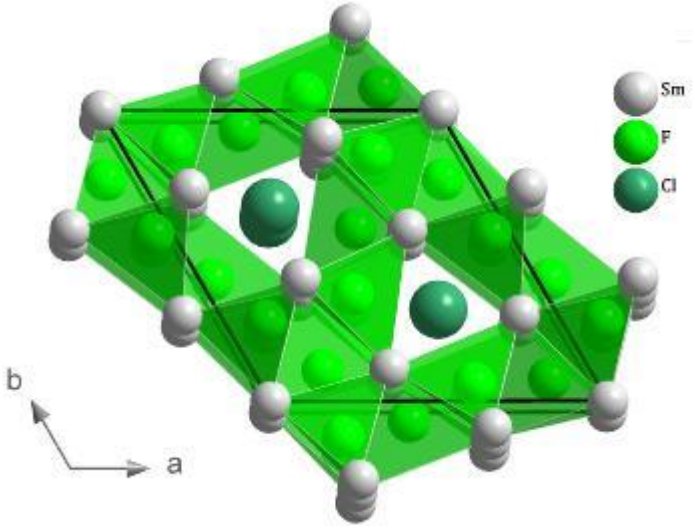

Back to Table of contents

MS15 Mineralogical and inorganic crystallography

MS15-1-3 Copper – cyano – thiocyanato anionic frameworks
#MS15-1-3

E. Goreshnik [1], S. Petrusenko [2]
[1]Jožef Stefan Institute - Ljubljana (Slovenia), [2]Taras Shevchenko National University of Kyiv - Kyiv (Ukraine)

Abstract
The reaction of CuCN and CuSCN with manganese(II) nitrate in DMSO (DMSO - dimethyl sulfoxide) affords to produce a novel coordination compound of composition $[Mn(DMSO)_4(H_2O)_2][Cu_8(SCN)_4(CN)_6](DMSO)$ (**1**) (Figure). The crystal structure of **1** (sp. gr. $P4_2/n$) contains a unique anionic $\{[Cu_8(SCN)_4(CN)_6]^{2-}\}_n$ network of unknown topology with infinite square channels of about 12 x 12 Å, filled by solvated Mn^{2+} complex cations and partially disordered DMSO molecules. The related compounds with Cu^{2+} (**2**), Co^{2+} (**3**) and Ni^{2+} (**4**) instead of Mn^{2+} possess similar structure (space groups: $P4_2/n$ **2**, $P4_2/ncm$ **3**, **4**), but their complex $[M(DMSO)_4(H_2O)_2]^{2+}$ cations are strongly disordered.

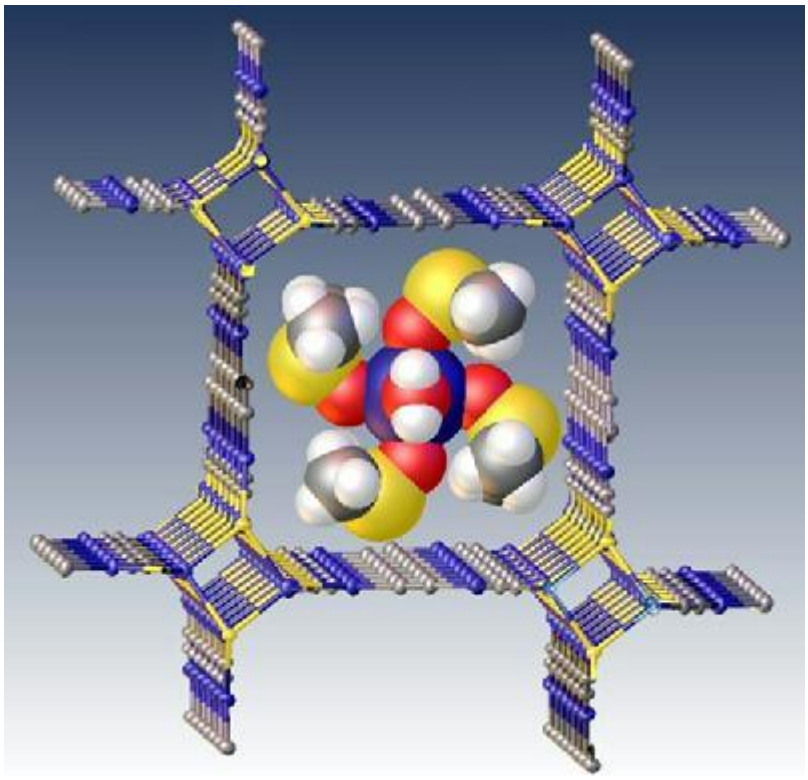

Back to Table of contents

MS15 Mineralogical and inorganic crystallography

MS15-1-4 $SmBi_2O_4Cl$: The First Single-Crystal Study in the Systems $LnBi_2O_4X$
#MS15-1-4

M.V. Kurz [1], R.J.C. Locke [1], A. Erden [1], T. Schleid [1]
[1]University of Stuttgart - Stuttgart (Germany)

Abstract
A mixture of Bi_2O_3, Sm_2O_3 and $SmCl_3$ reacted at 800 °C in an eutectic mixture of NaCl and CsCl as flux in a fused silica ampoule and resulted in yellow plates of the title compound. $SmBi_2O_4Cl$ crystallizes in the tetragonal space group *P*4/*mmm* with the lattice parameters *a* = 388.91(3) pm and *c* = 895.16(7) pm with *Z* = 4 and hitherto its structure was only known from X-ray powder diffraction data [1]. The corresponding antimonate(III) $SmSb_2O_4Cl$ with the real composition $Sm_{1.3}Sb_{1.7}O_4Cl$ offers a mixed occupation of the antimony position with samarium [2,3] for the same crystal structure. In contrast to this, $SmBi_2O_4Cl$ shows no mixed occupation, but one samarium and one bismuth position with regular occupation.
The structure features one crystallographic samarium (1*a*: 0, 0, 0), one bismuth (2*h*: 1/2, 1/2, 0.28294(9)), one oxygen (4*i*: 0, 1/2, 0.1582(9)) and one chlorine position (1*b*: 0, 0, 1/2) each. Sm^{3+} is coordinated by eight oxygen atoms (*d*(Sm–O) = 240.6(5) pm) forming a $[SmO_8]^{13-}$ cube. Each cube is connected via edges with four other cubes, resulting in a layer $^2_\infty\{[SmO^e_{8/2}]^{5-}\}$ parallel to the (001) plane (Figures 1 and 2). Bismuth is coordinated as ψ^1-square pyramid $[BiO_4]^{5-}$ by $^2_\infty\{[BiO^v_{4/4}]^{+}\}$ four oxygen atoms (*d*(Bi–O) = 224.2(4) pm), which are connected via four vertices to infinite layers $^2_\infty\{[SmO^e_{8/2}]^{5-}\}$ sandwiching the layers from both sides. The Cl^- anions are not efficiently connected to the Bi^{3+} cations (*d*(Cl···Bi) = 336.7(1) pm), but located in the gaps between the lone pairs at the Bi^{3+} centers.

References
[1] M. Schmidt, H. Oppermann, C. Henning, R. W. Henn, E. Gmelin, N. Söger, *Z. Anorg. Allg. Chem.* **2000**, *626*, 125–135.
[2] F. C. Goerigk, Th. Schleid, *Z. Anorg. Allg. Chem.* **2019**, *645*, 1079–1084.
[3] F. C. Goerigk, *Doctoral Dissertation*, Univ. Stuttgart **2021**.

Extended unit cell of SmBi2O4Cl.

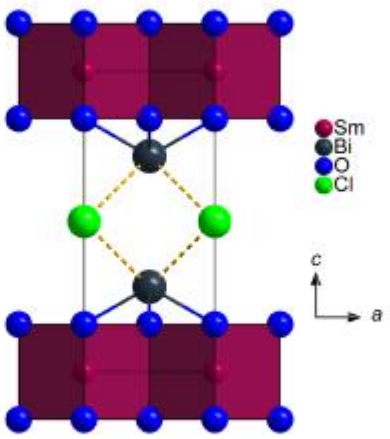

[SmO8]13– cube (left) and Bi–O layer (right).

Back to Table of contents

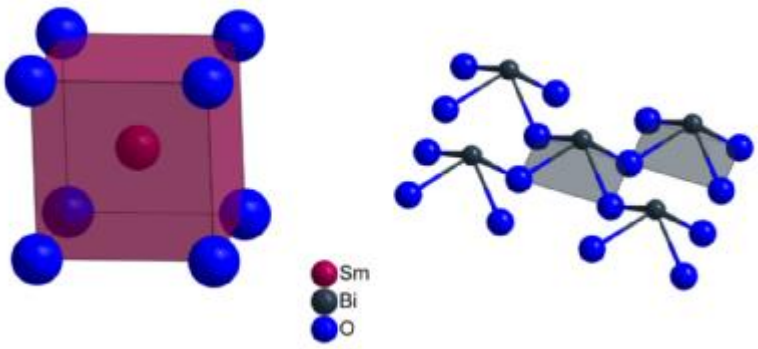

Back to Table of contents

MS15 Mineralogical and inorganic crystallography

MS15-1-5 Structure, texture and residual strain in Al/W/Al heterostructures
#MS15-1-5

D. Vinci [1], U. Lüders [2], C. Guillaume [3], M.D. Lemrhari [4], F. Le Cornec [4], D. Chateigner [2]
[1]European XFEL - Schenefeld (Germany), [2]CRISMAT (UMR 6508 CNRS ENSICAEN Université de Caen Normandie, Normandie Université) - Caen (France), [3]CRISMAT (UMR 6508 CNRS ENSICAEN Université de Caen Normandie, Normandie Université) & Murata Integrated Passive Solutions - Caen (France), [4]Murata Integrated Passive Solutions - Caen (France)

Abstract
Thick metallic films are widely used in microelectronics, as for example for interconnection purposes and metallic contacts. The structural properties of these films have a certain influence on their performances, but even more, residual strains are to be evaluated and controlled, as they can lead to local distortions and deformations of the die, and in the worst case to reliability issues.
This contribution reports on the structural and textural characterization of a heterostructure of Aluminium-Tungsten-Aluminium (AWA) by means of X-ray diffraction. The layered stack is obtained by sputtering, on a Si-(001) substrate covered by a 30 nm thermal SiOx layer. The bottom Al layer has a thickness of 3 µm, and the top Al-layer a thickness of 10 µm. The two Al layers are separated by a W layer of 300 nm. The structure, texture and microstructure of the three layers composing the heterostructure have been investigated by interpreting the diffraction diagrams using the so-called “Combined Analysis” formalism [1] implemented in the MAUD software [2]. This method is based on cyclic Rietveld refinements [3] of the diffraction patterns measured for 864 different sample orientations. In this study, the texture is quantified through the refinement of the Orientation Distribution Function (ODF) of crystallites using the E-WIMV method [1], the anisotropic crystallite sizes and microstrains using the Popa anisotropic formalism [4] and the residual stress biaxial tensor using tensor homogeneization by geometric mean of single-crystal elastic constants weighted by the ODF [5]. We carried out the measurements with a ThermoFisher Scientific 4-circles X-ray diffractometer, Cu Kα radiation (λCu= 1.5418nm), equipped with a curved position sensitive detector (INEL CPS 120).
Strong fiber-like textures are evidenced in all Al and W layers, the fiber axes corresponding to the main crystal directions ([111] and [001] resp.), being perpendicular to the sample plane with a maximum orientation density on the corresponding pole figures of 30 m.r.d. and 6 m.r.d.. While the tungsten layer exhibits relatively large residual stresses s11 = 3.36 GPa and s22 = 3.32 GPa, the aluminium appears free of residual stress.
An overview of the main results will be given in this contribution.

References
[1] D. Chateigner (Ed): Combined analysis, ISTE-Wiley, London (2010).
[2] L. Lutterotti, H.-R. Wenk, S. Matthies, in: J.A. Szpunar (Ed.), Textures of Materials, 2, NRC Research Press, Ottawa, 1599 (1999).
[3] H.M. Rietveld, J. Appl. Crystallogr. 2, 65 (1969).
[4] N.C. Popa, J. Appl. Crystallogr. 31, 176 (1998).
[5] S. Matthies, M. Humbert, J. Appl. Crystallogr. 28, 254 (1995).

XRD measured data and fit.

Back to Table of contents

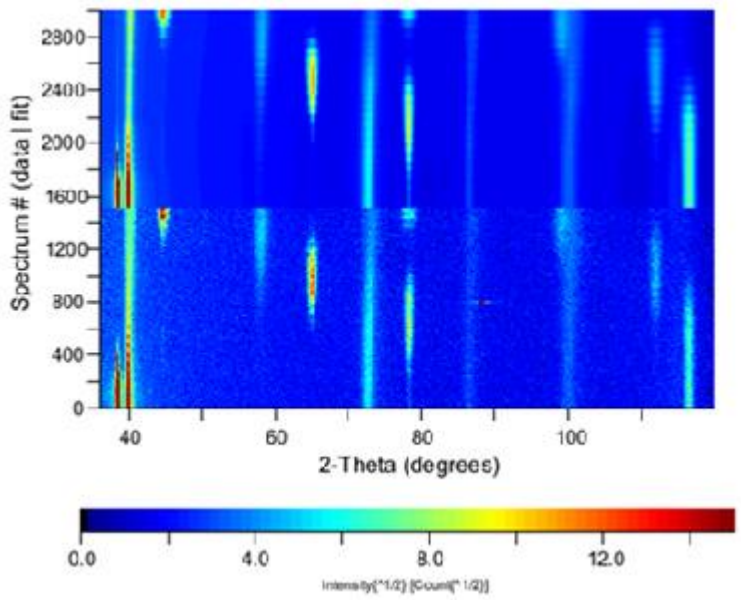

Back to Table of contents

MS15 Mineralogical and inorganic crystallography

MS15-1-6 Synthesis and Characterization of the solid solution series NaYb1–xLuxS2 in the α-NaFeO2 structure type
#MS15-1-6

E. Häußler [1], J. Sichelschmidt [2], M. Baenitz [2], T. Doert [1]
[1]Technische Universität Dresden - Dresden (Germany), [2]Max Planck Institute for Chemical Physics of Solids - Dresden (Germany)

Abstract
Materials with the *α*-$NaFeO_2$ structure have lately attracted considerable interest in quest of a unique magnetic ground state – the quantum spin liquid (QSL) state. In this structure type antiferromagnetically interacting trivalent rare earth ions with J_{eff} = ½ can be arranged on a regular triangular sublattice (see Figure 1) thus providing the perfect geometrical basis for studying this kind of frustrated spin system. Indeed, no magnetic order was found in $NaYbCh_2$ (*Ch* = S, Se) down to 260 mK [1,2].To investigate the interplay of the electron spins with respect to the magnetic properties in detail, we subsituted the Yb^{3+} ions in $NaYbS_2$ with non magnetic Lu^{3+} to dilute the magnetic sublattice. As the spin-spin interactions are influenced by the geometric confinements of the structure we had a detailed look on the structural parameters before determining the magnetic susceptibility and the electron spin resonance (ESR) properties. We characterized the samples of the solid solution series $NaYb_{1-x}Lu_xS_2$ with $0 \leq x \leq 1$ with respect to their chemical composition, analyzed their structural parameters in single crystal and powder X-ray diffraction experiments and evaluated the structural changes (see Figure 2 for the lattice parameters) throughout the whole substitution series. In this contribution, we report on the synthesis and the crystallographic details of the structure and give an insight into the physical properties obtained via ESR spectroscopy and magnetization measurements.

References
[1] M. Baenitz, Ph. Schlender, J. Sichelschmidt, Y. A. Onykiienko, Z. Zangeneh, K. M. Ranjith, R. Sarkar, L. Hozoi, H. C. Walker, J.-C. Orain, H. Yasuoka, J. van den Brink, H. H. Klauss, D. S. Inosov, Th. Doert, *Phys. Rev. B* **2018**, 98, 220409.
[2] W. Liu, Z. Zhang, J. Ji, Y. Liu, J. Li, X. Wang, H. Lei, G. Chen, Q. Zhang, *Chin. Phys. Lett.* **2018**, 35, 117501.

Crystal structure of NaYbS2 in R-3m.

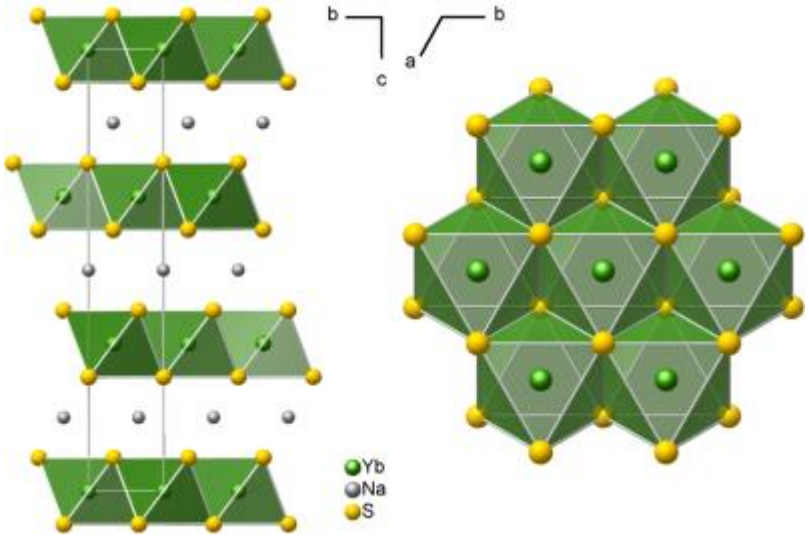

Refined lattice parameters of NaYb1–xLuxS2 samples

Back to Table of contents

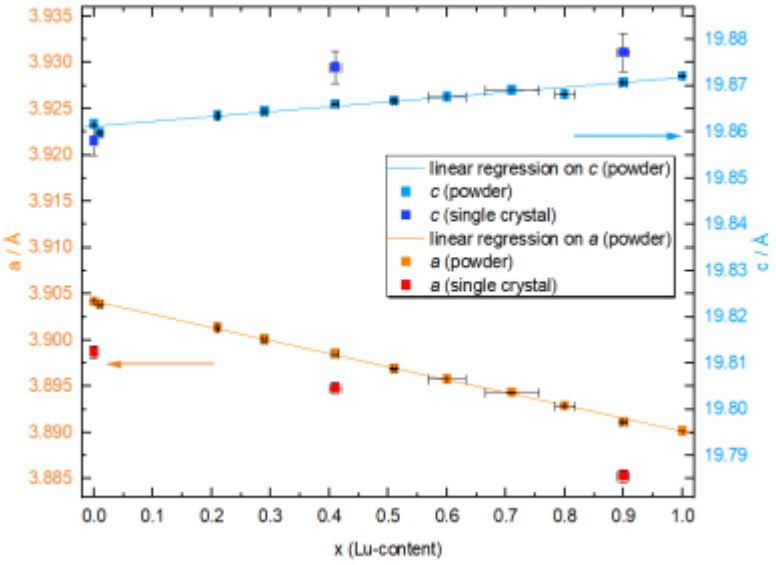

Back to Table of contents

MS15 Mineralogical and inorganic crystallography

MS15-1-7 Isolated $[SiO_4]^{4-}$ Tetrahedra in the Chloride-Poor Oxosilicate $Ce_3Cl[SiO_4]_2$
#MS15-1-7

R.J.C. Locke [1], I. Hartenbach [1], T. Schleid [1]
[1]University of Stuttgart - Stuttgart (Germany)

Abstract
In an attempt to synthesize $CeSb_2O_4Cl$, rod-shaped colorless single crystals with the composition $Ce_3Cl[SiO_4]_2$ were obtained as a by-product from glassy silica ampoules. $Ce_3Cl[SiO_4]_2$ crystallizes isotypically to the A-type $Ln_3Cl[SiO_4]_2$ series with *Ln* = La, Pr and Nd[1–4] in the monoclinic space group *C*2/*c* with *a* = 1439.13(9) pm, *b* = 646.24(4) pm, *c* = 877.96(6) pm and *β* = 98.341(3)° for *Z* = 4 (CSD-2124078).
The crystal structure of $Ce_3Cl[SiO_4]_2$ contains isolated $[SiO_4]^{4-}$ tetrahedra (Figure 1) as the defining building blocks, showing a slight distortion with angles O–Si–O in the range from 105.9(2) to 118.4(2)°. The Si–O distances reside between 160.6(5) and 164.2(4) pm, which are quite typical oxosilicate values. Furthermore, two crystallographically distinct Ce^{3+} cations are present with $(Ce1)^{3+}$ being surrounded by one Cl^- anion plus another more distant Cl^- one as well as eight oxygen atoms forming a 9+1-fold coordination sphere. The $(Ce2)^{3+}$ cations show a tricapped trigonal prismatic coordinative environment, built up by one Cl^- anion and eight oxygen atoms. The distances *d*(Ce–O) = 243.2(4) – 290.8(4) pm and *d*(Ce–Cl) = 287.6(1) – 295.4(2) pm plus 350.8(1) pm range in common intervals, when compared with PbFCl-type CeOCl[5] (*d*(Ce–O) = 237 pm (4×) and *d*(Ce–Cl) = 312 pm (1×) and 319 pm (4×)) for example. The Cl—Ce^{3+} partial structure with infinite chains 1D-$\{[ClCe^{t}_{2/1}Ce^{v}_{2/2}]^{8+}\}$ of *trans*-vertex linked kites $[ClCe_{3+1}]^{11+}$ propagating along [010] is shown in Figure 2 displaying one short and one long $(Ce1)^{3+}$–Cl distance.

References
[1] P. Gravereau, B. Es-Sakhi, C. Fouassier, *Acta Crystallogr.* **1988**, *C 44*, 1884.
[2] G.-C. Guo, Y.-G. Wang, J.-N. Zhuang, J.-T. Chen, J.-S. Huang, Q.-E. Zhang, *Acta Crystallogr.* **1995**, *C 51*, 2471.
[3] C. Sieke, I. Hartenbach, Th. Schleid, *Z. Anorg. Allg. Chem.* **2000**, *626*, 2236.
[4] C. Sieke, *Doctoral Thesis*, Univ. Stuttgart, Germany, **1998**.
[5] M. Wolcryz, L. Kepinski, *J. Solid State Chem.* **1992**, *99*, 409.

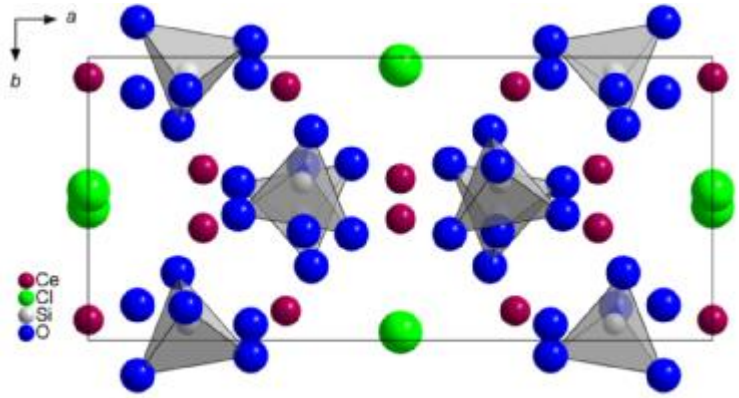

Figure 1. Projection of the monoclinic crystal structure of $Ce_3Cl[SiO_4]_2$ onto (001) emphasizing the isolated $[SiO_4]^{4-}$ tetrahedra.

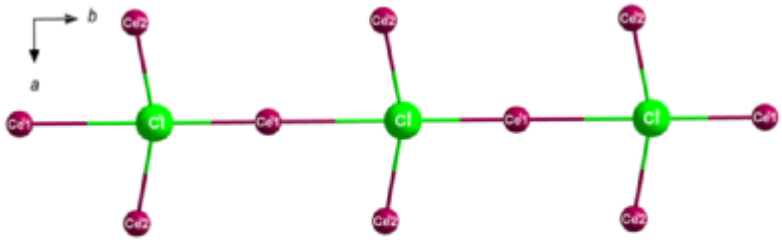

Figure 2. Cl^-–Ce^{3+} partial structure of $Ce_3Cl[SiO_4]_2$ with infinite chains 1D-$\{[ClCe^{t}_{2/1}Ce^{v}_{2/2}]^{8+}\}$.

Back to Table of contents

MS15 Mineralogical and inorganic crystallography

MS15-1-8 Gd_3PS_3 and Gd_3PSe_3: Two Gadolinium Phosphide Chalcogenides with Th_3P_4-Type Crystal Structure #MS15-1-8

P. Djendjur [1], N. Atmaca [1], T. Schleid [1]
[1]University of Stuttgart / Institute for Inorganic Chemistry - Stuttgart (Germany)

Abstract
Chalcogenides of the rare-earth elements with the Th_3P_4-type structure are well-known throughout the chemical and crystallographic community. Several representatives of the binary sesquisulfides, -selenides and -tellurides RE_2Ch_3 (*RE* = La – Nd, Sm, Gd – Tb; *Ch* = S – Te) crystallize with this structure motif [1–2] and represent a cation-deficient variant of the Th_3P_4 prototype, occupying only 10.667 of the 12 possible cationic positions in the cubic unit cell to satisfy charge-neutrality according to $(RE^{3+})_{2.667}\square_{0.333}(Ch^{2-})_4$ for $Z = 4$. On the other hand, this allows for insertions of further metal cations like Na^+ to yield $NaRE_8Ch_{12}$ (metallic according to $(Na^+)(RE^{3+})_8(Ch^{2-})_{12}(e^-)$) [3] or even additional RE^{3+} cations leading to the composition RE_3Ch_4 (also metallic according to $(RE^{3+})_3(Ch^{2-})_4(e^-)$) [4]. Another example for the versatility of this structure is shown by the series of europium pnictogenide chalcogenides Eu_4Pn_2Ch (*Pn* = P – Bi, *Ch* = S – Te) [5], which crystallize in the *anti*-type arrangement of the Th_3P_4 structure. Here, divalent Eu^{2+} cations occupy the former sixfold surrounded anion site and the former cation site is hosting a 2:1 mixture of pnictogenide and chalcogenide anions according to $(Eu^{2+})_4[(Pn^{3-})_2(Ch^{2-})_1]$.The two new gadolinium phosphide chalcogenides Gd_3PS_3 (CSD-2169111) and Gd_3PSe_3 (CSD-2169112) could be obtained by replacing part of the Ch^{2-} anions in gadolinium sulfide and -selenide Gd_3Ch_4 with P^{3-}, resulting in formally ionic compounds with a statistically occupied mixed-anion site and a fully occupied cation site according to $(Gd^{3+})_3[(P^{3-})_1(Ch^{2-})_3]$. So both compounds crystallize in the cubic space group $I\bar{4}3d$ (no. 220) with $Z = 4$. They exhibit the lattice parameters $a(Gd_3PS_3)$ = 841.45(6) pm and $a(Gd_3PSe_3)$ = 868.79(6) pm, respectively, which are slightly larger for the sulfide, but somewhat smaller for the selenide than those of the corresponding C-type gadolinium sesquichalcogenides (a(C-Gd_2S_3) = 838.47(9) pm [6] and a(C-Gd_2Se_3) = 872.56(5) pm [7] for $Z = 5.333$). Gd^{3+} is surrounded by eight anions (P^{3-} and Ch^{2-} in a statistic fashion with a molar ratio of 1:3) forming a trigonal dodecahedron (d(Gd–P/S = 282 – 301 pm, d(Gd–P/Se = 290 – 312 pm), whereas the anionic site exhibits a trigonal hemiprismatic coordination sphere with six Gd^{3+} cations in its vicinity (Figure 1, see Table 1 for the atomic coordinates). Energy dispersive X-ray spectroscopy (EDXS) measurements were conducted to verify the composition of Gd_3PS_3 and Gd_3PSe_3 successfully.

Table 1. Atomic positions, equivalent isotropic displacement parameters and coordination numbers (*C.N.*) for Gd_3PS_3 and Gd_3PSe_3.

Atoms		***x/a***	***y/b***	***z/c***	U_{eq} **/ pm²**	***C.N.***
Gd_3PS_3						
Gd	(12*a*)	3/8	0	1/4	132(2)	8
P/S	(16*c*)	0.07268(12)	*x/a*	*x/a*	96(5)	6
Gd_3PSe_3						
Gd	(12*a*)	3/8	0	1/4	175(3)	8
P/Se	(16*c*)	0.17803(8)	*x/a*	*x/a*	81(4)	6

References
[1] L. N. Eatough, A. W. Webb, H. T. Hall, *Inorg. Chem.* **1969**, *8*, 2069–2071.[2] Th. Schleid, *Habilitationsschrift*, University of Hannover, Hannover, Germany, **1993**.[3] T. Heinze, W. Urland, *Z. Anorg. Allg. Chem.* **1994**, *620*, 1698–1701.[4] P. D. Dernier, E. Bucher, L. D. Longinotti, *J. Solid State Chem.* **1975**, *15*, 203–207.[5] F. Hulliger, *Mater. Res. Bull.* **1979**, *14*, 259–262.[6] Th. Schleid, F. A. Weber, *Z. Anorg. Allg. Chem.* **1998**, *624*, 557–558.[7] M. Folchnandt, Th. Schleid, *Z. Anorg. Allg. Chem.* **2001**, *627*, 1411–1413.

Cubic unit cell of Gd3PS3 and Gd3PSe3.

Back to Table of contents

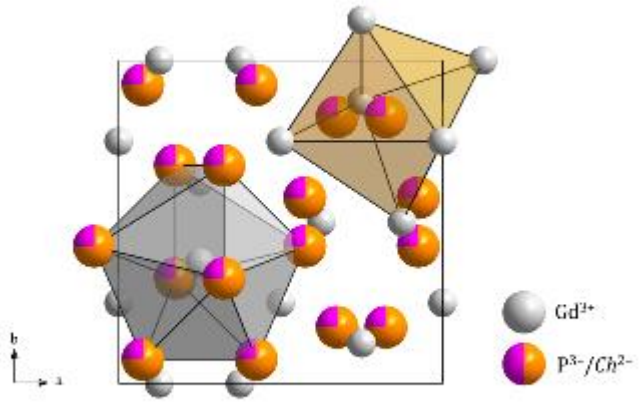

Back to Table of contents

MS15 Mineralogical and inorganic crystallography

MS15-1-9 Closing Some Gaps of Knowledge: Single Crystals of $Pr_2O[SiO_4]$ and $Sm_2O[SiO_4]$ with the A-Type Structure
#MS15-1-9

R.C. Locke [1], M.C. Schäfer [1], P. Djendjur [1], T. Schleid [1]
[1]University of Stuttgart / Institute for Inorganic Chemistry - Stuttgart (Germany)

Abstract
Syntheses with lanthanoid metals in glassy silica ampoules often tend to yield oxosilicates as by-products. Thus, the two presented silicates $Pr_2O[SiO_4]$ and $Sm_2O[SiO_4]$ were also obtained from different reactions including the elemental lanthanoids, but with other target compounds. Both crystallize isostructurally to the $Ln_2O[SiO_4]$ series with *Ln* = La, Nd, Eu, Gd, Ho – Tm and Lu [1–6] in the monoclinic space group $P2_1/c$ with the lattice parameters a = 925.49(8) pm, b = 733.97(6) pm, c = 692.06(5) pm, β = 108.382(3)° for $Pr_2O[SiO_4]$ (CSD-2127743) and a = 915.92(8) pm, b = 717.19(6) pm, c = 679.42(5) pm, β = 107.825(3)° for $Sm_2O[SiO_4]$ (CSD-2127807) adapting the $Gd_2O[SiO_4]$- or A-type structure with Z = 4.
The Ln^{3+} cations occupy two crystallographically different positions (Figure 1). $(Ln1)^{3+}$ resides in a distorted capped square hemiprism with 8+1 oxygen atoms, while $(Ln2)^{3+}$ centers a capped trigonal prism with just seven of them. The lanthanoid-oxygen distances, namely d(Pr–O) = 234 – 269 pm and d(Sm–O) = 231 – 259 pm, fall into the usual range when compared with similar praseodymium and samarium oxosilicates such as apatite-type $Ln_{4.667}O[SiO_4]_3$ (*Ln* = Pr and Sm) [7], for example. Silicon is surrounded by a slightly distorted tetrahedron of four oxygen atoms as *ortho*-oxosilicate anion $[SiO_4]^{4-}$ with silicon-oxygen distances ranging from 159 to 166 pm, which remains isolated. The fifth oxygen atom works as an O^{2-} anion, which is coordinated by four Ln^{3+} cations as $[OLn_4]^{10+}$ tetrahedron (d(O–*Ln*) = 230 – 243 pm). Their connectivity via edges and corners leads to corrugated $^2_\infty\{[O(Ln1)_{1/1}(Ln2)_{3/3}]^{4+}\}$ layers spreading out parallel to the (100) plane (Figure 2).

References
[1] K. Fukuda, T. Iwata, E. Champion, *Powd. Diffr.* **2006**, *21*, 300–303.
[2] L. Leon-Reina, J. M. Porras-Vazquez, E. R. Losilla, L. Moreno-Real, M. A. G. Aranda, *J. Solid State Chem.* **2008**, *181*, 2501–2506.
[3] M. E. Bohem, Th. Schleid, *Z. Anorg. Allg. Chem.* **2016**, *642*, 1055–1055.
[4] Yu. I. Smolin, S. P. Tkachev, *Kristallografiya* **1969**, *14*, 22–25.
[5] I. Hartenbach, S. F. Meier, J. Wontcheau, Th. Schleid, *Z. Anorg. Allg. Chem.* **2002**, *628*, 2907–2913.
[6] H. Müller-Bunz, Th. Schleid, *Z. Anorg. Allg. Chem.* **1999**, *625*, 613–618.
[7] I. Hartenbach, Th. Schleid, *Z. Kristallogr.* **2005**, *220*, 206–210.

Coordination polyhedra of $(Ln1)^{3+}$ and $(Ln2)^{3+}$.

Back to Table of contents

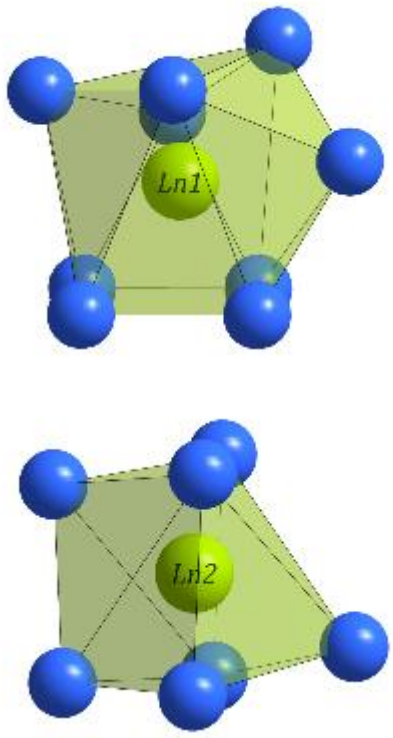

Unit cell of the A-type structure of $Ln_2O[SiO_4]$.

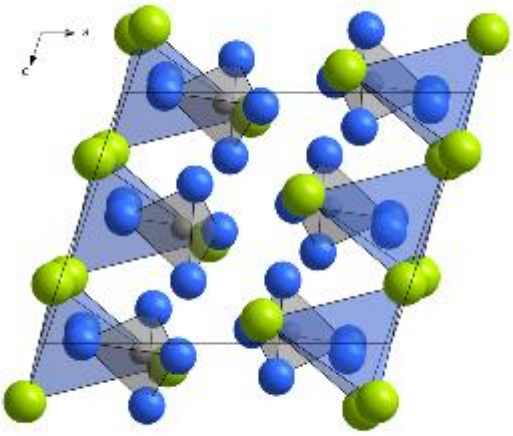

Back to Table of contents

MS15 Mineralogical and inorganic crystallography

MS15-2-1 $Cu_{0.9}Pb_{1.2}Sb_{2.9}Se_6$, an incommensurably modulated $^{4'4}$L-lillianite
#MS15-2-1

L. Staab [1], M. Grauer [1], K. Ueltzen [1], C. Benndorf [1], C. Paulmann [2], O. Oeckler [1]
[1]Institute of Mineralogy, Crystallography and Materials Science, Leipzig University - Leipzig (Germany), [2]Mineralogical-Petrographical Institute, Hamburg University - Hamburg (Germany)

Abstract
Lillianites are a structural family derived from the crystal structure of the mineral lillianite $Pb_3Bi_2S_6$ and belong to the sulfosalts.[1,2] The structures are built up by tilted and distorted NaCl type slabs that are interconnected by cations in bicapped trigonal prisms formed by anions (see Fig. 1). The numbers N1 and N2 in the symbol ^{N1,N2}L denote the number of edge-sharing octahedra across the NaCl type slabs.[3]
^{4,4}L-type $Cu_{0.9}Pb_{1.2}Sb_{2.9}Se_6$ can be described as an incommensurably modulated structure with the (3+1)-dimensional superspace group $Cmc2_1(\alpha 00)000$ with unit-cell dimensions a = 4.155(6) Å, b = 14.081(5) Å, and c = 19.842(11) Å, and a modulation vector of 0.68379(16) a^*.
The crystal structure features combined positional and occupational modulation on two sites where octahedral vacancies are either occupied by Sb atoms or Cu atoms that are displaced towards an edge of the octahedra, thus adopting a distorted tetrahedral coordination (see Fig. 2). The feature induces positional modulation of different extent of all other atoms in the structure.
In addition to the structure determination at ambient conditions, temperature induced structural changes were investigated. While cooling to 120 K had no effect on the symmetry, the satellite reflections disappear above 250 °C as the copper atoms lose their long-range order.

References
[1] J. Takagi, Y. Takéuchi, *Acta Crystallogr. Sect. B* **1972**, *28*, 649–651.
[2] K. Ohsumi, K. Tsutsui, Y. Takéuchi, M. Tokonami, *Acta Crystallogr. Sect. A* **1984**, *40*, C255-C256.
[3] E. Makovicky, S. Karup-Møller, *N. Jb. Miner. Abh.* **1977**, *130*, 264–287.

Fig. 1: Projection along [001].

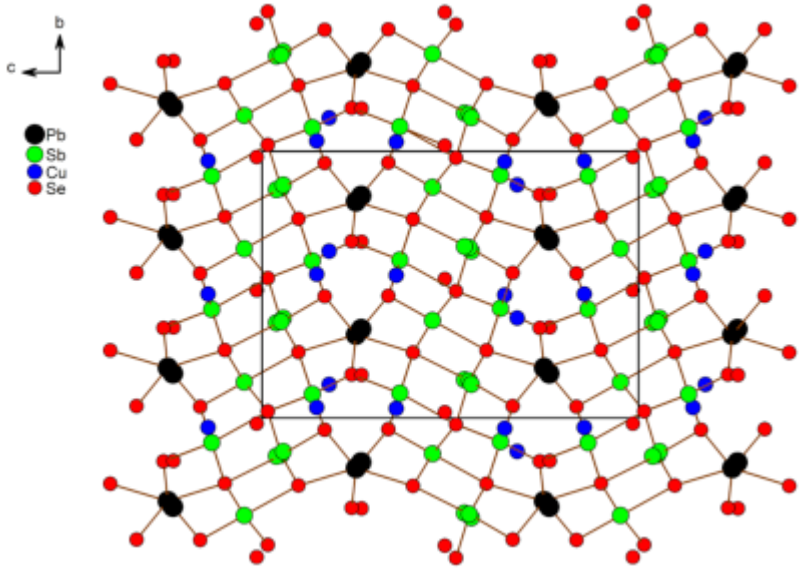

Fig. 2: Cutout of the modulated site.

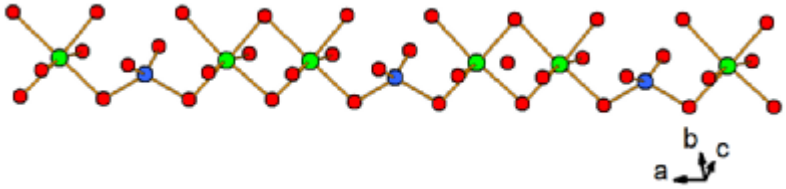

Back to Table of contents

MS15 Mineralogical and inorganic crystallography

MS15-2-10 Supertetrahedra and cation distribution in the strontium aluminium oxonitridophosphate $SrAl_5P_4N_{10}O_2F_3$ by SCXRD and STEM
#MS15-2-10

M. Pointner [1], O. Oeckler [2], W. Schnick [1]
[1]LMU Munich - Munich (Germany), [2]Leipzig University - Leipzig (Germany)

Abstract
Multinary nitrides have received much attention because of their structural diversity and several important applications, e.g. as host lattices for luminescent materials. In addition to the anionic substructure built up from tetrahedra, octahedral building blocks may complement the structural entities like the first nitridic micas $AESi_3P_4N_{10}(NH)_2$ (*AE* = Mg, Ca, Sr), which show typical tetrahedra-octahedra-tetrahedra layers.[1] The strontium aluminum oxonitridophosphate $SrAl_5P_4N_{10}O_2F_3$:Eu^{2+}, which shows green luminescence, was obtained by a mineralizer-assisted high-temperature high-pressure route (1400 °C, 5 GPa) with a Walker-type multianvil press starting from $Sr(N_3)_2$, $SrCO_3$, P_3N_5, AlN, EuF_3 and NH_4F as mineralizer.[2] $SrAl_5P_4N_{10}O_2F_3$ crystallizes in space group *I*-4*m*2 [*a* = 11.179, *c* = 5.148 Å]. The structure was elucidated by single-crystal X-ray diffraction (SCXRD). The metrics were confirmed by a tilt series of selected area electron diffraction patterns. EDX spectra (TEM and SEM) agree with the element ratio suggested by SCXRD, in particular the Al:P ratio of 1.25:1. The structure can be described as a variant of a joint *fcc* packing of all anions and Sr atoms with filled octahedral and tetrahedral voids. Possible disorder of Al and P atoms on these octahedral and tetrahedral sites was investigated by *Z*-contrast imaging (STEM-HAADF) and STEM-EDX mapping with atomic resolution. The corresponding intensities of the *Z*-contrast image as well as the spatial separation of STEM-EDX signals identify the Sr positions and confirm the allocation of Al and P on separate Wyckoff positions. Figure 1 shows a combination of a STEM-HAADF image and the corresponding STEM-EDX maps of the three cation columns Sr, Al and P along [001]. Aluminum exclusively occupies octahedral sites whereas phosphorus occupies the single tetrahedral site. Vertex-sharing PN_4 tetrahedra build up a three-dimensional network together with a new type of supertetrahedra-like building blocks composed of ten edge-sharing $Al(N,O,F)_6$ octahedra (Fig. 2, alternating opaque and transparent supertetrahedra for better visibility). $Sr(N/O/F)_{12}$ cuboctahedra share faces and form chains along [001]. Based on the known cation distribution, BVS calculations suggest the anion distribution in a straightforward way.

References
[1] L. Eisenburger, P. Strobel, P.J. Schmidt, T. Bräuniger, J. Wright, E. Lawrence Bright, C. Giacobbe, O. Oeckler, W. Schnick, *Angew. Chem.* **2022**, *134*, e202114902; *Angew. Chem. Int. Ed.* **2022**, *61*, e202114902.[2] S. Merlino, C. Biagioni, E. Bonaccorsi, N. V. Chukanov, I. V. Pekov, S. V. Krivovichev, V. N. Yakovenchuk, T. Armbruster, *Mineral. Mag.* **2015**, *79*, 145.

STEM-HAADF image and -EDX map in [001].

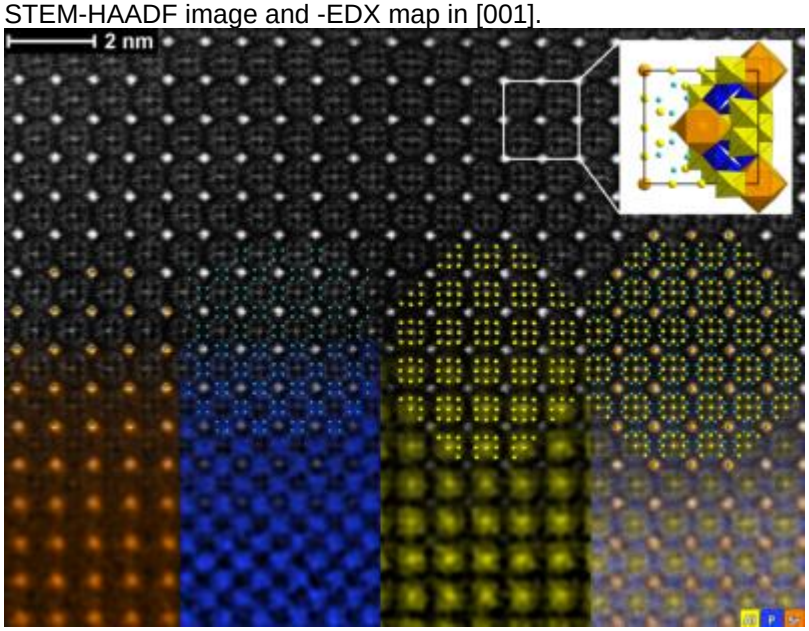

Interconnected supertetrahedra-like elements.

Back to Table of contents

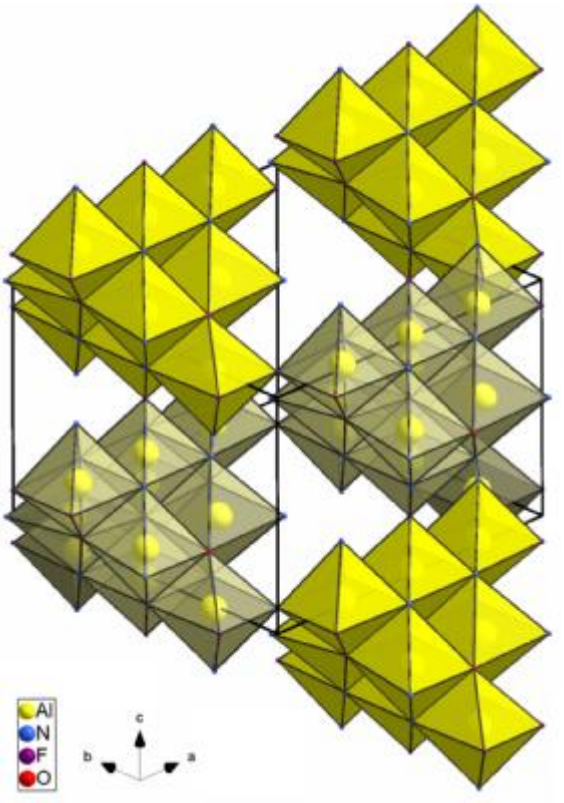

Back to Table of contents

MS15 Mineralogical and inorganic crystallography

MS15-2-11 Cesium oxide mercurides – a new class of double salts
#MS15-2-11

L. Nusser [1], C. Hoch [1]
[1]Ludwig-Maximilians-Universität - München (Germany)

Abstract
While its neighbouring elements Pt, Au and Tl reportedly form anions in combination with electropositive metals in compounds such as Cs_2Pt [1], CsAu [2] and NaTl [3], Hg does not form anions that easily. When reacted with electropositive metals, mercury tends to form amalgams, which feature negatively polarised Hg atoms or atom groups $[Hg_n]^{\delta-}$, but no 'true' mercuride anions, therefore resulting in the *bad metal* behaviour of these amalgams. This may be due to its closed shell configuration $4f^{14}5d^{10}6s^26p^0$, illustrated by the fact that mercury does not form a stable atomic anion in the gas phase [4].
By ternary combinations of Cs, Hg and O a series of double salts with the first mercuride anions now has been made accessible. We present $Cs_{18}Hg_8O_6$ (*I*23, *a* = 13.3920(10) Å, *V* = 2401.8(5) Å^3, *Z* = 2) featuring the mercuride anion $[Hg_8]^{6-}$ next to isolated oxide anions [5]. $[Hg_8]^{6-}$ has a slightly distorted cubic shape and is coordinated by cesium atoms, capping faces and edges (Fig. 1, left. Cesium atoms in blue, Hg atoms in green. All atoms are shown with their thermal displacement ellipsoids at 99% probability). The ionic character of the double salt is confirmed by DFT calculations of the electronic structure. Due to very close structural relations, $Cs_{18}Hg_8O_6$ can be described as homeotypic to the thallide oxide $Cs_{18}Tl_8O_6$ [6].
Cs_8Hg_8O is dimorphic: α-Cs_8Hg_8O (*R*3, *a* = 10.0844(11) Å, *c* = 46.475(6) Å), *V* = 4093.1(8) Å^3, *Z* = 6) transforms at ~220 °C into the β modification (*R*3, *a* = 10.080(6) Å, *c* = 116.71(7) Å, *V* = 10270(11) Å^3, *Z* = 12). Both Cs_8Hg_8O modifications represent a new structure type, again containing cubic $[Hg_8]^{6-}$ anions and oxide anions, coordinated by cesium cations.
The structure of '$Cs_{58}[Hg_8]_6O_{12}$' (*P*1, *a* = 16.360(2) Å, *b* = 18.888(2) Å, *c* = 19.120(2) Å, *α* = 61.779(4)°, *β* = 69.705(4)°, *γ* = 68.431(4)°, *V* = 4749.5(7) Å^3, *Z* = 1) shows a still unresolved twinning problem, resulting in the formal charge of '5⅔–' for the $[Hg_8]$ anion.
$Cs_{14}Hg_{12}O_4$ (*P*2$_1$/*c*, *a* = 10.734(3) Å, *b* = 15.688(3) Å, *c* = 17.378(3) Å, *β* = 128.146(10)°, *V* = 2301.4(9) Å^3, *Z* = 4) contains the cluster anion $[Hg_{12}]^{6-}$, which can be described as stack of two face-sharing $[Hg_8]$ cubes. Analogous to the $[Hg_8]^{6-}$ anion, the edges and faces of the $[Hg_{12}]^{6-}$ anion are capped by cesium cations (Fig. 1, right. Cesium atoms in blue, Hg atoms in green. All atoms are shown with their thermal displacement ellipsoids at 99% probability), while the oxide anions are octahedrally coordinated.

References
[1] A. Karpov, J. Nuss, U. Wedig, M. Jansen, *Angew. Chem.* **2003**, *115*, 4966; *Angew. Chem. Int. Ed.* **2003**, *42*, 4818.
[2] A. Sommer, *Nature* **1943**, *152*, 215.
[3] E. Zintl, W. Dullenkopf, *Z. Phys. Chem.* **1932**, *16B*, 195.
[4] J. H. Simons, R. P. Seward, *J. Chem. Phys.* **1938**, *6*, 790.
[5] L. Nusser, T. Hohl, F. Tambornino, C. Hoch, *Z. Anorg. Allg. Chem.* **2022**, e202100389.
[6] U. Wedig, V. Saltykov, J. Nuss, M. Jansen *J. Am. Chem. Soc.* **2010**, *132*, 12458.

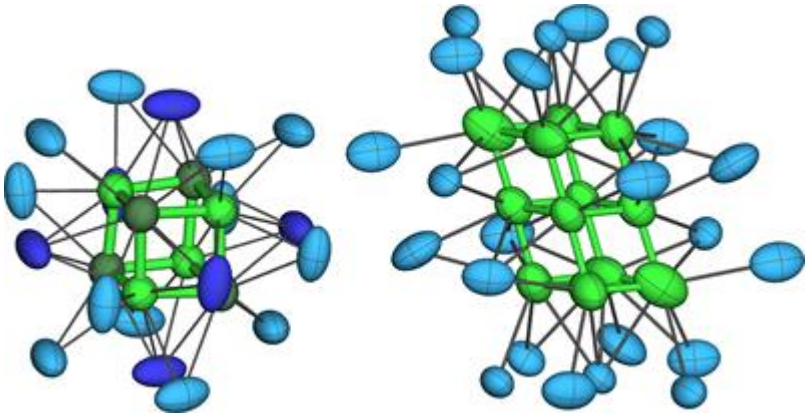

Back to Table of contents

MS15 Mineralogical and inorganic crystallography

MS15-2-12 Ammonothermal synthesis of new cation-deficient Antiperovskites
#MS15-2-12

T. Chau [1], S. Rudel [1], W. Schnick [1]
[1]University of Munich (LMU), Department of Chemistry - Munich (Germany)

Abstract
Inorganic antiperovskites with the formula X_3AN (X^{2+} = Ba, Sr, Ca, Mg; A^{3-} = As, Sb) have recently been reported to exhibit excellent optoelectronic properties like small carrier effective masses, suitable direct bandgaps, high optical absorption coefficients as well as allowed optical transitions at band edges. These properties can be tuned depending on the *X*- and *A*-site. Extending the composition to quaternary antiperovskites ($X_6AA'N_2$) enables enlarging the theoretical maximum solar cell efficiencies to above 29%.[1-2]
Here we report on the ammonothermal synthesis of $X_5Sb_2(NH)_2$ (*X* = Ca, Sr), starting from XH_2 (*X* = Ca, Sr) and Sb. The crystal structures of $X_5Sb_2(NH)_2$ were solved and refined by single-crystal X-ray diffraction (scXRD). $X_5Sb_2(NH)_2$ crystallizes in the orthorhombic space group *Pbam* ($Ca_5Sb_2(NH)_2$: *a* = 6.7980(16) Å, *b* = 13.327(4) Å, *c* = 4.9213(11) Å, *R*1 = 0.016, *wR*2 = 0.027; Sr5Sb2(NH)2: *a* = 7.2257(12) Å, *b* = 13.9816(4) Å, *c* = 5.2195(7) Å, *R*1 = 0.026, *wR*2 = 0.052). SEM-EDX (scanning transmission electron microscopy, energy dispersive X-ray spectroscopy) confirm the *X*/Sb-ratio obtained by scXRD. The obtained structures were further confirmed using powder X-ray diffraction and Raman spectroscopy.
The new compounds feature a square-pyramidal-like coordination geometry around the imide-group (X_5NH), forming ordered defects in the antiperovskite-derived structure. They crystallize as an inverse variant of $Ca_2Mn_2O_5$, where the effect of the oxygen vacancies and structural order have been correlated to their electrocatalytic properties.[3]

References
[1] D. Han, C.Feng, M.-H. Du, T. Zhang, S. Wang, G. Tang, T. Bein, H. Ebert *J. Am. Chem. Soc.* **2021**, *143*, 31, 12369–12379.[2] Y. Mochizuki, H.-J. Sung, A. Takahashi, Y. Kumagai, F. Oba *Phys. Rev. Mater.* **2020**, *4*, 044601-1–14.[3] J. Kim, X. Yin. K. C.Tsao, S. Fang, H. Yang *J. Am. Chem. Soc*. **2014**, *136*, 14646-14649.

Ca5Sb2NH2 crystal structure along [001]

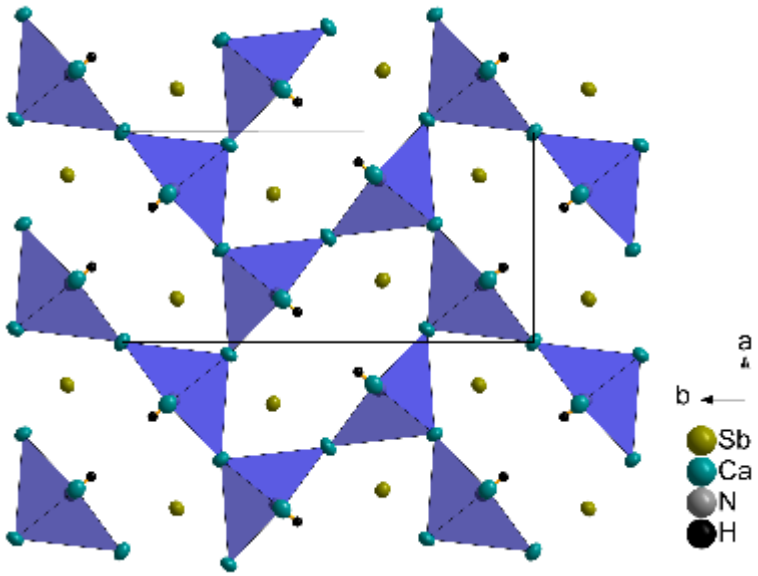

Back to Table of contents

MS15 Mineralogical and inorganic crystallography

MS15-2-13 Charge density studies of single and transient (single to double) Boron-Oxygen bonds #MS15-2-13

R. Gajda [1], A. Piekara [1], D. Tchoń [1], K. Woźniak [1], W. Sławiński [1]
[1]University of Warsaw - Warszawa (Poland)

Abstract
Issues in boron chemistry are still less described than those of the chemistry of carbon. One of such issue seems to be bonds between boron and oxygen. It is already known that except singular, double and triple B-O bonds, there are also claimed a transient type between a single and double B-O bonds [1]. To analyze this phenomena topologically, DFT calculations and electron localization function (ELF) were adopted on wide set of relatively simple molecules containing boron [2,3]. Those theoretically optimized structures were also characterized from the point of view of properties at their bond critical points (BCPs). In this work, on the basis of $(H_4B_4O_9)^{2-}$ ion, we would like to look deeper into the phenomenon of existence of single and multiple bonds. Presented result originate from high-resolution, single crystal, X-ray diffraction experiment. High quality of collected data allowed to obtain experimental charge density distribution. Multipole model refinement according to Hansen-Coppens theory was adopted.
In a nutshell, the ion $(H_4B_4O_9)^{2-}$, which is a component of $(NH_4)_2B_4O_5(OH)_4 \times 2H_2O$ crystal structure, has two types of boron-oxygen bond, i.e. single B-O bond and the other one intermediary between single and double B-O bond. Differences between those two bond types are visible not only cause they differ by their lengths but also a topology of electron density distribution differs. Experimental results based on multipole model refinement give excellent agreement with theoretical DFT calculation as well as with literature data. Properties such as electron density and Laplacian of electron densitycal obtained at bond critical points for both types of B-O bonds could work also as a kind of hint helping us to categorise B-O bonds previously reported in the literature (in the case when electron density and Laplacian at bond critical points are known).

References
[1] Straub, D. Lewis Structures of Boron-Compounds Involving Multiple Bonding. J. Chem. Educ. 1995, 72 (6), 494–497.
[2] Mierzwa, G.; Gordon, A. J.; Latajka, Z.; Berski, S. On the Multiple B-O Bonding Using the Topological Analysis of Electron Localisation Function (ELF). Comput. Theor. Chem. 2015, 1053, 130–141.
[3] Michalski, M.; Gordon, A. J.; Berski, S. Theoretical Insights and Quantitative Prediction of the Nature of Boron-Chalcogen (O, S, Se, Te) Interactions Using the Electron Density and the Electron Localisation Function (ELF). Polyhedron 2021, 210, 115495.

The investigated ion.

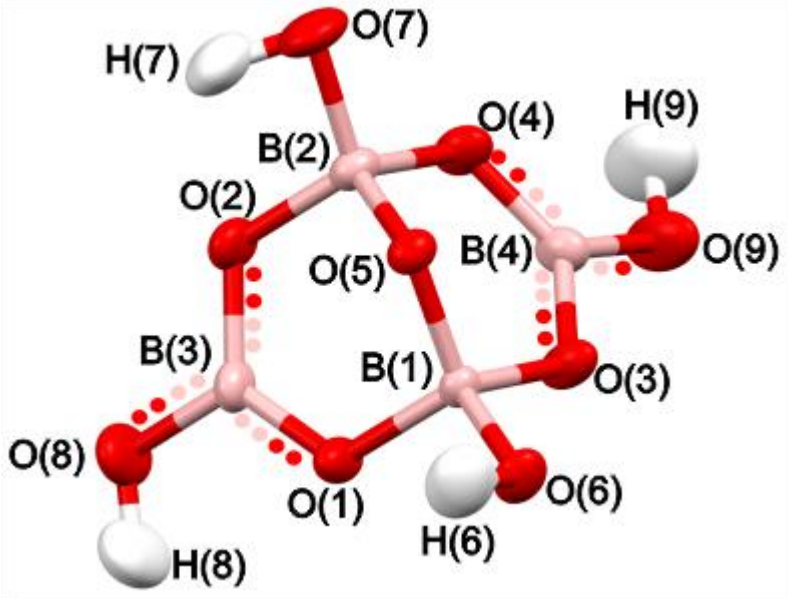

Laplacian of the experimental electron density.

Back to Table of contents

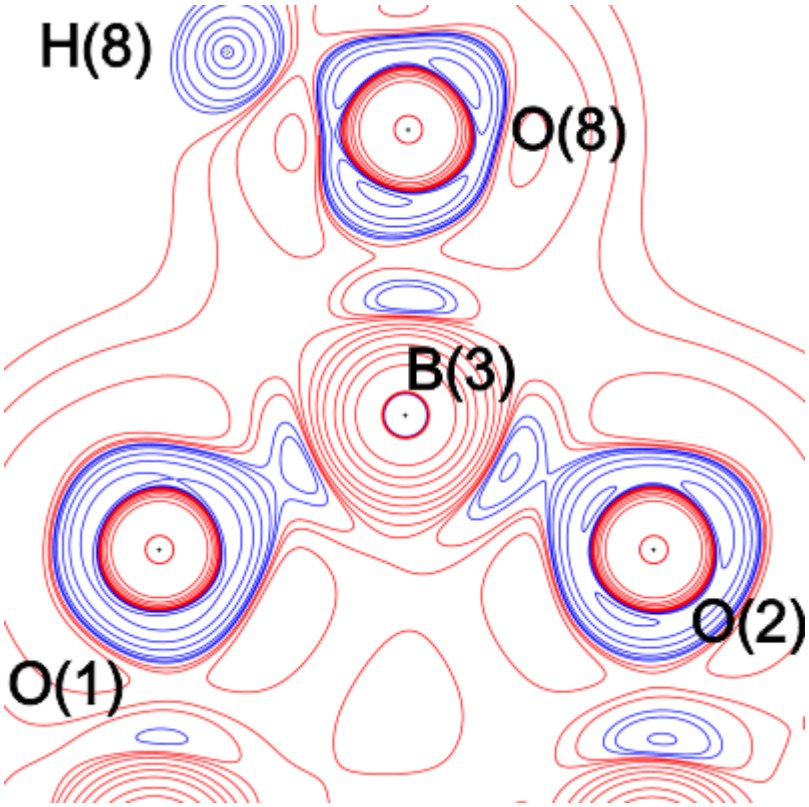

Back to Table of contents

MS15 Mineralogical and inorganic crystallography

MS15-2-14 Molten-salt growth of ruthenate quantum materials
#MS15-2-14

D.A. Fernandes De Almeida [1], A.J. Browne [1], M. Pelly [1], B. Gade [1], A.W. Rost [1], A.S. Gibbs [1]
[1]University of St. Andrews - St. Andrews (United Kingdom)

Abstract
Quantum materials are highly topical because their macroscopic properties cannot be understood simply by semi-classical descriptions of their constituent particles [1]. An essential part of understanding those properties is careful crystal growth and structural characterisation [2]. We are currently exploring the influence of different crystal growth techniques on the quantum states of materials with highly sensitive structure-property relationships.
Of particular interest are strontium ruthenates such as $Sr_3Ru_2O_7$. Careful crystal growth and structure characterisation was essential in determining the intrinsic properties of this material due to elements of structural disorder, such as stacking faults [3], and structural distortions [4]. One route to high quality crystals that has not yet been explored for $Sr_3Ru_2O_7$ is alkali metal molten-salt growth, which we are doing for the first time.
We are also exploring other materials in the Sr–Ru–O phase diagram and have succeeded in growing high quality single crystals of $Sr_4Ru_2O_9$. We are using these to determine its physical properties in a more informative manner than has previously been undertaken [5, 6], and thus are advancing the understanding of an exciting quantum material.

References
[1] “The rise of quantum materials,” Nature Physics, 2016, V. 12, p. 105
[2] Browne, A. J., Krajewska, A., and Gibbs, A. S. “Quantum materials with strong spin–orbit coupling: challenges and opportunities for materials chemists,” Journal of Materials Chemistry C, V. 9, 2021, p. 11640–54
[3] Huang, Q., Lynn, J. W., Erwin, R. W., Jarupatrakorn, J., and Cava, R. J. “Oxygen displacements and search for magnetic order $Sr_3Ru_2O_7$,” Physical Review B, V. 58, 1998, p. 8615-8521
[4] H. Shaked, J.D. Jorgensen, O. Chmaissem, S. Ikeda, Y. Maeno “Neutron Diffraction Study of the Structural Distortions in $Sr_3Ru_2O_7$,” Journal of Solid State Chemistry, V. 154, 2000, p. 361-367
[5] Dussarrat, C., Fompeyrine J. and Darriet, J. “$Sr_4Ru_2O_9$, a Structural Model Resulting from the Stacking of [Sr_3O_9] and [Sr_3O_6] Mixed Layers. Structural Relationships to Related Perovskite-Type Structures”, European Journal of Solid-State Inorganic Chemistry, V. 26, 1995, p. 3-14
[6] Sundar Manoharan, S., Singh, B., Driscoll, J., et al. “Magnetism and electronic transport in $Sr_{4-x}La_xRu_{2-x}Mn_xO_9$: Interplay of Mn and Ru redox chemistry,” Journal of Applied Physics, V. 97, 2005, p. 10A304

Single crystal grown of Sr4Ru2O9

Back to Table of contents

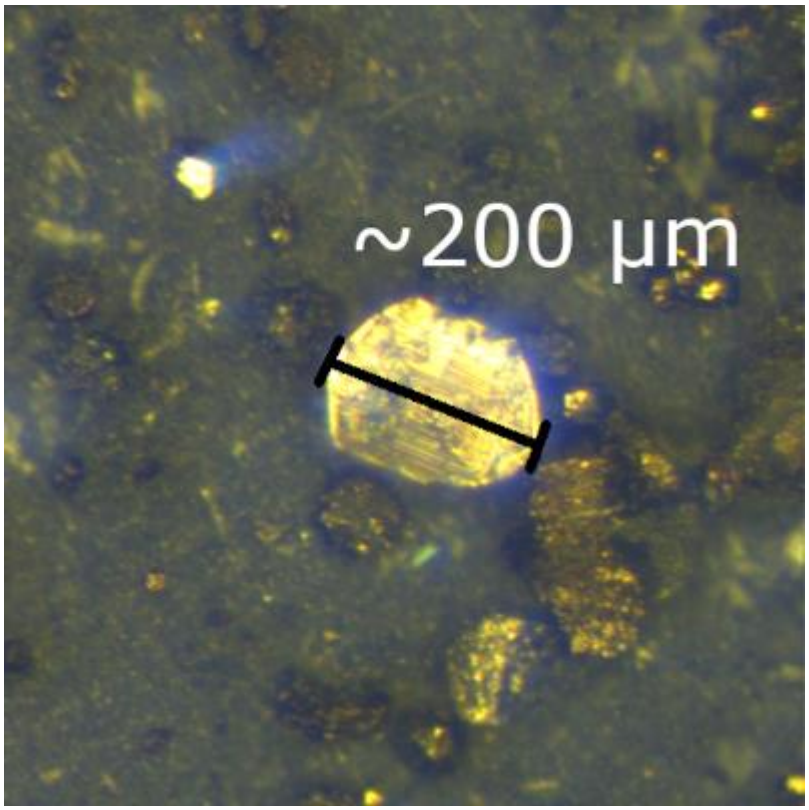

Back to Table of contents

MS15 Mineralogical and inorganic crystallography

MS15-2-15 Dypingite: The phase identification and transformation
#MS15-2-15

A. Sednev-Lugovets [1], Y. Lu [2], P. Carvalho [3], Ø. Vistad [3], H. Friis [2], H. Austrheim [4], M. Guzik [1]
[1]University of Oslo - Kjeller (Norway), [2]Natural History Museum - Oslo (Norway), [3]SINTEF Industry - Oslo (Norway), [4]University of Oslo - Oslo (Norway)

Abstract
Dypingite is a naturally occurring mineral, with an empirical formula $Mg_5(CO_3)_4(OH)_2{\cdot}5H_2O$, and a member of the hydrocarbonate mineral group. It was named in 1970 by Gunnar Raade, after the Dypingdal serpentine-magnesite deposit in Norway [1]. Recently, it was reported that this mineral can effectively remove heavy metals (e.g., Cr, Cd, Cu, Pb, Ni [2]) from water and cause their long-term immobilisation [3]. It is expected that the unique desert rose morphology of the compound or/and peculiarities of its crystal structure are the reasons of the dypingite remarkable sorption properties. Despite the fact that this mineral has been known for 50 years, the information about its unit cell parameters, or even Bragg peak positions, is inconsistent and surprisingly limited. To partly fill this gap, we have been performing comprehensive structural and microstructural studies on the natural and synthetic dypingite powder samples to: i) identify a crystalline phase called dypingite; ii) correctly index powder X-ray diffraction (PXD) patterns so as to determine the compound unit cell parameters and to solve its crystal structure; iii) investigate the dypingite phase transformation occurring upon the compound hydration/dehydration.

References
1. Raade G, Dypingite, a new hydrous basic carbonate of magnesium, from Norway, Am. Mineral., 55 (1970) 14572. Uzair MN, Feasibility Study on Heavy Metal Adsorption by Weathered Dunites with Emphasis on the Minerals Pyroaurite and Dypingite, Master thesis, University of Oslo, Norway, 2014.3. Hooper JC, Tracking the fate of nickel during transformation of nesquehonite to dypingite at 35°C, Bachelor thesis, Queen's University, Canada, 2019.

The desert rose morphology of dypingite

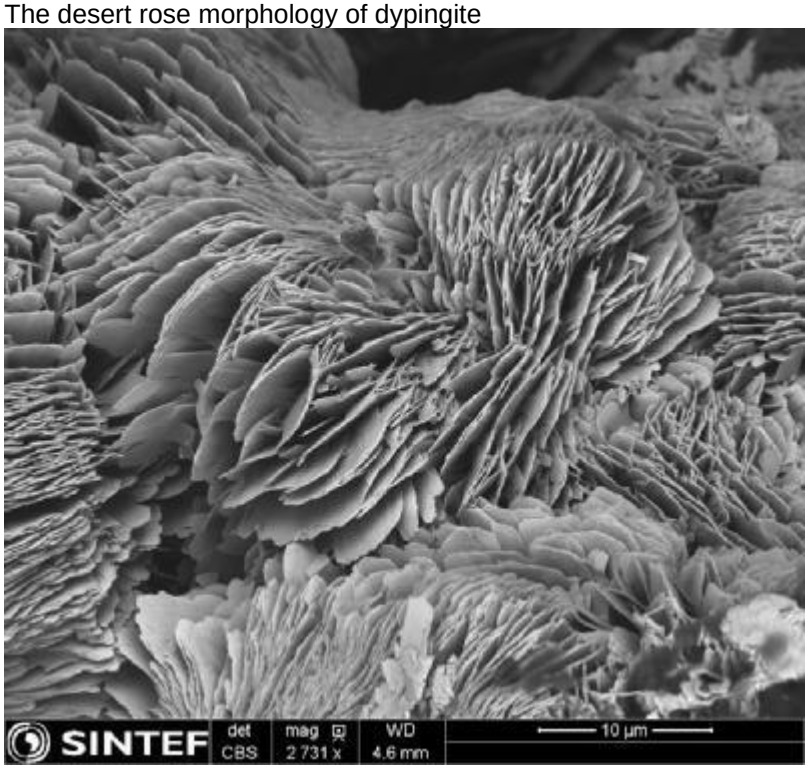

The PDX pattern of the dypingite mineral

Back to Table of contents

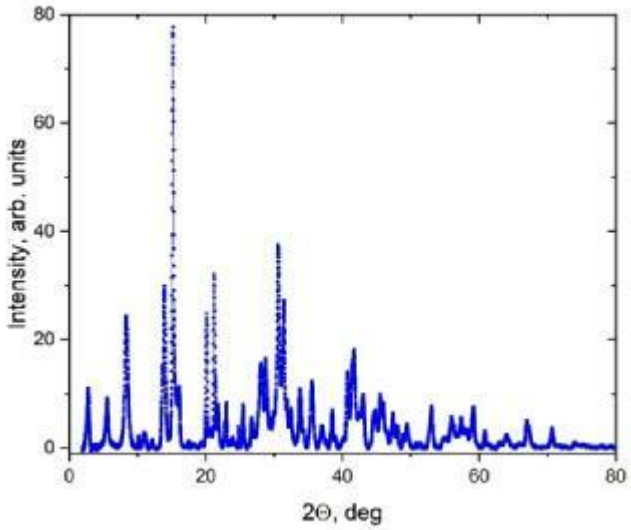

Back to Table of contents

MS15 Mineralogical and inorganic crystallography

MS15-2-2 $Cs_3La[AsS_4]_2$: A Cesium-Containing Lanthanum Thioarsenate(V)
#MS15-2-2

P. Lange [1], K. Engel [1], T. Schleid [1]
[1]University of Stuttgart - Stuttgart (Germany)

Abstract
The structural diversity of alkali-metal thiophosphates with transition or even rare-earth metal participation has been studied intensively in the past years. However, only few investigations on thioarsenates(V) were conducted although they might as well exhibit a large variety of different stoichiometries and structures.
The target compound was synthesized from metallic lanthanum (La), cesium polysulfide (Cs_2S_x, $x \approx 3$), arsenic sesquisulfide (As_2S_3) and elemental sulfur in a stoichiometric ratio of 1:1:1:6. Cesium polysulfide was prepared from the elements (two equivalents of cesium with three equivalents of sulfur) via ammonothermal synthesis in an autoclave for two days until the complete conversion of the elemental cesium. The starting materials were filled into a fused glassy silica ampoule in an argon-filled glove box and sealed under dynamic vacuum. The ampoule was placed inside a muffle furnace and heated to 600 °C with 30 °C/h, held for 4 days and then cooled back to room temperature with 3 °C/h. Afterwards, the bulk product was inspected for suitable single crystals since the powder X-ray diffraction pattern revealed more than one phase.
Here we present a cesium-containing lanthanum thioarsenate(V) with the composition $Cs_3La[AsS_4]_2$ (CSD number: 2156995). This stoichiometric formula seems familiar as $K_3RE[AsS_4]_2$ compounds with *RE* = Nd, Sm, Gd and Dy have previously been published by Bensch et al. [1,2]. The novel cesium compound $Cs_3La[AsS_4]_2$ does not share the same structure type ($K_3Gd[AsS_4]_2$: a = 1034.84(7) pm, b = 1880.39(14) pm, c = 882.38(6) pm, β = 117.063(7)°, Z = 4; monoclinic, *C*2/*c*) [2], however. $Cs_3La[AsS_4]_2$ crystallizes monoclinically as well, but with the non-centrosymmetric space group *P*21 and the lattice parameters a = 1014.71(6) pm, b = 702.68(4) pm, c = 1192.35(7) pm, β = 90.232(3)° for Z = 2. There is only one unique La^{3+}-cation position within the asymmetric unit surrounded by eight S^{2-} anions (d(La^{3+}–S^{2-}) = 295.5 – 299.9 + 325.4 + 327.3 pm) building a bicapped trigonal prism. Connected via corners, these $[LaS_{6+2}]^{13-}$ prisms form one-dimensional infinite chains propagating along the *b*-axis, which are separated from each other by three crystallographically independent Cs^+ cations in 9- to 11-fold sulfur coordination. Moreover, all sulfur atoms participate in the arsenic(V) coordination forming isolated $[AsS_4]^{3-}$ tetrahedra (d(As^{5+}–S^{2-}) = 212.2 – 218.9 pm, (S–As–S) = 97.3 – 123.2°).

References
[1] Y. Wu, C. Näther, W. Bensch, *Inorg. Chem.* **2006**, *45*, 8835–8837.[2] Y. Wu, W. Bensch, *Solid State Sci.* **2009**, *11*, 1542–1548.

Extended unit cell of Cs3La[AsS4]2, along [010].

Back to Table of contents

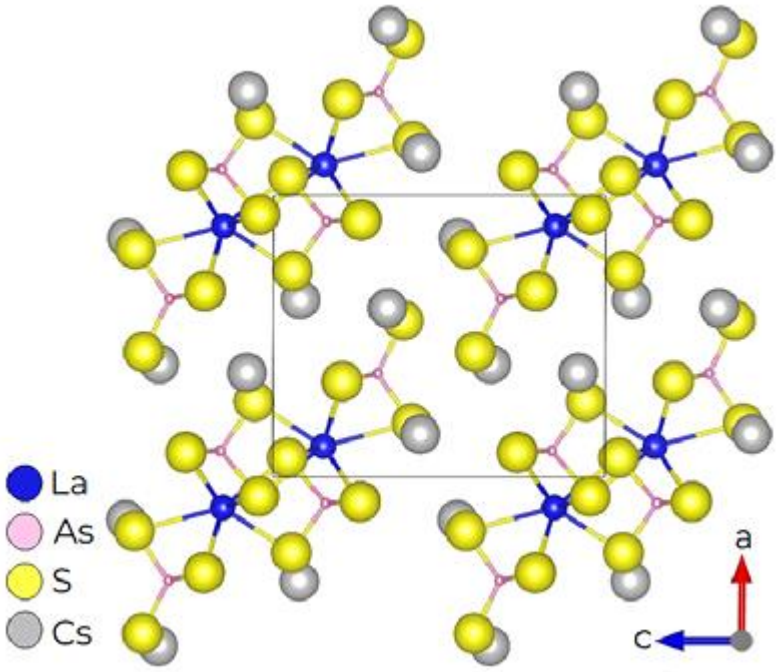

(001) projection to emphasize chains along [010]

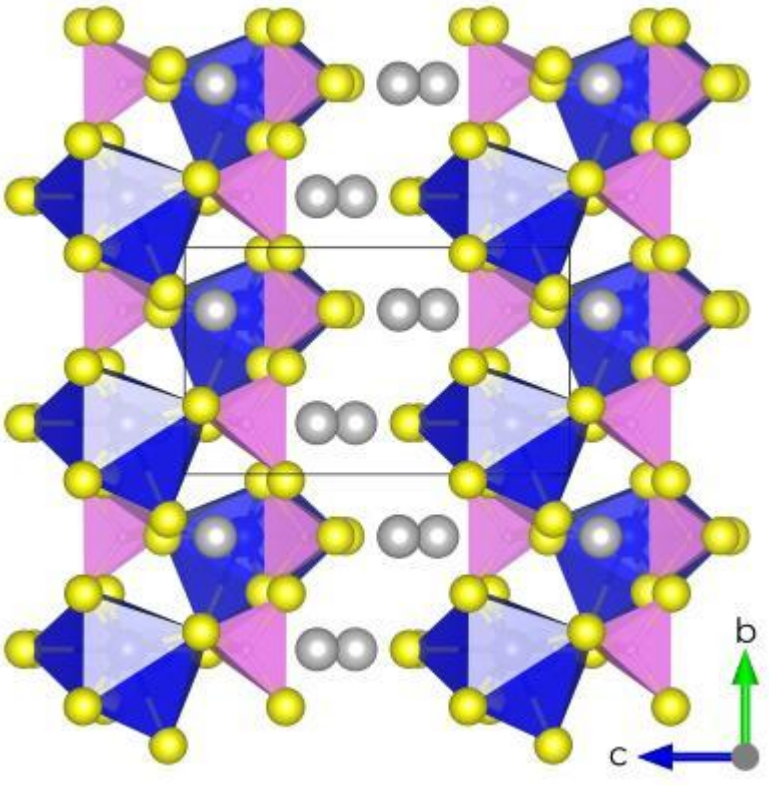

Back to Table of contents

MS15 Mineralogical and inorganic crystallography

MS15-2-3 Crystal chemistry of extracted brownmillerite from sulfate resisting Portland cement
#MS15-2-3

A. Mériot [1], M.N. De Noirfontaine [1], L. Izoret [2], M. Courtial [1], S. Tusseau-Nenez [3], S. Gauffinet [4], S. Diliberto [5], F. Dunstetter [1]
[1]Laboratoire des Solides Irradiés, CEA-DRF-IRAMIS, CNRS, Ecole Polytechnique, Institut Polytechnique de Paris - Palaiseau (France), [2]Syndicat Français de l'Industrie Cimentière - Clichy (France), [3]Laboratoire de Physique de la Matière Condensée, CNRS, Ecole Polytechnique, Institut Polytechnique de Paris - Palaiseau (France), [4]Laboratoire Interdisciplinaire Carnot de Bourgogne, CNRS, Université de Bourgogne Franche-Comté - Dijon (France), [5]Institut Jean Lamour, UMR 7198, CNRS, Université de Lorraine - Nantes (France)

Abstract
Brownmillerite, the so-called ferrite phase, is the iron bearing phase of ordinary Portland cement clinker and represents typically 7-8% wt% of the its total mass. It is a wide solid solution between $Ca_2Fe_2O_5$ and $Ca_2Al_{1.3}Fe_{0.7}O_5$, often written $Ca_2Al_xFe_{2-x}O_5$ with 0<x<1.4. The crystal structure is orthorhombic with two distinct space groups: Pnma for 0<x<0.4-0.6 and Ibm2 for 0.4-0.6<x<1.4 [1-3]. In usual Portland cement, it is well established that brownmillerite crystallizes in space group Ibm2, with Al/Fe ratio in the range 1 to 2 approximately [4]. At the present time, only few studies have analyzed brownmillerite phase of more specific sulfate resisting Portland cements (SRPC) [5-7]. It is known that the brownmillerite phase is richer in iron [4] but there is a lack of recent and accurate crystal structure parameters on industrial brownmillerite, that are of particular importance for further study of cement reactivity.
Brownmillerite, resulting from the crystallisation of the liquid phase, is one the less abundant of the four major phases of Portland cement clinker. It constitutes the interstitial phase in which calcium silicates are embedded. Its crystals are with small sized particles (~1 µm), frequently dendritic, eventually mixed with tricalcium aluminate. Studying the crystal chemistry directly from the cement leads to an overly complex interpretation due to the Bragg lines overlap and the lack of accuracy of chemical analysis (SEM/EDS). The proposed approach to overcome this drawback is to extract brownmillerite by selective chemical dissolution.
Four SRPC (A-D samples) were used to extract brownmillerite, then systematically studied by powder X-ray diffraction (XRD), electron microprobe (EPMA), X-ray fluorescence spectroscopy and ^{57}Fe Mössbauer spectroscopy. Two extraction steps were used: the first is the salicylic acid/methanol (SAM) protocol that leaves a residue rich in brownmillerite, tricalcium aluminate and sulfate phases. The second, which was developed in this study, uses acetic acid (AcA) to dissolve tricalcium aluminate and sulfates phases. On the other hand, eight synthetic brownmillerite samples with similar Al/Fe ratio were used to compare their crystal chemistry with the industrial ferrites.
The selective extraction clearly appears of particular importance to obtain a correct estimation of Al/Fe content in ferrite phase, consistent with EPMA analysis. The influence of the extraction protocol is deeply discussed. The Rietveld refinements show that all the brownmillerite samples of this study crystallize in space group Ibm2. Two families of brownmillerite (A&C and B&D) are distinguished by their cell parameters and aluminium content (Figure 1), depending on the presence or the lack of tricalcium aluminate phase in cement. Mössbauer spectroscopy is used to evaluate the iron repartition in octahedral and tetrahedral sites in extracted and synthetic brownmillerite.

References
[1] A. A. Colville and S. Geller, "The crystal structure of brownmillerite, Ca_2FeAlO_5," Acta Crystallographica B, 27 2311-15 (1971).[2] A. A. Colville and S. Geller, "The crystal structure of $Ca_2Fe_{1.43}Al_{0.57}O_5$ and $Ca_2Fe_{1.28}Al_{0.72}O_5$," Acta Crystallographica B, 28 3196-200 (1972).[3] G. Redhammer, G. Tippelt, G. Roth, and G. Amthauer, "Structural variations in the brownmillerite series $Ca_2(Fe_{2-x}Al_x)O_5$: single-crystal X-ray diffraction at 25°C and high-temperature X-ray powder diffraction (25 °C ≤ T ≤ 1000 °C)," American Mineralogist, 89 405–20 (2004).[4] H. F. W. Taylor, "Cement Chemistry." 2nd edition, Thomas Telford Edition: London, (1997).[5] A. R. Landa-Canova and S. Hansen, "Transmission electron microscopic study of ferrite in sulfate-resisting Portland cement clinker," Cement and Concrete Research, 29 679-86 (1999).[6] R. S. Gollop and H. F. W. Taylor, "Microstructural and microanalytical studies of sulfate attack. II. Sulfate resisting Portland cement: ferrite composition and hydration chemistry," Cement and Concrete Research, 24[7] 1347-58 (1994).[7] E. Backström and S. Hansen, "X-ray mapping of interstitial phases in sulphate resisting cement clinker," Physical Review B, 9[33] 17-23 (1997).

Figure 1: Brownmillerite unit cell volume

Back to Table of contents

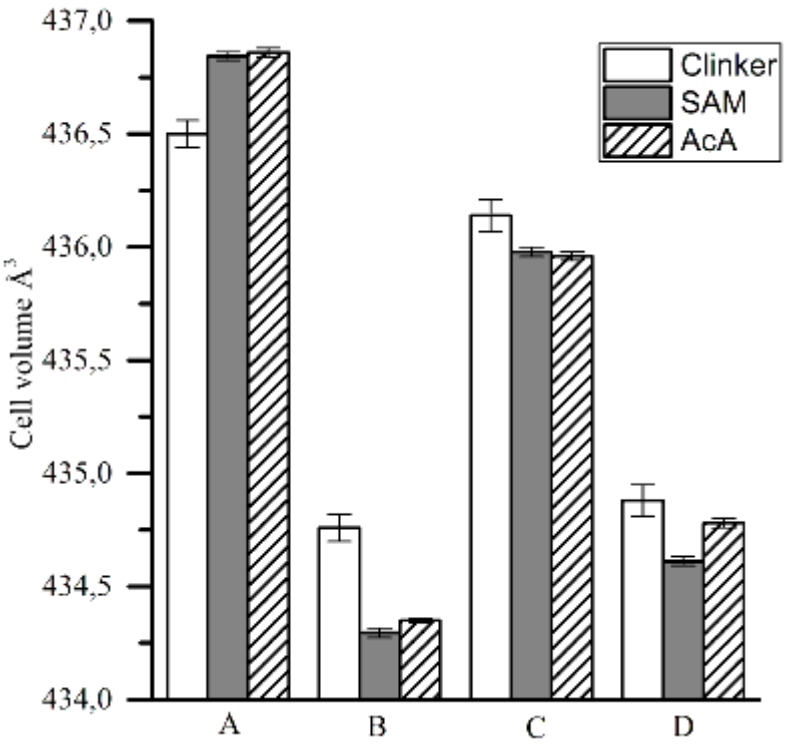

Back to Table of contents

MS15 Mineralogical and inorganic crystallography

MS15-2-4 The crystal structures of Sn6TO8 (T = Si or Ge): tin(II)-cluster containing zinc blende structural analogues #MS15-2-4

D. Parsons [1], A. Nearchou [2], J. Hriljac [1]
[1]Diamond Light Source Ltd - Didcot (United Kingdom), [2]University of Birmingham - Birmingham (United Kingdom)

Abstract
A cubic tin(II) silicate, *α*-Sn_6SiO_8, and a cubic tin(II) germanate, *α*-Sn_6GeO_8, have been synthesised by hydrothermal methods and the crystal structures of these materials have been elucidated by Rietveld refinement of synchrotron PXRD data.[1][2] The crystal structures are analogous to the zinc blende structure: comprising a face-centred cubic array of $[Sn_6O_8]^{4-}$ anionic clusters with Si^{4+} or Ge^{4+} cations occupying half of the tetrahedral holes, giving rise to a 3-dimensional framework of clusters joined by bridging orthosilicate or orthogermanate moieties. The crystal structure of the cubic tin(II) germanate is depicted in Figure 1.
Applying variable temperature PXRD studies to both the tin(II) silicate and tin(II) germanate have revealed thermal decomposition and oxidation to tin(IV) occurs at *ca*. 600 °C and 675 °C, respectively.[1][2] Thermal decomposition is observed at significantly higher temperatures than for tin(II) oxide, *α*-SnO, which decomposes over the range 300 – 500 °C,[3] demonstrating the superior stability of the framework structures of the silicate and germanate. Variable temperature PXRD has also revealed the formation of a tetragonal polymorph upon cooling the tin(II) silicate to 170 K. The crystal structure of the tetragonal tin(II) silicate polymorph, *γ*-Sn_6SiO_8, has also been elucidated by Rietveld refinement of synchrotron data. While a phase transition occurs upon cooling the tin(II) silicate, no such transition occurs upon cooling the tin(II) germanate and the cubic structure is instead retained at 100 K. By comparing the crystal structures of *α*-Sn_6SiO_8, *γ*-Sn_6SiO_8 and *α*-Sn_6GeO_8 (at both ambient temperature and 100 K), a structural argument based on strain is presented for why a transition occurs in the silicate system upon cooling but not in the germanate system. In this poster, the crystal structures of the cubic and tetragonal tin(II) silicate and the cubic tin(II) germanate are presented, along with structural explanations for the temperature behaviour of these materials.

References
[1] D. S. Parsons, S. N. Savva, W-C. Tang, A. Ingram and J. A. Hriljac, *Inorg. Chem.*, 2019, **58**, 16313 – 16316.
[2] D. S. Parsons, A. Nearchou and J. A. Hriljac, manuscript in preparation.
[3] M. S. Moreno, R. C. Mercader and A. G. Bibiloni, *J. Phys.: Condens. Matter*, 1992, **4**, 351 - 355.

The crystal structure of α-Sn6GeO8.

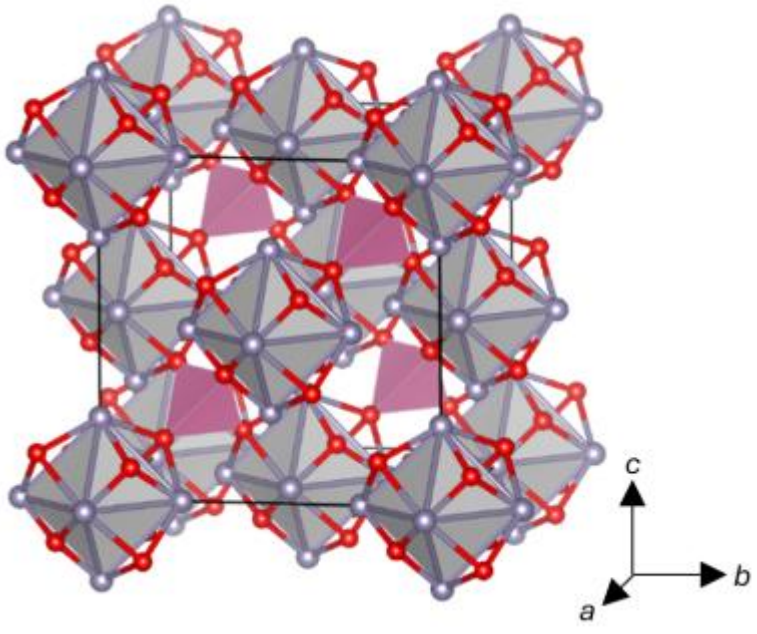

Back to Table of contents

MS15 Mineralogical and inorganic crystallography

MS15-2-5 Again for the choice of space group for the crystal structures of the scapolite group representatives #MS15-2-5

V. Kostov-Kytin [1], M. Kadiyski [1], R. Nikolova [1]
[1]IMC Bulgarian Academy of Sciences, VAT ID: BG 831906364 - Sofia (Bulgaria)

Abstract
Scapolites are rock-forming minerals with well-pronounced crystal chemical complexity. The interest in such compounds is determined by the possibility of their use as geothermometers, as well as by their potential for greenhouse gas storage. Their crystal structure is composed of a $[(Si,Al)_nO_{2n}]$ framework containing eight- and four-membered rings. Calcium and sodium cations are located in the channels formed by the eight-membered rings, and carbonate, sulphate and chlorine anions are located in those formed by the four-membered rings (Fig. 1). There are three types of heterovalent isomorphism for group members, which can generally be represented as follows: Si⇔Al (framework cations); Ca⇔Na and CO_3⇔SO_4⇔Cl (extra-framework species). Relations between the three schemes are not always explicit and unambiguous, but in general their joint manifestation leads to electroneutrality. The use of routine practices applicable to other aluminosilicates are often resorted to during investigations of the crystal chemical peculiarities of scapolites, especially with regard to their framework construction. These are: Lowenstein's rule referring to the aluminium and silicon order; the dependence of size of the framework tetrahedra on the type of their central cations (Si, Al). The latter indicates the preferred population in the tetrahedral positions. The highest symmetry space group used in solving crystal structures in the marialite-meyonite series $Na_4Al_3Si_9O_{24}Cl$ (Me0) – $Ca_4Al_6Si_6O_{24}CO_3$ (Me100), is the tetragonal *I4/m*. It is applicable to the representatives falling within the compositional range of the two end members. In the middle region, however, additional reflexes are observed in the diffraction patterns, which require the use of the primitive *P42/n* of the tetragonal syngony. Drawing boundaries between the representatives of the two space groups, especially those with high calcium content, is still controversial.

This work presents results of single-crystal X-ray investigations of scapolites from three localities, two of which are reported for the first time. The studies samples have been identified as Me71; Me75, and Me80. Their crystal chemical characteristics relate them to the disputed area for selection of a space group. In search of an opportunity to refine the arrangement of framework cations, the structure of each phase has been solved in three space groups: *I4/m*, *P42/n*, and the monoclinic *I2/m*. The obtained results shed new light on the choice of space group for description of scapolites crystal structures, as well as on the preferred by silicon and aluminium ions positions and hence for their ordering in the framework construction.
Acknowledgments: This work was funded by the Operational Program “Science and Education for Intelligent Growth” by the Bulgarian Ministry of Education and Science, co-financed by the European Union through the European Structural and Investment Funds under grant BG05M2OP001-1.001-0008 of National Centre for Mechatronics and Clean Technology.

Schematic presentation of scapolite structure

Back to Table of contents

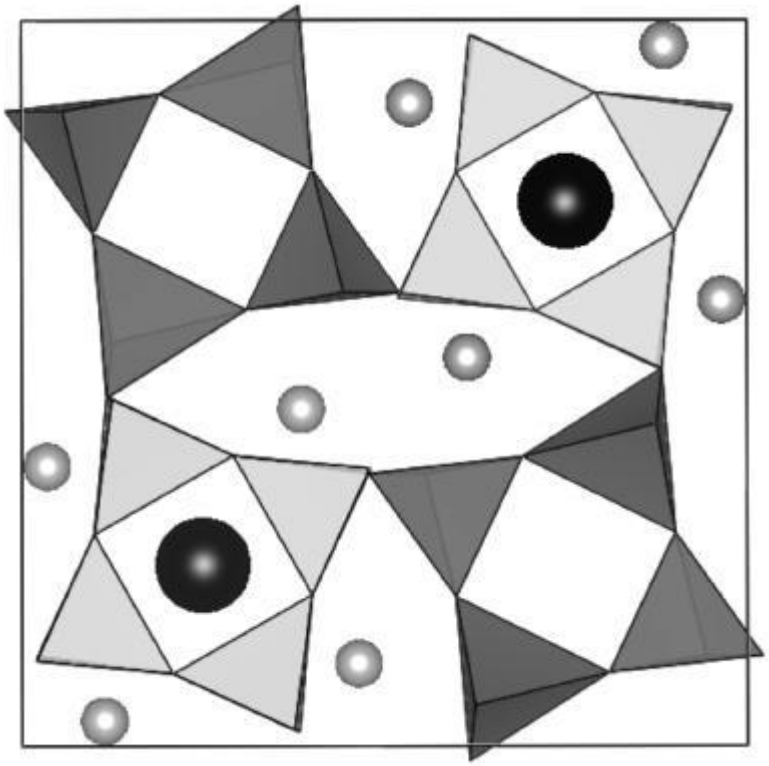

Back to Table of contents

MS15 Mineralogical and inorganic crystallography

MS15-2-7 From AM_5 to A_2M_{17}: New crystallographically related intermetallics
#MS15-2-7

M. Otteny [1], K. Köhler [1], M. Wendorff [1], C. Röhr [1]
[1]Institut für Anorganische und Analytische Chemie, Albert-Ludwigs-Universität - Freiburg (Germany)

Abstract
In the systems Sr-Mg-Cd and Ba-Mg-Cd [1], three new ternary intermetallics A_2M_{17} [2] were obtained, which are crystallographically related to the $CaCu_5$-type structure. The corresponding relations will be demonstrated applying the Bärnighausen group-subgroup formalism [3]. Besides the common $CaCu_5$-type ($P6/mmm$, a≈511, c≈405 pm), which is not observed for eather of the border phases of the ternary systems, the trigonal Th_2Zn_{17} ($R\bar{3}m$, a≈906, c≈1323 pm) and the hexagonal Th_2Ni_{17} ($P6_3/mmc$, a≈836, c≈816 pm) structure type as well as a new related structure ($P6_3/mmc$, a≈1033 c≈2021 pm) were synthesised.Their syntheses were performed by heating the elements under Ar atmosphere up to 750/800 °C (for A=Sr/Ba) followed by cooling with rates of 5-10 K/h.
The $CaCu_5$-type compounds (Fig. 1, a) are build up from |:AA:| stacked Mg/Cd kagomé nets (*M*, green), forming trigonal bipyramids M_5 (rose), connected via all vertices. Within the resulting large hexagonal channels running along [001] the Sr/Ba cations (pink, CN=18+2) are located. In the system Ba-Mg-Cd, the $CaCu_5$-type structure appears close to the composition $BaMg_{3.5}Cd_{1.5}$ only. Herein, both crystallographic *M* sites are statistically occupied by Mg and Cd.
In the structures forming the Th_2Zn_{17}-type (Fig. 1, b) each third of the *A* cations is replaced by M_2 dumbbells (blue-magenta). In the Ba system, this structure type was already known from older film data - which has been similarly verified by a recent single crystal structure refinement - for Ba_2Mg_{17} [4], in which up to 41.7% of the Mg atoms could be replaced by Cd. For *A*=Sr, it was only found in ternary phases with an approximate equimolar Mg:Cd ratio.
The Th_2Ni_{17} (Fig. 1, c) and the new structure type (Fig. 1, d) exhibit two different types of channels: For Th_2Ni_{17}, 1/3 of the channels are occupied by *A* cations exclusively, the remaining channels are alternatingly stuffed by *A* cations and M_2 dumbbels. For *A*=Sr, the latter structure type is yet known for Sr_2Mg_{17} [5], which hence has been reinvestigated herein. For *A*=Ba, a single Mg-rich Th_2Ni_{17} phase with the composition $Ba_2Mg_{14.4}Cd_{2.6}$ was obtained.In the newly characterized A_2M_{17} structure of this family 1/3 of the channels are alternatingly occupied by A/M_2, whereas in the remaining channels every 5th *A* cation is replaced by an M_2 dumbbell. This new structure type was obtained for *A*=Sr and with Cd proportions between 26 and 36%.
For the structures containing M_2 dumbbells, a preferred occupation of the concerning positions with Mg is observed. This can be explained by it's decreased electronegativity, which is confirmed by the Bader charges obtained by lo+APW-DFT bandstructure calculations. The crystal-chemical parameters determining the stability of the three different A_2M_{17} structure types as well as the 'coloring' (Mg/Cd distribution at the *M* sites) will be discussed in this contribution.

References
[1] K. Köhler, C. Röhr, Z. Kristallogr. Suppl. 42, 162 (2022).[2] W. Steurer, J. Dschemuchadse, Intermetallics: Structures, Properties, and Statistics, 2016, Oxford University Press (vol 26, ed 2)[3] H. Bärnighausen, Match, Com. in Math. Chem. 9, 139 (1980).[4] E. Gladyshevskii, Sov. Phys. Crystallogr. 6, 207-208 (1961).[5] P. Kripyakevich, Kristallografiya, 7, 31-42 (1962).

Back to Table of contents

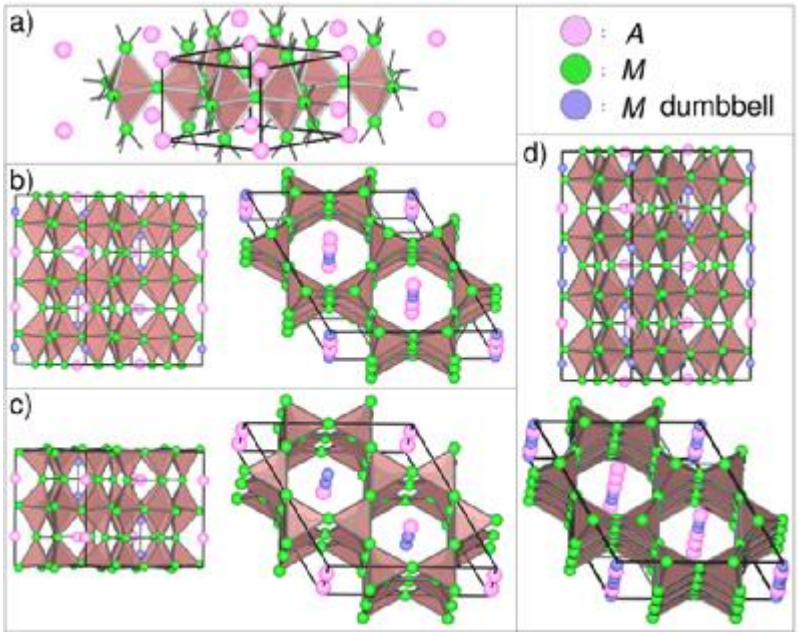

Back to Table of contents

MS15 Mineralogical and inorganic crystallography

MS15-2-8 $Rb_2I_8Nd_4Sb_{16,667}O_{28}$: A Quinary Oxoantimonate(III) Iodide with Rubidium and Neodymium #MS15-2-8

R.J.C. Locke [1], K.N. Bozenhardt [1], T. Schleid [1]
[1]University of Stuttgart - Stuttgart (Germany)

Abstract
In attempts to synthesize $NdSb_2O_4I$ in analogy to $NdBi_2O_4I$[1], with $Rb_2I_8Nd_4Sb_{16.667}O_{28}$ the first flux-containing rare-earth metal(III) oxoantimonate(III) iodide could be obtained via solid-state reactions, which forms pale violet, long thin, needle-shaped crystals. It crystallizes in the monoclinic space group *C*2/*m* with *a* = 2269.98(17) pm, *b* = 415.27(3) pm, *c* = 1284.56(9) pm and *β* = 96.559(3)° for *Z* = 1 (CSD-2169526).
Four out of five crystallographically distinct Sb^{3+} cations (Sb1–Sb4) form square ψ^1-pyramids $[SbO_4]^{5-}$ (Figure 1, *right*) together with four oxygen atoms and a stereochemically active non-bonding electron pair each. These pyramids exhibit Sb^{3+}–O^{2-} distances from 196 to 228 pm and are linked either by two edges or by two edges and one corner. The fifth Sb^{3+} cation (Sb5) forms rather a ψ^1-tetrahedron $[SbO_3]^{3-}$ (Figure 1, *right*) with only three oxygen atoms at similar distances and its lone pair. There is some disorder present, which causes to be the Sb4 and Sb5 positions only partially occupied. In this new structure, for the first time, a triple and a quadruple coordination mode of the Sb^{3+} cations with oxygen atoms occurs simultaneously. The ψ^1-pyramids are each linked by edges, while the ψ^1-tetrahedra are connected by corners, resulting in infinite strands of so-called “halfpipes” (Figure 1, *left*) propagating along [010].
The structure displays $[NdO_8]^{13-}$ hemiprisms, which share by four skew edges to form a kind of staircase structure. These polyhedra are located within antimony-oxygen “halfpipes” with each oxygen atom of a hemiprism also belonging to the “halfpipe”. The Rb^+ cations, occupying only one half of their crystallographic positions, have six iodide anions as neighbors to form trigonal prisms $[RbI_6]^{5-}$, which share two trans-oriented faces to form endless chains according to 1D-$\{[RbI^f_{6/2}]^{2-}\}$ (Figure 2).

References
[1] M. Schmidt, H. Oppermann, C. Henning, R. W. Henn, E. Gmelin, N. Söger, M. Binneweis, *Z. Anorg. Allg. Chem.* **2000**, *626*, 125–135.
[2] R. J. C. Locke, *Doctoral Dissertation* **2024**, University of Stuttgart, *in preparation.*
[3] K.-N. Bozenhardt, *Master Thesis* **2022**, University of Stuttgart.

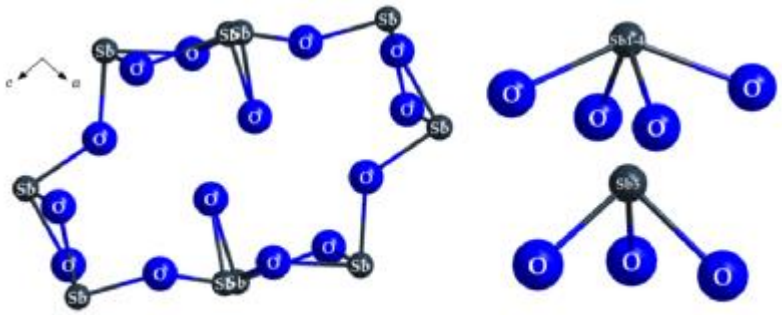

Figure 1. Antimony-oxygen "halfpipes" (*left*) and their building blocks (ψ^1-pyramids $[(Sb1–4)O_4]^{5-}$ and ψ^1-tetrahedra $[(Sb5)O_3]^{3-}$, *right*).

Back to Table of contents

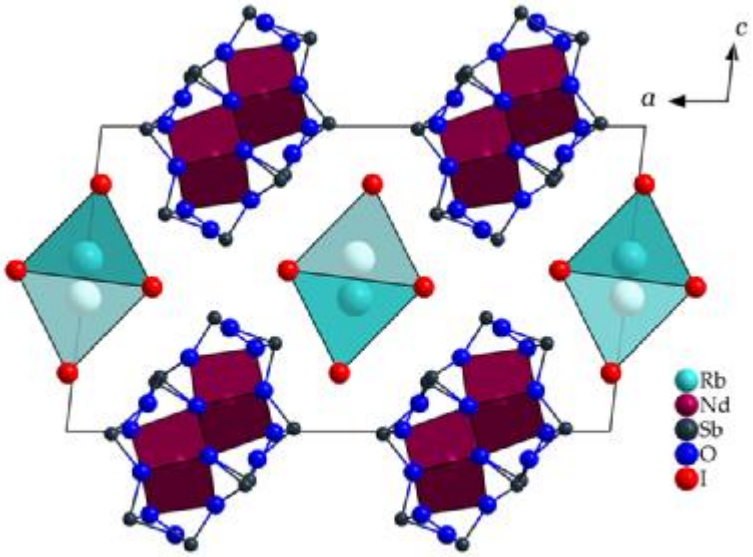

Figure 2. Projection of the monoclinic crystal structure of $Rb_2I_8Nd_4Sb_{16.667}O_{28}$ onto [010] emphasizing the antimony-oxygen "halfpipes" filled with $[NdO_8]^{13-}$ polyhedra.

Back to Table of contents

MS15 Mineralogical and inorganic crystallography

MS15-2-9 Crystal structures of AB_2 pnictogen compounds related to the diamond structure type – An overview #MS15-2-9

N. Langer [1], A. Feige [1], L. Bradaczek [1], O. Oeckler [1]
[1]Institut für Mineralogie, Kristallographie und Materialwissenschaft - Leipzig (Germany)

Abstract
Structures representing coloring variants of cubic or hexagonal diamond or containing cutouts of these follow the Grimm-Sommerfeld or Zintl concepts. Binary pnictides MPn_2 (*Pn* = P, As, Sb) related to diamond are formed by only few cations *M* such as Be, Zn, Cd, Si and Ge. Crystal structures of MPn_2 typically contain tetrahedral coordination spheres and pnictogen polyanions that are part of six-membered rings. Most MPn_2 compounds are semiconductors and theoretical calculations suggest favorable transport properties for thermoelectric or photovoltaic applications.[1–4]
Structures of $BePn_2$ compounds can be derived from cubic diamond by group-subgroup relations. Literature on these compounds seems rather superficial, probably due to experimental and crystallographic complications. BeP_2,[5] $BeAs_2$ and $BeSb_2$ adopt two different structure types. Neglecting stacking disorder, the atom sites of BeP_2 and $BeAs_2$ correspond to a distorted diamond structure with eight-membered pnictogen rings interconnected by Be atoms. The ordered diamond-like structure of $BeSb_2$, which has also been observed for a new polymorph of $BeAs_2$, contains twisted polyanionic chains. Be atoms complete this Sb substructure to produce six-membered rings with chair conformation.
Although for Zn and Cd, the VEC of MPn_2 is 4, these compounds do not form coloring variants of diamond but closely related structures. All atoms are fourfold coordinated with *Pn* forming polyanionic chains. Black ZnP_2 and β-$CdAs_2$ share the $ZnAs_2$ type,[6–8] which contains As helices. These form parts of six- and five-membered rings. Zn atoms complete the rings and interconnect the As helices. One translation period of these helices comprises five atoms. The structure of red ZnP_2 (also adopted by β-CdP_2) is closely related,[6,9] but its P-atom helices exhibit four atoms per translation period. Such helices are also present in orthorhombic α-CdP_2 as well as in α-$CdAs_2$ and the isotypic tetragonal α'-CdP_2.[10–12] Whereas α-CdP_2 is rather similar to β-CdP_2, the tetrahedra in α-$CdAs_2$ are extremely distorted and do not form a dense network.
Whereas GeP_2 and polymorphs of SiP_2 and $SiAs_2$ crystallize in the pyrite type,[13–15] the layered structure of $GeAs_2$ contains motifs of cubic diamond that comprise rows of pairs of chair-like six-membered rings.[16] In these rows, As zigzag chains are integrated. One fragment is connected to two others by six-membered rings in distorted chair or boat conformation, giving rise to the formation of additional five-membered rings. Although the structure does not form a 3D network, all Si atoms are tetrahedrally coordinated by As. The As atoms of the zigzag chains are bound to one additional Ge atom, the other As atoms are coordinated by three Ge atoms. Whereas $SiAs_2$ and one polymorph of SiP_2 adopt the $GeAs_2$ type with space group *Pbam*,[17] there is another closely related polymorph of SiP_2 with *Pnma*.[18]

References
[1] Soshnikov E., Trukhan V., Haliakevich T., Soshnikava H., *Mold. J. Phys. Sci.* **2005**, *4*, 201.
[2] F. Q. Wang, Y. Guo, Q. Wang, Y. Kawazoe, P. Jena, *Chem. Mater.* **2017**, *29*, 9300.
[3] A. Živković, B. Farkaš, V. Uahengo, N. H. de Leeuw, N. Y. Dzade, *J. Phys.: Condens. Matter* **2019**, *31*, 265501.
[4] S. Bai, C.-Y. Niu, W. Yu, Z. Zhu, X. Cai, Y. Jia, *Nanoscale Res. Lett.* **2018**, *13*, 404.
[5] P. L'Haridon, J. David, J. Lang, E. Parthé, *J. Solid State Chem.* **1976**, *19*, 287.
[6] I. E. Zanin, K. B. Aleinikova, M. Y. Antipin, *Crystallogr. Rep.* **2003**, *48*, 199.
[7] Y. A. Ugai, K. B. Aleinkova, T. A. Marshakova, N. S. Rabotkina, *Inorg. Mater.* **1985**, *21*, 650.
[8] M. E. Fleet, *Acta Crystallogr. Sect. B* **1974**, *30*, 122.
[9] J. Horn, *Bull. Acad. Pol. Sci., Ser. Sci. Chim.* **1969**, 69.
[10] O. Olofsson, J. Gullman, *Acta Crystallogr. Sect. B* **1970**, *26*, 1883.
[11] L. Červinka, A. Hrubý, *Acta Crystallogr. Sect. B* **1970**, *26*, 457.
[12] N. Eckstein, I. Krüger, F. Bachhuber, R. Weihrich, J. E. Barquera-Lozada, L. van Wüllen, T. Nilges, *J. Mater. Chem. A* **2015**, *3*, 6484.
[13] J. Osugi, R. Namikawa, Y. Tanaka, *Rev. Phys. Chem. Japan* **1967**, *37*, 81.
[14] T. K. Chattopadhyay, H. G. von Schnering, *Z. Kristallogr.* **1984**, *167*, 1.
[15] P. C. Donohue, W. J. Siemons, J. L. Gillson, *J. Phys. Chem. Solids* **1968**, *29*, 807.
[16] J. H. Bryden, *Acta Crystallogr.* **1962**, *15*, 167.
[17] T. Wadsten, M. Vikan, C. Krohn, Å. Nilsson, H. Theorell, R. Blinc, S. Paušak, L. Ehrenberg, J. Dumanović, *Acta Chem. Scand.* **1967**, *21*, 593.
[18] X. Zhang, S. Wang, H. Ruan, G. Zhang, X. Tao, *Solid State Sci.* **2014**, *37*, 1.

Crystal structures of MPn_2 compounds.[5-18]

Back to Table of contents

MPn_2	Be	Zn	Cd	Si	Ge
P	BeP_2 *I*4$_1$/*amd* (average structure)	black ZnP_2 → $ZnAs_2$ type	α-CdP_2 *Pna*2$_1$	SiP_2 *Pnma*	GeP_2 → pyrite type
		red ZnP_2 P4$_1$2$_1$2	β-CdP_2 → red ZnP_2 type	SiP_2 → $GeAs_2$-type	
			CdP_2 → α-$CdAs_2$ type	SiP_2 → pyrite type	
As	$BeAs_2$ → BeP_2 type	$ZnAs_2$ *P*2$_1$/*c*	α-$CdAs_2$ *I*4$_1$/22	$SiAs_2$ → $GeAs_2$ type	$GeAs_2$ *Pbam*
	$BeAs_2$ → $BeSb_2$ type		β-$CdAs_2$ → $ZnAs_2$ type	$SiAs_2$ → pyrite type	
Sb	$BeSb_2$ *I*4$_1$/*a*	-	-	-	-

Back to Table of contents

MS16 Time-resolved diffraction and scattering techniques

MS16-1-1 Photoinduced charge density wave phase in 1T-TaS2: growth and coarsening mechanisms #MS16-1-1

A. Jarnac [1], V. Jacques [2], L. Cario [3], E. Janod [3], S.L. Johnson [4], S. Ravy [2], C. Laulhé [5]
[1]Synchrotron SOLEIL - Gif-sur-Yvette (France), [2]Université Paris-Saclay, CNRS, Laboratoire de Physique des Solides - Orsay (France), [3]Institut des Matériaux Jean Rouxel, Université de Nantes, CNRS - Nantes (France), [4]Institute for Quantum Electronics, Eidgenossische Technishe Hochschule (ETH) Zürich - Zürich (Switzerland), [5]Université Paris-Saclay, Synchrotron SOLEIL - Gif-sur-Yvette (France)

Abstract
Charge density wave (CDW) states are broken symmetry states of metals arising from electron-phonon interactions, which are characterized by a periodic modulation of both atomic positions and electron density. Diffraction techniques are especially well adapted to studying such compounds, since the structural modulation gives rise to so-called satellite peaks those intensity is proportional to the square of the atomic displacement amplitude.
The CDW states are gapped, which makes those sensitive to excitations with infrared laser pulses. In the two-dimensional tantalum disulfide 1T-TaS_2, we found that an intense laser pulse can induce a phase transition between two distinct CDW states, namely the incommensurate (I) and nearly commensurate (NC) CDW states. A detailed description of the NC → I photoinduced phase transition was achieved using pump-probe X-ray diffraction measurements **[1,2]**. Above the threshold fluence for the NC → I transition, the NC-CDW melts within 400 fs. A broad satellite peak corresponding to the photoinduced I phase (denoted I*) could be detected 2 ps after laser excitation. The analysis of its intensity and width allows identifying a nucleation/growth mechanism of the photoinduced I* phase (**Fig. 1a**). At a pump-probe delay of 100 ps, the photoinduced I* phase has fully developed at sample's surface. However, it is fragmented into several small domains (< 30 nm) corresponding each to a given phase Φ of the I-CDW modulation. The dynamics observed in the 100 - 500 ps pump-probe delay range is dominated by the coarsening of this domain pattern (**Fig. 1b**). The latter result was confirmed by low-energy electron diffraction **[3]**.
It can be further shown that the photoinduced I*-CDW phase differs from the I-CDW phase at equilibrium not only by its limited correlation length, but also by a larger period of the CDW modulation (shorter wave vector of the CDW) **[4]**. We propose that the increased period of the I*-CDW modulation would be due to a smaller number of conduction electrons involved in the collective CDW state, some of them being trapped at CDW-dislocation sites.

References
[1] C. Laulhé, T. Huber et al., Phys. Rev. Lett. 118, 247401 (2017).
[2] G. Lantz, C. Laulhé et al., Phys. Rev. B 96, 224101 (2017).
[3] S. Vogelgesang, G. Storeck et al., Nature Phys. 14, 184-190 (2018).
[4] A. Jarnac, V.L.R. Jacques et al., Comptes Rendus. Physique 22, 139-160 (2021).

Fig.1 - (a) Nucleation/Growth. (b) Coarsening

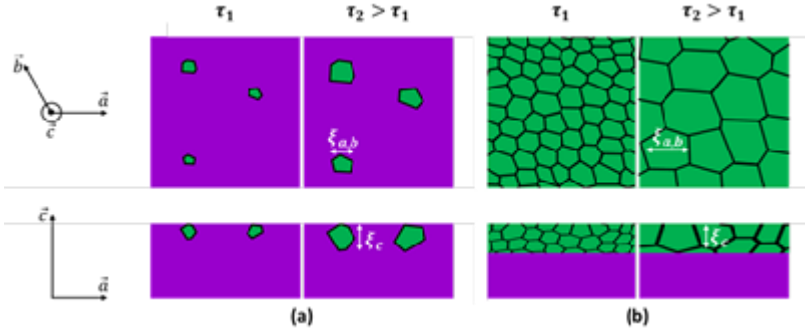

Back to Table of contents

MS16 Time-resolved diffraction and scattering techniques

MS16-1-2 CFEL TapeDrive 2.0: A conveyor belt-based sample delivery system for multi-dimensional serial crystallography
#MS16-1-2

A. Henkel [1], J. Maracke [1], A. Munke [1], M. Galchenkova [1], A. Rahmani Mashhour [1], P. Reinke [1], M. Domaracky [1], H. Fleckenstein [1], J. Hakanpää [2], J. Meyer [2], A. Tolstikova [2], J. Carnis [1], P. Middendorf [1], L. Gelisio [1], O. Yefanov [1], H.N. Chapman [1], D. Oberthür [1]
[1]Center for Free-Electron Laser Science, DESY - Hamburg (Germany), [2]Deutsches Elektronen-Synchrotron DESY - Hamburg (Germany)

Abstract
Serial crystallography (SX) at both X-ray free-electron lasers (XFELs) and synchrotrons offers the possibility to collect data at non-cryogenic temperature almost radiation damage free and enables time-resolved crystallography of irreversible reactions. The necessary steady delivery of new micron-sized crystals of biological macromolecules sets it apart from traditional single crystal macromolecular crystallography (MX). For this, many new means of sample delivery have been developed [1]. Described here is a novel conveyor belt-based sample delivery system, the completely re-designed and re-engineered second generation of the CFEL TapeDrive. It is optimized for fast installation at beamlines, ease of use, low sample consumption and precise adjustment of several sample delivery parameters, like ligand concentration, pH and sample temperature. Through combination of these parameters and the additional possibility for time-resolved experiments (delay times of 50 ms – 180 s), CFEL TapeDrive 2.0 enables multidimensional serial crystallography experiments. It can now be used as standard instrumentation at beamline P11 at PETRA III (DESY, Germany) and is suitable for serial Laue crystallography with polychromatic X-rays. Additionally, it can be used at XFELs in air (e.g. at SwissFEL and LCLS), offering the possibility to combine the advantages of jet-based injection with those of fixed target-based systems. In the future, parts of the system will be automated to achieve rapid ligand screening with micron-sized crystals in various sample environments.
By introducing the CFEL TapeDrive 2.0, a platform for user-friendly multi-dimensional serial crystallography, we provide a novel approach for structural biology to further reveal details about how macromolecules keep our biological world turning.

References
[1] Sierra R.G. et al. (2018) Sample Delivery Techniques for Serial Crystallography. In: Boutet S., Fromme P., Hunter M. (eds) X-ray Free Electron Lasers. Springer, Cham. https://doi.org/10.1007/978-3-030-00551-1_5

Detailed drawing of the CFEL TapeDrive 2.0

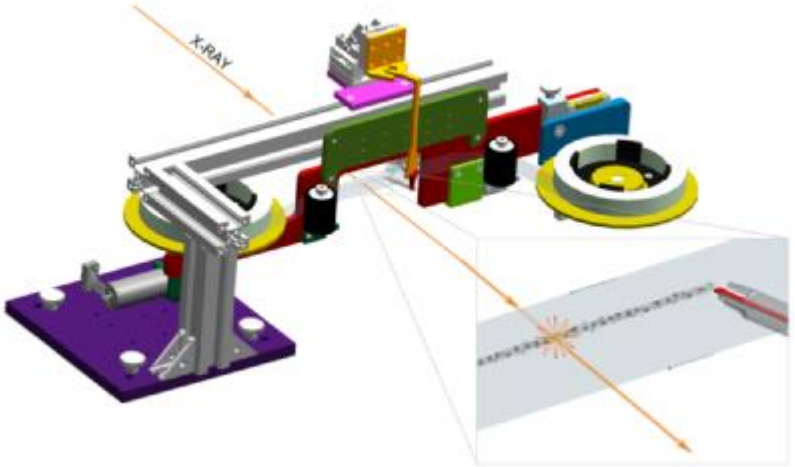

Back to Table of contents

MS16 Time-resolved diffraction and scattering techniques

MS16-1-3 Novel in situ powder neutron diffraction setups – The creation of a modern magnetic compound #MS16-1-3

J.V. Ahlburg [1], F.H. Gjørup [1], T. Kessler [1], R. Smith [2], P. Henry [2], M. Christensen [1]
[1]Department of chemistry, Aarhus University - Aarhus (Denmark), [2]Rutherfor Appleton laboratories, ISIS neutron source - Didcot (United Kingdom)

Abstract
In order to take full advantage of the significantly increased data collection rates expected at the European Spallation Source (ESS), it is paramount that new sample environments are developed to match the performance of the coming instruments. Here, we present two newly developed sample environments for neutron powder diffraction:
1. A single crystal Sapphire Air gun Heater Setup (SAHS), specially designed for solid-gas in situ angular dispersive neutron powder diffraction, has been developed [1] (Fig 1.1 and 1.2). Heating is provided by an air gun heater, allowing the sample to reach temperatures of up to 700 °C within less than 5 minutes. The setup is based on a single crystal sapphire tube, which offers a very low and smooth background. Fig. 1.1-2 shows: Schematic and picture of the SAHS. Gas flows through the system in the following order: A Quick fit connector, B Fused silica tube, C SCS sample container, D Outlet valve. The heater airflow goes through: E Hi-Heater airgun, F heat confinement quartz dome, G Ceramic insulator with air outlet grooves. H Thermocouple.
2. An induction furnace has been developed in a collaboration with: Chalmers University in Sweden, ISIS at the Rutherford Appleton Laboratory in England, the ESS in Sweden and Aarhus University in Denmark (Fig 1.3, 1.4 and 1.5). A fully functioning prototype has been built for the Time of Flight (ToF) diffractometer POLARIS at ISIS and will lead to a second version for the diffractometer/Small Angle Neutron Scattering (SANS) instrument HEIMDAHL at the ESS. The heating is based on an induction element, which allows an extremely fast and efficient way of heating and can reach temperatures of up to 1600 °C in less than 5 minutes. Furthermore, the setup works both in vacuum and under ambient conditions and requires no heat shielding, thus reducing the beam attenuation and lowering the level of background scattering. Fig. 2 shows: 1-2 The induction furnace heat element. 3 The full induction furnace setup.
Both setups offer: high temperatures, fast temperature stability, large sample volumes, and offer a very low attenuation of the beam. The setups have proven to be ideal for carrying out investigations of advanced materials under realistic conditions [2]. The ability to investigate real materials, in real time under realistic conditions, is a huge advantage for scientific investigations as well as for industrial applications.

References
[1] Ahlburg, J. V., et.al., J. Appl. Cryst. (2019), 52, 761-768, [2] Ahlburg. J.V., et.al., Nanoscale, Bind 12, Nr. 17, 2020, s. 9440-9451.

Reduction setup

Back to Table of contents

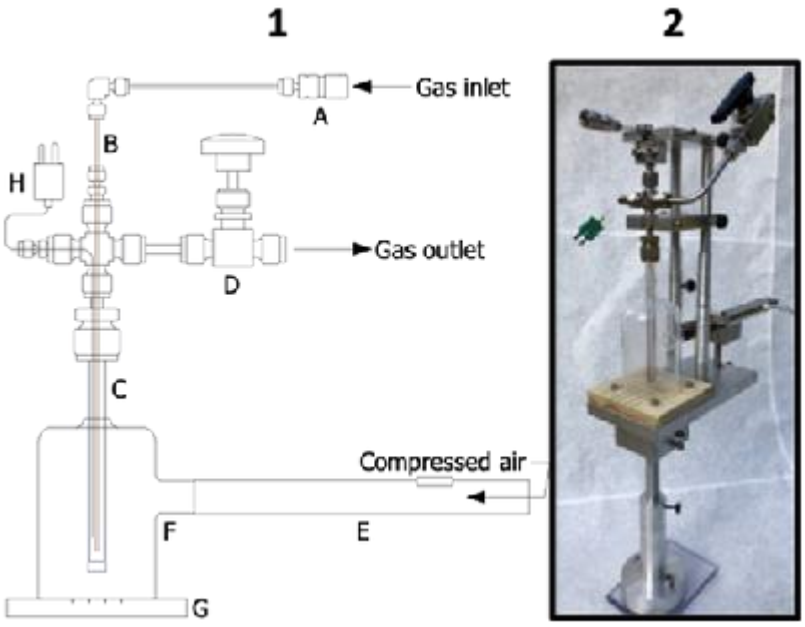

Induction furnace

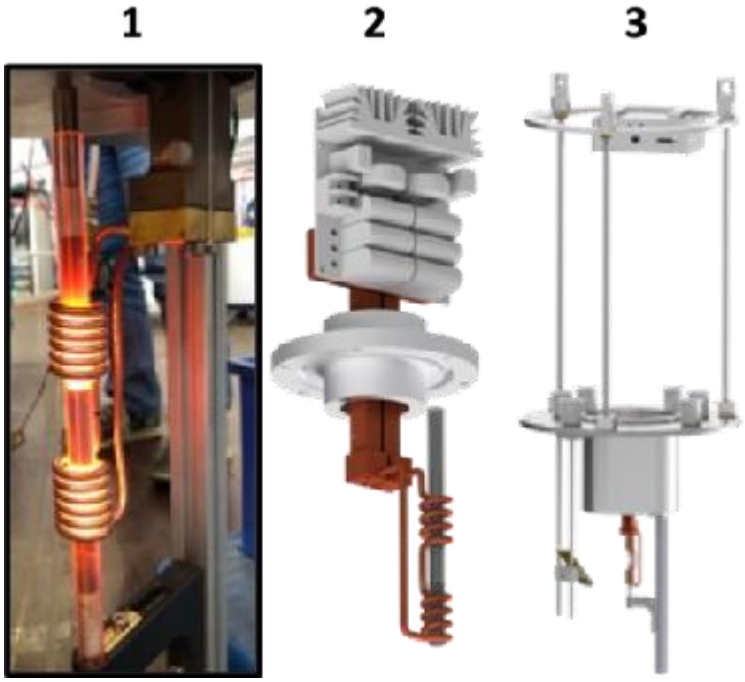

Back to Table of contents

MS16 Time-resolved diffraction and scattering techniques

MS16-1-4 Controlled reactive assembly of colloidal nanocrystal superlattices: mechanism and kinetics #MS16-1-4

D.M. Balazs [1], J. Cimada Da Silva [2], T. Dunbar [2], T. Hanrath [2]
[1]Institute of Science and Technology Austria (ISTA) - Klosterneuburg (Austria), [2]Cornell University (United States)

Abstract
Crystallization through attachment on nanoscale building blocks represents a novel way of creating 'designer materials'. The opportunity to tune the structure, and hence the quality and degree of interaction between the building blocks creates a wide parameter space for tailoring the ensemble-level properties, eventually reaching truly purpose-built materials. Traditionally, bottom-up synthesis meant using nanocrystals as a feedstock for conventional materials processing. The approach of controlled assembly through intermolecular forces, however, seems more promising for the ability to restrict particular degrees of freedom and to shift the energy- and timescales into the soft matter regime.[1] Moreover, working at interfaces of liquids (solvent-solvent or solvent-air), confines the assembly into a plane, enabling the formation of 2D-confined structures.[2]
Assembly and oriented attachment of colloidal quantum dots into a superlattice with long range order both at the atomic and multi-nanometer scale carries the promise of creating novel properties, particularly for semiconductor devices and related applications.[3,4] Additionally, the established reaction mechanism, control approaches and general behavior can be translated into many other systems. The general approach to created ordered lattices has been established, but a knowledge gap persists in our ability to control the assembly and attachment process.[5,6] Filling these knowledge gaps is essential to establish the energetic-kinetic framework of a representative system that can be later generalized.
In this work, we report the results of our efforts to understand and control the formation of superlattices of PbSe colloidal nanocrystals. Using a combination of structural characterization techniques, such as electron microscopy and synchrotron-based X-ray scattering, we describe the process from the introduction of a droplet of a colloidal dispersion through an assembly of nanoparticles at a liquid surface into a correlated superlattice to an epitaxially connected hierarchical system. We describe the physics and chemistry of spreading, drying and reactive assembly, and establish the guidelines for applying the method to other systems.

References
[1] G. M. Whitesides, B. Grzybowski, Science 2002, 295, 2418.
[2] R. Dong, T. Zhang, X. Feng, Chem. Rev. 2018, 118, 6189.
[3] K. Whitham, J. Yang, B. H. Savitzky, L. F. Kourkoutis, F. Wise, T. Hanrath, Nature Materials 2016, 15, 557.
[4] D. M. Balazs, M. A. Loi, Advanced Materials 2018, 30, 1800082.
[5] A. Abelson, C. Qian, T. Salk, Z. Luan, K. Fu, J.-G. Zheng, J. L. Wardini, M. Law, Nat. Mater. 2019, 1. doi:10.1038/s41563-019-0485-2
[6] T. Hanrath, Nat. Mater. 2019, 1. doi:10.1038/s41563-019-0515-0

Back to Table of contents

MS16 Time-resolved diffraction and scattering techniques

MS16-1-5 Amyloid beta 42 fibrils: a small-angle X-ray scattering view of the growth kinetics and its variability #MS16-1-5

S. Da Vela [1], T. Cheremnykh [1], M. Shafiq [2], M. Glatzel [2], D. Svergun [1]
[1]EMBL Hamburg Unit - Hamburg (Germany), [2]Universitätsklinikum Hamburg-Eppendorf - Hamburg (Germany)

Abstract
Aggregation of the peptide amyloid beta 42 (Aβ42) into fibrils is a key event in the pathogenesis of Alzheimer's disease. During this aggregation process, smaller neurotoxic Aβ42 oligomers are formed, which, despite their relevant role in neurodegeneration, are insufficiently characterized [1]. We employed synchrotron time-resolved Small-angle X-ray Scattering (TR-SAXS) to monitor the kinetics of Aβ42 aggregation in solution including structural information. Multiple TR-SAXS datasets spanning several hours of the aggregation process were collected and could be adequately described in terms of a minimal set of coarse-grained structures, revealing the overall features of the oligomers. Moreover, the inherent variability of the process was addressed, and the Aβ42 fibrils present at late stages were compared with those present in the literature [2,3,4].

References
[1] Haass, Christian, and Dennis J. Selkoe. "Soluble protein oligomers in neurodegeneration: lessons from the Alzheimer's amyloid β-peptide." Nature reviews Molecular cell biology 8.2 (2007): 101-112.
[2] Langkilde, Annette E., et al. "The architecture of amyloid-like peptide fibrils revealed by X-ray scattering, diffraction and electron microscopy." Acta Crystallographica Section D: Biological Crystallography 71.4 (2015): 882-895.
[3] Wälti, Marielle Aulikki, et al. "Atomic-resolution structure of a disease-relevant Aβ (1–42) amyloid fibril." Proceedings of the National Academy of Sciences 113.34 (2016): E4976-E4984.
[4] Lattanzi, Veronica, et al. "Amyloid β 42 fibril structure based on small-angle scattering." Proceedings of the National Academy of Sciences 118.48 (2021).

Amyloid growth kinetics monitored by SAXS

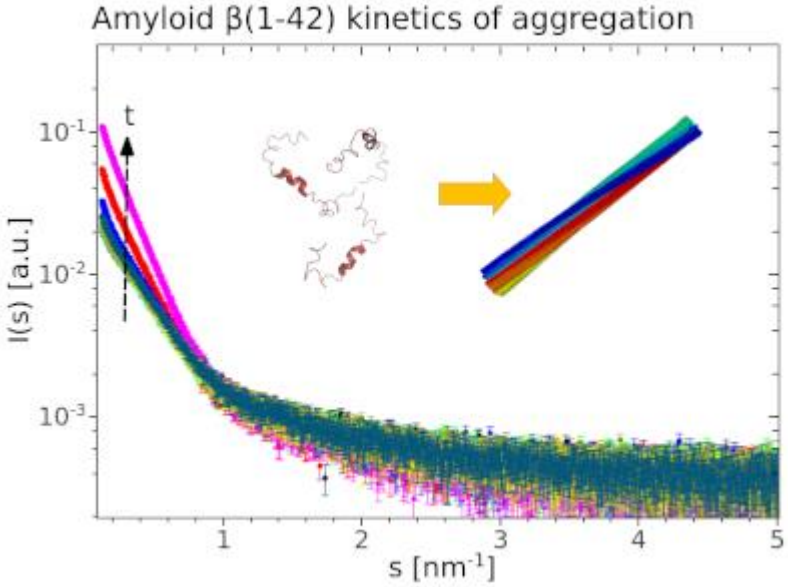

Back to Table of contents

MS16 Time-resolved diffraction and scattering techniques

MS16-1-6 Spin and Charge Density Wave coupling in chromium studied through the Spin-Flip transition: statics and ultrafast dynamics
#MS16-1-6

V.L.R. Jacques [1], C. Laulhé [2], A. Gallo-Frantz [1], D. Ghoneim [1], E. Bellec [3], S. Ravy [1], D. Le Bolloc'h [1]
[1]Laboratoire de physique des Solides - Universite Paris-Saclay/CNRS - Orsay (France), [2]Synchrotron SOLEIL - Gif-sur-Yvette (France), [3]European Synchrotron Radiation Facility - Grenoble (France)

Abstract
Chromium is a very peculiar system in condensed matter, as it develops both a spin-density-wave (SDW) and a charge-density-wave (CDW) despite its 3D cubic structure [1]. They appear concomitantly below the Néel transition temperature TN=311K with a large-period modulation (>50 nm for the SDW) and are found to be linked by a harmonic relationship, the CDW period being half the SDW period. Their orientation is also similar, and as the three <100> directions of the crystal are equivalent, they are found to be oriented along one of them in different domains called Q-domains. The description of the SDW requires going a step further: the magnetic moments are modulated with a linear polarization along the SDW, and their orientation abruptly flips from transverse to longitudinal with respect to the direction of the modulation, at the so-called spin-flip transition (SFT) that takes place at TSF=123K.
Although this description has been known for many years, a question remains concerning the mechanism that accounts for the CDW formation. The origin of the SDW is clearly attributed to a magnetic instability resulting from the pairing of a large number of electron and hole states at the Fermi level, favored by a peculiar Fermi surface geometry that allows good nesting between electron and hole pockets. The origin of the CDW is less clear, and two main scenarii are found in the literature. The first one relies on magnetostritive coupling that would lead to a periodic lattice distortion and hence to a CDW with half the SDW period due to the interaction between the SDW and the lattice [2]. The other scenario involves a second nesting of unnested bands remaining after the SDW formation, that would lead to a CDW instability [3]. Those two scenarii have a fundamental difference: the first one involves the lattice, while the other one only involves electronic states.
In order to clarify the link between SDW, CDW and atomic lattice, we performed several experiments through the SFT. Indeed, at this transition, the magnetic domains merge to form magnetic domains with a single orientation, while the CDW and lattice should be unaffected. We first probed the local structure of SDW, CDW and lattice using coherent x-ray diffraction (CXRD) that is particularly sensitive to local phase defects of these modulations, and show that the CDW 'feels' the SFT, the correlation lengths becoming smaller at the transition [4]. We then use time-resolved x-ray diffraction (TR-XRD) in synchrotron and XFEL, with time resolutions down to 50fs, to probe the apparition dynamics of the CDW after laser excitation that destroys the density waves [5]. After showing that there is a threshold effect for the excitation, we will present a comparison of the CDW dynamics above and below the SFT. We will then discuss the relevance of the different scenarii found in the literature, in the light of our results.

References
[1] E. Fawcett, Spin-density-wave antiferromagnetism in chromium, Rev. Mod. Phys. 60, 209-283 (1988)
[2] W. Cowan, Strain and the spin-flip transition in chromium: Laudau theory, Journal of Physics F: Metal Physics 8, 423 (1978)
[3] Young and Sokoloff, The role of harmonics in the first order antiferromagnetic to paramagnetic transition in order, Journal of Physics F: Metal Physics 4, 1304 (1974)
[4] V.L.R. Jacques et al., Charge- and spin-density waves observed through their spatial fluctuations by coherent and simultaneous x-ray diffraction, Phys. Rev. B 89, 245127 (2014)
[5] V.L.R. Jacques et al, Laser-Induced Charge-Density-Wave Transient Depinning in Chromium,
Phys. Rev. Lett. 117, 156401 (2016)

Back to Table of contents

MS16 Time-resolved diffraction and scattering techniques

MS16-1-7 FemtoMAX – A beamline for ultrafast pump/x-ray probe experiments
#MS16-1-7

J.C. Ekström [1], A. Jurgilaitis [1], D. Kroon [1], V.T. Pham [1], J. Larsson [1]
[1]MAX IV Laboratory - Lund (Sweden)

Abstract
The FemtoMAX beamline[1] is designed for ultrafast pump/x-ray probe experiments with 200 fs time resolution. The beamline is now open for regular user calls. FemtoMAX is driven by the linear accelerator at MAX IV. We will show some of the experiments performed at the FemtoMAX beamline to give a flavour of the experiments that can be performed at the beamline.
Since the end of 2020 the FemtoMAX beamline is operating at a repetition rate of 10 Hz. The x-ray spot size diameter at the sample position has been measured to be 50 µm (FWHM). The two in-vacuum undulators provides x-ray photon energies between 1.8-12 keV and based on the selected energy the number of photons per pulse is ~10^6-10^7, using a multilayer monochromator with 1% bandwidth. An ultrafast laser system delivers ultrashort pump pulses to the sample end station spanning from UV to THz frequencies. The relative timing of the laser and x-ray pulses are measured with an accuracy of < 150 fs using post sorting.
We will show various experiments performed at the FemtoMAX beamline that includes ultrafast studies.

References
[1] H. Enquist, A. Jurgilaitis, A. Jarnac, A. U. J. Bengtsson, M. Burza, F. Curbis, C. Disch, J. C. Ekstrom, M. Harb, L. Isaksson, M. Kotur, D. Kroon, F. Lindau, E. Mansten, J. Nygaard, A. I. H. Persson, V. T. Pham, M. Rissi, S. Thorin, C. M. Tu, E. Wallen, X. C. Wang, S. Werin and J. Larsson, J Synchrotron Radiat 25, 570-579 (2018).

Back to Table of contents

MS16 Time-resolved diffraction and scattering techniques

MS16-2-1 Seed-skewness algorithm paired with instrument model refinement for signal detection in time-resolved Laue photocrystallography
#MS16-2-1

P. Łaski [1], D. Szarejko [1], R. Kamiński [1], K. Jarzembska [2]
[1]Department of Chemistry, University of Warsaw - Warsaw (Poland), [2]Department of Chemistry, University of Warsaw - Warszawa (Poland)

Abstract
An efficient 1-dimensional seed-skewness (SS) algorithm adapted for X-ray diffraction signal detection along with signal integration procedure is presented. The method performs well for both the standard single-crystal X-ray diffraction data, as well as for time-resolved (TR) Laue photocrystallographic data collected at the Advanced Photon Source and European Synchrotron Radiation Facility. It enables efficient separation of signal from the background in single 1-dimentional data vectors, it is capable of determining small changes of reflection shapes and intensities resulting from exposure of the sample to laser light, and it is especially attractive for extracting relatively weak reflections from the background. The last is possible through the adjustment of “trust level” and “signal level” parameters in the algorithm.Performance of the algorithm is compared with the already reported Kruskal-Wallis test method[1]. Both methods perform competitively in terms of speed and determining the intensity of strong reflections, while the parameterization of the SS method allows for more efficient tuning of the algorithm to improve its sensitivity towards weak reflections.Furthermore, a novel instrument model refinement approach which allows to obtain precise detection parameters, such as detector distance and X-ray beam centre is presented. It is shown that relatively small adjustments in these parameters can significantly improve orientation-matrix matching procedures used during TR Laue data processing.Finally, a series of TR Laue experiments was carried out on selected model small molecule complexes, and the resulting data was processed with the use of the novel algorithm. The obtained results are presented and discussed.

References
[1] J. A. Kalinowski, et al., J. Synchrotron Rad. 2012, 19, 637.

Back to Table of contents

MS16 Time-resolved diffraction and scattering techniques

MS16-2-2 Dynamic XRD measurements with new features of the EIGER2 detector
#MS16-2-2

D. Sisak Jung [1], M. Burian [1]
[1]DECTRIS - Baden (Switzerland)

Abstract
Over the last two decades, the dynamic nature of synchrotron experiments was manifested in three ways: (i) increasing the temporal resolution of classical PXRD experiments without compromising data quality, (ii) further development of scanning techniques, such as ptychography, coherent diffractive imaging, and XRD computed tomography, and (iii) performing time-resolved scanning techniques. Such dynamic measurements typically require a large amount of data to be collected in a short time. Consequently, the ideal experimental setup would include a detector with a very large sensor area, high frame rate, negligible readout time, high efficiency and the ability to discern very weak and very strong signals. Over the last several years, EIGER2 detectors were extensively used for such dynamic measurements. However, the large sensor area and high frame rates were sometimes mutually exclusive. In 2022, the new features of EIGER2 detectors allowed for an even more flexible optimization between detector area and speed, and with this enabled new, interesting dynamic experiments.
The first part of this work will address the newly released features that enable faster and cleaner data collection: 8-bit readout mode, lines ROI region-of-interest mode, and double-gating mode. In the second part, we will demonstrate how these features were put to use for various X-ray applications: fast scanning modes for high-resolution PXRD studies [1], increased scan speed for low-dose ptychography [2], sub-millisecond time-resolved PXRD [3], suppression of higher harmonics and cosmics, and shot-to-shot background correction in pump-probe-type experiments. The highlighted experiments cover proof-of principle and scientific studies, and they are carried out as collaborative projects at several synchrotron sources: ESRF (Grenoble, France), BSRF (Bejing, China), Elettra (Trieste, Italy) and the Australian synchrotron (Melbourne, Australia).

References
[1] Fitch, A., Dejoie, C. (2021) J. Appl. Cryst. 54, 1088-1099.
[2] Jones, M.W.M. et al. (2021) J. Syn. Rad. 29(2).
[3] Zhang, D. et al. (2022) Rev. Sci. Instrum. 93, 033902

Back to Table of contents

MS17 Total scattering studies and disorder

MS17-1-1 Structure and morphology of C-S-H-based hardening accelerator nanoparticles by X-ray total scattering techniques
#MS17-1-1

G. Dal Sasso [1], M.C. Dalconi [2], G. Ferrari [3], J.S. Pedersen [4], S. Tamburini [5], F. Bertolotti [6], A. Guagliardi [7], M. Bruno [8], L. Valentini [2], G. Artioli [2]
[1]Institute of Geosciences and Earth Resources, National Research Council of Italy - Padova (Italy), [2]Department of Geosciences and CIRCe Centre, University of Padova - Padova (Italy), [3]MAPEI Spa, R&D Laboratory - Milan (Italy), [4]Department of Chemistry and Interdisciplinary Nanoscience Center (iNANO), Aarhus University - Aarhus (Denmark), [5]nstitute of Condensed Matter Chemistry and Technologies for Energy, National Research Council of Italy - Padova (Italy), [6]Department of Science and High Technology and To.Sca.Lab, University of Insubria - Como (Italy), [7]Institute of Crystallography and To.Sca.Lab, National Research Council of Italy, - Como (Italy), [8]Department of Earth Sciences, University of Turin - Turin (Italy)

Abstract
Calcium silicate hydrate (C-S-H) is the main binding phase in Portland cement. The addition of C-S-H nanoparticles as nucleation seeds has successfully been used to accelerate the hydration process and the precipitation of binding phases either in conventional Portland cement or in alternative binders. Indeed, the modulation of the hydration kinetics during the early-stage dissolution-precipitation reactions, by acting on the nucleation and growth of binding phases, improves the early strength development. The fine-tuning of concrete properties in terms of compressive strength and durability by designed structural modifications can be achieved through the detailed description of the reaction products at the atomic scale. The nano-sized, chemically complex and structurally disordered nature of these phases hamper their thorough structural characterization. To this aim, we implement a novel multi-scale approach by combining forefront small-angle X-ray scattering (SAXS) and synchrotron wide-angle X-ray total scattering (WAXTS) analyses for the characterization of Cu-doped C-S-H nanoparticles dispersed in a colloidal suspension, used as hardening accelerator. SAXS and WAXTS data were analysed under a unified modelling approach by developing suitable atomistic models for C-S-H nanoparticles to be used to simulate the experimental X-ray scattering pattern through the Debye scattering equation [1]. The optimization of atomistic models against the experimental pattern, together with complementary information on the structural local order from ^{29}Si solid-state nuclear magnetic resonance and X-ray absorption spectroscopy, provided a comprehensive description of the structure, size and morphology of C-S-H nanoparticles from the atomic to the nanometre scale. C-S-H nanoparticles were modelled as an assembly of layers composed of 7-fold coordinated Ca atoms and decorated by silicate dimers and chains. The structural layers are a few tens of nanometres in length and width, with a crystal structure resembling that of a defective tobermorite, but lacking any ordering between stacking layers [2].

References
[1] A. Cervellino, R. Frison, F. Bertolotti, A. Guagliardi, DEBUSSY 2.0 : the new release of a Debye user system for nanocrystalline and/or disordered materials, J. Appl. Crystallogr. 48 (2015) 2026–2032. doi:10.1107/S1600576715020488.
[2] G. Dal Sasso, M.C. Dalconi, G. Ferrari, J.S. Pedersen, S. Tamburini, F. Bertolotti, A. Guagliardi, M. Bruno, L. Valentini, G. Artioli, An Atomistic Model Describing the Structure and Morphology of Cu-Doped C-S-H Hardening Accelerator Nanoparticles, Nanomaterials. 12 (2022) 342. doi:10.3390/nano12030342.

Back to Table of contents

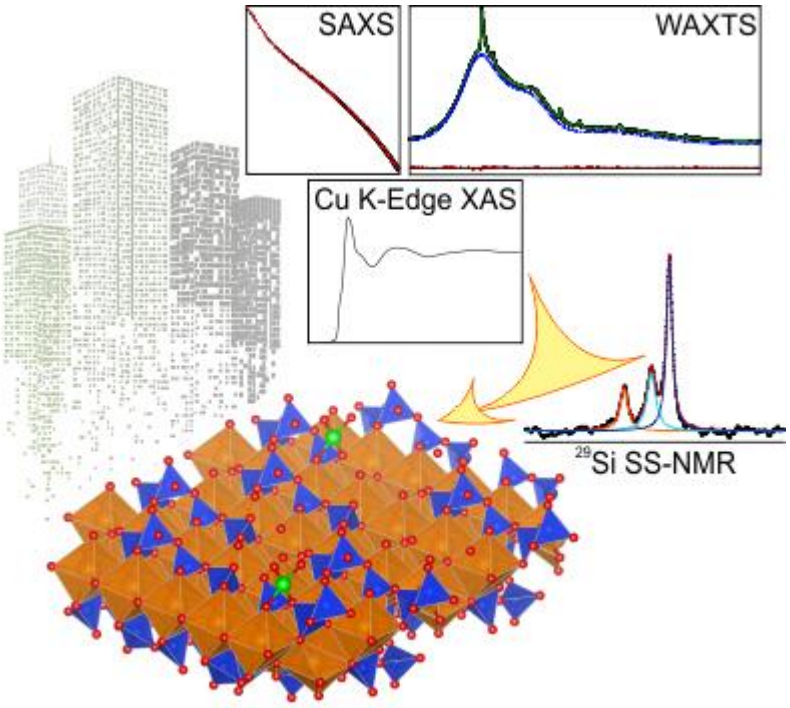

Back to Table of contents

MS17 Total scattering studies and disorder

MS17-1-2 Structural study of metallic nanoparticles: two challenging cases
#MS17-1-2

P. Lecante [1]
[1]CEMES/CNRS - Toulouse (France)

Abstract
From a structural point of view, two very different classes of materials are still challenging for conventional X-ray and electron based techniques. Very small size objects obviously fall below the current limits of XRD and are even challenging for TEM studies, not only because of their small size (typically less than 2 nm) but also of their reduced phase contrast, related to a less compact structure [1, 3, 6].
Surprisingly, much bigger objects are also challenging and sometimes classified as amorphous despite a purely metallic very strong local order.For these two classes, spontaneous or radiation induced metastability can make structural studies even more tricky [2, 4-5] and these materials often remain non described, despite their potentially important magnetic or catalytic properties. PDF analysis can still bring insights in such conditions, however a complete and accurate description is still unachieved. Different published case studies based on in-lab measurements will be presented.

References
[1] M. Respaud., J.-M. Broto, H. Rakoto, A.-R. Fert & al., Phys. Rev. B, 1998, 57, 2925-2935.
[2] C. Desvaux, C. Amiens, P. Fejes & al., Nat. Mater., 2005, 4, 750-753.
[3] L.-M. Lacroix, S. Lachaize, A. Falqui & al., J. Appl. Phys., 2008, 103, 1-3.
[4] N. Liakakos, B. Cormary, X.-J. Li, P. Lecante & al., J. Am. Chem. Soc., 2012, 134, 17922-17931.
[5] J. G. Mattei, F. Pelletier, D. Ciuculescu, P. Lecante & al., J. Phys. Chem. C, 2013, 117, 1477-1484.
[6] B. Morcos, P. Lecante, R. Morel, P.-H. Haumesser, C. Santini, LANGMUIR, 2018, 34, 7086-7095.

Back to Table of contents

MS17 Total scattering studies and disorder

MS17-1-4 Elucidating the local structure of poorly crystalline and amorphous carbon nitride materials using energy-filtered electron radial distribution function analysis and low electron dose HRTEM
#MS17-1-4

N. Tarakina [1], D. Piankova [1], A. Tyutyunnik [2], H. Zschiesche [1], M. Antonietti [1]
[1]Max Planck Institute of Colloids and Interfaces - Potsdam (Germany), [2]Institute of Solid State Chemistry - Ekaterinburg (Russian Federation)

Abstract
Understanding the structure of carbon nitrides is a long-standing challenge, since many of them are complex, often poorly crystalline or even amorphous materials, which are usually difficult to characterize by standard diffraction methods. Still, detailed knowledge about their structure (especially local ordering) is key to control properties of existing carbon nitrides and design new compounds. In this respect, electron radial distribution function (eRDF) analysis is becoming more and more attractive as a fast, easy accessible tool to quantitatively describe and compare the local structure of materials. The eRDF is usually obtained from electron total scattering data, which can be collected on any standard transmission electron microscope within a few seconds making this technique easily accessible to a lot of users. The zero-loss-energy filtering method that we applied allows mainly elastically scattered electrons to contribute to the diffraction signal, improving the signal-to-noise ratio about 5 times and thus allowing to obtain reliable energy-filtered eRDFs even from amorphous materials. Here, I present the application of energy-filtered electron radial distribution function (EF-eRDF) analysis, combined with low-dose transmission electron microscopy imaging and X-ray powder diffraction, to study several members of the carbon nitride family (from poorly crystalline poly(heptazine imide) salts (M-PHI, M=K, Na, Mg) to amorphous nitrogen doped carbons (a-CN)).
Starting structural models of M-PHI (M=K, Na, Mg) salts were created based on HRTEM data and a general assumption about the structure. A stacking of polyheptazine imide layers on top of each other with M atoms placed within and in between the layers allows the formation of channels along the c-direction. However, problems with determining the exact metal positions, as well as particular anisotropic broadening of the peaks, clearly pointed to the presence of defects in the systems. A detailed analysis of the eRDFs showed that the average coherence length (ACL) of M-PHI (M=K, Na, Mg) salts is about 5 nm. Peak positions in the eRDFs coincide with the models obtained from XRD Rietveld refinement only up to 4.2 Å. As found by Reverse Monte Carlo refinement of the eRDFs and HRTEM image analysis, the layers are not stacked perfectly but display 2-8 degrees of rotational disorder and also partial disorder of the polyheptazine backbone within the layer. The presence of this disorder without breaking the main channel structure of M-PHI, promotes their high catalytic activity. One can see the striking difference in the ACL of M-PHIs compared to a-CN, for which it is around 7 Å, indicating that only short-range order up to the 3rd coordination sphere is present in the amorphous CN covalent framework. The main C-N and C-C peak positions are common for both M-PHI and a-CN up to 4.5 Å, but in the case of a-CN, the peaks are broader. The limited size of the ordered regions in a-CN facilitates their high sorption capabilities.
The authors acknowledge support by the Max Planck Society. We are grateful to Dr. I. Teixeira, Dr. A. Savateev and Dr. J. Kossmann for their support with photocatalytic and CO2 sorption characterization

Back to Table of contents

MS17 Total scattering studies and disorder

MS17-2-1 Tuning electronic and phonon bands through disorder
#MS17-2-1

N. Roth [1], A.L. Goodwin [1]
[1]Inorganic Chemistry Laboratory, University of Oxford - Oxford (United Kingdom)

Abstract
Disorder in crystals is often far from random, and in some cases the local correlations of disorder can be tuned. The tuning of disorder allows a new handle to tune properties. By using simple models for electronic interactions and force constants, it is shown how crystals with identical average crystal structures, but different types of correlated disorder, can have different electronic and phonon band structures. It is further shown that by changing the type of disorder from random to correlated, it is possible to open band gaps, allowing for drastic changes to electronic properties. Single-crystal diffuse x-ray scattering is used as an effective way to distinguish between different types of local correlations, and the diffuse scattering is related to the changes to the band structures.

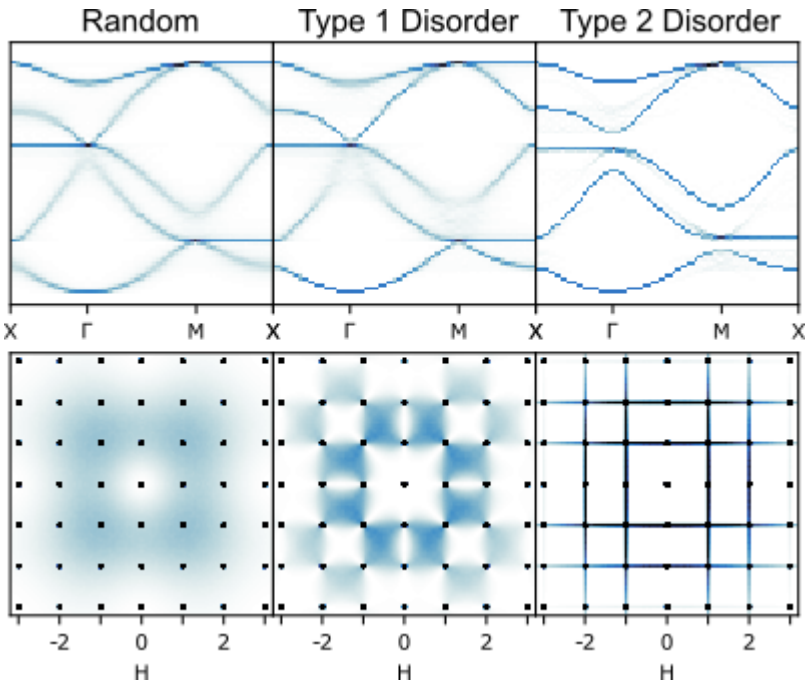

Back to Table of contents

MS17 Total scattering studies and disorder

MS17-2-2 Quantitative analysis of diffuse electron scattering in the lithium-ion battery cathode material $Li_{1.2}Ni_{0.13}Mn_{0.54}Co_{0.13}O_2$
#MS17-2-2

R. Poppe [1], D. Vandemeulebroucke [1], R.B. Neder [2], J. Hadermann [1]
[1]University of Antwerp - Antwerp (Belgium), [2]Friedrich-Alexander-Universität Erlangen-Nürnberg - Erlangen (Germany)

Abstract
Materials with short-range order produce diffraction patterns that contain both Bragg reflections and diffuse scattering. The average crystal structure can be determined from analysis of the Bragg reflections. To obtain information about the short-range order, it is necessary to analyse the diffuse scattering.
Our study shows, for the first time, a refinement of short-range order parameters from the diffuse scattering in single-crystal electron diffraction data. The approach was demonstrated on the lithium-ion battery cathode material $Li_{1.2}Ni_{0.13}Mn_{0.54}Co_{0.13}O_2$, for which the crystals are too small to be investigated with single-crystal X-ray or single-crystal neutron diffraction. Both the amount of stacking faults and the percentage of the different twins in the crystal were refined from the intensity distribution of the diffuse streaks using a differential evolutionary algorithm in DISCUS [1].
The approach was applied on reciprocal space sections reconstructed from three-dimensional electron diffraction (3D ED) data (Figure 1) since they exhibited less dynamical effects compared to in-zone precession electron diffraction (PED) patterns. The effect of dynamical scattering and thermal diffuse scattering on the intensity distribution of the diffuse streaks will also be discussed.

References
[1] Proffen, T., & Neder, R. B. (1997). J. Appl. Crystallogr. 30, 171-175.

Figure caption (the box below is too small): [-210] reciprocal space section (a) reconstructed from three-dimensional electron diffraction (3D ED) data, (b) calculated for the refined short-range order parameters.

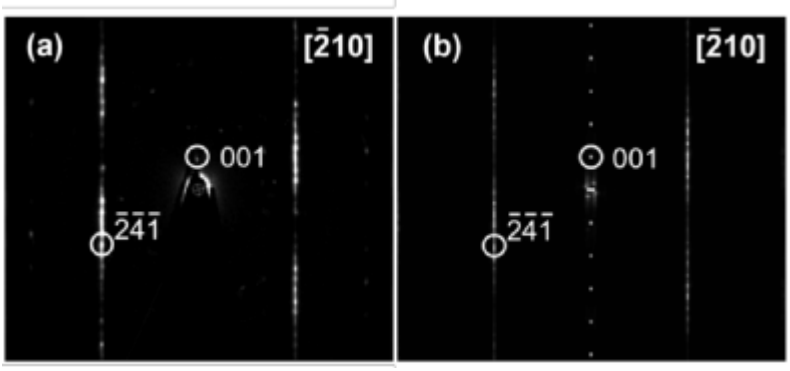

Back to Table of contents

MS17 Total scattering studies and disorder

MS17-2-3 Cross-shaped diffuse scattering in K2Cu3Te4O12 and Na2Cu3Te4O12
#MS17-2-3

F. Eder [1], M. Weil [1], B. Stöger [1]
[1]TU Wien - Wien (Austria)

Abstract
$K_2Cu_3Te_4O_{12}$ and $Na_2Cu_3Te_4O_{12}$ were obtained in solid state reactions with water as a mineralizer. Both crystal structures can be derived from a tetragonal family structure ($P4/ncc$; a_0 = 8.426(9) Å, c_0 = 6.403(6) Å ($K_2Cu_3Te_4O_{12}$) and a_0 = 8.298(2) Å, c_0 = 6.1633(12) Å ($Na_2Cu_3Te_4O_{12}$)) with positional disorder of Te and K/Na around the same crystallographic site, and of the O atoms. In the diffraction patterns of $K_2/Na_2Cu_3Te_4O_{12}$, diffuse streaks in two perpendicular directions resulting in cross-like shapes on the $l = n + ⅓$ and $l = n + ⅔$ ($n \in \mathbb{Z}$) planes are observed (Figure 1). Even though the family structures of $K_2Cu_3Te_4O_{12}$ and $Na_2Cu_3Te_4O_{12}$ are isotypic, the orientation of the streaks is different: In $K_2Cu_3Te_4O_{12}$ they are parallel to $[100]$, in $Na_2Cu_3Te_4O_{12}$ parallel to $[110]$ with respect to the family structure.
The crystal structure of $K_2Cu_3Te_4O_{12}$ is built from ordered $^1_\infty[K_2Te_4O_{12}]$-rods with the sequence […K-Te-Te-K-Te-Te…] oriented along $[001]$, which are connected by the Cu atoms. These rods have a translational period c_{rod} of $3c_0$ and the rod group $P2/c11$. The $^1_\infty[K_2Te_4O_{12}]$-rods have two possible orientations, which differ by a rotation of 90° around $[001]$ (Figure 2; K/Te at different z values are drawn lighter/darker).
The cross-shaped diffuse scattering can be explained by dividing the structure into two substructures, each consisting of all rods with the same orientation, which are disordered independently from each other. For each substructure, the disorder can be modelled by a variable stacking of layers oriented in (100) or (010). The rods of an adjacent layer are translated by ±⅙ c_{rod} or +½ c_{rod}, though the +½ contact is not realized since it would lead to a K⋯K distance of only 3.301(9) Å. The ±⅙ layer pairs are symmetrically equivalent and therefore the stacking can be described by order-disorder (OD) theory [1]. One of the two maximum degree of order (MDO) polytypes [2] (consisting of only either +⅙ or -⅙ contacts; space group $P\bar{1}$, $a = a_0$, $b = 3b_0$, $c=3c_0$) is in accordance with the characteristic reflections, making it the preferred stacking.
For $Na_2Cu_3Te_4O_{12}$, the situation is more complicated. The smaller size of the Na atoms allows +½ c_{rod} contacts as well. It is not possible to use OD-theory for modelling because not all pairs of layers are equivalent. For both structures the disordered stacking of layers is modelled using DIFFAX [3] and is compared with precession images of the single crystal diffraction studies.

References
[1] Dornberger-Schiff, K., Grell-Niemann, H. On the Theory of Order-Disorder (OD) Structures. *Acta Crystallogr*. **14**, 167–177 (1961).
[2] Dornberger-Schiff, K., Grell, H. Geometrical Properties of MDO Polytypes and Procedures for Their Derivation. II. OD Families Containing OD Layers of M > 1 Kinds and Their MDO Polytypes. *Acta Crystallogr*. **A38**, 491–498 (1982).
[3] Treacy, M. M. J., Newsam, J. M., Deem, M. W. A General Recursion Method for Calculating Diffracted Intensities From Crystals Containing Planar Faults. *Proc. Roy. Soc. Lond*. **A433**, 499–520 (1991).

(hk⅓)* plane of K2(left)/Na2(right)Cu3Te4O12

Back to Table of contents

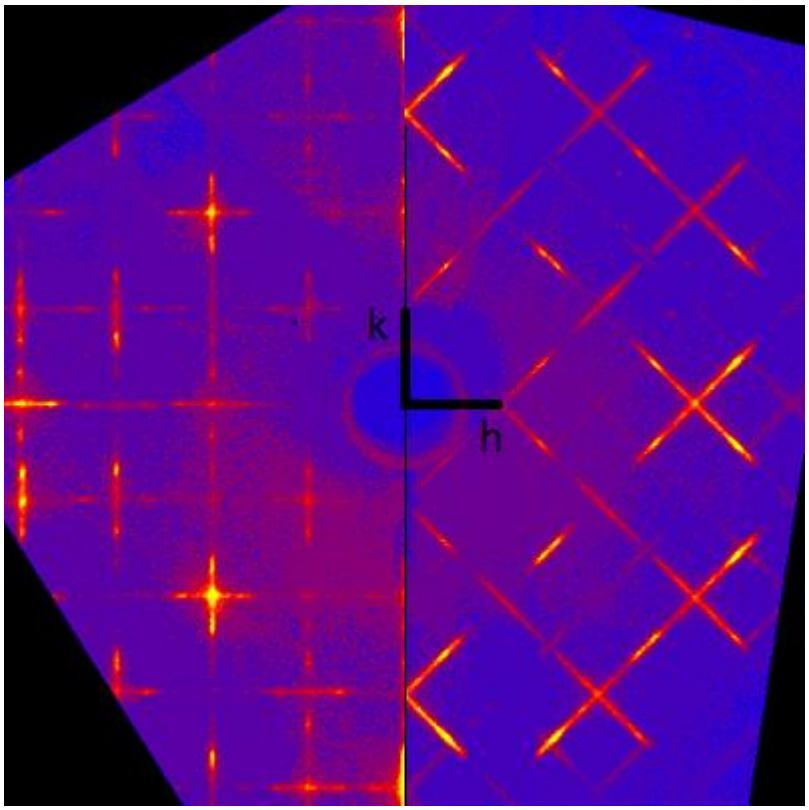

Simplified family structure of K2Cu3Te4O12

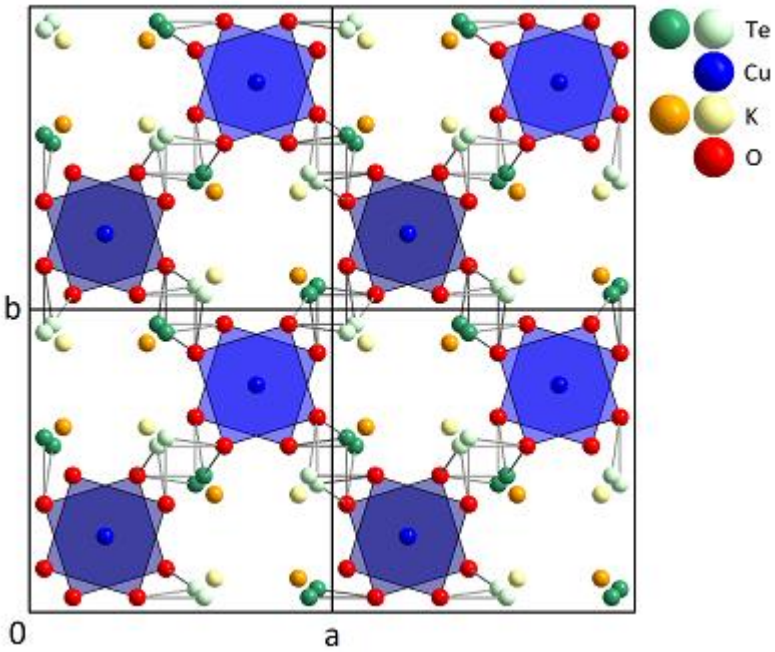

Back to Table of contents

MS17 Total scattering studies and disorder

MS17-2-4 Ordered and disordered structural variety in supposedly simple beryllium arsenide and beryllium phosphide
#MS17-2-4

L. Bradaczek [1], A. Feige [1], M. Michak [1], D. Günther [1], C. Benndorf [1], C. Giacobbe [2], E. Lawrence Bright [2], C. Paulmann [3], B. Stöger [4], O. Oeckler [1]
[1]Institute for Mineralogy, Crystallography and Materials Science - Leipzig (Germany), [2]European Synchrotron Radiation Facility - Grenoble (France), [3]Deutsches Elektronen-Synchrotron - Hamburg (Germany), [4]X-Ray Centre TU Wien - Vienna (Austria)

Abstract
A broad range of AB_2-type crystal structures containing main-group element anions in combination with divalent cations has been characterized for more than 100 years. Thus, one would expect that the crystal structure of $BeAs_2$ is well known.[1] However, pronounced stacking disorder, polymorphism and microcrystallinity have impeded structure elucidation for decades. Microfocused synchrotron radiation in combination with electron microscopy now allowed us to understand the structural variety of $BeAs_2$ including diffraction phenomena such as twinning and diffuse scattering.
The structural variety of $BeAs_2$ can be described and understood recognizing its relation to the diamond structure, considering group-subgroup relations. All polymorphs derive from an average structure model in space group $I4_1/amd$. Different possibilities of atomic ordering lead to two hettotypes. In comparison with the diamond structure, structures with significantly higher complexity are expected due to partially ionic interactions between beryllium and arsenic next to covalent As–As bonding. In $BeAs_2$, every beryllium atom is coordinated by four arsenic atoms whilst the coordination sphere of the arsenic atoms comprises two beryllium and two arsenic atoms, creating a diamond-like framework. The formation of arsenic rings or chains is in accordance with the 8–N rule and the Zintl concept. Two completely different polymorphs were found in the product of the same synthesis.
The structural motif of the first polymorph is an As_8 ring. These rings are arranged in long-range ordered layers while showing characteristic stacking disorder. This can be described in a classical way based on *OD* theory. Hypothetical long-range order, i.e. a *MDO* polytype, which is observed only in domains, corresponds to an ordered structure model in space group $C2/c$. The layers with As_8 rings feature a higher layer symmetry in comparison with the whole structure. Thus, there are energetically equivalent stacking variants that lead to disorder based on varying interconnection of the As_8 rings by Be atoms. A complex disorder model was developed to simulate sections through reciprocal space with diffuse streaks that can be compared to experimental data.[2] Crystallites exhibit different degrees of disorder which can be approximately quantified. In addition to this disorder, which leads to twin boundaries and various hypothetical polytypes, further twinning effects need to be considered in “single” crystals. These correspond to the symmetry reduction from the cubic diamond type to the tetragonal average structure. The average degree of disorder in a specific sample has been evaluated from powder diffraction data by comparing them to simulated ones. The domain structure as well as the local structure of e.g. twin boundaries have been investigated by HRTEM, which confirms that the results of X-ray diffraction can deliver valuable information for simulations. The structural features of this first polymorph are also present in BeP_2, which has been investigated in the same way.[3]
The second polymorph of $BeAs_2$ has a completely ordered crystal structure governed by chain-like As polyanions. They form a complex ordered arrangement in space group $I4_1/a$ containing twisted As chains that are separated by beryllium atoms to form a coloring variant of the diamond structure.

References
[1] R. Gerardin, J. Aubry, *J. Solid State Chem.* **1976**, *17*, 239.
[2] M. M. J. Treacy, J. M. Newsam, M. W. Deem, *Proc. Roy. Soc. Lond. A* **1991**, *433*, 499.
[3] J. F. Brice, R. Gérardin, M. Zanne, *Mater. Res. Bull.* **1975**, *10*, 1237.

Back to Table of contents

MS17 Total scattering studies and disorder

MS17-2-5 Probing hidden order in ferroelectric oxide thin films with single crystal diffuse X-ray scattering #MS17-2-5

J. Bang [1], N. Strkalj [2], M. Sarott [1], M. Trassin [1], T. Weber [1]
[1]ETH Zurich - Zurich (Switzerland), [2]Cambridge University - Cambridge (United Kingdom)

Abstract
Ferroelectric thin films have attracted great attention for its rich applications in energy-efficient electronic devices because of their relevant physical properties such as high dielectric constants, electrically switchable polarization, and high piezoelectric coefficients[1]. In fact, the growing demand for miniaturized microelectronics has inspired diverse research efforts towards the engineering of ferroelectric properties and domain architectures in the ultrathin regime[2]. Thus, comprehending the structural and electrical properties of ferroelectric thin films on the nanoscale became crucial. Recently, a lot of effort has been put into studying ferroelectric oxide superlattices with complex topologies such as long-range vortex-antivortex arrays of polarization[3]. These works have called for an in-depth structural investigation of the superlattice structures, since the orientation and arrangement of ferroelectric domains define the macroscopic ferroelectric properties in ferroelectric thin films. Here, we report on a newly discovered local order state in superlattices consisting of ferroelectric lead titanate and dielectric strontium titanate using a complete three-dimensional diffuse X-ray scattering data analyzed with 3D-deltaPDF method[4]. The data was collected with single crystal diffuse X-ray scattering technique, which, to the best of our knowledge, was used for the first time to study local order in single crystalline thin films. This work will not only contribute to gaining useful insights on structure-property correlations of ferroelectric oxide superlattices, but also lay groundwork for developing a novel non-disruptive solid-state characterization technique for analyzing local structures of thin films.

References
[1] Setter, N., et al. "Ferroelectric thin films: Review of materials, properties, and applications." Journal of applied physics 100.5 (2006): 051606
[2] Fong, Dillon D., et al. "Ferroelectricity in ultrathin perovskite films." Science 304.5677 (2004): 1650-1653; Kornev, Igor A., et al. "Ferroelectricity of perovskites under pressure." Physical review letters 95.19 (2005): 196804; Schlom, Darrell G., et al. "Strain tuning of ferroelectric thin films." Annu. Rev. Mater. Res. 37 (2007): 589-626.
[3] Yadav, A. K., et al. "Observation of polar vortices in oxide superlattices." Nature 530.7589 (2016): 198-201; Damodaran, Anoop R., et al. "Phase coexistence and electric-field control of toroidal order in oxide superlattices." Nature materials 16.10 (2017): 1003-1009; Das, S., et al. "Observation of room-temperature polar skyrmions." Nature 568.7752 (2019): 368-372.
[4] Weber, Thomas, and Arkadiy Simonov. "The three-dimensional pair distribution function analysis of disordered single crystals: basic concepts." (2012): 238-247.

Out-of-plane reciprocal space reconstruction

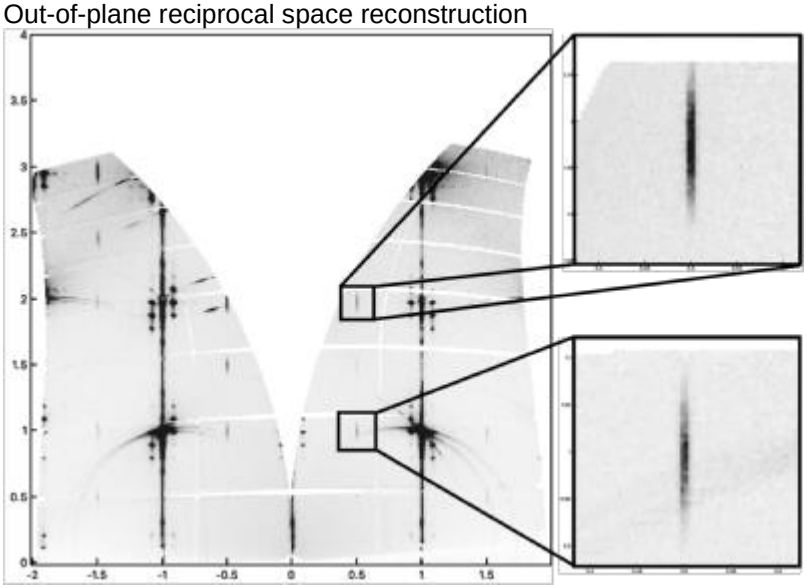

Back to Table of contents

In-plane reciprocal space reconstruction

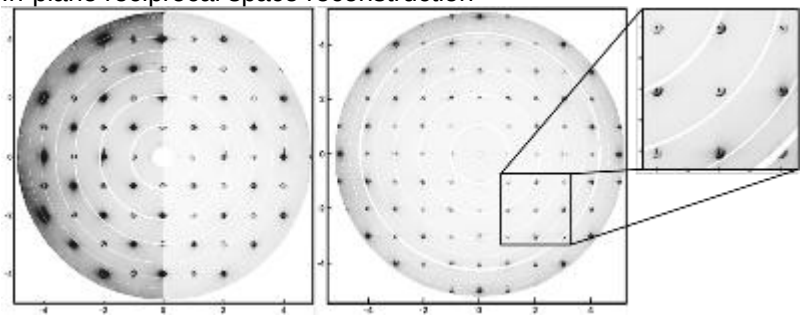

Back to Table of contents

MS17 Total scattering studies and disorder

MS17-2-6 Tuning local structure in Prussian Blue Analogues (PBAs)
#MS17-2-6

Y. Kholina [1], A. Simonov [1]
[1]ETH Zurich - Zurich (Switzerland)

Abstract
Frontier research seeks to control the local structure of disordered crystals to optimize their functional properties. We apply this approach to the Prussian Blue Analogue (PBA) system with the chemical formula Mn[Co(CN)6]2/3*xH2O, which we abbreviate as Mn[Co]. The structure of this material contains 33% of Co(CN)6 vacancies. These vacancies create a highly connected porous network, making PBAs attractive for hydrogen storage applications. It was theoretically shown that the connectivity and the accessible volume of such a network depend on vacancy distribution [1]. Therefore, to optimize mass transport properties, we need to grow material with a particular local structure. In this work, we show how to tune the local structure of PBA crystals grown in gel by varying the crystallization parameters: type of gel, crystallization temperature, the concentration of reactants, and concentration of chelating agents. We probe defect distribution by measuring the single crystal x-ray diffuse scattering, which allows quantitative characterization of local structure. All above-mentioned parameters allow smooth continuous control of diffuse scattering and thus of local order in Mn[Co] PBA crystals.

Back to Table of contents

MS17 Total scattering studies and disorder

MS17-2-7 Nano Materials Analysis by Combination of PDF und (U)SAXS
#MS17-2-7

L. Maze [1], D. Beckers [2], V. Kogan [2], A. Kharchenko [2], M. Gateshki [2]
[1]Malvern Panalytical - 91120 (France), [2]Malvern Panalytical - Almelo (Netherlands)

Abstract
X-ray powder diffraction is one of the most important techniques for material analysis with applications in areas ranging from pharmaceuticals to mining and from semiconductors to building materials. Each material presents its own challenges, and this creates a constant demand for improved data quality and shorter measurement times. Despite its long history, instrumentation for laboratory X-ray diffraction is in continuous development and recent years have marked significant progress in practically every component involved in the X-ray diffraction experiments.
The highly versatile Empyrean instrument enables a variety of X-ray scattering techniques for the structural and dimensional characterization of matter on multiple length scales. The Empyrean makes accessible on laboratory high-performance ultra-small-angle X-ray scattering (USAXS), small- and wide-angle X-ray scattering (SAXS/WAXS) as well as total scattering (atomic pair distribution function analysis; PDF) experiments. It covers Bragg spacings from sub-Angstroms to 1.7 microns, thus allowing the analysis of dimensions and complex structures in (nano-)materials on multiple length scales. The accessible scattering vector q-range spans over almost five decades (qmin = 0.0036 nm-1 to qmax = 215 nm-1), without any gaps.
SAXS and USAXS allow to investigate the size distribution, internal structure, and shape of nanoparticles and macromolecules and to determine characteristic repeat distances in nanostructured materials. On the other hand, with the total scattering (PDF) technique, the local atomic structures in (partially) disordered materials can be studied. The combination of all scattering techniques thus enables the investigation of complex structures on the atomic and nano- and meso- (length) scales, which is essential for a better understanding of and control over the macroscopic properties of a given material.

Back to Table of contents

MS18 Biomineralogy and bioinspired materials

MS18-2-1 Texture and Microstructure of the outer layer of a brachiopod fossil from the Terebratulida order (-155 My)
#MS18-2-1

D. Vinci [1], B. Maestracci [2], S. Gascoin [2], M. Gauduchon [3], P. Gauduchon [3], D. Chateigner [2]
[1]European XFEL, Holzkoppel 4 - Schenefeld (Germany), [2]Laboratoire CRISMAT-CNRS, IUT GON, Université de Caen Normandie, Normandie Université, 6 Bd. M . Juin - Caen (France), [3]Ré Nature Environnement, 14 rue de Montamer - Sainte Marie de Ré (France)

Abstract
Quantitative analysis of the crystallographic texture and microstructure of the biomineral layers of some invertebrates provide a better understanding of the species' phylogenetic placement, as well as they specify the purely mineral impact on their shell growth. For example, in current molluscs, the phylogenetic signal due to the strong and varied textures of the aragonitic layers helps to specify certain hypotheses [1], and in extinct fossilized species with calcitic layers to establish possible kinship relations [2]. The textures of the biomineral layers of the mollusc clade have been extensively studied, unlike to the brachiopod and bryozoan clades.
In this contribution, we present the outer calcitic layer of a fossilised brachiopod species of the Upper Jurassic (Kimmeridgien stage), belonging to the order Terebratulida. The sample was collected in Loix-en-Ré, Charente-Maritime, France. The layer was measured using 4-circles X-ray diffraction, then the texture was estimated by using the Combined Analysis method [3]. It exhibits a fibre texture with the <001> fiber axis perpendicular to the layer plane. The absence of preferred orientations perpendicular to <001> indicates a behaviour already observed in the fossil calcite layers and current molluscs, as well as in bryozoans.

References
[1] D. Chateigner et al., Materials Science and Engineering A, 528, (2010), 37-51
[2] D. Chateigner et al., Materials Science Forum, 408, (2002), 1687-1692
[3] D. Chateigner (Ed.), Combined Analysis, ISTE-Wiley (2010).

{0012} and {300} pole figures of calcite.

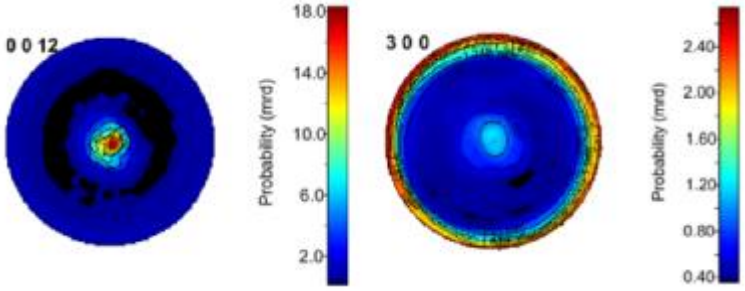

Back to Table of contents

MS18 Biomineralogy and bioinspired materials

MS18-2-2 NMR, Kinetic-Mechanistic and SC-XRD Study of Carbon Dioxide Capturing Model Molecular Materials #MS18-2-2

A. Roodt [1], J. Venter [1], S. Redgard [1]
[1]University of the Free State - Bloemfontein (South Africa)

Abstract
The effects of climate change, also brought upon by environmental pollution, has been gaining significant international awareness over the past decade and motivated many governments to upscale their efforts to achieve greenhouse gas (GHG) neutrality. A pollutant at the forefront of the GHGs is carbon dioxide (CO_2), which is considered the leading contributor (74.4%) to global warming. Global emissions of CO_2 from fossil fuels were at record levels in 2019 (36.6 $GtCO_2$ – down to 34 $GtCO_2$ in 2020), with China and the USA emitting 10.37 and 4.71 $GtCO_2$ respectively, in 2020. [1,2].
In this study, Platinum Group Metal (PGM) complexes and other nucleophiles were identified which displayed activities as entities which exhibit potential as CO_2 capturing/conversion catalysts to further drive the process. It firstly focused on the synthesis of a range of PGM complexes [Rh, Pt, Pd] which incorporates 1,5-cyclooctadiene (COD) as a ligand (a known π-accepting modality) in the system to offer a different probe for evaluating structural changes induced at the metal centres. The essence of this is focused primarily on utilizing accurate single-crystal X-ray diffraction (SC-XRD) to evaluate the COD conformation in the complexes and scrutinise distortions therein, as for example, described by the so-called Venus fly-trap parameters, the jaw, twist and bite dihedral angles (ψ, τ, χ). [3,4] Special focus was given to the influence the ligands have on the coordinated COD, “mimicking” the Venus fly-trap plant, see below.
The SC-XRD was then supplemented by evaluating the organometallic PGM complexes and associated nucleophiles for catalytic potential in the cycloaddition of CO_2 to an epoxide (epichlorohydrin, EPI) under ambient conditions as initially introduced by Arayachukiat et al. and Yingcharoen et al., [5,6] but focusing on detailed mechanistic and possible kinetic pathways involved. Several carefully studied parameters will be discussed in this presentation, which include the effects of (i) a range of acids based on their Bronsted acidity (pKa values) and number of acidic protons, (ii) [(Bu_4N)I], (iii) [EPI], (iv) [CO_2] under atmospheric pressure, and (v) [Metal complex].

References
[1] N. US Department of Commerce, NOAA Global Monitoring Laboratory - The NOAA Annual Greenhouse Gas Index (AGGI), 2021, (Accessed 11/12/2021). https://gml.noaa.gov/aggi/aggi.html.
[2] C. Le Quéré, G. P. Peters, P. Friedlingstein, R. M. Andrew, J. G. Canadell, S. J. Davis, R. B. Jackson, M. W. Jones, Nature Climate Change, 2021, 11, 197–199.
[3] T. N. Hill, A. Roodt, G. Steyl, Polyhedron, 2013, 50, 82–89.
[4] T. N. Hill, A. Roodt, Zeitschrift für Anorganische und Allgemeine Chemie, 2018, 644, 763–774.
[5] S. Arayachukiat, C. Kongtes, A. Barthel, S. V. C. Vummaleti, A. Poater, S. Wannakao, L. Cavallo, V. D’Elia, ACS Sustainable Chemistry & Engineering, 2017, 5, 6392–6397.
[6] P. Yingcharoen, C. Kongtes, S. Arayachukiat, K. Suvarnapunya, S. V. C. Vummaleti, S. Wannakao, L. Cavallo, A. Poater, V. D’ Elia, Advanced Synthesis & Catalysis, 2019, 361, 366–373.

Venus fly-trap leaf mimicking COD ligand

Back to Table of contents

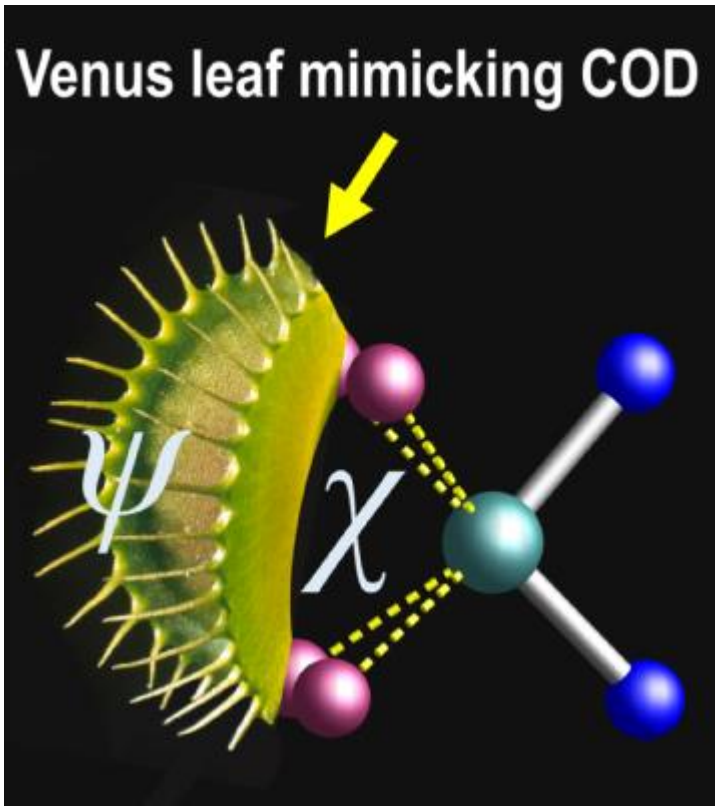

Back to Table of contents

MS19 Experimental and theoretical advances in quantum crystallography

MS19-1-1 Theoretical considerations of radiation damage effects in mercury containing compounds #MS19-1-1

L. Bucinsky [1], S. Grabowsky [2]
[1]Slovak University of Technology - Bratislava (Slovakia), [2]University of Bern - Bern (Switzerland)

Abstract
Radiation damage in mercury compounds [1] will be examined theoretically. Since mercury (5d elements in general) has the K-edge energy levels below the energy of X-ray and usually used synchrotron radiation, absorption is a natural phenomena. This can be either manifested in higher residual densities around the heavy element atoms [2,3], or can lead to further disintegration of the crystal. Herein, we will consider the hypothesis that radiation damage is driven by a gross change of geometry of Hg containing model compounds in the excited state, which is promoted by absorption.

Acknowledgements: APVV-20-0213, VEGA 1/0718/19, VEGA 1/0139/20

References
[1] L. Bucinsky, D. Jayatilaka, S. Grabowsky. J. Phys. Chem. A 2016, 120, 6650-6669.
[2] A. Grytsiv, P. Rogl, E. Bauer, H. Michor, E. Royanian, G. Giester. Intermetallics 2010, 18, 173-178. https://doi.org/10.1016/j.intermet.2009.07.009.
[3] S. Pawlędzio, M. Malinska, M. Woińska, J. Wojciechowski, L. A. Malaspina, F. Kleemiss, S. Grabowsky K. Woźniak. IUCrJ (2021). 8, 608-620.

Back to Table of contents

MS19 Experimental and theoretical advances in quantum crystallography

MS19-1-2 Correlating Chemical Bonds with Glass Formation in Coordination Polymers: A Combined X-ray Electron Density and High-pressure Single Crystal X-ray Diffraction Study
#MS19-1-2

S. Sarkar [1], E.S. Vosegaard [1], B.B. Iversen [1]
[1]Aarhus University - Aarhus C (Denmark)

Abstract
Amorphous metal-organic frameworks (MOF)/coordination polymer (CP) represents a new class of hybrid functional materials with novel short-range structures and potential applications such as gas mixture separations (H_2/CH_4, CO_2/N_2), optical luminescence materials, anode material in lithium ion batteries.[1] Pioneering work on amorphous MOFs is carried out on melt-quenched glasses formed especially by the zeolitic imidazolate frameworks (ZIFs).[2] In our recent work[3], we have demonstrated the key roles of the metal–ligand bonds and the internal imidazole bonds in controlling the subtle balance between melting and decomposition process in prototypical glass forming ZIF-zni MOF. In addition to melt-quenched MOFs, mechanically induced amorphization which directly converts crystals into a glassy state was first demonstrated in CdTz CP.[4] To understand the root of mechanically induced amorphization in CP, the role of chemical bonds and structural changes under pressure should be investigated.
In this work, we compare the electron density distribution of two isostructural CP molecules-MnTz and ZnTz ([M(II)(1,2,4-triazole)2(H_2PO_4)$_2$], using high-resolution single-crystal X-ray diffraction data measured at 100 K. MnTz undergoes a direct crystal-to-glass phase transition through mechanical milling whereas ZnTz retains its crystalline form under similar mechanical treatment.[5] Quantitative chemical bonding analysis using several topological parameters based on Bader's QTAIM theory[6] shows that Mn–ligand bonds are primarily closed shell ionic in nature with a spherical $3d^5$ electron density of Mn atom (Figure 1). On the other hand, aspherical electron density features are seen on Zn atom (Figure 1). The respective Zn–ligand bonds in ZnTz have partial polar covalent features.
High-pressure single crystal diffraction study was carried out at several pressure points upto 3.5 GPa and 7.5 GPa for MnTz and ZnTz respectively. The metal–ligand bonds shows higher linear compressibility in MnTz (~9.5 TPa^{-1}) as compared to ZnTz (~8 TPa^{-1}) (Figure 2). Interestingly, both molecules exhibit pressure induced phase transition from orthorhombic (*Pbcn*) to monoclinic ($P2_1/c$) phase at elevated pressures (3.1-3.6 GPa for MnTz, 4.6-5.9 GPa for ZnTz). These high-pressure monoclinic phases are similar to the ambient crystal structure of CdTz CP which also form glass under mechanical milling.[4]

References
1. Horike, S.; Ma, N.; Fan, Z.; Kosasang, S.; Smedskjaer, M. M., Mechanics, Ionics, and Optics of Metal–Organic Framework and Coordination Polymer Glasses. Nano Letters 2021, 21 (15), 6382-6390.
2. Bennett, T. D.; Horike, S., Liquid, glass and amorphous solid states of coordination polymers and metal–organic frameworks. Nat. Rev. Mater. 2018, 3 (11), 431-440.
3. Sarkar, S.; Grønbech, T. B. E.; Mamakhel, A.; Bondesgaard, M.; Sugimoto, K.; Nishibori, E.; Iversen, B. B., X-ray Electron Density Study of the Chemical Bonding Origin of Glass Formation in Metal–Organic Frameworks**. Angew. Chem. Int. Ed. 2022, n/a (n/a), e202202742.
4. Chen, W.; Horike, S.; Umeyama, D.; Ogiwara, N.; Itakura, T.; Tassel, C.; Goto, Y.; Kageyama, H.; Kitagawa, S., Glass Formation of a Coordination Polymer Crystal for Enhanced Proton Conductivity and Material Flexibility. Angew. Chem. Int. Ed. 2016, 55 (17), 5195-5200.
5. Ohara, Y.; Hinokimoto, A.; Chen, W.; Kitao, T.; Nishiyama, Y.; Hong, Y. l.; Kitagawa, S.; Horike, S., Formation of Coordination Polymer Glass by Mechanical Milling: Dependence on Metal Ions and Molecular Doping for H+ Conductivity. Chem. Commun. 2018, 54, 6859.
6. Bader, R. F. W., Atoms in Molecules. A Quantum Theory. Atoms in Molecules. A Quantum Theory, Clarendon Press, Oxford, New York: 1990.

2D deformation maps plotted at ± 0.1eÅ-3 level.

Back to Table of contents

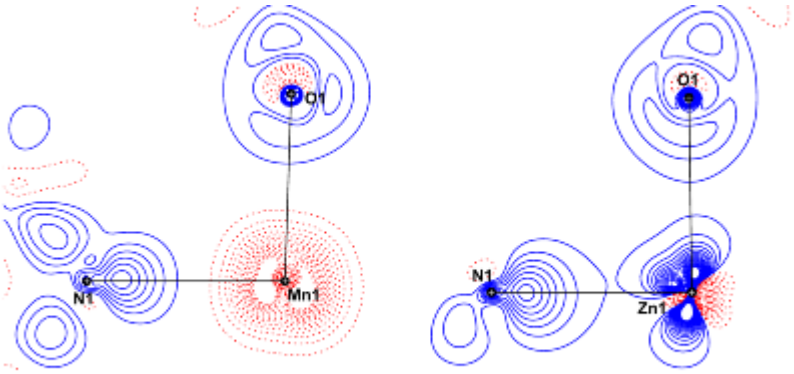

Figure 1. 2D deformation maps along N_1–M_1–O_1 plane plotted at a contour level of + 0.1 eÅ^{-3}. Blue represents charge concentration, and red represents charge depletion regions

Variation in metal-ligand bond lengths with pressu

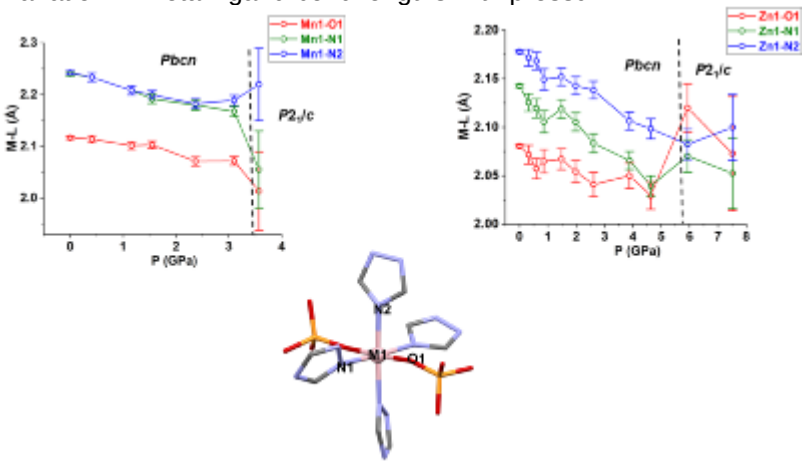

Figure 2. Variation in metal–ligand bond lengths with pressure

Back to Table of contents

MS19 Experimental and theoretical advances in quantum crystallography

MS19-1-3 Comparative study of in-house and synchrotron X-ray electron densities on molecular crystals #MS19-1-3

E.S. Vosegaard [1], J.V. Ahlburg [1], S. Takahashi [2], E. Nishibori [2], B.B. Iversen [1]
[1]Aarhus University - Aarhus (Denmark), [2]University of Tsukuba - Tsukuba (Japan)

Abstract
In this study, the data quality of a range of available in-house single crystal x-ray diffractometers was tested against synchrotron data on their ability to produce an accurate Multipolar Model (MM) of the electron density of the archetypical molecular crystal melamine. The instruments tested include the BL02B1 beamline at the SPring-8 synchrotron, state-of-the-art in-house diffractometers Rigaku Synergy-S, STOE Stadivari and the older Agilent Supernova. The specific details for obtained datasets can be seen in the table.

Overview of the six different datasets used for the MM comparison. At SPring8 data was collected at two different temperatures, and two different sources were tested at the Synergy-S.

	SPring8		Synergy-S		Stadivari	Supernova
Detector	Pilatus CdTe		HyPix arc100		Eiger CdTe	CCD
Wavelength [Å]	0.25		0.71 (Mo)	0.56 (Ag)	0.71 (Mo)	0.71 (Mo)
Temperature [K]	25	100	100	100	100	100

Preliminary analysis show that even though the data quality varies slightly between the six data sets, there is virtually no difference between the resulting multipole models. All datasets provide a reliable MM with great data quality (>20 (>7 for supernova) and redundancy >7), high resolution (>1.18 $Å^{-1}$), low R-factors (<3%) and low min/max residuals (<0.3 $e/Å^3$). Residual density map (ρ_{obs}-ρ_{calc}) and deformation density map (ρ_{MM}-ρ_{IAM}) for the six different datasets can be seen in the figure. Contour lines are shown at 0.1 $e/Å^3$. The residual density maps are shown at the highest common resolution cutoff of 1.18 $Å^{-1}$. Deformation density maps are calculated to the full resolution.The noise level is significantly higher for the Supernova with an old CCD detector as seen in the residual density map in the figure, but it has a random nature, suggesting low impact on the validity of the MM. The deformation density map in the figure obtained from the SPring8 100K dataset has some abnormal features in the upper part of the ring, suggesting minor systematic flaws. In the present case the SPring8 25K, Synergy Mo and Ag datasets seem to be of (slightly) higher quality among six quite excellent MMs.

Residual- and deformation density maps.

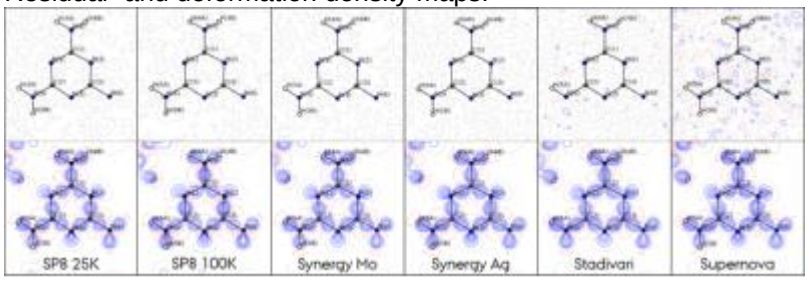

Back to Table of contents

MS19 Experimental and theoretical advances in quantum crystallography

MS19-2-1 X-ray constrained wavefunction approach: furhter developments and future outlooks
#MS19-2-1

A. Genoni [1]
[1]1Laboratory of Theoretical Physics and Chemistry, CNRS & University of Lorraine - Metz (France)

Abstract
The X-ray constrained wavefunction (XCW) technique [1-4] is a modern quantum crystallographic method that aims at extracting plausible electronic wavefunctions from X-ray diffraction data. This is done by minimizing the energy of the system under exam and simultaneously maximizing the statistical agreement between calculated and experimental structure factor amplitudes.
In this presentation, two unsolved problems of the XCW technique will be addressed: i) the possibility of introducing a weight for each considered reflection; ii) the need of determining a clear halting point during the XCW calculations (also known as the long-standing problem of determining the value of the parameter).
Pertaining to the former problem, we have recently proposed [5] a weighting scheme based on the results of a previous investigation on the capability of extracting electron correlation effects through X-ray constrained wavefunctions [6]. In that study we observed that the high-angle data largely predominate and are already very well described at unconstrained level (i.e., when =0), with the consequence that the significant electron correlation effects contained in the low- and medium-angle reflections cannot be fully captured by the XCW method. Based on these observations, we introduced a weighting scheme to up-weight the low- and medium-angle data and to down-weight the high-angle ones. The results obtained by means of this strategy will be shown and discussed, both in the case in which we exploited theoretically generated data and in the one in which we used experimental reflections.
Concerning the second point, we will present how the X-ray constrained wavefunction method can be revisited if the stationary condition of the Jayatilaka functional with respect to the auxiliary variable is introduced [7]. In fact, following a reasoning analogous to the one used in constrained Density Functional Theory [8, 9], regains its original meaning of Lagrange multiplier and it is possible to prove that the correct value of is always a maximum stationary point of the functional to optimize. Based on this finding, we will propose a reformulation of the XCW method that will be intrinsically more physically meaningful since it will enable to straightforwardly evaluate the highest level of confidence with which the experimental X-ray diffraction data can be reproduced. Finally, the new variant of the XCW technique will allow to better distinguish between “X-ray constrained” and “X-ray restrained” wavefunctions.

References
[1] D. Jayatilaka, Phys. Rev. Lett. 1998, 80, 798-801.
[2] D. Jayatilaka, D. J. Grimwood, Acta Cryst. A 2001, 57, 76-86.
[3] D. J. Grimwood, D. Jayatilaka, Acta Cryst. A 2001, 57, 87-100.
[4] D. J. Grimwood, I. Bytheway, D. Jayatilaka, J. Comp. Chem. 2003, 24, 470-483.
[5] G. Macetti, A. Genoni, Acta Cryst. A, submitted.
[6] A. Genoni, L. H. R. Dos Santos, B. Meyer, P. Macchi, IUCrJ 2017, 4, 136-146.
[7] A. Genoni, Acta Cryst. A, submitted.
[8] Q. Wu, T. Van Voorhis, Phys. Rev. A 2005, 72, 024502.
[9] B. Kaduk, T. Kowalczyk, T. Van Voorhis, Chem. Rev. 2012, 112, 321-370.

Back to Table of contents

MS19 Experimental and theoretical advances in quantum crystallography

MS19-2-2 Influence of modelling of disorder on results of Hirshfeld atom refinement of an organo-gold(i) compound #MS19-2-2

S. Pawlędzio [1], M. Malinska [1], F. Kleemiss [2], S. Grabowsky [3], K. Woźniak [1]
[1]Biological and Chemical Research Centre, Department of Chemistry, University of Warsaw, Żwirki i Wigury 101, 02-089 Warsaw - Warsaw (Poland), [2]Faculty for Chemistry und Pharmacy, University of Regensburg, Universitätsstr. 31, 93053 Regensburg, Germany - Regensburg (Germany), [3]3Department of Chemistry, Biochemistry and Pharmaceutical Sciences, University of Bern, Freiestrasse 3, Bern 3012, Switzerland - Bern (Switzerland)

Abstract
Almost 30% of deposited structures in the Cambridge Structural Database (CSD) are disordered[1]. Usually, it affects only some parts of the molecule, such as freely rotating functional groups, solvents molecules or long side chains. Detecting and modelling of the disorder are important not only in crystallography but also in other related branches of science, including material chemistry, mineralogy, pharmaceutical industry or structural biology. For example, it has been reported that disordered proteins are of important role in binding DNA and signalling cascades[2].
Hirshfeld atom refinement (HAR)[3a],b is a method that uses tailor-made aspherical atomic scattering factors, obtained from the quantum mechanical calculations, to refine atomic positions and their ADPs in the standard least-square refinement. It has been shown that HAR overcomes all the shortcomings of the Independent Atom Model (IAM), yielding more accurate hydrogen atom positions[4] and enabling refinement of hydrogen atom ADPs[5]. Furthermore, HAR was successfully applied to small[6] and big[7], light[6] and heavy[8] molecules. During the last few years, new software for HAR was extensively developed and nowadays modelling of disorder, even for structures with heavy elements, is possible[9a,b].
Our previous study on organo-gold(I) compound and relativistic HAR[10] did not include modelling of disorder. Therefore, here, we will show the reinvestigation of this study with NoSpherA2[9a]. The validation of modelling of disorder with HAR, where wavefunctions were computed using either HF or DFT methods. In some cases also relativistic DKH2 Hamiltonian was used. The impact of modelling of disorder on the results of HAR is analysed in terms of differences of dynamic structure factors, which were calculated from the obtained thermally smeared electron density based on wavefunctions that were computed with or without electron correlation and relativistic effects. The role of modelling disorder is also compared with the effect of treatment of hydrogen atom ADP values, which were obtained from SHADE and as well as from HAR, and atomic anharmonicity of the gold atom.

Acknowledgements: Support from the National Science Centre Poland within PRELUDIUM grant No. UMO-2018/31/N/ST4/02141 is gratefully acknowledged.

References
References:
[1] C. R. Groom, I. J. Bruno, M. P. Lightfoot, S. C. Ward, Acta Crystallographica B, 2016, 72, 171–179.
[2] J. D. Atkins, S. Y. Boateng, T. Sorensen, L. J. McGuffin, Int J Mol Sci., 2015, 16, 19040–19054.
[3] a) D. Jayatilaka, B. Dittrich, Acta Crystallographica Section A, 2008, 64, 383–393. b) S. C. Capelli, H.-B. Bürgi, B. Dittrich, S. Grabowsky, D. Jayatilaka, IUCrJ, 2014, 1, 361–379.
[4] L. A. Malaspina, A. A. Hoser, A. J. Edwards, M. Woińska, M. J. Turner, J. R. Price, K. Sugimoto, E. Nishibori, H.-B. Bürgi, D. Jayatilaka, S. Grabowsky, CrystEngComm, 2020, 22, 4778–4789.
[5] M. Wanat, M. Malinska, A. A. Hoser, K. Woźniak, Molecules, 2021, 26, 3730.
[6] M. Woińska, S. Grabowsky, P. M. Dominiak, K. Woźniak, D. Jayatilaka, Science Advances, 2016, 2, e1600192.
[7] L. A. Malaspina, E. K. Wieduwilt, J. Bergmann, F. Kleemiss, B. Meyer, M. F. Ruiz-López, R. Pal, E. Hupf, J. Beckmann, R. O. Piltz, , A. J. Edwards, S. Grabowsky, A. Genoni, J Phys Chem Lett., 2019, 10, 6973–6982.
[8] L. Bučinský, D. Jayatilaka, S. Grabowsky, The Journal of Physical Chemistry A, 2016, 120, 6650–6669.
[9] a) F. Kleemiss, O. V. Dolomanov, M. Bodensteiner, N. Peyerimhoff, L. Midgley, L. J. Bourhis, A. Genoni, L. A. Malaspina, D. Jayatilaka, J. L. Spencer, F. White, B. Grundkötter-Stock, S. Steinhauer, D. Lentz, H. Puschmann, S. Grabowsky, Chem. Sci., 2021, 12, 1675–1692. b) M. Chodkiewicz, S. Pawledzio, M. Woinska, K. Wozniak, IUCrJ, 2022, 9, 298-315.
[10] S. Pawlędzio, M. Malinska, M. Woińska, J. Wojciechowski, L. Andrade Malaspina, F. Kleemiss, S. Grabowsky, K. Woźniak, IUCrJ, 2021, 8, 608–620.

Back to Table of contents

MS19 Experimental and theoretical advances in quantum crystallography

MS19-2-3 Selenium in Charge Density Investigations
#MS19-2-3

R. Herbst-Irmer [1]
[1]**Georg-August-Universität - Göttingen (Germany)**

Abstract
Selenium compounds pose a challenge for X-ray structure analysis and especially for charge density studies because, on the one hand, selenium has a relatively high absorption coefficient at the Mo wavelength (λ = 0.71073 Å) and, on the other hand, shows X-ray fluorescence.
In spite of these problems, we were interested in the investigation of non-covalent interactions in the compounds dibenzyl diselenide BnSeSeBn (**1**) [1] and 1-mesitylselanyl-8-(dimethylsilyl)naphthalene (**2**) [2]. In **1** very short intermolecular Se···Se distances of 3.44 Å were observed, while in **2** the Si–H···Se contact caught our attention.
Several datasets for **1** were collected at different in-house diffractometers with various X-ray wavelengths, intensities and detectors at 100 K. Unfortunately, all multipole refinements ended up with two relatively high residual density peaks in the proximity of selenium at similar positions for all datasets. At the end, these peaks could be explained as disorder with radiation-induced radical species BnSeSe•/•Bn. This made a charge density investigation impossible, but extended DFT methods and solid state EPR showed that not only organo-selenide radicals like RSe• may occur, but also organo diselenide BnSeSe• radicals and organic radicals R•, which is particularly important to know in structural biology.
Also, the investigation on **2** was challenging. Resolution dependent errors need to be cured to model the Se atom properly and to characterize the Si–H···Se contact as chalcogen–hydride bond.

References
[1] Schürmann, C. J., Teuteberg, T. T., Stückl, A. C., Ruth, P. N., Hecker, F., Herbst-Irmer, R., Mata, R. A. & Stalke, D. (2022). *Angew. Chem. Int. Ed*., e202203665.
[2] Keil, H., Herbst-Irmer, R., Rathjen, S., Girschik, C., Müller, T. & Stalke, D. (2022). *Inorg. Chem*. **61**, 6319–6325.

Back to Table of contents

MS19 Experimental and theoretical advances in quantum crystallography

MS19-2-4 NoSpherA2 - From Inorganic to Protein Crystallography
#MS19-2-4

F. Kleemiss [1], O. Dolomanov [2], H. Puschmann [2], M. Bodensteiner [1]
[1]University of Regensburg - Regensburg (Germany), [2]OlexSys Ltd. - Durham (United Kingdom)

Abstract
NoSpherA2 [1] – the interface for non-spherical atoms in *Olex2* [2] – was initially capable of performing Hirshfeld Atom Refinement (HAR) [3] for ordered and disordered, mostly molecular, crystal structures. The recent extension of the interface to include databases of multipoles [4] or combine approaches in a “hybrid” mode allow unprecedented speeds of refinements, where known parts of the structure can be described by tabulated or low-level methods, while the remainder can be described using tailor made scattering factors.
The treatment of heavy elements and very large structures like proteins remained time consuming. Two recently implemented methods aim to make these structures refinable using *NoSpherA2* with affordable computational equipment. fragHAR [5] can calculate wavefunctions for large molecules with linear scaling time requirements (see Fig. 1) and help tackle time consuming disorder treatments by describing disordered regions as individual fragments without the need to recompute a wavefunction of the whole structure. While conventional HAR needs exponentially increasing amounts of time with rising numbers of atoms for the wavefunction calculations the fragHAR approach can be fitted using a linear dependence on the atom number. (Fig. 1) Additionally, the use of Effective Core Potentials (ECPs) was introduced into *NoSpherA2*-HAR based on the tight-core treatment of density modelled by ECPs as used in other charge density analysis.[6] This approach allows treatment of large structures and especially heavy elements with relatively little computational resources, since for example Pt can be modelled using 60 electrons in the effective core and therefore reducing the number of orbitals to be calculated and evaluated by 30 in the case of restricted SCF procedures.

References
[1] F. Kleemiss, O. V. Dolomanov, M. Bodensteiner, N. Peyerimhoff, L. Midgley, L. J. Bourhis, A. Genoni, L. A. Malaspina, D. Jayatilaka, J. L. Spencer, F. White, B. Grundkötter-Stock, S. Steinhauer, D. Lentz, H. Puschmann, S. Grabowsky, *Chem. Sci.*, **2021**, 12, 1675-1692.
[2] a) O. V. Dolomanov, L. J. Bourhis, R. J. Gildea, J. A. K. Howard, H. Puschmann, *J. Appl. Cryst.*, **2009**, 42, 339-341. b) L. J. Bourhis, O. V. Dolomanov, R. J. Gildea, J. A. K. Howard, H. Puschmann, Acta Cryst., **2015**, A71, 59-75.
[3] a) S. C. Capelli, H.-B. Bürgi, B. Dittrich, S. Grabowsky, D. Jayatilaka, *IUCrJ*, **2014**, 1, 361-379. b) M. Woinska, S. Grabowsky, P. M. Dominiak, K. Wozniak, D. Jayatilaka, *Sci. Adv.*, **2016**, 2(5).
[4] M. L. Chodkiewicz, S. Migacz, W. Rudnicki, A. Makal, J. A. Kalinowski, N. W. Moriarty, R. W. Grosse-Kunstleve, P. V. Afonine, P. D. Adams, P. M. Dominiak, *J. Appl. Cryst.,* **2018**, 51, 193-199.
[5] J. Bergmann, M. Davidson, E. Oksanen, U. Ryde, D. Jayatilaka, *IUCrJ*, **2020**, 7, 158-165.
[6] T. A. Keith, M. J. Frisch, *J. Phys. Chem. A*, **2011**, 115, 12879-12894.

Timing of calculations versus size of structure.

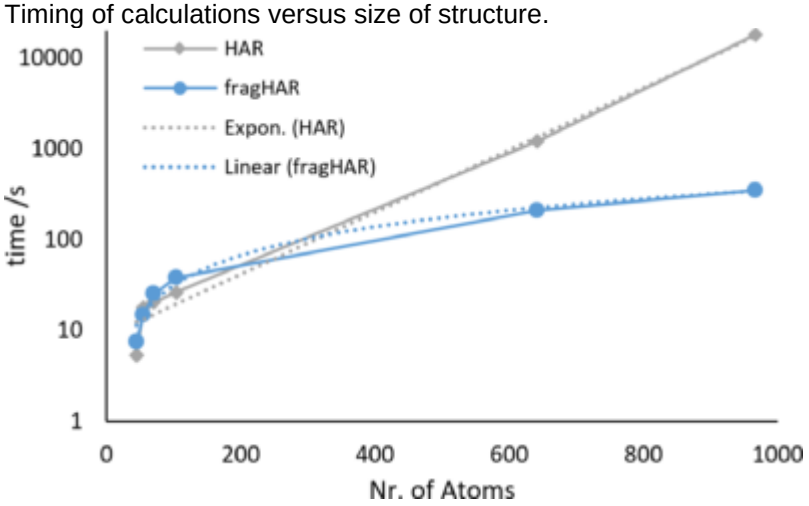

Back to Table of contents

MS19 Experimental and theoretical advances in quantum crystallography

MS19-2-5 Thermal motion and position of hydrogen bonded to transition metals in coordination complexes studied with HAR combined with SHADE3 or NoMoRe
#MS19-2-5

M. Woinska [1], A. Hoser [1], C. Michal [1], W. Krzysztof [1]
[1]Biological and Chemical Research Centre, Chemistry Department, University of Warsaw, Żwirki i Wigury 101, 02-089 Warszawa, Poland - Warsaw (Poland)

Abstract
Hirshfeld Atom Refinement (HAR) is a method which, based on X-ray data, yields more accurate positions of hydrogen atoms bonded to light chemical elements and – if data quality allows – also to heavy metals [1]. Nevertheless, treatment of hydrogen thermal motions is more problematic and HAR often yields ADPs which are N.P.D. or produces thermal ellipsoids with distorted shapes. Therefore, tools enabling estimation of hydrogen ADPs such as SHADE3 [2] or Normal Mode Refinement (NoMoRe) [3] are helpful. Transition metal (TM) hydride complexes are particularly challenging for X-ray crystallography. On the one hand, obtaining high quality data is hindered by problems such as high absorption and radiation damage. Access to neutron data which could be used as a benchmark is even more limited. On the other hand, using an advanced model of electron density such as HAR involves time-consuming calculations. This problem is even more exacerbated in the case of SHADE3 or NoMoRe, for which periodic wave function has to be computed.
In this contribution we present the results of HAR performed for five structures of TM (Fe, Nb, Rh and Os) and metalloid (Sb) hydride complexes for which both neutron and X-ray data were available in the CSD. Refinements were performed in three versions: (1) hydrogen thermal motions refined with HAR (usually isotropically, except the Fe and Rh complexes for which anisotropic refinement of C-bonded H atoms was possible), (2) H ADPs fixed at the SHADE3-derived values and (3) H ADPs obtained in the course of NoMoRe. The influence of the method of obtaining hydrogen thermal motions on the positions of hydrogen atoms derived by HAR, particularly TM-H bond lengths, will be analyzed. Changes of statistical parameters characterizing refined models will also be discussed. Differences between hydrogen ADPs obtained with various methods will be studied using the similarity index (S) [4]. For the Sb complex, for which neutron and X-ray data collection temperatures are the same, thermal motions derived from the neutron experiment and the three methods applied to X-ray data will be compared.
Acknowledgements: We are grateful for the financial support from the Polish National Science Centre (NCN) under Opus grant DEC-2018/31/B/ST4/02142 and the Core Facility for crystallographic and biophysical research to support the development of medicinal products sponsored by the Foundation for Polish Science (FNP). Wroclaw Centre for Networking and Supercomputing of Wroclaw University of Technology and the PL-Grid infrastructure are gratefully acknowledged for providing computational facilities.

References
[1] M. Woińska, M. L. Chodkiewicz, K. Woźniak, Chem. Commun., 2021, 57, 3652-3655.[2] A. A. Hoser, A. Ø. Madsen, Acta Cryst., 2016, A72, 206–214.[3] (a) A. A. Hoser, A. Ø. Madsen, Acta Cryst., 2016, A72, 206–214; (b) A. A. Hoser, A. Ø. Madsen, Acta Cryst., 2017, A73, 102–114.[4] Spackman, M. A. Chem. Rev., 1992, 92, 1769–1797.

HAR+NoMoRe crystal structure of the Rh complex.

Back to Table of contents

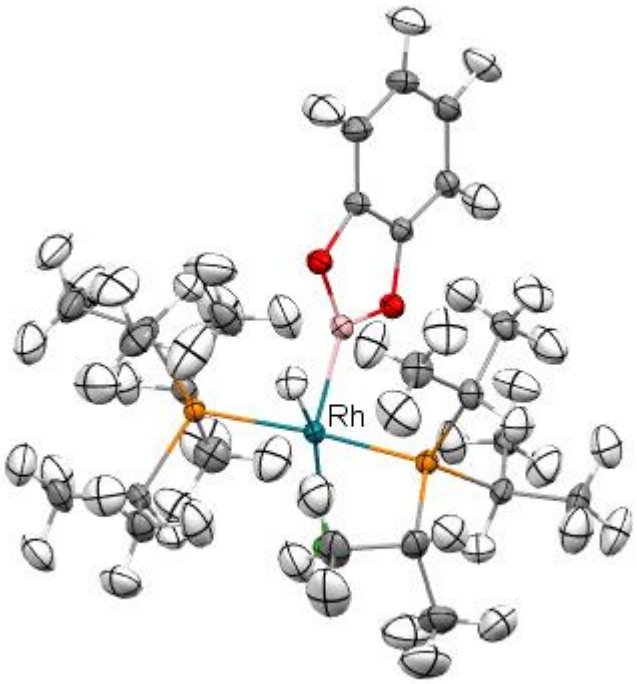

Back to Table of contents

MS19 Experimental and theoretical advances in quantum crystallography

MS19-2-6 A rush to explore protein–ligand electrostatic interaction energy with Charger #MS19-2-6

V. Vukovic [1], T. Leduc [1], C. Didierjean [1], F. Favier [1], B. Guillot [1], C. Jelsch [1]
[1]CRM2 CNRS Univ Lorraine - Nancy (France)

Abstract
The mutual penetration of electron densities between two interacting molecules complicates the computation of an accurate electrostatic interaction energy based on a pseudo-atom representation of electron densities. The numerical exact potential and multipole moment (nEP/MM) method is time-consuming since it performs a 3D integration to obtain the electrostatic energy at short interaction distances. Nguyen et al. (2018) recently reported a fully analytical computation of the electrostatic interaction energy (aEP/MM). This method performs much faster than nEP/MM (up to two orders of magnitude) and remains highly accurate. A new program library, Charger, contains an implementation of the aEP/MM method. Charger (Vukovic et al., 2021) has been incorporated into the MoProViewer software (Guillot et al., 2014). Benchmark tests on a series of small molecules containing only C, H, N and O atoms show the efficiency of Charger in terms of execution time and accuracy. Charger is also powerful in a study of electrostatic symbiosis between a protein and a ligand. It determines reliable protein–ligand interaction energies even when both contain S atoms. It easily estimates the individual contribution of every residue to the total protein–ligand electrostatic binding energy. Glutathione transferase (GST) in complex with a benzophenone ligand was studied due to the availability of both structural and thermodynamic data (Schwarz et al., 2018). The resulting analysis highlights not only the residues that stabilize the ligand but also those that hinder ligand binding from an electrostatic point of view. This offers new perspectives in the search for mutations to improve the interaction between protein and ligand partners.

References

Guillot, B., Enrique, E., Huder, L., & Jelsch, C. (2014). MS19. O01. MoProViewer: a tool to study proteins from a charge density science perspective. Acta Cryst, 70, C279.
Schwartz, M., Perrot, T., Aubert, E., Dumarçay, S., Favier, F., Gérardin, P., ... & Gelhaye, E. (2018). Molecular recognition of wood polyphenols by phase II detoxification enzymes of the white rot Trametes versicolor. Scientific reports, 8(1), 1-11.
Vuković, V., Leduc, T., Jelić-Matošević, Z., Didierjean, C., Favier, F., Guillot, B., & Jelsch, C. (2021). A rush to explore protein–ligand electrostatic interaction energy with Charger. Acta Crystallographica Section D: Structural Biology, 77(10).

Binding of benzophenone to GST

Back to Table of contents

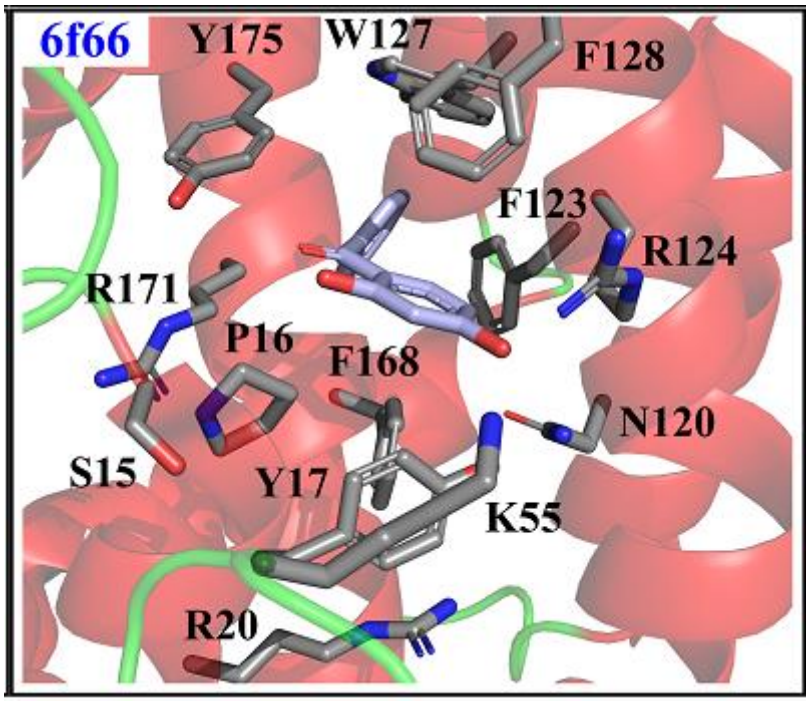

Energy contribution of residues to binding

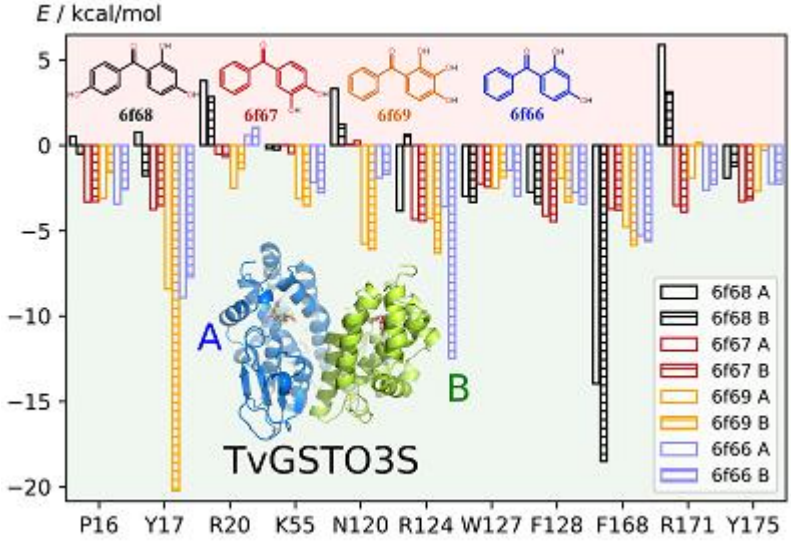

Back to Table of contents

MS20 Electric, opto-electronic and magnetic properties from elastic and inelastic scattering plus properties of materiels from quantum crystallography

MS20-2-1 Superexchange Mechanism In M(II) Formate Dihydrate Series And Charge Density Study Of The Co(II) Formate Dihydrate
#MS20-2-1

T.B.E. Grønbech [1], L. Krause [1], D. Ceresoli [2], B.B. Iversen [1]
[1]Centre For Integrated Materials Research, Department of Chemistry and iNANO, Aarhus Univesity - Aarhus (Denmark), [2]Istituto di Scienze e Tecnologie Chimiche "Giulio Natta" (SCITEC), National Research Council (CNR) - Milano (Italy)

Abstract
The Co(II) formate dihydrate (Co-formate) system exhibits a two-dimensional antiferromagnetically ordered structure intercalated by paramagnetic Co ions below [1]. Structurally, the magnetic planes are composed of Co-sites linked by formate ligands, while the paramagnetic Co ions do not exhibit the same two-dimensional structure. However, signs of short-range ferromagnetic order between the magnetic planes and paramagnetic ions have been observed upon further cooling [2].
Following a polarised neutron scattering experiment on the structural congener Mn-formate [3], it has been proposed that the two-dimensional magnetic order can be explained by superexchange facilitated by the formate ligands. Herein, this is further studied by analysing the charge density of Co-formate derived from a single crystal X-ray scattering experiment where it is observed from Laplacian maps that the formate ligands can coordinate into d-orbitals of t_{2g}-symmetry through a π-symmetric interaction. Correlating the possible interactions with extracted d-orbital populations, and interpreting these in terms of relative orbital energies, the interaction can be understood as back-donation.
This opens up the possibility of superexchange facilitated via π-symmetric interactions in addition to σ-symmetric interactions over the delocalised formate electron system. Applying the superexchange symmetry rules of Kanamori [4] together with the observed d-orbital populations allows for a mechanistic description of the antiferromagnetic 2-dimensional order and the short-range ferromagnetic order where the former is facilitated by σ-symmetric interactions and the latter by π-symmetric interactions. Furthermore, the short-range interaction is influenced by competing superexchange mechanisms in agreement with the lower ordering temperature.

References
[1] D. G. Kellerman et al., Phys. Status Solidi B, 2016, 253, 2209-2216
[2] H. Yamakawa, M. Matsuura, J. Phys. Soc. Jpn., 1976, 41, 798-803
[3] P. Radhakrishna et al., J. Phys.: Condens. Matter, 1993, 5, 6447-6460
[4] J. Kanamori, J. Phys. Chem. Solids, 1959, 10, 87-98

Orbital ordering based on extracted d-populations.

Back to Table of contents

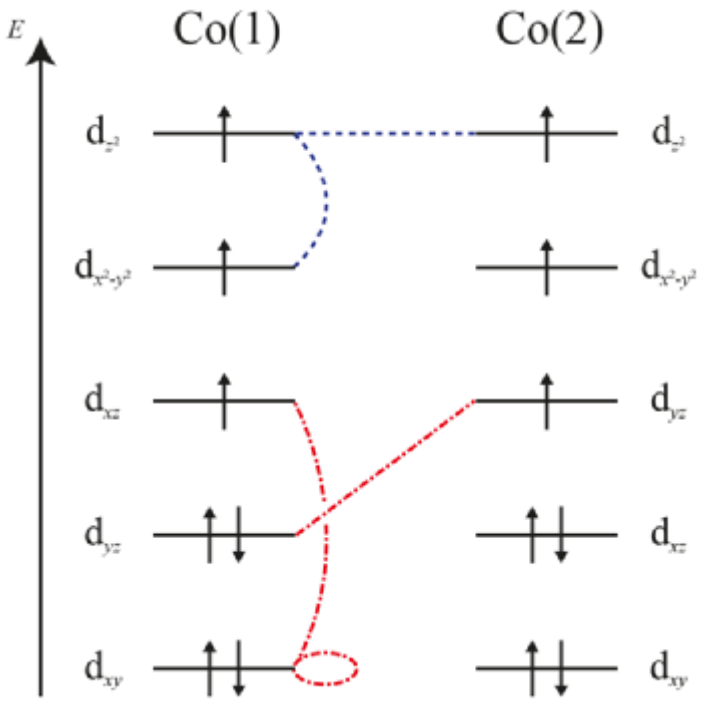

Superechange mechanism through pi-orbitals.

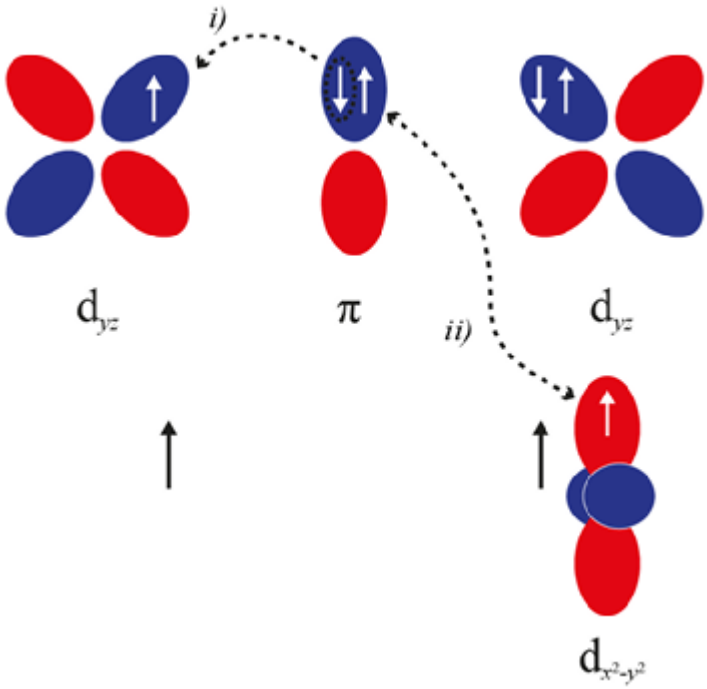

Back to Table of contents

MS20 Electric, opto-electronic and magnetic properties from elastic and inelastic scattering plus properties of materiels from quantum crystallography

MS20-2-2 Guiding antiferromagnetic transitions in Ca2RuO4
#MS20-2-2

D.G. Porter [1], F. Forte [2], V. Granata [2], M. Cannavacciuolo [2], R. Fittipaldi [2], M. Cuoco [2], A. Bombardi [1], A. Vecchione [2]

[1]Diamond Light Source Ltd - Didcot (United Kingdom), [2]University of Salerno - Salerno (Italy)

Abstract
Ca_2RuO_4 (CRO), the close neighbour of the famous superconductor Sr_2RuO_4 displays surprisingly different behaviour to its neighbour, exhibiting insulating behaviour below an irreversible metal-insulator transition at T_{MI} = 357K. In the insulating state CRO displays orbital ordering at T_{OO} = 260K and antiferromagnetic ordering at low temperature. Two magnetic ground states have been reported in this system with either an A-centred or B-centred order and moments predominately pointed along the b-axis. Many reports have been made altering the chemical composition of the system, including doping the atomic sites with elements of various oxidation states and atomic radii. In each case the behaviour is the same - any modification of the stoichiometric distorted structure through even low doping results in a change in magnetic ground state from the A-centred to the B-centred phase. Here we add to these results with characterisation measurements of CRO doped with manganese. We combine x-ray diffraction measurements of the crystal structure with resonant elastic x-ray scattering (REXS) measurements to determine the magnetic structure. We then use this doping regime to create a microscopic model of the system and use this to determine the nature of the transition between these two magnetic ground states. While our analysis focuses on a specific case of substitution, we show that any perturbation that can impact in a similar way on the crystal structure, by reconstructing the induced spin-orbital exchange, is able to drive the antiferromagnetic reorganization.

Back to Table of contents

MS21 Aperiodic crystals in organic and inorganic compounds and soft condensed matter

MS21-1-1 {R}Pt2Si2 family: a modulated story
#MS21-1-1

E. Duverger-Nédellec [1], M. Falkowski [2], P. Doležal [3], V. Buturlim [3], A.V. Andreev [3], L.M. Chamoreau [4], J. Forté [4], L. Havela [3]
[1]ICMCB-UMR5026 - Pessac (France), [2]IFMPAN - Poznan (Poland), [3]Charles University, Condensed Matter Department - Prague (Czech Republic), [4]IPCM, Sorbonne université - Paris (France)

Abstract
Materials with low electronic dimensionality are currently widely studied due to their natural tendency to exhibit remarkable properties such as thermoelectricity, high electron mobility or superconductivity. Moreover, this low dimensionality is also at the origin of another phenomenon: the charge density wave instability (CDW). This instability can be described by Peierls' theory [1] as a gap opening at the Fermi Surface of the material leading to the modulation of its electronic density accompanied by a periodic distortion of its atomic lattice. Therefore, a transition to a CDW state is characterized by the appearance of an anomaly in the electron transport properties and of additional reflections in the X-ray diffraction pattern, called satellite reflections.
An anomaly in the resistivity measurements, signature of a CDW transition, was reported at 112 K, 77 K and 88 K for the compounds {R}Pt_2Si_2, with R = La, Nd and Pr respectively [2,3]. However, no structural transition was evidenced by powder X-ray diffraction [4] and only one approximate modulation vector has been determined for $LaPt_2Si_2$ by electron diffraction: **q** = 1/3 **a*** [3]. To understand the structural impact of these CDWs we performed a single-crystal X-ray diffraction study on these materials at low temperature. This study reveals not only the appearance of satellite reflections associated with the reported CDW transitions but also the existence of an additional transition, at higher temperature, leading from an unmodulated structure to a modulated structure [4 ,5]. This unexpected phase transition, corresponding to no reported resistive anomaly, leads to an incommensurate structural modulation characterised by the wave vectors $\mathbf{q_1}$ = 0.360 **a***, 0.323 **a*** and 0.326 **a*** for $LaPt_2Si_2$ (160 K < T_1 < 150 K), $NdPt_2Si_2$ (300 K < T_1 < 260 K) and $PrPt_2Si_2$ (290 K < T_1 < 120 K) respectively. In the case of $LaPt_2Si_2$, this vector is very similar to the nesting vector of a CDW transition determined by ab initio calculations [6]. This observation stands in favor of a CDW-nature of the first structural transition. At lower temperature, a new set of satellites appears, coexisting with the first one, corresponding to the CDW transition observed in the resistivity measurements. This additional modulation is characterized by the wave vectors $\mathbf{q_2}$ = α **a*** + α **b*** + 0.5 **c***; with α = 0.187; 0.158 and 0.168 for $LaPt_2Si_2$ (115 K > T_2 > 100 K), $NdPt_2Si_2$ (90 K > T_2 > 40 K) and $PrPt_2Si_2$ (110 K > T_2 > 90 K) respectively. Last but not least, a third set of satellite reflections, with the wave vector $\mathbf{q_3}$ = 0.094 **a*** + 0.094 **b*** + 0.25 **c***, is observed on the XRD pattern of $LaPt_2Si_2$ at 50 K, showing that this familly is still full surprises and deserves more investigations.
Acknowledgments : This study was funded by the ERDF project NANOCENT : Nanomaterials Centre for Advanced Applications (CZ.02.1.01/0.0/0.0/15_003/0000485).

References
[1]: Peierls, R.E. (1955). Quantum Theory of Solids. London, Oxford Univ. Press.
[2]: Gupta, R., Dhar, S.K., Thamizhavel, A., Rajeev, K.P., & Hossain, Z. (2017). J.Phys.: Condens. Matter 29, 255601.
[3]: Nagano, Y., Araoka, N., Mitsuda, A., Yayama, Y., Wada, H., Ichihara, M., Isobe, M., & Ueda, Y. (2013) J. Phys. Soc. Jpn. 82, 064715.
[4]: Falkowski, M., Doležal, P., Andreev, A.V., Duverger-Nédellec, E., & Havela, L. (2019). Phys. Rev. B 100, 064103.
[5] : Falkowski, M., Doležal, P., Duverger-Nédellec, E., Chamoreau L.-M., Forté J., Andreev, A.V., & Havela, L. (2020), Phys. Rev. B 101, 174110
[6]: Kim, S., Kim, K., Min, B.I. (2015). Sci. Rep. 5, 15052.

Back to Table of contents

MS21 Aperiodic crystals in organic and inorganic compounds and soft condensed matter

MS21-1-2 Quasicrystalline Ultrathin Oxides films : model structures & properties
#MS21-1-2

T. Dorini [1], F. Brix [1], C. Ruano Merchan [1], M. Sicot [1], V. Fournee [1], E. Gaudry [1]
[1]Univ. Lorraine CNRS IJL - Nancy (France)

Abstract
Recently, the discovery of the quasiperiodic order in ultra-thin perovskite films reinvigorated the field of 2-dimensional oxides on metals, and raised the question of the reasons behind the emergence of the quasiperiodic order in these systems [1]. In this talk, we focus on a theoretical approach based on Density Functional Theory to investigate quasicrystalline ultrathin oxide films grown on metallic single crystal substrates [2]. The crystalline structure of these 2D phases can be described by specific tilings using a few elementary tiles (squares, triangles and rhombuses) [3] as observed by Scanning Tunneling Microscopy (STM). Calculations point the exothermic formation of these systems, which interact quite strongly with the underlying metal support, but more weakly than less complex structures. The optimization of the atomic positions shows a significant relaxation in the direction perpendicular to the surface, which could alleviate the strain due to the lattice mismatch between the substrate and the oxide layer. The interaction between the film and the underlying metal is ensured by hybridization of electronic states and by charge transfer from the oxide layer to the underlying metal. The calculated STM images are in perfect agreement with the experimental images, which confirm both the atomic structure model and the two-dimensional character of the oxide formed. Compared to the initial perovskite structure, the 2D oxide films obtained after reduction are under stoichiometric both in oxygen and in strontium. Electronic effects are found important parameters that influence the formation of quasicrystalline ultra-thin oxides. Up to now, experimentalists have mainly focused on BaTiO 3 /Pt and SrTiO 3 /Pt, because of the small size mismatch with Pt. We strongly believe that many complex 2D oxide quasiperiodic or approximant systems remain to be discovered.

References
[1] T. T. Dorini et al., Two-dimensional oxide quasicrystal approximants with tunable electronic and magnetic properties, Nanoscale, 13, 10771 (2021)
[2] C. Ruano Merchan et al., Two-dimensional square and hexagonal oxide quasicrystal approximants in SrTiO 3 films grown on Pt(111)/Al 2 O 3 (0001), Phys. Chem. Chem. Phys., 24, 7253 (2022)
[3] E. Cockayne et al., Structure of Periodic Crystals and Quasicrystals in Ultrathin Films of Ba-Ti-O, Phys. Rev. B, 93, 020101 (2016)

Structural model of a 2D quasicrystal approximant

Back to Table of contents

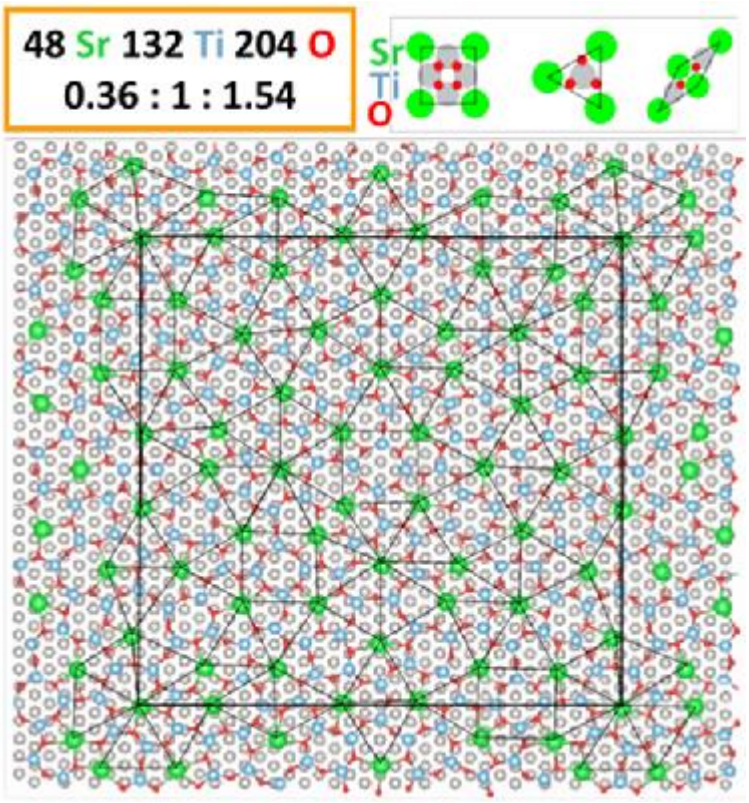

Back to Table of contents

MS21 Aperiodic crystals in organic and inorganic compounds and soft condensed matter

MS21-1-3 Towards understanding of structure modulation in macromolecular system of Hyp-1/ANS protein complex
#MS21-1-3

J.M. Smietanska [1], I.I.I. Buganski [1], J. Sliwiak [2], M. Jaskolski [2], M. Gilski [2], Z. Dauter [3], R. Strzalka [4], J. Wolny [4]
[1]AGH University of Science and Technology - Krakow (Poland), [2]Center for Biocrystallographic Research, Institute of Bioorganic Chemistry, Polish Academy of Sciences - Poznan (Poland), [3]3Synchrotron Radiation Research Section, MCL, National Cancer Institute, Argonne National Laboratory, Argonne - Argonne (United States), [4]AGH University of Science and Technology - Kraków (Poland)

Abstract
The phenomenon of crystal structure modulation is quite widespread and well-understood in small-molecule crystallography, but in macromolecular crystallography is almost unheard of [1]. Modulated structures are characterized by the disappearance of short-range translational order restored in long-range by an atomic modulation function (AMF). Rigorous analysis of incommensurate modulation requires interpretation of diffraction pattern as a three dimensional projection of a higher dimensional reciprocal lattice [2]. Existing, routinely used procedures for solving and refinement of protein structures are not suitable for complex analysis of modulated structures. In cases of incommensurate modulation even the data processing might be an insurmountable problem. Our research include analysis of Hyp-1/ANS protein complexes using a higher-dimensional approach with modulation vector implemented as another dimension. Any assumptions of commensurateness were rejected and special corrections for twinning, pseudosymmetry and structural disorder such as phonons were introduced to improve structure model and reduce high R factors values. Deviation of atom position relative to its average position in three-dimensional space can be reconstructed by shape of the AMF. As a model structures, unique Hyp-1/ANS modulated protein complexes were chosen [1,3]. The re-integration of raw data was performed in CrysAlisPro software with detailed analysis of weak satellite reflections, while phase problem was resolved using Superflip – software based on charge flipping algorithm. For structure modelling and refinement, original software written in Matlab environment with introduced corrections for structural disorder was used. Optimization method used during refinement based on metaheuristics and genetic algorithms against traditional maximum likelihood targets. Therefore, new software dedicated to structure analysis of modulated macromolecular systems will be shared to other users.

References
[1] Sliwiak, J., Dauter, Z., McCoy, A., Jaskolski, M. & Read, R.J. (2014). Acta Cryst. D70, 471-480.
[2] Wolny, J., Buganski, I., Kuczera, P. & Strzalka, R. (2016). J. Appl. Crystallogr. 49, 2106-2115.
[3] Sliwiak, J., Dauter, Z., Kowiel, M., McCoy, A., Read, R.J & Jaskolski, M. (2015). Acta Cryst. D71, 829-843.

Back to Table of contents

MS21 Aperiodic crystals in organic and inorganic compounds and soft condensed matter

MS21-1-4 Resonant „forbidden" reflections in aperiodic crystals
#MS21-1-4

G. Beutier [1], M. De Boissieu [1], G. De Laitre [1], G. Chahine [1], N. Blanc [2], S.P. Collins [3], G. Nisbet [3], S.R. Kotla [4], S. Van Smaalen [4], P. Gille [5], E.N. Ovchinnikova [6], V.E. Dmitrienko [7]
[1]Univ Grenoble Alpes - CNRS - SIMaP - Grenoble (France), [2]CNRS - Institut Néel - Grenoble (France), [3]Diamond Light Source - Grenoble (United Kingdom), [4]Universität Bayreuth - Bayreuth (Germany), [5]Universität München - München (Germany), [6]Moscow State University - Moscow (Russian Federation), [7]Shubniov Institute of Crystallography - Moscow (Russian Federation)

Abstract
Some symmetries in crystal structures are responsible for systematic extinctions of reflections (for instance, in crystals with face-centered lattice, it is well known that reflections are allowed only if h, k and l are of the same parity). Nevertheless, in the case of glide plane and screw axes symmetries, the forbidden reflections can be observed at an X-ray absorption edge of the material, thanks to the anisotropy of the tensor of scattering, which encodes the local electronic anisotropy of the resonant atoms [1,2]. Such resonant "forbidden" reflections are well known for periodic crystals.
In this contribution, we present the first experimental demonstration (to our knowledge) of such reflections in aperiodic crystals. We present results on crystals from two classes of aperiodic crystals: d-AlCoNi, a decagonal quasicrystal (Figure 1), and Rb2ZnCl4, an incommensurately modulated crystal (Figure 2). In the former case, the forbidden reflections are mostly due to the intrinsic symmetry of the quasicrystal. In the latter case, however, the intensity of forbidden reflections can be related to atomic displacements with respect to the symmetric (commensurate) structure [3], similarly to the case of a few periodic crystals [4–9].

References
[1] Dmitrienko, Acta Cryst. A 39, 29–35 (1983).
[2] Templeton & Templeton, Acta Cryst. A 41, 133-142 (1985).
[3] Dmitrienko & Ovchinnikova, Acta Cryst. A 56, 340-347 (2000).
[4] Kokubun et al, Phys. Rev. B 64, 073203 (2001).
[5] Kirfel et al, Phys. Rev. B 66, 165202 (2002).
[6] Collins et al, Phys. Rev. B 68, 064110 (2003).
[7] Beutier et al, Eur. Phys. J. Special Topics 208, 53–66 (2012).
[8] Richter et al, Phys. Rev. B 89, 094110 (2014).
[9] Beutier et al, Phys. Rev. B 92, 214116 (2015).

(1 0 0 -1 3) forbidden reflection in Al-Co-Ni

Back to Table of contents

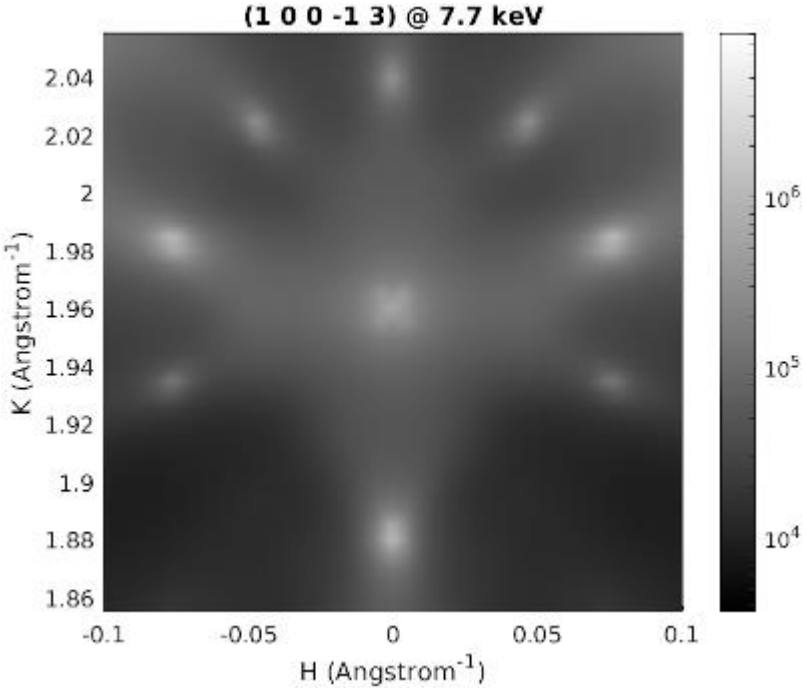

Spectrum of the 700 reflection of Rb2ZnCl4.

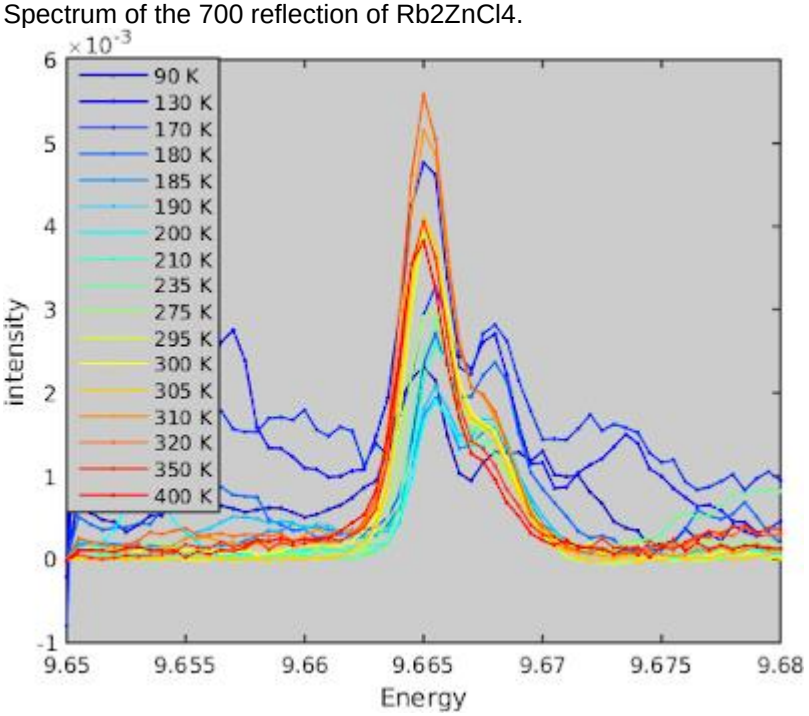

Back to Table of contents

MS21 Aperiodic crystals in organic and inorganic compounds and soft condensed matter

MS21-1-5 The incommensurate composite structure of the misfit layer compound PbS1.12VS2 #MS21-1-5

C. Antunes Correa [1], J. Volný [2], K. Uhlířová [2], T. Verhagen [2]
[1]Institute of Physics of the Czech Academy of Sciences - Prague (Czech Republic), [2]Faculty of Mathematics and Physics, Charles University - Prague (Czech Republic)

Abstract
Transition metal dichalcogenides (TMD) have been attracting attention due to their promising use in photonic [1,2], biological [3], and chemical applications [4]. As an alternative to the standard light-emitting devices (LEDs), which lacks the emission of chirally polarized light at room temperature, TMD semiconductors can be used to obtain intrinsically and controllable chiral LEDs. One of the configurations of chirally polarized LED configurations is the stacking of different types of semiconductors [5]. The whole spectral range from the far-infrared to the ultraviolet can be spanned by creating heterostructures formed by superlattices of two layers of semiconductors. Misfit layer compounds (MLC) [6] intrinsically form a superlattice consisting of stacking of a layer of a transition metal monochalcogenides (TMM) and one of a TMD, with a general composition of $(MS)_{1+x}TX_2$, where, M is Sn, Pb, Sb, Bi, or a rare earth element; T is Ti, V, Cr, Nb or Ta; X is S or Se; $0.08<x<0.28$.
In this work, single-crystals of t$PbS_{1.12}VS_2$ were prepared by chemical vapor transport, which were measured using single-crystal x-ray diffraction. The crystal structure is an incommensurate composite with alternated stacking of the subsystems PbS and VS_2, with the stacking perpendicular to the ab plane. The interaction between the sublattices corresponds to a perturbating potential, which causes the modulation of each of the sublattices and, consequently, satellite reflections are present on the diffraction patterns. The crystal structure will be described using the superspace group formalism, where a wave vector **q** is the reciprocal lattice vector **b*** from the subsystem VS_2 and is a modulation of the subsystem PbS.

References
[1] Krasnok, A.; Lepeshov, S.; Alú, A. Nanophotonics with 2D Transition Metal Dichalcogenides [Invited]. Opt. Express 2018, 26 (12), 15972. https://doi.org/10.1364/OE.26.015972.
[2] Mak, K. F.; Shan, J. Photonics and Optoelectronics of 2D Semiconductor Transition Metal Dichalcogenides. Nature Photon 2016, 10 (4), 216–226. https://doi.org/10.1038/nphoton.2015.282.
[3] Hu, H.; Zavabeti, A.; Quan, H.; Zhu, W.; Wei, H.; Chen, D.; Ou, J. Z. Recent Advances in Two-Dimensional Transition Metal Dichalcogenides for Biological Sensing. Biosensors and Bioelectronics 2019, 142, 111573. https://doi.org/10.1016/j.bios.2019.111573.
[4] Lv, R.; Robinson, J. A.; Schaak, R. E.; Sun, D.; Sun, Y.; Mallouk, T. E.; Terrones, M. Transition Metal Dichalcogenides and Beyond: Synthesis, Properties, and Applications of Single- and Few-Layer Nanosheets. Acc. Chem. Res. 2015, 48 (1), 56–64. https://doi.org/10.1021/ar5002846.
[5] Withers, F.; Del Pozo-Zamudio, O.; Mishchenko, A.; Rooney, A. P.; Gholinia, A.; Watanabe, K.; Taniguchi, T.; Haigh, S. J.; Geim, A. K.; Tartakovskii, A. I.; Novoselov, K. S. Light-Emitting Diodes by Band-Structure Engineering in van Der Waals Heterostructures. Nature Mater 2015, 14 (3), 301–306. https://doi.org/10.1038/nmat4205.
[6] Wiegers, G. A. Misfit Layer Compounds: Structures and Physical Properties. Progress in Solid State Chemistry 1996, 24 (1–2), 1–139. https://doi.org/10.1016/0079-6786(95)00007-0.

Back to Table of contents

MS21 Aperiodic crystals in organic and inorganic compounds and soft condensed matter

MS21-2-1 Incommensurately Modulated Rb2ZnCl4
#MS21-2-1

S. Kotla [1], S. Van Smaalen [1], S. Ramakrishnan [2], T. Rekis [3], J. Bao [4], A. Schaller [1], C. Eisele [1], M. De Boissieu [5], G. De Laitre [5], L. Noohinejad [6]
[1]Laboratory of crystallography, University of Bayreuth - Bayreuth (Germany), [2]Department of Quantum Matter, Hiroshima University - Higashihiroshima (Japan), [3]Department of Pharmacy, University of Copenhagen - København (Denmark), [4]Department of Physics, Materials Genome Institute and International Center for Quantum and Molecular structures, Shanghai University - Shanghai (China), [5]University of Grenoble Alpes, CNRS,Grenoble INP - Saint-Martin-d'Hères (France), [6]DESY - Hamburg (Germany)

Abstract
Rubidium Zinc Chloride (Rb_2ZnCl_4) is isostructural to β-K_2SO_4 and shows ferroelectric behavior below 192K [1]. It belongs to A_2BX_4 crystal family and exhibits successive phase transitions which are characteristic of this family. At high temperature it has an orthorhombic structure with Pmcn as its space group with some disorder associated with $ZnCl_4$ tetrahedra, then an incommensurate modulation develops along c-axis at 303K with the wavevector q = (1/3 – δ) c*, where 'δ' is the parameter which shows the incommensurability and it decreases with decreasing temperature. At around Tc = 192K, 'δ' becomes zero and thus Rb_2ZnCl_4 goes from an incommensurately modulated structure to a commensurately modulated structure [2]. Finally, Rb_2ZnCl_4 undergoes an additional phase transition around 75K [3] with a probable monoclinic distortion and additional satellites in a*b* plane. In the incommensurate phase the modulation wave function goes from a harmonic sinusoidal function to a highly anharmonic function as it approaches lock-in phase transition at Tc. The modulation function in the incommensurate phase of Rb_2ZnCl_4 is not only given by displacive modulation but also by the modulations of atomic displacement parameters (ADPs) and anharmonic ADPs [4-5]. In the low temperature phase (T<75K), the additional modulation arises in the ab plane with the wavevector q = 0.5a*+0.5b*. The detailed structural analysis in each phase, especially near the lock-in transition along with the lattice dynamics studies help us to understand the relation between aperiodic order and physical properties.

References
[1] Sawada, S., Shiroshi, Y., Yamamoto, A., Takashige, M., & Matsuo, M. (1977). J. Phys. Soc. Japan 43(6), 2099-2030.[2] Gesi, K. & Iizumi, M. (1979). J. Phys. Soc. Japan 46(2), 697-698.[3] Bagautdinov B. Sh., Shekhtman, V. Sh., (1999) Phyics of Solid State, 41(6): 987-993.[4] Aramburu, I., Friese, K., Perez-Mato, J. M., Morgenroth, W., Aroyo, M., Breczewski, T. & Madariaga, G. (2006). Phy. Rev. B 73, 014112.[5] Li, L., Wölfel, A., Schönleber, A., Mondal, S., Schreurs, A. M. M., Kroon-Batenburg, L. M. J. & van Smaalen, S. (2011). Acta. Cryst. B 67, 205-217.

Back to Table of contents

MS21 Aperiodic crystals in organic and inorganic compounds and soft condensed matter

MS21-2-2 Incommensurately modulated charge density wave phase transition in EuAl2Ga2 #MS21-2-2

H. Agarwal [1], S.R. Kotla [1], S. Ramakrishnan [2], C. Eisele [1], L. Noohinejad [3], M. Tolkiehn [3], B. Bag [4], S. Ramakrishnan [4], S. Van Smaalen [1]
[1]Laboratory of Crystallography, University of Bayreuth, Bayreuth, 95444, Germany - Bayreuth (Germany), [2]Department of Quantum Matter, AdSM, Hiroshima University, Higashi-Hiroshima, 739-8530, Japan - Hiroshima (Japan), [3]P24, PETRA III, Deutsches Elektronen-Synchrotron DESY, Hamburg, 22607, Germany - Hamburg (Germany), [4]Department of Condensed Matter Physics and Materials Science, Tata Institute of Fundamental Research, Mumbai, 400005, India - Mumbai (India)

Abstract

Rare-earth-based intermetallics show superconductivity, magnetic order, and heavy fermionic behavior due to 4f electrons [1]. In Eu-based intermetallics, Eu offers two types of valance states of Eu^{2+} (magnetic) and Eu^{3+}(nonmagnetic) due to an unstable 4-f shell. $EuAl_4$ shows the charge density wave (CDW) at T_{CDW}= 140 K and orders antiferromagnetically below T_N = 15.4 K; however, $EuGa_4$ represents the characteristic of CDW above 1GPa, not at ambient pressure, and orders antiferromagnetically below T_N = 16.4 K [2],[3]. A recent study on $EuAl_2Ga_2$ shows an out-of-plane CDW below ~ 51 K while the magnetic propagation vector lies in-plane below T_N = 19.5 K [4].
The present study reports on the incommensurately modulated charge density wave in $EuAl_2Ga_2$. We have performed a Single-crystal X-ray diffraction (SXRD) experiment at beamline P24 of PETRA-III at DESY (Hamburg, Germany) in the temperature range of 300 K – 20 K. $EuAl_2Ga_2$ possesses tetragonal symmetry with space group I4/mmm at room temperature. Temperature-dependent SXRD experiment reveals the presence of satellite reflections below T_{CDW} with a 1-D modulation vector (0, 0, 0.113). These satellites are used to study the incommensurately modulated charge density wave transition in the material. Our recent study on $EuAl_4$ shows the tetragonal to incommensurately modulated orthorhombic CDW phase transition [5]. We will present the CDW modulated crystal structure as a function of temperature in $EuAl_2Ga_2$.

References

[1]. Ramarao, S. D., Singh, A. K., Subbarao, U. & Peter, S. C. An overview on the structural diversity of europium based ternary intermetallics. J. Solid State Chem. 281, 121048 (2020).
[2]. Nakamura, A. et al. Transport and magnetic properties of $EuAl_4$ and $EuGa_4$. J. Phys. Soc. Japan 84, (2015).
[3]. Stavinoha, M. et al. Charge density wave behavior and order-disorder in the antiferromagnetic metallic series $Eu(Ga_{1-x}Al_x)_4$. Phys. Rev. B 97, 195146 (2018).
[4]. Moya, J. M. et al. Incommensurate magnetic orders and possible field-induced skyrmions in the square-net centrosymmetric $EuGa_2Al_2$ system. (2021) doi:10.48550/arxiv.2110.11935.
[5]. Ramakrishnan, S. et al. Orthorhombic charge density wave on the tetragonal lattice of $EuAl_4$. (2022) doi:10.48550/arxiv.2202.10282.

Back to Table of contents

MS21 Aperiodic crystals in organic and inorganic compounds and soft condensed matter

MS21-2-3 An incommensurately modulated composite structure in the Nd-Ru system
#MS21-2-3

J.M. Hübner [1], S. Lidin [1]
[1]Centre for Analysis and Synthesis, Department of Chemistry,Lund University - Lund (Sweden)

Abstract
Despite the interesting magnetic and superconducting properties of the phases in the binary systems RE-Ru (RE = La, Pr, Nd), the compounds at about 35-38 at.% Ru have remained uncharacterized due to their complex crystal structure [1,2]. High-resolution diffraction experiments (beamline Cristal, synchrotron Soleil, France) on single crystals of the Nd compound revealed a composite structure comprising observable satellites up to very high order (Fig. 1). The partial overlap required manual indexing and processing of the satellite reflections which will be explained in detail in this contribution.The resulting 3D+1 structure was solved in space group *X*4/*nbm*(00*g*)00*ss* with *a* = 15.6130(8) Å, *c* = 6.3258(4) Å, *q* ≈ 2/23. In [001] direction, Nd atoms form chimneys, hosting linear Ru-Ru chains (Fig. 2). This structural arrangement is closely related to that of $Y_{44}Ru_{25}$ [3] and in turn to that of Nd_5Ir_3 (Pu_5Rh_3-type, [4]).
Acknowledgments: The authors are grateful to Pierre Fertey for comprehensive support during beamtime.

References
[1] A. Palenzona, F. Canepa, J. Less-Common Met., 157 (1990) 307 – 313.[2] A. Palenzona, F. Canepa, J. Less-Common Met., 162 (1990) 267-272.[3] M. L. Fornasini, A. Mugnoli, A. Palenzona, J. Less-Common Met., 154 (1989) 149 – 156.[4] D. Paccard, J. Le Roy and J. M. Moreau, Acta Crystallogr. Sect. B, 35 (1979) 1315.

Fig.1. Diffraction pattern of the (h0l) layer.

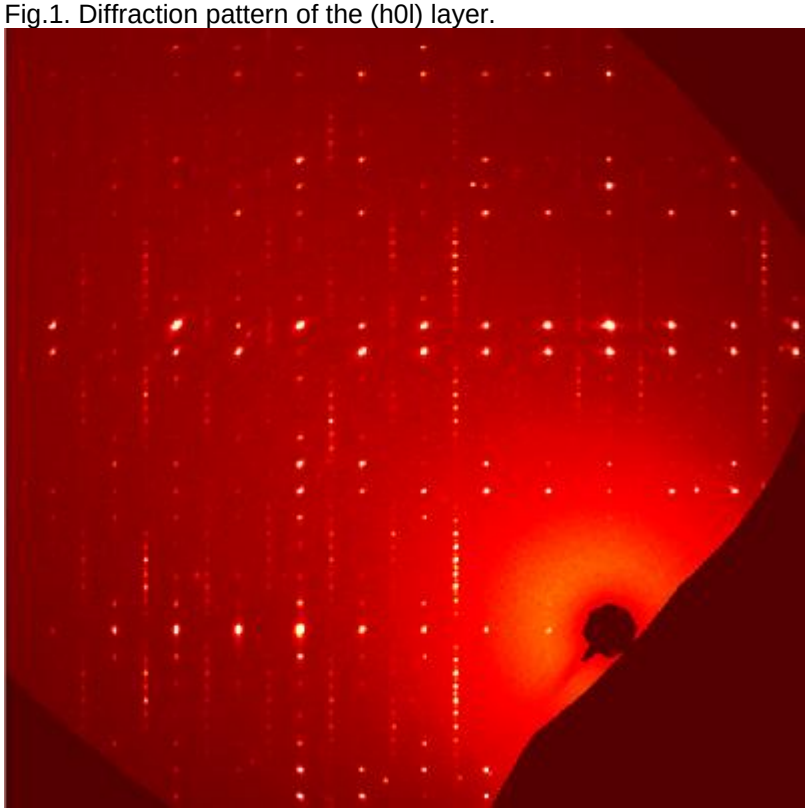

Fig. 2. Nd-chimneys with linear Ru-chains.

Back to Table of contents

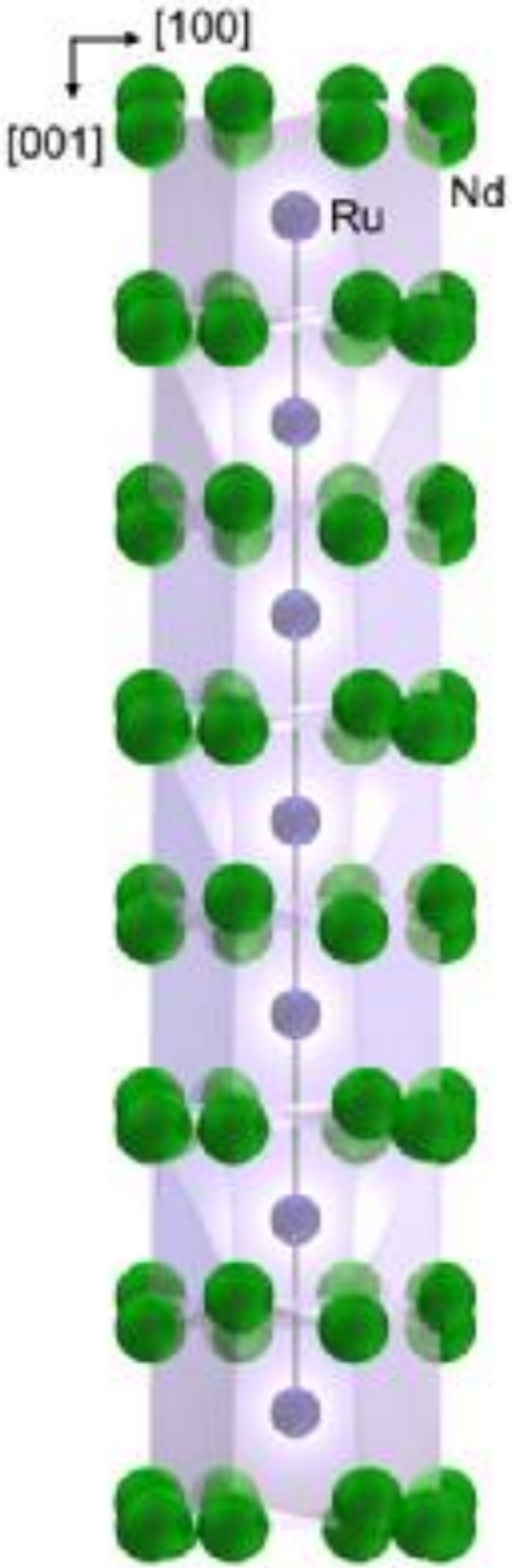

Back to Table of contents

MS23 Quasicrystals and complex intermetallic materials

MS23-1-1 Quasicrystalline structure modelling with the statistical method
#MS23-1-1

J. Wolny [1], R. Strzałka [1], I. Bugański [1], J. Smietańska [1]
[1]AGH University of Science and Technology - Krakow (Poland)

Abstract
Since the discovery of quasicrystals, the higher-dimensional method was extensively used to model the atomic structure of quasicrystals and refinement. The basic idea behind this method is a considering of a quasicrystal as a multidimensional object with periodicity. Only by projecting it on the 3D real space, a quasiperiodic arrangement of atoms is obtained. Higher-dimensional method combined with a cluster approach was used to model a vast majority of quasicrystalline systems [1]. An alternative method, named a statistical method, working in real space only and making use of the concept of the average unit cell, was proposed [2]. Results of using both methods are equivalent to some extent, but some differences, e.g., in modeling structural defects, may appear [4].
Over the last years, the statistical method has found its application in the structure refinement of numerous decagonal and icosahedral quasicrystals (e.g., [1, 2] or very recently [3]). For the very last result of icosahedral CdYb phase, no assumptions on the cluster type were not made, but only 3D Penrose quasilattice was used to refine the structure. In addition, the influence of phasonic flips on the atomic structure at high temperatures was recently discussed. Finally, the macromolecular system with modulation of the atomic positions was investigated [ASIA].
In this presentation, a short introduction to the statistical method will be followed by some exemplar applications of the approach to real systems, including modeling of phonons and phasons.

References
[1] W. Steurer, Acta Cryst. A 74 (2018) 1.
[2] J. Wolny, B. Kozakowski, P. Kuczera, R. Strzalka, J. Wnek, Isr. J. Chem. 51 (2011) 1275.
[3] R. Strzalka, I. Buganski, J. Wolny, Crystals 6 (2016) 104.
[4] J. Wolny, I. Buganski, P. Kuczera, R. Strzalka, J. Appl. Cryst. 49 (2016) 2106.
[5] P. Kuczera, J. Wolny, W. Steurer, Acta Cryst. B 68 (2012) 578.
[6] I. Buganski, J. Wolny, H. Takakura, Acta Cryst. A 76 (2020) 180.
[7] I. Buganski, R. Strzalka, J. Wolny, et al., in preparation.
[8] J. Smietanska, J. Sliwiak, M. Gilski, Z. Dauter, R. Strzalka, J. Wolny, M. Jaskolski, acta Cryst. D 76 (2020) 653.

Back to Table of contents

MS23 Quasicrystals and complex intermetallic materials

MS23-1-2 1/1 and 2/1 QC approximant in the Ce-Au-Al System
#MS23-1-2

J. Valentin [1], P. Boulet [1], G. Lengaigne [1], J. Ledieu [1], V. Fournée [1]
[1]Institut Jean Lamour - Nancy (France)

Abstract
Since the discovery of the stable binary $Cd_{5.7}Yb$ [1] and $Cd_{5.7}Ca$ [2] icosahedral quasicrystals (QCs), there has been an increasing interest in these quasicrystalline structures and their approximants. These quasicrystalline phases, known as Tsai-type QCs, and their related approximants (1/1: $YbCd_6$ Type, SG: *Im-3*, and 2/1: $Yb_{13}Cd_{76}$ SG : *Pa-3*) are built from similar clusters consisting of concentric shells of disordered tetrahedra, dodecahedra, icosahedra, icosidodecahedra and defected triacontahedra from the inside out.
Similar approximant structures, called 1/1 QC approximant, crystallizing with the body centered space group *Im-3*, have been reported in ternary systems like RE-Au-X [3-5], RE-Ag-X [6] with RE = Rare earth, Ca [7] or Na [8] and X a metalloid element or in Sc-Mg-Zn system [9]. All these systems have similar clusters but differ significantly by their respective composition. For example, gold systems usually crystallize with composition around $RE_{15}Au_{65}X_{20}$, for silver it is approximately around $RE_{20}Ag_{40}In_{40}$ and for the Sc-Mg-Zn the 1/1 composition is $Sc_{14}Mg_{0.8}Zn_{84}$ [10]. The same behavior can be observed for the 2/1 approximant.
In this frame, we will concentrate here on the Ce-Au-Al systems, where Kondo effect behavior have been reported recently [10], but without complete structural determination. Indeed to date both quasicrystal approximants have been only reported in the Sc-Mg-Zn [9] and in the Ca-Au-Sn[7] systems. Therefore, this paper will report the structural characterization of both 1/1 and 2/1 approximants in a ternary system where magnetic element like cerium is involved. In both cases, the two approximants' structures have been characterized by powder and single crystal X-ray diffraction.
The single crystal XRD analysis performed on the as-cast sample reveals the existence of two types of structure. First, a body centered cubic structure (Im-3) isotypic to those previously reported for the Ge or Sn-containing systems [3,4] was observed with $a_{1/1}$ = 14.927 Å for the 1/1 approximant. In agreement with the X-ray powder diagram a second crystal analysis reveals the existence of a primitive cubic unit cell with $a_{2/1}$ = 24.12 Å, crystallizing with the *Pa-3* space group and in agreement with the 2/1 approximant reported for the Sc-Mg-Zn and Ca-Au-Sn systems. This paper will precisely describe these two related structures explaining their structural relationship and differences with those already reported in similar systems.

References
[1] A.P. Tsai, J. Q. Guo, E. Abe, H. Takakura and T.J. Sato, Nature 408 (2000) 537.
[2] J. Q. Guo, E. Abe and AP Tsai, Phys. Rev. B 62 (2000) R14605.
[3] P. Boulet, D. Mazzone, H. Noel, P. Rogl R. Ferro, J Alloys and Compds 317-318 (2001), 350.
[4] P. Boulet, M.C. de Weerd, M. Krnel, S. Vrtnik, Z. Jagličić and J. Dolinšek, Inorg. Chem. 60 (2021), 2526.
[5] G. Gebresenbut, R. Tamura, D. Eklöf , C.P. Gomez, J. Phys.: Condens Matter 25 (2013), 135402.
[6] C.P. Gomez, Y Morita, A. Yamamoto, AP Tsai J. Phys Conf Ser 165 (2009), 012045.
[7] Q. Lin and J. D. Corbett, Inorg. Chem. 49 (2010), 10436.
[8] Q. Lin, V. Smetana, G.J. Miller, J.D. Corbett, Inorg. Chem. 21 (2012), 8882.
[9] Q. Lin, J. D. Corbett, J. Am. Chem. Soc. 128,(2006), 13268.
[10]Y. Muro T. Fukuhara, T. Namiki, T. Kuwai, A. Sakurai, A. Ishikawa, S. Suzuki R. Tamura Materials Transactions 62 (2021), 321.

Back to Table of contents

MS23 Quasicrystals and complex intermetallic materials

MS23-2-1 Architecture of rare earth-rich complex intermetallics based on polyicosahedral clusters #MS23-2-1

P. Solokha [1], S. De Negri [1], R. Freccero [1]
[1]Università di Genova - Genova (Italy)

Abstract
The rare earth (*RE*)–transition metal (*T*)–Mg ternary systems are characterized by numerous intermetallic compounds, spread all over the concentration range. Particularly, the rare-earth rich ones make up a large family of compounds, distributed among some characteristic stoichiometries, such as 4:1:1 (*cF*96-Gd_4RhIn), 23:7:4 (*hP*68-$Pr_{23}Ir_7Mg_4$, *hP*68-$Yb_{23}Cu_7Mg_4$), 15:5:2 (*hR*132-$La_{15}Rh_5Cd_2$) and 9:1:4 (*hP*28-Hf_9BMo_4) [1-3] (see figure 1). These complex intermetallics possess common structural features: 1) *T*-centered trigonal prisms with *RE*s at vertices; 2) absence of Mg-*T* interactions; 3) binary core-shell polyicosahedral clusters (PCs), consisting by a core of Mg (formed by one to few atoms) icosahedrally coordinated by *RE*s (see figure 1).In this work, some new members of this family are presented:The RE_4CuMg (*RE* = Yb, Ca) compounds show the very common 4:1:1 stoichiometry but crystallize in a new structure type (*hR*144-Ca_4CuMg, space group *R*-3*m*, *a*=10.376(2) Å, *c*=51.2790(6) Å). Binary core-shell PCs are indeed present, with Mg7@*RE*32 composition, found in this structure for the first time.The $Y_{37}Ni_{13}Mg_4$ compound is the first representative of a *hP*108 structure (space group $P6_3/mmc$, *a*=9.688(2) Å, *c*=34.423(7) Å), corresponding to a stoichiometry never reported before. Binary core-shell PCs of Mg3@*RE*20 and Mg@*RE*12 compositions highlight a similarity with 23:7:4 compounds of $Yb_{23}Cu_7Mg_4$ type.Data on these new compounds, together with those in the literature, evidence that, with the same stoichiometry, some structures, the cubic 4:1:1 and the hexagonal 23:7:4 ($Pr_{23}Ir_7Mg_4$ type), are preferred by typical trivalent *RE*s, instead, the rhombohedral 4:1:1 and the hexagonal 23:7:4 ($Yb_{23}Cu_7Mg_4$ type) are formed by the divalent ones. These structural differences are reflected in the Mg-centered PCs (Mg4 tetrahedral cores for trivalent *RE*s, Mg isolated atoms + Mg3 triangular cores for divalent *RE*s). On the other hand, known Y-rich phases show similarities with both groups, depending on composition.All compounds under consideration stay on the compositional line indicated in pink in figure 1: in fact, their compositions can be described as simple linear combinations of RE_7T_3 and RE_9TMg_4 parent types, as follows:$RE_{37}T_{13}Mg_4$ = RE_9TMg_4 + $4RE_7T_32RE_{15}T_5Mg_2$ = RE_9TMg_4 + $3RE_7T_3RE_{23}T_7Mg_4$ = RE_9TMg_4 + $2RE_7T_34RE_4TMg$ = RE_9TMg_4 + RE_7T_3This fact allows to rationalize the apparently weird and random observed stoichiometries.A deeper crystal structure analysis will be presented leading to a unified description of the architecture of these *RE*-rich intermetallics according to an elegant structural principle. This generalization is useful to guide discovery of new representatives as well as revision of inconsistent data.

References
[1] P. Villars, K. C. Pearson's Crystal Data - Crystal Structure Database for Inorganic Compounds; ASM International, Materials Park, Ohio, USA, 2019/20
[2] P. Solokha et al., Chemistry of Metals and Alloys 2 (2009) 39
[3] S. De Negri et al., Inorganic Chemistry 55 (2016) 8174

Binary core shell PCs in RE-T-Mg compounds

Back to Table of contents

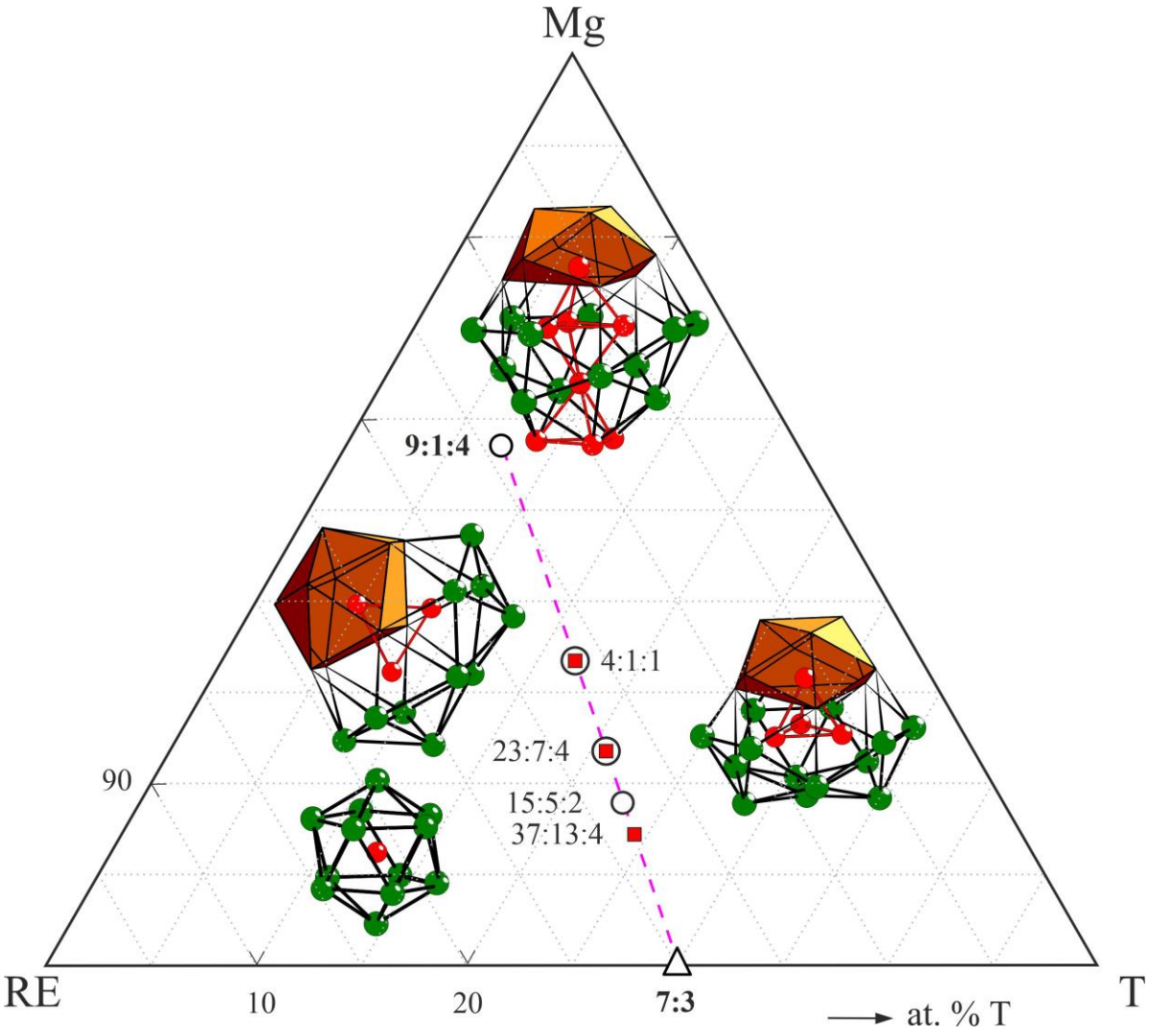

Back to Table of contents

MS23 Quasicrystals and complex intermetallic materials

MS23-2-2 Dual nature od CdYb quasicrystal: The strucutre with Bergman or Tsai clusters?
#MS23-2-2

I. Buganski [1], R. Strzalka [1], J. Wolny [1]
[1]AGH - Krakow (Poland)

Abstract
The atomic structure model of CdYb [1] quasicrystal became a universal standard for all icosahedral quasicrystals with Tsai clusters. The model is praised for its geometrical simplicity and chemical order. Atoms cluster in simple shapes like icosahedron, triacontehedron, etc. Clusters are linked via rhombic faces of triacontahedron along 2-fold axis (b-linkage) and interpenetrate along 3-fold axis (c-lnkage). The unaviodable gaps between clusters are filled with rhombohedral units decorated according to the simple-decoration scheme derived based on identity to existing approximiant periodic strucutres with cubic unit cell.
Recently, a structural model of ZnMgTm icosahedral quasicrystal was developed [2]. The model was founded on different principia than the CdYb model. The unique decoration of rhombohedra in Amman-Kramer-Neri tiling was found and exploited for strucutral study. When the model was interpreted for atomic clusters, the linkage along 5-fold axis was found, that does not exist in periodic approximant crystals. Not only that. The additional linkage discards the neccessity of having interstitial atoms occupying positions outside of clusters making the model interpretable as a covering of triaconsthedral clusters with Bergman inner shells.
Due to the fact that the principia standing behind the model of ZnMgTm are not reserved exclusively to Bergman quasicrystals, we decided to apply the model to CdYb icosahedral quasicrystal. We found out the model can be successfully solved in the tiling-and-decoration scheme with Tsai clusters as a covering. The crystallographic R-factor of the model reached 11.5% for over 5000 symmetry-independent diffraction amplitudes. Not only that. The model can be equally well interpreted as the covering with Bergman clusters what is also evidnet in the electron density maps recovered based on the experimental diffraction aplitudes phased with charge flipping algorithm. Both models will be discussed during the presentation.

References
[1] Takakura, H., et al., Nature Mat. 6 (2007), 58-63
[2] Buganski, I., et al., Acta Cryst. A76 (2020), 180-196

Back to Table of contents

MS23 Quasicrystals and complex intermetallic materials

MS23-2-3 A49Ga2Tl108 (A = K, Rb), examples of mixed trielides of the K49Tl108 structure type.
#MS23-2-3

B.L. Lehmann [1], C.R. Röhr [1]
[1]Albert-Ludwigs Universität - Freiburg (Germany)

Abstract
In the course of our studies on the structures of ternary trielides with mixed triel positions (Ga/In) [1] and (Ga/Tl) [2], we succeeded to synthesize the new compounds $K_{49}Ga_2Tl_{108}$ and $Rb_{49}Ga_2Tl_{108}$. Beside A_8GaTl_{10} (*A* = K, Rb, Cs) [2] with isolated clusters $[Ga@Tl_{10}]^{8-}$, these compounds represent a further example of a structure containing Ga-centered polyhedra, which in this case however are not isolated but part of a three-dimensional network. For the synthesis of both compounds the elemental metals were used in a ratio of $K_{47}Ga_5Tl_{105}$ and $Rb_{49}Ga_{10}Tl_{100}$ respectively. $K_{49}Ga_2Tl_{108}$ could be obtained in pure phase, whereas $Rb_{49}Ga_2Tl_{108}$ was yielded as a byproduct beside the main phase $Rb_{15}Tl_{27}$ [3]. Both compounds are isotypic with the known thallides $K_{49}Tl_{108}$ [4] and $Rb_{49}Tl_{109.7}$ [5] and crystallize in the cubic space group *Pm*-3 ($K_{49}Ga_2Tl_{108}$, *a* = 1722.8 pm, *R*1 = 0.045; $Rb_{49}Ga_2Tl_{108}$, *a* = 1752.7 pm, *R*1 = 0.055). The Ga atoms occupy the Wyckoff positions 1*a* and 1*b*, which are empty in $K_{49}Tl_{108}$ and statistically occupied by Tl in $Rb_{49}Tl_{109.7}$. The trielide polyanion thus consits of Ga-centered icosahedra (Fig. 1. c.) which are all-exo bonded to monocapped Tl-centered hexagonal antiprisms of Tl (Fig. 1. b.). Each of those antiprisms is connected via exo-bonds to four icosahedra and nine neighbouring antiprisms, whereby the exo-bond between the capping atoms is connecting the antiprisms to dumbbells (Fig. 1. a.). The two cluster types are arranged in a hierarchic variant of the Cr_3Si-type with the icosahedra occupying the Si positions and the antiprisms taking the Cr positions. The latter are thus forming non-intersecting chains running parallel to the cell axes. The monocapping of the antiprisms causes a symmetry reduction from the space group *Pm*-3*n* to *Pm*-3, which is described by a Bärnighausen group-subgroup tree. The incorporation of Ga into the icosahedra leads to an increase of the volumes ofthese polyhedra from $71.1 \cdot 10^6$ pm^3 to 74.2 resp. $75.4 \cdot 10^6$ pm^3. The Ga-Tl distances amount to 309 pm and are thus enlarged with respect to the Ga-Tl bond lenghts in A_8GaTl_{10} (290 pm). However, the distances nicely correspond to the value of 313 pm expected on the basis of the metallic radii of Ga and Tl. This indicates considerable metallic bonding contributions. The bonding situation in both the binary and the ternary compounds was analyzed on the basis of band structure calculations.

References
[1] M. Falk, C. Röhr, Stacking polytypes of mixed alkali gallides/indides $A_{1\text{-}2}(Ga/In)_3$ (*A* = K, Rb, Cs), synthesis, crystal chemistry and chemical bonding. *Z. Kristallogr.* 234, 623-646 (2019).
[2] B. Lehmann, C. Röhr, Endohedral ten-vertex clusters $[Ga@Tl10]^{8-}$ in the mixed trielides A_8GaTl_{10} (*A* = K, Rb, Cs). *Z. Anorg. Allg. Chem.* (submitted).
[3] Z. Dong, J. D. Corbett, $A_{15}Tl_{27}$: A Structural Type Containing Both Isolated Clusters and Condensed Layers Based on the Tl_{11} Fragment, Syntheses, Structure, Properties and Band Structure, *Inorg. Chem.* 35(6), 1444-1450 (1996).
[4] V. Müller, G. Cordier, Darstellung und Kristallstruktur von $K_{49}Tl_{108}$. *Z. Naturforsch.* 48b, 1035-1040 (1993).
[5] V. Schwinghammer, S. Gärtner, Effects upon Substitution in Alkali Metal Thallides: How far can X-Ray Structure Determination of Strongly Absorbing Compounds go? *Acta Cryst.* A76 Suppl. (2021).

a. Unit Cell b. Hexagonal Antiprism c. Icosahedron

Back to Table of contents

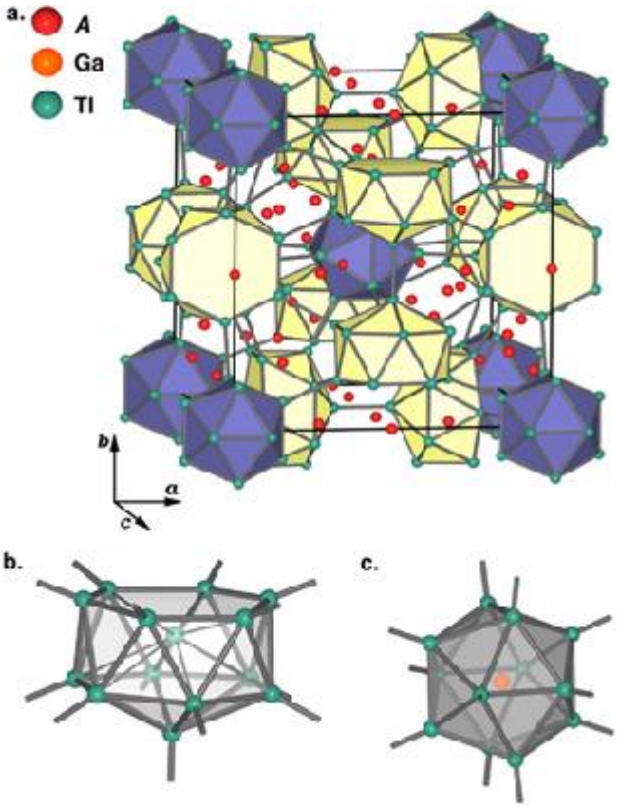

Back to Table of contents

MS23 Quasicrystals and complex intermetallic materials

MS23-2-4 Phase transformation in a decagonal Al-Cu-Rh quasicrystal induced by phasons #MS23-2-4

R. Strzałka [1], I. Bugański [1], J. Wolny [1]
[1]AGH University of Science and Technology - Krakow (Poland)

Abstract
Since the beginning of research on the structure of quasicrystals, the challenging question about the stability of these phases has not been answered with a clear answer [1]. The use of two competing mechanisms of structure stabilization (through entropy or energy minimization) in quasicrystals finds only partial theoretical and experimental verifications. In our presentation, we will present the results of the refinement of the Al-Cu-Rh decagonal structure model based on high-temperature data [2] using a new phason approach [3,4] and a generalized Penrose tiling (GPT) as a quasilattice [5]. Diffraction data were collected at temperatures 293 K and 1013-1223 K. A correlation was observed between lattice parameters and the maximum residual electron density was observed, indicating a phase transformation at around 1083-1153 K. At the same temperatures, the minima of values of moments, which model the phasonic flips, are observed, leading to the conclusion that the transition to a more stable phase is related to phason disorder.
The occurrence of the additional 5th atomic surface in GPT can be obtained by phasonic fluctuation in the ideal structure. In the consecutive refinement we observed that the atomic distribution of an 5th atomic surface correlates with the stability of a structure at the temperature of approximately 1153 K, which could indicate the influence of the phason disorder on the stabilization of the structure [6].

References
[1] M. de Boissieu, Chem. Soc. Rev. 20 (2012) 6778.
[2] P. Kuczera, J. Wolny, W. Steurer, Acta Cryst. B 70 (2014) 306.
[3] I. Buganski, R. Strzalka, J. Wolny, Acta Cryst. A 75 (2019) 352.
[4] I. Buganski, R. Strzalka, J. Wolny, J. App. Cryst. 53 (2020) 904.
[5] M. Chodyn, P. Kuczera, J. Wolny, Acta Cryst. A 71 (2015) 161.
[6] I. Bugański, R. Strzałka, J. Wolny, Acta Cryst. A (submitted, in revision).

Back to Table of contents

MS23 Quasicrystals and complex intermetallic materials

MS23-2-5 A tale of two closely related 1/1 Tasi-type quasicrystal approximants in the RE–Au–M (RE = rare-earth elements, M = p-block elements) systems
#MS23-2-5

S. Ghanta [1], U. Haussermann [2]
[1]Dr. - Stockholm (Sweden), [2]Prof - Stockholm (Sweden)

Abstract
In this work, we review our current understanding of atomic structures, formation conditions, compositions, and temperatures for Tsai and pseudo-Tsai phases 1/1 ACs in the RE–Au–M (RE = rare-earth elements, M = p-block elements) systems. The atomic structures of the 1/1 ACs have been determined from single-crystal X-ray diffraction data and described using concentric atomic clusters with icosahedral symmetry. We hypothesize the presence of pseudo-Tsai phases is a more common phenomenon that occurs in more systems[1,2]. The pseudo-Tsai phases are structurally similar yet physically different from the Tsai phases[3–5]. Tsai-type phases are distinguished by a cluster unit made up of five concentric polyhedral shells: the disordered tetrahedron, a pentagonal dodecahedron, an icosahedron, an icosidodecahedron, and an outer-most triacontahedron. The Tsai phase contains disordered tetrahedron decorated with Au/M mixed sites, Pseudo Tsai phase contains a RE site at the center. Both cluster types can be found coexisting in the approximants. The structural differentiations between Tsai and pseudo-Tsai phases exhibit strong correlations between lattice parameters, cluster sizes, particular site occupancies, and valence electron counts.

References
(1) Gebresenbut, G.; Shiino, T.; Eklöf, D.; Joshi, D. C.; Denoel, F.; Mathieu, R.; Häussermann, U.; Pay Gómez, C. Atomic-Scale Tuning of Tsai-Type Clusters in RE–Au–Si Systems (RE = Gd, Tb, Ho). Inorg. Chem. 2020, 59 (13), 9152–9162. https://doi.org/10.1021/acs.inorgchem.0c01023.
(2) Lin, Q.; Corbett, J. D. M 3 (Au,Ge) 19 and M 3.25 (Au,Ge) 18 (M = Ca, Yb): Distinctive Phase Separations Driven by Configurational Disorder in Cubic YCd 6 -Type Derivatives. Inorg. Chem. 2010, 49 (10), 4570–4577. https://doi.org/10.1021/ic100118q.
(3) Sato, T. J.; Ishikawa, A.; Sakurai, A.; Hattori, M.; Avdeev, M.; Tamura, R. Whirling Spin Order in the Quasicrystal Approximant Au72Al14Tb14. Phys. Rev. B 2019, 100 (5), 054417. https://doi.org/10.1103/PhysRevB.100.054417.
(4) Miyazaki, H.; Sugimoto, T.; Morita, K.; Tohyama, T. Magnetic Orders Induced by RKKY Interaction in Tsai-Type Quasicrystalline Approximant Au-Al-Gd. Phys. Rev. Mater. 2020, 4 (2), 024417. https://doi.org/10.1103/PhysRevMaterials.4.024417.
(5) Gebresenbut, G. H.; Andersson, M. S.; Nordblad, P.; Sahlberg, M.; Pay Gómez, C. Tailoring Magnetic Behavior in the Tb-Au-Si Quasicrystal Approximant System. Inorg. Chem. 2016, 55 (5), 2001–2008. https://doi.org/10.1021/acs.inorgchem.5b02286.

Back to Table of contents

MS23 Quasicrystals and complex intermetallic materials

MS23-2-6 Investigation of chemical order in Gd14AuxAl86-x quasicrystal 1/1 approximants #MS23-2-6

Y.C. Huang [1], G.H. Gebresenbut [1], U. Häussermann [2], C. Pay Gómez [1]
[1]Uppsala University - Sweden - Uppsala (Sweden), [2]Stockholm University - Stockholm (Sweden)

Abstract
Quasicrystals (QCs) exhibit crystallographically forbidden symmetries and aperiodic long range atomic order. whereas approximants of quasicrystals (ACs) possess conventional periodic crystal structures with similar chemical composition and local atom arrangments as their related QCs. For the past 40 years, there has been considerable interest in finding new QCs and ACs, and investigating their physical properties. The effect of chemical composition on magnetic behavior has been recently reported for ACs Gd14AuxAl86-x. [1]. In particular it was found that with increasing Au concentration magnetism changes from spin glass behavior to FM to AFM. In order to better understand the underlying reasons for the observed magnetic properties, it was deemed necessary to determine the crystal structures in detail of Gd14AuxAl86-x. 1/1 ACs for a broader range of x. Therefore, high quality single crystals with different Au/Al ratio have been synthesized using the self-flux method. The phase purity of the samples have been confirmed by EDX and powder XRD techniques. The crystal structures were refined from single crystal XRD data. As a result, some atomic sites show strong chemical preference while others are resilient. The specifics of the chemical ordering phenomenon in Gd14AuxAl86-x 1/1 ACs will be discussed.

References
[1] A. Ishikawa et al., Composition-driven spin glass to ferromagnetic transition in the quasicrystal approximant Au-Al-Gd., Phys. Rev. B 93, 024416 (2016).

Back to Table of contents

MS24 3D electron diffraction

MS24-1-1 In-situ Liquid Phase 3D ED/MicroED for Studying Polymorphism
#MS24-1-1

E. Broadhurst [1], T. Mailk [2], E.C.S. Jensen [2], M.N. Yesibolati [2], K.S. Mølhave [2], H. Xu [1], X. Zou [1]
[1]Stockholm University - Stockholm (Sweden), [2]Technical University of Denmark - Copenhagen (Denmark)

Abstract
In materials, chemistry, and medicine, small molecules can form different crystal structures of the same compound, called polymorphs.[1] Determining the specific atomic structure of a complex molecule and the many polymorphs is echallenging, often requiring X-ray synchrotron or neutron facilities.[2] Understanding how these polymorphs behave in a variety of conditions is crucial to their potential applications. In this work, we aim to combine 3D electron diffraction methods[3] with a novel nanofluidic microchip system[4] and establish a foundational platform to solve new crystal structures of molecular organic crystals and their polymorphs in-situ.

References
1. A. J. Cruz-Cabeza, S. M. Reutzel-Edens, J. Bernstein, Chemical Society Reviews, 2015, 44, 8619-8635.
2. M. Gemmi, E. Mugnaioli, T. E. Gorelik, U. Kolb, L. Palatinus, P. Boullay, S. Hovmöller, J. P. Abrahams, ACS central science, 2019, 5, 1315-1329.
3. L. Samperisi, X. Zou, Z. Huang, CrystEngComm, 2022, 24, 2719-2728.
4. T. Malik, E. C. Stillhoff, M. S. Larsen, M. N. Yesibolati, & K. Mølhave, Microscopy and Microanalysis, 2021, 27, 99-100.

Crystallization of polymorphs of glycine

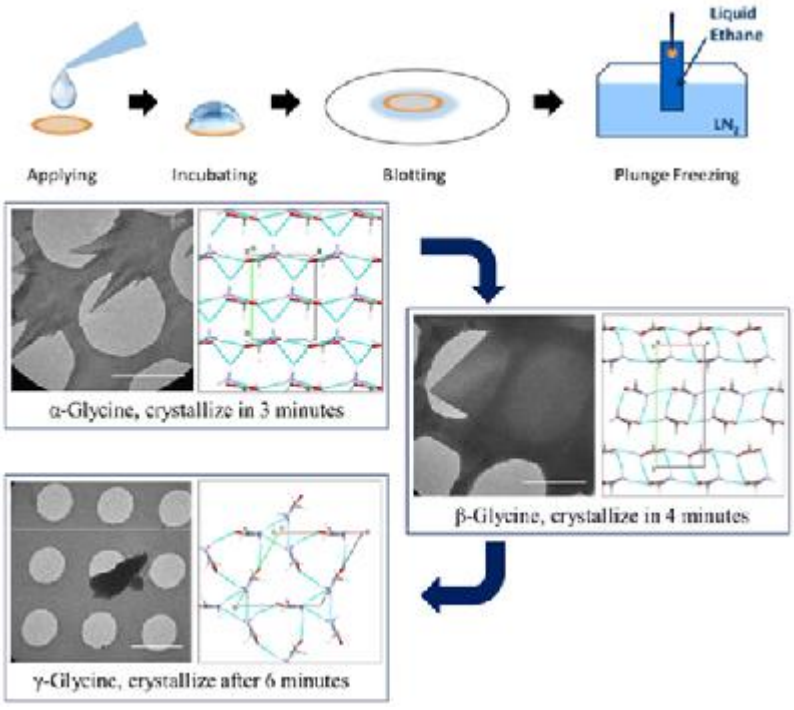

Design of the nanochannel for liquid cell TEM

Back to Table of contents

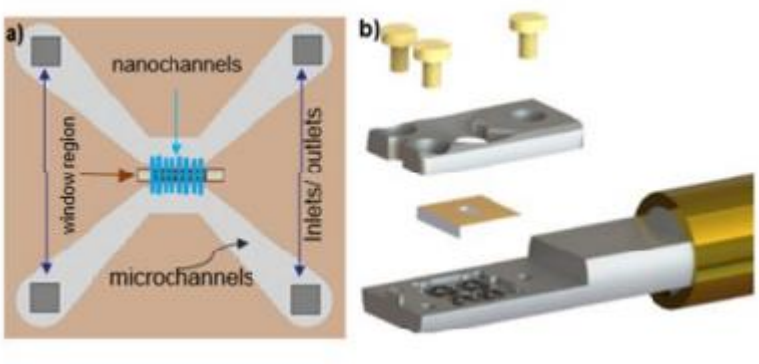

Back to Table of contents

MS24 3D electron diffraction

MS24-1-2 On the Cutting Edge of Electron Diffraction Quality
#MS24-1-2

E. Hovestreydt [1], J. Merkelbach [1], C. Jandl [1], D. Stam [1]
[1]ELDICO Scientific AG - Villigen (Switzerland)

Abstract
Electron diffraction (3D ED) has recently emerged as a powerful tool for structure determina-tion on crystallites in the nanometer range, as it allows to bypass the common bottleneck of growing single crystals, big enough for x-ray diffraction. 3D-ED, using both the continuous rota-tion method and software as we know from X-ray crystallography, is gaining a lot of attention in all fields of research from organic and inorganic molecules, over polymorphism, geological sciences, natural products, biomolecules, material sciences to energy-storage materials and many others.

Here we showcase results from our electron diffractometer, the first entirely dedicated device for 3D ED, on representative case studies dealing with challenging organic compounds to demonstrate the benefits over TEM-based MicroED experiments. Pioneers in the field of electron diffraction already agree that a dedicated device is of great advantage for all fields of nano-crystallography.

As a benchmark and to show the capabilities of a dedicated electron diffractometer, we recently performed 3D ED experiments on Metaxalone, $C_{12}H_{15}NO_3$. Sold as Skelaxin, it is a muscle relax-ant, but its exact mechanism of action is still not known. Metaxalone exhibits various poly-morphic forms with substantial effects on e.g. solubility and bioavailability, one of which could only be obtained[1] as nanometer-sized needles and thus required electron diffraction for accurate structure elucidation.

The data quality obtained is clearly superior to previously reported[1], despite room-tempera-ture data collection, indicating a higher performance of a dedicated diffractometer compared to equipment commonly used until today.

References
[1] V. Hamilton et al., Cryst. Growth Des., 20, 7, 4731–4739 (2020)

Fig.1 Metaxalone from nano-crystal

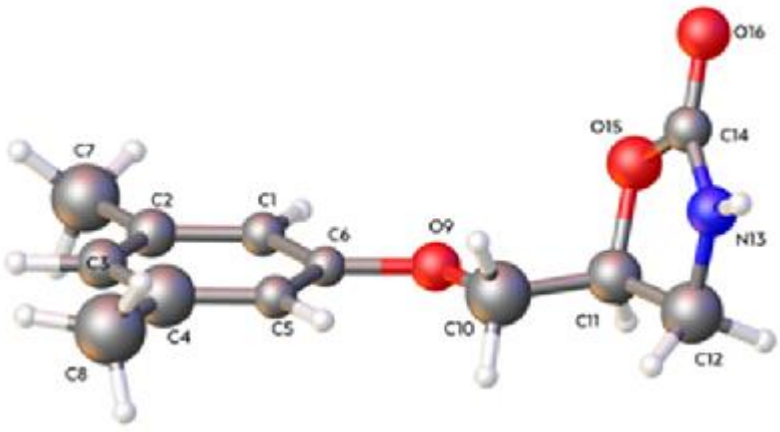

Back to Table of contents

MS24 3D electron diffraction

MS24-1-3 Refinement parameters in dynamical electron diffraction
#MS24-1-3

R. Beanland [1], A. Cleverley [1]
[1]University of Warwick - Coventry (United Kingdom)

Abstract
The structure factor equation elegantly captures the effect of atomic structure on diffracted intensities:
The only parameters are the Miller indices of the diffracted beam g = hkl, the atomic coordinates rj, scattering factor fj, and thermal factor Tj for all N atoms in the unit cell. In X-ray diffraction (XRD), the structure factor Fhkl is chosen to be the point of contact between theory and experiment, taking the diffracted intensity to be given by Ihkl = FhklF*hkl, where F*hkl is the complex conjugate of Fhkl. Other effects such as absorption, extinction, background, mosaicity, scaling, fluctuations in the incident X-ray beam intensity, Lorentz factors and polarisation are taken to be experimental issues, which can be corrected to obtain the 'true' diffracted intensity Ihkl.
In electron diffraction (ED) although the structure factor equation is still important, coupling between different diffracted beams and multiple scattering means that a calculated Ihkl is only approximated by FhklF*hkl, and can be very different when these dynamical diffraction effects are strong. This does not mean that diffracted intensities in ED are fundamentally unreliable – they can be calculated with reasonable accuracy, if the geometry is known to very high precision (<0.5 mrad) at all times (due the exquisite sensitivity of multiple scattering to orientation of the crystal). Furthermore, it is no longer possible to consider scattering effects such as extinction, absorption, background and mosaicity as experimental parameters and they must instead be brought into the calculation of a diffracted intensity.
As a result, the point of contact between experiment and simulation in a dynamical electron diffraction refinement should in principle be rather different to that of X-rays. Here, the experimental corrections in a continuous rotation electron diffraction (cRED) experiment are evaluated for crystals of silicon and tyrosine in comparison with dynamical electron diffraction simulations performed using the Bloch-wave method. (Fig. 1)

Structure Factor Equation

$$F_{hkl} = \sum_{j=1}^{N} f_j(\theta) T_j \exp\left(2\pi i \mathbf{g} \cdot \mathbf{r}_j\right)$$

Fig. 1

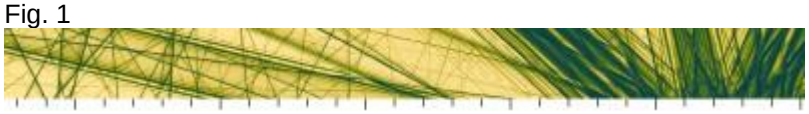

Back to Table of contents

MS24 3D electron diffraction

MS24-1-4 3D ED on isolated nanoparticles: exploring the size limit of crystals
#MS24-1-4

E. Cordero Oyonarte [1], L. Rebecchi [2], V. Pralong [1], I. Kriegel [2], P. Boullay [1]
[1]Normandie Université, ENSICAEN, UNICAEN, CNRS, CRISMAT - CAEN (France), [2]Functional Nanosystems, Italian Institute of Technology - GENOVA (Italy)

Abstract
3D ED [1] brings together different approaches to collect diffraction data on single crystals of much smaller size than those usable for single crystal X-ray diffraction. But what is the minimum crystal size at which it is possible to collect 3D ED data suitable for structure solution and refinement?
In order to address this issue, it is necessary to explore some instrumental constraints. Having a transmission electron microscope (JEOL F200) with a condenser system capable to preserve parallel beam illumination condition for a wide range of beam size and brightness is definitely a plus. Smaller particles mean weaker diffraction signals and the use of a hybrid-pixel detector (M3 Cheetah ASI) is certainly interesting here. Having a goniometer with low movement upon tilting is also nice.
In this contribution, we will show our first results obtained on TiO2 brookite nanorods (about 20 nm x 80 nm in size) where it has been possible to collect PEDT (Precession Electron Diffraction Tomography) data and successfully solve the structure. Taking both precession and dynamical diffraction effects into account [1], the structural model was then refined with very good Robs values (about 8%). From our experimental setup, the accurate structure of nanoparticles above 20 nm is obtained quite straightforward. However, the situation becomes more difficult as the particle size decreases as illustrated here (Fig. 1) in the case of 10 nm ITO nanoparticles. Particle tracking, beam sensitivity and weak diffraction signal are the issues I would like to present and discuss with you.
These results are obtained within the framework of the European project NanED (Electron Nanocrystallography – H2020-MSCA-ITN GA956099).

References
[1] L. Palatinus et al., “Structure refinement using precession electron diffraction tomography and dynamical diffraction: tests on experimental data”, Acta Cryst. B71 (2015) 740–751.

Figure 1

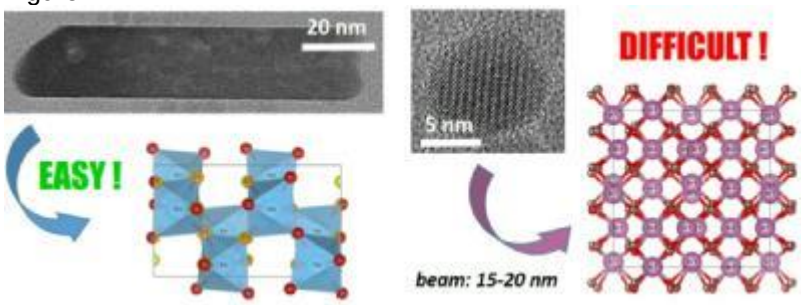

Back to Table of contents

MS24 3D electron diffraction

MS24-1-5 The influence of energy-filtering on kinematical and dynamical structure refinement from 3D ED data #MS24-1-5

M. Cabaj [1], L. Palatinus [1], I. Andrusenko [2], M. Gemmi [2]
[1]Department of Structure Analysis, Institute of Physics, Czech Academy of Sciences, Prague, Czech Republic - Prague (Czech Republic), [2]Istituto Italiano di Tecnologia, Center for Materials Interfaces, Electron Crystallography, Pontedera, Italy - Pontedera (Italy)

Abstract
X-ray diffraction data is a well-established and reliable approach of solid-state structure solution and refinement. Compared to it, electron diffraction is still not as commonly used due to various reasons, one of them being higher figures of merit indicating poorer accuracy of structure refinement. There are many ways to address this problem, ranging from using more complex theoretical approach for structure refinement, to installing additional parts of equipment, which enable collection of higher quality data.
In this work we investigate the influence of energy-filtering on data refined with kinematical and dynamical approach.
Four sets of data – two filtered and two unfiltered – were collected from two crystals of metal-organic polymer containing Zn(II), water and 4,4'-biphenyldicarboxylic acid. For first crystal, the unfiltered data were collected first and the filtered – second. For the other crystal the order of data collection was reversed. This protocol ensures that the observed differences are not due to the radiation damage.
All datasets were processed with PETS2 [1], and then solved and refined with JANA2020 [2]. We processed all four data set in an identical manner to ensure a reliable and unbiased comparison.
In each case we observed some differences in R-factors. For kinematical refinement the R factors were slightly lower for the unfiltered data (less than 1% of difference), with the except of R(all), which was higher for the filtered data. The situation was different for the dynamical approach – all R factors were higher for the unfiltered data, and again – the difference was usually less than 1%.
The obtained results confirm the preliminary hypothesis that the energy-filtering affects the kinematical and dynamical data refinement process in a different way. The change in all R factors is not considerable, but still measurable. Adding an energy-filter negatively affects kinematical refinement, but improves the dynamical one.

	Crystal 1			Crystal 2		
	Filter off	Filter on	Difference(filter off - filter on)	Filter off	Filter on	Difference(filter off - filter
Kinematical refinement						
R(obs)	24.94	25.13	-0.19	26.11	25.95	-0.16
wR(obs)	29.00	29.51	-0.51	30.02	28.91	-1.11
R(all)	32.47	30.78	1.69	29.35	31.46	2.11
wR(all)	29.91	30.35	-0.44	30.37	29.36	-1.01
Dynamical refinement						
R(obs)	10.27	9.78	0.49	12.46	12.94	0.48
wR(obs)	11.73	11.12	0.61	14.16	15.33	1.17
R(all)	16.71	16.24	0.47	15.35	16.26	0.91
wR(all)	13.34	12.78	0.56	14.82	15.94	1.12

This work was supported by the Czech Science Foundation, project number 21-05926X.

References
[1] L. Palatinus, P. Brázda, M. Jelínek, J. Hrdá, G. Steciuk and M. Klementová, "Specifics of the data processing of precession electron diffraction tomography data and their implementation in the program PETS2.0," Acta Cryst. B, vol. B75, pp. 512-522, 2019.
[2] V. Petricek, M. Dusek and L. Palatinus, "Crystallographic Computing System JANA2006: General features," Z. Kristallogr., vol. 229, no. 5, pp. 345-352, 2014.

Back to Table of contents

MS24 3D electron diffraction

MS24-1-6 Crystal Structure Study of Xenon Compounds Using 3D Electron Diffraction.
#MS24-1-6

K. Gurung [1], P. Brázda [1], L. Palatinus [1]
[1]Czech Academy of Sciences - Prague (Czech Republic)

Abstract
The low stability of the xenon compounds in the atmosphere and under the electron beam makes it quite a challenge for their crystal-structure studies using electron diffraction. At the same time, some of these compounds are difficult to crystallize in large crystals, and electron diffraction is the only way to elucidate their structure. Recent progress in 3D electron diffraction (3D ED) makes it a promising technique for studying the crystal structures of these largely unexplored compounds. To verify the feasibility of the application of 3D ED to these compounds, we investigated XeF2 and [XeF][TaF6]. Sample loading was achieved by the use of a glovebox and a homemade construct that utilized liquid nitrogen, preventing the exposure of the sample to moisture. Energy-dispersive X-ray spectroscopy (EDS) confirmed the presence of xenon and fluorine in the loaded sample. The electron diffraction on XeF2 confirmed the presence of this phase. However, the crystal quality was not sufficient to obtain a full single crystal 3D ED data set. However, the compound turned out to be sufficiently stable under the electron beam to potentially permit a 3D ED data collection. These results, albeit preliminary, demonstrate that it is possible to investigate nanocrystalline xenon-containing compounds as well as other air-sensitive and reactive materials by 3D ED.

References
[1] Hargittai, I. Neil Bartlett and the First Noble-Gas Compound. Struct. Chem. 2009, 20 (6), 953.
[2] Levy H., Agron P. The Crystal and Molecular Structure of Xenon Difluoride by Neutron Diffraction, J. Am. Chem. Soc, 1963, 85, 241-242

Back to Table of contents

MS24 3D electron diffraction

MS24-2-1 TAAM refinement in dynamical approach against electron diffraction data
#MS24-2-1

B. Gruza [1], P. Brázda [2], L. Palatinus [2], P. Dominiak [1]
[1]Department of Chemistry, University of Warsaw - Warsaw (Poland), [2]Institute of Physics of the Czech Academy of Sciences - Prague (Czech Republic)

Abstract
In recent years we observe spectacular development of the methods for 3D electron diffraction (3D ED). People learn how to improve data collection, among others how to diminish radiation damage and how to deal with dynamical scattering. Currently, there are available structures from 3D ED with R-factors below 10% and resolution around dmin=0.5Å. For such data and refinement with dynamical approach [1] residual density on bonding paths or lone electron pairs regions can be observed. It led us to the necessity to use more sophisticated, aspherical models of electrostatic potential.
We already proposed TAAM refinements against 3D ED data in kinematic approximation [2]. Now TAAM is coupled with dynamical refinement and available in Jana2020 [3]. Here we present refinements of 1-methyluracil crystal structure against dmin=0.56 Å data with TAAM model in dynamical approach. There is a visible clearing of the residual density map (Figure 1.), also lowering of the maximum and minimum values and further lowering of R-factor. ADPs for non-H atoms become systematically bigger and X-H bonds shorter. In the future we should also be able to go beyond TAAM and refine parameters of the multipole model.
Acknowledgments: This research was funded by National Science Centre, Poland 2020/39/I/ST4/02904

References
[1] L. Palatinus, V. Petricek, and C. A. Correa, Acta Crystallogr. Sect. A Found. Adv., 2015, vol. 71, pp. 235–244.
[2] B. Gruza, M. L. Chodkiewicz, J. Krzeszczakowska, and P. M. Dominiak, Acta Crystallogr. Sect. A Found. Adv., 2020, vol. 76, pp. 92–109.
[3] V. Petrícek, M. Dusek, and L. Palatinus, Zeitschrift für Krist. - Cryst. Mater., 2014, vol. 229, pp. 345–352.

Residual denisty maps

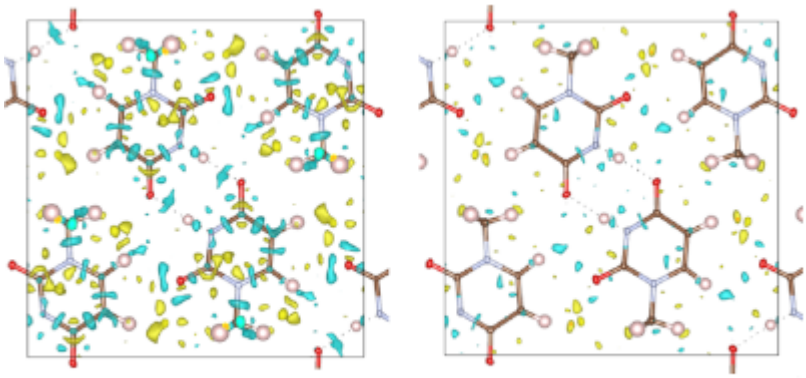

Dynamical IAM refinement (left) and dynamical TAAM refinement (right).
Contour level 0.04 e/Å, yellow: positive, cyan: negative

Back to Table of contents

MS24 3D electron diffraction

MS24-2-2 Implementation of a Dose-Symmetric Tomography Scheme in 3D Electron Diffraction #MS24-2-2

E. Yörük [1], H. Klein [2], S. Kodjikian [2]
[1]Institute of Physics of the Czech Academy of Sciences, Na Slovance 2, Prague, Czech Republic and CNRS, Institut Néel and Université Grenoble-Alpes – Grenoble – France - Prague/Grenoble (Czech Republic), [2]CNRS, Institut Néel and Université Grenoble-Alpes – Grenoble – France - Grenoble (France)

Abstract
3D electron diffraction (3DED) has established itself as a powerful technique to elucidate atomic structures of nano-sized crystals[1]. One of the most commonly encountered issues in the 3DED field is beam damage to crystals under electron exposure, which causes diffraction intensity loss and a decay in data resolution from sensitive crystals[2]. Here we implement the technique of dose-symmetric tomography (DST)[3] employed in the field of cryo-electron tomography (cryoET) into low-dose electron diffraction tomography (LD-EDT)[4] to further improve the signal-to-noise ratio in 3DED.
Starting the acquisition in the low-tilt region, which often provides high-resolution data due to lower apparent thickness, assures that these data are recorded while the crystal is not beam yet damaged (**Figure 1**). The high-tilt frames of the damaged crystal are used for unit cell determination only. Damage-free low-tilt data from multiple particles is then merged for structure determination (**Figure 2**).
We present results obtained on two test samples $Sr_5CuGe_9O_{24}$ and Mn-formiate. Results on $Sr_5CuGe_9O_{24}$, containing 9 independent cation and 13 independent oxygen positions, show that it is possible to get an accurate structure by solely using frames in the +/-10° range from 3 particles. Model accuracy often improves with data completeness by merging more particles, but this is not always the case. Particles that yield only very weak diffraction intensities generate difficulties in the rescaling process and tend to worsen the data quality. The same is true for thick crystals subjected to higher dynamical scattering effects. For Mn-formiate the high tilt diffraction frames clearly showed beam damage effects and it was possible to reduce the range to +/- 8° for the structure solution in SIR2014. All non-hydrogen atom positions were directly obtained with a high accuracy (average distance to the DRX refined positions of 0.1 Å). Dynamical refinement is possible on dose symmetric electron diffraction tomography (DS-EDT) data but requires a certain amount of data completeness.Instead of a tilt range of around 100° in standard 3D ED, DS-EDT only needs a tilt range of 20° or less on an individual crystal to obtain exploitable data. At the same signal-to-noise ratio, the necessary dose can therefore be reduced by an order of magnitude.

References
[1] Mauro Gemmi et al., “3D Electron Diffraction: The Nanocrystallography Revolution,” ACS Central Science 5, no. 8 (2019): 1315–29.
[2] R.F. Egerton, “Radiation Damage to Organic and Inorganic Specimens in the TEM,” Micron 119 (2019): 72–87.
[3] Wim J.H. Hagen, William Wan, and John A.G. Briggs, “Implementation of a Cryo-Electron Tomography Tilt-Scheme Optimized for High Resolution Subtomogram Averaging,” Journal of Structural Biology 197, no. 2 (2017): 191–98.
[4] Stéphanie Kodjikian and Holger Klein, “Low-Dose Electron Diffraction Tomography (LD-EDT),” Ultramicroscopy 200 (2019): 12–19.

Figure 1: Representation of dose-symmetric tomogra

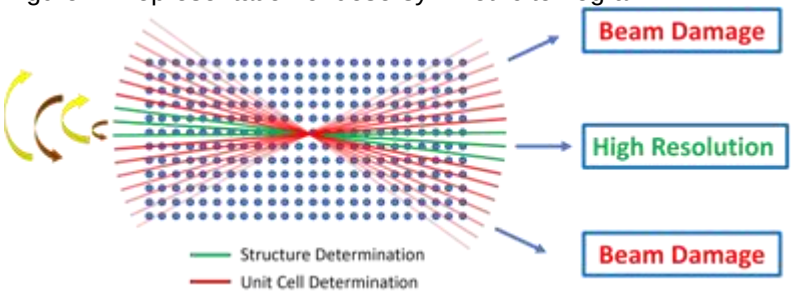

Figure 2: Representation of sub-tomogram averaging

Back to Table of contents

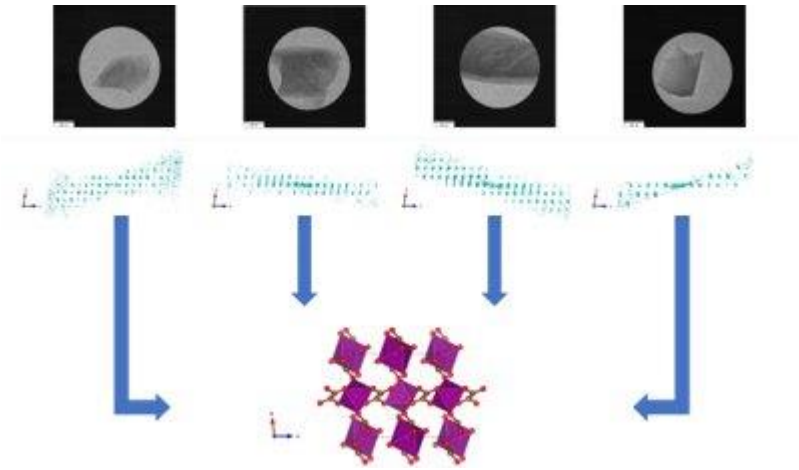

Back to Table of contents

MS24 3D electron diffraction

MS24-2-3 3D scanning precession electron diffraction analysis of nanodomains in thin films
#MS24-2-3

S. Passuti [1], E.F. Rauch [2], A. David [1], P. Boullay [1]
[1]Normandie Université, ENSICAEN, UNICAEN, CNRS, CRISMAT - CAEN (France), [2]SIMAP, Grenoble INP, Université Grenoble Alpes, CNRS - GRENOBLE (France)

Abstract
Strain engineering is an efficient way to modify the ground state of epitaxial thin films in order to induce new features or improve existing properties. One of the challenges in this approach is to quantify structural changes occurring in these films. While X-ray diffraction is the most widely used technique to obtain accurate structural information on bulk materials, severe limitations appear in the case of epitaxial thin films due to the presence of a thick substrate (mm range) for a film thickness usually well below 100 nm.
This last decade, 3D electron diffraction (3D ED) [1], and notably precession electron diffraction tomography (PEDT), has shown its usefulness in the determination of new, metastable, phases stabilized in the form of thin films. While challenging, the determination of unknown structures does actually not represent the major need for thin films. In most cases, the deposited materials have a known structure. The question is not to solve the structure but to know how it differs from the bulk [2].
In this context, our aim is to develop a standard dataset acquisition technique in order to accurately quantify the structure of nano-sized domains in thin films. This can be done by combining the standard PEDT procedure with, for each tilt angle, a line or an area scan across the film section (Fig. 1). Known as scanning precession electron diffraction tomography (SPEDT) and already used for nanocrystalline microstructures analysis [3], this approach has the potential to become the standard procedure to characterize films as thin as 10 nm thanks to constant improvements in the illumination and detection systems of transmission electron microscopes. For thicker films, where strain relaxation might occur, line scan shall be sufficient to obtain structural information about the evolution of the structure versus thickness (Fig. 1a). Executed on an area of the film containing several domains (Fig. 1b), diffracted intensities related to each domain could be recorded and used for structure solution and refinement, increasing in this way the amount of information that can be obtained from a single acquisition.
These results are obtained within the framework of the European project NanED (Electron Nanocrystallography – H2020-MSCA-ITN GA956099).

References
[1] M. Gemmi et al., “3D Electron Diffraction: The Nanocrystallography Revolution”, ACS Central Science 5 (2019) 1315-1329.
[2] G. Steciuk et al., “Precession electron diffraction tomography on twinned crystals: application to CaTiO3 thin films”, J. Appl. Cryst. 52 (2019) 626-636.
[3] E. F. Rauch et al., “New Features in Crystal Orientation and Phase Mapping for Transmission Electron Microscopy”, Symmetry 13 (2021) 1675.

figure 1

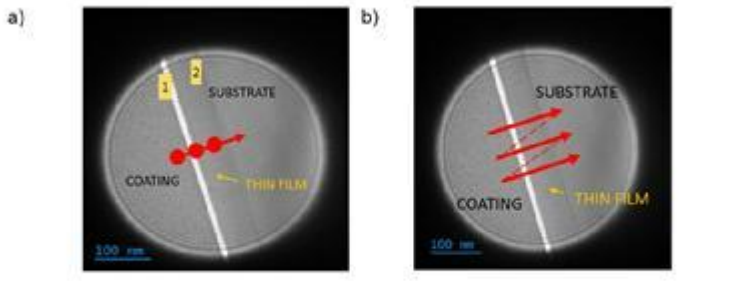

Figure 1: a) Scheme representing a line scan across the sample. The red arrow indicates the direction of the electron beam, while the red dots represent the electron beam at every step where a diffraction pattern is acquired. b) Scheme representing an area scan across the sample. In this case, the electron beam scanned on lines (red arrows) going from the coating to the substrate while acquiring the diffraction patterns.

Back to Table of contents

MS24 3D electron diffraction

MS24-2-4 Dynamical Diffraction Simulations of Continuous Rotation Electron Diffraction Data #MS24-2-4

A. Cleverley [1], R. Beanland [1]
[1]University of Warwick - Coventry (United Kingdom)

Abstract
Structure solution utilizing 3D-ED (three dimensional electron diffraction) has grown in interest since the turn of the 21st century. The interest and accessibility of the technique is due to the increase in computing power, TEM control, detector advances and method developments. However, the R–factor for ED refinements remain far above that of X–ray or neutron diffraction measurements. This is often referred to as the 'R-factor gap'. The cause of this problem is still not completely understood, however the most significant contributing factor is probably multiple scattering, which requires dynamical theory rather than the kinematic models appropriate for other methods such as X-ray diffraction.Here, we use Bloch-wave dynamical electron diffraction simulations using the f elix (Beanland et al., 2019) code to produce large–angle convergent beam electron diffraction (LACBED) patterns that correspond to a continuous rotation electron diffraction (cRED) experiment. In combination with experimental corrections to integrated intensities[1], we find significant reductions in R–factor when comparing experimental data with dynamical intensities rather than kinematical ones.

Fig. 1. Two examples of rocking curves in cRED data taken from a single crystal silicon (110) lamella. Most rocking curves are a simple peak like the $\bar{9}\bar{3}\bar{3}$ reflection in (a). A few rocking curves showed complex (dynamical) structure such as the 311 reflection shown in (b). Corresponding LACBED simulations for a specimen 170nm thick are shown in c) and d), with the nominal beam path marked as a red line and frame numbers marked in yellow. Intensity profiles along the red line give the rocking curves (e) and (f). Applying the angular range of the incident beam as a convolution to the simulation gives simulated rocking curves that are a good match to experiment.

References
Beanland, R., Evans, K., R¨omer, R. A. & Hubert, A. J. M., (2019). Felix bloch wave simulation:Source code. URL: https://github.com/WarwickMicroscopy/Felixx

Fig 1

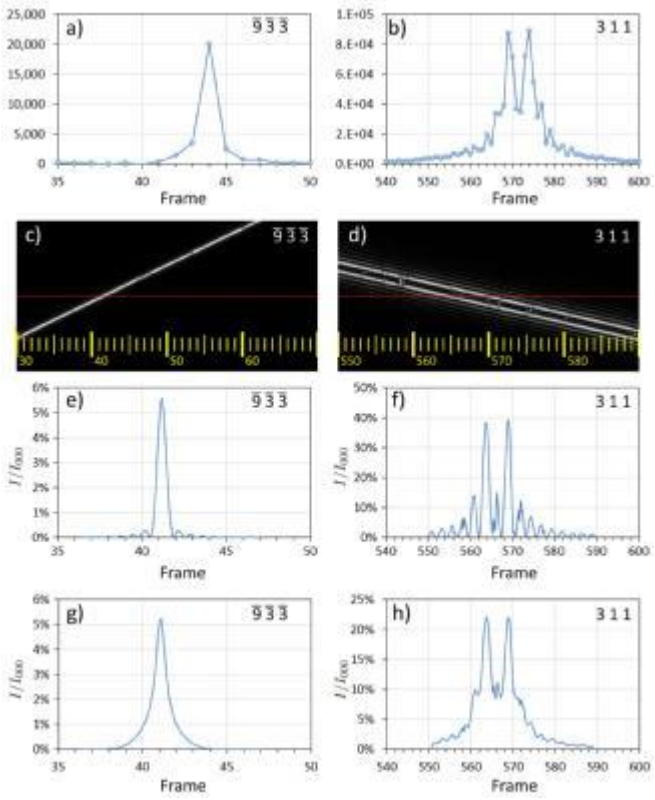

Back to Table of contents

MS24 3D electron diffraction

MS24-2-5 The XtaLAB Synergy-ED: Progress and latest results
#MS24-2-5

F. White [1], R. Bücker [1], M. Meyer [2], M. Jasnowski [2], A. Yamano [3], S. Ito [3], J. Ferrara [4], E. Okunishi [5], Y. Aoyama [5]
[1]Rigaku Europe SE - Neu-Isenburg (Germany), [2]Rigaku Polska - Wrocław (Poland), [3]Rigaku Corporation - Tokyo (Japan), [4]Rigaku Americas Corporation - The Woodlands (United States), [5]JEOL Ltd - Tokyo (Japan)

Abstract
Recognizing the potential of Single-Crystal Electron Diffraction (SC-ED), also known as 3DED and MicroED, Rigaku and JEOL announced a collaboration in 2020 to develop a product designed in a fashion that will make it easy for any crystallographer to use. The resulting product, the XtaLAB Synergy-ED[1], a new and fully integrated electron diffractometer, was released around one year later in May 2021. Many materials only form nanosized crystals or are challenging to produce in large quantities. Before the development of the SC-ED technique, synthetic chemists were forced to rely on other techniques, such as NMR, often in combination with each other, to postulate 3D structure. Unfortunately, the NMR results can be difficult to interpret for complicated molecules such as natural products. SC-ED has become a revolutionary technique for the advancement of structural science. The XtaLAB Synergy-ED is an electron diffractometer operated via CrysAlisPro for a seamless workflow from data collection to structure determination of three-dimensional molecular structures from nanocrystals.
Since its launch, our demo lab XtaLAB Synergy-ED has generated over 160 structures of various samples, see Figure 1, from organics to MOFs, with a range of compositions and cell dimensions. In this presentation, we will provide an overview of the capabilities of the Synergy-ED and review some of more interesting structures that have been determined since May of 2021.

References
[1] Ito, S.; White, F.J.; Okunishi, E.; Aoyama, Y.; Yamano, A.; Sato, H.; Ferrara, J.D.; Jasnowski, M.; Meyer, M; CrystEngComm 2021, 23, 8622-8630

Back to Table of contents

MS24 3D electron diffraction

MS24-2-6 Dynamical Refinement of 3D ED data: comparison of CCD and HPD data
#MS24-2-6

H. Chintakindi [1], L. Palatinus [1]
[1]Department of Structure Analysis, Institute of Physics, Czech Academy of Sciences, - Prague (Czech Republic)

Abstract
Electron crystallography has gained a significant impact and interest over the last few years due to the development of 3D data acquisition techniques and analysis of the obtained 3D Electron diffraction data. The introduction of new, direct detectors provided a significant boost to the speed and data quality of 3D ED data. However, direct comparison of the data quality coming from these new detectors and from more traditional detectors has rarely, if ever, been done on real-life data. Therefore, we decided to profit from our microscope setup which allows easy switching between two detectors and compare the data collection, and structure refinement from both under otherwise identical conditions
The analysis was done on a TEM FEI Tecnai G2 20 with an accelerating voltage of 200 kV, equipped with a CCD detector Olympus SIS Veleta, dynamic range 14 bit, and a hybrid pixel detector Medipix 3 ASI Cheetah. Both detectors are retractable, mounted at the same height at opposite side-entry ports of the microscope, having an almost identical field of view. Therefore, data can be collected on both without changing any alignment settings of the microscope.
Three data sets were collected on a selected crystal of Lutetium Aluminum Garnet ($Lu_3Al_5O_{12}$, LAG) in continuous rotation mode, with varying exposure times.
All the data sets were processed with PETS2[1] software, and the processing parameters like the rocking curve width and mosaicity were kept constant for all data sets. The structure was then solved and refined in JANA2020[2] using the dynamical refinement. Even though results indicate that after kinematical and dynamical refinement, data collected from the CCD detector (C1) has very good R-values, the number of observed reflections was low compared to the other two datasets (H1 and C2). The obtained results depict some differences in the R-factors, Fourier maps, and atomic displacement parameters of the dynamical refinement between the detector systems, but they are still inconclusive to identify the best among the two.

References
1. Palatinus, Lukáš & Brázda, Petr & Jelínek, Martin & Hrdá, Jaromíra & Steciuk, Gwladys & Klementova, Mariana. (2019). Specifics of the data processing of precession electron diffraction tomography data and their implementation in the program PETS2.0. Acta Crystallographica Section B Structural Science, Crystal Engineering and Materials. 75. 512-522. 10.1107/S2052520619007534.
2. Petrícek, Václav & Dusek, Michal & Palatinus, Lukáš. (2014). Crystallographic Computing System JANA2006: General features. Zeitschrift für Kristallographie - Crystalline Materials. 229. 10.1515/zkri-2014-1737.

Comparison of R-factors between HPD and CPD

DETECTORS	HPD	CCD	
	H1	C1	C2
Exposure time	500	1000	2828
KINEMATIC REFINEMENT			
N(obs)	310	231	310
N(all)	310	310	310
R(obs)	30.16	24.34	32.88
wR(obs)	40.64	25.71	46.12
R(all)	30.16	26.85	32.33
wR(all)	40.64	25.89	46.12
DYNAMIC REFINEMENT			
N(obs)	3758	1560	3687
N(all)	3814	3953	3704
R(obs)	9.89	7.88	10.24
wR(obs)	11.12	7.81	11.71
R(all)	9.94	13.48	10.24
wR(all)	11.13	8.22	11.71

Back to Table of contents

MS25 3D electron diffraction for structure solution of organics and proteins

MS25-1-1 Structure determination of a protein-peptide complex using microcrystal electron diffraction #MS25-1-1

A. Shaikhqasem [1], L. Machner [2], F. Hamdi [3], C. Parthier [1], F.L. Kyrilis [3], S.M. Feller [2], P.L. Kastritis [3], M.T. Stubbs [1]
[1]Institute for Biochemistry und Biotechnology, Charles Tanford Protein Center, Martin Luther University Halle-Wittenberg - Halle (Saale) (Germany), [2]Institute of Molecular Medicine (Tumor Biology), Charles Tanford Protein Center, Martin Luther University Halle-Wittenberg - Halle (Saale) (Germany), [3]ZIK HALOmem, Charles Tanford Protein Center, Martin Luther University Halle-Wittenberg - Halle (Saale) (Germany)

Abstract
Developments in microcrystal electron diffraction (MicroED) allow the determination of protein structures from crystals that are too small to be analyzed by conventional X-ray crystallography [1]–[3]. Although the method has been used to determine novel protein structures, it is limited to micro/submicron ultra-thin protein crystals [4], [5]. Due to the limited rotation range of the sample stage in a MicroED setup, completeness of the collected data is restricted by crystal shape, symmetry and orientation on the grid [4], [6]. Here we applied MicroED to determine the structure of a novel complex between an enzyme regulatory domain and an intrinsically disordered peptide. Needle-like crystals in the space group $P2_12_12_1$ were grown using the hanging drop vapor diffusion method. Diffraction data were collected on a 200 kV Thermo Scientific Glacios Cryo-TEM equipped with a CetaD detector. Data were collected along multiple sections of several crystal needles within the limiting rotation range of the sample stage. The performed collection strategy allowed data processing from only two crystals that were oriented perpendicular to each other on the grid, resulting in a 3.2 Å resolution dataset with a merged completeness of 89.3%. Our work represents an effective workflow for obtaining a complete electron diffraction dataset from needle-like protein crystals.

References
[1] B. L. Nannenga, D. Shi, A. G. W. Leslie, and T. Gonen, “High-resolution structure determination by continuous-rotation data collection in MicroED,” Nat. Methods 2014 119, vol. 11, no. 9, pp. 927–930, Aug. 2014.

[2] B. L. Nannenga and T. Gonen, “The cryo-EM method microcrystal electron diffraction (MicroED),” Nat. Methods 2019 165, vol. 16, no. 5, pp. 369–379, Apr. 2019.

[3] M. T. B. Clabbers, A. Shiriaeva, and T. Gonen, “MicroED: conception, practice and future opportunities,” urn:issn:2052-2525, vol. 9, no. 2, pp. 169–179, Jan. 2022.

[4] H. Xu et al., “Solving a new R2lox protein structure by microcrystal electron diffraction,” Sci. Adv., vol. 5, no. 8, pp. 4621–4628, Aug. 2019.

[5] C. Nguyen and T. Gonen, “Beyond protein structure determination with MicroED,” Curr. Opin. Struct. Biol., vol. 64, p. 51, Oct. 2020.

[6] B. L. Nannenga, “MicroED methodology and development,” Struct. Dyn., vol. 7, no. 1, p. 014304, Feb. 2020.

Back to Table of contents

MS25 3D electron diffraction for structure solution of organics and proteins

MS25-1-2 Protein Crystallization 'De-optimization' for MicroED
#MS25-1-2

L. Wang [1], G. Hofer [1], X. Zou [1], H. Xu [1]
[1]Stockholm University - Stockholm (Sweden)

Abstract
Understanding interactions between the protein-active sites and small molecule ligands will provide insights into structure-based drug discovery and following drug development[1]. Recently, the micro-crystal electron diffraction (MicroED) method, developed on the widely available transmission electron microscope (TEM), has shown advantages in providing high-quality structural information[2,3]. Compared with the traditional single X-ray diffraction (SXRD) method, it only needs tiny crystals and enables the investigation of proteins that are difficult to crystalize. Furthermore, micro-crystals may have fewer defects and lower mosaicity than larger ones, which improves stability during ligand soaking or rapid cooling[4–6].
In the previous study, SXRD researchers focused on growing a formidable and well-ordered protein crystal, while protein crystals used for MicroED, on the other hand, are supposed to be small and thin. These plate-like crystals allow the penetration of electrons and minimize multiple scattering. To this aim, methods such as cryo-FIB[7] and fragmentation[8] were introduced to obtain protein crystals with suitable size and morphology. However, direct crystallization without mechanical modification is still challenging. Here we developed a 'de-optimization' crystallization strategy to grow micro-crystals from the protein solution. This general protocol shows the potential to prepare a large concentration of micro-crystals for MicroED experiments.

References
1. Blundell, T. L. Protein crystallography and drug discovery: recollections of knowledge exchange between academia and industry. IUCrJ 4, 308–321 (2017).
2. Clabbers, M. T. B. et al. MyD88 TIR domain higher-order assembly interactions revealed by microcrystal electron diffraction and serial femtosecond crystallography. Nat. Commun. 12, 2578 (2021).
3. Xu, H. et al. Solving a new R2lox protein structure by microcrystal electron diffraction. Sci. Adv. 5, eaax4621 (2019).
4. Wolff, A. M. et al. Comparing serial X-ray crystallography and microcrystal electron diffraction (MicroED) as methods for routine structure determination from small macromolecular crystals. IUCrJ 7, 306–323 (2020).
5. Clabbers, M. T. B., Fisher, S. Z., Coinçon, M., Zou, X. & Xu, H. Visualizing drug binding interactions using microcrystal electron diffraction. Commun. Biol. 3, 417 (2020).
6. Cusack, S. et al. Small is beautiful: protein micro-crystallography. Nat. Struct. Biol. 5, 634–637 (1998).
7. Duyvesteyn, H. M. E. et al. Machining protein microcrystals for structure determination by electron diffraction. Proc. Natl. Acad. Sci. 115, 9569–9573 (2018).
8. de la Cruz, M. J. et al. Atomic-resolution structures from fragmented protein crystals with the cryoEM method MicroED. Nat. Methods 14, 399–402 (2017).

Back to Table of contents

MS25 3D electron diffraction for structure solution of organics and proteins

MS25-1-3 3DED Experimental Parameter Optimization to Metal Organic Frameworks
#MS25-1-3

M. Santucci [1], L. Gemmrich Hernandéz [1], E. Alkhnaifes [2], U. Kolb [1], N. Stock [2]
[1]Centre for High Resolution Electron Microscopy (EMC-M), Johannes Gutenberg University - Mainz (Germany), [2]Institute of Inorganic Chemistry, Kiel University - Kiel (Germany)

Abstract
3D Electron Diffraction (3DED) is nowadays one of the best techniques for structure determination of nano crystalline material. The basis for a successful crystal structure analysis are the acquired data quality and the completeness of expected reflections in the reciprocal space. Dependent on the materials beam sensitivity, micro-crystallinity, agglomeration state and crystal structure complexity, it can be challenging to perform. MOFs usually require cryo-handling, due to electron beam and vacuum sensitivity, and hybrid pixel detectors to maximize the signal-to-noise (S/N) ratio in order to achieve higher quality data, minimize experimental time and electron dose on the sample, avoiding structure modifications. [3,4]
Metal-Organic Frameworks (MOFs) are a class of porous materials with physicochemical properties strictly related to their crystal structure. These compounds, usually display pores of tunable sizes and a 3D crystalline network composed by the interaction between inorganic metal cations and organic ligands through coordination bonds. [1] Thanks to their porous structure, these materials are widely used for small molecules adsorption or guest replacement, heterogeneous catalysis, drug delivery, gas storage, sensing. [2]
In this work, we report a systematic investigation of Pyrazole-3,5-dicarboxylic acid-(acetate)(sulphate)/Iron MOF as synthetized and thermally activated, achieved from ED patterns acquired by a common CCD camera, in a FEI Tecnai F30/S-TWIN Transmission Electron Microscope (TEM), operating at 300 kV. In a first step, the crystal structure of both, the as synthesized and activated material, was solved. Both the previously unknown structures crystallize in the orthorhombic space group $Pna2_1$ and they are characterized by the presence of three iron cations, in a triangle shape and sharing an oxygen in the middle of it. There are two types of interconnections between the irons cations. The first type is bonding two irons by a sulphate and an acetate. Instead, the second one is bonding two irons by the acetate group of two linkers as shown in fig.1. Subsequently, a series of different data acquisition protocols (e.g. illumination, acquisition and camera parameters) were applied and the quality of the collected data sets were compared (fig.2).
Due to this optimization, Fast-Automated Diffraction Tomography (Fast-ADT), a semi-automatic tool for 3DED data acquisition and crystal tracking, could be applied more efficiently. [5] In this way, the electron dose could be minimized for the given setting especially if a CCD camera is used. It could be shown that the quality of crystal structure refinement of a beam sensitive and vacuum sensitive material was improved.

References
[1] M. Gemmi, E. Mugnaioli, T.E. Gorelik, U. Kolb, L. Palatinus, P. Boullay, S. Hovmöller, J.P. Abrahams, 3D Electron Diffraction: The Nanocrystallography Revolution, ACS Cent. Sci. 5 (2019) 1315–1329. https://doi.org/10.1021/acscentsci.9b00394.
[2] A.A. Adeyemo, I.O. Adeoye, O.S. Bello, Metal organic frameworks as adsorbents for dye adsorption: overview, prospects and future challenges, Toxicol. Environ. Chem. 94 (2012) 1846–1863. https://doi.org/10.1080/02772248.2012.744023.
[3] U. Kolb, T. Gorelik, E. Mugnaioli, Automated diffraction tomography combined with electron precession: a new tool for ab initio nanostructure analysis, MRS Online Proc. Libr. 1184 (2009) 38–50. https://doi.org/10.1557/PROC-1184-GG01-05.
[4] N. Portolés-Gil, A. Lanza, N. Aliaga-Alcalde, J.A. Ayllón, M. Gemmi, E. Mugnaioli, A.M. López-Periago, C. Domingo, Crystalline Curcumin bioMOF Obtained by Precipitation in Supercritical CO2 and Structural Determination by Electron Diffraction Tomography, ACS Sustain. Chem. Eng. 6 (2018) 12309–12319. https://doi.org/10.1021/acssuschemeng.8b02738.
[5] S. Plana-Ruiz, Y. Krysiak, J. Portillo, E. Alig, S. Estradé, F. Peiró, U. Kolb, Fast-ADT: A fast and automated electron diffraction tomography setup for structure determination and refinement, Ultramicroscopy. 211 (2020) 112951. https://doi.org/10.1016/j.ultramic.2020.112951.

Fig.1 Structure solution of FeMOF, view along c

Back to Table of contents

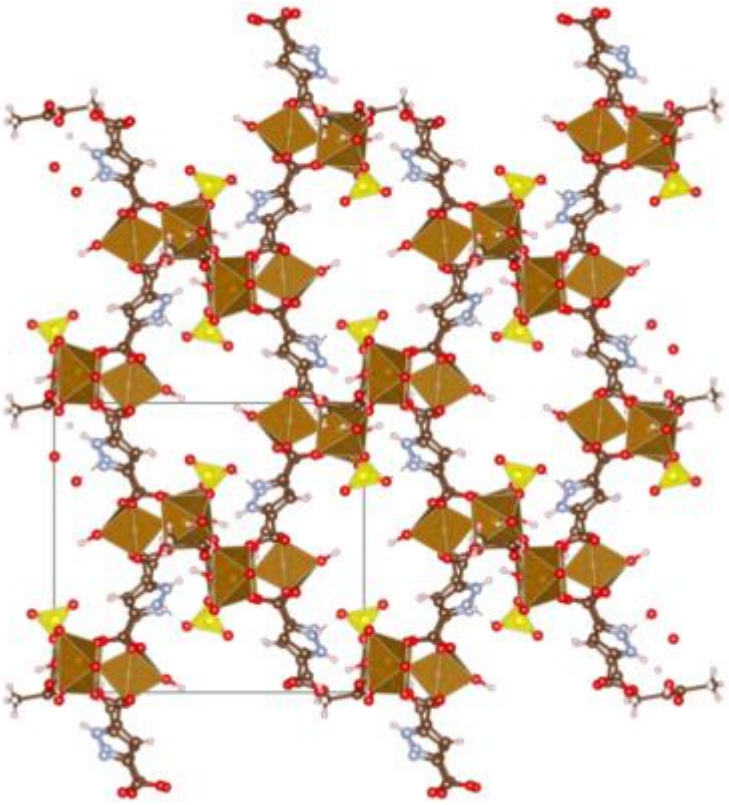

Fig.2 Static ED patterns at different time

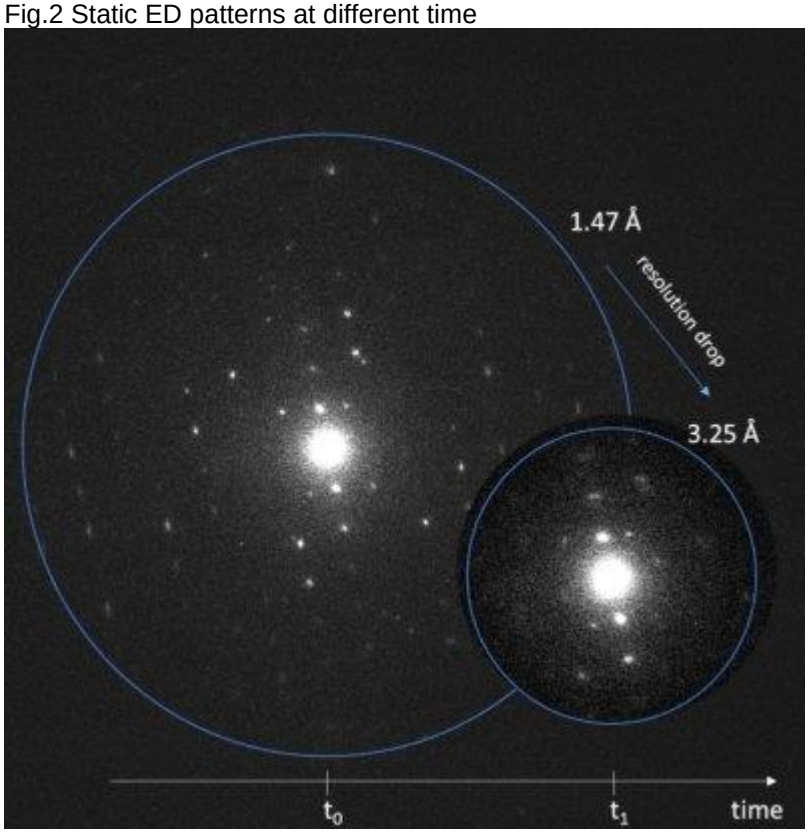

Back to Table of contents

MS25 3D electron diffraction for structure solution of organics and proteins

MS25-1-4 Structure determination study of beam sensitive organics with 3D electron diffraction #MS25-1-4

M. Bauer [1], U. Kolb [1]
[1]Johannes-Gutenberg-Universität - Mainz (Germany)

Abstract
Three dimensional electron diffraction has been proven suitable for a large range of materials including highly beam sensitive crystals [1][2]. In order to speed up data acquisition thus decresing the electron beam damage the majority of these crystal structures have been performed using fast hybrid pixel detectors. Here we demonstrate different settings for successful data acquisition using a slow CCD camera. One of the examples used to demonstrate this is the crystal structure solution of Vitamin B2 (riboflavin) [3] also known as lactoflavin. Riboflavin is a naturally occurring yellow pigment that was first isolated from whey and egg white in 1933 [4]. Riboflavin has the function of a vitamin and is commonly found in milk, liver, kidney, muscle, yeast and plant matter. The human body is supplied with vitamin B2 through nutrition [5]. Depending on which of the eight riboflavin polymorph is present [6], the solubility and thus the bioavailability of the vitamin changes. 3D Electron Diffraction (3DED) combined with electron precession technique was used to determine the structure of the anhydrate riboflavin polymorph.
The three-dimensional electron diffraction data was collected by using Fast-Automated Diffraction Tomography (Fast-ADT) in a FEI Tecnai F30/S-TWIN Transmission Electron Microscope (TEM) equipped with a ULTRASCAN4000 CCD camera. Fast-ADT is a straightforward method and allows a quick data acquisition and crystal tracking with no need for a manual crystal pre-orientation. This can reduce the electron dose during the acquisition and therefore the technique has been proven suitable for beam-sensitive organic materials like the riboflavin [7].
The polymorph A of riboflavin occurs in the orthorhombic space group P212121. Each unit cell contains four riboflavin molecules showing an elaborated hydrogen bonding network where the sugar alcohol D-Ribit side chains of the molecules face each other. Moreover the molecules in the unit cell occur twisted against each other so they are not stacked but appear similar as a herringbone pattern.

References
[1] K. Takaba, S. Maki-Yonekura et al., „Protein and Organic-Molecular Crystallography With 300kV Electrons on a Direct ElectronDetectors", Frontiers in Molecular Biosciences Volume 7, Article 612226, 2021.
[2] B. Bammes, „Sub-Ångström-Resolution MicroED Using a Direct Detection Camera", Microsc. Microanal. 26 (Suppl 2), 2020.
[3] M. Guerain et al., „Structure determination of riboflavin by synchrotron high-resolution powder X-ray diffraction", Acta Cryst. C77, 800–806, 2021.
[4] R. Kuhn, P. György und T. Wagner-Jauregg, „Über Lactoflavin, den Farbstoff der Molke," 1933. [5] J. B. Perkins und J. G. Pero, „Biosynthesis of Riboflavin, Biotin, Folic Acid, and Cobalamin", 1933.
[5] G. F. M. Ball, Vitamins Their Role in the Human Body, Oxford: Blackwell Publishing Ltd, 2004.
[6] E. D. f. t. Q. o. M. &. H. o. t. C. o. E. (EDQM), European Pharmacopoeia Volume 1, Straßburg: Council of Europe, 2019.
[7] S. Plana-Ruiz, Y. Krysiak, J. Portillo, E. Alig, S. Estradé, F. Peiró, U. Kolb, „Fast-ADT: A fast and automated electron diffraction tomography setup for structure determination and refinement", Ultramicroscopy 211, 1129512009, 2020.

Structure solution model of Riboflavin Polymorph A

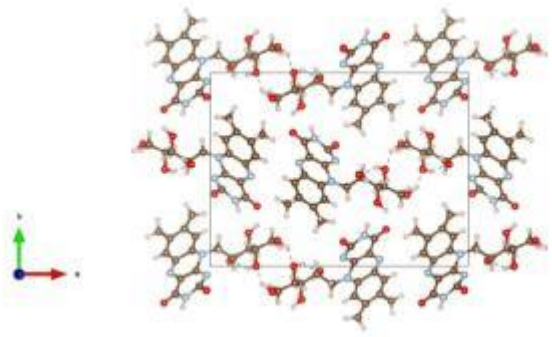

Back to Table of contents

MS25 3D electron diffraction for structure solution of organics and proteins

MS25-1-5 Structural Basis of Higher-order Assembly Formation In Toll-Like Receptor 1 and 2 Signaling Pathway #MS25-1-5

B.B.O.S. Kobe [1], N. Jeff [1], Y.A.N.L. Yan [1], X. Hongyi [2], P. Laura [2]
[1]The University of Queensland - Brisbane (Australia), [2]Stockholm University - Stockholm (Sweden)

Abstract
Toll-like receptors (TLRs) detect pathogens and endogenous danger-associated molecules, initiating innate immune responses that lead to the production of pro-inflammatory cytokines. Signaling by TLRs is initiated by dimerization of their cytoplasmic TIR (Toll/interleukin-1 receptor [IL-1R]) domains, followed by recruitment of the TIR-containing adaptor proteins, including MyD88 (myeloid differentiation primary response gene 88) and MAL (MyD88 adaptor-like/TIRAP). In previous works, we showed the MAL TIR domain can reversibly and spontaneously form filaments in vitro. They also form co-filaments with TLR4 TIR domain and nucleate the assembly of MyD88 TIR domain into crystalline arrays. These results suggest signaling by cooperative assembly formation (SCAF), a prevalent mechanism in innate immunity and cell death pathways. The structural basis of higher-order assembly formation in the TLR1/2 signaling pathways remains obscure.
Here, we show that TLR2 TIR domain directly interacts with the MyD88 TIR domain, and nucleates the assembly of MyD88 TIR domain in vitro. Microcrystal electron diffraction (Micro-ED) is the crucial technique to address the assembly structure. The structure shares a high similarity with the previous MAL TIR domain induced MyD88 TIR domain higher-order assembly. Conformational changes are found at key regions for signaling (e.g., BB loop) compared to the monomeric X-ray structure. We also found that TLR1 TIR domain can co-assemble with MAL into filaments, electron microscopy (EM) studies indicate that the filaments have a different morphology compared with MAL filaments alone. The results shed lights on a conserved SCAF model in the TLR1/2 signaling pathway but may involve more complicated TIR: TIR interactions.

Back to Table of contents

MS25 3D electron diffraction for structure solution of organics and proteins

MS25-2-1 Charge refinement of metal ion cofactors in protein crystals using MicroED
#MS25-2-1

L. Pacoste [1], G. Hofer [1], R. Kumar [1], H. Lebrette [2], C. Choo Lee [3], H. Xu [1], M. Högbom [1], X. Zou [1]
[1]Stockolm University - Stockholm (Sweden), [2]UPS - Tolouse (France), [3]Umeå University - Stockholm (Sweden)

Abstract
Microcrystal electron diffraction (MicroED) is an attractive alternative to X-ray diffraction for studying micro and sub-micron sized protein crystals. In contrast to X-ray diffraction, electron diffraction probes electrostatic potential distribution within the specimen and not electron density. Because of this, MicroED can be used to determine charge states in residues and metal cofactors within metalloenzymes. In the broader perspective, determining charge state of metal cofactors in different states of an enzymatic reaction could provide insight into the charge transfer at the enzyme active site. However, more insight is needed in how different charge states of a metal cofactor are reflected in the electron diffraction data and if this difference is within the accuracy of the experiment.
In this study, the R2 protein of class I ribonucleotide reductase (R2a) containing a diiron center (FeIIIFeIII) has been used as a model protein to simulate electron diffraction data. Data was simulated by calculating the structure factors from an available R2a structure model. The simulated data was further used for structural refinement in SHELXL, using different oxidation states of the iron ions in the refinement model. The refinement outcome could successfully detect the correct charge of the iron in the metal centre. Furthermore, MicroED data has been collected on R2a crystals. Two different strategies, namely cryo-FIB milling and optimization of microcrystals, were explored for preparing crystals. The later method produced ideal plate-like crystals for MicroED data collection up to 2 Å resolution. Future work will focus on optimizing sample preparation for MicroED, collecting high quality data and refining the charge states of diiron centre against experimental data.

Back to Table of contents

MS25 3D electron diffraction for structure solution of organics and proteins

MS25-2-2 Structural Study of Organic Cocrystals Using 3D Electron Diffraction
#MS25-2-2

V.E. Agbemeh [1], D. Sonaglioni [2], I. Andrusenko [2], E. Husanu [2], M. Gemmi [2]
[1]Istituto Italiano Tecnologia (IIT) & University of Parma - Pontedera (Italy), [2]Istituto Italiano Tecnologia (IIT) & University of Pisa - Pontedera (Italy)

Abstract
One of the main limitations on the effectiveness of Active Pharmaceutical Ingredients (APIs) is their low solubility in water resulting in low oral bioavailability. To improve this, one of the proposed solution is cocrystallization with compounds known as Generally Recognized As Safe (GRAS) [1]. APIs cocrystals are composed of two molecules in the same lattice bonded by noncovalent bonds[2].
This work addresses the structural study of lamotrigine and oxyresveratrol cocrystals formed by mechanosynthesis. Ethyl maltol, isonicotinamide, and nicotinamide were used as GRAS coformers.
Mechanosynthesis often leads to the formation of crystals too small for single-crystal x-ray diffraction (SCXRD) hence finding structural information is an extremely hard task.
3D electron diffraction is the most suitable to solve this task with some unique advantages in the analysis of small crystals. In 3D ED single crystal diffraction data of structure solution quality can be collected on grains as small as few hundreds of nanometers[3,4,5]. Thanks to a new generation of single electron detectors this kind of experiment can be performed in low dose, therefore beam sensitive crystals like organics do not amorphized during the duration of the experiment. With the knowledge obtained from the crystal structure, modifications can be made during the intermediate crystallization steps or to the final compounds which can be crucial for the commercialization of APIs.
Our preliminary results show changes in the unit cell parameters of the newly formed cocrystals with respect to their initial precursors which indicate that the process of cocrystallization was achieved.
PXRD has been performed to cross-check the structure derived with electrons diffraction. Despite submicrometric crystals size and a strong stacking disorder their unit cell parameters were successfully determined and used for further crystal structure elucidations.
The authors acknowledge the support from the European Union's Horizon 2020 research and innovation programme under the Marie Skłodowska-Curie grant agreement No 956099 (NanED – Electron Nanocrystallography – H2020-MSCA-ITN).

References
Reference
1. Sakamoto N., Tsuno N., Koyama R., Gato K., Titapiwatanakun V., Takatori K., Fukami T. Four Novel Pharmaceutical Cocrystals of Oxyresveratrol, Including a 2 : 3 Cocrystal with Betaine. Chem Pharm Bull (Tokyo). 2021;69(10):995-1004. doi: 10.1248/cpb.c21-00375. PMID: 34602581.2. Aitipamula S., Banerjee R., Bansal K. A. et. al Polymorphs, Salts, and Cocrystals: What's in a Name? Crystal Growth & Design 2012 12 (5), 2147-2152 doi: 10.1021/cg30029483. Andrusenko I., Potticary J., Hall S.R., Gemmi M. A new olanzapine cocrystal obtained from volatile deep eutectic solvents and determined by 3D electron diffraction. Acta Crystallogr B Struct Sci Cryst Eng Mater. 2020 Dec 1;76(Pt 6):1036-1044. doi: 10.1107/S2052520620012779. Epub 2020 Nov 12. PMID: 33289715.4. Gemmi, M., Mugnaioli, E., Gorelik, T. E., Kolb, U., Palatinus, L., Boullay, P., Hovmöller, S., & Abrahams, J. P. (2019). 3D Electron Diffraction: The Nanocrystallography Revolution. ACS central science, 5(8), 1315–1329. https://doi.org/10.1021/acscentsci.9b003945. Brázda P, Palatinus L. Babor M. Electron diffraction determines molecular absolute configuration in a pharmaceutical nanocrystal 2019J Science P667-669 V 364 6441 doi:10.1126/science.aaw2560

Back to Table of contents

MS26 Quantum mechanical models for dynamics and diffuse scattering

MS26-2-3 Dynamics and disorder: on the stability of pyrazinamide polymorphs
#MS26-2-3

A. Østergaard Madsen [1], T. Rekis [1], A. Hoser [2]
[1]University of Copenhagen - Copenhagen (Denmark), [2]University of Warsaw - Warsaw (Poland)

Abstract
We focus on structures and the relative stability of four pyrazinamide polymorphs. We present new single crystal X-ray diffraction data collected for all forms at 10 K and 122 K. By combining periodic ab-initio DFT calculations with normal mode refinement against X-ray diffraction data, we calculate both enthalpic and entropic contributions to the free energy of all polymorphs. Based on the estimated free energies, we anticipate the stability order of the polymorphs at a given temperature and predict the phase transition temperatures. We conclude that α and γ forms have higher vibrational entropy than that of β and δ and therefore they are significantly more stabilized at higher temperatures. Due to the entropy, which arises from the disorder in γ form, it overcomes form α and is the most stable form at temperatures above c.a. 500 K. Our findings are in qualitative agreement with the experimental calorimetry results.

The four pyrazinamide polymorphs

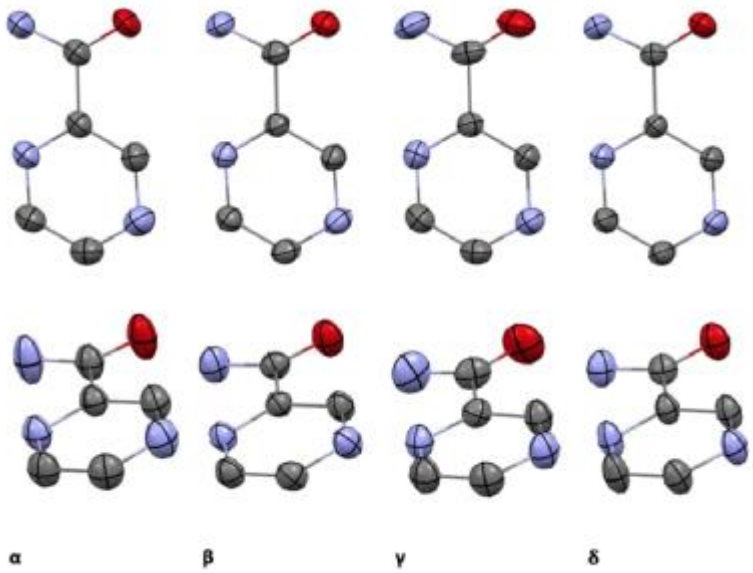

Back to Table of contents

MS27 Minerals and Materials Under Extreme Conditions

MS27-1-1 Behavior of Occupied and Void Space in Molecular Crystal Structures at High Pressure #MS27-1-1

C. Wilson [1], T. Cervenka [1], P. Wood [2], S. Parsons [1]
[1]University of Edinburgh - Edinburgh (United Kingdom), [2]Cambridge Crystallographic Data Centre - Cambridge (United Kingdom)

Abstract
We report a Monte Carlo algorithm for calculation of occupied ("network") and unoccupied ("void") space in crystal structures.[1] The variation of the volumes of the voids and the network of intermolecular contacts with pressure sensitively reveals discontinuities associated with first- and second-order phase transitions, providing insights into the effect of compression (and, in principle, other external stimuli) at a level between those observed in individual contact distances and the overall unit cell dimensions. The method is shown to be especially useful for the correlation of high-pressure crystallographic and spectroscopic data, illustrated for naphthalene, where a phase transition previously detected by vibrational spectroscopy, and debated in the literature for over 80 years, has been revealed unambiguously in crystallographic data for the first time. Premonitory behavior before a phase transition and crystal collapse at the end of a compression series has also been detected. The network and void volumes for 129 high-pressure studies taken from the Cambridge Structural Database (CSD)[2] were fitted to equation of state to show that networks typically have bulk moduli between 40 and 150 GPa, while those of voids fall into a much smaller range, 2–5 GPa. These figures are shown to reproduce the narrow range of overall bulk moduli of molecular solids (ca. 5–20 GPa). The program, called CellVol, has been written in Python using the CSD Python API and can be run through the command line or through the Cambridge Crystallographic Data Centre's Mercury interface.[3] The in situ use of the program shall also be demonstrated by presenting recent results from a high pressure study on glyphosate and the immidiate appearence of phase behaviour when compared to classical methods discussed.

References
1. Wilson, C.J.G., Cervenka, T., Wood, P.A. and Parsons, S., 2022. Behavior of Occupied and Void Space in Molecular Crystal Structures at High Pressure. Crystal Growth & Design.
2. Giordano, N., Beavers, C.M., Kamenev, K.V., Marshall, W.G., Moggach, S.A., Patterson, S.D., Teat, S.J., Warren, J.E., Wood, P.A. and Parsons, S., 2019. High-pressure polymorphism in l-threonine between ambient pressure and 22 GPa. CrystEngComm, 21(30), pp.4444-4456.
3. Groom, C. R.; Bruno, I. J.; Lightfoot, M. P.; Ward, S. C., The Cambridge structural database. Acta Crystallogr. 2016, B72, 171-179.

Back to Table of contents

MS27 Minerals and Materials Under Extreme Conditions

MS27-1-2 In-situ characterization of liquids at high pressure combining x-ray tomography, x-ray diffraction and x-ray absorption using the white beam station of PSICHE.
#MS27-1-2

J-P. Itié [1], L. Henry [1], N. Guignot [1], A. King [1]
[1]Synchrotron-soleil - Gif sur Yvette (France)

Abstract
Study of liquids at extremes conditions has shown a constantly growing interest over the last decades, whether regarding geological and planetary science or more specifically, for the study of polyamorphism in pure substances. The liquid (or amorphous state) is characterized by the lack of long range order. Consequently, characterization of the liquid state often requires to combine two or more techniques in order to obtain different macroscopic and microscopic properties. Among those, the determination of the density at extreme conditions of pressure and temperature may be one of the most widely used as it provides a straightforward diagnosis on elastic properties (such as bulk modulus) of the liquid.
In the early nineties, density measurements using synchrotron radiation and an absorption contrast method based on the Beer-Lambert law was proposed. This technique is designed as follows: two photodiodes are placed below and after the sample position and record respectively the incident and transmitted x-ray intensities as the sample is translated perpendicular to the beam. For a monochromatic x-ray source, the density is obtained through the Beer-Lambert law. The monochromaticity of the x-ray incident beam is of crucial importance as the mass absorption coefficient varies strongly with x-ray energy (e.g. low energies are more absorbed than high energies, far away from the absorption edges). This method is commonly used in the Paris-Edinburgh Press (PEP) and the Multi-Anvils press (MA). Here we describe a new technique allowing the measurement of density taking avantages of the intensity of the white beam. The experiments were carried out on liquid gallium at high pressure using the UToPEC (Ultrafast Tomography Paris Edinburgh Cell) on the white-beam station of the PSICHE beamline at Soleil. Figure 1 shows the experimental setup developed for the density measurements using x-ray white beam and figure 2 the results obtained on liquid gallium.
The strength of the technique is that it can be combined on the beamline PSICHE to other high speed techniques quasi-simultaneously: ultra-fast x-ray computed tomography (XCT), high-speed radiography for imaging and viscosity measurements, fast energy dispersive XRD that can be extended to combined angle and energy XRD (CAESAR [4]) for reliable structural measurements. Such a multi-technical approach, ideally suited to the study of liquid and amorphous materials, has already been described in the past [5], but the addition of this new technique allowing for independent density measurements as well as the speed of acquisitions give totally new options to experimenters.

Psiché experimental setup

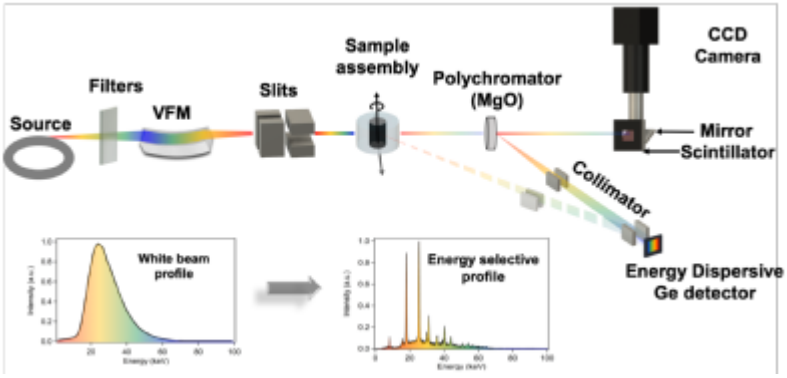

a) XRD pattern of MgO b) absorption results

Back to Table of contents

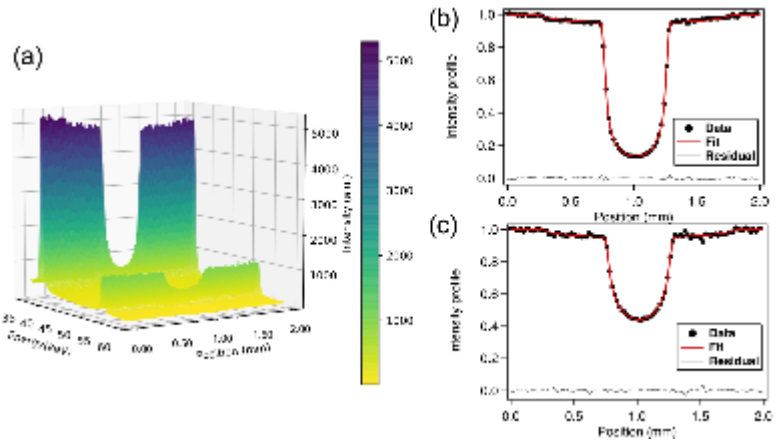

Back to Table of contents

MS27 Minerals and Materials Under Extreme Conditions

MS27-1-3 High-pressure structure and phase behaviour of naphthyl end-capped oligothiophene #MS27-1-3

N. Giordano [1], S. Guha [2], B. Stewart [3], J. Kjelstrup-Hansen [4], M. Knaapila [5]
[1]DESY - Hamburg (Germany), [2]University of Missouri - Columbia (United States), [3]University of Bradford - Bradford (United Kingdom), [4]University of Southern Denmark - Sønderborg (Denmark), [5]Norwegian University of Science and Technology - Trondheim (Denmark)

Abstract
Pressure provides a clean tool to modify molecular packing without chemical interference, including intermolecular separation and relative displacements as shown for optically active materials like π-conjugated molecules.[1] Understanding macromolecular self-organisation is essential in the physics and materials science of π-conjugated molecules giving rise to their intriguing opto-electronic properties and applications.[2,3,4] Brédas and others studied thiophenes including sexithienyls and other π-conjugated molecules and established fundamental principles in how the charge transport and other properties depend on their intermolecular separation and the relative displacements between molecules.[5,6]
Here, we present high-pressure crystal structures of naphthyl end-capped oligothiophene, 5,5′-bis(naphth-2-yl)-2,2′-bithiophene (NaT2), derived from single-crystal X-ray diffraction synchrotron experiments supported by high pressure optical and Raman spectroscopy and molecular modelling. First, we report high pressure crystal structures to 0.8 Å resolution and show reversible unit cell modifications with increasing pressure ending up with a new high-pressure phase at 3 GPa. Second, we describe interaction directionalities and identify new sulfur-hydrogen contacts that demonstrate the fundamental difference between thiophenes and acenes and other fuzed-ring molecules. Our results complement both earlier ambient condition studies of NaT2 and other thiophenes as well as earlier high-pressure studies of small π-conjugated molecules, polymers and other materials.

References
(1) Schmidtke, J. P.; Friend, R. H.; Silva, C. Tuning Interfacial Charge-Transfer Excitons at Polymer-Polymer Heterojunctions under Hydrostatic Pressure. Phys. Rev. Lett. 2008, 100 (15), 157401. https://doi.org/10.1103/PhysRevLett.100.157401.
(2) Da Como, E.; von Hauff, E. The WSPC Reference on Organic Electronics: Organic Semiconductors. Materials and Energy Series. Volume 1: Basic Concepts, Volume 2: Fundamental Aspects of Materials and Applications. Edited by Jean-Luc Brédas and Seth R. Marder. Angew. Chem. Int. Ed. 2017, 56 (18), 4915–4916. https://doi.org/10.1002/anie.201701913.
(3) Mishra, A.; Ma, C.-Q.; Bäuerle, P. Functional Oligothiophenes: Molecular Design for Multidimensional Nanoarchitectures and Their Applications. Chem. Rev. 2009, 109 (3), 1141–1276. https://doi.org/10.1021/cr8004229.
(4) Zhang, L.; Colella, N. S.; Cherniawski, B. P.; Mannsfeld, S. C. B.; Briseno, A. L. Oligothiophene Semiconductors: Synthesis, Characterization, and Applications for Organic Devices. ACS Appl. Mater. Interfaces 2014, 6 (8), 5327–5343. https://doi.org/10.1021/am4060468.
(5) Brédas, J.-L.; Beljonne, D.; Coropceanu, V.; Cornil, J. Charge-Transfer and Energy-Transfer Processes in π-Conjugated Oligomers and Polymers: A Molecular Picture. Chem. Rev. 2004, 104 (11), 4971–5004. https://doi.org/10.1021/cr040084k.
(6) Mannebach, E. M.; Spalenka, J. W.; Johnson, P. S.; Cai, Z.; Himpsel, F. J.; Evans, P. G. High Hole Mobility and Thickness-Dependent Crystal Structure in α,ω-Dihexylsexithiophene Single-Monolayer Field-Effect Transistors. Adv. Funct. Mater. 2013, 23 (5), 554–564. https://doi.org/10.1002/adfm.201201548.

Reversible yellow to red colour change in NaT2

Back to Table of contents

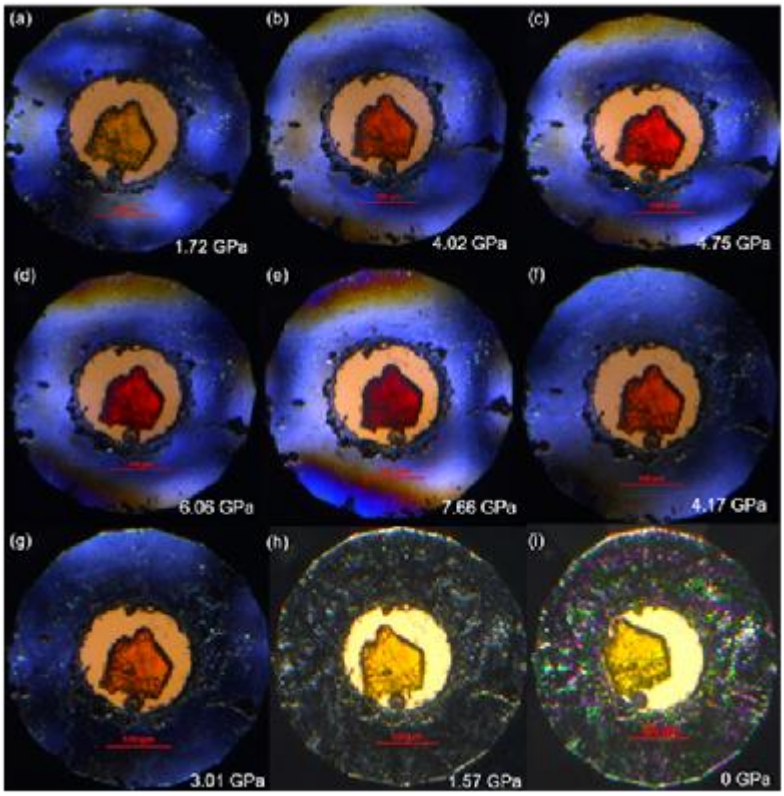

Back to Table of contents

MS27 Minerals and Materials Under Extreme Conditions

MS27-1-4 It's been a long time coming - Temperature dependent structure solution of Rb[SCN] #MS27-1-4

L.C. Folkers [1], F. Tambornino [2]
[1]STOE & Cie GmbH - Darmstadt (Germany), [2]Department of Chemistry and Material Sciences Center, Philipps-Universität Marburg - Marburg (Germany)

Abstract
K[SCN] was the first compound comprising the thiocyanate anion that was crystallographically determined just after the advent of single crystal X-ray diffraction, also introducing its own structure type [1]. The elucidation of the Na and Cs thiocyanates followed in the 1970ties, where the Cs compound was found to show a phase transition at high temperature [2-3]. Surprisingly the structure of Li[SCN] was not published until 2014, even though its hydrate had already been commercially available for years [4].
The synthesis of Rb[SCN] had been established as well in the 1970ties and its phase transition was discovered in the 1990ties [5-6]. However, its low and high temperature structures were only assigned to the K[SCN] structure type and not further investigated.
Rb[SCN] crystallizes in the orthorhombic *Pbcm* space group type at temperatures below 432 K and in the tetragonal *I*4/*mcm* space group type at higher temperatures [7]. The structural details of the low and high temperature phases and their relations to other alkali-metal thiocyanates will be discussed.

References
[1] H. P. Klug, *Z. Krist. – Cryst. Mater.*, **1933**, *85*, 214 – 222.
[2] S. Manolatos, M. Tillinger, B. Post, *J. Solid State Chem*., **1973**, *7*, 31–35.
[3] P. H. van Rooyen, J. C. A. Boeyens, *Acta Crystallogr*., **1975**, *B31*, 2933–2934.
[4] O. Reckeweg, A. Schulz, B. Blaschkowski, Th. Schleid, F. J. DiSalvo, *Z. Naturforsch. B Chem. Sci.*, **2014**, *69*, 17–24.
[5] S. S. Ti, S. F. A. Kettle, Ø. Ra, *Spectrochim. Acta Mol. Spectrosc*., **1976**, *32*, 1603–1613.
[6] A. Fuith, *Phase Trans.*, **1997**, *62*, 1–93.
[7] A. Shlyaykher, T. Pippinger, T. Schleid, O. Reckeweg, F. Tambornino, *Z. Krist. - Cryst. Mater.*, **2022**, *237*, 69 – 75.

Back to Table of contents

MS27 Minerals and Materials Under Extreme Conditions

MS27-1-5 Charge density study on α-glycine under high pressure
#MS27-1-5

S. Sutula [1], M. Malinska [1], R. Gajda [1], A. Makal [1], M. Stachowicz [2], P. Fertey [3], K. Woźniak [1]
[1]Biological and Chemical Research Center, Department of Chemistry, University of Warsaw - Warsaw (Poland), [2]Department of Geology, University of Warsaw - Warsaw (Poland), [3]Synchrotron SOLEIL - Saint-Aubin (France)

Abstract
Nowadays tools for high-pressure experiments become more and more advanced and allow for better quality experiments. Some information, however, is lost during the measurement with the use of diamond anvil cell (DAC), but part of it can be retrieved with a proper data collection and model refinement.
Main objective of this work is to collect high-quality data on α-glycine ($NH3^{+}$–CH2–COO^{-}, $P2_1/n$) at room-temperature under ambient pressure with in-house diffractometer and another under high pressure with the use of synchrotron radiation. Performing refinements of the multipole model against those datasets should give some insights into what are the main challenges of performing charge density studies under high pressure.
In-house diffractometer data was collected with the MoKα radiation with the full completeness up to 1.2 $Å^{-1}$ resolution and high-pressure experiment was carried out under 1.5 GPa and gave completeness of 65% up to the resolution of 1.1 $Å^{-1}$. The collected datasets were reduced, merged and used for refinement of electron density distribution with the application of the multipole model in MoPro[1]. As those abovementioned datasets do not allow for direct comparison, additional file has been artificially created, where the reflections of the high-angle experiment were limited only to those present in the high-pressure experiment. Comparing a model refined on such a dataset with the two based on the original experiments allows for drawing some conclusions on what information is lost when the completeness sharply drops and when the collected raw frames are contaminated with the signal from diamonds and other parts of DAC.
Discrepancies between the obtained models are best illustrated on the differential electron density maps, where two corresponding maps have been subtracted from each other. Employing such a powerful tool, however, should first be preceded with miniscule manual alteration of the final structure files. There are some clearly visible differences between the obtained models refined against the three datasets and they regard the structural, thermal and electronic parameters.
This work was supported by the Foundation for Polish Science, TEAM-TECH Core facility for crystallographic and biophysical research to support the development of medicinal products (co-financed by the European Union under the Regional Development Fund).

References
[1] Guillot, B. et al., J. Appl. crystallogr., 2001, 34, 214-223.

Back to Table of contents

MS27 Minerals and Materials Under Extreme Conditions

MS27-1-6 Highly sensitive, self-healing metal-organic framework
#MS27-1-6

A. Półrolniczak [1], A. Katrusiak [1]
[1]Adam Mickiewicz University - Poznań (Poland)

Abstract
Self-healing of materials is the phenomenon of restoring a damaged material to its primary properties without any external intervention. Wrinkles, cracks and other types of damage appearing on the crystals' surface have been shown to change the physicochemical properties of materials, and their propagation can lead to the eventual destruction of the material. At this point, this type of gradual degradation is almost undetectable and requires manual intervention for eventual repairs. In contrast, the self-healing materials counter degradation through the initiation of a repair mechanism that responds to the micro-damage which can be of invaluable importance for the more durable materials. It is thus important to further explore the concept of self-repair.
We have focused our scientific interest on a porous metal-organic network, $[Cd(BDC)(AZPY)]_n$ (BDC = terephthalic acid; AZPY = 4,4' - azobispyridine) exhibiting the excellent ability to self-repair its single-crystal features. When subjected to a mechanical force, as a result of tilts and conformational changes of the AZPY linkers, the crystals faces of $Cd(BDC)(AZPY)]_n$ becomes fractured and the scratches on the crystal surface start appearing. However when the pressure is released, all arose damages disappear. This process can be efficiently repeated in many compression and decompression cycles.
Appearing damages of the crystal surfaces are strongly connected to the structural changes of $[Cd(BDC)(AZPY)]_n$ under high-pressure. To compensate the mechanical stresses the crystal lattice distorts, leading to a ferroelastic phase transition from the atmospheric phase α of the orthorhombic space group *Cmce* to a high pressure phase β of monoclinic space group $P2_1/n$. The pressure induced transformation orders the –N-N- bridge of the azopyridine, which significantly reduces the lattice strain. Interestingly, depending on the guest molecules filling the voids and the type of used hydrostatic fluid, the phase transition can be observed in the range between 0.2 and 0.9 GPa.
The pleochroic [Cd(BDC)(AZPY)]n crystals exhibits several features attractive for sensor applications. They are sensitive to guest molecules, crystal environment and pressure, but they are almost unaffected by temperature. We have proven that the interplay of the framework topology with the flexibility of linkers can lead to specific types of structural transformations of MOFs.
Acknowledgements: This work was supported by funding from the Polish National Science Centre: PRELUDIUM 18 No. UMO-2019/35/N/ST5/01838 and grant POWR.03.02.00-00-I026/16 co-financed by the EU European Social Fund under the Operational Program Knowledge Education Development.

References
References:
1) G. Wypych, Self-Healing materials: Principles and technology, ChemTec Publishing, 1st edn, 2017. 802) M. D. Hager, S. van der Zwaag and U. S. Schubert, Self-healing Materials, Springer International Publishing, 1st edn, 2016. 813) S. K. Ghosh, Self-healing Materials: Fundamentals, Design Strategies, and Applications, Wiley-VCH, 2008.4) A. Półrolniczak, A. Katrusiak, Mater. Adv. 2021, 2, 4677.

Back to Table of contents

MS27 Minerals and Materials Under Extreme Conditions

MS27-1-7 Temperature mapping, beamshaping and indirect laser heating in diamond anvil cells on the PSICHE beamline, synchrotron SOLEIL
#MS27-1-7

N. Guignot [1], G. Morard [2], D. Antonangeli [3], S. Boccato [3], N. Jaisle [2], R. Pierru [3], L. Xie [4], P. Bouvier [5], J. Dominique [2], J.P. Deslandes [1]
[1]Synchrotron SOLEIL - Gif sur Yvette (France), [2]ISTerre - Grenoble (France), [3]IMPMC - Paris (France), [4]UCL - Londres (United Kingdom), [5]Institut Néel - Grenoble (France)

Abstract
The laser heated diamond anvil cell (LHDAC) technique is widely used to generate temperatures of more than several thousands of K for pressures reaching tens and even hundreds of GPa. It is very common on synchrotron beamlines over the world, allowing for in-situ studies of phase transitions, thermoelastic properties of new materials, etc. The X-ray micro-focused beam dimensions are generally perfectly compatible with the hot spot dimensions (~10/20 µm in diameter).
Despite this popularity, this technique generates high radial temperature gradients, that are detrimental for several reasons: 1/ they generate chemical diffusion (Soret effect) that are very problematic in the case of chemically complex samples; 2/ a very small X-ray beam is required, which can be an issue when a good grain statistics is required for example in the case of X-ray diffractions; 3/ kinetics studies are very difficult to do with such gradients; 4/ the sample microstructure may be difficult to interpret correctly. Moreover, the sample is heated via a direct absorption of the laser. That often generates instabilities, particularly during melting when sample absorbance can change drastically. Of course, on many occasions the sample can't even be heated with the laser wavelength available.
For all these reasons, we have developed and implemented on the PSICHE beamline (SOLEIL) a new combination of techniques:
- Real-time sample surface temperature and emissivity mapping using an adapted 4 color pyrometry technique [1].- Laser beamshaping: to modify the shape of the laser focused spot and to control the effect of that shape on the temperature distribution via the 4 color pyrometry mapping.- Indirect laser heating: the technique is based on a development introduced by [2]. The sample is loaded inside a drilled boron-doped diamond (BDD) disk, opaque and laser absorber. We use here a "donut" laser shape to heat only the BDD, which thus acts as a simple heater. Direct laser absorption by the sample is minimized.
We will give details on how this combination of techniques can improve the quality of experimental results using the LHDAC technique. We will present first results and some perspectives.

References
[1] Campbell, A.J., Measurement of temperature distributions across laser heated samples by multispectral imaging radiometry. Rev. Sci. Instrum. 79, 015108 (2008).[2] Weck G. et al., Determination of the melting curve of gold up to 110 GPa. Phys. Rev. B, 101, 014106, 1–8 (2020).
[3] Rainey E.G.S and Kavner A., J. Geophys. Res. Solid Earth, 119(11), p. 8154-8170 (2014).

Temperature mapping of a BDD assembly

Back to Table of contents

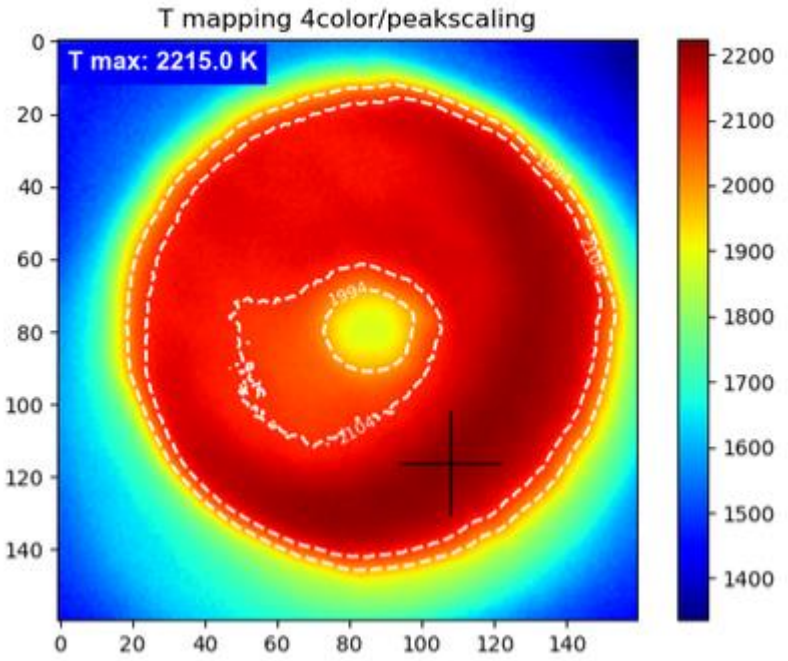

Back to Table of contents

MS27 Minerals and Materials Under Extreme Conditions

MS27-2-1 High pressure, high temperature crystallography of silicon
#MS27-2-1

A. Courac (kurakevych) [1], S. Pandolfi [2], W. Crichton [3], Y. Le Godec [4]
[1]IMPMC - Sorbonne university - Paris (France), [2]SLAC National Accelerator Laboratory - Stanford (United States), [3]ESRF - Grenoble (France), [4]IMPMC - CNRS - Paris (France)

Abstract
HP research on Si started more than 50 years ago and since then several allotropes, displaying a wide variety of physical properties, have been reported. The narrow-bandgap semiconductor Si-III with BC8 structure (originally believed to be semimetal) can be obtained from the high-pressure tetragonal metallic phase, Si-II, formed during compression of common silicon according to Si-I→Si-II. Such a transformation during decompression can be either direct, Si-II→Si-III, or with an intermediate step Si-II→Si-XII→SiIII. Our in situ studies of pure Si in oxygen-free environment indicated that in the absence of pressure medium, Si-I remains metastable at least up to ~14 GPa, while the pressure medium allows reducing the onset pressure of transformation to ~10 GPa. Upon heating Si-III at ambient pressure a hexagonal structure, named Si-IV, was observed. This allotrope was believed to be a structural analogue of the hexagonal diamond found in meteorites (called also lonsdaleite) with the 2H polytypestructure. Calculations have predicted several hexagonal polytypes of Si and of other Group-IV elements to be metastable, such as 2H (AB), 4H (ABCB) and 6H (ABCACB). Exhaustive structural analysis, combining fine-powder X-ray and electron diffraction, afforded resolution of the crystal structure. We demonstrate that hexagonal Si obtained by high-pressure synthesis correspond to Si-4H polytype (ABCB stacking), in contrast with Si-2H (AB stacking) proposed previously. The sequence of transformations Si-III→Si-IV(4H)→Si-IV(6H) has been observed in situ by powder X-ray diffraction. This result agrees with prior calculations that predicted a higher stability of the 4H form over 2H form. Further physical characterization, combining experimental data and ab-initio calculations, have shown a good agreement with the established structure. Strong photoluminescence emission was observed in the visible region, for which we foresee optimistic perspectives for the use of this material in Si-based photovoltaics. The study of silicon allotropic transformation in Na-Si and K-Si systems at high pressure, high temperature conditions indicated new interesting results on the second-order character of Si-II→Si-XI transformation and will be discussed in the presentation. The impact of the second order character on the topology of the pressure-temperature phase diagram of silicon will be analyzed.

References
Kim, Duck Young, Stevce Stefanoski, Oleksandr O Kurakevych, and Timothy A Strobel. 2015. 'Synthesis of an open-framework allotrope of silicon', Nat. Mater., 14: 169-73.
Kurakevych, Oleksandr O., Yann Le Godec, Wilson A. Crichton, Jeremy Guignard, Timothy A. Strobel, Haidong Zhang, Hanyu Liu, Cristina Coelho Diogo, Alain Polian, Nicolas Menguy, Stephen J. Juhl, and Christel Gervais. 2016. 'Synthesis of Bulk BC8 Silicon Allotrope by Direct Transformation and Reduced-Pressure Chemical Pathways', Inorg. Chem., 55: 8943–50.
Kurakevych, Oleksandr O., Timothy A. Strobel, Duck Young Kim, Takaki Muramatsu, and Viktor V. Struzhkin. 2013. 'Na-Si Clathrates Are High-Pressure Phases: A Melt-Based Route to Control Stoichiometry and Properties', Cryst. Grow. Des., 13: 303-07.
Pandolfi, S., C. Renero-Lecuna, Y. Le Godec, B. Baptiste, N. Menguy, M. Lazzeri, C. Gervais, K. Spektor, W. A. Crichton, and O. O. Kurakevych. 2018. 'Nature of Hexagonal Silicon Forming via High-Pressure Synthesis: Nanostructured Hexagonal 4H Polytype', Nano Lett., 18: 5989-95.

Silicon allotropes by HPHT synthesis

Back to Table of contents

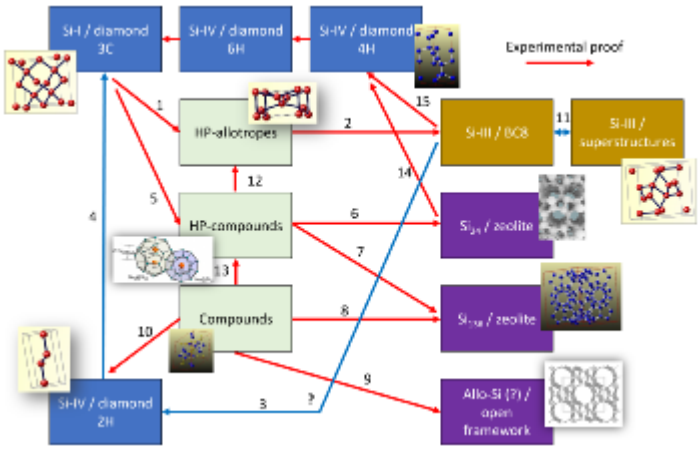

Back to Table of contents

MS27 Minerals and Materials Under Extreme Conditions

MS27-2-2 In-situ single-crystal neutron diffraction of a high-pressure phase of sodium chloride hydrate #MS27-2-2

K. Yamashita [1], K. Komatsu [2], T. Ohhara [3], K. Munakata [4], T. Irifune [5], T. Shinmei [5], K. Sugiyama [6], T. Kawamata [6], H. Kagi [2]
[1]Institute of Physical Chemistry, University of Innsbruck - Innsbruck (Austria), [2]Graduate School of Science, The University of Tokyo - Tokyo (Japan), [3]Japan Atomic Energy Agency - Ibaraki (Japan), [4]Comprehensive Research Organization for Science and Society - Ibaraki (Japan), [5]Geodynamics Research Center, Ehime University - Ehime (Japan), [6]Institute for Materials Research, Tohoku University - Sendai (Japan)

Abstract
Salt-water system has been studied from the perspectives of physical chemistry and planetary science. Its unique phenomena, such as salt-bearing ice [1,2], are found under pressured conditions, however, its phase behaviour, even possible crystalline phases, are not fully understood yet. Some salts have unique high-pressure phases, not only stacking differences of anhydrous salt, but also variation in composition ratio; *e.g.* $MgCl_2$ and $MgSO_4$ take unique hydration numbers under high pressure [3,4]. Sodium chloride (NaCl) is a major salt in nature. It has only one hydrate at ambient pressure: dihydrate at low temperatures [5]. Our group found its new hydrate under high pressure like the case of previously reported salt hydrates [3,4]. Its structure without the hydrogen positions was determined from single-crystal x-ray diffraction experiments. However, powder neutron diffraction techniques could not accomplish the full determination of the structure with hydrogen positions. Here, I will present the result of single-crystal neutron diffraction experiments to reveal the crystal structure of the new hydrate.
The diffraction patterns were collected at 298 K and 1.7 GPa using the Laue-TOF diffractometer at the BL18 (SENJU) beamline of the MLF J-PARC [6]. Single-crystalline specimens of the hydrate were directly grown from a NaCl saturated D_2O solution under high pressure using a newly-developed diamond anvil cell [7]. The observed diffraction patterns were analysed based on the initial structure derived from the previous diffraction experiments.
The new hydrate has a monoclinic structure with $\beta \sim 119°$. It contains thirteen water molecules per pair of sodium chloride, a much larger hydration number than the other NaCl hydrate. The sodium atoms are coordinated by six water molecules forming octahedral units. The crystal structure of the hydrate consists of the hydrogen-bonding network binding the $Na(D_2O)_6$ octahedra, interstitial water molecules, and chlorine atoms. Considering the restriction of symmetry and stoichiometry, the water molecules are not in definitive orientations but orientationally disordered like those in ice. This is contrast to other known hydrates in which water molecules are restricted to face ionic species due to their strong electrostatic interactions. The structure with large numbers of water molecules and hydrogen-bonded structure can provide an insight to understand the structural features of salt-water systems in solid phases.

References
[1] Frank, M. R., Runge, C. E., Scott, H. P., Maglio, S. J., Olson, J., Prakapenka, V. B. & Shen, G. (2006). *Phys. Earth Planet. Inter.* **155**, 152–162.
[2] Klotz, S., Bove, L. E., Strässle, T., Hansen, T. C. & Saitta, A. M. (2009). *Nat. Mater.* **8**, 405–409.
[3] Komatsu, K., Shinozaki, A., Machida, S., Matsubayashi, T., Watanabe, M., Kagi, H., Sano-Furukawa, A. & Hattori, T. (2015). *Acta Crystallogr. B***71**, 74–80.
[4] Fortes, A. D., Knight, K. S. & Wood, I. G. (2017). *Acta Crystallogr. B***73**, 47–64.
[5] Klewe, B. & Pedersen, B. (1974). *Acta Crystallogr. B***30**, 2363–2371.
[6] Ohhara, T., Kiyanagi, R., Oikawa, K., Kaneko, K., Kawasaki, T., Tamura, I., Nakao, A., Hanashima, T., Munakata, K., Moyoshi, T., Kuroda, T., Kimura, H., Sakakura, T., Lee, C. H., Takahashi, M., Ohshima, K. I., Kiyotani, T., Noda, Y. & Arai, M. (2016). *J. Appl. Crystallogr.* **49**, 120–127.
[7] Yamashita, K., Komatsu, K., Klotz, S., Fernández-Díaz, M. T., Fabelo, O., Irifune, T., Sugiyama, K., Kawamata, T. & Kagi, H. (2020). *High Press. Res.* **40**, 88–95.

Back to Table of contents

MS27 Minerals and Materials Under Extreme Conditions

MS27-2-3 Crystal structure and equation of state of Al-bearing bridgmanite at high-pressure and high-temperature #MS27-2-3

G. Criniti [1], A. Kurnosov [1], K. Glazyrin [2], R. Husband [2], Z. Liu [3], T. Boffa Ballaran [1], D. Frost [1]
[1]University of Bayreuth - Bayreuth (Germany), [2]DESY - Hamburg (Germany), [3]Jilin University - Changchun (China)

Abstract
MgSiO3-rich bridgmanite is the most abundant mineral phase in pyrolitic and basaltic phase assemblages at the pressure and temperature conditions of Earth's lower mantle. Al is typically incorporated in the crystal structure of bridgmanite through the Fe3+AlO3 and AlAlO3 charge coupled (CC) mechanisms, and through MgAlO2.5 oxygen vacancy (OV) mechanism. MgO-saturated systems, such as pyrolite (Mg/Si ~ 1.3) stabilize the OV mechanism at shallow lower mantle conditions, while the CC mechanisms become more and more abundant with increasing pressure and become dominant at mid- and deep-lower mantle conditions. It has been argued that the formation of oxygen vacancies in bridgmanite would cause a substantial softening of its bulk modulus. However, so far experimental studies have not provided a definite proof to such hypothesis due to the lack of well characterized samples.
In this study, we synthesized several Fe-free Al-bearing bridgmanite crystals with different compositions in a multi-anvil apparatus. The recovered samples were then characterized using an electron probe microanalyzer to accurately determine the degree of OC and CC substitution of each sample. Single-crystals of bridgmanite with different CC and OV contents were then tested and selected by means of single-crystal X-ray diffraction. High-pressure and high-temperature diffraction measurements were conducted in resistively-heated diamond anvil cells at the Extreme Conditions Beamline P02.2 of PETRA-III (DESY, Habmurg). By fitting equations of state to the pressure-volume-temperature datasets and by refining the crystal structure of the three samples, the stability and elasticity of bridgmanite solid solutions at lower mantle conditions will be discussed.

Back to Table of contents

MS27 Minerals and Materials Under Extreme Conditions

MS27-2-4 Estimating completeness in single-crystal high-pressure diffraction experiments
#MS27-2-4

D. Tchon [1], A. Makal [1]
[1]Biological and Chemical Research Centre, Faculty of Chemistry, University of Warsaw - Warsaw (Poland)

Abstract
The invention of Diamond anvil cell (DAC) has revolutionised many fields of science by providing a way to introduce high pressure (HP) while keeping the sample accessible to radiation. [1] Any decent single crystal can be encased inside a DAC, pressurised, and investigated by the means of X-ray diffraction (XRD) without a need for additional equipment or software. Structure factors collected in this way can be used to identify and solve numerous crystal structures, but their quality and quantity are never quite on par with even routine ambient-condition experiments. [2–6]
The geometry of a modern symmetrical DAC can be described using just a single parameter called the opening angle. Anvil cells commonly feature an opening angle of 35° or less, rendering up to 97% of otherwise collectable reflections inaccessible to the XRD experiment. Consequently, diffraction patterns collected in HP conditions are routinely incomplete, especially so in materials with low internal symmetry, which as a result are under-represented in HP studies. [7] Furthermore, this limitation affects the applicability of quantum-crystallographic techniques, as they often require abundant information on the reciprocal space. [8–10]
The above issue can be circumvented in two different ways: either by merging datasets collected on multiple crystals or by utilising the inherent symmetry of one crystal. The first approach, while innately simpler, requires special infrastructure such as well-focused incident beam or a gas membrane cells to avoid merging problems. [11,12] Meanwhile, the other solution calls only for a precise control over crystal orientation, which to some degree can be performed in any laboratory. [13]
In present work, a potency – maximum attainable completeness of collected data – was numerically calculated as a function of crystal orientation, DAC opening angle, resolution, and incident radiation wavelength. Static figures and tables describing the most common experimental set-ups were prepared and general conclusions were drawn. Crystal orientation was found to influence the potency far more than the opening angle or wavelength. In particular, it was shown that an unfortunately placed cubic sample can offer lower percent of data than a well-oriented crystal belonging to the orthorhombic system.
The exact values of potency vary between individual anvil cells and samples. In order to easily evaluate every diffraction set-up and predict best experimental strategies in each case, a dedicated python library was prepared. [14] A web-server “hikari-toolkit” was launched to allow every user to easily calculate the potency of their experimental set-up with ease.

References
[1] Katrusiak, A. Lab in a DAC – high-pressure crystal chemistry in a diamond-anvil cell. Acta Cryst B 75, 918–926 (2019).
[2] Angel, R. J. Absorption corrections for diamond-anvil pressure cells implemented in the software package Absorb6.0. J Appl Cryst 37, 486–492 (2004).
[3] Katrusiak, A. Shadowing and absorption corrections of single-crystal high-pressure data. Zeitschrift für Kristallographie - Crystalline Materials 219, 461–467 (2004).
[4] Katrusiak, A. High-pressure crystallography. Acta Cryst A 64, 135–148 (2008).
[5] Merrill, L. & Bassett, W. A. Miniature diamond anvil pressure cell for single crystal x-ray diffraction studies. Review of Scientific Instruments 45, 290–294 (1974).
[6] Binns, J., Kamenev, K. V., McIntyre, G. J., Moggach, S. A. & Parsons, S. Use of a miniature diamond-anvil cell in high-pressure single-crystal neutron Laue diffraction. IUCrJ 3, 168–179 (2016).
[7] Tchoń, D. & Makal, A. Completeness of data in XRD experiments using diamond anvil cell. Acta Crystallogr A Found Adv 77, C1212–C1212 (2021).
[8] Casati, N., Kleppe, A., Jephcoat, A. P. & Macchi, P. Putting pressure on aromaticity along with in situ experimental electron density of a molecular crystal. Nature Communications 7, 10901 (2016).
[9] Jayatilaka, D. & Dittrich, B. X-ray structure refinement using aspherical atomic density functions obtained from quantum-mechanical calculations. Acta Cryst A 64, 383–393 (2008).
[10] Pawlędzio, S. et al. Relativistic Hirshfeld atom refinement of an organo-gold(I) compound. IUCrJ 8, 608–620 (2021).
[11] Tchoń, D. & Makal, A. Structure and piezochromism of pyrene-1-carbaldehyde at high pressure. Acta Cryst B 75, 343–353 (2019).
[12] Casati, N., Genoni, A., Meyer, B., Krawczuk, A. & Macchi, P. Exploring charge density analysis in crystals at high pressure: data collection, data analysis and advanced modelling. Acta Cryst B 73, 584–597 (2017).
[13] Tchoń, D. & Makal, A. Maximizing completeness in single-crystal high-pressure diffraction experiments: phase transitions in 2°AP. IUCrJ 8, 1006–1017 (2021).

Back to Table of contents

[14] Tchoń, D. hikari-toolkit – A high-level tool for manipulating crystallographic files. (2022). at <https://pypi.org/project/hikari-toolkit/>

Crystal orientation affects potency in HP XRD

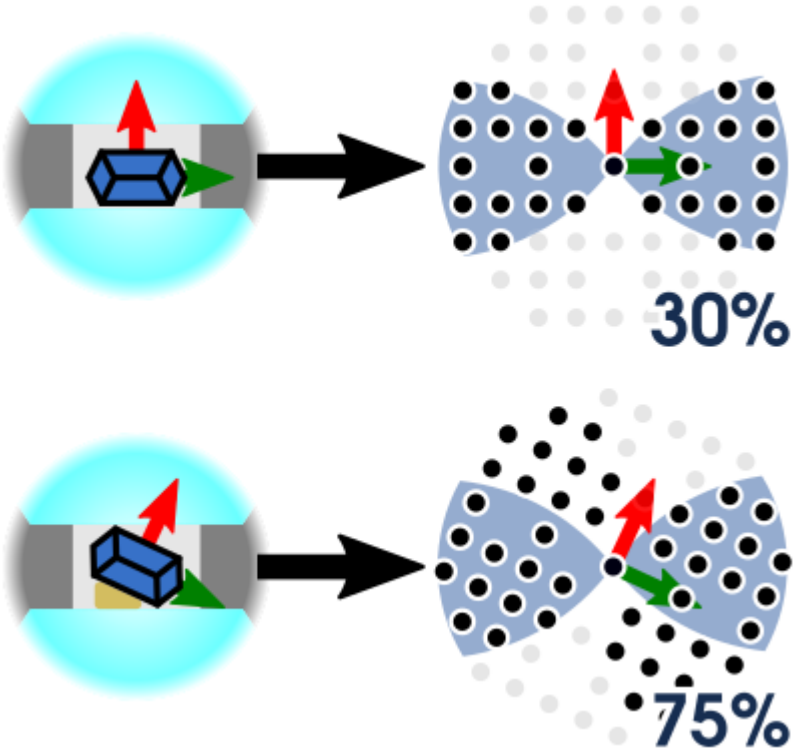

Potency as a function of crystal orientation

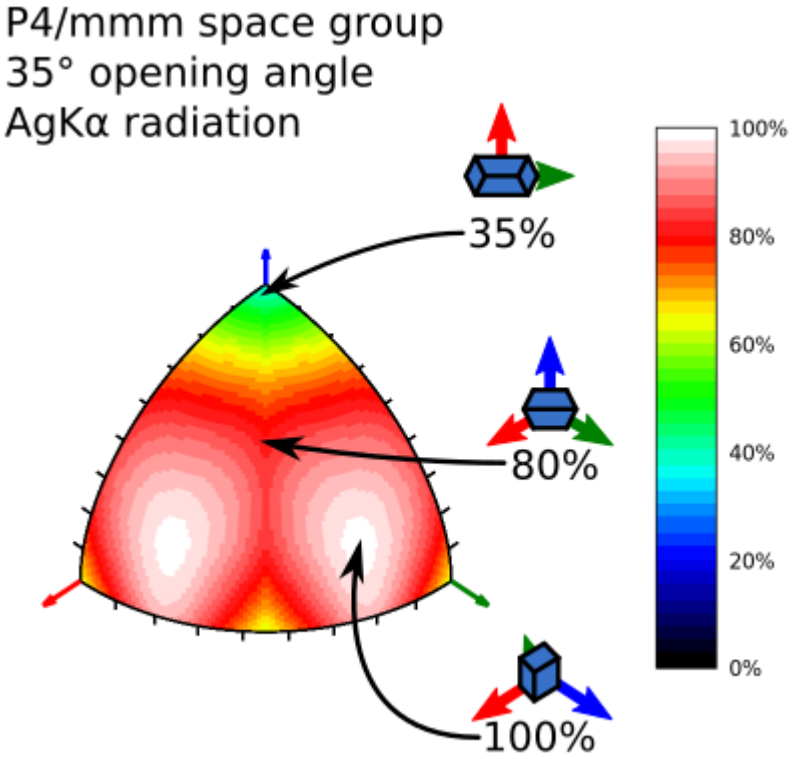

Back to Table of contents

MS27 Minerals and Materials Under Extreme Conditions

MS27-2-5 High-Pressure Polymorphs of Osmocene and Ruthenocene
#MS27-2-5

I. Moszczyńska [1], A. Katrusiak [1]
[1]Adam Mickiewicz University - Poznań (Poland)

Abstract
Ruthenocene ($RuCp_2$)[1] and osmocene ($OsCp_2$)[2] are isostructural, at ambient conditions they both crystalize in the orthorhombic space group *Pnma*. However, high pressure conditions reveal phase transitions to two different polymorphs, space groups *Pcmb* at 3.9 GPa[3] and *Pcab* at 3.5 GPa for $RuCp_2$ and $OsCp_2$ respectively. In both cases there is a large pressure hysteresis (about 3.15 GPa) in which *α* and *β* phases can coexists (Figure 1). *α*-phases of both compounds are mostly stabilize by C-H···π contacts. High-pressure phase transformations occure because of competitive impact of C-H···π and C-H···M contacts. Non-identical way of high pressure transitions of this two compounds arise from different preference to create anagostic M···H-C interactions. In *β*-$OsCp_2$ there are 4 different anagostic contacts, while in *β*-$RuCp_2$ only one H···Ru distance is shorter than the sum of van der Waals radii (Figure 2). The arrangement of short contacts around osmium cation in *β*-$OsCp_2$ leads to eliminate mirror plane symmetry in the crystal structure. In *β*-osmocene the shortest Os···H contact is longer than the shortest Ru···H contact in *β*-ruthenocene. All phase transitions of metallocenes published already in the literature involve changes in molecular conformations, which differ from transformation of $RuCp_2$ and $OsCp_2$.

References
1. Hardgrove, G. L.; Templeton, D. H. The Crystal Structure of Ruthenocene. Acta Crystallogr. 1959, 12 (1), 28–32. DOI: 10.1107/S0365110X59000081.
2. Bobyens, J. C. A.; Levendis, D. C.; Bruce, M. I.; Williams, M. L. Crystal Structure of Osmocene, Os(η-C_5H_5)$_2$. J. Crystallogr. Spectrosc. Res. 1986, 16 (4), 519–524. DOI: 10.1007/BF01161040.
3. Moszczyńska, I.; Katrusiak, A. Competition between Hydrogen and Anagostic Bonds in Ruthenocene Phases under High Pressure. J. Phys. Chem. C 2022. DOI: 10.1021/acs.jpcc.1c10249.

Isochoric crystallization of ruthenocene phases

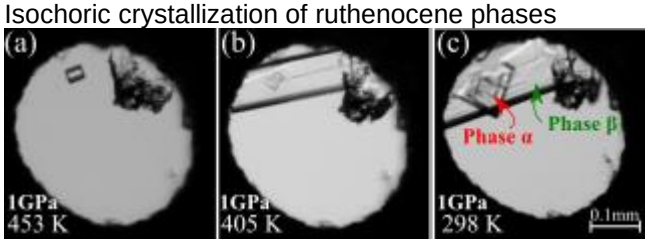

Anagostic M-H contacts in ruthenocene and osmocene

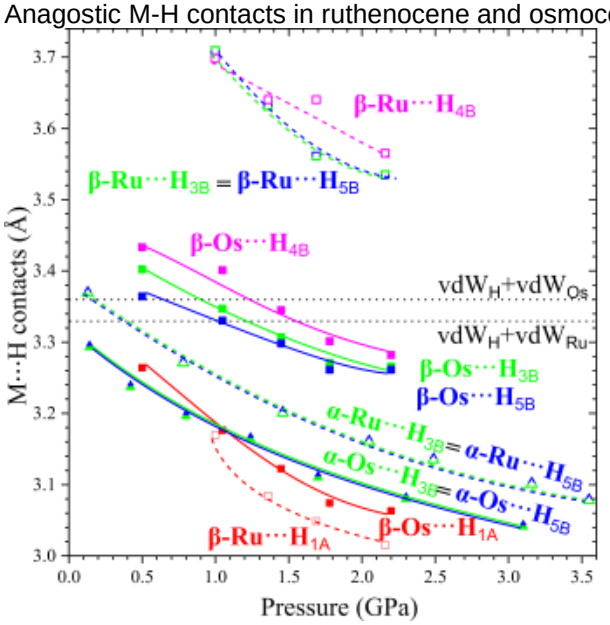

Back to Table of contents

MS27 Minerals and Materials Under Extreme Conditions

MS27-2-6 Interplay between H-bonding proton dynamics and Fe valence fluctuation in Fe3(PO4)2(OH)2 barbosalite at high pressure
#MS27-2-6

G. Hearne [1], V. Ranierei [2], P. Hermet [2], J. Haines [2], O. Cambon [2], J.L. Bantignies [3], M. Poienar [4], C. Martin [5], J. Rouquette [2]
[1]Department of Physics, University of Johannesburg PO Box 524, Auckland Park 2006, Johannesburg - Johannesburg (South Africa), [2]ICGM, Univ Montpellier, CNRS, ENSCM, Montpellier, France - Montpellier (France), [3]L2C, Univ Montpellier, CNRS, ENSCM, Montpellier, France - Montpellier (France), [4]National Institute for Research and Development in Electrochemistry and Condensed Matter, Renewable Energies - Photovoltaic Laboratory, Str. Dr. A. Paunescu Podeanu, nr.144, 300569, Timis¸oara, Timis¸, Romania - Timisoara (Romania), [5]CRISMAT, CNRS UMR 6508, 6 bvd Maréchal Juin, 14050 CAEN CEDEX, France - Caen (France)

Abstract
Pressure dependence of mixed-valence barbosalite Fe2+Fe3+2(PO4)2(OH)2 is investigated based on a combination of single crystal X-ray diffraction, DFT calculations, infrared and Mössbauer spectroscopy to determine how the change in H-bonding, i.e. O-H…O, may influence Fe2+→(OH)-→Fe3+ intervalence electron transfer and vice-versa.
Recently, the original P21/n space group of barbosalite was questioned as n-glide plane reflection conditions (h0l:h+l=2n) were found to be violated based on TEM and single crystal X-ray diffraction. A doubled unit-cell barbosalite structure in the P21 space group, i.e. along the c axis, was proposed[1]. However, subsequent analysis reveals that such reflections thought to be attributable to the doubled unit-cell, are in fact due to a non-merohedral twinning with a 90° rotation angle. The barbosalite structure is clearly still centrosymmetric with the P21/n space-group as either suggested by the cumulative probability distribution curves and the use of a polar twinning law in the P21 space group solution. Moreover, contrary to what was originally proposed, the presence of an additional non-stoechiometric iron statistically connects the face sharing FeO6 octahedra trimers, i.e. Fe2+-Fe3+-Fe2+, to form infinite chains along <110> as observed in the lipscombite-like structure[2]. Based on DFT calculations, hydrogen atoms are located in the octahedral volume of this additional non-stoechiometric atom iron site and forms a hydrogen bond O–H···O between the (OH)- common vertex of three octahedra and one of the oxygens of a PO4 group, i.e. as part of Fe-O–H···O-P structural sequences. This means that the FeO6 octahedral trimers are either connected by a hydrogen bond or by this non stoichiometric iron site.
Pressure triggers proton delocalization involving a P21/n-Cc phase transition in a 2a×2b×c supercell at ~5 GPa in hydrogen bonds of the Fe-O-H…O-P structural segments. Hydrogen bond reinforcement and anticipated proton dynamics, discerned by IR spectroscopy and symmetrization of lattice parameters, impact on the crystal field at proximate Fe cations. This triggers dynamical minority-spin electron exchange along Fe2+®L®Fe3+ pathways (ligand L = O or (OH)- of shared octahedral faces), discerned by 57Fe Mössbauer spectroscopy at 10-30 GPa. The pressure response of these mixed-valence hydroxy phosphates exemplify the interplay between proton (THz) and electron (MHz) dynamics on two disparate time scales in the same condensed phase. This is of widespread relevance to charge dynamics in hydrogen bonded systems (e.g., biomolecular complexes and planetary interiors).

References
[1] M. Poienar, F. Damay, J. Rouquette, V. Ranieri, S. Malo, A. Maignan, E. Elkaim, J. Haines, C. Martin, Structural and magnetic characterization of barbosalite Fe-3(PO4)(2)(OH)(2), J. Solid State Chem., 287 (2020).
[2] I. Vencato, E. Mattievich, Y.P. Mascarenhas, CRYSTAL-STRUCTURE OF SYNTHETIC LIPSCOMBITE - A REDETERMINATION, American Mineralogist, 74 (1989) 456-460.

Barbosalite structure in (P21/n)

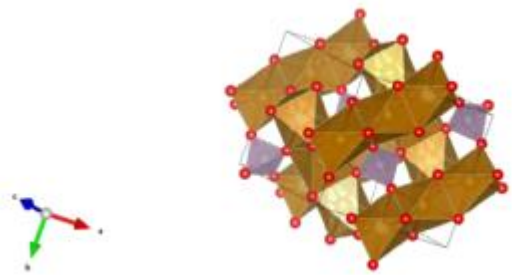

Back to Table of contents

HP-structure of barbosalite at 9.9 GPa (Cc)

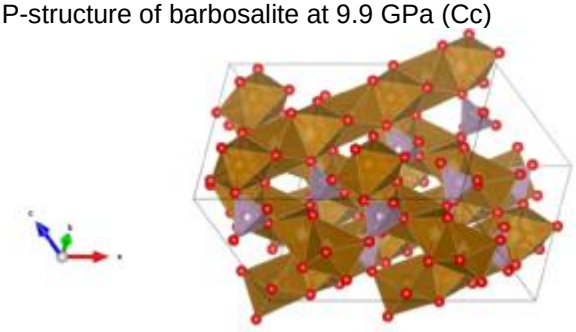

Back to Table of contents

MS27 Minerals and Materials Under Extreme Conditions

MS27-2-7 Decoupling spin-crossover and structural phase transition in iron(II) molecular complex #MS27-2-7

D. Paliwoda [1], L. Vendier [1], G. Molnár [1], A. Bousseksou [1]
[1]LCC, CNRS & Université de Toulouse (UPS, INP), - 31077 Toulouse (France)

Abstract
Spin-crossover (SCO) materials are sensitive to external stimuli. SCO transition arouses curiosity because the change of the spin state of metal ion involves appearance of serious structural perturbation related to changes of metal-ligand distances. The interest in Fe(II) spin crossover systems is enhanced by the fact that the spin state can be conveniently switched by changing the temperature, applying pressure, light irradiation or by the action of a chemical agent[1]. Hence, these compounds are considered as materials for potential applications[2] for example in medicinal diagnostic[3], as sensors[4], displays[5] and memory devices[6].
We have recently investigated pressure induced spin-crossover (SCO) transitions in Fe(II) molecular complexes: **(1)** [$Fe^{II}(H_2B(pz)_2)_2(bipy)$] and **(2)** [$Fe^{II}(H_2B(pz)_2)_2(phen)$] pz: pyrazole; bipy: 2,2'-bipyridine; and phen: phenanthroline).
We have performed a series of high-pressure measurements of **(1)** and **(2)** using wide-opening angle diamond anvil cell (One20DAC) and four-circle Rigaku Synergy-S XtaLab diffractometer equipped with Hypix6000 hybrid pixel Si detector. At normal conditions **(1)** and **(2)** form monoclinic crystals of space group *C*2/*c*. Both complexes undergo SCO transition when cooled down to 160 K, which is manifested indirectly by abrupt shortening of Fe-N(ligand) distance of about 0.2 Å. While **(1)** remains monoclinic upon further cooling, the low temperature high spin (HS) to low spin (LS) transition in **(2)** is accompanied by the structural transformation from monoclinic *C*2/*c* form to triclinic $P\bar{1}$ phase.
Compression of **(2)** decouples SCO and structural transition which allows to detect monoclinic LS form, so far undetectable upon cooling[7,8].
Acknowledgements: Financial support from regional Nanomat PRRI Project and ERC "E-MOTION" Advanced Grant is gratefully acknowledged.

References
[1] A. B. Gaspar, G. Molnár, A. Rotaru; H. J. Shepherd, *C.R. Chimie*, 2018, **21**, 1095.
[2] A. Bousseksou, G. Molnár, L. Salmon, W. Nicolazzi, *Chem. Soc. Rev.* 2011, **40,** 3313.
[3] R. N. Muller, L. V. Elst and S. J. Laurent, *J. Am. Chem. Soc.,* 2003, **125**, 8405.
[4] C. Bartual-Murgui, A. Akou, C. Thibault, G. Molnar, C. Vieu, L. Salmon, A. Bousseksou, *J. Mater. Chem. C*, 2015, **3**, 1277.
[5] O. Kahn, C. J. Martinez, *Science,* 1988, **279**, 44.
[6] J.-F. Letard, P. Guionneau, L. Goux-Capes, *Top. Curr. Chem*., 2004, **235**, 221;
[7] J. A. Real, M. Carmen Muñoz, J. Faus, X. Solans, *Inorg. Chem.,* 1997, **36**, 3008.
[8] A. L. Thompson, A. E. Goeta, J. A. Real, A. Galet, M. Carmen Muñoz, *Chem. Comm*., 2004, **12**, 1390.

Unit cell angles α/γ of (2) and av. Fe-N distances

Back to Table of contents

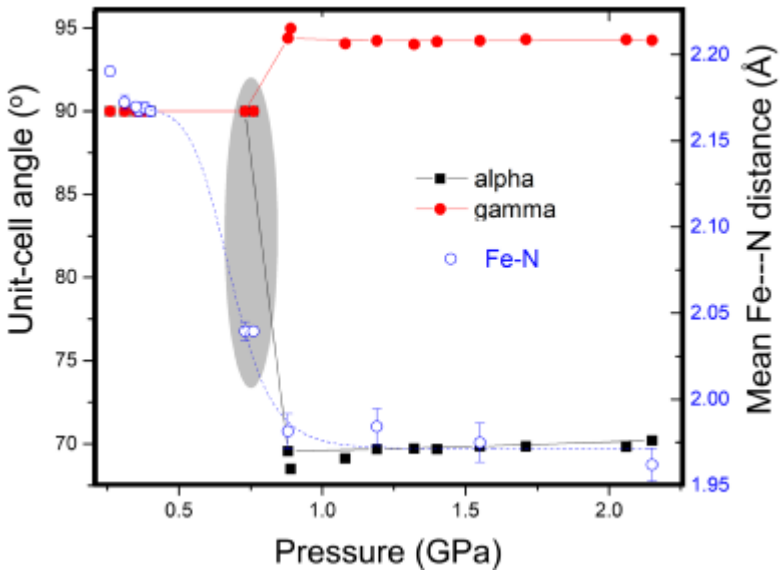

Back to Table of contents

MS27 Minerals and Materials Under Extreme Conditions

MS27-2-8 Crystallography at extreme conditions at the CRISTAL beamline@SOLEIL
#MS27-2-8

P. Fertey [1], V. Baledent [2], G. Guillier [2], F. Legrand [1], P. Foury [2]
[1]synchrotron SOLEIL - Gif-sur-Yvette (France), [2]Université Paris-Saclay, CNRS, Laboratoire de Physique des Solides - Orsay (France)

Abstract
Pressure as a thermodynamic potential has long been a subject of a large interest since it can drives main interesting phenomena like structure–property relations, conformational and structural transformations of molecules, polymerization, structural and electronic phase transitions, polymorphism or triggering new chemical reactions.
Understanding the crystal structure under compression is a key step to elucidate the underlying mechanisms. Structure determination of single crystals under pressure is commonly performed at room temperature, both in the laboratory and at synchrotron radiation facilities [1]. The sample is placed in a Diamond Anvil Cell which strongly constrains the completeness of the acquired data sets for structural model resolution/refinement. Devices that allow measurements under pressure and at low temperature are much less common. Most of them are based on cryostats that limit the number of degrees of freedom of the sample orientation to a single degree of rotation. If this limitation is not constraining for powder samples, it however drastically reduces the completeness of the datasets in the case of a single crystal, often involving the need to introduce more or less strong constraints to reach a satisfying structural model.
A new cryostat specifically designed for the acquisition of the most possible complete data sets will be presented. Thanks to an additional degree of freedom allowing the rotation of the DAC around its axis, the completeness of datasets can be significantly increased allowing the release of constraints in the refinement stage. Furthermore, the pressure can be adjusted in situ at any temperature between 8K and the room temperature, avoiding warming the sample to change the pressure, which is mandatory if, for example, the pressure induces an irreversible phase transition.
The performance and relevance of this new sample environment for the study of the structural properties of single crystals in the (P ,T) phase diagram will be illustrated through different examples as well as the possibility of high pressure diffraction at the CRISTAL beamline at synchrotron SOLEIL [2].

References
[1] McMahon, Top Curr Chem 315, 69–110 (2012)
[2] https://www.synchrotron-soleil.fr/en/beamlines/cristal

Back to Table of contents

MS27 Minerals and Materials Under Extreme Conditions

MS27-2-9 Crystal structures of V2O5 and V6O13 at high pressures: implications for the Wadsley phase family behaviour at extreme conditions
#MS27-2-9

B.V. Hakala [1], D.K. Manousou [2], K. Glazyrin [3], W.A. Crichton [4], K. Friese [1], A. Grzechnik [5]
[1]Jülich Centre for Neutron Science-2 and Peter Grünberg Institute-4 (JCNS-2/PGI-4), Forschungszentrum Jülich GmbH - Jülich (Germany), [2]Section of Condensed Matter Physics, Department of Physics, National and Kapodistrian University of Athens - Athens (Greece), [3]Deutsches Elektronen-Synchrotron DESY - Hamburg (Germany), [4]European Synchrotron Radiation Facility - Grenoble (France), [5]Institute of Crystallography, RWTH Aachen University - Aachen (Germany)

Abstract
The so-called *Wadsley* phases with general formula V_nO_{2n+1} form a homologous series of compounds [1–3]. They have arisen much interest due to the observed metal-insulator transitions and their potential application as battery materials. [4–7] The crystal structures of the parent compound V_2O_5 and of V_6O_{13} (n=3) at ambient conditions are closely related, especially if we assume sixfold coordination of vanadium in an α-V_2O_5 with one V-O distance being longer. The crystal structures of the α-V_2O_5 (space group *Pmmn*) and α-V_6O_{13} (space group *C2/m*) polymorphs can be described as built of single layers and alternating layers of single and double layers of VO_6 polyhedra respectively. [8,9]
We have now studied single crystals of V_2O_5 and V_6O_{13} as a function of pressure at Petra III, DESY. Our study [10] shows a complete irreversible amorphization of the α-V_2O_5 sample above 7.3 GPa. Further investigation of the HP-HT behaviour of α-V_2O_5 was performed at the large volume press at ID06 at the ESRF, where we followed the evolution of the sample with in-situ synchrotron radiation. Heating of the amorphous phase led to the formation of the δ-V_2O_5 polymorph with Sb_2O_5 structure, which can be recovered at ambient conditions. High-pressure single crystal diffraction experiments α-V_6O_{13} show an anomalous behaviour between 2 and 3 GPa, yet the ambient pressure polymorph seems to be stable up to the highest pressures reached in the experiment.
Opposed to the ambient polymorph, the δ-V_2O_5 polymorph, which crystallizes from the amorphous material, consists of only double layers of VO_6 polyhedra. This configuration is similar to the one of a metastable VO_2(B). [11] Comparing higher stability of the hybrid single-double layered α-V_6O_{13} to the single layered structure of α-V_2O_5 which collapses under pressure, we propose that the binary oxides in the *Wadsley* series would tend to transform to the stable double-layer like configuration of the VO_2(B) type at extreme conditions. [10] This hypothesis requires further confirmation by performing HP measurements on V_6O_{13} at higher than previously attained pressures as well as closer investigation of the other members of the *Wadsley* series.

References
[1] Schwingenschlögl, U. et al. Ann. der Phys. 13, 475–510 (2004)
[2] Eguchi, R. et al. Phys. Rev. B - Condens. Matter Mater. Phys. 65, 1–4 (2002)
[3] Katzke, H. et al. Phys. Rev. B - Condens. Matter Mater. Phys. 68, 1–7 (2003)
[4] Bhatia, A. et al. Chem. Mater. 34, 1203–1212 (2022)
[5] Averianov, T. et al. J. Alloys Compd. 903, 163929 (2022)
[6] Andrews, J. L. et al. Chem 4, 564–585 (2018)
[7] He, P. et al. J. Mater. Chem. A 8, 10370–10376 (2020)
[8] Enjalbert, R. et al. Acta Crystallogr. Sect. C Cryst. Struct. Commun. 42, 1467–1469 (1986)
[9] Wilhelmi, K.-A. et al. Acta Chem. Scand. 25, 2675–2687 (1971)
[10] Hakala, B. V. et al. J. Alloys Compd. 911, 164966 (2022)
[11] Théobald, F. et al. J. Solid State Chem. 17, 431–438 (1976)

Back to Table of contents

MS27 Minerals and Materials Under Extreme Conditions

MS27-2-10 Understanding the behaviour of spin crossover materials for barocaloric applications: (P,T) phase diagrams
#MS27-2-10

P. Rosa [1], M. Marchivie [1], P. Guionneau [1], B. Vignolle [1], J.P. Itié [2]
[1]ICMCB, CNRS-Université de Bordeaux-Bordeaux INP - Pessac (France), [2]SOLEIL synchrotron - St Aubin (France)

Abstract
Climate change preoccupations motivates researching alternatives to energy-intensive vapor-compression thermodynamic machines, which use gases with tremendous greenhouse effect and are of limited thermodynamic efficiency. Roughly 3 billion systems (refrigeration, air-conditioning, heat pumps) consume roughly about 1/6th of the whole global electricity production, with greenhouse gas emissions equivalent to the whole EU emissions.[1] The mechanocaloric effect, which refers to adiabatic temperature changes induced by stress or pressure, is one of the most promising energy-saving new technology for cooling systems. Mechanocaloric research produced in the last decade highly performing materials, overcoming easily electrocaloric and magnetocaloric materials.[2] Most interestingly, mechanocaloric materials use non-critical, cheap, abundant and non-toxic elements. In 2016 a milestone paper identified molecular Spin CrossOver (SCO) complexes as showing promising mechanocaloric potential.[3] Following papers evidenced large to colossal barocaloric effects around the SCO temperatures,[4] which were reviewed recently in a very favourable light as compared to other materials being investigated.[5] Indeed SCO corresponds to a stimulus-induced (T, P, light,…) electronic configuration change, leading to a switch of optical/magnetic/electronic/structural properties concomitant with configurational, magnetic and phonon entropy changes[6] that may be sensitive to very small pressure perturbations of a few kilobars or even less.
Understanding the properties of such systems is of interest for the design of improved systems. To do so it is most informative to cross data gathered from structural determinations under varied conditions (temperature, light irradiation or pressure) and properties determination under similar conditions (magnetism, spectroscopy,…). We will present studies on two spin crossover complexes. SCO compounds show a change of spin state under application of an external stimuli (pressure, temperature, photoexcitation). This change goes together with modification of the population of molecular orbitals, with anti-bonding orbitals corresponding to longer metal-ligand bond lengths being populated in the High Spin (HS) state. Pressure is thus naturally one of the relevant thermodynamic constraints to consider: in SCO materials based on Fe2+ (d6) ions, it usually favors the diamagnetic low-spin (LS) state, which has a lower volume than the paramagnetic HS state. Diffraction studies, on single crystals or polycrystalline powder, are a powerful tool to study and understand the nature of the species observed when combining pressure and temperature changes (Fig. 1), allowing the mapping of the phase diagram of those complexes.

References
[1] D. Coulomb et al., IIR Inf. 2017, 17.
[2] L. Mañosa et al. Appl. Phys. Lett. 2020, 116, 050501.
[3] K. G. Sandeman APL Mater. 2016, 4, 1.
[4] P. J. Von Ranke Appl. Phys. Lett. 2017, 110, 18. P. J. Von Ranke et al. Phys. Rev. B 2018, 98, 224408. S. P. Vallone et al. Adv. Mater. 2019, 31, 1.
[5] P. Loveras, J.-L. Tamarit MRS Energy&Sustainability 2021, 8, 3.
[6] W. Nicolazzi et al., Comptes Rendus Chim. 2018, 21, 1060.

Fig. 1 Diffraction pattern evolution up to 2.2 GPa

Back to Table of contents

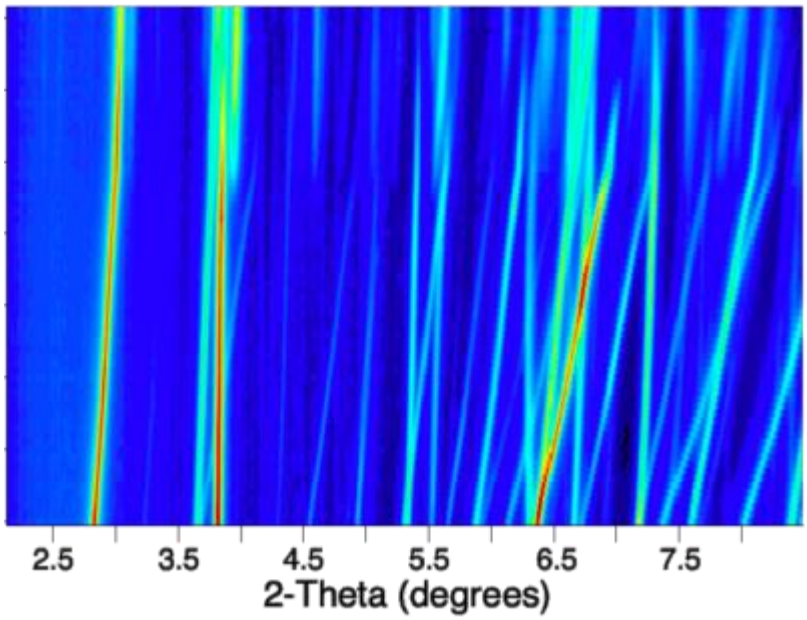

Back to Table of contents

MS27 Minerals and Materials Under Extreme Conditions

MS27-2-11 Intermolecular Interactions, Polymorphism and Properties of Primary Amines at High Pressure #MS27-2-11

N. Sacharczuk [1], A. Olejniczak [1], M. Bujak [2], M. Podsiadło [1]
[1]Faculty of Chemistry, Adam Mickiewicz University - Poznań (Poland) - Poznań (Poland), [2]Faculty of Chemistry, University of Opole - Opole (Poland) - Opole (Poland)

Abstract
A series of the simplest primary amines: ethylamine (EA), propylamine (PA), butylamine (BA), and pentylamine (PEA), has been studied at high pressure by single-crystal X-ray diffraction. EA is gaseous, while PA, BA, and PEA are liquids at ambient conditions. They represent an important class of compounds, used in organic chemistry, and their crystal structures have been previously determined only at ambient pressure and low temperature.[1] We have obtained single crystals of particular amines in a diamond-anvil cell (DAC) in the range between their freezing pressures at ambient temperature to *ca*. 6 GPa. EA at high pressure crystallizes in phase II of space group $P2_1/c$. For the series from PA to PEA six new polymorphs at high pressure have been found: two of PA (phases II and III, both in $P2_1/c$ space group), two of BA (phases II and III, space group $Pbc2_1$), and two of PEA (phase II and III, space group $Pbc2_1$ and $P2_1cn$). We have explained the structural transformations of primary amines at high pressure by analysing the NH···N and CH···N intermolecular interactions. We have also found the structure-symmetry relations for new polymorphs and we have correlated them with the melting temperature, freezing pressure, and molecular symmetries. Phase diagrams of studied amines have been also outlined up to *ca*. 6 GPa.

Acknowledgments: this study was supported by the National Science Centre (grant No. 2020/37/B/ST4/00982).

References
1.Maloney, A. G. P.; Wood, P. A.; Parsons, S. Competition between Hydrogen Bonding and Dispersion Interactions in the Crystal Structures of the Primary Amines. CrystEngComm 2014, 16, 3867−3882

Back to Table of contents

MS27 Minerals and Materials Under Extreme Conditions

MS27-2-12 Phase transitions and thermal expansion in a niobium oxyfluoride solid solution
#MS27-2-12

E.K. Dempsey [1], J. Cumby [1]
[1]University of Edinburgh - Edinburgh (United Kingdom)

Abstract
The control of thermal expansion is key for any engineering materials which undergo significant temperature changes, for instance by improving thermal shock resistance or reducing strain in solid oxide fuel cells.[1, 2] ReO3-type structures, such as ScF3, can exhibit negative thermal expansion through thermally-induced octahedral tilting.[3] Many ReO3-type trifluorides and oxyfluorides also show an octahedral tilting pressure phase transition, from Pm-3m to R-3c.[4] The octahedral tilting, therefore, creates a clear link between the temperature-pressure behaviour of ReO3-type structures.[5]
The variable oxidation state of niobium in NbO2F allows the formation of a ReO3-type oxygen-fluorine solid solution.[6] This provides an excellent model system for exploring the impact of anionic composition on physical properties. Initial ab initio calculations predict the pressure phase transition is strongly dependent on anionic composition. A similar dependence is therefore expected for thermal expansion, opening the potential for control of thermal expansion through anion doping.
A full pressure-temperature phase diagram for both pure and fluoride-doped NbO2F has been measured experimentally at the ESRF. Combining ab initio predictions with x-ray diffraction at extreme conditions provides insight into the fundamental relationship between anionic composition, thermal expansion and pressure phase transitions. This presents a new pathway for the design of functional mixed-anion materials with controllable pressure and temperature responses.

References
1. J. Chen, L. Hu, J. Deng and X. Xing, Chem. Soc. Rev., 2015, 44, 3522-3567.
2. J.-H. Kim and A. Manthiram, Chem. Mater., 2010, 22, 822-831.
3. B. K. Greve, K. L. Martin, P. L. Lee, P. J. Chupas, K. W. Chapman and A. P. Wilkinson, J. Am. Chem. Soc., 2010, 132, 15496-15498.
4. S. Carlson, J. Appl. Crystallogr., 2000, 33, 1175-1176.
5. C. R. Morelock, L. C. Gallington and A. P. Wilkinson, J. Solid State Chem., 2015, 222, 96-102.
6. F. J. Brink, L. Norén and R. L. Withers, J. Solid State Chem., 2004, 177, 2177-2182.

Figure 1:The (a) Pm-3m and (b) R-3c phase of NbO2F

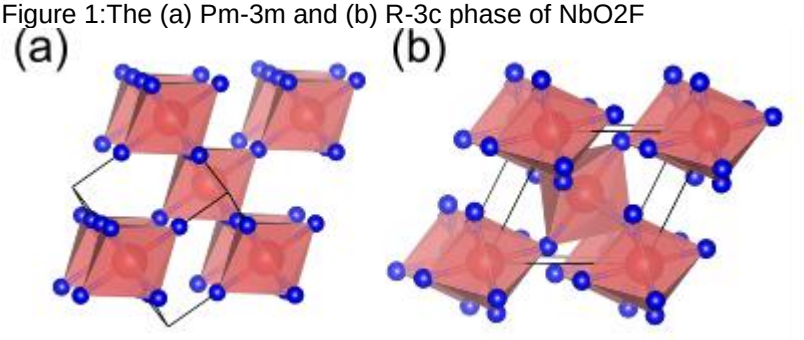

Back to Table of contents

MS27 Minerals and Materials Under Extreme Conditions

MS27-2-13 Crystal Structure of High Pressure Modification of Gold(III) Trifluoride
#MS27-2-13

S. Ivlev [1], K. Eklund [2], A. Karttunen [2], F. Kraus [3]
[1]Philipps-Universität Marburg - Marburg (Germany), [2]Aalto University - Aalto (Finland), [3]Aalto University - Marburg (Germany)

Abstract
Gold(III) trifluoride is a binary compond of gold and fluorine. At standard conditions the compound crystallizes in the hexagonal space group $P6_122$ (or $P6_522$) [1]. A few phase transitions at higher pressures were predicted and observed in the Raman spectra of AuF_3 by Kurzydowski and coworkers [2]. To the best of our knowledge, no crystal structure of any of the high pressure modifications of AuF_3 was so far determined experimentally.
Here we will present our latest data on the first experimental determination of the crystal structure of gold(III) trifluoride at higher pressure. The crystals of AuF_3 were synthesized in a fluorine oven by interaction of gold metal powder with fluorine-argon mixture at increased temperatures. The crystals grown in the colder part of the fluorine oven were transferred and stored in a glove box and were used for single crystal X-ray diffraction later.
The diffraction experiment was carried out using a One20DAC diamond anvil cell by Almax easyLab. The pressure in the DAC was controlled using the ruby fluorescence method and was set to be equal to approximately 2 GPa. At the conditions of the experiment we observed the phase transition predicted and observed in the Raman spectra of AuF_3 by Kurzydowski and coworkers [1]. We confirm that the high pressure polymorph modification of gold trifluoride crystallizes in the hexagonal space group $P6_1$ (or $P6_5$). The following unit cell parameters were determined from the diffraction data: a = 4.9195(4), c = 16.3956(13) Å, V = 343.64(6) Å^3, Z = 6 at 293 K and ca. 2 GPa.

References
[1] F. W. B. Einstein, P. R. Rao, James Trotter, Neil Bartlett. *J. Chem. Soc. A*, **1967**, 478-482.
[2] D. Kurzydłowski, S. Kobyakov, Z. Mazej, S. B. Pillai, B. Chakraborty, P. K. Jha. *Chem. Commun.*, **2020**, *56*, 4902-4905

Back to Table of contents

MS27 Minerals and Materials Under Extreme Conditions

MS27-2-14 High-pressure polymerisation of CS2 : "Bridgman's black" revisited
#MS27-2-14

S. Klotz [1], B. Baptiste [1], T. Hattori [2], S. Feng [3], C. Jin [3], K. Béneut [1], J.M. Guigner [1], I. Estève [1]
[1]IMPMC - Paris (France), [2]J-PARC Centre - Tokai (Japan), [3]IOP-CAS - Beijing (China)

Abstract
It is known since decades that carbon disulphide (CS2) transforms under pressure of a few GPa and under moderate high temperatures irreversibly into a polymeric 3-dimensional solid ("Bridgman black") with complex structure containing multiple-types of C-C, C-S and S-S bonds [1-5]. Here we show that by compression at 300 K to ~7 GPa using large-volume Paris-Edinburgh devices, an instantaneous reaction leads to a mixture of pure sulphur and a well-defined compound with stoichiometry close to C2S (Fig. 1). The availability of macroscopic sample quantities enables an in-depth characterisation of the reaction product by applying a variety of techniques, in particular x-ray and neutron diffraction, Raman scattering, infrared absorption, density and resistivity measurements [6]. We find that this material is fundamentally different to Bridgman black and consists of sulphur bonded to sp2 graphite layers of nanometric dimension, with some similarity to graphene oxide (Fig. 2). The compound is a semiconductor with a gap of 45 meV and a conductivity 13 orders of magnitude higher than found in the 3D C-S polymer known so far. The material can be easily produced in cm3 quantity and may have technological applications.

References
[1] P.W. Bridgman, Proc. Amer. Acad. Arts Sci. 74, 399-424 (1942).
[2] B. Ochiai, & T. Endo, Prog. Polym. Sci. 30, 183-215 (2005).
[3] E. Whalley, Can. J. Chem. 38, 2105 (1960).
[4] E.G. Butcher, M. Alsop, J.A. Weston & H.A. Gebbie, Nature 199, 756 (1963).
[5] W.S. Chan & A.K. Jonscher, Phys. stat. sol. 32, 749 (1969).
[6] S. Klotz, B. Baptiste, T. Hattori, S.M. Feng, Ch. Jin, K. Béneut, J.M. Guigner, I. Estève, Carbon 185, 194 (2021)

Fig 1: Sample of CS2 (black sphere in the centre)

Fig. 2 Structural model of CxS

Back to Table of contents

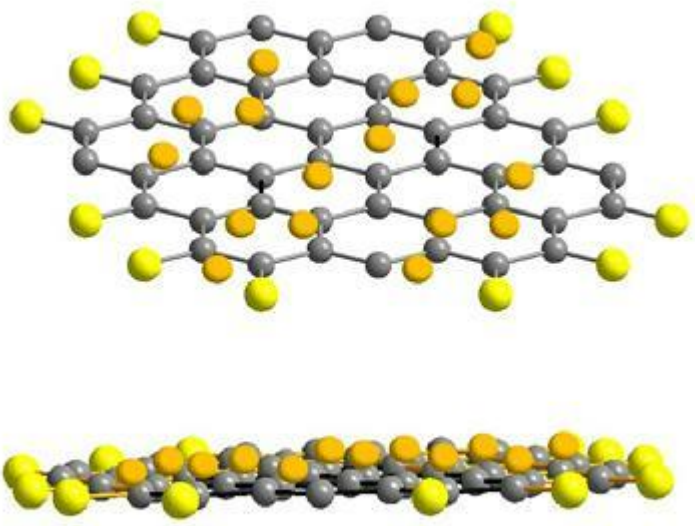

Back to Table of contents

MS27 Minerals and Materials Under Extreme Conditions

MS27-2-15 Pressure as switch for ionic conductivity in minerals of the pearceite-polybasite group
#MS27-2-15

C. Hejny [1], A. Wierer [1], A. Venturi [1]
[1]University of Innsbruck - Innsbruck (Austria)

Abstract
Pearceite-polybasite group minerals (PPGM), $[(Ag,Cu)_6(As,Sb)_2S_7][Ag_9CuS_4]$, are intriguing materials with Ag^+ fast ion conduction character that have attracted a lot of interest in the recent years. The notation of the chemical formula reflects the fact, that PPGM are composed of two different layers: layer A with general composition $[(Ag,Cu)_6(As,Sb)_2S_7]^{2-}$ and layer B with general composition $[Ag_9CuS_4]^{2+}$, whereat layer B is the place where the ionic conductivity takes places (BINDI et al. 2007). The root-name pearceite is given to minerals where As is dominant over Sb and the root-name polybasite for Sb-dominant phases. In addition, a suffix is attached to the root-name to give crystallographic information on the superstructure variant. Trigonal polytypes with lattice parameters a ~ 7.5, c ~ 12.0 Å are given the hyphenated italic suffix -*Tac*, trigonal polytypes with lattice parameters a ~ 15.0, c ~ 12.0 Å have -*T2ac* and monoclinic polytypes with a ~26.0, b ~» 15.0 c ~ 24.0 Å, β ~ 90° have -*M2a2b2c* as suffix. Depending on the exact chemical composition and disorder of the Ag and Cu atoms within the crystal structure a number of different crystal structures and their temperature-induced phase transitions are known (e.g. BINDI et al. 2006).

In order to test the possibility to use pressure as a switch for superconductivity, i.e. to induce phase transitions from the ionic conduction form to an ordered or partially ordered superstructure form with Ag ions “frozen-up” into fixed atomic positions, in-situ single-crystal diffraction experiments of PPGM have been performed in the diamond anvil cell.

A crystal fragment of pearceite-*Tac*, $Ag_{13.3}Cu_{3.8}As_{1.5}Sb_{0.4}S_{11}$, *a* = 7.3510(6), *c* = 11.892(1) Å, *V* = 556.5(1) Å^3, *P*-3*m*1, from the Clara Mine, Oberwolfbach, Schwarzwald, Germany, shows strong diffuse diffraction features parallel to *c** at ambient conditions that are characteristic for the high temperature fast ion conduction form. On pressure increase the appearance of additional reflections at *h*/2 and *k*/2 reveals a phase transition to the *T2a*c superstructure between 0.1 and 1.2 GPa (1.2GPa: *a* = 7.3137(5), *c* = 11.723(4) Å, *V* = 542.8(2) Å^3). Furthermore, diffuse maxima condense within the originally uniform diffuse diffraction features and a number of sharp satellite reflections appear at 1.2 GPa and move their position with increasing pressure. These features are in accordance with the explanation of a composite modulated structure model for the PPGM superstructures (WITHERS et al. 2008). A crystal of polybasite-*T2ac*, $Ag_{15.0}Cu_{1.7}Sb_{1.8}As_{0.2}S_{11}$, *a* = 15.1006(5), *c* = 11.9329(4) Å, *V* = 2356.5(1) Å^3, *P*321, from the Husky Mine, Elsa, Yukon Territory, Canada, transforms to the *M2a2b2* superstructure variant, *a* = 14.785(5), *b* = 22.643(9), *c* = 25.48(2) Å, α = 89.94(5), β = 90.69(5), γ = 89.98(3), V = 8531(9) Å3 between 3.5 and 5.4 GPa.

References
BINDI, L., EVAIN, M., PRADEL, A., ALBERT, S., MENCHETTI (2006) Phys. Chem. Minerals 33, 677-690.

BINDI, L., EVAIN, M., SPRY, P.G., MENCHETTI, S. (2007) Amer. Mineral. 92, 918-925.

WITHERS, R.L., NORÉN, L., WELBERRY, T.R., BINDI, L., EVAIN, M., MENCHETTI, S. (2008) Solid State Ionics 179, 2080-2089.

Back to Table of contents

MS28 Navigating crystal forms in molecular and pharmaceutical materials

MS28-1-1 Exploring the unknown world of the virosphere
#MS28-1-1

I. Cormack [1], E. Tarrant [1], E. Pohl [1]
[1]Durham University - Durham (United Kingdom)

Abstract
Biotechnology plays an ever-increasing role in the production of everyday products, from food ingredients to vaccine development. Many of the key tools in biotechnology have been discovered from the study of viruses as their genomes are packed with novel nucleic acid-processing enzymes.1 However, the vast majority of viruses have not been characterised.2 Therefore, the European Virus-X consortium sampled viruses from extreme environments to sequence and characterize their proteins.2 From this, several hundred gene products have been characterised. A number of viral proteins sourced from these extreme environments were identified with the potential to enhance a wide range of current molecular biology techniques. One group of proteins, single-stranded DNA binding proteins, show potential to enhance loop-mediated isothermal amplification specification and assay time.2 These binding proteins await characterisation using a range of biophysical and structural techniques which include X-ray crystallisation and cryogenic electron microscopy.

References
1. G. Ofir and R. Sorek, Cell, 2018, 172, 1260-1270.
2. Aevarsson, A. et al., FEMS Microbiology Letters, 2021, DOI: https://doi.org/10.1093/femsle/fnab067.

Back to Table of contents

MS28 Navigating crystal forms in molecular and pharmaceutical materials

MS28-1-2 Probing the effect of non-/hydrostatic pressures on ofloxacin and levofloxacin #MS28-1-2

J. Gasol Cardona [1], M.R. Ward [1], D. Markl [1], A.G.P. Maloney [2], I.D.H. Oswald [1]
[1]University of Strathclyde - Glasgow (United Kingdom), [2]Cambridge Crystallographic Data Centre - Cambridge (United Kingdom)

Abstract
Pharmaceutical tablets are the most widely used oral solid dosage (OSD) form worldwide. They have a convenient design that favours high patient compliance, display good stability to atmospheric conditions, and can be manufactured at a large scale with the correct formulation. [1] Currently, an iterative process is often needed to determine an OSD formulation with optimum mechanical properties for tablet compaction. Iterative processes require greater amounts of starting material, additional funding and prolonged research time. To make OSD formulation more efficient, a deeper understanding of the structural characteristics of pharmaceutically relevant materials and their behaviour under pressure is needed.
Ofloxacin and levofloxacin are the racemic mixture and L-enantiomer, respectively, of the effective antibiotic drug molecule 9-fluoro-3-methyl-10-(4-methylpiperazin-1-yl)-7-oxo-2,3-dihydro-7H-[1,4]oxazino[2,3,4-ij]quinoline-6-carboxylic acid. The chiral difference between the levo and dextro isomers causes not only a significant variation in antibacterial activity [2], but also differing solid state landscapes for ofloxacin and levofloxacin. [3][4]
In our study, we perform high-pressure X-ray diffraction on ofloxacin, levofloxacin hemihydrate and levofloxacin anhydrous γ-form to determine the impact of chirality, hydration and slip planes on their structural behaviour under pressure. Pressure is applied using hydrostatic and non-hydrostatic pressure transmitting media (PTM) to compare and model the differences in behaviour under these different pressure regimes. Additional Raman spectroscopic studies are carried out to complement the observations reported *via* X-ray diffraction. The materials are compressed up to 5 GPa to study their compressibility and phase behaviour above the tableting pressure range.

References
1. A. Advankar, D. Kapoor, R. Maheshwari, N. Raval, V. Tambe, R. K. Tekade and P. Todke, in *Drug Delivery Systems*, ed. R. K. Tekade, Elsevier, Amsterdam, 1 edn., 2019, ch. 13, pp. 615-664.**2.** D. N. Fish and A. T. Chow, *Clin. Pharmacokinet.*, 1997, **32**, 101-119.**3.** S. Mahapatra, K. N. Venugopala and T. N. G. Row, *Cryst. Growth Des.*, 2010, **10**, 1866-1870.**4.** N. Wei, L. N. Jia, Z. R. Shang, J. B. Gong, S. G. Wu, J. K. Wang and W. W. Tang, *CrystEngComm*, 2019, **21**, 6196-6207.

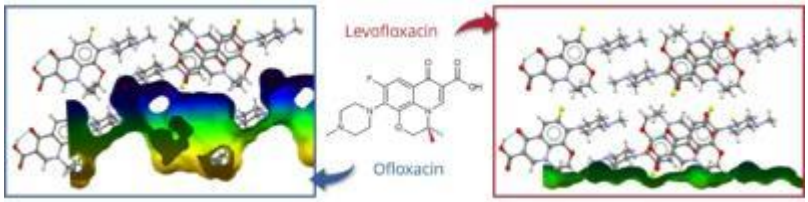

Back to Table of contents

MS28 Navigating crystal forms in molecular and pharmaceutical materials

MS28-1-3 Structural study of copper and zinc complexes of monoquinolines potentially active against Alzheimer's disease
#MS28-1-3

L. Vendier [1], M. Nguyen [1], B. Meunier [1], A. Robert [1]
[1]CNRS - Toulouse (France)

Abstract
Loss of homeostasis of redox metals, particularly copper, in the brain of patients with Alzheimer's disease (AD) and the scavenging of copper by the amyloid peptide Aβ are responsible for oxidative damage leading to death of the cells neurons. To restore this copper homeostasis, without disturbing the abundant zinc in the brain, we have developed tetradentate chelators specific for copper, the TDMQs (for TetraDentate MonoQuinolines), formed of an 8-aminoquinoline unit substituted, on position 2, by a chelating side chain. In the metal complexes of TDMQ, the coordination of copper(II), provided by a square plane formed by the two nitrogen atoms of the 8-aminoquinoline unit and by the two nitrogens of the side chain, is very strong. The coordination of zinc, ensured only by the side chain, is much weaker. TDMQs are capable of completely extracting copper from Cu-Aβ complexes, and making it available to copper proteins. The complete structural characterization, by single-crystal X-ray diffraction, of eight TDMQ copper-zinc complexes is described here. The crystallographic structure is correlated with the affinity of the ligands for Cu(II) and Zn(II), and with their capacity to inhibit in vitro an oxidative stress induced by the Cu-Aβ complex. Such specific copper chelators should be able to regulate copper homeostasis in brain tissue and can therefore be considered as potential therapeutic agents for Alzheimer's disease.

References
[1] W. Zhang, D. Huang, M. Huang, J. Huang, D. Wang, X. Liu, M. Nguyen, L. Vendier, S. Mazères, A. Robert, Y. Liu, B. Meunier, ChemMedChem 2018, 13 (7), 684-704.
[2] Y. Li, M. Nguyen, M. Baudoin, L. Vendier, Y. Liu, A. Robert, B. Meunier, Eur. J. Inorg. Chem. 2019 (44), 4712-4718.
[3] Y. Liu, M. Nguyen, A. Robert, B. Meunier, Acc. Chem. Res. 2019, 52 (7), 2026-2035.
[4] Y. Li, M. Nguyen, L.Vendier, A.Robert, Y. Liu, B. Meunier, J. Mol. Struc., 1251 (2022) 132078

Restoration of copper homeostasis by TDMQs, specif

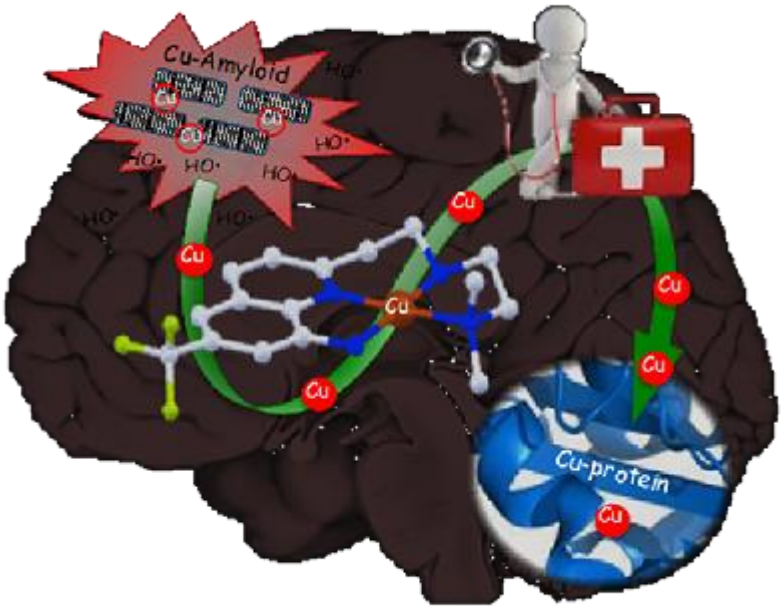

Back to Table of contents

MS28 Navigating crystal forms in molecular and pharmaceutical materials

MS28-1-4 RESI, Steady, Go!, Using the RESI tool in SHELX to help refine high Z' structures.
#MS28-1-4

M. Elsegood [1], M. Smith [1], P. De'ath [1]
[1]Loughborough University - Loughborough (United Kingdom)

Abstract
Crystal structures with more than one molecule in the asymmetric unit have been of interest in recent years, for example via collating projects run by Prof. Jon Steed at Durham University in the UK. In this work, new polymorphs or entirely new structures with moderate to high Z' values will be presented.
The Z' = 1 structure of trimellitic acid appears twice in the CSD, in both cases from the early 1970's and measured at room temperature [1,2 & Fig 1 (left)]. Here, new polymorphs with Z' = 6 and 10 will be discussed. Intriguingly, these both originate from crystallisations in the presence of lanthanide salts.
There is also a Z' = 1 entry in the CSD for 4-(methoxycarbonyl)benzoic acid, which is mono-methylated terephthalic acid. [3 & Fig 1 (right)] Here, a new polymorph with Z' = 3 is discussed.
The last structure is a new Pd-phosphine complex incorporating a long C_{18} chain and having a remarkable Z' = 20. Crystallising compounds with long greasy chains is often troublesome, but has been achieved for this and several similar compounds.
Clearly, the mechanics of refining such high Z' structures is a challenge. This starts with atom labelling to incorporating H atoms, and then analysing geometrical features, etc, and so the RESI command in SHELX has been explored to see how it might help in such cases. As a novice user of this command, even after nearly 30 years in crystallography, some discussion with more experienced users of RESI would be welcomed.

References
1. F. Takusagawa, K. Hirotsu, and A. Shimada, *Bull. Chem. Soc., Jpn*., (1973), 46, 2960.
2. F. G. Beltran and J. M. F. Marquina, *Rev. Acad. Cienc. Ex. Zaragoza*, (1970), 25, 183.
3. Y. Li and J. Wang, *Z. Kristallgr. - New Cryst. Struct*. (2019), 234, 349.

Figure 1.

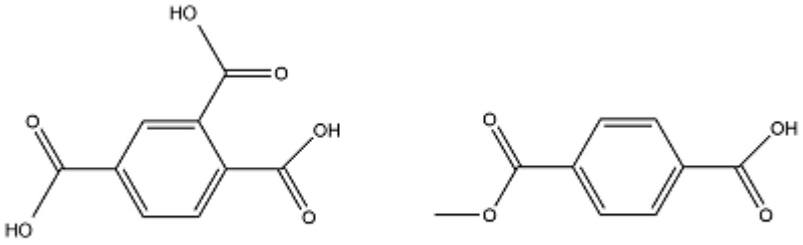

Trimellitic acid. 4-(Methoxycarbonyl)benzoic acid

Back to Table of contents

MS28 Navigating crystal forms in molecular and pharmaceutical materials

MS28-1-5 Ribavirin at High Pressure
#MS28-1-5

B. Tiwari [1], N. Giordano [1]
[1]DESY - Hamburg (Germany)

Abstract
Exhaustive characterisation of polymorphism and phase transitions in active pharmaceutical ingredients (APIs) is of critical importance to pharmaceutical companies in the development of 'solid forms' used in patient therapy. Polymorphs of the same API may differ in their physical properties e.g. solubility, kinetic stability, or tabletability; affecting everything from bioavailability to manufacture and storage.[1] We are interested in characterising polymorphism in APIs using high pressure to mediate phase transitions. New polymorphs realised by high pressure may have improved therapeutic properties or identify limitations of the marketed form.
Ribavirin, a broad-spectrum antiviral agent,[2] was studied to 10 GPa using single crystal X-ray diffraction in the diamond anvil cell with synchrotron radiation (λ=0.2916 Å). Full structure determinations and refinements have been performed for the ambient pressure phase (P212121) which is stable to 5.6 GPa and its pressure-volume equation-of-state determined. The emergence of twinning at 6.3 GPa indicates the formation of a new phase, and efforts are underway to solve the new high-pressure crystal structure.

References
[1] Jie Lu, Xiaolan Zhan, Lianwei Chen, Lijuan Zhang, and Shimin Mao J. of Chem. & Eng. Data 2014 59 (8), 2665-2669
[2] Prusiner, P. & Sundaralingam, M. (1976). Acta Cryst. B32, 419-426.

Molecular structure of ribavirin at 5.62 GPa

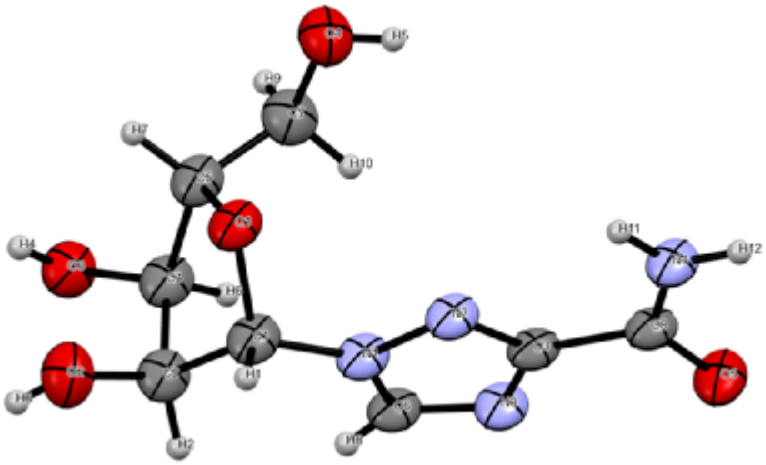

Back to Table of contents

MS28 Navigating crystal forms in molecular and pharmaceutical materials

MS28-1-6 Solid form characterization of pharmaceutical compounds enhanced by Electron Diffraction experiments #MS28-1-6

D. Stam [1], J. Merkelbach [1], C. Jandl [1], G. Steinfeld [1], E. Hovestreydt [1]
[1]ELDICO Scientific AG - Villingen (Switzerland)

Abstract
Solid state screening of Active Pharmaceutical Ingredients (APIs) is essential for selecting the most adequate solid form for development into a drug product. Therefore, it is always recommended to conduct a thorough search to establish the landscape of the crystalline solid forms and to assess the associated development risks.
For each solid-state form of an API, the arrangement of the molecules in the crystal determines its physical properties and therefore, knowledge of crystal structure is important in order to fully understand and optimize the pharmaceutical performance of the drug.
Consequently, an effective approach for solid form screening combined with crystal structure determination is of considerable importance across the drug development process (Figure 1). However, as growth of suitable crystals for X-ray crystallography may be time consuming for complex molecules, using Electron diffraction (ED) on nano-sized crystals represents a significant advantage to the solid-state studies.
This contribution aims to offer different case studies of the importance of crystal structure determination for the pharmaceutical industry. Particularly, the capability of the new ELDICO ED-1 electron diffractometer (Figure 2) to efficiently provide crystal structures will be explored in the case of pharmaceutical nanocrystals.

Solid form screening during drug development

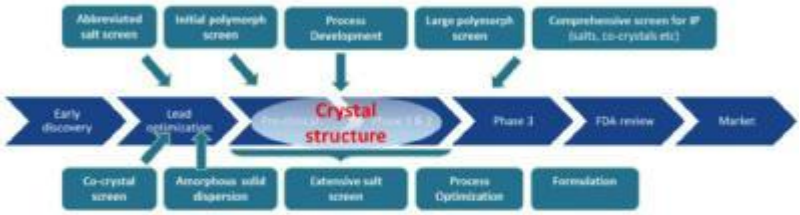

ELDICO ED-1 electron diffractometer

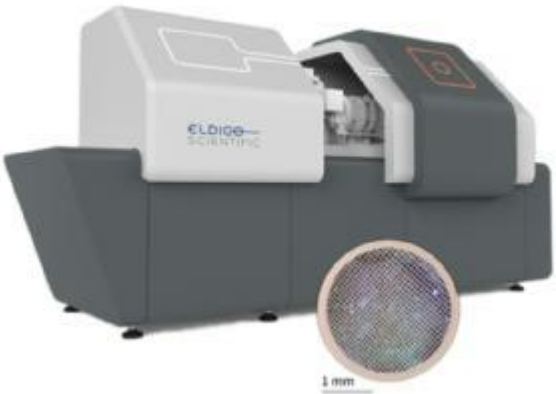

Back to Table of contents

MS28 Navigating crystal forms in molecular and pharmaceutical materials

MS28-1-7 New Drug-Drug Salt Forms of Ciprofloxacin with Fenamic Acids
#MS28-1-7

A. Sevillano-Páez [1], C. Alarcón-Payer [2], F.J. Acebedo-Martínez [1], J.M. González-Pérez [3], A. Domínguez-Martín [3], D. Choquesillo-Lazarte [1]
[1]Laboratorio de Estudios Cristalográficos, IACT, CSIC-UGR - Granada (Spain), [2]Hospital Universitario Virgen de las Nieves - Granada (Spain), [3]Department of Inorganic Chemistry, University of Granada - Granada (Spain)

Abstract
Crystal engineering has provided an efficient approach for tuning physicochemical properties of active pharmaceutical ingredients (APIs), and therefore has a direct application in the pharmaceutical industry. For instance, salt formation is a widely used strategy to improve the solubility of ionizable drugs [1]. This work reports on the preparation and solid-state characterization of two new drug-drug salts of ciprofloxacin in a 1:1 stoichiometry, using mefenamic and tolfenamic acids as the second component. Low aqueous solubility and moisture sensitivity of the parent drug molecules used in this study have motivated us to investigate the possibility of forming novel salts of existing drugs for enhanced physicochemical properties and better biological activity. The new pharmaceutical salts were prepared by mechanochemical methods and characterized by thermal, spectroscopic and diffractometric techniques. Their crystal structures have been determined to evaluate the role of intermolecular interactions on the improvement of physicochemical properties. Stability studies at 40 ºC and 75% RH, solubility determination and preliminary *in-vitro* studies contributed to complete the whole picture of these multicomponent molecular materials. Significant results of our study will be presented.

References
[1] Kasim, N. A.; Whitehouse, M.; Ramachandran, C.; Bermejo, M.; Lennerna, H.; Hussain, A. S.; Junginger, H. E.; Stavchansky, S. A.; Midha, K. K.; Shah, V. P.; Amidon, G. L. *Mol. Pharmaceutics*, 1 (2004) 85.

Back to Table of contents

MS28 Navigating crystal forms in molecular and pharmaceutical materials

MS28-1-8 New multicomponent crystals as a method to improve the physicochemical properties of active pharmaceutical ingredients – three case studies
#MS28-1-8

E. Pindelska [1], I. Madura [2], K. Znajdek [3], A. Sarna [3], C. Martin [3]
[1]Department of Analytical Chemistry and Biomaterials, Faculty of Pharmacy, Medical University of Warsaw - Warsaw (Poland), [2]Department of Inorganic Chemistry, Faculty of Chemistry, Warsaw University of Technology - Warsaw (Poland), [3]Scientific Circle "Spektrum" at Department of Analytical Chemistry and Biomaterials, Faculty of Pharmacy, Medical University of Warsaw - Warsaw (Poland)

Abstract
Multicomponent pharmaceutical crystals, consisting of cocrystals and salts, have found use as an alternative solid form of drugs with better physicochemical properties compared to the corresponding parent drugs. The purpose of creating multicomponent crystals is to improve the solubility profiles and dissolution rate of drug molecules, but also to help overcome other problems such as hygroscopicity, poor tabletting, instability, and bitter taste. We aimed to obtain new salts of memantine (MEM) with reduced hygroscopicity and improved taste compared to currently used memantine hydrochloride, which is slightly hygroscopic and has a bitter taste. Another goal was to improve the solubility and release profile of two poorly soluble drugs: febuxostat (FEB) and erlotinib (ETB) by creating new multicomponent systems.
The synthesis was performed by reacting MEM free base with sweet-tasting acids: acesulfame, saccharin, and anthranilic acid. In a case of FEB and ETB, the liquid assisted milling method has been used successfully to obtain new multicomponent crystals. Fourier transformed infrared spectroscopy and powder X-ray diffraction were used to provide information about the formation of new substances. The crystal structure of the new obtained crystals was determined by single crystal X-ray studies. Structural studies were supported by solubility and dissolution rate tests. In the case of MEM, also taste tests.
Each of new MEM salts has an improved taste and is less hygroscopic than memantine hydrochloride. Solubility and dissolution research show that newly obtained multicomponent crystals of FEB and ETB exhibit almost three times higher solubility and dissolution rate than their free bases.
Acknowledgments: These studies were financially supported by Medical University of Warsaw, grants number FW231/2/F/GW/N/21 and FW231/1/F/MG/N/21.

Crystal structures of memantine salts.

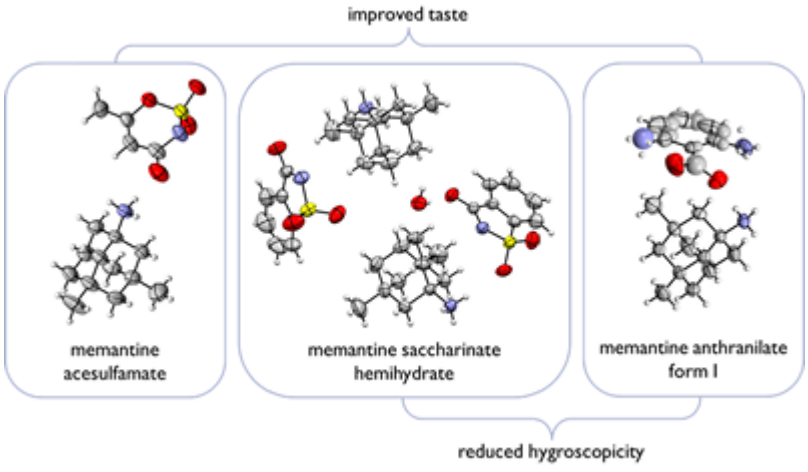

Back to Table of contents

MS28 Navigating crystal forms in molecular and pharmaceutical materials

MS28-1-9 Navigating crystal forms in pharmaceutical compounds by 3DED/MicroED
#MS28-1-9

M. Lightowler [1], S. Li [2], X. Ou [2], G. Hofer [1], J. Cho [1], X. Zou [1], M. Lu [2], H. Xu [1]
[1]Stockholm University - Stockholm (Sweden), [2]Sun Yat-sen University - Guangzhou (China)

Abstract
Three-dimensional electron diffraction (3DED), also known as microcrystal electron diffraction (MicroED) has recently emerged as a promising method for crystal structure determination of pharmaceutical compounds[1,2]. The method complements existing methods by providing the opportunity to study small organic molecules from crystals too small for conventional single crystal X-ray diffraction and too complex for powder X-ray diffraction. In our lab, structures of several pharmaceutical compounds have been determined and various studies indicate that 3DED/MicroED is capable of (i) rapid structure determination at atomic resolution[2,3], (ii) solving crystal structures of new polymorphs[4,5], (iii) studying polymorphism evolution[6,7], and (vi) phase analysis by high-throughput 3DED/MicroED. However, comparing to X-ray diffraction, 3DED/MicroED is still in its infancy. Further optimization and innovations in new software and hardware are required to make it more robust and more accessible to the structural chemistry and pharmaceutical research community. In EMC33, I would like to present our latest development in specimen preparation, data collection and processing routine, and future perspective of 3DED/MicroED.

Figure Caption - A summary of 3DED/MicroED applications in studying crystal forms of pharmaceutical compounds in our lab. a) structure determination of API bismuth Subgallate[8], b) Polymorphism evolution of glycine[6], c) Crystallization of carbamazepine[7], d) Discovery of indomethacin form θ, correcting a 47-year-old misunderstanding[5], e) Structure determination of five phases of vemurafenib, and f) Phase analysis by high throughput 3DED/MicroED.

References
1. Clabbers, M. T. B. & Xu, H. Microcrystal electron diffraction in macromolecular and pharmaceutical structure determination. Drug Discov. Today Technol. S1740674920300354 (2020) doi:10.1016/j.ddtec.2020.12.002. 2. Jones, C. G. et al. The CryoEM Method MicroED as a Powerful Tool for Small Molecule Structure Determination. ACS Cent. Sci. 4, 1587–1592 (2018). 3. Gruene, T. et al. Rapid Structure Determination of Microcrystalline Molecular Compounds Using Electron Diffraction. Angew. Chem. Int. Ed. 57, 16313–16317 (2018). 4. Andrusenko, I. et al. Structure determination, thermal stability and dissolution rate of δ-indomethacin. Int. J. Pharm. 608, 121067 (2021). 5. Lightowler, M. et al. Indomethacin Polymorph δ Revealed To Be Two Plastically Bendable Crystal Forms by 3D Electron Diffraction: Correcting a 47-Year-Old Misunderstanding**. Angew. Chem. Int. Ed. 61, (2022). 6. Broadhurst, E. T. et al. Polymorph evolution during crystal growth studied by 3D electron diffraction. IUCrJ 7, 5–9 (2020). 7. Broadhurst, E. T., Xu, H., Parsons, S. & Nudelman, F. Revealing the early stages of carbamazepine crystallization by cryoTEM and 3D electron diffraction. IUCrJ 8, 860–866 (2021). 8. Wang, Y. et al. Elucidation of the elusive structure and formula of the active pharmaceutical ingredient bismuth subgallate by continuous rotation electron diffraction. Chem. Commun. 53, 7018–7021 (2017).

Back to Table of contents

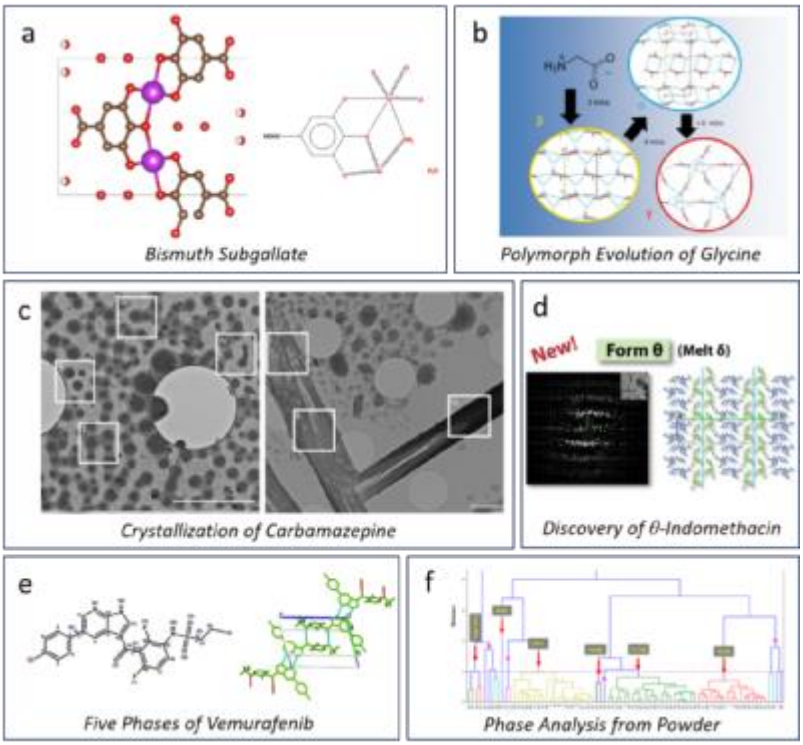

Back to Table of contents

MS28 Navigating crystal forms in molecular and pharmaceutical materials

MS28-1-10 Polymorphic landscape of pharmaceutical solid solutions
#MS28-1-10

M. Lusi [1]
[1]University of Limerick - Limerick (Ireland)

Abstract
In the pharmaceutical industry, polymorphism represents both a potential issue as well as an opportunity to isolate a solid form with improved properties, for manufacturing, storage or administration. Indeed polymorph screening is common practice in the early stage of drug development. The phenomenon is well documented for single component and multicomponent molecular crystals. For almost a century, practical rules of thumbs for the design of solid solutions have overlooked the possibility of polymorphism for these phases. In recent years though, the occurrence of polymorphism in mixed crystals and solid solutions has been highlighted.
Here novel examples of polymorphism are presented for substitutional solid solutions and mixed cocrystals. In most cases the crystal structure of the mixed product depends on the composition i.e. it is chemically controlled. In other instances real polymorphism occurs at the same composition due to variation of crystallization methods (synthetic controlled) or external conditions (physical controlled). Finally the relationship between physical properties (solubility and stability), crystallography (solid form) and chemistry (composition) is discussed to determine the potential use of solid solutions to probe and control the polymorphic landscape of pharmaceutical solid solutions.

Solid state landscape of a racemic mixed cocrystal

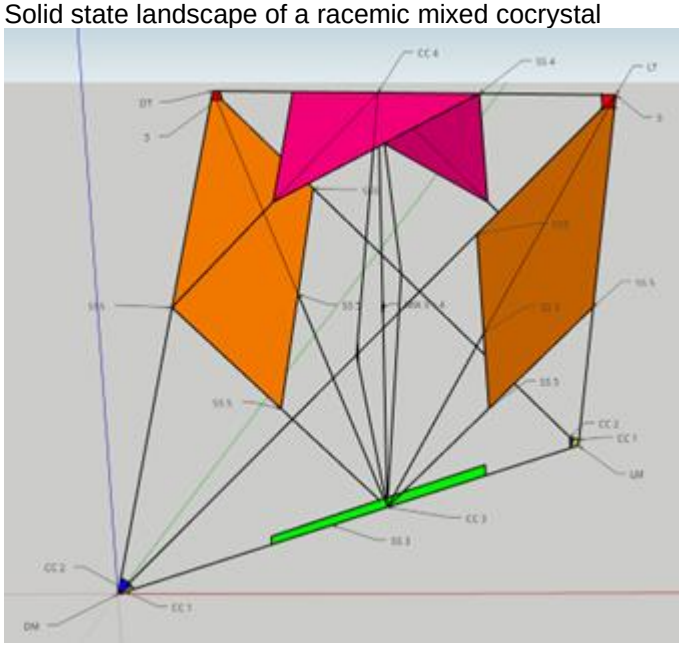

Back to Table of contents

MS28 Navigating crystal forms in molecular and pharmaceutical materials

MS28-1-11 Integrating machine learning in crystal structure prediction for pharmaceutical compounds #MS28-1-11

A. Anelli [1], H. Dietrich [2], P. Ectors [1], F. Stowasser [1], T. Bereau [3], M. Neumann [2], J. Van Den Ende [4]
[1]Hoffmann La Roche - Basel (Switzerland), [2]Avant-garde Materials Simulation - Merzhausen (Germany), [3]University of Amsterdam - Amsterdam (Netherlands), [4]Hoffman La Roche - Basel (Switzerland)

Abstract
Organic molecules can crystallize into various solid forms, which generates a polymorphic degree of freedom[1]. Since the different solid forms have distinct physico-chemical behavior (e.g. solubility, compressibility etc…), it is paramount to know which crystalline packings an active pharmaceutical ingredient (API) can aggregate into. A promising route to characterize the crystalline landscape of APIs is to perform quantum mechanical atomistic simulations of each potential polymorph, so as to obtain a much needed ranking of the observable crystals[2]. While this routine is fully general and applicable to any class of compounds, it requires a substantial computational investment, allowing its use mostly for molecules in the later drug development stages. To decrease the computational overhead of such approaches, we propose an integrated machine learning crystal structure prediction (ML-CSP) framework. We combine on the fly machine learning potentials[3] with a Bayesian selection scheme to accurately sample the crystal structure landscape of a target API. In Figure 1, we show how the accuracy of a model trained on PBE-DFT energies for fentanyl molecular crystals improves as we progress our ML-CSP routine. By using our method, we report a 3 to 5 fold increase in performances, paving the way for crystal structure prediction to penetrate in the earlier development stages or target more complex compounds.

References
[1] : Cruz-Cabeza, A.J., Feeder, N. and Davey, R.J., 2020. Open questions in organic crystal polymorphism. Communications Chemistry, 3(1) DOI : https://doi.org/10.1038/s42004-020-00388-9
[2] : Hoja, J., Ko, H.Y., Neumann, M.A., Car, R., DiStasio Jr, R.A. and Tkatchenko, A., 2019. Reliable and practical computational description of molecular crystal polymorphs. Science advances, 5(1) DOI : 10.1126/sciadv.aau3338
[3] Sivaraman, G., Krishnamoorthy, A.N., Baur, M., Holm, C., Stan, M., Csányi, G., Benmore, C. and Vázquez-Mayagoitia, Á., 2020. Machine-learned interatomic potentials by active learning: amorphous and liquid hafnium dioxide. npj Computational Materials, 6(1) DOI : https://doi.org/10.1038/s41524-020-00367-7

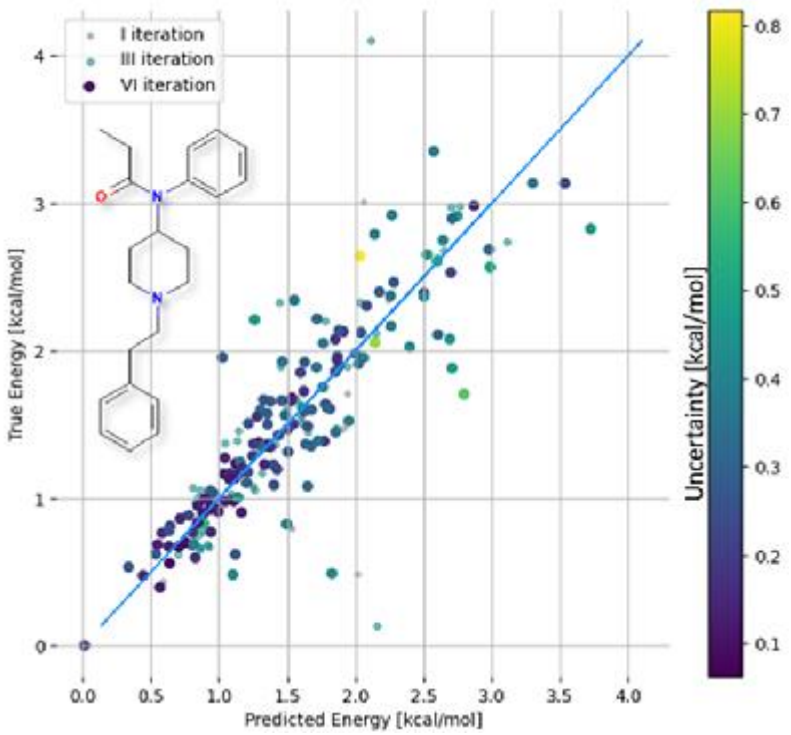

Back to Table of contents

MS28 Navigating crystal forms in molecular and pharmaceutical materials

MS28-1-12 On the selectivity of methylation of the amidine system and stereoisomerism of 3-alkylated derivatives of 5-metoxycarbonylmetylidene-4-phenylimino-1,3-thiazol-2(5H)-one
#MS28-1-12

A. Pyrih [1], M. Jaskolski [2], R. Lesyk [3], A. Gzella [4]
[1]Adam Mickiewicz University in Poznan - Poznań (Poland) - Poznań (Poland), [2]Institute of Bioorganic Chemistry, Polish Academy of Science - Poznań (Poland), [3]Danylo Halytsky Lviv National Medical University - L'viv (Ukraine), [4]Poznań University of Medical Sciences - Poznań (Poland)

Abstract
The following four methylated derivatives of 5-metoxycarbonylmetylidene-4-phenylamino-1,3-thiazol-2(5H)-one, with the potential to form N=C-NH ↔ NH–C=N tautomeric equilibria, were synthesized and studied by X-ray crystallography in order to determine the selectivity of methylation of the amidine system:
3-methyl-5-methoxycarbonylmetylidene-4-phenylimino-2-thiazolidione;3-methyl-5-methoxycarbonylmetylidene-4-(4-bromophenylimino)-2-thiazolidione;3-methyl-5-methoxycarbonylmetylidene-4-(4-chlorophenylimino)-2-thiazolidione;3-methyl-5-methoxycarbonylmetylidene-4-(4-fluorophenylimino)-2-thiazolidione.
The crystal structures show that the methylation takes place in each case selectively at the nitrogen atom of the heterocycle. It was found that the presence of a bulky methyl group in that position causes a change in the conformation of the molecule with respect to the substrates - 5-methoxycarbonylmethylidene-4-phenylamino-2-thiazolinones, which are characterized by a very stable synperiplanar conformation. At the same time, due to the shift in the position of the double bond in the amidine group, the molecules of all four products adopt the E configuration. The latter observation is particularly interesting, as this is the first time it has been reported for 4-phenylamino-1,3-thiazol-2(5H)-one derivatives. It is also worth noting that in the newly prepared methylated derivatives of 5-methoxycarbonylmethylidene-4-phenylimino-2-thiazolidinone, the thiazolidinone and phenyl rings are approximately perpendicular, in contrast to the coplanar orientation in the substrate molecules. The flat 5-methoxycarbonylmethylidene moiety in both, the substrate and products molecules has the Z configuration and lies approximately in the plane of the heterocycle.
The work was supported by grant no. POWR.03.02.00-00-I020/17 co-financed by the European Union through the European Social Fund under the Operational Program Knowledge Education Development.

Back to Table of contents

MS28 Navigating crystal forms in molecular and pharmaceutical materials

MS28-1-13 Rationalising the formation of co-crystals of nicotinamide and isonicotinamide
#MS28-1-13

J. Adjimani [1], Y. Khimyak [1], L. Fabian [1]
[1]University of East Anglia - Norwich (United Kingdom)

Abstract
The creation of multicomponent crystals forms has provided an avenue that has become increasingly important in improving many physiochemical drug properties, such as aqueous solubility and bioavailability[1]. To further enhance the discovery of new multi-component forms, understanding intermolecular interactions, particularly hydrogen bonding is pivotal. We selected two common, GRAS (generally recognised as safe) cocrystal coformers from the Cambridge Structural Database (CSD)[2]; Nicotinamide (NA) and Isonicotinamide (INA) which have 178 and 233 cocrystals respectively. These coformers have the same chemical composition, except for the position of the nitrogen in the pyridine ring. Interestingly, they exhibit different hydrogen bonding, even with the same cocrystal coformer. This phenomenon is unexpected, as conventional cocrystal formation is synthon based[3], and with NA and INA having the same synthons, one would expect the same hydrogen bonding patterns. We analysed the hydrogen bonding of the cocrystals reported in CSD, and determined which synthons are preferred in NA and INA. To probe this further, we synthesized cocrystals of these coformers with 7 Active Pharmaceutical Ingredients (APIs) via liquid assisted grinding in different stoichiometric ratios, namely 1:1, 1:2, 2:1 and 1:3. The results of these crystallization experiments were analysed using DSC, PXRD, Solid-state NMR and SCXRD to ascertain the effect the varying of stoichiometry has on cocrystal formation.

References
1. Kavanagh, O. N.; Croker, D. M.; Walker, G. M.; Zaworotko, M. J., Pharmaceutical cocrystals: from serendipity to design to application. Drug Discovery Today 2019, 24 (3), 796-804.
2. Groom, C. R.; Bruno, I. J.; Lightfoot, M. P.; Ward, S. C., The Cambridge Structural Database. Acta Crystallogr. Sect. B-Struct. Sci.Cryst. Eng. Mat. 2016, 72, 171-179
3. Desiraju GR. Supramolecular Synthons in Crystal Engineering—A New Organic Synthesis. Angewandte Chemie International Edition in English. 1995;34(21):2311-27.

Structure of Nicotinamide and Isonicotinamide

Back to Table of contents

MS28 Navigating crystal forms in molecular and pharmaceutical materials

MS28-1-14 Polymorphism in Lithium ionic cocrystals
#MS28-1-14

Y. Hjiej Andaloussi [1], M. Zaworotko [1]
[1]University of Limerick - Limerick (Ireland)

Abstract
The use of lithium as a highly effective therapeutic for the treatment of bipolar disorder and major depressive disorder has been historically hindered by a narrow therapeutic window between efficacy and toxicity. In 2013, lithium was modified to have improved pharmacokinetic properties through the use of an ionic cocrystal with salicylate and L-Proline, known as LISPRO, that has since been taken through to phase 2 clinical trials for the treatment of Alzheimer's disease. But did we get the right crystal form? Polymorphism in ionic cocrystals is an understudied phenomenon. As such this was investigated in LISPRO which found that the previously reported cocrystal polymorph of LISPRO, LISPRO(α), is in fact metastable. LISPRO(α) was found to transform under slurry conditions to the more thermodynamically stable polymorph, LISPRO(β), which possesses a highly similar Powder X-ray diffraction (PXRD) pattern. We assessed the polymorphism of a similar lithium L-Proline cocrystal with 4-methoxybenzoate (L4MPRO) which was shown to form the kinetically hindered but thermodynamically more stable L4MPRO(α) form, and the metastable L4MPRO(β) and (γ) forms. These case studies in the polymorphism of pharmaceutically-relevant agents offer cautionary tales and lessons on the mechanochemical and solution-based methods to study polymorphism in ionic cocrystals.

References
Sanii, R.; Andaloussi, Y. H.; Patyk-Kaźmierczak, E.; Zaworotko, M. J., Polymorphism in Ionic Cocrystals Comprising Lithium Salts and l-Proline. Crystal Growth & Design 2022.
Smith, A. J.; Kim, S.-H.; Duggirala, N. K.; Jin, J.; Wojtas, L.; Ehrhart, J.; Giunta, B.; Tan, J.; Zaworotko, M. J.; Shytle, R. D. Improving Lithium Therapeutics by Crystal Engineering of Novel Ionic Cocrystals. Mol. Pharm. 2013, 10, 4728– 4738
Schou, M.; Baastrup, P. C.; Grof, P.; Weis, P.; Angst, J. Pharmacological and Clinical Problems of Lithium Prophylaxis. Br. J. Psychiatry 1970, 116, 615– 619
Habib, A.; Sawmiller, D.; Li, S.; Xiang, Y.; Rongo, D.; Tian, J.; Hou, H. Y.; Zeng, J.; Smith, A.; Fan, S. N.; Giunta, B.; Mori, T.; Currier, G.; Shytle, D. R.; Tan, J. LISPRO mitigates beta-amyloid and associated pathologies in Alzheimer's mice. Cell Death Dis. 2017, 8, e2880

Back to Table of contents

MS28 Navigating crystal forms in molecular and pharmaceutical materials

MS28-2-1 Dry amorphization of itraconazole: extrusion and crystallinity
#MS28-2-1

E. Berthier [1], S. Welzmiller [2], M. Richter [3]
[1]Thermo Fisher Scientific - Artenay (France), [2]Thermo Fisher Scientific - Ecublens (Switzerland), [3]Thermo Fisher Scientific - Karlsruhe (Germany)

Abstract
In the development of active pharmaceutical ingredients (APIs), their bioavailability is of main concern. The metastable amorphous state of APIs can reduce the dissolution time and therefore increase bioavailability, but it needs to be stabilized by a matrix material. Polymers are predominantly used to form solid dispersions with APIs and therefore stabilize the amorphous state. Solid dispersions are mostly prepared by hot melt extrusion (HME) and spray drying. HME requires temperatures above the glass transition temperature of the polymer which often can lead to decomposition or structural change of the API, whereas spray drying requires tedious handling of a solvent.
An alternative route to stabilize the amorphous state of APIs is the usage of porous silica with a well-defined pore size distribution. Recent studies [1]-[3] have shown that solvent-free ball-milling of API/porous silica mixtures at moderate temperatures can improve the dissolution rate. Nonetheless, extensive milling times and batch processing is required. Twin-screw compounding technology is a mature process which can synthesize material in a constant flow with increased reproducibility and flexibility.[4][5]
In this study, itraconazole is used as a model drug which is stabilized by a mesoporous silica matrix. Processing is carried out by a laboratory sized pharmaceutical twin screw extruder with varying screw configurations and process parameters.
To analyze the quality of the processed material, powder X-ray diffraction (XRD) is used to quantify the amorphous to crystalline ratio by means of standard-less combined whole pattern refinements. Full amorphization is reached at 70°C, whereas up to 97% of amorphized API (1:1 blend) is achievable at room temperature, which is in good agreement to Differential Scanning Calorimetry (DSC) measurements. Additional Scanning Electron Microscopy (SEM) investigations clearly indicate a decrease in particle size of both, silica and itraconazole.

References
[1] A. Baán et al., “Dry amorphisation of mangiferin, a poorly water-soluble compound, using mesoporous silica,” Eur. J. Pharm. Biopharm., vol. 141, no. March, pp. 172–179, 2019.
[2] D. Bahl, J. Hudak, and R. H. Bogner, “Comparison of the ability of various pharmaceutical silicates to amorphize and enhance dissolution of indomethacin upon co-grinding,” Pharm. Dev. Technol., vol. 13, no. 3, pp. 255–269, 2008.
[3] F. Monsuur et al., “Solvent free amorphisation for pediatric formulations (minitablets) using mesoporous silica,” Int. J. Pharm., vol. 511, no. 2, pp. 1135–1136, 2016.
[4]C. Vervaet and J. P. Remon, “Continuous granulation in the pharmaceutical industry,” Chem. Eng. Sci., vol. 60, no. 14, pp. 3949–3957, 2005.
[5] J. Vercruysse et al., “Stability and repeatability of a continuous twin screw granulation and drying system,” Eur. J. Pharm. Biopharm., vol. 85, pp. 1031–1038, 2013

Back to Table of contents

MS28 Navigating crystal forms in molecular and pharmaceutical materials

MS28-2-2 Structure Determination of Pharmaceutical Cocrystals by Three-dimensional Electron Diffraction #MS28-2-2

J.Y. Xu [1], H.Y. Xu [1], X.D. Zou [1], C.C. Sun [2]
[1]Stockholm University - Stockholm (Sweden), [2]University of Minnesota - Minnesota (United States)

Abstract
Three-dimensional Electron Diffraction (3D ED), also known as MicroED, is becoming a powerful method for structure determination of nano-/micro- sized crystals. Owing to the strong interaction between electrons and matters, crystals that are too small for single-crystal X-ray diffraction and too complex for powder X-ray diffraction, can be studied by 3D ED. Thanks to the ease of beam manipulation, fast rotation as well as sensitive detectors, low-dose 3D ED becomes possible. With the assistance of a cryo-holder, further protection of the specimen against vacuum and electron beam damage can be achieved, which extends the application of electron crystallography to the structure determination of beam-sensitive crystals[1,2].
Herein, we show a series of pharmaceutical cocrystals solved by 3D ED[3,4]. With this method, more structures of pharmaceutical crystals can be solved efficiently, which will accelerate the development of structural pharmacology and drug discovery.

References
1.Gruene, T. etal. Rapid Structure Determination of Microcrystalline Molecular Compounds Using Electron Diffraction. Angew. Chemie - Int. Ed. (2018).
2.Jones, C. G. etal. The CryoEM Method MicroED as a Powerful Tool for Small Molecule Structure Determination. ACS Cent. Sci. (2018).
3.Wan, W., Sun, J., Su, J., Hovmöller, S. & Zou, X. Three-dimensional rotation electron diffraction: software RED for automated data collection and data processing. J. Appl. Crystallogr. (2013).
4.Cichocka, M.O., Ångström, J., Wang, B., Zou, X. & Smeets, S. High-throughput continuous rotation electron diffraction data acquisition via software automation. J. Appl. Crystallogr. (2018).

Scheme. The structures of pharmaceutical cocrystal

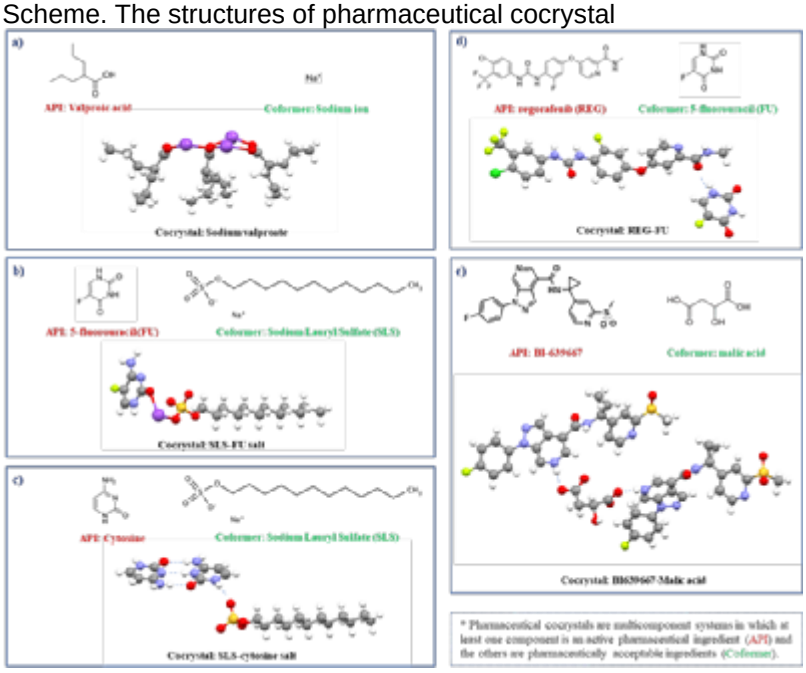

Back to Table of contents

MS28 Navigating crystal forms in molecular and pharmaceutical materials

MS28-2-3 Piperazine scaffold in drugs –structural and pharmaceutical points of view
#MS28-2-3

I.D. Madura [1], E. Pindelska [2]
[1]Warsaw University of Technology, Faculty of Chemistry - Warsaw (Poland), [2]Medical University of Warsaw, Faculty of Pharmacy - Warszawa (Poland)

Abstract
Knowledge of the conformational stability of compounds with potential biological activity is essential for studying ligand-receptor interactions. Typically, such interactions are simulated computationally, which gives insight into both the nature of the ligand-receptor interactions and indicates the most efficiently interacting molecular fragment of the ligand. This knowledge, in turn, allows the design of new generic ligands that act more selectively, for example. Usually, the results of experimentally characterized ligand crystal structures are used as a starting point for such studies. It should be noted that the ligand rarely binds to the receptor with strong covalent bonds; rather, weak reversible non-covalent interactions such as hydrogen or halogen bonds, or aromatic interactions are involved. Hence, a detailed analysis of intermolecular interactions a given molecule can exhibit is often beneficial. What is more, a combined techniques approach, involving X-ray diffraction, spectroscopic, thermal, and computational studies, seems to be a value-adding methodology as well.
This contribution concerns ligands containing a piperazine fragment in their structure. Such scaffold is present in a variety of active pharmaceutical molecules (over 300 crystals in the CSD drug subset [1]), to mention only antibiotics (e.g. levofloxacin [2]), antidepressants (e.g. trazadone [3]), antifungal (e.g. posaconazole [4]) and anticancer drugs (e.g. imatinib [5]). Noteworthy is a variety of crystal forms determined so far, like polymorphs, co-crystals, salts and solvates.
We will show the intermolecular interactions analysis, and the basis for the discussion will be their hierarchy established on the analysis of large molecular synthons and estimated interaction energy. The data for the analysis will be retrieved from CSD database and supplemented with our own research results. Correlation to ligand activity and certain receptors affinity will be addressed. Particular attention will be paid to multi-component crystals, which may show better pharmaceutical properties than pure drugs.
Acknowledgments
IDM is grateful to the Scientific Council of Chemical Sciences at Warsaw University of Technology for the NChem3_2022 grant.

References
[1] M.J. Bryant, S.N. Black, H. Blade, R. Docherty, A.G.P. Maloney, S.C. Taylor, *The CSD Drug Subset: The Changing Chemistry and Crystallography of Small Molecule Pharmaceuticals*, J. Pharm. Sci. 108, **2019**, 1655-1662. doi: 10.1016/j.xphs.2018.12.011;
[2] J.T.J. Freitas, C.C. de Melo, O.M.M.S. Viana, F.F. Ferreira, A.C. Doriguetto, C*rystal Structure of Levofloxacin Anhydrates: A High-Temperature Powder X-ray Diffraction Study Versus Crystal Structure Prediction* Cryst. Growth Des. 18, **2018**, 3558-3568. doi: 10.1021/acs.cgd.8b00363;
[3] J. Jaśkowska, P. Zaręba, A. Drabczyk, A. Kozak, I.D. Madura, Z. Majka, E. Pindelska, *New Pharmaceutical Salts of Trazodone* Molecules, 26, **2021**, 769. doi.org/10.3390/molecules26030769;
[4] G.Kuminek, K.L.Cavanagh, M.Fatima M.da Piedade, N.Rodriguez-Hornedo, *Posaconazole Cocrystal with Superior Solubility and Dissolution Behavior* Cryst. Growth Des. 19, **2019**, 6592-6602. doi:10.1021/acs.cgd.9b01026;
[5] J.P. Jasinski, R. J.Butcher, Q. N. M.Hakim Al-Arique, H. S. Yathirajan, B. Narayana, *Imatinibium dipicrate* Acta Cryst. E66, **2010**, o411-o412. doi: 10.1107/S1600536810000577.

Back to Table of contents

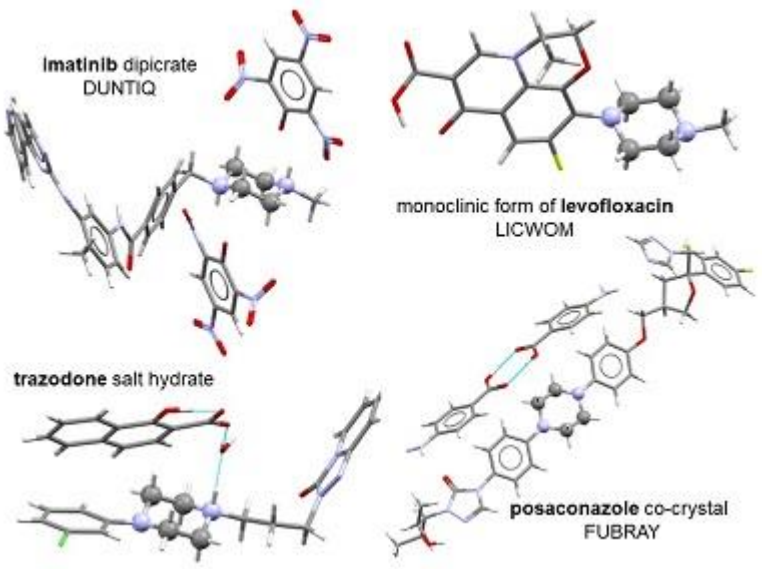

Back to Table of contents

MS28 Navigating crystal forms in molecular and pharmaceutical materials

MS28-2-4 GABA & Gabapentin - Commonalities and Distinctions in (Co-)Crystallization behaviour from molecular conformation to crystal lattice
#MS28-2-4

D. Komisarek [1], V. Vasylyeva [1], F. Demirbas [1], K. Merz [2], C. Schauerte [3]
[1]Heinrich Heine University - Düsseldorf (Germany), [2]Ruhr University Bochum - Bochum (Germany), [3]SOLID-CHEM - Bochum (Germany)

Abstract
γ-amino butanoic acid (GABA) is a simple non-essential amino acid from which manifold active pharmaceutical ingredients (APIs) are derived. The antiepileptic drug Gabapentin (2-(1-(aminomethyl)-cyclohexyl) acetic acid) is one of its most commercially successful analogues. In this work commonalities and distinctions in their crystallization behavior are elucidated on. In the past, various publications have established indicators of stability for either single molecular conformations or crystal entities of either GABA[1-3] or Gabapentin[4, 5]. Identification of common structure motifs in congruence with an analysis of lattice energies and molecular conformations are performed on single- and multicomponent crystalline entities. First, two polymorphs of GABA and Gabapentin as well as the Gabapentin hydrate are analyzed in the described manner. In the second step, multicomponent forms of both compounds with either fumaric or succinic acid are used for comparison. It is attempted to answer the questions: Can a favourable molecular conformation be an indicator for crystal phase stability in single and multicomponent crystalline species? Are structural properties of crystalline solid GABA species necessarily comparable to those of a similar derivative? What indicators for a reliably stable GABA related crystalline phase might there be? Lattice energies are calculated via Quantum Espresso PWSCF v. 6.6[6] and analysis of molecular and crystal structure properties is conducted via Mercury 2020.2.0[7] and PLATON[8].
Work in preparation, D. Komisarek, F. Demirbas, K. Merz, C. Schauerte and V. Vasylyeva 2022.

References
[1] Song, I. K.; Kang, Y. K. Conformational preferences of γ-aminobutyric acid in the gas phase and in water. J. Mol. Struct. 2012, 1024, 163–169. DOI: 10.1016/j.molstruc.2012.04.080.
[2] Wang, L.; Sun, G.; Zhang, K.; Yao, M.; Jin, Y.; Zhang, P.; Wu, S.; Gong, J. Green Mechanochemical Strategy for the Discovery and Selective Preparation of Polymorphs of Active Pharmaceutical Ingredient γ-Aminobutyric Acid (GABA). ACS Sustain. Chem. Eng. 2020, 8 (45), 16781–16790. DOI: 10.1021/acssuschemeng.0c04707.
[3] Lamkowski, L.; Komisarek, D.; Merz, K. GABA-Controlled Synthesis of the Metastable Polymorphic Form and Crystallization Behavior with a Chiral Malic Acid. Cryst. Growth Des. 2022, 22 (1), 356–362. DOI: 10.1021/acs.cgd.1c00991.
[4] Liu, Y.; Wang, Y.; Huang, X.; Li, X.; Zong, S.; Wang, N.; Hao, H. Conformational Selectivity and Evolution Affected by the Desolvation Process. Cryst. Growth Des. 2022, 22 (2), 1283–1291. DOI: 10.1021/acs.cgd.1c01253.
[5] Delaney, S. P.; Smith, T. M.; Korter, T. M. Conformation versus cohesion in the relative stabilities of gabapentin polymorphs. RSC Adv. 2014, 4 (2), 855–864. DOI: 10.1039/C3RA43887B.
[6] Giannozzi, P.; Baseggio, O.; Bonfà, P.; Brunato, D.; Car, R.; Carnimeo, I.; Cavazzoni, C.; Gironcoli, S. de; Delugas, P.; Ferrari Ruffino, F.; Ferretti, A.; Marzari, N.; Timrov, I.; Urru, A.; Baroni, S. Quantum ESPRESSO toward the exascale. Chem. Phys. 2020, 152 (15), 154105. DOI: 10.1063/5.0005082.
[7] Macrae, C. F.; Sovago, I.; Cottrell, S. J.; Galek, P. T. A.; McCabe, P.; Pidcock, E.; Platings, M.; Shields, G. P.; Stevens, J. S.; Towler, M.; Wood, P. A. Mercury 4.0: from visualization to analysis, design and prediction. J. Appl. Crystallogr. 2020, 53 (Pt 1), 226–235. DOI: 10.1107/S1600576719014092. Published Online: Feb. 1, 2020.
[8] Spek, A. L. Single-crystal structure validation with the program PLATON. J. Appl. Crystallogr. 2003, 36 (1), 7–13. DOI: 10.1107/S0021889802022112.

Back to Table of contents

MS28 Navigating crystal forms in molecular and pharmaceutical materials

MS28-2-5 Salt Formation between Two Frontline Antitubercular APIs: from Mechanochemistry to Spontaneous Formation
#MS28-2-5

V. Smith [1]
[1]Rhodes University - Makhanda (South Africa)

Abstract
The discovery of novel active pharmaceutical ingredients (APIs) used to treat diseases like tuberculosis has slowed in recent years. First- and second-line therapies recommended by the world health organization (WHO) were introduced more than 50 years ago while the youngest member of the first line medicines consisting of rifampin, isoniazid, (S,S)-ethambutol and pyrazinamide were introduced in 1970. Issues relating to the rise of resistant strains, solubility, bioavailability, the 'pill burden' and the need to diversify the available treatments are paramount to producing new and effective treatments.[1,2] Cocrystallization is an area of enormous interest owing to the facile manner in which it can be used to enhance the physicochemical properties of the parent APIs.[3] Herein we report on the salt formation between frontline antitubercular APIs (S,S)-ethambutol (free base) (ETMBTL) and pyrazinecarboxylic acid (PCBA), the active metabolite of pyrazinamide. Our attempts at preparing the salt included neat grinding, liquid-assisted grinding, solvent evaporation and co-sublimation. Moreover, the salt forms spontaneously when a 1:2 physical mixture of ETMBTL and PCBA is exposed to a relative humidity of 75% at 20 °C (see Figure 1).[4] The resulting salt was characterized by differential scanning calorimetry (DSC), powder X-ray diffraction (PXRD), Fourier transform-infrared spectroscopy (FTIR) and single-crystal X-ray diffraction (SCXRD).[1–5]

References
[1] Pai, M.; Behr, M.A.; Dowdy, D.; Dheda, K.; Divangahi, M.; Boehme, C.; Ginsberg, A.; Swaminathan, S.; Spigelman, M.; Getahun, H.; Menzies, D. and Raviglione, M., *Nat. Rev. Dis. Primers*, **2016**, 2, 1-23.
[2] Villemagne, B.; Crauste, C.; Flipo, M.; Baulard, A.R.; Déprez, B. and Willand N., *Eur. J Med. Chem*., **2012**, 51, 1-16.
[3] Sarceviča, I.; Orola L.; Nartowski K.P.; Khimyak Y.Z.; Round A.N.; and Fábián L., *Mol. Pharmaceutics*, **2015**, 12, 2981-2992.
[4] Maheshwari C.; Jayasankar A.; Khan N.A.; Amidona G.E.; and Rodríguez-Hornedo N., *CrystEngComm*, **2009**, 11, 493-500.
[5] Duggirala, N.K.; Perry, M.L.; Almarsson Ö. and Zaworotko, M.J., *Chem. Commun.*, **2016**, 52, 640-655.

Figure 1. Cocrystal formation

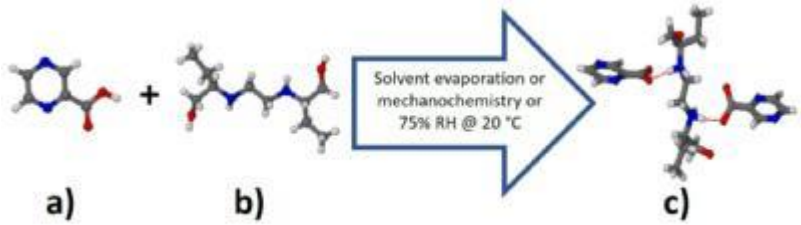

Back to Table of contents

MS28 Navigating crystal forms in molecular and pharmaceutical materials

MS28-2-6 Stability of Co-crystals a Density Functional Theory study
#MS28-2-6

R. Fox [1], J. Klug [1], D. Thompson [2], A. Kellett [1], A. Reilly [1]
[1]Dublin City University - Dublin (Ireland), [2]Dublin City University - Limerick (Ireland)

Abstract
Co-crystals are crystals of more than one molecule held together through dispersion interactions such as Hydrogen bonding, dipole-dipole interactions, and Van der Waals interactions. Co-crystals have also been more stable than their single-crystal counterparts, as indicated by their higher lattice enthalpy.[1] In literature, hydrogen bonding has been the main focus to account for the stability of co-crystals.[2] However, other dispersion interactions like Van der Waals could be necessary for stabilising co-crystals.
Various Density functional theory (DFT) methods have been used to calculate the lattice enthalpy of experimentally made thermodynamically stable co-crystals. These methods include Tkatchenko and Scheffler (TS) and Many-Bodied dispersion (MBD) dispersion corrections. This co-crystal set includes simpler molecules, 4,4'-bipyridine and oxalic acid, and more complex active pharmaceutical ingredients, aspirin and paracetamol; these are all experimentally made structures. Previous work has shown that most co-crystals are thermodynamically stable, so calculations are expected to have a negative enthalpy.[1]
Using the DFT method, simple systems of oxalic acid and 4,4'-bipyridine were calculated to be more stable than their single-component counterparts, with the calculations predicting negative lattice enthalpies. Whereas with more complex systems of aspirin and paracetamol, the DFT methods predict that some of the co-crystals are less stable than their single-component counterparts, with some co-crystals producing positive lattice enthalpies.
The prediction might not predict might not accurately calculate the lattice energy of the complex systems by the DFT methods. However, the geometry optimisation does not consider that kinetic effects might play a role in the stability of these co-crystals.

References
1 C. R. Taylor and G. M. Day, Evaluating the Energetic Driving Force for Cocrystal Formation, Cryst. Growth Des., , DOI:10.1021/acs.cgd.7b01375.
2 A. V. Yadav, A. S. Shete, A. P. Dabke, P. V. Kulkarni and S. S. Sakhare, Co-crystals: A novel approach to modify physicochemical properties of active pharmaceutical ingredients, Indian J. Pharm. Sci., 2009, 71, 359–370.

Back to Table of contents

MS29 Crystal engineering: structural flexibility, phase transitions and non-standard manipulation of synthons

MS29-1-1 Structure-directing Ag···π interactions in coordination complexes
#MS29-1-1

T. Theunissen [1], S.A. Bourne [1], C. Esterhuysen [2]
[1]University of Cape Town - Cape Town (South Africa), [2]University of Stellenbosch - Stellenbosch (South Africa)

Abstract
The Ag-π interaction can be considered as one of the most widely used metal-π interactions [1]. The interactions have been applied to a number of fields, including catalysis [2], molecular recognition [3], and polymer/material design [4]. In spite of the usefulness of Ag-π interactions, a better understanding of the orbital interactions that govern the stability trends is still required. This information could assist in guiding design of new materials and applications that exploit this interaction. The reaction of silver(I) nitrate with sodium benzoate (NaBn) and a pyridyl yielded three binuclear complexes: $[Ag_2(Bn)_2]$ (I) and $[Ag_2(Bn)_2(2\text{-Pic})_2]$ (II) and $[Ag_2(Bn)_2(3\text{-ClPic})_2]$ (III) where 2-Pic is 2-picoline and 3-ClPic is 3-chloropyridine. All three of these complexes have been characterized by IR, thermal analysis, and X-ray single crystal and powder diffraction. Complexes (I), (II), and (III) are all linked into Ag-Ag (<2.885 Å) dimers with the silver(I) ions being bridged by the benzoate ligands. Additionally, complexes (II) and (III) each had the silver(I) ion bound to one monodentate picoline-derived ligand. Complex (I) packs as a two-dimensional polymer structure, while complexes (II) and (III) each form one-dimensional chains connected by weak intermolecular interactions. These weak intermolecular Ag···π, π···π, and H···π interaction systems are expected to lead to the assembly and by extension the stability of the three-dimensional crystal frameworks. The nature of these interactions, namely the Ag···π, was further examined by DFT calculations. The Ag···π interactions were found to be driven by favourable molecular orbital interactions, between an aromatic π-donor orbital and the Ag LP* acceptor orbital (a (π) → LP* interaction). The Ag···π interactions displayed the classical preferential alignment of the Ag LP* toward the ring carbons and/or nitrogen and an aromatic π orbital rather than toward the aromatic centroid. These results describe a potential understanding of the weak interactions of silver(I) with π systems.

References
[1] (a) Griffith, E. A. H.; Amma, E. L. J. Am. Chem. Soc. 1974, 96, 743− 749. (b) Pierre, J.-L.; Baret, P.; Chautemps, P.; Armand, M. J. Am. Chem. Soc. 1981, 103, 2986. (c) Dias, H. V. R.; Wang, Z.; Jin, W. Inorg. Chem. 1997, 36, 6205−6215. (d) Munakata, M.; Wu, L. P.; Ning, G. L. Coord. Chem. Rev. 2000, 198, 171−203. (e) Lindeman, S. V.; Rathore, R.; Kochi, J. K. Inorg. Chem. 2000, 39, 5707−5716.
[2] (a) Curran, D. P.; Hongyan, Q.; Geib, S. J.; DeMello, N. C. J. Am. Chem. Soc. 1994, 116, 3131−3132. (b) Rebek, J., Jr. Chemtracts: Org. Chem. 1989, 2, 337−352.
[3] Omoto, K.; Tashiro, S.; Kuritani, M.; Shionoya, M. J. Am. Chem. Soc. 2014, 136, 17946−17949.
[4] (a) Chebny, V. J.; Rathore, R. J. Am. Chem. Soc. 2007, 129, 8458−8465. (b) Gao, C.-Y.; Zhao, L.; Wang, M.-X. J. Am. Chem. Soc. 2012, 134, 824−827. (c) Zang, S.-Q.; Han, J.; Mak, T. C. W. Organometallics. 2009, 28, 2677−2683. (d) Côte, A. P.; Shimizu, G. K. H.´ Inorg. Chem. 2004, 43, 6663−6673.

Silver(I) complexes with benzoate and pyridines

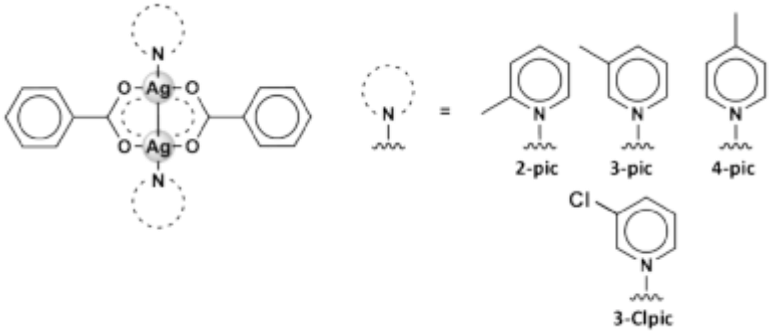

Back to Table of contents

MS29 Crystal engineering: structural flexibility, phase transitions and non-standard manipulation of synthons

MS29-1-2 Crystal engineering of phenol-phenolate supramolecular heterosynthon
#MS29-1-2

S. Jin [1], M. Zaworotko [1]
[1]University of Limerick - Limerick (Ireland)

Abstract
"Crystal engineering" is defined as "the field of chemistry that studies the design, properties and applications of crystals". One application of crystal engineering is prevalent in the study of cocrystals. Cocrystals have gained much attention, particularly in the pharmaceutical industry, due to their ability to modify physicochemical properties of drug molecules without changing their biological efficacy. Cocrystals are solids that are crystalline single-phase materials composed of two or more different molecular and/or ionic compounds generally in a stoichiometric ratio which are neither solvates nor simple salts.[1] Cocrystals can be classified into molecular cocrystals (MCCs) that contain only neutral components (coformers) in the crystal lattice and ionic cocrystals (ICCs)[2] comprising of at least one ionic coformer that is a salt. ICCs involving inorganic salts (e.g., alkali and alkaline earth halides etc.) can also be viewed as a coordination complex between organic type ligands and metal cations. Ionic cocrystals have generated widespread interest as they exhibit strong hydrogen bonding or coordination bonding and have more components suggesting greater diversity of physicochemical properties.

The study of supramolecular synthons to investigate their amenability to crystal engineering will enable efficient discovery of new cocrystals. Supramolecular synthon is further classified into supramolecular homosynthon and heterosynthon.[3] Phenols are well-established in crystal engineering as they have demonstrated their ability to form robust supramolecular heterosynthons. They are also a common functionality found in many pharmaceutical and nutraceutical molecules. Phenol-phenolate ($PhOH\cdots PhO^-$) complexes have been studied in solution and gas phases but it remains understudied as a supramolecular heterosynthon in crystal engineering.

Statistical analysis on this $PhOH\cdots PhO^-$ supramolecular heterosynthon was conducted on relevant structures deposited on the Crystal Structural Database (CSD) and the novel ICCs reported in this work.

References
[1] Aitipamula, S. et al., Crystal Growth & Design, 2012, 12, 2147-2152.
[2] Braga, D. et al., Chem. Commun., 2010, 46, 7715-7717.
[3] Walsh, R. D. B. et al., Chem. Commun., 2003, 186-18.

Back to Table of contents

MS29 Crystal engineering: structural flexibility, phase transitions and non-standard manipulation of synthons

MS29-1-3 Polymorphism in a series of dipodal N-donor ligands containing a biphenyl core
#MS29-1-3

S. Chaudhary [1], D. Kędziera [1], Z. Rafiński [1], L. Dobrzańska [1]
[1]Nicolaus Copernicus University - Torun (Poland)

Abstract
Polymorphism[1] is the ability of a substance to form various crystalline phases that differ for example by their molecular arrangement (packing polymorphism)[2] or by the molecular conformation they adopt (conformational polymorphism)[3]. It is known that varying the conditions (change of solvent, level of supersaturation, temperature, pressure) during the crystallization process is the main factor responsible for this phenomenon to occur, leading to the formation of products displaying different physical properties, including thermodynamic, spectroscopic, kinetic and mechanical characteristics[4]. Unfortunately, polymorphism is far from being clearly understood. Computational studies such as crystal structure predictions (CSP), which are under continuous development to complement the experimental screening of solid forms, help to identify the most likely formed polymorphic phases and to understand the crystallization behavior at the molecular level[5]. Herein, we would like to present the polymorphic behavior of a series of flexible dipodal N-donor ligands containing a biphenyl core, namely 4,4′-bis(pyridin-4-ylmethyl)-1,1′-biphenyl **(1)**, 4,4′-bis(1H-imidazol-1-ylmethyl)-1,1′-biphenyl **(2)** and 2,2′-bis(1H-imidazol-1-ylmethyl)-1,1′-biphenyl **(3)**. Crystals of these heterocyclic ligands were grown from a range of solvents such as THF, MeOH, DCM, EtOH, acetonitrile, and acetone. Two different forms for each of the ligands were isolated and their crystal structures were determined by SCXRD analysis. These were further profiled by various techniques such as TGA/DTA, powder XRD, FT-IR and computational methods, with the latter providing better understanding of the interplay of the intermolecular interactions.

References
1. a) Cruz-Cabeza, A. J., Feeder, N., Davey, R. J. *Commun Chem*, **2020**, 3, 142, b) Brog, J. P., Chanez, C. L., Crochet A., Fromm, K. M. *RSC Adv*, **2013**, 3, 16905–1693.2. Cruz-Cabeza, A. J., Reutzel-Edens, S. M., Bernstein, *J. Chem. Soc. Rev*, **2015**, 44, 8619–8635.3. a) Cruz-Cabeza, A. J., Bernstein J. *Chemical Reviews*, **2014**, 114 (4), 2170-2191, b) Nangia, A. *Accounts of Chemical Research*, **2008**, 41 (5), 595-604.4. Purohit, R., Venugopalan, P. *Reson*, **2009**, 14, 882.5. a) Ryan, K., Lengyel, J., Shatruk, M. *J. Am. Chem. Soc,* **2018**, 140, 32, 10158–10168, b) Price, S. L. *Chem. Soc. rev*, **2014**, 43, 2098-2111.

Conformational flexibility of 2

Back to Table of contents

MS29 Crystal engineering: structural flexibility, phase transitions and non-standard manipulation of synthons

MS29-1-4 Crystal Engineering of Pharmaceutical ICCs Involving NH+···N heterosynthons: Antifungal agents as Case Studies
#MS29-1-4

M. Rahmani [1], M. Zaworotko [1]
[1]University of Limerick - Limerick (Ireland)

Abstract
During recent decades, crystal engineering, which is the understanding and exploitation of intermolecular interactions to design molecular solids [1], has shown to be a very successful strategy for the formation of new materials with desired properties. In this context, the discovery of multi-component molecular solid forms of active pharmaceutical ingredients (APIs) [2], particularly ionic cocrystals (ICCs) [3], expands the possibilities for improving API physicochemical properties without requiring chemical modification. Herein we report the design and synthesis of a new family of ionic cocrystals (ICCs) containing miconazole (MC) and econazole (EC) (the imidazole-based antifungal drugs with poor aqueous solubility). Fourteen new ICCs of MC and EC, formed by combining a series of imidazole/ 1, 2, 4-triazole-based coformers with hydrobromic acid or hydrochloric acid, were identified, as well as five new salt forms of these APIs. A charge-assisted $NH^{+}\cdots N$ supramolecular heterosynthon is detected in all but one of them. Detailed investigations of the crystal structures and packing of these ICCs demonstrated that the nature of the model compounds used in ICCs could play a significant influence in modifying physicochemical properties. This novel design strategy can pave a facile route for designing and synthesizing novel multi-component crystals of several clinical medicines containing azole rings that suffer from poor physicochemical properties.

References
[1] G. R. Desiraju and G. W. Parshall, *Materials science monographs* **1989**, 54.
[2] Ö. Almarsson and M. J. Zaworotko, *Chemical Communications* **2004**, 1889-1896.
[3] D. Braga, F. Grepioni, L. Maini, S. Prosperi, R. Gobetto and M. R. Chierotti, *Chemical Communications* **2010**, 46, 7715-7717.

Back to Table of contents

MS29 Crystal engineering: structural flexibility, phase transitions and non-standard manipulation of synthons

MS29-1-5 Experimental study of dynamic structural transformations between copper(II) coordination polymers with 5-fluorouracil-1-acetic acid and 4,4-bipyridine
#MS29-1-5

J. Perles [1], P. Amo-Ochoa [1], N. Maldonado [1], A. García [1], V.G. Vegas [1]
[1]Universidad Autónoma de Madrid - Madrid (Spain)

Abstract
The study of chemical systems where slight changes in the synthetic conditions give rise to multiple phases can be very enlightening, especially those where several competing factors are at play (1). In these systems, small variations in solvent ratio, temperature or stoichiometry yield different compounds, which can also undergo phase transformations themselves. These phase transformations, sometimes reversible, as a response to external stimuli (2-3) can be useful to apply these compounds as sensors.
The design of the reported coordination compounds include copper(II) as the metal centre and 4,4-bipyridine and 5-fluorouracil-1-acetic acid (5-FUAcO), a modified nucleobase, as ligands. The use of two ligands with different coordination possiblities allows the formation of compounds with different dimensionality. Furthermore, the interactions of biomolecules with metal ions have proved useful to synthesize biomimetic artificial systems for the development of advanced functional materials that can be applied in therapeutic medicine and materials science (4-5). Biomolecules are also fascinating tools in supramolecular chemistry, as they are well known for their self-recognition ability and stablish a wide variety of non-covalent interactions. Nucleobases in particular have been successfully used as bioligands that can form synthons through supramolecular bonds among themselves, both by hydrogen bonding and π-π stacking interactions, as well as with other molecules (6-8).
In this communication, the different crystal phases (in particular, the six copper coordination polymers obtained), and their transitions are described.

References
1. *Experimental and Theoretical Study of Dynamic Structural Transformations between Sensing Copper(II)-Uracil Antiferromagnetic and Metamagnetic Coordination Compounds.* Maldonado, N.; Perles, J.; Martínez, J. I.; Gómez-García, C. J.; Marcos, M.-L.; Amo-Ochoa, P. Crystal Growth & Des., 2020, 20 (8), 5097-5107.2. *Smart composite films of nanometric thickness based on copper–iodine coordination polymers. Toward sensors.* Conesa-Egea, J.; Nogal, N.; Martínez, J. I.; Fernández-Moreira, V.; Rodríguez-Mendoza, U. R.; González-Platas, J.; Gómez-García, C. J.; Delgado, S.; Zamora, F.; Amo-Ochoa, P., Chem. Sci. 2018, 9 (41), 8000-8010.3. *Multistimuli Response Micro- and Nanolayers of a Coordination Polymer Based on Cu_2I_2 Chains Linked by 2-Aminopyrazine.* Conesa-Egea, J.; Gallardo-Martinez, J.; Delgado, S.; Martinez, J. I.; Gonzalez-Platas, J.; Fernandez-Moreira, V.; Rodriguez-Mendoza, U. R.; Ocón, P.; Zamora, F.; Amo-Ochoa, P., Small 2017, 13 (33).4. *Copper(II)–Thymine Coordination Polymer Nanoribbons as Potential Oligonucleotide Nanocarriers.* Vegas, V. G.; Lorca, R.; Latorre, A.; Hassanein, K.; Gómez-García, C. J.; Castillo, O.; Somoza, Á.; Zamora, F.; Amo-Ochoa, P. Angew. Chem. Int. Ed., 2017, 56 (4), 987-991.5. *Rational Design of Copper(II)–Uracil Nanoprocessed Coordination Polymers to Improve Their Cytotoxic Activity in Biological Media,* Vegas, V. G.; Latorre, A.; Marcos, M.-L.; Gómez-García, C.J.; Castillo, O.; Zamora, F.; Gómez, J.; Martínez-Costas, J.; Vázquez López, M.; Somoza, A.; Amo-Ochoa, P. ACS Applied Materials & Interfaces, 2021,13 (31), 36948-36957.6. *Theophylline alkaloid as glue of paddle-wheel copper(II)-adenine entities to afford a rhomboid chain.* Pascual-Colino, J.; Beobide, G.; Castillo, O.; Luque, A.; Pérez-Yáñez, S., Inorg. Chim. Acta, 2019, 484, 437-442.7. *Reactivity of homoleptic and heteroleptic core paddle wheel Cu(II) compounds.* Sánchez-Férez, F.; Guerrero, M.; Ayllón, J. A.; Calvet, T.; Font-Bardia, M.; Planas, J. G.; Pons, J.,. Inorg. Chim. Acta 2019, 487, 295-306.8. *Coordination polymers with nucleobases: From structural aspects to potential applications.* Amo-Ochoa, P.; Zamora, F., Coord. Chem. Rev. 2014, 276, 34-58.

Structural diversity in the polymeric compounds

Back to Table of contents

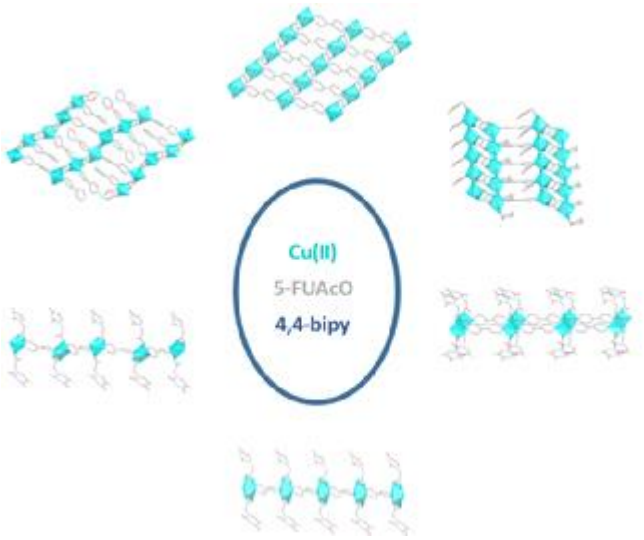

Back to Table of contents

MS29 Crystal engineering: structural flexibility, phase transitions and non-standard manipulation of synthons

MS29-1-6 Fractal transitions of selenourea
#MS29-1-6

K. Roszak [1], A. Katrusiak [1]
[1]Faculty of Chemistry, Adam Mickiewicz University - Poznan (Poland)

Abstract
Fractal phase transitions have been found in the crystal lattices of selenourea, $SeC(NH_2)_2$, At room temperature, selenourea crystallizes in phase α, of the enantiomorphic space-group type $P3_1$ and the unit cell containing nine symmetry-independent molecules, i.e. the Z' number equal to 9 [1-3]. The lattice of phase α is similarity-related to that of a 3-fold smaller unit-cell (Z'=3), which in turn is likewise related to another 3-fold smaller unit-cell (Z'=1), all of the same space-group type. Indeed, at 374 K, phase α transforms to phase γ, for which the space-group type $P3_1$ is retained, and the Z' number is reduced to 3. The same similarity fractal rule relating phases α and γ, also applies to the lattice of a hypothetical phase δ (Z'=1). Analogous fractal rules like this between the α-γ-δ phases of selenourea have been identified also for other compounds described in the literature. The unit-cell dimensions in crystals naturally limit the down-scaling of all natural fractals. The temperature-induced fractal transitions described for selenourea α-γ-δ phases, contrast with the high-pressure transition at 0.21 GPa to phase β, which is centrosymmetric and for which the aggregation of molecules is significantly different [1]. Relations between crystallographic macroscopic and microscopic fractals will be discussed.

References
[1]. Roszak K, Katrusiak A. High-pressure and environment effects in selenourea and its labile crystal field around molecules. Acta Crystallogr Sect B 2021, 77, 449–455. DOI: DOI: 10.1107/S205252062100398X
[2]. Luo Z, Dauter Z. Embarras de richesses–It is not good to be too anomalous: Accurate structure of selenourea, a chiral crystal of planar molecules. PLoS One. 2017, 12, e0171740(1–13). DOI:10.1371/journal.pone.0171740
[3]. Rutherford JS, Calvo C. The crystal structure of selenourea. Z. Kristallogr. 1969, 128, 229–258. DOI: 10.1524/zkri.1969.128.3-6.229

Back to Table of contents

MS29 Crystal engineering: structural flexibility, phase transitions and non-standard manipulation of synthons

MS29-1-7 The Elastic Properties of Postulated Solid Forms from First Principles
#MS29-1-7

R. Zwane [1]
[1]**Dublin City University - Dublin (Ireland)**

Abstract
The elastic properties of a crystal contain extensive information about the response of a material to applied stress and strain and influence key properties such as hardness, powder flexibility, and tabletability. Different polymorphs and solid forms of an active pharmaceutical ingredient (API) can exhibit markedly different elastic and mechanical properties, and therefore understanding the mechanical properties of different solid forms would greatly aid pharmaceutical solid-form development. In crystal structure predictiion, the analysis of a crystal energy landscape in a pharmaceutical setting can aid the understanding of polymorphism of an API across a landscape and assist in identifying mechanical properties accessible to an API. In this contribution, mechanical properties of postulated solid forms of 2-((4-(3,4-Dichlorophenethyl)phenyl)amino)benzoic acid DPAB, utilized for the treatment of Alzheimer's disease and the XXIIIth molecule in the sixth CSP blind test, are characterized using first-principles and first-principles based methods (density-functional theory). The assessment of mechanical stability, elastic moduli and the anisotropy of the elastic moduli of DPAB will potentially enable the screening of putative solid forms for a polymorph(s) that exhibits improved compression properties.
image caption

References
S. Price, D. Braun and S. Reutzel-Edens, Chemical Communications, 2016, 52, 7065-7077.A. M. Reilly, R. I. Cooper, Acta Crystallographica Section B: Structural Science, Crystal Engineering and Materials, 2016, 72, 439–459.L. J. Simons, B.W. Caprathe,M. Callahan, J.M. Graham, T. Kimura, Y. Lai, H. LeVine,
W. Lipinski, A. T. Sakkab, Y. Tasaki, L. C. Walker, T. Yasunaga, Y. Ye, N. Zhuang and
C. E. Augelli-Szafran, Bioorganic &Medicinal Chemistry Letters, 2009, 19, 654–657.

Back to Table of contents

MS29 Crystal engineering: structural flexibility, phase transitions and non-standard manipulation of synthons

MS29-1-8 Crystallization and structural investigations of 1,2-cyclopentanediol analogues and their co-crystallization with ethylenediamine.
#MS29-1-8

J. Gajda [1], M.K. Cyrański [1], R. Boese [2], Ł. Dobrzycki [1]
[1]Faculty of Chemistry, University of Warsaw - Warsaw (Poland), [2]Universität Duisburg Essen - Essen (Germany)

Abstract
Amine and hydroxyl groups, due to the complementarity of interactions, can form relatively strong hydrogen bonds, where the OH or NH2 fragments can be both donor and acceptor [ref. 1]. Such interactions can be a driving force for the formation of a crystalline phase. However, the resulting structure can be affected by a presence of additional functional groups.
Presented here results are based on the crystal engineering of analogues of 1,2-cyclopentanediol and ethylenediamine. Since all the examined diols (*cis* and *trans* isomers of 1,2cyclopentanediol and 1,4-anhydroerythritol) and their mixtures with ethylenediamine are liquids under normal conditions, the crystallizations experiments were performed *in situ* directly on the goniometer of the single crystal diffractometer with the use of an IR laser [ref. 2]. During the experiments a plastic and crystalline phase of *cis*-1,2-cyclopentanediol, a plastic phase of *trans*-1,2-cyclopentanediol and cocrystals of ethylenediamine with cis *cis*-1,2-cyclopentanediol and 1,4-anhydroerythritol were obtained and characterized by singe crystal diffraction technique. For the neat diols DSC measurements were also performed. On their basis, the melting points of the compounds and temperature of the phase transition in the solid *cis*-1,2-cyclopentanediol were determined.

References
Ref. 1. O. Ermer and A. Eling, “Molecular recognition among alcohols and amines: supertetrahedral crystal architectures of linear diphenol–diamine complexes and aminophenols”, *J. Chem. Soc. Perkin Trans. 2*, 1994, 925944.Ref. 2. R. Boese, “Special issue on *In Situ* Crystallization”, *Z. Für Krist. - Cryst. Mater.*, 2014, 229, 595601.

Back to Table of contents

MS29 Crystal engineering: structural flexibility, phase transitions and non-standard manipulation of synthons

MS29-2-1 Co-crystals of n-alcohols with propyl-, allyl- and propargylamine. Effect of C-C bond saturation on the structural motifs.
#MS29-2-1

B. Prus [1], R. Boese [2], M. Cyrański [2], J. Zachara [3], Ł. Dobrzycki [2]
[1]University of Warsaw and Warsaw University of Technology - Warsaw (Poland), [2]University of Warsaw - Warsaw (Poland), [3]Warsaw University of Technology - Warsaw (Poland)

Abstract
Amines and alcohols can act as good ingredients for the co-crystallization experiments. This is due to the complementarity of their functional groups in terms of hydrogen bonds formation. In the literature there are known some examples of such structures but they are mostly limited to diamine-diol co-crystals [1] or aromatic systems [2]. The presented here results are focused on the influence of C-C bond saturation in the small amine molecules on the co-crystals formation with n-alcohols. As the simplest and stable unsaturated compounds allylamine and propargylamine were chosen. The reference molecule was propylamine. In such model systems, both intra- and intermolecular interactions are not affected by the presence of additional substituents and functional groups.
The examined mixtures are liquid under ambient conditions, therefore an IR laser-assisted in situ crystallization technique was used to obtain desired co-crystals directly on the goniometer of the single crystal diffractometer [3]. The X-Ray measurements were complemented by DFT periodic calculation in CRYSTAL17 program.
During the research 30 mixtures were tested (ten alcohols in methanol-decanol range with three amines) for which 25 co-crystals were obtained. In the structures three types of hydrogen bonds motifs are observed. Two different layers of L4(4)8(8) and L6(6) types and ribbon T4(2) [4]. Elongation of the aliphatic chain of the alcohol causes the change of the motif in a systematic way. However the point of transition is different for various amine, due to the influence of the C-C bond saturation.
To elucidate the influence of the saturation of the C-C bond on the formation of co-crystals, several periodical calculations were performed. They were based on the cohesive energy calculation combined with its partition to the interactions within structural motifs and among them. This type of computation allows to compare structures with 1D and 2D motifs and help to understand the reasons why a particular architecture is observed. A finite number of potential motifs made it possible to model the structures of unobtained co-crystals, to verify their energy properties.
Systematic research of amine-alcohol co-crystals shows that changes in structural motifs are predictable in the studied group. The known properties can be used to design similar systems.

The research was supported by the National Science Center in Poland (Grant SONATA BIS 6 NCN, 2016/22/E/ST4/00461). Project implemented under the Operational Program Knowledge Education Development 2014-2020 co-financed by the European Social Fund.

References
[1] S. Hanessian, A. Gomtsyan, M. Simard, and S. Roelens, J. Am. Chem. Soc., 1994, 116, 4495–4496
[2] A. R. Choudhury, D. S. Yufit, and J. A. K. Howard, Z. Für Krist. - Cryst. Mater., 2014, 229, 625–634
[3] R. Boese, Z. Kristallogr., 2014, 229, 595-601.
[4] L. Infantes, S. Motherwell, CrystEngComm, 2002, 4, 454−461.

Back to Table of contents

MS29 Crystal engineering: structural flexibility, phase transitions and non-standard manipulation of synthons

MS29-2-2 A temperature-dependent flexible proton transfer system
#MS29-2-2

L. Saunders [1], P. Edwards [2], J. Taylor [3], D. Nye [3], D. Grinter [4], D. Allan [4], S. Thompson [4]
[1]Diamond Light Source - Didcot (United Kingdom), [2]University of Leeds - Leeds (United Kingdom), [3]STFC - Didcot (United Kingdom), [4]Diamond - Didcot (United Kingdom)

Abstract
Molecular crystals are formed from the association of discreet organic molecules via intermolecular interactions and may be single or multi-component. Crystal engineering is used in their design to target specific structural features resulting from molecular association, including voids, stacking or charged species, with related material properties such as guest uptake, colour and switchable forms.
Hydrogen bonding interactions play an important role in the molecular assembly of organic components in the solid state. Proton transfer events may occur within molecular crystals when formed of organic acids and bases and is favoured across the shorter of the hydrogen bonding interactions, often those that are charge assisted and where a significant covalent component is found.[1] The proton transfer may be static, occurring on crystal formation and resulting in oppositely charge species connected by charge assisted hydrogen bonds, or be variable, such that multiple positions across the hydrogen bond are energetically favourable and/or are susceptible to external crystal environment.[2] Determining proton transfer state in the salt-cocrystal continuum has impact in pharmaceutical regulation whilst a shifting proton position as a function of an external variable can result in sensor (where a colour change is induced) or switchable (polarisation change) technology. It's study and where this type of behaviour is found is therefore of interest, to aid in incorporation into or its control within functional materials.
In this work, we present a study of the temperature dependent behaviour of multi-component molecular salt (1) 4,4'-bipyridinium 2,4-dinitrobenzoate (1:3), probed using a range of characterisation techniques. System (1) has resulted from a co-crystallisation study based on introducing a third-component to alter the proton transfer states and colour properties of the 4,4'-bipyridinium hydrogen squarate.[3, 4] We use differential scanning calorimetry alongside synchrotron single crystal and powder X-ray diffraction methods to characterise the thermal behaviour of (1). In the crystal structure of (1), molecular association of components occurs via charge assisted N^{+}—H···O^{-} hydrogen bonds across which proton disorder is evident. Due to the weak scattering signal of the H-atoms from the X-rays, it is not possible to accurately resolve the nature of the disorder or how, if at all, it evolves as a function of temperature. In light of this, we implement a number of spectroscopic techniques including Near Edge X-ray Absorption Fine Structure and X-ray Photoelectron spectroscopy to explore the proton disorder of this system to determine what role, if any, it has in the thermally induced crystallographic phase transition.

References
1. L. K. Saunders, A. R. Pallipurath, M. J. Gutmann, H. Nowell, N. Zhang and D. R. Allan, CrystEngComm, 2021, 23, 6180-6190.
2. L. K. Saunders, H. Nowell, L. E. Hatcher, H. J. Shepherd, S. J. Teat, D. R. Allan, P. R. Raithby and C. C. Wilson, CrystEngComm, 2019, 21, 5249-5260.
3. D. M. S. Martins et al., J. Am. Chem. Soc., 2009, 131, 3884-3893.
4. J. S. Stevens, Cryst. Growth Des., 2022, 22, 779-787.

Back to Table of contents

MS29 Crystal engineering: structural flexibility, phase transitions and non-standard manipulation of synthons

MS29-2-3 Rare low spin to high spin transition by cooling a desolvated [2x2] Fe (II) metallogrid revealed by crystallographic studies.
#MS29-2-3

J.D.J. Velazquez-Garcia [1], K. Basuroy [1], D. Storozhuk [1], J. Wong [2], S. Demeshko [2], F. Meyer [2], S. Techert [1]
[1]Deutsches Elektronen Synchrotron - Hamburg (Germany), [2]Institut für Anorganische Chemie, Georg-August-Universität Göttingen - Göttingen (Germany)

Abstract
Spin crossover (SCO) complexes are prototypes of materials with bi- or multi-stability in the solid state. The structural evolution during their spin transition is a key feature to establish the foundations of how to utilize this type of material. Here, we used single crystal X-ray crystallography to study the molecular reorganisation during the thermal SCO of a solvated and a desolvated [2 × 2] tetranuclear metallogrid of the form $[FeII_4LMe_4](BF_4)_4$ ($[LMe]^-$ = 4-methyl-3,5-bis{6-(2,2′-bipyridyl)}pyrazolate), here called **FE4**. A multi-temperature crystallographic investigation exhibits the influence of the solvent effect in the number of spin transitions that occur in the solid sample, observed by the expansion of the average Fe-N bond length of one crystallographic-symmetry independent metal atoms where the SCO take place. While the solvated crystals show a single gradual phase transition from a 3HS-1LS to a 2HS-2LS configuration in the 400K to 250K range, the desolvated crystals show two SCO: a gradual 3HS-1LS to 2HS-2LS transition in the 400K to 140K range and the reverse transition from 2HS-2LS to 3HS-1LS by further cooling to 80K. The present work highlights the importance of the solvent effect in SCO complexes and open new questions about the control of the bi-/multi-stability in SCO solids.

References
[1] J. de J. Velazquez-Garcia, K. Basuroy, D. Storozhuk, J. Wong, S. Demeshko, F. Meyer, R. Henning and S. Techert, Dalton Trans, 2022, 51, 6036–6045.
[2] B. Schneider, S. Demeshko, S. Neudeck, S. Dechert and F. Meyer, Inorg. Chem., 2013, 52, 13230–13237.
[3] J. A. Real, A. B. Gaspar and M. C. Muñoz, Dalton Trans., 2005, 2062.
[4] P. Guionneau, Dalton Trans, 2014, 43, 382–393.

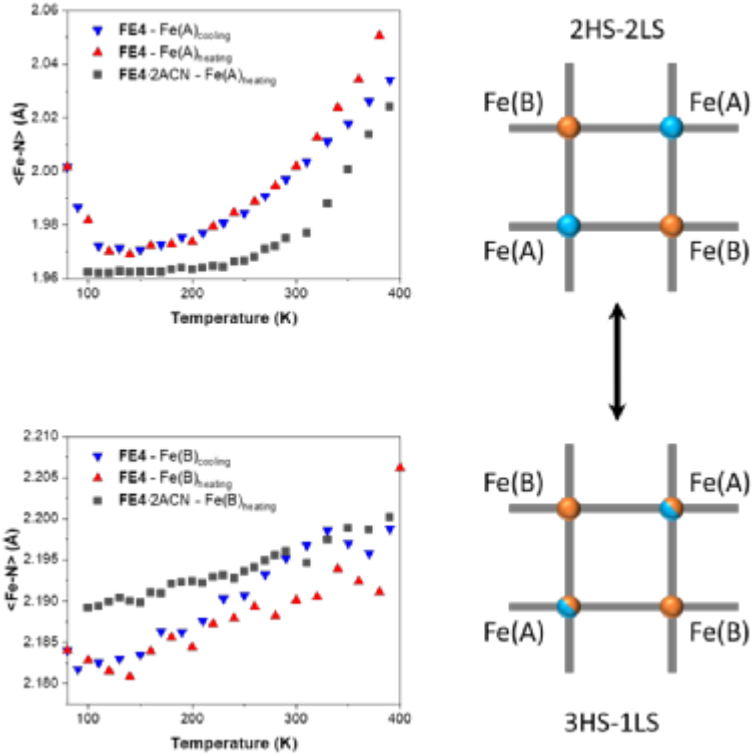

Back to Table of contents

MS29 Crystal engineering: structural flexibility, phase transitions and non-standard manipulation of synthons

MS29-2-4 The role of halogen bonding in sulfonamide co-crystals: π···X preferred over O···X?
#MS29-2-4

T. Heinen [1], S. Merzenich [1], A. Kwill [1], V. Vasylyeva [1]
[1]Heinrich-Heine University - Düsseldorf (Germany)

Abstract
Sulfonamides are one of the most important pharmaceutical compound classes.[1] It started in 1935 with Prontosil one of the first synthetic antibacterial drugs which was later honoured with the noble price.[2] Today there are over 70 active pharmaceutical ingrediencies (APIs) with various applications in use. Herein we present the first systematic study on the role of halogen bonding in sulphonamides multicomponent systems. Co-crystals of four sulfonamides in the range from simple ones to more complex APIs were designed and structurally characterized. Model halogen bond co-formers 1,4-diiodotetrafluorobenzene and/or 1,2-diiodotetrafluorobenzene were used to implement halogen bonds into the systems with N-phenyl-methane sulfonamide, N-methylbenzene sulfonamide, N-phenyl-benzene sulfonamide and Chlorpropamide.[3] In our study we consider general binding patterns, geometrical considerations of the overall crystal packing, perform calculations of lattice energies and energies of intermolecular interaction based on plain wave functions.[4] We finally resolve the question why halogen bonding seems to prefer interactions with π-systems over electron rich N- or O-moieties within these systems.

References
[1] a) İ. Gulçin, P. Taslimi, Expert opinion on therapeutic patents 2018, 28, 541; b) K. P. Rakesh, S.-M. Wang, J. Leng, L. Ravindar, A. M. Asiri, H. M. Marwani, H.-L. Qin, Anti-cancer agents in medicinal chemistry 2018, 18, 488; c) A. S. Kalgutkar, R. Jones, A. Sawant in Drug Discovery (Ed.: D. A. Smith), Royal Society of Chemistry, Cambridge, 2010, pp. 210–274; d) A. Ovung, J. Bhattacharyya, Biophysical reviews 2021, 13, 259.
[2] a) M. Wainwright, J. E. Kristiansen, Dyes and Pigments 2011, 88, 231; b) H. Ellis, British journal of hospital medicine (London, England : 2005) 2014, 75, 231.
[3] T. Heinen, S. Merzenich, A. Kwill, V. Vasylyeva, in prep. 2022.
[4] a) P. Giannozzi, S. Baroni, N. Bonini, M. Calandra, R. Car, C. Cavazzoni, D. Ceresoli, G. L. Chiarotti, M. Cococcioni, I. Dabo et al., Journal of physics. Condensed matter : an Institute of Physics journal 2009, 21, 395502; b) P. Giannozzi, O. Andreussi, T. Brumme, O. Bunau, M. Buongiorno Nardelli, M. Calandra, R. Car, C. Cavazzoni, D. Ceresoli, M. Cococcioni et al., Journal of physics. Condensed matter : an Institute of Physics journal 2017, 29, 465901.

Back to Table of contents

MS29 Crystal engineering: structural flexibility, phase transitions and non-standard manipulation of synthons

MS29-2-5 Co-crystallization of organic chromophore roseolumiflavin and effect on its optical characteristics #MS29-2-5

T. Haj Hassani Sohi [1], F. Maaß [1], C. Czekelius [1], V. Vasylyeva [1]
[1]Heinrich-Heine University - Duesseldorf (Germany)

Abstract
Recent advances on organic solid-state chromophores have led to several potential applications in diverse fields like organic or polymeric light-emitting diodes (OLEDs/PLEDs)[1,2], solid-state lasers[3,4] or fluorescent chemosensors[5], promising great interest from a broad range of research. Moreover, tunability, flexibility and low cost characterize and add to a great advantage for potential usability of organic chromophores[6]. A substance group of interest is alloxazine including its isomer isoalloxazine, the latter being the basis for flavins. While their important role in biological processes has been established[7,8], flavins also act as chromophores. Mainly considered in solution, their solid-state characteristics, especially structural characterization remains almost unstudied. With the isoalloxazine derivative roseolumiflavin we were able to successfully design three robust binary co-crystals with hydrogen and halogen bonding motives[9]. The co-crystals further exhibit altered optical properties in the solid state confirming easily accessible luminescence modification via a crystal engineering approach. Structural characterization of roseolumiflavin and its multicomponent crystals display differences in crystal packing with rearranged π ⋯ π stacking motifs being noticeable as a result of the co-crystal formation. Our findings thus render new possibilities to investigate on flavins in the aspect of crystal engineering to tune optical properties of organic chromophores.

References
1 C. W. Tang and S. A. VanSlyke, Organic electroluminescent diodes, Appl. Phys. Lett., 1987, 51, 913–915.

2 R. H. Friend, R. W. Gymer, A. B. Holmes, J. H. Burroughes, R. N. Marks, C. Taliani, D. D. C. Bradley, D. A. D. Santos, J. L. Brédas, M. Lögdlund and W. R. Salaneck, Electroluminescence in conjugated polymers, Nature, 1999, 397, 121–128.

3 A. J. C. Kuehne and M. C. Gather, Organic Lasers: Recent Developments on Materials, Device Geometries, and Fabrication Techniques, Chemical Reviews, 2016, 116, 12823–12864.

4 J. Gierschner, S. Varghese and S. Y. Park, Organic Single Crystal Lasers: A Materials View, Advanced Optical Materials, 2016, 4, 348–364.

5 J. Wu, W. Liu, J. Ge, H. Zhang and P. Wang, New sensing mechanisms for design of fluorescent chemosensors emerging in recent years, Chem. Soc. Rev., 2011, 40, 3483–3495.

6 M. K. Bera, P. Pal and S. Malik, Solid-state emissive organic chromophores: design, strategy and building blocks, J. Mater. Chem. C, 2020, 8, 788–802.

7 S. O. Mansoorabadi, C. J. Thibodeaux and H. Liu, The diverse roles of flavin coenzymes--nature's most versatile thespians, J. Org. Chem., 2007, 72, 6329–6342.

8 H. Grajek, Review - Flavins as photoreceptors of blue light and their spectroscopic properties, Current Topics in Biophysics, 2011, 34, 53–65.

9 Takin Haj Hassani Sohi, Felix Maaß, Constantin Czekelius, Vera Vasylyeva, Co-crystallization of organic chromophore roseolumiflavin and effect on its optical characteristics, CrystEngComm, 2022, submitted.

Back to Table of contents

MS29 Crystal engineering: structural flexibility, phase transitions and non-standard manipulation of synthons

MS29-2-6 Supramolecular Synthon Promiscuity in Phosphoric Acid–Dihydrogen Phosphate Ionic Cocrystals #MS29-2-6

M.M. Haskins [1], M. Lusi [1], M. Zaworotko [1]
[1]University of Limerick - Limerick (Ireland)

Abstract
The majority of active pharmaceutical ingredients (APIs) studied as lead candidates in drug development exhibit with poor aqueous solubility, which typically results in such APIs being poorly absorbed and exhibiting low bioavailability. Salts and pharmaceutical cocrystals can address low solubility and other relevant physicochemical properties of APIs. Pharmaceutical cocrystals are amenable to design through crystal engineering because supramolecular synthons, especially those sustained by hydrogen bonds, can be anticipated through computational modelling or Cambridge Structural Database (CSD) mining.
In this contribution, we report a combined experimental and CSD study on a class of ionic cocrystals (ICC) containing dihydrogen phosphate (DHP) salts and phosphoric acid (PA). This type of ICC is present in marketed drug product, but remains understudied from a crystal engineering perspective. Ten novel DHP:PA ICCs were prepared comprising nine organic bases and one anticonvulsant API, lamotrigine. From the resulting crystal structures and a CSD search of previously reported DHP:PA ICCs, 46 distinct hydrogen bond motifs (HBMs) have been identified between DHP anions, PA molecules, and, in some cases, water molecules. Our results indicate that although DHP:PA ICCs are a challenge from a crystal engineering perspective, they are formed reliably and, given that phosphoric acid is a pharmaceutically acceptable coformer, this makes them relevant to pharmaceutical science.

References
Haskins M. M., Lusi M. and Zaworotko M. Crystal Growth & Design 2022, 22, 5, 3333-3342

Back to Table of contents

MS29 Crystal engineering: structural flexibility, phase transitions and non-standard manipulation of synthons

MS29-2-7 Crystal Engineering in the Design of Cocrystals / Salts of Quinoline Drugs
#MS29-2-7

S.Z. Grabowski [1], A. Skórska-Stania [1]
[1]Faculty of Chemistry, Jagiellonian University in Krakow - Kraków (Poland)

Abstract
Quinoline derivatives exhibit a very wide spectrum of biological activity, such as: antibacterial, antimalarial, antiviral. Compounds containing the quinoline system in their structure, such as Cinchona alkaloids, chlororoquine and mefloquine, have been used in the treatment of malaria for many years [1]. However, the growing resistance of malaria parasites to these drugs and the lack of a vaccine till 2021 mobilized chemists to applicate new solutions to the old drugs.
In modern drug chemistry, one of the approaches to achieving improved drugs is the formation of a co-crystal. It allows for a change in the physical properties of the parental drug, and hence the pharmacokinetic profile, without changing the main activity of the drug molecule itself. This is highly advantageous when the properties such as solubility, toxicity, and bioavailability can be improved. It also allows investigations into multiple drug therapies, in which two drug molecules could be co-crystallized, creating drug-drug co-crystal. This type of drugs combination can be very useful because it allows synergistic action, so it can highly improved pharmacological effect on the organism.
Recently, we have engineered series of quinoline drugs designing crystalline phases with modified important properties. We have selected coformers using in sillico statistical methods based on the CSD Materials module from the CSD database. We have used statistical methods for prediction of interactions between molecules using Full Interaction Maps, molecular complementarity tools, synthon analysis and estimating the possibility of formation of hydrogen bond. These methods give opportunity to predict occurrence of the most important factor in organic molecular crystals – intermolecular interactions – and how they affect on crystal structure formation. Combining of such tools gave us possibility to design new crystal phases with high probability of formation [3].
Based on initial engineering, co-crystallization or coupling of the above-mentioned drugs with selected coformers using modern crystal engineering methods were carried out under various pressure and temperature conditions. Obtained crystals were examined using X-ray diffraction studies to behold if new phases crystallized and to understand how intermolecular interactions affect on crystal packing. Thanks to this knowledge we better understand molecule behaviour in the crystalline state, so we can design and obtain more crystal phases with better and better properties until the satisfactory effect is achieved.
Our results will contribute to obtain new crystal phases with enhanced physical and/or pharmacological properties which will be used as drugs without undesirable side effects and another often presented common problems. It can clearly help todays medicine in treatment of many diseases and pharmacology in the production of improved drugs.

References
1. Krafts K, Hempelmann E, Skórska-Stania A. From methylene blue to chloroquine: a brief review of the development of an antimalarial therapy. Parasitol Res. 2012 Jul;111(1):1-6.
2.Tiekink ERT,Vittal J, Zaworotko M (2010-01-11). Organic Crystal Engineering: Frontiers in Crystal Engineering. Organic Crystal Engineering: Frontiers in Crystal Engineering

Back to Table of contents

MS29 Crystal engineering: structural flexibility, phase transitions and non-standard manipulation of synthons

MS29-2-8 Trimorphic Ionic Cocrystals Sustained by the Phenol-Phenolate Supramolecular Heterosynthon #MS29-2-8

S. Jin [1], M. Zaworotko [1]
[1]University of Limerick - Limerick (Ireland)

Abstract

"Crystal engineering" is defined as "the field of chemistry that studies the design, properties and applications of crystals". One application of crystal engineering is prevalent in the study of cocrystals. Cocrystals have gained much attention, particularly in the pharmaceutical industry, due to their ability to modify physicochemical properties of drug molecules without changing their biological efficacy. Cocrystals are solids that are crystalline single-phase materials composed of two or more different molecular and/or ionic compounds generally in a stoichiometric ratio which are neither solvates nor simple salts.[1] Cocrystals can be classified into molecular cocrystals (MCCs) that contain only neutral components (coformers) in the crystal lattice and ionic cocrystals (ICCs) comprising of at least one ionic coformer that is a salt. ICCs involving inorganic salts (e.g., alkali and alkaline earth halides etc.) can also be viewed as a coordination complex between organic type ligands and metal cations. Ionic cocrystals have generated widespread interest as they exhibit strong hydrogen bonding or coordination bonding and have more components suggesting greater diversity of physicochemical properties.

The study of supramolecular synthons to investigate their amenability to crystal engineering will enable efficient discovery of new cocrystals. Supramolecular synthon is further classified into supramolecular homosynthon and heterosynthon.[2] Phenols are well-established in crystal engineering as they have demonstrated their ability to form robust supramolecular heterosynthons. They are also a common functionality found in many pharmaceutical and nutraceutical molecules. Recently, we have conducted crystal engineering studies on ICCs of phenol and substituted phenol derivatives with their conjugate bases, establishing the phenol···phenolate ($PhOH\cdots PhO^-$) supramolecular heterosynthon.[3]

Afterwards, by exploiting $PhOH\cdots PhO^-$ heterosynthon, novel trimorphic ICCs of a phenolic nutraceutical with its conjugate base were isolated and characterized. Structural analysis and conversion relationship were conducted on the three polymorphs in this work.

References

[1] Aitipamula, S. *et al.*, *Cryst. Growth Des.*, **2012**, 12, 2147-2152.
[2] Walsh, R. D. B. *et al.*, *Chem. Commun.*, **2003**, 186-187.
[3] Jin, S. *et al.*, *Cryst. Growth Des.*, **2022**.

Back to Table of contents

MS29 Crystal engineering: structural flexibility, phase transitions and non-standard manipulation of synthons

MS29-2-9 Synthesis and structural studies of cocrystals of cis and trans isomers of 1,2-cyclohexanediol with selected amines
#MS29-2-9

A. Sadocha [1], Ł. Dobrzycki [1], G. Cichowicz [1], M.K. Cyrański [1], R. Boese [2]
[1]University of Warsaw, Faculty of Chemistry - Warszawa (Poland), [2]University of Duisburg-Essen, Faculty of Chemistry - Essen (Germany)

Abstract
Presented work is dedicated to crystal engineering [1] of aliphatic and aromatic amines and isomers of 1,2-cyclohexanodiol. When crystallization experiments with small molecule aliphatic amines or aniline are performed at ambient conditions the formation of neat crystalline diol is observed. The only exception is formation of co-crystal with *trans*-1,2-cyclohexanediol and 4-fluoroaniline at room temperature. Hence, to analyze crystallization behavior of the title diol with series of amines (cyclopropylamine, cyclobutylamine, cyclopentylamine, cyclohexylamine, propylamine, butylamine, isobutylamine, *tert*-butylamine, aniline, ethylenediamine) *in situ* method supported by IR laser was used [2]. The crystals grown directly on the goniometer head were characterized by single crystal X-ray diffraction technique. It is observed that the *trans* isomer of 1,2-cyclohexanediol forms cocrystals with amines more willingly than the *cis* variant. In some cases plastic phases are formed. In all the obtained cocrystals hydrogen bonds between amino and hydroxyl groups are the main intermolecular forces that determine the crystal structure. In the co-crystal of *cis*-1,2-cyclohexanediol with cyclobutylamine the molecules are arranged in columns. In the remaining twelve systems, the structural motifs can be classified as layers, among which it is possible to distinguish different topologies of N…O interactions. The similarity of the structural motifs in the resulting crystal phases suggests that some predictability can be expected in the organization of molecules in systems composed of similar diols and amines. This fact makes these compounds very useful building blocks for crystal engineering and supramolecular recognition [3].

References
[1] G. R. Desiraju, “Crystal engineering: the design of organic solids” Amsterdam ; New York: Elsevier, 1989.
[2] R. Boese, “Special issue on In Situ Crystallization”, Z. Kristallogr., 2014, 229, 595-601
[3] S. Hanessian, R. Saladino, R. Margarita, and M. Simard, “Supramolecular Chirons Based on Enantiodifferentiating Self-Assembly between Amines and Alcohols (Supraminols)” Chem. – Eur. J., 1999, 5, 2169–2183

Back to Table of contents

MS30 Advanced porous materials : MOFs, COFs, SOFs....and what else?

MS30-1-1 Benefits of Cu-Kβ radiation for the structure determination of sponge crystals
#MS30-1-1

F. Meurer [1], C. Von Essen [2], C. Kühn [2], H. Puschmann [3], M. Bodensteiner [1]
[1]University of Regensburg - Regensburg (Germany), [2]Merck KGaA - Darmstadt (Germany), [3]Durham University - Durham (United Kingdom)

Abstract
The Crystalline Sponge method enables the structural elucidation of scarce, small organic analytes and hard-to-crystallize compounds. By diffusion of solvent and analyte molecules into the cavities of a metal-organic framework (the crystalline 'sponge') and molecular orientation by the MOF's functional groups, an analyte becomes part of the crystal structure and thus observable through X-ray diffraction methods.[1]
Unfortunately, many problems inherent to the structural elucidation of MOFs limit the possibilities of this method. These include weak host-guest interaction, incomplete diffusion, twinning, disorder of both analyte and solvent and sample decay. As much as the physical and chemical aspects of the method have recently been improved, the crystallographic aspects pose challenging problems onto the method. As we have recently adopted the use of the very rarely used Cu Kβ radiation in our X-ray department and found promising results in the analysis of our small molecule data, we also applied Cu Kβ radiation to the Crystal sponge method and compared it to the more commonly used wavelength Cu Kα in a total of six comparison experiments. Cu Kβ inherits a shorter wavelength than Cu Kα radiation (1.39222 Å compared to 1.54187 Å) and thus results in up to 38 % more unique reflections and up to 136 % total reflections. This is mainly due to the maximum resolution of 0.72 Å is accessible for Cu Kβ radiation, compared to 0.80 Å for Cu Kα radiation. Less absorption by consistently 25 % in absorption coefficient for Cu Kβ leads to less background and absorption damage.[2]This results in better crystallographic models for the Cu Kβ data sets: Significantly lower quality parameters were obtained in every Cu Kβ experiment. Bond precision was mainly better and the compared residual electron density maps (Fig. 1) look much cleaner. Additionally, more solvent positions could be modelled in the Cu Kβ data sets. In total, way fewer restraints and no constraints had to be used in the models collected using Cu Kβ radiation. Our findings suggest a routine use of Cu Kβ radiation – not only for the crystalline sponge method. The same advantages are to be expected in general for the structural elucidations of metal-organic frameworks but also standard small molecule crystallography.

References
[1] Hoshino, M., Khutia, A., Xing, H., Inokuma, Y. & Fujita, M. (2016). IUCrJ. 3, 139–151[2] Meurer, F., von Essen, C., Kuehn, C., Puschmann, H., Bodensteiner, M. (2022). IUCrJ 9, DOI: https://doi.org/10.1107/S2052252522002147

Cu Kα (left) and Cu Kβ (right) of the same sponge

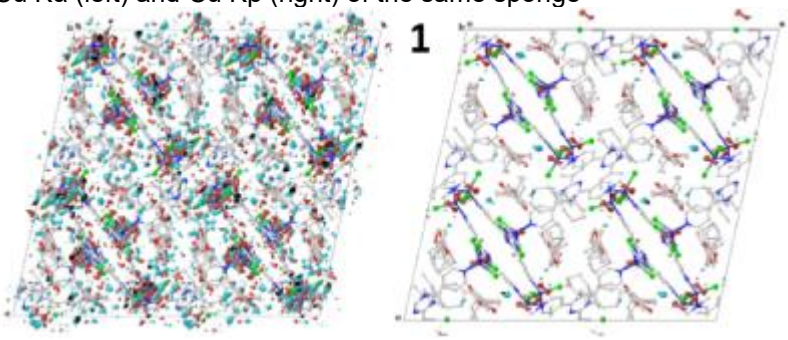

Back to Table of contents

MS30 Advanced porous materials : MOFs, COFs, SOFs....and what else?

MS30-1-2 Water cluster structure in the MOF CAU-10-H: a powder diffraction perspective
#MS30-1-2

G. Nenert [1], A. Pustovarenko [1], S. Canossa [2], D. Rega [3], M.A. Van Der Veen [3]
[1]Malvern Panalytical - Almelo (Netherlands), [2]Department of Nanochemistry, Max Planck Institute for Solid State Research - Stuttgart (Germany), [3]Catalysis Engineering, Department of Chemical Engineering, TU Delft - Delft (Netherlands)

Abstract
Several metal-organic frameworks (MOF) excel in harvesting water from the air or as heat pumps as they show a steep step in the water isotherm at 10-30 RH% [1]. Yet, a precise understanding of the water structure within the confined space of such MOF is still lacking. Here, we unravel the structural properties of CAU-10-H under various water content. We show that the water content can be tuned using the relative humidity, temperature and history of the sample. Previous studies have shown a structural phase transition from hydrated (non-centrosymmetric structure) to dry (centrosymmetric structure) [2]. Here in this contribution, we show that high resolution powder diffraction can allow to locate water molecules and the existence of various states of hydrated phases including centrosymmetric one.
This study besides bringing further insight into the water clusters present in this MOF enlights also the powerfulness of powder diffraction in the study of MOF materials.

References
[1] Wentao Xu, Omar M. Yaghi, ACS Cent. Sci. 2020, 6, 8, 1348–1354[2] Dominik Fröhlich et al. J. Mater. Chem. A, 2016,4, 11859-11869

In-situ relative humidity experiment on CAU-10-H

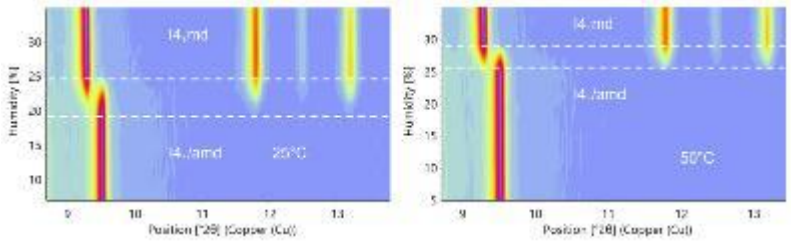

Back to Table of contents

MS30 Advanced porous materials : MOFs, COFs, SOFs....and what else?

MS30-1-3 Structural variability of MOFs built from a tetratopic phosphinate ligand
#MS30-1-3

P. Brazda [1], M. Kloda [2], J. Hynek [2], J. Demel [2]
[1]Institute of Physics of the Czech Academy of Sciences, Na Slovance 1999/2 - 18221 Prague 8 (Czech Republic), [2]Institute of Inorganic Chenistry of the Czech Academy of Sciences, Husinec-Rez 1001 - 25068 Husinec-Rez (Czech Republic)

Abstract
Metal organic frameworks (MOFs) using phosphinate ligands showed recently to be stable even under hydrothermal conditions [1]. Mixing ligand tricyclo[3.3.1.1^{3,7}]decane-1,3,5,7-tetrayltetrakis(phenyl-4-methylphosphinic acid (H_4TPATP(Me), Figure 1A) with ferric ions led to formation of three different phases. The major phase (ICR-11, space group *P*-3, a=24.3(1), c=9.50(5)Å) has significant proton conductivity because two out of four phosphinate groups are not coordinated to iron but form walls of the channels running parallel along *c* direction [2]. 3D electron diffraction (3D ED) experiments revealed two more minor phases. One has triclinic Bravais lattice and shows low level of crystallinity, which demonstrates itself in diffuse scattering features. The other phase is monoclinic (space group *C*2/*c*, a=15.48(1), b=29.03(1), c=23.75(1) Å, beta=91.1(1)°) and the structure was solved ab initio (Figure 1B). The iron cations form trimers interconnected by six phosphinate groups. Two other phosphinate groups are capping the terminal iron cations from both sides leading to eight coordinated phosphinate groups in total However, the three ferric ions have nine positive charges. This results in one positive charge per trimer, which is compensated by formic acid, which has only about 0.5 occupancy at both ends of the trimer. Even though the structure is very large (nearly 11000 Å^3), it was possible to perform dynamical refinement [3], which clearly revealed the position of the half-occupied carbon atom of the coordinated formic acid. The unit cell contains 488 non-hydrogen atoms, which makes it the largest dynamically refined structure.
Acknowledgement:
We thank Czech Science Foundation (project no. 20-04408S) for financial support.

References
[1] Hynek, J., Brazda, P., Rohlicek, J., Londesborough, M.G.S., Demel, J. Angew. Chem. Int. Ed. 57 (2018) 5016-5019.
[2] Kloda, M., Plechacek, T., Ondrusova, S., Brazda, P., Chalupsky, P., Rohlicek, J., Demel, J., Hynek, J., Inorg. Chem. under review.
[3] Palatinus, L., Petricek, V., Correa, C. A. Acta Crystallogr. A 71 (2015) 235.

Figure 1 Tetratopic phosphinate ligand H4TPATP(Me)

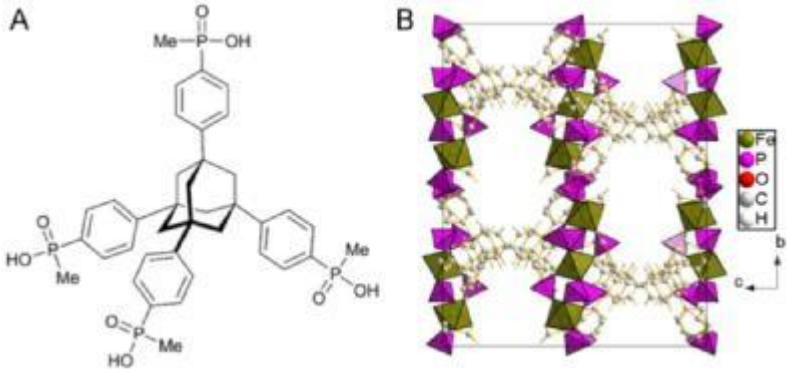

Back to Table of contents

MS30 Advanced porous materials : MOFs, COFs, SOFs....and what else?

MS30-1-4 Structure Determination of Nanocrystalline MOFs Using Electron Diffraction
#MS30-1-4

C. Jandl [1], J. Merkelbach [1], D. Stam [1], G. Steinfeld [1], E. Hovestreydt [1]
[1]ELDICO Scientific AG - Villigen (Switzerland)

Abstract
Electron diffraction (3D-ED, MicroED) is gaining more and more momentum as a technique for the structural elucidation of challenging compounds as it bypasses the main limitation of growing crystals of suitable size for single-crystal X-ray diffraction. As such it has already found applications in all fields of research from organic and inorganic compounds, over polymorphism, pharmacology, natural products, geological sciences, biomolecules, materials science to energy-storage materials and others.
As porous materials commonly obtained from solvothermal synthesis MOFs often pose a challenge for traditional X-ray crystallography as their inherent properties do not allow for a recrystallisation, which makes structural analysis dependent on obtaining suitable single crystals straight from the synthesis. Being able to use nanocrystalline as synthesized material makes electron diffraction the perfect tool to tackle this problem and determine structures from crystals that are too small even for synchrotron facilities.
We show a range of examples from recent literature measured on our ED-1 electron diffractometer demonstrating the reliability and potential of 3D-ED for applications in the field of porous coordination compounds and benefits of a dedicated electron diffractometer.

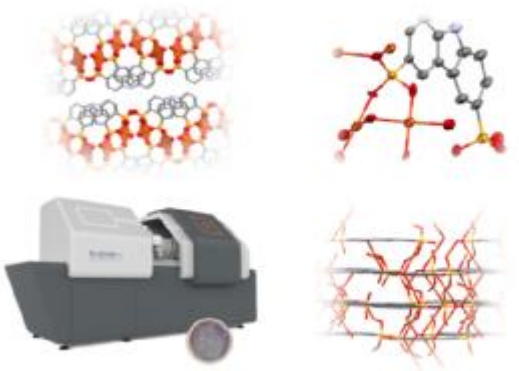

Back to Table of contents

MS30 Advanced porous materials : MOFs, COFs, SOFs....and what else?

MS30-1-5 Chiral 3D Metal-Organic Frameworks with Zinc and Hydroxy-Amino Acids
#MS30-1-5

D. Vušak [1], V. Idek [1], B. Prugovečki [1]
[1]Department of Chemistry, Faculty of Science, University of Zagreb - Zagreb (Croatia)

Abstract
Metal-organic frameworks are well explored class of materials with over 110000 datasets in Cambridge Structural Database (CSD, version 2021.3.0) [1]. Only 114 of those contain zinc and α-amino acid or amino acid derivative, and only 1 dataset is a 3D MOF containing zinc, 4,4'-bipyridine and amino acid (L-lysine) [2]. Introduction of a chiral molecule in MOF increases possibilities for their potential applications, e.g. for enantioselective catalysis or separation or for tuning magnetic properties [3].
As part of our investigation of porous materials involving essential metal atoms and biologically important compounds [4–7], we report four 3D chiral cationic MOFs with zinc, 4,4'-bipyridine (bipy) and L-serine (HSer) or L-threonine (HThr). One L-serinato, $\{[Zn_2(\mu\text{-Ser})_2(\mu\text{-bipy})_3](NO_3)_2\cdot(DMF/water)\}_n$ (**1**), and three L-threoninato MOFs were obtained: two solvates of the same framework formula unit $\{[Zn_4(\mu\text{-Thr})_4(H_2O)(\mu\text{-bipy})_4(DMF)](NO_3)_4\cdot(DMF/water)\}_n$ (**2a** and **2b**) and $\{[Zn_2(\mu\text{-Thr})_2(H_2O)(\mu\text{-bipy})_3](NO_3)_2\cdot 2bipy\cdot 2H_2O)\}_n$ (**2c**). **1** and **2c** have a higher volume ratio of crystallization solvent and/or bipyridine molecules (>40%) and form 2D channels, while in **2a** and **2b** 25–28% of the unit cell volume is occupied by solvent molecules forming 1D channels. The influence of solvent on crystallization and coordination modes is discussed, as well as a comparison of syntheses, crystal structures and properties of compounds.

References
[1] Groom, C. R., Bruno, I. J., Lightfoot, M. P., Ward, S. C. (2016) *Acta Cryst*. B**72**, 171–179.
[2] Li, S.-Q., Hu, N.-H. (2012) *Acta Cryst*. E**68**, m633–m634.
[3] Mendes, R. F., Almeida Paz, F. A. (2015) *Inorg. Chem. Front.* **2**, 495–509.
[4] Vušak, D., Prugovečki, B., Milić, D., Marković, M., Petković, I., Kralj, M., Matković-Čalogović, D. (2017) *Cryst. Growth Des*. **17** 6049–6061.
[5] Vušak, D., Prugovečki, B., Matković- Čalogović, D. (2018) *Acta Cryst*. A**74**, E337–E337.
[6] Vušak, D., Ležaić, K., Prugovečki, B., Matković-Čalogović, D. (2019) *Acta Cryst*. A**74**, E530–E530.
[7] Vušak, D., Smrečki, N., Muratović, S., Žilić, D., Prugovečki, B., Matković-Čalogović, D. (2021) *RSC Adv*. **11**, 23779–23790.

Figure 1. Channels of solvent and/or bipyridine

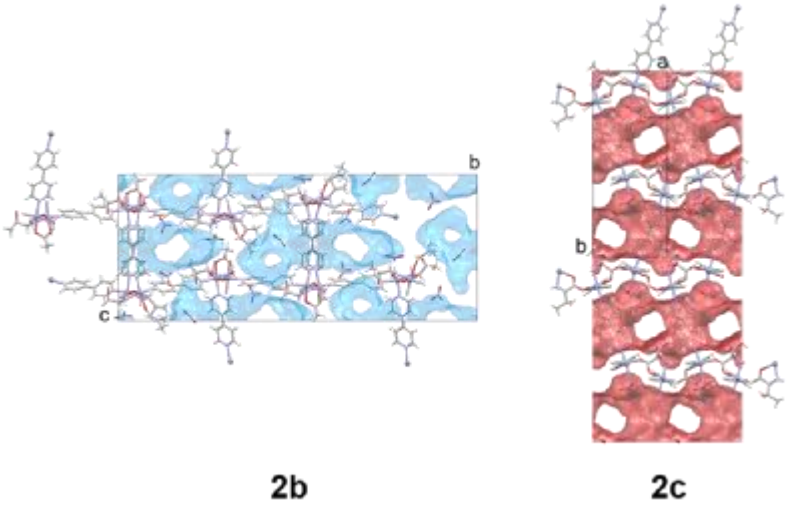

2b 2c

Back to Table of contents

MS30 Advanced porous materials : MOFs, COFs, SOFs....and what else?

MS30-1-6 Hydrogen-bonded organic frameworks based on luminescent rhenium octahedral cluster complexes #MS30-1-6

D.I. Konovalov [1], D.I. Konovalov [2], E. Cadot [3], M.A. Shestopalov [4]
[1]Institut Lavoisier de Versailles, UMR 8180, UVSQ, Université Paris-Saclay - Versailles (France) - Versailles (France), [2]Nikolaev Institute of Inorganic Chemistry SB RAS - Novosibirsk (Russian Federation), [3]Institut Lavoisier de Versailles, UMR 8180, UVSQ, Université Paris-Saclay - Versailles (France) - Versailles (France) - Versailles (France), [4]Nikolaev Institute of Inorganic Chemistry SB RAS - Novosibirsk (Russian Federation) - Novosibirsk (Russian Federation)

Abstract
Rhenium octahedral cluster complexes are compounds with common formula $[\{Re_6Q_8\}L_6]^n$ and set of interesting physical-chemical properties such as: (i) bright red luminescence at excitation by UV, visible, X-ray or electric current, (ii) photosensitivity properties, i.e. the ability to transfer the energy of the excited cluster state to triplet oxygen, thus converting it into a highly active singlet form, as well as (iii) high radiodensity properties due to the high local concentration of heavy atoms in the cluster core. The presence of such properties, which are certainly promising from a practical point of view, makes it possible to predict the possibility of using such compounds both in an individual form and as components for the creation of functional materials in various fields from sensorics to biomedicine.
Substitution of apical halide ligands in $[\{Re_6Se_8\}X_6]^{3-}$ (X = Cl, Br) by benzimidazole (bimzH) accompanied by a self-assembly process leads to the formation of microporous Re_6- based hydrogen-bonded organic frameworks (**Re_6-HOFs**) constructed on N−H···X hydrogen bonds and π−π-stacking interactions between bimzH ligands. **Re_6-HOFs** demonstrate sorption properties with a Brunauer−Emmett−Teller surface area of up to 443 m^2g^{-1} and luminescence with a quantum yield and an emission lifetime of up to 0.16 and 16 μs, respectively. The compounds obtained complement small groups of transitionmetal cluster-based HOFs, which are a perspective for the development of multifunctional frameworks.

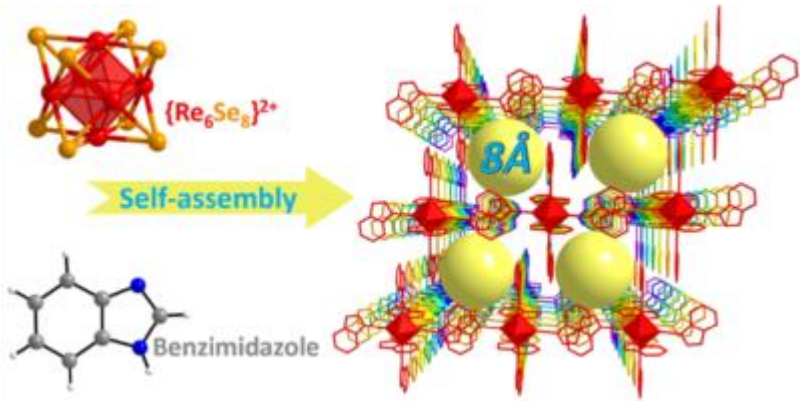

Back to Table of contents

MS30 Advanced porous materials : MOFs, COFs, SOFs....and what else?

MS30-2-1 Mixed-ligand metal-organic frameworks incorporating rigid and flexible linkers
#MS30-2-1

K. Muguru [1], C. Oliver [1]
[1]University of Cape Town - Cape Town (South Africa)

Abstract
Metal-organic frameworks (MOFs) form a class of inorganic-organic hybrid porous crystalline materials containing metal ions or metal clusters bridged by organic ligands via coordination bonds to form one-, two-, or three-dimensional networks with useful properties.[1,2] The flexibility of changing the metal centers and organic ligands allows a wide range of MOFs to be designed, and by careful selection of the constituents, MOFs with desired structures and tailored properties can be produced. Mixed-ligand MOFs have two or more different types of organic linkers that provide the possibility of tuning pore size or shape, since ligands of various sizes could be used to synthesize these materials, thus allowing further tailoring of properties.[3] We report the synthesis involving the reaction of 1,3,5-benzenetricaboxylic acid (H_3btc) and 1,3-bis(4-pyridyl)propane-N,N'-dioxide (bppdo) with $Co(NO_3)_2.6H_2O$ in N,N'-dimethylformamide (DMF), methanol (MeOH) and H_2O which afforded $[Co_{6.5}(btc)_4(bppdo)_2(OH)(H_2O)_{7.5}]n.\ n(H_2O)_{3.5}(DMF)$ (**1**). The compound was characterised by variable-temperature X-ray diffraction and thermal analysis and have showed high porosity (BET surface area, 548 m2/g). The gas sorption properties of **1** are dependent upon the activation method, for example, room-temperature and thermal evacuation, and activation involving solvent exchange. The MOF display high N_2, H_2, CO_2, gas uptake capacities at room temperature. Water vapour sorption of **1** show that it readily absorbs water vapour at low relative pressures The significant adsorption of different gas and vapour is due to the presence of micropores and unsaturated metal sites in the MOF. We further report the synthesis involving the reaction of H_3BTC and 1,2-bis(4-pyridyl)ethane-N,N'-dioxide (BPEDO) with $CuSO_4.5H_2O$ in dimethylacetamide (DMA), ethanol (EtOH) and H_2O which resulted in $[Cu_4(btc)(bpedo)_{0.5}(SO_4)_{0.5}(OH)(H_2O)]n.$ (**2**). Compound **2** exhibit a high uptake capacity for H_2O.

References
1. H. W. Langmi, J. Ren and N. M. Musyoka, in Compendium of Hydrogen Energy, ed. R. B. Gupta, A. Basile and T. N. Veziroğlu, Woodhead Publishing, 2016, p. 163-188.
2. T. Tahier and C. L. Oliver, CrystEngComm, 2015, 17, 8946-8956.
3. M. Du, C. Li, C. Liu and S. Fang, Coord. Chem. Rev., 2013, 257, 1282-1305.

Back to Table of contents

MS30 Advanced porous materials : MOFs, COFs, SOFs....and what else?

MS30-2-10 Efficient Eco-friendly Metal Organic Framework for Amoxycilline degradation from aqueous solution #MS30-2-10

R.M. Percoco [1], L. Bartella [1], P. Hajivand [1], T.F. Mastropietro [1], P. Escamilla [2], J. Ferrando-Soria [2], E. Pardo [2], L. Di Donna [1], D. Armentano [1]
[1]Dipartimento di Chimica e Tecnologie Chimiche (CTC), Università della Calabria - Arcavacata (Italy), [2]Instituto de Ciencia Molecular (ICMol), Universidad de Valencia - Paterna (Spain)

Abstract
Due to the scarcity of water and the growing industrialization, pharmaceutical wastewater treatment is of particular importance. Today's pharmaceutical residuals are suggested as an overgrowing portion of the emerging pollutants because of their broad usage. Antibiotics such as amoxicillin (AMX) are commonly found in the wastewater, reaching the environment through urine and excreta and one of the most known effects on the environment is the development of resistant pathogenic bacteria. Amoxicillin is an antibiotic of the betalactam family. This class of antibiotics interferes with the synthesis of the cell wall of bacteria by inhibiting the transpeptidase, an enzyme essential for the formation of peptidoglycan. Amoxicillin is characterized by chemical stability, low rate of biodegradation and high level of toxicity. It has been widely used in veterinary medicine to prevent various bacterial infections of the livestock due to their broad spectrum and lesser side effects used for disease treatment. To a lesser extent, it is used for the treatment of human infections.
For this reason, it is necessary to achieve an efficient method to eliminate this pollutant.[1] Metal−organic framework (MOFs) as a new class of nanoporous materials, due to their rich host-guest chemistry, has displayed high efficiency in various fields especially in the adsorption process. [2,3]
Taking the abovementioned into account, current work aimed to prepare, and evaluate the efficacy of of an eco- and bio-compatible water wastewater treatment as adsorbent for the removal of AMX from aqueous solutions. This novel MOF ($Ca^{II}Zn^{II}_6$[(S,S)- Mecysmox]$_3(OH)_2(H_2O)\}\cdot 15H_2O$ (1), is characterized by functional channels decorated with CH_2SCH_3 thioalkyl chain from L-methylcysteine amino acid-derived ligand (Figure 1). In this contribution its adsorption capacity, reusability and surprisingly its catalytic activity, in mild conditions, in degradation of AMX to penicilloic acid will be described. This combination of outstanding efficiency with low-cost straightforward synthesis places this material among the most promising adsorbents reported for the removal and degradation of this type of contaminants.

References
1. Kerkez-Kuyumcu, Ö., Ş.S. Bayazit, and M.A. Salam, Antibiotic amoxicillin removal from aqueous solution using magnetically modified graphene nanoplatelets. Journal of Industrial and Engineering Chemistry, 2016. 36: p. 198-205.2. M. Mon, R.Bruno, J.Ferrando-Soria, L. Bartella, L.Di Donna, M.Talia, R. Lappano, M. Maggiolini, D. Armentano, E. Pardo Mater. Horiz., 2018,5, 683-6903. C. Negro, H. Martínez Pérez-Cejuela, E. Simó-Alfonso, J. Manuel Herrero-Martínez*, R.Bruno, D. Armentano, J. Ferrando-Soria, E. Pardo ACS Appl. Mater. Interfaces 2021, 13, 24, 28424–28432

View of the porous crystal structure of 1

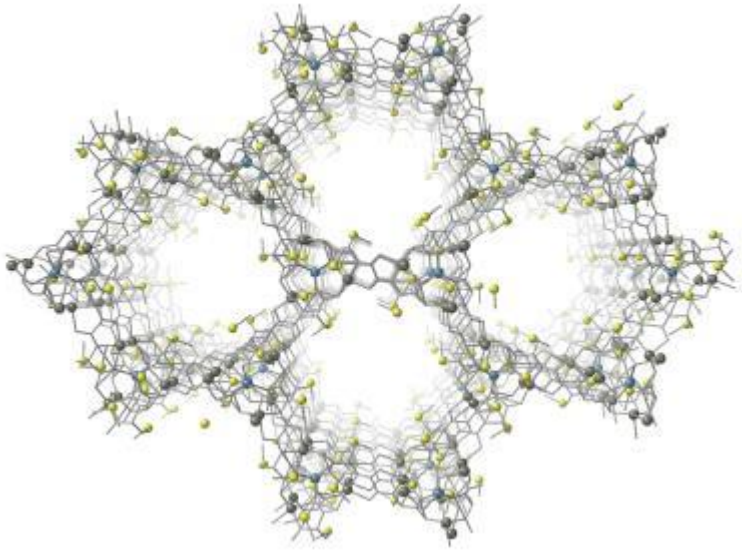

Back to Table of contents

MS30 Advanced porous materials : MOFs, COFs, SOFs....and what else?

MS30-2-2 Structure determination of a highly disordered 2D MOF by continuous rotation electron diffraction method
#MS30-2-2

G. Zhou [1], Z. Huang [1]
[1]Department of Materials and Environmental Chemistry - Stockholm University (Sweden)

Abstract
As a combination of metal-organic frameworks and 2D materials, 2D MOFs have garnered increasing attention due to the uniformed porosity, tunable structures, exfoliation property. These features make 2D MOFs exhibit in potential application catalysis, gas storage, gas separation, luminescence, et al. However, the structure determination is challenging for conventional X-ray diffraction technology. Data collection is hindered by the small size of the crystals (< 1 μm) and data processing, structure refinement often suffers from disorders caused by displacement of the layers.
Herein, we present the successful structure determination of a novel 2D MOF with Zr12 as node and 2,2'-Bipyridine-5,5'-dicarboxylic acid as linker based on continuous rotation electron diffraction method[1]. The data set suffers from the ambiguous value of c axis length caused by the interlayer disorders (Figure 1b, 1b). We first refine the structure with c axis equals to 28.75 Å. The double-layered hxl net can be nicely refined (Figure 2a), while interlayer structure can not be solved. The inter layer distance is 15 Å, longer than the ligand. There remain obvious residues between the layers which can not be assigned. These residues look just like the Zr12 cluster. By using cryo-holder, the data quality has been improved slightly still showing severe disorders. By adjusting XDS parameters[2], the c axis can be confirmed to be 15.92 Å and the interlayer structures thus can be solved.

References
1. J. Appl. Cryst. (2018). 51, 1094-1101.
2. J. Appl. Cryst. (1988). 21, 67-72.

Figure 1

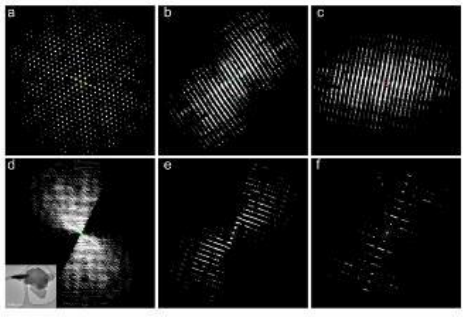

Figure 2

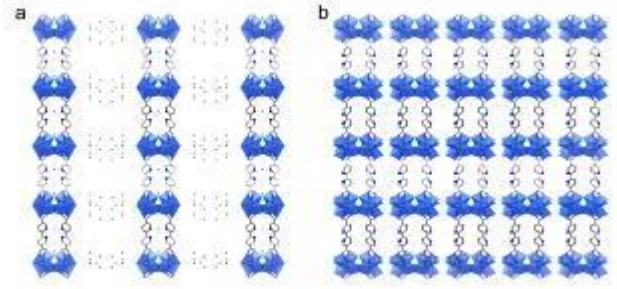

Back to Table of contents

MS30 Advanced porous materials : MOFs, COFs, SOFs....and what else?

MS30-2-3 Graphene Oxide as a Structural Directing Agent of MOFs
#MS30-2-3

A. Saad [1], N. Guillou [1], N. Menguy [2], C. Sicard [1], N. Steunou [1]
[1]Institut Lavosier de Versailles - Versailles (France), [2]Sorbonne Univeriste - Paris (France)

Abstract
Due to their huge surface areas, topological diversity, and functional tunability, MOFs have sparked a high interest for different applications including gas storage/separation, catalysis, sensing or biomedicine **[1]**. However, these porous hybrid materials are mostly obtained in the form of a polycrystalline powder or spherical nanospheres. One of the main challenges for their practical application is to control the crystal size, morphology and multiscale porosity of these materials while developing adequate shaping methods. For that purpose, one of the strategies reported in literature consists of combining MOFs with different carbon-based materials (polymers, graphene, carbon nanotubes, ...) **[2]**. A recent work investigated the use of GO nanoscrolls as structure directing agents to form single crystal aluminum based MOF nanowires (NWs) **[3]**. Following this approach, it was possible to obtain hierarchical porous MOF/GO composites with a specific microstructure that allowed a homogeneous dispersion of MOF NWs in the GO matrix, without any agglomeration of MOF NPs or restacked GO layers (Figure 1.). Hence, throughout this PhD project, we were able to extend this concept to another aluminum based MOF with a higher permanent porosity. Furthermore, through certain experimental conditions, a solvent-induced flexibility behavior was observed for these single crystal MOF nanowires. In this communication, we will present the synthesis optimization of this MOF/GO composite, their microstructural characterization by advanced techniques and their solvent induced flexibility behavior.

References
[1] Zhenjie Zhang, Ha Thi Hoang Nguyen, Stephen Miller, Seth Cohen, Angewandte Chemie 54 (2015) 6152.
[2] Liang Feng, Kun-Yu Wang, Joshua Powell, Hong-Cai Zhou, Matter, 1 (2019) 801.
[3] Mégane Muschi, Anusha Lalitha, Saad Sene, Damien Aureau, Mathieu Fregnaux, Imène Esteve, Lucie Rivier, Naseem Ramsahye, Sabine Devautour-Vinot, Clémence Sicard, Nicolas Menguy, Christian Serre, Guillaume Maurin, Nathalie Steunou, Angewandte Chemie 59 (2020) 10353.

Formation mechanism of single crystal MIL69(Al) NW

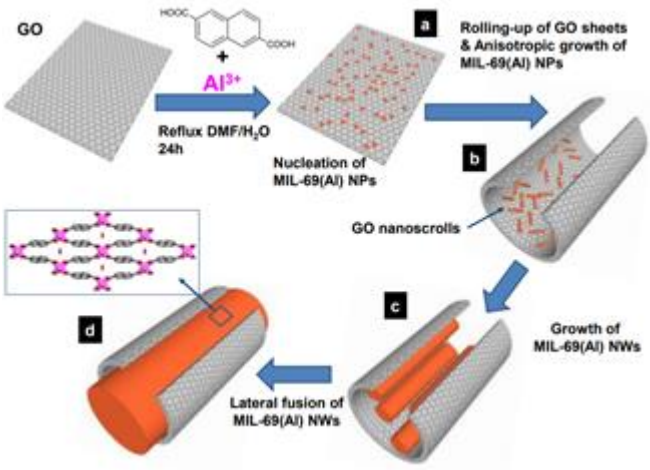

Back to Table of contents

MS30 Advanced porous materials : MOFs, COFs, SOFs....and what else?

MS30-2-4 In-situ characterizations of the selective CO2 adsorption in free-template nanosized zeolites RHO and CHA
#MS30-2-4

N. Barrier [1], M. Debost [1], J. Grand [2], P. Boullay [1], E. Clatworthy [3], A. Päcklar [1], P. Klar [4], P. Brázda [4], N. Nesterenko [2], J.P. Dath [2], J.P. Gilson [3], L. Palatinus [4], S. Mintova [3]
[1]Normandie Université, ENSICAEN, UNICAEN, CNRS, Laboratoire de Cristallographie et Science des Matériaux (CRISMAT) - Caen (France), [2]Total Research and Technologies, Feluy - Seneffe (Belgium), [3]Normandie Université, ENSICAEN, UNICAEN, CNRS, Laboratoire Catalyse et Spectrochimie (LCS) - Caen (France), [4]Institute of Physics of the Czech Academy of Sciences - Prague (Czech Republic)

Abstract
Natural gas is a mixture of hydrocarbon gas, mostly containing methane, used as a fossil fuel or source of carbon chain compounds. During one of the natural gas processing steps, methane (CH_4) must be separated from CO_2. One of the methods is to use materials with high adsorption and selectivity as separating membranes. Of the porous materials used as membranes, reduced pore cage type zeolites such as RHO or CHA are very good candidates. Indeed, these porous materials have narrow pores connecting large cages, whose access can be blocked or reduced by the cations (Cs, Li, Na,...) present in their networks. This is the trap-door effect, which gives the material increased selectivity. For example, CO_2 being less voluminous than CH_4, it will have easier access to these pockets.
The influence of different cations has been studied by many research groups.[1] It has a direct impact on the hydrothermal stability of these zeolites. These studies also attributed the high selectivity to the high surface polarity of zeolite RHO, which favors interactions with polar molecules such as CO_2. In addition, it has been found that the high absorption of CO_2 is due to the high pore volume of this zeolite, and not caused by the repositioning of the cations. The increase in the pore volume can be obtained by the synthesis of nanoscale RHO and CHA zeolites, but all the previous studies of the trap-door effect have been carried out on micrometric zeolites.
In this presentation, we will show our results on the CO_2 adsorption/desorption process followed in situ by X-ray (synchrotron and laboratory), neutron and 3D electron diffraction technics. Different free-template CHA [2] and RHO [3] zeolites based on caesium, potassium and sodium whose crystallite sizes vary from 50 to 300 nm have been studied. Our study demonstrates how the cationic distributions in the zeolite framework, or the flexibility of the framework itself influence the CO_2 adsorption-desorption process.

References
[1] (a) M. M. Lozinska, E. Mangano, J. P. S. Mowat, A. M. Sheperd, R. F. Howe, S. P. Thomson, J. E. Parker, S. Brandani, P. A. Wright, J. Am. Chem. Soc. 134, 17628 (2012); (b) Y. Lee, J. A. Hriljac, T. Vogt, J. B. Parise, M. J. Edmonson, P. A. Anderson, D. R. Corbin, T. Nagai, J. Am. Chem. Soc. 123, 8418 (2001); (c) T. Nenoff, J. B. Parise, G. A. Jones, L. G. Galya, D. R. Corbin, G. D. Stucky, J. Phys. Chem. 100, 14256 (1996); (d) J. B. Parise, D. E. Cox, J. Phys. Chem. 88, 1635 (1984).
[2] Debost, M.; Klar, P. B.; Barrier, N.; Clatworthy, E. B.; Grand, J.; Laine, F.; Brazda, P.; Palatinus, L.; Nesterenko, N.; Boullay, P.; Mintova, S. Synthesis of Discrete CHA Zeolite Nanocrystals without Organic Templates for Selective CO_2 Capture. Angew. Chem.-Int. Edit. 2020, 59 (52), 23491–23495.
[3] Grand, J.; Barrier, N.; Debost, M.; Clatworthy, E. B.; Laine, F.; Boullay, P.; Nesterenko, N.; Dath, J.-P.; Gilson, J.-P.; Mintova, S. Flexible Template-Free RHO Nanosized Zeolite for Selective CO_2 Adsorption. Chem. Mat. 2020, 32 (14), 5985–5993.

The trap-door effect for a Cs-RHO zeolite allowing

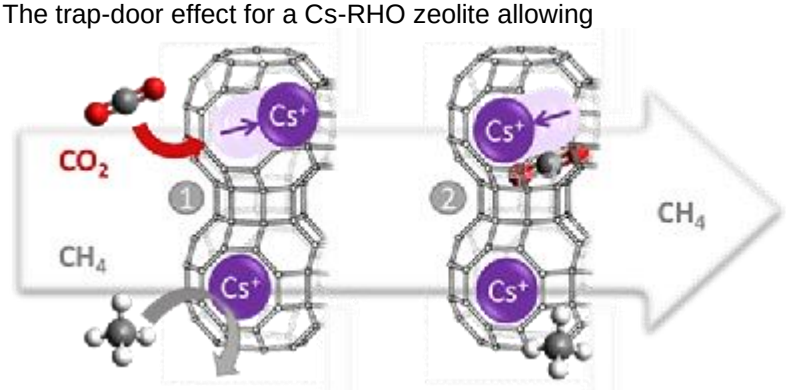

Back to Table of contents

MS30 Advanced porous materials : MOFs, COFs, SOFs....and what else?

MS30-2-5 Structure solution using 3DED of beam and vacuum sensitive carbazole-based di-phosphonic acid Metal Organic Frameworks.
#MS30-2-5

L. Gemmrich Hernandez [1], F. Steinke [2], U. Kolb [1], N. Stock [2]
[1]JGU - Mainz (Germany), [2]Institute of Inorganic Chemistry - Kiel (Germany)

Abstract
Metal-Organic Frameworks (MOFs) are characterized by metal nodes (inorganic building units, IBUs) linked by organic molecules (linker) resulting in a 3D network with pores that allow them to easily interact, absorb and release liquid and gas phases such as moisture, solvents... [1]. These materials are very challenging to investigate due to their tendency to crystallize as microcrystalline powders. Therefore, methods such as 3-dimensional electron diffraction (3DED) and XRPD are excellent tools to achieve structure determination [2]. In this research, we report the use of Transmission Electron Microscopy (TEM) to attain the structure solution of two new MOFs (Cu- and Zn-DPC), built by a new linker molecule. Both compounds were initially characterized using XRPD with the aim of determining their crystal structure. However, this approach was not successful. Therefore, 3DED was used to achieve the crystal structure through direct methods. One of the challenges of the study of these DPCs using 3DED is their beam and vacuum sensitivity. Since they contain guest molecules, upon introducing them inside the TEM, their structure starts to change due to water and/or solvent loss. These alterations result in a decrease in crystallinity, variation of length of the crystallographic axes, shearing of the cell, loss of volume and coordination change of the metallic cations. Therefore, in order to enable an ab initio structure solution, fast data acquisition is essential. In this project, using Fast Automated Electron Diffraction Tomography (Fast-ADT) we were able to achieve structure solution of such complex samples with room temperature measurements in an FEI TECNAI-F30 STWIN transmission electron microscope equipped with a ULTRASCAN4000 CCD camera. While the structures of these compounds feature similar building blocks, there are significant differences in their resulting networks; CuDPC can be described as a layered 2D coordination polymer, while ZnDPC features a layered IBU, but the interconnection through the linker molecules results in a 3D network. Both materials change within the TEM environment as a function of the time: the CuDPC shows a reduction of the distance between the IBUs accompanied with a shrinking of the lattice parameter b, and overall cell volume reduction upon removal of H_2O from the IBU and the coordination environment of the copper ions (which changes from square pyramidal to square planar), while ZnDPC also shows lattice shrinking and volume reduction to a smaller extent, with β-angle changes being the more evident variation in the structure.

References
[1] Yang, F. Xu, G. Dou, Y. Wang, B. Zhang, H. Wu, H. Zhou, W. Li, J. and Chen, B. “A flexible metal–organic framework with a high density of sulfonic acid sites for proton conduction”, Nature Energy (2017), 2(11), 877–883.
[2] T. Rhauderwiek, H. Zhao, P. Hirschle, M. Döblinger, B. Bueken, H. Reinsch, D. De Vos, S. Wuttke, U. Kolb and N. Stock. “Highly stable and porous porphyrin-based zirconium and hafnium phosphonates – electron crystallography as an important tool for structure elucidation “, Chemical Science (2018), 9, 5467–5478.

Fig 1. Structure solution model of the ZnDPC

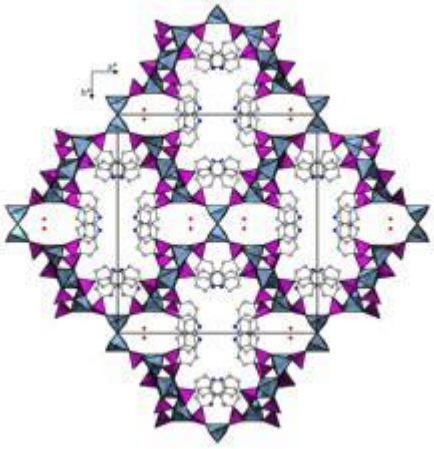

Fig 2. ADT3D volume reconstruction ZnDPC

Back to Table of contents

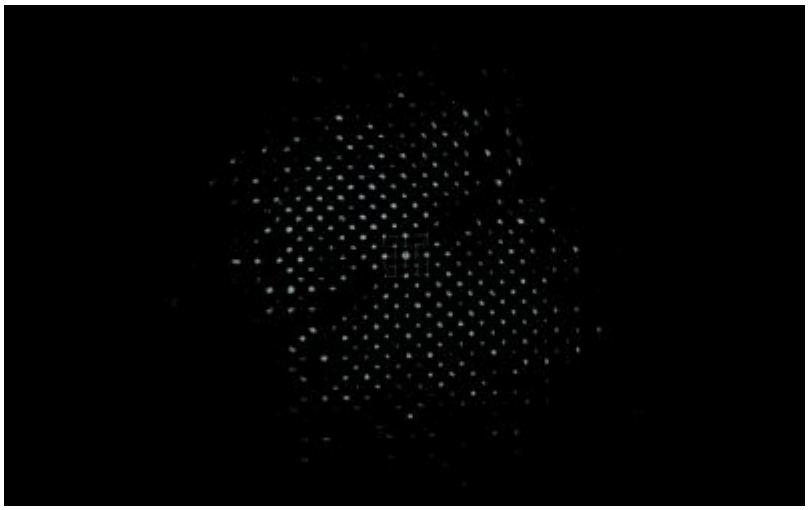

Back to Table of contents

MS30 Advanced porous materials : MOFs, COFs, SOFs....and what else?

MS30-2-6 Mesoporous MOF-based scaffolds for catalysis
#MS30-2-6

C.M.L. Vande Velde [1], R. Fucci [1], L. Esrafili [1]
[1]University of Antwerpen - Antwerpen (Belgium)

Abstract
Homogeneous and heterogeneous catalysts are known to have opposite characteristics: the main advantage of the first (selectivity/activity) is the main disadvantage of the second, and vice versa (recovery/reuse) [1]. Given their complementarity, merging their properties by heterogenizing the homogeneous catalyst would create a super catalyst.For practical use, the catalyst should be characterizable, cheap, easy to quantitatively recover, as well as environmentally sustainable.Mesoporous Metal Organic Frameworks can be used as heterogeneous substrate for this purpose. Most of the MOF structures that are based on commercially available linkers have micropores (up to 2nm), and this limits their application when considering their use in fields where substrate size is important (e.g. synthesis of APIs).The organic linkers do not only directly affect the final size of the pores but they also contribute, together with the metal core, to the final morphology of the MOFs. The combination of morphology and pore size is crucial for the final application of MOFs.The direct engineering of novel MOFs structure presenting a specific morphology and pore size is possible. To facilitate this, advanced synthetic techniques have been developed to achieve large molecules in a cheap and fast synthesis.[2]According to the isoreticular synthesis principle [3], libraries of MOFs that share the same morphology can be generated by increasing the size of organic linkers but keeping the same metal core.
Basing our approach on this principle, we generated libraries of star-shaped organic linkers (3 and 4-topic) that can be turned into a series of honeycomb (hnb) MOFs. This novel series of MOFs has the characteristics of pore size and morphology that are specifically chosen to better tackle the problem of diffusion of reagents and products, generating a class ofnovel advanced catalysts.

References
[1] J. Čejka, R. E. Morris, P. Nachtigall. (2017). Catalysis Series, Zeolites in Catalysis , DOI: 10.1039/9781788010610-FP001[2] R. Fucci, C. M. L. Vande Velde. (2021). Faraday Discuss., 97. DOI: 10.1039/D1FD00026H[3] H. Deng, S. Grunder, K. E. Cordova, C. Valente, H. Furukawa, M. Hmadeh, F. Gándara, A. C. Whalley, Z. Liu, S. Asahina, H. Kazumori, M. O'Keeffe, F. Stoddart, O. M. Yaghi. (2012). Science, 6084, 1018. DOI: 10.1126/science.1220131

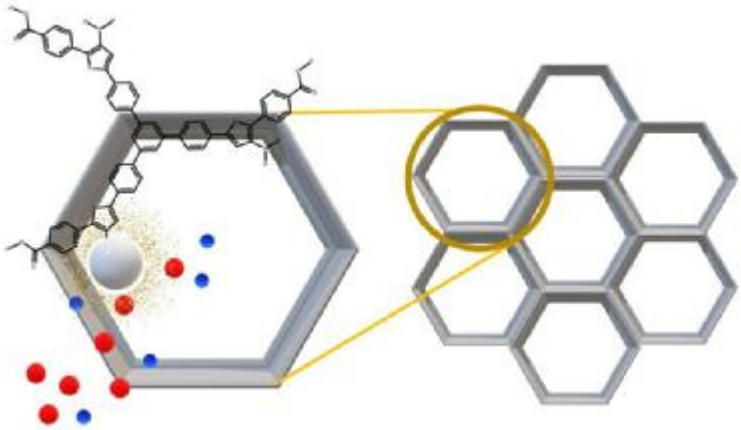

Back to Table of contents

MS30 Advanced porous materials : MOFs, COFs, SOFs....and what else?

MS30-2-7 Pillarplexes - Porous Organometallic Synthons in Crystal Engineering
#MS30-2-7

A. Pöthig [1]
[1]Technical University of Munich - Garching (Germany)

Abstract
Pillarplexes[1] (Fig. 1A), supramolecular organometallic complexes (SOCs),[2] are self-assembled by two macrocyclic NHC ligands and eight coinage metal ions (AgI and AuI) and can act as tubular metallocavitands with remarkable properties (Fig. 1B): intrinsical photoluminescence, tunable solubility via anion exchange and shape-selective host abilites towards linear molecules. Furthermore, they can also be applied as building blocks in mechanically interlocked rotaxanes[2] (Fig. 1C) and show potential in the biological context.[3]The pillarplexes can also be potentially applied as synthons in crystal engineering. Hereby, a variety of non-covalent interactions can occur, ranging from hydrogen bonding, pi-stacking to metallophilic contacts (Fig. 2A).[4] Via chemical modification of the rim of the pillarplexes a higher flexibility can be introduced while preserving the porosity of the cavitand.[5] In detail, we were able to observe a shape-adaptive behavior of the pillarplex in the solid state, mainly driven by hydrogen bonding. The modified rim of the pillarplexes induces less steric repulsion, resulting in a lower energy penalty upon compression as rationalized by DFT calculations.

References
[1] P. J. Altmann, A. Pöthig*, J. Am. Chem. Soc. 2016, 138, 13171-13174.
[2] P. J. Altmann, A. Pöthig*, Angew. Chem., Int. Ed. 2017 129, 15939–15942.
[3] A. Pöthig*, S. Ahmed, H. C. Winther-Larsen, S. Guan, P. J. Altmann, J. Kudermann, A. M. Santos Andresen, T. Gjøen, O. A. Høgmoen Åstrand*, Front. Chem. 2018, 6, 584.
[4] A. A. Heidecker*, M. Bohn, A. Pöthig*, Z. Kristallogr. – Cryst. Mater. 2022, 237(4-5), 167-177, doi.org/10.1515/zkri-2021-2076.
[5] S.Guan‡, T. Pickl‡, C. Jandl, L. Schuchmann, X.-Y. Zhou, P. J. Altmann, A. Pöthig*, Org. Chem. Front. 2021, 8, 4061-4070.

Back to Table of contents

MS30 Advanced porous materials : MOFs, COFs, SOFs....and what else?

MS30-2-8 Structure Determination of a Mechanochemically Synthesised Metal-Organic Framework Using 3D Electron Diffraction
#MS30-2-8

M. Faye [1], A. Sala [1], D. Marchetti [1], V.E. Agbemeh [1], M. Gemmi [1]
[1]Istituto Italiano di Tecnologia, Center for Materials Interfaces, Electron Crystallography - Pontedera (Italy)

Abstract
3D Electron Diffraction (3D ED) is an emerging technique for structural characterization of crystals of up to ten's of nanometers in size thanks to the strong interaction between electrons and matter, thus overcoming the main limitation of Single Crystal X-Ray Diffraction (SCXRD)[1].
Metal-Organic Frameworks (MOFs) on the other hand, are hybrid porous materials that have been receiving much attention in the recent years by reason of their versatility as well as tunability, leading to a wide variety of applications such as catalysis, separation, sensing, storage, amongst others. The crystal structure of the MOFs plays an important role on their properties and applications. However, it is often very difficult to grow crystals large enough for conventional SCXRD, making them great candidates for characterization by 3D ED[2].
In this work, we describe the structure solution of a MOF with particle size of approximately 250nm synthesized through an environmentally friendly technique: Liquid Assisted Grinding mechanosynthesis, using water as solvent and biocompatible precursors. Using protocatechuic acid as ligand we have been able to obtain a mixed-metal MOF containing both Mn and Cu in the structure. The structure solution using 3D ED data was obtained ab-initio and required a low dose experiment to avoid amorphization. The structure, which is monoclinic exhibits a relevant porosity. Interestingly, in the vacuum of the microscope, the channels seem to be completely solvent free.

References
1. Gemmi, M. et al. 3D Electron Diffraction: The Nanocrystallography Revolution. ACS Cent. Sci. 5, 1315–1329 (2019).
2. Huang, Z., Grape, E. S., Li, J., Inge, A. K. & Zou, X. 3D electron diffraction as an important technique for structure elucidation of metal-organic frameworks and covalent organic frameworks. Coord. Chem. Rev. 427, 213583 (2021).

Back to Table of contents

MS30 Advanced porous materials : MOFs, COFs, SOFs....and what else?

MS30-2-9 Nanoporosity control by molecule-loaded nanofiber filters for residual water treatment #MS30-2-9

B.A. Paez-Sierra [1], D.K. López-Gómez [2]
[1]Universidad Militar Nueva Granada, Campus Nueva Granada - Cajiá (Colombia), [2]Universidad Militar Nueva Granada, Campus Nueva Granada - Cajicá (Colombia)

Abstract
One of the technologies that have grown the most in the last two decades for wastewater treatment uses filtration membranes. This work presents molecule-loaded nanofiber mats produced by the electrospinning process. The nanofibers consist of polycaprolactone (PCL) acting as a thermoplastic, while the load molecule is a chalcone derivative with varying concentrations from 0.0% to 1.0%. Analysis of electron scanning microscopy (SEM) images reveals average fiber diameter from about 90 nm to about 400 nm and diameters in inverse relation to the chalcone concentration. In addition, from FT-IR analysis it was determined that quantum confinement is achieved for the loaded molecules and increases in proportion to the chalcone molecule. This finding is correlation with the diameter of the PCL:Chalcone nanofibers. Based on a two-dimensional Poisson distribution, the porous diameter of the filters was about 1400 nm for 0.0 % molecule-loaded nanofibers while for 10%, concentration went down to about 110 nm. Interestingly, the pore size is proportional to the nanofiber diameter for specific surface mass density per porosity of the filters. Finally, all filters were tested with acid mine drainages (AMD), and ionic charge retention is related to the concentration of the loaded molecule and nanofiber diameter.

Acknowledgements
This work was supported from funding provided by Vice-Rector for Research – Universidad Militar Nueva Granada, Campus Nueva Granada, grant number IMP-CIAS 3115.

References
[1] Diana, E.J., Kanchana, U.S., Mathew, T.V., Anilkumar, G., 2020. Recent developments in the metal catalysed cross-coupling reactions for the synthesis of the enone system of chalcones. Applied organometallic chemistry 34, n/a.
[2] Figueroa Ariza, L., Duarte Espinosa, M. and Páez Sierra, B., 2020. Low-cost microwave reactor for green synthesis of nanomaterials. Ingeniería Solidaria, 16(2).
[3] Páez-Vélez, C., Castro-Mayorga, J.L., Dussán, J., 2020. Effective Gold Biosorption by Electrospun and Electrosprayed Bio-composites with Immobilized Lysinibacillus sphaericus CBAM5. Nanomaterials (Basel, Switzerland) 10, 408.

Back to Table of contents

MS31 Unconventional interactions or symmetries for optimized and new properties, including chirality

MS31-1-1 Chirality determination in single crystals using XNCD and MChD
#MS31-1-1

M. Atzori [1], M. Cortijo [2], E. Hillard [3], G. Rikken [1], A. Rogalev [4], P. Rosa [3], P. Sainctavit [5], C. Train [1], F. Wilhelm [4]
[1]LNCMI - Grenoble (France), [2]Madrid Complutense - Madrid (Spain), [3]ICMCB - Pessac (France), [4]ESRF - Grenoble (France), [5]IMPMC - Pessac (France)

Abstract
Octahedral tris(bidentate) coordination complexes are chiral due to the propeller-like arrangement of the ligands around the metal core. The enantiomers of $[M(en)_3](NO_3)_2$ (M = Mn(II), Co(II), Ni(II), Zn(II); en = ethylenediamine) spontaneously resolve to form a mixture of conglomerate crystals in the space group $P6_322$ at room temperature [1].
Although conglomerate formation allows crystals of only one or the other enantiomer to be effortlessly obtained, resolution can only truly be accomplished after the identification and triage of the two crystal forms. For this, we have implemented an original method for determining the handedness of individual crystals in a mixture using a tightly-focused, circularly polarized X-ray beam [2]. The X-ray natural circular dichroism (XNCD) spectra measured at the metal K-edge on $[Co(en)_3](NO_3)_2$ and $[Ni(en)_3](NO_3)_2$ show maxima at the metal pre-edge. Mapping of a crystal assembly was performed by setting the X-ray energy to the peak maximum and determining the sign of the difference in absorption for the two polarizations, directly yielding the crystal handedness.. Interestingly, small amounts of ascorbic acid present in the crystallization flask appear to bias the conglomerate, in the lambda direction for $[Co(en)_3](NO_3)_2$ and in the delta direction for $[Ni(en)_3](NO_3)_2$.
Using the same model compounds, we have obtained experimental magneto-chiral dichroism (MChD) spectra on single crystals in the UV-visible energy range. MChD manifests as the differential absorption of chiral systems under a magnetic field using unpolarized light. The paramagnetic nickel and cobalt derivatives demonstrate an enormous optical anisotropy with MChD on the order of 10^{-1} with respect to the isotropic absorption spectra [3]. State-of-the-art quantum chemical calculations of the MChD spectra for the Ni(II) derivative were able to simulate the experimental results. This opens the way to new tools to assign chirality using unpolarized light and the development of MChD as a potent spectroscopic tool.

References
(1) Cortijo, M.; Valentín-Pérez, Á.; Rouzières, M.; Clérac, R.; Rosa, P.; Hillard, E. A. Crystals 2020, 10 (6), 472.
(2) Cortijo, M.; Valentín-Pérez, Á.; Rogalev, A.; Wilhelm, F.; Sainctavit, Ph.; Rosa, P.; Hillard, E. A. Chem. Eur. J. 2020, 26 (59), 13363–13366.
(3) M. Atzori, H.D. Ludowieg, Á. Valentín-Pérez, M. Cortijo, I. Breslavetz, K. Paillot, P. Rosa, C. Train, J. Autschbach, E.A. Hillard, G.L.J.A. Rikken, Sci. Adv., 7 (2021) eabg2859.

Figure

Back to Table of contents

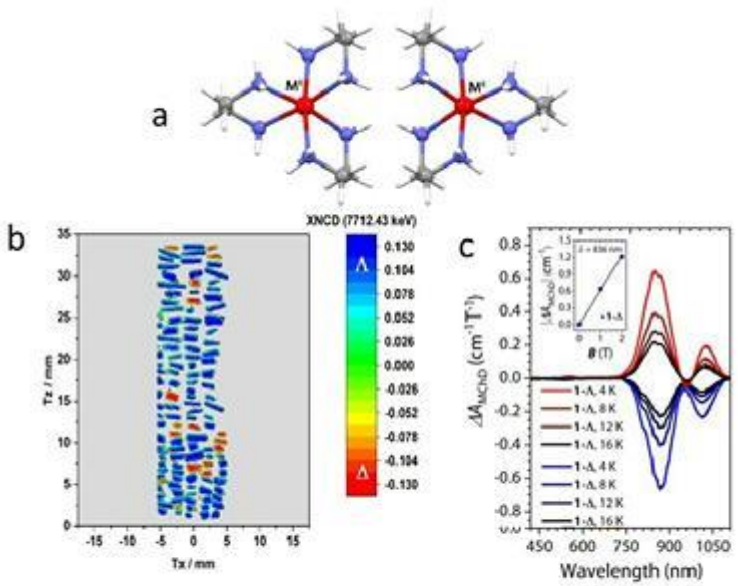

(a) View of the molecular structure of Λ-$[M^{II}(en)_3]^{2+}$ (left) and Δ-$[M^{II}(en)_3]^{2+}$ (right) (M^{II} = Ni, Co) complex cations; (b) XNCD mapping of an assembly of $[Co^{II}(en)_3](NO_3)_2$ crystals; (c) Orthoaxial ΔA_{MChD} spectra for Λ and Δ single crystals of $[Ni^{II}(en)_3](NO_3)_2$ at several temperatures. The inset shows the MChA strength as a function of the inverse temperature.

Back to Table of contents

MS31 Unconventional interactions or symmetries for optimized and new properties, including chirality

MS31-2-1 Pseudo and real symmetries for structural optimization of chromeno[4,3-b]quinoline derivatives #MS31-2-1

P. Bombicz [1], K. Aradi [2], G.T. Gál [3], S. De [3], T. Holczbauer [3], N.V. May [3], Z. Novák [2], L. Bereczki [3]
[1]Centre for Structural Science, Research Centre for Natural Sciences - Budapest (Hungary) - Budapest (Hungary), [2]Institute of Chemistry, Eötvös University - Budapest (Hungary), [3]Centre for Structural Science, Research Centre for Natural Sciences - Budapest (Hungary)

Abstract
A novel synthetic method was developed for the construction of chromenoquinoline derivatives from arylpropynyloxy-benzonitriles and diaryliodonium triflates via an oxidative arylation−cyclization path [1]. The method enables the synthesis of chromenoquinoline derivatives with high modularity due to the ease with which variable functional groups can be built into the reaction.
In the presented study the 7-phenyl-6H-chromeno[4,3-b]quinoline is substituted on the phenyl ring at *para* position by a methyl, a methoxy, an acetyl or a carboxymethyl group. The crystal structures have undergone on a gradual modification while the nature of the substituents has been changing (alkyl => ether => ketone => ester) averting the mutual orientation and the point group symmetry of the molecular pairs, as well as the Z value. The effect of the increasing size of the derivatives of the molecules and the increasing number of acceptor atoms on the crystal structures are discussed. None of the derivatives has any classical hydrogen bond donor atom, only C-H...O or C-H...N hydrogen bonds are possible in the structures. However, the 7-phenyl-6H-chromeno[4,3-b]quinolines have an extended hetero-aromatic ring system with potential π... π stacking affinity. The stacking of the molecules is found to be significantly influenced by the electronic effect of the substituents in para position on the phenyl ring. The moderately electron withdrawing groups influence the electron distribution of the aromatic rings in the way that the centrosymmetric stacking of the molecules becomes favourable [2].

References
[1] Klára Aradi, Petra Bombicz, Zoltán Novák: Modular Copper-Catalyzed Synthesis of Chromeno[4,3-b]quinolines with the Utilization of Diaryliodonium Salts *J. Org. Chem*. 2016, 81, 920−931.
[2] Laura Bereczki, Klára Aradi, Gyula Tamás Gál, Sourav De, Tamás Holczbauer, Nóra Veronika May, Zoltán Novák, Petra Bombicz: in preparation

Formulas of the chromenoquinoline derivatives

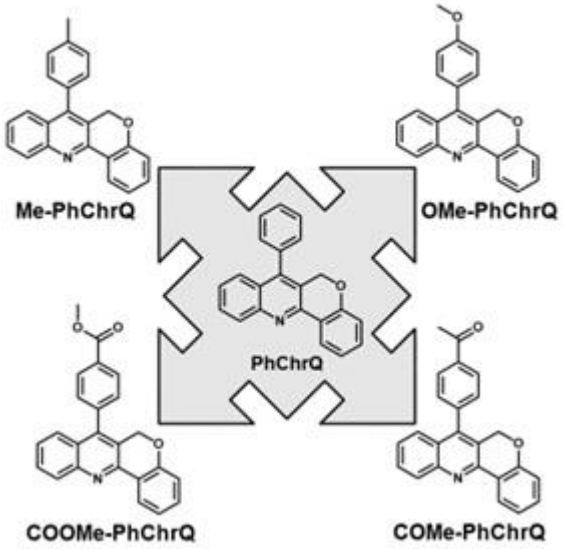

Back to Table of contents

MS31 Unconventional interactions or symmetries for optimized and new properties, including chirality

MS31-2-2 Chalcogen Bond in Bioactive Compounds
#MS31-2-2

G. Resnati [1], A. Pizzi [1], K. Konidaris [1], A. Daolio [1], M. Jane S. [2], P. Politzer [2]
[1]Politecnico di Milano - Milan (Italy), [2]University of New Orleans - New Orleans (United States)

Abstract
The Chalcogen Bond (ChB) is the attractive interaction wherein elements of group 16 of the periodic table act as electrophiles [1]. The interaction is receiving major attention thanks to the role and applications in the structure and functions of molecular materials and compounds of biological and pharmacological relevance [2]. For instance, thiazole and benzo[d]thiazole derivatives are used in many drugs and in vivo imaging agents [3] and in this communication we will present the crystal structures of some N-alkyl thiazolium and benzo[d]thiazolium compounds of biopharmacological interest. Among others, we will report the structure of thiamine monophosphate, a vitamin B1 coenzyme. In these crystal structures the sulphur atom is chalcogen bonded with different nucleophiles, as proven by the geometric features of the interactions. The ability of the thiazolium and benzothiazolium moieties to form ChBs is confirmed by analyses of the Cambridge Crystallographic Database (CSD) and computational studies.

References
[1] Scilabra P., Terraneo G., Resnati G., Acc. Chem. Res., 2019, 52, 5, 1313-1324
[2] Daolio, A.; Scilabra, P.; Di Pietro, M. E.; Resnati, C.; Rissanen, K.; Resnati, G. New J. Chem. 2020, 44, 20697–20703.
[3] Chhabria, M. T.; Shivani, P.; Modi, P.; Brahmkshatriya, P. S. Curr. Top. Med. Chem. 2016, 16, 2841–2862.

Back to Table of contents

MS32 Advanced techniques to disclose Structure-Property Relationships

MS32-1-1 Identification of a coherent twin relationship in functional perovskites from high-resolution reciprocal-space maps
#MS32-1-1

S. Semën [1], D. David [1], G. Guanjie [2], D. Carsten [3], N. Nan [2]
[1]Department of Materials Science and Engineering, Tel Aviv University - Tel Aviv (Israel), [2]Electronic Materials Research Laboratory, Key Laboratory of the Ministry of Education and International Center for Dielectric Research, School of Electronic and Information Engineering, Xi'an Jiaotong University - Xi'An (China), [3]European Synchrotron Radiation Facility - Grenoble (France)

Abstract
Twinning is a common crystallographic phenomenon, related to the formation and coexistence of several orientation variants of the same crystal structure. It may occur during symmetry-lowering phase transitions or crystal growth itself. Once formed, twin domains play an important role in defining physical properties of functional materials: for example, they underpin the giant piezoelectric effect in ferroelectrics, superelasticity in ferroelastics and the shape-memory effect in martensitic alloys. Unfortunately, there is still a lack of experimental methods for the characterization of twin domain patterns. Although single crystal X-ray diffraction could fill this methodological gap, its implementation for the case of diffraction from multi-domain crystal is far from trivial especially for the case of the so-called pseudomerohedral twinning. Specifically, it is hard to assign various components of split Bragg peaks to the particular set of domains.
Here we propose a theoretical framework and an algorithm for the recognition of ferroelastic domains and the identification of the coherent twin relationship using high-resolution reciprocal space mapping of X-ray diffraction intensity around split Bragg peaks. We adapt the geometrical theory of twinned ferroelastic crystals [1] for the analysis of the X-ray diffraction patterns. We derive the necessary equations and outline an algorithm for calculation of the separation between the Bragg peaks, diffracted from possible coherent twin domains, connected to one another via mismatch-free interface. We demonstrate that such separation is always perpendicular to the planar interface between mechanically matched domains. As examples, we present the analysis of the separation between the peaks diffracted from tetragonal and rhombohedral domains in the high-resolution reciprocal space maps of BaTiO3 and PbZr1-xTixO3 crystals of functional ferroelectric perovskites. We collected three-dimensional reciprocal space maps at the custom-built home-laboratory four-circle X-ray diffractometer [2], equipped with large (PILATUS 1M) pixel area detector. The example of such reciprocal space map of diffraction intensity distribution around 102 Bragg peak of BaTiO3 is presented in the Figure 1. The analysis (see [3] for full details) results in the assignment of the present peaks to specific sets of ferroelastic domains as well as establishing the orientation of domain walls between them.
The method can be used to analyse the response of multi-domain patterns to external perturbations such as electric field, change of a temperature or pressure.

References
[1]. Fousek, J. & Janovec, V. (1969). J. Appl. Phys. 40, 135–142.
[2]. Gorfman, S., Spirito, D., Cohen, N., Siffalovic, P., Nadazdy, P. & Li, Y. (2021). J. Appl. Cryst. 54, 914–923.
[3]. Gorfman, S., Spirito, D., Zhang, G., Detlefs, C. Zhang N. (2022). Acta Cryst A78 (3), 158-171.

Figure 1

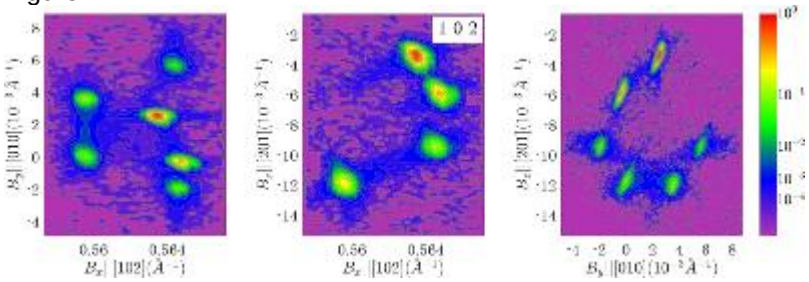

Back to Table of contents

MS32 Advanced techniques to disclose Structure-Property Relationships

MS32-2-1 Octahedral Distortion through the CSD database to reveal structure-properties relationship in spin crossover complexes.
#MS32-2-1

M. Marchivie [1], P. Guionneau [1], G. Chastanet [1], R. Ketkaew [2], Y. Tantirungrotechai [2], P. Harding [3], D.J. Harding [3]
[1]CNRS, Univ. Bordeaux, Bordeaux INP, ICMCB, UMR 5026 - Pessac (France), [2]Computational Chemistry Research Unit, Fac. of Science and Tech., Thammasat Univ. - Pathum Thani (Thailand), [3]Functional Materials and Nanotechnology Center of Excellence, Walailak Univ. - Nakhon Si Thammarat (Thailand)

Abstract
Spin crossover (SCO) compounds are molecules, mainly based on transition metal complexes in an octahedral geometry, that can adopt two electronic states depending of their surrounding environment. SCO compounds can thus switch **from a Low Spin (LS) state to a High Spin (HS) state upon an external stimulus** like temperature pressure, light, or many others, what lead to a great interest from the scientific community due to their potential applications as captors, actuators, memories, smart pigments and many others. One of the key point, nevertheless, is to synthesize the right complex with optimal and controlled properties. From this point of view, **the very high versatility of molecular materials is an evident advantage to obtain several complexes with very different switching properties** such as large range of transition temperatures, smooth to very abrupt transitions or the apparition of large hysteresis loops… This high versatility can however turn into a drawback to properly identify the key structural parameters that will guide the chemist to design the right material with the expected properties as the implied structural parameters are numerous and subtle.
For decades, researchers of the SCO community have explored the structure-properties relationships of several families of SCO compounds, and some trends are now well established[1]. The role of octahedral distortion, for example, has been identified as a key parameter to obtain long lifetimes in photo-induced systems and is also linked to the thermal transition temperature[2]. Several distortion parameters have then been proposed: from the simplest analysis of metal to ligand bond lengths (d_{M-L}) to more sophisticated ones such as Θ, that measures the trigonal distortion of an octahedral geometry and require more complicated calculations. In order to make the evaluation of the octahedral geometry distortion accessible to a large scale of exploration, it appeared mandatory to unify its calculation as it was not straightforward. Also, we recently proposed a new program called **OctaDist** (**Octa**hedral **Dist**ortion calculator) leading to an universally agreed method that allows to make comparisons across the increasingly diverse structural SCO databases[3]. This program has been then used to explore the huge CSD database to extract a clear chemical meaning related to the distortion parameters using, in our example, **more than 6000 iron complexes** (figure 1).
This new approach clearly open the way to use such a program, conjointly with Artificial Intelligence (AI), to go beyond the limited number of complexes generally used within the different families to find structure-properties relationships. It should lead to new wider correlations combining, for example, several parameters or even new totally not envisaged ones, by deep learning methods.

References
[1] M. A. Halcrow Spin-Crossover Materials (John Wiley & Sons Ltd, 2013). in 147–169 ; E. Collet & P. Guionneau Comptes Rendus Chim. 2018, 21, 1133–1151
[2] G. Chastanet, C. Desplanches, C. Baldé, P. Rosa, M. Marchivie & P. Guionneau Chem. Squared 2018, 2, 2
[3] R. Ketkaew, Y. Tantirungrotechai, P. Harding, G. Chastanet, P. Guionneau, M. Marchivie & D. J. Harding Dalt. Trans. 2021, 50, 1086–1096

Mean Fe-N distance vs Θ for 6546 Fe complexes

Back to Table of contents

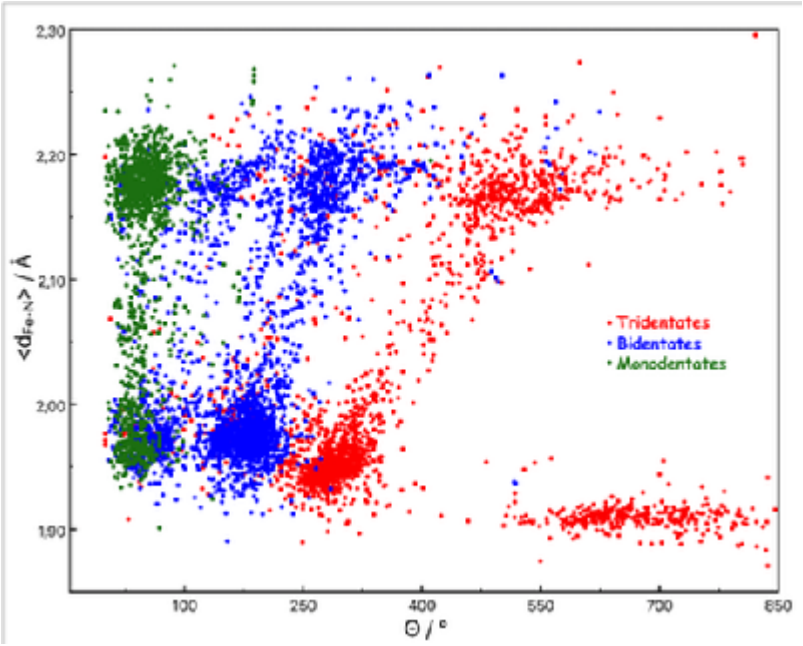

Back to Table of contents

MS32 Advanced techniques to disclose Structure-Property Relationships

MS32-2-2 Mapping the Space of Two-Dimensional Lattices
#MS32-2-2

M. Bright [1], V. Kurlin [1], A. Cooper [1]
[1]University of Liverpool - Liverpool (United Kingdom)

Abstract
Crystallographic unit cells are traditionally classified discretely (for example, into Bravais classes). We are interested in finding a continuous classification. By this we mean the derivation of some quantity from the geometric parameters of a unit cell, which does not vary under transformations giving rise to the same lattice (for example, rotation and translation), and a real number associated with pairs of these quantities which defines a 'distance' between them (for example, it is zero between two identical lattices), that takes small values between two unit cells that differ only by a small geometric perturbation.

One can use such a metric to associate the precise position of a structure in the resulting space of, and continuously measured physical properties such as conductivity or opacity.

A barrier to this approach is that the same lattice can be described by an infinite number of different basis vectors. We can impose a list of inequalities on the geometric parameters of a lattice which gives a provably unique selection – Niggli's reduced cell [1] being the most well known. However, it is proved in [2] that any such selection will be discontinuous - a small perturbation of the lattice can lead to a large change in the geometry of the unit cell.

Building on work in [3], we prove in [4] that a unique invariant can be derived for 2 dimensional lattices, and in [5] we use this invariant to develop a measure of 'chirality distance' – the closeness of a lattice to its nearest neighbour with higher symmetry – and from this a distance between any two lattices that satisfies the desired conditions, giving the first representation to our knowledge of all 2D lattices as points in a metric space. In Figure 1 we represent this space as a square with opposite edges identified where each point represents (up to scaling) a unique lattice, and show the density of millions of lattices derived from the Cambridge Crystallographic Structural Database [6].

A practical application is to look at the growing number of materials which could potentially be crystallised as monolayers. To date the most extensive database of such materials be found in [7], a subset of which have had their theoretical monolayer lattice structures computed. Figure 2 shows a plot of this data in the same square as Figure 1, which suggests that monolayer structures cluster strongly in areas of high symmetry.

References
[1] Niggli, P. *Krystallographische und strukturtheoretische Grundbegriffe*, v1. Akademische verlagsgesellschaft mbh (1928).
[2] Widdowson, D., Mosca, M.M., Pulido, A., Kurlin, V., Cooper, A.I. *Average Minimum Distances of periodic point sets - fundamental invariants for mapping all periodic crystals.* MATCH Communications in Mathematical and in Computer Chemistry,.87(3), .529-559, (2022). Available at http://kurlin.org/projects/periodic-geometry-topology/AMD.pdf
[3] Conway, J. H. & Sloane, N. J. *Low Dimensional Lattices (VI)* Proceedings of the Royal Society A, 436(1896), 55–68 (1992).
[4] Kurlin, V. Mathematics of 2-dimensional lattices. arxiv:2201.05150 (2022). The latest version is at http://kurlin.org/projects/periodic-geometry-topology/lattices2Dmaths.pdf
[5] Bright, M., Cooper, A.I., Kurlin, V. Geographic-style maps for 2-dimensional lattices. arxiv:2109.10885 (2022). The latest version is at http://kurlin.org/projects/periodic-geometry-topology/lattices2Dmap.pdf
[6] C. R. Groom, I. J. Bruno, M. P. Lightfoot, S. C. Ward. *The Cambridge Structural Database.* Acta Cryst. B 72, 171-179. (2016) DOI: 10.1107/S2052520616003954
[7] Mounet, N., Gibertini, M., Schwaller, P., Campi, D., Merkys, A., Marrazzo, A., Sohier, T., Castelli, i.E., Cepellotti, A., Pizzi, G., Marzari, N. *Two-dimensional materials from high-throughput computational exfoliation of experimentally known compounds.* Materials Cloud Archive 2020.158 (2020)

Density Map of Lattices in the Metric Space

Back to Table of contents

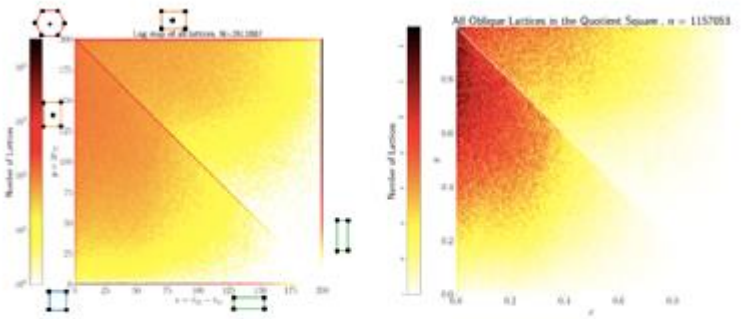

Figure 1: Density plot of all 2D unit cells derived from the Cambridge Crystallographic Structural Database in a metric space defined by geometric invariants. **Left**: All cells - position of cells with particular symmetries in the space are marked. **Right**: Cells with no reflection/rotation symmetries only.

Position of Lattices from [7] in the Metric Space

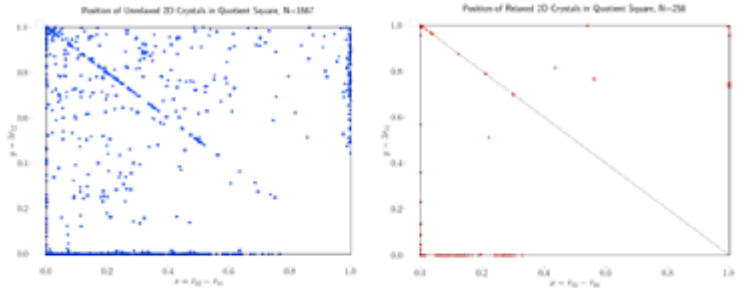

Figure 2: Plot of 2D unit cells from monolayer structures in [7], in the representation of the metric space shown in Figure 1. **Left** 'Unrelaxed' lattices, whose 2 dimensional unit cell is derived from the parent 3 dimensional lattice. **Right** 'Relaxed' lattices, where the structure of the 2 dimensional cell in isolation from its parent structure has been simulated.

Back to Table of contents

MS33 Supramolecular recognition

MS33-1-1 Self-assembly and conformation of three novel benzothiazolyl azo dyes
#MS33-1-1

L. Racané [1], M. Herceg [1], M. Relić [1], M. Cetina [1]
[1]Department of Applied Chemistry, Faculty of Textile Technology, University of Zagreb, Prilaz baruna Filipovića 28a - Zagreb (Croatia)

Abstract
The majority of synthetic aromatic dyes are azo dyes (65-70 %), in which one or more N=N groups are linked to aromatic or heteroaromatic ring substituted with some functional groups. Azo dyes are mostly used in textile industry (80%), because of their low cost, high stability and colour variety, but also for colouring different substrates in many other industrial fields. Besides, they are used in a number of high-tech applications such as for optical data storage and non-linear optics [1,2]. Compounds which contain heterocyclic ring, compared to those that have aromatic ring, are used in the design of new azo dyes due to the fact that they exhibit better colour strength and brightness. From variety of such dyes interest for those with benzothiazole ring is growing.We have previously reported synthesis and structural studies of several azo dyes that comprise benzothiazole ring [3,4]. Herein we present the synthesis and X-ray structures of three novel benzothiazolyl azo derivatives that have potential to be used as textile disperse dyes. These derivatives differ in the substituent at 2-position of the benzothiazole ring (Fig. 1). The focus in this study is on conformation of the molecules and especially on their supramolecular assembling as it is known that small difference on surface of the molecule may significantly influence its supramolecular architecture. The results reveal that hydrogen-bonding in all structures is governed by two strong intermolecular hydrogen bonds, one O-H···N and one O-H···O. While both interactions in **1** form dimers, in **2** and **3** they link neighbouring molecules into infinite chains. Further difference in the supramolecular aggregation arise from a number of weaker C-H···O hydrogen bonds. Thus, two bifurcated C-H···O hydrogen bonds are present in **2** and **3**, while only one is observed in **1**. Interestingly, hydrogen-bonded dimers generated by O-H···N and O-H···O hydrogen bonds in **1** give rise to a parallel arrangement of aromatic rings and formation of π···π interactions (Fig. 2), which are completely absent in **2** and **3**. All above mentioned interactions in these three structures are reinforced by C-H···π interactions, so forming three-dimensional networks.Acknowledgement. This work has been supported by University of Zagreb research grants PP1/15 and PP1/22 and Croatian Science Foundation under the project IP-2018-01-4379.

References
[1] Bamfield P. & Hutchings M. (2010). Chromic phenomena: Technological applications of colour chemistry, 3rd ed., Royal Society of Chemistry.[2] Samsami, S., Mohamadi, M., Sarrafzadeh, M.-H., Rene, E. R., Firoozbahr, M. (2020). Process Saf. Environ. Protect. 143, 138–163.[3] Pavlović, G., Racané, L., Čičak, H. & Tralić-Kulenović, V. (2009). Dyes Pigments 83, 354–362.[4] Racané, L., Mihalić, Z., Cerić, H., Popović J. & Tralić-Kulenović, V. (2013). Dyes Pigments 96, 672–678.

Fig. 1.

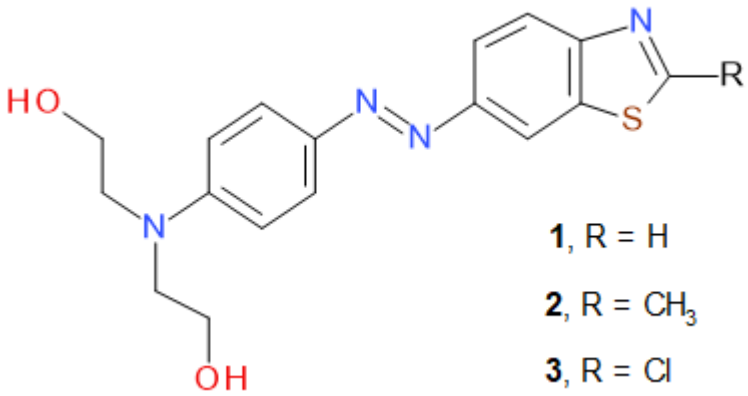

Fig. 2.

Back to Table of contents

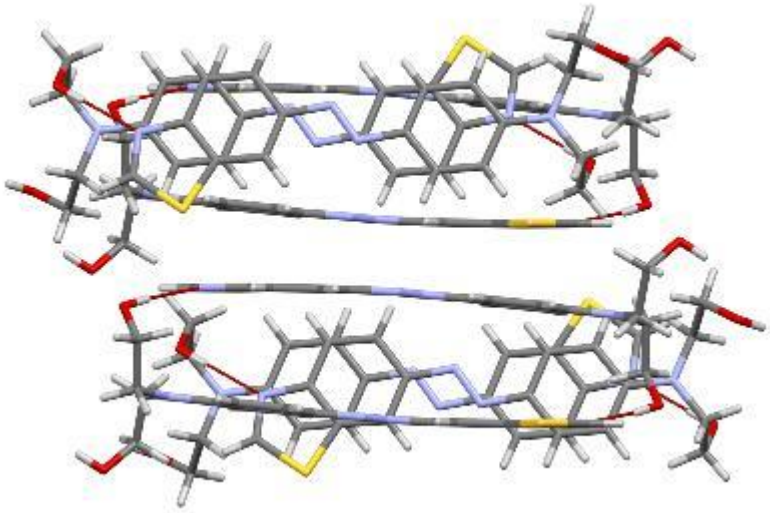

Back to Table of contents

MS33 Supramolecular recognition

MS33-1-2 Solid state stabilization of water clusters by polyamide macrocyclic frameworks #MS33-1-2

M. Ceborska [1], K. Dąbrowa [2], J. Jurczak [2]
[1]Faculty of Mathematics and Natural Sciences, Cardinal Stefan Wyszynski University - Warsaw (Poland), [2]Institute of Organic Chemistry, Polish Academy of Sciences - Warsaw (Poland)

Abstract
Unclosed Cryptands (UCs) are neutral macrocyclic organic compounds which contain several amide groups connected by alkyl linkers and flexible lariat arm resulting in their structural flexibility [1-2]. Both in solution and in the solid state, UCs are characterized by high water affinity and their conformation is very sensitive to traces of water. We designed and synthesized three UCs of type **1** differing only in the *p*-positioned substituent in the lariat arm (electron-withdrawing nitro group, electron donating methoxy group, and proton), and UC of type **2** characterized by the reversed positioning of amide group in the lariat arm. The crystal structures of so designed macrocycles revealed various water structures, such as water chain and the octameric water clusters built from cyclic tetramer with four pendulous H_2O molecules (Figure 1) [3-5].

References
1. Dąbrowa, K., Niedbała, P., Majdecki, M., Duszewski, P., Jurczak J. *Org. Lett*. 17, 4774 (2015) **2.** Dąbrowa, K., Ceborska, M., Jurczak, J. *Cryst. Growth Des*. 17, 701 (2017) **3.** Dąbrowa, K., Ceborska, M., Jurczak, J. *Cryst. Growth Des*. 14, 4906 (2014) **4.** Dąbrowa, K., Ceborska, M., Jurczk, J. *Supramol. Chem*. 30, 464 (2018) **5.** Dąbrowa, K., Ceborska, M., Jurczak, J. *Molecules*, 2021, 26(9), 2787.

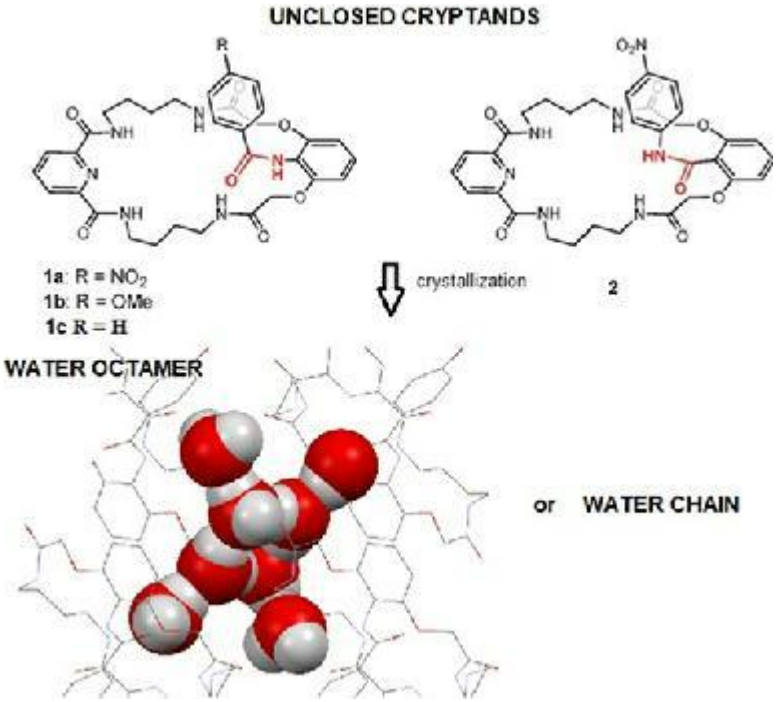

Back to Table of contents

MS33 Supramolecular recognition

MS33-1-3 The dicyanoaurate supramolecular chemistry: a pletora of opportunities
#MS33-1-3

E. Priola [1], A. Giordana [1], A. Luca [1], D. Eliano [1], O. Lorenza [1], M. Godrath [2], F. Antonio [3]
[1]University of Turin - Turin (Italy), [2]University of Maragheh, - Maragheh (Iran, Islamic Republic of), [3]Universitat de les Illes Balears - Palma de Mallorca (Spain)

Abstract
The supramolecular chemistry of dicyanoaurate anion have shown an explosion, with the discovery of materials with impressive properties like vapochromism,[1] strong luminescence[2] and non-classical response to pression and temperature.[3] Most of the previous work has been focalized on the construction and engineering of materials through the coordination ability of the terminal cyanides and on the incredibly strong Au(I)…Au(I) aurophilic interactions that this complex can show. In more recent years, it has been more and more clear that a series of other energetic components of the crystal packing that are not necessarily weaker than the previous ones have not yet been considered. One of these contributions is the coinage bonding, very different in nature from aurophilic interaction, but also more exotic metallophilic interactions have been rarely studied. In this contribution, we will speak about the results on some more exotic interaction, like Au(I) …Cu(II),[4] Au(I) …π[5] and Au(I) …Ag(I), that we analyzed in a series of bimetallic crystalline compounds through QTAIM theory, NCI plots and NBO computational tools, demonstrating their strength and defining their nature.

References
[1] Cairns A. B., Catafesta J., Levelut C., Rouquette J., van der Lee A., Peters L., Thompson A. L., Dmitriev V., Haines J., Goodwin A. L., Nat. Mater., 2013, 12, 212–216.
[2] Lefebvre J., Batchelor R. J. , Leznoff D. B., J. Am. Chem. Soc., 2004, 126, 16117–16125.
[3] Goodwin A. L., Kennedy B. J., Kepert C. J., J. Am. Chem. Soc., 2009, 131, 6334–6335.
[4] Priola E., Mahmoudi G., Andreo J., Frontera A., Chem. Commun., 2021, 57, 7268–7271.
[5] Priola E., Giordana A., Mazzeo P. P., Mahmoudi G., Gomila R. M., Zubkov F. I., Pokazeev K. M., Valchuk K. S., Bacchi A., Zangrando E., Frontera A., Dalton Trans., 2021, 50, 16954-16960

Au...pi interaction

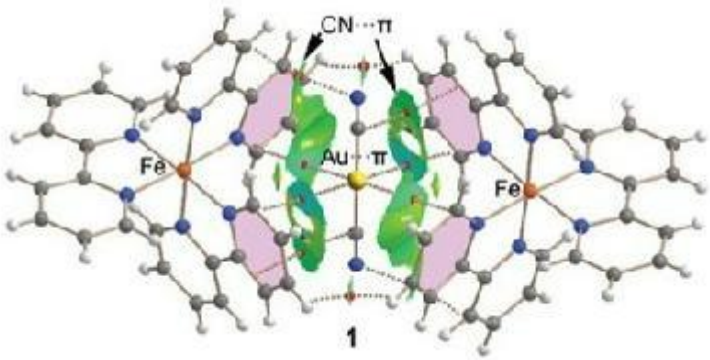

1

Au...Cu coinage bonding

Back to Table of contents

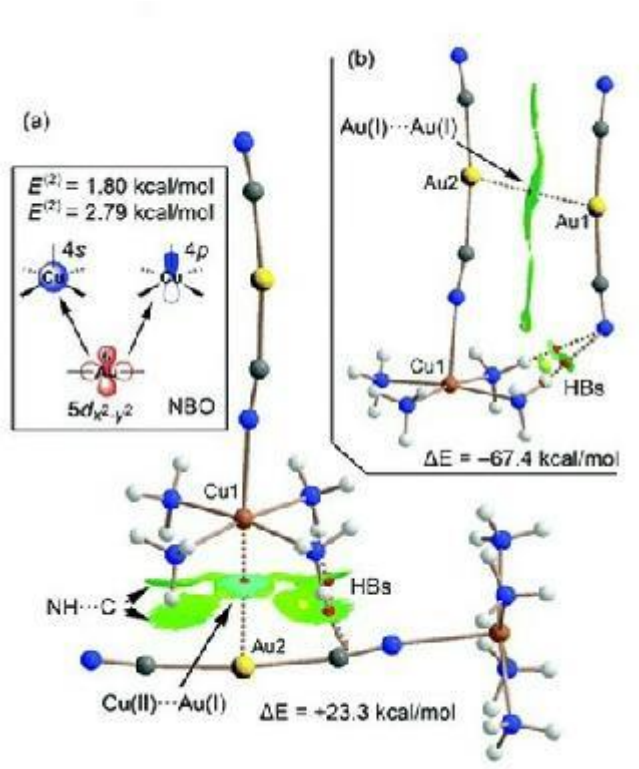

Back to Table of contents

MS33 Supramolecular recognition

MS33-2-1 quasi-pentagonal shape of carboxylated pillar[6]arene in its host-guest crystalline complexes #MS33-2-1

H. Butkiewicz [1], S. Kosiorek [1], V. Sashuk [1], O. Danylyuk [1]
[1]Institute of Physical Chemistry Polish Academy of Sciences - Warsaw (Poland)

Abstract
Carboxylated Pillar[6]arene (CPA6), first reported by Guocan Yu in 2012 [1], is highly symmetrical pillar-shaped macrocyclic compound, composed of six hydroquinone units linked by methylene bridges at the para-positions, modified by twelve carboxylic acid groups. Its hydrophobic, electron-rich cavity combined with its water solubility makes it great candidate as host molecule for various electron-deficient guest or other cationic molecules. Moreover, carboxyl groups, that can take part in proton transfer, are located at the terminal positions of flexible aliphatic chains, so they can adjust to the size and shape of guests.
All we know about the shape of CPA6 or its host-guest complexes is based on the theory, solution studies or relying on the crystal structures of already known members of pillar[6]arene derivatives. But can we believe the assumptions?
Herein, we want to present, for the very first time, our results on the X-ray structures of CPA6 in the form of its host-guest complexes with N,N′-dimethyl-4,4′-bipyridinium cation (paraquat) and pentamidine. Our studies show that roughly hexagonal molecule can change shape and simulate the symmetry of a pentagon, adapting to the shape of the guest molecule. These results shed a new light on the self-assembly and properties of the host-guest complexes of CPA6 in the solid state.

References
[1] Yu G., Xue M., Zhang Z., Li J., Han C., Huang F., *J. Am. Chem. Soc*. 2012, **134**, 19489–19497

Back to Table of contents

MS33 Supramolecular recognition

MS33-2-2 Host-guest crystals with a flexible structure
#MS33-2-2

K. Kravets [1], A.W. Coleman [2], K. Suwinska [3], O. Danylyuk [1]
[1]Institute of Physical Chemistry Polish Academy of Sciences, Kasprzaka 44/52, 01-224 Warsaw, Poland - Warsaw (Poland), [2]LMI, CNRS UMR 5615, Université Lyon 1, 43 bvd 11 Novembre, 69622 Villeurbanne, France - Villeurbanne (France), [3]Faculty of Mathematics and Natural Sciences, Cardinal Stefan Wyszynski University, Wóycickiego 1/3, 01-938 Warsaw, Poland - Warsaw (Poland)

Abstract

Soft crystals have structural order, but they are able to change their structure in response to some gentle stimuli. [1] The structural transformations can be induced by mechanical stimuli, temperature, vapor exposure, light, etc. The structural response can be accompanied with the change of color, shape, size, or optical properties. The category of soft crystals embraces organic, inorganic, and inorganic-organic hybrid crystals. Depending on their structure and properties, these crystals have potential applications in sensors, semiconductors, photosynthetic systems, etc.

Herein, we report a soft host-guest crystal complex obtained from macrocyclic host p-sulfonatocalix[8]arene and iproniazid. p-Sulfonatocalix[8]arene is a water-soluble anionic macrocycle with good flexibility due to the large size of the cavity. The host-guest cocrystallization from aqueous solution gave nice crystals suitable for single-crystal X-ray diffraction analysis. The host-guest supramolecular interaction is guided mainly by the ionic forces and charge-assisted hydrogen bonds between cationic iproniazid and anionic sulfonate groups of calix[8]arene. The crystal packing revealed large water channels between layers of calix[8]arenes and iproniazid molecules acting as pillars in the structure. In order to check the structural flexibility of this complex, the loss of solvent water molecules from the crystal was examined. The air-dried crystals of the host-guest complex have the same space group but different arrangement of guest iproniazid molecules in the structure. The desolvation (dehydration) of the host-guest crystal complex proceeds as single crystal to single crystal transformation. The host-guest framework changes from the channel-type to closed structure, and also the change in hydrogen bonding between host and guest is observed.

References

[1] M. Kato, H. Ito, M. Hasegawa, K. Ishii. Soft Crystals Flexible response systems with high structural order. Chem - A Eur J., 25 (2019), pp. 5105-5112.

Back to Table of contents

MS33 Supramolecular recognition

MS33-2-3 The interplay of strong and weak intra and intermolecular hydrogen bonds in Sparfloxacin multicomponent forms: how it affects stability and solubility
#MS33-2-3

M.T.T. Duarte [1], M. Djaló [1], M. Arpacıoğlu [1], T. Neuparth [1], A. Cunha [1], V. André [1]
[1]Centro Quimica Estrutural, Dept. Engenharia Química - LISBOA (Portugal)

Abstract
Hydrogen bonds are known to be determinant in the supramolecular arrangement of multicomponent drug crystal forms. The main goal of the present study is to correlate these crystal engineering principles with the improvement of Sparfloxacin (SPAR) stability and solubility.1 SPAR is an antibiotic from the class of the fluoroquinolones, used in the treatment of bacterial infections.

Stable homo and hetero synthons between SPAR carboxylic acid moiety and carboxylic acid/amides/amines/ moiety's of some generally recognized as safe(GRAS) co-formers led to the formation of cocrystals and salts.
Attempts were performed in order to rationalize the formation of strong and directing intermolecular interactions with shelf and room humidity stability as well as solubility. SPAR molecules present a strong intramolecular pattern, N-H…O(C=O)…H-O(COOH), maintained in the majority of the supramolecular arrangements, promoting or preventing further SPAR-SPAR intermolecular contacts. 2,3
Results will be present and discussed here.
Acknowledgement: FCT - Project UID/QUI/00100/2019 and PTDC/QUI-OUT/30988/2017

References
[1] Desiraju, G. R., JACS, 2013, 135, (27), 9952-9967.
[2] Shemchuk, O.; Andre, V.; Duarte, M. T.; Taddei, P.; Rubini, K.; Braga, D.; Grepioni, F., Crystal Growth & Design 2017,176, 3379-3386
[3] Djaló, M.; Cunha, A., Luís, João; Quaresma, S.; Fernandes, A.; André, V.; Duarte, M. T., Crystal Growth & Design, 2021, 21, 2, 995–1005

Figure1. The illustration of SPAR:AA crystal struc

Back to Table of contents

MS33 Supramolecular recognition

MS33-2-4 Shape and Volume – Molecular Recognition Rules of Big Calixarene Rings
#MS33-2-4

M. Malinska [1]
[1]**Faculty of Chemistry, University of Warsaw - Warsaw (Poland)**

Abstract
Calixarenes are vase-shaped host molecules that can form complexes with one or more guest molecules. To establish molecular recognition rules, the hosts p-tert-butylcalix[6]arene (TBC6) and p-tert-butylcalix[8]arene (TBC8) were crystallized with different guest molecules (cyclohexane, anisole, heptane, toluene, benzene, methyl acetate, ethyl acetate, dichloromethane, chloroform, tetrahydrofuran, acetonitrile, dimethyl sulfoxide, dimethylformamide, and pyridine) and the obtained structures were characterized by X-ray diffraction (1,2). With most solvents, 1:1 and/or 1:3 TBC6–guest complexes were formed, although other stoichiometries were also observed with small guest molecules, and crystallization from ethyl acetate produced the unsolvated form. A common structural feature of most TBC(4/6/8)-guest structures is off-set bilayer packing, which is built by the strongest dimers (for TBC6 dimers energies are lower than −110 kJ mol^{-1}). This structural feature was also present in pure TBC6 crystal structure. The incorporation of solvent molecules with volumes <100 Å^3 in TBC6 crystal structures leads to the separation of the off-set bilayers, whereas larger solvent molecules prevent the formation of this layer. Even though the formation of a structural motif with the tert-butyl group in the TBC6 cavity is energetically favoured, its slow rate of formation possibly limits the formation of pure TBC6 crystals. Hence, the crystal structure of a high macrocycle-to-solvent ratio system can transform into a more thermodynamically stable crystal structure with a lower ratio through solvent evaporation or recrystallization(3). The calculated fill percentage of the TBC6 cavity was ~55% for apolar guests and significantly lower for polar solvents, indicating that polar molecules can bind to apolar cavities with significantly lower packing coefficients. All guest molecules that occupy the TBC6 cavity interact with the host with an energy close to −50 kJ mol^{-1}; therefore, this property does not determine molecular recognition. The ratio between the apolar surface area and the volume was used to predict the formation of inclusion versus exclusion complexes, with inclusion complexes observed at ratios <40. These findings allow the binding of potential guest molecules to be predicted and a suitable crystal packing for the designed properties to be obtained.

References
(1) Malinska, M. Insights into Molecular Recognition from the Crystal Structures of *p-tert*-Butylcalix[6]arene Complexed with Different Solvents. IUCrJ 2022, 9 (1), 55–64. https://doi.org/10.1107/S2052252521010678.(2) Kieliszek, A.; Malinska, M. Conformations of *p-tert*-Butylcalix[8]arene in Solvated Crystal Structures. Cryst. Growth Des. 2021, 21 (12), 6862–6871. https://doi.org/10.1021/acs.cgd.1c00773.(3) Malinska, M. Temperature- and Solvent-Induced Crystal-Form Transformations of the Pyridine@*p-tert*-Butylcalix[6]arene Host–Guest System. Cryst. Growth Des. 2021, 21 (2), 1103–1112. https://doi.org/10.1021/acs.cgd.0c01422.

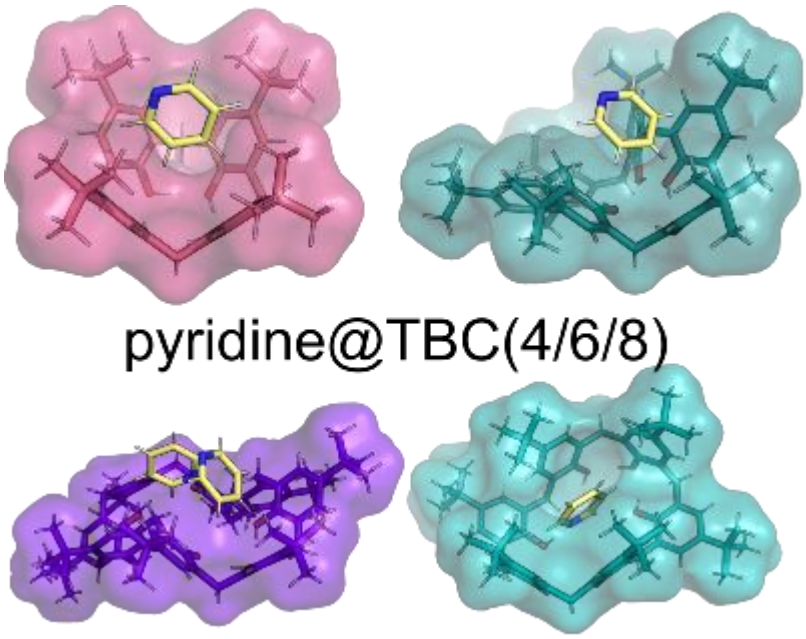

Back to Table of contents

MS34 Crystallization Techniques and chemical reactions driven by solid state interactions

MS34-1-1 Preparation and characterization of Apremilast multicomponent solid forms
#MS34-1-1

Y. Naumkina [1], J. Čejka [1], E. Korotkova [1]
[1]University of Chemistry and Technology, Prague - Prague (Czech Republic)

Abstract
Apremilast is indicated for the treatment of psoriatic arthritis, atopic dermatitis and rheumatoid arthritis. The Apremilast is a Biopharmaceutical Classification System class IV drug, which has low permeability and low solubility. It is known that Apremist cocrystals and solvates with aromatic compounds increase the solubility. The components are held preferably by aromatic-aromatic interactions over hydrogen bond formations. The object of this research is to study the types of interactions in Apremilast multicomponent systems with amino acids and different acids. This includes preparation of the Apremilast multicomponent systems with a slow evaporation method, a physical-chemical properties evaluation and determination of structure by the Single Crystal X-ray Diffraction. This research was supported by the Czech Science Foundation grant No. 21-05926X.

Back to Table of contents

MS34 Crystallization Techniques and chemical reactions driven by solid state interactions

MS34-1-2 Nucleation & Growth of α-Ti(HPO4)2·H2O Single Crystal and its Unprecedented Structure Determination from X-ray Single–Crystal Data
#MS34-1-2

Z. Amghouz [1], R. Mendoza-Merono [2], S. García-Granda [2], A. Adawy [3]
[1]Department of Material Science and Metallurgical Engineering, University of Oviedo - Gijon (Spain), [2]Department of Physical and Analytical Chemistry, University of Oviedo - Oviedo (Spain), [3]Unit of Electron Microscopy and Nanotechnology, Institute for Scientific and Technological Resources, University of Oviedo - Oviedo (Spain)

Abstract
α-titanium phosphate phase α-$Ti(HPO_4)_2 \cdot H_2O$ (α-TiP) is a tetravalent metal phosphate that has recently gained a special interest in biomedical application owing to its exceptional biocompatibility and ability to be loaded with antimicrobial agents [1-4]. As reported earlier, α-TiP tends to crystallize into microcrystalline powder that allowed its structural determination using neutron powder diffraction [5]. Here, we report that nucleation and crystallization of single α-TiP crystals with suitable dimensions (>50μm) for single-crystal X-ray diffraction could be effectuated using a hydrothermal treatment of a metallic titanium (Ti-6Al-4V alloy) in high concentrations of phosphoric acid solutions. Accordingly, the single-crystal X-ray diffraction analysis could be performed and revealed its crystalline structure in a monoclinic space group, P21/c, with a= 8.6288(5) Å, b= 5.00546(17) Å, c= 19.1468(11) Å, and β=127.555(9)°. Although the space group is similar to that previously reported from the neutron powder diffraction [5], the obtained unit cell is considerably larger. A bulk of the obtained crystals were subjected to through analyses using polarization microscopy, scanning electron microscopy combined with energy dispersive X-ray spectroscopy (SEM-EDX), and thermal analysis (TG/SDTA-MS, DSC) and the results confirmed that the obtained crystals bear the general structural properties of the polycrystalline powder.

References
1. García, I.; Trobajo, C.; Amghouz, Z.; Adawy, A. (2021). Nanolayered metal phosphates as biocompatible reservoirs for antimicrobial silver nanoparticles. Materials, 14(6), 1481.
2. García, I.; Trobajo, C.; Amghouz, Z.; Alonso-Guervos, M.; Díaz, R.; Mendoza, R.; Mauvezín-Quevedo, M.; Adawy, A. (2021). Ag-and Sr-enriched nanofibrous titanium phosphate phases as potential antimicrobial cement and coating for a biomedical alloy. Materials Science and Engineering: C, 126, 112168.
3. Adawy, A.; Amghouz, Z.; Trobajo, C.; García, J. R. (2021). Antimicrobial nanolayered and nanofibrous metal phosphates for prospective biomedical applications. Foundations of Crystallography, 77, C1072.
4. Amghouz, Z.; García, J. R.; Adawy, A. (2022). A Review on the Synthesis and Current and Prospective Applications of Zirconium and Titanium Phosphates. Eng, 3(1), 161-174.
5. Salvadó, M. A.; Pertierra, P.; García-Granda, S.; García, J. R.; Rodríguez, J.; Fernandez-Diaz, M. T. (1996). Neutron powder diffraction study of α-Ti $(HPO_4)_2 \cdot H_2O$ and α-Hf $(HPO_4)_2 \cdot H_2O$; H-atom positions. Acta Crystallographica Section B: Structural Science, 52(5), 896-898.

Back to Table of contents

MS34 Crystallization Techniques and chemical reactions driven by solid state interactions

MS34-2-1 A Sustainable Approach to Disulfide Bond Exchange in Aryl Disulfides at High-Pressure #MS34-2-1

S. Sobczak [1], A. Katrusiak [1]
[1]Adam Mickiewicz University - Poznan (Poland)

Abstract
The aim of 'green' chemistry focuses on improving existing and exploring new techniques leading to the sustainable synthesis of chemical compounds. Traditionally, many materials are manufactured by solvothermal and solution-based methods - both requiring considerable amounts of energy and generating a lot of waste. To overcome these problems inspiration can be taken from nature. Mankind has always been dependent on mineral resources, many of which were formed in the unique high-pressure and high-temperature environment in Earth's crust. What is more, the energy required for compressing a sample to a considerable pressure of about 500 MPa (5 times higher than that at the bottom of the Mariana Trench) is a small fraction, about an order of magnitude less, compared to the energy needed for heating the sample by about 100 K. The high-pressure technologies have already paved their way in the food industry, thus it can be expected that mimicking such extreme conditions will soon become more common to synthesize novel materials. too.
The application of pressure in the aryl disulfide exchange reaction allows excluding catalysts or any reducing agents in the process.[1] Owing to the confined reaction space of the high-pressure reactor or diamond anvil-cell, the entropy of the system can be increased in a controlled manner to a stage when the substrates are dissolved and the molecules are excited into high energy conformers, involving rota-vibrational states.[2] The mechanical energy absorbed by homodimeric aryl disulfide molecules allows and facilities the homolytic cleavage of the S-S bonds. Then the unique process of high-entropy nucleation and subsequent kinetic crystallization offsets the thermodynamic equilibrium accelerating the exchange reaction.[3] This combination of effects provides an environmentally responsible method, in which pure heterodimeric disulfides can be attained with high yields, in a form of single crystals, with a smaller number of steps, in shorter times, requiring less energy and producing less or no waste at all.[4]

References
[1] Sobczak, S.; Drożdż, W.; Lampronti, G. I.; Belenguer, A. M. A.; Katrusiak, A.; Stefankiewicz, A. R. Dynamic Covalent Chemistry under High-Pressure: A New Route to Disulfide Metathesis. Chem. - A Eur. J. 2018, 24 (35), 8769–8773.
[2] Sobczak, S.; Katrusiak, A. Colossal Strain Release by Conformational Energy Up-Conversion in a Compressed Molecular Crystal. J. Phys. Chem. C 2017, 121 (5), 2539–2545.
[2] Sobczak, S.; Ratajczyk, P.; Katrusiak, A. High-pressure Nucleation of Low-Density Polymorphs. Chem. – A Eur. J. 2021, 27 (24), 7069–7073.
[4] Sobczak, S.; Ratajczyk, P.; Katrusiak, A. Squeezing Out the Catalysts: A Sustainable Approach to Disulfide Bond Exchange in Aryl Disulfides. ACS Sustain. Chem. Eng. 2021, 9 (20), 7171–7178.

The pressure-induced radical-mediated mechanism

Back to Table of contents

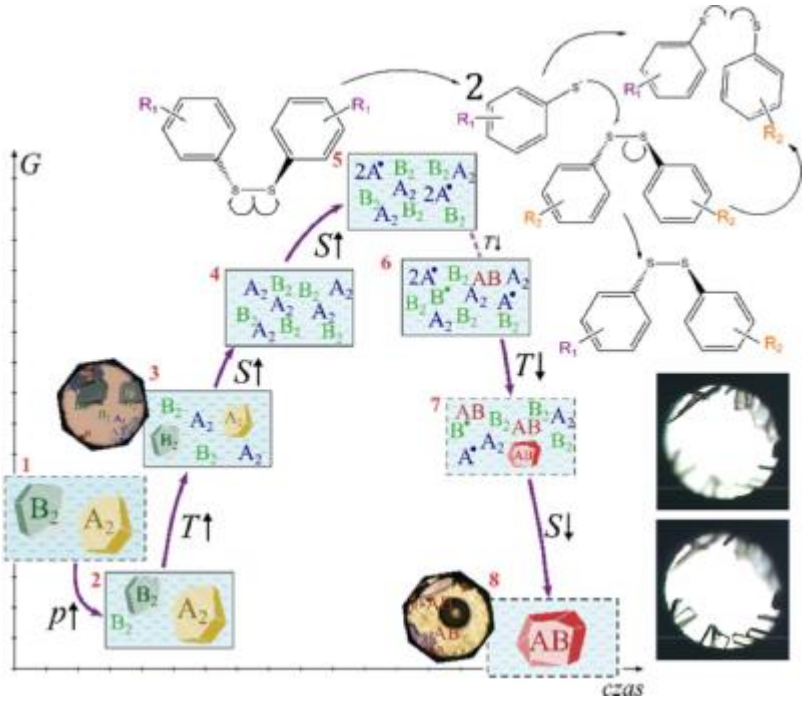

Back to Table of contents

MS34 Crystallization Techniques and chemical reactions driven by solid state interactions

MS34-2-2 Phase diagram p/T of resorcinol and the stabilization of high-pressure polymorphs by rational doping #MS34-2-2

A. Katrusiak [1], F. Safari [1]
[1]Adam Mickiewicz University - Poznan (Poland)

Abstract
Resorcinol, $C_6H_6O_2$, apart from being an important natural product and chemical agent of many applications [1,2], it was also the first compound, for which the structures of two polymorphs were determined in the 1930s [3,4]. These polymorphs α and β were puzzling, because they crystallized in the same space-group type $Pnc2_1$ and the high-temperature polymorph β was more dense than the low-temperature phase α. Moreover, the conformation of the molecules was different: anti-anti in polymorph α and anti-syn in polymorph β. Under high pressure resorcinol either transformed from phase α to β at about 0.5 GPa or no such a transformation was observed; at the same time new high-pressure phases γ and δ of resorcinol were postulated, but their structures were not determined [5]. Finally, a new polymorph ε of resorcinol, of space group $P2_12_12_1$ and Z=8, was obtained under ambient pressure by doping resorcinol with tartaric acid [6]. Most surprisingly, the density of polymorph ε was higher compared to those of polymorphs α and β. We grew single crystals of polymorph ε in a diamond-anvil cell (DAC), however these crystals could not be recovered to normal conditions, as they transformed back to form α below 0.2 GPa [7]. It showed that polymorph ε in its pure form is unstable in ambient pressure, where it was observed in the doped mixtures [6]. Above 0.7 GPa, we also obtained another polymorph ζ, monoclinic space group $P2_1/c$, Z=8 [7]. The outlined phase diagram of resorcinol explains its puzzling behavior. The behavior of resorcinol indicates the methods for stabilizing the high-pressure polymorphs of various compounds at ambient conditions. We also showed the preference for obtaining resorcinol solvates under high-pressure [8].

References
[1] Durairaj, R. B. Resorcinol: Chemistry, Technology, and Applications; Springer: Berlin, Germany, 2005.
[2] Dressler, H. Resorcinol: Its Uses and Derivatives; Plenum Press: New York, 1994.
[3] Robertson, J. M. The Structure of Resorcinol a Quantitative X-ray Investigation. Proc. R. Soc. London A 1936, 157, 79–99.
[4] Robertson, J. M.; Ubbelohde, A. R. A new form of resorcinol. II. Thermodynamic properties in relation to structure. Proc. R. Soc. London A 1938, 167, 136– 147.
[5] Kichanov, S. E.; Kozlenko, D. P.; Bilski, P.; Wąsicki, J.; Nawrocik, W.; Medek, A.; Hancock, B. C.; Lukin, E. V.; Lathe, C.; Dubrovinsky, L. S. N. The polymorphic phase transformations in resorcinol at high pressure. J. Mol. Struct. 2011, 1006, 337– 343.
[6] Zhu, Q.; Shtukenberg, A. G.; Carter, D. J.; Yang, T.; Yu, J.; Chen, M.; Raiteri, P.; Oganov, A. R.; Pokroy, B.; Polishchuk, I., Bygrave P.J., Day, G.M., Rohl, A.L., Tuckerman, M.E., Khar, B. Resorcinol Crystallization from the Melt: A New Ambient Phase and New Riddles. J. Am. Chem. Soc. 2016, 138, 4881– 4889.
[7] Safari, F., Katrusiak, A. High-Pressure Polymorphs Nucleated and Stabilized by Rational Doping under Ambient Conditions. J. Phys. Chem. C 2021, 125, 42, 23501–23509.
[8] Safari, F.; Olejniczak, A.; Katrusiak, A. Pressure-promoted Solvation of Resorcinol. Cryst. Growth Des. 2020, 20, 3112–3118.

Back to Table of contents

MS35 Artificial intelligence in photon and neutron crystallography, data mining, machine learning

MS35-1-1 Data-driven approach for the solution of the phase problem in crystallography: first insights #MS35-1-1

T. Rekis [1], A.S. Larsen [1], A.Ø. Madsen [1]
[1]University of Copenhagen - Copenhagen (Denmark)

Abstract
For a crystal structure to be solved from the diffraction data, it is necessary to obtain the complex structure factors, $\boldsymbol{F}_{\mathbf{H}}$, of the measured reflections. Their squared moduli, $|\boldsymbol{F}_{\mathbf{H}}|^2$, are proportional to the measured intensities, but the phase angles to reconstruct the complete complex numbers cannot be determined experimentally. Since the exact solution to this phase problem is not known, several methods to overcome this crucial step in crystal structure determination have been developed over time. For example, direct methods or charge flipping algorithm can be used for most organic, inorganic, and metal-organic structures. Nevertheless, these methods fail if, for example, the available data resolution is not sufficiently high. Furthermore, they cannot be used to solve protein structures intrinsically having large unit cells with hundreds of atoms in the asymmetric units.
In our study, we have attempted to solve the phase problem using a neural network. We focused on small organic molecule and metal-organic structures in the most common space group $P2_1/c$. Millions of fictive structures containing metal atoms and/or molecular fragments were generated to train the neural network. Validation set consisted of over a thousand structures retrieved from the Cambridge Structural Database for which the structure factor amplitudes, $|\boldsymbol{F}_{\mathbf{H}}|$, were generated at several resolution limits and fed into the trained network to output phases. The phases could be retrieved with a striking accuracy leading to correct structure solutions for over 99% of the validation set entries. Furthermore, the phase accuracy was also high if the resolution limit was chosen to be low, i.e. d_{min} = 1.9 Å. Several dozen of experimentally measured diffraction data sets were also used for validation. Our results hint that deep learning could be used to obtain electron density maps of structures for which only a limited resolution data can be obtained and which are problematic to solve using currently available methods.

Back to Table of contents

MS36 Software development in quantum mechanics-based methods of crystallography

MS36-2-1 HirshFrag: a new software tool for automatic molecular fragmentation
#MS36-2-1

L. Patrikeev [1], M. Chodkiewicz [1], K. Woźniak [1]
[1]University of Warsaw - Warszawa (Poland)

Abstract
Hirshfeld Atom Refinement (HAR) [1, 2] is becoming more and more important in the refinement of single crystal X-ray data. However, the use of quantum chemical calculations in the main bottleneck in HAR. It is well-known that the computational chemistry methods are still very limited in applicability to many systems of interests such as proteins and polymers. One of the most effective strategies to make such computations feasible is to use the fragmentation methods [3-6]. By the fragmentation method, we mean the partition of a large system into effective overlapping or non-overlapping subsystems (fragments), performing quantum chemical calculations for each fragment, and combining the fragments together to compute properties of the whole system.We have developed a new code called HirshFrag, which is intended for the automatic molecular fragmentation. The code employs several different methods of molecular fragmentation including the Systematic Molecular Fragmentation [4, 5] with some improvements, and an approach developed in our group [6]. The current version of HirshFrag is able to interact with the discamb2tsc program from the DiSCaMB software package [7].
In this presentation, we will discuss how different fragmentation approaches, available from HirshFrag, influence on HAR. In addition, we will discuss the speed up that can be achieved thanks to the fragmentation.
Acknowledgements: The authors thank the Polish National Science Centre for a financial support within the OPUS grant number 2018/31/B/ST4/02142.

References
[1] Jayatilaka, D. & Dittrich, B. (2008). Acta Cryst. A64, 383–393.[2] Capelli, S. C., Bürgi, H.-B., Dittrich, B., Grabowsky, S. & Jayatilaka, D. (2014). IUCrJ, 1, 361–379.[3] Gordon M. S., Fedorov D. G., Pruitt S. R. & Slipchenko L. V. (2012). , Chem. Rev., 112, 632–672.[4] Deev V. & Collins M. A. (2005). J. Chem. Phys. 122, 154102:1-12.[5] Collins M. A., Cvitkovic M. W. & Bettens R. P. A. (2014). Acc. Chem. Res., 47, 2776−2785.[6] Chodkiewicz M., Pawlędzio S. , Woińska M. & Woźniak K. (2022). IUCrJ., 9, 298-315.[7] Chodkiewicz M. L., Migacz S., Rudnicki W., Makal A., Kalinowski J. A., Moriarty N. W., Grosse-Kunstleve R. W., Afonine P. V., Adams P. D. & P. M. Dominiak. (2018). J. Appl. Cryst., 51, 193-199.

Back to Table of contents

MS37 Advances in Structure determination of new materials by multi-technique approach including imaging techniques (2)

MS37-2-1 Complementarity of hyperspectral XAS imaging and Raman spectroscopy for studying the impregnation and drying of supported CoMoP/ Al2O3 HDS catalysts
#MS37-2-1

B. Barata [1], C. Legens [2], E. Devers [2], O. Delpoux [2], L. Barthe [3], C. La Fontaine [3], O. Roudenko [3], V. Briois [3]
[1]SOLEIL, IFPEN - Saint-Aubin, Solaize (France), [2]IFPEN - Solaize (France), [3]SOLEIL - Saint-Aubin (France)

Abstract
With strengthened environmental regulations in oil fractions[1], there is a demand for more efficient hydrodesulfurization (HDS) catalysts. The preparation of these catalysts starts with the impregnation of a solution containing Mo and Co and usually P on an alumina support, followed by maturation and drying. Upon impregnation/maturation, there is a change in the equilibria between the Mo-species in the acidic impregnation solution due to the contact with basic alumina, leading to an heterogeneous distribution of different Mo species further transformed upon drying into mono, polymolybdates and P-HPAs (Heteropolyanions)[2]. As the catalytic activity is improved with P-HPAs[3], a rational design of the catalyst requires an *in situ* spatially and time-resolved chemical speciation to better understand the underlying adsorption processes for *in fine* mastering those unitary preparation steps.
Our methodology is based on the complementary use of *in situ* X-ray Absorption Spectroscopy (XAS) and *ex situ* Raman spectroscopy hyperspectral imaging. At the ROCK-SOLEIL beamline, Full Field (FF) time-resolved Mo K edge XAS imaging has been developed, consisting in the recording of space-energy resolved 3D data cubes using a pixelated CMOS camera (1.625µm pixel size)[4]. The rate of spectra collection is 1 cube/11s, each cube corresponding to 580 images/energies, recorded with a Field of View of 1.6mm x 1.2mm. These performances perfectly match the resolution required for the characterization of the preparation of a mm-sized industrial alumina extrudate. Optimized cells for *in situ* impregnation/maturation and *in situ* drying have been specifically developed. The first one allows the injection of ~0.1µL solution inside the cell cavity containing an extrudate (1.5mm x 1.6mm), followed by 3h-maturation. Inside the drying cell, the same extrudate is heated from RT to 120°C followed by 1h isothermal plateau.
Processing of the hyperspectral XAS data is performed in Jupyter notebooks followed by linear combination fitting (LCF) of the EXAFS spectra using a library of EXAFS spectra of bulk references[5], results in the quantification of Mo-based species dispersed on the support, given in relative fraction of spectrum.
The work presented herein enables for the first time the dynamic monitoring of the Mo-speciation changes during the key preparation steps of a catalyst with 8 wt.% MoO_3, Co/Mo 0.4, P/Mo 0.56 after a dry impregnation (Fig.1(a)-(b)). Whereas only the Strandberg's HPA is measured in the impregnation solution, the speciation obtained by FF XAS imaging shows that Anderson's $AlMo_6O_{24}$, Dawson monomer's, lacunary Keggin's HPAs, monomolybdate and the pristine Strandberg's HPA are dispersed on the extrudate after *in situ* impregnation/maturation (3h). The maps suggest an heterogeneous spatial distribution of the species, with an increasing HPAs concentration from the core to the edges of the extrudate (Fig.1(c)-(d)). After drying (2h, 120°C), the dispersion of species reflects the heterogeneity obtained at the end of the maturation.

References
(1) United Nations Environment Program (2020); **(2)** Catita, L. et al. A. Catal. A 547 (2017) 164-175; **(3)** Frizi, N. et al. Catal. Today 130 (2008) 272–282; **(4)** La Fontaine, C. et al. Synch. Rad. News 33(1) (2020) 20-25; **(5)** Lesage, C. PhD Thesis (2019)

Back to Table of contents

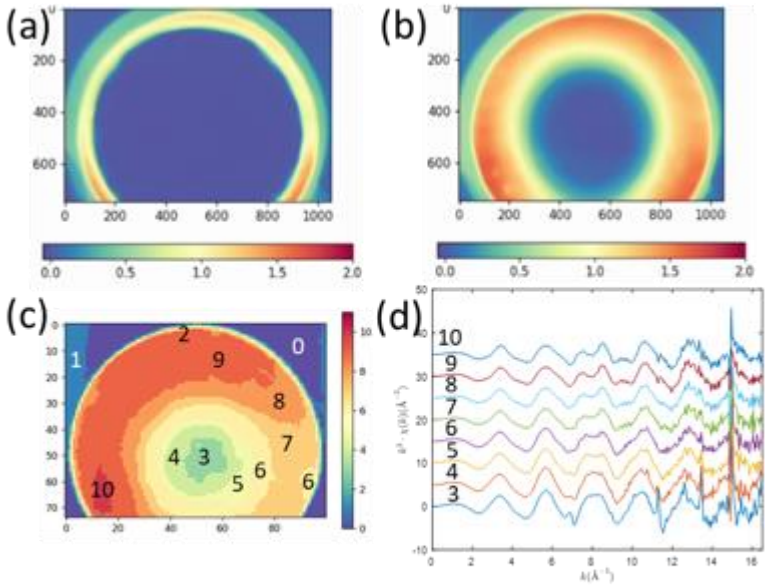

Fig. 1: Approximate absorption maps at (a) 2 min (b) 46 min after impregnation. (c) Edge jump slicing of a map at the end of 3h maturation and (d) EXAFS spectra from the slices in (c).

Back to Table of contents

MS37 Advances in Structure determination of new materials by multi-technique approach including imaging techniques (2)

MS37-2-2 Electron Diffraction and Nanocrystallography: Crystal Mapping of nanoscale Crystals with a dedicated Electron Diffractometer
#MS37-2-2

J. Merkelbach [1], C. Jandl [1], G. Steinfeld [1], E. Hovestreydt [1], D. Stam [1]
[1]ELDICO Scientific AG - Villigen (Switzerland)

Abstract
In recent years, Electron Diffraction (ED) established itself as an emerging technology in the fields of inorganic molecules, material sciences, geological sciences, energetic materials, bioorganic chemistry, and many others.[1-4] Diffraction experiments are done with (modified)-Electron Microscopes and performing these experiments require special expertise and efforts. Pioneers in the field of Electron Diffraction[5] all agree that a dedicated device for the realization of such experiments would be a significant step forward for the crystallographic community.
With the “ED-1”, such a device is now on the market and ELDICO Scientific AG will present latest results from its dedicated Electron Diffractometer, built and optimized for diffraction experiments. Electron Diffraction in conjunction with STEM imaging can be used for crystal mapping with a seamless transition to structure analysis of crystals with different morphology. The possibilities of this dual-technique workflow will be shown on different examplifying experiments performed on our device.

References
U. Kolb, Y. Krysiak, S. Plana-Ruis. *Acta Cryst.* (2019), **B75**, 463, and references therein.
D. Bowden, Y. Krysiak, L. Palatinus, D. Tsivoulas, S. Plana-Ruiz, E. Sarakinou, U. Kolb, D. Stewart, M, Preuss. *Nature Communications*, (2018), **9**, 1374.
R. Bücker, P. Hogan-Lamarre, P. Mehrabi, E. C. Schulz, L. A. Bultema, Y. Gevorkov, W. Brehm, O. Yefanov, D. Overthür, G. H. Kaisser, R. J. Dwayne Miller. *Nature Communications*, (2020), **11**, 996.
E. T. Broadhurst, H. Xu, M. T. B Clabbers, M. Lightowler, F. Nudelman, X. Zou, S. Parsons. *IUCrJ*, (2020), **7**, 5.
M. Gemmi et al. *ACS Cent Sci.* (2019) **5**, 1315.

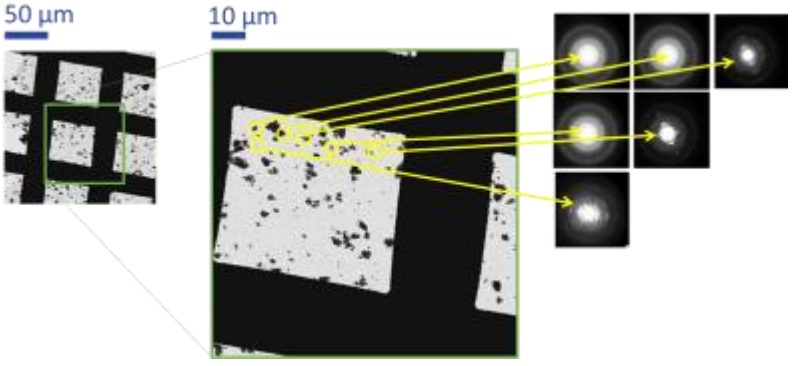

Back to Table of contents

MS38 Computations with/for Pair Distribution Functions

MS38-1-1 Error Bounds of Pair Distribution Function Analysis in Characterization of Thermal Disorder in Nanocrystals
#MS38-1-1

M. Batyrow [1], H. Ozturk [1]
[1]Ozyegin university - Istanbul (Turkey)

Abstract
Pair distribution function (PDF) analysis is a novel tool that is becoming popular in structural characterization of nanocrystals from their diffraction signature. However, there are no established accuracy bounds of the recovered structural parameters from PDF analysis [1]. In this work, we present a self-consistent computational workflow to address this question. By performing PDF analysis on simulated diffraction profiles of realistic gold nanocrystals at various temperatures, we compare temperature induced structural parameters such as lattice parameters and atomic displacements from PDF analysis to those from direct atomistic calculations [2,3] at finite temperatures.

References
[1] Abolfazl BALOOCHIYAN, Merdan BATYROW, Hande ÖZTÜRK, Accuracy limits of pair distribution function analysis in structural characterization of nanocrystalline powders by X-ray diffraction. Journal of the Turkish Chemical Society Section A: Chemistry: (in press).
[2] Xiong, Shangmin & Lee, Seung-Yub & Noyan, Ismail. (2019). Average and local strain fields in nanocrystals. Journal of Applied Crystallography. 52. 10.1107/S1600576719000372.
[3] A. Stukowski, J. Markmann, J. Weissmüller, and K. Albe, “Atomistic origin of microstrain broadening in diffraction data of nanocrystalline solids,” Acta Materialia, vol. 57, no. 5, 2009, doi: 10.1016/j.actamat.2008.12.011.

Back to Table of contents

MS38 Computations with/for Pair Distribution Functions

MS38-2-1 Investigation of Pair Distribution Function Method on Structural Analysis of Nanocrystalline Powders #MS38-2-1

A. Baloochiyan [1], H. Ozturk [1]
[1]Ozyegin University - Istanbul (Turkey)

Abstract
This self-consistent computational work presents the minimum errors of structural parameters (e.g. lattice parameters, crystalline size, atomic displacement parameters) expected from Pair Distribution Function (PDF) analysis of nanocrystalline gold powders. Recently, PDF analysis has gained momentum in naocrystalline powder characterization by X-rays, however, current literature does not contain expected error bounds of the resulting structural parameters. For an accurate interpretation of X-ray diffraction data, the error bounds must be analyzed. We aim to address this problem in three steps: 1. Simulation of ideal powderdiffraction experiments with the use of the Debye scattering equation, 2. PDF analysis of the diffraction data, and 3. Determination of the errors from PDF analysis by comparing them with real-space analysis of spherical gold nanocrystals with sizes of 30 nm and smaller. Our results demonstrate that even for the ideal nanocrystals in ideal diffraction conditions, the extracted structural parameters from PDF analysis diverge from their true values. These deviations are dependent on the average size of the nanocrystals and the wavelengths of the illuminating X-rays. In diffraction analyses of nanocrystalline powders, lower X-ray energies and smaller crystal sizes are prone to greater uncertainties in extracted structural parameters.

References
1. Prasad N, Karhikeyan B. Tunable bandgap and blue emission of ZnS nanoparticles induced by controlled S vacancies. Journal of Applied Physics 2019; 125: 085702. < 10.1063/1.5083656>.
2. Tran N, Zhao W, Carlson F, Davidson JH, Stein A. Metal Nanoparticle-Carbon Matrix Composites with Tunable Melting Temperature as Phase-Change Materials for Thermal Energy Storage. ACS Applied Nano Materials 2018; 1: 1894-1903. <10.1021/acsanm.8b00290>.
3. Ingham B. X-ray scattering characterisation of nanoparticles. Crystallography Reviews 2015; 21(4): 229-303. < 10.1080/0889311X.2015.1024114>.
4. Kang S-JL, Park J-H, Ko S-Y, Lee H-Y. Solid-State Conversion of Single Crystals: he Principle and the State-of-the-Art. Journal of the American Ceramic Society 2015; 98(2): 347-360. < 10.1111/jace.13420>.
5. Neder RB, Proffen T. Exact and fast calculation of the X-ray pair distribution function. Journal of Applied Crystallography 2020; 53: 710-721. <10.1107/S1600576720004616 >.
6. Rietveld HM. A profile refinement method for nuclear and magnetic structures. Journal of Applied Crystallography 1969; 2: 65-71. < 10.1107/S0021889869006558>.
7. Juhas P, Farrow C, Yang X, Knox K, Billinge S. Complex modelling: a strategy and software program for combining multiple information sources to solve ill posed structure and nanostructure inverse problems. Acta Crystallographica 2015; A71: 562-568. < 10.1107/S2053273315014473>.
8. Petkov V, Bedford N, Knecht MR, Weir MG, Crooks RM, Tang W, Henkelman G, Frenkel A. Periodicity and atomic ordering in nanosized particles of crystals. Nanoscale 2008; 112 (24):8907-8911. < 10.1021/jp801195c>.
9. Popa NC, Balzar D. Size-broadening anisotropy in whole powder pattern fitting. Application to zinc oxide and interpretation of the apparent crystallites in terms of physical models. Journal of Applied Crystallography 2008; 41: 617:627. < 10.1107/S0021889808012223>.
10. Bugaev AL, Guda AA, Lomachenko KA, Shapovalov VV, Soldatov AV, Lazzarini A et al. Core-Shell Structure of Palladium Hydride Nanoparticles Revealed by Combined X-ray Absorption Spectroscopy and X-day Diffraction. The Journal of Physical Chemistry C 2017; 121: 18202-18213. < 10.1021/acs.jpcc.7b04152>.
11. Xiong S, Öztürk H, Lee S-Y, Mooney P, Noyan IC, The nanodiffraction problem. Journal of Applied Crystallography 2018; 51:1102-1115. < 10.1107/S1600576718007719>.
12. Toby BH, Egami T. Accuracy of pair distribution function analysis applied to crystalline and non-crystalline materials. Acta Crystallographica 1992; A48: 336-346.
< 10.1107/S0108767391011327>.
13. Farrow CL, Billinge SJL. Relationship between the atomic pair distribution function and small-angle scattering: implications for modelling of nanoparticles. Acta Crystallographica 2009; 65(3): 232-239. < 10.1107/S0108767309009714 >.
14. Plimpton S. Fast Parallel Algorithms for Short-Range Molecular Dynamics. Journal of Computational Physics 1995; 117 (1): 1-19. < 10.1006/jcph.1995.1039>.

Back to Table of contents

15. Sheng HW, Kramer MJ, Cadien A, Fujita T, Chen MW. Highly optimized embedded-atom-method potentials for fourteen fcc metals. Physical Review B, 2011; 83 (13): 134118. < 10.1103/PhysRevB.83.134118>.
16. Öztürk H., Yan H., Hill JP, Noyan IC. Sampling statistics of diffraction from nanoparticle powder aggregates. Journal of Applied Crystallography 2014; 47: 1016-1025. < 10.1107/S1600576714008528>.
17. Debye P. Zerstreuung von Röntgenstrahlen. Annalen der Physik 1915; 46: 809-823. < 10.1002/andp.19153510606>.
18. Warren BE, X-ray Diffraction. New York, NY, USA: Courier Corporation, 2012. ISBN: 978-0486663173
19. Juhas P, Davis T, Farrow CL, Billinge SJL. PDFgetX3: A rapid and highly automatable program for processing powder diffraction data into total scattering pair distribution functions. Journal of Applied Crystallography 2013; 46: 560-566. < 10.1107/S0021889813005190>.
20. Trueblood KN, Bürgi HB, Burzlaff H, Dunitz JD, Gramaccioli CM, Schulz HH, Shmueli U, Abrahams SC. Atomic Displacement Parameter Nomenclature. Report of a Subcommittee on Atomic Displacement Parameter Nomenclature. Acta Crystallographica 1996; A52: 770-781. < 10.1107/S0108767396005697>.
21. Dippel A-C, Roelsgaard M, Boettger U, Schneller T, Gutowski O, Ruett U. Local atomic structure of thin and ultrathin films via rapid high-energy X-ray total scattering at grazing incidence. IUCrJ 2019; 6: 290-298. < 10.1107/S2052252519000514 >.
22. Gilbert B. Finite size effects on the real-space pair distribution function of nanoparticles. Journal of Applied Crystallography 2008; 41: 554-562. < 10.1107/S0021889808007905>.
23. Guinier A. X-Ray Diffraction: In Crystals, Imperfect Crystals, and Amorphous Bodies. Mineola, NY, USA: Dover Publications, 2013.
24. Huang WJ, Sun R, Tao J, Menard LD, Nuzzo RG, Zuo JM. Coordination-dependent surface atomic contraction in nanocrystals revealed by coherent diffraction. Nature Materials 2008; 7(4): 308-313. < 10.1038/nmat2132 >.
25. Xiong S, Lee S-Y, Noyan IC. Average and local strain fields in nanocrystals. Journal of Applied Crystallography 2019; 52: 262-273. < 10.1107/S1600576719000372 >.
26. Least-Square Atomic Strain, Li Group. <http://li.mit.edu/Archive/Graphics/A/annotate_atomic_strain/Doc/main.pdf>
27. Stukowski A, Markmann J, Wissmüller J, Albe K. Atomistic origin of microstrain broadening in diffraction data of nanocrystalline solids. Acta Materialia 2009; 57(5): 1648:1654. < 10.1016/j.actamat.2008.12.011>.

Back to Table of contents

MS38 Computations with/for Pair Distribution Functions

MS38-2-2 The Pointwise Distance Distribution is stronger than the Pair Distribution Function
#MS38-2-2

V. Kurlin [1], D. Widdowson [1]
[1]University of Liverpool - Liverpool (United Kingdom)

Abstract
A periodic crystal is usually given in a Crystallographic Information File as a pair of a (primitive, conventional, or reduced) unit cell and a motif of atoms with fractional coordinates with respect to a cell basis. This traditional representation of crystals doesn't allow us to quickly and continuously quantify the similarity [1] between nearly identical crystals because a reduced cell can discontinuously increase under almost any tiny displacement of atoms.
The Pair Distribution Function (PDF) was a convenient tool [2] to distinguish periodic crystals up to rigid motion or isometry maintaining all interatomic distances. The exact PDF can be defined as the infinite distribution of pairwise distances between all atomic centers with multiplicities for repeated distances but avoiding all repetitions due to lattice translations. For convenience, this exact PDF can be written as an infinite sequence of increasing distances.
Figure 1 (left) shows the classical example of non-isometric sets of 4 points in the plane that have the same PDF of 6 distances: root(2), root(2), 2, root(10), root(10), 4. Figure 1 (right) shows a similar example of 1-dimensional periodic sequences S(r) and Q(r), which both have the unit cell [0,8] with 4 points in their motifs and depend on a parameter 0<r<1. These are examples of homometric sets that have the same PDF and the Patterson function [3].
The recently discovered Pointwise Distance Distribution (PDD) extends PDF to a stronger isometry invariant that is provably continuous under any small perturbations of points [4].
The PDD(S;k) of a periodic point set S is a matrix of rows consisting of increasing distances from every motif point of S to its k neighbors within the infinite set S, see Figure 2 (left).
PDD matrices are cpntinuously compared by the Earth Mover's Distance in Figure 2 (right).
All periodic sets in general position, including the sets in Figure 1, are provably distinguished by PDD for a large enough k with an explicit upper bound [4]. The PDF can be reconstructed from PDD, not vice versa. These theoretical results have been confirmed by 200B+ pairwise comparisons of all 660K+ periodic crystals in the Cambridge Structural Database.
This huge experiment took only a couple of days on a modest desktop [4] and detected five pairs of unexpected duplicate structures that are truly isometric to the last decimal place, but one atom is replaced by a different one, for example, Cd by Mn in HIFCAB vs JEPLIA.

References
[1] Sacchi, P., Matteo Lusi, M., Cruz-Cabeza, A.J., Nauhac, E.Joel Bernstein, J. Same or different – that is the question: identification of crystal forms from crystal structure data. CrystEngComm 22 (43), 7170-7185, 2020.
[2] Terban, Maxwell and Billinge, Simon. Structural analysis of molecular materials using the pair distribution function. Chemical Reviews 122 (2022), 1208-1272.
[3] Patterson, AL. Homometric structures, Nature 143 (1939), 939-940.
[4] Widdowson, D., Kurlin, V., Pointwise Distance Distributions of finite and periodic point sets. Arxiv.org:2108.04798. The latest version is at http://kurlin.org/projects/periodic-geometry-topology/PDD.pdf

Non-isometric sets with the same PDF

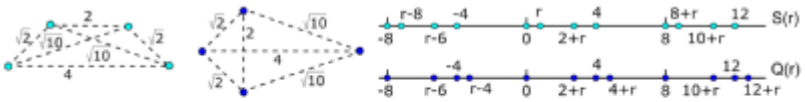

Figure 1: **Left**: the sets $K = \{(\pm 2, 0), (\pm 1, 1)\}$ and $T = \{(\pm 2, 0), (-1, \pm 1)\}$ can not be distinguished by their six pairwise distances $\sqrt{2}, \sqrt{2}, 2, \sqrt{10}, \sqrt{10}, 4$. **Right**: the 1D periodic sets $S(r) = \{0, r, 2+r, 4\} + 8\mathbb{Z}$ and $Q(r) = \{0, 2+r, 4, 4+r\} + 8\mathbb{Z}$ for $0 < r \leq 1$ have the same Patterson function and Pair Distribution Function. Both pairs are distinguished by the Pointwise Distance Distribution.

Pointwise Distance Distribution with a metric

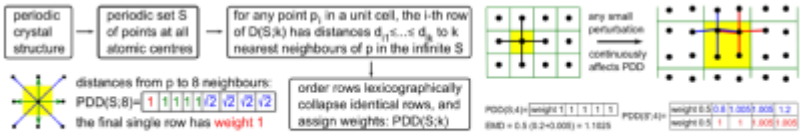

Figure 2: **Left**: pipeline of the Pointwise Distance Distribution (PDD). **Right**: example computation of the Earth Mover's Distance (EMD) between PDDs of a square lattice and its perturbation for $k = 4$ neighbors.

Back to Table of contents

MS39 Crystallography at the nanoscale

MS39-1-1 In memory of R. J. Haüy
#MS39-1-1

G. Shpenkov [1]
[1]Retired - Bielsko-Biala (Poland)

Abstract
R.J. Haüy's (1743-1822) contribution to science is enormous. He is the creator of the first theory of the structure of crystals. He approved the idea of symmetry in the science of crystals. According to Haüy, crystalline bodies are masonry of polyhedral-bricks-"molecules". Each crystalline substance is characterized by its characteristic form of the molecules. As a result, Haüy established a general principle according to which all varieties of one crystalline substance enclose, as an elementary cell, a part of a crystal that has a "primitive and original form of a certain kind". He called these unit cells "integrated molecules". Thus Haüy considered the atoms of any substance as elementary molecules, the structure of which determines the shape of the crystals. The discoveries of Haüy became the basis for the creation of the atomic theory adequate to reality. Unfortunately, in 1848, Augusto Bravais replaced the molecular "bricks-molecules" with their centers of gravity (dots), which ultimately led to spatial lattices, which now underlie the modern concept of crystal structures. In the end this led to the modern atomic model, according to which atoms are, actually, empty spherical spaces and in their centers are superdense tiny nuclei. Such identical structural elements (physical points - atoms), obviously, cannot lead to the variety of structures that exist in nature, which was observed by Haüy. Haüy proved that each crystalline substance is characterized by an individual structure, which is expressed, in particular, in the repeatability of its typical interfacial angels. In the framework of the Wave Model, which we have developed, we proved that atoms are elementary nucleon molecules and characteristic polar angles of the arrangement of nodes in them completely coincide with the mentioned characteristic angles of crystals measured by Haüy. The nodal structure of the atomic spherical shells, following from the solution of the wave equation, for the first time obtained by us, is presented in Fig.1. So, Haüy's idea of a molecular-crystal-like structure of elementary "bricks" (atoms), of which crystalline substances are made up (put forward by him almost 250 years ago), was at last developed and its adequacy to reality was finally confirmed. This became possible thanks to a new theory, based on dialectical philosophy and its logic - Wave Model [1-3].

References
1. G.P. Shpenkov, An Elucidation of the Nature of the Periodic Law, Chapter 7 in "The Mathematics of the Periodic Table", edited by Rouvray D.H. and King R.B., Nova Science Publishers, NY, 119-160, 2006.
2. G.P. Shpenkov, Physics and Chemistry of Carbon in the Light of Shell-Nodal Atomic Model, Chapter 12 in "Quantum Frontiers of Atoms and Molecules", edited by Putz M.V., Nova Science Publishers, NY, 277-323, 2011.
3. George Shpenkov, Discovery of the wave nature of crystals, Keynote speech at the Annual Meeting of the German Crystallographic Society (DGK) 25-28 March 2019, Leipzig; https://shpenkov.com/pdf/CrystalsNature.pdf.

Back to Table of contents

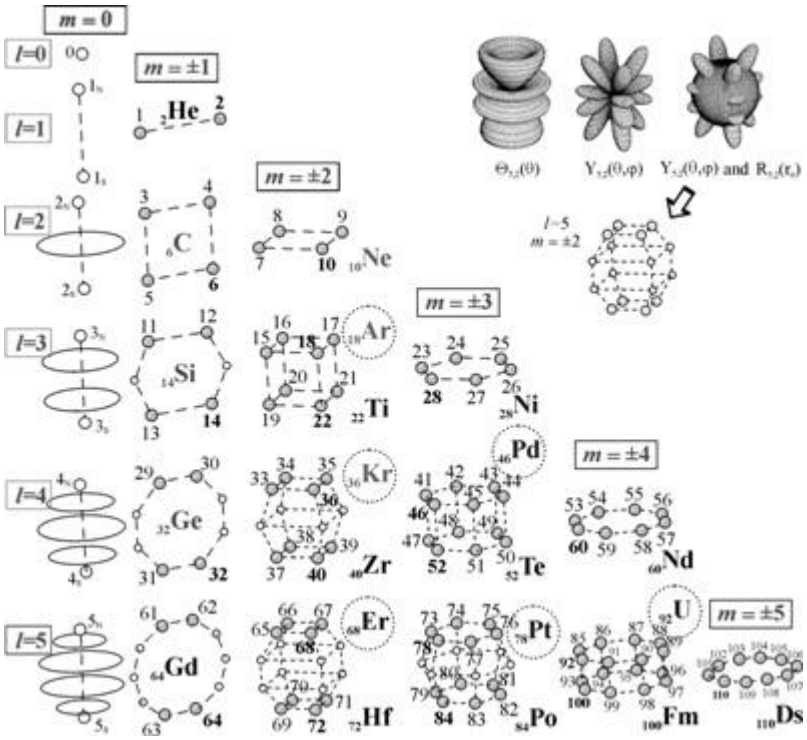

Back to Table of contents

MS39 Crystallography at the nanoscale

MS39-1-2 Thermal evolution of bilayers composed of fcc nanoparticles studied by x-ray scattering methods #MS39-1-2

T. Košutová [1], L. Horák [1], Z. Krtouš [1], A. Kuzminova [1], N. Khomiakova [1], D. Nikitin [1], J. Hanuš [1], O. Kylián [1], M. Dopita [1]

[1]Charles University, Faculty of Mathematics and Physics - Prague (Czech Republic)

Abstract

In our study, we investigated thin layers consisting of face-centered cubic metallic nanoparticles. First, copper, silver and gold nanoparticle layers were studied individually. Subsequently, bilayers of these nanoparticles were deposited and analyzed. The deposition of studied nanoparticles was performed by the Haberland type gas aggregation cluster sources, which are using magnetron sputtering of single metallic targets. This physical bottom-up preparation method is environmentally friendly, scalable to industrial demands and provides high cleanness of the process.

Copper, silver and gold nanoparticles belong to plasmonic nanoparticles, in which it is possible to couple electromagnetic field with the collective oscillations of conduction electrons - plasmons. These nanoparticles have a great application potential because, for all of them, the localized surface plasmon resonance is in the region of visible light.

Our study is focused on the thermal stability of described nanoparticle layers in the air atmosphere and temperature changes in their optical properties. The thermal evolution of morphology, chemical and phase composition, size distribution and microstructure of Cu, Ag and Au nanoparticles was determined by combining in-situ x-ray diffraction (XRD) and ex-situ small angle x-ray scattering and electron microscopies (SEM, TEM). The optical properties of layers were analyzed by UV-Vis spectroscopy and ellipsometry.

Copper nanoparticles are not stable in the air atmosphere, the oxidation process starts immediately after removal from the deposition chamber and core-shell Cu@Cu_2O nanoparticles are formed. Cu nanoparticles further oxidize during the heating procedure, but the size of nanoparticles is almost constant up to 200 °C. The additional layer of Au nanoparticles at the top of copper nanoparticles slows down the oxidation process. In contrast to copper nanoparticles, no oxidation was observed during the annealing of silver and gold nanoparticles up to 800 °C. SAXS and SEM measurements showed that the morphology of silver nanoparticles is less stable than for the gold ones, Ag nanoparticles start to coalesce around 100 °C. During annealing, the size of the crystallites increases but much slower in comparison to the overall size of nanoparticles. The amount of microstructural defects (microstrain, stacking faults) is reduced by annealing for all types of layers. It has been observed that the final layer architecture depends on the sequential order of the bilayers.

SEM images of individual layers of nanoparticles

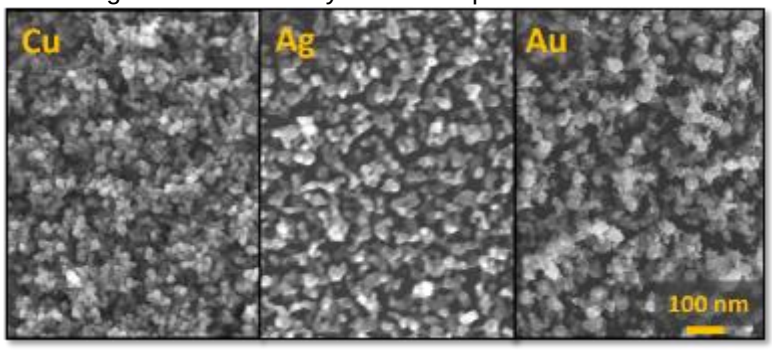

XRD patterns measured during in-situ annealing

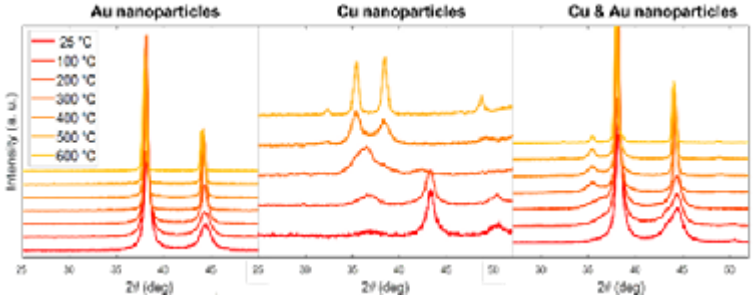

Back to Table of contents

MS39 Crystallography at the nanoscale

MS39-1-3 Rapid High-Throughput Crystallisation of Dihydropyridines
#MS39-1-3

J. Metherall [1], M. Probert [1], M. Hall [1], J. Mccabe [2], P. Corner [2]
[1]Newcastle University - Newcastle upon Tyne (United Kingdom), [2]AstraZeneca - Macclesfield (United Kingdom)

Abstract
Within pharmaceutical drug development, there is a strong drive to obtain the active pharmaceutical ingredients (APIs) in the solid-state, as this enables convenient tablet or capsule drug formulation, ensuring easy usage, aiding patient compliance, and improving API stability.[1] As different solid-forms have different physical properties (including solubility), solid-form screening is an essential part of early drug development, and the ability to undertake rapid crystallisation screening is therefore very beneficial.[2]
Modern materials characterisation can be heavily dependent on the availability of suitable, high-quality crystals for analysis, as such crystals enables analysis by single crystal X-ray diffraction (SCXRD), providing atomic level structural resolution. Success in growing crystals is proportional to the amount of experimental crystallisation space explored. Approaches to the investigation of crystallisation space have undergone a 'step-change' in recent years with new techniques[3-5] becoming available *via* the use of technological advancements in liquid handling.[6] One of these 'step-change' developments is high-throughput encapsulated nanodroplet crystallisation (ENaCt). This technique permits large numbers of experimental crystallisation conditions to be screened in parallel with low overall quantities of analyte consumed. The method allows for the initiation of hundreds of individual crystallisation experiments within a few minutes of preparing solutions of the analyte in question.
We have shown that ENaCt is a capable tool for the crystallisation and subsequent SCXRD analysis of a set of six API analogues, belonging to the dihydropyridine class. Dihydropyridines are calcium channel blockers, used in the treatment of hypertension. The high-throughput crystallisation experiments presented herein were performed using a liquid-handling robot (SPT Labtech Mosquito®)[6] on the microgram scale, reducing the overall material demand to a few milligrams of total analyte. Crystals were grown from nanolitre-scale droplet solutions with each compound prepared for crystallisation in twelve common laboratory solvents. Oils were used to encapsulate the samples, with the aim to reduce the rate of solvent loss and allow a slow increase in the sample concentration up to and beyond the point of saturation. The oil encapsulation combined with the restricted number of nucleation sites available in such small droplets, aids the growth of high-quality single crystals.[1]
The six dihydropyridine compounds were successfully crystallised using the developed ENaCt protocol; single crystals of dimensions ≥ 50 µm being obtained within 2 weeks, and have been analysed via SCXRD. The results clearly demonstrate that the high-throughput crystallisation screening methods employed are beneficial in obtaining high-quality single crystals, suitable for SCXRD, in short timeframes with low overall sample requirements (~20 mg), hence providing a valuable technique for use in the drug development process.

References
1. S.L. Morissette, O. Almarsson, M.L. Peterson, J.F. Remenar, M.J. Read, A.V. Lemmo, S. Ellis, M.J. Cima and C.R. Gardner, *Adv. Drug Delivery Rev.*, 2004, **3**, 275-300.2. L.F. Huang and W.Q. Tong, *Adv. Drug Delivery Rev*. 2004, **56**, 321-334.3. A.R. Tyler, R. Ragbirsingh, C.J. McMonagle, P.G. Waddell, S.E. Heaps, J.W. Steed, P. Thaw, M.J. Hall and M.R. Probert, *Chem*., 2020, **6**, 1755-1765.4. P.P. Nievergelt, M. Babor, J. Cejka and B. Spingler, *Chem. Sci.*, 2018, **9**, 3716-3722.5. M. Hoshino, A. Khuita, H. Xing, Y. Inokuma and M. Fujita, *IUCrJ*, 2016, **3**, 139-151.6. SPL Labtech Mosquito®, https://www.sptlabtech.com/company.

Back to Table of contents

MS39 Crystallography at the nanoscale

MS39-1-4 Multiscale characterization of Spin Crossover complexes
#MS39-1-4

M. Penicaud [1], P. Rosa [2], M. Gonidec [2], L. Poggini [3], L. Squillantini [3], F. Carlà [4]
[1]ICMCB - Université de Bordeaux - Pessac (France), [2]ICMCB - CNRS - Pessac (France), [3]University of Florence - Florence (Italy), [4]Diamond Light Source - Didcot (United Kingdom)

Abstract
Spin CrossOver (SCO) complexes are a family of materials displaying two stable electronic configurations (low spin and high spin), that can be reversibly tuned using appropriate stimuli (temperature, pressure, light irradiation, magnetic field etc…). In bulk materials, the switching properties are also highly dependent on the crystal packing and the interactions between complexes[1]. SCO transition metal complexes have been proposed to be employed in molecular electronic and in multifunctional spintronic devices. The assembly of SCO complexes on a solid support is the fundamental first step before any device fabrication: for this scope high-vacuum sublimation deposition allows obtaining high quality nanometric films, with a good control of the final thickness[2]. In nanostructured SCO thin films, due to the fragile nature of the spin transition involved (both in terms of stability of the molecules and of robustness of the SCO process to external constraints), it is often observed that the interaction with the surface can bring the system in a total or a partial loss of SCO properties. This may originate from a strong interaction with the substrate[3] or a partial degradation of the molecular structure[4]. We will present the study of two Fe(II) SCO complexes, first in bulk (powder and single crystals) to establish structure-properties relationships, then in ultra thin films evaporated on Si(100) and on polycristalline metallic substrates (Au, Ag). The structure and morphology of the ultra thin films were investigated by AFM imaging, X-Ray Reflectometry and Grazing Incidence X-ray Diffraction (GIXRD).

References
1. S. Ossinger, C. Näther, A. Buchholz, M. Schmidtmann, S. Mangelsen, R. Beckhaus, W. Plass, and F. Tuczek., *Inorg. Chem*. **2020**, 59, 12, 7966–7979
2. M. Atzori, L. Poggini, L. Squillantini, B. Cortigiani, M. Gonidec, P. Bencok, R. Sessoli and M. Mannini, *J. Mater. Chem. C*, **2018**, 6, 8885–8889.
3. T. Miyamachi, M. Gruber, V. Davesne, M. Bowen, S. Boukari, L. Joly, F. Scheurer, G. Rogez, T. K. Yamada, P. Ohresser, E. Beaurepaire and W. Wulfhekel, *Nat. Commun.*, **2012**, 3, 938.
4. T. G. Gopakumar, M. Bernien, H. Naggert, F. Matino, C. F. Hermanns, A. Bannwarth, S. Mühlenberend, A. Krüger, D. Krüger, F. Nickel, W. Walter, R. Berndt, W. Kuch and F. Tuczek, *Chem. - A Eur. J.*, **2013**, 19, 15702–15709.

Back to Table of contents

MS39 Crystallography at the nanoscale

MS39-2-1 Encapsulated Nanodroplet Crystallisation: Expanding Solution-Phase Crystallisation Methodologies for Polymorph Screening
#MS39-2-1

J. Weatherston [1], M. Probert [1], M. Hall [1]
[1]Newcastle University - Newcastle Upon Tyne (United Kingdom)

Abstract
Polymorphism is a solid-state phenomenon where a chemical species may adopt different conformational or packing arrangements, therefore allowing for the formation of more than one distinct crystal structure. As a result of these different packing arrangements, crystal polymorphs can exhibit varying physical and chemical properties. These properties such as solubility, hardness, colour, and melting point can all be important in the design of a compound.[1]
In the pharmaceutical and crystal engineering fields, a thorough understanding of the polymorphic landscape of a chemical species is critical to reliably select and grow crystal forms with suitable properties for their intended functionality. For example, the bioavailability of an active pharmaceutical ingredient can be drastically altered by the crystal form in which it is formulated.[2] Whilst computational crystal structure prediction can be used to highlight likely crystal forms of a given chemical species[1], manual crystallisation screens remain the only way to effectively assess the impact of polymorphism on a compound. The techniques classically applied to grow high-quality single crystals are often time-consuming and require significant quantities of the sample compound.[3] In the pharmaceutical industry, this often leaves crystal form screening to a later stage of drug development when large quantities of material are available for such experiments. This has led to significant demand for rapid, small-scale crystallisation techniques that would permit crystal form screening at a much earlier phase of drug development.[3]
Herein, we describe how encapsulated nanodroplet crystallisation (ENaCt), a small-scale, high-throughput, robot-assisted crystallisation technique, can be applied to probe areas of the polymorphic landscape that were previously inaccessible to solution-phase crystallisation techniques. Polymorph screens of 5-methyl-2-[(2-nitrophenyl)amino]-3-thiophenecarbonitrile (ROY) and nicotinamide resulted in the growth of high-quality single crystals of polymorphs only previously known to crystallise from melt-based experiments, demonstrating the capability of ENaCt for probing a large area of the polymorphic landscape.[4-7]

References
1. A. J. Cruz-Cabeza, N. Feeder and R. J. Davey, *Commun Chem*., 2020, **3**, 1-4.2. E. H. Lee, *Asian Journal of Pharmaceutical Sciences*., 2014, **9**, 163-1753. A. R. Tyler, R. Ragbirsingh, C. J. McMonagle, P. G. Waddell, S. E Heaps, J. W. Steed, P. Thaw, M. J. Hall, and M. R. Probert, *Chem*, 2020, **6**, 1851-1853.4. S. Chen, I. A. Guzei, and L. Yu, J. Am. Chem. Soc., 2005, **127**, 9881–9885.5. X. Li X. Ou, H. Rong, S. Huang, J. Nyman, L. Yu and M. Lu, *Cryst. Growth Des.*, 2020, **20**, 7093– 7097.6. A. Levesque, T. Maris, and J. D. Wuest, *J. Am. Chem. Soc*., 2020, **142**, 11873–11883.7. X. Li, X. Ou, B. Wang, *Commun. Chem*., 2020, **3**, 152.

Back to Table of contents

MS40 Operando and in-situ crystallographic studies

MS40-1-1 The effect of auxiliary ligands on nitrite group linkage isomerization reaction in a series of nickel(II) complexes
#MS40-1-1

K. Deresz [1], K. Potempa [2], A. Krówczyński [2], R. Kamiński [2], D. Schaniel [3], K. Jarzembska [1]
[1]Univeristy of Warsaw - Warsaw (Poland), [2]Univeristy of Warsaw - Warszawa (Poland), [3]Univeristy of Lorraine - Nancy (France)

Abstract
Molecular switches are materials that undergo chemical transformation (isomerization, cyclisation etc.) upon some external stimuli (light pulse, temperature, high pressure). Such systems can be used in many ways, for example in optoelectronics, medicine or solar energetics. A good example of compounds of this kind are transition-metal complexes with ambidentate ligands, such as: -NO2, -SO2, -DMSO, that undergo photoisomerisation reaction. Switchable systems' behaviour upon light irradiation can be readily examined photocrystallographically. Understanding of factors governing such processes in crystals and their mechanisms will contribute to later conscious design of efficient molecular switches, and further to development of new technologies.
The current study is a part of our wider project dedicated to design and thorough investigations of novel photoswitchble transition-metal systems with small ambidentate ligands [1]. The series of compounds presented here differ by the type of the chelating N,N,O-donor ligand (different amine fragment or aliphatic substituents), which affects the Ni-NO2 bond strength. This effect along with crystal packing and intermolecular interaction influence on the photo-induced isomerization were deeply investigated. The examined compounds switch from nitro to nitrito binding mode under 405 nm - 530 nm LED light irradiation, with good conversion rates close to 100%, and the generated linkage isomers are stable in a wide temperature range. The reaction is proven reversible, the systems relax back to the ground state around 220 K. The isomerization reactions were examined using solid-state photoIR spectroscopy and photocrystallography, which also enabled structural evaluation of the light-induced metastable-state species. Intermolecular interactions were characterized using DFT calculations and Hirshfeld surface approach. Theoretical calculations were also used to determine relative stability of various linkage isomers under consideration.
The authors thank the PRELUDIUM-BIS grant (2019/35/O/ST4/04197) of the NCN (Poland) for financial support and the Wrocław Centre for Networking and Supercomputing, Wrocław, Poland (Grant No. 285) for providing computational facilities. The X-ray diffraction experiments were carried out at the Department of Physics, UW, on a Rigaku Oxford Diffraction SuperNova diffractometer, which was co-financed by the EU within the European Regional Development Fund (POIG.02.01.00-14-122/09). The IR spectroscopy experiments were carried out at the University of Lorraine.

References
[1] Kutniewska, S. E., Krowczynski, A., Kaminski, R., Jarzembska, K. N., Pillet, S., Wenger, E. & Schaniel, D. (2020). IUCrJ 7, 1188-1198.

Back to Table of contents

MS40 Operando and in-situ crystallographic studies

MS40-1-2 3DED in situ single crystal studies on submicron sized particles during redox reactions in gas environments and electrochemical reactions
#MS40-1-2

J. Hadermann [1], M. Batuk [1], D. Vandemeulebroucke [1]
[1]University of Antwerp - Wilrijk (Belgium)

Abstract

Oxidation and reduction processes are important in the field of energy materials. Changes in crystal structures during such processes dictate ion conduction paths and reversibility, thus efficiency, capacity and lifetime of different technologies. Such structural changes are currently followed in situ using X-ray and neutron powder diffraction techniques, because the materials are usually only active as submicron particles, making in situ single crystal X-ray or neutron diffraction studies non-applicable. Although in situ powder diffraction can uncover very important structural changes, it can be hindered by peak overlap of different phases and peak broadening due to the small crystal sizes, leaving some structures unsolved or unrefined. Using instead electron diffraction allows performing in situ single crystal experiments on the individual particles within a powder sample, due to the much stronger interaction between electrons and matter, and allows uncovering information and determining structures out of reach of in situ powder diffraction techniques. In literature, in situ transmission electron microscopy is so far mainly used for imaging, but the possibilities of in situ electron diffraction and especially the advanced technique of 3DED (in which reciprocal space is reconstructed from a series of electron diffraction patterns taken at different angles such that the data can be used for solution and refinement, similar to other single crystal diffraction techniques) are unexplored. In this lecture we will demonstrate our pioneering results on in situ 3DED, where we have monitored how the crystal structures of materials change under oxidizing and reducing gas atmospheres, or under electrochemical oxidation and reduction.

Oxidation of SrFeO2.5

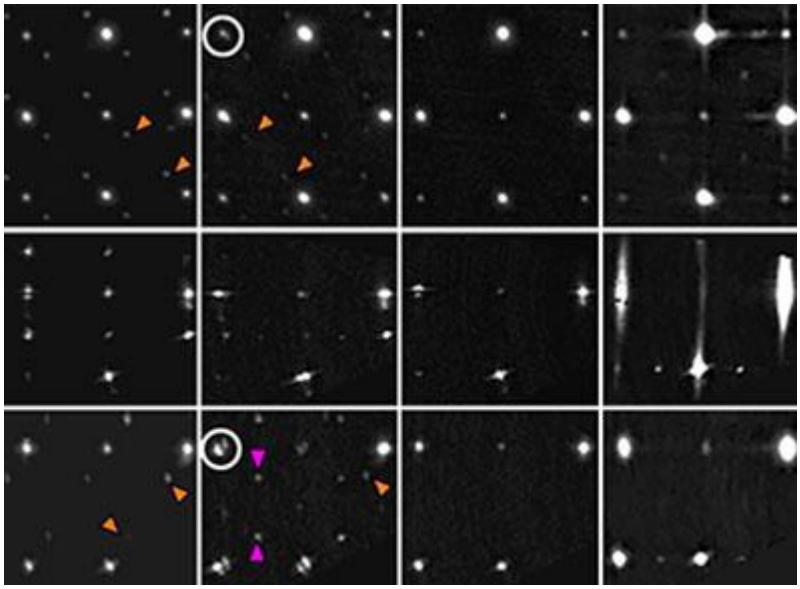

Back to Table of contents

MS40 Operando and in-situ crystallographic studies

MS40-1-3 Insights on Selective Gas Sorption Behavior in a Family of MOF-like Materials from Operando Crystallographic Studies with DFT Calculations
#MS40-1-3

A. Allen [1], E. Cockayne [1], W. Wong-Ng [1]
[1]NIST - Gaithersburg (United States)

Abstract
Design and development of new solid gas-sorbent materials, having adjustable structures to accommodate high densities of adsorbed gas solvent molecules, continues to be of major interest. This is driven by universal needs for molecular sorption and gas detection, enhanced oil and gas recovery, various gas storage and separation applications, as well as the need for increasingly efficient, inexpensive gas sorbents to address climate change through carbon dioxide reduction (CDR) [1]. In this context, metal organic frameworks (MOFs) and similar materials show promise. These comprise metal ions or clusters linked into highly porous 3D networks by coordinated organic ligands. Their behavior can include an ability to exhibit hysteresis in reversible structural transitions between low- and high-porosity states during adsorption/desorption cycles. One group of microporous compounds possessing such MOF-like structures is the pillared cyanonickelate ("PICNIC") family of Hofmann compounds, based on square planar sheets of $Ni(CN)_2$ bridged by organic ligands terminated by N atoms at each end [2]. Since the network is not inherently rigid against shearing of $Ni(CN)_2$ planes against to each other, some PICNIC materials are flexible, although not all. Experimental results based on X-ray and neutron diffraction (XRD and ND), as well as small-angle scattering (SAXS and SANS) will be presented for several generic members of the PICNIC family, including operando studies under dual gas flow conditions (CO_2 with N_2, CH_4 and H_2) and supercritical CO_2 conditions [3-5]. Significant insights have been gained regarding the different structural and microstructural gas sorption responses for different members of the PICNIC family by comparing these experimental results to the predictions of density functional theory (DFT) calculations [6].

References
[1] Trickett, C.A. et al. (2017). Nature Rev. Mater. 2, art. no. 17045.
[2] Hagrman, D. et al. (1999). Angew. Chem. Int. Ed. 38, 3165-3168.
[3] Allen, A.J. et al. (2015). J. Alloys Compd. 647, 24-34.
[4] Allen A.J. et al. (2019). Nanomaterials. 9, art. no. 354.
[5] Wong-Ng, W. et al. (2021). Polyhedron. 200, art. no. 115132.
[6] Cockayne, E. et al. (2021). J. Phys. Chem. C. 125, 15882-15889.

Back to Table of contents

MS40 Operando and in-situ crystallographic studies

MS40-1-4 A unique laboratory experimental setup for single crystal X-ray diffraction under electric field #MS40-1-4

E. Wenger [1], E. Tailleur [1], C. Palin [1], P. Alle [1], S. Pillet [1], D. Schaniel [1]
[1]CRM2-UMR UL-CNRS 7036 - Vandoeuvre-lès-Nancy (France)

Abstract
In the context of studies of multi-functional materials with piezo-ferro-electric properties, we are developing a device for the characterization of structural changes under static and alternating electric fields (of the order of 30 kV.cm-1) [1].
In this kind of materials, structural changes related to the application of an electric field take place at different physical scales, from the microscopic (atomic displacements, symmetry changes, crystal lattice distortion) to the macroscopic (microstructure, formation and displacement of domain walls, polarization switching). Single crystal X-ray diffraction is a well-adapted technique for exploring these structural changes. Accurate and complete mapping of the reciprocal space under electric field is an instrumental and methodological challenge. It can be achieved with the use of a 4-circles goniometer and a 2D detector such as the Cegitek RebirX 540 hybrid pixel detector [2]. Indeed, this detector has all the necessary specifications for this type of measurements (absence of readout noise, electronic shutter, fast readout time, adapted firmware).
The device developed in our laboratory [3] allows the generation of an alternating electric field and the positioning of the goniometer to be synchronized with the X-ray photons detection by the RebirX detector. The recorded diffraction images are multiplexed and summed directly in the detector using the firmware precisely developed for these experiments.
Applying an electric field in different directions to a single crystal suitable for XRD requires specific sample holders. They must be compact, adaptable to a usual goniometric head and allow a complete exploration of the reciprocal space. Different types of sample holders have been designed and built in the CRM2 laboratory and allow crystals of different size, morphology and nature to be subjected to an electric field according to chosen crystallographic orientations, with or without direct contact of the electrodes on the sample.
This experimental setup has been tested in different configurations, on an inorganic quartz crystal [3] but also on a molecular compound [4].

References
[1] Studies of electric field induced structural and electron-density modifications by X-ray diffraction: N. K. Hansen, P. Fertey and R. Guillot, Acta Cryst. (2004), A60, 465-471.
[2] Cegitek Innovation: 13830 Roquefort la Bedoule, France
[3] Diffraction studies under in-situ electric field using a 2D hybrid pixel XPAD detector: Fertey P., P. Allé, E. Wenger, B. Dinkespiler, S. Hustache, K. Medjoubi, F. Picca, C. Lecomte and C. Mazzoli. J. Appl. Cryst. (2013), 46.
[4] An electric field cell for performing in situ single-crystal synchrotron X-ray diffraction: L. K. Saunders, H. H.-M. Yeung, M. R. Warren, P. Smith, S. Gurney, S. F. Dodsworth, I. J. Vitorica-Yrezabal, A. Wilcox, P. V. Hathaway, G. Preece, P. Roberts, S. A. Barnett and D. R. Allan J. Appl. Cryst. (2021), 54, 1349-1359.

Setup for SC-XRD studies under electric field

Back to Table of contents

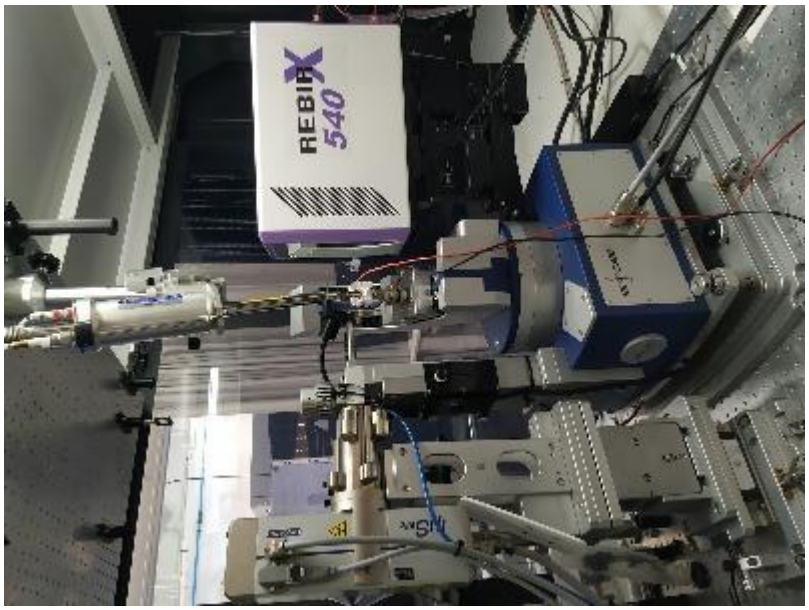

Back to Table of contents

MS40 Operando and in-situ crystallographic studies

MS40-1-5 Differential scanning diffraction and differential scanning imaging as novel methods for in situ studies of organic eutectic systems
#MS40-1-5

M. Lopresti [1], M. Milanesio [1], L. Palin [1], M. Bonomo [2], C. Barolo [2]
[1]Dipartimento di Scienze ed Innovazione Tecnologica, Università of the Eastern Piedmont "Amedeo Avogadro" - Vercelli (Italy), [2]Department of Chemistry and NIS Interdepartmental Center and INSTM Reference Centre, University of Torino - Torino (Italy)

Abstract
In the last decade, hot/cold stages have been made available to laboratories, which allowed scientist to carry out in situ X-ray diffraction experiments at non-environmental conditions [1], without having to rely on large-scale structures such as synchrotrons. This, combined with the increasingly improved detectors and data collection systems, allow to collect huge amounts of data in a few hours of experiments, also at lab facilities. With this new instrument configuration available, numerous in situ experiments were performed in non-ambient temperature conditions collecting simultaneous imaging and diffraction data, thus studying structural and morphology features in one shot [2]. The advantage of experiments in presence of temperature gradients lies in the possibility of observing step by step the transformations of the samples being analyzed along the entire transformation, being it a phase transition from one physical state to another, or formation of one polymorph into another or a chemical reaction. Exploiting in situ imaging and X-ray diffraction data, coupled to PCA multivariate analysis [3], we introduce two new techniques called differential scanning diffraction and differential scanning imaging respectively. These two techniques allow to obtain, in addition to the information related to the structure of the samples, information related to the transformations induced by temperature in a very similar way to those that can be obtained using differential scanning calorimetry. The technique has been applied in the study of different materials of interest, e.g. inorganic (as test case) and organic-based eutectic mixtures known as deep eutectic solvents (DES) .

References
[1] Conterosito, E.; Lopresti, M.; Palin, L. In Situ X-ray Diffraction Study of Xe and CO2 Adsorption in Y Zeolite: Comparison between Rietveld and PCA-Based Analysis. Crystals 2020, 10, 483. https://doi.org/10.3390/cryst10060483.
[2] Haoxiang Y., Shangshu Q., Lei Y., Peng L., Xiaoting L., Minghe L., Nengbing L., Miao S., Jie S. Morphological, electrochemical and in-situ XRD study of LiNi0.6Co0.2Mn0.1Al0.1O2 as high potential cathode material for rechargeable lithium-ion batteries. Journal of Alloys and Compounds, 667, 2016, 58-64. https://doi.org/10.1016/j.jallcom.2016.01.199.
[3] Guccione, P.; Lopresti, M.; Milanesio, M.; Caliandro, R. Multivariate Analysis Applications in X-ray Diffraction. Crystals 2021, 11, 12. https://doi.org/10.3390/cryst11010012
[4] Benworth B. Hansen, Stephanie Spittle, Brian Chen, Derrick Poe, Yong Zhang, Jeffrey M. Klein, Alexandre Horton, Laxmi Adhikari, Tamar Zelovich, Brian W. Doherty, Burcu Gurkan, Edward J. Maginn, Arthur Ragauskas, Mark Dadmun, Thomas A. Zawodzinski, Gary A. Baker, Mark E. Tuckerman, Robert F. Savinell, and Joshua R. Sangoro. Deep Eutectic Solvents: A Review of Fundamentals and Applications. Chemical Reviews 2021 121 (3), 1232-1285. https://doi.org/10.1021/acs.chemrev.0c00385

DSD profile of a DES eutectic mixture.

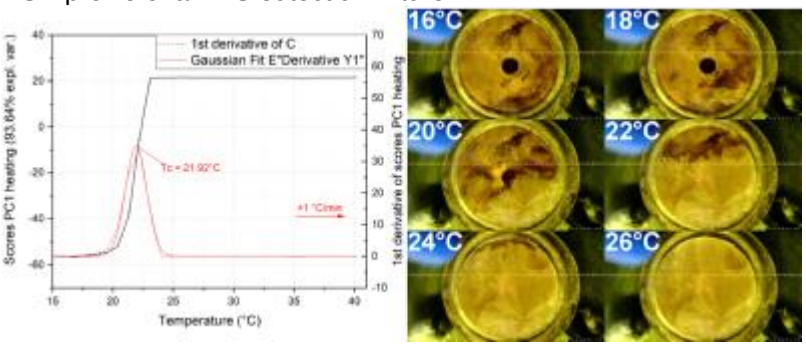

Back to Table of contents

MS40 Operando and in-situ crystallographic studies

MS40-1-6 High temperature phase transitions and twinning in polycrystals probed by in situ 3D reciprocal space mapping
#MS40-1-6

R. Guinebretière [1], D. Fowan [1], E. Thune [1], R. Raj Puroshit Purushottam Raj [2], S. Arnaud [3], G. Chahine [4], N. Blanc [3], O. Castelnau [5]
[1]IRCER - Limoges (France), [2]Université Grenoble Alpes, CEA, IRIG - Grenoble (France), [3]Université Grenoble Alpes, CNRS, Institut Néel - Grenoble (France), [4]Université Grenoble Alpes, SIMaP, Grenoble INP, CNRS - Grenoble (France), [5]5Laboratoire PIMM, UMR CNRS 8006 - Paris (France)

Abstract
Solid-state phase transitions (SPT) are fundamental processes that are driving a large part of the effective physical properties of single crystals as well as polycrystalline materials. In addition to the structural evolutions that can be described by space group transitions, SPTs are often associated with transformations that occur at the mesoscale and generate structural defects such as dislocations, twinning, stacking faults, strain fields, etc. Such defects can be detected and quantitatively studied in the reciprocal space through high-resolution x-ray diffraction experiments. Originally developed to study defects in epitaxial layers, the Reciprocal Space Mapping (RSM) method has been extended to cover everything from imperfect single crystals to complex polycrystals. Over the past decade, the widespread use of 2D solid-state detectors at synchrotron radiation sources has promoted the development of 3D-RSM on timescale that enables to follow the sample evolutions as a function of external stimuli. In the case of polycrystals, it has been shown that this approach allows to select the crystals of interest in reciprocal space from all the crystals constituting the probed volume. We have recently shown that this method can be used even at very high temperature (over 1000 °C) [1, 2]. We will show during the conference that high temperature 3D-RSM can be extended to in situ observation of solid-state phase transition allowing to evidence the formation of crystallographic variants and twins.
The potential of this approach will be illustrated by the in situ study of two successive phase transitions in pure zirconia dense polycrystal. Under atmospheric pressure, pure zirconia solidifies into a cubic crystal structure (c) (space group Fm m). Upon cooling it transforms first to tetragonal (t) (space group P42/nmc) and then to monoclinic (m) (space group P21/c). We will show that the method allows following the temperature induced splitting of an initially unique Reciprocal Lattice Node (RLN) into 24 RLNs generated by the loss of symmetry axis through two successive phase transitions (see Fig. 1). Moreover, since the SPT occurs under huge stresses [3], the RLNs are embedded in a large, 3-dimensional, diffuse scattering signal that is very clearly evidenced (see Fig. 2). The crystallographic interpretation of RLN splitting and the diffuse scattering signal associated with the phase transitions in pure zirconia polycrystal will be discussed during the talk.

References
[1] R. Guinebretière, S. Arnaud, N. Blanc, N. Boudet, E. Thune, D. Babonneau and O. Castelnau, “Full reciprocal-space mapping up to 2000 K under controlled atmosphere: the multipurpose QMAX furnace,” J. Appl. Cryst. 53, 650-661 (2020).
[2] R. Guinebretière, T. Ors, V. Michel, E. Thune, M. Huger, S. Arnaud, N. Blanc, N. Boudet and O. Castelnau, “Coupling between elastic strains and phase transition in dense pure zirconia polycrystals,” Phys. Rev. Mater. 6, 013602 (2022).
[3] T. Ors, F. Gouraud, V. Michel, M. Huger, N. Gey, J.S. Micha, O. Castelnau and R. Guinebretière “Huge local elastic strains in bulk nanostructured pure zirconia materials” Mater. Sci. Eng. A 806, 140817 (2021).

Splitting of the cubic zirconia 111 node

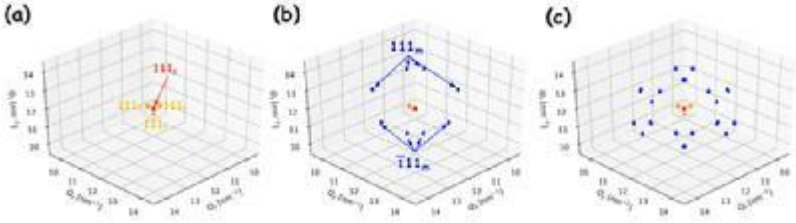

RSMs recorded near the zirconia 111t node

Back to Table of contents

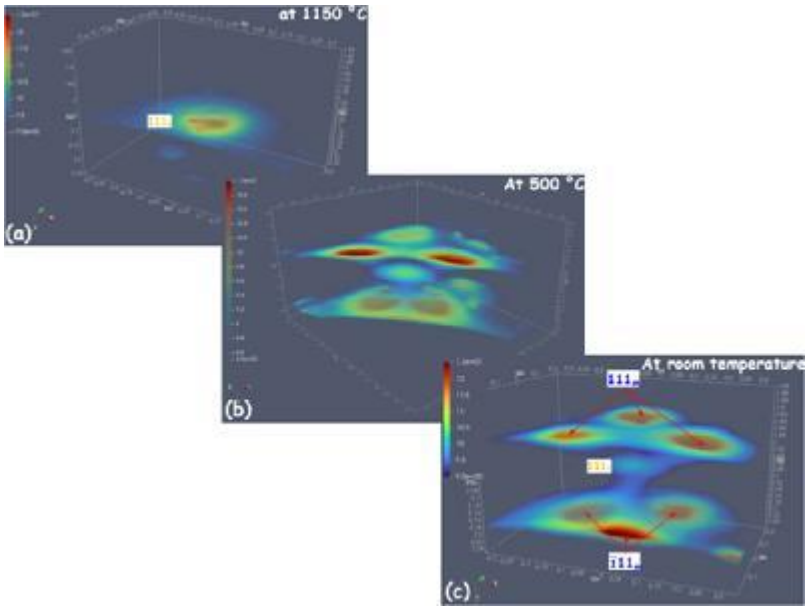

Back to Table of contents

MS40 Operando and in-situ crystallographic studies

MS40-1-7 Low-temperature study in the mixed crystal series Ni(1-x)Cu(x)Cr2O4
#MS40-1-7

M. Tovar [1], M. Reehuis [1], N. Stüßer [1], S. Schorr [2]
[1]Helmholtz-Zentrum Berlin - Berlin (Germany), [2]Freie Universität Berlin - Berlin (Germany)

Abstract
Members of the mixed crystal series $Ni_{1-x}Cu_xCr_2O_4$ crystallize in a distorted spinel struture [1,2,3]. For the end members $NiCr_2O_4$ and $CuCr_2O_4$ strong Jahn-Teller activities on the Ni^{2+} and Cu^{2+} ions at the A site lead to an elongation and a flattening of the NiO_4 and CuO_4 tetrahedra, respectively. Two structural phase transitions where caused by the local distortion, where the crystal structure first undergoes a change from cubic (Fd3m) to tetragonal symmetry (I41/amd) followed by a change to orthorhombic space group Fddd at or below room temperature, depending on the Cu-Ni substitution. Low-temperature X-ray diffraction by means of a Guinier diffractometer, hosted at the HZB X-ray Corelab, was applied in combination with neutron powder diffraction data to elucidate the interplay between structural and magnetic distortion in the complex spinel system.

References
[1] Dollase, W.A.; O'Neill, H.S.C., Acta Crystallographica C (1997) 53, 657
[2] Reehuis et al., Phys. Rev. B 91 (2015) 024407
[3] Suchomel et al., Phys. Rev. B 86 (2012) 054406

Lattice parameters of Ni0.82Cu0.18Cr2O4

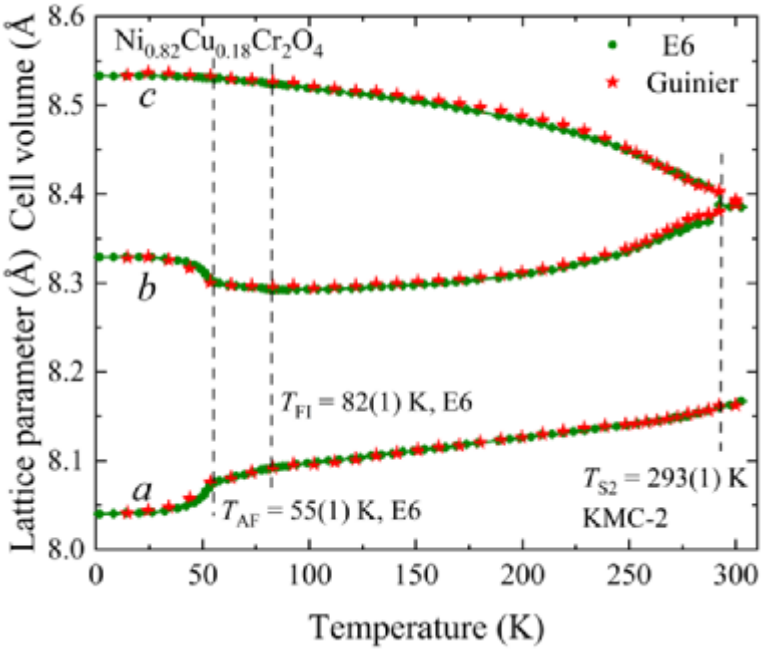

Low temperatur Guinier diffractometer

Back to Table of contents

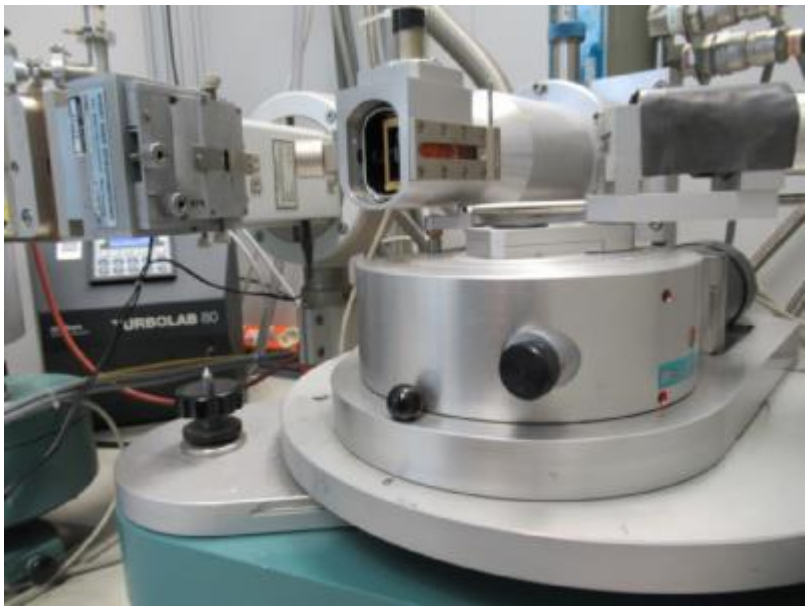

Back to Table of contents

MS40 Operando and in-situ crystallographic studies

MS40-1-8 Tracking the high temperature synthesis of LiNiO2 under oxygen gas flow by laboratory-based X-ray diffraction
#MS40-1-8

D. Weber [1], H. Gesswein [2], M. Bianchini [3], T. Brezesinski [1]
[1]Karlsruhe Institute of Technology, Institute for Applied Materials - Eggenstein-Leopoldshafen (Germany), [2]Karlsruhe Institute of Technology, Institute for Applied Materials - Eggenstein-Leopoldshafen (Germany) - Eggenstein-Leopoldshafen (Germany), [3]University of Bayreuth - Bayreuth (Germany)

Abstract
Tracking the formation process of cathode active materials for lithium ion batteries can shed a light on product properties and the role of dopants during crystallization in this highly relevant class of materials. The mechanism of formation can be elucidated directly via high temperature in-situ synchrotron experimentation under gas flow or by indirect inference over a series of synthesis. Both methods are costly, as synchrotron time is precious and a large number of solid state synthesis can easily occupy experimenters for weeks.
Here, we describe a gas flow reactor for in-situ diffraction (GRID) on a laboratory X-ray diffractometer based on a modified design by Chupas *et al.*[1] including initial studies on the synthesis of $LiNiO_2$.[2] As a product, $LiNiO_2$ that is highly sensitive to small variations in Li^+ content as well as oxygen partial pressure during synthesis.[3] Utilizing an in-situ reactor on a laboratory diffractometer allows iterating experimental conditions, which is critical in order to observe the formation of good materials. Thus, the loss of resolution compared to synchrotron experiments can be offset with improved measurement procedures specifically adjusted to the material at hand. Standardized measurement procedures and cross instrument calibration allow knowledge transfer from the in-situ experiment directly to lab-based bulk synthesis. Observables include the lattice parameters as well as crystallite size broadening at the initial stages of crystallization up to approximately 50 nm. Additionally, we performed a series of isothermal kinetic experiments, thus quantifying the energetic barrier for crystal growth in two regimes. Our study shows opportunities and challenges in lab-based high temperature in-situ diffraction measurements and highlights possible pathways towards higher resolution in time and space in PXRD at the lab scale.

References
[1] P. J. Chupas, K. W. Chapman, C. Kurtz, J. C. Hanson, P. L. Lee and C. P. Grey: "A versatile sample-environment cell for non-ambient X-ray scattering experiments", J. Appl. Cryst., **2008**, *41*, 822-824; https://doi.org/10.1107/S0021889808020165.
[2] H. Gesswein, P. Stüble, D. Weber, J. R. Binder, R. Mönig: "A multipurpose laboratory diffractometer for operando powder X-ray diffraction investigations of energy materials", J. Appl. Cryst., **2022**, *55*, in press, https://doi.org/10.1107/S1600576722003089.
[3] M. Bianchini, F. Fauth, P. Hartmann, T. Brezesinski, Jürgen Janek: "An in situ structural study on the synthesis and decomposition of $LiNiO_2$", J. Mater. Chem. A, **2020**, *8*, 1808-1820, https://pubs.rsc.org/en/content/articlehtml/2020/ta/c9ta12073d

Elucidation of high T reaction mechanisms.

Back to Table of contents

Laboratory-based in-situ diffraction:

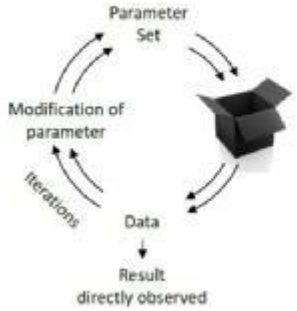

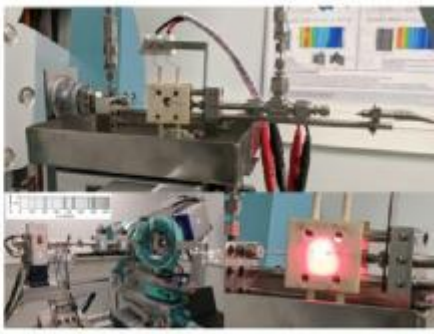

Convenstional solid state synthesis:

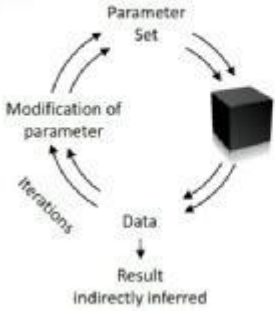

Synchrotron-based in- situ diffraction:

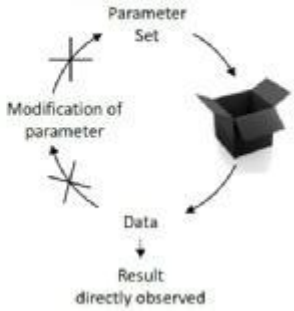

Back to Table of contents

MS40 Operando and in-situ crystallographic studies

MS40-2-1 Photocrystallographic and spectroscopic studies of a simple photoswitchable Co(acac)2(imidazole)NO2 complex.
#MS40-2-1

P. Borowski [1], R. Kamiński [1], D. Schaniel [2], K.N. Jarzembska [1]
[1]University of Warsaw - Warsaw (Poland), [2]Universite de Lorraine, CNRS, CRM2 - Nancy (France)

Abstract
The importance of transition-metal photoswitchable complexes owing molecular fragments that can exist in multiple isomeric forms (e.g. NO2, NO or SO2) is constantly increasing. Hence, in the current study new photoactive bis(acetyloacetonato-O,O')(imidazole)nitrocobalt(III) complexes was designed and synthesized. Crystals of both cis and trans isomers of the studied compounds were obtained and structurally analysed. Multi-temperature X-ray diffraction and solid-state IR/UV-Vis spectroscopic experiments were conducted to determine optimal photoisomerisation reaction conditions. It occurred that almost full nitro-nitrito conversion was observed for the cis isomer after 365-405 nm LED irradiation in the 100 – 290 K temperature range, while for the trans isomer only small changes were observed in the solid-state IR spectra. The isomerization reaction progress was monitored using selected bands corresponding to the NO2 vibrations, which were assigned based on normal-mode frequencies calculated at the DFT(B3LYP)/6-311++G** level of theory and literature contributions. Spectroscopic results were confirmed photocrystallographically using our homemade light-delivery device[i], which also enabled evaluation of the molecular structure of the metastable product – the exo-nitrito linkage isomer. The stability of the light-induced species was thoroughly examined.
(a)
(b)
(c)

Figure (a) Schematic representation of the cis isomer of title compound; (b) IR absorption spectra in the solid state after 405nm LED irradiation at room temperature; (c) schematic representation of the trans isomer of title compound.

The authors thank the The Best of the Best! 4.0 project – Ministry of Education and Science (Poland) – for financial support. The Wrocław Centre for Networking and Supercomputing (grant No. 285) is gratefully acknowledged for providing computational facilities. The in-house X-ray diffraction experiments were carried out at the Department of Physics, University of Warsaw, on Rigaku Oxford Diffraction SuperNova diffractometer, which was co-financed by the European Union within the European Regional Development Fund (POIG.02.01.00-14.122/09).

References

[1] Kamiński R. Jarzembska K.N. Kutyła S.E. Kamiński M. J.Appl.Cryst.2016, 49, 1383-1387

Figure1

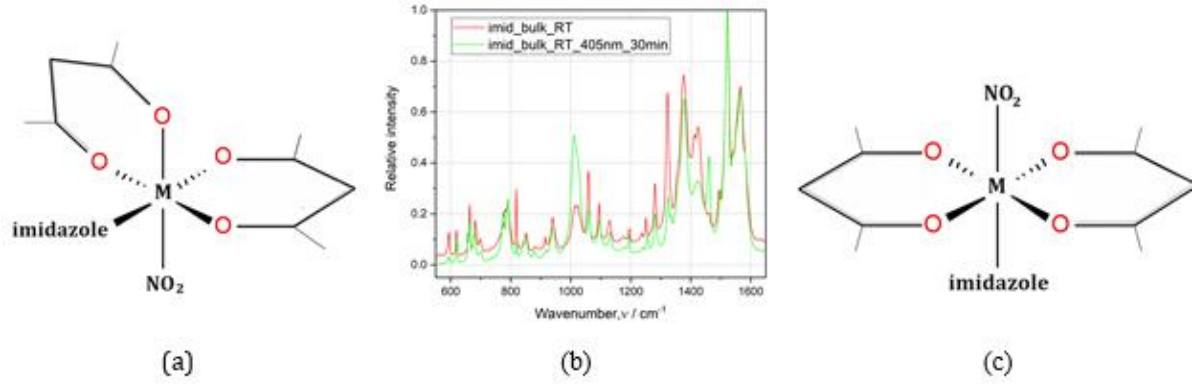

Back to Table of contents

MS40 Operando and in-situ crystallographic studies

MS40-2-2 Factors governing photoswitchability of selected nickel(II) nitro complexes #MS40-2-2

K. Potempa [1], K.A. Deresz [1], A. Krówczyński [2], D. Schaniel [3], R. Kamiński [1], K.N. Jarzembska [1]
[1]Department of Chemistry, University of Warsaw - Warsaw (Poland), [2]Department of Chemistry, University of Warsaw - Warsaw (Poland) - Warsaw (Poland), [3]Université de Lorraine, CNRS, CRM2 - Nancy (France)

Abstract
Development of effective photoswitchable compounds has gained great amount of interest in recent years due to their applicability in optoelectronics, photonics and photovoltaics [1]. The most desirable materials are characterised by high efficiency of the light-induced reaction in the solid, close to ambient working temperature and stability.
Amongst many types of structure-altering processes induced by external factors such as temperature, pressure and/or electromagnetic radiation, system undergoing linkage isomerism are suitable candidates for photoswitchable materials. Essential for this phenomenon to occur is the presence of ambidentate ligands such as NO, NO_2, SO_2 that provide many different coordination modes.
Apart from external factors which may trigger linkage isomerism reactions, there are also internal factors which may facilitate or hamper this process, including crystal packing and intermolecular interactions. Especially important here are hydrogen bonds involving the ambidante groups which have decisive influence on their freedom of movement during linkage isomerism reaction [2]. Another important factor is the reaction cavity volume i.e. the amount of space available for the ambidentate ligand.
In order to find effective photoswitchable compounds there was prepared a series of nickel complexes with nitrite group serving as an ambidentate ligand that were thoroughly investigated crystalographically and spectroscopically. Three nickel complexes with various photoswitchable properties are presented here. Great amount of attention was paid to structural analysis that would contribute to design of this kind of compounds in the future. The examined compounds varied in amount of nitrite groups present in the structure and by the size and structure of ancillary ligands. Compounds with less favourable potential to undergo photoisomeration possessed two smaller ancillary ligands – derivatives of ethylenediamine. In comparison, it turned out that bulky (N,N,O) chelating ligand are much more beneficial. Structural investigations were supported by Hirshfeld surface analysis and computational modelling at the B3LYP/6-311++G** level of theory.

References
[1] J. M. Cole, Zeitschrift Fur Kristallographie, 2008, 223, 4-5/2008.
[2] Hatcher, L. E., Bigos, E. J., Bryant, M. J., MacCready, E. M., Robinson, T. P., Saunders, L. K., … Raithby, P. R., CrystEngComm, 2014,16(35), 8263–8271.

Back to Table of contents

MS40 Operando and in-situ crystallographic studies

MS40-2-3 Photocrystallographic studies on linkage isomers using an ensemble of complementary methods #MS40-2-3

D. Schaniel [1], A. Mikhailov [2], G. Kostin [2], T. Woike [1], A. Gansmuller [1]
[1]CRM2 - Nancy (France), [2]Nikolaev Institute of Inorganic Chemistry SB RAS - Novosibirsk (Russian Federation)

Abstract
We present results on the structure and properties of photoinduced linkage isomers (PLI), corresponding to nitrosyl (GS) and isonitrosyl (MS1) configurations of the NO ligand, in ruthenium nitrosyl compounds using in-situ X-ray diffraction (XRD) and NMR [1]. The solid-state NMR investigations of the PLI in trans-[Ru(py)$_4$(^{15}NO)^{19}F](ClO$_4$)$_2$ were performed at temperatures below T = 250 K using a dedicated setup [2]. The results are analyzed in combination with periodic DFT calculations and compared to the results of XRD [3] . The obtained results show the applicability of solid-state multinuclear NMR technique for the investigation of PLI in nitrosyl complexes. The sensitivity and resolution of the NMR technique provides clearly resolved signals from two chemically identical but structurally independent complex cations in both ^{19}F and ^{15}N NMR spectra. These measurements allow determining independently both achieved populations of PLI and the rates of reverse transformation for two crystallographic sites. Measurement of ^{19}F T_1 relaxation show that the compounds are diamagnetic in MS1 as well as in GS. Structural details and changes of the electron density were obtained by measuring the chemical shift tensors of ^{15}N, ^{19}F as well as the two bond 2J(^{19}F-Ru-^{15}N) and three bond 3J(^{19}F-Ru-O-^{15}N) couplings in GS and MS1. Analysis of the NMR results by DFT calculations allowed the assignment of the NMR signals and showed the consistency of the results with the X-ray based structural models. Calculation of the spin-spin ^{15}N-^{19}F J-couplings showed that the relative direction of the nuclear spins on ^{15}N and ^{19}F are the same in GS and MS1 after the rotation of the NO-ligand, and charge density analysis indicates that there is only a small re-distribution of the charges going from GS to MS1. Globally, these results show that the solid-state NMR technique well complements other photocrystallographic methods such as in-situ X-ray diffraction, IR spectroscopy, and calorimetry in the investigation of solid-state light-induced isomers. In that respect the approach presented here opens the door to new NMR studies of such photo-commutating complexes. This should allow the comparison of commutation activation energies of different sites within the same crystals, and open new perspectives on future studies with different ligands and counterions in order to understand the effect of structure and electrostatic interactions on the photocommutation properties.

References
[1] This work was financially supported by a joint ANR-RSF project, grants no ANR-21-CE30-0045-0 and RSF-22-43-09001, respectively.
[2] A. Gansmuller, A. A. Mikhailov, G. A. Kostin, J. Raya, C. Palin, T. Woike, D. Schaniel, Anal. Chem. 2022, 94, 4474.
[3] A. A. Mikhailov, E. Wenger, G. A. Kostin, D. Schaniel, Chem. Eur. J. 2019, 25, 7569.

Back to Table of contents

MS40 Operando and in-situ crystallographic studies

MS40-2-4 XRDynamic 500: The Automated Multipurpose Powder X-Ray Diffractometer from Anton Paar #MS40-2-4

A. Jones [1], M. Kremer [1], T. Müller [1], B. Puhr [1], B. Schrode [1], P. Vir [1]
[1]Anton Paar GmbH - Graz (Austria)

Abstract
With the launch of the XRDynamic 500 automated multipurpose powder X-ray diffractometer, Anton Paar is breaking new ground in XRD and taking materials research to the next level. In this presentation the key features and benefits of XRDynamic 500 will be presented.
The core of XRDynamic 500 is the TruBeam™ concept. TruBeam™ comprises a large goniometer radius and evacuated optics units, automatic change of the beam geometry and all optics components, and automated instrument and sample alignment routines. All of these features combine to deliver outstanding data quality (in terms of both resolution and signal-to-noise ratio) that can be measured with high efficiency in a straight-forward manner; even users new to XRD can measure excellent quality XRD data every time. The high level of automation means that you can perform measurements on one or many samples with different geometries and instrument configurations in one batch with no user intervention needed.
In addition to the key instrument features and benefits, application examples will also be presented. XRDynamic 500 is suitable for powder XRD (in reflection and transmission), grazing incidence XRD, non-ambient XRD, PDF analysis, SAXS and more, covering a huge range of sample types and application fields. A wide variety of sample stages and sample holders ensures that there is an optimized instrument configuration available no matter the type of sample.

XRDynamic 500

Back to Table of contents

MS40 Operando and in-situ crystallographic studies

MS40-2-5 How to do it? On-line single crystal irradiation and spectroscopic measurements at in-house X-ray diffraction laboratory
#MS40-2-5

K. Konieczny [1], A. Hasil [2], D. Schaniel [2], S. Pillet [1]
[1]Laboratoire de Cristallographie, Résonance Magnétique et Modélisations CRM2, CNRS, Université de Lorraine - Nancy (France), [2]Laboratoire de Cristallographie, Résonance Magnétique et Modélisations CRM2, Université de Lorraine - Nancy (France)

Abstract
With the development of hardware and ideas in crystallography field single-crystal studies becomes more and more demanding, thus more and more often a need of use complementary techniques in order to support X-ray diffraction data occurs.
Ideally, all complementary techniques should be used on the exactly same sample, in the exactly same conditions as for X-ray diffraction measurement. This however requires all the experimental set-ups mounted within the diffractometer, what creates difficulties due to limited space and goniometer movements during x-ray diffraction measurement. On the other hand, goniometer allows a crystal orientation in chosen direction, what is crucial for spectroscopic measurements.
In the literature most of on-line experimental set-ups are mounted at synchrotron facilities,[1–14] where space requirements are not that demanding, and very often hardware capabilities are greater. In- house solutions are rarely described.[15,16]
In this presentation we will focus on techniques requiring proper wavelength guiding from UV-IR range acting as external stimulus inducing structural changes within a crystal or to perform spectroscopic measurements on a single crystal. Our set-up is designed by crystallographers for crystallographers. We tried to find user friendly solutions, providing high efficiency and universal applications avoiding compromises.
We will discuss mostly the practical aspects when building on-line set-ups from sample preparation, through the selection of optics and data processing, to the analysis of the results. We will point out the biggest difficulties and most challenging topics with presentation of ready apparatus solutions with description of used components and applications, such as optical absorption and photoluminescence measurements on a single crystal.

References
[1] Nanao, M. H. & Ravelli, R. B. G., Structure 14, 791–800 (2006).
[2] Carpentier, P., Royant, A., Ohana, J. & Bourgeois, D., J. Appl. Crystallogr. 40, 1113–1122 (2007).
[3] Orville, A. M. et al., J. Synchrotron Radiat. 18, 358–366 (2011).
[4] Von Stetten, D. et al., Acta Crystallogr. Sect. D Biol. Crystallogr. 71, 15–26 (2015).
[5] Pompidor, G., Dworkowski, F. S. N., Thominet, V., Schulze-Briese, C. & Fuchs, M. R., J. Synchrotron Radiat. 20, 765–776 (2013).
[6] Weik, M., Vernede, X., Royant, A. & Bourgeois, D., Biophys. J. 86, 3176–3185 (2004).
[7] De la Mora-Rey, T. & Wilmot, C. M., Curr. Opin. Struct. Biol. 17, 580–586 (2007).
[8] Ellis, M. J., Buffey, S. G., Hough, M. A. & Hasnain, S. S., J. Synchrotron Radiat. 15, 433–439 (2008).
[9] McGeehan, J. E., Carpentier, P., Royant, A., Bourgeois, D. & Ravelli, R. B. G., J. Synchrotron Radiat. 14, 99–108 (2007).
[10] Owen, R. L. et al., J. Synchrotron Radiat. 16, 173–182 (2009).
[11] Pearson, A. R. & Owen, R. L., Biochem. Soc. Trans. 37, 378–381 (2009).
[12] Royant, A. et al., J. Appl. Crystallogr. 40, 1105–1112 (2007).
[13] Sakai, K., Matsui, Y., Kouyama, T., Shiro, Y. & Adachi, S. I., J. Appl. Crystallogr. 35, 270–273 (2002).
[14] Shimizu, N. et al., J. Synchrotron Radiat. 20, 948–952 (2013).
[15] Kamiński, R., Jarzembska, K. N., Kutyła, S. E. & Kamiński, M. A., J. Appl. Crystallogr. 49, 1383–1387 (2016).
[16] Yufit, D. S., J. Appl. Crystallogr. 50, 1556–1558 (2017).

Fig. 1. The design of the experimental set-up

Back to Table of contents

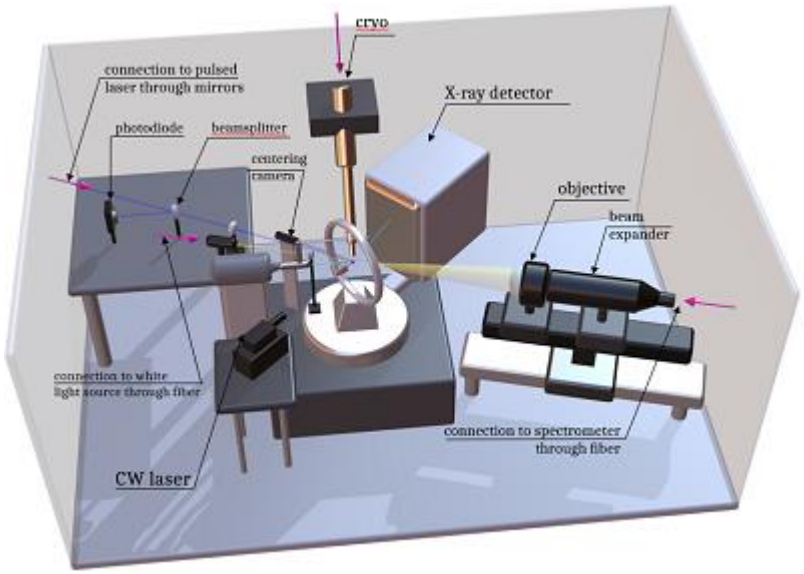

Back to Table of contents

MS40 Operando and in-situ crystallographic studies

MS40-2-6 In situ 3D observations of a core-shell volume transition in a Ni_3Fe nanocrystal using Bragg Coherent X-ray Diffraction Imaging
#MS40-2-6

C. Chatelier [1], C. Atlan [1], M. Dupraz [1], N. Li [1], E. Rabkin [2], S. Labat [3], J. Eymery [4], M.I. Richard [1]
[1]CEA Grenoble - ESRF - Grenoble (France), [2]Technion-Israel Institute of Technology - Haifa (Israel), [3]IM2NP - Aix Marseille Université - Marseille (France), [4]CEA Grenoble - Grenoble (France)

Abstract
Coherent X-ray Diffraction Imaging (CDI) [1] allows for the *in situ* 3D mapping of the structural changes during phase transitions and chemical reactions, with a fair spatial resolution of the order of magnitude of 10 nm [2]. Using this technique in multi-Bragg conditions (Bragg CDI on multiple reflections), it was possible to follow the structural evolution (change in morphology, variation of the displacement and strain fields) as a function of temperature in a 300 nm Ni_3Fe nanocrystal. During this volume transition, which happens between 500°C and 600°C, a core-shell structure is progressively observed with two distinct lattice parameters (difference of 0.39%, corresponding to two different Ni:Fe ratios), leading to highly strained and coherent domains. A rounding of the particle is also observed, with a disappearing of the initial facets. Static molecular calculations (LAMMPS) of different systems, such as faceted and core-shell nanoparticles, complete this work and allow for the confirmation of a core-shell structure. This study shows the perfect ability of modern phase retrieval methods to reconstruct highly strained systems such as core-shell nanoparticles.

References
[1] I. Robinson and R. Harder, Coherent X-Ray Diffraction Imaging of Strain at the Nanoscale, Nat. Mater. 8, 291 (2009).
[2] S. Labat, M.-I. Richard, M. Dupraz, M. Gailhanou, G. Beutier, M. Verdier, F. Mastropietro, T. W. Cornelius, T. U. Schülli, J. Eymery, and O. Thomas, Inversion Domain Boundaries in GaN Wires Revealed by Coherent Bragg Imaging, ACS Nano 9, 9210 (2015).

BCDI analysis (a) before and (b) after annealing

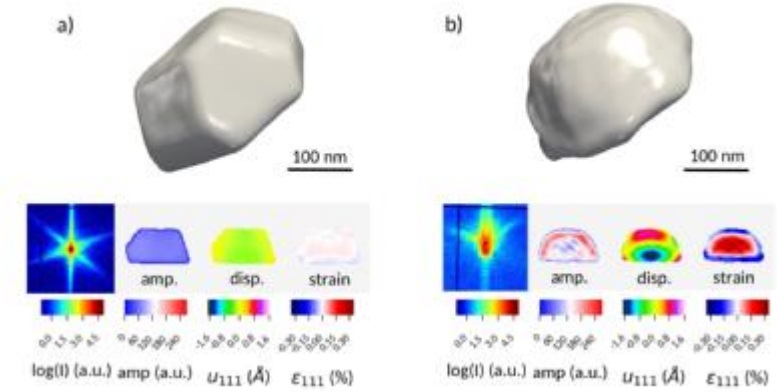

LAMMPS simulations: (a) faceted and (b) core-shell

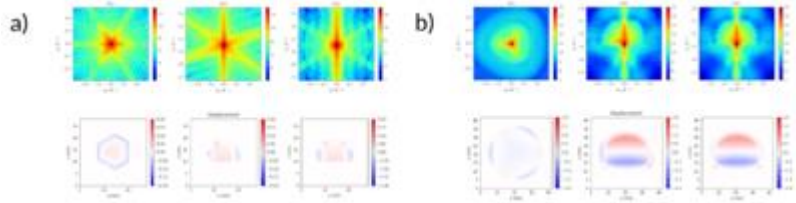

Back to Table of contents

MS40 Operando and in-situ crystallographic studies

MS40-2-7 Operando potential-induced strain heterogeneity of a breathing Pt nanoparticle
#MS40-2-7

C. Atlan [1], C. Chatelier [1], A. Viola [2], M. Dupraz [3], S. Leake [4], J. Eymery [1], F. Maillard [2], M.I. Richard [1]
[1]Univ. Grenoble Alpes, CEA Grenoble, IRIG, MEM, NRS - Grenoble (France), [2]Univ. Grenoble Alpes, CNRS, Grenoble INP, Univ. Savoie Mont Blanc, LEPMI - Saint-Martin-d'Hères (France), [3]Univ. Grenoble Alpes, CNRS - Saint-Martin-d'Hères (France), [4]ESRF - The European Synchrotron - Grenoble (France)

Abstract
Pt nanoparticles and their alloys are frequently used as catalysts in a large number of (electro)chemical processes. Understanding how the structure of these catalysts evolve during the reaction is a major challenge to optimize their catalityc performance and activity. Since coherent X-ray diffraction imaging [1, 2] is a non-destructive technique, it allows for the *in situ* and *operando* 3D mapping of the sctuctural response of single nanoparticles during electrochemical reaction (*i.e.* for diffferent electrode potentials) and for different types of electrolyte.
Here, we show that the use of this technique allows to follow the 3D evolution of the strain of a Pt nanoparticle during an electrochemical reaction (see Figure 1). More precisely, we show evidence of heterogeneous and potential-dependent strain distribution between highly-coordinated ({100} and {111} facets) and under-coordinated atoms (edges and corners) as well as evidence of strain propagation from the surface to the bulk of the nanoparticle (see Figure 2). The heterogeneity of strain distribution depends on the electrode potential and reaches as large as 0.08 % at oxygen reduction reaction-relevant potential. These results provide dynamic structural insights to better simulate and design efficient nanocatalysts for energy storage and conversion applications.

References
[1] I. Robinson and R. Harder, Coherent X-Ray Diffraction Imaging of Strain at the Nanoscale, Nat. Mater. 8, 291 (2009).
[2] J. Carnis, L. Gao, S. Fernández, G. Chahine, T. U. Schülli, S. Labat, E. J. M. Hensen, O. Thomas, J. P. Hofmann, and M.-I. Richard, Facet-Dependent Strain Determination in Electrochemically Synthetized Platinum Model Catalytic Nanoparticles, Small accepted (2021).

1: Electrode potential influence on surface strain

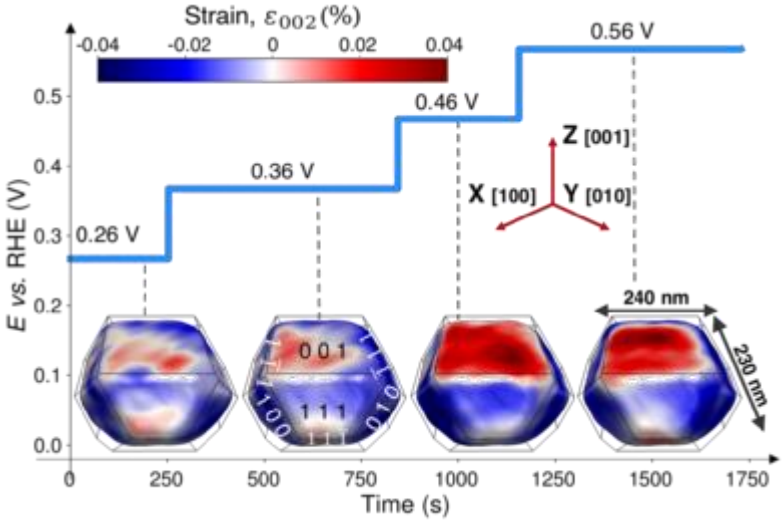

2: strain - displacement relationship

Back to Table of contents

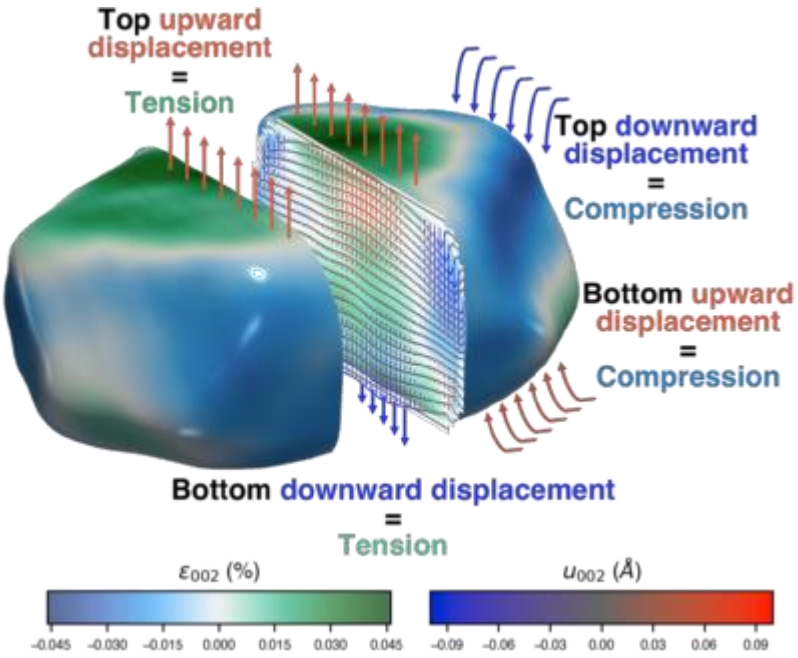

Back to Table of contents

MS40 Operando and in-situ crystallographic studies

MS40-2-8 Stoichiometry and C-rate impact on NMC/Graphite lithiation : an in situ and operando study #MS40-2-8

S. Tardif [1], T. Jousseaume [1], J.F. Colin [1], M. Chandesris [1], S. Lyonnard [1]
[1]CEA - Grenoble (France)

Abstract
Recent developments in the Li-ion technology have triggered a paradigm shift in the automotive industry and the rise of the electric vehicle (EV). Yet, to fully eclipse fossil fuels, electrochemical batteries must improve their energy capacity, power density, safety and cost efficiency. Focusing here on the electrode materials, the layered compound family $LiNi_xMn_yCo_zO_2$ (NMCxyz) holds great promise. Increasing the Ni content allows to extract more lithium in a potential window compatible with standard electrolytes. However, it also results in a destabilisation of the crystal structure, leading to irreversible capacity losses. A clear understanding of the lithiation mechanism as a function of the Ni content is thus much needed to later optimize the electrode design for better performances. A second factor for irreversible capacity losses is the charge rate. Whereas fast charging is of paramount importance for the EV, the large electric currents implied can lead to and/or enhance the heterogeneous behaviour of the electrode, resulting in premature aging. Rate dependence and material phases evolution are closely related by the chemical potential [1]. That is why the coupled analysis of these two aspects is necessary and the comparison of dynamic (*operando*) and static (*in situ*) mechanisms could distinguish new models from literature [2].
In this study, we followed the lithiation and delithiation mechanism in graphite and NMC electrodes with three different stoichiometries (Ni fraction from 0.6 to 1) in the exact same experimental conditions (setup, cycling conditions) to evidence the lithiation mechanisms. Synchrotron operando X-ray diffraction (XRD) was performed to have both high temporal resolution, angular resolution and wide-angle range required for a precise description of the lithiation and delithiation of the investigated materials. Both graphite and NMC materials were analysed by pattern-matching to follow their crystallographic structure, and thus the lithiation pathway. The comparison was further performed with the dynamics at lower rates (i.e. equilibrium or quasi-equilibrium, as investigated on a Cu-K_α diffractometer with Bragg-Brentano geometry.
We highlight similarities and differences in the insertion mechanisms of the different NMC materials, as a function of the C-rate. We also reveal the impact of the charge rate on the intercalation mechanism of NMC as well as of graphite, showing the importance of the layered compound nature, and supported by numerical simulations. For the first time, the confrontation of lithiation models under either dynamic (with no electrochemical reactions pause) or static (system at equilibrium) conditions broaden our knowledge of lithium insertion thanks to the parallel utilisation of *in situ* and *operando* techniques.

References
[1] Tardif, S. et al, J. Mater. Chem. A, 2021, 9, 4281-4290[2] Park, J. et al, Nature Materials, 2021

Back to Table of contents

MS41 Automation in data collection and processing

MS41-1-1 SOLEIL ongoing development using industrial robots for beamline automation.
#MS41-1-1

Y.M. Abiven [1], L.E. Muñoz [1], J. Da Silva Castro [1], G. Correc [1], E. Elkaim [1], P. Fertey [1], F. Legrand [1], K. Medjoubi [1], A. Noureddine [1], F. Ribaud [1], A. Somogyi [1], V. Jacques [2]
[1]Synchrotron SOLEIL - Saint Aubin (France), [2]Laboratoire de Physique des Solides - Orsay (France)

Abstract
SOLEIL [1] already provides a large variety of experimental techniques, and sample environments to its user communities throughout its 29 beamlines. Looking towards the future, SOLEIL teams are currently working towards a technical proposal of an ambitious upgrade of SOLEIL [2], aiming at an improvement in brilliance, coherence and flux. The upgrade of the facility will be accompanied by the offer of new access mode to benefit efficiently from these new performances.
Following actual trends, the new sources will bring up a data deluge especially resulting from multi-technique, fast 2D detectors, and automatization improvement. To address these scientific challenges, a Data-driven approach has been adopted as strategy in technical and scientific fields. In this perspective, new automated processes are currently under development involving industrial robot [3] to improve samples throughput or to manipulate the detectors in multiple positions through large working spaces and complex end-stations. These new applications can benefit from robotization, in particular for diffraction techniques This automatization will integrate Artificial Intelligence (AI) algorithms to complete acquisition scanning technics allowing optimization of complex feedbacks and data processing.
Over the last decade, the beamlines such as PROXIMA1[4] and PROXIMA2[5] at SOLEIL, for macromolecular crystallography, have implemented industrial robots with their dedicated control system. Recently, a SOLEIL standard to integrate STAUBLI [6] robots into TANGO [7] control system has been built and is ready to be declined in the applications identified in the roadmap. A first system for picking and placing samples has been deployed in the powder instrument at CRISTAL [8] beamline. Currently under commissioning, another robot to automate the positioning of a detector was installed at the NANOSCOPIUM [9] beamline in order to add wide-angle nano-diffraction to its X-ray imaging modalities.

References
[1] Synchrotron SOLEIL, https://www.synchrotron-soleil.fr/
[2] https://www.synchrotron-soleil.fr/fr/actualites/avant-projet-sommaire-pour-lupgrade-de-soleil
[3] Y. M. Abiven, L. E. Munoz, F. Briquez, M. E. Couprie, E. Elkaim, K. Medjoubi, A. Noureddine, A. Somogyi & M. Valléau (2021) SOLEIL'S Process Automation Improvement Using Industrial Robots, Synchrotron Radiation News, 34:4, 10-17, DOI: 10.1080/08940886.2021.1968268
[4] Chavas, L. M. G., et al., "PROXIMA-1 beamline for macromolecular crystallography measurements at Synchrotron SOLEIL", Journal of Synchrotron Radiation, vol. 28, pp 970-976, 2021.
[5] PROXIMA 2 beamline, https://www.synchrotron-soleil.fr/en/beamlines/proxima-2a
[6] Stäubli Robotics, https://www.staubli.com/en-fr/robotics
[7] Tango Controls, https://www.tango-controls.org
[8] CRISTAL beamline, https://www.synchrotron-soleil.fr/en/beamlines/cristal
[9] NANOSCOPIUM beamline, https://www.synchrotron-soleil.fr/en/beamlines/nanoscopium

Back to Table of contents

MS41 Automation in data collection and processing

MS41-1-2 Data treatment at Synchrotron SOLEIL: automation, IA, on-demand computing, packaging #MS41-1-2

E. Farhi [1], O. Roudenko [1], F.E. Picca [1], A. Bellachehab [1], S. Bac [1], M. Ounsy [1]
[1]Synchrotron SOLEIL - Saint-Aubin (France)

Abstract
We shall present the reduction and analysis initiatives undertaken at Synchrotron SOLEIL. In terms of data treatment automation, we have implemented automatic data reduction pipe-lines for surface diffraction (using libHKL and Binoculars), auto-processing for MX beamlines, and a set of Jupyter Notebooks for absorption spectroscopy data.
We are also developing new AI algorithms targeted to automatic data reduction. Examples include de-noising of microscopy images as well as inelastic ARPES data sets, classifying SAXS datasets into scatterer model groups for further fit (based on SASmodels and McXtrace [1]). Further studies include an element identification and oxidation state estimator for absorption spectroscopy (XANES), as well as a Bravais lattice/space group estimator for powder diffraction.
Last, we provide computing resources in the form of a JupyterHub portal, and the DARTS service [2] with virtual machine on-demand for data treatment computing. Our strategy is to keep in touch with beam-lines to inquire for their software needs, feed these services with this software that we push as X/neutron Debian packages [3], and always favour simplest solutions.

References
[1] McXtrace <http://mcxtrace.org/>
[2] DARTS/qemu-web-desktop <https://gitlab.com/soleil-data-treatment/soleil-software-projects/remote-desktop>
[3] Photons-and-Neutrons Debian packaging <https://salsa.debian.org/pan-team/soleil-packaging-overview>

McXtrace beam-line modelling

DARTS on-demand computing

Back to Table of contents

MS41 Automation in data collection and processing

MS41-1-3 DARTS on-demand computing
#MS41-1-3

E. Farhi [1]
[1]Synchrotron SOLEIL - Saint-Aubin (France)

Abstract
The Data Analysis Remote Treatment Service (DARTS) [1] is a remote desktop service that launches virtual machines in the cloud, and displays them in your browser. These machines can be used for e.g. scientific data treatment. A user indicates how many CPU cores and how much memory he wishes, can optionally request a GPU for heavy-duty computations, and can be customized at start-up. The sessions typically start in about 10 seconds, and can be shared with colleagues within their life-time (typically 4 days). Each user can manage all his active sessions (connect, stop, share). This service can be installed and configured within a few minutes (sudo apt install qemu-web-desktop), and it requires minimal maintenance. The source code is fully open-source, and relies on very simple elements (Apache web-server and QEMU). Give it a try !
We provide at Synchrotron SOLEIL a set of prepared environments with plenty of scientific software for e.g. crystallography, spectroscopy, imaging, tomography, etc. A specialized environment has also been set-up for AlphaFold protein structure prediction.

References
[1] DARTS https://gitlab.com/soleil-data-treatment/soleil-software-projects/remote-desktop

DARTS on-demand computing

Create a data treatment session

Back to Table of contents

MS41 Automation in data collection and processing

MS41-1-4 Automated high-throughput X-ray PDF data collections on the I15-1 beamline at Diamond Light Source #MS41-1-4

P. Chater [1]
[1]**Diamond Light Source - Oxfordshire (United Kingdom)**

Abstract
The I15-1 XPDF beamline at Diamond Light Source is committed to the fast and reliable production of total scattering and pair distribution function (PDF) data. Since becoming operational in 2017, I15-1 has welcomed users from a diverse range of disciplines such as materials science, energy materials, earth sciences and pharmaceuticals. Over the last few years I15-1 has undergone significant changes to improve the beamline hardware and software.
A robotic sample changing system has been implemented which allows up to 440 samples to be loaded at one time for high-throughput or remote access experiments at temperatures from 100 to 1000 K. A new bespoke detector is currently in commissioning which will dramatically improve both the speed and quality of the PDF data produced.
Software developments have delivered improved LIMS and we are currently testing novel automatic PDF processing capabilities. These developments allow aspects of experiments to be tracked in real-time, both while at Diamond and off-site, and offer an improved user experience.

Robotic sample changing system on I15-1.

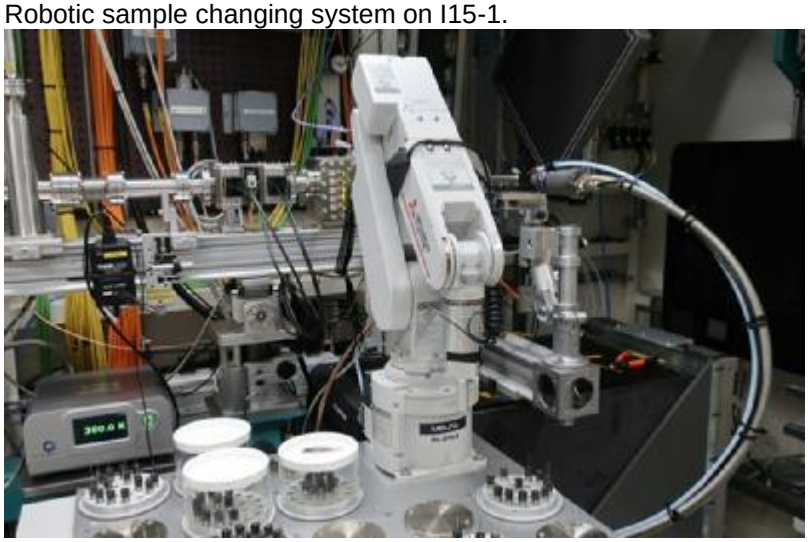

Back to Table of contents

MS41 Automation in data collection and processing

MS41-2-1 Introducing the XtaLAB Synergy Flow
#MS41-2-1

P. Le Magueres [1], M. Del Campo [1], J. Ferrara [1], M. Meyer [2], D. Kucharczyk [3], A. Wisniewski [4], P. Stec [4], J. Gordon [1]
[1]Rigaku Americas Corporation - The Woodlands (United States), [2]RigakuEurope SE - Wroclaw (Poland), [3]Rigaku Polska - Wroclaw (Poland), [4]Rigaku Polska - Wrocław (Poland)

Abstract
The XtaLAB Synergy Flow turns any Synergy cabinet diffractometer into an automated, high-throughput machine by incorporating a 6-axis UR3 Universal Robot and a 3-puck dewar. The Flow system can automatically screen and collect 48 crystal samples with minimal human intervention. CrysAlisPro has been upgraded with tools to control all aspects of robotics and sample queuing. A unique X-ray safe dewar-drawer system allows loading and unloading of pucks without opening the X-ray enclosure or disturbing data collection. Ultimately, the XtaLAB Synergy Flow system is the perfect solution to allow full-time use of your diffractometer during a time when human interaction and contamination must be minimized.

Back to Table of contents

MS41 Automation in data collection and processing

MS41-2-2 Algorithms for automated detection of (near-)duplicate periodic crystals
#MS41-2-2

V. Kurlin [1]
[1]**Materials Innovation Factory, University of Liverpool - Liverpool (United Kingdom)**

Abstract
A periodic crystal is usually given in a Crystallographic Information File as a pair of a (primitive, conventional, or reduced) unit cell and a motif of atoms with fractional coordinates with respect to a cell basis. This traditional representation is highly ambiguous because the same crystal can be given by infinitely many pairs of a cell basis and a motif of atoms.
Since crystal structures are determined in a rigid form, their most practical equivalence is rigid motion (a composition of translations and rotations) or isometry (including reflections), which maintain all inter-atomic distances. The most natural definition of a periodic crystal is not a single set of points given but an isometry class of infinitely many periodic point sets that are all equivalent to each other up to isometry.
This new definition clarifies the key question “same or different” that remained unresolved [2] by classical tools such as the powder diffraction pattern (PXRD) and packing similarity (RMSD implemented by Mercury). Both similarities RMSD and 1-PXRD fail the triangle inequality [3], which should be satisfied by any well-defined metric. Figure 1 (left) shows that almost any tiny displacement (thermal vibration) of atoms discontinuously affects classical invariants based on symmetry groups or reduced (conventional) cells that can double in size.
To reliably detect (near-)duplicates appearing in all experimental databases and paper mills [1], periodic crystals should be compared by their complete isometry invariants, which are crystal descriptors with no false negatives and no false positives. The first complete invariants of all periodic crystals are the isosets [4] whose key ingredients are local clusters of a radius alpha around motif points. Figure 1 (middle and right) shows how these clusters grow when the radius alpha is increasing. Isometry classes of all alpha-clusters are arranged into a hierarchical isotree showing their evolution for all alpha, see Figure 2. The isotree always stabilizes for any periodic point set and algorithmically detects an isometry in a time cubically depending on the size of a motif.
A continuous metric on isosets was approximated with a factor of only 4 in 3-space [5]. These results were confirmed by 200B+ pairwise comparisons of all 660K+ periodic crystals in the Cambridge Structural Database, which took a couple of days on a modest desktop [6] and detected five pairs of isometric duplicates where one atom is replaced by a different one, for example, Cd by Mn in HIFCAB vs JEPLIA.

References
[1] Bimler, David. Better Living through Coordination Chemistry: A descriptive study of a prolific papermill that combines crystallography and medicine, IUCr Newsletter April 2022
https://www.chemistryworld.com/news/800-crystallography-related-papers-appear-to-stem-from-one-paper-mill/4015589.article.
[2] Sacchi, P., Matteo Lusi, M., Cruz-Cabeza, A.J., Nauhac, E.Joel Bernstein, J. Same or different – that is the question: identification of crystal forms from crystal structure data. CrystEngComm 22 (43), 7170-7185, 2020.
[3] Widdowson, D., Kurlin, V., Pointwise Distance Distributions of finite and periodic point sets. Arxiv.org:2108.04798. The latest version is at http://kurlin.org/projects/periodic-geometry-topology/PDD.pdf
[4] Anosova, O., Kurlin, V. An isometry classification of periodic point sets. Peer-reviewed Proceedings of Discrete Geometry and Mathematical Morphology 2021, p. 229-241. Available at http://kurlin.org/projects/projects/periodic-geometry-topology/crystal-isosets-complete.pdf
[5] Anosova, O., Kurlin, V. Algorithms for continuous metrics on periodic crystals. Arxiv: 2205.15298. The latest version is available at http://kurlin.org/projects/projects/periodic-geometry-topology/isoset-metric.pdf
[6] Widdowson, D., Mosca, M.M., Pulido, A., Kurlin, V., Cooper, A.I. Average Minimum Distances of periodic point sets - fundamental invariants for mapping all periodic crystals. MATCH Communications in Mathematical and in Computer Chemistry, v.87(3), p.529-559, 2022. Available at http://kurlin.org/projects/periodic-geometry-topology/AMD.pdf

Discontinuity of most invariants under vibration

Back to Table of contents

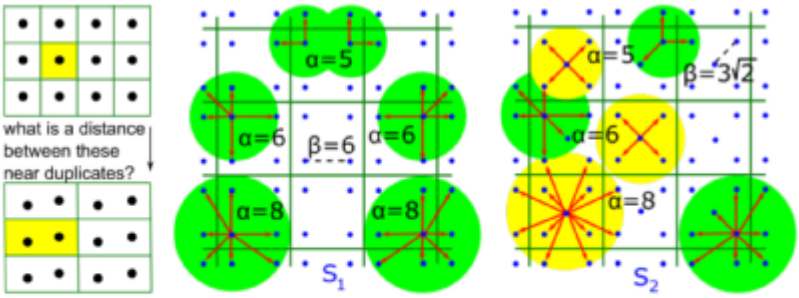

Figure 1: **Left**: most invariants based on symmetry groups and reduced or conventional cells are discontinuous under tiny perturbations. **Middle**: the periodic set $S_1 \subset \mathbb{R}^2$ has the square unit cell $[0,10)^2$ containing the four points $(2,2),(2,8),(8,2),(8,8)$. All local α-clusters of S_1 are isometric, shown by red arrows for $\alpha = 5,6,8$. **Right**: in comparison with S_1, the set S_2 has the extra point $(5,5)$ in the center of the cell $[0,10)^2$, so S_2 has green and yellow isometry types of α-clusters.

Isotree visualizing the complete invariant isoset

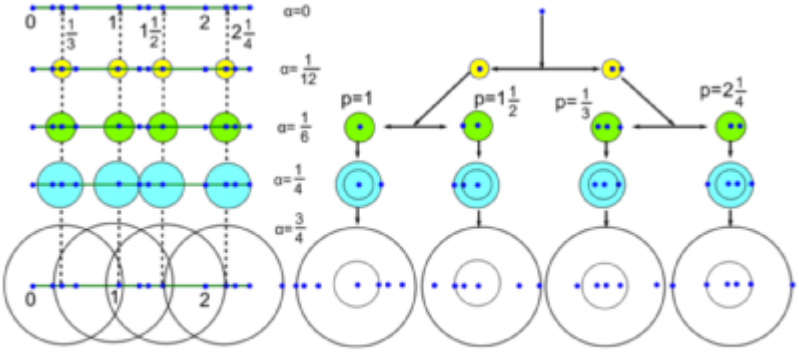

Figure 2: **Left**: the 1-dimensional periodic set $S_4 = \{0, \frac{1}{4}, \frac{1}{3}, \frac{1}{2}\} + \mathbb{Z}$ has four points in the unit cell $[0,1)$. **Right**: the isotree $\mathrm{IT}(S_4)$ consists of isometry classes of the local α-clusters of radius α around the points of $S_4 \subset \mathbb{R}$ with radii $\alpha = 0, \frac{1}{12}, \frac{1}{6}, \frac{1}{4}, \frac{3}{4}$. The α-clusters are intervals shown by colored disks.

Back to Table of contents

MS42 Solving Structures Through Combination of Reciprocal and Direct Space Methods

MS42-1-1 Data-driven approach for the solution of the phase problem in crystallography: first insights #MS42-1-1

T. Rekis [1], A.S. Larsen [1], A.Ø. Madsen [1]
[1]University of Copenhagen - København Ø (Denmark)

Abstract
For a crystal structure to be solved from the diffraction data, it is necessary to obtain the complex structure factors, $\boldsymbol{F}_{\mathbf{H}}$, of the measured reflections. Their squared moduli, $|\boldsymbol{F}_{\mathbf{H}}|^2$, are proportional to the measured intensities, but the phase angles to reconstruct the complete complex numbers cannot be determined experimentally. Since the exact solution to this phase problem is not known, several methods to overcome this crucial step in crystal structure determination have been developed over time. For example, direct methods or charge flipping algorithm can be used for most organic, inorganic, and metal-organic structures. Nevertheless, these methods fail if, for example, the available data resolution is not sufficiently high. Furthermore, they cannot be used to solve protein structures intrinsically having large unit cells with hundreds of atoms in the asymmetric units.
In our study, we have attempted to solve the phase problem using a neural network. We focused on small organic molecule and metal-organic structures in the most common space group $P2_1/c$. Millions of fictive structures containing metal atoms and/or molecular fragments were generated to train the neural network. Validation set consisted of over a thousand structures retrieved from the Cambridge Structural Database for which the structure factor amplitudes, $|\boldsymbol{F}_{\mathbf{H}}|$, were generated at several resolution limits and fed into the trained network to output phases. The phases could be retrieved with a striking accuracy leading to correct structure solutions for over 99% of the validation set entries. Furthermore, the phase accuracy was also high if the resolution limit was chosen to be low, i.e. d_{min} = 1.9 Å. Several dozen of experimentally measured diffraction data sets were also used for validation. Our results hint that deep learning could be used to obtain electron density maps of structures for which only a limited resolution data can be obtained and which are problematic to solve using currently available methods.

Back to Table of contents

MS43 Crystallography for cultural heritage materials

MS43-1-1 New insights on the composition of complex-shape Cultural Heritage objects obtained with an X-ray mobile instrument
#MS43-1-1

V. Poline [1], P. Martinetto [1], P. Bordet [1], O. Leynaud [1], N. Blanc [1]
[1]CNRS - Grenoble (France)

Abstract
Investigations in Cultural Heritage (CH) research have always been facing the major issue of the fragility of the objects studied. There is an utter need for developments in mobile non-invasive and non-destructive analysis. We will show the performances of a new mobile instrument using X-ray powder diffraction (XRPD) and fluorescence (XRF) at the same point in reflection geometry. These two techniques are well-known in the CH field allowing the identification of the elements and the resulting crystalline structures without disrupting the objects' integrity [1, 2]. Moreover, the joint use of a linear and 2D detector for XRPD allows to gain insight into the microstructure of the analysed phases. We first present the analysis of an unusual metallic cover found around the neck of a burried abbot recently found in the Saint-Médard-de-Soissons abbey (13th century) [3]. The complex-shape cover is made of several lead foils with areas showing evidences of soldered joints. 2D-XRPD investigations revealed the surface carbonatation of the lead foils and two different micro-structures of lead carbonate between the foils and the soldered joints with a brazing filler material made of Pb-Sn. In addition, we present the investigations of five late medieval polychrome sculptures with sophisticate relief decoration called "applied-brocade" [4]. The instrument allowed to detect/confirm the presence of these multilayered decorations, to identify the associated phases and the main differences between their stratigraphy [5, 6]. These results show the benefits of the combined use of XRPD (1D-2D) and XRF and the importance of well-designed degrees of freedom for in situ measurements of complex-shape objects.

References
[1] A. Gianoncelli, J. Castaing, L. Ortega, E. Dooryhée, J. Salomon, P. Walter, J.-L. Hodeau, and P. Bordet, "A portable instrument for in situ determination of the chemical and phase compositions of cultural heritage objects," X-Ray Spectrometry, vol. 37, no. 4, pp. 418–423, 2008.[2] S. D. Meyer, F. Vanmeert, R. Vertongen, A. V. Loon, V. Gonzalez, J. Delaney, K. Dooley, J. Dik, G. V. der Snickt, A. Vandivere, and K. Janssens, "Macroscopic x-ray powder diffraction imaging reveals vermeer's discriminating use of lead white pigments in Girl with a Pearl Earring," Science Advances, vol. 5, no. 8, p. eaax1975, 2019.[3] ARC-Nucléart, "Prélèvement d'une sépulture à Soissons." https://www.arc-nucleart.fr/Pages/Actualites/2020/Alb%C3%A9ric.aspx, Apr. 2021. Accessed : 2021-01-03.[4] I. Geelen and D. Steyaert, Imitation and illusion : applied brocade in the art of the Low Countries in the fifteenth and sixteenth centuries. KIK-IRPA Royal Institute for Cultural Heritage, 2011. Publication Title : Scientia Artis 6.[5] P. Martinetto, N. Blanc, P. Bordet, S. Champdavoine, F. Fabre, T. Guiblain, J. L. Hodeau, F. Lelong, O. Leynaud, A. Prat, E. Pouyet, E. Uher, and P. Walter, "Non-invasive X-ray investigations of medieval sculptures : New insights on "applied tin-relief brocade" technique," Journal of Cultural Heritage, vol. 47, pp. 89–99, Jan. 2021.[6] F. Lelong, E. Pouyet, S. Champdavoine, T. Guiblain, P. Martinetto, P. Walter, H. Rousselière, and M. Cotte, "Des « brocarts appliqués » dans la sculpture savoyarde, vers une caractérisation interdisciplinaire," CeROArt, 2021.

Applied brocade examples

Mobile instrument measuring the metallic cover

Back to Table of contents

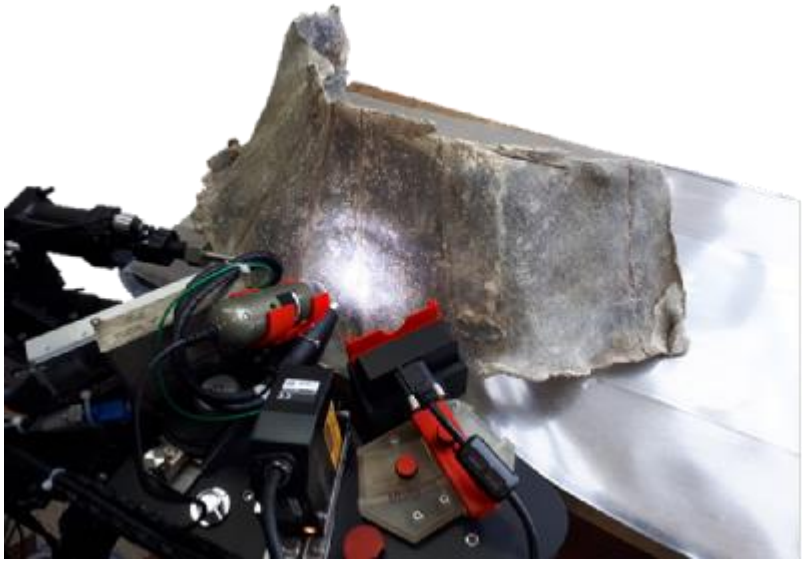

Back to Table of contents

MS43 Crystallography for cultural heritage materials

MS43-1-2 2D high lateral resolution XRPD mapping and micro-Raman analyses for the in-depth characterization of red stains on heritage marbles
#MS43-1-2

A. Suzuki [1], E. Cantisani [1], M. Ricci [2], S. Vettori [1]
[1]Institute of Heritage Science-National Research Council ISPC-CNR - Sesto fiorentino (FI) (Italy), [2]Department of Chemistry "Ugo Schiff", University of Florence - Sesto fiorentino (FI) (Italy)

Abstract
Red stains are a common alteration phenomenon on heritage marbles all over the world, very difficult to remove and affecting the aesthetical appearance and cultural and economic values of manufacts. The causes of this phenomenon have been debated for decades and several possible origins were identified (such as microorganisms, previous restoration treatments etc.). In the context of the main Florentine monuments, previous multi-analytical studies demonstrated that the red staining in these cases is due to the presence of minium (lead tetraoxide) concentrated prevalently in the calcite crystal boundaries, but also the presence of other Pb crystalline phases was suggested by preliminary micro-Raman analyses. Possible sources of Pb, the role of microorganism, the environmental conditions and physical characteristics of marbles were also evaluated [1].
In order to identify the presence of other Pb compounds and their distribution in the red stained areas, samples were collected from the marble cladding facades of the Baptistery of San Giovanni and Santa Maria del Fiore Cathedral in Florence (Italy). Thin sections of these samples were analysed with 2D high lateral resolution (few microns) X-Ray Powder Diffraction (XRPD) mapping (map size of 400 x 400 um2) available at ID13 (ESRF synchrotron facility) [2] and the same areas were analysed with micro-Raman spectroscopy. The mapping at the micrometre scale of the crystalline phases with both techniques has been successful in shedding light in the in-depth distribution of the several lead oxide phases present in the marble red stains.

References
[1] Cantisani E., et al., Analyst, 2019, 144 (7), 2375 – 2386
[2] Cotte M., et al., Molecules, 2022, 27, 1997.

Macroscopic appearance of a marble red stain.

Cross section of a red stain sample.

Back to Table of contents

Back to Table of contents

MS43 Crystallography for cultural heritage materials

MS43-2-1 Strain mapping of metallic cultural heritage objects with synchrotron microbeams #MS43-2-1

A. Schoekel [1], M. Etter [1], L. Glaser [2], A. Rothkirch [1], M. Wendt [1]
[1]Deutsches Elektronen-Synchrotron DESY - Hamburg (Germany), [2]Universitätsklinikum Hamburg Eppendorf - Hamburg (Germany)

Abstract
Diffraction mapping of metallic objects by high energy X-ray beams is a well-established method in order to spatially resolve their macroscopic and/or microscopic strain. Modern synchrotron sources allow to collect diffraction patterns with micrometer sized beams, resulting in high quality strain maps with an unprecedented resolution. So far, these methods were mostly used to study the influence of manufacturing processes and treatments on metallic components as well as symptoms of aging or fatigue on specimen.
Here we present a proof of principle of radiographic strain mapping as tool to retrieve erased hallmarks in metallic objects. We collected strain maps of different metal sheets marked with punch letters. Half of the letters were mapped as produced by powder X-ray diffraction, while the other half was erased by grinding until the letter could not be visually identified anymore before measurement. We could prove that in both cases an unambiguous strain pattern can be measured in the materials, which can be analyzed by Whole Powder Pattern Fitting methods (WPPF), Rietveld refinement or even decorrelated by Principal Component Analysis of the integrated raw data.
Based on these results, we believe that also illegible letters or hallmarks in metallic cultural heritage objects can be identified in a non-destructive way.

Back to Table of contents

MS43 Crystallography for cultural heritage materials

MS43-2-2 New insights on composition of complex-shape Cultural Heritage objects obtained with an X-ray mobile instrument
#MS43-2-2

V. Poline [1], P. Martinetto [1], P. Bordet [1], O. Leynaud [1], N. Blanc [1]
[1]Institut Néel - Grenoble (France)

Abstract
Investigations in Cultural Heritage (CH) research have always been facing the major issue of the fragility of the objects studied. There is an utter need for developments in mobile non-invasive and non-destructive analysis. We will show the performances of a new mobile instrument using X-ray powder diffraction (XRPD) and fluorescence (XRF) at the same point in reflection geometry. These two techniques are well-known in the CH field allowing the identification of the elements and the resulting crystalline structures without disrupting the objects' integrity [1, 2]. Moreover, the joint use of a linear and 2D detector for XRPD allows to gain insight into the microstructure of the analysed phases. We first present the analysis of an unusual metallic cover found around the neck of a burried abbot recently found in the Saint-Médard-de-Soissons abbey (13th century) [3]. The complex-shape cover is made of several lead foils with areas showing evidences of soldered joints. 2D-XRPD investigations revealed the surface carbonatation of the lead foils and two different micro-structures of lead carbonate between the foils and the soldered joints with a brazing filler material made of Pb-Sn. In addition, we present the investigations of five late medieval polychrome sculptures with sophisticate relief decoration called "applied-brocade" [4]. The instrument allowed to detect/confirm the presence of these multilayered decorations, to identify the associated phases and the main differences between their stratigraphy [5, 6]. These results show the benefits of the combined use of XRPD (1D-2D) and XRF and the importance of well-designed degrees of freedom for in situ measurements of complex-shape objects.

References
[1] A. Gianoncelli, J. Castaing, L. Ortega, E. Dooryhée, J. Salomon, P. Walter, J.-L. Hodeau, and P. Bordet, "A portable instrument for in situ determination of the chemical and phase compositions of cultural heritage objects," X-Ray Spectrometry, vol. 37, no. 4, pp. 418–423, 2008.[2] S. D. Meyer, F. Vanmeert, R. Vertongen, A. V. Loon, V. Gonzalez, J. Delaney, K. Dooley, J. Dik, G. V. der Snickt, A. Vandivere, and K. Janssens, "Macroscopic x-ray powder diffraction imaging reveals vermeer's discriminating use of lead white pigments in Girl with a Pearl Earring," Science Advances, vol. 5, no. 8, p. eaax1975, 2019.[3] ARC-Nucléart, "Prélèvement d'une sépulture à Soissons." https://www.arc-nucleart.fr/Pages/Actualites/2020/Alb%C3%A9ric.aspx, Apr. 2021. Accessed : 2021-01-03.[4] I. Geelen and D. Steyaert, Imitation and illusion : applied brocade in the art of the Low Countries in the fifteenth and sixteenth centuries. KIK-IRPA Royal Institute for Cultural Heritage, 2011. Publication Title : Scientia Artis 6.[5] P. Martinetto, N. Blanc, P. Bordet, S. Champdavoine, F. Fabre, T. Guiblain, J. L. Hodeau, F. Lelong, O. Leynaud, A. Prat, E. Pouyet, E. Uher, and P. Walter, "Non-invasive X-ray investigations of medieval sculptures : New insights on "applied tin-relief brocade" technique," Journal of Cultural Heritage, vol. 47, pp. 89–99, Jan. 2021.[6] F. Lelong, E. Pouyet, S. Champdavoine, T. Guiblain, P. Martinetto, P. Walter, H. Rousselière, and M. Cotte, "Des « brocarts appliqués » dans la sculpture savoyarde, vers une caractérisation interdisciplinaire," CeROArt, 2021.

Applied-brocade examples

Mobile instrument measuring an artefact

Back to Table of contents

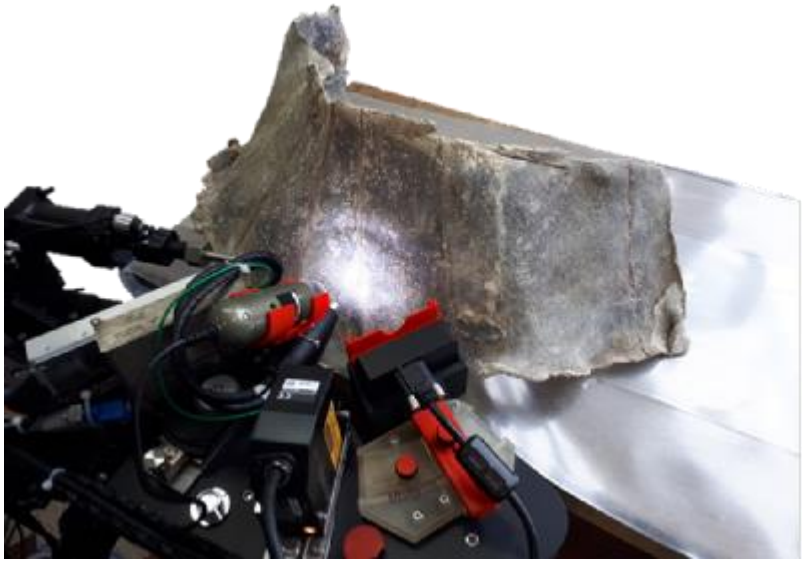

Back to Table of contents

MS43 Crystallography for cultural heritage materials

MS43-2-3 Insight into thermally-induced reduction of Plattnerite into Red Lead pigment #MS43-2-3

A. Suzuki [1], W. Oberhauser [2], I. Osticioli [3], C. Riminesi [3]
[1]Institute of Heritage Science-National Research Council ISPC-CNR - Sesto fiorentino (FI) (Italy), [2]Institute of Chemistry of OrganoMetallic Compounds ICCOM-CNR - Sesto fiorentino (FI) (Italy), [3]Institute of Applied Physics IFAC-CNR - Sesto fiorentino (FI) (Italy)

Abstract
Red lead, mixed valence state lead oxide (Pb3O4), is a bright red pigment particularly appreciated and widely used since antiquities. In mural paintings this pigment may darken due to the degradation to plattnerite (b-PbO2), which is a brown-black pigment. Up to now, no well-established conversion methods to restore darkened red lead in wall paintings have been reported. In this context, the thermally induced lead dioxide conversion into red lead can bring about new insights. In fact, in recent research the thermal effect of Near Infrared (NIR) Continuous Wave (CW) laser irradiation has been exploited and tested on mural painting mock-ups [1].
However, the apparent contradictory results reported in the literature concerning the decomposition of lead dioxide [2-4] is a strong hint for the dependence of the new lead oxide formation on temperature, heating rate and duration of the heat treatment. The formation of non-stoichiometric lead oxides as intermediate species in the plattnerite conversion has, to the best of our knowledge, not been monitored by a close analysis of the crystalline phases. Therefore, a detailed analysis of the suitable heating conditions is required to define an efficient thermal conversion method.
In the present work, a high-temperature X-ray diffraction study has been carried out on plattnerite powder samples with different temperature, heating rates, quenching or annealing and environment conditions. Each crystalline phase was then characterized by micro-Raman spectroscopy allowing the identification of specific spectral features of intermediate non-stoichiometric lead oxides. The combination of X-ray diffraction pattern with the corresponding Raman spectrum of the same crystalline phase allowed to shed light on the laser induced degradation mechanism that occur during irradiation of plattnerite with NIR CW lasers.

References
[1] de Seauve T., et al. (2021), App. Phys. B 127, 162.
[2] Otto E. M. (1966), J. Electrochem. Soc. 113 525.
[3] Aleksandrov V. V., et al. (1978), J. Therm. Anal. 205-212.
[4] Gavrichev, et al. (2008), J. Therm. Anal. Calorim. 857-863.

Back to Table of contents

MS44 Crystallography in large scale facilities

MS44-1-1 Photoactivation in a Fluorescent Protein Proceeds via the Hula-Twist : Mechanism Revealed through TR-SFX
#MS44-1-1

A. Fadini [1], J. Van Thor [1]
[1]Imperial College London - London (United Kingdom)

Abstract
The light-induced cis/trans isomerization of a chromophore double bond is a fundamental reaction in photochemistry and it has been shown to be the primary activation event for a variety of protein photoreceptors. A detailed understanding of the reaction pathway and of how it is steered by protein environment is key for the rational design of more effective photosystems.
In the 1980s, Liu&Asato coined and proposed a mechanism for chromophore photoisomerization in proteins: the hula twist. This was supposed to be volume conserving and therefore favorable inside a sterically-crowded binding pocket. By exploiting the time resolution available at XFELs and the insertion of a heavy atom to break the symmetry of the chromophore ring, we capture the ultrafast photoproduct of the trans-to-cis reaction in a fluorescent protein. This, to our knowledge, is the first direct experimental structural evidence that unequivocally supports hula-twist chromophore photoisomerization in a protein, more than 30 years after it was first hypothesized. By analyzing data from time points that span from 300 fs to 1 µs, we also resolve how photoisomerization leads to the sequential movement and relaxation of secondary structure elements. This data demonstrates the power of time-resolved crystallography for elucidating the ultrafast dynamical response in photoactivated systems.

References
Work so far unpublished.
Key relevant references :
Liu, R. S. H. & Asato, A. E. The primary process of vision and the structure of bathorhodopsin: A mechanism for photoisomerization of polyenes* (lumirhodopsin/hypsorhodopsin/binding site/concerted twist). Proc. Nail. Acad. Sci. USA 82, 259–263 (1985)
Chang, J., Romei, M. G. & Boxer, S. G. Structural Evidence of Photoisomerization Pathways in Fluorescent Proteins. J. Am. Chem. Soc. 141, 15504–15508 (2019)
Colletier, JP., Schirò, G., Weik, M. (2018). Time-Resolved Serial Femtosecond Crystallography, Towards Molecular Movies of Biomolecules in Action. In: Boutet, S., Fromme, P., Hunter, M. (eds) X-ray Free Electron Lasers. Springer, Cham. https://doi.org/10.1007/978-3-030-00551-1_11

graphical abstract

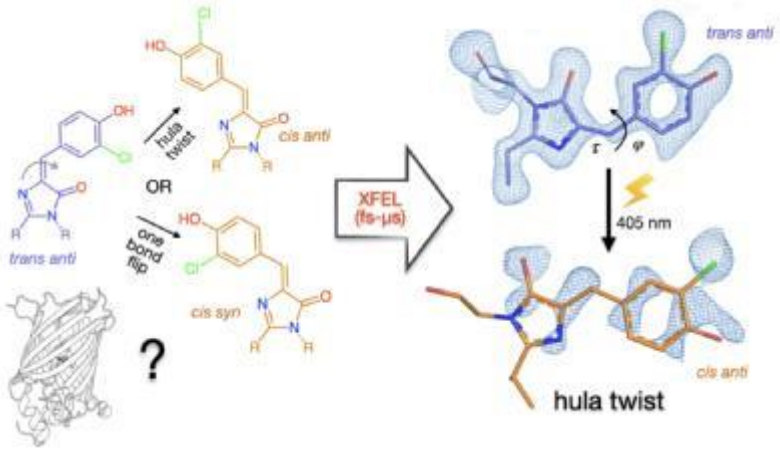

Back to Table of contents

MS44 Crystallography in large scale facilities

MS44-1-2 The High-throughput Macromolecular Crystallography Beamline P11
#MS44-1-2

H. Taberman [1], C. Borges [1], E. Crosas [1], S. Chatziefthymiou [1], A. Gruzinov [1], B. Kistner [1], G. Pompidor [1], J. Song [1], J. Hakanpää [1]
[1]DESY - Hamburg (Germany)

Abstract
P11 at PETRA III (DESY, Hamburg) is a high-throughput instrument for macromolecular crystallography (1). P11 has tuneable photon energy between 5.5 - 28 keV having the Eiger2 X 16M as the stationary detector and the possibility of using a CdTe-detector for higher energies. Beam size from 200 x 200 µm to 4 x 9 µm can be used with a maximum photon flux of 1.3 x 1013 ph/s at 12 keV energy. The automatic sample changer at P11 is based on the unipuck format with a total capacity of 23 pucks (368 samples) having a mount-unmount cycle of approximately 36 s, which brings the beamtime spent per sample down to ca. 2min. Furthermore, in close proximity of the beamline, P11 has a user laboratory with e.g. a crystal shifter for semi-automated crystal harvesting.
During the past two years mode of operation at P11 has changed from fully on-site to almost exclusively remote. Remote connection using FastX-access via a dedicated remote machine was established in 2020, which has enabled near normal user operation throughout the pandemic. Users are supported by a virtual meeting and the scientific accounts can be used during and after the beamtime for manual data processing on Maxwell, the central computational cluster, where the autoprocessing is also migrated to the dedicated P11 nodes.
P11 is a very diverse environment and allows the adjustment to various non-standard experiments e.g. via the long term proposal (LTP) scheme. For example, serial synchrotron crystallography at P11 is enabled with sample delivery through various types of solid supports or the tape-drive setup, which enables time-resolved experiments by the mix-and diffuse method (2), and has been developed through the LTP scheme along with the real-time autoprocessing of serial data with CrystFEL (3).
This year MXCuBE will be employed as the default control software with the integration to ISPyB for tracking shipments, communicating the sample details to MXCuBE, as well as acting as a data archive. The establishment of parallel autoprocessing pipelines in addition to the currently used, XDSAPP-based (4) pipeline, and the implementation of strategy calculation including dose estimation are also planned. Furthermore, these software developments are synchronising P11 with the EMBL PETRA III beamlines for the future foundation of a uniform structural biology village at PETRA IV.

References

[1] Burkhardt A., et al. Status of the crystallography beamlines at PETRA III Eur. Phys. J. Plus, 131, 56 (2016)
[2] Beyerlein KR, et al., Mix-and-diffuse serial synchrotron crystallography. IUCrJ 4, 769-777 (2017)
[3] White TA, et al., Recent developments in CrystFEL. J. Appl. Cryst. 49, 680-689 (2016)
[4] Sparta KM, et al., XDSAPP2.0 J. Appl. Cryst. 49 1085-1092 (2016)

Back to Table of contents

MS44 Crystallography in large scale facilities

MS44-1-3 Ultrafast X-ray Diffraction and Scattering at the Femtosecond X-ray Experiment (FXE) Instrument at the European XFEL: present status and future perspectives
#MS44-1-3

D. Vinci [1], Y. Jiang [1], R. Schubert [1], P. Zalden [1], D. Khakhulin [1], P. Frankenberger [1], F. Alves Lima [1], F. Ardana-Lamas [1], C. Deiter [1], M. Biednov [1], X. Huang [1], M. Knoll [1], D.D. Jimenez [1], F. Otte [1], S. Paul Dutta [1], H. Wang [1], H. Yousef [1], C. Milne [1]
[1]European XFEL - Schenefeld (Germany)

Abstract
Time-resolved X-ray methods are widely used for monitoring time-resolved electronic and structural dynamics over the course of photochemical reactions. Since fundamental processes in physics, chemistry and biology occur in ultrashort time range (from 10^{-12} to 10^{-15} s), X-ray free electrons lasers (XFELs) development received much more attention in the last ten years. Several experiments have successfully demonstrated that this new generation of light sources provides unprecedented insight into structural and electronic dynamics occurring during photo-induced reactions in various condensed-matter systems [1-2]. The EuXFEL allows to investigate these types of mechanisms thanks to the extremely brilliant (>10^{12} photons $pulse^{-1}$), ultra-short pulses (<100 fs), transversely coherent X-ray radiation, high repetition rate of up to 4.5 MHz, and extreme focusing (<10 um).
In this contribution, we present an overview of the present status and future perspectives of time-resolved diffraction and scattering techniques at the FXE beamline in EuXFEL. The instrument uses femtosecond optical laser pulses to pump the samples while the ultrafast X-ray FEL pulses probe their dynamical evolution in the so-called pump-probe method. The FXE instrument enables a femtosecond temporal resolution down to about 115 fs FWHM [4]. One unique scientific capability of FXE is to study ultrafast dynamics with various X-ray methods simultaneously in the photon energy range from 5 to 20 keV [3-4]. X-ray diffraction and scattering experiments on liquid and solid systems have been achieved at FXE [3]. For instance, ultrafast photochemistry studies in solution phase are performed by combining the wavelength-dispersive 16-crystal von Hamos X-ray emission spectrometer (XES) and X-ray solution scattering (XSS) recorded the Large Pixel Detector (LPD) [5-6]. Starting with non-resonant simultaneous Ka and Kb XES on Fe complexes [7-9] the capability was extended to a variety of other metal complexes including Co-, Ni- and Cr-based systems. The FXE beamline have also achieved successful sold-state experiments, including XES on thin films, single-crystal XRD with the Jungfrau detector motion, and polycrystalline scattering with the LPD.
The next step at the FXE beamline is to enable further solid-state experiments. In this perspective, the XTRAS project (ultrafast X-ray crystallography with diverse sAmple delivery) will be developed to provide femtosecond atomic “movies” of molecular crystals by means of single crystal XRD experiments and to reconstruct ultrafast intermediate state structures. The objective is to upgrade the existing vacuum chamber, and thereby provide rotation XRD, simultaneous XRD and XES, and cryogenic conditions for experiments requiring diverse sample delivery methods.

References
[1] Abela, R. et al. Struct. Dyn. 4, 061602 (2017).
[2] Chergui, M. & Collet, E. Chem. Rev. 117, 11025–11065 (2017).
[3] Galler, A. et al. J. Synchrotron Rad. 26, 1432–1447 (2019).
[4] Khakhulin, D. et al. Appl. Sci. 10, 995 (2020).
[5] Hart, M. et al. IEEE NSS/MIC 534 (2012).
[6] Veale, M. et al. JINST 12, P12003 (2017).[7] Bacellar, C. et al. PNAS 117, 21914-21920 (2020).
[7] Bacellar, C. et al. PNAS 117, 21914-21920 (2020).
[8] Naumova, M. et al. J. Phys. Chem. Lett. 11, 6, 2133–2141 (2020).
[9] Naumova, M. et al. J. Chem. Phys. 152, 214301 (2020).

Back to Table of contents

MS44 Crystallography in large scale facilities

MS44-1-4 The Powder Diffraction and Total Scattering Beamline P02.1 at PETRA III, DESY
#MS44-1-4

A. San Jose Mendez [1], V. Baran [1], H. Jeppesen [1], S. Alexander [1], S. Tim [1], W. Mario [1], W. Sergej [1], E. Martin [1]
[1]DESY - Hamburg (Germany)

Abstract
Powder Diffraction is a well-established method which allows to investigate long-range order structural properties of crystalline materials. On the other hand, Total Scattering measurements in combination with the Pair Distribution Function method is an expanding and powerful technique which allows to investigate the short-range and/or long-range order at the same time, making it possible not only to investigate crystalline materials, but also amorphous solids or liquids. Therefore, the combination of both methods provides a detailed insight into the structure of a wide range of material systems, including organic materials such as pharmaceuticals, co-crystals, covalent-organic frameworks, polymers and fibers, metal-organics such as metal-organic frameworks and inorganic materials such as nanoparticles, ceramics, cements, battery materials, metals and steels, metallic glasses, minerals and mineral glasses, superconductors, strongly (electron-)correlated materials, corrosion products, melts, liquids and so forth. For this huge range of crystalline and non-crystalline materials, structural properties, phase transitions or phase mixtures can be investigated at synchrotron facilities in ex situ, in situ or operando experiments utilizing either beamline-offered or user-developed sample environments.
The Powder Diffraction and Total Scattering Beamline P02.1 at the PETRA III synchrotron at the DESY facility in Hamburg, Germany, is a specialized station, where researchers from science and industry have the possibility to collect Powder Diffraction and Total Scattering data simultaneously with a fixed energy of 60 keV [1, 2]. With a custom-made tandem detector setup consisting of two large area detectors, users can, among others, perform in situ crystal growth experiments from the amorphous and nanocrystalline state up to the microcrystalline state, collecting simultaneously high-resolution Powder Diffraction data and Total Scattering / Pair Distribution Function data on the same sample. The P02.1 beamline offers a variety of sample environments for high-temperature (gas blowers, ceramic heater, Linkam furnace) and low-temperature (cryostreamer, cryostat) studies, as well as for mechanical treatments (stress rig, ball mills, etc.). While the aforementioned sample environments are available at the beamline, others like gas-flow cells, battery setups, etc., are provided on a collaborative basis with DESY users. Besides regular on-site synchrotron experiments, users can also apply for mail-in / rapid access services for Powder Diffraction and/or Total Scattering / Pair Distribution Function measurements of samples packed in capillaries. These measurements can be then automatically performed using a robotic system either at room-temperature or at temperatures in the range between 100 K and 1200 K, achieved by the employment of a liquid nitrogen cryostreamer and a hot-air blower.
In this presentation, we will inform the scientific community as well as industrial customers about the latest developments at beamline P02.1.

References
[1] Dippel A.-C. et al., Z. Anorg. Allg. Chem. 2014, 640, 3094.
[2] Dippel A.-C. et al., J. Synchrotron Radiat. 2015, 22, 675.

Back to Table of contents

MS44 Crystallography in large scale facilities

MS44-1-5 Live monitoring onsite, remote and unattended data collection on synchrotron MX beamlines #MS44-1-5

D. Aragao [1], N. Elliot [1]
[1]Diamond Light Source - Didcot (United Kingdom)

Abstract
Macromolecular crystallography instruments around the world run more and more in a remote access or unattended configuration. This results in less contact between humans and the hardware as well as less awareness of software and hardware states. Beamline failures that were in the past routinely reported by humans are now missed and lost in the noise of other issues. On another hand there is a need to have a chain of triggers from the beamline failure to the call out of a synchrotron staff that can assess and fix an issue. Finally, although most facilities have constant monitoring tools such has text messages or emails on catastrophic failures like loss of vacuum or cooling in the DCM, they tend to not monitor less important information due to the incapacity of a human being to deal with excessive amounts of information including false positives. Here we present a beamline monitoring software that intents to monitor EPICS PVs as well as other systems via HTTP restful interfaces, database connections or on disk file analysis and report in a configurable way to systems such as Slack, Email, Signal/WhatsApp or others. The use of a Slack bot allows update of configuration notifications as well as query some beamline states remotely before a support remote connection is required. Concepts as beamline mode as well as custom notifications for different staff members as well as a dependency chain of failures help reduce the number of notifications to a level which can be dealt with. The expectation is that this will be part of the on call / callout system, monitor the beamline live for upcoming possible problems as well as provide a log of the beamline states for the last day(s).

References
[1] https://networkx.org/ [2] R. Flaig et all, Acta Cryst. (2017). A73, a71

Live monitoring of an EPICS beamline

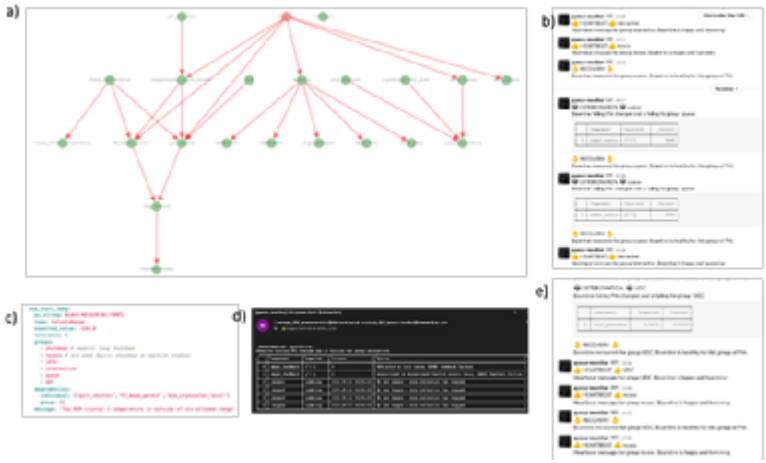

Back to Table of contents

MS44 Crystallography in large scale facilities

MS44-1-6 Beamline setup & calibration quality control for synchrotron MX beamlines #MS44-1-6

D. Aragao [1], N. Cowieson [1]
[1]Diamond Light Source - Didcot (United Kingdom)

Abstract
Macromolecular crystallography instruments around the world are mostly set on a single or handful of configurations. These makes them more predictable and more reliable. At the same time, current throughput demand on MX beamlines squeezes more and more the time for a careful regular maintenance and calibration of the instrument. The latter is extremely important to maximize data quality, protect equipment from failure and detect degradation that can lead to both degradation of performance and unexpected component breakdown down the track with consequence loss of beam hours. Across the world instrument scientists and software engineers have, with success, automated the daily setup & calibration but often neglected the need for quality control (QC) database recording. Proper QC systems allow a maintenance record of checks with numerous advantages namely: optimizing time by not doing all tests everyday but also guaranteeing that certain tests are done in regular intervals; plot beamline degradation or improvements particularly when new software or hardware is implemented; guarantee that beamline performance is not dependent of synchrotron staff doing the checks because they are all done the same way and recorded the same way; help train new staff into instrument scientist positions and many others. Here we present the next generation of a software tool initially developed at the Australian Synchrotron [1] in Python 2 and using GTK but in recent years re-written with more modern software including Python 3 and QT 5 (DLS internal Gitlab). It is currently in beta tests at Diamond Light Source I04 [2] beamline. The tool attempts to represent the checks currently done (Figure 1a) using visual cues pointing to when the check was last performed as well as provide some guidance on how to do the step-by-step checks. It will then database and file record the result of that check for future reference, tracking and baseline QC (Figure 1 b-c).
Figure 1. a) Main window showing the different steps as configured for DLS i04 beamline. b) Stored image for Rotation axis QC step showing a needle aligned at orthogonal angles 0 degrees (top left) and 180 degrees (top right); 90 degrees (bottom left) and 270 degrees (bottom right). c) Stored image for Align Beam QC step showing crosshair and beam position for 9 different zoom levels.

References
[1] https://github.com/AustralianSynchrotron/BeamlineSetup [2] R. Flaig et all, Acta Cryst. (2017). A73, a71

Beamline setup quality control GUI in action

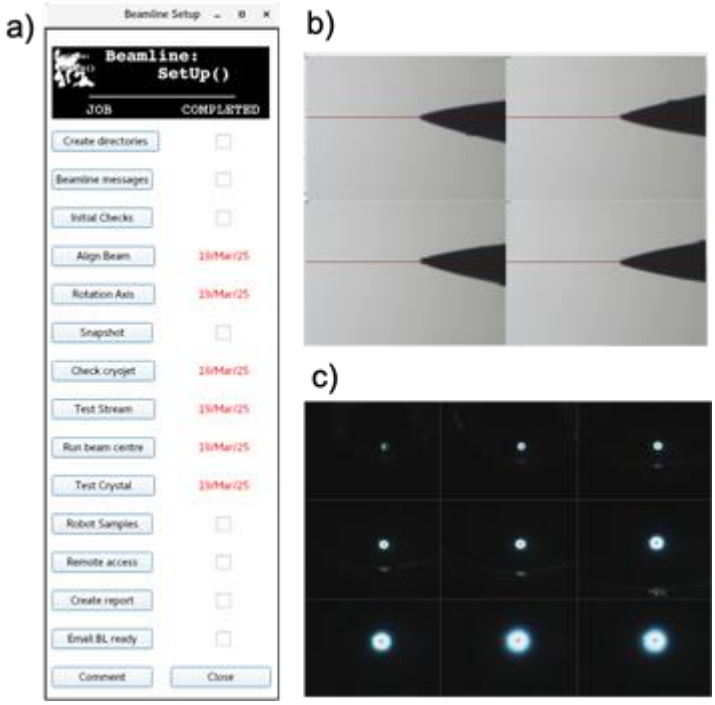

Back to Table of contents

MS44 Crystallography in large scale facilities

MS44-1-7 Powder diffraction on beamline CRISTAL: faster measurements and automation #MS44-1-7

E. Elkaim [1], P. Fertey [1], F. Legrand [1], L. Munoz [1], Y.M. Abiven [1], A. Noureddine [1]
[1]Synchrotron SOLEIL - Gif sur Yvette (France)

Abstract
In 2017, a "fast" curved detector consisting of 9 linear modules (Mythen, Dectris) was mounted on the 2-Circles diffractometer at the CRISTAL beamline, thus completing the multi-analyzer intended for high angular resolution measurements. With this detector, the time required to record a diagram has been greatly reduced from about 1 hour to less than 5 minutes in most cases.
To improve the efficiency of experiments, samples mounting was automated: for standard measurements at room temperature, mounting and then centering the capillaries are time-consuming repetitive tasks that required the permanent presence of a user during the experiments. To make better use of the available beam time, a robotic sample changer(capillaries) has been installed on the Cristal beamline. Equipped with a 36 samples magazine, this new device makes it possible to carry out automatic experiments adapted to mail-in or remote access. This poster describes the powder diffraction instrument and the automatic samples centering procedure. Characteristics of the diffractometer with its 2 detectors systems and some results are also presented.

Back to Table of contents

MS44 Crystallography in large scale facilities

MS44-1-8 Local strains in aluminum titanate polycrystalline materials
#MS44-1-8

D.P. Fowan [1], M. Mouiya [2], M. Huger [1], E. Thune [1], R. Guinebretière [1], R. Purushottam Raj Purohit [3], J.S. Micha [3], O. Castelnau [4]
[1]Université de Limoges-IRCER - Limoges (France), [2]University Mohammed VI-MSN/Université de Limoges-IRCER - Ben Guerir/Limoges (Morocco), [3]Université de grenoble Alpes-CEA-IRIG-MEM-CNRS - Grenoble (France), [4]Laboratoire PIMM - Paris (France)

Abstract
Polycrystalline materials based on aluminum titanate exhibit very low thermal expansion [1] and therefore have a very good thermal shock resistance [2]. Accordingly, they are mainly used for very high temperature applications.The β-Al_2TiO_5 phase crystallizes under the orthorhombic *Cmcm* space group and has anisotropic thermal expansion related to its structural characteristics, with a negative linear thermal expansion along the lattice axis [3]. This strong thermal anisotropy leads to a complex system of internal stresses and cracks (see Fig.1a) in polycrystalline aluminum titanate materials synthesized by high temperature sintering [4]. Moreover, β-Al_2TiO_5 phase decomposes into α-Al_2O_3 (alumina) and TiO_2 (rutile) by eutectoid reaction at 1300 °C [5]. However, it can be stabilized at room temperature through the formation of residual stresses or solid solutions containing various cation (Fe^{3+}, Mg^{2+}, etc.). In polycrystalline materials, the strains and the formation of solid solutions thus leads to metastable states, which are usually far from thermodynamic equilibrium. Understand the influence of such out of equilibrium situation on the decomposition process of β-Al_2TiO_5 and the formation of microcracks require multiscale investigations from the crystal size to the microstructure scale [2,6].
We investigated local strains on polycrystalline aluminum titanate samples by X-ray Laue microdiffraction at room temperature. Experiments were performed on ESRF beamline BM32 [7]. Thanks to the development of a new data reduction method based on the use of a neural network [8], we were able to index and extract the components of the deviatoric strain tensor online. Mapping at the sub-micrometric scale of the spatial evolutions of the strain tensor was measured (see Fig. 1b) and the strain components level distributions over the probed sample area are reported in Fig. 2.
We will illustrate through this communication, the influences on the strain state of both nature of the doping cations (Si^{4+}, Mg^{2+}, Fe^{3+}, Zr^{4+}) and the thermal treatments used in the elaboration process of different powdered or bulk samples.

References
[1] W., R. Buessem, N. R. Thielke, R. V. Sarakauskas, “Thermal Expansion Hysteresis of Aluminum Titanate”, *Ceram. Age, 60 (1952) 38-40*
[2] C. Babelot, A. Guignard, M. Huger, C. Gault, T. Chotard, T. Ota, N. Adachi, “Preparation and thermomechanical characterization of aluminum titanate flexible ceramics”, *J. Mater. Sci., 46 (2011) 1211-1219.*
[3] A. Doncieux, K. Ninomiya, N. Ishizawa, T. Ota, M. Huger, “Structural Basis for the Anisotropic Thermal Expansion of Aluminum Titanate, Al2TiO5, at Elevated Temperatures”, *11. (unpublished)*
[4] R. D. Skala, D. Li, I. Low, “Diffraction, structure and phase stability studies on aluminum titanate”, *J. Europ. Ceram. Soc., 29 (2009) 67-75.*
[5] S. M. Lang, C. L. Fillmore, L. H. Maxwell, “The system beryllia-alumina-titania: Phase relations and general physical properties of three-component porcelains”, *J. Res. Nat. Bur. Stand., 48 (1952) 298-312.*
[6] G. Bruno, A. M. Efremov, B. R. Wheaton,J. E. Webb, “Microcrack orientation in porous aluminum titanate”, *Acta. Mat.,58 (2010) 6649-6655.*
[7] O. Ulrich, X. Biquard, P. Bleuet, O. Geaymond, P. Gergaud, J. S. Micha, O. Robach, F. Rieutord, “A new white beam x-ray microdiffraction setup on the BM32 beamline at the European synchrotron radiation facility”, *Rev. Sci. Instrum., 82 (2011) 1-6.*
[8] R. R. P. Purushottam Raj Purohit, S. Tardif, O. Castelnau, J. Eymery, R. Guinebretiere, O. Robach, T. Ors, J.S. Micha, “LaueNN: Neural network based hkl recognition of Laue spots and its application to polycrystalline materials”, *in press in J. Appl. Cryst.*

Observation of a crack

Back to Table of contents

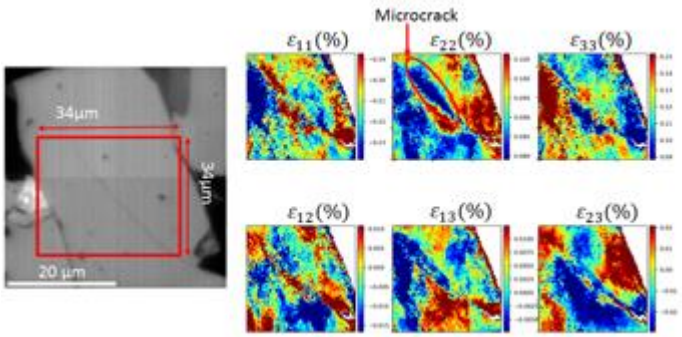

Deviatoric strain distributions

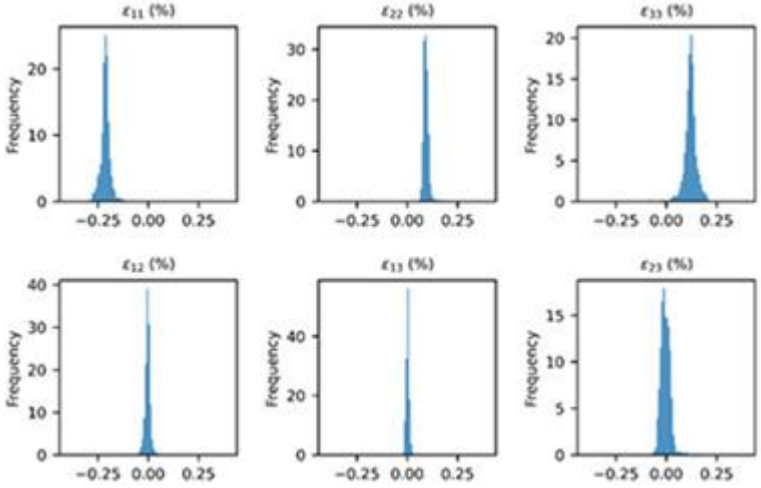

Back to Table of contents

MS44 Crystallography in large scale facilities

MS44-1-9 Coherent X-ray Diffraction Imaging on the D2AM (BM02) beamline
#MS44-1-9

M. Dupraz [1], G. Chahine [2], N. Blanc [1], S. Arnaud [1], F. Livet [2]
[1]Institut Néel - Grenoble (France), [2]SIMaP - Grenoble (France)

Abstract
Coherent diffraction imaging (CDI) is a lensless imaging technique[1], allowing to reconstruct isolated two- or three-dimensional objects from their measured diffraction pattern using computational inversion algorithms. In Bragg geometry (BCDI), the technique relies on the measurement of the 3D intensity distribution around a Bragg peak to recover the displacement and strain fields within finite crystals[2]. A strong reason for developing the capability to image strain in nanocrystals in the context of materials science is that it can be altered substantially by processing of the material, either as part of its design function or to test fundamental materials science principles.
Coherent x-ray beams are typically obtained from synchrotron sources, whose high brilliance and small source size allows to obtain coherent x-ray beams of reasonable intensity and of nearly macroscopic spatial extension. The intensity Ic available from a source in a coherent scattering experiment is connected to the average source brilliance B. The brilliance achieved by BM sources is significantly lower (typically 2 orders of magnitude) than the brilliance offered by undulator sources [3]. However, the large reduction of the source size after the EBS upgrade opens new avenues for the use of coherence on BM beamlines. Here, we explore the use of coherence and in particular of Bragg Coherent x-ray Diffraction Imaging (BCDI) on the D2AM beamline. We used Platinum nanoparticles (NPs, 100 nm to 1 µm in size) on a Yttria-stabilized zirconia (YSZ) obtained by solid-state dewetting to evaluate the feasibility of the technique. We managed to reconstruct 5 NPs using two Bragg reflections, clearly demonstrating the potential of the beamline for such measurements (Fig. 1). This is the first demonstration of BCDI on a bending magnet (BM) beamline, opening new avenues for the use of coherence on this type of beamlines. In order to optimize the experimental setup for future experiments, we evaluated the coherent properties of the beam using different approaches, i.e., diffraction from a 5 microns pinhole, analysis of the scattering from an aerogel sample, and ptychography on a Siemens star sample to reconstruct both the sample and the incoming X-ray beam.

References
1. Miao, J., Charalambous, P., Kirz, J. & Sayre, D. Extending the methodology of X-ray crystallography to allow imaging of micrometre-sized non-crystalline specimens. Nature 400, 342–344 (1999).
2. Robinson, I. & Harder, R. Coherent X-ray diffraction imaging of strain at the nanoscale. Nature Materials 8, 291–298 (2009).
3. Livet, F. Diffraction with a coherent X-ray beam: dynamics and imaging. Acta Crystallographica Section A Foundations of Crystallography 63, 87–107 (2007).

Reconstructed electron density and u222 displaceme

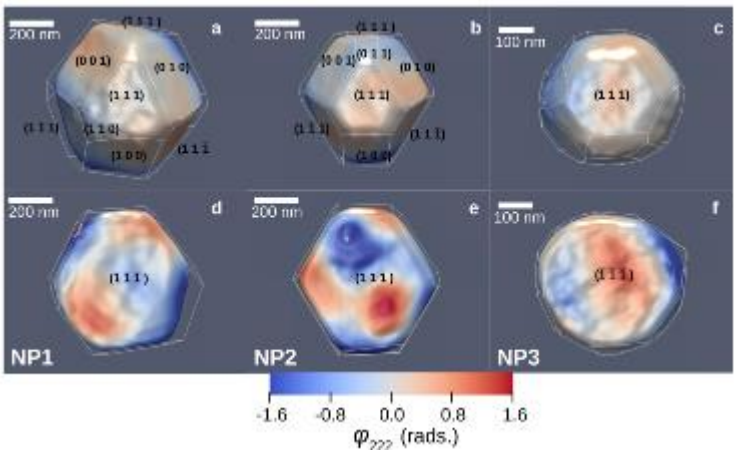

Back to Table of contents

MS44 Crystallography in large scale facilities

MS44-1-10 Implementation of a crystallographic fragment screening pipeline at the Swiss Light Source #MS44-1-10

D. Eris [1], J. Kaminski [1], L. Vera [1], K. Smith [1], C.Y. Huang [1], N. Meier [1], M. Wang [1], J. Wojdyla [1], M. Sharpe [1]
[1]Paul Scherrer Institute - Villigen (Switzerland)

Abstract
In recent years, fragment-based drug discovery (FBDD) has emerged as a viable strategy to develop lead compounds against protein targets. The “start small, elaborate efficiently” directive that defines FBDD stands in contrast to more traditional high-throughput drug discovery campaigns. FBDD has been used successfully in both industry and academics, delivering several drugs to the clinic with many more candidates currently in clinical trials. One of the most useful and informative techniques for FBDD is X-ray crystallography, employed most effectively as a primary screen to detect the binding of fragment hits to protein target sites, while simultaneously elucidating binding poise and identifying possibilities for fragment development.
In recent years, technological advances at macromolecular crystallography beamlines in terms of instrumentation, beam intensity, and robotics have enabled the development of dedicated platforms at synchrotron sources for FBDD using X-ray crystallography. Here, we report the development of the Fast Fragment and Compound Screening (FFCS) platform at the Swiss Light Source (SLS): an integrated pipeline for crystal soaking, handling, and data collection, which allows crystallography-based screening of protein crystals against hundreds of fragments and compounds.

References
Kaminski, J. W., Vera, L., Stegmann, D., Vering, J., Eris, D., Smith, K. M. L., Huang, C.-Y., Meier, N., Steuber, J., Wang, M., Fritz, G., Wojdyla, J. A. & Sharpe, M. E. (2022). Acta Cryst. D78, 328-336.

Back to Table of contents

MS44 Crystallography in large scale facilities

MS44-1-11 Azimuthal integration for fast X-ray area detectors on FPGAs
#MS44-1-11

Z. Matej [1], K. Skovhede [2], C.P. Johnsen [2], A. Barczyk [1], C. Weninger [1], A. Salnikov [1], B. Vinter [2]
[1]MAX IV Laboratory, Lund University - Lund (Sweden), [2]Niels Bohr Institute, University of Copenhagen - København (Denmark)

Abstract
Developments in X-ray detectors and increasing brightness of new generation light sources as X-ray free electron lasers and diffraction limited storage rings allow faster diffraction experiments. In order to catch up with the high data rates and to provide feedback to experiments with the lowest possible latency a compute acceleration of azimuthal integration (AZINT) of scattering data from X-ray area detectors is done here on field-programmable gate arrays (FPGAs). FPGA is a sort of computer chip hosted on a computer board which is often connected directly to external electronic devices as detector readout circuits or network transceivers. Modern “compute” FPGAs can be equipped with large memory and hosted in a computer exactly the same way as graphical processing units (GPUs). Moreover they can be programmed, beside other options, with the same programming language. In particular with OpenCL – the standard programming model used e.g. in the pyFAI azimuthal integration toolbox. OpenCL and synchronous message exchange (SME) were used to implement AZINT on FPGAs and to process data from X-ray diffraction experiments. Compute FPGAs are excellent candidates for processing high throughput detector data. All the tasks of receiving, decompressing the camera image stream and the final AZINT computation can be handled on a single device. The FPGA implementation allows for fixed and extremely short latencies in receiving integrated diffraction patterns that can be fitted in other parts of the configurable pipeline and provide a real-time feedback to the experiment. The solution can be integrated with compute infrastructures at large scale facilities or as an embedded device it can increase capabilities of handling high throughput detector data in any lab. It is available in the DevCloud [1] as well now. It is demonstrated the FPGA implementation can process several (>6) Giga-pixels per second on the mid-range FPGAs. That matches well the maximum frame-rates of detectors at MAX IV nowadays and it is well comparable with capabilities of high-end GPUs.

References
[1] https://gitlab.com/MAXIV-SCISW/compute-fpgas/bincount (last visited, July 4th, 2022)

Back to Table of contents

MS44 Crystallography in large scale facilities

MS44-2-1 A rigid-compact-multi-analyzer system for accurate powder diffraction analysis in the laboratory and/or on a synchrotron source to extract high resolution and low-noise patterns
#MS44-2-1

J-L. Hodeau [1], A. Prat [1], N. Boudet [1], N. Blanc [1], S. Arnaud [1], J.L. Hazemann [1], O. Proux [1], M. Jacquet [2], P. Martinetto [1]

[1]Institut Neel - Grenoble (France), [2]LAL-Univ Paris-sud - Orsay (France)

Abstract
Diffraction instruments using analyzer-filtering have existed since the 1990s for Synchrotron Radiation (SR) sources, (but are hardly practicable on laboratory sources), they have an efficiency that makes them used on the world's SR sources [1-6]. We present the realization/efficiency of a small rigid-compact-multi-analyzer system which allows to filter in parallel 20-50-100 measurements on SR sources, but also on laboratory X-ray sources (AgKα). This filtering is carried out by a diffractive filtering curved surface consisting of either a crystal, a thin layer, or multiple crystals supported on a fixed and rigid log-spiral curved surface. The geometry of this surface is calculated to allow filtration over a large angular range (2Θ) and using an X-ray spectral range to be usable by various sources [7]. The rigid-compact-multi-analyzer block completes and makes full use of the qualities of new "pixel" detectors which have a very low intrinsic noise [6]. When used together, they can drastically exceed the measurement detection thresholds (from 2-1% to 0.1%) alloying to detect minor phases in studies of heterogeneous "real" materials.
The tested rigid-compact-multi-analyzer system consists of a rigid-compact-multi-analyzer comb that contain 20-50 Si(111) single crystals and an associated block of 20-50 Soller slits. The angle between each crystal being 0.1°, its measuring range is 2-5°. This geometry has been calculated to operate an X-ray source having an energy ranging from 22KeV to 46KeV. Figure 1 shows a picture of the system on D2AM diffractometer at the ESRF. Figure 2 shows the total diagram (and the corresponding residual noise) of a LaB6 sample measured at 22KeV(AgKα) ; contributions of each analyzer is also shown for the low angle (110) LaB6 reflection ; the peaks have a FWHM: 0. 008°; the signal-to-noise ratio is 1/1000. The Rietveld refinement of these LaB6 diagram gives Bragg Rf 1.544 and Rf 1.046. The strong diffraction peak has an intensity of 60,000 cps while the residual noise is 60cps! (i.e. 3.5 to 2.5 cps. per analysis channel!) [8]. Using the same set-up and alignment, we collected data of some complex heterogeneous samples of the PatrimAlp culture heritage program [9]. Thanks to this set-up, we can quantify their components, the width of the lines of each phase is only related to the crystallinity of the phases and the fluorescence is suppressed. After the measurements of these "real" samples, we re-measured the LaB6 reference, without modifying the settings, we found the same intensities and profiles as before.

References
[1] Hodeau J-L. et al. (1998). Crystal and Multilayer Optics, Proc. SPIE 3448, 353-361; doi: 10.1117/12.332525[2] Siddons D.P. et al. (1998). Crystal and Multilayer Optics, Proc. SPIE 3448, 120-131; doi: 10.1117/12.332499[3] Gozzo F. et al. (2006). J. Appl. Cryst. 39, 347-357.; DOI: 10.1107/S0021889806009319[4] Lee P.L. et al. (2008). J. Synchrotron. Rad. 15, 427-432.; DOI: 10.1107/S0909049508018438[5] Parker J.E. et al. (2011). J. Appl. Cryst. 44, 102-110.; DOI: 10.1107/S0021889810044948[6] Dejoie C. et al. (2018). J. Appl. Cryst. 51, 1721-1733.; DOI: 10.1107/S1600576718014589[7] Prat A. et al. (2022). J. Appl. Cryst. submitted[8] Hodeau J-L. et al. (2022). J. Appl. Cryst. submitted[9] PatrimAlp. https://patrimalp.univ-grenoble-alpes.fr

Rigid-compact-analyzer-comb on D2AM diffractometer

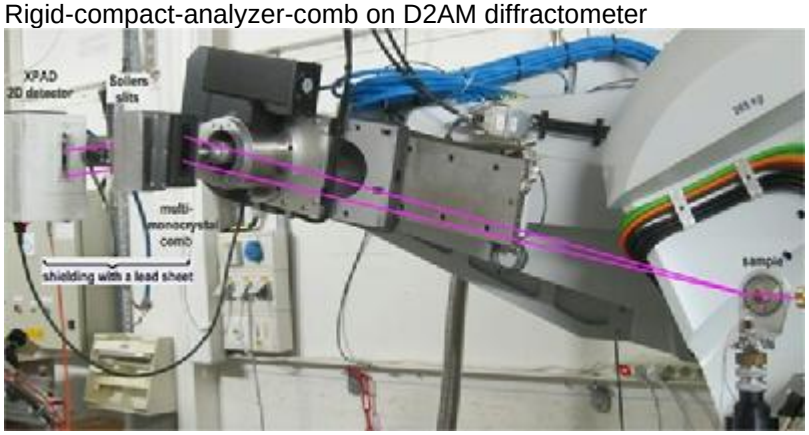

Back to Table of contents

LaB6 pattern using filtering by a 20 crystals comb

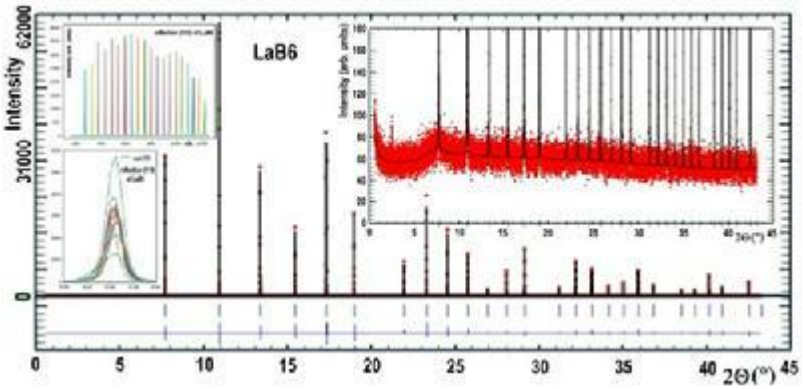

Back to Table of contents

MS44 Crystallography in large scale facilities

MS44-2-2 Koala, Echidna and Wombat – the neutron crystallography instruments at the Australian Centre for Neutron Scattering
#MS44-2-2

H. Maynard-Casely [1], M. Avdeev [1], A.J. Edwards [1], J.R. Hester [1], V. Peterson [1], R.O. Piltz [1], A. Studer [1], C.W. Wang [1]
[1]ANSTO - Sydney (Australia)

Abstract
The Australian Centre for Neutron Scattering is a neutron scattering facility located 35 km south of Sydney, Australia – using neutrons from the OPAL reactor. OPAL has now run for over 15 years, with exceptional availability – allowing allocation of ~200 days of instrument time to user proposal each year. Within the suite of 15 neutron instruments we have three that are dedicated for crystallographic studies under a wide range of conditions; the single-crystal Laue instrument Koala [1] (soon to be Koala 2.0), the high-resolution powder diffraction instrument Echidna [2] and the high-intensity diffraction instrument Wombat [3]. The poster will detail the capabilities of each of the instrument, recent upgrades [4] as well as some recent scientific highlights.
Our instruments are available for merit-based proposals from all researchers, with the deadlines for proposals on the 15th of March and 15th September. Echidna also runs a mail-in program open for proposals continually. Do please contact one of the team if you would be interested in applying for time.

References
1. Edwards, A.J., Neutron diffraction - recent applications to chemical structure determination. 2011. Website: https://www.ansto.gov.au/our-facilities/australian-centre-for-neutron-scattering/neutron-scattering-instruments/koala-laue (accessed 27/04/2022)
2. Avdeev, M. and Hester J.R., ECHIDNA: a decade of high-resolution neutron powder diffraction at OPAL. Journal of Applied Crystallography, 2018. 51(6): p. 1597-1604. Website https://www.ansto.gov.au/our-facilities/australian-centre-for-neutron-scattering/neutron-scattering-instruments/echidna-high (accessed 27/04/2022)
3. Studer, A.J., Hagen M.E., and Noakes T.J., Wombat: The high-intensity powder diffractometer at the OPAL reactor. Physica B: Condensed Matter, 2006. 385–386, Part 2(0): p. 1013-1015. Website https://www.ansto.gov.au/our-facilities/australian-centre-for-neutron-scattering/neutron-scattering-instruments/wombat-high (accessed 27/04/2022)
4. Edwards, A.J. and Piltz. R.O. Finding the Goldilocks zone for chemical crystallography via Laue single-crystal neutron diffraction–what have we learned from KOALA to improve KOALA 2.0? Acta Crystallographica A – Foundation and advances, 2021.

Back to Table of contents

MS44 Crystallography in large scale facilities

MS44-2-3 Protein crystallization and characterization for serial femtosecond crystallography at the European XFEL #MS44-2-3

H. Han [1], L. Brings [1], A. Chretien [1], I. De Diego [1], E. Round [1], C. Schmidt [1], R. Schubert [1], J. Schulz [1], K. Lorenzen [1]
[1]European XFEL - Schenefeld (Germany)

Abstract
The highly intense and short pulsed X-ray free electron laser (XFEL) beams enabled the measurement of nano- and micro-crystals as well as the study of protein dynamics by overcoming radiation damage through 'diffraction before destruction' (1). However, its application is still limited due to the difficulties in production and characterization of highly ordered nano- and micro-crystals, which are essential for the success of SFX experiments. To obtain high amount of microcrystal slurry requires conversion and optimization of vapor diffusion crystallization to batch crystallization, and this process can be sped up by systematic approach (2). The characterization of protein microcrystals in terms of size, density, homogeneity, and crystalline ordering necessitates the use of equipment not available in every laboratory, such as DLS, SONICC, and TEM. The bio lab of the European XFEL is an integrated user facility connected to the beamlines for supporting biological experiments (3). The laboratory was financed and built by a collaboration between the European XFEL and the XBI (XFEL biology infrastructure) User Consortium. It is equipped with various state of the art equipment for bio-sample preparation and characterization, including the equipment listed above. We also offer the possibility to test different sample delivery methods in order to select the optimal one that maximizes the success of the experiments at the XFEL instruments.
In this presentation, we would show process of protein microcrystal preparation and characterization in the XBI lab at the European XFEL with examples of beamtime preparation.

References
1. Neutze, R., Wouts, R., van der Spoel, D., Weckert, E. & Hajdu, J. Potential for biomolecular imaging with femtosecond X-ray pulses. *Nature* (2000). 406, 752–757.2. Beale, J.H. et al. Successful sample preparation for serial crystallography experiments *J. Appl. Cryst.* (2019). 52, 1385–1396.3. Han, H. et al. The XBI BioLab for life science experiments at the European XFEL. *J. Appl. Cryst.* (2021). 54, 7–21.

The layout of the XBI BioLab in European XFEL

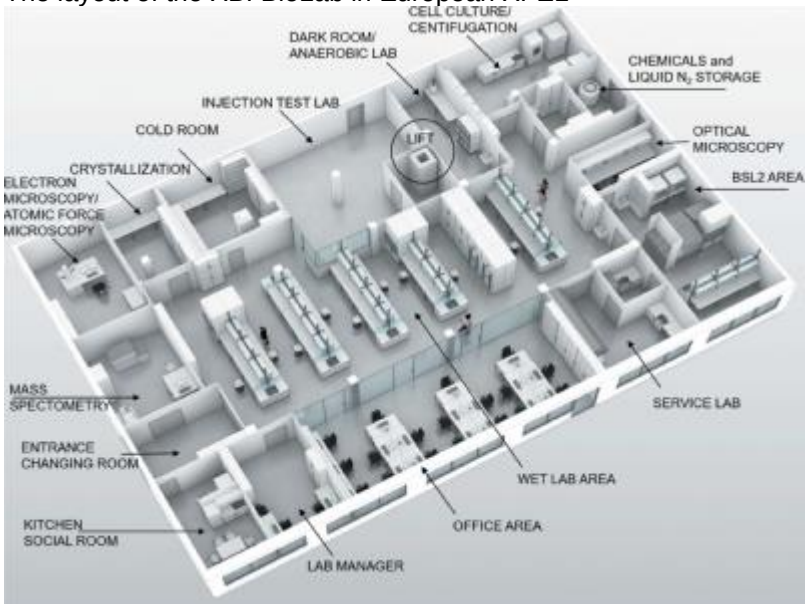

Back to Table of contents

MS44 Crystallography in large scale facilities

MS44-2-4 Chemical crystallography at PETRA III and IV
#MS44-2-4

M. Tolkiehn [1], L. Noohinejad [1]
[1]DESY - Hamburg (Germany)

Abstract
P24 at PETRA III (DESY, Hamburg) is a beamline dedicated to chemical crystallography, which started user operation in 2018. It is optimized for diffraction experiments on single crystals of small molecules and gives the opportunity to study complicated structures including quasiperiodic, modulated crystals, phase transition in non-ambient conditions, charge density and in-situ electrical filed measurements. We present some new updates of the instrumentation of the beamline and show our plans for a new beamline at the diffraction limited storage ring PETRA IV.

Back to Table of contents

MS44 Crystallography in large scale facilities

MS44-2-5 High Energy X-Ray Diffraction for Physics and Chemistry at beamlines P07 and P21.1 at PETRA III, DESY #MS44-2-5

I.G. Nielsen [1], O. Ivashko [1], O. Gutowski [1], A.C. Dippel [1], M.V. Zimmermann [1]
[1]Deutsches Elektronen-Synchrotron DESY - Hamburg (Germany)

Abstract
High energy X-ray diffraction and scattering based techniques play a major role in many scientific fields incl. physics, chemistry, and materials science. In particular, they enable complex in situ and operando experiments and the analysis of local (dis)order on atomic scale. The high-energy scattering and diffraction beamlines P07-DESY and P21.1 are operated jointly with a focus on exploiting the capabilities of high energy X-rays for a wide spectrum of scientific applications.

High photon energies of 50-100 keV allow for measuring with complex sample environment while maintaining the possibility to access a wide q-range. This makes it possible to perform diffraction and total scattering experiments in a variety of conditions such as temperatures, magnetic or electric field, and other in situ and operando modes for numerous types of materials.

The beamline P21.1 is a multipurpose versatile high energy X-ray diffraction beamline. Standard experiments include studies of single crystals, amorphous materials, liquids and nanocrystalline matter at various conditions. Several sample environments are available at the beamline such as a displex cryostat with temperatures down to 10 K, heaters for flat samples and capillaries up to 800 °C and the possibility to combine total scattering and small-angle scattering.

The P07-DESY branch is a high energy X-ray diffraction beamline specializing in small-beam experiments as the X-ray beam is routinely focused down to 2 µm × 30 µm (vertically × horizontally) at the sample position. The focusing capabilities enable spatially resolved techniques such as computed tomography (CT) with diffraction and PDF contrast (XRD/PDF-CT) as well as grazing incidence scattering studies of surfaces and thin films. In situ chambers for film deposition and heating in grazing incidence are available at the beamline.

The possibilities at the beamlines are presented to showcase the offered available techniques to the crystallographic user community.

Back to Table of contents

MS44 Crystallography in large scale facilities

MS44-2-6 Advanced diffraction techniques at the PSICHE beamline, Synchrotron SOLEIL
#MS44-2-6

A. King [1], N. Guignot [1], P. Piault [1], L. Henry [2], Y. Le Godec [3], H. Proudhon [4], J.P. Itie [1]
[1]Synchrotron SOLEIL - Gif-sur-Yvette (France), [2]Synchrotron SOLEIL/CEA - Gif-sur-Yvette (France), [3]IMPMC - Paris (France), [4]Centre des Matériaux MINES ParisTech - Corbeil-Essonnes (France)

Abstract
The PSICHE beamline of Synchrotron SOLEIL uses both imaging and diffraction to investigate materials, with a particular emphasis on in-situ experiments under extreme conditions. To meet the particular requirements of these measurements, we have developed or implemented a range of advanced diffraction techniques. Here we will present a number of the most important developments: Combined Angle and Energy-dispersive Structural Analysis and Refinement (CAESAR) [1,2], Diffraction Contrast Tomography (DCT) [3], and recent developments to improve the reliability of residual strain measurements. The CAESAR technique is particularly suited to the study of amorphous or liquid samples at extreme conditions. We have optimised both the acquisition and data analysis strategies in order to minimise the acquisition time and obtain correctly normalised data. DCT and related approaches are used for study multi- or polycrystals. First experiments have focused on the onset of plastic deformation, while in future we hope to apply these techniques to phase transitions at extreme conditions. Finally, a recurrent problem in the materials science community is the difficulty of measuring residual elastic strain reliably in large-grained materials. We present a strategy inspired by the Friedel-pair approach used in DCT for minimising the pseudostrain problem.

References
1. Wang, Y., Uchida, T., Von Dreele, R., Rivers, M.L., Nishiyama, N., Funakoshi, K., Nozawa, A. and Kaneko, H. (2004). J. Appl. Cryst. 37, 947-956.
2. King, A., Guignot, N., Henry, L., Morard, G., Clark, A., Le Godec, Y., Itié, J.P. J. Appl. Cryst. 55(2): 218-227. (2022).
3. Ludwig, W., Reischig, P., King, A., Herbig, M., Lauridsen, E.M., Johnson, G., Marrow, T.J., Buffière, J.-Y. Rev. Sci. Instrum. 80, 033905 □2009□

Back to Table of contents

MS44 Crystallography in large scale facilities

MS44-2-7 Long Wavelength Crystallography
#MS44-2-7

K. El Omari [1], R. Duman [1], V. Mykhaylyk [1], O. Christian [1], W. Armin [1]
[1]Diamond Light Srouce - Didcot (United Kingdom)

Abstract
The I23 Long wavelength MX beamline at the Diamond Light source is a unique instrument dedicated to experimental phasing and optimised to operate at wavelengths between 1.5 to 4 Å [1]. The beamline enables users to exploit the increased anomalous signal specific to scatterers naturally present in proteins such as S, P, Cl, Ca and K. This renders obsolete the need for selenomethionine incorporation or heavy-atom derivatisation of protein crystals, which represents a significant barrier in the process of experimental phasing. In addition to the long wavelength phasing experiments, I23 is the sole beamline where identification and localisation of biologically important ions, such as K, Ca, Cl is feasible by generation of anomalous difference Fourier maps below and above the element absorption edge [2,3,4]. Recent results of native phasing and ion identification/localisation demonstrating the capability and potential of the beamline will be presented.

References
[1] Wagner, A. et al. (2016). Acta Crystallogr D Struct Biol.
[2] Langan, P.S. et al. (2018). Nature Communications
[3] Rozov, A. et al (2019). Nature Communications
[4] Herdman, M. et al (2022). Structure

Back to Table of contents

MS44 Crystallography in large scale facilities

MS44-2-8 The BM07-FIP2 beamline for macromolecular crystallography at ESRF #MS44-2-8

E. Mathieu [1], C. Berzin [1], P. Jacquet [1], Y. Sallaz-Damaz [1], P. Israel-Gouy [1], F. Borel [1], D. Cobessi [1], J.L. Ferrer [1], A. Royant [1]
[1]IBS - Grenoble (France)

Abstract
BM07-FIP2 is available to users since October 1st, 2021. It is the follow-up of beamline FIP-BM30A [1] which ended operation in 2018 upon ESRF-EBS upgrade. FIP2 (French beamline for the Investigation of Proteins) is located on the Bending Magnet section 07 (BM07) of the ESRF. It is especially dedicated to crystallography of biological macromolecules. Its optics can deliver a focused beam on a fixed sample position in a large energy range (7-17 keV, to be extended to 5-25 keV). The beam size can be adjusted between 50 x 50 and 250 x 250 um^2. Data collection is controlled using the browser-based MXCuBE3 user interface, and sample (meta)data are handled and stored by ISPyB. FIP offers the following capabilities:
- High-throughput screening of cryocooled crystals
- (Multiwavelength) anomalous diffraction experiments
- In situ (in plate) crystal screening and data collection [2]
- On-line UV-Vis absorption microspectrophotometry [3]
- Humidity-controlled experiments [4]

References
[1] Roth M, Carpentier P, Kaïkati O, Joly J, Charrault P, Pirocchi M, Kahn R, Fanchon E, Jacquamet L, Borel F, Bertoni A, Israel-Gouy P, Ferrer JL (2002) FIP: a highly automated beamline for multiwavelength anomalous diffraction experiments. Acta Cryst. D58, 805-914.
[2] Jacquamet L, Ohana J, Joly J, Borel F, Pirocchi M, Charrault P, Bertoni A, Israel-Gouy P, Carpentier P, Kozielski F, Blot D, Ferrer JL. (2004) Automated analysis of vapor diffusion crystallization drops with an X-ray beam. Structure 12, 1219-1225.
[3] von Stetten D, Giraud T, Carpentier P, Sever F, Terrien M, Dobias F, Juers DH, Flot D, Mueller-Dieckmann C, Leonard GA, de Sanctis D, Royant A (2015) In crystallo optical spectroscopy (icOS) as a complementary tool on the macromolecular crystallography beamlines of the ESRF. Acta Cryst. D71, 15-26
[4] Sanchez-Weatherby J, Bowler MW, Huet J, Gobbo A, Felisaz F, Lavault B, Moya R, Kadlec J, Ravelli RB, Cipriani F (2009) Improving diffraction by humidity control: a novel device compatible with X-ray beamlines . Acta Cryst. D65, 1237-1246

Back to Table of contents

MS45 What is inside the black box?

MS45-1-1 Hybrid Photon Counting detectors - black boxes or powerful tools?
#MS45-1-1

M. Müller [1]
[1]DECTRIS Ltd. - Baden (Switzerland)

Abstract
Detectors play a key role for the data quality that can be achieved in a diffraction experiment. Their mode of operation and detector specific data corrections are important factors to consider when choosing data acquisition strategy and parameters in order to achieve best possible data quality. To use Hybrid Photon Counting (HPC) detectors not just as black boxes but as extremely powerful tools for X-ray detection, it is helpful to understand the underlying mode of operation and the data corrections performed by the detector and analysis software.
In this presentation I will outline the mode of operation of modern HPC detectors, providing a basic understanding of the critical steps from initial X-ray detection to corrected images provided to the experimenter. This basic understanding will help any experimenter to choose data acquisition strategy and parameters that fully exploit the advantages of modern HPC detectors and provide optimal data quality.

Back to Table of contents

MS45 What is inside the black box?

MS45-1-2 Olex2: What's in the black box?
#MS45-1-2

H. Puschmann [1], O. Dolomanov [1]
[1]OlexSys - Durham (United Kingdom)

Abstract
Olex2 [1] is now firmly established as a major software package in the field of small-molecule crystallography and it is safe to claim that the majority of structures are now processed with Olex2.
For many, Olex2 is a convenient interface to the ShelX software, and rightly so: users can concentrate on what matters in their structures and there is no need to be overly familiar with the computer language that interfaces the structure with the refinement program.
But there is so much more to Olex2, and recent developments have seen the coming-of-age of our native refinement program olex2.refine [2]. Recent developments have seen an enormous increase in speed and it is now also fully compatible with ShelXL refinements (you can switch easily between the two). But in addition, with olex2.refine we can now also
-- refine using non-spherical form factors (NoSpherA2) [3,4]
-- access constantly evolving new Quantum Crystallographial functionality [5]
-- refine atoms anharmonically
-- refine the anomalous dispersion parameters f' and f'' [6]
-- use various unique constraints and restraints
Olex2 is extensible on many levels: be it through simple macros, small python scripts, fully functional complex extension modules (which anyone can create) and, at a deeper level, powerful new developments on the level of the underlying cctbx.
In this contribution, I will dissect what is in Olex2, and explain how it is all organised. You will be interested in this if you
-- would like to get an overview of what's new in Olex2
-- are interested in gaining a deeper understanding of how it all works
-- would like to learn how to teach Olex2 new tricks
-- would like to contribute new science to Olex2
Olex2 is open-source, multi-platform and free of charge for all users

References
[1] OLEX2: a complete structure solution, refinement and analysis program Oleg Dolomanov, Luc Bourhis, Richard Gildea, Judith Howard, Horst Puschmann J. Appl. Cryst. (2008) 42(2), 339-341
[2] The anatomy of a comprehensive constrained, restrained refinement program for the modern computing environment–Olex2 dissected Bourhis, Dolomanov, Gildea, Howard, Puschmann, Acta Cryst. (2015) A71 (1), 59-7
[3] Accurate crystal structures and chemical properties from NoSpherA2, Florian Kleemiss et al., Chemical Science (2021); 12(5): 1675–1692.
[4] Vanishing of the atomic form factor derivatives in non-spherical structural refinement – a key approximation scrutinized in the case of Hirshfeld atom refinement, Laura Midgley et al, Acta Cryst. (2021). A77, 519-533
[5] https://gow.epsrc.ukri.org/NGBOViewGrant.aspx?GrantRef=EP/W029588/1
[6] Refinement of dispersion correction parameters in single-crystal structure determinations, Florian Meurer et al, [submitted, April 2022]

Back to Table of contents

MS45 What is inside the black box?

MS45-1-3 Pushing the Limits of Microfocus X-Ray Sealed Tube Sources for Crystallography
#MS45-1-3

J. Graf [1], T. Stuerzer [2], R. Durst [2], K. Atak [1], P. Radcliffe [1], C. Michaelsen [1]
[1]Incoatec GmbH - Geesthacht (Germany), [2]Bruker AXS GmbH - Karlsruhe (Germany)

Abstract
The structure determination on ever smaller and weakly diffracting crystals is one of the biggest challenges in the development of in-house X-ray analytical equipment for chemical and biological crystallography, which continuously raises the requirements for modern X-ray sources and detectors. Nowadays, modern low power microfocus X-ray sealed tube sources define the state-of-the-art for most in-house X-ray diffraction equipment, as they deliver intensities in the range of rotating anodes, yet maintain all the comfort of a sealed tube system.
Throughout the past years, we have continuously explored the physical limitations of impact ionization sources in order to find ways to push or even overcome some of the limitations, such as the heat transfer in the anode, leading to brighter X-rays sources with solid targets. The brightness of an X-ray tube is mainly limited by the thermal conductivity of the bulk anode material. As the thermal conductivity of diamond is up to about 5 times higher than that of copper and the highest known conductivity of all bulk materials [1], industrial diamond is increasingly replacing traditional materials for the thermal management in challenging applications [2], in which a high local heat load needs to be dissipated, such as in heat sinks for high-power microelectronic devices [3, 4]. In X-ray sources, diamond can be used as a heat sink directly coupled to the anode material, resulting in a significantly higher thermal conductivity compared to a conventional metallic anode and, hence, allowing for an increase in tube brilliance by applying a higher power load on the anode [5].
As a result of our efforts, we recently introduced a unique new class of microfocus sealed tube X-ray sources that uses a novel anode technology, the diamond hybrid anode [6]. It consists of a thin layer of metal deposited onto a bulk industrial diamond which acts as a heat spreader and significantly improves the heat dissipation in the anode. Consequently, the anode can accept a higher power density in the focal spot on the target without damaging the surface of the target layer. The balanced heat management allows the source to be air-cooled, while assuring that the intensity loss over time is only a few percent over 10,000 h of full power operation, which is significantly lower than the intensity degradation observed for microfocus rotating anodes [7, 8]. Along with this, optimizing the take-off angle of the anode and the parameters of the cathode to match the requirements of the X-ray optics enables a significant increase in the intensity on the sample. In combination with the latest developments in multilayer mirror technology, the IµS DIAMOND delivers an intensity in the range of $1 \cdot 10^{11}$ phts/s/mm^2 with a divergence that matches the typical mosaicity of weakly diffracting samples.
We will be reviewing the latest innovations in microfocus sealed tube X-ray sources and multilayer optics and be presenting selected results from protein and pharmaceutical crystallography that demonstrate the impact of these recent developments on the data quality.

References
[1] Moore, A.L. & Shi L. (2014). Materials Today 17, 163.
[2] Dischler B. & Wild C. (1998). Low-Pressure Synthetic Diamond Manufacturing and Applications. Berlin: Springer.
[3] Obeloer T., Bolliger B., Han Y., Long Lau B., Tang G. & Zhang X. (2015). IMAPS, 1.
[4] Pu S., Luo W., Shuai Y., Wu C. & Zhang W. (2016). ICMIA, 184.
[5] Li X., Wang X., Li Y. & Liu Y. (2020). Materials 13, 241.
[6] Durst R. D., Michaelsen C., Radcliffe P. & Schmidt-May J. (2020). US Patent 10,847,336.
[7] Mehranian A., Ay M. R., Riyahi Alam N. & Zaidi H. (2010). Med. Phys. 37, 742.
[8] Kákonyi R., Erdélyi M. & Szabó G. (2010). Med. Phys. 37, 5737.

Back to Table of contents

MS45 What is inside the black box?

MS45-2-1 Photon-counting detectors in the space domain and the time domain
#MS45-2-1

R. Durst [1], A. Abboud [1], B. Becker [2], T. Stuerzer [1]
[1]Bruker AXS GmbH - Karlsruhe (Germany), [2]Bruker AXS LLC - Madison, WI (United States)

Abstract
Conventionally, photon-counting detectors have operated in the time domain, in which X-rays are counted one-by-one as they hit the detector. However, this type of serial detection has limitations. It has been proposed that photon counting in the space domain should have significant advantages. In this approach the detector produces a fast 'movie' of the evolving X-ray diffraction pattern and then a processor looks for individual events in each frame of the movie. We describe the advantages of space-domain versus time-domain photon counting and explain how space-domain photon counting can be implemented using the latest generation of real-time processors.

PHOTON III X-ray detector

Back to Table of contents

MS46 Reproducibility in crystallography

MS46-1-1 Tensor of radiation expansivity – a proposed measure of structural susceptibility to radiation damage #MS46-1-1

C. Mcmonagle [1], S. Grabowsky [2], L.A. Malaspina [2], Y. Balmohammadi [2], D. Chernyshov [1]
[1]Swiss-Norwegian Beam Lines at European Synchrotron Radiation Facility - Grenoble (France), [2]Departement für Chemie, Biochemie und Pharmazie, Universität Bern - Bern (Switzerland)

Abstract
The advent of 4th generation synchrotron radiation sources of extreme brightness opens new possibilities for time resolved crystallography. However, with more routine accesses to extremely high doses of radiation during typical diffraction measurements, observable effects from radiation are increasingly observed for small molecule systems. Reproducibility and reliability of lattice parameters is of key concern for small molecule X-ray diffraction (SMX). (Christensen et al., 2019) They are commonly measured as a function of pressure and/or temperature to give thermal expansivities and bulk modulus but undetected dose effects can at best muddy the waters or at worst render these studies lacking. Negative X-ray expansion, (Coates et al., 2021) modification of polar properties, (Bogdanov et al., 2021) shift of spin equilibria in spin-crossover solids (Chernyshov et al., 2021) under irradiation serve as examples where different results might be observed as a function of energy and dose.
Here we present a set of observation of the lattice response of the radiation damage that concern dicyano-bis(triphenylphosphine)-mercury(II) [$Hg(CN)_2(PPh_3)_2$]. Repeated single crystal x-ray diffraction collections were made at fixed temperatures using synchrotron radiation on BM01, ESRF EBS. This enabled us to characterize the radiation expansivity independent of the thermal expansion.
We show that, at least in the beginning of the damage, the lattice response can be parametrized with help of a tensor, similar to the thermal expansion or compressibility. We propose that new tensorial property may serve as a measure of structural susceptibility to the radiation damage that can be spotted during a SMX experiment.

References
Bogdanov, N. E., Zakharov, B. A., Chernyshov, D., Pattison, P. & Boldyreva, E. V. (2021). Acta Crystallographica Section B 77, 365-370.
Christensen, J., Horton, P. N., Bury, C. S., Dickerson, J. L., Taberman, H., Garman, E. F. & Coles, S. J. (2019). IUCrJ 6, 703-713.
Chernyshov, D., Dyadkin, V, and Toernroos K. W., (2022) Acta Cryst. B , accepted
Coates, C. S., Murray, C. A., Boström, H. L. B., Reynolds, E. M. & Goodwin, A. L. (2021). Materials Horizons 8, 1446-1453.

Back to Table of contents

MS46 Reproducibility in crystallography

MS46-1-2 CODATA, IUCr, PDBj collaboration for medical-protein crystal structure definitive versions of data files #MS46-1-2

J. Helliwell [1], G. Kurisu [2], L. Kroon-Batenburg [3]
[1]University of Manchester - Manchester (United Kingdom), [2]PDBj - Osaka (Japan), [3]University of Utrecht - Utrecht (Netherlands)

Abstract
Envisaging a process akin to a journal's peer review we have set up an IUCr and PDBj collaboration for medical-protein crystal structure definitive versions of data files within the CODATA GOSC Case Studies (see https://codata.org/initiatives/decadal-programme2/global-open-science-cloud/case-studies/diffraction-data/). Quoting from our Case Study webpage "The overall reproducibility of the diffraction data and their linked molecular model is the overarching guide. The scope of this challenge, in general terms, can be judged by the fact that the FAIR movement (FAIR=Findable, Accessible, Interoperable, Reusable) did not include data quality in its criteria. In the spirit of scientific reproducibility, we introduce a term somewhere between reusability and reproducibility, namely definitive reusability." That PDBj had launched a raw diffraction images data archive XRDa https://xrda.pdbj.org/ was pivotal as it would allow a combined evaluation of raw data, processed structure factors and derived protein molecular model. This also would lead to general community benefit beyond medical pandemic challenges, although of course very important, to the whole of macromolecular crystallography. Feedback on a PDBj deposition is made by JRH and LKB to GK and who then can decide, like a journal editor exactly what feedback is made to a depositor to PDBj for a possible reversioning of a PDBj deposition. Progress of this initiative will be described and spans covid-19 and other medically important proteins (e.g. see Brink and Helliwell (2022), Hanau and Helliwell, 2022, Helliwell 2021).

References
Brink, A. and Helliwell, J.R. (2022) IUCrJ 9, 180-193.

Hanau, S. and Helliwell, J.R. (2022) Acta Cryst. (2022). F78, 96–112.

Helliwell, J R (2021) Acta Cryst F77, 388-398.

Back to Table of contents

MS47 New horizons in teaching crystallography in the 21st century

MS47-2-1 Expanding horizons - the use of crystallographic structures in high school chemistry classes #MS47-2-1

E. Irmer [1]
[1]**Georg-August-Universität - Göttingen (Germany)**

Abstract
The role of molecular models for visualising the “invisible” particle-level in chemistry education cannot be underestimated, especially for younger students in high school chemistry classes. Results from X-ray diffraction experiments can be used to introduce students into a “realistic” understanding of the structure of molecules and intermolecular forces. Especially the Cambridge Structural Database (CSD) houses many structures, which are relevant for chemical issues in undergraduate student courses (Battle *et al.*, 2010) or in school chemistry classes. However, often teachers or teacher students have little knowledge of crystallographic techniques. Therefore, they do not dare to use these results in their chemistry classes.
We make a proposal for educational reconstruction of the basics of X-ray diffraction and the process of crystal structure determination to enable teachers to work with the results. We will show which aspects are needed for this task and where problems and pitfalls may lurk.
We use the CSD teaching subset from the CCDC educational resources via the Mercury structure visualizer for an easy access to structures, which are relevant for chemical issues in school chemistry classes. We will show which program features are most important for exploring the structure of molecules and of intermolecular forces.
We will discuss examples for using CSD structures in different class levels of school chemistry lessons, from classical subjects as bonding types and aromaticity or conformations of hydrocarbons to intermolecular forces or hydrogen bonding.

References
Battle, G. M., Ferrence, G. M. & Allen, F. H. (2010). J. Appl. Cryst. **43**, 1208–1223, doi:10.1107/S0021889810024155.

Back to Table of contents

MS47 New horizons in teaching crystallography in the 21st century

MS47-2-2 CRISTAL-ITE: a single crystal X-ray diffractometer scale model for scientific dissemination #MS47-2-2

M. Giorgi [1], Y. Berchadsky [1]
[1]Aix Marseille University - Marseille (France)

Abstract
In a recent article entitled 'Teaching and Education highlighted' the authors report: 'In editing Teaching and Education articles… it is usually not the novelty of the scientific content that is important but the novelty in the way in which established crystallographic ideas and concepts are presented, especially with reference to the expected level of the target audience'[1]. Indeed development of modern digital tools in the 21st century is an undeniable asset for teaching crystallography toward students and the wider public[2,3] but encounters between people, physical links and thus 'teaching by the hands' remain as important as ever. Moreover, our own experience in disseminating knowledge demonstrates that the wider public and school/college students are always very enthusiastic about the idea of meeting laboratory staff, researchers and engineers, to discuss their research or more general scientific subjects. With this in mind we thought it would be interesting to 'take out' of the laboratory some 'mysterious' and complex equipment, bringing it to the attention of people who don't usually have the opportunity to see it - or even know that it exists - and use it as a basis for explaining various phenomena and concepts of crystallography in a playful way. The various technologies used in the design and operation of a four-circle single crystal X-ray diffractometer make it a very visual apparatus, likely to attract the eye and allowing to explain many physical phenomena or mathematical concepts - electromagnetic radiation, diffraction, interferences, Fourier transform - and to talk about crystallography in the broadest sense - state of matter, crystals, chemistry, biology etc... -. Tabletop diffractometers exist but are still very heavy and out of financial reach for schools or scientific associations for educational projects. We have therefore chosen to design and create a scale model of this type of diffractometer with the most common characteristics with the laboratory equipment, but safe, cheap and easily transportable in classrooms or public space[4]. Our poster will describe the main technical specifications of the apparatus that will also be present on site for demonstrations in action.

References
1. Dawe, L. N., Garcia-Ruiz, J. M., Hadju, J., McIntyre, G. J., Meilleur, F. & Stephenson, L. '(2022). J. Appl. Cryst. 55, 215-217.
2. Ferrara, J. D., Cochran, A., Del Campo, M., Göb, C. R., Le Maguerès, P., Meyer, M., Puschmann, H., Schürmann, C., Stanley, A., Swepston, P. N., Tripathi, A.,White, F. & Wojciechowski, J. (2021). Struct. Dyn. 8, 010401.
3. Kantardjieff, K. (2010). J. Appl. Cryst. 43, 1276-1282.
4. Giorgi, M. & Berchadsky, Y. J. Appl. Cryst. 55, 149-153.

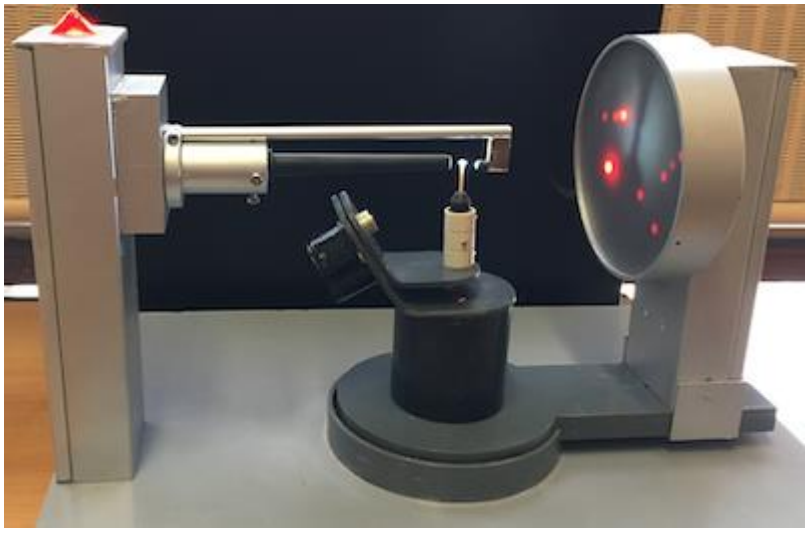

Back to Table of contents

MS47 New horizons in teaching crystallography in the 21st century

MS47-2-3 EASY GOV: Innovative Platform for Laboratory Management
#MS47-2-3

M. Benvenuti [1], M. Corsini [1]
[1]University of Siena _ Italy_ Dipartimento di Biotecnologie Chimica e Farmacia - Siena (Italy)

Abstract
The pandemic situation of COVID-19 demonstrated the need to integrate technologies with the capacity to perform rapid and intelligent data analysis to support laboratory management. Laboratory activities will be more successful as more attention is devoted to redesigning their processes systematically, using the best management practices.The development of a Platform, which supports the management of needs and services related to laboratories, is the ambitious project of the EASY GOV European Project.
The goal is to provide an easy-to-use, efficient and innovative tool, to be implemented with the collaboration of university institutions, which need to manage the laboratories. The main aspects on which the project focuses are: the management of spaces, instruments, materials and waste, paying specific attention to laboratory safety.
Greater attention devoted to the systematic redesign of laboratory activities, using more efficient management practices, will ensure a better organization of collective work. Therefore, by reducing the time required for the timely scheduling and planning of laboratory activities, the EASY GOV Platform will be a valuable support to the daily work of technicians and researchers.
EASYGOV Platform promotes correct actions within the laboratories through mandatory online tests, which also allow adequate supervision and which provide the basic requirements in terms of good laboratory practices.
Participating in the EASY GOV Project also means promoting collaboration and the exchange of knowledge at an international level between European technicians and researchers, thus helping to develop and standardize new procedures that make use of innovative practices for the management of laboratories.
Modules of the project:
Management of laboratory equipmentChemicals managementManagement of Biological ResourcesWaste ManagementManagement of laboratory materialManagement of laboratory spacesService managementLaboratory Safety ManagementTraining management
Objectives of EASY GOV project are: to promote an innovative practice in a digital era, capable of meeting expectations/needs and experiences in a European/international context face to COVID-19 pandemic; to promote an easy, effective and efficient management tool at the level of institutions with laboratory facilities; to promote internationalization; to promote transparency and recognition of skills and qualifications; to contribute to organizational modernization.
EASY GOV European Project Website: https://easygov.bio.uminho.pt/

References
THE PROJECT
EASY GOV is a European Project (Project No. 2020-I-PT0I-KA226-HE-094702) in which participate five partners from four European countries (Universidade do Minho, Portugal; University of Siena, Italy; Panepistimo Thessalias, Greece; New Consulting-Information Systems, Lda, Portugal; Rigas Stradina Universitate, Latvia) with a budget of 262.040,00 €.
Project Team for the University of Siena unit: Manuela Benvenuti and Maddalena Corsini (Department of Biotechnology, Chemistry and Pharmacy).

Back to Table of contents

Co-funded by the Erasmus+ Programme of the European Union

Back to Table of contents